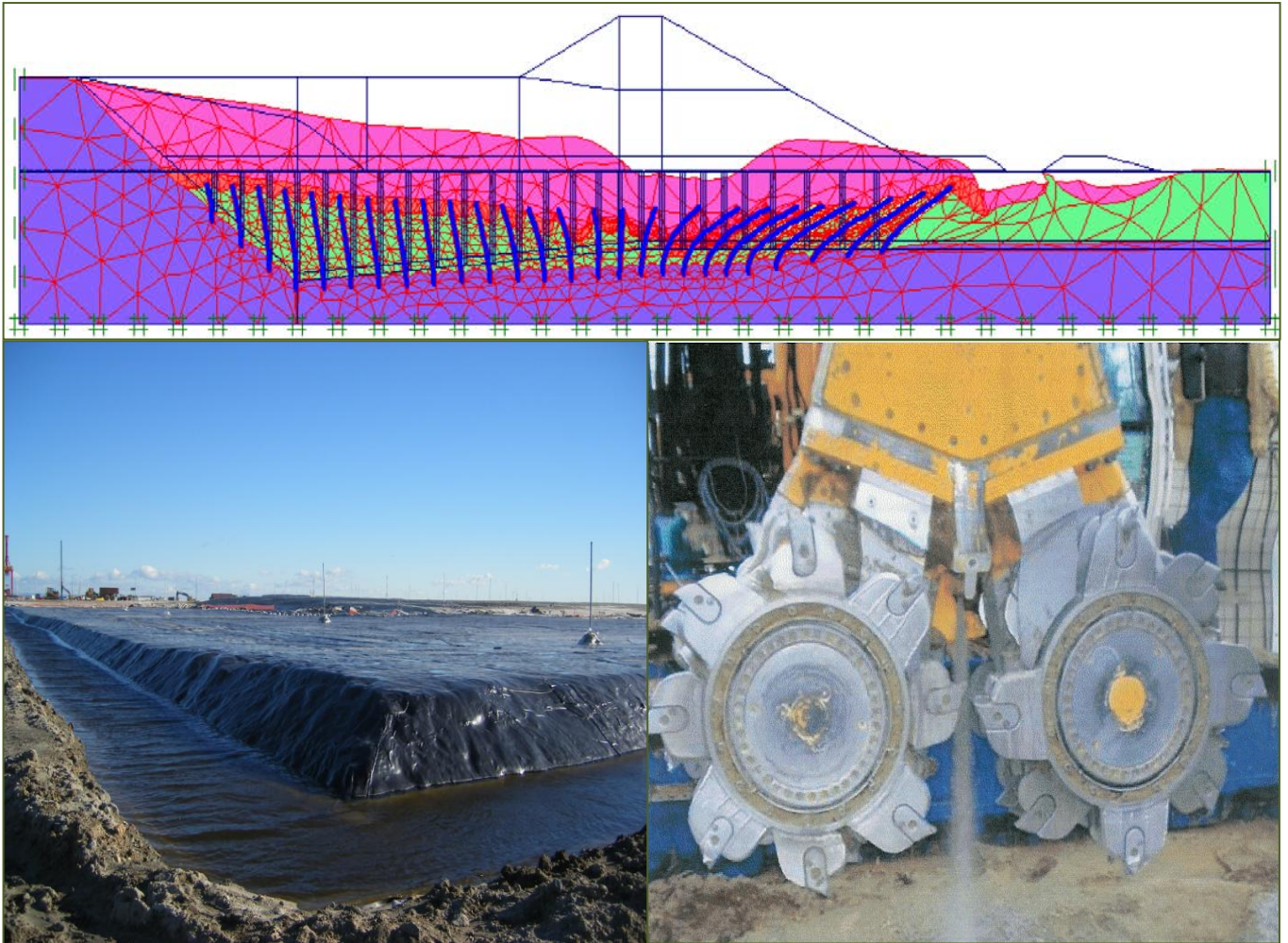# PROCEEDINGS OF THE INTERNATIONAL SYMPOSIUM

TC 211 IS-GI Brussels 2012

Recent Research, Advances & Execution Aspects of
GROUND IMPROVEMENT WORKS
31 May – 1 June 2012, Brussels, BELGIUM

VOLUME II

Organised by:

ISSMGE Technical Committee TC 211 Ground Improvement

Belgische Groepering voor Grondmechanica en Geotechniek
Groupement Belge de Mécanique des Sols et de la Géotechnique

Comité Français de Mécanique des Sols

Edited by:

Nicolas Denies & Noël Huybrechts

SIMSG ISSMGE

GBMS
BGGG

CFMS

Recent Research, Advances & Execution Aspects of Ground Improvement Works

Edited by

Dr. Ir. Nicolas Denies
Belgian Building Research Institute (BBRI-CSTC-WTCB), Belgium

Ir. Noël Huybrechts
Belgian Building Research Institute (BBRI-CSTC-WTCB), Belgium

Editorial address

Ground Improvement is a large and important domain in soil mechanics and geotechnical engineering and consists in a wide variety of techniques and methods adapted to a broad range of problems. The amount of contributions to the proceedings of this symposium is certainly a proof of that.

It cannot be denied that during the last decades the importance of the ground improvement market has enormously increased. New methods, tools and procedures have been developed and applied in practice.
In order to support this evolution in a scientific way, research programs have been and are being carried out worldwide, leading to more and better insights and delivering the basis for the establishment of design methods, quality control procedures and standards.

Due to the increasing interest of the construction sector for Ground Improvement techniques, the Belgian Building Research Institute (BBRI) has got more and more involved in projects addressing ground improvement during the last decade, most of them in a fruitful partnership with the Belgian Association of Foundation Contractors (ABEF).
In line with this evolution, the Geotechnical Division of the BBRI supports since 2005 the activities of the ISSMGE TC 211 Ground Improvement, which results today in the organization of an international symposium with more than 1600 pages of publications spread out over 4 Volumes:

- *Volume 1* of the proceedings contains the contributions of the 7 General Reporters, the Louis Ménard lecture held by *Patrick Mengé*, and the specialty lecture of the ISSMGE president *Jean-Louis Briaud*.
- *Volumes 2 to 4* contain more than 140 papers, subdivided in 7 Sessions, each of them dealing with a particular domain of Ground Improvement.

It can be noted that 40% of the papers deal with soil stabilisation and deep mixing, proving the huge interest in these techniques. This is not surprising, as they are outstanding and competitive sustainable construction methods.

We believe that the content of the present proceedings gives a very good overview of recent and on-going research actions and practices with regard to Ground Improvement. Moreover, we are convinced that they will contribute significantly to the further development of quality control procedures and standards.

Finally we would like to thank the Belgian Federal Public Service Economy, the NBN (Belgian standardization organization) and the Flemish Governmental Agency for Innovation by Science and Technology (IWT) for their financial support of the BBRI research programs addressing Ground Improvement techniques.

The Editors,

Nicolas Denies & Noël Huybrechts
Geotechnical Division, Belgian Building Research Institute, Brussels, Belgium

Table of contents of VOLUME II

CONTRIBUTIONS

SESSION 1
VIBRO & IMPACT COMPACTION

Soil dynamic response after ground improvement by heavy dynamic compaction or vibrocompaction

Stéphane Brûlé and Emmanuel Javelaud, MENARD, France, stephane.brule@menard-mail.com

ABSTRACT

Soil improvement work by dynamic compaction or vibrocompaction improves the granular soils' mechanical characteristics obtained by in situ investigations. The shear wave velocity parameter V_s could increase as well but in a much smaller proportion than those measured by mean of the cone penetration test or the pressurmeter test. Parameters tested within the elastic range of deformation, as V_s for instance, could increase enough and lead to a soil classification change. First experiences feedback points out the geotechnical conditions which are able to induce an Eurocode 8 ground type change after dynamic compaction or vibrocompaction works.

1. INTRODUCTION

This article presents the geotechnical conditions convenient to the change of the initial ground type, preliminary defined according to the European Standard EN 1998 (2005) for design structures for earthquake resistance, after works of densification of granular soil by methods such as dynamic compaction or vibrocompaction. To date, the ground densification leading to such result is clearly not the objective of the treatment but could become it, in particular if it brings an economic advantage in term of reinforced concrete for building project.

The analysis of the soils' mechanical characteristics before and after treatment could indeed lead to hold a different ground elastic spectrum, according to Eurocode 8 statuory point of view. It is well known that ground densification increases the mechanical characteristics of soils tested with cone penetration test (CPT) or pressurmeter test (PMT). To rule on the relevance of an effective change of class of ground, the classical site investigation is not sufficient. In fact, it is necessary to prefer shear wave velocity measurement (V_s) more adapted to the soil small strain parameters inferred by seismic waves ($\varepsilon \ll 10^{-4}$). Most of the worksites in Western Europe are concerned with a small strain seismicity (Semblat and al. 2009).

For the evaluation of soil liquefaction risk during an earthquake, there are studies based on the correlation between the soil shear wave velocity and the soil shear strength. Indeed, the compactness of sandy soils, used to appreciate their susceptibility to liquefaction can be appreciated through the V_s parameter (Andrus and al. 2000).

However, as described in European Standard EN 1998 (2005), the measurement of V_s has a promising future as an in situ liquefaction indicator, especially when it is difficult to obtain undisturbed and representative soil core samples (silty gravel soils for instance). Although significant progress on V_s measurement for subsurface investigations, the liquefaction analysis by means of V_s parameter requires the technical support of senior engineer. The content of this article is the following. First we define the study's validity domain (§2), then we appreciate the soils' parameter change after compaction with few case studies (§3). The argumentation is based on geotechnical investigation consisted of CPT, PMT and geophysical survey with V_s parameter obtained with modal analysis of surface waves (MASW). These worksites examples allow an accurate description of the initial ground type and no equivoque evolution after treatment (§4).

2. VALIDITY DOMAIN OF STUDY

2.1. Ground densification

This article is only about ground improvement techniques essentially for granular soil as dynamic compaction and vibrocompaction (figure 1). In both case we analyse the ground densification for some meters to several tens of meters thick. It could be a treatment to mitigate either an insufficient soil bearing capacity either incompatible settlements for the project or liquefaction mitigation. Vibrocompaction is a method using a vibratory probe inserted into ground. It was carried out to a depth of more than 60 m for onshore and offshore projects. The method is mainly applied to the densification of hydraulic sandfill

with various carbonate contents (Chu and al. 2009). Dynamic compaction consists on dropping a heavy weight from air onto ground. Dynamic compaction and vibrocompaction are classified as "ground improvement without admixtures in non-cohesive soils or fill materials" according to the TC 17 ground improvement meeting (www.bbri.be/go/tc17).
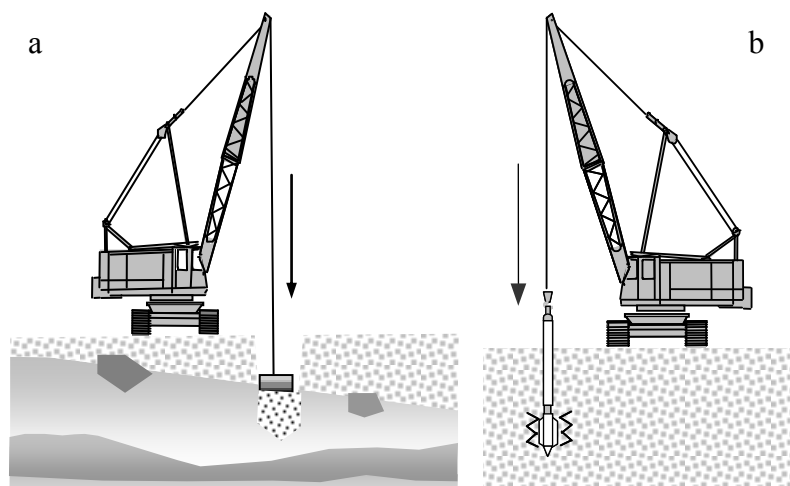
Figure 1: Dynamic compaction (a) et vibrocompaction (b).

2.2.   Soil texture

Soils in this study are mostly sands and gravels. The efficiency of vibrocompaction techniques is optimum if the fine content (passing through the n°200 sieve or grain size smaller than 75 µm) doesn't exceed 10 to 15% of the total weight of the soil sample (Mitchell and al. 2002) and less than 2% of clay (grain size smaller than 2 µm). Figure 2 shows validity domain for each technique versus grain size. Some authors suggest using CPT results to judge the suitability of the vibrocompaction method (Massarsch, 1991).

	Soil types	
Size range	**Sands**	**Gravels to cobbles**
ASTM	> 0.074 mm < 4.75 mm	> 4.75 mm < 350 mm
British/European Standard	> 0.06 mm < 2.0 mm	> 2.0 mm < 200 mm
Ground improvement without admixtures in non-cohesive soils or fill materials	Dynamic compaction Vibrocompaction	

Figure 2: Soil particle size main condition for ground densification techniques as dynamic compaction or vibrocompaction.

2.3.   Site effect

The amplification of seismic waves at the free surface, namely « site effects » may strengthen the impact of an earthquake in specific areas (e.g. Mexico 1985). Indeed, when seismic waves propagate through alluvial layers or scatter on strong topographic irregularities, refraction/scattering phenomena may strongly increase the amplitude of the ground motion. It is then possible to observe stronger motions further away from the epicenter. At the scale of an alluvial basin, the analysis of seismic wave propagation is a complex problem involving as various phenomena as resonance of the whole basin,

propagation in heterogeneous media, generation of surface waves on the basin edges, nonlinear behaviour of geomaterials. The analysis of seismic wave propagation and amplification in complex geological structures requires efficient numerical methods. At this stage of the analysis, we simply consider the 1D soil model and we do not question its effectiveness for earthquake ground motion description. We neglect 2D/3D effects.

Damage due to seismic excitation is often directly correlated to local site condition in the form of motion amplification and/or liquefaction induced ground deformation. Ground type induces directly the elastic response spectrum and this is an important hypothesis considering that mean value of the shear wave velocity $V_{s,30}$ (1) is reliable to relate site effects. Strong motion earthquakes are not analysed in this paper. In fact this type of earthquakes induces non reversible deformation. Topographic amplification are not analysed too because most of the ground improvement worksites are located on large size horizontal surfaces, on alluvium basin or near the shore line.

2.4. Eurocode 8 ground types

Geotechnical investigation CPT, SPT test ($\varepsilon>10^{-4}$) or geophysical methods ($\varepsilon<<10^{-4}$) based on V_s measures can be used for Eurocode 8 ground type. Results from both methods are depicted in this article. The geophysical method is Multichannel Analysis of Surface Wave method (Bitri and al. 1998). Soil classes are defined with the harmonic mean, formula (1), calculated for thirty meter of soil below the ground surface. Ground densification works are often concerned with A, D, E, S_1 and S_2 ground type (table 1).

$$V_{s,30} = \frac{30}{\sum_{i=1}^{n} \frac{h_i}{V_{si}}}$$

(1)

Table 1: Eurocode 8 ground types.

Ground type and description of stratigraphic profil
A : Rock or other rock-like geological formation, including at most 5 m of weaker material at the surface. $V_{s,30}$> **800 m/s.**
D : Deep deposits of dense or medium dense sand, gravel or stiff clay with thickness from several tens to many hundreds of metres. $V_{s,30}$< **180 m/s.**
E : A soil profile consisting of a surface alluvium layer with V_s values of type C or D and thickness varying between about 5 m and 20 m, underlain by stiffer material with $V_s > 800$ m/s.
S_1, S_2 : Soils potentially concerned with liquefaction (see EN 1998).

Table 2: Site characteristics
a – Brûlé and al. (2010a), b – Liausu (2010), c – Lauzon and al. (2006) and Karray and al. (2008).

	City Country	Surface (m²)	Maximum depth of densification (m)	Size range	Technique
a	Givors France	65 000	15	Well graded gravels backfill	Dynamic compaction
b	Dakar Senegal	70 000	13	Sand	Vibrocompaction
c	Peribonka Dam Canada	> 100 000	52	Sands and gravels	Vibrocompaction

3. WORKSITE BACKGROUND

3.1. Description

We selected three construction sites among Menard's recent ones where the granular soils' densification led to significant modifications of the soils' mechanical characteristics. For each site, the soil improvement was carried out over several thousand square meters. Note that the purpose of the works were to reach some settlement criteria for the superficial foundations, not to obtain the maximum possible densification of the soil.

The first project concerns the Givors' former Glass factory in France. Heavy dynamic compaction (HDC[TM]) was performed to improve 7 to 15 m well graded gravels backfills (Brûlé et al., 2010). This 85,000 m² building project has been subjected to energy level up to 5 000 kJ/impact.

The second project is the extension of the terminal container within the Port of Dakar in Senegal (Liausu, 2010), which was gained against the sea. Vibrocompaction works (figure 2) was carried out to improve 12 to 13 m of hydraulic sandy fill laying over marl. Soil improvement had been performed over an area of about 70,000 m^2.

The third project had been carried out by Geopac during the construction of a dam over the Peribonka river (Karry et al., 2008; Lauzon et al., 2006) in Northern Québec (Canada). The Peribonka Dam's construction involved deep compaction of the river's sand over 30 m at its foundation. Vibrocompaction (figure 2) was performed to compact the sand and as a remediation method for liquefaction risk.

3.2. Data

Regarding the Givors' project (table 2), the soil parameters are obtained from investigations carried out within a specific investigation area (35 x 150 m), and repeated exactly at the same positions before and after the soil densification. The tip resistance (q_c) and the pressuremeter limit pressure (PMT) given in table 3 are respectively the arithmetic and harmonic means of values from several borings over the whole improved depth (Brûlé et al., 2010). The shear wave velocity $V_{s,30}$ over the first 30 meters results from 10 M.A.S.W. profiles.

In Dakar, the tip resistance (q_c) and Standard penetration test values SPT (blows per 30 cm) given in table 3 are the arithmetic averages of values determined over the improved depth at the boreholes located within a sample area.

Data relative to the Péribonka Dam are given by Lauzon et al. (2006) and Karray et al. (2008). The main information is the shear wave velocity increase consecutively to the soil densification work, from about 150 - 250 m/s before the vibrocompaction work of the dam's foundation soil, to 250 – 350 m/s after the compaction work.

It is actually quite difficult to gather, from different sites, information that are obtained by using exactly the same procedures. Therefore, in this manuscript, our main objective is to investigate the parameters' range of variations. The results of soil tests and geophysical surveys are summarized in table 3.

Table 3: Results of site investigations done before and after densification.

Project	Site investigation				$V_{s,30}$ (m/s)	
	CPT	SPT	MASW	PMT	Before	After
Givors	x		x	x	244	252
Dakar	x	x			-	-
Peribonka Dam	x		x		Non calculated	

Project	N_{SPT}		CPT q_c (MPa)		PMT p_{l*} (MPa)	
	Before	After	Before	After	Before	After
Givors	-	-	3.7	7.3	0.5	2.4
Dakar	< 15	> 50	< 8	> 15	-	-
Peribonka Dam	-	-	< 10	> 10	-	-

3.3.   Data's analysis

The site investigation results show that the mechanical parameters obtained from in situ tests can increase by a factor of two after soil improvement works. The shear wave velocity V_s increases also but in a smaller proportion. At Givors were dynamic compaction work was performed from the surface, the shear wave velocity over the first five meters increased by about 20%. Calculated according to (1), the $V_{s,30}$ increases by about 3%. Regarding the Péribonka Dam, we note that the shear wave velocity increase can be greater than 15% over the whole improved layer. The vibrocompaction technique's effect on the $V_{s,30}$ can therefore be important even if the soil is not improved down to 30 m depth.

Basing the classification on in situ parameters, a modification of the ground type is possible. Modifying the ground type is however more difficult when the proxy used is the shear wave velocity, although it may be possible if the soil compaction is carried out for that purpose.

3.4.   Main information

The ground type according to the European Standard EN 1998 must be done appropriately so that the soil class is representative of the geologic context. It must indeed realistically take into account the site amplification effect: the lithology and the thickness of the soft layer laying on the seismic bedrock. The figure 3 shows the difference between the Eurocode 8 elastic response spectra calculated for C and D ground type. Assuming that some soil improvement work makes the soil ground type shift from a D class to a C class, the design of the structure must be adjusted, especially for structures with a natural period over 0.2 sec.

For example, if we use the formula (2) to estimate the natural period of a building whose height is less than 40 m, and constituted of reinforced concrete frames, it may have an impact on the design for buildings having at least two floors.

$$T_1 = C_t . H^{3/4} \tag{2}$$
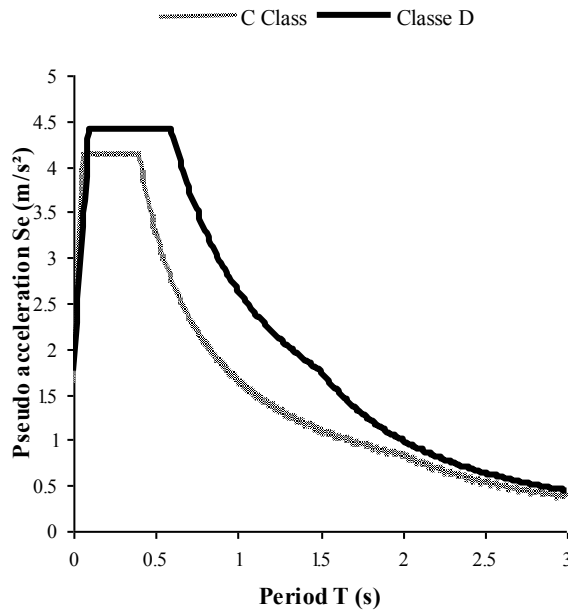
*Figure 3: Ground spectrum shape comparison for a D and C ground type with a 5% damping ratio (ξ).
The specific category of the structure is II (γ_I=1).*

4. CONCLUSIONS

Based on the possible variation range of soil's shear wave velocity, we identified the geotechnical contexts for which soil improvement work may lead to soil class' modifications (table 4). We also included in table 4 the cases where specific site studies, based on 1D numerical model shaked at their bedrock by real seismogram for example, may lead to a modification of the dynamic response of the soil.

Table 4: Geotechnical conditions convenient to a EC8 ground type change after ground densification.

Ground type	Comments
A	Even with a strong densification of the top 5 m soil, the statuory ground type can't change. However, the ground response can be affected in case of numerical modelling with new soil dynamic parameters.
D	Ground type can change if the soil is cohesionless and if V_s is close to the 180 m/s threshold. Ground type can shift from D to C if the ground densification modified 10 to 30 m of soil : $V_{s,30}$ can be modified. Site effect calculated by computational modelling for a two layers model could be modified. For example, let consider a natural 30 m thick D soil underlain by stiffer material with $V_s > 800$ m/s. If the ground treatment densify these 30 m by means of deep vibrocompaction, it is realistic to hope a significant change of the ground elastic response. In case of very thick alluvial basin (> 100 m) with D soil laying on a deep rock formation, the impact of the densification on the ground dynamic response, even for a 30 m treatment, could be minimized.
E	For soil profile consisting of a surface alluvium layer with V_s values of type D and thickness varying between about 5 m and 20 m, underlain by stiffer material with $V_s > 800$ m/s, see above comments for D ground type.
S_1, S_2	Specific studies must be led because European Standard EN 1998 doesn't supply any spectrum. If the soil survey only identify some lenticular deposits of sandy material (C or D type) suspect to local liquefaction risk and if the goal of the ground improvement is only to mitigate this phenomena, surface ground response will be hardly modified. However, a global deep densification for over consolidated granular soils, will directly define the new ground type, and then the elastic ground spectrum.

REFERENCES

Andrus, D.R. and Stokoe, K.H. (2000), "Liquefaction resistance of soils from shear wave velocity", ASCE, Journal of Geotechnical and Geoenvironmental Engineering, vol. 126, no. 11, 1015-1025.

Bitri, A., Le Bégat, S. and Baltassat, J.M. (1998), "Shear wave velocity determination of soils from in-situ Rayleigh waves measurements", Proceedings of the 4th Meeting EEGS, Barcelona, Spain, 503-506.

Brûlé, S., Javelaud, E. and Birtri, A. (2010a), " Seismic response analysis of a site after soil improvement by heavy dynamic compaction", Franco-Maghreb Conference in Geotechnical Engineering, Gammarth, Tunisia.

Brûlé, S., Javelaud, E.H., Ohmachi, T., Nakamura, Y. and Inoue S. (2010b), "H/V method used to qualify the modification of dynamic soil characteristics due to ground improvement work by means of heavy compaction process. A case study : the former Givors's glass factory area", 7th International Conference on Urban Earthquake Engineering and 5th International Conference on Earthquake Engineering, Tokyo, Japan, 02-26, 451-455.

Chu, J., Varaksin, S., Ulrich, K. and Mengé, P. (2009), "Construction Processes, State of the Art Report", 17th International Conference on Soil Mechanics and Geotechnical Engineering, TC17 meeting ground improvement, Alexandria, Egypt.

Eurocode 8 (2005) Design of structures for earthquake resitance – Part 1 : General rules, seismic actions and rules for buildings. The European Standard EN 1998-1.

Karray, M. and Lefebvre, G. (2008), "Control of deep compaction using Modal-Analysis-of-Surface-Wave "MASW" for the Péribonka dam foundation", International Conference on Geotechnical Engineering.

Lauzon, M., Gagné, B., Rattue, A.D, Bigras, A. and Hammamji, Y. (2006), "Vibrocompaction of the foundation soils of Peribonka hydro-electric dam ", Congrès annuel de l'Association Canadienne des Barrages.

Liausu, Ph. (2010), "Control of hydraulic sandfill vibrocompaction", Journées Nationales de Géotechnique et de Géologie de l'Ingénieur, Grenoble, France, 689-696.

Massarsch, K.M. (1991), "Deep Soil Compaction Using Vibratory Probes", Proceedings of Symposium Design, Construction and Testing of Deep Foundation Improvement: Stone Columns and Related Techniques, Bachus, R.C. Ed ASTM Special Technical Publication, STP 1089, Philadelphia, 297-319.

Mitchell, J.M. and Jardine, F.M. (2002), "A Guide to Ground Treatment ", CIRIA.

Semblat, J.F. and Pecker, A. (2009), "Waves and vibrations in soils: Earthquakes", Traffic, Shocks, Construction works, IUSS Press.

Ground improvement tank terminal Amsterdam - The Netherlands

J.W. Dijkstra, Cofra B.V., Netherlands, j.dijkstra@cofra.nl
A.H. Nooy van der Kolff, Hydronamic B.V., Netherlands, a.h.nooyvanderkorff@boskalis.nl

ABSTRACT

In the western part of the Port of Amsterdam a new storage terminal of oil products is being built. The site investigation revealed that underneath a single tank the thickness of the compressible layers could differ up to 3 meters. It was concluded by the client that ground improvement was required to avoid excessive differential settlements of the storage tanks and associated maintenance costs. The initial ground improvement design proposed by the client consisted of the application of dynamic replacement (DR). A trial showed that the traditional DR method as well as the CDC technique did not achieve sufficient improvement. Therefore, a full ground improvement was made, with large excavations up to a depth of 8 meters below the surface, removing more than 1,000,000m3 of material. The excavations were backfilled with sand. This very loose sand was compacted in one phase using the CDC technique. This paper presents an overview of the initial trial results and the final work method with a focus on the method of compaction and the compaction results.

1. INTRODUCTION

In the western part of the Port of Amsterdam a large new storage terminal for gasoline and related products is being built. An impression of the terminal is given in Figure 1. Before the storage tanks could be built, a large ground improvement was required. The ground improvement was required because of the large risk of differential settlements underneath the storage tanks and the high direct and indirect costs involved with the jacking and backfilling of differentially settled tanks. During the ground improvement, the highly compressible layers were removed within the zone of influence of the tanks and replaced by sand. This sand was compacted in one phase from the surface using the world largest rapid impact compaction hammers. This paper presents an overview of the ground improvement works with a focus on the method of compaction and the results obtained.

Figure 1: Artist impression terminal

2. GEOLOGY

The extensive site investigation data at the location of the terminal, with numerous CPT tests underneath one single tank, revealed compressible Holocene deposits with varying thicknesses underneath a continuous sand layer of 3 to 5 meters in thickness. The sand layer was placed in the 1960s during a large scale reclamation of the port of Amsterdam and was placed on top of the agricultural areas. The area was raised further during the dredging operations of the new 'Afrika' harbor at the beginning of this century,

adding about 1 meter to the sand thickness. Underneath a single tank, the layer thickness of the compressible material, consisting of a distinct layer of peat on top of a clay layer, could differ a couple of meters. The local thickening of the layer is contributed to an infilled channel, which presumably formed in the underlying clayey sand deposits on top of the Pleistocene sands. Figure 2 presents the interpolated bottom of the compressible layers. The creek is recognizable through the red coloring.
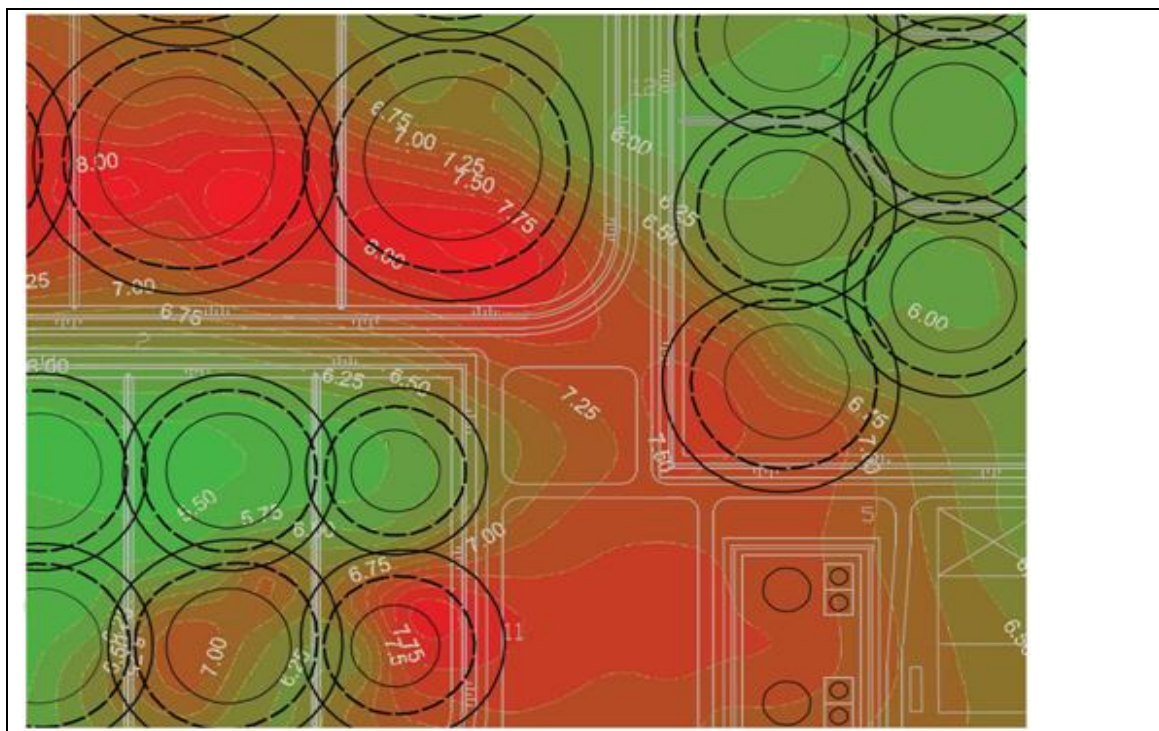
Figure 2: Interpolated bottom of the compressible peat and clay layer from the CPT information

3. INITIAL DESIGN

The large differences in the thickness of the compressible layer made that, without any ground improvement, the design did not comply with the PG29 guideline. The filling of the tanks, founded on raft foundations, would initiate differential settlements exceeding the maximal allowable 2.5% skew.

As a solution, the client proposed to use dynamic compaction to create sand columns inside the soft deposits, which is also known as Dynamic Replacement (DR). Through the installation of the sand columns it was anticipated to create shorter drainage paths, thereby allowing the excess pore water pressures to dissipate quickly during the loading of the tanks. The accompanying design made by the client consisted of dropping a 12.5 ton weight 4 times from a height of 6m in a grid of 3.5m by 3.5m. A compaction trial was initiated by the client and two contractors were invited to demonstrate their technique. Next to the design solution (DR) requested by the client, an alternative dynamic compaction technique was proposed by Cofra B.V. This was the CDC method.

4. CDC METHOD

The CDC method is a relative simple but effective compaction method. A weight of 9 or 16 tonnes is hydraulically accelerated within a frame. It drops from a height of 1.2 meters, with a frequency of minimal 40 times a minute, onto a foot which remains in contact with the ground. The foot is hammered into the ground till the stop criterion is met or when the maximum stroke of 1 meter is reached. Because the used feet have a large diameter ranging from 1.5m to 2.6m, they experience enough resistance in the granular soil to transfer the kinetic energy into compression and shear waves. The energy of the waves exceeds, in the non saturated zone, the shear resistance between the particles, making them rearrange into a denser structure. In the saturated zone, the compaction is achieved by the combination of the compression and shear waves. The pore pressures are momentarily raised during the passage of the compression wave. This results in a temporary lowering of the effective stresses and contact forces between the sand particles. When the shear waves passes, the excess pressures have not yet dissipated completely and the particles are moved into a denser structure. As a result of the dense compaction grid used during the compaction operations, with overlapping zones of influence, a single location is repeatedly vibrated, leading to homogeneous and effective compaction.
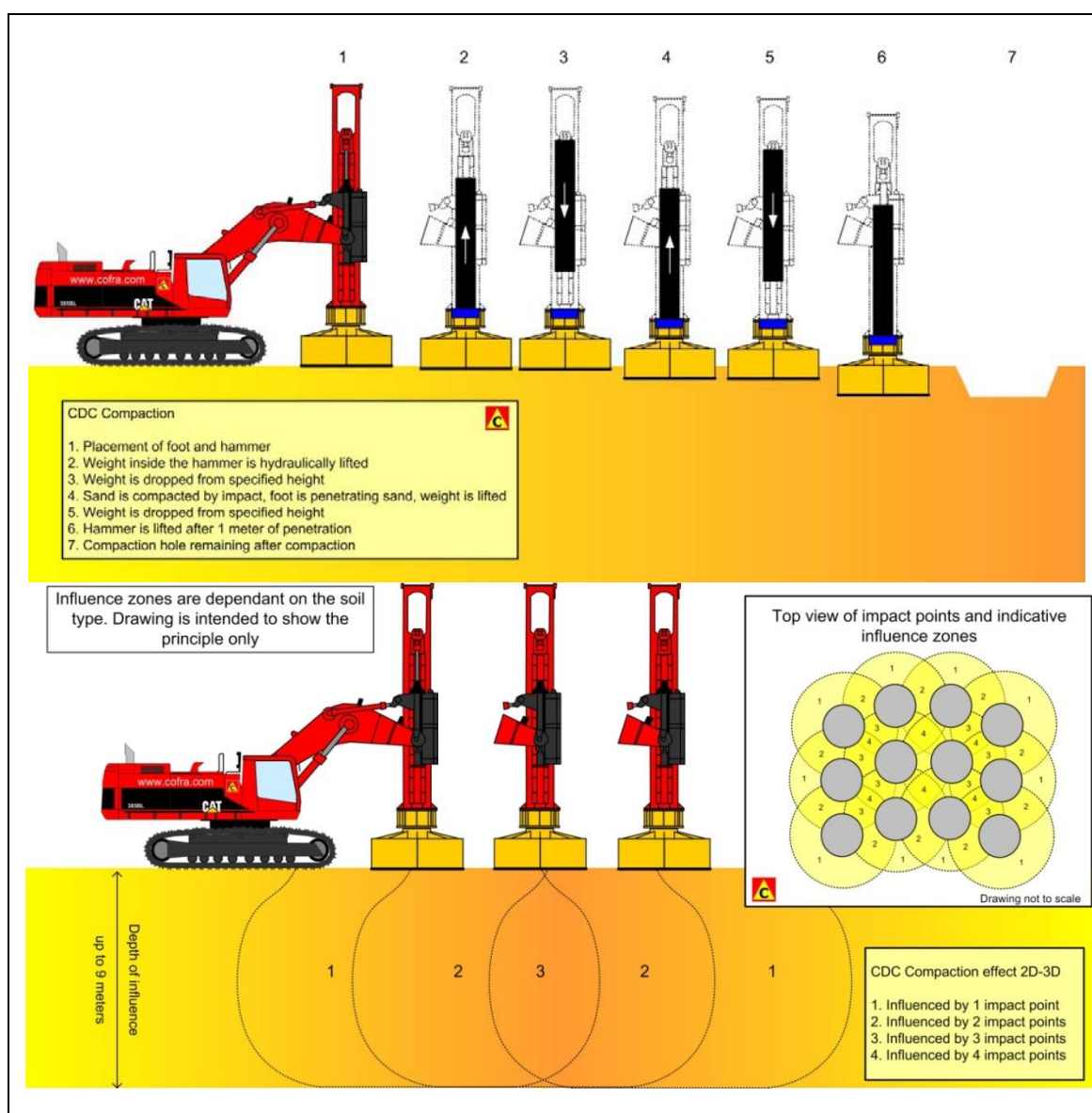
Figure 3: CDC principle

5. GROUND IMPROVEMENT TRIAL

The testing of DR and CDC techniques was performed during a compaction trial. The compaction trial was executed in march 2009. Before the trial was commenced a detailed method statement was made discussing the tests to be performed and how the alternative CDC method would be able to accomplish the same effect as the proposed Dynamic Compaction, as the CDC method is not capable to produce the same amount of energy per blow compared to the falling weight method.

It was proposed to test two compaction methods using the CDC hammers. The first method was similar to conventional dynamic replacement: a column of sand is pounded into the softer layer creating a stiff column transferring the load to the bearing layers below the soft layer. It was anticipated that in total 4 compaction runs were required to be able to create the column of sand.
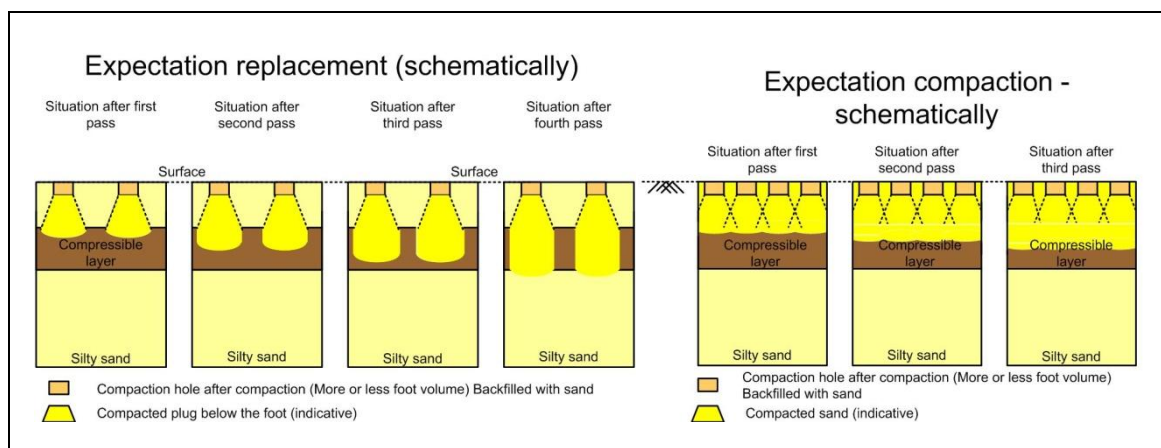
Figure 4: Principle of creating sand columns in the compressible peat and clay layer (left) and compaction on top of the peat and clay layers (right).

The second method tested was the regular CDC compaction method, where the complete surface area is treated in an overlapping grid. This was brought forward in order to accommodate the clients wish to "crack the peat and allow for a fast consolidation upon loading". Both principles are depicted in Figure 4.

The dynamic replacement operations were executed using 9 compaction locations in a square grid of 3.5m. Each phase of the compaction consisted of the compaction of all 9 locations and the compaction of each location till the compaction foot with a diameter of 1.5m was fully penetrated into the ground, i.e. 1m of displacement. After each phase CPT tests were performed to monitor the compaction levels and possible penetration of sand into the peat layer. Photo 1 shows the execution of the trial. During the trial massive amounts of water were forced to the surface, inundating the trial area.

Photo 1: Compaction of a trial location. Note the subsidence on the surface and the water in the previously compacted location

The second stage of the trial, compacting the area using a standardized grid, was performed by downsizing the diameter of the foot and grid spacing in every following compaction phase. The following compaction method was used:

- The first phase was executed using a 2.0m diameter foot with a grid spacing of 2.5m by 2.5m.
- The second phase was executed using a 1.5m diameter foot with a grid spacing of 2.0m by 2.0m.
- The last phase was executed using a 1.0m diameter foot and a grid spacing of 1.6m by 1.6m.

The changes were made to the grid and the foot diameter as the CPT testing of each previous phase showed no clear reduction of the thickness of the peat layer and compaction of the overlying sand layer. With the reduction of the foot diameter it was tested if the compaction of the top layer could be "broken" by the higher energy-surface ratio of the smaller diameter foot.

During the execution of the trial it became clear that for both trial methods:

- tremendous amounts of water were forced to the surface inundating the trial area,
- the top layer showed clear increases in cone resistance,
- no sand was forced into the peat layer.

The reason for the results became only apparent in the next stage of the project and will be discussed in a following section. It should however be noted that, even with a peat layer underneath, a clear increase in cone resistance was measured in the sand layer overlying the peat, as shown in Figure 6.
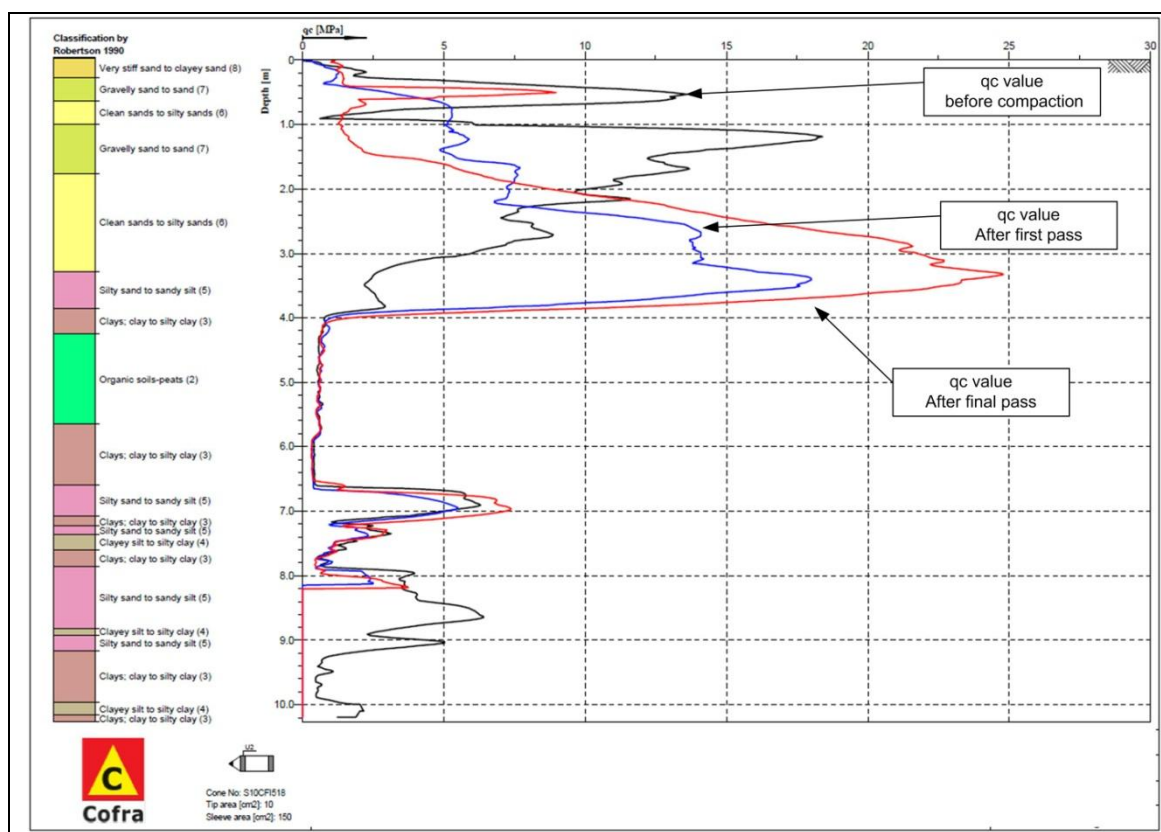
Figure 6: CPT results after the different compaction stages. The compaction after the first phase shows a clear change in the CPT profile, a clear increase in cone resistance in the zone 2-4m below the surface. The top section is disturbed by the penetration of the foot and reworking of material into previously compacted locations. The compaction of the final phase shows a further increase in cone resistance in the section from 2-4m below the surface. The low cone resistance in the top 1.4m is due to the backfilling of the compaction location.

6. NEW DESIGN

As the trial with the traditional DR method was also not successful, the client requested the contractors involvement in the design. After several consultations between the client, advisor and contractor, in which several ground improvement solutions were reviewed and priced within given boundary conditions, a simple solution was chosen to reduce the risk of the differential settlement: the removal of the compressible layers and their replacement with sand. This solution was economically most attractive, as right next to the new terminal, a new dock was required to be built providing a source of sand.

After the award of contract, a detailed operational plan was made in cooperation with the dredging company Boskalis to allow for a fast excavation and backfill. The sand was compacted from the surface after backfilling only. In total an area of 125,000m2 was compacted with a production of 2,000m2 per working day. The complete work, including excavations from 5 up to 8 meters deep, backfilling and compaction, was executed within 4 months time. Photo 2 and 3 give an impression of the project.

Photo 2: Photograph of the excavation of the compressible layers underneath the sand layer

Photo 3: aerial overview of the project with the different phases

7. EXCAVATION

During the excavation of the material it became clear why the replacement of the peat had not worked during the initial trial. The peat and clay layers were found to be very compact and almost dry. The peat could be excavated in large dry lumps. This was however of major advantage to the excavation process as the peat was strong enough for vertical excavation, as can be seen in Photo2. With the considerable strength of the peat, it is clear that the penetration of material into the peat was not possible.

8. COMPACTION REQUIREMENTS

The compaction requirements of the backfill material were set by the client, and required a cone resistance of minimal 5 MPa throughout the newly placed fill. Newly placed dry fill is generally compacted using vibratory rollers together with a slow filling process in layers. In this project it was chosen to abandon this principle and compact the placed material, with a maximum thickness of 8 meters, in one phase from the final surface using the CDC method. This was of major benefit to the speed of execution of the project and frequency of testing. Moreover the pumping period to lower the water table was reduced to only the excavation period, which also reduced the impact on the surrounding of the works. During the filling and compaction the pumps were not operational.

Photo 4: excess pore water escaping to the surface during the compaction

9. EXECUTION

The required compaction energy and compaction method was determined during a compaction trial, executed at the start of the project. In the trial two regularly used grid spacings were used, a 3.3m and a 2.5m center to center distance with a two meter foot diameter. Each grid spacing was used on a single tank footprint to incorporate the lateral variability in the fill in the trial and be sure the chosen method would be able to compact the sand in one pass. The compaction results were reviewed on the basis of CPT testing. The results indicated that the 2 meter diameter foot and a grid spacing of 2.5m was the most optimal configuration of the compaction with regards to the production and the requirement of reaching 5 MPa over the complete height of the fill. An example of a CPT test performed during the trial is given in Figure 7. The shown CPT was performed on the section compacted using the 3.3m grid. This specific CPT did not comply with the specification at 6 meter below the surface and required recompaction. The CPT result after recompaction is also shown in the figure.
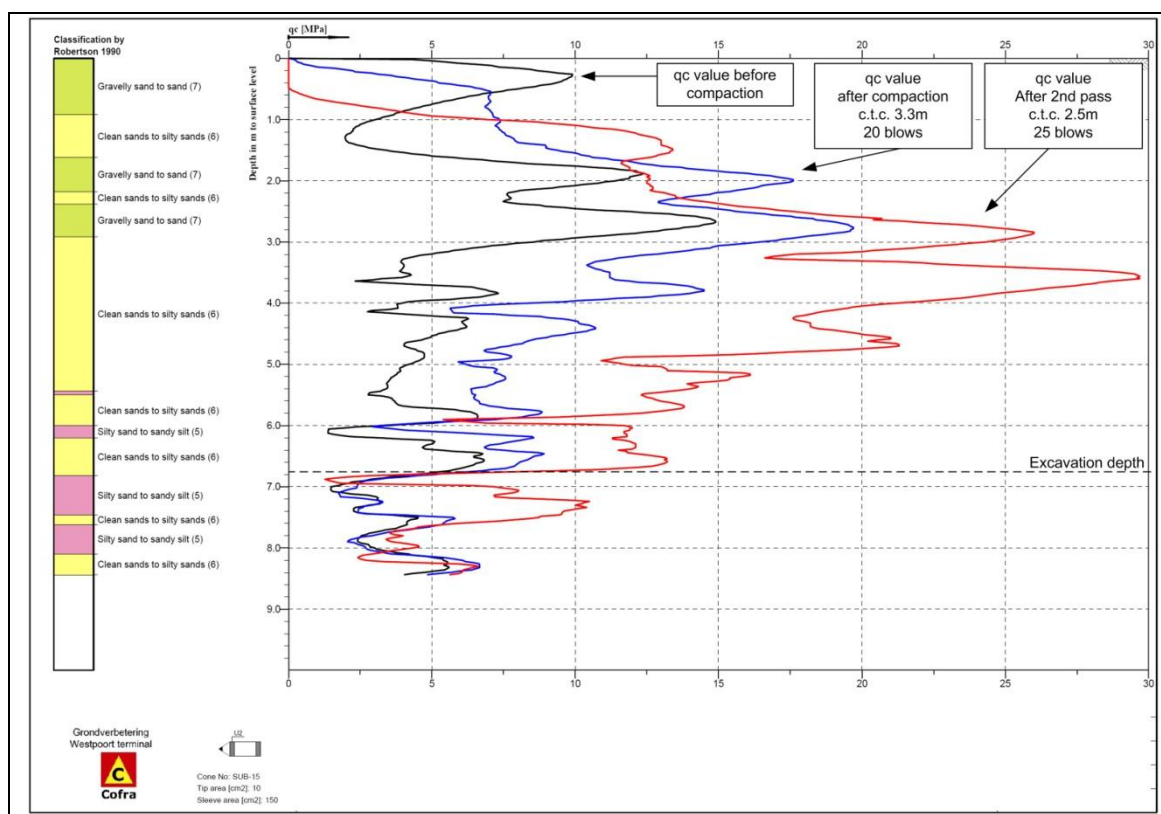
Figure 7: CPT test of initial trial area where the grid spacing was determined before and after compaction and after recompaction with the final grid.

10. QUALITY AND EFFECT OF PLACEMENT OF THE SAND

Due to the varying quality of the sand and the different methods of filling (in smaller layers and in lifts of several meters thick) the initially determined fixed number of blows per grid point was not a practical method to achieve homogeneous compaction. It was therefore chosen to change the work method to a more advanced system using the induced settlement as a stopping criterion. The induced settlement is measured during the compaction operations and displayed on the GPS guided loggers. This method was, after a statistical analysis of the performed handover CPT tests, able to deal with the varying filling methods and deliver a more homogeneous terrain after compaction. The used criterion was a settlement of the foot of 23mm per blow. When the criterion was met, the chance that the subsoil was compacted to the specification was more than 95%. The average surface level drop after compaction was, depending on the filling method and depth of excavation, after one pass, between 0.25m and 0.50m. Figure 8 presents a part of the obtained loggerdata. In the example a section of the compaction data is shown. The example shows the effect of the filling method. The left side of the compacted area was filled in one stage, the right side in multiple stages. The one stage filling results in much higher settlements before the criterion is met and hence a lower relative density before compaction.
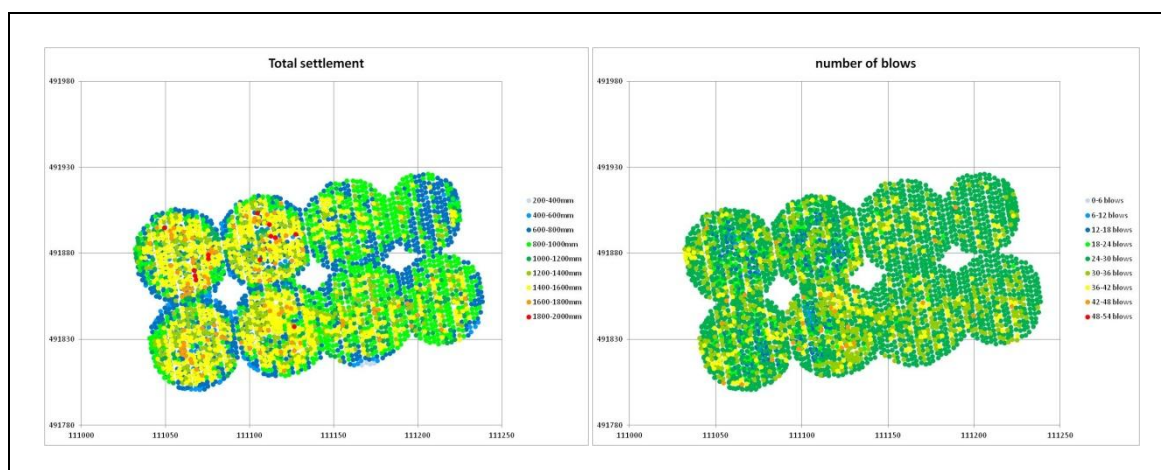
Figure 8: Logger data from one of the tank pits showing the effect of the placement method of the sand, where the left hand tank sites have been filled in one stage and hence show more settlement upon compaction

As described above, the method of filling and the quality of the sand had a large influence on the results of the compaction. This was especially noticeable during the compaction of the tank excavations backfilled with dredged North Sea sand. This sand, with a fines content of about 0%, compacted much better than the local sand with fines content above 10% using similar compaction energy. An example of a CPT taken after before and after compaction in the North Sea sand is given in Figure 9. In the silty sand CPT profiles where reached similar to Figure 9 but with cone resistances ranging between 10 and 15 MPa. Maximum cone resistance values above 30MPa were reached at sections with higher initial relative densities.
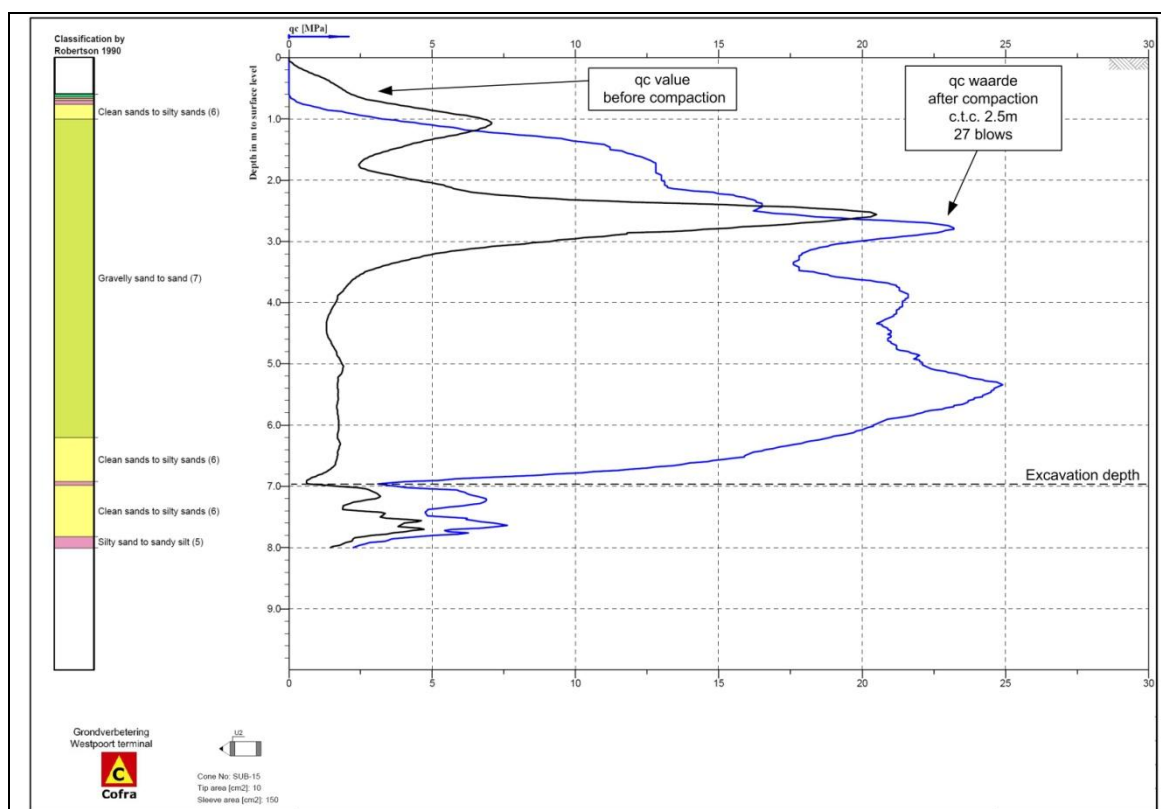
Figure 9: CPT test of area where North sea sand was used as fill material.

The surface settlement after compaction was in-between 30 and 50cm depending on the location and excavation depth.

11. QUALITY CONTROL TESTING

After the compaction and an analysis of the logger data, the compaction results were checked using CPT tests. CPTs results from before and after compaction were analyzed, where it should be noted that many more tests were available from after the compaction than from before the compaction. The compaction was checked with 17 cone penetration tests within each tank, equaling a CPT every 225m2 The CPT's were also used to check the excavation dimensions and the removal of all the compressible material. All CPT's were compliant to the contractual criterion.

The water load testing, i.e. the filling of a finished tank with water to simulate the loading conditions and test the integrity of the tanks, recently performed after the construction of the tanks, showed a compliance to the PG29 guideline.

12. INFLUENCE ON SURROUNDING STRUCTURES

Next to the area 4 windmills were located. As they were within the zone of influence of the compaction works, with minimal distances to the compaction front of 16 to 25m. They were actively monitored during the excavation and during the compaction operations. The displacement and the vibrations remained within the tolerances requested. Figure 10 gives the vibrations measured on the foundation of the windmill closest to the compaction operations. The vibrations were very low due to the large weight of the slab and the special working method, with compaction towards the windmill leaving always a section of very loose sand between the compaction and the windmill, reducing the vibrations.
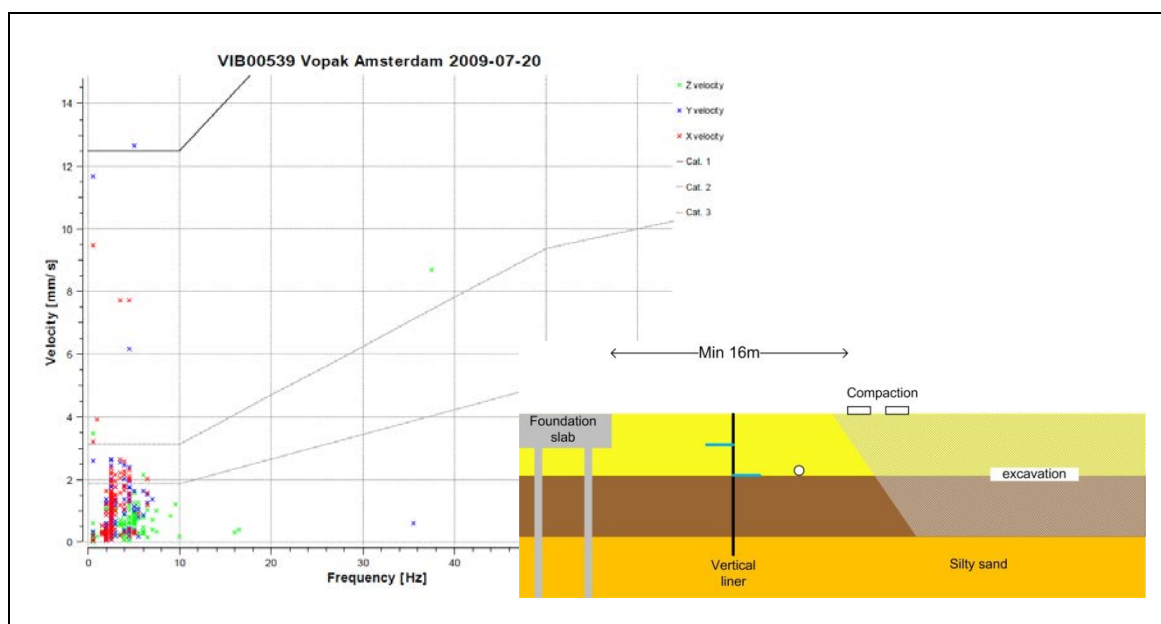
Figure 10: Vibration measurements on the foundation of the windmill

13. CONCLUSION

The CDC method was successfully applied at a large ground improvement project in the Western part of the harbor of Amsterdam. Due to the stiff characteristics of the peat and clay layer at a depth of 4 to 5 meter below the surface, the execution of DR using both CDC as well as the traditional method were not successful. This lead to the excavation of the compressible peat and clay layers within the influence zones of the tanks. After the backfilling of the excavations, with a depth up to 8 meters deep, the CDC compaction reached the required minimal cone resistance 5MPa over the full depth of the excavation. After compaction the CPT profile reached in general between 10 and 15 MPa. Maximum peak values of over 30 MPa were reached in sections with an initial higher cone resistance using a grid spacing with center to center distances of 2.5m.

The surrounding structures were not influenced by the excavation and compaction works with vibration velocities in general below 3mm/s.

REFERENCES

P. Meijers et al, 2009, Gedrag van zand onder cyclische belasting, Geotechniek nr 1 p30-35 (Dutch)
H.J.A. Berendsen, 2004, De vorming van het land, Gorcum b.v., Koninklijke Van
PGS 29 guideline, 2008, Vloeibare aardolieproducten - bovengrondse opslag in verticale cilindrische installaties, Ministerie van VROM, Den Haag (Dutch)
Lunne et al, 1997, Cone penetration testing in geotechnical practice

Laboratory study of disc rotation for densification of loose sands

Feng Tao-Wei, Chung Yuan Christian University, TAIWAN, R. O. C., twfeng@cycu.edu.tw

ABSTRACT

Thin layer of loose sands near the ground surface is likely unavoidable as a result of vibratory or impact compaction. In developing a method for densification of such loose sands, the disc rotation method was examined in the laboratory with a test tank of 600-mm in diameter and two discs of 150-mm and 200-mm in diameter. Both Ottawa sand and native Mai-Liao sand, with much difference in particle characteristics, were used in the test program. The disc was loaded on loose sand specimen and then was rotated about its central axis. Rotation of the disc induces shear stress on sand particles and causes them to rearrange so that a denser state may be achieved. Significant factors involved in the disc rotation operation include static vertical pressure on the disc, amplitude of disc roration, and accumulated angle of disc rotation. Disc settlement and specimen heaving as a result of disc loading and shearing were measured. Sand density measurements were made at various locations within the specimen for evaluation of effectiveness of the disc rotation method. Test results show that both the static vertical pressure and the subsequent disc rotation can improve the relative density of loose sands. The effectiveness of disc rotation is found to be a function of sand particle characteristics, magnitude of vertical stress on the disc, and angle of disc rotation.

1.   INTRODUCTION

Experiences show that, after ground improvement by vibratory compaction method, dynamic compaction method, and sand compaction pile method of dynamic nature, loose sands are commonly found near ground surface. For example, D'Appolonia et al. (1969) reported that in many cases the relative density of the last lift of backfill under vibratory compaction was still less than the required value of 75%. The main reason for such condition is likely that the confining pressure acting on sands at shallow depths is small so that ground vibration generated by compaction tends to loosen up the previously compacted sands. A laboratory experimental study has been made to evaluate a disc shearing method for densification of shallow sands (Feng et al. 2007). This method involves using a disc for applying both static surcharge loads and shear forces to the loose sand specimens. The shear forces are applied by rotating the disc so as to induce shear displacements of sand particles beneath the disc. With such movements, the density of loose sands will be increased.

The laboratory study of a disc rotation method utilizes a test tank of 600 mm in diameter and 600 mm in depth (Feng and Huang 2009). Loose dry sand specimen is prepared by using air pluviation method. The specimen is incrementally loaded to a selected value of static vertical pressure, under which the disc is rotated on the specimen to induce sand compression or disc settlement. In the mean time, heaving of sand specimen may appear in the area surrounding the disc. Typical static vertical pressure-settlement relationship derived from the disc rotation test is illustrated in Figure 1.
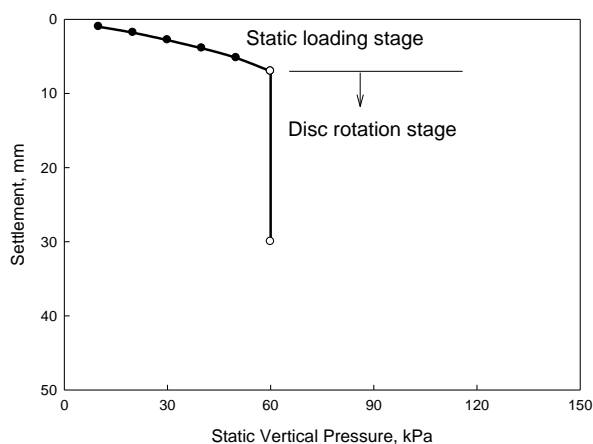
Figure1: Illustration of static vertical pressure-settlement relationship from the disc rotation test

Critical operating factors considered for the disc rotation test include static vertical pressure on the disc, amplitude of angle of disc rotation, and accumulated angle of disc rotation. Based on the results of previous studies (Feng et al. 2010), it can be tentatively concluded that the static vertical pressure utilized should be somewhat less than the ultimate bearing capacity value, the disc rotation should be of reversal type, and the efficiency of disc rotation in inducing sand compression decreases with increasing the accumulated angle of disc rotation.

A direct indication of sand densification after disc rotation would be a net decrease of sand volume which can be evaluated from the data of settlement and heaving. Such data obtained from several series of laboratory disc rotation tests show a net decrease in specimen volume for both the Ottawa sand and a native Mai-Liao sand. In addition, the volume decrease of Mai-Liao sand is much more than that of the Ottawa sand, which is likely attributed to the smaller and platy-shaped particles of Mai-Liao sand. Effect of disc rotation on sand density has also been evaluated with laboratory data of mini-cone penetration resistance from specimens with and without disc rotation (Feng et al., 2010). Such data obtained from several series of disc rotation tests on two Ottawa sand specimens clearly show that the mini-cone penetration resistance (in kPa) can be increased ~~~~~~
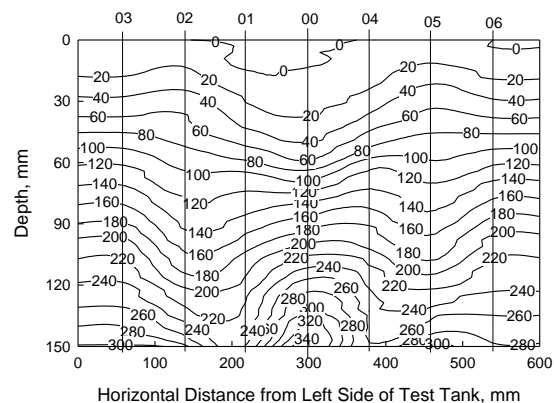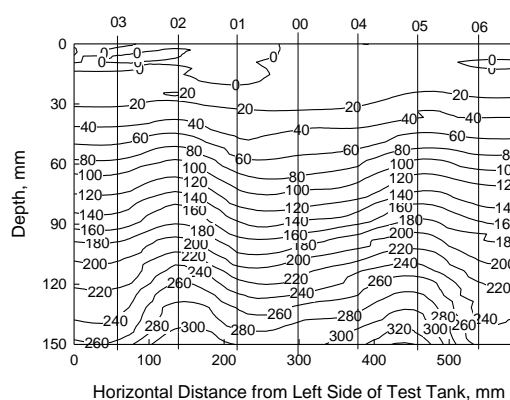
Figure2: Mini-cone resistance without disc rotation   Figure 3: Mini-cone resistance with disc rotation

Furthermore, with the mini-cone penetration resistance data, an influence zone below the disc for greater than zero increase in penetration resistance can be evaluated. It has been tentatively found that this influence zone generated by disc rotation at the central point on the specimen has approximately a side slope with 30° to the horizontal plane and a depth of half of the disc diameter. Although the mini-cone penetration resistance data is useful for evaluation of the influence zone by disc rotation, a question can be raised as to what is the magnitude of sand density increase by disc rotation. This question is thus investigated in this study through several series of laboratory disc rotation tests with direct measurement of sand density. Especially, in addition to the single point of disc rotation, multiple points of disc rotation are also conducted so that the area of densification covered by disc rotation is increased. In this paper, part of the laboratory test results are presented and discussed.

2.   SOILS TESTED AND TEST PROCEDURES

Although the disc rotation method is conceived for general application on granular soils, only two granular soils are tested. One is the Mai-Liao sand which is native alluvial sand with predominantly platy particles and the other is Ottawa sand which is the ASTM standard sand with round particles. Average grain size of the Mai-Liao sand is 0.17 mm and of the Ottawa sand is 0.33 mm. The Mai-Liao sand sample contained about 6% of fines and the Ottawa sand sample was clean sand. As these two sands have very different particle characteristics, they are also suitable for studying whether or not the effectiveness of disc rotation is a function of particle shape. This study used two different diameters of emery wheels as the discs, one is 150 mm and the other is 200 mm, to study the effect of disc diameter on sand densification. The 600-mm diameter test tank was used to contain dry loose sand specimens of initial relative density of 50%. To determine local relative density of the specimen, prior to and after disc rotation, a stainless steel tube sampler of 30 mm in height, 30 mm in diameter, and 1 mm in wall thickness was made. The tube sampler has two open ends and is carefully pushed downward with the aid of a glass plate and a level placed on top of it. After the tube sampler is completely pushed into the sand, part of the sand surrounding the tube sampler is slowly and carefully excavated down to the bottom of the sampler, and then a thin cutting stainless steel blade is pushed horizontally across the bottom of the tube

sampler. During the process, little or no heaving occurs in the sand within the tube sampler and that is considered an indication of little or no disturbance on the sand specimen. Results of many verification tests on freshly prepared sand specimens show that the relative densities measured by using this technique were rather accurate with about $\pm 5\%$ deviations. Several series of disc rotation tests were conducted until the discs settled about 40~50 mm, i.e. before exceeding the 50-mm travel of the displacement measuring device. After moving the loading frame with the disc away from the test tank, a total of 52 post-disc rotation relative density measurements at different locations were made for each specimen. This enables an evaluation of the effect of disc rotation on the whole specimen. The following paragraphs present some significant test results and evaluations.

3. TEST RESULTS AND EVALUATIONS

3.1. Static pressure versus settlement relationships

In a few tests conducted at the begining of the study, incremental static loading was applied to the disc to determine the relationship between static pressure and settlement for each sand. The obtained relationship was used to evaluate the bearing capacity of the disc for each sand tested. It would not be effective in sand densification to induce bearing capacity failure prior to rotating the disc. On the other hand, less static pressure on the disc would induce less shear displacement and therefore less particle rearrangement in the sand specimen. Therefore, a static pressure slightly less than the bearing capacity was preferred for conducting the disc rotation. Figure 4 shows the data of static pressure and settlement of the Ottawa sand, and Fig. 5 shows the data of static pressure and settlement of the Mai-Liao sand. For those curves with maximum static pressures of either 90 kPa or 100 kPa, they were obtained first for the purpose of determining the suitable static pressures for conducting the disc rotation test. The rest of the curves all end at static pressures under which the disc rotation tests were conducted. The good agreement among the abundant number of curves for each sand reflects a good reproducibility in specimen preparation.
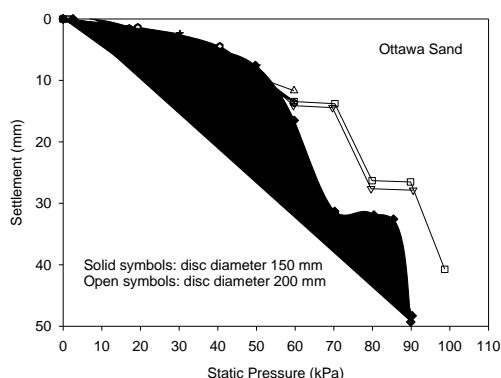
Figure 4: Data of static pressure versus settlement of the disc on Ottawa san
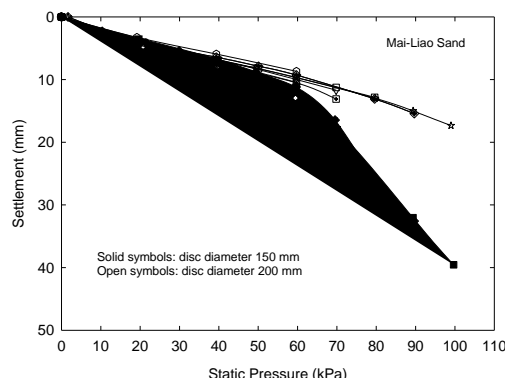
Figure 5: Data of static pressure versus settlement of the disc on Mai-Liao sand

The bearing capacities of the 150-mm and 200-mm diameter discs on Ottawa sand were evaluated from Fig. 4 as 56 kPa and 68 kPa, respectively. Thus, it was decided for some tests to use 50 kPa and 60 kPa as the static pressures for the respecitve discs during disc rotation on Ottawa sand. The bearing capacity of the 150-mm disc on Mai-Liao sand was evaluated from Fig. 5 as 65 kPa. Thus, it was decided to use 60 kPa as the static pressures for the 150-mm disc during disc rotation on Mai-Liao sand. For the 200-mm disc on Mai-Liao sand, it can be seen from Fig. 5 that the obtained static pressure versus settlement curves remain rather flat up to the maximum staitc pressure applied. Therefore, since the larger size of 200-mm as compared to the size of 150-mm, it was decided to used 70 kPa as the static pressures for the 150-mm disc during disc rotation on Mai-Liao sand.

It is interesting to note that the data shown in Fig. 4 an Fig. 5 demonstrate the effect of grain characteristics on deformation volumetric behavior of granular soils. The most significant differences between these two sands are probalby in both size and shape. The Ottawa sand is coarser than the Mai-Liao sand. The Ottawa sand grains are mainly rounded, whereas the Mai-Liao sand grains are mainly platy. It can be seen from Fig. 4 and Fig. 5 for static pressures less than about 50 kPa that the slope of the curves is flatter for the Ottawa sand as compared to that for the Mai-Liao sand. The Ottawa sand yields at smaller static pressures and the slope of the curves is steeper than those of the Mai-Liao sand. It was

observed during the tests on Ottawa sand that yielding occurred more suddenly that was followed by little settlement under next loading increment.

3.2.   Changes in relative density as result of disc rotation operation

Before disc rotation operation, the specimen was prepared to have an initial relative density of 50%. In addition, local relative density was measured within the specimen for two purposes. One was to assess the uniformity of relative density across the whole specimen. The other was to obtain data for evaluation of effectiveness of disc rotation operation in increasing the relative density. The measured local initial relative density data for Ottawa sand and Mai-Liao sand are shown in Fig. 6 and Fig. 7, respectively. Although these data do show some variations across the whole specimen, it can be computed from them that the average value is very close to 50%.
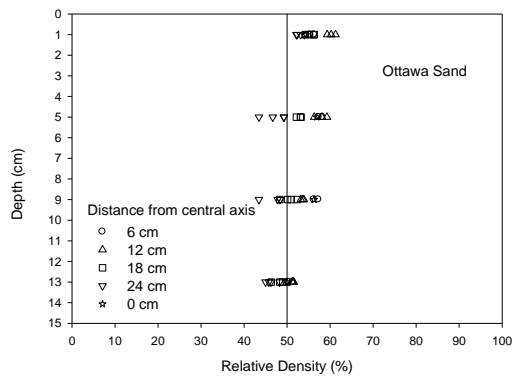
Figure 6: Measured data of relative density before disc rotation on Ottawa sand
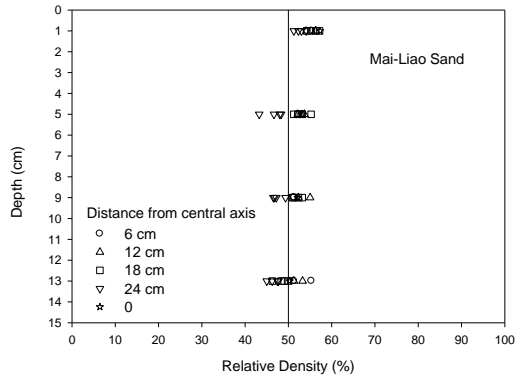
Figure 7: Measured data of relative density before disc rotation on Mai-Liao sand

To investiagte the effect of disc rotation operation on the relative density, another specimen for each sand was prepared in the test tank to have also an initial relative density of 50%. Then the disc rotation operation was applied to the surface of each specimen at four localities next to each other. For the Ottawa sand specimen, the disc was rotated under 50 kPa static pressure and back and forth once with $10°$ accumulated angle of rotation. For the Mai-Liao sand specimen, the disc was rotated under 70 kPa static pressure and back and forth once with $10°$ accumulated angle of rotation. Figures 8 and 9 show data of measured local relative density within the Ottawa sand specimen and the Mai-Liao sand specimen, respectively. An increase in the relative density is obvious for both sands and is more for the Ottawa sand as compared to the Mai-Liao sand. These data clearly demonstrate that the disc rotation method is effective in increasing the relative density of loose sands. Further study is underway to collect more data for verification of the disc rotation method.
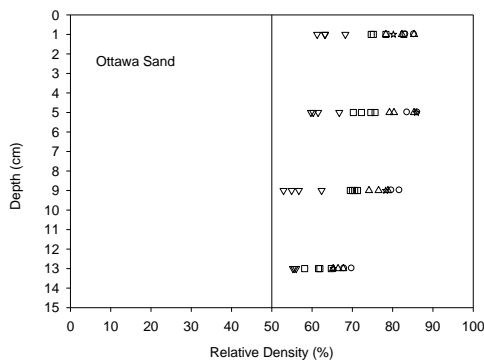
Figure 8: Data of relative density after disc rotation on Ottawa sand
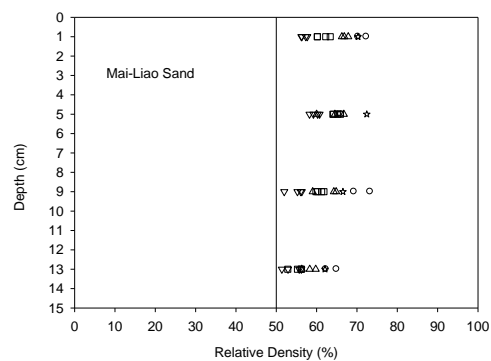
Figure 9: Data of relative density after disc rotation on Mai-Liao sand

4.   CONCLUSIONS

The following conclusions are based on data and discussions presented in previous paragraphs. The disc rotation method has been applied successfully in this laboratory study for densification of two sands. These two sands are different in grain size and shape which are likely responsible for their different

volumetric behaviors due to disc rotation. The small tube sampler has been used successfully in measureing local relative density within the specimen. The obtained test results show that, under only 50 ~ 70 kPa of static pressure, the disc rotation method can increase the relative density of loose sands to about 70 ~ 85%.

5. ACKNOWLEDGEMENTS

REFERENCES

Feng, T. W., Tzeng, C. S., Huang, Y. H., and Li, S. C. (2010), "Disc Rotation for Improving Loose Sands," Proc. of the 17ᵗʰ Southeast Asian Geotechnical Conference, Vol. 1, pp. 79-82.

D'Appolonia, D.J., Whitman, R.V., and D'Appolonia, E., "Sand Compaction with Vibratory Rollers," Journal of the Soil Mechanics and Foundation Division, ASCE, Vol 95, No SM1, 1969, pp 263-284.

Feng, T.W. and Huang, Y.H., "Disc Shear of Loose Sands in a Test Tank," Proc. of ISOPE 2009 International Conference, Vol. 1, 2009, pp 51-55.

Feng, T.W., Yang, J.H., and Huang, J.Y., "A Laboratory Study on Densification of Loose Sands by Disc Shearing," Proc. of ISOPE 2007 International Conference, Vol. 2, 2007, pp 1597-1600.

Lessons Learned from Millions of Square Metres of Ground Improvement

Babak Hamidi, GFWA, Australia, b.hamidi@gfwa.com.au
Serge Varaksin, Menard, Menard, France, serge.varaksin@menard-mail.com

ABSTRACT

Ground improvement can be applicable to projects of any size; however there are certain delicacies that necessitates special attention when ground treatment is implemented in large size projects. It is the authors' experience from performing millions of square meters of ground improvement that soil treatment of mega and giga size projects can be optimised if specifications and testing methods have been developed properly, the ground improvement solution has been adapted according to the in-situ ground conditions and project requirements, and that allocation of equipment and working teams have been planned and managed appropriately. Unsuitable acceptance criteria can veer the ground improvement campaign into an unnecessarily costly and time consuming and sometimes impossible endeavour. This paper will review the ground improvement works of several very large size projects including Abu Dhabi Corniche (900,000 m^2), Al Quoa New Township (1,135,000 m^2), King Abdulla University of Science and Technology (2,600,000 m^2) and Al Falah New Township (4,840,000 m^2).

1.   INTRODUCTION

Ground improvement includes numerous methods that are applicable to a very wide range of ground conditions, load conditions and project sizes. While a number of soil improvement solutions may all be feasible in a project, the usually the selection of the method is driven by cost or schedule.

Although it should be the intention of the engineers to develop the most economical acceptable foundation solution when dealing with any project, the sensitivity of this intent appears to be more critical in large size projects where the repetition and summation of even the smallest extras can ultimately lead to large costs and additional execution time. Thus, it may be beneficial to study the key parameters that will impact cost and programming.

2.   PARAMETERS OF SIGNIFICANCE

Although all ground improvement works should be designed, performed and tested properly the chances that flaws in any of these processes in a large mega or giga size project could lead to a larger financial loss is greater, and hence it is essential that application of ground improvement in projects of considerable size be robust and flexible, well tailored to the problem, properly designed and executed and tested in accordance to the requirements.

2.1.   Suitability of Technique

Regardless of the project size and all other conditions, constraints and parameters the intended ground improvement method should suit the problem.

Any one ground improvement technique is not suitable and applicable to all ground conditions. Regardless of cost, schedule and any other issues, if the wrong or inappropriate technology is used, it will not perform satisfactorily, and ultimately alternative solutions will have to be taken into consideration.

For example while particulate (permeation) grouting is less costly than other grouting techniques (Mitchell, 1981), this technology is mainly suitable for sands and gravels, and for coarse silts using chemical solutions (Semprich and Stadler, 2003, Chu et al, 2009) and cannot be used in clays. Ultra fine grout mixes can be used in medium to coarse sands, but will not permeate silts and suspensions with regular cement, at best will permeate into coarse sand. Hence, if an unsuitable grout mix is used permeation will not be realised, the project's objectives will not be met, and the project will face delays and extra costs.

In Umm Al Quwain Marina the preliminary geotechnical investigations that were based on SPT boreholes suggested that the site was composed of several layers of loose sands with fines content in the range of less than 10% to 20%. Once the ground improvement project was awarded to a specialist ground improvement contractor who had proposed dynamic compaction, further geotechnical testing revealed a different soil profile and the presence of a previously unidentified very soft very silty sand to sandy silt (fines content in the range of 40 to 60%) layer. Consequently, the ground improvement technique was modified to pre-excavated dynamic replacement (Hamidi et al, 2012a).

Although it would be ideal if it was possible to efficiently apply one ground improvement technique with similar parameters to an entire large size project in reality this is almost never the case. Even if the application of one technique to the entire site was possible, it is very doubtful that ground conditions, loading, and design criteria would be the same everywhere. Consequently the ground improvement parameters will also have to be manipulated accordingly.

The ground conditions of Al Jazira Steel Pipe Factory in Abu Dhabi Industrial City was fairly consistent with the top 5 m being loose silty to very silty sand. Although dynamic replacement was implemented as the only soil improvement technique, due to the numerous load conditions and design requirements (point loads from 300 to 2,500 kN and uniform loads from 40 to 200 kPa, acceptable total settlements from 25 to 75 mm and differential settlements from 1/500 to 1/1000) the footings locations and dynamic replacement print locations of heavily loaded footings and slabs were pre-excavated (Hamidi et al., 2011b).

Ground improvement of Oso II NGL in Bonny Island, Nigeria was even more challenging and a combination of techniques including dynamic replacement, dynamic compaction, jet grouting, controlled modulus columns, and prefabricated vertical drains were utilised.

2.2.   Concept of Acceptance Criteria

The adoption of suitable acceptance criteria is probably almost as important as selecting the appropriate ground improvement technique itself, and unsuitable criteria can erroneously fail or pass a treatment programme.
    Acceptance criteria can be envisaged to be in three main forms based on quality of work, minimum test values or directly on design criteria (Hamidi et al, 2011a).

2.2.1.   *Acceptance criteria based on quality of work*

Sometimes the responsibility of the contractor is only to provide the working team, equipment, material and execution of the works according to the specification's and drawings that have been prepared by others.

In this type of project, acceptance criteria is generally non-technical and based on performing the works correctly. Testing is generally specified, but meeting predetermined results will not be the contractor's responsibility because others have developed the methodology and design.

Should works be performed correctly, but test results fail to meet expectations, then the contractor may be required to perform additional work, but will be exempted from all other responsibilities and consequences. Correction of the works to meet the project's needs will be the responsibility of others.

This type of specifications can be useful in small projects and in the absence of specialist ground improvement and geotechnical contractors. However, its use in large size projects and in the presence of specialist contractors is questionable.

2.2.2.   *Acceptance criteria based on minimum test values*

Sometimes acceptance criteria is based on minimum test values or a correlations to test values. At times, the specified testing method is practically infeasible. For example, it may be specified to carry out in-situ density tests for the ground improvement works of a road that is to be constructed on a thick reclamation. Although density testing may be applicable to dry, shallow and thin layers of roller compacted soil in a typical road construction project, it is very impractical to perform such tests in saturated deep treated soils.

Sometimes specifications stipulate an impractical testing method, but attempt to resolve the problem by correlating the specified test to a practical testing method. For example the specifications may state a certain percentage of in-situ density and stipulate a correlation to CPT cone resistance. However, it CPT on its own should suffice and there is no need to reduce accuracy by introducing a density correlation.

Although previously specified in many projects, implementation of relative density is also a poor choice and there is overwhelming evidence that this parameter must not be used as acceptance criteria of ground improvement projects. Hamidi et al. have reviewed the inaccuracies associated with the concept of relative density (Hamidi et al., in review a) and relative density correlations (Hamidi et al., in review b). In extreme cases, application of relative density can be as accurate as making a wild guess.

The above discussions have been recognised by many geotechnical engineers, and thus a trend has been realised whereas minimum values for practical, efficient and economical field tests such as SPT, CPT or PMT (Menard Pressuremter Test) have been stipulated as acceptance criteria.

This, itself, is a positive step forward as it recognises that establishing acceptance criteria based on direct measurement of parameters is more rational and beneficial than making correlations; however it is not enough. What lies behind these types of acceptance criteria are calculations that have been carried out by geotechnical engineers to ensure certain design requirements such as bearing capacity, total and differential settlements, liquefaction mitigation or long term consolidation have been satisfied. However, the condition in which the test values of the soil layers just reach the minimum value is only one of countless possibilities that may satisfy the design criteria, and statistically speaking, the least probable of all of them. Furthermore, in techniques with inclusions such as dynamic replacement, stone columns, jet grouting, deep soil mixing and controlled modulus columns, where loads are distributed between the in-situ soil and the inclusions by arching (Hamidi et al., 2009) the concept of minimum value concept becomes meaningless as the in-situ soil improves negligibly and it is only the added elements that improve the ground's behaviour.

2.2.3. Acceptance criteria based on design criteria

There is no better way of making sure that a certain aspect of design has been fulfilled than directly verifying that specific criterion itself; hence it would be very rational to assume that optimised results can be achieved when acceptance is based on design criteria.

Acceptance criteria for Nakilat Ship Repair Yard that was undertaken as part of Port of Ras Laffan expansion in Qatar was initially based on a relative density correlation with a calcarenite correction factor. Alternative specifications based on design criteria were later proposed by a ground improvement specialists contractor who was awarded the project. Calculations were able to demonstrate that test results that had not satisfied the relative density requirements in total were able to provide better safety factors for bearing capacity and lesser settlements than the relative density specifications (Hamidi et al, 2010b).

Similarly, acceptance criteria for Madina A'Zarqa (Blue City) in Oman was initially based on minimum CPT values, but was later modified to include PMT and analyses of bearing capacity and settlements. In this project, it was also observed that it was possible to meet design criteria without strictly complying to the specified minimum test values (Hamidi et al, 2012b).

2.3.   Availability and Mobilisation

While mobilisation costs can be a major expenditure in small size projects, its percentage of project costs becomes lesser and lesser as the project's size grows. Hence while mobilisation costs may be a determining parameter for selecting a soil improvement technique in a small project, even transcontinental mobilisation of equipment may be very justifiable in large projects.

Hamidi et al. (2011e) have reported the ground improvement works for two tanks in Dubai's Palm Jumeira Sewerage Treatment Plant. While dynamic compaction would have been the preferred treatment method, due to unavailability of plant with sufficient lift capacity, the project was performed using dynamic surcharging.

As will be seen in the case studies, importation of multiple number of rigs to meet construction schedules can be considered in mega and giga size projects if proper planning is performed.

3.   CASE STUDIES

A number of very large size projects have recently been constructed on soil that had been subject to improvement using dynamic compaction, dynamic replacement and dynamic surcharging. All these projects were subject to challenging ground conditions and specifications and required thoughtful design, proper planning and allocation of sufficient plant and equipment, and suitable testing to allow completion of ground improvement works within the very limited allocated time frames. These projects were from 900,000 to 4,840,000 m^2.

3.1.   Abu Dhabi New Corniche

Abu Dhabi New Corniche is a 6 km long reclamation with an area of 900,000 m^2 that has been hydraulically reclaimed from the Persian Gulf (Hamidi et al., 2010a). The reclamation began at the face of the original beach road and on average extended 160 m into the sea. The maximum width of the reclamation was 300 m and the maximum reclamation thickness of about 12 m at the sea facing is supported by sheet piles.

The geotechnical investigation that was performed after reclamation reported that the seabed was composed of medium dense fine grained sand followed by a dense layer of sand, shells and ultimately the limestone bedrock.

Project specifications stipulated that reclaimed material had to contain less than 10% fines. Based on this expectation, acceptance criteria required that relative density be at least 80% with an SPT blow count, N, correlation.

Once the ground was reclaimed, testing indicated that the fill, was loose to very loose with N in the range of 1 to 10; hence ground improvement was stipulated and the project was awarded to a specialist ground improvement contractor who has proposed dynamic compaction.

Further testing during the works revealed that the hydraulic fill had segregated and a soft silty layer of at least 0.5 m thick was covering the seabed.

This project is an excellent example of one of many problems associated with relative density. Noting that relative density is applicable to soils with less than 15% fines (ASTM, 2006a, 2006b), the project's specifications were no longer applicable. It should be noted that relative density correlations are also subject to doubt (Hamidi et al., 2012b).

Thus, in addition to the non-functional criteria of relative density and the SPT correlation, PMTs were carried out for the design of sheet piles and further verification of the work.

The works were carried out with a maximum number of 7 rigs in two working shifts with a peak production rate of 200,000 m^2 of improved ground per month.

The energy per unit area of treatment, pounder weight, drop height and number of phases were varied based on the treatment thicknesses. Pounder weights were from 12.5 to 25 tons and maximum drop height was 20 m. In areas with less than 6 m thickness, two phases of deep treatment using 12.5 and 16 ton pounders were utilized. In deeper areas three phases of deep compaction using 25 ton pounders were carried out. Sometimes due to the build up of pore pressure, the phases had to be broken down into sub phases.

Figure 1 shows the completed project facing Abu Dhabi city. As can be seen this project was performed in close proximity to hundreds of buildings. Although dynamic compaction generated waves can damage structures if they are in close proximity of the works, it is possible to estimate vibration parameters (Hamidi et al., 2011c), and to implement measures to reduce vibrations such as installing isolation barriers (Hamidi et al., 2012).

Figure 1: Aerial view of Abu Dhabi New Corniche

3.2.   Al Quoa'a New Township

Al Quoa'a is a remote and isolated desert township that is located about 100 km from Al Ain and on the border of the United Arab Emirates and Oman (Hamidi et al, 2010d). The second phase of Al Quoa'a, consisting of 450 two floor villas and associated infrastructure has been constructed on a site with an area of more than 3.8 million m^2. As shown in Figure 2, the dune hills were cut and dumped into the lower level areas to provide a level platform.

The fill areas covered an area of 1,135,000 m^2. More detailed assessments revealed that 44% of the fill material was placed at depths less than 6 m, 35% were from 6 to 12 m deep, 13% were from 12 to 16 m deep and the remaining 8% were located at depths deeper than 16 m from the finished working platform (±0.0 m RL). The maximum depth of the fill was 28 m.

CPT results indicated that the ground in the cut areas was satisfactory enough to support the structures and infrastructures, but the dumped dune sands in the fill areas were in a loose state and except for the upper 2 m, cone resistance, q_c, was in the range of 2 to 4 MPa. PMTs that were later carried out as part of the post ground improvement programme indicated that limit pressure, P_l, was in the range of 0.1 to 0.5 MPa. Sieve analyses of the dune sand showed that the soil was poorly graded fine clean sand, and groundwater was not observed down to the maximum testing termination depth of about 30 m.

Figure 2: Backfilling and construction of the working platform by dumping

It was understood by the project's designers that in addition to settlements originating from structural loads, the very young fill could have also been subject to settlements under its own weight, or to subsidence due to vibration or washing and densification of material.
Ground improvement was deemed as a possible solution for the treatment of the very loose fill, and consequently a design and construct project was awarded to a specialist geotechnical contractor who had

proposed dynamic compaction. Although original acceptance criteria were based on minimum q_c values, alternative acceptance criteria based on design bearing capacity, acceptable settlements and elimination of self weight creep were proposed and approved.

As bearing capacity, load induced and creep settlements can all be calculated using PMT (Menard, 1975), this testing method was chosen for verification of results. P_l is also a suitable characteristic for evaluating soil creep. Thus, acceptance criteria as shown in Tables 1 and 2 were approved. It is the author's opinion that acceptance criteria could have been further optimised if acceptance was only agreed and approved to be based on design criteria.

Table 1: Acceptance criteria for villa areas

Criteria for Villa Areas	Safe bearing	Self bearing
Thickness where parameters prevail	-0.75 to-5.50 m RL	From -5.50 m RL
PMT limit pressure	750 kPa	600 kPa
Menard Modulus	4.8 MPa	4 MPa

Table 2: Acceptance criteria for non-villa areas

Criteria for Non-Villa Areas	Safe bearing	Self bearing
Thickness where parameters prevail	From ±0.00 m RL	From ±0.00 m RL
PMT limit pressure	600 kPa	600 kPa
Menard Modulus	4 MPa	4 MPa

A total of 6 rigs were used for this10 month long project. Utilizing heavy duty cranes could have provided sufficient lift capacity to treat about one half of the project; however the remaining areas were deeper than what could have been treated by such equipment and specialised rigs including the specially designed Menard 700 t.m rig were mobilised to perform deeper treatment by dropping 25 ton pounders. These rigs were able to treat up to about 90% of the site. The innovative MARS (Menard Accelerated Release System) technology was developed and patented to drop a 35 ton pounder in actual free fall (Figure 3).

Dynamic compaction energy was optimised based on the treatment thickness and acceptance criteria. MARS and special rigs were used for the first phase treatment of the deep fill areas. Heavy duty cranes were used for the treatment of subsequent phases of those areas and the remaining zones.

250 PMT were carried out at the site. For comparison purposes, 50 tests were carried out before dynamic compaction, and the remaining 200 tests were performed after the works. Depth of testing was based on the fill thickness and depth of dense in-situ soil. Figure 4 shows P_l values before and after dynamic compaction in four locations.

Figure 3: MARS automated drop and grab system
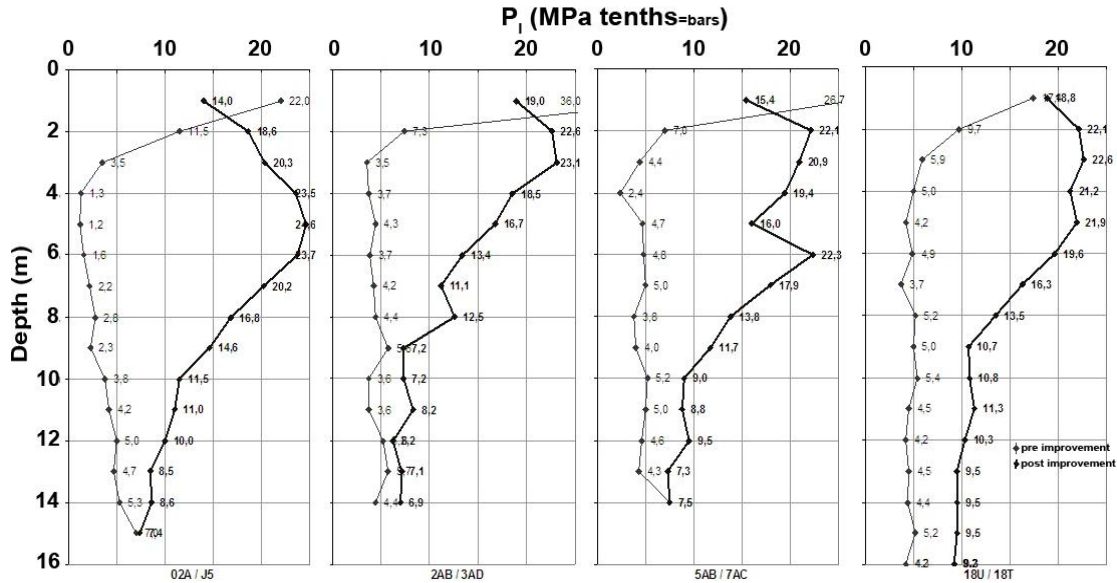
Figure 4: PMT limit pressure before and after dynamic compaction at 4 locations

3.3.   King Abdulla University of Science and Technology

The 5.6 million m² King Abdulla University of Science and Technology (KAUST) is located in Rabigh on the coast of the Red Sea and near the city of Jeddah in Saudi Arabia (Hamidi et al., 2010c). KAUST, originally anticipated to have buildings with at most two to three storeys.

The project was fast track and according to the schedule, master planning, architectural and structural design and construction all had to be completed in less than three years. Thus there was great need for flexibility, coordination and overlapping of tasks.

The preliminary geotechnical investigation that was carried out rather sparingly indicated that the ground was very heterogeneous loose or soft soils with rapid variations within short distances. This investigation and further testing during the works indicated that more than 2,600,000 m² of the construction area was to be built on soil consisting of up to 9 m of loose silty sand or soft sandy silt (locally called sabkah).

As groundwater level was less than 1 m below in-situ ground level it was decided to raise the ground by about 3 m to be safely above high tide. Approximately 1 to 1.5 m of this granular fill was placed before ground improvement.

Only a well worked out schedule that incorporated design and construction could have met the project's deadline. However, the problematic soil posed as a serious obstacle to this programme as it was not possible to design the foundations without finalisation of the buildings' locations and architectural drawings.

The design and construct ground improvement proposal that met the project manager's technical requirements, schedule and budget was based on the below design criteria:
o Footing location: Any place within the treatment area
o Maximum footing load: 1,500 kN
o Allowable bearing capacity: 200 kPa
o Maximum total settlement: 25 mm
o Maximum differential settlement between two adjacent footings: 1/500
o Liquefaction mitigation for an earthquake with PGA= 0.07g
o Level: 0.8 m below final ground level, but in any case at least 2 m above sabkah level

The construction method was a combination of dynamic compaction and dynamic replacement. Major changes to loads of some buildings later introduced the need to utilise dynamic surcharging as well. Dynamic compaction pounders used in this project weighed up to 21 tons.

Dynamic replacement was used in areas where the maximum depth of sabkah was 5 m. High energy dynamic replacement was used when the sabkah layer's depth was more than 5 m. In such a case, , in

addition to the engineered fill required for reaching final ground level, a 3 m surcharge was placed over the area for 3 weeks.

After completion of ground treatment in some areas, it became known that the revised master plan incorporated 20 six storey buildings. Hence, dynamic surcharging was also used to consolidate the deep sabkah layers. In this technique a combination of preloading and vibration is used to re-introduce pore pressure in the soil-water system and consequently to accelerate settlement rates. In addition to the engineered fill required for reaching final ground level a 3 m high surcharge was placed and dynamic compaction was performed on it.

Differences in ground behaviour due to pounder impact enabled the site supervisors to assess the rapidly varying ground conditions and to apply the appropriate ground improvement technique as needed. It was observed that while the first dynamic compaction pounder impact penetrated the ground by about 0.25 m, the dynamic replacement pounder penetration was substantially more and in the range of about 1 m. Also, performing dynamic compaction frequently resulted in the seepage of groundwater to the surface, but this phenomenon was rarely encountered in dynamic replacement areas. Ground rest periods in between dynamic compaction phases were 1 to 3 days, but considerably longer and from 7 to 21 days when dynamic replacement had to be performed. Also, ground heave due to pounding was not observed in dynamic compaction areas but was observable in dynamic replacement zones.

The allocated time frame for mobilization, execution and testing of ground improvement works was set at 10 months. Ground improvement was carried out basically over a period of 8 months using a total of 13 rigs working two shifts per day. To the knowledge of the authors, this is the world record for the number of dynamic compaction/dynamic replacement rigs working at the same time on a single project. A review of the treatment rates shows that at its peak, about 600,000 m^2 of ground was treated in one month.

A total of 180 PMT tests were carried out to confirm that the bearing and settlements had been achieved. A number of CPT is also performed for verification of liquefaction mitigation.

3.4. Al Falah Community Development

Al Falah Community Development is a 12.7 million m^2 town that is being constructed on the outskirts of Abu Dhabi (Hamidi et al, 2011f). The geotechnical investigation of the project indicated that the site was covered with a layer of silty sand with a variable thickness of only a few centimetres to more than 18 m followed by sandstone or siltstone. The soil in a large portion of the site was very dense and it was possible to construct shallow foundations without any geotechnical issues. SPT blow counts in these areas were consistently more than 50 and CPT penetration would generally reach refusal within the first metre.

However, the ground conditions were not suitable for construction throughout the entire site, and test results indicated the presence of loose soil layers in an area of 4,840,000 m^2. In these areas N in the superficial layer were generally from 7 to 12 and occasionally as low as 2, and q_c was mostly from 2 to 3 MPa. Fines content of the soil was usually less than 25% but occasionally higher, and the CPT friction ratio was generally less than 1% but occasionally as high as 3%.

It was observed that while the groundwater level was relatively deep and from 11 to 18 m below the ground surface, the moisture content of the ground varied from 8 to 35% in the non-saturated layers.

Further study revealed that the thickness of loose soil deposits was less than 3 m in 64% of the site. 23% of the loose soils had a thickness of 3 to 6 m, 8% had a thickness of 6 to 10 m and 5% had a thickness of more than 10 m and exceptionally up to 18 m. Consequently, a study and assessment of the geotechnical report and preliminary calculations indicated that the mentioned above areas with poor ground conditions could not support shallow foundations the below design criteria
o Allowable bearing capacity: 150 kPa for conventional strip or pad foundations with maximum dimensions of 1.5m×1.5m^2 (villa areas) or 3×3 m^2 (heavy loads).
o Maximum total settlement: 25 mm for a maximum pressure of 150 kPa applied to the above mentioned footings.
o Differential settlement: 1:500 measured between surface points not closer than 8 m apart.
o Liquefaction mitigation: for an earthquake with magnitude 6 and PGA= 0.15g.

The 240 day design and construct ground improvement contract was awarded to a specialist contractor who had proposed dynamic compaction. It was expected that the average and peak ground improvement

production rate during the contract period had to respectively exceed 700,000 m^2 and 900,000 m^2 per month for the project to be delivered on time.

A key target for optimisation was the treatment energy. This was achieved by taking a number of parameters into account, such as:
o Depth of improvement: geotechnical information indicated that the treatment depth was variable from less than 3 m to more than 10 m and exceptionally up to 18 m. Hence, it was logical to divide the treatment zones according to treatment thicknesses (0 to 3 m, 3 to 6 m, 6 to 10 m, and 10$^+$ m).
o Amount of improvement: The amount of load that the soil had to support was not the same throughout the project. Thus, it was rational to improve the soil in each area based on the requirements of that specific area.
o Treatment energy: Once the requirements for depth of treatment and energy intensity have been established it will be necessary to design the number of blows per print or unit area. Achieving the same energy intensity will require lesser blows with a heavier pounder; however lifting pounders heavier than about 13 to 16 tons requires special lifting rigs. Experience of KAUST indicated that it was possible to mobilise large numbers of rigs in a relatively short period.

Thus, with the intention to optimise production a combination of different pounders weighing up to 23 tons were utilised by 11 rigs working in two shifts.

The optimisation of dynamic compaction design and ability to provide sufficient number of rigs allowed the completion of the project before the handover date, i.e. in 7 months. The maximum ground improvement monthly production rate was 966,000 m^2 which to the knowledge of the authors is the current world record.

PMT was used as the main testing tool. CPT was also carried out for verification of liquefaction mitigation and as an additional control measure. In addition to the tests that were performed during the calibration programme, a total of 282 PMT and 1,029 CPT were also carried out to confirm the project requirements had been met.

It can be calculated that the ratios of treated ground to PMT and CPT are respectively about 1 in 17,000 m^2 and 1 in 4,700 m^2. These ratios are larger than what is occasionally requested in project specifications. However, this was made possible due to the nature of dynamic compaction works. In this technique each impact point in itself can represent a pseudo test whereas the amount of ground and crater settlement can be correlated to the soil parameters. The successful application of dynamic compaction in other large size projects with similar area to test ratios (for example 180 PMT tests or 1 test per 14,400 m^2 was carried out in KAUST) and the development of methods for predicting soil parameters using imposed ground subsidence (Hamidi et al., 2010d, 2011g) and continuous successful experiences justify the logic of such testing programmes. Without such an optimised approach, testing in itself could become a critical task rather than a means of verification.

4.   CONCLUSION

Experience gained from performing millions of square metres of ground improvement projects suggests that it is possible to optimise large mega and giga size projects by implementing a robust and flexible solution that has been well designed and tailored to meet the specific requirements of the project. The intended methodology may include more than one soil treatment technique; however even if one technique is deemed as being the optimal solution, it is unlikely that one pattern will be suitable for the entire site. It is best to divide the site into subdivisions and to take the treatment thickness, loadings and design criteria into consideration. Merging of design and construction will further improve efficiency.

Acceptance criteria is an equally important issue, and if not possible, it is indeed very difficult to optimise a project with criteria based on quality of work, minimum tests values, and correlations that have been developed for other soils. The most suitable approach is to base the acceptance requirements directly on the design criteria.

Although availability of equipment will directly affect the schedule, it is possible to allocate considerable number of rigs to a project by planning ahead.
The number of tests have to be kept in balance, and it is possible to utilise pounder penetration of dynamic compaction and dynamic replacement as a monitoring tool.

REFERENCES

ASTM (2006a) D4253-00 (Reapproved 2006): Standard Test Methods for Maximum Index Density and Unit Weight of Soils Using a Vibratory Table

ASTM (2006b) D4254-00 (Reapproved 2006): Standard Test Methods for Minimum Index Density and Unit Weight of Soils and Calculation of Relative Density

Chu, J., Varaksin, S., Klotz, U. and Menge, P. (2009) State of the Art Report: Construction Processes. 17th International Conference on Soil Mechanics & Geotechnical Engineering: TC17 meeting ground improvement, Alexandria, Egypt, 7 October 2009, 130.

Hamidi, B., Nikraz, H. and Varaksin, S. (2009) Arching in Ground Improvement. Australian Geomechanics Journal, 44, 4 (December), 99-108.

Hamidi, B., Nikraz, H. and Varaksin, S. (2010a) Treatment of Thick Saturated Loose Subgrades Using Dynamic Compaction. 3rd International Conference on Problematic Soils (PS10), Adelaide, 7-9 April, 121-128.

Hamidi, B., Varaksin, S. and Nikraz, H. (2010b) Treatment of a Hydraulically Reclaimed Port Project by Dynamic Compaction. 3rd International Conference on Problematic Soils (PS10), Adelaide, 7-9 April, 113-120.

Hamidi, B., Varaksin, S. and Nikraz, H. (2010c) Implementation of Optimized Ground improvement techniques for a Giga Project. GeoShanghai 2010 Conference, ASCE Geotechnical Special Publication No 207: Ground Improvement and Geosynthetics, Shanghai, 3-5 June, 87-92.

Hamidi, B., Varaksin, S. and Nikraz, H. (2010d) Predicting Soil Parameters by Modelling Dynamic Compaction Induced Subsidence. 6th Australasian Congress on Applied Mechanics (ACAM6), Perth, Australia, 12-15 December, Paper 1150.

Hamidi, B., Nikraz, H. and Varaksin, S. (2011a) Ground Improvement Acceptance Criteria. 14th Asian Regional Conference on Soil Mechanics and Geotechnical Engineering Hong Kong, 23-27 May, Paper No. 404.

Hamidi, B., Nikraz, H. and Varaksin, S. (2011b) Application of Dynamic Replacement in a Steel Pipe Factory. International Conference on Advances in Geotechnical Engineering (ICAGE), Perth, 7-9 November, 867-872.

Hamidi, B., Nikraz, H. and Varaksin, S. (2011c) Dynamic Compaction Vibration Monitoring in a Saturated Site. International Conference on Advances in Geotechnical Engineering (ICAGE), Perth, 7-9 November, 267-272.

Hamidi, B., Nikraz, H. and Varaksin, S. (2010d) Soil Improvement of a Very Thick and Large Fill by Dynamic Compaction. 3rd International Conference on Problematic Soils (PS10), Adelaide, 7-9 April, 129-138.

Hamidi, B., Varaksin, S. and Nikraz, H. (2011e) Application of Dynamic Surcharging for Construction of Tanks on Reclaimed Ground. International Conference on Advances in Geotechnical Engineering (ICAGE), Perth, 7-9 November, 873-878.

Hamidi, B., Varaksin, S. and Nikraz, H. (2011f) Dynamic Compaction for Treating Millions of Square Meters of Sand. International Conference on Advances in Geotechnical Engineering (ICAGE), Perth, 7-9 November, 475-480.
Hamidi, B., Varaksin, S. and Nikraz, H. (2011g) Predicting Menard Modulus using Dynamic Compaction Induced Subsidence. International Conference on Advances in Geotechnical Engineering (ICAGE), Perth, 7-11 November, 221-226.

Hamidi, B., Varaksin, S. and Nikraz, H. (2012a) The Effectiveness of Vibration Reduction Trenches in a Dynamic Replacement Project. 11th Australia New Zealand Conference on Geomechanics - Ground Engineering in a Changing World, Melbourne, 15-18 July, in review.

Hamidi, B., Varaksin, S. and Nikraz, H. (2012b) Application of Dynamic Compaction in a Project with Smart Acceptance Criteria. International Conference on Ground Improvement and Ground Control - Transport Infrastructure Development and Natural Hazards Mitigation (ICGI2012), Wollongong, 30 October - 2 November, in review.

Hamidi, B., Varaksin, S. and Nikraz, H. (2012c) The Effectiveness of Vibration Reduction Trenches in a Dynamic Replacement Project. 11th Australia New Zealand Conference on Geomechanics - Ground Engineering in a Changing World, Melbourne, 15-18 July, in review.

Hamidi, B., Varaksin, S. and Nikraz, H. (in review) Relative Density Concept is not a Reliable Criterion. Ground Improvement.

Hamidi, B., Varaksin, S. and Nikraz, H. (in review) Relative Density Correlations are not Reliable Criteria. Ground Improvement.

Menard, L. (1975) The Menard Pressuremeter: Interpretation and Application of Pressuremeter Test Results to Foundation Design, D.60.AN. Sols Soils, 26, 5-43.

Mitchell, J. K. (1981) Soil Improvement State-of-the-Art Report. 10th International Conference on Soil Mechanics and Foundation Engineering, 4, Stockholm, 509-565

Semprich, S. & Stadler, G. (2003) Grouting in Geotechnical Engineering, in Geotechnical Engineering Handbook, 2: Procedures, Smoltczyk, U. (ed), 57-90.

Quantifying the Zone of Influence of the Impact Roller

M. B. Jaksa, B. T. Scott, N. L. Mentha, A. T. Symons, S. M. Pointon, P. T. Wrightson and E. Syamsuddin
School of Civil, Environmental and Mining Engineering, University of Adelaide, Australia
mark.jaksa@adelaide.edu.au

ABSTRACT

Rolling dynamic compaction (RDC) involves traversing the ground by means of a non-circular module consisting of 3, 4 or 5 sides. Over the last few decades, a number of studies have been carried out in an effort to quantify the effectiveness of RDC. In this study, the zone of influence of the 4-sided 'impact roller' was measured in a systematic fashion in the field by means of a series of earth pressure cells (EPCs) embedded in the ground, in situ density measurements and dynamic cone penetration tests. Measurements obtained from the field trial, which was conducted at an open-cut mine in South Australia, suggest that the depth of influence for which there is significant and quantifiable improvement with the roller is approximately 2.1 m below the ground surface and this corresponded to soil stress readings of between 150 and 200 kPa. Positive pressure readings due to RDC were also measured by the EPCs buried up to 3.85 m below the ground surface, indicating that the actual zone of influence (for which there is improvement) extends beyond this depth.

1. INTRODUCTION

Ground improvement is a fundamental and essential part of civil construction and comprises approximately 30 different methods of ground treatment, including modification, chemical alteration, reinforcement with steel or geosynthetic, strengthening by drainage, densification by vibration or consolidation and the use of electro-osmosis (Phear & Harris 2008). Of these, compaction is by far the most prevalent and involves increasing the density of the ground by means of mechanically applied energy such as static compaction, which employs drum, padfoot, sheepsfoot and tyre rollers or dynamic compaction, which makes uses of vibratory rollers and plates, rammers, heavy tamping, vibroflotation and rolling dynamic compaction (Hausmann 1990). The advantage of dynamic compaction is that it enables the ground to be improved to a much greater depth (>10 m as compared to 0.3 m for static compaction), with the depth of improvement depending on the energy applied (Mayne et al. 1984). When compared to other ground improvement techniques dynamic compaction is one of the most cost effective (Lukas 1995), but its use is limited by the large ground vibrations it induces, so that it is not suitable on small sites or adjacent to buildings and other infrastructure.

This paper is concerned with a specific type of dynamic compaction, known as rolling dynamic compaction (RDC), which involves traversing the ground with a non-circular 'roller'. RDC is a relatively new technology and is becoming more popular because it is able to compact the ground more effectively, i.e. to greater depths than its static and vibrating roller counterparts, and more efficiently because of its greater speed – 12 km/h compared with 4 km/h using traditional rollers (Pinard 1999). RDC was originally developed by Aubrey Berrangé in South Africa in the late 1940s, but its value was not fully appreciated until the mid-1980s. Since then RDC has been successfully implemented worldwide with different module designs having 3, 4, and 5 sides (Photo 1). RDC involves towing these heavy (6–12 tonnes) non-circular modules, which rotate about a corner and fall to impact the ground. Due to the combination of kinetic and potential energies, and the relatively large mass of the module, RDC has demonstrated compactive effort to more than one metre below the ground surface (and more than 3 m in some soils) (Avalle & Carter 2005) – far deeper than conventional static or vibratory rolling (Clegg & Berrangé 1971, Clifford 1976, 1978), which is generally limited to depths of less than 0.5 m. In addition, RDC is unique in that it is able to compact large areas of open ground at depth, both effectively and efficiently. As a result, it has been used successfully in large reclamation projects such as the Palm Islands in Dubai, in the compaction of sites with un-engineered fill, such as industrial land or brownfield sites; in the agricultural sector to reduce water loss (Avalle 2004b), in the mining sector to improve haul roads and tailings dams, in general civil construction works (Avalle 2004a) and for an 80 km highway rehabilitation project (Jumo & Geldenhuys 2004).

This paper seeks to quantify the zone of influence, that is the depth and lateral extent, of the 4-sided 'impact roller', by means of a field trial involving in situ and laboratory testing and extends previous work by Avalle et al. (2009).

Photo 1: Rolling dynamic compaction modules: (a) 4-sided (Broons), (b) 3-sided (Landpac), (c) 5-sided (Infratech).

2.   FIELD STUDY

The field trial was conducted in June 2011 at the Project Magnet Tailings Storage Facility at the Iron Duke Mine, which, as shown in Figure 1, is located 49 km west of the South Australian city of Whyalla. RDC was achieved by means of Broons' 8 tonne, 4-sided impact roller (BH-1300), traversing over three adjacent lanes in order to compact three loose lifts of approximately 1,200 mm thickness of coarse, magnetite iron tailings. Surveying, soil sampling and a suite of in situ tests were performed at intervals of 8 passes of the impact roller to measure ground improvement. The in situ testing included dynamic cone penetration testing in the form of the Perth penetrometer, sand replacement field density tests and the spectral analysis of surface waves (SASW) geophysical technique. In order to classify the soil and quantify its compaction characteristics, laboratory testing was undertaken which involved standard and modified Procter compaction tests, particle size distribution and Atterberg limits tests. In addition, earth pressure cells (EPCs) were installed at different depths to measure dynamic pressures induced by RDC.

2.1.   Test Pad Construction

In order to measure the zone of influence and effectiveness of the impact roller a test pad was constructed in three separate lifts of 1,200, 1,530 and 1,460 mm in thickness, as illustrated in Figure 2(a), which also shows the locations of the embedded earth pressure cells (EPCs). These are discussed later. Figure 2(b) shows a plan view of the test pad, which enabled the impact roller module to compact the soil in three adjacent lanes. In each case, as shown in Figure 2(b), the direction of travel of the module was to the top of the page.

The first lift of the test pad was constructed by mine dump trucks end-tipping loose material adjacent to the pad, whereby a large front-end loader subsequently spread the material over the pad. This process caused the soil to be partly compacted by the weight of the loader. This was repeated until a lift height of

approximately 1,200 mm was achieved. For the remaining two lifts, the soil was placed by dump truck and then leveled using a 30 tonne excavator (Photo 2), which meant that the placed material was slightly less compact than the first lift, since the excavator did not pass over the surface as much, since it used a combination of spreading the soil with its bucket and tracking over the top layer to level the surface.
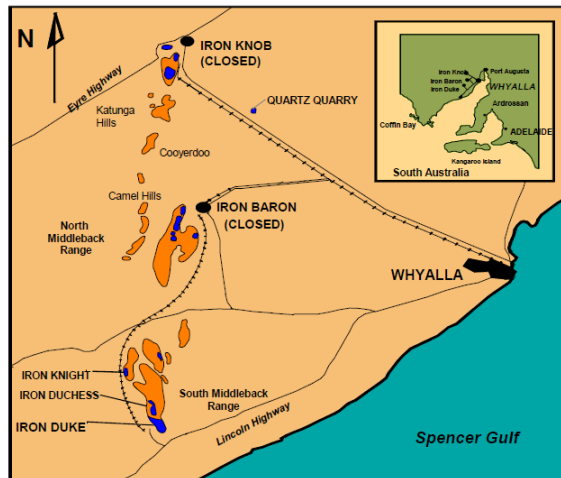
Figure 1: Location of field study site – Iron Duke Mine, South Australia (OneSteel, 2004).

(a)

(b)
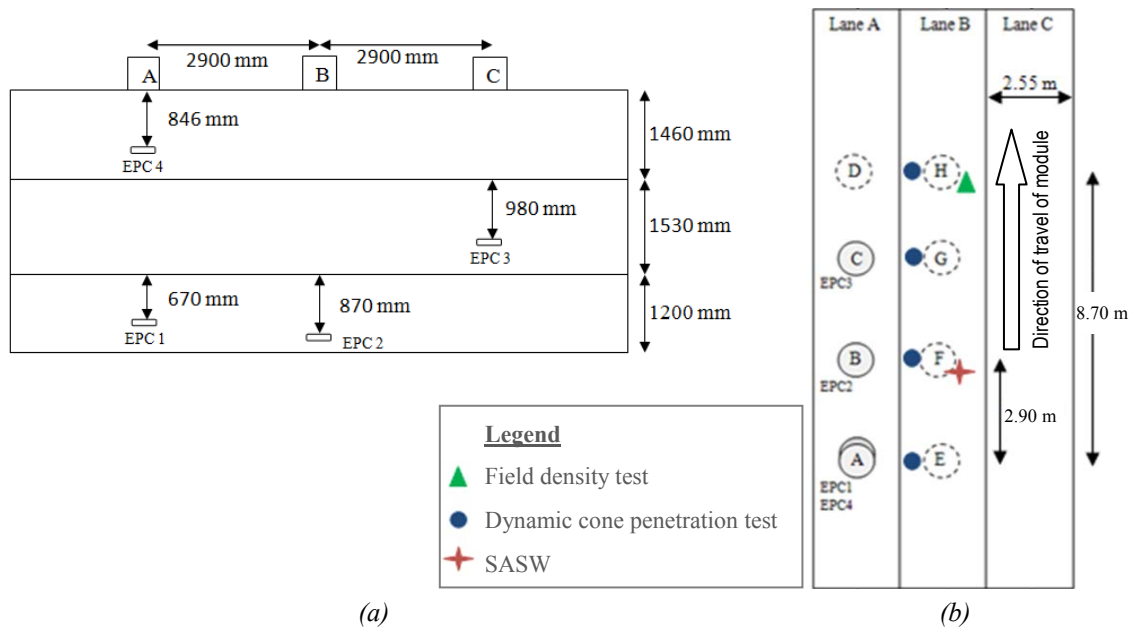
Figure 2: Details of test pad: (a) cross-sectional view, (b) plan view.

Photo 2: Test pad construction showing excavator used.

2.2.   **Material Characteristics**

The material used to construct the test pad consisted of coarse iron magnetite tailings. In order to classify the tailings and to determine its compaction characteristics, a series of index tests (i.e. particle size distribution and Atterberg limits tests) were performed, as well as standard and modified Proctor compaction tests. Figure 3 shows the average grading curve obtained from 9 particle size distribution tests, which were performed in accordance with AS 1289.3.6.1 (Standards Australia 2009). The 9 tests exhibited a very tight distribution about the average. The Atterberg limits tests and the particle size distributions suggest that the soil is a well-graded sand (SW) with some clay fines of low plasticity.

Standard and modified Proctor compaction tests were performed in accordance with AS 1289.5.1.1 and AS 1289.5.2.1 (Standards Australia 2003a, b), respectively. The results are summarised in Figure 4. The large dry unit weights are a consequence of the sand consisting of crushed magnetite.

2.3.   **In Situ Testing**

The locations of the in situ tests were shown previously in Figure 2(b) and consisted of field density tests, dynamic cone penetrometer tests, and geophysical testing in the form of the spectral analysis of surface waves (SASW). Due to space constraints, the SASW results are not presented here, but will be the topic of a future paper.

2.3.1.   *Field Density Testing*

In order to obtain direct measurements of in situ density, sand replacement tests were performed in accordance with AS 1289.5.3.1 (Standards Australia, 2004). Three tests were performed at depths of approximately 300 mm below the surface of each lift, approximately at Location H [Figure 2(b)]; prior to rolling, and after 8 and 16 passes. These are time consuming tests, which limited the number that could be carried out within the available time.
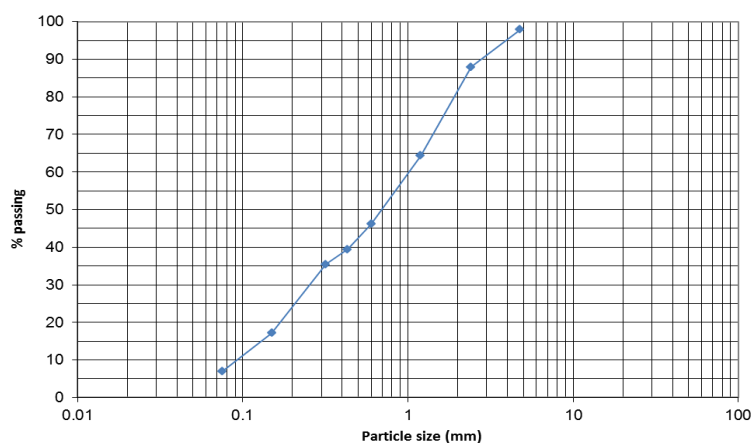
Figure 3: Average particle size distribution from 9 tests.
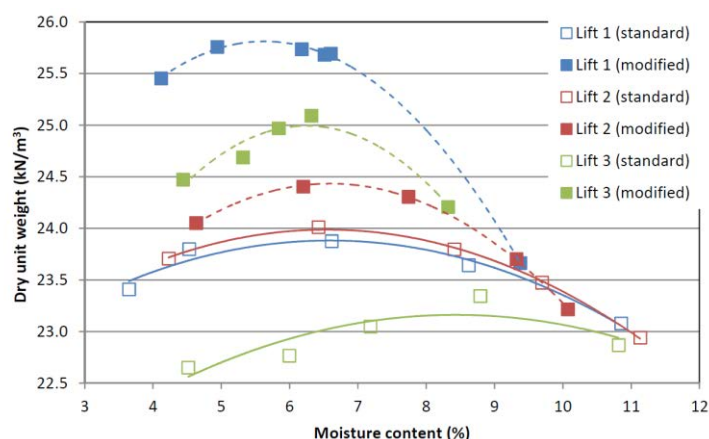
Figure 4: Results of standard and modified Proctor compaction tests for each lift.

The field dry density results are shown in Figure 5. Neglecting the measurements for Lift 2, which are inconclusive, and may be the result of surface disturbance, the measurements indicate that the majority of the increase in soil density occurred in the first 8 passes, with a diminishing rate of increase thereafter. These results are consistent with settlement measurements obtained by surface levelling.

Figure 6 combines all field density test data for the site and shows a plot of the average modified dry density ratio against the depth below ground surface for 8 passes of the impact roller and can be used to determine the depth at which a target dry density ratio (e.g. 95% with respect to modified compaction) is expected to be achieved. Extrapolating the trend line obtained from the data shown in this figure, it can be estimated that the effective depth for 8 passes is approximately 1.3 m (i.e. 8 passes of the impact roller will achieve a dry density ratio of 95%, provided that the layer thickness does not exceed 1.3 metres).
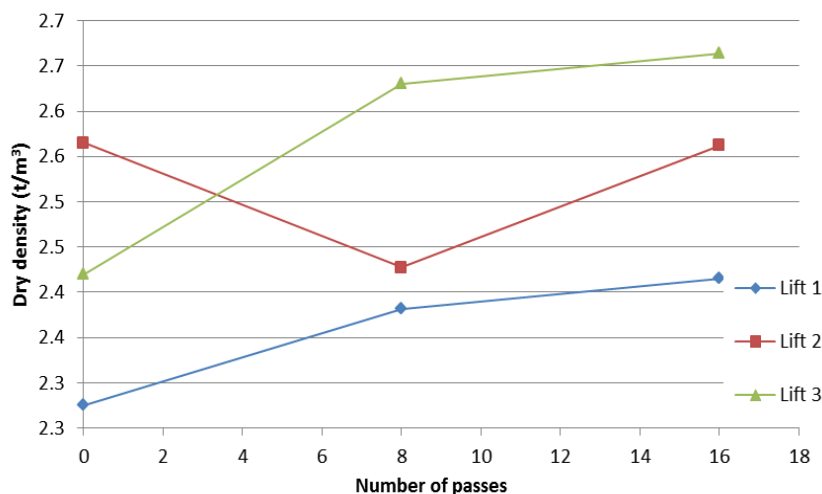
Figure 5: In situ dry density plotted against number of passes.
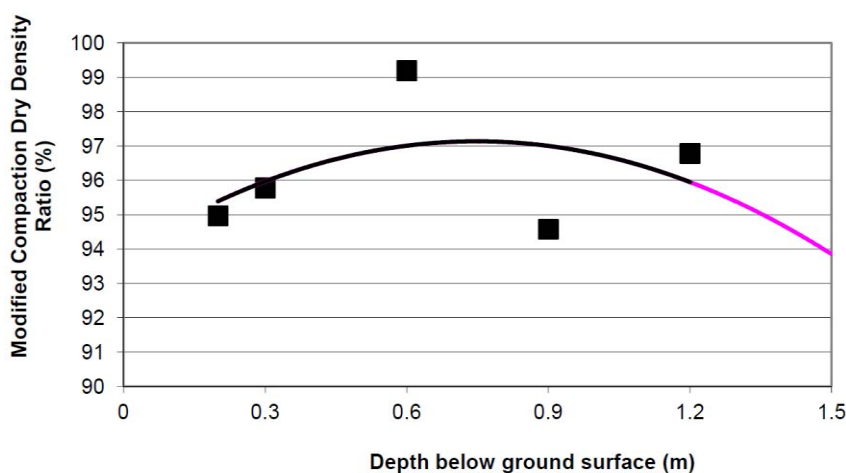
Figure 6: Modified dry density ratio versus test depth (8 passes of the impact roller).

2.3.2. Dynamic Cone Penetrometer Testing

In order to assess density improvement with depth, the Perth penetrometer test (PPT) was performed with blows recorded every 50 mm, in accordance with the standard procedure AS 1289.6.3.3 (Standards Australia 1997). Figure 7 summarises the average results across all tests undertaken (i.e. all lifts), so as to determine a general trend with increasing passes and also to determine the depth of influence of the impact roller. Each test was terminated at a depth of 850 mm due to the physical limit of the equipment. Between depths of 0.3 to 0.85 m, there is a noticeable increase in the number of blows with greater number of passes of the impact roller. Above a depth of 0.3 metres, results are inconclusive, again likely due to surface disturbance caused by the roller. Figure 7 suggests that the impact roller is effective in improving the in situ density of the tailings from 0.3 metres to beyond the penetrometer depth of 0.85 m.
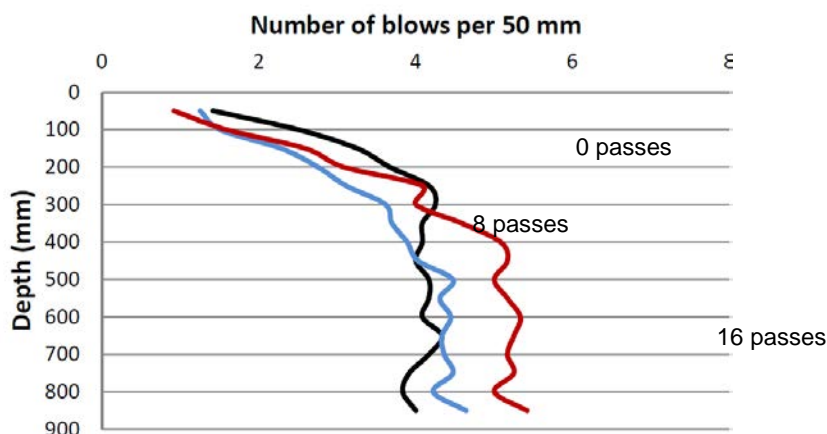
Figure 7: Results of dynamic cone penetrometer tests.

3.   EARTH PRESSURE CELLS

Each time the impact roller strikes the ground, it creates a pressure wave which travels through the soil from the surface. A key aspect of this research project was to gain knowledge about how that pressure wave propagates through the soil and to use that understanding to develop a model of the zone of influence of the impact roller. A total of $4 \times$ Geokon 3500 earth pressure cells (EPCs) were buried at different depths and used to measure pressure within the ground, as shown previously in Figure 2(a). The EPCs were offset horizontally by a half turn of the roller (2.90 m) to prevent stress shadowing. Measurements from the EPCs were acquired at a sampling frequency of 2 kHz (i.e. one sample every 0.0005 seconds). That frequency proved appropriate to balance the conflicting requirements, on the one hand to detect the sudden increase in pressure caused by the roller striking the ground and, on the other, without generating overly excessive data.

The EPCs were installed at each depth by using the excavator to create a trench. As suggested by Rinehart and Mooney (2009), coarse bedding sand was used when positioning the EPCs in the trench, as shown in Photo 3. The sand was used to form a solid base beneath the cell so that it was less likely to move and yielded more accurate measurements. Given that the test pad material itself consisted of coarse sand, this detail may have been unnecessary. The soil was then replaced in the trench by the excavator and it was then compacted slightly by means of its bucket. This process replicated the virgin construction of each lift.

The EPC testing program consisted of 16 passes per lane, 3 lanes per lift and a total of 3 lifts, as shown previously in Figure 2. Each of the passes was considered separately, thereby producing a total of 144 data sets characterising an individual pass of the impact roller. An indication of the depth of influence can be obtained by determining how pressure induced by a strike of the roller varies with depth.

Photo 3: Preparing the EPCs in situ on bedding sand.

To develop that relationship, data from all three lifts were used. Again, as shown in Figure 2, two EPCs were installed in Lift 1, 3 in Lift 2 and 4 in Lift 3, together providing pressure readings at 9 different depths below the surface, as the test pad is progressively constructed, each lift in succession.

An example of the data obtained from the EPCs is shown in Figure 8. Here a direct impact is measured by the impact roller striking the ground immediately above the embedded EPC, where a single main pressure peak of over 200 kPa is recorded. Two smaller peaks are also measured either side of the main peak, at intervals of approximately half a second, which corresponds to the module striking the ground each quarter revolution before and after the location of the EPC. In this particular pass, the two adjacent peaks were readily visible; however all other peaks were barely detectable since the pressure dissipates rapidly through the soil as the impacts occur farther away. In contrast, Figure 9 shows an example of measurements obtained when the roller did not impact the ground directly above an EPC.

An example of superimposed data from each EPC is given in Figure 10. As shown previously in Figure 2(a), EPC1 was located immediately below EPC4, at respective depths of 3,337 and 846 mm below the ground surface; EPC2 was located 3,850 mm below the ground; and EPC3 2,512 mm below the ground surface, once all 3 lifts had been placed. These depths account for non-uniformity of the ground surface and were established by on site levelling. Figure 10 clearly shows the decay in maximum imposed dynamic pressure as the depth increases, as well as the increase in static pressure with depth recorded by each EPC, which represents the overburden stress.
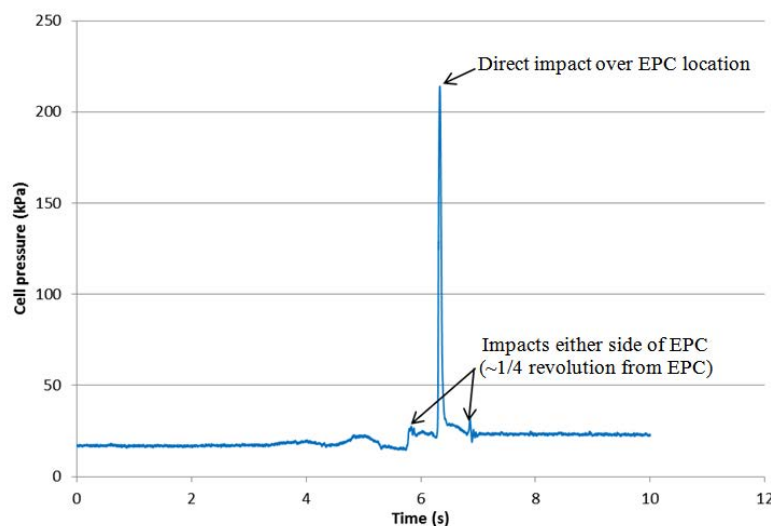
Figure 8: Example results obtained from direct impact over an EPC (EPC3, Lift 2, Lane A, Pass 2).
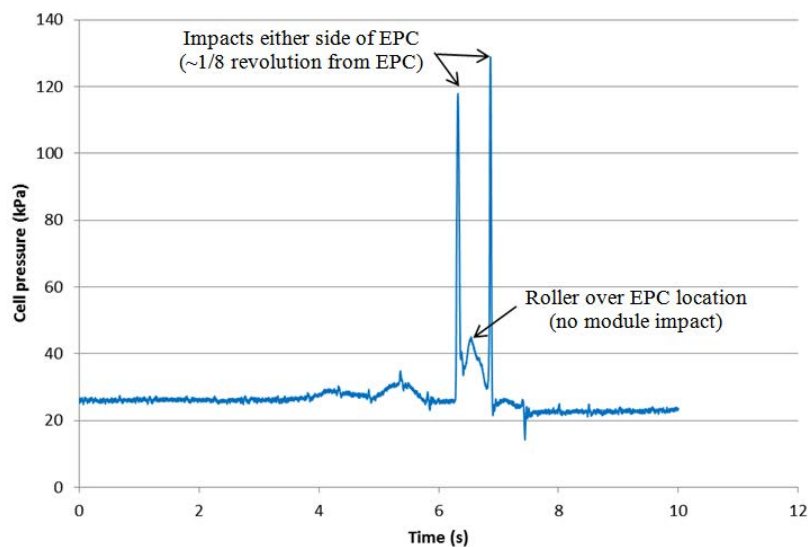
Figure 9: Example data from an impact not directly over an EPC (EPC3, Lift 2, Lane A, Pass 7).

Figure 11 shows the measured peak pressures averaged over all of the EPCs plotted against depth below ground. Only peak pressures corresponding to module impacts striking the ground directly over an EPC were used to develop this and the remaining figures. The plot shows that the highest pressure reading obtained in the field trial was 604 kPa at 0.67 m depth. The pressure then quickly dissipated, decreasing by over 50% to around 260 kPa at 1 m depth. By 2 m depth the pressure had again halved to 120 kPa, just over double the overburden pressure at that depth. The deepest EPC, located 3.85 m below ground, measured a pressure of 38 kPa. That value represents less than 10% of the highest value recorded, but was still nearly equivalent to the static pressure of the roller at the surface, suggesting that, even at that depth, the roller was having some influence.

The pressure measurements from the 3 test lanes were combined to produce a cross section showing the zone of influence in the plane perpendicular to the direction of travel. Figure 12 shows a summary contour plot of peak pressure imparted by the impact roller with depth after 16 passes of the impact roller. It can be observed that the highest pressure readings recorded (> 200 kPa) are located in the upper 2 m; supporting other test data that suggests most of the quantifiable ground improvement occurs within this zone. Even the deepest pressure cells (buried at 3.85 metres below the ground surface) registered positive pressure readings due to the impact roller; suggesting that the zone of influence extended beyond this depth.
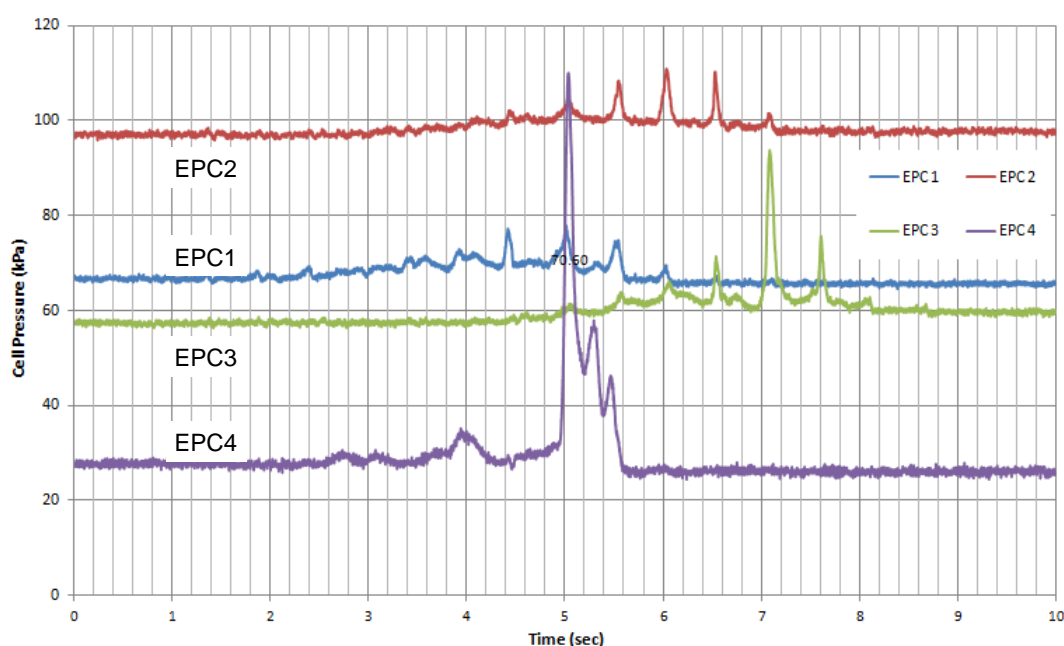
Figure 10: Example of superimposed results from all 4 EPCs.
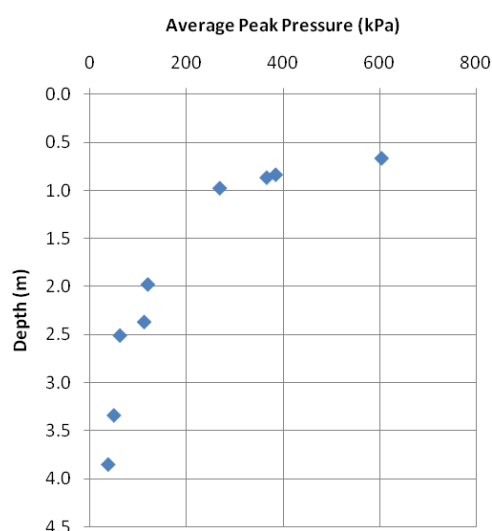
Figure 11: Average peak pressure versus depth below ground.

Figure 13 shows a summary contour plot of pressure imparted by the impact roller with depth after 16 passes in the plane parallel to the direction of travel. It can be observed that the highest pressure readings recorded (> 200 kPa) are located within the upper 1.5 m.

4.   CONCLUSIONS

This paper has presented the results of a field study, conducted at Iron Duke Mine, near Whyalla, South Australia, which aimed to measure the zone of influence of the 4-sided impact roller. Instrumentation and testing confirmed that quantifiable ground improvement occurs within the upper 2 m below the ground, although influence was measured at a depth of 3.85 m by means of earth pressure cells. Contour plots were developed which quantified the influence zone at various stress levels. Future work will focus on measuring the ratio of density improvement with depth and lateral extent.
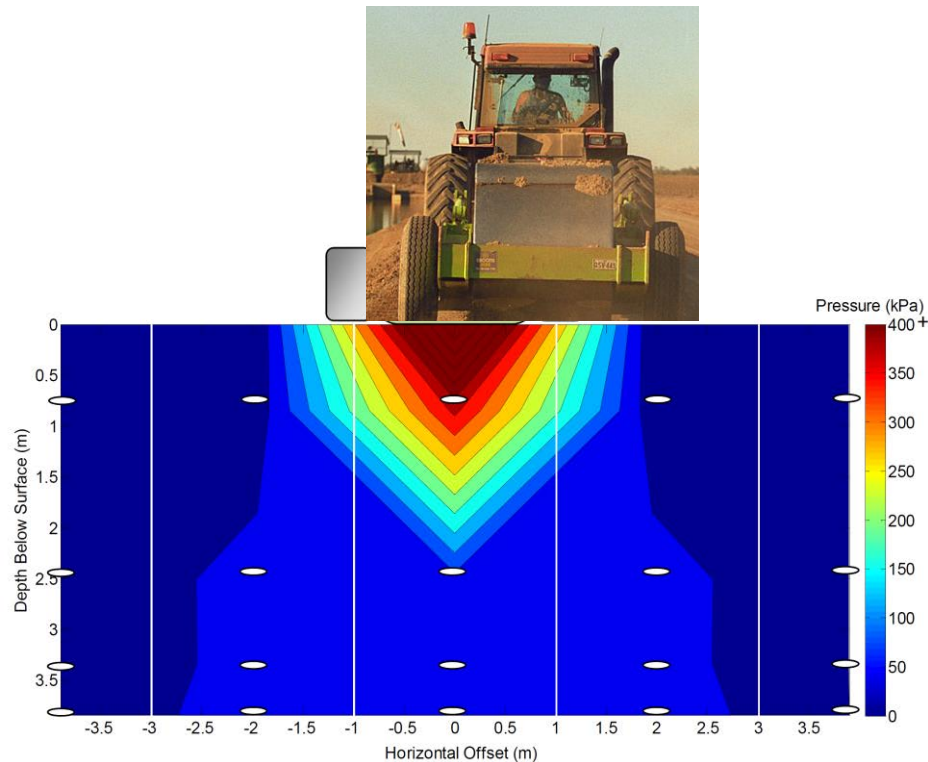
Figure 12: Pressure contours with depth after 16 passes in plane perpendicular to direction of travel.
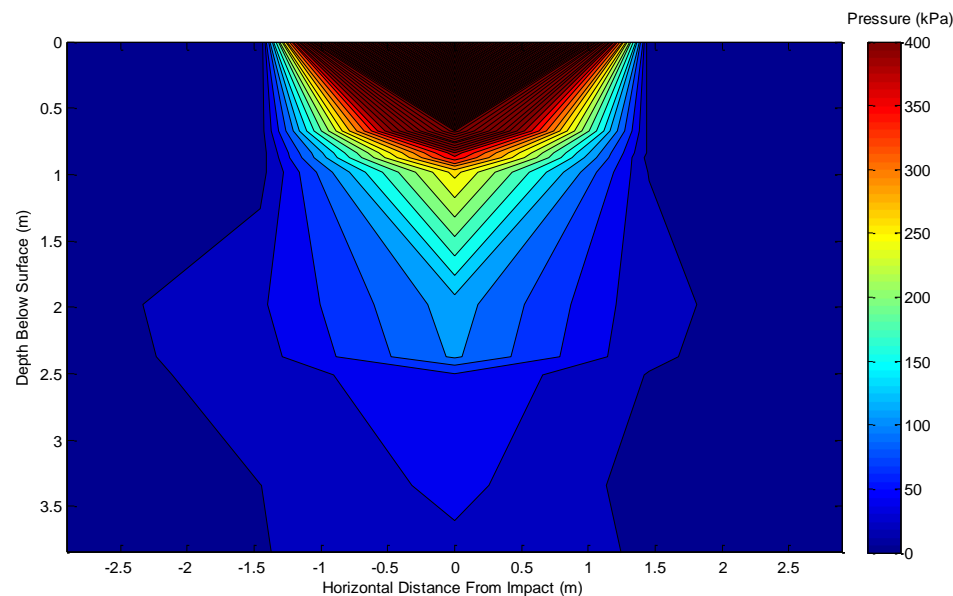
Figure 13: Pressure contours with depth after 16 passes in plane parallel to direction of travel.

5.   ACKNOWLEDGEMENTS

REFERENCES

Avalle, D. L., 2004a, Ground improvement using the 'square' impact roller – case studies, Proc. 5th Int. Conf. on Ground Improvement Techniques, Kuala Lumpur, 101–108.

Avalle, D. L., 2004b, Use of the impact roller to reduce agricultural water loss, Proc. 9th Australia New Zealand Conf. on Geomechanics, Auckland, 513–518.

Avalle, D. L. and Carter, J. P., 2005, Evaluating the improvement from impact rolling on sand, Proc. 6th Int. Conf. on Ground Improvement Techniques, Coimbra, Portugal, 8pp.

Avalle, D. L., Scott, B. T. and Jaksa, M. B., 2009, Ground energy and impact of rolling dynamic compaction – results from research test site, Proc. XVII Int. Conf. on Soil Mechanics and Geotech. Engrg., Alexandria, Egypt, October 5–9, Vol. 3, 2228–2231.

Clegg, B. and Berrangé, A. R., 1971, The development and testing of an impact roller, The Civil Engineer in South Africa, 13(3), 65–73.

Clifford, J. M., 1976, Impact rolling and construction techniques, Proc. ARRB Conf., Vol. 8, 21–29.

Clifford, J. M., 1978, The impact roller – problems solved, The Civil Engineer in South Africa, 20(12), 321–324.

Hausmann, M. R., 1990, Engineering Principles of Ground Modification, McGraw-Hill, New York.

Jumo, I. and Geldenhuys, J., 2004, Impact compaction of subgrades-experience on the Trans-Kalahari Highway including continuous impact response (CIR) as a method of quality control, Proc. 8th Conf. on Asphalt Pavements for Southern Africa, Paper 19.

Lukas, R. G., 1995, Dynamic compaction, Geotechnical Engineering Circular No 1, Report, FHWA-SA-95-037.

Mayne, P. W, Jones, J. S and Dumas, J. C., 1984, Ground response to dynamic compaction, Journal of Geotechnical Engineering, ASCE, 110(6): 757–774.

OneSteel, 2004, Iron Ore Mines: Welcome to OneSteel's Mining Operations, http://www.onesteel.com/ images/db_images/presentations/Mining%20Operations%20Analyst%20Presentation%201%20apr%200 4.pdf [accessed 04/05/2011].

Phear, A. G. and Harris, S. J., 2008, Contributions to Géotechnique 1948–2008: Ground improvement, Géotechnique, 58(5): 399–404.

Pinard M. I., 1999, Innovative developments in compaction technology using high energy impact compactors, Proc. 8th Australia New Zealand Conf. on Geomechanics, Hobart, Vol. 2, 775–781.

Rinehart, R. V., Mooney, M. A., 2009, Measurement of roller compactor induced triaxial soil stresses and strains, Geotechnical Testing Journal, 32(4): 347–357.

Standards Australia, 1997, Methods of testing soils for engineering purposes – Soil strength and consolidation tests – Determination of the penetration resistance of a soil – Perth sand penetrometer test, AS 1289.6.3.3, Sydney.

Standards Australia, 2003a, Methods of testing soils for engineering purposes – Soil compaction and density tests – Determination of the dry density/moisture content relation of a soil using standard compactive effort, AS 1289.5.1.1, Sydney.

Standards Australia, 2003b, Methods of testing soils for engineering purposes – Soil compaction and density tests – Determination of the dry density or moisture content relation of a soil using modified compactive effort, AS 1289.5.2.1, Sydney.

Standards Australia, 2004, Methods of testing soils for engineering purposes – Soil compaction and density tests – Determination of the field density of a soil – Sand replacement method using a sand-cone pouring apparatus, AS 1289.5.3.1, Sydney.

Standards Australia, 2009, Methods of testing soils for engineering purposes – Soil classification tests – Determination of the particle size distribution of a soil – Standard method of analysis by sieving, AS 1289.3.6.1, Sydney.

A comparison of soil improvement achieved using different vibro methods

Rafael Jimenez and Fernando Roman, Technical University of Madrid (UPM), Spain (rafael.jimenez@upm.es; fernando.roman@upm.es)

José Miguel Garcia-Gutierrez, ENAGAS. jmgarcia@enagas.es

ABSTRACT

A liquefied natural gas (LNG) plant is currently being constructed on a hydraulic fill in El Musel Port (Gijon, Northern Spain). The hydraulic fill is mainly composed of marine sands dredged from nearby locations, and it was placed on site using the rainbow and pipeline discharge and the bottom dump methods. The dynamic loads imposed by some of the plant elements suggested the need to conduct soil improvement using vibro-methods. To identify the most suitable method among those available, several options (including vibro compaction, and vibro-substitution using the bottom and top feed methods) were considered in a trial field. Monitoring and control methods included the use of geophysical methods as well as DPSH and SCPTU tests. This paper presents the results of the monitoring conducted at such trial field before and after the different treatments were employed, and it illustrates the degrees of improvement achived using each one.

1. INTRODUCTION

"Vibro" methods (with or without addition of stone) have been commonly employed in practice for densification of granular soils since the 1930´s (Slocombe et al., 2000). The main uses of the technique with granular soils have been to densify the soil, which leads to increasing stiffness and strength (hence reducing settlements and increasing stability; see e.g., Hughes et al. 1975; Hughes & Withers, 1974) and also to reduced liquefaction risk and reduced ground deformations during seismic events (see e.g., Adalier & Elgamal, 2004). The technique has been proven to be effective without addition of stone in soils with up to 15% fines (and less than approximately 2% fine silts to clays); and the addition of stone is usually required to increase the densification efficiency in soils with higher fines contents (Slocombe et al, 2000). In addition to soil type and type of stone added, the results obtained with the technique depend mainly on the total energy introduced into the soil by the vibrator (which itself depends on grid spacing, vibrator type and power, number of repetitions, etc.), and also on the quality of workmanship and on personnel's experience (Slocombe et al, 2000).

Because of the complexity of phenomenon and the number of factors involved, and despite some very interesting contributions and case histories (see e.g., Slocombe et al. (2000) and references therein), there is not much guidance in the literature on how to assess the degrees of densification that can be achieved in a specific project. For that reason, it is usually necessary to resort to the *observational method*, so that several improvement alternatives are tested to see how they perform at each site.

In this paper, we report the results of a recent experience of application of vibro-methods in a hydraulic fill made of marine sands (with a varying but generally small amount of silt) that were dredged from nearby locations. Three vibro-methods for soil improvement are compared: *(i)* stone columns executed by the water-flushing technique ("wet method") with stone added from the surface ("top-feed"); *(ii)* stone columns ("wet method") with bottom-feed delivery of stone; and *(iii)* vibro-compaction (with addition of the same sand to increase efficiency and to maintain site level). Three field tests were developed (one for each treatment type indicated above) and a series of in-situ tests were employed to compare the conditions before and after treatment. (In-situ tests included dynamic penetration using DPSH penetration tests; seismic cone penetration tests or SCPTU; and seismic wave velocity analyses.)

2. DESCRIPTION OF THE PROJECT

In this paper, we present results of a field tests conducted at a reclaimed port facility constructed by the hydraulic fill method (mainly using "rainbow" and "pipeline" discharge methods, as well as "bottom dumping" from barges; for a description see Lee et al. (1999) and Lee (2001)). The purpose of the project is to construct a Liquefied Natural Gas (LNG) regasification plant for ENAGAS in El Musel Port (Gijon, Spain). (ENAGAS is the Technical Manager of the Gas System and Common Carrier for the high

pressure gas network in Spain; for further details, see http://www.enagas.es). Photo 1 shows an aerial photograph with the specific location of the project.

Photo 1: Location of the project

The material used for the hydraulic fill is a marine sand obtained by dredging from nearby locations. The sands have a variable silt content (although in most cases it is smaller than 30%), and particles are mainly composed of shell fragments. The composition and properties of the fill sand are discussed in more detail in a companion paper (see Roman *et al.* (2012) "Preloading of a hydraulic fill for foundation of LNG tanks", Proceedings of ISSMGE - TC 211 International Symposium on Ground Improvement IS-GI Brussels 31 May & 1 June 2012) Table 1 shows a typical column of soil at the site, whereas Photograph 2 illustrates the aspect of the hydraulic fill as observed at a temporary cut in the same site. Note that some compositional variability can be observed due to the type of materials employed, as well as the variability of construction methods; for further discussion of characteristics of hydraulic fills, see Witman (1970), Sladen & Hewitt (1989).

Table 1: Typical soil column at the hydraulic fill site

Material	Depth <m>	SPT <N30>	N_{20} DPSH	CPTU Qc <MPa>	Water content ω <%>	Density γ_d <t/m³>
Hydraulic Fill (Level I)	0 – 3,5	10	7	7	8	1.44
Hydraulic Fill (Level II)	3,5 – 10	5	3	5	23	1.68
Hydraulic Fill (Level III)	10 – 20	12	10	8	23	1.68
Cuaternary (Level IV)	20 – 25	20	20	10	23	1.70
Bedrock	> 25	R	R	R	-	-

Photo 2: View of typical soil column

To provide an adequate foundation for the tanks, preloading was selected as the main ground improvement technique (see Roman et al. (2012) for details); however, there were some locations in which more strict requirements for the foundation material were specified, such as areas where critical structures (e.g., a very high torch) or dynamic equipment (such as compressors, etc.) were going to be founded. The vibro-compaction and vibro-replacement methods for ground improvement were considered for such locations. To make a selection among the available options, a trial field was designed at the compressor's area to compare the degrees of improvement achieved by three different "vibro" methods: *(i)* stone columns constructed with the "wet" method and top feed; *(ii)* stone columns constructed with the "wet" method and bottom feed; and *(iii)* vibro-compaction (with addition of the same sand with which the fill is constructed). The details of the trial field design, as well as the methods employed and results obtained, are presented below.

3.   GROUND IMPROVEMENT BY VIBRO METHODS

To compare the relative performances of the different vibro-methods employed, three trial fields (or test sites) were developed, and seven (7) treatments of each type were conducted at each site (the central "column" was constructed first). Treatments were situated within a triangular grid with a theoretical area replacement ratio of approx. 12% (a 80cm "target" diameter for treatments, and 2,15m distances between centres). Control tests conducted at the sites included continuous dynamic penetration values (using DPSH N20 values); (seismic) cone penetration values (qc of SCPTU); and measurement of seismic wave velocities (cross-hole). The three trial fields were developed adjacent to each other to minimize the likelihood of changes in the underlying materials, and also to reduce the need for boreholes in the development of a "continuous" profile using the cross-hole method. Figure 1 shows a plan view of the theoretical locations of treatments at each of the three test sites, and also of the geotechnical tests conducted at each site (preliminary; before treatment; or after treatment). In the discussion below, Test Site 1 corresponds to stone columns executed with the "wet" bottom-feed method; Test Site 2 corresponds to stone columns executed with the "dry" top-feed method; and Test Site 3 corresponds to vibro-compaction (with sand addition).
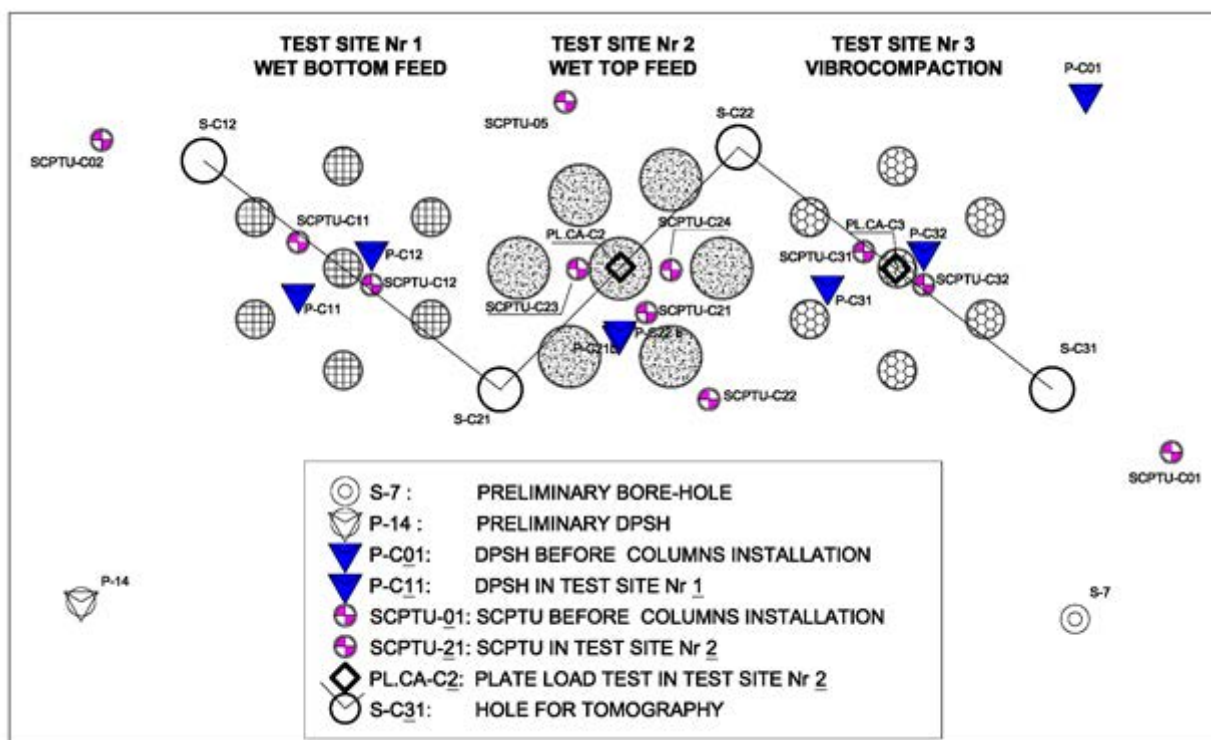
Figure 1: Location of treatments and of control tests at test sites

4.   COMPARISON OF FIELD TEST RESULTS

By comparing the situations before and after improvement, it is possible to assess the degree of improvement achieved by each of the methods considered at Tests sites 1 to 3.

For instance, Figure 2 presents a comparison between DPSH N_{20} dynamic penetration values measured before and after treatment for each of the test sites. (There were two DPSH available before treatment --- one at the lower-left corner and one at the upper-right corner---; since their results are very similar, they have been considered as representative of "before treatment" conditions in all test sites.) It can be observed that the vibro-treatments produce a significant increase in the compacity (as measured by penetration resistance) of the fill, and they are also shown to produce a more "homogeneous" material in the vertical direction. (Note that the increase with depth is less significant in the case after treatment). DPSH N_{20} values in the order of 15-20 are obtained in all cases (there seems to be no large difference between methods) and, in some cases, even higher values have been observed for tests conducted at a very short distance to the treatment. (Such values would correspond to SPT N-values in the order of 25-40, which suggests that a "medium" to "dense" sand condition is being achieved.)

Similarly, Figure 3 presents the comparison of SCPTU tip resistances measured before and after the tests. In general, it can be observed that the three tests available before the ground improvement (one on the upper-left part; one on the top; and one n the lower-right part) show very similar results, hence suggesting the homogeneity of fill initial conditions. (Note also that cone tip resistance values agree with other values reported in the literature for other hydraulic fill projects; see e.g., Lee (2001)) As in the DPSH case, it seems clear that the ground improvement techniques have the consequence of producing a vertical homogenization of ground conditions, and also that tests that are closer to the "as-built" column location tend to give higher values of tip penetration resistance. (Increases of qc tip resistance values ranging from 100% to 500% ---and probably more in some cases—have been obtained in most cases; such values compare well with values presented in the literature for other case histories (see *e.g.*, Slocombe *et al.* (2000))
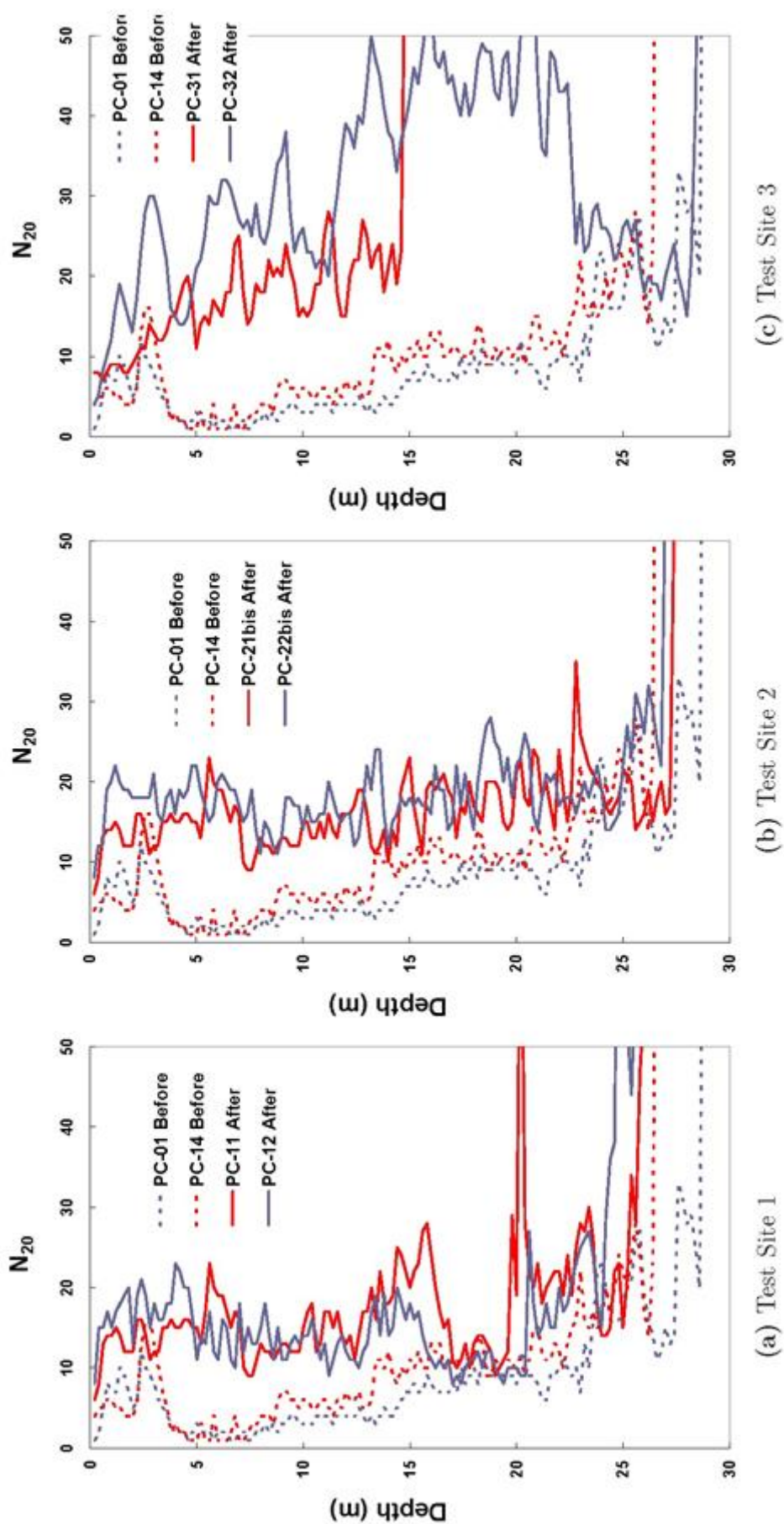
Figure 2: Comparison of DPSH values
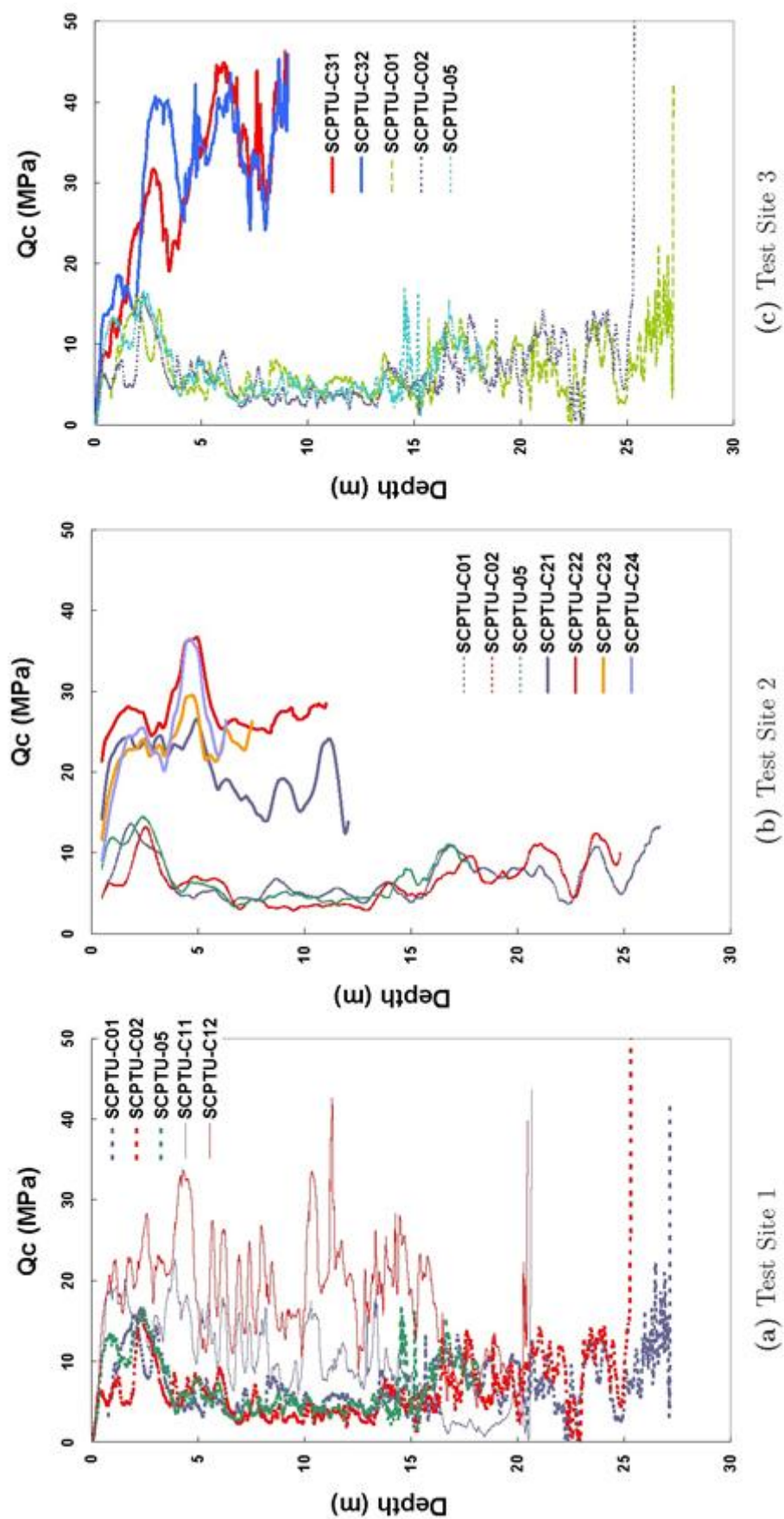
Figure 3: Comparison of SCPTU tip resistance

Figure 4 presents the results of seismic velocities of S-waves measures with the SCPTU. It can be observed that available data again suggest that there is a significant increase (in the order of 25% to 100% higher, with most common increases in the order of 50-100%) of measured wave velocities after treatment, and also that velocities measured across the actual "columns" are higher.
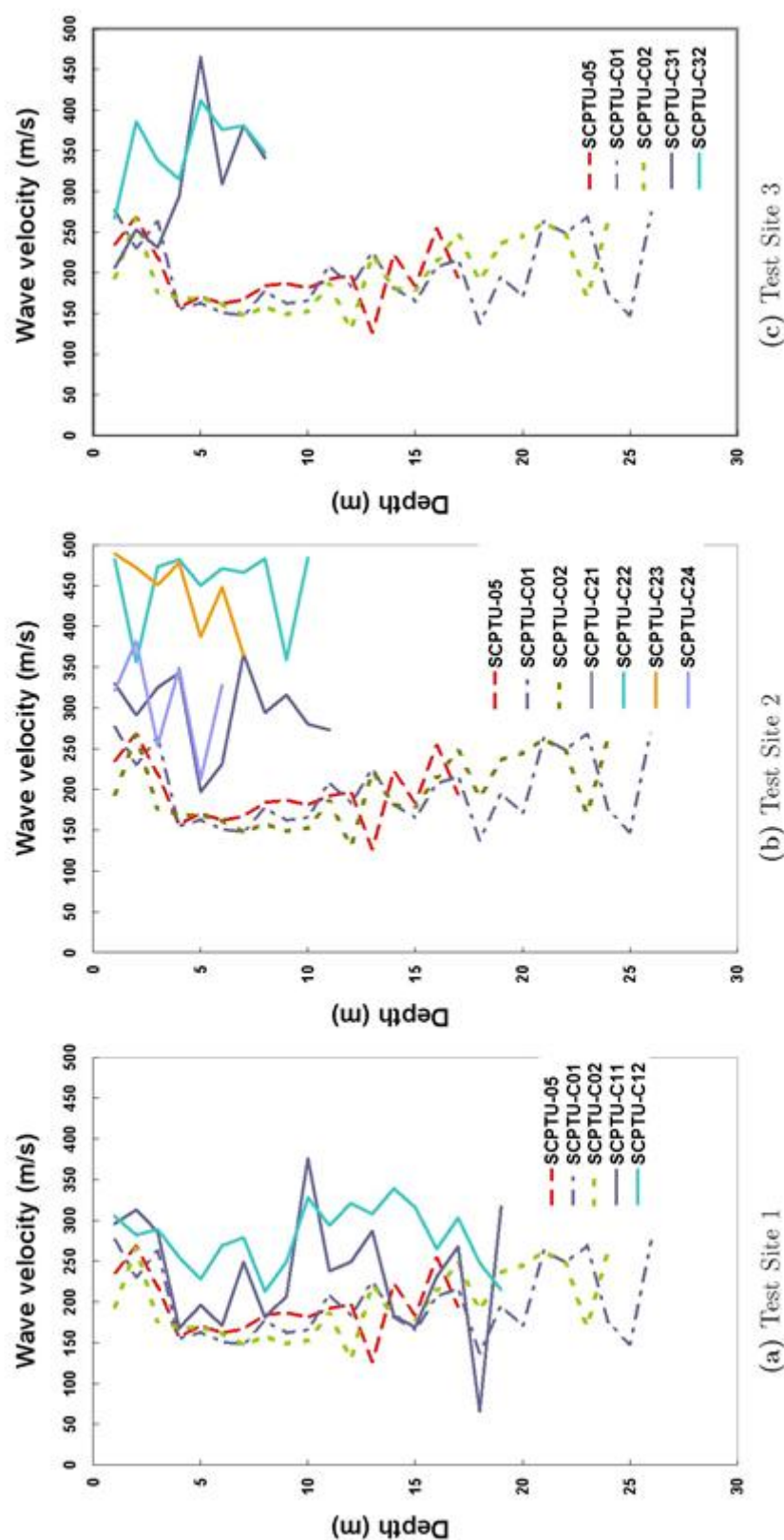
Figure 4: Comparison of wave velocities (vs) measured with SCPTU
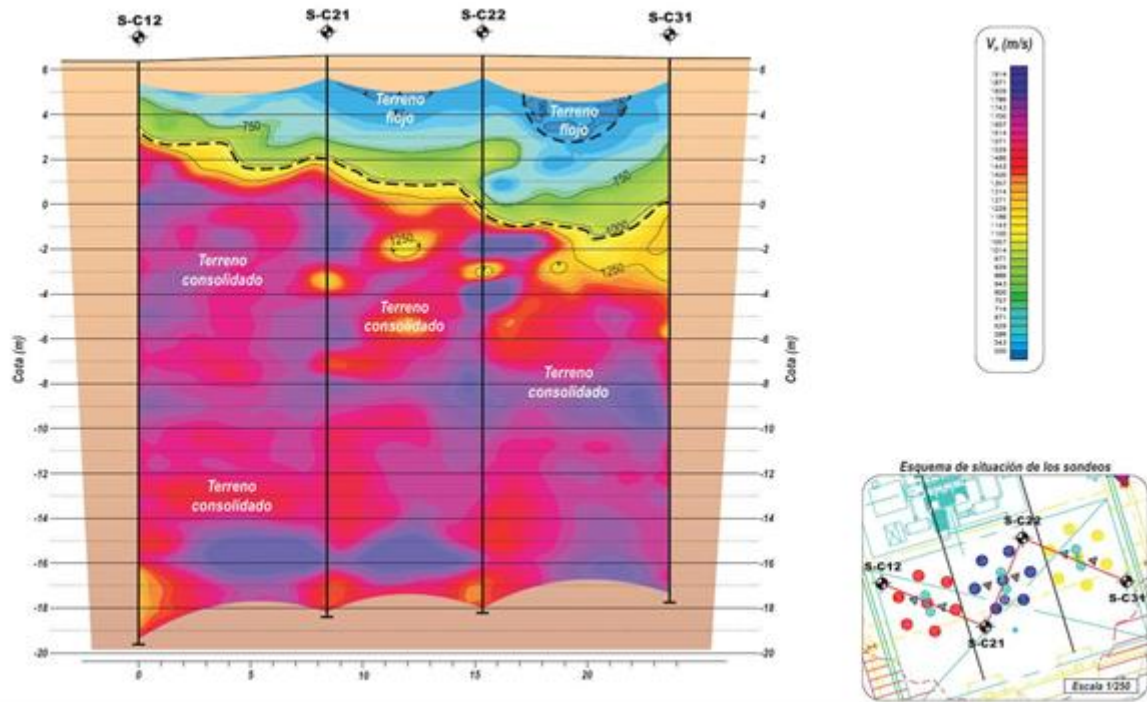
Figure 5: Profiles of seismic velocities (vp) across test sites (GEOCISA-ICT, 2010)

Figure 5 shows the result of a seismic tomography (using the cross-hole method) that has been developed employing the boreholes indicated in Figure 1. It can be noted that, in all cases, a "loosened" zone remains at locations close to the surface. (In this case, and to fulfil the required design specifications, the surface had to be excavated and replaced by a granular and compacted material.) . It is also observed that areas treated with stone columns tend to produce higher seismic velocities than those observed in the area treated with vibro-densification (with sand addition). Similarly, and although differences are not very high, results suggest that the bottom-feed method employed at Test Site 1 provides higher (and more uniform) seismic velocities. (Note the "gaps" observed at the location of the bottom feed treatment at Test Site 2.) This is probably due to the higher diameter control achieved with the bottom-feed method (in agreement with previous observations of Slocombe et al. (2000), our experience suggests that a more controlled and uniform shape is obtained), although more research is probably needed on this topic to verify this observation.

5. CONCLUSIONS

This paper presents the results of recent field tests executed in El Musel Port to select the "best" vibro-method for soil improvement (among those available) in the context of a LNG regasification plant project. The need for vibro methods was because some parts of the plant (compressors, torch) needed special requirements for their foundation material, so that the preloading technique that was employed in the rest of the plant (see Roman *et al.* (2012)) was considered not sufficient. To compare the relative performances of the different vibro-methods employed, three trial fields (or test sites) were developed, and seven (7) treatments of each type were conducted at each site. Treatments were situated within a triangular grid with a theoretical area replacement ratio of approx. 12%. The vibro-methods considered for soil improvement were: *(i)* stone columns constructed with the "wet" method and top feed; *(ii)* stone columns constructed with the "wet" method and bottom feed; and *(iii)* vibro-compaction (with addition of the same sand with which the fill is constructed).

Tests conducted at the site to verify the degree of improvement achieved included dynamic penetration (DPSH) tests; seismic cone penetration (SCPTU); and seismic wave velocity measurements (using the cone and also the cross-hole method). Results indicated that (except for a limited depth in the vicinity of the surface, the extent of which was dependant on the type of method employed) a significant improvement is achieved by the use of vibro methods in this case, and that such achievement has been verified by all testing methods employed. In addition, they show that the soil densification achieved by the vibro methods has the additional advantage of being quite homogeneous in the vertical direction. (The

densification effect decreases as the distance to the treatment increases.) In addition, the seismic tomography obtained by the seismic cross-hole method suggests that the improvement obtained by the bottom-feed method is more "uniform" than that obtained by the top-feed method. (This is probably a result of the more "uniform" columns that are obtained due to the better diameter control provided by the bottom-feed method.)

Based on the results available from the test sites, both types of stone columns were considered acceptable to provide the required "target" material, and the top feed approach was selected in this case on the basis of economic considerations. (The vibrator employed was the Pennine 400 vibroflot; see http://www.penninevibropilin.com for details.) Furthermore, to avoid the "loosened" zone at the surface, columns were constructed from the "original" ground surface; in that way, the "looser" material at the surface was later excavated and substituted by a compacted granular material. (The bottom of the excavation was also compacted.)

Finally, it should be emphasized that conclusions presented herein can only be taken as guidance in similar projects since, as explained above, there are multiple variables that influence the performance of ground improvement techniques by vibro methods.

6. ACKNOWLEDGEMENTS

REFERENCES

Adalier, K., & Elgamal, A. 2004. Mitigation of liquefaction and associated ground deformations by stone columns. Engineering Geology, 72: 275–291.

Hughes, J. M. O., & Withers, N. J. 1974. Reinforcing of soft cohesive soils with stone columns. Ground Engineering, 7(3): 42–44 & 47–49.

Hughes, J. M. O., Withers, N. J., & Greenwood, D. A. 1975. A field trial of the reinforcing effect a stone column in soil. Geotechnique, 25(1): 31–44.

Lee, K. M. 2001. Influence of placement method on the cone penetration resistance of hydraulically placed sand fills. Canadian Geotechnical Journal, 38(3): 592-607.

Lee, K. M., Shen, C. K., & Mitchell, J. K. 1999. Effects of Placement Method on Geotechnical Behavior of Hydraulic Fill Sands. Journal of Geotechnical & Geoenvironmental Engineering (ASCE), 125(10): 832–846.

Sladen, J. A., & Hewitt, K. J. 1989. Influence of placement method on the in situ density of hydraulic sand fills. Canadian Geotechnical Journal, 26: 453–466.

Slocombe, B. C., Bell, A. L., & Baez, J. I. 2000. The densification of granular soils using vibro methods. Geotechnique, 50(6): 715–725.

Whitman, R. V. 1970. Hydraulic Fills to Support Structural Loads. Journal of the Soils Mechanics and Foundations Division (Proceedings of the American Society of Civil Engineers), 96(SM1): 23–47.

Sand Compaction Pile Technology and its Performance in both Sandy and Clayey Grounds

Hiroki Kinoshita, Fudo Tetra Corp., Japan, hiroki.kinoshita@fudotetra.co.jp
Kenji Harada, Fudo Tetra Corp., Japan, kenji.harada@fudotetra.co.jp
Mitsuo Nozu, Fudo Tetra Corp., Japan, mitsuo.nozu@fudotetra.co.jp
Jun Ohbayashi, Fudo Tetra Corp., Japan, jun.ohbayashi@fudotetra.co.jp

ABSTRACT

Sand Compaction Pile (SCP) technology has been developed in Japan since the 1950s and has been widely applied to various structures on both clayey and sandy grounds (as liquefaction mitigation). In this paper, various projects that verify the effectiveness of the SCP method in past intense earthquakes including the 2011 huge earthquake are discussed and the following observations are made: (1) strong sand pile with consistent diameter is possible to be installed even with using top vibrator and vertical vibration sequence; (2) SL-gauge system which has been developed in Japan is able to secure uniform diameter sand pile installation; (3) top vibrator system has many advantages, such as sand and other materials can be used, and addition of water is not necessary for installation; and (4) SCP method has also non-vibratory system using forced lifting/driving device.

1. INTRODUCTION

The sand compaction pile (SCP) method is a method of improving soft ground by means of installing well-compacted sand piles in the ground. It combines such fundamental principles of ground improvement as densification and drainage. It can be applied to all soil types, from sandy to clayey soils, and it has therefore been widely used in Japan for improvement of soft ground. In sandy ground, the SCP method is often used as a countermeasure against liquefaction and the effectiveness of compaction to prevent liquefaction has been confirmed in past intense earthquakes, showing this to be one of the most reliable improvement methods.

This paper describes the outline, classification and history of SCP method and concludes by discussing its features through comparison with the stone column method, which is used worldwide as vibratory gravel pile method. The paper also demonstrates the improvement effectiveness of the SCP method for both sandy and clayey ground. Furthermore, some cases that demonstrate the difference in the degree of damage suffered through past intense earthquakes between unimproved ground and ground compacted by the SCP method are shown.

2. OUTLINE OF SCP METHOD

Figure 1 shows the classification and history of the SCP method, including some relevant geotechnical issues. The SCP method has both vibratory system with vibro-hammer and non-vibratory system with forced lifting/driving device. It also can be implemented both on land and off-shore using an exclusive barge. Although the vibratory SCP was developed more over 50 years ago and has been implemented in more than 380,000 km of improved ground, the vibro-hammer used has a negative effect in the form of vibration and noise on the surrounding environment, making it difficult to utilize the method in urban sites or at locations close up to existing structures. To address this issue, a non-vibratory SCP method (with the commercial name 'SAVE Compozer') was therefore developed, which does not require impact or vibration on the driving device to penetrate the ground. The implementation volume of the non-vibratory SCP has reached more over 7,000 km to date.

The equipment consists mainly of an SCP driving device used as a base machine and a forced lifting/driving device with a rotary drive motor or hydraulic-powered geared motor to rotate the casing pipe as shown in Figure 2. Two types of forced lifting/driving device are used: the pin rack-sprocket type and the rack-pinion type. In both cases, the necessary reaction force for the forced lifting/driving device comes from the total equipment weight, and the sprocket or pinion gear is rotated by a hydraulic motor. The operating procedure for the non-vibratory SCP method, shown in Figure 3, is discussed below and is identical to that adopted in the conventional SCP method. A 400~500 mm diameter casing pipe is used to create well compacted sand piles of 700 mm diameter and as a result, the surrounding ground is densified.

	1940s	1950s	1960s	1970s	1980s	1990s	2000s	2010s
Items related to sand compaction pile method		development period(1955-1969)		spread period(1970-1989)		turning period(1990-)		
		'56 ▼Beginning of On-shore Work				'95▼Development of Non-vibratory SCP(On-shore)		
			'65▼Beginning of Off-shore Work			'02▼Development of Non-vibratory SCP (Off shore)		
implementation volume (thousand km)			12	80	180	330	380	

Average sea depth of artificial islands for off-shore work (m): Tokyo Bay Trans Road; Kansai International Airport (Phase II); Kansai International Airport (Phase I); Nagasaki Airport; Kobe Port Island; Port Southern Osaka; Ohgi Island.

Geotechnical issues: Stability; Settlement(Deformation); Tohoku Pacific Earthquake '11▼; '95▼Hyogo-ken Nambu earthquake; Earthquake resistance; Environment; '64▼Niigata Earthquake.

Figure 1: Geotechnical issues and history of SCP method

(1) Set the casing pipe to the predetermined place.
(2) By operating the forced lifting/driving device, install the casing pipe into the ground while rotating.
(3) After the casing pipe reached the required depth, feed sand through the upper hopper.
(4) By drawing up the casing pipe, the sand in the casing pipe is pressed out to the void by compressed air.
(5) Extract the casing while compacting the pressed out sand pile to enlarge it.
(6) Form the sand pile to the ground surface by repeating the above procedure.

Table 1 compares the features between the SCP method and the stone column method. The main point of difference is the location of vibrator and this gives the SCP method an increase in penetration ability and can penetrate without water.

Recordings of vibration associated with the vibratory methods (vibratory SCP method and stone column method) and non-vibratory SCP method are shown in Figure 4. As clearly seen from the figure, vibrations are greatly reduced in the non-vibratory method compared with the vibratory methods, making it suitable for applications in urban areas and close to existing structures.

A	Base machine
B	Base machine Leader part
C	Forced lifting/driving device
D	Rotary drive motor
E	Casing pipe
F	Hopper
G	Bucket
H	Compresser
I	Receving tank
J	Swivel
K	Power generator
L	Wheel loader
M	Noise suppresser

(a) Pin rack and sprocket type (b) Rack and pinion type
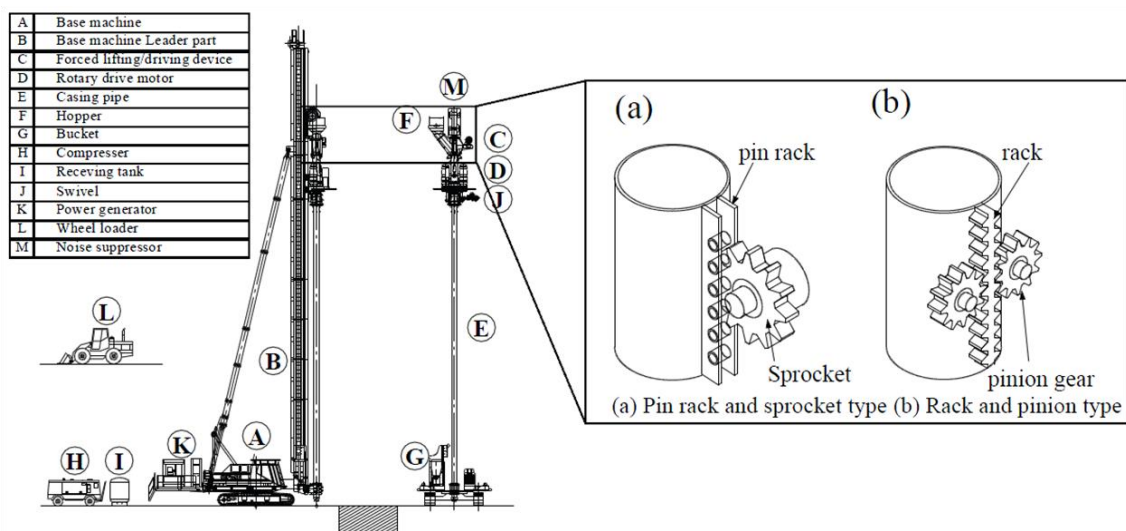
Figure 2: Non-vibratory SCP equipment and main components of forced lifting/driving device
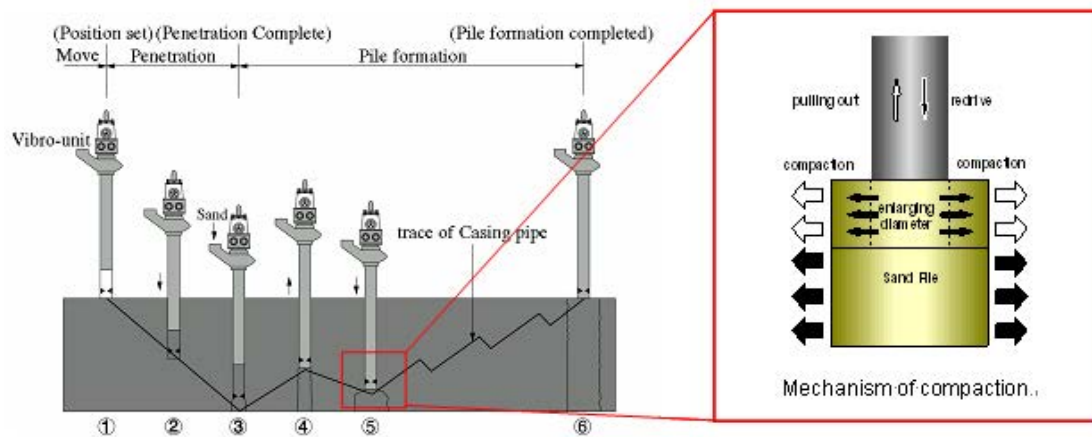
Figure 3: Operating procedure of non-vibratory SCP method

Table 1: Comparison between SCP method and stone column method

	Sand Compaction Pile method	Stone Column method (dry-bottom feed)
Location of vibrator	Upper part	lower part
Vibration direction	vertical	horizontal
Supply way of material	lower part	lower part
Use of air/water	air no water	air/water
Infilling material	sand/gravel	gravel only
Quality control	sand/gravel volume	Intensity of electric current
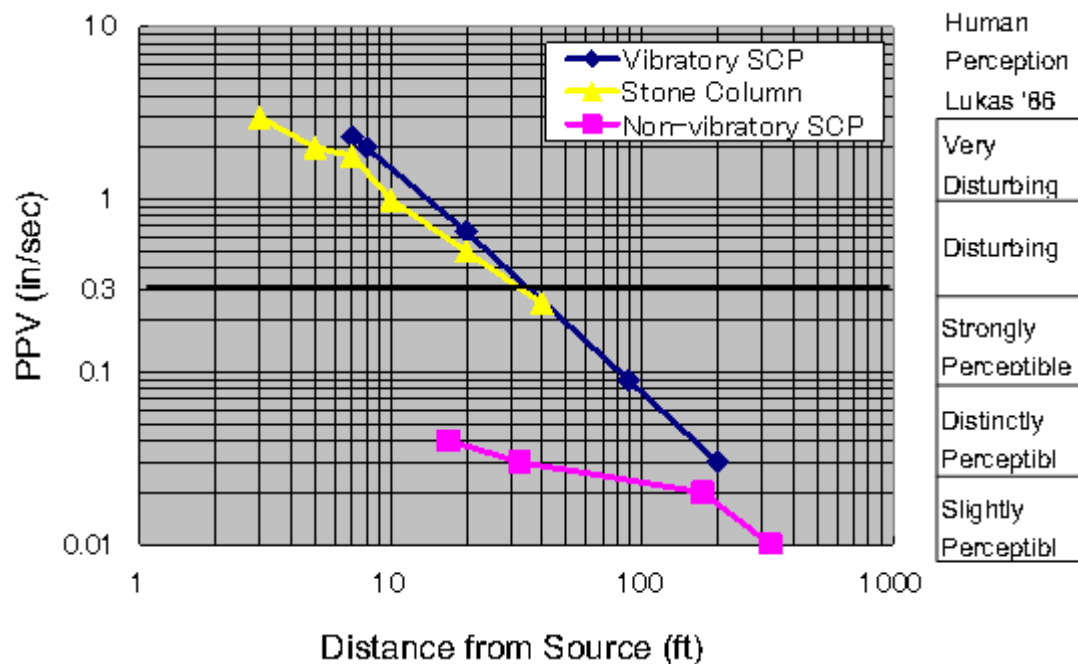
Figure 4: Decrease over distance of vibration of vibratory and non-vibratory SCP methods

To summarize, the features of the SCP method are as follows:

(1) Strong sand pile with consistent diameter is possible to be installed even with using top vibrator and vertical vibration sequence.
(2) SL-gauge system which has been developed in Japan is able to secure uniform diameter sand pile installation.
(3) Top vibrator system has lot of advantages, such as sand and other material can be used, and addition of water is not necessary during installation.
(4) SCP method has also a non-vibratory system using forced lifting/driving device.

3.   IMPROVEMENT EFFCTIVENESS BY SCP METHOD

3.1.   Improvement effectiveness for clayey ground

An example of application to embankment on clayey ground is discussed. Figure 5 indicates the cross-section of the embankment with the SCP improvement specification and soil boring log. From the properties of the area, the top 5 meters consist of peat layer with natural water content of $w_n = 400 - 1000\%$. Figure 6 shows the construction process along with the amount of settlement in the central portion of the embankment over time. In the figure, the unconfined compressive strengths q_u are also plotted. The embankments were completed up to 8m in height with no failure in the SCP section. The unconfined compressive strength increased as the settlement progressed.
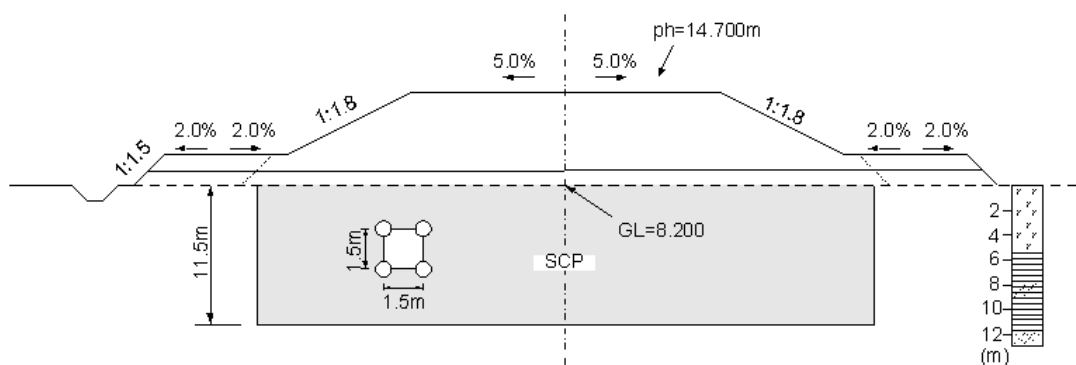
Figure 5: Cross-section of embankment
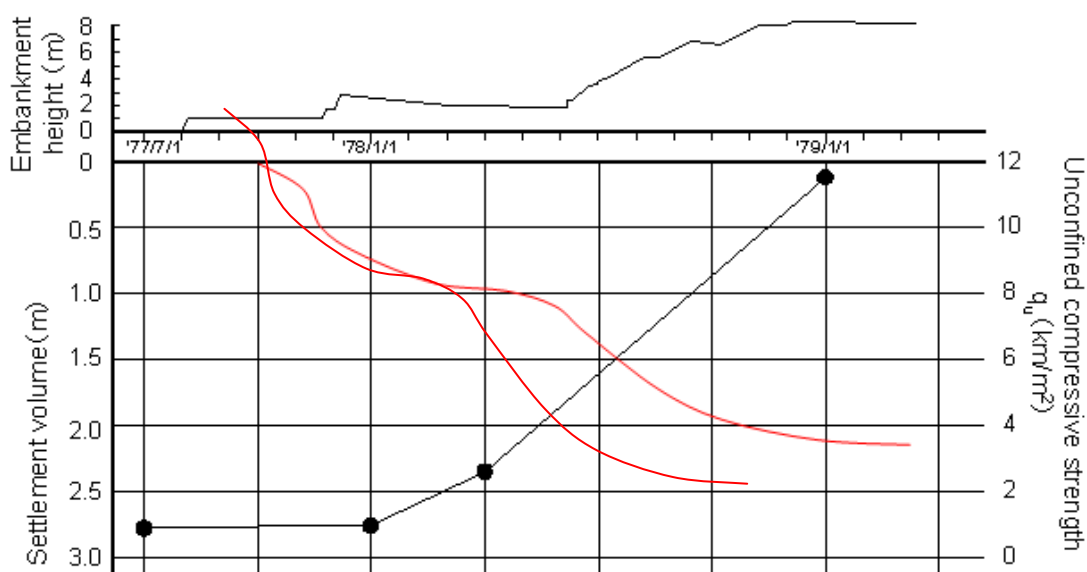
Figure 6: Elapsed time of consolidation settlement and unconfined compressive strength

---

3.2. Improvement effectiveness for sandy ground

Next, an example of application for sandy ground is shown. To illustrate the increase in density of sand, typical SPT N-values obtained from sites improved by both vibratory SCP and non-vibratory SCP procedures are shown in Figure 7(a) while examples of CPT q_c values from vibratory SCP–improved ground are illustrated in Figure 7(b). It is observed that penetration resistances obtained between sand piles installed increased as the piles pushed and displaced the adjacent ground.

Moreover, results of cases where various instruments (e.g., pressuremeters and dilatometers) were used to measure the lateral stresses before and after implementation of both vibratory and non-vibratory SCP methods are presented in Figure 8. In the figure, the relation between the lateral stress ratio, K_C, and replacement ratio, a_s, are plotted 1 month and 2 years after the SCP operation. Note that the data points corresponding to improvement ratio a_s=0 refer to the condition prior to the implementation of SCP method. It can be observed that substantial increase in K_C–values is observed 2 years after implementation, with larger increase in K_C values occurring at higher a_s.
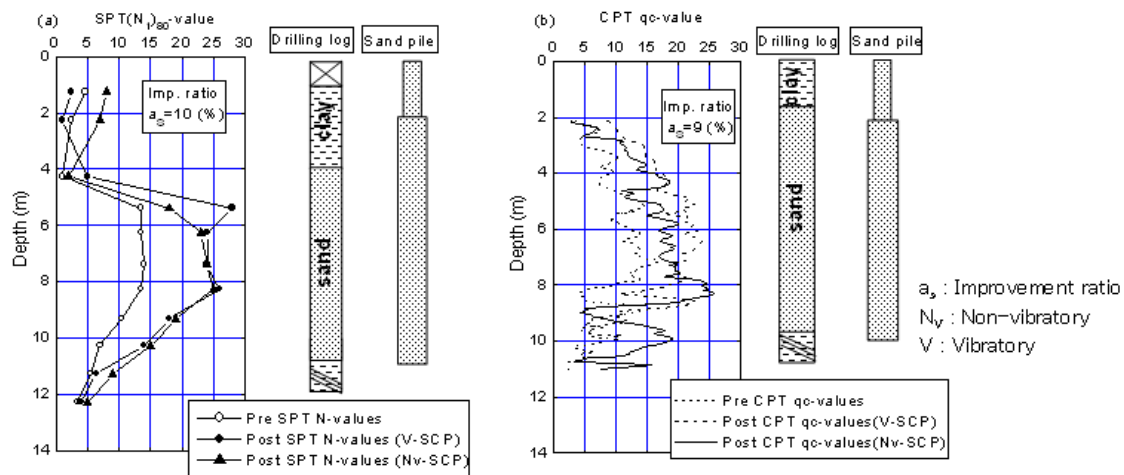
Figure 7: Examples of increased penetration resistances in grounds improved by SCP method in terms of: (a) SPT N–values; and (b) CPT q_c–values
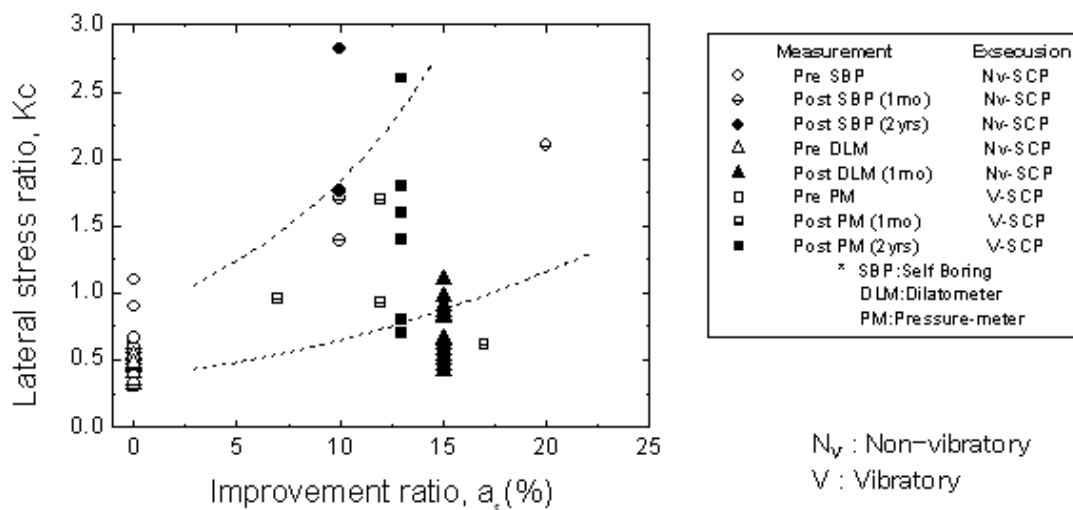
Figure 8: Example of results showing increase in K_C–values due to SCP implementation

4. CASES WHERE IMPROVEMENT EFFECT OF SCP METHOD HAS BEEN VERIFIED IN INTENSE EARTHQUAKES

Figure 9 shows the epicenter locations and characteristics of the 1974 Miyagiken-oki earthquake and seven other large-scale earthquakes which occurred later, including the 2011 Tohoku Pacific earthquake, and gives information on the performance of SCP-improved ground as a result of these earthquakes. As the figure shows, there has been no report of major disruption to structures erected on SCP-compacted ground, thus confirming in a qualitative sense the validity of compaction-type ground improvement. The following are some representative cases of ground improvement performance related to important structures.

4.1. Improvement effectiveness in port facility structures (1993 Kushiro-oki Earthquake)

Figure 10 shows a standard section of the Kushiro West Port that was affcted by the 1993 Kushiro-oki Earthquake (Yamada et al. 1990). At this location, countermeasures to resist earthquakes, mostly compaction by the vibratory SCP method, were implemented in the ground behind the quay walls. In areas adjacent to steel structures, gravel drain method was adopted to avoid any negative effects of vibration or displacement from the improvement work. SPT N-values in areas between sand piles in the compaction-improved areas were around 20~30. The maximum horizontal acceleration recorded at the Kushiro Port Construction Office, located about 1.5 km from the quay walls, was 470 gal but no damage due to the earthquake was observed, and port activities resumed the day following the earthquke. However, in unimproved grounds within the same wharf area, large cracks appeared in quay walls (approx. 10 cm wide, 20 cm vertical offset) and the quays could not be used.
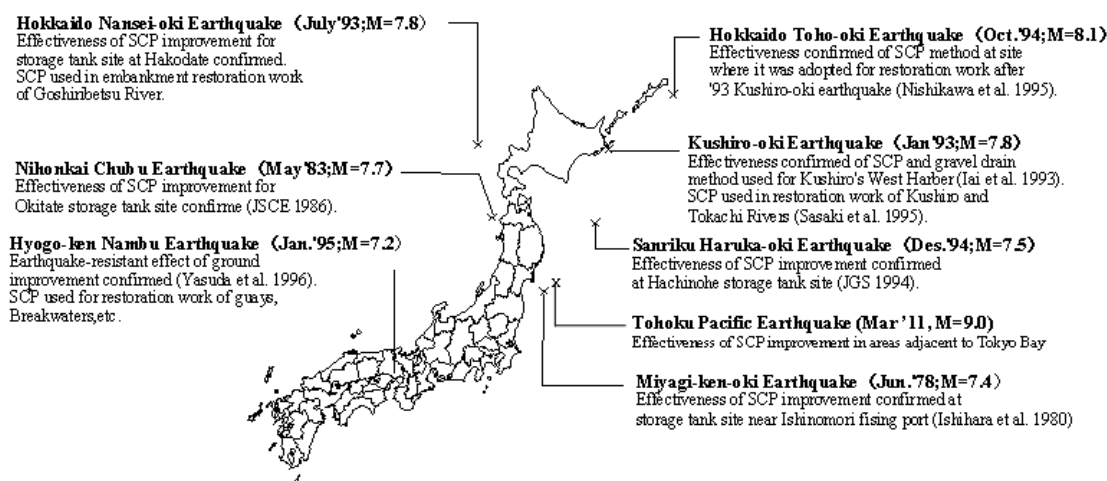
Figure 9: Recent intense earthquakes and information gained on ground improvement performance
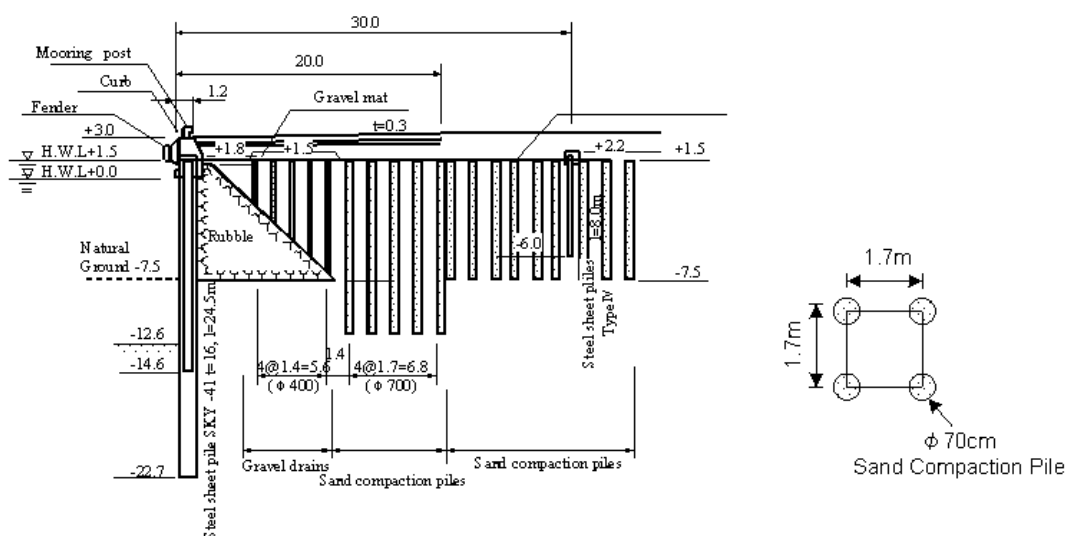
Figure 10: Standard section of revetment

4.2. Improvement effectiveness in river embankments (1993 Kushiro-oki Earthquake)

The 1993 Kushiro-oki Earthquake caused serious damage to many parts of eastern Hokkaido. River embankments, particularly those along the Kushiro River, suffered damage that included lateral cracking, cross cracking, slope collapse and cave-ins. The Kushiro River embankments suffered intermittent collapse over a section of several hundred meters, attributed to liquefaction in the al luvial sand layer and in the embankment itself below groundwater level.

In the restoration work, vibratory SCP method was adopted for the first time for foundation ground improvement in the restoration of iver embankments. Figure 11 shows a standard section (Sasaki et al. 1993). One year and nine months after the restoration work was completed, the Hokkaido-Toho-oki Earthquake occurred, and again the region suffered massive seismic impact. In the locations where the SCP method had been used there was no damage, but cracking re-occurred at locations where the embankment had been restored after the Kushiro-oki Earthquake only by compact-tamping because the cracking at that time had been light.
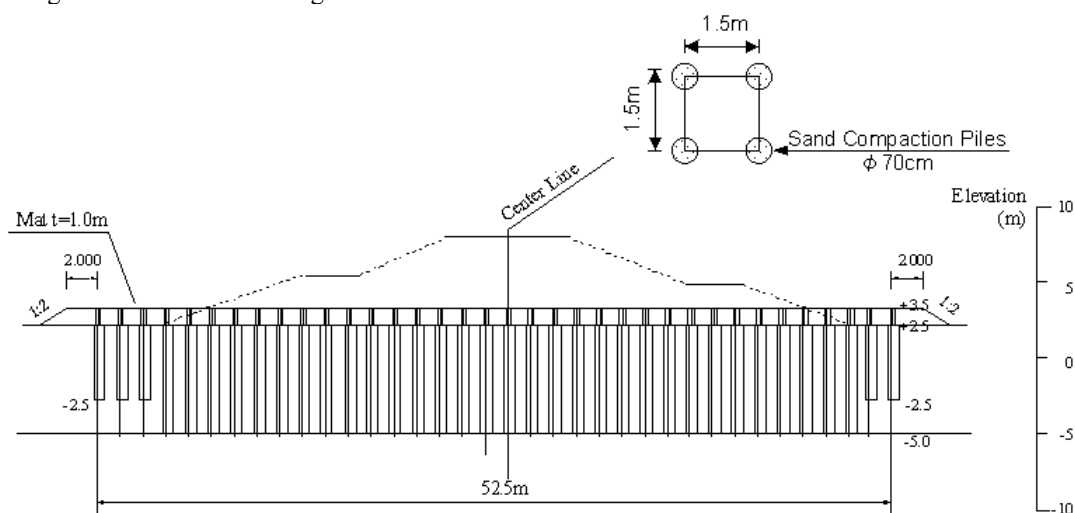
Figure 11: Standard section of river embankment

4.3. Improvement effectiveness in a storage ta nk facility (1993 Hokkaido Nansei -oki Earthquake)

In the 1993 Hokkaido Nansei-oki Earthquake a remarkable difference was observed between the areas of improved ground, including the vibrator y SCP-improved tank base ground, and the adjacent unimproved areas. Figure 12 shows the locations of sand boil marks in the improved tank base ground and the adjacent non-improved ground areas. The tanks themselves, installed on ground that had been improved against liquefaction using the SCP method, did not suffer damage, but evidence of sand boiling could be observed at a distance of approximately 1/2 of the improvement depth from the improved section.
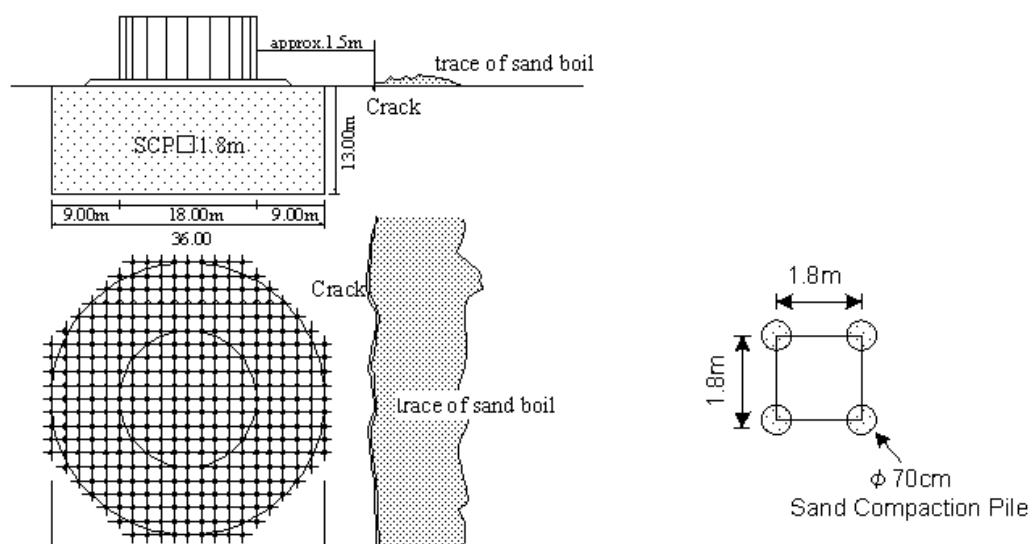
Figure 12: Standard section and plan of storage tank facility

4.4. Improvement effectiveness in buildings (1995 Hyogo-ken Nambu Earthquake)

Large scale liquefaction occurred in the two man-made islands, Port Island and Rokko Island, in the Kobe Port area as a result of the 1995 Kobe Earthquake. For structures in both islands, various types of ground improvement were undertaken as measures to accelerate consoliation settlement in the alluvial clay layer due to excess weight, and to increase the bearing capacity of the landfill soil layer. In the improved sections, there was little damage caused by settlement etc. as compared wit h the damage in unimproved areas. Figure 13 shows the measured post-earthquake settlements of the buildings with pile foundations in the areas of improved grounds. In both islands, 40-50 cm settlement occurred in the unimproved areas, but in the areas improved by compaction methods, including SCP, the settlement was negligible (Yasuda et al. 1996).
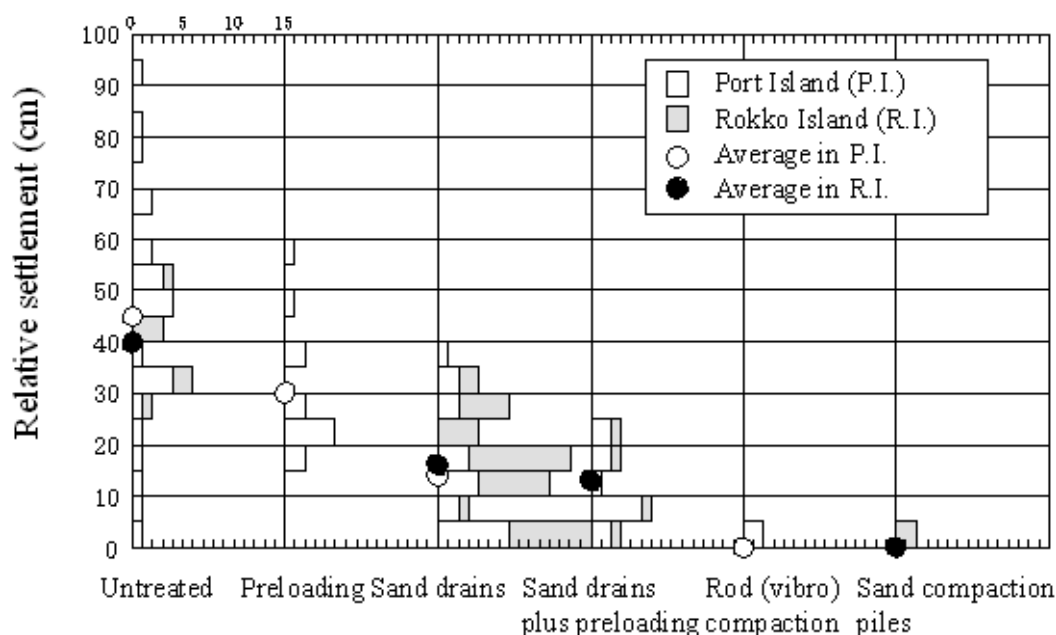
Figure 13: Relative settlement and methods of ground improvement Buildings with pile foundation)

During the 1995 Hyogoken Nambu earthquake, six cases of subsidence measurement of buildings on spread foundations located in the man-made islands were conducted before and after the earthquake (Kakurai et al. 1996). Figure 14 shows the cross-sections of these buildings. The foundation ground

beneath buildings a~e were improved by partial compaction, while no improvement was implemented under building f. Also indicated in each figure are the total bearing load from each of the building, the amount of absolute settlement measured and the improvement ratio. As shown in the figure, the settlement following the earthquake of building f with unimproved foundation ground was about 20cm whereas the amount of settlement in buildings a~d was in the order of several centimeters, depending on the extent of improvement.
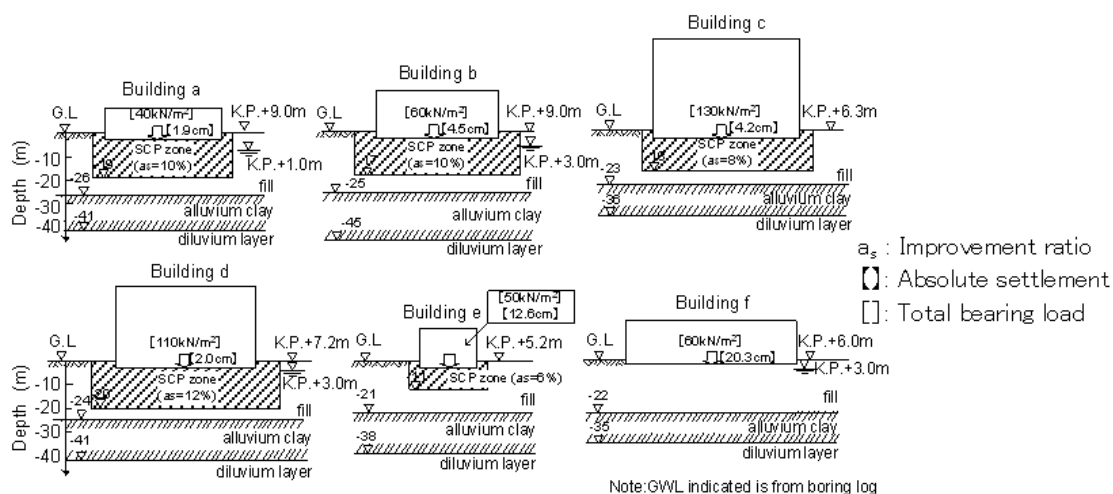
Figure 14: Absolute settlement and SCP improved area (Buildings on spread foundation)

4.5. Improvement effectiveness in buildings (2011 Tohoku Pacific Earthquake)

Following the 11 March 2011 Tohoku Pacific Earthquake (M_w 9.0), liquefaction was observed in many areas adjacent to Tokyo Bay, about 390 km from the epicentre, as shown in Figure 15. Manholes were uplifted, grounds settled, and buildings and bridges were damaged as a result of liquefaction.

Figure 15: Liquefied zones along Tokyo Bay (Ishikawa et al, 2011)

 A medical center building is located in reclaimed land along the Tokyo Bay as shown in Figure 16. The building is 5 stories high and supported by piles. After the liquefaction assessment, it was judged that there is a high potential for liquefaction and consequently, non-vibratory SCP was adopted at this site as a countermeasure against liquefaction. The imrovement specification is square arrangement with pitch of 1.5m (a_s=16.7%) and the length of the pile is 12m. In the surrounding area of the improved site, gravel instead of sand was used to dissipate the excess water pressure from liquefied area. The effectiveness of this method was verified for a building in Rokko Island during the 1995 Hyogo-ken Nambu Earthquake. As shown in Photo 1, although liquefaction-induced damage was observed outside the improved area, no damage was observed within the improved area.
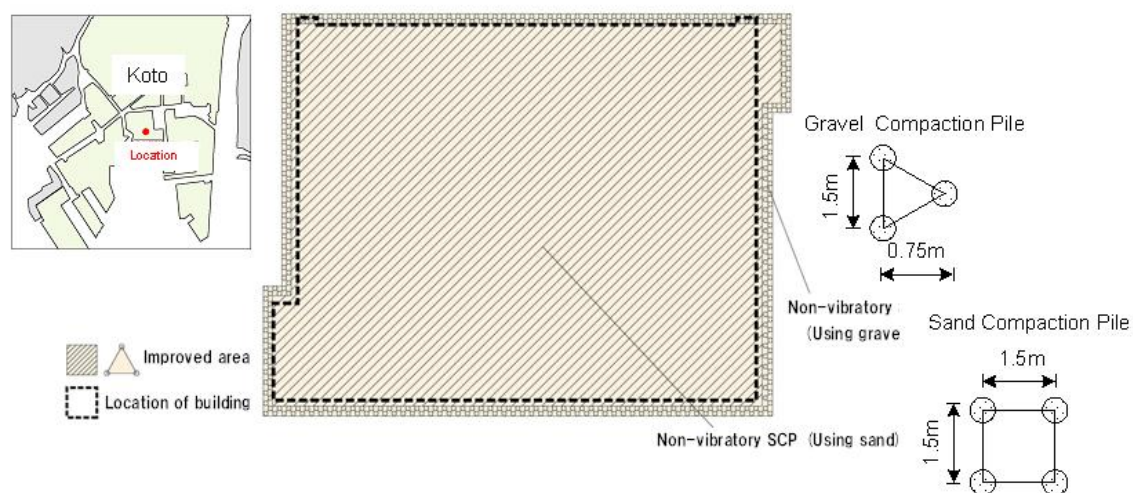
Figure 16: Plan view of the SCP improved area of the building

5.   CONCLUDING REMARKS

This paper highlighted the features of the SCP method and its improvement effectiveness though investigation of the implementation and performance of improved grounds during actual large earthquakes in Japan.
 There was no damage on the improved area during the 2011 Tohoku Pacific Earthquake. This showed that the improved ground by SCP method is effective not only against intense earthquakes such as the 1995 Hyogo-ken Nambu Earthquake but also against earthquakes having long duration time. A qualitative understanding of these factors and analyses should be undertaken in future studies.

Photo 1: Successful ground improvement in Tatsumi area

REFERENCES

Architectural Institute of Japan, AIJ, 2001, Recommendations for Design of Building Foundations (in Japanese).

Harada, K., Orense, R.P., Ishihara, K. and Mukai, J., 2010, Lateral Stress Effects on Liquefaction Resistance Correlations, New Zealand Society for Earthquake Engineering Bulletin, Vol. 43, pp. 13-23.

Harada, K., Nozu, M. and Orense, R.P., 2011, Liquefaction-proofing through sand compaction pile method : Case studies from recent gigantic earthquakes in Japan, 7th APRU Research on Multi-hazard the Pacific Rim, Auckland, New Zealand (to be presented).

Ishihara, K., Kawase, Y. and Nakajima, M., 1980, Liquefaction Characteristics of Sand Deposits at Oil Tank Site during the Miyagiken-oki Earthquake, Soils and Foundations, Vol. 20, No. 2, pp. 97-111.

Ishihara, K. and Harada, K., 1992, Sand compaction pile method - a ground technique for soft soils, Proc. of the International Geotechnical Conference, Vietnam, pp.471-480.

Ishikawa, K. and Yasuda, S., 2011, Liquefaction along Tokyo Bay during the 2011 Tohoku-Pacific Ocean Earthquake in Japan, 2nd International Conference on Performance-Based Design in Earthquake Geotechnical Engineering (to be submitted).

Japanese Geotechnical Society, 2009, Manual of Sand Compaction Pile Method by Re-driven System (in Japanese).

Kakurai, M., Aoki, M., Hirai, Y. and Matano, H., 1996, Investigation of spread foundations on liquefied man-made islands, Tsuchi-to-Kiso, 44-2, pp.64-66 (in Japanese).

Sasaki, Y., Tamura, K., Yamamoto, M. and Ohbayashi, J., 1995, Soil Improvement Work for River Embankment Damaged by 1993 Kushiro-oki Earthquake, Proceedings of 1st International Conference on Earthquake Geotechnical Engineering, Vol. 1, pp. 43-48.

Yamada, H. and Sato, M., 1990, Site Tests related to Work to Implement Countermeasures to Liquefaction at Kushiro Port, Presentation Outlines 4th set, of 34th Hokkaido Development Agency Technical Research Meeting, pp. 259-264 (in Japanese).

Yasuda, S., Ishihara, K., Harada, K. and Shinkawa, N., 1996, Effect of Soil Improvement on Ground Subsidence due to Liquefaction, Soils and Foundations, Special Issue, pp. 99-107.

Yasuda, S. and Harada, K., 2011, Liquefaction-induced Damage in the Reclaimed Lands along Tokyo Bay," Journal of Japanese Geotechnical Society, 59-7, pp.38-41 (in Japanese).

Ground improvement works on large scale projects in the North of Morocco

Benoît Meulewaeter and Dirk Bourlon, Besix Design Department Brussels,
Jan Maertens, Jan Maertens BVBA and KU Leuven

ABSTRACT

During the past years Morocco has launched many important industrial maritime and infrastructure works especially in the North of the country. Tanger Med, Tanger Roulier and Tanger Med 2 harbors have for instance change the face of the North Morocco offering great opportunities in the maritime transport and services. Those projects involve further developments as highways and railways facilities.

Building such a new harbor (Tanger Med 2 is a 2.8 km length quaywall) implies large ground works for the platform where for instance the equipment for the containers transport should come. Beyond the classical problems, the scale of the project and the ground structure in Tanger Med pushed the vibrocompaction technique to its limits.

Bouregreg in Rabat is another example of the development's will and involvement in major projects. Bouregreg could be compared to building an entire new city on an old waste storage. The general soil conditions were weak and not able to sustain any classical building loading.

This paper presents the ground improvement works applied at this large project scale in the North of Morocco for the projects that have seen the Belgian company Besix involved.

1.   INTRODUCTION

Morocco has seen over the last years a series of large scale projects with ground improvement involved. A clear and determined development thinking seen over the last years lead the country to invest in important infrastructure projects. Such projects do involve ground improvement techniques in a scale not common. This article deals with the application of those techniques on projects in which the Belgian Company Besix has been involved.

Tangier is by far the most developed Moroccan city over the last years. The complex of Tanger Med will offer more than three new harbors with container terminals and Ro-Ro terminals. It will offer the opportunity for the largest container vessels in the world to lean on the Moroccan coast. The realization of the nearshore quaywalls and the working platforms required the use of vibrocompaction technique.

In another infrastructure type of project, Rabat was also the theatre of an uncommon development. The project called Bouregreg had the intention of building a whole new city in the vicinity of Rabat on a soft soil area along the Bouregreg River. Stone columns have been used as foundation technique for the project.

The vibrocompaction technique has also been used for the Mazagan project. The foundations of this luxury hotel complex development close to the city of Al Jadida were initially designed with piles. An alternative proposal with vibrocompaction has been proposed accepted and realized.

Outside of Morocco, Besix has been involved in Algeria for the project Hamma (desalination plant). The stone column technique has here been used.

2.   BOUREGREG

As part of the urban development of the region around Rabat, a new neighborhood is to be build between Rabat and Salé in the Bouregreg valley close to the open sea. The project AMWAJ is the second sequence of a huge development project in the Bouregreg valley. The master plan on figure 1 gives the general layout of the project. The area includes many different structures as buildings, places, canals... The final function (administrative, public, offices, stores, hotels) of each building is not yet defined.

Figure 1: Master Plan

Sector SIB is the first part of the project to be built. The site is characterized by very poor geotechnical conditions as illustrated by the typical CPT test of Figure 3. So a foundation with stone columns installed with the wet method has been adopted for the project. 52000 stones columns concentrated under the foundations of the buildings have been installed following a scheme of figure 2.
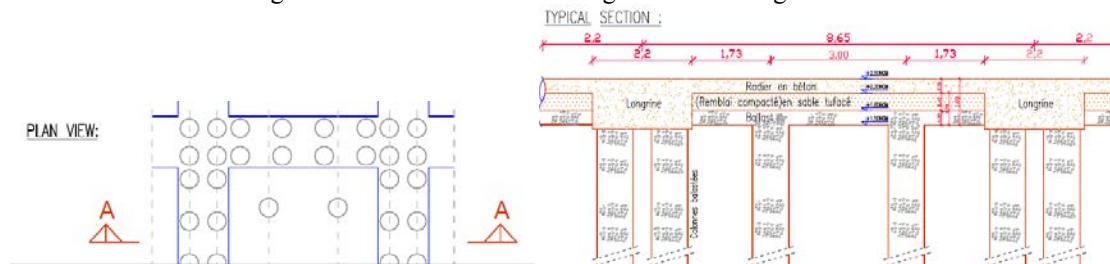
Figure 2: Plan view and typical cross section A-A

The depth has been determined based on the soil investigation CPT tests. It was possible to reach the resistant layer about 10m below ground level as show on the following typical CPT. The material used for the realization of the stone columns was a 10-80mm gravel.
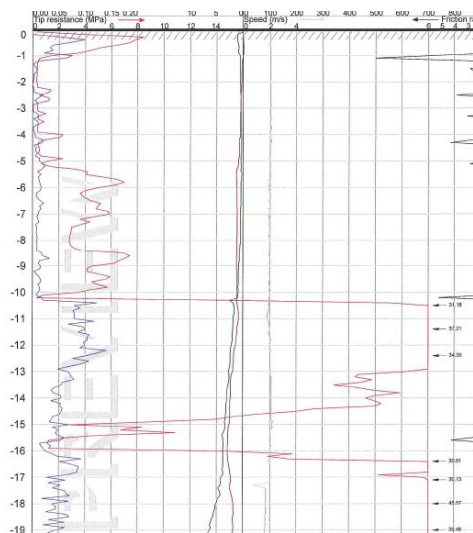
Figure 3: Typical CPT test result for the project Amwaj

Due to the presence of compressible layers underneath the bottom level of the stone columns (-15.00 m/-16.00 m), preloading has been necessary to limit the settlements to the allowed value of 50mm.

3.   MAZAGAN

The realization of the luxury Mazagan beach resort in Morocco close to the city of Al Jadida has seen ground improvement works under the different buildings of this entertainment center.

Figure 4: Overview of the beach resort

The specifications in terms of settlement are quite stringent to make sure the luxury buildings would not suffer from settlements. The subsoil consists of relatively clean sand with 5 to 15% particles < 74 □m but the cone resistance in the upper layers was smaller than the minimum value of 6 MPa normally required for strip footings. The original design consisted of a pile foundation. As alternative, the vibrocompaction technique has been proposed. In order to validate the solution proposed and determine the distance between the compaction points, two preliminary tests have been completed. The typical execution procedure is shown on figure 5 where three grids are tested.
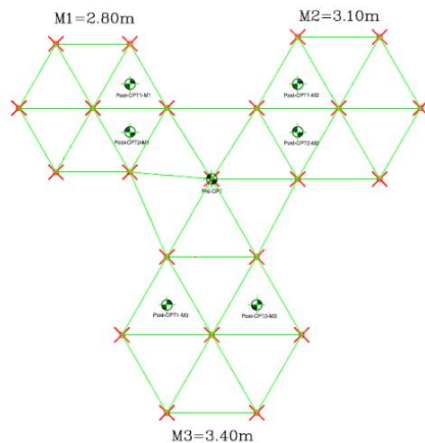
Figure 5: Preliminary test grid and post CPT's positions

During execution of the vibrocompaction a crater is formed on top of the layer as seen in figure 6. It has been decided to study the influence on the results if the crater's fill is made with sand or gravel. Therefore one test field has been realized with addition of in situ sand during compaction. For the other test field gravel has been added during compaction. The tests gave comparable results and it has been decided to do the fill with sand.

Figure 6: Crater due to execution

CPT's are used to control the works by comparing results before and after compaction. During the beginning of the execution it was not possible to reach the specified depth. Looking at the site investigations, it was thought that the probe should be able to reach a depth of 6 to 7 m. The first tests done were blocked at a depth of 3 to 4 m. This was probably due to the presence of old pavements but mainly due to an inappropriate execution method. In fact the water flushing was not sufficient. The ground is then compacted rapidly and prevents the probe to go deeper. A bigger pump allowing more flushing has been used during the further works and the predicted depths could be reached.
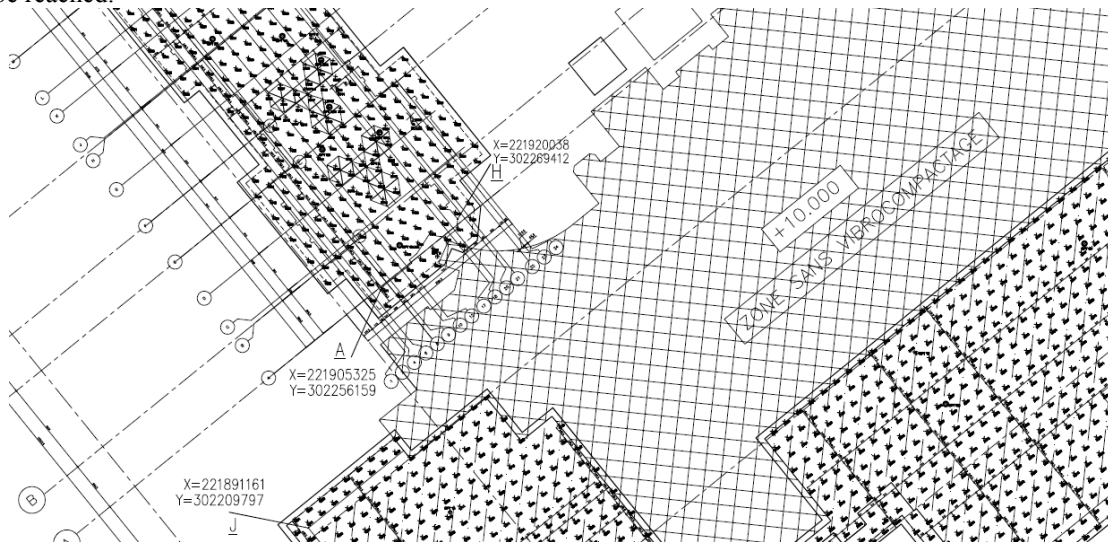
Figure 7: Example of the compaction points localisation

4. TANGER MED

The complex of Tanger Med consists of building three harbours in front of Gibraltar on the Moroccan coast where the Atlantic Ocean meets the Mediterranean Sea. The container terminals of Tanger Med Port 1 and Tanger Med Port 2 should accommodate the largest container vessels in the world.
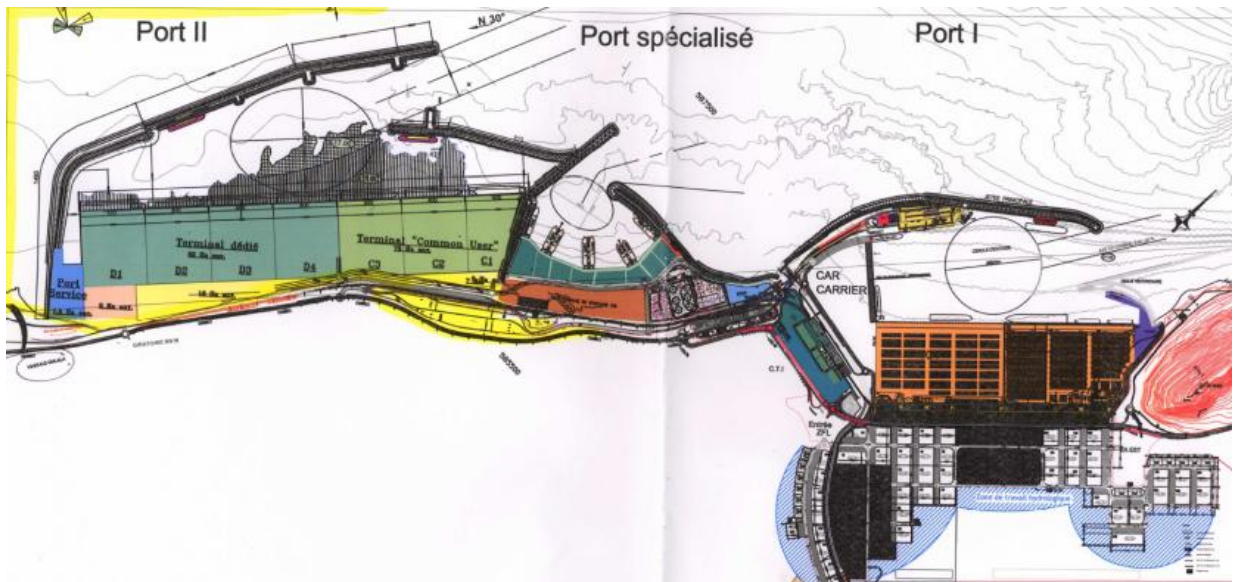
Figure 8: Complex of Tanger Med

The working platforms is made in sand backfill that is vibrocompacted to obtain a CPT cone resistance qc = 10 MPa. More than 2 million square meters are to be compacted. The details of the realisation are not discussed here. The intention is to focus on a more specific ground improvement problem encountered in some areas for the foundation of the quaywall at Tanger Med1. The main quaywall is made of concrete prefab blocks on top of each other from level -18mZH/-16mZH up to +4.5 mZH.

Such a gravity quaywall generates important foundation stresses which require a strong foundation layer especially in a high seismicity region as Tanger. In general the existing subsoil in the vicinity of the harbors is very stiff to rock. The rock is mainly composed of mudstone and sandstone. It is typical in the region to find in some areas the rock dug by ancient rivers coming from the hills on land to the sea. Tanger Med 1 quaywall was thought at first to be build with the bedrock at foundation level but additional site investigations have shown the bedrock level as seen on figure 9. Three areas with soft soil under the foundation level have been found.
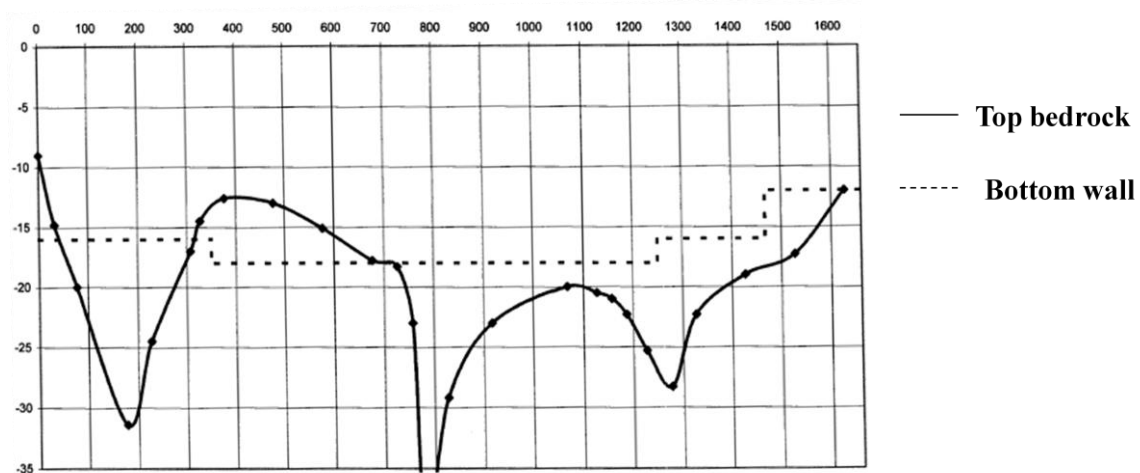
Figure 9: bedrock level along TM1 quaywall

Since such a soft soil would not be able to sustain the stresses at the foundation location, the following solution had to be adapted. The soft layers have been removed by dredging and replaced by stones (max.200mm) until foundation level. To avoid major settlements and differential settlements of this stone layer vibrocompaction has been applied.
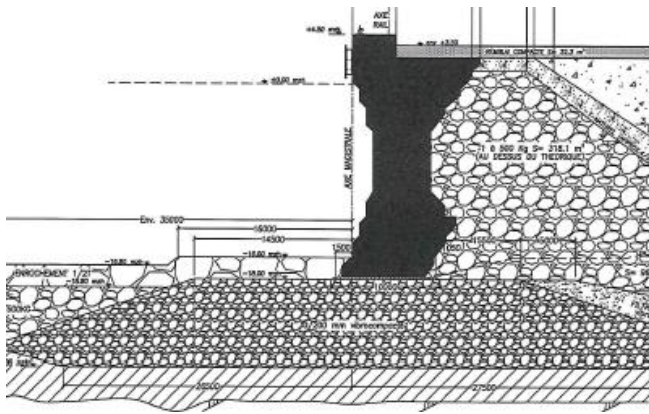
Figure 10: Typical cross section + foundation gravel vibrocompacted

A large vibro probe has been used in Tanger Med 1 to be able first to go to the required depth and second to vibrocompact gravel with important stones of 200mm. The sieve analysis from this gravel was situated on the limit of the applicability of the vibro technique. The intermediate distance between the compaction points has been chosen based on available experience (from the extension of the Monaco harbour) on similar works with large depths together with a large thickness of the fill to be compacted. A triangular pattern of 3.10 m has been adopted.

To control the works, the realization of CPT's was not possible due to the size of the stones. Therefore, the method adapted is to measure the settlements on the top of the fill. It was expected to have a relative density Dr of the fill of approx. 45 % for the stones dropped in the water. This Dr is increased to 75 % due to the vibrocompaction. This leads to approx 7 to 8% of settlement.

The differential settlements were avoided and the quaywall realized with the same foundation level for parts on bedrock or on a former loose layer replaced by vibrocompacted stones.

5.   HAMMA

Hamma Water Desalination Spa (HWD) has awarded the construction of a Desalination Plant to provide potable water to the city of Algiers, Algeria. The facility is located close to the port of Algiers, on the site named '' les sablettes'', district of Hussein Dey, municipality of Belouizdad. Hamma seawater desalination facility will produce 200.00 m³/day of potable water for municipal distribution. The main features of the plant are: offshore, undersea screened seawater intake, onshore seawater pumping station, pre-treatment of raw seawater, reverse osmosis desalting, remineralization for potable water delivery, product storage and delivery. The general layout with the different structures is given on the figure 11.
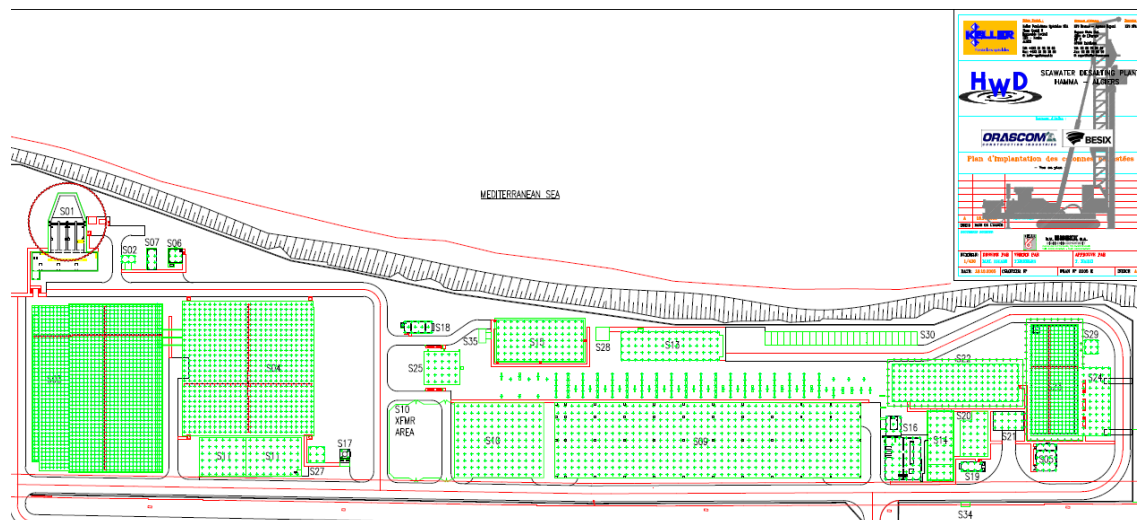
Figure 11: General layout and stone columns localisation

From the site investigation (CPT and dynamic penetrometer on figure 12) it has been deduced that the upper layers consists of loose fills and soft layers with a thickness of about 5m. So a ground improvement was necessary for the foundations of the different structures. Seeing the depth needed to reach the resistant layer, stone columns installed according to the wet method were chosen. The design has been kept simple. The number of stone columns and intermediate distance is determined taking the weight of the structure divided by the capacity of one column limited to 350 kN whithout doing a trial test before the works.
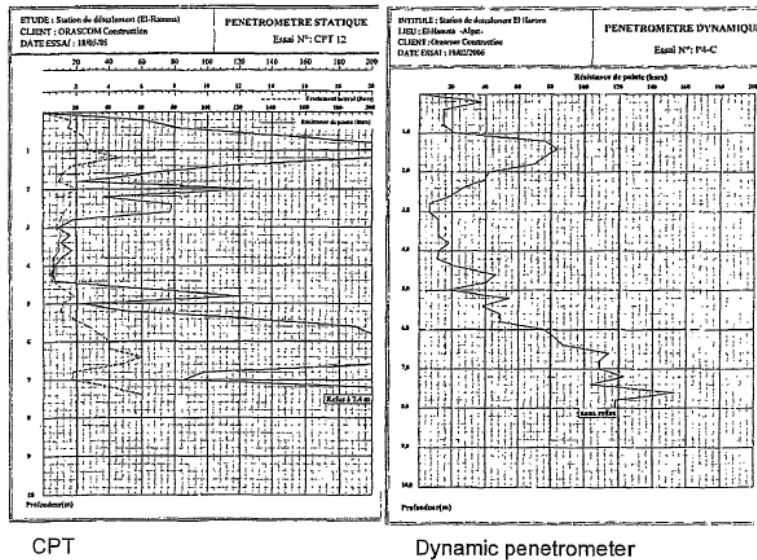
Figure 12: typical CPT and dynamic penetrometer result

The coarse material used for the stone columns did not allow the CPT tests for the control. A control on the energy comsumption during the placing of the stone columns is done but also loading tests have been performed. Two different procedures were used for the loading tests: one following the Keller procedure and one following the Terracon. The two procedures are shown on figure 13. The Keller procedure consists of loading the column at the top by means of a steel plate having the same diameter as the stone column and the Terracon procedure consists of loading the column and some gound around the column.
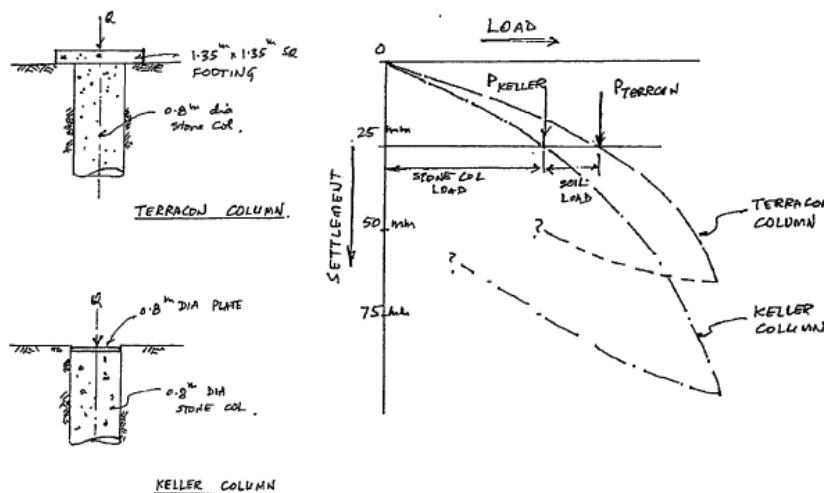
Figure 13: Plate load test Keller and Terracon procedure

Appropriate acceptance criteria had to be defined for the interpretation of the results of the loading tests realized according to the two methods.

6. CONCLUSION

The examples given above clearly illustrate the applicability of ground improvement techniques for different problems and applications. It should however be clear that every application of ground improvement necessitates a detailed study and preparation of the execution and a specific control. Only in this way the quality of the realized ground improvement works can be guaranteed.

Assessment of Grid Spacing for Dynamic Compaction

Richard Moyle, Coffey Geotechnics, United Kingdom & University of Sydney, Australia
richard_moyle@coffey.com
Robert Turner, Coffey Geotechnics, Australia, robert_turner@coffey.com

ABSTRACT

Dynamic compaction is a ground improvement technique that involves dropping a tamper from a predetermined height in a coordinated grid pattern over the required treatment area. Previous applications of dynamic compaction have used a tamper weighing up to 40 tonnes dropped from a height of up to 40m. Multiple passes are generally used commencing with a wide primary spacing (pass 1) which is in-filled by secondary (pass 2) and tertiary passes (pass 3).

The final distance between the midpoints of impact on the grid pattern, referred to as the grid spacing, has a significant effect on the ground improvement achieved by dynamic compaction (Lucas, 1992); and also the rate at which dynamic compaction can be applied over the required treatment area. As such, the grid spacing becomes an important design parameter when assessing dynamic compaction.

This paper presents the results of a full scale dynamic compaction trial on a site underlain by uncontrolled fill, where a specific investigation was undertaken to select an appropriate grid spacing. The results of geotechnical investigations and site monitoring were used to assess the effect, both vertically and laterally, of the grid spacing on the compaction of the underlying soil. Furthermore, a comparison is made between the results achieved in the trial to those found in previous research to enable further refinement of the work carried out by Poran and Rodriguez (1992).

1. INTRODUCTION

1.1. The Process of Dynamic Compaction

Dynamic compaction is a ground improvement technique that involves dropping a tamper from a predetermined height in a coordinated grid pattern over the treatment area. The improvement in soil behaviour due to the compaction process depends upon factors such as the grid pattern and spacing, the tamper shape and weight, the number of passes and the number of drops used at each grid point.

The grid pattern adopted for the dynamic compaction process is usually formed by undertaking multiple passes, commencing with a wide primary spacing (pass 1) which is in-filled by secondary (pass 2) and tertiary passes (pass 3). An illustration of a typical grid pattern used in dynamic compaction is presented in Figure 1.

LEGEND

■ PASS 1 DROP LOCATION

✚ PASS 2 DROP LOCATION

✚ PASS 3 DROP LOCATION
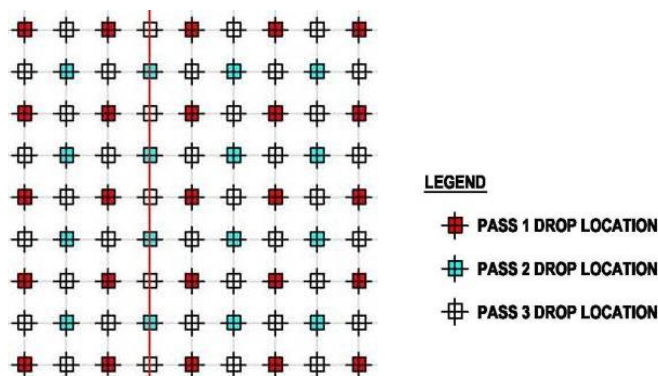
Figure 1: Example of Grid Pattern for Dynamic Compaction

The orthogonal distance between adjacent points on the grid pattern after pass 3, referred to as the grid spacing, has a significant effect on the ground improvement achieved by dynamic compaction (Lukas, 1992); and also the rate at which dynamic compaction can be applied over a given area. As such, the grid spacing becomes an important design parameter when assessing dynamic compaction.

1.2.   Previous Studies

The influence of grid spacing in dynamic compaction has been the subject of numerous numerical studies. Poran and Rodriguez (1992) investigated both the vertical and lateral extent of the influence of dynamic compaction on cohesionless soils and filled ground. They postulated that at each impact location the zone of influence may be represented by a semi-spheroid shape with *a* (horizontal radius) and *b* (vertical depth); where *a* and *b* are function of the drop mass, drop height and number of impacts (refer to Figure 2 below).
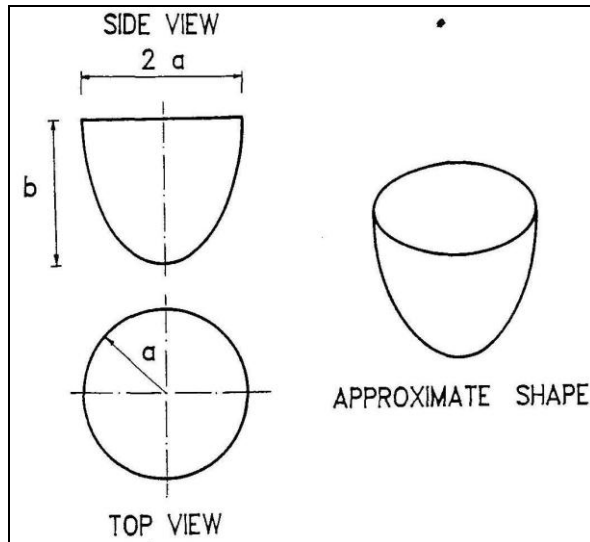
Figure 2: Shape of zone effected by Dynamic Compaction (Poran and Rodriguez, 1992)

Poran and Rodriguez (1992) presented relationships between the horizontal radius and the vertical depth of the semi-spheroid and the equipment dependent factors as follows:

$$\frac{b}{D} = j + k \log\left(\frac{NWH}{Ab}\right) \qquad (1)$$

$$\frac{a}{D} = l + m \log\left(\frac{NWH}{Ab}\right) \qquad (2)$$

where   *a* is the horizontal radius
           b is the vertical depth
           j, *k*, *l* & *m* are empirical factors
           N = Number of drops;
           W = Pounder mass (tonnes);
           H = Drop Height (metres);
           A = Contact area between the tamper and the soil (meters^2)
           D = pounder diameter (meters).

The empirical factors *j*, *k*, *l* and *m* as presented by Poran and Rodriguez (1992) depend on the relative density of the soil and were found to vary as follows:
- Parameter *j*: -12.59 to -15.27;
- Parameter *k*: 6.25 to 8.08
- Parameter *l*: -4.43 to -2.49
- Parameter *m*: 1.90 to 2.32

Chow, Yong, Yong and Lee (1994) also investigated the effect of print spacing (distance between drop locations) on ground improvement using dynamic compaction. They presented a different approach to Poran and Rodriguez (1992) that estimated the lateral extent of the ground improvement based on assessment of the increase in friction angle in cohesionless materials.

The depth of influence (or the *b* parameter noted above) of dynamic compaction has been the focus of studies by Menard (1977), Luongo (1992), Lukas (1992) and others. Lukas (1992) presented the depth of influence of the dynamic compaction process to be as follows:

$$D = n \, (W \times H)^{\frac{1}{2}} \tag{3}$$

where   n = empirical coefficient

         W = weight of the pounder (tonnes)

         H = drop height (metres)

The studies by Menard (1977), Luongo (1992) and Lukas (1992) relate the depth of influence to the pounder weight and drop height but do not consider the effect of the grid spacing.

1.3. This Study

The effect of grid spacing on the compaction of the soil was examined as part of a full scale dynamic compaction trial at a site containing 15m depth of uncontrolled fill overlying shale bedrock. The fill comprised various mixtures of silt, sand and clay that had been excavated from alluvial deposits. Perched groundwater occurred at various locations within the fill.

This paper presents an initial discussion of the geotechnical investigation and monitoring methods used to assess the effect of the grid spacing of the soil. The results of the geotechnical investigation and monitoring are also presented with the assessment of the impact of the different grid spacing on the site. A comparison is also made to previous works undertaken to enable further refinement of the dynamic compaction process.

2. ASSESSMENT OF GRID SPACING

2.1. General

Dynamic compaction was undertaken to compact the fill using a 20-tonne tamper dropped from 23m height over a square grid pattern with grid spacings that ranged from 4.2m to 6.0m, as shown on Figure 1.

The purpose of this investigation was to assess the influence of grid spacing on the degree of compaction of the material between the drop points (termed here "interaction"). The compaction requirements for the project were set to achieve a density of at least $2t/m^3$ over the upper 6m of fill.

The assessment of the "interaction" between drop points was based on a series of key monitoring indicators namely:
- Heave/Penetration Tests;
- Subsurface settlement monitoring (extensometers); and,
- Downhole Gamma Density testing.

These indicators are described in the following section.

2.2. Key Monitoring Indicators

2.2.1. Heave / Penetration Tests

Heave/penetration testing was typically carried out at the commencement of each pass within each area of different grid spacing. A heave/penetration test involves dropping the pounder on a single location up to 40 times and the measurement of the volume generated by a) the penetration of the pounder and b) the soil heave above original soil level prior to, during and after the test adjacent to the pound location.

This was measured through the establishment of 12 survey stations around a drop location along three equally spaced axes where the change in level was monitored. Four stations were established on the pounder to monitor the depth of penetration. This configuration is shown on Figure 3.
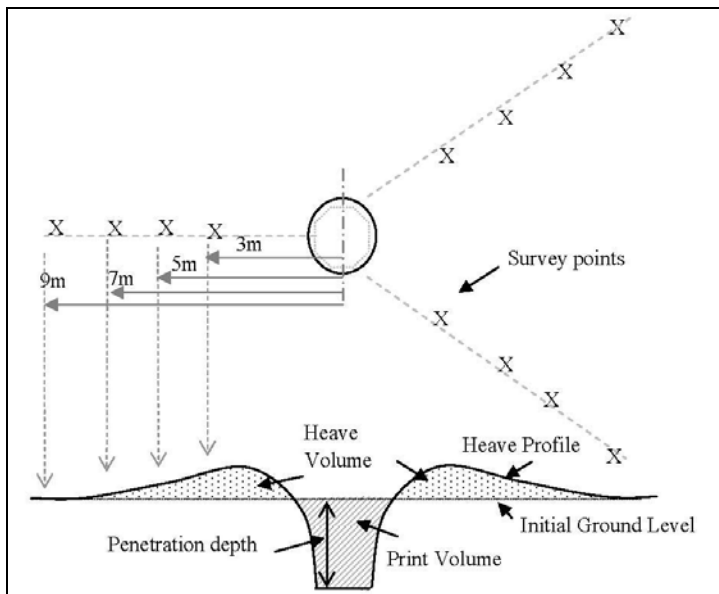
Figure 3: Typical Configuration of Heave / Penetration Test

The survey stations were monitored prior to the commencement of the heave/penetration test and then generally after every 4 blows, up to a maximum of 40 blows. In addition, the diameter of the resultant crater was monitored.

The results of the heave/penetration tests can be used to calculate:
1. The volume of heave calculated from monitoring the 12 survey stations surrounding the pounder.
2. The volume of the crater formed by the dynamic compaction works with blow count (calculated from monitoring the survey stations on the pounder and the diameter of the crater).
3. The net volume with blow count; that is, the volume of the crater minus the volume of heave.
4. The amount of penetration per blow; that is, the amount the pounder goes into the ground at each blow.
5. The amount of heave per blow, calculated from 1 above; and,
6. The ratio of penetration to heave, calculated from the ratio of items 2 and 1 above

Further information on the Heave / Penetration testing and the results obtained from the testing are provided in Moyle and Redman (2009).

The premise of assessing whether there is "interaction" between drop points is that the results of the heave / penetration tests for the tertiary pass should show a large heave volume and a subsequent small volume of the crater formed during the dynamic compaction process. Conversely, where there is no interaction, there should be relatively little heave and the amount of penetration recorded should be large.

2.2.2. Extensometer Monitoring

Extensometer monitoring involves the installation of magnets along a hollow tube, which can be monitored to assess ground movements as a result of the dynamic compaction process. Extensometers were installed in each area of different grid spacing at the mid-point between drop locations.

A typical result of the extensometer monitoring is presented on Figure 4. As can be seen, there are distinct zones of heave (or negative settlement) and compression (or settlement).
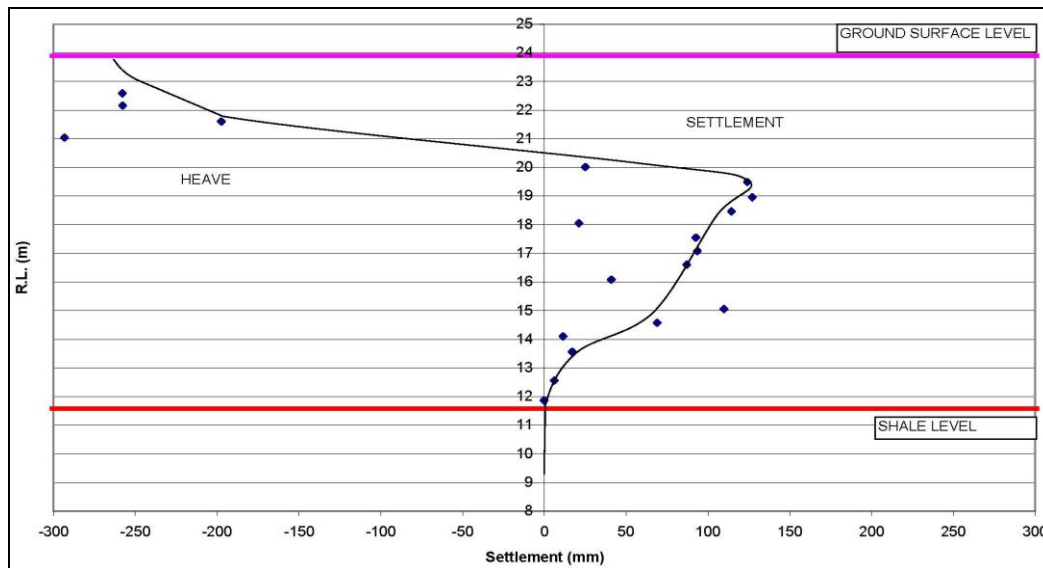
Figure 4: Typical Result of Extensometer Monitoring

In the context of this study, extensometer monitoring can provide an indication of the "interaction" of dynamic compaction as follows:

- If there is limited interaction between drop points, the expected results from the monitoring would be a either a large or small settlement with a small heave;
- If there is interaction between drop points, the expected results from the monitoring would be either a large or small settlement with a large heave.

The extensometer monitoring results are also used to assess the depth of influence of the dynamic compaction process. This is done by assessing the depth to which the lowest magnet on the extensometer has recorded settlement resulting from the dynamic compaction process.

2.2.3. Downhole Gamma Density Testing

Downhole Gamma Density (DHGD) testing consists of lowering of a probe, approximately 3.8m long, down to the base of a borehole, then raising it to the surface progressively while recording the Natural Gamma and Wet Density of the sidewall profile of the borehole in 10mm depth intervals.

Photographs of the down-hole gamma density meter are presented on Figure 5.

Figure 5: Photographs of Downhole Gamma Density Meter

Of particular importance to this study, the DHGD probe contains a focussed density system to record the apparent Wet Density of the soil, based on a back-scatter approach, where rays emitted from a Caesium source in the probe are either absorbed or reflected depending on the density characteristics of the material. A receiver on the DHGD tool records how many rays are reflected from the soil, thus assessing

the wet density of the soil. The Wet Density is recorded in grams per cubic centimetre, or tonnes per cubic metre (t/m^3).

The results of the DHGD testing were used to assess whether the ground improvement process achieved the required density within the subsurface profile (which was typically above 2.0t/m^3 in the upper 6m).

2.3.   Results of the Key Monitoring Indicators

2.3.1.   *Heave / Penetration Test Results*

The results of the heave / penetration tests have been presented on Figures 6 and 7. Presented on Figure 6 is a plot of the penetration per blow (in m/blow); and of the heave volume per blow (in m^3/blow). Presented on Figure 7 is the ratio of the print volume to the heave volume.

The results of the heave / penetration testing indicate the following:
- The average penetration per blow remains nearly constant for the different grid spacing;
- The amount of heave volume per blow decreases with increasing grid spacing;
- The ratio of the penetration volume to heave volume increases with increasing grid spacing.

The results of the monitoring show a clear trend of decreasing interaction between drop locations with increasing grid spacing.
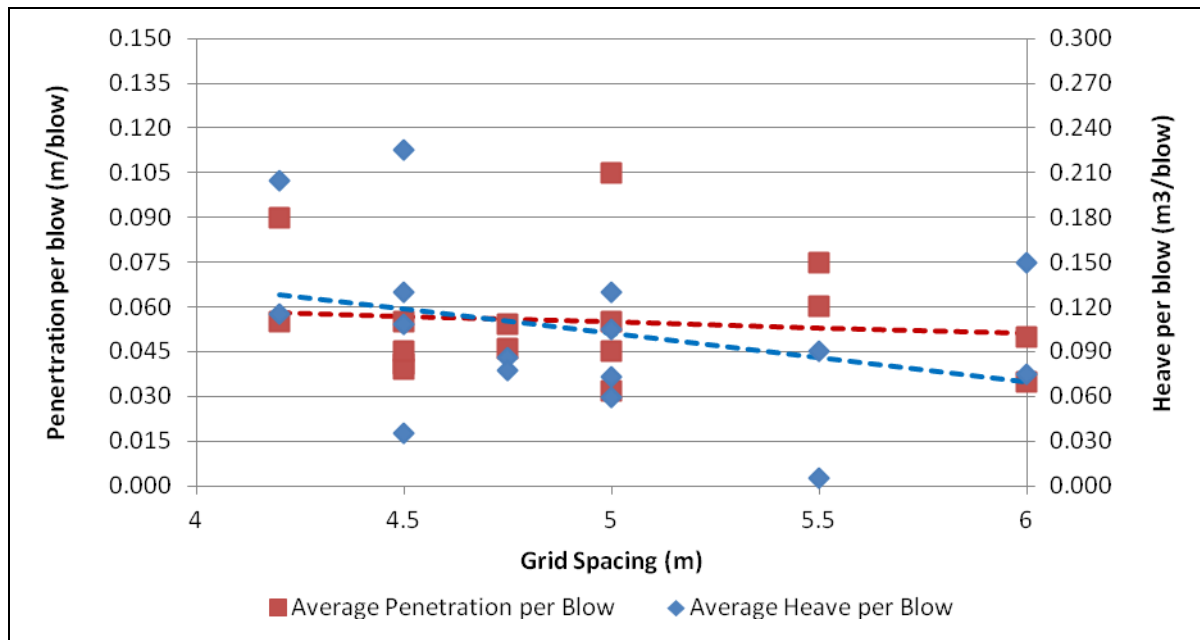
Figure 6: Results of Heave Tests – Penetration and Heave Volume per Blow
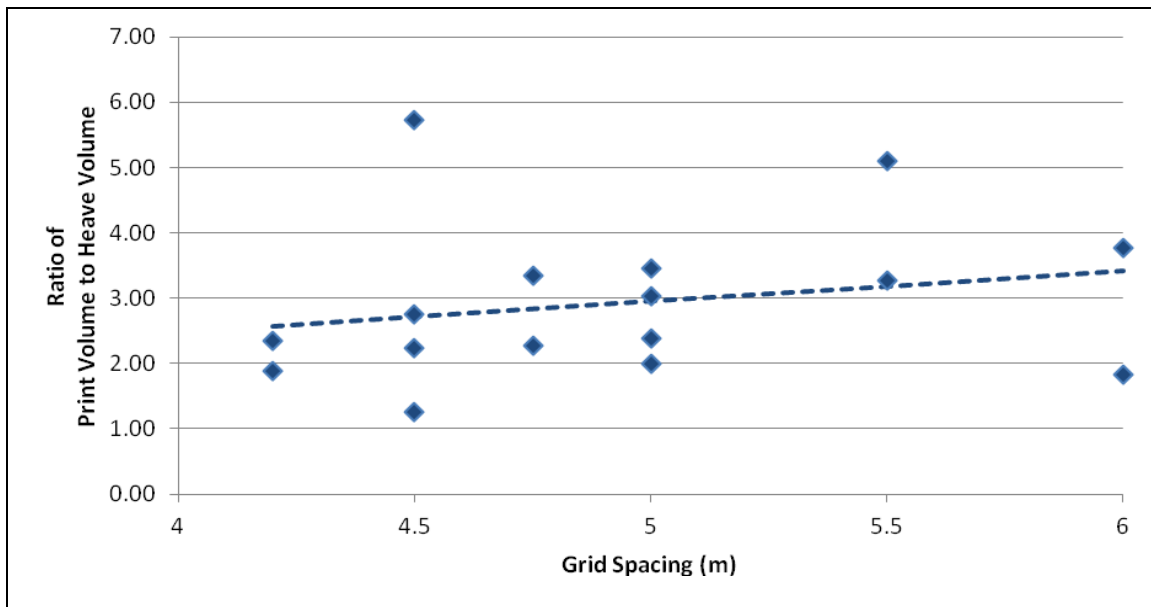
Figure 7: Results of Heave Tests – Ratio of Print Volume to Heave Volume

2.3.2. Extensometer Monitoring Results

The results of the extensometer monitoring are presented on Figure 8 as a plot of the maximum recorded heave and settlement for each of the extensometers recorded in areas of different grid spacing.
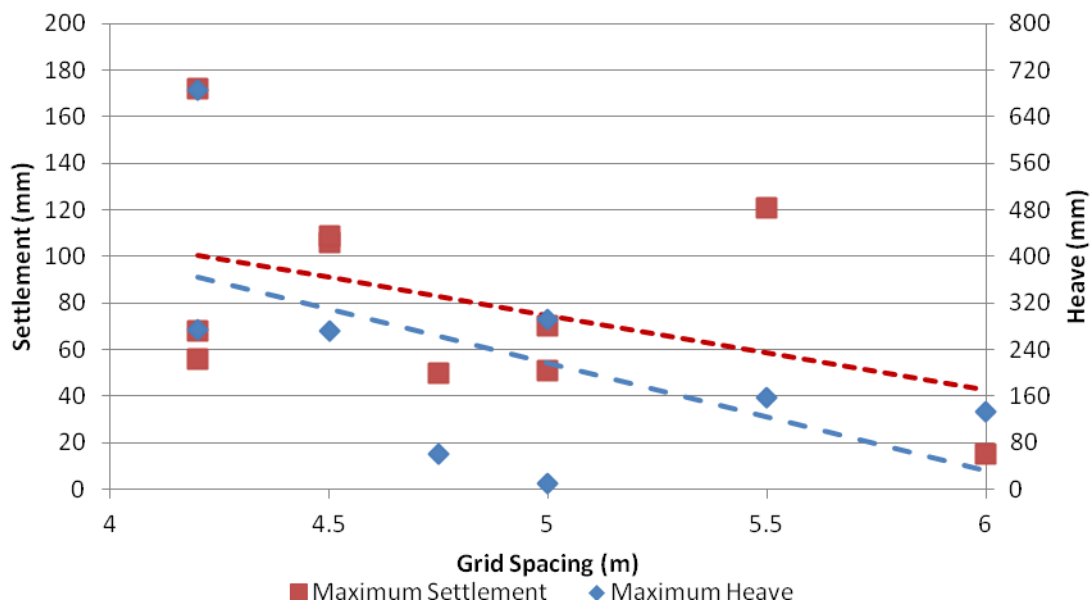
Figure 8: Results of Extensometer Monitoring

The results of the extensometer monitoring show a consistent trend of decreasing settlement and heave with increasing grid spacing. The amount of settlement recorded in the area with a 5.5m grid spacing shows a significant amount of settlement, however this is assessed to be associated with a localised area where the extensometer was installed consisting of loose material (prior to the commencement of dynamic compaction).

The results of the extensometer testing have also been used to assess the depth of influence resulting from dynamic compaction. Presented on Figure 9 is a plot showing the assessed depth of influence for different grid spacings.
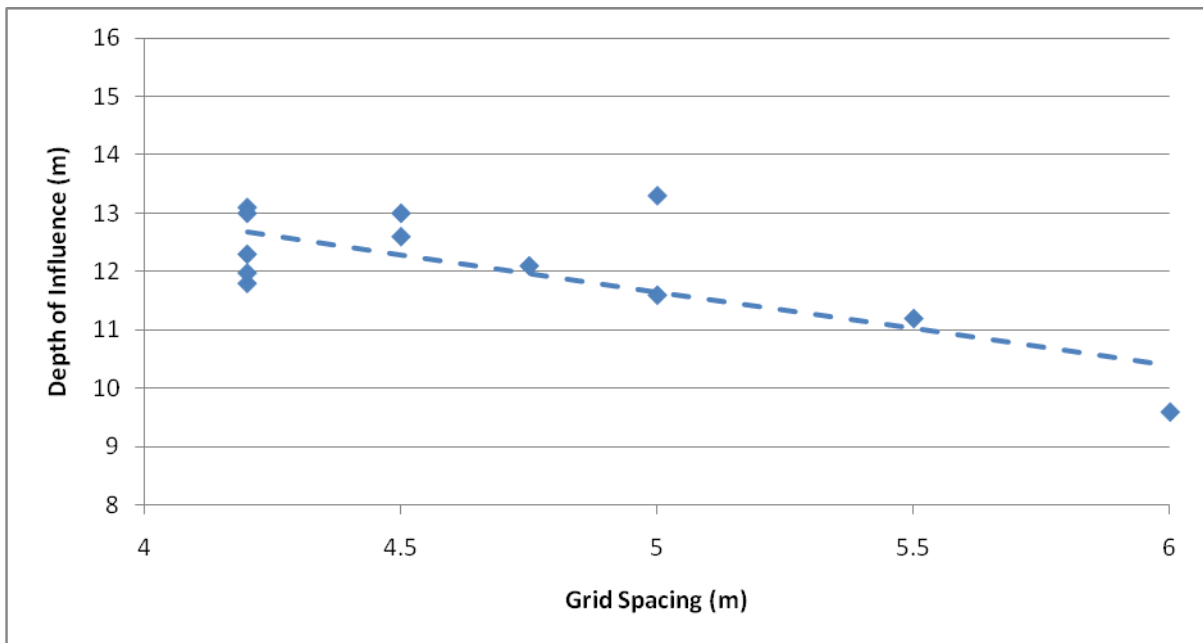
Figure 9: Assessed Depth of Influence

As can be seen from the results, the depth of influence from the dynamic compaction process decreases with increasing grid spacing. This trend is consistent with that presented by Poran and Rodriguez (1992) and that of Chow et al (1994) where the zone of influence is postulated to be conical in shape and diminishes with distance from the drop location. It should be noted that previous postulations about the depth of influence, such as from Menard (1977), are considered at the drop location; whereas the results presented herein are for the midpoint between drop locations.

2.3.3. *Downhole Gamma Density Test Results*

The results of the Downhole Gamma Density Testing are presented in Figure 10 below. The results have been plotted showing the average wet density in the upper 6m, and the average wet density in the lower 6 to 13m.

As can be seen from the results the highest wet density appears to have been achieved where there is a spacing of 4.5m.
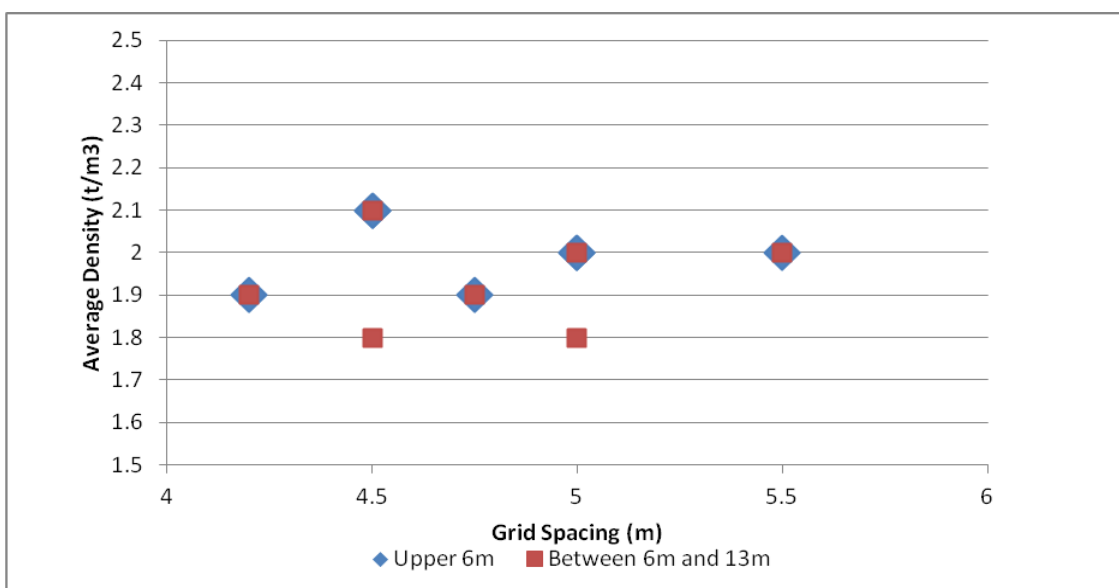
Figure 10: Results of Density Testing

3.   SUMMARY AND CONCLUSIONS

The results of the monitoring and testing of dynamic compaction being carried out using a drop weight of 20 tonne and a drop height of 23m, can be summarised as follows:

- The results of the heave / penetration testing show a decreasing interaction between drop locations as the grid spacing is increased from 4.2m to 6.0m;
- The extensometer results also show a decreasing interaction between drop locations as the grid spacing increases from 4.2m to 6.0m;
- The extensometer results showed a decrease in the depth of influence of the dynamic compaction process with increasing grid spacing; and,
- The density test results show a higher density recorded for a grid spacing of 4.5m, which decreases slightly with an increasing grid spacing.

Based on the results of the trial, and the monitoring it was concluded that a grid spacing of 4.5m had sufficient interaction between drop locations and the required density criterion was achieved.

Using the formulae presented by Poran and Rodriguez (1992) and the results of the dynamic compaction trial, relationships have been established between parameters *j* and *k*; and between parameters *l* and *m*; which are as follows:

$$j = 3.410k - 1.25 \tag{4}$$

$$l = 3.410m - 5.55 \tag{5}$$

The relationships presented above are different to those postulated by Poran and Rodriguez (1992). The main difference identified is that the dataset supporting the work done by Poran and Rodriguez (1992) was predominantly derived from work on cohesionless fill. The data set could be correlated with data of similar soil types in order to refine the work carried out thus far.

Based on the results of the extensometer monitoring assessing the depth of influence of the dynamic compaction process, should be a function of the grid spacing, as well as the drop height and pounder weight. Based on the result presented herein, the following is recommended as a revised equation for assessing the depth of influence of dynamic compaction:

$$D = 0.58(WH)^{1/2} - 1.3(S - 4.5) \tag{6}$$

where   D = Depth of Influence (m)
         W = Pounder Weight (tonnes)
         H = Drop Height (metres)
         S = Grid Spacing (m)

4.   ACKNOWLEDGMENTS

REFERENCES

Chow Y. K., Yong D. M., Yong K. Y. and Lee S. L. (1994). Dynamic Compaction of Loose Granular Soils: Effect of Print Spacing. Journal of Geotechnical Engineering, Vol 120 No 7, pages 1115 – 1133.

Lukas R. G. (1992). Dynamic Compaction Engineering Considerations. Conference Proceeding from Grouting, Soil Improvement and Geosynthetics, Volume 2, Louisiana USA, 1992, pages 889 – 901.

Luongo V., (1992). Dynamic compaction: predicting depth of improvement. Geotechnical special publication Vol.2, No. 30, 1992, pages 927 – 939.

Menard L and Broise Y (1975), "Theoretical and Practical Aspects of Dynamic Compaction", Geotechnique 25, No 1, March pp 3 – 18.

Moyle R. and Redman P. G. (2009), "Optimization of Dynamic Compaction Processes – A Case Study", Ground Improvement Technologies and Case Histories, December 2009, Singapore, pages 739 – 746.

Poran C. J. and Rodriguez J. A. (1992). Design of Dynamic Compaction. Canadian Geotechnical Journal, Vol 29, pages 796 – 802.

The Effect of Different Tamper Geometries on the Dynamic Compaction of Sandy Soils

Yahya Nazhat, School of Civil Engineering, University of Sydney, Australia, yahya.nazhat@sydney.edu.au
David Airey, School of Civil Engineering, University of Sydney, Australia, david.airey@sydney.edu.au

ABSTRACT

Dynamic Compaction is a ground improvement technique mainly used to densify loose granular soil deposits above the water table by systematically dropping flat bottomed tampers of 5 -20 tons from heights of 10 -40 m on a selected impact grid to compact the underlying soil layers. While the dynamic compaction method appears to be simple, it requires careful consideration of the tamper mass, number of drops, drop height and grid spacing if the desired degree of improvement is to be achieved. This paper reports the results of a series of 2-D dynamic compaction experiments that have investigated the effect of the tamper shape on the response of the underlying granular soils using high-speed photography.
Flat, conical, shell and convex shaped tampers have been used. Each tamper shape has been dropped on two soil types, uniform sand and a sand-silt mixture. The photographic data are used to evaluate the effect of the shape of the tampers on the compaction efficiency, depth of improvement and the internal densification mechanism. The results indicate the different tamper shapes lead to significant differences in the magnitude of densification and depth of improvement, and reveal unique patterns of propagating shock waves.

1.   INTRODUCTION

Modern dynamic compaction (DC) was developed as a useful ground improvement method around the mid 1970s (*Menard and Broise, 1975*). DC was initially considered to be suitable only for granular soils, but the technique has been applied in the treatment of silty sand and uncontrolled fill sites. Large numbers of case studies have demonstrated that DC can increase the density and bearing capacity of treated sand deposits and improve their resistance to liquefaction. The technique is widely used as it can be successfully applied to different types of soils, is economically competitive, relatively simple, and does not add chemicals to the treated environment. In practice, DC takes place over a grid of tamping locations and several tamping cycles are performed until the target ground improvement is achieved. For ground improvement engineers, the depth of influence (D_{max}) is one of the most uncertain aspects of the DC process. Menard and Broise suggested the following well-known formula to estimate the DC depth of improvement:

$$D_{max} = \sqrt{W.H} \tag{1}$$

This equation was later revised to account for different soil types (*Lukas, 1979*) as:

$$D_{max} = n\sqrt{W.H} \tag{2}$$

where W=tamper weight (tonnes), H=drop height (m) and n=an empirical coefficient (typically 0.3-0.8)

However, this simple approach has its limitations as there is no rational procedure for determining *n,* and thus it is not clear if a single coefficient is sufficient to account for the effects of site specific factors, such as varying soil properties and profile, and tamper geometry and spacing. The wide range of values that have been suggested for the empirical factor *n* also result in uncertainty in the application of this equation.

The effect of footing base profile on failure mechanisms and bearing capacity has been investigated in classical geotechnical research (*Cassidy, et al., 2002, White, et al., 2008*) using physical model tests and numerical limit analysis. In physical model tests on sand the bearing capacity of 130° and 150° conical spudcan-type footings in dry sand has been reported to differ significantly from that of a flat footing (*White, et al., 2008*), with the conical shape causing a reduction in the operative friction angle owing to a progressive failure mechanism. However, using aluminium rods to model soil grains, shell foundations demonstrated higher surface and embedded bearing capacities compared with conventional flat foundation (*Yamamoto, et al., 2009*).

Previous studies of tamper geometry in DC have suggested that there may be an influence of shape on the soil response. This has been primarily assessed by the displaced volume at the surface, expressed in terms of the crater geometry through the shape, area, depth and heave around the crater *(Mullins et al., 2000 and Feng et al., 2005)*, but these quantities are not obviously related to the densification at depth. For example, empirical correlations between depth of improvement and initial shear strength of soils, crater depth (penetration) and impact energy per unit area were proposed *(Mullins et al., 2000)*. The effect of different tamper geometries on the depth of improvement has been quantified mainly by conducting physical subsurface investigations using cone penetration tests and/or portable nuclear density gauge before and after certain numbers of DC impacts. In physical models using Mai-Liao and Ottawa sands with 90º apex angle conical based tampers the conical tampers were claimed to provide better DC efficiency than flat-based tampers in the Mai-Liao sand, but to provide similar performance in the Ottawa sand *(Feng et al., 2000)*. Like the conventional footing studies mentioned above the difference was considered to arise from the different dilatancy of the two sands. Conical and flat-based tampers were reported to provide near identical depths of improvement, as interpreted from cone penetration tests *(Feng et al., 2005)*, when Mai-Liao sand was mixed with fines for fines contents between 3.4% and 14%. However, the authors claimed that better overall performance was gained in the case of conical-based tampers as a result of more lateral densification. In another study using well graded Sakarya River sand, results showed that conical-based tampers reached deeper levels than flat-bottomed tampers creating greater crater depths and crater areas, suggesting that tamper shape could influence the efficiency of dynamic compaction *(Arslan, et al, 2007)*. Using cylindrical, oval, square and conical tampers in DC tests of loose Arak sand *(Ghazavi, et al., 2010)*, a greater depth of improvement was claimed from flat, cylindrical tampers over flat square and conical tampers for the same dropped mass, but the method used to assess the depth of improvement was not specified.

Clearly, the size of the zone influenced by DC, the effects of different tamper geometries and the influence of soil properties on the mechanics of the DC process itself, are not well understood. One of the reasons for this ongoing debate is the difficulty of observing and measuring the dynamic behaviour of the underlying target soils. In this work, the kinematics occurring due to different tampers geometries and subsurface soil dynamic responses during plain strain DC model experiments using high speed photography and digital image correlation (DIC) techniques are presented. The use of high speed digital photography has enabled characterisation of distinctive flow patterns, calculation of soil strains and observation of different strain localisation that are key issues in understanding the response of granular soils to DC.

2. EXPERIMENTAL SET UP

2.1. Testing Apparatus

The testing apparatus, shown in Photo 1, consists of a fabricated container (350 mm x 150 mm x 750 mm) fixed to a steel frame open at the top with a 25 mm thick clear acrylic (Perspex) sheet bolted to the front of the frame. A thinner, replaceable, 5 mm sheet of Perspex was placed between the sand and the front face to prevent scratching and damage of the main Perspex sheet. An electromechanical motor and gearbox is mounted on a steel frame affixed to the container platform. The gearbox and motor allows the tamper, and the 25mm diameter shaft connected to it, to be lifted to a pre-specified height at which the gearbox clutch is engaged allowing the freefall of the tamper and shaft. The switch operating the clutch is also used to synchronise the activation of the high speed camera. The frame was isolated from the floor to minimise vibrations being transmitted through the laboratory floor to the camera. The high speed camera was mounted on a tripod placed on the floor and positioned 1.2m from the testing apparatus. The tamper is able to free fall up to 600 mm, although a constant drop height of 300 mm was chosen throughout the tests discussed here. A typical DC test involved 6 drops of the tamper, with high speed photography taken over 3.2 seconds for each drop. Control markers were placed between the Perspex sheets for camera calibration, and to validate the conversion from image space to real space measurements. The soil container can be rotated through 90º to the horizontal via two hinges at its base to facilitate sample preparation. Steel bolts secure the hinges to the steel frame once the container is vertical prior to testing.
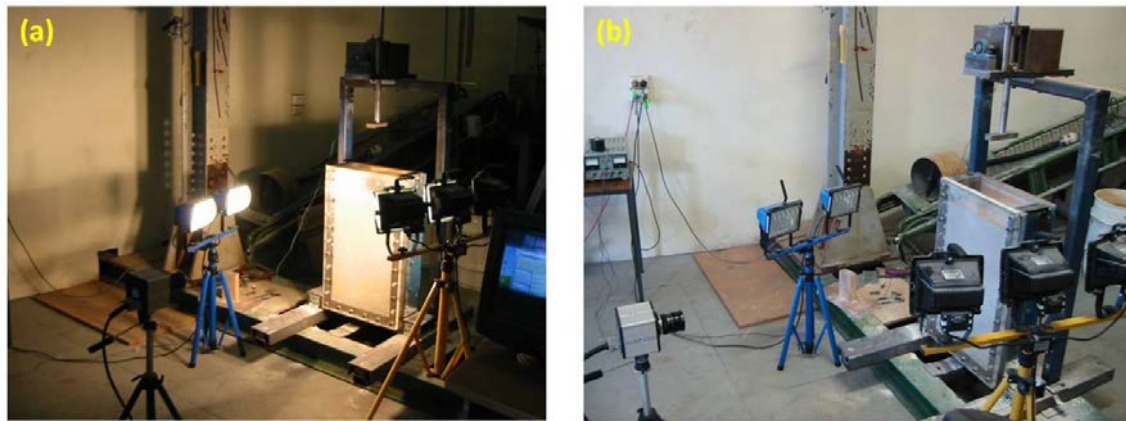
Photo 1: Testing apparatus and camera set up-sand model (a) and sand-silt model (b).
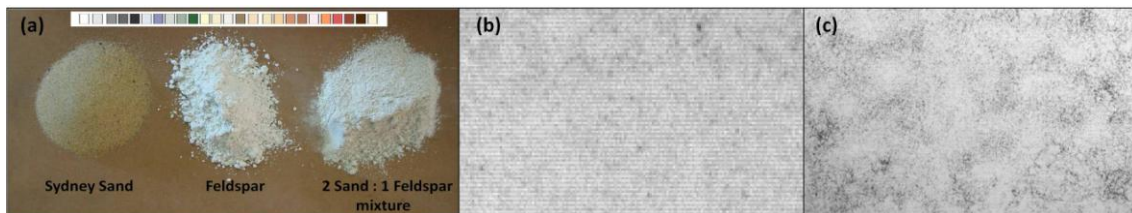
Photo 2: Natural colours of Sydney sand, feldspar silt and sand-silt mixture (a), texture of sand grains in a sand image (b) and texture by speckled black embossing powder on the face of a sand-silt mixture (c).

2.2.   Tested Materials

Medium to fine grained dry Sydney sand and a mixture of 2 parts sand and 1 part feldspar silt were used in this experimental work. The sand is poorly graded with a uniformity coefficient (d_{60}/d_{10}) of 3.0, and maximum and minimum void ratios of 0.8 and 0.58, respectively. Grading curves of Sydney sand and sand-feldspar mixture are shown in Figure 1. To prepare the sand specimens the container was fixed in its vertical position, and sand was dry-rained into the container from specific heights to produce uniform beds of sand. The variability in the colour of the sand grains provided sufficient texture for the GeoPIV-DIC algorithm tracking the displacement of the sand particles. The relatively pale colour, and small grain size, of the sand/feldspar mixture required an artificial texture to be added on the face of the soil. This was performed by unfastening the hinges, rotating the tank 90° to horizontal, removing the back of the container, placing a plug to form the upper surface of the model, sprinkling black, embossing powder, target markers on the Perspex window followed by dry-raining the sand-feldspar mixture, and then replacing the back of the container and rotating the tank back to its vertical position and securing it to the steel frame. Sand models were prepared with a pre-compaction void ratio of 0.63 (relative density of 63% and a unit weight of 15.8 kN/m³). Dry sand-silt models were prepared with a pre-compaction void ratio of 0.67 (relative density of 58% and unit weight of 15.6 kN/m³). Photo 2, shows samples of Sydney sand, feldspar silt, sand-silt mixture together with captured photographs of sand and sand-silt mixture with embossing powder target markers.

2.3.   High Speed Camera

A high speed digital camera, model FASTCAM 1024PCI manufactured by Photron Inc (http://www.photron.com), fitted with a Navitron 50 mm lens with focal length of 0.95 m was used in this work. Images were captured at a rate of 1000 fps (frames per second) at full 1024 x 1024 pixel resolution. A Shutter speed of 1/3000 second and 1000 fps provided the optimum frame sequence, field of view and image brightness for the 1024 x 1024 pixel image resolution. The field of view of the 1024 x 1024 pixel image was 403 mm x 403 mm giving an object space pixel size of 0.39 mm. To avoid undesirable reflections and shadowing during photography, lighting was provided by two sets of 2 x 500W spotlights located to the sides between the camera and the apparatus. The camera was connected to a computer via PCI bus, and controlled using the Photron Fastcam Viewer (PFV) software provided by the manufacturer.
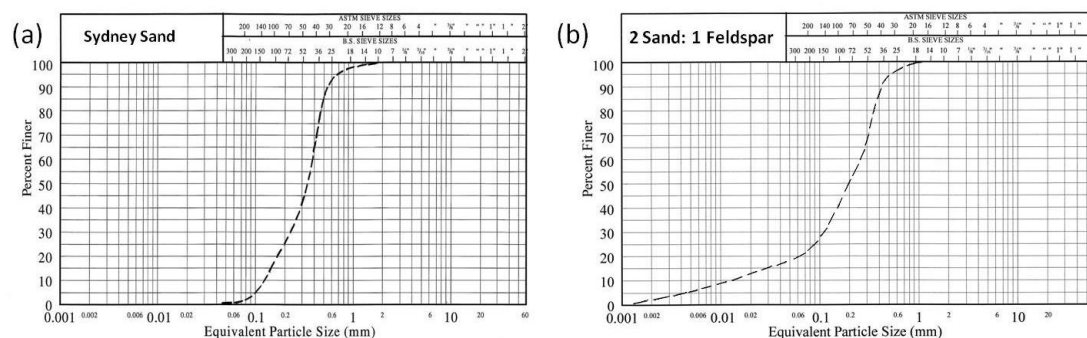
Figure 1: Grading curves of Sydney sand (a) and mixture of 2 sand: 1 feldspar (b).

2.4.   Tampers

Four steel tampers with the geometries shown in Figure 2, that is flat-based, 120° apex angle conical-based, 120° shell-based and curve-based tampers labelled here as types A, B, C and D respectively, were used. The tamper depth is equal to the width of the container to ensure a 2-D, plane strain configuration. The free falling assembly (the tamper and shaft) weighs 57.9N, 55.7N, 55.7N and 56.2N for tamper types A, B, C and D respectively. For a 300mm free fall, the impact energy varied between 16.7N.m and 17.4N.m per drop (a difference of less than 5% between the different tampers) with a total energy of about 100 Nm due to six impacts. The fall height was kept constant in each test by adjusting the elevation at which the clutch was activated to allow for the deformation of the soil surface.

3.   PHOTOGRAMMETRY

3.1.   Digital image correlation and PIV algorithm

The digital image correlation (DIC) method is a non-contact analysis method that obtains incremental displacements and strain fields on the surface of planar specimens by comparing a set of digital images taken before and after specimen deformation. DIC as a strain measurement technique was first introduced in 1980s (*Peters et al., 1982*) and has since been widely used in experimental strain analysis. Due to rapid developments in high resolution digital cameras and computer technology, the use of this measurement method has proven to be a flexible and useful tool for deformation analysis in several engineering applications. The DIC analysis presented in this paper was carried out using the MATLAB module called GeoPIV (*White et al.,2003*). The GeoPIV code has been established as a reliable and flexible tool for deformation measurement in the field of experimental soil mechanics. Precisions of 0.05 and 0.02 pixels, for GeoPIV patches greater than 16x16 pixels and 50x50 pixels respectively, were obtained from examining images of rigid body movements of sand and textured clay samples (*White et al.,2005*). In dynamic applications, precisions of 0.0039 pixels and 0.0815 pixels for patches of 32x32 pixels were obtained for static and free falling objects respectively (*Chow et al., 2010)*. The validation of the GeoPIV algorithm for dynamic and large strain applications, the calibration of the high speed camera and the effect of the image quality in measuring large transient deformations have been reported previously by the authors (*Nazhat et al., 2011a and 2011b*).

3.2.   Application of high speed photography in DC tests

Studying geotechnical models using high speed photography and DIC enables continuous monitoring of displacement fields and internal strains at, and directly after, tamper impact. The photographic analysis provides continuous and smooth fields of motion of the soil particles and detailed information on the evolving patterns of strain localisation resulting from the rapid impact loading. Figures 3 and 4 show the cumulative displacements, captured by 1000 fps digital photographs, resulting from 6 impacts for each of the tamper shapes on sand and sand-silt mixture models, respectively. Figure 5 shows the corresponding total shear strains for the sand models and Figure 6 the corresponding total volumetric strains for the sand-silt mixtures. The results show distinct differences in the responses between the two different soils and between the different tamper shapes. Details of the different internal kinematics and of the effectiveness of the different tamper geometries are discussed in the following section.
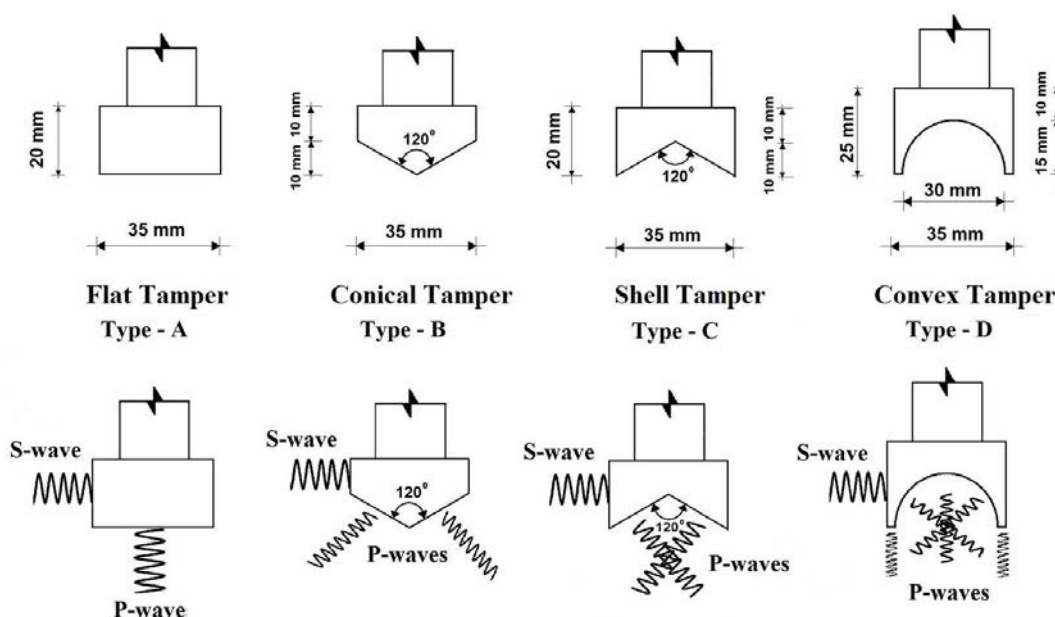
Figure 2: Geometries of studied tampers and directions of their anticipated body waves

4. RESULTS AND DISCUSSION

4.1. The Kinematics of Dynamic Compaction

4.1.1. Displacement Patterns

Irrespective of tamper geometry or type of soil, the displacement fields from DC, shown in Figures 3 and 4, are generally comprised of two significant regions. In the upper region the soil deformation pattern consists of a general bearing capacity failure type mechanism where the soil is being pushed to the side and upwards, whereas in the lower region beneath the tamper the soil is pushed downwards and a confined soil compression takes place. The features of the bearing capacity mechanism, such as the inclined shear planes and radial shear zones, are more evident in the case of sand models where the tampers generally penetrated less than for the sand-silt mixture models. For the sand-silt tests, the amount of soil heave around the tampers was significantly less and as the tampers penetrated deeper into the model this resulted in more of a local or punching shear failure mechanism. In these tests the inclined side shear planes only developed in later impacts with increasing impacting efforts. For the sand-silt mixture a bigger portion of the imparted energy is utilised by the compaction mechanism beneath the tamper rather than being wasted in pushing the soil aside and upwards, suggesting that DC will be more effective in compressible soils. It is also evident from Figures 3 and 4 that the extent of the region beneath the tamper experiencing significant displacement varies with the tamper geometry. For the sand Figure 3 shows that tamper shapes A and D affect the greatest amount of soil, and of these the curved tamper, which concentrates the deformation beneath the tamper, appears to be the most effective. For the sand-silt mixture Figure 4 shows that tamper shape B penetrates further, affects a much greater region and appears to be the most effective.

4.1.2. The Compaction Mechanism

It is widely believed that the densification of a soil following dynamic compaction occurs in a semi-prolate-spheroidal region with the largest density increase directly beneath the point of impact and the density change gradually decreasing with distance from the tamper. The reduction in cumulative displacement with distance from the tamper shown in Figures 3 and 4 supports this view, however, the results from the photographs, shown in Figures 5 and 6, are not consistent with this interpretation. They show an alternative phenomenon of progressive but not homogeneous densification of the region beneath the tamper. Each tamper impact generates one or more shock bands, which are associated with high shear and volumetric strains, which pass down through the soil and eventually come to rest. The soil through which the shocks pass experiences a cycle of contraction and dilation, which produces little net change to the soil density. However, the soil in the shock band is significantly denser and this compacted band of soil is effectively locked in place when the shock band comes to a halt. With further impacts additional

shock bands are generated and as these come to rest in different locations more of the soil is effectively compacted, however, even after six impacts much of the soil with the region bounded by the furthest travelled compaction band experiences little if any densification.
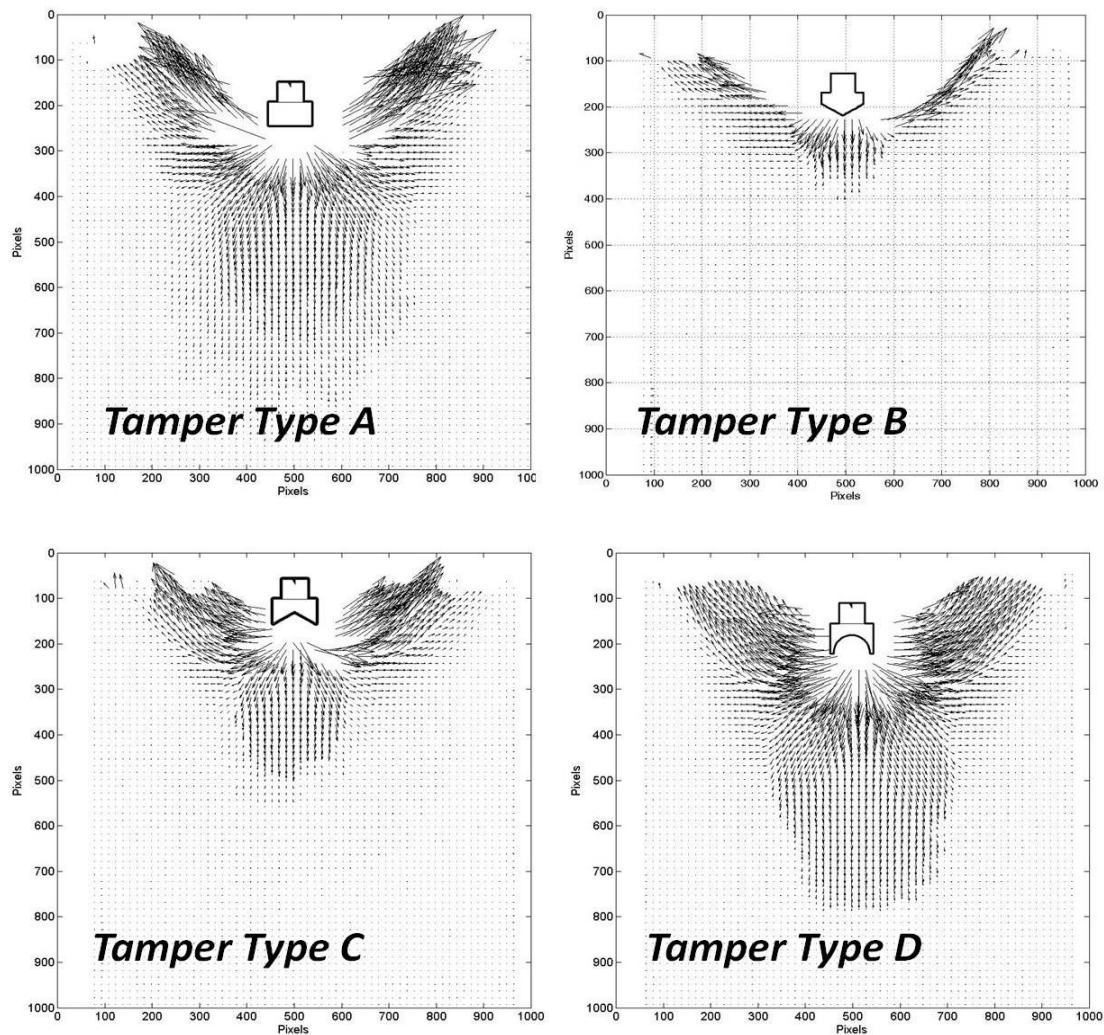
Figure 3: Cumulative displacement vectors (magnified x 2 for clarity) after 6 impacts – Sand models (1000 pixels = 400mm)

The propagation of the compaction shock bands and the extent of the region affected by dynamic compaction differs between the two soil types and between the different tamper geometries. For the sand models the compaction bands reach their furthest extent in the first or second impact, and subsequent impacts create additional compaction bands that fill the region between the tamper and the outer band. This evolution of the compaction bands is shown in Figure 7 for the flat-bottomed tamper as it is dropped onto the sand. Although only shear strains are shown in Figure 7, the areas of high shear strain are also areas of high volume strain. It may also be noted from Figure 7 that the small region of very high strains directly beneath the tamper also grows with successive impacts. The compaction bands developed similarly in the other tests on sand using the different shaped tampers. In contrast, the evolution of the compaction bands for the sand-silt models occurs differently, with the distance travelled by the compaction bands increasing with number of blows as shown in Figure 8, at least for the six blows used here. The evolution of the compaction band patterns was similar in all the sand-silt mixture models for all four tamper shapes.
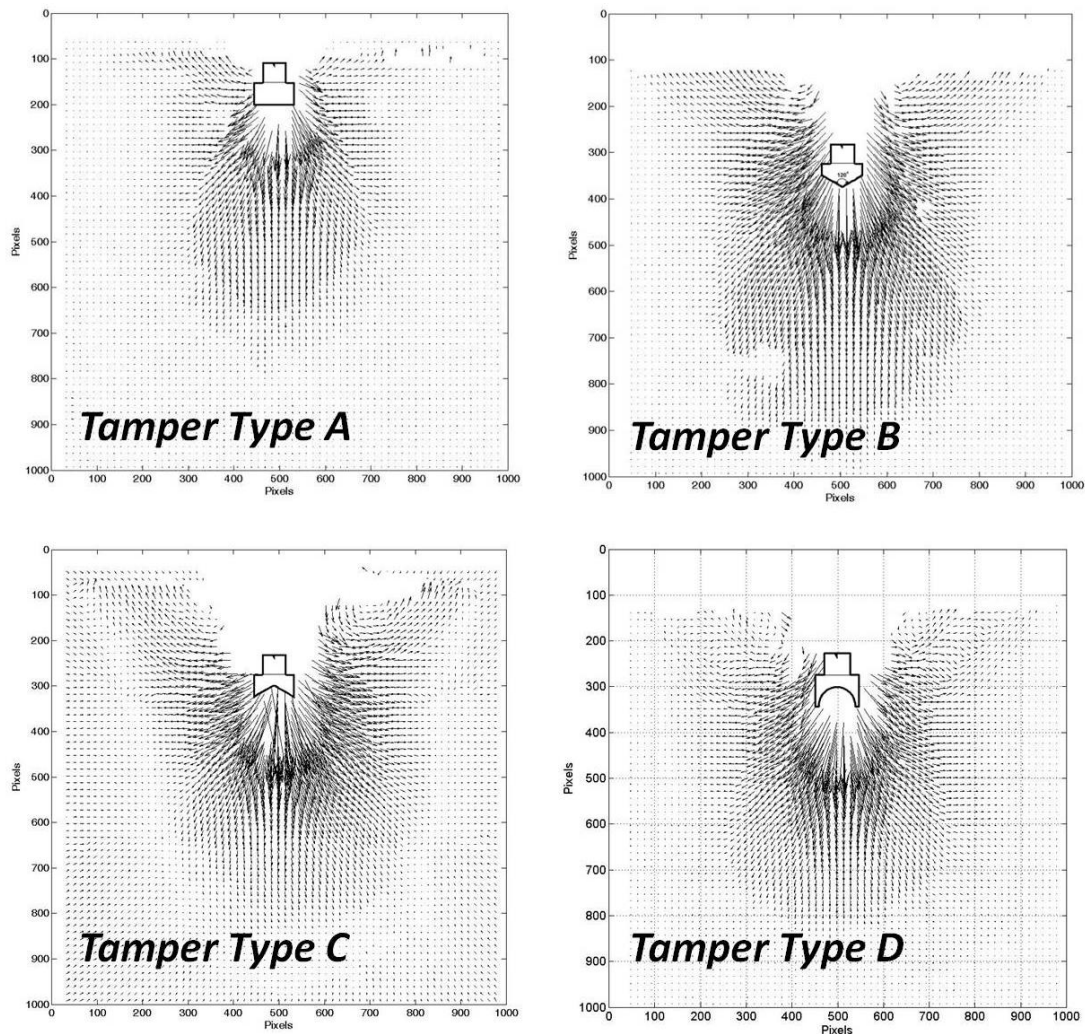
Figure 4: Cumulative displacement vectors (magnified x 2 for clarity) after 6 impacts – Sand- Silt mixture models (1000 pixels = 400mm)

4.2. The Effect of Tamper Geometry on Dynamic Compaction

The high speed photography technique enables measurements of the depth of influence, the lateral extent of the impacted zone at depth, and the magnitude of the strains within the influence zone to be obtained and to enable a quantified assessment of the effect of different tamper geometries on dynamic compaction. The following parameters have been chosen to assist in this process:

I.   Dimensions and characteristic features after 6 impacts as illustrated in Figure 9 including:
  i.   Z1: Maximum depth of penetration (equivalent to tamper crater depth)
  ii. Z2: Depth of highly sheared region below the tamper, measured from the original soil surface
  iii. Z3: Maximum depth of localised strain bands (equivalent to DC influence depth, D_{max})
  iv. Z4: Primary zone of interest for DC. Taken to start at a depth equal to the tamper width (B) below the tamper base's final position.
  v.   WS: Maximum width of region within the outermost strain band
  vi. Aspect ratio Z3/Z1 (influence depth/crater depth)
  vii. Aspect ratio Z3/Z2
  viii. Aspect ratio Z3/WS (influence depth/influence lateral extent)

II. Global volumetric strain (GVS, %) due to 6 impacts as defined in Figure 10
III. After 6 impacts the difference between the percentages of the area experiencing contraction and dilation within the region of Z4 x the width of the model, referred to as the net contraction (NC, %) determined as shown in Figure 11.
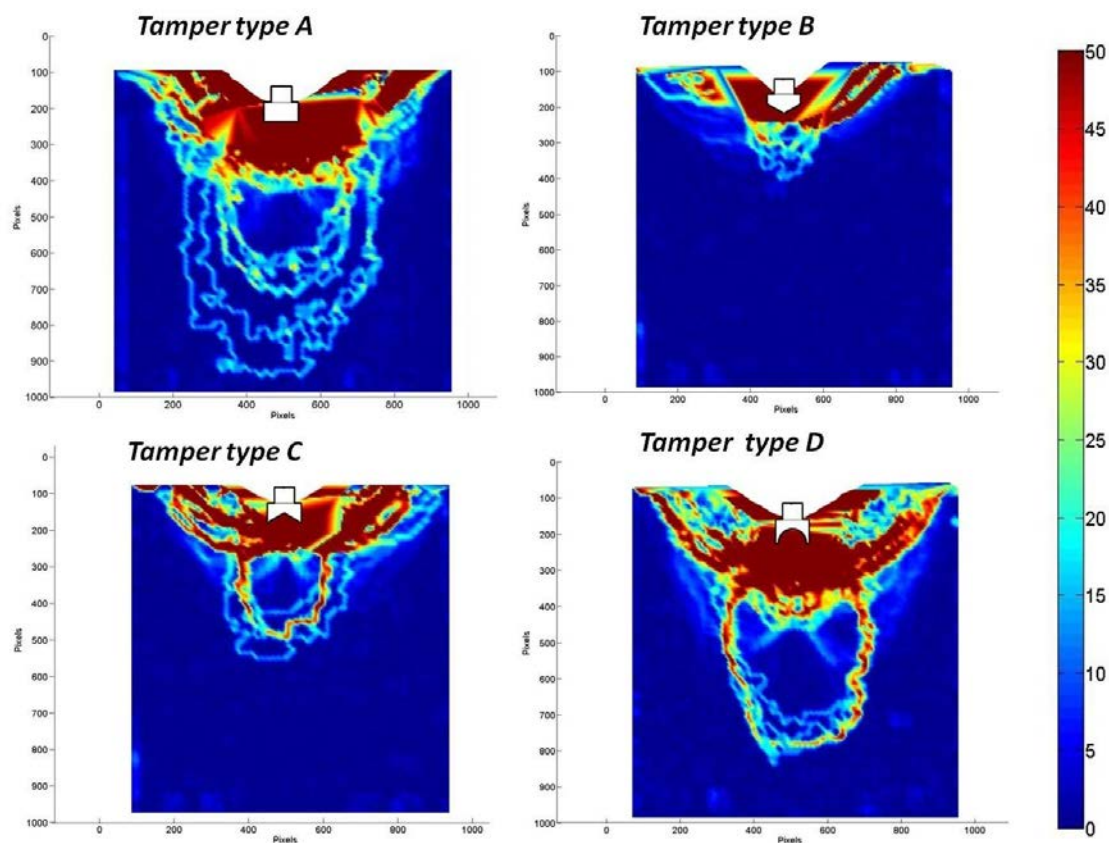
Figure 5: Total Shear Strain at end of 6 impacts on dry sand models using four types of tampers

The selection of the DC primary zone of interest starting at a depth of B (tamper width) below the tamper's final position was based on observations from the GeoPIV displacement fields and strain plots that showed the region above Z4 was primarily a region of dilative volumetric strains and thus little densification would be expected, and this is also consistent with observations from impact compaction (*Berry, 2001*) which showed highly variable densification directly beneath the tamper.

As discussed previously there are significant differences in the amount and extent of densification produced by the different tamper geometries and between the responses of the two investigated target materials. Despite the essentially identical pre-impact relative densities of the models of either material, there were noticeable differences in all characteristic feature measurements as well as the estimated global volume strain (GVS) and percentage net contraction (NC). In the sand models, there was 26% difference between the smallest and largest depths of penetration (Z1) and these were associated with variations of 150% in Z3 and 180% WS. The greatest and smallest Z3 were produced by tamper types D and B, while the widest WS was achieved by tamper type A. For the sand-silt mixtures there was a greater difference of 54% difference between smallest and largest depths of penetration (Z1) but these were associated with smaller variations in Z3, 26% and WS, 24% . In the sand-silt mixtures the greatest and smallest (Z3) were produced by tamper types A and C, and the widest (WS) was achieved by tamper type B. The effects of different tamper base profiles on the studied characteristic features as well as on the GVS and NC adjudicator parameters are summarised in Figures 12 and 13. These figures show that all the selected quantities vary significantly with tamper geometry and soil type, despite the similar impact energies and similar relative densities of tests for each soil type.
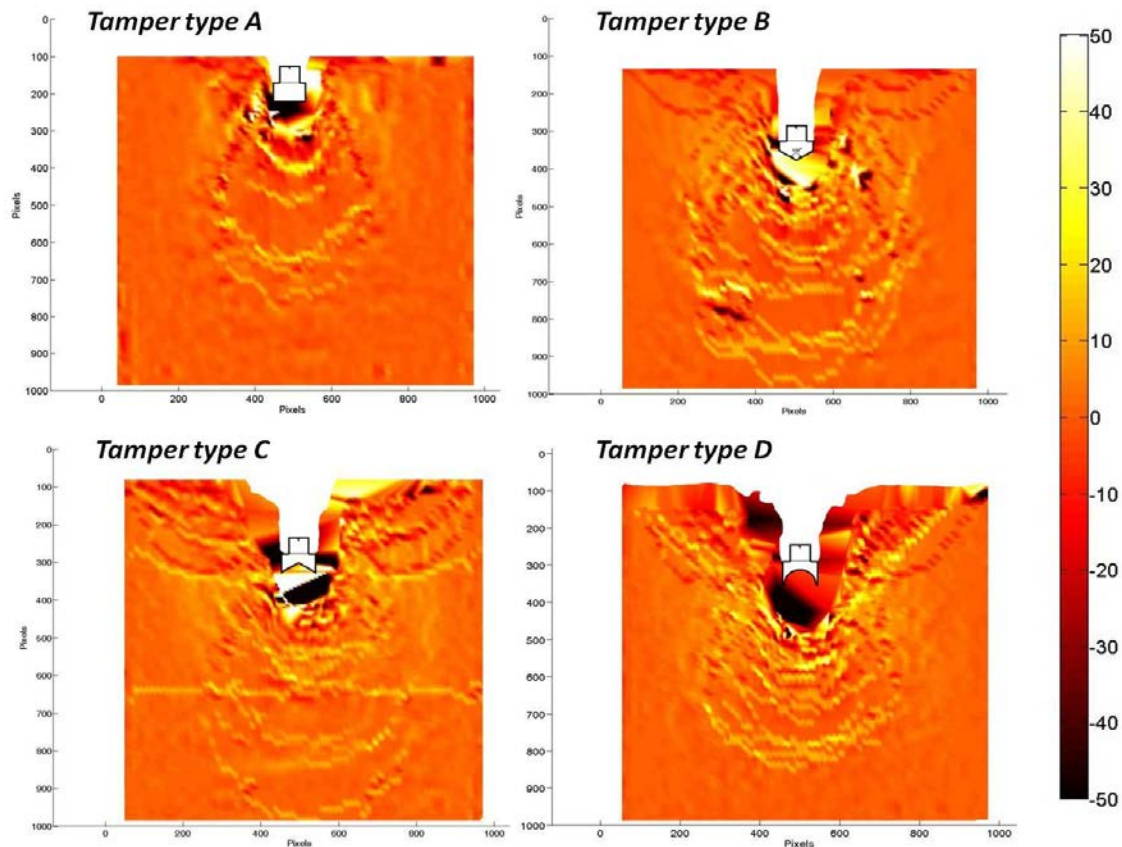
Figure 6: Total Volumetric Strain at end of 6 impacts on sand-silt models using four types of tampers
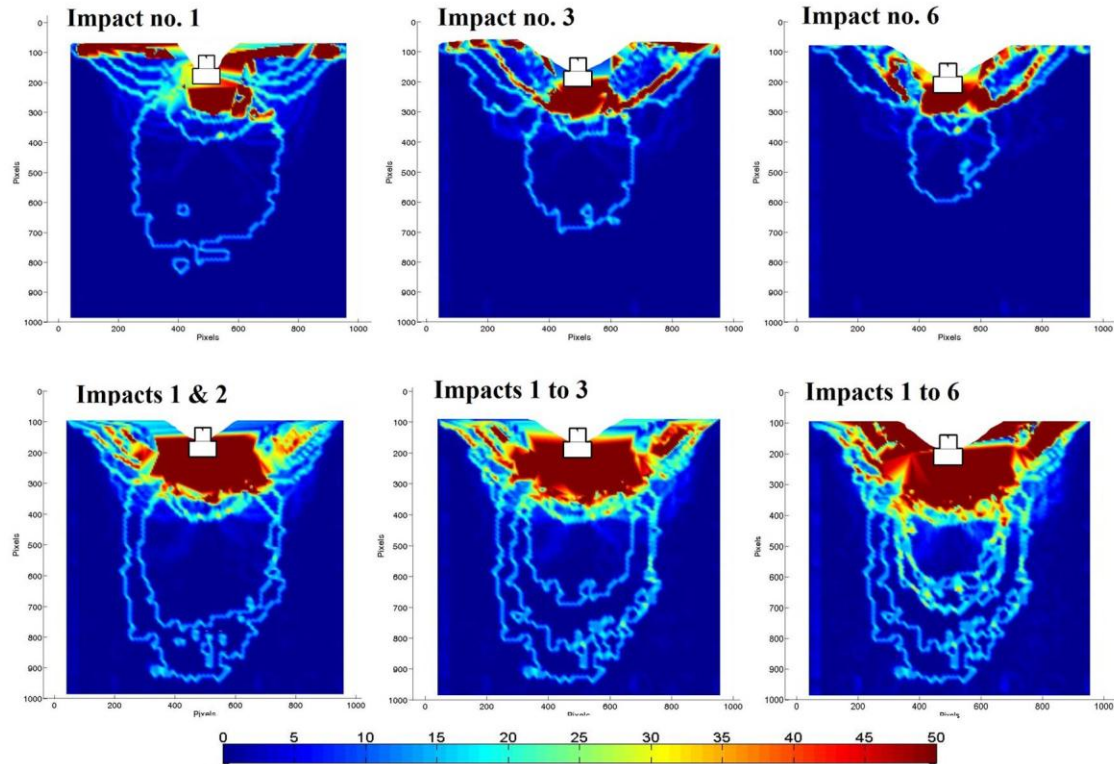
Figure 7: Incremental shear strains and history of total shear strain over the course of 6 impacts on a sand model using tamper type A
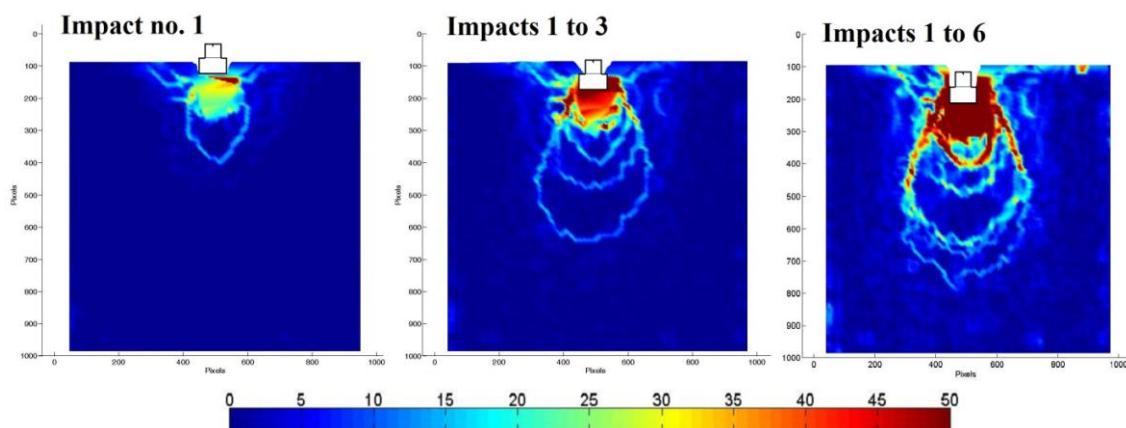
Figure 8: History of total shear strain over the course of six impacts on a sand-silt model using tamper type A
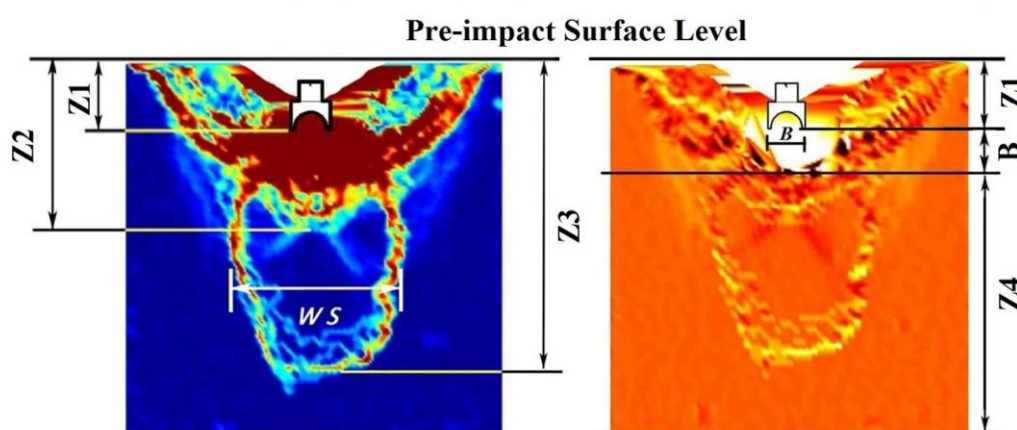
B: Width of Tamper
Z1: Maximum Depth of Tamper Penetration
Z2: Depth of Major Shearing
Z3: Maximum Depth of Localised Strain Front
Z4 : Primary Zone of DC
WS: Maximum width of Strain Bulb

Figure 9: Characteristic features of DC selected measurements

The results show that the use of crater dimension measures such as the displaced volume and crater depth (expressed here by the global volumetric strain GVS, and tamper penetration depth Z1) to estimate the tamper efficiency and DC degree of improvement may provide misleading results particularly in the case of loose sand. For example, the results show a difference of less than 1% in the penetrations (crater depths) of tamper types A and B in near identical sand models, however the GVS from tamper type A is 3.4 times greater than the GVS of tamper type B. On the other hand, the GVS due to tamper type B is about three times the GVS of tamper type C while the difference between their depths of penetration is less than 15%. The precise values are not important as there are important differences between these small scale laboratory tests and field tests, but they indicate the limitations of surface measurements for predicting compaction at depth. Apart from the different scales between the laboratory and the field, the use of loose, dry materials has affected the estimates of the depth of penetration (Z1), the shape of the deformed surface and the subsequent calculation of GVS. This is because the dry sand is able to flow freely into the crater, and to partially fill in the crater between impacts, in contrast to typical field behaviour where suctions in moist natural soil prevent collapse of the soil into the formed crater.

Pre-impact Model Volume ($V_{initial}$): 33,075,000 mm³
Volume of Zone I: 214,512 mm³
Volume of Zone II: 613536 mm³
Global Volumetric Strain, % = ($V_{initial}$ + $V_{zone\ I}$ - $V_{zone\ II}$) / $V_{initial}$
= (33,075,000 + 214,512 − 613536) / 33,075,000 = 1.206 %
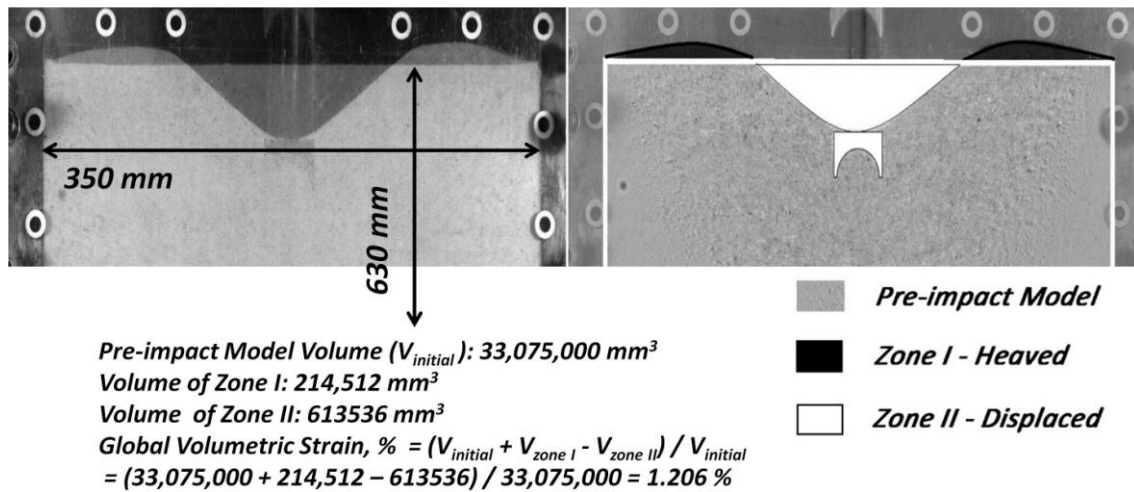
Figure 10: Calculation example of global volumetric strain

Percentage of area having positive volumetric strain (0-20%) - Contraction 38.06% of the analysed area

Percentage of Net Contraction (NC) due to 6 impacts is : 13.51%

Percentage of area having of negative volumetric strain (-20 - 0%) - Dilation 24.55% of the analysed area
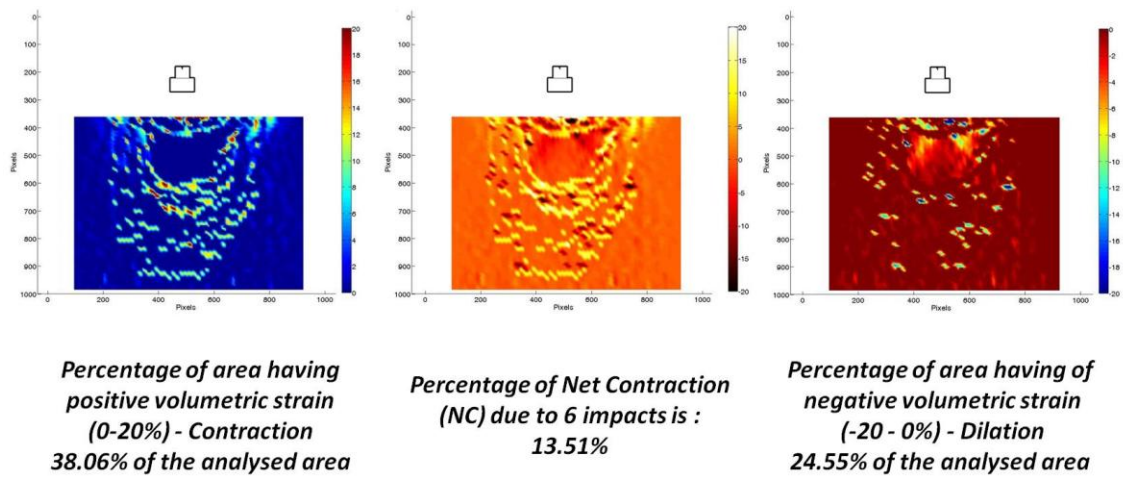
Figure 11: Calculation example of percentage of net contraction (NC) within the Z4 region

In the authors' opinion, the percentage of area experiencing compression (NC) in the primary zone of interest, over depth Z4, provides a more meaningful and accurate measure for quantifying soil mass displacement and densification in the studied models. This quantity is preferred to a sum of the volume strains at each point due to the simplicity of the NC calculation and its good agreement with the volumetric strains from pixel-by-pixel data. In all the tests significant areas in the zone of interest are indicated to experience both compression and dilation, and there is generally more compression than dilation as would be expected. It is interesting to observe from Figure 12a that a much greater area experiences compression with the silty sand mixture when compared to the loose sand, and tamper B in the loose sand produces almost no net compaction at depth. Although this trend is reflected in the global volume strains, GVS, measured from the surface measurements shown in Figure 13, the GVS provides a poor indication of the response at depth. For tamper B in the loose sand, the poor densification at depth was reflected in all the measured parameters like Z3, WS and NC, and the majority of the GVS was a result of the larger sideways and upward (heaving) displacements of its dart front rather than any significant compaction at depth as also illustrated by the GeoPIV displacement vectors and strain map shown in Figures 3 and 5 respectively.

Figure 12 shows the penetration depths, Z1, in the sand-silt models were almost double the corresponding depths in the sand models for all tampers except the flat base tamper type A, and from Figure 13 it is clear that there is no correlation between Z1 and GVS. Figure 13b shows a reasonable correlation between GVS and the NC values from sand-silt models, but not for the sand, which suggests that the surface heave in the sand tests is an important factor limiting the usefulness of the surface measures in estimating DC effectiveness.
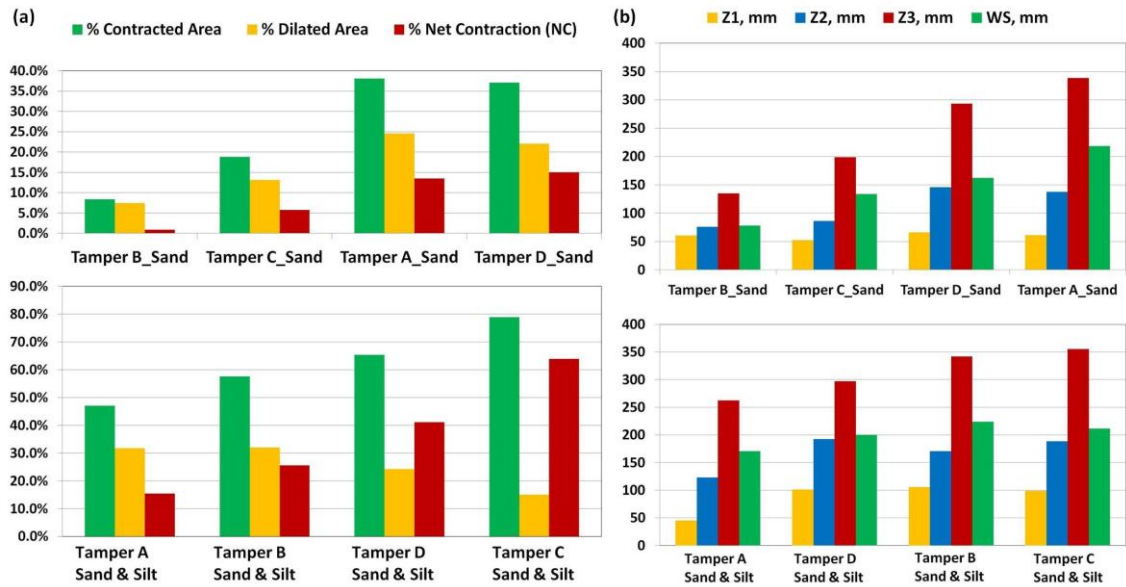
Figure 12: Variation in volumetric strain intensities - arranged from smallest to largest NC (a) and DC measured characteristic features - arranged from smallest to largest Z3 (b)
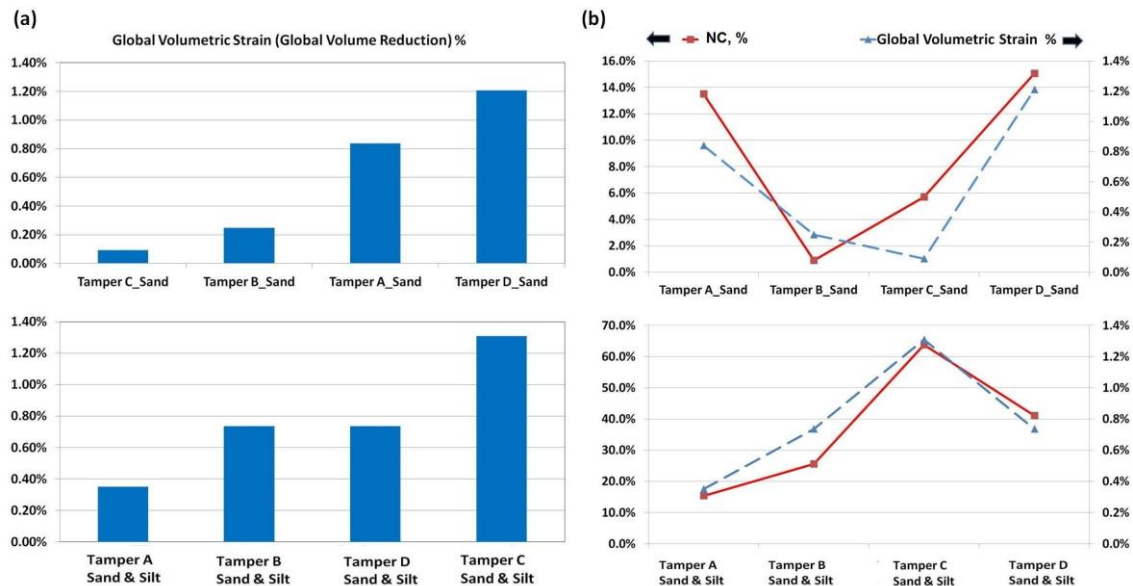
Figure 13: Variation in global volumetric strain with respect to tamper geometries (a) and correlation between the global volumetric strains (GVS) and net contraction (NC) within the region of Z4 (b.)

Relationships between various aspect ratios and NC are presented in Figure 14. These relationships address the diverse responses of the two target materials to the different tamper geometries during DC model tests. The aspect ratio Z3/Z1, the ratio of depth of soil improvement to penetration depth was found to be more affected by the type of the target material in the cases of tamper types B and D while it was less affected in the cases of tamper types A and C. Nevertheless, the higher Z3/Z1 ratio did not necessarily imply that greater densification has taken place as can be seen from the trend relationships between Z3/Z1 and NC in the cases of tamper types C and D. The aspect ratios Z3/Z2 and Z3/WS were found to be less sensitive to the soil type or the tampers geometry.
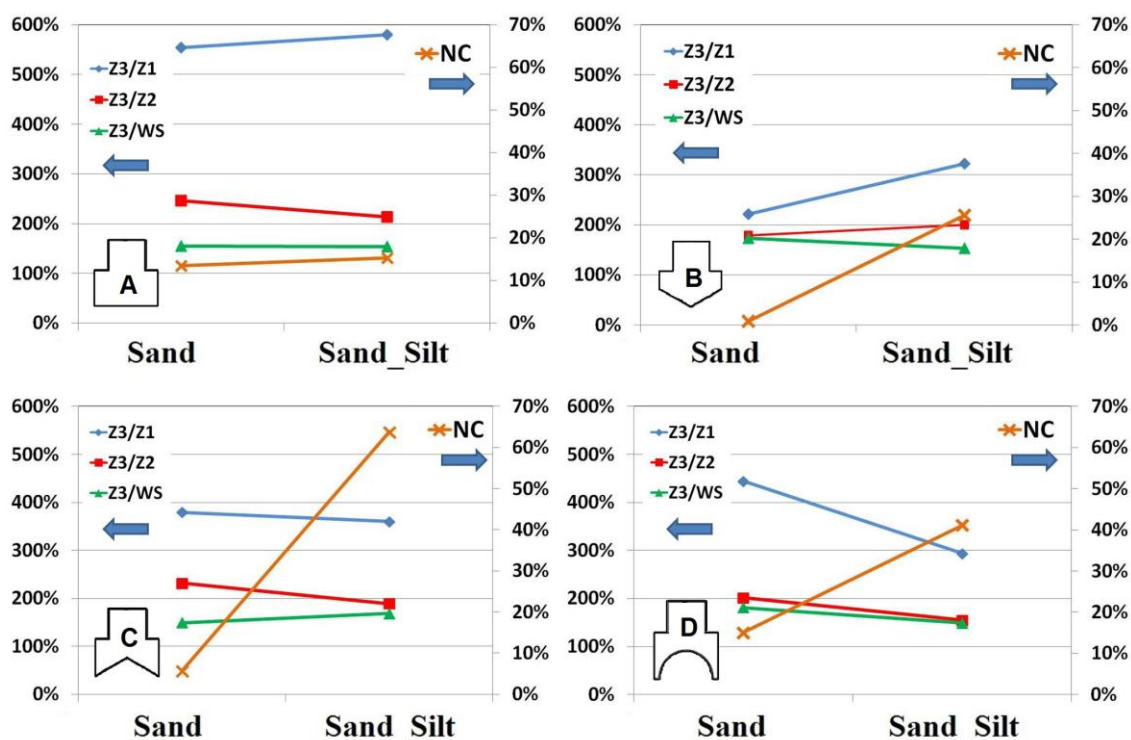
Figure14: Correlations between tamper geometries, key DC aspect ratios and intensities of areas of net contractions (NC) in sand and sand-silt models

5. CONCLUSIONS

High speed photography and DIC have been used to characterise the response of two types of soil to dynamic compaction using four different tamper profiles. As a quantitative tool, digital high speed photography has allowed the propagation of localised deformation and strain fields to be identified and has suggested that compaction shock bands control the kinematics of dynamic compaction. The results have revealed distinctive internal densification mechanisms that depend on the tamper geometry and the type of target soil.

The direct applicability of the results may be limited by the small scale and low stress levels in the model tests, however, they indicate that the response of soil to dynamic compaction is likely to be strongly influenced by the soil type and tamper geometry. The results show that there are significant differences in the extent and magnitude of the compacted zone at depth, and suggest that there may be significant benefits from considering different tamper shapes in future field studies. It was found that no single tamper shape performed well across both soil types investigated.

The results may benefit the ground improvement industry where dynamic compaction is usually applied in systematically controlled passes on a grid pattern with the application of typically 5 to 15 impacts per grid point. The tests suggest potential to improve dynamic compaction practice by using combinations of different tamper geometries on alternate grids to achieve the most effective densification. The effect of tamper geometry on the dynamic compaction process should be further investigated, both experimentally by employing larger scale models and in field trials using in situ before and after testing to scale the effect of the tamper geometry on the efficiency of dynamic compaction.

REFERENCES

Arslan, H., Baykal, G. and Ertas, O., 2007, Influence of tamper weight shape on dynamic compaction, Ground Improvement, Vol. 11, No. 2, pp 61–66.

Berry, A. D., 2001, Development of volumetric strain influence ground improvement prediction model with special reference to impact compaction. Master of Engineering Thesis, University of Pretoria, South Africa

Cassidy, M.J. and Houlsby, G.T., 2002, Vertical bearing capacity factors for conical footings on sand, Geotechnique, Vol. 52, No. 9, pp 687–692

Chow, S.H., Nazhat, Y. And Airey, D.W., 2010, Applications of high speed photography in dynamic tests, Proceeding of 7th International Conference on Physical Modelling in Geotechnics, ICPMG, Zurich, pp 313-318

Ghazavi, M. and Niazipour, M., 2010, An experimental setup for the investigation of tamper geometry effects, Proceedings of the 7th International Conference on Physical Modelling in Geotechnics, Zurich, pp 235-238.

Feng, T.W., Chen, K.H., Su, Y.T., and Shi, Y.C , 2000, Laboratory investigation of the efficiency of conical based tampers for dynamic compaction, Geotechnique, Vol. 50, No. 2, pp 667-674.

Lukas, R. G., 1979, Densification of loose deposits by pounding, Journal of Geotechnical Engineering, ASCE, Vol. 106, No GT4, p435-446.

Menard, L. and Broise, Y., 1975, Theoretical and practical aspects of dynamic consolidation, Geotechnique, Vol. 25, No.1, pp 3-18.

Mullins, G., Gunaratne, M., Stinnette, P., and Thilakasiri,S., 2000. "Prediction of Dynamic Compaction Tamper Penetration," Soils and Foundations, Japanese Geotechnical Society, Vol. 40, No. 5, pp. 91-97.

Nazhat, Y. & Airey, D.W., 2011(a), Applications of high speed photography and X-ray computerised tomography (Micro CT) in dynamic compaction tests, International Symposium on Deformation Characteristics of Geomaterials, Seoul, Korea, pp 421-427.

Nazhat, Y. & Airey, D., 2011(b), Validation of High Speed Photography and PIV in Large Strain Measurements of Granular Materials, 9th International Symposium on Particle Image Velocimetry – PIV'11, Kobe, Japan.

Peters, W.H. and Ranson, W.F., 1982, Optical Engineering, Vol. 21, No. 3, pp. 427-431.

Tao-Wei Feng and Chih-Chung, Ke, 2005, A Study on Using Conical Bottom Tamper for Dynamic Compaction in Platy Sand, Proceedings of the Fifteenth International Offshore and Polar Engineering Conference, Seoul, Korea, pp 674-678.

White, D.J., Take, W.A. and Bolton M.D., 2003, Soil deformation measurement using particle image velocimetry (PIV) and photogrammetry, Geotechnique, Vol. 53, No. 7, pp 619–631.

White, D., Randolph, M. and Thompson, B, 2005, An Image-Based Deformation Measurement System For The Geotechnical Centrifuge, International Journal of Physical Modelling in Geotechnics, Vol. 5, No. 3, pp 01-12.

White, D.J., Teh, K.L., Leung, C.F. & Chow, Y.K., 2008, A comparison of the bearing capacity of flat and conical circular foundations on sand, Geotechnique, Vol. 58, No. 10, pp 781–792

Yamamoto, K., Lyamin, A.V., Abbo, A.J., Sloan. S.C. & Hira, M, 2009, Bearing capacity and failure mechanism of different types of foundations on sand, Soils and Foundations, Vol. 49, No.2, pp 305-314

Vibro Ground Improvement Techniques – A UK Perspective

Colin J. Serridge, Balfour Beatty Ground Engineering Ltd, United Kingdom. colin.serridge@bbge.com

ABSTRACT

Of the various ground improvement techniques available in the UK, vibro techniques employing vibroflots (vibrating pokers) to construct (vibro) stone columns are the most commonly used and have been applied in the UK since the 1950's. Introduction of the vibro stone column technique permitted the application of vibro techniques to a much wider range of soil types. As the soil conditions have a large influence on the result, stone column techniques require an appropriate level of site and ground investigation to permit satisfactory geotechnical characterisation of the soil profile and in turn performance prediction. An understanding of where the differing stone column techniques work and how, to ensure correct and appropriate application, together with consideration of the most appropriate design approach, are essential, as are quality control and monitoring procedures during stone column installation, to ensure successful implementation and performance. Vibro stone column techniques permit the adoption of relatively simple shallow foundations and ground bearing floor slabs. Furthermore, they can also provide significant sustainability advantages in comparison to more traditional deep foundation methods and techniques. Discussion of these aspects together with experiences and recent research activity, from a UK perspective, is provided.

1. INTRODUCTION AND HISTORY

The development of the vibro stone column method in the 1950's permitted the application of vibro techniques to a much wider range of soil types, most notably finer-grained soils (cohesive and mixed cohesive and granular soils), thus increasing the range of soils which could be treated by vibro techniques. Vibro stone column techniques were introduced into Great Britain in the late 1950's and have been used extensively worldwide.The principal piece of equipment used to carry out vibro ground improvement techniques is the vibroflot (also referred to as a vibrating poker or depth vibrator), which is either suspended from a crawler crane or mounted on a leader attached to a base machine, dependent upon the specific application. Whilst the basic components of the equipment have changed very little over the years, there have been significant developments in the reliability (with extended lifespans and reduced maintenance) and power ratings of the equipment with the objective of achieving greater efficiency in densification and stone column production.

2. APPLICABILITY OF VIBRO TECHNIQUES

The vibroflot may be used for both in situ compaction/densification of cohesionless soils and for forming stone columns in fine-grained soils (Figure 1.). The actual mechanism of improvement is a function of whether the soils are essentially granular (coarse-grained) or cohesive (fine-grained).

It is generally recognised that in situ vibro compaction is appropriate for granular soils with a total fines (particles finer than 0.06 mm) content of up to 15% of which the clay and fine silt content (particles smaller than 5 μm) should be less than 2% (Slocombe et al., 2000). The principles of vibro techniques in granular soils is based upon particles of coarse grained soil being rearranged into a denser state by means of dominantly horizontal vibration from the vibroflot (vibrating opoker). The resultant void ratio and corresponding increased angle of shearing resistance then permit the adoption of higher imposed design loadings at lesser settlement and increased seismic resistance.

For higher fines content, the stone column technique is employed. With fine-grained soils the cohesion between the soil particles dampens the vibrations and prevents rearrangements and compaction occurring. Improvement is achieved by 'reinforcing' the soil with relatively rigid stone columns. During the stone column construction the introduced coarse granular column material is pressed radially into the soil so that it is displaced beyond the diameter of the vibrator. The column of compacted dense granular material forms, together with the surrounding soil, a composite stone column − soil mass, with enhanced shear strength and bearing capacity, together with a corresponding reduction in settlements, attributed to the 'stiffening' effect of the stone columns. Stone columns in fine-grained soils also assist in the dissipation

of excess pore water pressure under applied load or surcharge, which accelerates the consolidation process, together with providing enhanced slope stability parameters.
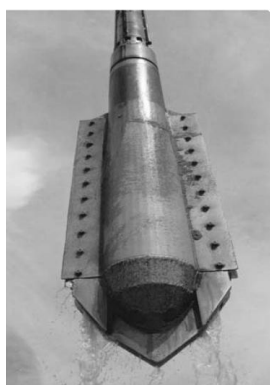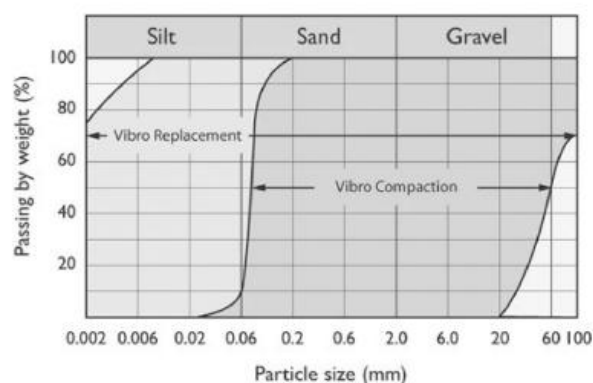
Figure 1a: Top-feed Vibroflot

Figure 1b: Range of soils treatable by vibrocompaction and vibro stone columns

3.   VIBRO STONE COLUMN TERMINOLOGY

Terminology for vibro stone column techniques has not always been applied in a consistent manner and some attempt at addressing this can be found in BRE Document BR 391, Specifying Vibro Stone Columns (2000). This specification employs terms that reflect the fundamental principles of top-feed or bottom-feed to describe the method of stone aggregate supply, and wet or dry to describe the 'jetting' medium. This has given rise to the following terminology in the UK:

- dry top-feed technique
- dry bottom-feed technique
- wet top feed-technique

The technique adopted is a function of ground conditions, bore stability and environmental constraints. Historically, in the UK the literature has suggested that the dry top-feed technique should not be used in fine-grained soils with undrained shear strengths of less than around 30 kN/m2. For soils weaker than this the dry bottom-feed technique (or historically the wet top-feed technique) has been used. In terms of a lower-bound undrained shear strength, a value of 15 kN/m2 has typically been used for vibro stone column applications. However, developments in vibroflot technology (together with monitoring and quality control systems), have allowed weaker soils to be treated in certain applications. Consideration also needs to be given to soil sensitivity when selecting the appropriate (installation) technique, as saturated sensitive soils can undergo significant remoulding when exposed to vibrations. For soft soils, settlement tends to be more of an issue than bearing capacity. All three vibro stone column techniques described above use similar types of vibroflot, normally hydraulically or electrically driven, the main differences being the dry bottom-feed equipment which has a stone (aggregate) feed tube attached to the vibroflot to permit the stone aggregate to be introduced to the tip of the vibroflot without it having to be removed from the bore, thus overcoming any instability issues in weak ground or treatment to beneath the water table. The stone aggregate is typically handled by front end loaders with a side tip facility. All the vibro stone column techniques are aimed at constructing well-compacted granular columns, typically of crushed stone or gravel aggregates in the void formed in the ground by the vibrating poker, thus improving bearing capacity and drainage while reducing total and differential settlements. Within the UK, the dry top and dry bottom-feed techniques (Figure 2) are the most comonly used, with the wet top- feed technique having been largely superseded by the dry bottom-feed technique on environmental grounds.
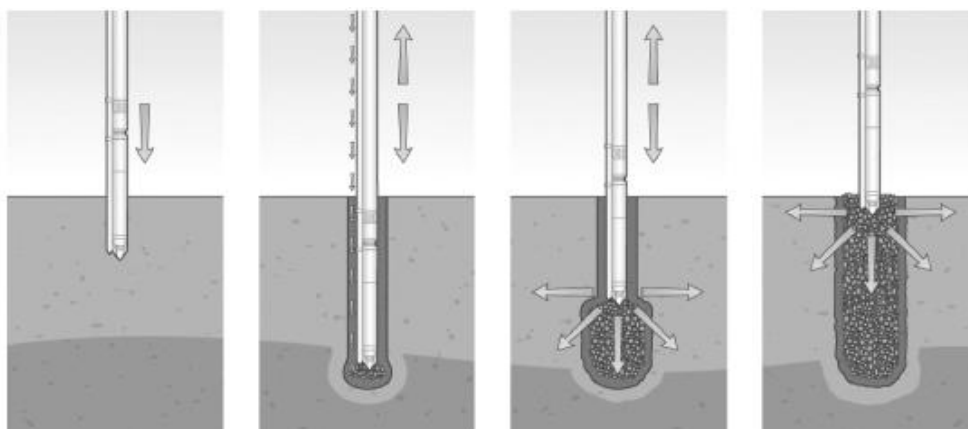
Figure 2: Installation sequence for dry bottom-feed stone columns

4. SOIL GEOTECHNICAL PROPERTIES AND CHARACTERISATION

Because of the large influence of the soil conditions on performance, ground improvement using virbo techniques requires a more extensive site and ground investigation programme compared with more conventional deep foundation(s) solutions (Serridge, 2008). The most common types of ground-related problems encountered concern soil strata boundaries, i.e. geometry not as anticipated, and the geotechnical properties of the soil profile. Cone penetration tests (CPT's) using the piezocone (CPTU) are being increasingly used for geotechnical characterisaton of soft fine-grained deposits in the UK (with regard to soil type and stratification and also parameters such as stress history, undrained shear strength, small strain shear modulus and coefficient of consolidation), and where vibro stone column techniques have been subsequently adopted. Continued development of high-quality databases of CPTU results and soil properties has contributed to development of new and improved correlations, Powell and Lunne (2005). In addition to satisfactory site geo-characterisation, important steps in achieving successful ground improvement implementation and performance include: an appropriate design and review process; consideration of the interfacing with other ground improvement techniques (or deep foundation techniques); preliminary trials (where applicable); monitoring; quality control and testing (Figure 3). Management of geotechnical risk is discussed by Clayton (2001).
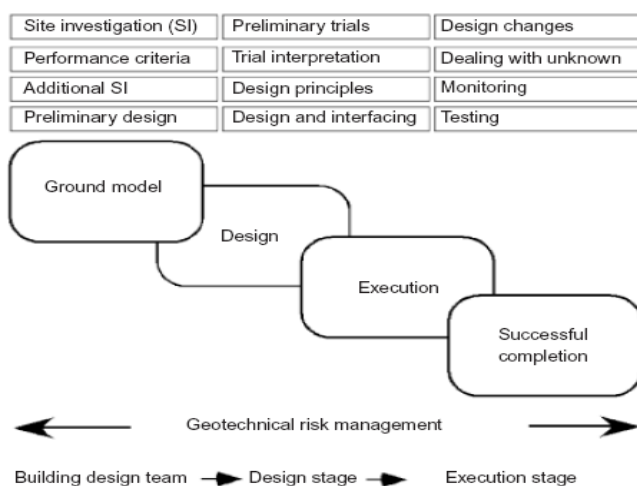
Figure 3: Important steps for successful ground improvement implementation (after Serridge and Synac 2007)

5. VIBRO STONE COLUMN DESIGN

Within the UK design is typically based on Hughes and Withers (1974) for determination of stone column length and load-carrying capacity of an individual stone column. The guidance of Baumann and Bauer (1974) is frequently adopted for analysis of stress distribution between columns and soil. Foundation settlement (without ground improvement) is first estimated using available geotechnical parameters and then applying appropriate settlement reduction factors (within the treated depth), according to Priebe

(1995), to allow for the 'reinforcing' effect of the stone columns. Although primarily applicable to embankment loadings over soft fine-grained/organic soils, it is important that secondary consolidation is considered as in some instances it may contribute to a significant part of the total settlement.

5.1. Research Activity in the UK

Increasing pressure to develop marginal soft clay sites has focussed attention on investigation of the application of vibro stone columns to deep soft clay deposits both in the UK and Ireland. This has prompted increased research activity, particularly over the last 10-15 years, in an attempt to improve overall understanding of stone columns in this application and faciltate more economic foundation design. The investigations adopted have included (physical) laboratory modelling (for example, Mc Kelvey (2002); Mc Kelvey *et al.,* (2004) (see Figure 4) and full scale field trials - Watts and Serridge (2000); Serridge and Sarsby (2008), together with numerical modelling - Killeen and Mc Cabe (2010)). These have involved evaluations of bearing capacity (including column deformation and bulging) and settlement control/reduction using different stone column spacings, diameters and depths (including length to diameter ratio), of stone columns. Historically, research attention has focussed on widespread loads, with more recent research activity having focussed on narrow footings to more closely model low-rise structures over soft clay.

Field trials reported by Watts and Serridge (2000) and Serridge and Sarsby (2008) have demonstrated that partial depth vibro stone columns can be satisfactorily constructed using the dry bottom-feed technique in soft sensitive clay soils (i.e. Bothkennar Carse Clay), (see Figure 4), to support conventional narrow footings. However, a high level of quality control is required to avoid any potential problems, and is reliant upon there being good supervision, having experienced rig operators and implementation of appropriate monitoring systems (rig instrumentation). It was also clear from these field trials that the vibroflot (vibrating poker) should not remain in the ground for longer than is necessary to achieve an acceptable level of workmanship with regard to stone column construction, to avoid excessive soil disturbance. Air jetting should be kept to the minimum necessary to obviate soil suction effects on the vibroflot whilst at the same time minimising soil disturbance (remoulding). The requirement for large end bulbs at the toe of partially penetrating ('floating') stone columns was considered questionable, as the benefits are offset by the extent of disturbance caused by imparting excessive energy to the ground at the toe/base of the column. For this reason construction of stone columns to a more uniform diameter over their length, without imparting excessive energy at the toe was considered a better approach particularly in soft sensitive clays and silts.
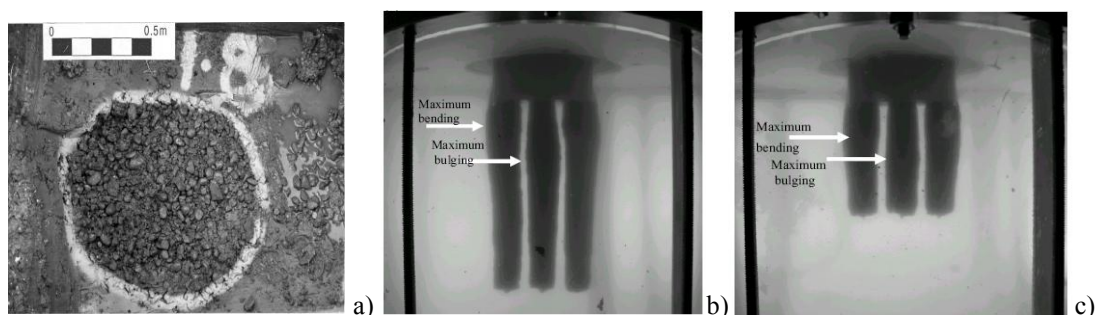
Figure 4 a) Exposed stone column at 1.8 m depth in soft sensitive Bothkennar clay (after Watts and Serridge, 2000) b) and c) Laboratory modelling of 'floating' long and short stone columns (afterMc Kelvey et al., 2004).

6. SPECIFICATIONS

Within the UK the main specification documents and guidance notes covering vibro stone column techniques include:

- Institution of Civil Engineers (ICE) *Specification for Ground Treatment* (1987).
- Building Research Establishment (BRE) BR 391 *Specifying Vibro Stone Columns* (2000).
- BS EN 14731 *Ground Treatment by Deep Compaction* (BSI, 2005).
- NHBC Standards, Chapter 4.6: *Vibratory Ground Improvement Techniques* (2011).

7. STONE AGGREGATE REQUIREMENTS

All the above-mentioned specifications convey a similar message with regard to stone aggregate requirements for vibro stone columns – that aggregates used in stone column construction should be sufficiently hard (i.e. must withstand the vibratotory impact of the vibroflot); inert; free draining (typically less than 5% fines); and of appropriate grading, shape and angularity to form dense granular columns with high angles of internal friction. Acceptable particle shapes for stone column material include rounded, angular and irregular. Unacceptable materials would be flaky and elongated. Minimum Los Angeles Abrasion (LAA) values in the range 30 to 40 are recognised within the industry as being acceptable for use in vibro stone columns, dependent upon specific applications and subject to approval on a job specific basis. Typical grading requirements for stone column aggregate are given in BS EN 14731 *Ground Improvement by Deep Compaction* (BS1, 2005).

7.1. Recycled aggregates (sustainability)

Natural (primary) aggregate resources are not unlimited within the UK and their extraction causes increasingly unacceptable geo-environmental impacts. As part of achieving environmentally sustainable development within the ground improvement sector, there is an increasing desire to utilise recycled (and secondary) aggregates in vibro stone columns. However, where such materials are considered for use it is important that there are appropriate specifications and quality control/assurance procedures in place to ensure 'fitness-for-purpose' Spent railway track ballast and crushed concrete currently have the greatest potential for this application in the UK and other materials have been investigated. Further information on these aspects can be found in Slocombe (2003) and Serridge (2005) among others.

8. ENVIRONMENTAL CONSIDERATIONS

8.1. Noise and Vibration

Whilst it is rare for noise level issues to be a problem with vibro techniques, vibration levels need to be considered when working close to existing structures and services/ultilities so that these are not adversely affected. The safe working distance which can be adopted will depend on a number of factors including type of ground, the vibroflot power rating, the nature and repair of the structure and also plant access, and particularly if any basement structures are present. However, each situation must be assessed on its own merits and delapidation and precondition surveys should be considered, in addition to appropriate risk assessments and vibration monitoring.

8.2. Contaminants

Appropriate risk assessment and precautions is required on contaminated sites and to avoid exposure to the atmosphere of chemicals and materials such as asbestos, and in accordance with appropriate legislation.

8.3. Vibro concrete plugs

Penetrative ground improvement techniques such as vibro stone columns can generate potential pathways for contaminant migration on brownfield contaminated sites. This raises environmental concerns, particularly if sensitive groundwaters or underlying aquifers are present, due to potential pollutant linkages (i.e. source-pathway-receptor linkages). An innovative approach to address this issue has been the development of 'vibro concrete plug' technology, incorporating the introduction of lean mix concrete into the basal section (toe) of the stone column, thereby isolating any pathways for downward migration of contaminants via the stone columns. Further guidance on pollution prevention in this context can be found in the UK Environment Agency Report NC/99/73 (2001). The above technology has also been utilised to bridge thin peaty deposits within the treated depth.

9. MONITORING, QUALITY CONTROL AND TESTING

Close monitoring of ground response, quality control and testing throughout the duration of the vibro ground improvement works is essential. The majority of vibro stone column projects in the UK involve the support of structures. Therefore, in addition to the monitoring and recording of installation parameters, some form of validation testing using load testing and/or penetration testing, dependent upon soil type, is normally required. Load tests typically include:
- short-term plate load tests;

- zone load tests or skip tests;
- embankment load tests (surcharge load tests).

In essentially granular soils pre and post treatment SPT , CPT or DP (dynamic probing) may be carried out. A useful suitability rating for test methods applied to vibro techniques is provided by Moseley and Priebe (1993).

10.   PRACTICAL ISSUES

There are a number of practical issues to take into consideration in the context of vibro stone column techniques, based upon the UK experience. The more pertinent ones are: Dealing with obstructions - dense granular made ground (fill), obstructions and remnant foundations from previous developments can be an issue in terms of preventing vibroflot penetration and potential for forming hard spots. These should be suitably remediated (e.g. pre-loosening/excavation with removal and/or screening/crushing of oversize granular material before returning to excavation) and with provision of an appropriate cushion of granular material between underside of foundation or ground bearing floor slab and top of buried remnant foundation; Working platforms and stabilised platforms - provision of a safe granular working platform is essential for safe access and execution of vibro ground improvement. Stabilised platforms (lime/cement) can be used, but due consideration needs to be given to implications of 'spragging' of rig tracks and ponding of water in inclement weather, which may necessitate placement of a surface granular layer; Pre-boring - many historic heterogeneous fills in the UK are quite competent, particularly in their uppermost layers. This, together with placement of any engineered/stabilised upfill in advance of vibro ground improvement, can impede vibroflot penetration, necessitating the use of pre-boring. Arisings are/will be generated which then need to be dealt with; Slopes and interceptor drains - for construction at the base of slopes, it is important that there is appropriate drainage at the toes to intercept water draining off the slope, to avoid any detrimental effects on the treated ground; Lateral forces - vibro techniques (vibrocompaction and vibro stone columns) as with driven piling, can generate lateral forces that can act on existing retaining structures, sheet piles and quay walls. Consideration of these effects requires specialist input ; Gas venting - on historic landfill sites, stone columns can actively vent any gases trapped in the fill. Therefore considerataion of provision of gas venting measures may be required follwing appropriate risk assessment; Installation tolerances - Accepted positional tolerances for vibro stone columns are more flexible than for piles and are typically quoted at 150 mm.

11.   CONDITIONS WHERE CAUTION TO BE EXERCISED

Within the UK there are recogonised ground conditions within the ground improvement industry which are either considered not appropriate/suitable for vibro stone column techniques, or where caution should be exercised. Some of the more significant ones are : Excessive degradable materials – on sites where the made ground (fill) contains excessive quantities of degradable domestic refuse, this would decay with time and cause loss of support to the stone columns and hence induce settlement. Generally, where degradable refuse content is less than about 10% (by volume) and fairly evenly distributed, sites can be considered for treatment, but the design approach has to be conservative and whether or not vibro is adopted is dependent upon the building, its function, appropriate risk assessment and also the client's (performance) requirements; Non-engineered recent clay fills – this is a situation where self-weight movement will not be complete. Whilst introduction of stone columns may well improve the situation it is very difficult to control self-weight movements. Typically, significant depths of clay fill (up to 5-8 m) should not be considered suitable for treatment if less than around eight to ten years old. Each site has to be judged on its own merits, however, and with due consideration of settlement performance requirements and any residual self weight consolidation in the clay fill; Opencast mineworkings – a variant on the backfilled clay pit is the backfilled opencast mineworking, where in addition to differential settlement implications for structures spanning the pit edge or buried wall, there is the issue of restoration of the groundwater table (inundation), the timing of which is totally unpredictable. When the groundwater does re-establish itself there is breakdown of the clay fill and further settlement, which can be in excess of self-weight movements. Vibro can be considered if careful attention is given to sealing the tops of the stone columns with clay immediately following their installation and during subsequent foundation excavation by concrete blinding, thus inhibiting surface water ingress due to, for example, heavy rain; Thick peat deposits – thin peat layers can be accommodated (see BRE BR 391 *Specifying Vibro Stone Columns* (2000)). Thickness, depth and lateral variations have to be considered very carefully in relation to the size of foundation and its loading. Situations where peat is at or close to founding level (where stresses will be highest) or at or below the anticipated toe of the stone column(s) should be avoided. On some sites covered by up to 2.0 m of peat, the peat has been excavated along the lines of the foundation

over a 2.0 to 3.0 m width and replaced with granular fill, vibratory stabilisation then being caried out in the normal way.

12. DESIGN OF FOUNDATIONS AFTER VIBRO GROUND IMPROVEMENT

The bearing pressures achievable with vibro techniques are a function of the engineering/geotechnical properties of the soils prior to ground improvement. Slocombe (2001) quotes bearing pressures in the range 50-100 kN/m2 for soft alluvial clays, increasing to values in the range 165-500 kN/m2 in natural sands or sands and gravels. However, each site has to be assessed on its own merits, particularly with regard to post treatment settlements achievable, to ensure compatability with required tolerances for the structure. Following adoption of vibro stone column techniques, conventional shallow pad/strip foundations and ground bearing floor slabs can be adopted, which provides a more cost effective solution, when compared to deep foundation piles, where more robust pile caps and ground beams, together with suspended floor slabs have to be adopted. Because the stone columns are formed by working against the overburden pressure the stone aggregate at the top of the constructed column is not as compact as at depth. For this reason the main load-bearing foundations should be/are typically placed at a minimum depth of 600 mm below the level from which the vibro was carried out in order to fully realise the enhanced performance. In cohesive soils in particular there should be appropriate allowance for minimum top and bottom mesh reinforcement. Levelling off and proofrolling of the sub-grade following completion of vibro ground improvement is normally acceptable prior to construction of groundbearing floor slabs.

13. CONCLUDING REMARKS

Where knowledge of a particular vibro technique is lacking, or there is uncertainty as to the applicability of vibro techniques to a specific set of site circumstances and performance requirements, then specialist advice should be sought to ensure appropriate vibro ground improvement selection/application and specification. Ideally (but dependent upon the specific contractual arrangements) involvement of the Specialist Ground improvement Contractor(s) at an early stage in the design process should be encouraged.

Satisfactory site geotechnical characterisation is essential to facilate satisfactory predictions of vibro ground improvement performance. In order to achieve this it is also important that new developments in site investigation technology such as developments in cone penetration testing (CPT/CPTU) and other investigative tools are embraced, particularly in softer ground.

Vibro techniques are employed in difficult ground conditions. Close monitoring, testing and quality control throughout the duration of the ground improvement works is therefore important, as is rig operator experience.

REFERENCES

Baumann, V. and Bauer, G.E.A. (1974) The performance of foundations on various soils stabilized by the vibro-compaction method. Canadian Geotechnical Journal, 11,pp. 509-530.

British Standards Institution (2005) Execution of Special Geotechnical Works – Ground Treatment by Deep Vibration. London: BSI, BS EN 14731.

Building Research Establishment (2000). Specifying vibro stone columns. BR 391. Garston, UK: CRC.

Clayton, C.R.I.(2001). Managing Geotechnical Risk. London: Thomas Telford, ICE.

Environment Agency (2001). Piling and Penetrative Ground Improvement Methods on Land Affected by Contamination: Guidance on Pollution Prevention. Environment Agency, 2001, NC/99/73.

Hughes, J.M. and Withers, N.J.(1974) Reinforcing of soft cohesive soils with stone columns. Ground Engineering, 7(3), pp. 42-49

Institution of Civil Engineers (1987) Specification for Ground treatment. London: Thomas Telford, ICE.

Killeen, M.M and McCabe, B.A. (2010) A numerical study of factors affecting the performance of stone columns supporting rigid footings on soft clay, Proceedings of the 7th European Conference on Numerical Methods in Geotechnical Engineering. Trondheim (Norway), pp. 833-838.

Mc Kelvey, D., Sivakumar, V., Bell, A., Graham, J. (2004) Modelling vibrated stone columns in soft clay. Journal of Geotechnical Engineering,157 (GE3), Proceedings of the Institution of Civil Engineers, London: Thomas Telford, pp. 137-149

Moseley, M.P. and Priebe, H.J. (1993) Vibro techniques. In Ground Improvement (ed. Moseley, M.P), pp. 1-19, Blackie, Glasgow.

NHBC Standards (2011). Chapter 4.6 Vibratory Ground Improvement Techniques, NHBC, UK.

Powell, J.J.M. and Lunne, T. (2005). Use of CPTU data in clays/fine-grained soils. Proceedings of the Second International Workshop. Studia Geotechnica et Mechanica, Baranowo near Boznan, 23-35 May 2004, Wroclaw University of Technology Vol. XXVII, No. 3-4, pp. 29-65.

Priebe, H.J. (1995) The design of vibro-replacement. Ground Engineering, 28, pp. 31-7.

Serridge C.J. (2005) Achieving sustainability in vibro stone column techniques. Journal of Engineering Sustainability, 158 (ES4), Proc. of the Inst. of Civil Engineers, London: Thomas Telford, pp, 211-22..

Serridge, C.J. and Synac, O (2007) Ground Improvement Solutions for motorway widening schemes and new highway embankment construction over soft ground. Ground Improvement, 11 (4), 219-28.

Serridge, C.J (2008) Site characterization and ground improvement applications for embankment construction over soft ground. In Proceedings of the BGA International Conference on Foundations, Dundee, Scotland, 24-27 June 2008, IHS BRE Press, pp. 1403-14.

Serridge, C.J. and Sarsby, R.W. (2008) A review of field trials investigating the performance of partial depth vibro stone columns in soft clay. Proceedings of the 2nd International Conference on the Geotechnics of soft soils, Glasgow, pp. 293-298.

Slocombe, B.C., Bell, A.L. and Baez, J.I. (2000) The densification of granular soils using vibro methods. Geotechnique, 50(6), pp 715-725.

Slocombe, B.C.(2003) Ground Improvement (nature versus nurture).Ground Engineering,36(5) pp.20-23.

Watts, K.S. and Serridge (2000) A trial of vibro bottom-feed stone column treatment in soft clay soil. Proceedings of the 4th International Conference on Ground Improvement Geosystems – Grouting, Soil Improvement and Geosystems including Reinforcement, Helsinki, June 2000, pp. 549-556.

Effects of Fines on Vibro-compaction

C. H. Wong, AECOM, Hong Kong, herman.wong@aecom.com,
K. C. Yeo, AECOM, Hong Kong, ken.yeo@aecom.com
S. H. Yung, AECOM, Hong Kong, eric.yung@aecom.com
S. J. Liu, CHEC, Peoples's Republic of China, sjliu@chec.bj.cn

ABSTRACT

This paper presents a case study of vibro-compaction ground improvement work on soils with different grain size distribution properties. The project site is located at Suez Canal of Port Said East in Egypt where a container terminal was proposed. The stratigraphies of the proposed site consists of 5 to 6m of hydraulically placed silty sand to sandy silt materials derived from excavations for the nearby Suez Canal by-pass channel over an approximate 5m-thick layer of medium dense to dense, fine to medium naturally occurring sand with many sand-sized shell fragments. This soil stratum became inter-layered with clay at some localized area within the site. The remaining underlying materials at deeper depth were generally very soft to very stiff clayey material with occasional dense to very dense, slightly silty to silty, fine to medium sand.

It is determined that the upper 10m-thick layer site soils are weak and susceptible to liquefaction under design earthquake shaking based on the in-situ pre-CPTs results. In order to prevent liquefaction hazard, soil replacement and vibro-compaction were proposed as the ground improvement measures. The ground improvement works include soil replacement of the upper hydraulic placed soils and vibro-compaction of the replaced soils as well as the underlying liquefiable silty sand layer. The replaced soils are relatively clean granular material with minimum amount of plastic fines, while the underlying silty sand layer consist of about 20% of fines with various plasticity.

Factor of Safety against liquefaction were determined before and after the vibro-compaction to verify improvement. The results indicate that vibro-compaction is an effective mean to increase the compaction of sandy soils while its effectiveness tends to reduce as the fines content of the improved soils increase.

1.　　INTRODUCTION

1.1.　　Project Description

A 1200m long quay wall was proposed in Port Said Container Terminal, Phase 2 extension work along the Suez Canal in Egypt. **Figure 1** shows the site plan of the project. The works majorly included filling and ground improvement works, marine dredging and construction of quay wall and revetment structures.
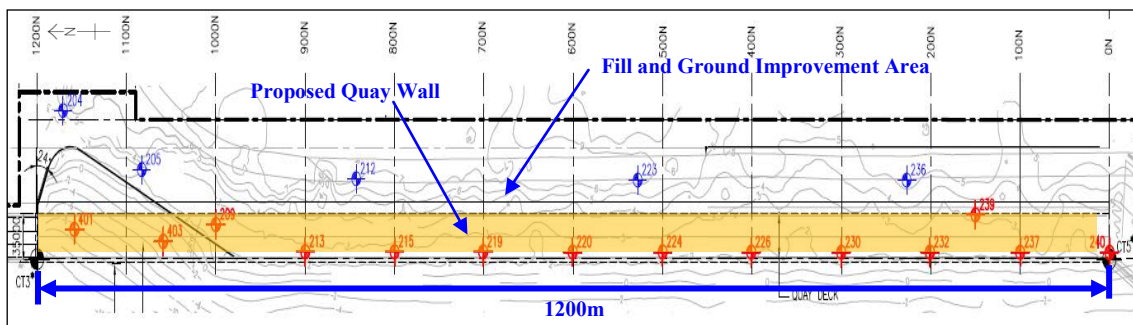
Figure 1 : Site Plan

1.2.　　Site Condition

Based on the available ground investigation information, groundwater table was detected at about 3m below existing ground. Besides, the site soils could be differentiated into 7 soil units down to large depth of more than 70m below the existing ground and are briefly described as follows:

Soil unit 1- Surcharge material placed on the Phase 2 site prior to the commencement of the previous work. The Unit generally comprises of silty sands with shell fragments but may also contain layers of silt and clay. This Unit has been overlain in parts by sands, silts and clays removed from the area of the Phase 1 works during construction over few years back. Thickness varies but generally over 2m.

Soil unit 2 - Hydraulically placed material derived from excavations for the nearby Suez Canal by-pass channels. The Unit variously comprises layers of very soft to soft clay, highly dilatant sandy silt and dilatant silty sand, sometimes with shell bands. Average thickness varies from 5 to 6m.

Soil unit 3 - Generally a medium dense to dense, fine to medium naturally occurring sand with many sand-sized shell fragments with SPT N-value between 19 to 26. The top level of this Unit tends to be deeper and the stratum tends to be thinner towards the south of the Site. The stratum becomes inter-layered with clay in the south. Average thickness varies from 5 to 6m.

Soil unit 4 - An inter-layered deposit of very soft to firm clay, clay/silt and clayey silty fine sand. The Unit is predominantly cohesive. Thickness varies from 3 to 5m.

Soil unit 5 - Consists of a considerable thickness of soft clay which becomes soft to firm and more plastic with depth. Thickness varies from 25 to 40m.

Soil unit 6 - Consists of generally dense to very dense, slightly silty to silty, slightly gravelly, fine to medium sand. Thickness varies and was about 9m.

Soil unit 7- Generally found as inter-bedded layers within Soil Unit 6 and comprises stiff to very stiff, highly plastic clay. Thickness detected over 20m.

The upper 3 types of soil units were involved in the ground improvement works. Based on the liquefaction analysis, soil unit 3 is considered liquefiable during the design earthquake and ground improvement has to be implemented. Details of liquefaction analysis are presented hereafter. In addition, in order to satisfy the requirement of bearing capacity and settlement as required by the project specification, soil units 1 & 2 needed to be improved as well.

2.   APPRECIATION OF PRE-CPTS TO LIQUEFACTION POTENTIALS

2.1.   Methodology

Pre-CPTs had been carried out at 25m interval grids over the site. Liquefaction analysis had been performed in accordance with Youd et. al. (2001) on the liquefaction potentials of the upper soils layers down to the bottom of soil unit 3 based on the pre-CPT results. The analysis adopted factors of safety of 2.0 and 1.25, depends on the tolerance of ground deformation effect associated with liquefaction. The results of liquefaction analysis are summarized in Figure 2 with highlighted results at CPT locations (with thickness of 0.2m as a unit) where are considered to be susceptible to liquefaction risk.

Based on the worst case of the analyses, the tentative improvement level of vibro-compaction for the intended area, which should not be more than 1m above the lowest level of liquefiable soil unit 3, is summarized as follows and is shown in Figure 2 (for part area showed as an example).

It has been observed in some of these pre-CPT results that unreasonably high porewater pressures (as large as about 1.6MPa) were detected in the sand layer (with friction ratio equals to about 1.0) at approximately 4m below the existing ground. In order to eliminate the re-occurrence of such inconsistency to the parameters (i.e. q_c, u and R_f), post-CPTs are to be carried out after the soil improvement works and results are to be closely monitored.
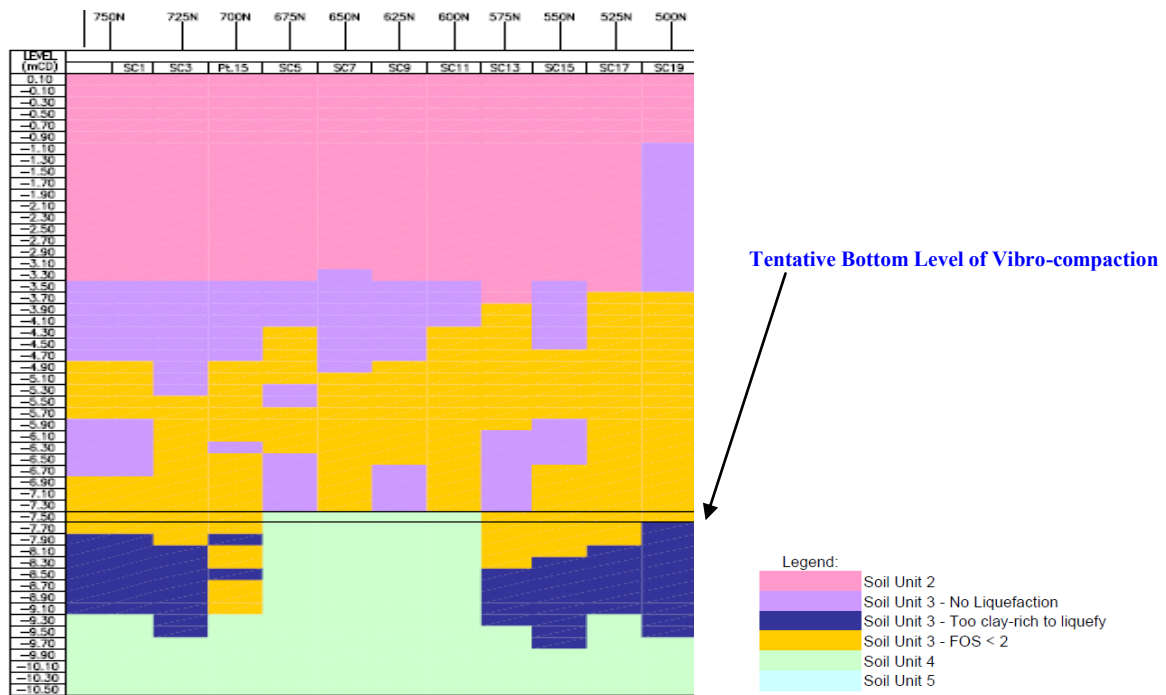
Figure 2: Summary of tentative improvement level of vibro-compaction, based on worst case of analysis

2.2. Results of Liquefaction Potential Analyses by Pre-CPTs

2.2.1. Pre-CPTs (N850-N500)

Four pre CPTs had been first carried out between N850 to N750, namely PRE-SC27A to PRE-SC30A. Twenty Pre-CPTs have been carried out between N750 and N500 at 25m spacing. The Pre-CPTs have been carried out at ground level between +1.74mCD to +3.17mCD, with ground water level located at +0.45mCD. The Pre-CPTs have been carried out to depth ranges from 8.6m to 14m. The locations of the Pre-CPT points, namely PRE-SC1 to PRE-SC20, are as shown in **Figure 3**.
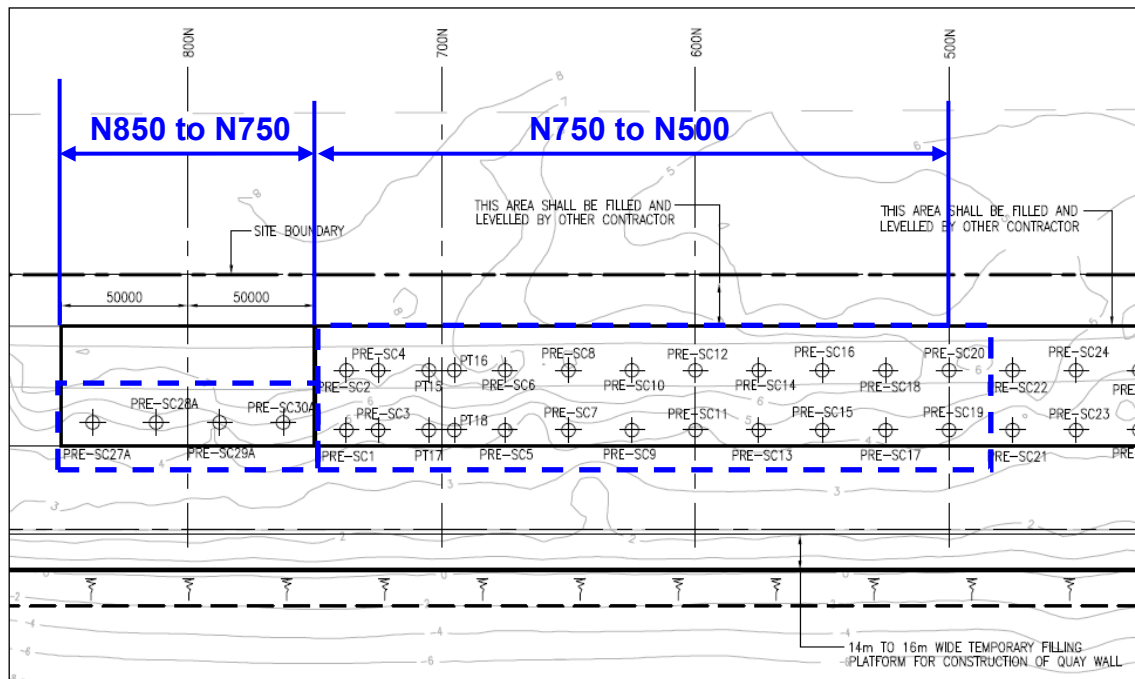
Figure 3: Summary Locations of the Pre-CPT points

The objective of carrying out these tests was to determine the depth of soil unit 3 where the factor of safety may fall below 2 with respect to the risk of liquefaction and hence, the maximum depth where soil improvement had to be carried out to eliminate this risk. Typical Results of PRE-SC27A to PRE-SC30A are shown in Figure 4. Interpretaion of the data can also be referred to as in Figure 5, using CPT classification diagram based on Robertson et al. (1986).
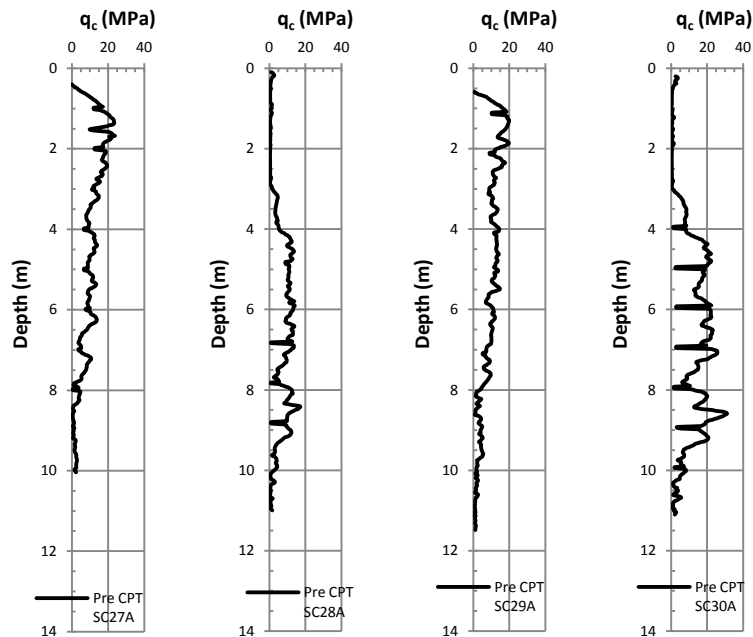
Figure 4: Typical Results of Pre-SC 27-30
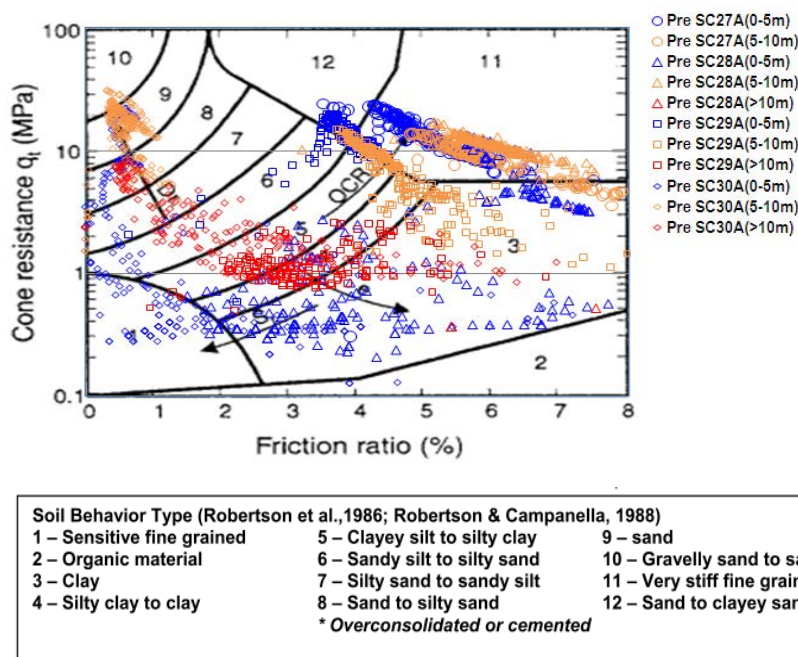
Figure 5: Classification Plot by CPT, based on qt and FR (Robertson et al., 1986)

It can be shown from Figure 5 that the top 5m of the soils are stiff fine grained sand to clayey sand. The underlying soils are mixed layers of silty sand, clayey silts and silty clay extending to over 15m below ground level.

3. GROUND IMPROVEMENT WORKS

3.1. Proposed Ground Improvement Scheme

The proposed ground improvement scheme involved replacement of soil units 1 & 2 by suitable fill from formation level to an acceptable depth, where the SPT 'N' value had been found adequate.

Soil replacement has been carried out for the upper layer of clayey silts with granular soils and vibro-compaction at 1.5m centre to centre spacing was conducted for the replaced soil and the liquefiable soil below down to the interface layer between soil unit 3 and soil unit 4.

3.2. Soils Compactability

Due to the relatively "clean" nature of the adopted suitable fill material, the compactibility of the suitable fill is not evaluated. In order to estimate the applicability of vibro-compaction to soil unit 3, its particle size distribution based on the laboratory test data were plotted against the typical range of compactable soils as shown in Figure 6 below.
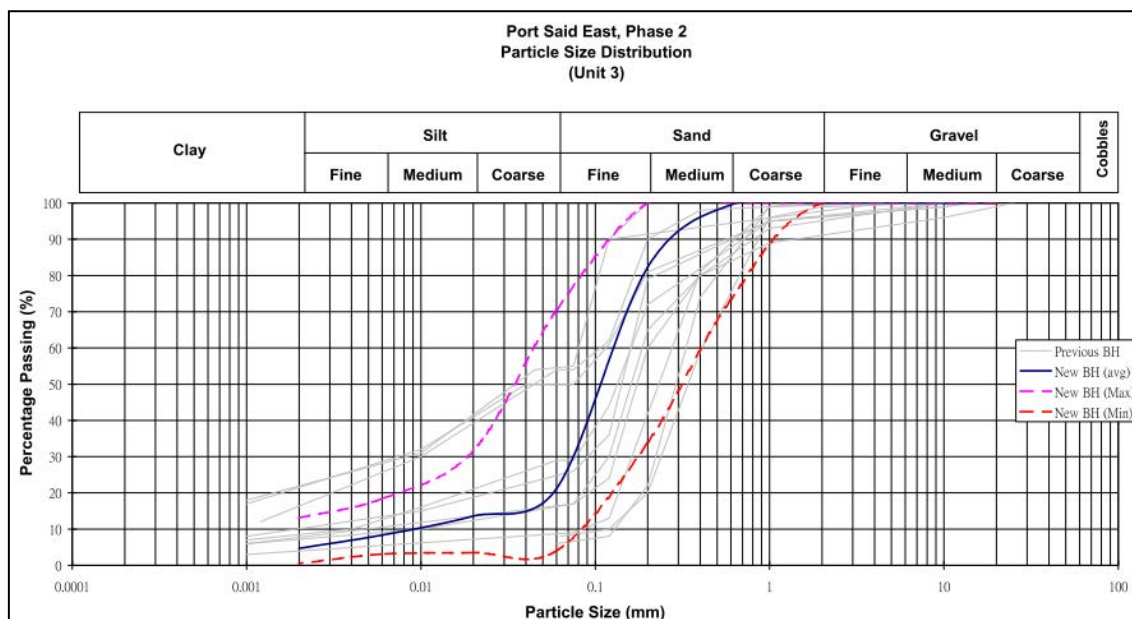
Figure 6: Particle Size Distribution of Soil Unit 3

It was found that the fines content of soil unit 3 was about 20%. Therefore, it was anticipated that soil unit 3 may not be effectively compacted by vibro-compaction. However, since the soil unit 3 required only small improvement to satisfy the required factor of safety against liquefaction, vibro-compaction was adopted to the bottom of the soil unit 3.

4. APPRECIATION OF POST-CPTS TO LIQUEFACTION POTENTIALS

4.1. Verification of Ground Improvement Scheme (initial section N750-N550)

Post-CPTs were carried out at 25m spacing after more than 1-2 weeks of completion of the ground improvement works, to verify the effect of the ground improvement works. Locations of the Post CPTs are shown in Figure 7. Typical Pre-CPTs & Post-CPT results are as shown in Figure 8. The Pre-CPTs includes CPT Nos. PRE-SC2, SC4, SC6, SC8, SC10, SC12 and SC14. The Post-CPTs includes CPT Nos. CPT-1, 2, 3b, 4, 5, 6, 7. Figure 9 shows a typical set of CPT results of Pre-CPT No. PRE-SC15 and Post-CPT No. CPTc for further elaboration.

It can be observed from Figure 8 that the soil improvement as resulted from the vibro-compaction for the top few meter of replaced soils has been very significant and the effect has gradually reduced with the extended depth of the granular sand layer (e.g. soil unit 3). The effect has become insignificant at the lower depth below the granular sand layer which has been considered as the interface layer between the upper granular soil layer and the lower cohesive soil layer (e.g. soil unit 4).

Figure 9 showed some inconsistent pre-CPT results of Pre-CPT SC15 that unreasonably high porewater pressures was detected in the sand layer. The post-CPTc results showed that the sand layer has not been improved significantly even after vibro-compaction has been carried out. For such situation, re-densification has been proposed to rectify the situation.
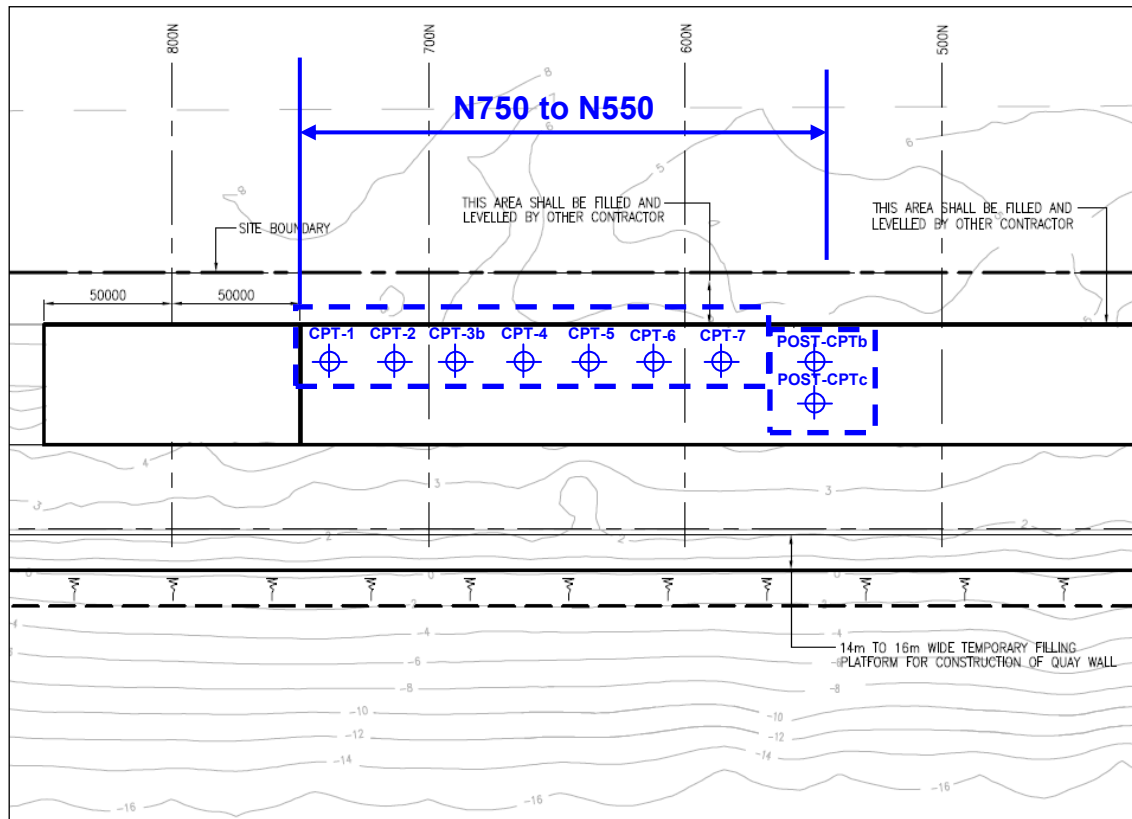
Figure 7: Locations of the Post-CPT points
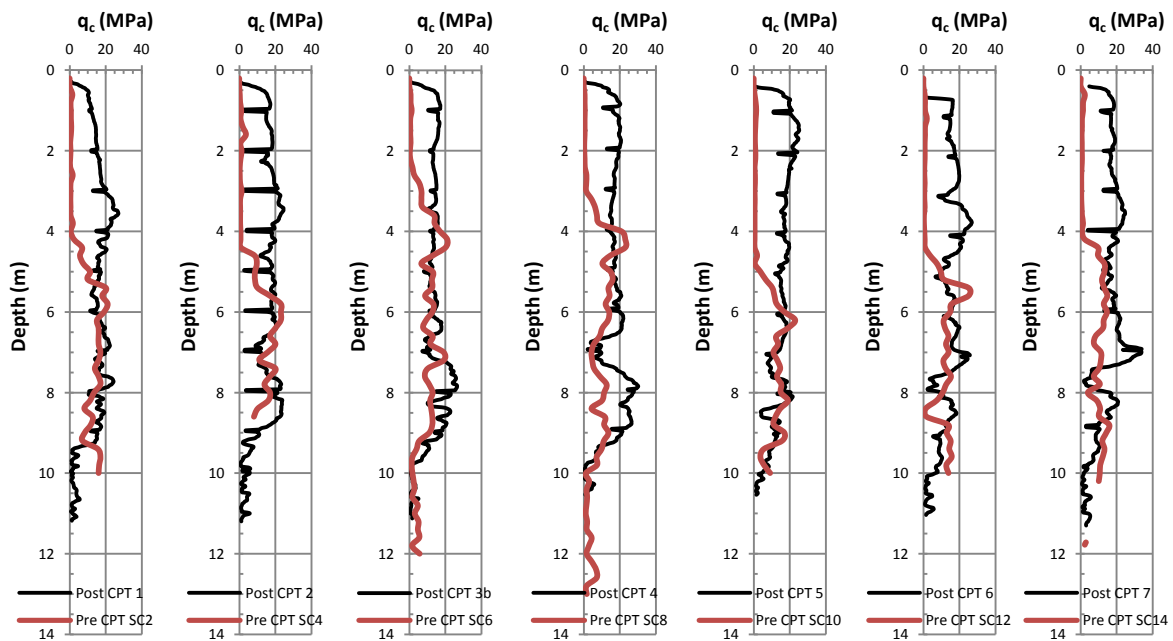
Figure 8: Pre-CPT and Post-CPT results near N750 and N550 before and after improvement implemented
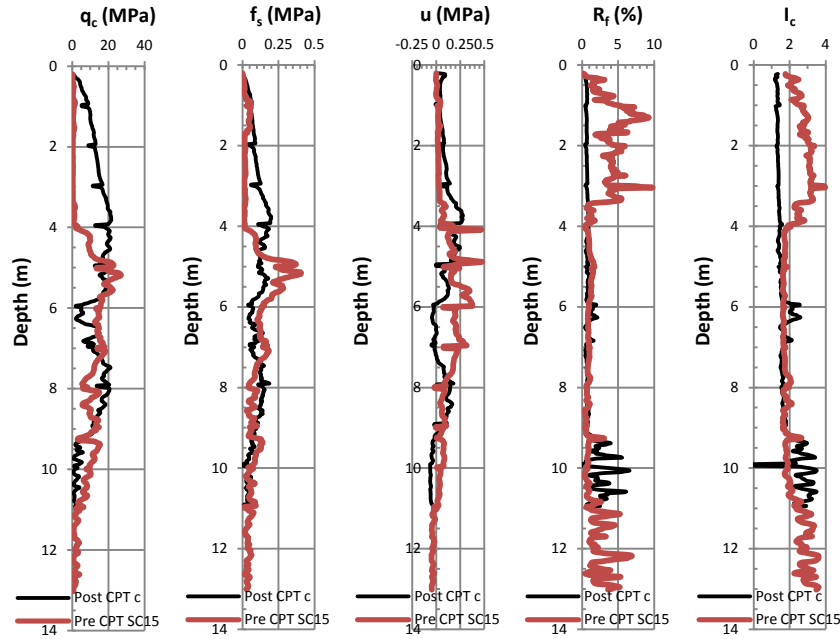
Figure 9: CPT results q_c, f_s, u and R_f of PRE-SC15 and POST-CPTc

5. COMPARISON OF PERFORMANCE

5.1. Replaced soil layers (where fines < 5%)

Base on Figure 8, major improvement of CPT tip resistance were observed after the soil was replaced by the relatively clean sandy fill (to about 4 to 4.5m below ground level) together with vibro-compaction. The improved tip resistance can achieve up to about 20MPa which ensures adequate resistance to liquefaction.

5.2. Existing soil unit 3 (where fines ~ 20%)

Improvement of tip resistance observed in the upper portion of soil unit 3 from about 4.5 to 7.5m below ground level where fines content are considered to be relatively high has not been very significant. Thin layer of liquefiable soils may exist due to the variation of fines content within the soil unit, but only exists in localized manner. Moreover it is clear that the sand layers above or below this thin layer are being improved by the vibroflotation process to achieve sufficient strength to comply with the required safety factor.

5.3. Interface of soil unit 3 & unit 4 (where fines exceed 40%)

Transition between soil unit 3 and soil unit 4 exists at level below -7.5mCD to about 9m below ground level (the level may vary at different locations) where ground improvement was proved to be less effective due to the increase in fines content contributed by soil unit 4. From the pre-CPTs data, the original materials had been classified as too clayey to liquefy.

6. DETAILED ANALYSES AND OBSERVATIONS

6.1. Using CPT Trend of changes in Ic

Robertson and Wride (1998) proposed that the Apparent Fines Content (FC) of soils may be estimated by the Soil Behavior Type Index (I_c). The determination of I_c is based on the equation below:

$$I_c = \left[(3.47 - Q)^2 + (\log(F) + 1.22)^2 \right]^{0.5} \tag{1}$$

Where Q is the normalized tip resistance and F is the normalized friction ratio.
Robertson and Wride (1998) suggested a simplified relationship between I_c and (FC %) as follows:

if $I_c < 1.26$ apparent fines content FC (%) = 0   (2)

if $1.26 \le I_c \le 3.5$ apparent fines content FC (%) = $1.75I_c^{3.25} - 3.7$ (3)

if $I_c > 3.5$ apparent fines content FC (%) = 100   (4)

Base on the above relationship, the CPT trend of the soil before and after the improvement by vibro-compaction is compared by plotting improvement index (i.e. q_c of Post-CPTs / q_c of Pre-CPTs) against I_c index.

In Figures 10 and 11, the improvement index against I_c plots of these depth ranges are plotted in different legends. Figure 10 shows the plot for Post-CPT-1 & Pre-SC3 and Figure 11 shows the plot for Post-CPTb & Pre-SC18.

It indicated that at fines content less than 15% (in contrast to a recommended value of 10% in practice), the soil improvement resulted from the vibro-compaction process can impose significant improvement of the soil strength of an average range of 1.5 to 2 times. No improvement can generally be made for soils where fines content are high, say over 20-25%.
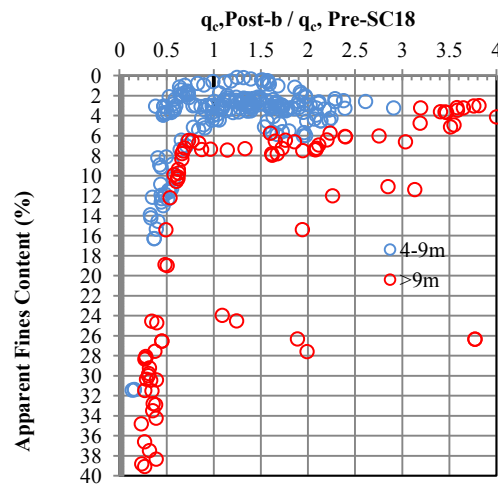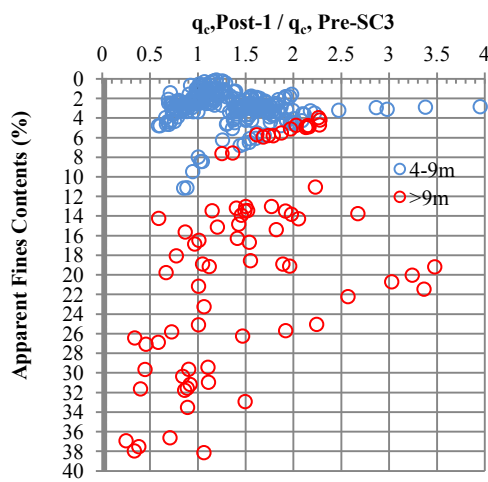
Figure 10: Improvement Index vs I_c , Post-CPT-1 & Pre-SC3

Figure 11: Improvement Index vs I_c , Post-CPTb & Pre-SC18

In order to understand the results of Pre-CPT SC15 and post-CPT c, Figure 12 has been plotted to detect the migration of fines before and after vibro-compaction. Based on Figure 12, the fines content of soils depth of 4 – 9m and at depth lower than 9m generally increased after the vibro-compaction. These may be due to the mixing effect of the vibro-probe during the ground improvement along the entire soil column for the interclay layer between the sand layers. As fines increase, the soil layers would become too clay to liquefy for the analysis.
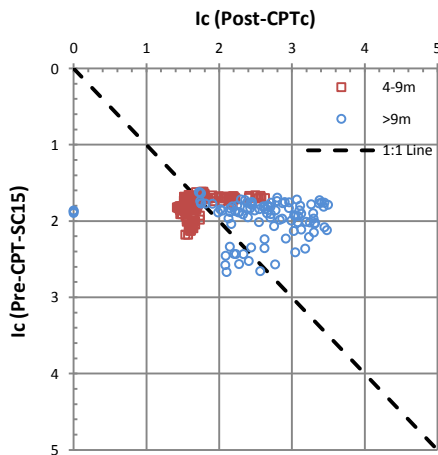
Figure 12: I_c value of POST-CPTc vs PRE-SC15

7.   CONCLUSIONS AND RECOMMENDATIONS

Liquefaction potential was determined before and after the vibro-compaction to verify improvement. The results indicate that vibro-compaction is an effective mean to increase the compaction of sandy soils while its effectiveness tends to reduce as the fines content of the improve soils increase.

Based on the CPT results, the liquefaction hazard was mitigated for the entire soil column. For soil unit 3 with less fines content, the soil was improved by densification effect provided by vibro-compaction. For soil unit 3 with more fines content or soils within the transition zone between soil unit 3 and soil unit 4, fines migration from the upper soils occurred and increased the fines content of the soil which have an effect to reduce the liquefaction risk.

REFERENCES

Youd et. al. (2001). "Liquefaction resistance of soils: summary report from the 1996 NCEER and 1998 NCEER/NSF workshops on evaluation of liquefaction resistance of soils", Journal of Geotechnical and Geoenvironmental Engineering, 127, 817-833.

Robertson. P.K., and Wride, C.E., 1998. "Evaluating Cyclic Liquefaction Potential Using The Cone Penetration Test" Canadian Geotechnical Journal, 35(1): 442-459

Robertson. P.K., Campanella, R.G., Gillespie, D., and Greig, J., (1986). "Use of Piezometer Cone data", In-Situ'86 Use of In-situ testing in Geotechnical Engineering, GSP 6 , ASCE, Reston, VA, Specialty Publication, pp 1263-1280.

Stone Column and Vibro-compaction of Soil Improvement for liquefaction

K. C. Yeo, AECOM, Hong Kong, ken.yeo@aecom.com
S. H. Yung, AECOM, Hong Kong, eric.yung@aecom.com
S. J. Liu, CHEC, People's Republic of China, sjliu@chec.bj.cn

ABSTRACT

This paper describes the site trials using stone columns and vibro-compaction to improve the ground performance against liquefaction potentials for site with sandy soils overlaid by clayey silts and assesses the effectiveness of both the methods using CPT analysis. Pre-CPTs were first conducted to determine the depth of soil where factor of safety fall below accepted limit, therefore the maximum depth where soil improvement has to be carried out to eliminate this risk. Two methods of improvements for trial were considered:(i)soil replacement for the clayey silts with granular soils and vibro-compacted the replaced soil and liquefiable soil underneath at 1.5m spacing;(ii)install stone columns with stone replacement ratio of 20% of 900mm in diameter and of 1.8m spacing, directly on the clayey silts and penetrate into the sandy soil layer. Two types of verification tests are carried out to check for compliance:(i)Post-CPTs to be conducted at centroids of the areas between the vibro-compaction or stone columns;(ii)Plate load tests (PLTs) on each trial area at 2 times of applied load of 75kPa, with measurements of load and deformation. The results of the verification tests are then compared and comments made on the effectiveness of both the methods. Some experiences of difficulties encountered in the construction work during the trial of both the improvement methods are presented. The paper concluded that the soil replacement with vibro-compaction method, for this particular site conditions, is more effective than the stone columns method. It indicated that stone columns, when installed in weak cohesive soil layer, may not be effective in mitigating the risk of liquefaction.

1.   INTRODUCTION

Ground improvement has been required to provide a continuous stable platform behind the quay wall constructed for Port Said Container Terminal, Phase 2 extension work of Egypt. Two methods of ground improvement were selected for trial, namely:

(i) Soil replacement for the upper layer of clayey silts with granular soils and vibro-compacted the replaced soil and the liquefiable soil below at 1.5m spacing;

(ii) Installation of stone columns with 900mm in diameter and 1.8m spacing (approximately with stone replacement ratio of 20%) directly on the upper clayey silts and penetrated into the liquefiable sandy soil layer below.

The objective of the work is to ensure that the improved ground is capable of supporting the required loads arising from the permanent works without liquefaction under all operating conditions, including the design earthquake for the site. In addition the settlement should be minimized to comply with the contract requirements.

Site trials were therefore carried out in testing areas selected with critical site conditions to determine the optimized configuration. Pre-CPTs and post-CPTs were conducted in the area before and after ground improvement to obtain cone resistance and to verify the effectiveness of the ground improvement work against liquefaction. Plate load tests (PLTs) were also conducted on the trial areas to 2 times of applied load (i.e. 2 times 75kPa) to assess the load-settlement characteristic of the improved ground for compliance.

2.   SITE CONDITIONS

Based on the available ground investigation information, the division of the level and thickness of each soil units as described on the borehole logs has been summarized in Table 1. Figure 1 shows the site plan with borehole locations.

It should be noted that the improved ground as specified in the contract should mean units 2 & 3 soils, in particularly unit 2 soils as it is basically sand silts with fines range from 25% to 65% and part exhibits high plasticity.

It was considered that partial removal of unit 2 soils down to an acceptable depth where the SPT 'N' value has been found adequate and replacement with suitable fill to formation level with vibro-

compaction may be the most effective means of ground treatment, particularly within the zone of lateral earth pressure on the quay wall.

Where the depth has been found unacceptable for soil replacement, vibro-stone column is to be considered for improving unit 2 soils and possible liquefiable unit 3 soils to meeting performance requirements of the specification.

Table 1: Soil units described on the borehole logs:

Type	Average Thickness (m)
Unit 1: Surcharge fill (as placed from Phase 1 work)	1.8
Unit 2: Hydraulically placed materials (with inter-layered of soft clay , sandy silt, dilatant silty sand, sometimes with shell bands)	4.5
Unit 3: Naturally deposited sand layer (inter-layered with clay)	5.1
Unit 4: Inter-layered soft to firm cohesive clay (with silty fine sand)	3.9
Unit 5: Soft to firm plastic clay	34.8
Unit 6: Dense to very dense, silty gravelly fine sand	7.9
Unit 7 Stiff to very stiff highly plastic clay inter-bedded within Unit 6	>19m
Ground water level generally located between: (applicable only at time of drilling)	3m below ground level
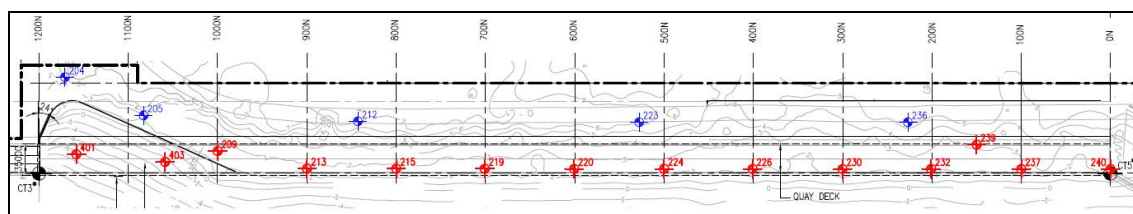
Figure 1: Site Plan

3.   DETAILS OF SITE TRIALS

The site trials are carried out at locations N400 and N560. Location N400 is a critical location where only soil unit 2 (and no soil unit 3) has been identified, and location N560 is a typical location with unit 2 soils that can be removed and replaced.

The size of the trial area for location N400 is designated to be 30m length x 12m width, with stone columns installed to -7.5mCD (tentative) from formation level of +2.5mCD. The final installation depth would be verified by pre-CPTs.

The size of the trial area for location N560 is designated to be 30m length x 15m width, with soil replacement with vibro-compaction implemented. The ground improvement measure comprises the removal of units 1 and 2 soils and replacement with suitable backfill to finished level. The fill and any unit 3 soils which is liquefiable will then be compacted by vibro-flotation for the area.

For each of the two selected site trial areas located at N400 and N560, pre-CPTs were carried out, namely PT11 to PT14 and Pre-SC15 to Pre-SC16. The penetration depth of the CPTs should be at least 1m into unit 4 soils. The location of the trial areas and the pre-CPT locations are as shown in Figure 2.

To verify the effect of the improved ground, post-CPTs were carried out about 3 days after completion of the ground improvement work, which is earlier than is normally recommended but which was done at this time to obtain an early indication of the improvement gained. Field compaction were carried out at top 2m of the backfill (above the ground water table), with additional PLTs of size 1.8m diameter carried out on each trial area to 150kPa (i.e. 2 times of applied load of 75kPa), with measurements of loads and deformations were also undertaken. The location of the trial areas and the post-CPT locations are as shown in Figure 3.
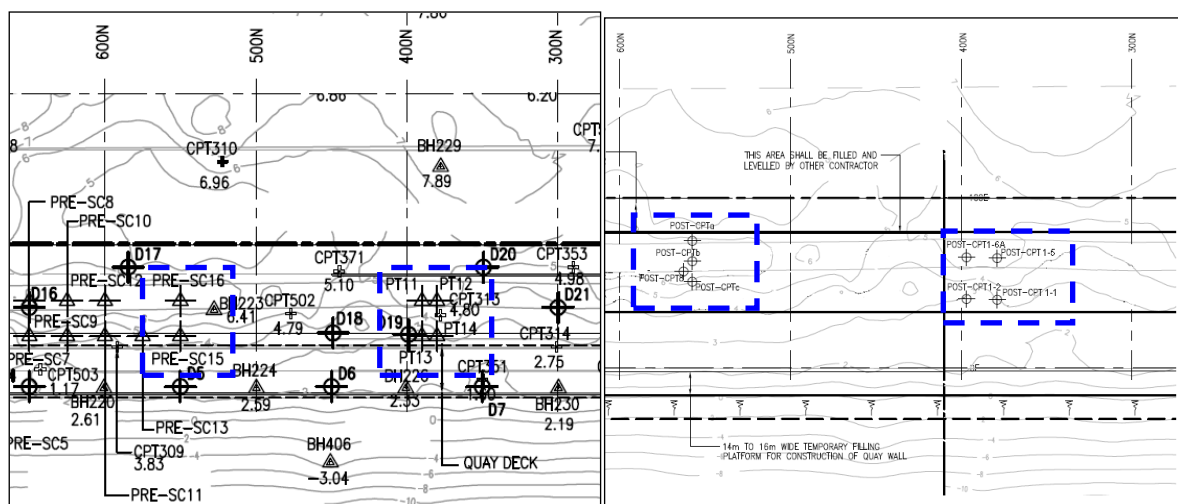
Figure 2: Pre-CPT carried out in the selected site trial areas

Figure 3: Post-CPT carried out in the selected site trial areas

4.   APPRECIATION OF PRE-CPTS TO LIQUEFACTION POTENTIALS

4.1.   Analysis on liquefaction potential

Liquefaction analysis has been carried out in accordance with Youd et al (2001) on the liquefaction potentials of the units 2 & 3 soils, using the pre-CPT results. The analysis is taking factors of safety of 2.0 and 1.25 for different application and highlighted results with CPT location (with thickness of 0.2m as a unit) which are considered to be susceptible to liquefaction risk.

4.2.   Results of analysis on liquefaction potential by Pre-CPTs

4.2.1   Zone at N400 of proposed stone columns

The results showed that for Pre-CPTs of point nos. PT11 & PT12 (at stacking area), if a factor of 1.25 is adopted for liquefaction assessment, it may be possible to replace unit 2 soils at 0mCD (where groundwater level is located at +0.5mCD) as unit 4 soils have been detected underneath by the CPT results. Therefore no stone columns are to be sunk.

The results also show that for Pre-CPTs of point nos. PT13 & PT14 (at area behind the quay wall), if a factor of 2.0 is adopted for liquefaction assessment, it is likely that the stone column are to be sunk to depth of -7.5mCD, seating on a thin layer of unit 3 soils of about 2m thick, before reaching unit 4 soils.

4.2.2   Zone at N560 of proposed soil replacement with vibro-compaction

Pre-SC15 and Pre-SC16 are the closest Pre-CPT to the selected section. The bottom level of unit 2 soil at the typical section is located at about -1.5mCD and sandy material is used to replace units 1 and 2 soils.

Based on the liquefaction assessment of Pre-CPTs, the ground treatment depths are estimated to be at approximately -9mCD (into liquefiable unit 3 soils before reaching unit 4 soils) in order to eliminate the resik of liquefaction to required standards.

5.   APPRECIATION OF POST-CPTS TO SOIL IMPROVEMENT

5.1.   Ground improvement by stone columns

The selected method of stone column using stone replacement ratio of 20% (initially) has been implemented for N400, with the diameter of the stone columns taken as 900mm with centre to centre spacing of 1.8m.

The installation was carried out by firstly excavate the existing ground level to +1.5m CD, and deposit a 1m thick granular filling material on top, then sunk the vibration probe with stone to -7.5mCD.

Post-CPT results, taking factors of safety of 2.0. The CPT results at the selected test locations, namely 1-1, 1-2, 1-5 and 1-6A (for N400). It is shown that the ground improvement by stone columns has limited effect on the q_c value of the improved soil. The factors of safety of the soil didn't reach the 2.0 requirement.

Typical Pre-CPT and Post-CPT results are shown in Figure 4(a) and 4(b).

5.2. Ground improvement by replacement and vibro-compaction method

The ground improvement measure comprises the removal of unit 1 and 2 soils and replacement with suitable backfill to finished level. The fill and any unit 3 soil which is liquefiable will then be compacted by vibro-flotation for the area.

In order to demonstrate the efficiency of vibro-flotation, typical section located approximately at N550 to N565 was selected to carry out the 4 Post-CPTs (Post-CPTs a, b, c and 8) between 28 February 2010 and 1 March 2010 which is about 4 days after completion of the ground improvement work, which is earlier than is normally recommended but which was done at this time to obtain an early indication of the improvement gained.

Typical Pre- and Post-CPT results are shown in Figure 5(a) and 5(b).
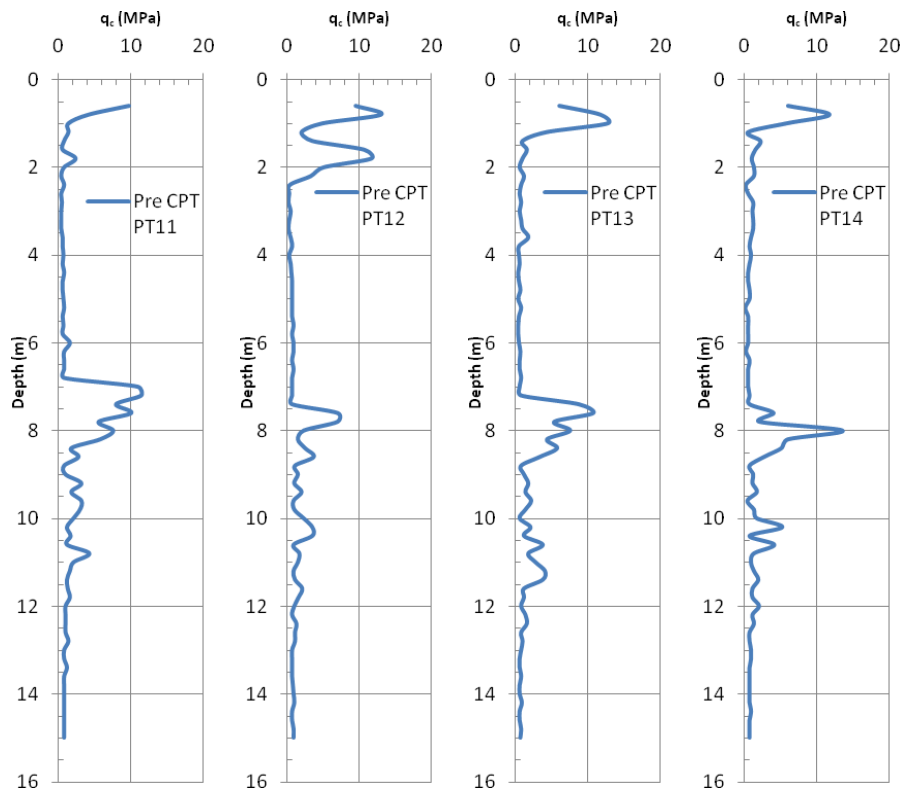
Figure 4(a): Pre-CPT results in Zone at N400 before improvement implemented
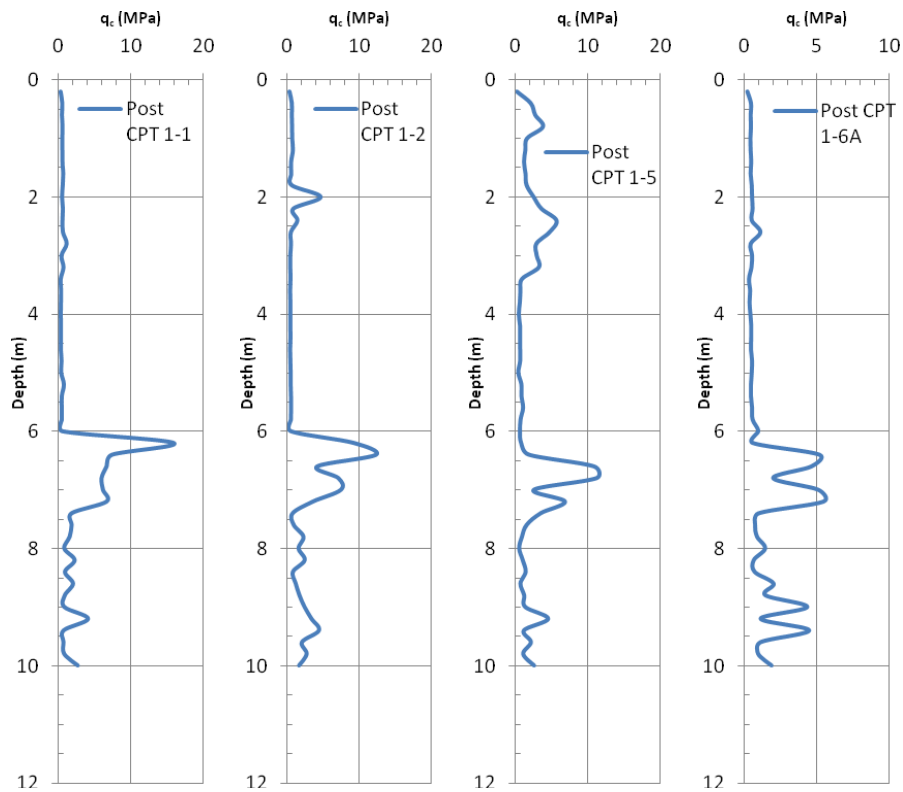
Figure 4(b): Post-CPT results in Zone at N400 after improvement implemented
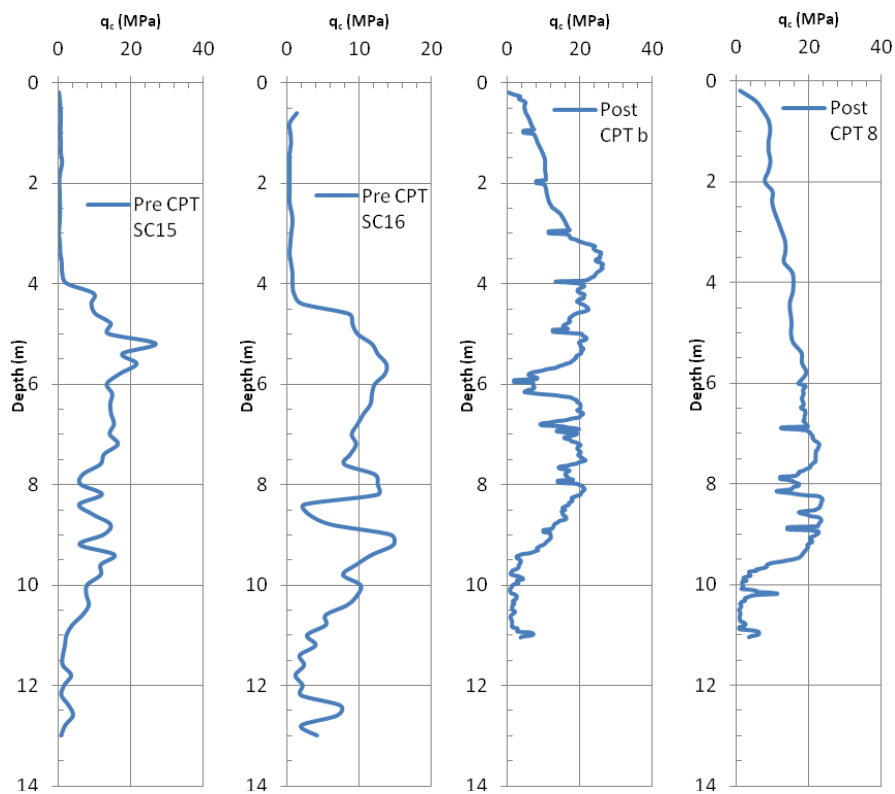
Figure 5: Pre-CPT and Post CPT results in Zone at N560 before and after improvement implemented

5.3.   Analysis on liquefaction potential

The analysis of the liquefaction is based on Youd et al (2001), using CPT results. The analytical procedures are as outlined in Appendix A for easy reference.

From Figures 4(a) and 4(b) and the analyses using the Post-CPT results, it can be noted that the Post-CPT 1-1, 1-2, 1-5. 1-6A showed there are localized liquefiable soil layer, located in unit 2 soils (Clayey material), and the soils are mainly too clayey to liquefy (this is as highlighted in part analysis of the post-CPT results of 1-6A using the methodology of Appendix A referred in Appendix B1).

Drainage path would be the major mechanisms for stone columns to mitigate liquefaction but not surrounding soil densification. However, drainage path is very difficult to assess as the permeability of the unit 2 soils cannot be quantified and in addition, the stone column may be clogged during the design life of the structure. Therefore it is concluded that the proposed ground improvement using stone columns is not very effective from the test results obtained. Photo 1 showed the water logging of the stone column immediately after construction.

In contrast, from Figures 5(a) and (b) and the analyses using Post-CPT results, it can be concluded that the proposed ground improvement of soil replacement with vibro-flotation is effective. As indicated, the vibro-flotation completely eliminated the liquefaction risk for the backfill material (this is as highlighted in part analysis of the Post-CPT results of CPT-8 using the methodology of Appendix A referred in Appendix B2). Photo 2 showed the operation of vibro-compaction in action.

Major improvement was identified in soil unit 3. Thin layer of liquefiable layer may exist due to the variation of fine contents within the layer. However, this layer is insignificantly thin and only exist in localized manner. Moreover it is clear that the sand layers below this thin layer are being improved by the vibroflotation process.

Transition between soil unit 3 and soil unit 4 exist at level below -7.5mCD (the level may vary at other ground improvement locations) where ground improvement is proved to be less effective due to the increase in clay content contributed by soil unit 4. From the Pre-CPTs data, the original materials had been classified as too clayey to liquefy.

| *Photo 1 : Water logging of stone column* | *Photo 2: Operation of vibro-compaction in action* |

6.   COMPARISON OF PERFORMANCE

To ensure if the improved ground is capable of supporting the required loads arising from the permanent works, plate load tests were carried out to determine the load-settlement behaviour of the ground.

The analysis based on FHWA (1993) indicated that for the stone columns under the applied load of 150 kPa would have a FOS of 1.2 under drained condition (ϕ' of 33 degrees) and would failed under undrained condition (S_u of 20kPa) for single column checks and end bearing.

Plate load test for compliance subsequently conducted indicated that the stone column exhibited excessive vertical settlement of about 50mm at 2 x 75kPa loads. Photo 3 shows excessive deformation of the improved ground during plate load test. This is evidently caused by lacking of confining pressure of the surrounding soils.

In contrast, the ground improved by soil replacement and compacted over the top 2m of soils satified the plate load test requirement with vertical settlement within the 25mm limits at 2 x 75 kPa loads.

7.   CONCLUSIONS AND RECOMMENDATIONS

The stone column sunked into sandy silts has not been able to dissipate pore water effectively and cause pore water to be logged in the columns (as showed in Photo 4 of the excavated stone column 2 weeks after construction). Lacking of effective drainage path has caused the surrounding soils incapable of proper consolidation, therefore increasing the confining pressure to eanble the efficienfy of stone column for improving the bearing capacity.

The trials demonstrated that soil replacement with vibro-compaction can be an effective means over the use of vibro-stone columns over sandy silts, with respect to both increasing load besring capacity and mitigating risk to liquefaction.

Photo 3 : Excessive vertical displacement of the improved ground during plate load test

Photo 4 : Excavated stone column 2 weeks after construction

REFERENCES

FHWA (1983). "Design and construction of stone columns, Volume I", FHWA/RD-83/026.

Youd et. al. (2001). "Liquefaction resistance of soils: summary report from the 1996 NCEER and 1998 NCEER/NSF workshops on evaluation of liquefaction resistance of soils", Journal of Geotechnical and Geoenvironmental Enginering, 127, 817-833.

APPENDIX A: ACCEPTANCE PROCEDURE FOR CPTS ASSESSMENT WRT LIQUEFACTION POTENTIALS OF SOILS

Procedure

The analytical procedures are outlined as follows:

1   Obtained CPT data (i.e. cone tip resistance, q_c and sleeve resistance, f_s)

2   Obtain normalizing factor for cone penetration resistance, $C_Q = (P_a/\sigma'_{vo})^n$.

    - use P_a = 1 atm and n = 1.0

3   Normalize q_c with C_Q and determine $Q = [(q_c - \sigma_{vo}) / P_a] [(P_a/\sigma'_{vo})^n]$

4   Determine $F = [f_s / (q_c - \sigma_{vo})] \times 100\%$

5   Determine Soil Behavior Type Index, $I_c = [(3.47 - \log Q)^2 + (1.22 + \log F)^2]^{0.5}$

    For $I_c > 2.6$, the soil is classed as "Too clay-rich to liquefy".   [Analysis Complete]

    - Chinese Criteria might be applied to confirm soil is non-liquefiable

    For $I_c < 2.6$, the soil is classed as "Sandy Material". Re-calculate $C_{Q (new)}$ [Refer to Step 6]

    - use P_a = 1 atm and n = 0.5

6   Normalize q_c and f_s with the re-calculated $C_{Q (new)}$

7   Re-determine $Q_{(new)}$ and $F_{(new)}$ using n = 0.5 and determine the $I_{c (new)}$

    For $I_{c (new)} < 2.6$, the soil is classed as "Non-plastic and granular". Calculate   [Refer to Step 12]
$CRR_{7.5}$

    For $I_{c (new)} > 2.6$, it is classed "Silty and possibly plastic". Recalculate $C_{Q (Inter)}$ [Refer to Step 8]

    - use P_a = 1 atm and n = 0.7

8   Normalize q_c and f_s with the re-calculated $C_{Q (Inter)}$

9   Re-determine $Q_{(Inter)}$ and $F_{(Inter)}$ using n = 0.7 and determine the $I_{c (inter)}$ [Refer to Step 12]

10   Determine Cone Penetration Resistance, $q_{c1N} = C_Q (q_c / P_a)$

11   Normalize q_{c1N} with Correction Factor for grain characteristics, K_c; $(q_{c1N})_{CS} = K_c q_{c1N}$

    Determine K_c based on either $I_{c(new)}$ or $I_{c(Inter)}$

    For $I_c \leq 1.64$, Kc = 1.0

    For $I_c > 1.64$, $K_c = -0.403I_c^4 + 5.581I_c^3 - 21.63I_c^2 + 33.75I_c - 17.88$

12   Determine
$CRR_{7.5}$

    For $(q_{c1N})_{CS} < 50$, $CRR_{7.5} = 0.833 [(q_{c1N})_{CS} / 1000] + 0.05$

    For $50 \leq (q_{c1N})_{CS} < 160$, $CRR_{7.5} = 93 [(q_{c1N})_{CS} / 1000]^3 + 0.08$

    For $(q_{c1N})_{CS} > 160$, the soil is "Non-Liquefiable"

13   Obtain $CSR = 0.65(a_{max} / g) (\sigma_{vo} / \sigma'_{vo}) r_d$

    The horizontal acceleration is taken as 0.12g.

    The soil factor is taken conservatively as Type D (refer to Table 3.1of EN1998-1:2004) with S =1.35 (refer Table 3.2of EN1998-1:2004), where Type D is defined as "Deposits of loose to medium cohesionless soil with or without cohesive layers or of soft to firm cohesive soils". Peak horizontal acceleration a_{max} = 0.12g x 1.35 = 0.162g.

    For $z \leq 9.15m$, r_d = 1.0 - 0.00765z

    For $9.15m < z \leq 23m$, r_d = 1.174 - 0.0267z

14   Determine Factor of Safety, $FOS = CRR_{7.5} / CSR$

    When FOS > 2.0 (at quay wall) or > 1.25 (other areas), the soil is non-liquefiable

    When FOS < 2.0 (at quay wall) or < 1.25 (other areas), soil improvement is required.

APPENDIX B1: ANALYSIS ON POST-CPT RESULTS OF POST-CPT 1-6A

CPT No.	G.L. (mCD)	Depth	q_c (MPa)	σvo (kPa)	σ'vo (kPa)	fs(MPa)	Ic	Ic>2.6?	$(q_{c1N})_{cs} = K_cQ_{c1N}$	Remark	CRR7.5	CSR	FoS	FoS > 2
1-6A	1.50	0.4	0.424	7.00	7.00	0.015	2.45	Sandy Material	29.11	(qc1N)cs<160, determine CRR7.5	0.07	0.10	0.71	N
1-6A	1.50	0.6	0.404	10.50	10.50	0.02	2.70	Too clay-rich to liquefy						
1-6A	1.50	0.8	0.424	14.00	14.00	0.017	2.72	Too clay-rich to liquefy						
1-6A	1.50	1	0.385	17.50	17.50	0.024	2.96	Too clay-rich to liquefy						
1-6A	1.50	1.2	0.404	21.00	19.47	0.031	3.04	Too clay-rich to liquefy						
1-6A	1.50	1.4	0.443	24.50	20.93	0.026	2.96	Too clay-rich to liquefy						
1-6A	1.50	1.6	0.404	28.00	22.39	0.023	3.01	Too clay-rich to liquefy						
1-6A	1.50	1.8	0.481	31.50	23.85	0.028	2.98	Too clay-rich to liquefy						
1-6A	1.50	2	0.501	35.00	25.31	0.038	3.07	Too clay-rich to liquefy						
1-6A	1.50	2.2	0.539	38.50	26.77	0.035	3.02	Too clay-rich to liquefy						
1-6A	1.50	2.4	0.481	42.00	28.23	0.037	3.13	Too clay-rich to liquefy						
1-6A	1.50	2.6	1.078	45.50	29.69	0.019	2.43	Sandy Material	56.77	(qc1N)cs<160, determine CRR7.5	0.10	0.16	0.61	N
1-6A	1.50	2.8	0.404	49.00	31.15	0.012	2.98	Too clay-rich to liquefy						
1-6A	1.50	3	0.501	52.50	32.61	0.018	2.96	Too clay-rich to liquefy						
1-6A	1.50	3.2	0.462	56.00	34.07	0.008	2.83	Too clay-rich to liquefy						
1-6A	1.50	3.4	0.289	59.50	35.53	0.007	3.16	Too clay-rich to liquefy						
1-6A	1.50	3.6	0.366	63.00	36.99	0.015	3.19	Too clay-rich to liquefy						
1-6A	1.50	3.8	0.327	66.50	38.45	0.017	3.33	Too clay-rich to liquefy						
1-6A	1.50	4	0.385	70.00	39.91	0.012	3.14	Too clay-rich to liquefy						
1-6A	1.50	4.2	0.443	73.50	41.37	0.018	3.16	Too clay-rich to liquefy						
1-6A	1.50	4.4	0.443	77.00	42.83	0.023	3.24	Too clay-rich to liquefy						
1-6A	1.50	4.6	0.424	80.50	44.29	0.017	3.21	Too clay-rich to liquefy						
1-6A	1.50	4.8	0.501	84.00	45.75	0.016	3.09	Too clay-rich to liquefy						
1-6A	1.50	5	0.481	87.50	47.21	0.018	3.17	Too clay-rich to liquefy						
1-6A	1.50	5.2	0.424	91.00	48.67	0.018	3.28	Too clay-rich to liquefy						
1-6A	1.50	5.4	0.424	94.50	50.13	0.012	3.19	Too clay-rich to liquefy						
1-6A	1.50	5.6	0.501	98.00	51.59	0.016	3.15	Too clay-rich to liquefy						
1-6A	1.50	5.8	0.539	101.50	53.05	0.015	3.10	Too clay-rich to liquefy						
1-6A	1.50	6	0.924	105.00	54.51	0.018	2.77	Too clay-rich to liquefy						
1-6A	1.50	6.2	0.558	108.50	55.97	0.012	3.05	Too clay-rich to liquefy						
1-6A	1.50	6.4	5.161	112.50	57.93	0.019	1.72	Sandy Material	76.58	(qc1N)cs<160, determine CRR7.5	0.12	0.19	0.63	N
1-6A	1.50	6.6	4.603	116.50	59.89	0.041	1.98	Sandy Material	83.98	(qc1N)cs<160, determine CRR7.5	0.14	0.19	0.69	N
1-6A	1.50	6.8	1.964	120.50	61.85	0.051	2.60	Sandy Material	99.43	(qc1N)cs<160, determine CRR7.5	0.17	0.19	0.88	N
1-6A	1.50	7	5.084	124.50	63.81	0.044	1.96	Sandy Material	86.65	(qc1N)cs<160, determine CRR7.5	0.14	0.19	0.72	N
1-6A	1.50	7.2	5.45	128.50	65.77	0.021	1.76	Sandy Material	76.60	(qc1N)cs<160, determine CRR7.5	0.12	0.19	0.63	N
1-6A	1.50	7.4	0.963	132.50	67.73	0.041	3.05	Too clay-rich to liquefy						
1-6A	1.50	7.6	0.713	136.50	69.69	0.036	3.25	Too clay-rich to liquefy						
1-6A	1.50	7.8	0.847	140.50	71.65	0.021	3.00	Too clay-rich to liquefy						
1-6A	1.50	8	1.406	144.50	73.61	0.018	2.62	Too clay-rich to liquefy						
1-6A	1.50	8.2	0.616	148.50	75.57	0.023	3.29	Too clay-rich to liquefy						
1-6A	1.50	8.4	0.674	152.50	77.53	0.022	3.22	Too clay-rich to liquefy						
1-6A	1.50	8.6	1.984	156.50	79.49	0.03	2.55	Sandy Material	72.94	(qc1N)cs<160, determine CRR7.5	0.12	0.19	0.60	N
1-6A	1.50	8.8	1.425	160.50	81.45	0.024	2.73	Too clay-rich to liquefy						
1-6A	1.50	9	4.314	164.50	83.41	0.036	2.12	Sandy Material	73.46	(qc1N)cs<160, determine CRR7.5	0.12	0.19	0.60	N
1-6A	1.50	9.2	1.098	168.50	85.37	0.046	3.10	Too clay-rich to liquefy						
1-6A	1.50	9.4	4.449	172.50	87.33	0.034	2.10	Sandy Material	71.81	(qc1N)cs<160, determine CRR7.5	0.11	0.19	0.60	N
1-6A	1.50	9.6	1.098	176.50	89.29	0.032	3.02	Too clay-rich to liquefy						
1-6A	1.50	9.8	0.924	180.50	91.25	0.015	2.98	Too clay-rich to liquefy						
1-6A	1.50	10	1.849	184.50	93.21	0.03	2.66	Too clay-rich to liquefy						

APPENDIX B2: ANALYSIS ON POST-CPT RESULTS OF POST-CPT-8

CPT No.	G.L. (mCD)	Depth	q_c (MPa)	σvo (kPa)	σ'vo (kPa)	fs(MPa)	Ic	Ic>2.6?	$(q_{c1N})_{cs} = K_cQ_{c1N}$	Remark	CRR7.5	CSR	FoS	FoS > 2
CPT8	1.50	0.6	7.198	10.80	10.80	0.051	1.25	Sandy Material	122.37	(qc1N)cs<160, determine CRR7.5	0.25	0.10	2.39	Y
CPT8	1.50	0.8	8.81	14.40	14.40	0.056	1.23	Sandy Material	149.77	(qc1N)cs<160, determine CRR7.5	0.39	0.10	3.75	Y
CPT8	1.50	1	9.199	18.00	18.00	0.054	1.25	Sandy Material	156.38	(qc1N)cs<160, determine CRR7.5	0.44	0.10	4.17	Y
CPT8	1.50	1.2	8.751	21.60	20.07	0.062	1.36	Sandy Material	148.77	(qc1N)cs<160, determine CRR7.5	0.39	0.11	3.44	Y
CPT8	1.50	1.4	8.78	25.20	21.63	0.069	1.41	Sandy Material	149.26	(qc1N)cs<160, determine CRR7.5	0.39	0.12	3.21	Y
CPT8	1.50	1.6	9.258	28.80	23.13	0.068	1.39	Sandy Material	157.39	(qc1N)cs<160, determine CRR7.5	0.44	0.13	3.43	Y
CPT8	1.50	1.8	8.661	32.40	24.75	0.055	1.38	Sandy Material	147.24	(qc1N)cs<160, determine CRR7.5	0.38	0.14	2.77	Y
CPT8	1.50	2	7.705	36.00	26.31	0.039	1.37	Sandy Material	130.99	(qc1N)cs<160, determine CRR7.5	0.29	0.14	2.04	Y
CPT8	1.50	2.2	9.856	39.60	27.87	0.063	1.38	Sandy Material	167.55	(qc1N)cs>160, no liquefaction	no Liquefaction			
CPT8	1.50	2.4	9.706	43.20	29.43	0.071	1.45	Sandy Material	165.00	(qc1N)cs>160, no liquefaction	no Liquefaction			
CPT8	1.50	2.6	10.363	46.80	30.99	0.079	1.46	Sandy Material	176.17	(qc1N)cs>160, no liquefaction	no Liquefaction			
CPT8	1.50	2.8	11.438	50.40	32.55	0.099	1.48	Sandy Material	194.66	(qc1N)cs>160, no liquefaction	no Liquefaction			
CPT8	1.50	3	12.484	54.00	34.11	0.098	1.44	Sandy Material	212.23	(qc1N)cs>160, no liquefaction	no Liquefaction			
CPT8	1.50	3.2	13.38	58.00	36.07	0.121	1.48	Sandy Material	222.78	(qc1N)cs>160, no liquefaction	no Liquefaction			
CPT8	1.50	3.4	13.439	62.00	38.03	0.132	1.53	Sandy Material	220.38	(qc1N)cs>160, no liquefaction	no Liquefaction			
CPT8	1.50	3.6	13.021	66.00	39.99	0.118	1.52	Sandy Material	207.07	(qc1N)cs>160, no liquefaction	no Liquefaction			
CPT8	1.50	3.8	15.291	70.00	41.95	0.14	1.49	Sandy Material	236.09	(qc1N)cs>160, no liquefaction	no Liquefaction			
CPT8	1.50	4	15.649	74.00	43.91	0.115	1.43	Sandy Material	236.16	(qc1N)cs>160, no liquefaction	no Liquefaction			
CPT8	1.50	4.2	15.47	78.00	45.87	0.129	1.48	Sandy Material	228.42	(qc1N)cs>160, no liquefaction	no Liquefaction			
CPT8	1.50	4.4	14.664	82.00	47.83	0.12	1.50	Sandy Material	212.03	(qc1N)cs>160, no liquefaction	no Liquefaction			
CPT8	1.50	4.6	14.783	86.00	49.79	0.112	1.49	Sandy Material	209.50	(qc1N)cs>160, no liquefaction	no Liquefaction			
CPT8	1.50	4.8	15.142	90.00	51.75	0.12	1.51	Sandy Material	210.49	(qc1N)cs>160, no liquefaction	no Liquefaction			
CPT8	1.50	5	14.963	94.00	53.71	0.113	1.51	Sandy Material	204.17	(qc1N)cs>160, no liquefaction	no Liquefaction			
CPT8	1.50	5.2	15.59	98.00	55.67	0.13	1.54	Sandy Material	208.95	(qc1N)cs>160, no liquefaction	no Liquefaction			
CPT8	1.50	5.4	17.889	102.00	57.63	0.155	1.52	Sandy Material	235.65	(qc1N)cs>160, no liquefaction	no Liquefaction			
CPT8	1.50	5.6	17.979	106.00	59.59	0.166	1.55	Sandy Material	232.91	(qc1N)cs>160, no liquefaction	no Liquefaction			
CPT8	1.50	5.8	19.203	110.00	61.55	0.188	1.56	Sandy Material	244.77	(qc1N)cs>160, no liquefaction	no Liquefaction			
CPT8	1.50	6	17.023	114.00	63.51	0.189	1.64	Sandy Material	222.79	(qc1N)cs>160, no liquefaction	no Liquefaction			
CPT8	1.50	6.2	18.517	118.00	65.47	0.15	1.52	Sandy Material	228.85	(qc1N)cs>160, no liquefaction	no Liquefaction			
CPT8	1.50	6.4	18.457	122.00	67.43	0.148	1.53	Sandy Material	224.77	(qc1N)cs>160, no liquefaction	no Liquefaction			
CPT8	1.50	6.6	18.935	126.00	69.39	0.153	1.53	Sandy Material	227.31	(qc1N)cs>160, no liquefaction	no Liquefaction			
CPT8	1.50	6.8	19.024	130.00	71.35	0.157	1.55	Sandy Material	225.22	(qc1N)cs>160, no liquefaction	no Liquefaction			
CPT8	1.50	7	20.398	134.00	73.31	0.167	1.53	Sandy Material	238.24	(qc1N)cs>160, no liquefaction	no Liquefaction			
CPT8	1.50	7.2	22.668	138.00	75.27	0.217	1.56	Sandy Material	261.28	(qc1N)cs>160, no liquefaction	no Liquefaction			
CPT8	1.50	7.4	21.802	142.00	77.23	0.18	1.53	Sandy Material	248.09	(qc1N)cs>160, no liquefaction	no Liquefaction			
CPT8	1.50	7.6	20.965	146.00	79.19	0.177	1.56	Sandy Material	235.59	(qc1N)cs>160, no liquefaction	no Liquefaction			
CPT8	1.50	7.8	17.113	150.00	81.15	0.129	1.59	Sandy Material	189.97	(qc1N)cs>160, no liquefaction	no Liquefaction			
CPT8	1.50	8	17.232	154.00	83.11	0.118	1.57	Sandy Material	189.02	(qc1N)cs>160, no liquefaction	no Liquefaction			
CPT8	1.50	8.2	16.306	158.00	85.07	0.2	1.77	Sandy Material	195.24	(qc1N)cs>160, no liquefaction	no Liquefaction			
CPT8	1.50	8.4	23.325	162.00	87.03	0.233	1.61	Sandy Material	250.03	(qc1N)cs>160, no liquefaction	no Liquefaction			
CPT8	1.50	8.6	18.845	166.00	88.99	0.226	1.74	Sandy Material	214.51	(qc1N)cs>160, no liquefaction	no Liquefaction			
CPT8	1.50	8.8	22.668	170.00	90.95	0.201	1.59	Sandy Material	237.69	(qc1N)cs>160, no liquefaction	no Liquefaction			
CPT8	1.50	9	22.13	174.00	92.91	0.209	1.62	Sandy Material	229.59	(qc1N)cs>160, no liquefaction	no Liquefaction			
CPT8	1.50	9.2	19.681	178.00	94.87	0.205	1.70	Sandy Material	210.39	(qc1N)cs>160, no liquefaction	no Liquefaction			
CPT8	1.50	9.4	18.188	182.00	96.83	0.148	1.65	Sandy Material	186.39	(qc1N)cs>160, no liquefaction	no Liquefaction			

SESSION 2
VERTICAL DRAINS, VACUUM CONSOLIDATION & PRELOADING

Numerical 3D comparison between real PVD and equivalent permeability in consolidation process

Belén M. Bacas. Terrasolum S.L. Santander, Spain, bacasb@terrasolum.es
Falko Schmidt. Terrasolum S.L. Santander, Spain., falko@terrasolum.es

ABSTRACT

Prefabricated vertical drains (PVDs) are often used for accelerating of the consolidation process in soft soils. In the field, it seems that the drainage behaviour of a single PVD is similar to axisymmetric condition, implying a three-dimensional study. This 3D effect has been analyzed using a small model of the unit cell. In this paper, a comparison between two unit cells is analyzed: one simulating soil with a real PVD installed, and the other one simulating soil with equivalent permeability (k_{ve}). This equivalent permeability is obtained from Jin-Chun Chai's investigation in 2001 (Simple Method of Modelling PVD-Improved Subsoil). The numerical simulation has been carried out using a three-dimensional explicit-different program. The objective is to analyze the 3D effect on pore pressure dissipation and settlement.

1.   INTRODUCTION

PVDs to improve consolidation of soft soil are widely used in civil works. In general, the studies about consolidation behaviour of this improved soil method are based on simplified models in 1D and 2D, that respond fairly well to the real behaviour of improved soil with PVDs (Barron, 1948, Hansbo 1981, Atkinson and Eldred 1981, Jamiolkowski et al. 1983, Priebe 1995, Chai et al. 1995, Chai and Miura, 1999 Almeida et al. 2000, Basu and Prezzi 2008, among others). These investigations pointed out that the most important factors that affect the consolidation rate with PVD-improved are the following one:

- the theoretical vertical and horizontal coefficient of consolidation of subsoil are based on one-dimensional vertical deformation and three-dimensional fluid flow
- the degree and radial extent of soil disturbance caused by pushing a hollow mandrel to the required depth in the ground (smear zone)
- the physical drain features: equivalent diameter, spacing and the layout pattern
- the mechanical drain features: well resistance (discharge capacity) and
- the drainage boundary conditions

In the last decade, some investigations are trying to predict the settlement and excess pore pressure variation versus the elapsed time taking into account the mentioned factors. Chai et al. (2001) proposed a simple method for modelling PVD improved subsoils, basing on the aim of installing PVDs to increase the mass hydraulic conductivity of the subsoil in the vertical direction. This method consists of obtaining an equivalent value of vertical hydraulic conductivity (k_{ve}) considering the soil hydraulic conductivities, the drain features, the boundary conditions and the smear zone. Furthermore, it is possible to analyze the improved subsoil in the same way as that for the unimproved case. Chai et al. indicate that the PVD-improved zone with an equivalent vertical hydraulic conductivity (k_{ve}) and subsoil horizontal hydraulic conductivity (k_h) can be analyzed in 1D, 2D or 3D, depending on the requirements. Therefore, the aim of this paper is to analyze two small models using 3D simulation by an explicit-different program. One model has been simulated with the equivalent vertical permeability and the other one has been simulated with a real PVD, comparing the settlements and excess pore pressure distribution in the vertical and horizontal direction.

The soil and PVD parameters as well as the load-time path was chosen from Chai et al. (2001) and Shen et al. (2005) investigations. Specifically, the case history of test embankment on soft mucky clay deposit in Eastern China. As Chai et al. the clay layer was modelled by a modified Cam-Clay model, the chosen soil parameters (very soft mucky clay) are presented in Table 1. PVDs characteristics are indicated in Table 2. Figure 1 displays the loading-time history relations of the embankment.

Table 1:Soil parameters for the model (Chai et al. 2001)

Layer	Thickness (m)	ν	κ	λ	M	e_0	γ (kN/m³)	k_h (10⁻⁶ cm/s)	k_v (10⁻⁶ cm/s)	k_{ve} (10⁻⁶ cm/s) without smear effect	k_{ve} (10⁻⁶ cm/s) with smear effect
Very soft mucky clay	10	0.35	0.028	0.28	0.8	1.36	17.3	2.94	1.96	114	13

Table 2: PVD parameters for the model (Chai et al. 2001)

Item	Symbol	Values
PVD cross-section (mm)	w x t	6 x 100
Length (m)	l	**10**
Layout pattern		Triangular
Spacing of PVDs (m)	S	1.5
Equivalent drain diameter (mm)	d_w	53.0
Unit cell diameter (m)	D_e	1.58
D_e/d_w	n	29.7
Smear zone diameter (mm)	d_s	355
Ratio of k_h over k_s in field	$(k_h/k_s)_f$	13.8
d_s/d_w	s	6.7
Discharge capacity (m³/year)	q_w	100
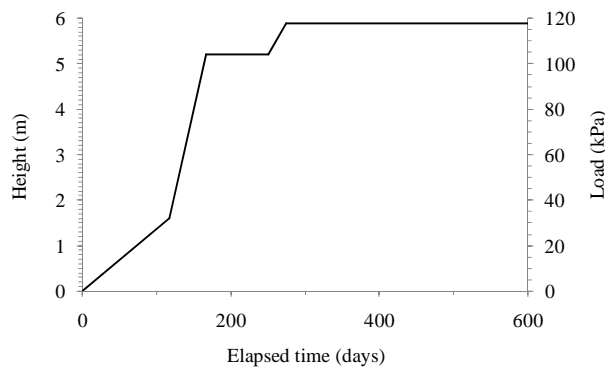
Figure 1: Load-time history of the model (Chai et al. 2001)

2.   ANALYSIS

As mentioned previously, the PVD pattern was triangular as shown in Fig. 2. For the 3D simulation of the unit cell has been considered a hexagonal cross-section the three different zones: unit cell, smear zone and equivalent PVD. Therefore, it is respected the hexagonal shape of the zone of influence for one PVD (Barron, 1948), as well as the hexagonal bounds of the smear zone and equivalent PVD adapt better to the unit cell bound. The dimensions of unit cell are detailed in Fig. 2 and the depth is 10 m. The four simulations have been carried out without well resistance effect: one with equivalent hydraulic conductivity (k_{ve}) and one with equivalent real PVD, each one with and without smear zone effect respectively (see table 3). Both soil and drain was modelled with Modified Cam-Clay mechanical model. The drain was simulated with the same mechanical model than the soil because during the consolidation that one settles going with the soil. Figure 3 plots the model of the unit cell, where the boundary conditions fitted the confining soil below the embankment, fixing the horizontal displacement. The vertical and horizontal displacements also were fixed at the bottom of the model. Regarding the drainage condition it was applied one-way drainage, being the top permeable and the bottom impermeable. Furthermore, for the simulation of unit cell with PVD it was fixed the static pore pressure in the drain, allowing the drainage through this drain without well resistance effect. As initial conditions a uniform vertical load of 90 kPa was considered. This was applied on the top of the unit cell, according to soil layer on the very soft mucky clay presented in the soil profile of Chai et al. 2001 research. The soil is in

normally consolidated state, and the groundwater level is on the upper face of the unit cell, so the soil column is saturated. The applied fluid-transport law corresponds to anisotropic permeability, table 3 summarizes the flow conditions for the four simulations carried out. Both horizontal and vertical hydraulic conductivities of the drain were taken from a commercial PVD with similar properties than PVD used by Chai. Another very important parameters of the fluid flow for 3D calculations are the Biot coefficient (α) and Biot modulus (M) (Biot, 1941). These parameters depend on the soil, therefore, it has been considered $\alpha=1$, assuming an incompressible solid constituent, and $M=1\cdot10^4$ kPa, defining $M=(K_u-K)/\alpha^2$, where K_u and K are undrained and drained bulk modulus of the soil.
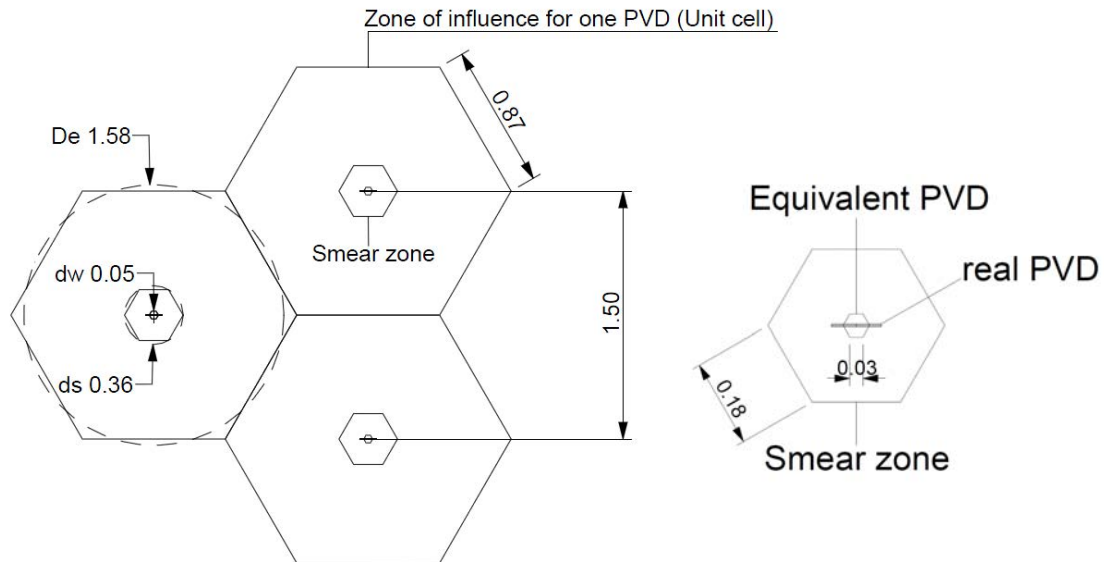
Figure 2: Plan of PVD pattern. Hexagonal unit cell, smear zone and equivalent drain.
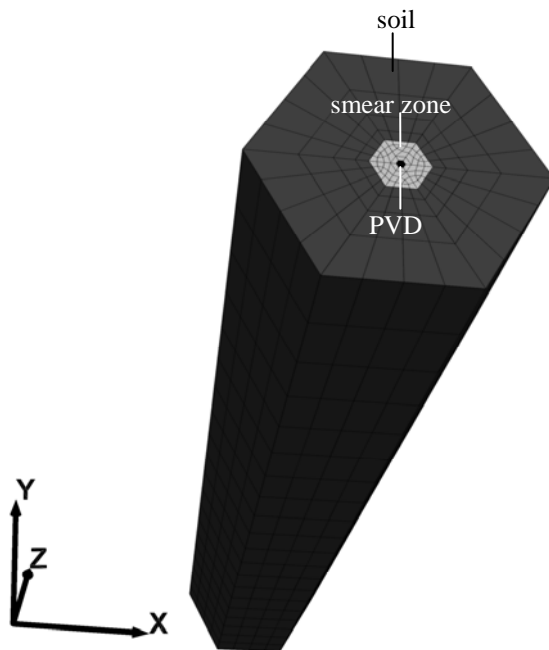
Figure 3: Model of the unit cell. Three areas: soil, smear zone and PVD.

Table 3: Anisotropic permeability conditions

Unit cell simulation	k_h (10^{-6} cm/s)	k_v (10^{-6} cm/s)	k_{ve} (10^{-6} cm/s)	k_s (10^{-6} cm/s)	k_{hdrain} (10^{-2} cm/s)	k_{vdrain} (10^{-2} cm/s)
with k_{ve}, without smear effect	2.94	–	114	–	–	–
with k_{ve}, with smear effect	2.94	–	13	–	–	–
with real PVD, without smear effect	2.94	1.96	–	2.94	1.4	13.7
with real PVD, with smear effect	2.94	1.96	–	0.21	1.4	13.7

3.   COMPARING SIMULATED RESULTS

Figure 5 compares the settlement curves for unit cell with smear effect. The equivalent vertical hydraulic conductivity k_{ve} simulation resulted in a slightly slower consolidation rate compared with that of using the real PVD. The maximum difference on settlement is around 5% (or 4 cm), as depth is increasing the difference decreases. Figure 6 specifically compares the settlement at depth of 0.5 m for simulations with and without smear effect. For the unit cell with k_{ve} the smear effect is more notable than unit cell with real PVD, that presents close curves. For the first one the maximum difference on settlement is about 13% (or 10 cm) and the difference of consolidation time is about 75 days. For the second one the maximum difference on settlement is about 5% (or 5 cm) and the difference of consolidation time is about 45 days.

Figure 7 compares the excess pore pressures, and it indicates that the model with k_{ve} and smear effect shows highest excess pore pressures and slower excess pore pressure dissipation rate, which is consistent with the results for settlement. In addition, Fig. 7 shows another important aspect as the influence of the smear zone, resulting a significant effect on the consolidation rate and predicting excess pore pressure.

Figure 8 contains the fluid discharge through the upper face, observing that models with k_{ve} the total fluid discharge is through the upper face (Fig. 9), and it presents a peak discharge when the load reaches 80% of total value. However, the simulation with real PVD and with smear effect presents a discharge of approximately of 20 % through the upper face and 80 % through the PVD, as can be seen in Fig. 9, demonstrating that the PVD works well. The vertical drainage presents more influence than radial drainage up to around 2 m depth, from this depth the radial drainage is predominant. This depth is halved (1 m) if it is simulated an ideal PVD (without smear effect and without well resistance), and the discharge through the upper and PVD is approximately 8 % and 92 % respectively.
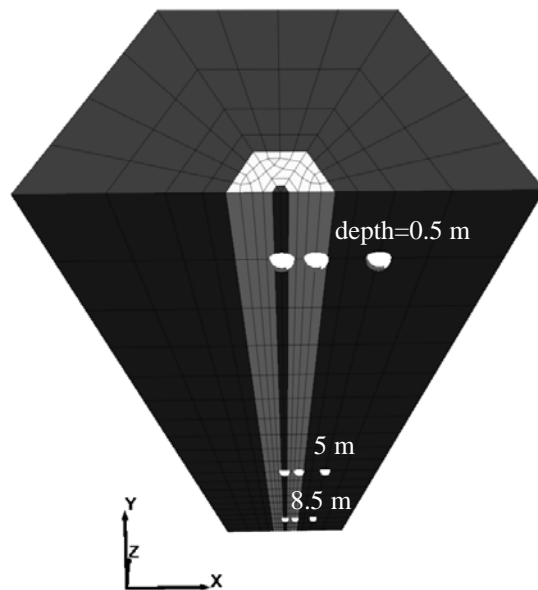
Figure 4: Location of measurement points
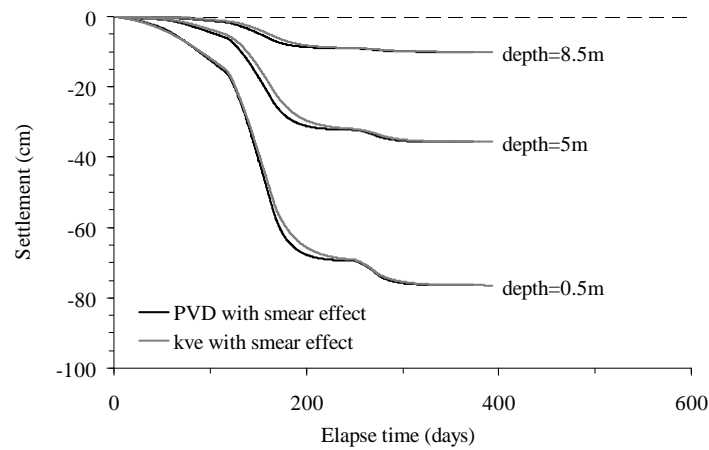
Figure 5: Comparison of settlement of unit cell with real PVD with unit cell with kve
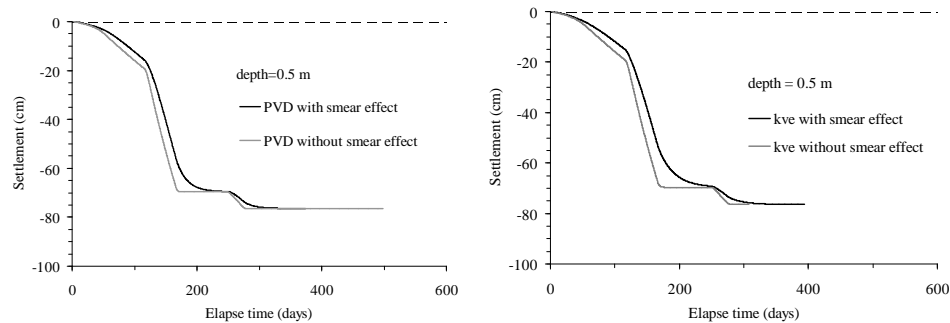
Figure 6: Settlement at depth of 0.5 m for the simulations with and without smear effect
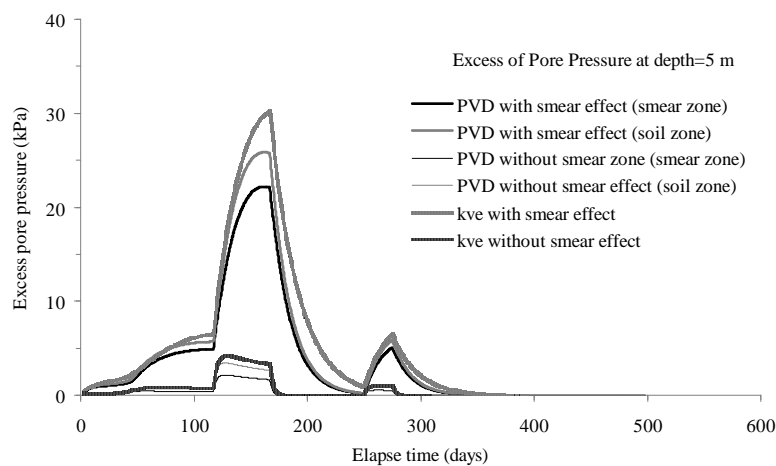
Figure 7: Comparison of excess pore pressure unit cell with and without smear
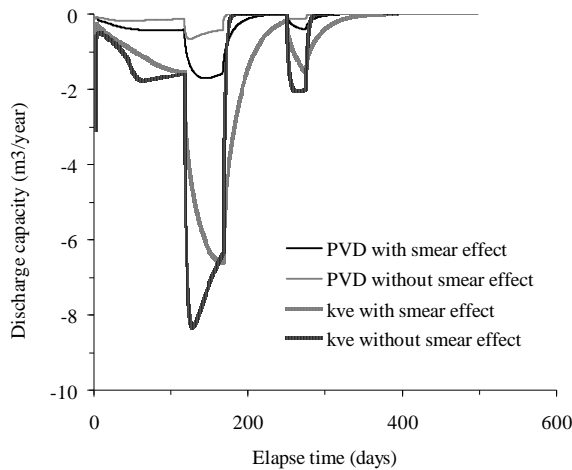
Figure 8: Comparison of fluid discharge at upper face

| k_{ve} simulation | *real PVD* simulation |
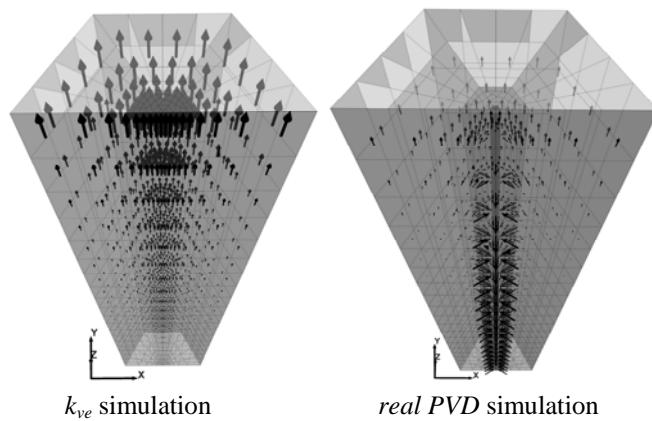
Figure 9: Discharge vectors (models with smear effect)

4.   CONCLUSIONS

The following conclusions are based on comparing the following numerical models: unit cell of improved soil with real PVD and unit cell of improved soil with equivalent hydraulic conductivity (k_{ve}) developed by Chai et al. (2001):

1. In general, the consolidation of soft soil during its improvement is a difficult issue, regarding the accurate predictions about consolidation rate and excess pore pressure. However, it normally seems that the final settlement predictions are quite close to the field measurements.

2. These unit cell models try to assess the 3D effect on consolidation considering the anisotropy fluid flow. Both unit cell with real PVD and unit cell with k_{ve} give similar final settlement results, but the consolidation rate and predicting excess pore pressure are somewhat different. The unit cell with real PVD simulation resulted in a faster consolidation rate and lower excess pore pressure prediction.

3. Considering the smear effect means that consolidation rate and excess pore pressure are considerably increasing.

4. In the modeled case with a real PVD with smear effect, 80% of the water coming out of the model during the entire consolidation process used the PVD.

REFERENCES

Almeida, M.S.S., Santa Maria, P.E.L., Martins, I.S.M., Spotti, A.P. y Coelho, L.B.M., 2000.Consolidation of a very soft clay with vertical drains. Géotechnique, 50(6), 633-643.

Atkinson, M. S. and Eldred P. J. L., 1981. Consolidation of soil using vertical drains. Geotechnique, Volume 31, Issue 1, pages 33 –43

Barron, R. A., 1948. Consolidation of fine-grained soils by drain wells. Trans. ASCE, 113, 718–742.

Basu, D. and Prezzi, M. (2008). "Effect of soil Disturbance on consolidation aided by prefabricated vertical drain." In Proceedings of EuroGeo4, 4th European Geosynthetics Conference, Edinburgh, U.K.

Biot, M. A., 1941. General theory of three dimensional consolidation. J. Appl. Phys., 12, 155–164.

Chai, J.C., Miura, N., Sakajo, S., Bergado, D.T., 1995. Behaviour of vertical drain improved subsoil under embankment loading. Soils and Foundations 35 (4), 49–61.

Chai, J. C., and Miura, N. 1999. Investigation of factors affecting vertical drain behavior. J. Geotech. and Geoenviron. Engrg., ASCE, 125(3), 216–226.

Chai, J.C., Shen, S.L., Miura, N., Bergado, D.T., 2001. A simple method of modeling PVD improved subsoil. Journal of Geotechnical and Geoenvironmental Engineering 127 (11), 965–972.

Hansbo, S., 1981. Consolidation of fine-grained soils by prefabricated drains. Proceedings of the Tenth International Conference on Soil Mechanics and Foundation Engineering, Stockholm, 3, pp. 677–682.

Jamiolkowski, M., Lancellotta, R., Wolski, W., 1983. Pre-compression and speeding up consolidation, general report. Special Session 6, Proceedings of Eight European Conference on Soil Mechanics and Foundation Engineering. Balkema, Rotterdam, pp. 1201–1226.

Priebe, H.J., 1995. Design of vibro replacement. Ground Engineering, 28(10), 31-37.

Shen, S. L., Chai, J. C., Hong, Z. S. and Cai, F. X., 2005. Analysis of field performance of embankments on soft clay deposit with and without PVD-improvement. Geotextiles and Geomembranes, Vol. 23, pp. 463- 485.

Performance and prediction of surcharge and vacuum consolidation via prefabricated vertical drains with special reference to highways, railways and ports

Buddhima Indraratna[1] Cholachat Rujikiatkamjorn[2], Geng Xueyu[3]

[1] Professor, Director, Centre for Geomechanics and Railway Engineering, Faculty of Engineering, University of Wollongong, NSW, Australia, email: indra@uow.edu.au

[2] Senior Lecturer, Centre for Geomechanics and Railway Engineering, Faculty of Engineering, University of Wollongong, NSW, Australia
Buddhima Indraratna[1]
[3] Research Fellow, Centre for Geomechanics and Railway Engineering, Faculty of Engineering, University of Wollongong, NSW, Australia

ABSTRACT

Much of the world's essential infrastructure is built along congested coastal belts that are composed of highly compressible and weak soils up to significant depths. Soft alluvial and marine clay deposits have very low bearing capacity and excessive settlement characteristics, with obvious design and maintenance implications on tall structures and large commercial buildings, as well as port and transport infrastructure. Stabilising these soft soils before commencing construction is essential for both long term and short term stability. A system of vertical drains combined with vacuum pressure and surcharge preloading has become an attractive ground improvement alternative in terms of both cost and effectiveness. This technique accelerates consolidation by promoting rapid radial flow which decreases the excess pore pressure while increasing the effective stress. Over the past 15 years, the Author and his co-workers have developed numerous experimental, analytical, and numerical approaches that simulate the mechanics of prefabricated vertical drains (PVDs) and vacuum preloading, including two-dimensional and three-dimensional analyses, and more comprehensive design methods. These recent techniques have been applied to various real life projects in Australia. The equivalent 2-D plane strain solution is described which includes the effects of smear zone caused by mandrel driven vertical drains. The equivalent (transformed) permeability coefficients are incorporated in finite element codes, employing the modified Cam-clay theory. Numerical analysis is conducted to predict the excess pore pressures, lateral and vertical displacements. Two case histories are discussed and analysed, including Port of Brisbane and Ballina and the predictions are compared with the available field data. These recent advances enable greater accuracy in the prediction of excess pore water pressure, and lateral and vertical displacement of the stabilised ground.

1.   INTRODUCTION

The booming population and associated development in coastal and metropolitan areas have necessitated the use of previously undeveloped low lying areas for construction purposes (Indraratna et al., 1992). Most of the Australian coastal belt contains very soft clays up to significant depths, especially in Northern Queensland and New South Wales. The low bearing capacity and high compressibility of these deposits affects the long term stability of buildings, roads, rail tracks, and other forms of major infrastructure (Johnson 1970). Therefore, it is imperative to stabilise these soils before commencing construction to prevent unacceptable differential settlement. However, attempts to improve deep bearing strata may not commensurate with the overall cost of the infrastructure (Bo et al. 2003). In the past, various types of vertical drains such as sand drains, sand compaction piles, PVDs (geo-synthetic), stone columns, and gravel piles have commonly been used. Certain types of granular piles and deep stone columns may indeed significantly enhance the intensity of the soil. However, because of the minimum risk of damage to utilities from lateral ground movement and a significant reduction in the price of flexible PVDs over the years, they have often been used to more conventional the original compacted sand drains, gravel piles stone columns etc. Their installation can significantly reduce the preloading period by decreasing the lesngth of the drainage path, sometimes by a factor of 10 or more. More significantly, PVDs can be installed quicker with minimum environmental implications and quarrying requirements.

Indraratna - Performance and prediction of surcharge and vacuum consolidation via prefabricated vertical drains with special reference to highways, railways and ports

II-145

Preloading (surcharge embankment) is one of the most successful techniques for improving the shear strength of low-lying areas because it loads the ground surface to induce a greater part of the ultimate settlement that it is expected to bear after construction (Richart 1957; Indraratna and Redana 2000; Indraratna et al. 2005a). In order to control the development of excess pore pressure, a surcharge embankment is usually raised as a multi-stage exercise, with rest periods between the loading stages (Jamiolkowski et al. 1983). Since most compressible low-lying soils have very low permeability and are often thick, a lengthy time period is usually needed to achieve the desired primary degree of consolidation (>95%). In these instances, the height of the surcharge can be excessive from an economic perspective and stability consolidation (Indraratna et al. 1994). One drawback of this surcharge technique is that the preload should be applied for a sufficiently long period, which may at times become impractical due to stringent construction schedules and deadlines. When PVDs combined with surcharge preloading is applied, vertical drains provide a much shorter drainage path in a radial direction which reduces the required preload period significantly. PVDs are cost effective and can be readily installed in moderate to highly compressible soils (up to 40m deep) that are normally consolidated or lightly over-consolidated. PVDs do not offer particular advantages if installed in heavily over-consolidated clays.

Apart from the method of drainage and PVDs combined with surcharge preloading, vacuum pressure has been used to enhance the efficiency of PVD when a desired degree of consolidation is required over a relatively short time period. Negative pore pressures (suction) distributed along the drains and on the surface of the ground accelerate consolidation, reduce lateral displacement, and increase the effective stress. This allows the height of the surcharge embankment to be reduced to prevent any instability and lateral movement in the soil. Today, PVDs combined with vacuum preloading are being used more and more in practical ground improvement all over the world.

This paper includes selected salient aspects of more than 15 years of active research conducted at the University of Wollongong in the area of soft soil stabilisation using PVDs and vacuum preloading, undoubtedly a vital Australian contribution to the field of soft soil improvement worldwide, plus offering a significant component of higher education training through almost a dozen doctoral studies to date, promoting the advancement of current industry practices in infrastructure development in coastal and low lying areas.

2. PRINCIPLES OF VACUUM CONSOLIDATION VIA PVDS

The vacuum preloading method for vertical drains was arguably first introduced in Sweden by Kjellman (1942). Since then, it has been used extensively to accelerate the consolidation of soft ground worldwide, for instance at the Philadelphia International Airport, USA; Tianjin port, China; North South Expressway, Malaysia; Reclamation world in Singapore and Hong Kong, China; Suvarnabhumi Second Bangkok International Airport, Thailand; Balina Bypass New South Wales and the Port of Brisbane, Queensland in Australia, among many other projects (Holtan 1965; Choa 1990; Jacob et al. 1994; Bergado et al. 2002; Chu et al. 2000; Yan and Chu 2003). When a high surcharge load is needed to achieve the desired undrained shear strength, and this cost becomes substantial due to an excessively high embankment and a long preloading period in order to achieve 95% or more consolidation, the optimum solution is to adapt to a combined vacuum and fill surcharge approach. In very soft clays where a high surcharge embankment cannot be constructed without affecting stability (large lateral movement) or having to work within a tight construction schedule, the application of vacuum pressure is quite often the most appropriate choice.

This PVD coupled system is designed to distribute the vacuum (suction) pressure to deep layers of the subsoil to increase the consolidation rate of reclaimed land and deep estuarine plains (e.g. Indraratna et al. 2005b; Chu et al. 2000). The mechanism for vacuum preloading can be explained by the spring analogy (Fig.1) described by Chu and Yan (2005), where the effective stress increases directly due to the suction (negative) pressure, while the total stress remains the same. This is in the context of conventional case surcharge preloading.

Indraratna - Performance and prediction of surcharge and vacuum consolidation via prefabricated vertical drains with special reference to highways, railways and ports

II-146

(a)
$$u_0 = q$$
$$\Delta p = q + \Delta q - (u_0 + \Delta u) = \Delta q - \Delta u$$

(b)
$$u_0 = q$$
$$\Delta p = q - (u_0 - \Delta u) = \Delta u$$
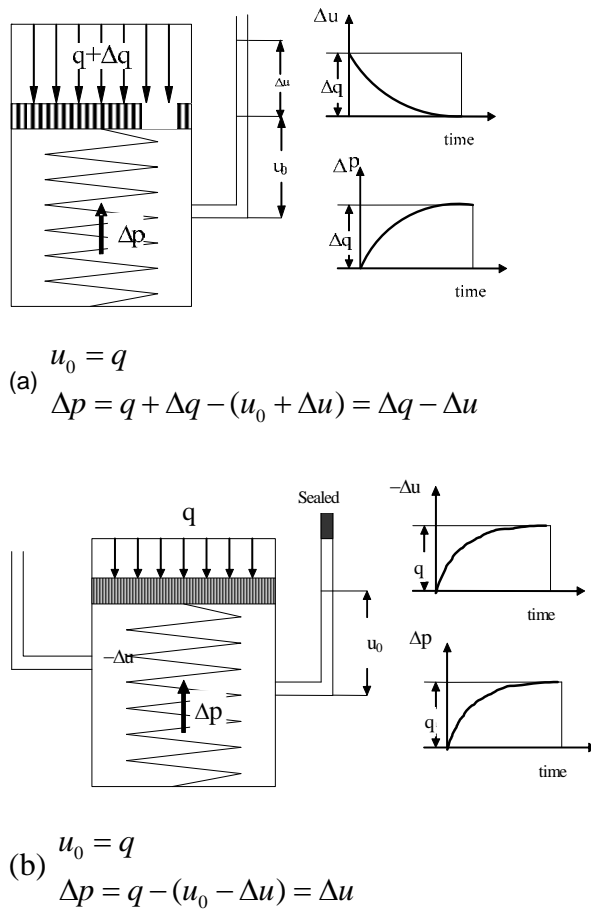
Figure 1: Spring analogy of vacuum consolidation process: (a) under fill surcharge; (b) under vacuum load (adopted from Chu and Yan 2005).

The general characteristics of vacuum preloading compared to conventional preloading are as follows (Qian et al. 1992; Indraratna and Chu 2005):

• The effective stress related to suction pressure increases isotropically, whereby the corresponding lateral movement is compressive. Consequently, the risk of shear failure can be minimised even at a higher rate of embankment construction, although any 'inward' movement towards the embankment toe should be carefully monitored to avoid excessively high tensile stresses.

• The vacuum head can propagate to a greater depth of subsoil via the PVD system and the suction can propagate beyond the tips of the drain and the boundary of the PVD.

• Assuming on air leaks and depending on the efficiency of the vacuum system used in the field, the volume of surcharge fill can be decreased to achieve the same degree of consolidation.

• Since the height of the surcharge can be reduced, the maximum excess pore pressure generated by vacuum preloading is less than the conventional surcharge method (Fig. 2).

• With the applied vacuum pressure, the inevitable unsaturated condition at the soil-drain interface may be partially compensated for.

• With field vacuum consolidation, the confining stress applied to a soil element may consist of two parts: (a) vacuum pressure and (b) lateral earth pressure (Chai 2005). Chai et al. (2008) demonstrated the possibility of improving clayey deposits by combining the cap-drain with a vacuum and the surface or subsurface soil as a sealing layer, in lieu of an air tight sheet on the ground surface. However, the efficiency of the method depends on preventing the surface sand from being affected by the pressure from pervious layers of sand and discontinuities in the ground.

Indraratna - Performance and prediction of surcharge and vacuum consolidation via prefabricated vertical drains with special reference to highways, railways and ports

II-147

(a)   (b)
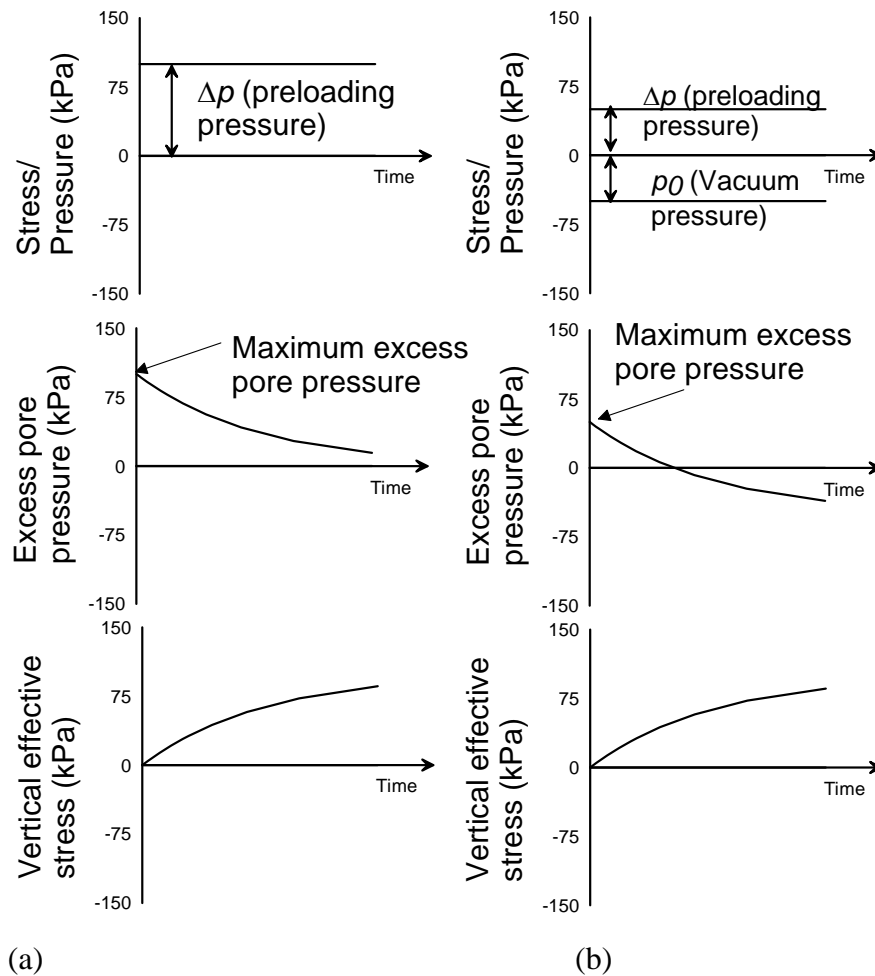
Figure 2: Consolidation process: (a) conventional loading；(b) idealised vacuum preloading (inspired by Indraratna et al. 2005c).

It is essential with vacuum assisted preloading that some horizontal drains be placed in transverse and longitudinal directions after installing the sand blanket, in order to uniformly distribute the surface suction. All vertical and lateral drains can then be connected to the edge of a peripheral Bentonite slurry trench, which is normally sealed by an impervious membrane system (Fig. 3a). The trenches can then be filled with water or Bentonite slurry to improve the intact sealing of the membrane around the boundary of the treated zone. The vacuum pumps are then connected to the prefabricated discharge system extending from the trenches (Fig. 3b). The suction head generated by the vacuum pump helps dissipate the excess pore water pressure via the PVDs.

When a reclaimed area has to be sub-divided into a number of sections to facilitate installation of the membrane (e.g. Port of Brisbane), vacuum preloading can only be effectively carried out in one section at a time. Vacuum preloading can become cumbersome over a very large area because the suction head may not be sustained due to the pressure of sand layers, or because it is too close to a marine boundary, in which case a cut off wall will often be used. An alternative method is to apply the vacuum directly to the individual PVD with flexible tubes without using a membrane. Here, each PVD is connected directly to the collector drain (Fig. 3b). Unlike the membrane system where an air leak can affect the entire PVD system, in this membrane-less system, each drain acts independently. However, installing an extensive tubing system for a large number of PVDs can increase the time and cost of installation (Seah 2006).

Indraratna - Performance and prediction of surcharge and vacuum consolidation via prefabricated vertical drains with special reference to highways, railways and ports

II-148

(a)   (b)

(c)
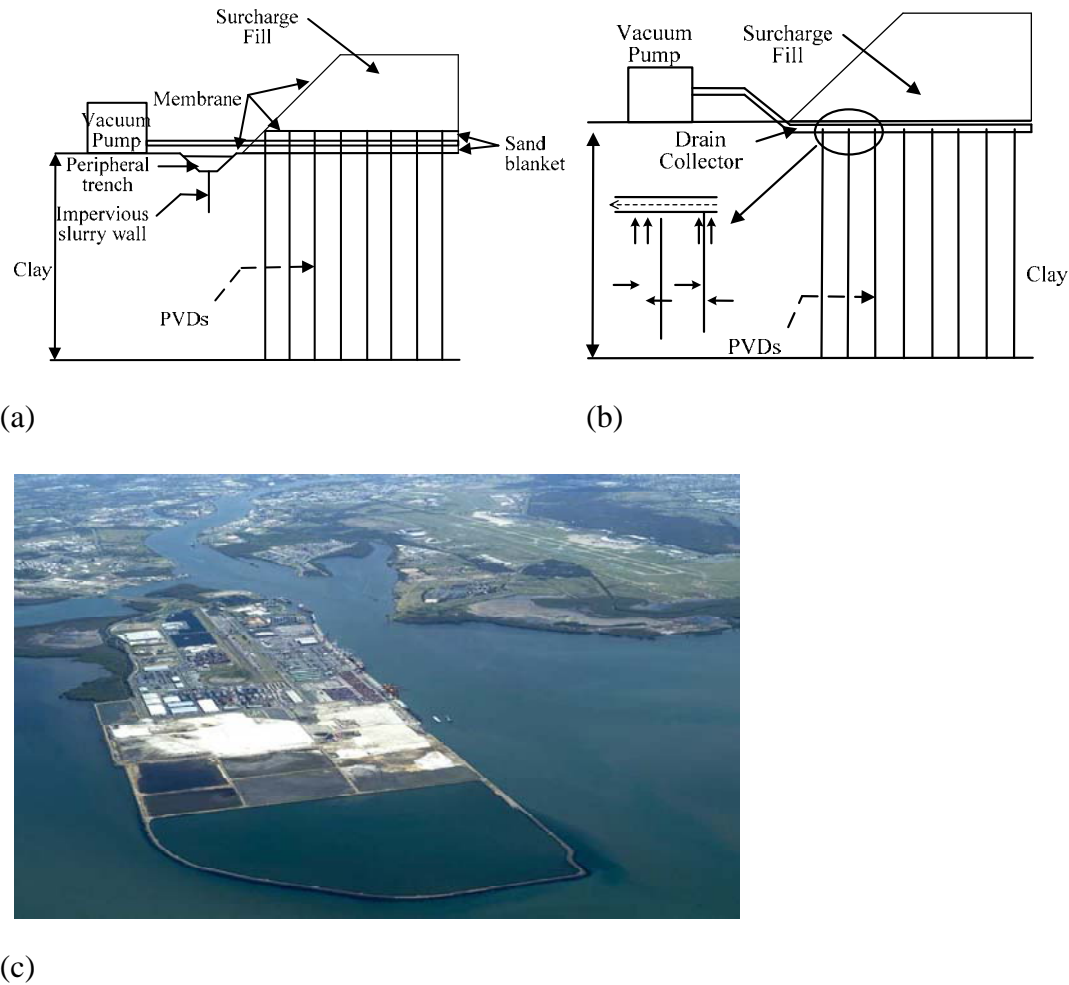
Figure 3: Vacuum-assisted preloading system: a) membrane system; (b) membrane-less system; and (c) vacuum at Port of Brisbane (Indraratna et al. 2005c).

Apart from the obvious inherent characteristics of these two vacuum systems, their effectiveness depends entirely on the properties of the soil, the thickness of the clay, the drain spacing, the type and geometry of PVDs, and the mechanical design and capacity of the vacuum pump. The selection and use of these systems are often based on empirical assessments that are invariably influenced by various aspects of the tender and/or the experience of the contractors, rather than detailed numerical studies. In this section, the analytical solutions to vertical drains incorporating the vacuum preloading of both systems (membrane and membrane-less) under time-dependent surcharge loading will be described.

The analytical modelling principles for both systems of the applied vacuum are shown in Fig. 4. The smear zone and well resistance are also considered in both models. The general solutions for excess pore water pressure, settlement, and degree of consolidation were derived through the Laplace transform technique. In addition, a time dependent surcharge preloading can be considered in lieu of an instantaneously applied constant load that can neither simulate the construction history of the embankment nor the variation of the applied vacuum pressure. The results elicited the need for correctly determining the permeability of the sand blanket in the membrane system, and the role of any variation in vacuum in the membrane-less system. The permeability of the sand blanket can significantly affect overall consolidation in the membrane system.

Indraratna - Performance and prediction of surcharge and vacuum consolidation via prefabricated vertical drains with special reference to highways, railways and ports

II-149

(a)   (b)
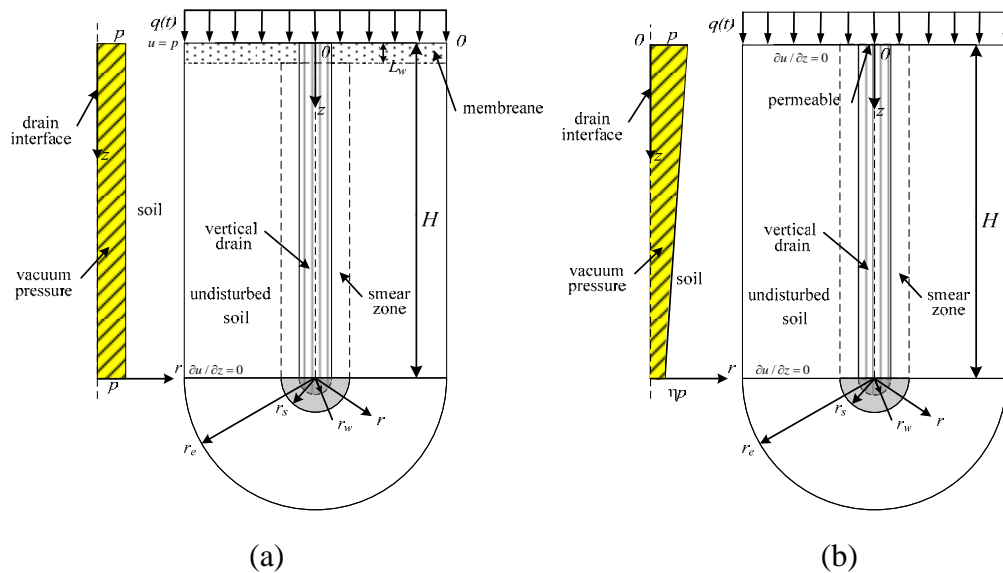
Figure 4: Analysis schemes of unit cell with vertical drain: (a) membrane system; and (b) membrane system.

With the Second Bangkok International Airport, various ground improvement schemes via PVDs with vacuum preloading and conventional surcharge preloading were studied by Indraratna and Redana (2000) and Indraratna et al. (2004). Consolidation with only surcharge preloading would take much longer than using vacuum preloading (Fig. 5). The corresponding settlements, excess pore water pressure, and lateral displacement, are presented in Figs. 5 and 6, respectively. As expected, the use of a vacuum pressure increased the rate of excess pore pressure dissipation. This is a direct result of an increased pore pressure gradient towards the drains due to negative pressure (suction) along the length of the drain. The use of sufficient vacuum pressure with properly sealed surface membranes accelerates the preconstruction settlement faster and better than the conventional surcharge preloading method. Moreover, a combination of embankment load with vacuum pressure can reduce the outward lateral displacement (Chai et al. 2005; Indraratna and Redana 2000).

Indraratna - Performance and prediction of surcharge and vacuum consolidation via prefabricated vertical drains with special reference to highways, railways and ports

II-150
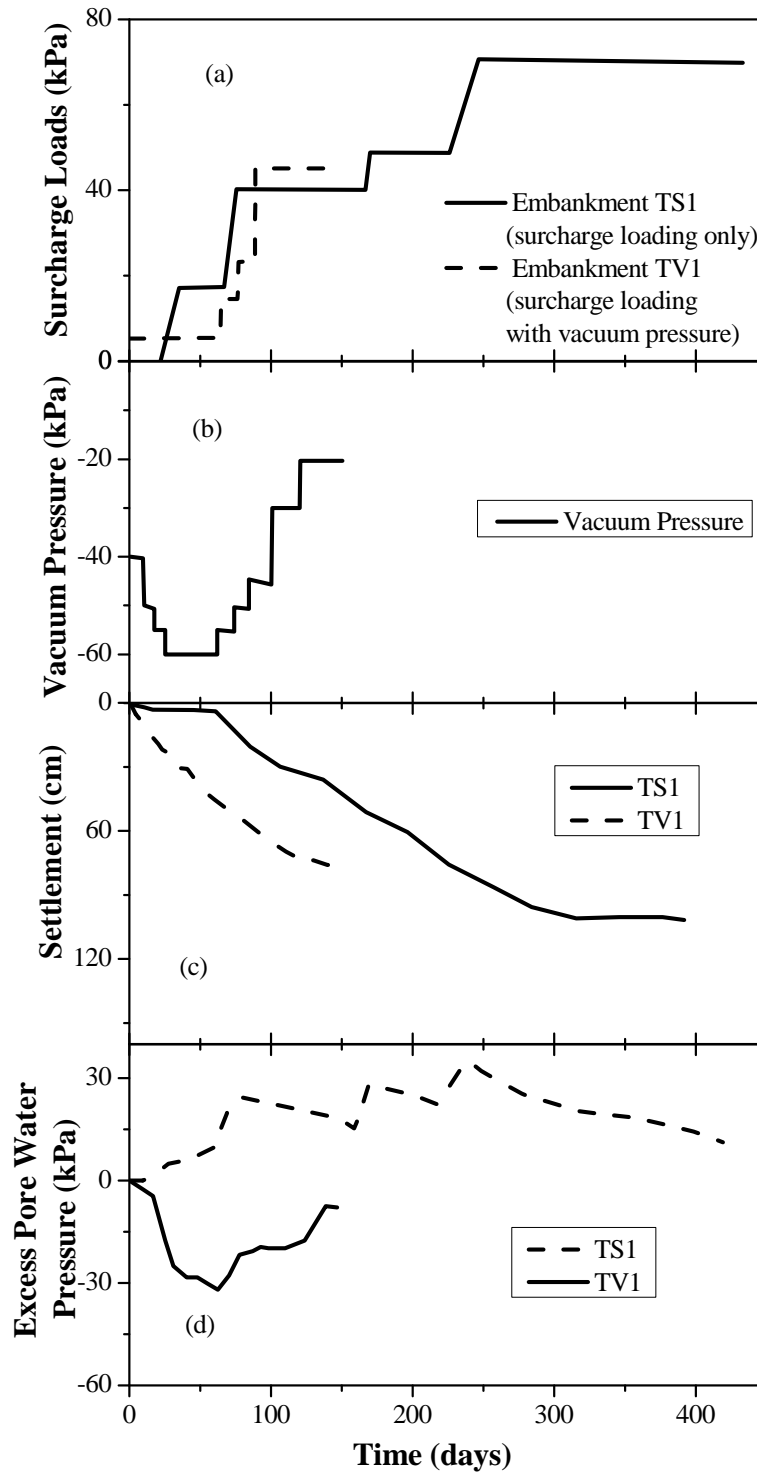
Figure 5: Second Bangkok International Airport (without vacuum pressure):(a) Construction loading history; (b) Surface settlement at the centreline of embankment; (c) Variation of excess pore-water pressure at 8m depth below ground level at the centreline for embankments (for surcharge only); (d) at 3m depth below ground level, 0.5 m away from the centreline for embankments (with surcharge and vacuum preloading together) (Indraratna et al. 2000, 2004).

Indraratna - Performance and prediction of surcharge and vacuum consolidation via prefabricated vertical drains with special reference to highways, railways and ports

II-151
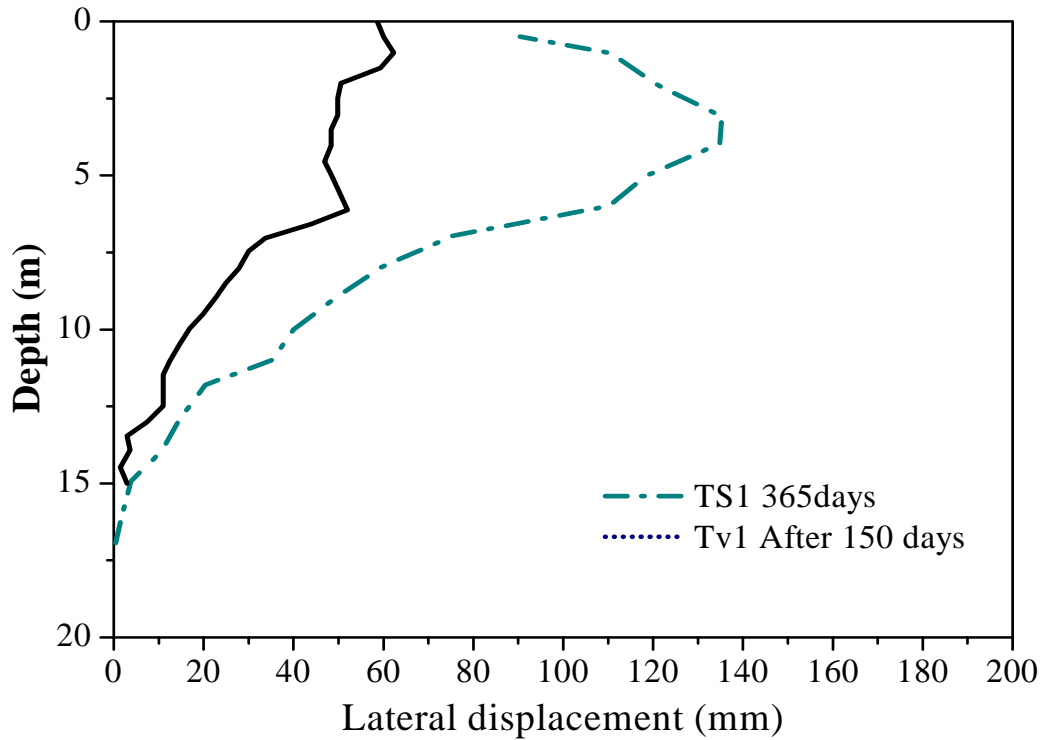
Figure 6: Lateral-displacement profiles 20m from the centreline of embankments (Indraratna et al. 2000, 2004).

3.   VACUUM CONSOLIDATION THEORY

Mohamedelhassan and Shang (2002) developed a combined vacuum and surcharge load system and adopted the one-dimensional Terzaghi's consolidation theory (Figure 7). The mechanism for the combined vacuum and surcharge loading (Fig. 7a) may be determined by the law of superposition (Figs. 7b and 7c). The average of degree of consolidation for combined vacuum and surcharge preloading can then be expressed by:

$$U_{vc} = 1 - \sum_{m=0}^{\infty} \frac{2}{M} \exp^{-M^2 T_{vc}} \tag{1}$$

$$T_{vc} = c_{vc} t / H^2 \tag{2}$$

where T_{vc} is a time factor for combined vacuum and surcharge preloading, and c_{vc} is the coefficient of consolidation for combined vacuum and surcharge preloading.

Indraratna et al. (2004) showed that when a vacuum is applied in the field through PVDs, the suction head along the length of the drain may decrease with depth, thereby reducing its efficiency. Laboratory measurements taken at a few points along PVDs installed in a large-scale consolidometer at the University of Wollongong clearly indicated that the vacuum propagates immediately, but a gradual reduction in suction may occur along the length of the drain. The rate at which the suction develops in a PVD depends mainly on the length and type of PVD (core and filter properties). However, some field studies suggest that the suction any develop rapidly even if the PVDs are up to 30 m long (Bo et al. 2003; Indraratna et al. 2005a).

Indraratna - Performance and prediction of surcharge and vacuum consolidation via prefabricated vertical drains with special reference to highways, railways and ports

II-152
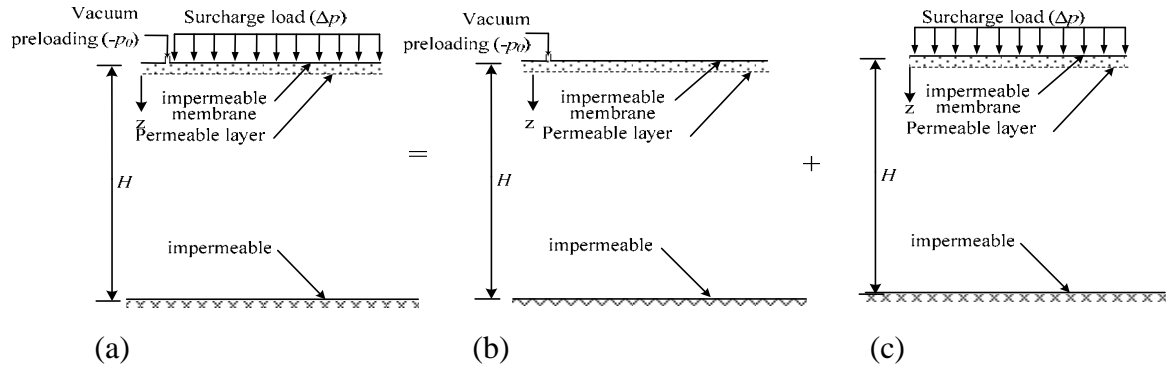
Figure 7: Schematic diagram of vacuum preloading system: (a) vacuum and surcharge combining load; (b) surcharge preloading; and (c) vacuum preloading (after Mohamedelhassan and Shang 2002).

Indraratna et al. (2004, 2005a) proposed a modified radial consolidation theory inspired by laboratory observations to include different distribution patterns of vacuum pressure (Fig. 8). These results indicated that the efficiency of the PVD depended on the magnitude and distribution of the vacuum. In order to quantify the loss of vacuum, a trapezoidal distribution of vacuum pressure along the length of the PVD was assumed.
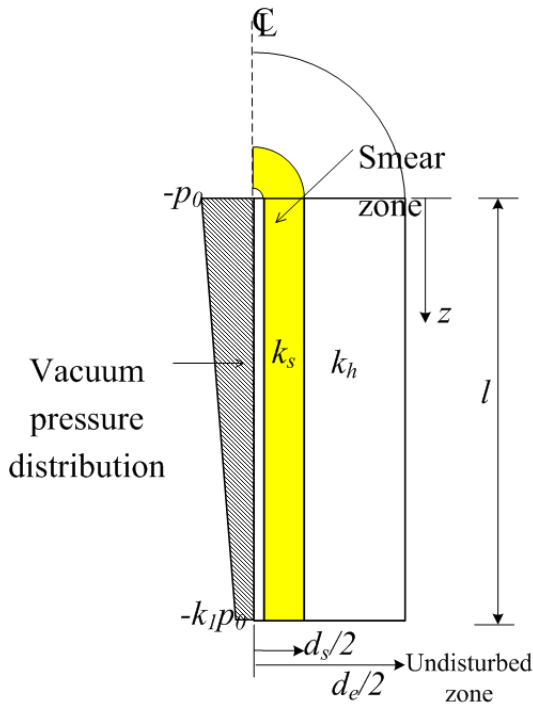
Figure 8: The distribution patterns of vacuum pressure in the vertical directions (after Indraratna et al. 2005a).

Based on these assumptions, the average excess pore pressure ratio ($R_u = \Delta p / \overline{u}_0$) of a soil cylinder for radial drainage that incorporates vacuum preloading can be given by:

$$R_u = \left(1 + \frac{p_0}{\overline{u}_o}\frac{(1+k_1)}{2}\right)\exp\left(-\frac{8T_h}{\mu}\right) - \frac{p_0}{\overline{u}_0}\frac{(1+k_1)}{2} \tag{3}$$

and

$$\mu = \ln\left(\frac{n}{s}\right) + \left(\frac{k_h}{k_s}\right)\ln(s) - 0.75 + \pi z(2l - z)\frac{k_h}{q_w}\left\{1 - \frac{k_h/k_s - 1}{(k_h/k_s)(n/s)^2}\right\} \tag{4}$$

Indraratna - Performance and prediction of surcharge and vacuum consolidation via prefabricated vertical drains with special reference to highways, railways and ports

II-153

where p_0 = the vacuum applied at the top of the drain, k_1 = ratio between the vacuum at the top and bottom of the drain, $\overline{u}_0$ = the initial excess pore water pressure, k_h = the horizontal permeability coefficient of soil in the undisturbed zone, k_s = the horizontal permeability coefficient of soil in the smear zone, T_h = the time factor, n = the ratio d_e/d_w (d_e is the diameter of the equivalent soil cylinder = $2r_e$ and d_w is the diameter of the drain = $2r_w$), s = ratio d_s/d_w (d_s is the diameter of the smear zone = $2r_s$), z = depth, l = the equivalent length of drain, q_w = the well discharge capacity.

4. NUMERICAL ANALYSIS

4.1. Two-dimensional plane strain conversion

For multi-drain simulation, plane strain finite element analysis can be readily adapted to most field situations (Indraratna and Redana 2000; Indraratna et al. 2005a). Nevertheless, realistic field predictions require that the axi-symmetric properties to be converted to an *equivalent* 2D plane strain condition, especially the permeability coefficients and drain geometry. Plane strain analysis can also accommodate vacuum preloading in conjunction with vertical drains. Indraratna et al. (2005b) proposed an equivalent plane strain approach to simulate vacuum pressure for a vertical drain system with modification to the original theory introduced by Indraratna and Redana (1997), as shown in Fig. 9.

(a) Axi-symmetric (b) Plane strain
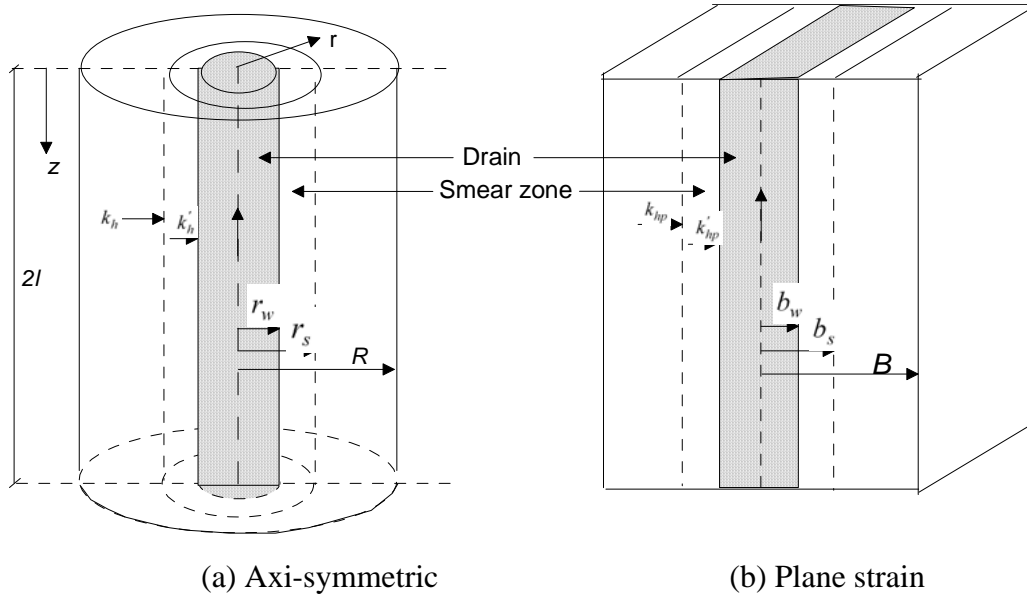
Figure 9: Conversion of an axi-symmetric unit cell into plane strain condition (Indraratna et al. 2005b).

Equivalent plane strain conditions can be fulfilled in three ways:

(1) Geometric approach where the PVD spacing varies, but the soil permeability remains constant;

(2) Permeability approach where the equivalent permeability coefficient is determined while the drain spacing remains unchanged;

(3) Combined permeability and geometric approach where plane strain permeability is calculated based on a convenient space between the drains.

Indraratna et al. (2005b) proposed an average degree of consolidation for plane strain by assuming that the plane strain cell (width of $2B)$, the half width of the drain b_w and the half width of the smear zone b_s may be kept the same as their axi-symmetric radii r_w and r_s, respectively. This implies that $b_w = r_w$ and $b_s = r_s$ (Fig.9). To excess pore pressure can be determined form:

$$\frac{\overline{u}}{\overline{u}_0} = \left(1 + \frac{p_{0p}}{\overline{u}_o}\frac{(1+k_1)}{2}\right)\exp\left(-\frac{8T_{hp}}{\mu_p}\right) - \frac{p_{0p}}{\overline{u}_0}\frac{(1+k_1)}{2} \tag{5a}$$

and

Indraratna - Performance and prediction of surcharge and vacuum consolidation via prefabricated vertical drains with special reference to highways, railways and ports

II-154

$$\mu_p = \left[\alpha + (\beta)\frac{k_{hp}}{k'_{hp}}\right] \tag{5b}$$

where $\bar{u}_0$ = the initial excess pore pressure, $\bar{u}$ = the pore pressure at time t (average values) and T_{hp} = the time factor in plane strain, and k_{hp} and k'_{hp} are the equivalent undisturbed horizontal and corresponding smear zone permeability, respectively. The geometric parameters α and β are given by:

$$\alpha = \frac{2}{3} - \frac{2b_s}{B}\left(1 - \frac{b_s}{B} + \frac{b_s^2}{3B^2}\right) \tag{6a}$$

$$\beta = \frac{1}{B^2}(b_s - b_w)^2 + \frac{b_s}{3B^3}\left(3b_w^2 - b_s^2\right) \tag{6b}$$

At a given level of effective stress, and at each time step, the average degree of consolidation for the axi-symmetric ($\overline{U}_p$) and equivalent plane strain ($\overline{U}p, pl$) conditions are made equal.

By making the magnitudes of R and B the same, Indraratna et al. (2005a) presented a relationship between k_{hp} and k'_{hp}. The smear effect can be captured by the ratio between the smear zone permeability and the undisturbed permeability, hence:

$$\frac{k'_{hp}}{k_{hp}} = \frac{\beta}{\dfrac{k_{hp}}{k_h}\left[\ln\left(\dfrac{n}{s}\right) + \left(\dfrac{k_h}{k'_h}\right)\ln(s) - 0.75\right] - \alpha} \tag{7}$$

Ignoring the effects of smear and well resistance in the above expression would lead to the simplified solution proposed earlier by Hird et al. (1992):

$$\frac{k_{hp}}{k_h} = \frac{0.67}{[\ln(n) - 0.75]} \tag{8}$$

Indraratna et al. (2005b) compared two different distributions of vacuum along a single drain for the equivalent plane strain (2D) and axi-symmetric conditions (3D). Varying the vacuum pressure in PVDs installed in soft clay would be more realistic for long drains, but a constant vacuum with depth is justified for relatively short drains

5. CASE HISTORIES

5.1. Port of Brisbane

The Port of Brisbane is located at the mouth of the Brisbane River at Fisherman Islands. An expansion of the Port includes a 235ha area to be progressively reclaimed and developed over the next 20 years using dredged materials from the Brisbane River and Moreton Bay shipping channels. The site contains compressible clays of over 30 m in thickness. At least 7 m of dredged mud capped with 2 m of sand was used to reclaim the sub-tidal area. Generally, the complete consolidation of the soft deep clay deposits may well take in excess of 50 years, if surcharging was the only treatment, with associated settlements of probably 2.5-4 m likely. To reduce the consolidation period, the method of PVDS and surcharge or PVD combined with vacuum pressure (at sites where stability is of a concern) was chosen to be trialled. Three contractors undertook the trial works being Austress Menard, Van Oord and Cofra/Boskalis. All three trialled prefabricated drains and surcharge with Austress Menard and Cofra/Boskalis also trialling their respective proprietary membrane and membrane-less vacuum systems. Figure 10 shows the final layout of a typical trial area with the PVD design results for each area.

The typical soil properties are summarised in Table 1.

Indraratna - Performance and prediction of surcharge and vacuum consolidation via prefabricated vertical drains with special reference to highways, railways and ports

II-155

Table 1: Typical Soil Properties (Port of Brisbane Corporation and Austress Menard 2008).

Soil layer	Soil type	γ_t (kN/m^3)	Cc/(1+e$_0$)	C$_v$ (m^2/yr)	C$_h$ (m^2/yr)	Cα/(1+e$_0$)
1	Dredged Mud	14	0.3	1	1	0.005
2	Upper Holocene Sand	19	0.01	5	5	0.001
3	Upper Holocene Clay	16	0.18	1	2	0.008
4	Lower Holocene Clay	16	0.235	0.8	1.9	0.0076

To compare two locations with a different loading history, the lateral displacement normalised by the applied effective stress at two inclinometer positions (MS24 and MS34) are plotted in Fig. 11. It was clear that the lateral displacements were largest in the upper Holocene shallow clay depths and were insignificant below 10m. From this limited inclinometer data, the membrane-less BeauDrain system (MS34) had controlled the lateral displacement more effectively than the surcharge only section (MS24). Settlement and excess pore water pressure predictions and field data for a typical settlement plate (TSP3) are shown in Fig. 12. The predicated settlement curve agreed with the field data. The excess pore water pressures were more difficult to predict than settlement, but they did indicate a slower rate of dissipation in the Holocene clays in every section monitored, in spite of the PVDs. From the perspective of stability, the incremental rate of change of the lateral displacement/settlement ratio (μ) with time can be plotted as shown in Fig. 13. This rate of change of μ can be determined for relatively small time increments where a small and decreasing gradient can be considered to be stable with respect to lateral movement, while a continuously increasing gradient of μ reflects potential lateral instability. In Fig. 13, the gradient in the non-vacuum area WD3 increased initially, which could be attributed to the final surcharge loading placed quickly, while the clay was still at early stages of consolidation. However, as the PVDs become fully active and settlement increased at a healthy rate, the gradient of μ decreased, as expected. In general, Figure 13 illustrates that the vacuum pressure provides a relatively unchanging gradient of μ with time.
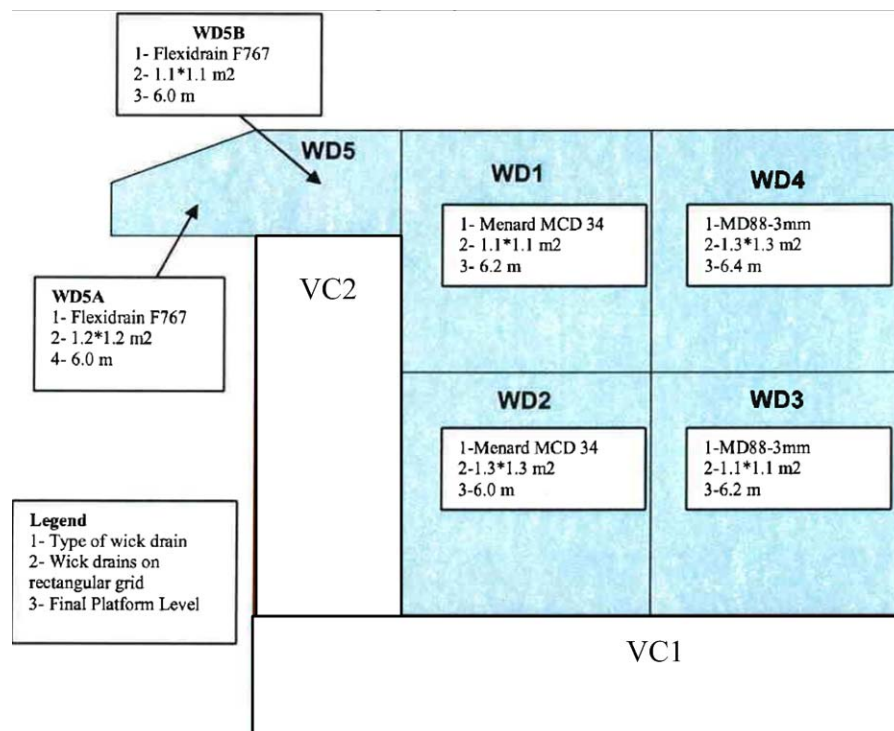
Figure 10: S3A Trial Area – Layout and detail design specifications (Port of Brisbane Corporation and Austress Menard 2008).

Indraratna - Performance and prediction of surcharge and vacuum consolidation via prefabricated vertical drains with special reference to highways, railways and ports

II-156

Lateral Displacement/Change in
Effective Stress with depth (mm/kPa)
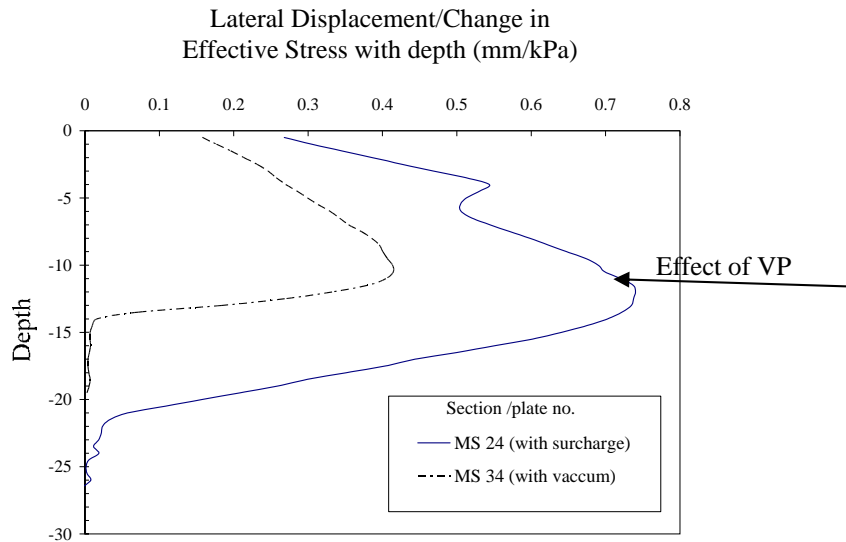
Figure 11: Comparison of lateral displacements in vacuum and non-vacuum areas.
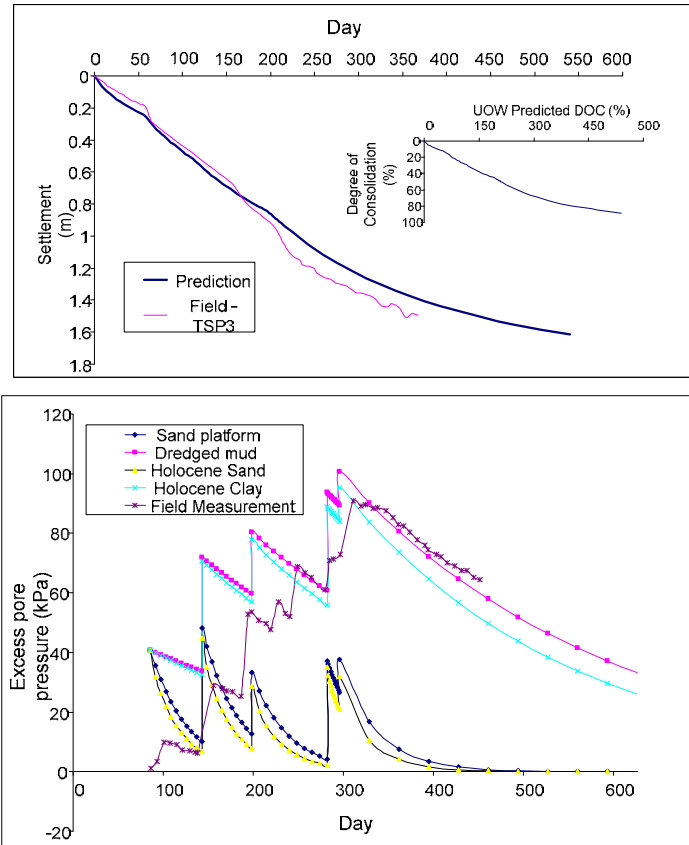
Figure 12: (a) Settlement; and (b) excess pore water pressure predictions and field data for a typical settlement plate location.

Indraratna - Performance and prediction of surcharge and vacuum consolidation via prefabricated vertical drains with special reference to highways, railways and ports

II-157
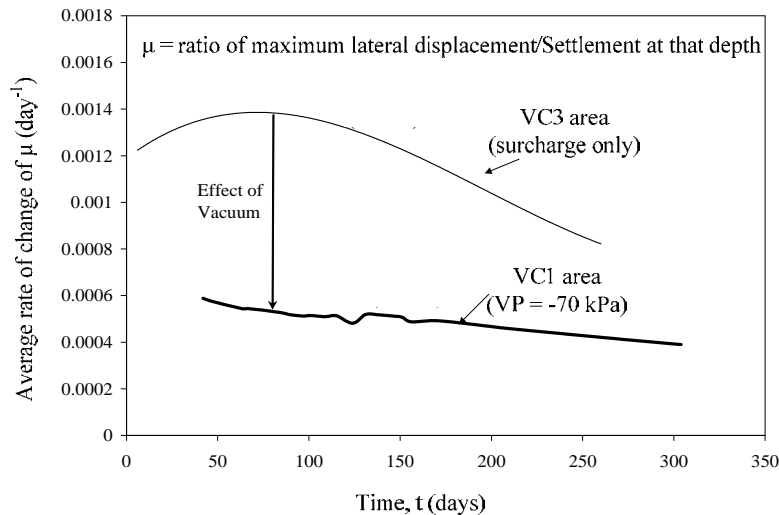
Figure 13: Rate of change of lateral displacement/settlement ratio with time.

Figure 14 provides approximately linear relationships between the long term residual settlement (RS) and the clay thickness of clay for an over-consolidation ratio (OCR) from 1.1 to 1.4, and for a degree of consolidation (DOC) that exceeding 80%. The reduced settlement (RS) was determined based on the theory secondary consolidation employing the secondary compression index C_α (Table 1). More detail on the computation of RS are given by Mesri and Castro (1987), Bjerrum (1972) and Yin and Clark (1994). As expected, when the OCR increased, the RS decreased substantially. In general, as the thickness of Holocene clay increased, the RS also increased. The corresponding regression lines and best–fit equations are also shown in Figure 14. In particular, the vacuum consolidation locations (VC1-2, VC2-2 and VC2-3) show a considerably reduced RS at an OCR approaching 1.4, which is well below the permissible limit of 250mm. At an OCR of approximately 1.3, the residual settlement associated with membrane-less BeauDrain consolidation (TA8) and membrane type (VC1-5) were also small.
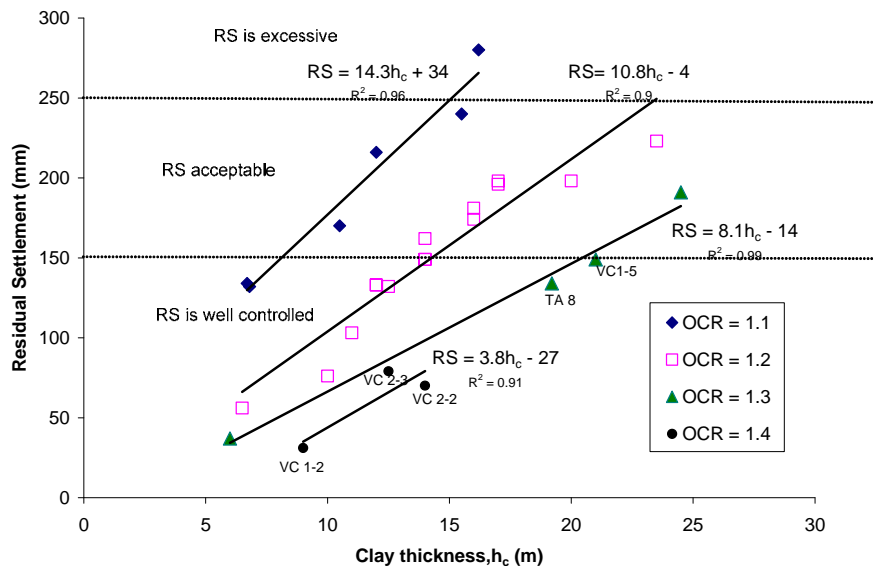
Figure 14: Effect of OCR and clay thickness on residual settlement.

5.2. Ballina Bypass

The Pacific Highway linking Sydney and Brisbane is constructed to reduce the high traffic congestion in Ballina. This bypass route has to cross a floodplain consisting of highly compressible and saturated marine clays up to 40 m thick. A system of vacuum assisted surcharge load in conjunction with PVDs

Indraratna - Performance and prediction of surcharge and vacuum consolidation via prefabricated vertical drains with special reference to highways, railways and ports

II-158

was selected to shorten the consolidation time and stabilise the deeper clay layers. To investigate the effectiveness of this approach, a trial embankment was built north of Ballina, 34mm diameter circular PVD at 1.0m spacing were installed in a square pattern. The vacuum system consisted of PVDs with an air and water tight membrane, horizontal transmission pipes, and a heavy duty vacuum pump. Transmission pipes were laid horizontally beneath the membrane to provide uniform distribution of suction. The boundaries of the membrane were embedded in a peripheral trench filled with soil-bentonite to ensure absolute air tightness. Figure 15 presents the instrument locations, including surface settlement plates, inclinometers and piezometers. The piezometers were placed 1m, 4.5m, and 8m below the ground level, and eight inclinometers were installed at the edges of each embankment. The embankment area was then divided into Section A (no vacuum pressure), and Section B, subject to vacuum pressure and surcharge fill. As the layers of soft clay fluctuated between 7m to 25 m (Table 2), the embankment varied from 4.3m to 9.0m high, to limit the post-construction settlement. A vacuum pressure of 70 kPa was applied at the drain interface and removed after 400 days. The geotechnical parameter of the three subsoil layers obtained from standard odometer tests are given in Table 3.
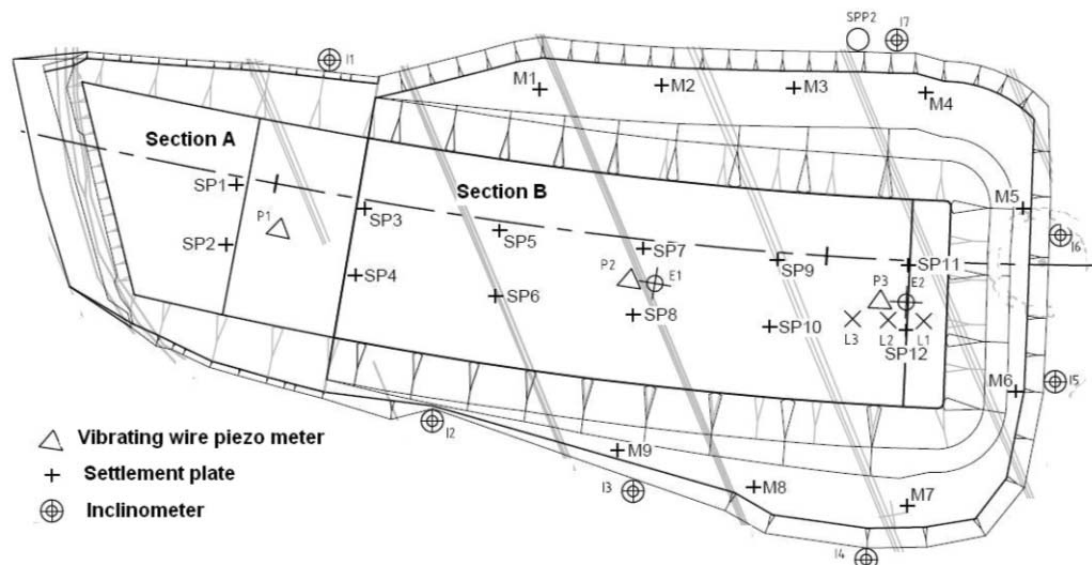
Figure 15: Instrumentation layout for the test embankments at Ballina Bypass (Indraratna et al. 2009).

Table 2: Bottom level of soft clay layer at each settlement plate (Indraratna et al. 2009)

Settlement plate	SP1 SP2	SP3 SP4	SP5 SP6	SP7 SP8	SP9 SP10	SP11 SP12
Bottom level of soft clay layer (m-RL)	2.7-6.7	6.7-9.7	9.7-11.7	11.7-14.7	14.7-17.7	20.7-24.7

Table 3: Soil parameters at SP12 (Indraratna et al. 2009).

Depth (m)	Soil Type	λ	κ	γ kN/m3	e_0	$k_{h,ax}$ 10^{-10} m/s	OCR
0.0-0.5	Clayey silt	0.57	0.06	14.5	2.9	10	2
0.5-15.0	Silty Clay	0.57	0.06	14.5	2.9	10	1.7
15.0-24.0	Stiffer Silty Clay	0.48	0.048	15.0	2.6	3.3	1.1

The soil profile with its relevant properties is shown in Fig. 16. A soft silty layer of clay approximately 10m thick was underlain by moderately stiff and silty layer clay located 10-30m deep, which was in turn underlain by firm clay. The groundwater was almost at the ground surface. The water content of the soft and medium silty clay varied from 80 to 120%, which was generally at or exceeded the liquid limit,

Indraratna - Performance and prediction of surcharge and vacuum consolidation via prefabricated vertical drains with special reference to highways, railways and ports

II-159

ensuring that the soils were fully saturated. The field vane shear tests indicated that the shear strength was from 5-40 kPa. The compression index ($C_c / (1 + e_0)$) determined by standard oedometer testing was between 0.30-0.50.
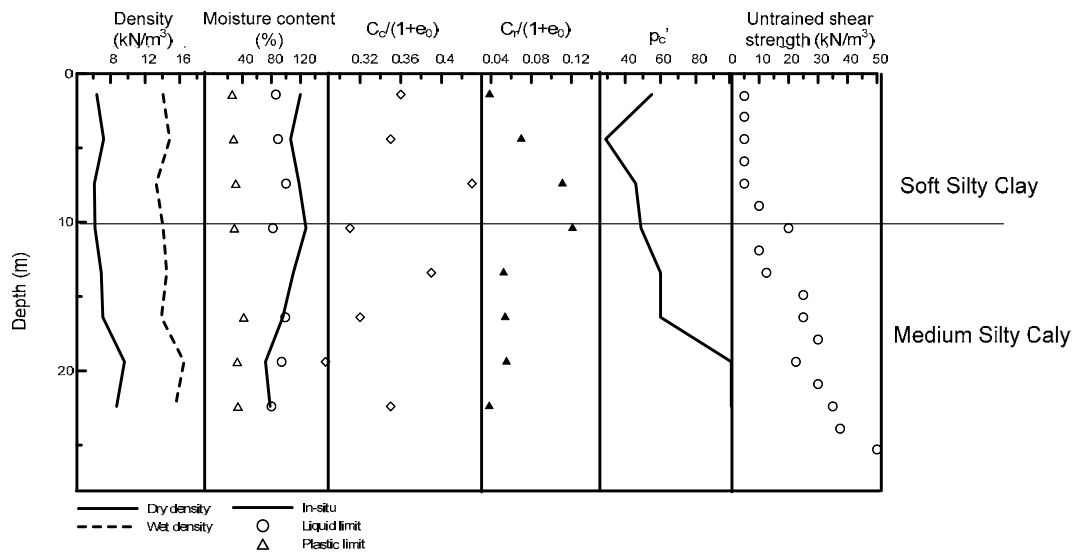
Figure 16: General soil profile and properties at Ballina Bypass (Indraratna et al. 2009).

Settlement and associated pore pressure recorded by the settlement plates and piezometers are shown in Fig. 17, with the embankment construction schedule. The actual suction varied from -70 kPa to -80 kPa, and no air leaks were encountered. Suction was measured by miniature piezometers embedded inside the drains.

Lateral displacement at the border of the embankments needed to be examined carefully, particularly the vacuum area where the surcharge loading was raised faster than that at the non-vacuum area. The soil properties and lateral displacement plots before and after vacuum are shown in Fig. 17. Inclinometer I1 was installed at the border of the vacuum area, whereas inclinometers I2-I4 were located at the edge of the vacuum area. Here the lateral displacement subjected to vacuum was smaller even though the embankments were higher. In Figure 17b the plot of lateral displacement normalised to embankment height showed that the vacuum pressure undoubtedly reduced lateral displacement.

Indraratna - Performance and prediction of surcharge and vacuum consolidation via prefabricated vertical drains with special reference to highways, railways and ports

II-160
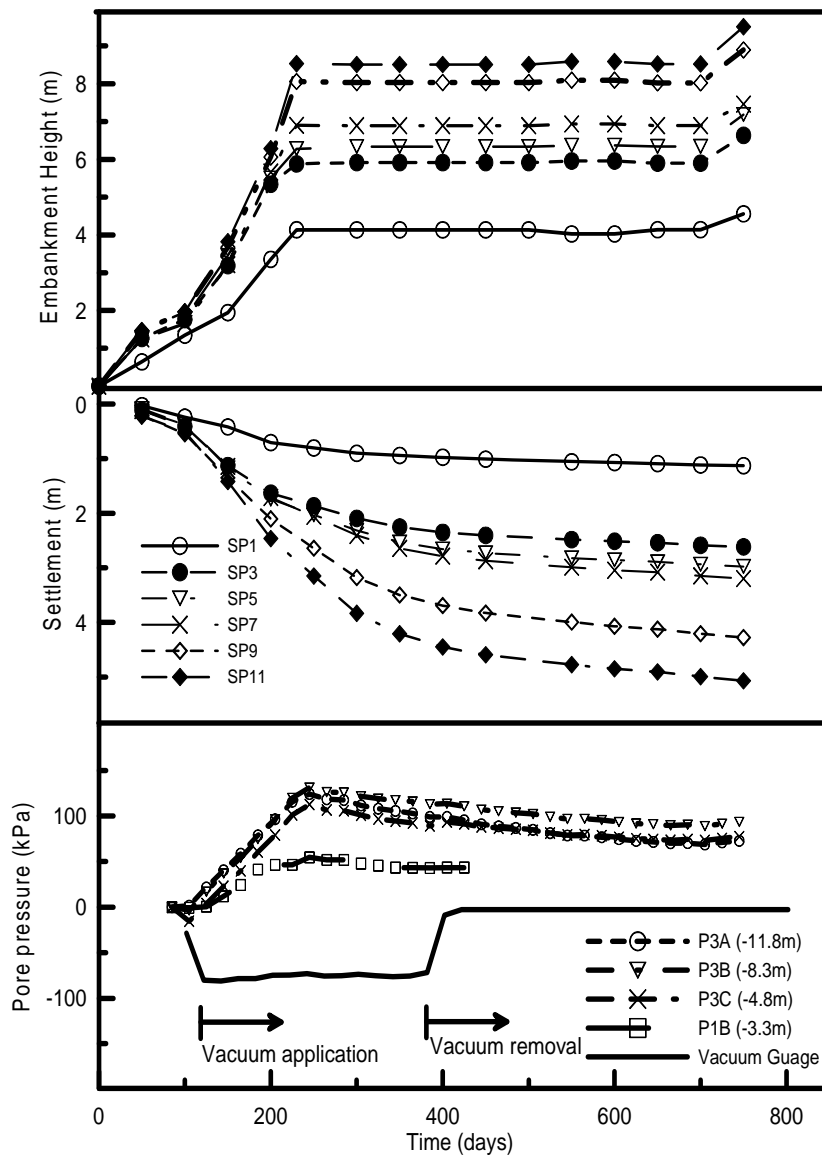
Figure 16: Embankment stage construction with associated settlements and excess pore pressures (Indraratna et al. 2009).

2D and 3D single drain analyses were used to compute the settlement at location SP-12. Typical 2D finite element mesh is shown in Fig. 18a. The construction history and measured settlement at the settlement plate SP-12 are shown in Fig. 18b. Here the clay was assumed to 24m thick, based on the CPT data. The analytical pattern was similar to Indraratna et al. (2005a). The predictions from 2D and 3D analyses agreed with the measured data, where the rate of settlement increased significantly after a vacuum was applied (Fig. 18c).

Indraratna - Performance and prediction of surcharge and vacuum consolidation via prefabricated vertical drains with special reference to highways, railways and ports

II-161

(a)   (b)
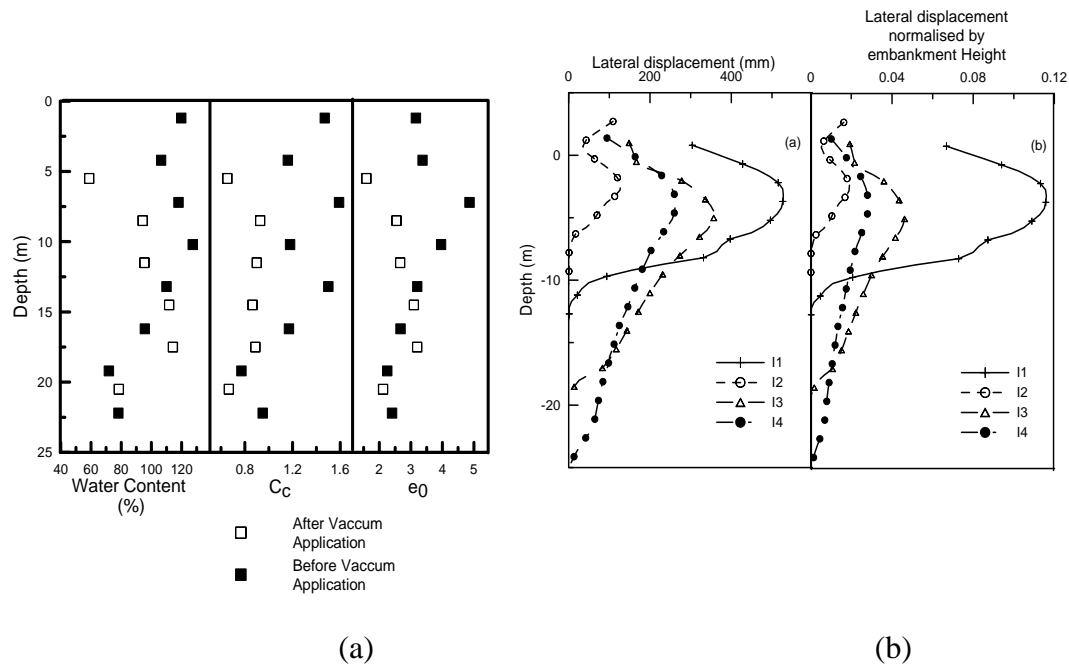
Figure 17: (a) Soil properties before and after vacuum application; and (b) Measured lateral displacement and lateral displacement normalised with embankment height (Indraratna et al. 2009).

(a)
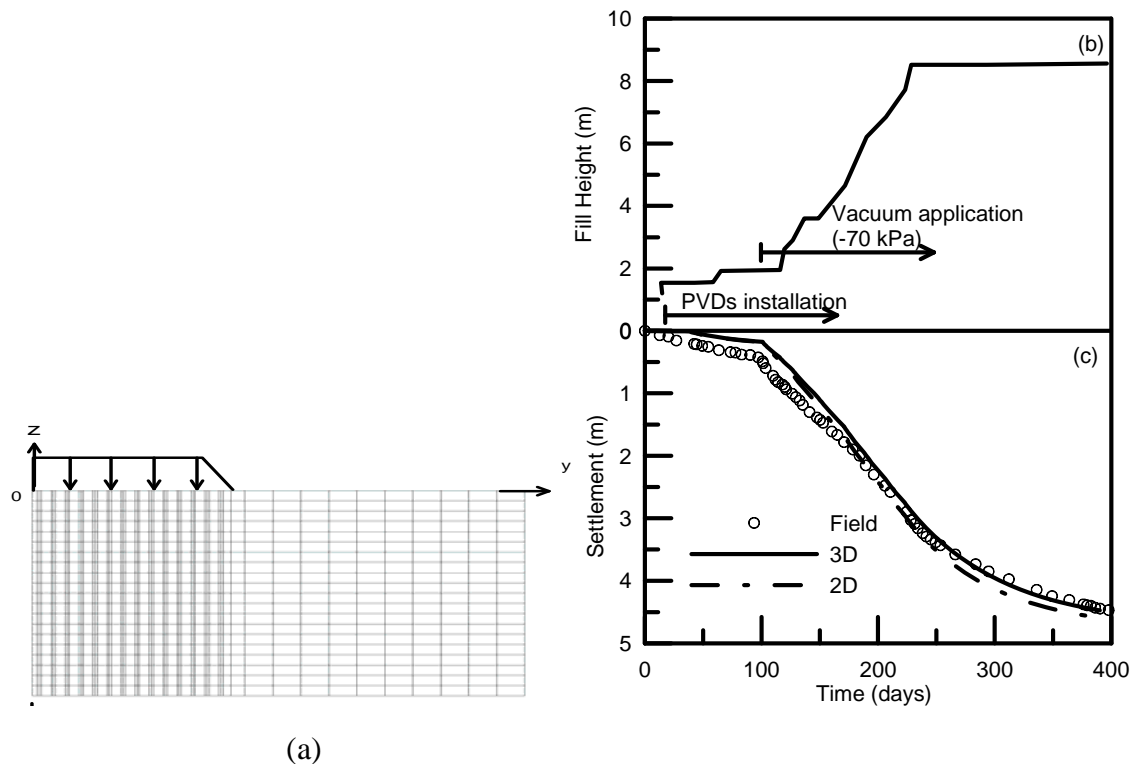
Figure 18: (a) 2D Finite element mesh; (b) loading history; and (c) consolidation settlements for settlement plate SP-12 (Indraratna et al. 2009).

5.3.   Sunshine Coast

The Sunshine Coast is one of Australia's fastest growing regions and the continued economic and population growth has increased the pressure on the region's main traffic corridor, the Sunshine Motorway. Site investigation at the proposed development route revealed that the subsoil consists of highly compressible, saturated marine clays of high sensitivity. In order to evaluate the effective ground improvement techniques, a fully instrumented trial embankment was constructed in 1992 and monitored by the Queensland Department of Main Roads (QDMR), Brisbane.

Indraratna - Performance and prediction of surcharge and vacuum consolidation via prefabricated vertical drains with special reference to highways, railways and ports

II-162

The subsoil conditions are relatively uniform throughout the site, consisting of silty or sandy clay about 10-11m thick, overlying a layer of dense sand approximately 6m thick. The value of $\lambda/(1+e_0)$ of the subsoil varies from 0.19 to 0.63, and the value of $\kappa/(1+e_0)$ was found to be about 10 times smaller than the compression index (QDMR, 1991, 1992).

The base area of the trial embankment was approximately 90m $\times$ 40m and incorporated 3 separate sections (Fig. 19a), identified as Sections A, B, and C, respectively. Sections A and B (each 35m in long) represented the zones of prefabricated vertical drains (installed at 1m intervals) and 'no drains' respectively. Vertical prefabricated drains were installed at a spacing of 2m in Section C. These prefabricated vertical drains (Nylex Flodrain, 100×4mm^2) in Sections A and C were installed in a triangular pattern.

(a)

(b)
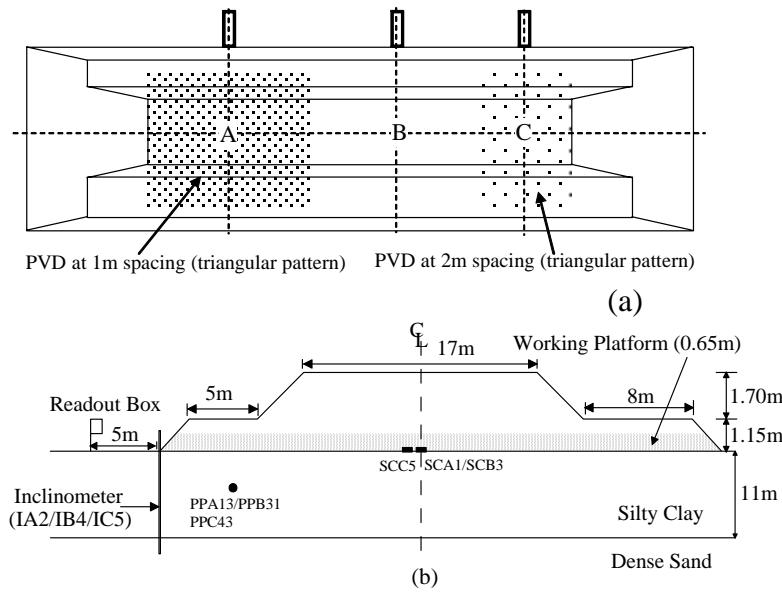
Figure 19: (a) Plan view of trial embankment, and (b) Typical cross-section of embankment with selected instrumentation points (adapted from QDMR, 1992)

A working platform 0.65m thick (500mm thick drainage layer composed of 7mm size gravel, plus 150mm of selected fill) was placed on top for construction traffic access. Prefabricated vertical drains (PVD) were installed from the working platform to a depth of 11m at Sections A and C. The embankment was constructed in stages using a loosely compacted granular material ($\gamma_t \approx 19$ kN/m^3) up to a height of 2.3m. Two berms, 5m in width on the instrumented side and 8m wide on the other side (Fig. 19) were constructed to increase the stability of the embankment. Half of the cross-section was intensively instrumented to capture the foundation response upon loading. A typical cross-section of the embankment with selected instrumentation points is shown in Fig. 19b. In this paper, the deformation and pore water pressure responses below Sections A, B and C were predicted using a plane strain finite element analysis and then compared with the available field data.

The multi-drain plane strain analysis was carried out using the finite element code PLAXIS, where the soil layers were divided into many elements (Sathananthan et al. 2008). In this paper, the soil layer close to the surface was modelled using the modified Cam-clay (MCC) properties determined by QDMR (1991). Given that the soil beneath the surface (up to 2.5m depth) is only lightly overconsolidated based on the results obtained from standard oedometer test (OCR=1.6), the authors have assumed that the application of MCC parameters for this soil layer is valid. Britto and Gunn (1987) and others clarify the validity of MCC for both normally consolidated and lightly overconsolidated clays. It is noted that for situations where the surface soil is heavily overconsolidated (compacted crust), the use of MCC parameters is inappropriate. The soft soil model based on Modified Cam-clay theory was also used to analyse the behaviour of normally consolidated clay layers beneath crust. Based on the oedometer test results on vertical and horizontal samples, the horizontal permeability (k_h) is approximately 2 times the vertical permeability (k_v) for all soil layers. For the embankment material which is silty sand, the Mohr-Coulomb model was used.

Indraratna - Performance and prediction of surcharge and vacuum consolidation via prefabricated vertical drains with special reference to highways, railways and ports

II-163

The finite element (PLAXIS) mesh contains 15-node triangular elements. The entire width of embankment was modelled because the loading was not symmetrical. The prefabricated vertical drains were modelled with zero thickness drain elements (the excess pore pressure along this element is assumed to be zero). The smear zone was modelled with the same modified Cam-clay properties ($\lambda/(1+e_0)$, $\kappa/(1+e_0)$, M) as the adjacent zone except for the reduced coefficient of lateral permeability. The locations of instruments including settlement gauges, piezometers and inclinometers were conveniently placed in the mesh in such a manner that the measuring points coincided with the mesh nodes. Only 11m depth of the foundation was considered due to the existence of the dense sand layer (below the overlying soft clay layer), which was stiff enough to assume a non-displacement boundary. Both the top (open boundary) and bottom surfaces of the subsoil foundation were assumed to be free draining and the water table coincided with the ground surface.
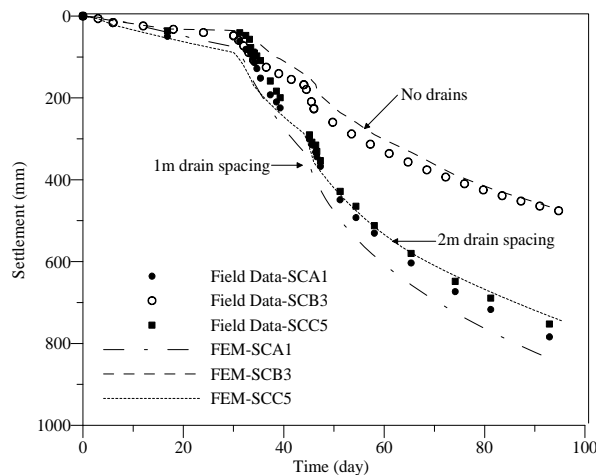
Figure 20: Centreline settlement of Sections A, B and C (Sathananthan et al. 2008).

The settlement gauges under Sections A, B and C, namely, SCA1, SCB3 (both under the centreline) and SCC5 (1m to the left of centreline) were selected for the purpose of comparing the field data with the numerical results. The predicted and measured surface settlements are illustrated in Fig. 20, which shows that the predicted values are in good agreement with the field data for Sections B and C. As expected, the rate of settlement increases due to the PVDs, where the plotted time-settlement at Section B (no drain) is only about 60% of that at Section A (drains at 1m spacing). This proves that the installation of vertical drains significantly decreases the consolidation time for a given settlement. Generally, the settlement rate is expected to be sensitive to drain spacing, but in this study, the difference in settlement-time plots for Sections A and C is small. The installation of closely spaced drains at Section A causes greater smear compared to that at Section C as well as the possible lateral variation of soil properties. In the finite element analysis, the soil properties are assumed constant along any lateral plane. For example, the total width of smear zone at Section A (drains @1m spacing) is about 18.9m compared to 9.7m at Section C (drains@2m spacing). This demonstrates that reducing the drain spacing excessively may only provide a marginal advantage due to increased smear.

Lateral deformation measured by the 3 inclinometers (IA2, IB4 and IC5) installed at the toe of the 5m wide berm at Sections A, B and C are compared with the numerical predictions in Fig. 21. As expected, the vertical drains significantly curtail the lateral deformation. For example, at 1m below the surface, the PVDs installed at 1m spacing (Section A) reduced the lateral displacement by 21% compared to Section B (no drains) and by 6% compared to Section C (drains installed at 2m spacing). Data for Section C indicate that there is not much reduction of lateral displacement below the crust as compared with Section B. These results also indicate that the predicted lateral displacement represents an acceptable match with the field data, but in some plots, a noticeable discrepancy is found approaching the ground surface within the upper most, lightly overconsolidated silty clay (OCR=1.6). For Section A plots (after 100 days) near the surface, the observed field displacements are larger than the predictions, even though the soil is lightly overconsolidated. This may suggest that the closely spaced drains at 1m spacing may have caused excessive smear. This is also supported by the observed excess pore water pressure as discussed below.

Indraratna - Performance and prediction of surcharge and vacuum consolidation via prefabricated vertical drains with special reference to highways, railways and ports

II-164
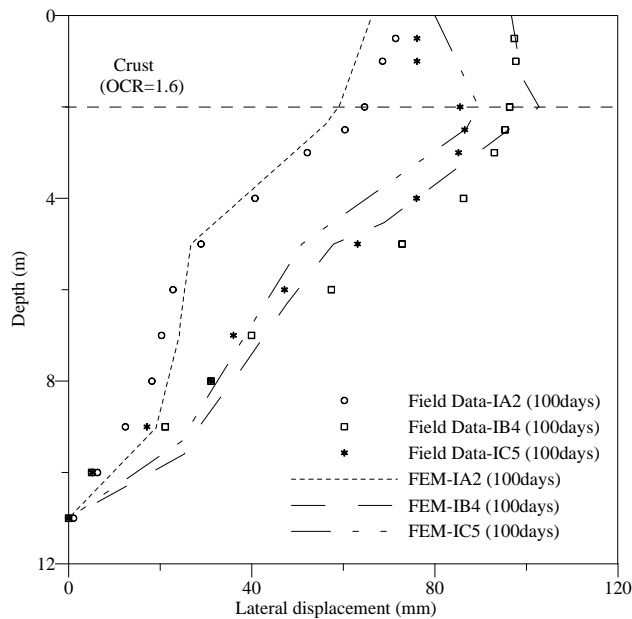
Figure 21: Lateral displacement profiles at the toe 5m berm of the embankment sections (Sathananthan et al. 2008).
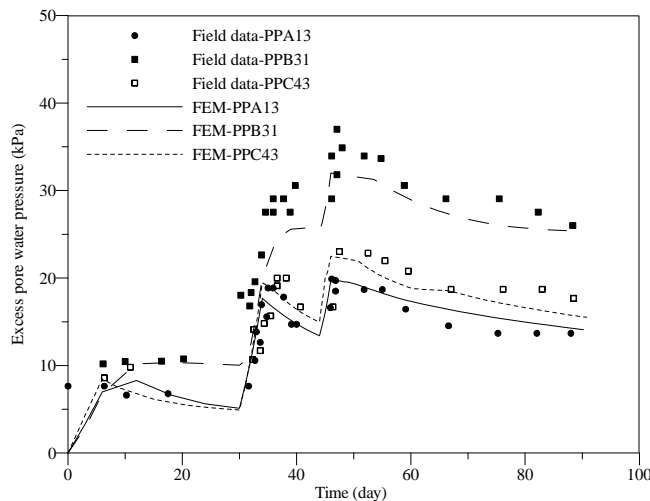
Figure 22: Excess pore pressure variation with time beneath the middle of the berm 5m (Sathananthan et al. 2008).

The predicted and observed variations of excess pore pressure at selected points beneath the middle of the berm are shown in Fig. 22. The selected pneumatic piezometers PPA13, PPB31 and PPC43 were installed at a depth of 5.0m at Sections A, B and C, respectively. Fig. 22 shows that significant excess pore pressures were generated due to embankment loading, and the predictions are in very good agreement with the field data. As expected, the induced excess pore pressure at Section B (no drains) is significantly higher (approximately 30%) than the other sections. Surprisingly, it is observed that at Section A where the drains are closely spaced, the excess pore water pressure is either slightly higher or nearly the same as at Section C before 40 days. After 40 days, rates of excess pore pressure dissipation in Sections A and C are the same. This can be attributed to excessive smear at Section A causing retarded pore pressure dissipation.

6.   CONCLUSION

It is clear that the application of PVDs combined with vacuum and surcharge preloading has become common practice, and is now considered to be one of the most effective ground improvement techniques. Analytical and numerical modelling of vacuum preloading is still a developing research area. There has always been a discrepancy between the predictions and observed performance of embankments stabilised with vertical drains and vacuum pressure. This discrepancy can be attributed to numerous factors such as

Indraratna - Performance and prediction of surcharge and vacuum consolidation via prefabricated vertical drains with special reference to highways, railways and ports

II-165

the uncertainty of soil properties, the effect of smear, inaccurate assumptions of soil behaviour and vacuum pressure distribution, and an improper conversion of axi-symmetric condition to plane strain (2D) analysis of multiply drains.

Vacuum assisted consolidation is an innovative method which has recently, and successfully, been used for large scale projects on very soft soils in reclamation areas. The extent of surcharge fill can be decreased to achieve the same amount of settlement and the lateral yield of the soft soil can be controlled by PVDs used in conjunction with vacuum pressure. The effectiveness of this system depends on (a) the air tightness of the membrane, (b) the seal between the edges of the membrane and the ground surface, and (c) the soil conditions and location of the ground water level. The exact role of membrane type and membrane-less systems for vacuum preloading requires detailed evaluation. In the absence of a comprehensive and quantitative analysis, the study of suitable methods to apply vacuum preloading becomes imperative, experimentally, numerically and in the field.

Analytical modelling of vertical drains that include vacuum preloading under axi-symmetric and plane strain conditions that simulate the consolidation of a unit cell surrounding a single vertical drain has been developed. The effects of vacuum propagation along the length of a drain and the occurrence of non-Darcian flow conditions have been incorporated in the proposed solutions to obtain a more realistic prediction. The elliptical cavity expansion theory provided further insight to evaluate the role that smear zone characteristics play on consolidation.

In large construction sites where many PVDs are installed, a 2D plane strain analysis is usually sufficient. The proposed conversion from axi-symmetric to a plane strain condition agreed with the data available from case histories, including Ballina Bypass and Port of Brisbane (Australia). These simplified plane strain methods can be readily incorporated in numerical (FEM) analysis. The conversion procedure from 3D to 2D based on the correct transformation of permeability and vacuum pressure, ensure that the time-settlement curves are the same as the true 3D analysis. Field behaviour and model predictions indicate that the efficiency of vertical drains depends on the magnitude and distribution of vacuum pressure as well as the degree of drain saturation during installation, and the extent of smear caused by the vertically penetrating mandrel.

7.   ACKNOWLEDGEMENT

Indraratna - Performance and prediction of surcharge and vacuum consolidation via prefabricated vertical drains with special reference to highways, railways and ports

II-166

REFERENCES

Bergado, D. T., Balasubramaniam, A. S., Fannin, R. J. and Holta, R. D. 2002. Prefabricated vertical drains (PVDs) in soft Bangkok clay: a case study of the new Bangkok International Airport Project, Canadian Geotechnical Journal. 39: 304-315.

Bo, M. W., Chu, J., Low, B. K., and Choa, V. 2003. Soil improvement; prefabricated vertical drain techniques, Thomson Learning, Singapore.

Chai, J. C., Cater, J. P., and Hayashi, S. 2005. Ground deformation induced by vacuum consolidation. Journal of Geotechnical and Geoenvironmental Engineering, ASCE, 131(12): 1552-1561.

Choa, V. 1990. Soil improvement works at Tianjin East Pier project. Proceedings 10th Southeast Asian Geotechnical Conference, Taipei, 1: 47-52.

Chu, J., and Yan, S.W. 2005. Application of vacuum preloading method in soil improvement project. Case Histories Book, Edited by Indraratna, B. and Chu, J., Elsevier, London. Vol. 3: 91-118.

Chu, J., Yan, S. W., and Yang, H. 2000. Soil improvement by vacuum preloading method for an oil storage station. Geotechnique, 50(6): 625-632.

Holtan, G.W. 1965. Vacuum stabilization of subsoil beneath runway extension at Philadelphia International Airport. In Proc. of 6th ICSMFE, 2.

Indraratna, B., Balasubramaniam, A. S. and Balachandran, S. 1992. Performance of test embankment constructed to failure on soft marine clay. Journal of Geotechnical Engineering, ASCE, 118(1): 12-33.

Indraratna, B., and Redana, I. W. 2000. Numerical modeling of vertical drains with smear and well resistance installed in soft clay. Canadian Geotechnical Journal, 37: 132-145.

Indraratna, B., Bamunawita, C., and Khabbaz, H. 2004. Numerical modeling of vacuum preloading and field applications. Canadian Geotechechnical Journal, 41: 1098-1110.

Indraratna, B., Rujikiatkamjorn C., and Sathananthan, I. 2005a. Analytical and numerical solutions for a single vertical drain including the effects of vacuum preloading. Canadian Geotechnical Journal, 42: 994-1014.

Indraratna, B., Sathananthan, I., Rujikiatkamjorn C. and Balasubramaniam, A. S. 2005b. Analytical and numerical modelling of soft soil stabilized by PVD incorporating vacuum preloading. International Journal of Geomechanics, 5(2): 114-124.

Indraratna, B., Rujikiatkamjorn C., Balasubramaniam. A. S. and Wijeyakulasuriya, V. 2005c. Predictions and observations of soft clay foundations stabilized with geosynthetic drains vacuum surcharge. Ground Improvement – Case Histories Book (volume 3), Edited by Indraratna, B. and Chu, J., Elsevier, London: 199-230.

Indraratna, B., and Rujikiatkamjorn, C., Kelly, R., and Buys, H. 2009. Soft soil foundation improved by vacuum and surcharge preloading at Ballina Bypass, Australia. International Symposium on Ground Improvement Technologies and Case Histories (ISGI09): 95-105.

Kjellman W. 1952. Consolidation of clayey soils by atmospheric pressure. Proceedings of a Conference on Soil Stabilisation, MIT, Boston, pp. 258–263.

Jacob, A., Thevanayagam, S. and Kavazajian, E., 1994. Vacuum-assisted consolidation of a hydraulic landfill. Vertical and Horizontal Deformations of Foundations and Embankments, Settlement'94, College Station. Geotechnical Special Publications No 40, ASCE: 1249-1261.

Jamiolkowski, M., Lancellotta, R., and Wolski, W. 1983. Precompression and speeding up consolidation. Proc. 8th ECSMFE: 1201-1206.

Johnson, S. J., 1970. Precompression for improving foundation soils. Journal of the Soil Mechanics and

Indraratna - Performance and prediction of surcharge and vacuum consolidation via prefabricated vertical drains with special reference to highways, railways and ports

II-167

Foundations Division, ASCE, 1: 111-114.

Mohamedelhassan E., and Shang, J.Q. 2002. Vacuum and surcharge combined one-dimensional consolidation of clay soils, Canadian Geotechnical Journal, 39: 1126-1138.

Port of Brisbane Corporation and Austress Menard (2008), personal communication internal report and confidential, 79p.

Queensland Department of Main Roads. (1991). Sunshine Motorway Stage 2 – Area 2 Geotechnical Investigation. Materials and Geotechnical Services Branch, June, R1765.

Queensland Department of Main Roads. (1992). Sunshine Motorway Stage 2 – Interim Report on the Performance of the Trial Embankment Area 2A (Ch 28490-28640). Materials and Geotechnical Services Branch, July, R1802.

Richart F.E. 1957. A review of the theories for sand drains. Journal of the Soil Mechanics and Foundations Division, ASCE, 83(3): 1-38.

Sathananthan, I., Indraratna, B., and Rujikiatkamjorn C., (2008). The evaluation of smear zone extent surrounding mandrel driven vertical drains using the cavity expansion theory. International Journal of Geomechanics, ASCE. 8(6), 355-365.

Seah, T.H. 2006. Design and construction of ground improvement works at Suvarnabhumi Airport. Geotechnical Engineering Journal of the Southeast Asian Geotechnical Society, 37: 171-188.

Yan, S.W. and Chu, J. 2003. Soil improvement for a road using a vacuum preloading method. Ground Improvement, 7(4): 165-172.

Indraratna - Performance and prediction of surcharge and vacuum consolidation via prefabricated vertical drains with special reference to highways, railways and ports

II-168

Use of Temporary Water Drawdown for Site Improvement

Richard A. Jewell, Fugro GeoConsulting, Belgium, rjewell@fugro.be

ABSTRACT

This paper describes examples where temporary drawdown of groundwater may be used as preload for fill construction over soft clay. The technique is effective in the right circumstances but is not frequently used for site improvement (Chu et al, 2009). The examples in this paper illustrate conditions where temporary groundwater lowering is beneficial for ground improvement. The equipment and methods are simple and tie in well with vertical drains. Combined with a suitable foundation engineering solution, the approach can be a highly effective component for site preparation.

This paper illustrates groundwater lowering for ground improvement purposes by means of three project examples on which the author was involved. Note that separate publication on the major case history CASE 1 is planned to provide full details on the soils data, site measurements and foundation performance.

1. Case 1 – large-scale onshore site improvement

A 35 hectare site located in a mangrove swamp next to a major river is to be used for the construction of petro-chemical facilities. The soil conditions comprise 35 m to 40 m of soft clay overlying stronger basal sands and silts. The existing ground level is at high water level (mangrove swamp). A final and stable site grade 2 m above high water level is required. The site grade should not undergo significant creep settlement during the design life of the plant.

Alternative solutions ranging from "offshore" construction at the unimproved site, to extensive deep soil mixing of the soft clay soil were considered. The optimal approach from the range of alternatives considered was to pre-load the site with sand fill combined with temporary groundwater lowering and vertical drains. A combination of shallow and piled raft foundations could then support the processing units and pipe racks. The large diameter tanks could be constructed with no further support such as piles.

The key geological feature that permitted groundwater lowering at this site was a continuous and permeable sand layer at about 14 m depth in the soft clay, called the middle sand layer. Relatively simple pumping tests measured the hydraulic properties of this sand layer and extensive CPT testing proved the continuity of the layer across the site.

A section through the improvement scheme is shown on Figure 1. The pumps are installed in the sand layer around the periphery of the site with some supplementary pumps installed within the site area to help remove the large volume of water resulting from clay consolidation as well as rain infiltration. The wells and submersible pumps were installed simply by jetting. Ejector pumps would have also been suitable for this project.

Vertical drains were installed to a short distance above the elevation of the more permeable basal soils below the clay so as not to provide a hydraulic connection, Figure 1. Larger drain spacing was used for vertical drains in the soft clay below the middle sand than in the more compressible and less permeable clay above, Photo 1.

The target drawdown level for the water was the top of the middle sand layer where the pumps are located. Groundwater modeling demonstrated that a cut-off in the sand layer outside the ring of pumps was not required; the pumps could handle the lateral flow of water through the sand layer from outside the area of site preparation. Any ground settlement resulting from temporary drawdown around the site would not cause damage. The exception was on one portion of the adjacent site where possible ground settlement had to be limited: a line of recharge wells installed in the middle sand layer at some distance from the pumps limited the drawdown in this area. A hydraulic cut-off through the sand layer outside the line of pumps on the site periphery would have been an alternative solution; but this was judged to involve higher risk and cost.

Creep testing of the soft clay indicated that preloading to achieve a minimum overconsolidation ratio in the clay OCR > 1.5 under final loading conditions would minimize future creep settlement at the site over the required design life. Combination of 90% consolidation in the soft clay loaded by the sand fill and the reduced groundwater level with subsequent removal of about 1 m of the sand (temporary surcharge) would permit the required preconsolidation. The case with no removal of sand surcharge is shown in Figure 2. In practice, 8 m of sand fill and the reduced groundwater level caused approximately 5m of settlement at the site. This enabled removal of about 1m thickness of sand while still achieving the desired 2 m change in grade elevation.

The removal of about 20 kPa sandfill loading significantly increases the achieved OCR in the upper soft clay layer. Where there is no physical removal of sandfill, it is only the difference between the total unit weight of the sandfill above water level during drawdown and the subsequent submerged unit weight once the sandfill is below the final groundwater level that provides the additional pre-loading at the top of the clay layer.

The foundation solution for the project was a combination of shallow foundations for more lightly loaded structures and piled-rafts for heavier units, Figure 3. The dominant factor in foundation design was to limit creep settlement between pipe racks and processing units. The piles distribute the applied loading to greater depth so as not to cause undue creep.

Note that no piling extended all the way to the stiffer basal soils. Any creep settlement at the site would transmit down drag to piles end-bearing in stiffer basal soils. There are many reasons why such an end-bearing pile design would be less satisfactory including the much larger quantity of piling that would be required (piles of great length attracting significant down drag), and differential settlement between piled units and the site grade.

2. Case 2 – Artificial Island Construction

A robust island is required to resist ice loading and permit the installation of equipment. A significant thickness of rockfill is required combined with outer sheet piling for the island. However, such construction was considered to be susceptible to two sources of settlement caused by the foundation conditions.

First, a variable thickness of relatively shallow soft clay below the island will cause differential settlement and ongoing creep settlement across the island, Figure 4. Second, the thick over-consolidated clay layer below the island will experience a significant increase in pore water pressure due to the island construction resulting in progressive settlement over the design life of the facilities. Note that while the stiffness of the deeper clay is relatively high, the size of the island and great thickness of the clay deposit causes a sufficient depth of clay to consolidate due to dissipation of positive pore water pressure, thereby causing significant settlement of the island.

At shallow depth there is sand layer containing a variable thickness of soft silty clay layers ranging from 0 m to 2.5 m thick. This sand layer containing soft clay of variable thickness overlies the deep stiff clay deposits. The sheet piles planned for construction of the island penetrate to the stiff clay soil and provide a hydraulic cut-off to surrounding water. Therefore, pumping from the base of the sand layer within the island would permit temporary drawdown of the water level to the top of the stiff clay and preloading of the variable soft clay and silty soils, Figure 5.

Further, several deep wells constructed to depth in the stiff clay would greatly reduce the time required for dissipation of positive excess pore-water pressure. In the absence of such drains, the horizontal drainage path length would be on the scale of the island diameter. Inclusion of some deep drains greatly reduces the drainage path length. Further, drainage in the stiff clay in the horizontal direction is likely to be much greater than in the vertical direction providing additional benefit by connecting more permeable horizontal layers, Figure 5.

There is a further benefit to be achieved. During the period of water drawdown to consolidate the upper soft silty clay soils, there will be additional hydraulic gradient applied to the deep drains causing faster dissipation of positive pore water pressure in the stiff clay. Depending on the period during which drawdown is maintained at the island, a volume of stiff clay soil around each deep well would dissipate pore water pressure to below the long term hydrostatic value. When pumping and drawdown at the island is stopped, a portion of the stiff clay nearer the vertical wells would experience increasing pore water

pressure (and volume expansion) as it moves toward the final hydrostatic equilibrium. This behaviour would counterbalance to an extent the remaining volume of stiff clay still dissipating positive pore water pressure and consolidating to reach hydrostatic conditions.

This second example illustrates how temporary reduction of water level can help mitigate settlement issues associated with both a soft layer of variable thickness across the site and settlement in stiff clay due to excess pore water pressure that develops t over the design life of the facility.

3.   Case 3 – Land reclamation nearshore

The third example is a near-shore land reclamation / artificial island construction over a significant thickness of soft estuarine clay. An important aspect for this reclamation was stability of the outer embankment (constructed over the soft estuarine clay) required to contain and protect the new sand fill. This is not described here.

The proposal to use temporary water drawdown in this case was to permit an efficient final working platform that would not be susceptible to significant creep settlement for the underlying soft clay and would be suitable for simple foundations.   An additional option provided by the method was that dry "onshore" construction methods could be used for the majority of the land reclamation (installation of drains and filling), if desired.

The main features for the site are shown diagrammatically in Figure 6.   The detail for stability and construction of the outer retaining embankment are not discussed here.   The land reclamation was proposed as follows:

(1)   During construction of the outer retaining and protective embankment an initial thickness of sand fill on the soft seabed would be placed through water.
(2)   A sheet pile (or similar) hydraulic cut-off would be placed through the outer embankment, or just inside it, to permit internal dewatering.
(3)   Pumps would reduce the water level inside the contained area down to the top of the soft clay. While significant pumping would be required in the short term, once the volume of water was removed, reduced pumping would be required to maintain drawdown.
(4)   Vertical drains would be installed in the soft clay by land based plant. The drains would stop just above the underlying stiff soil not to provide a hydraulic connection.
(5)   Sumps and pumps would be placed at the base of the sand fill.
(6)   Land based sand filling and compaction would be completed while maintaining drawdown to the top of the soft clay.
(7)   If additional preloading was desirable in some areas then an additional thickness of sand surcharge would be placed for subsequent removal.

The site preparation would also be applicable with vertical drains and initial sand filling placed through water with water drawdown only applied once the reclaimed area was above sea level.

Similar to project CASE 1 described earlier, the aim of the site preparation would be to pre-load the soft clay soil below the reclaimed land to reduce the tendency of creep to a minimum by means of achieving overconsolidation of the order OCR > 1.5 (which would be verified by laboratory testing for the particular clay soil).   This would then permit simple shallow foundations for most of the lighter structures. Heavier structures, if required, could be supported by piles bearing in the underlying stiffer basal soils. Benefit in that case would arise from reduced relative settlement between the site grade and the piled structure due to the site preparation.

4.   Concluding remarks

Three different projects have illustrated a wide range of ways that temporary groundwater lowering can be beneficial and efficient in ground improvement.   Common to all three examples is the use of groundwater lowering to pre-load soft clay so that overconsolidation of the order OCR > 1.5 under the final loading conditions can reduce creep settlement significantly. Where sand fill has been placed over relatively soft clay in such cases, shallow foundations and piled rafts for heavier loaded structures may be used to provide cost effective foundations.   Foundations may be designed to minimize differential settlement between more heavily and lightly loaded structures (as in CASE 1).

The benefit of temporary ground water drawdown was also illustrated to mitigate long-term settlement due to dissipation of construction induced excess pore water pressure in a large thickness of stiff clay. Although the compressive strain in the stiff clay is relatively small the resulting settlement can still be significant if there is a large thickness of clay that has been loaded.

The aim of this paper is to encourage the more extensive use of temporary ground water lowering as a tool that should be considered alongside physical surcharge and the use of vertical drains for ground improvement.

REFERENCES

Chu, J., Varaskin, S., Klotz, U. and Mengé, P. (2009). Construction Processes. Proc. 17th International Conference on Soil Mechanics and Geotechnical Engineering, Alexandria. pp 3006-3135

Photo 1: Installation of Deep Vertical Drains. Situation before Intermediate Drains in the Upper Clay are Installed down to the Middle Sand (CASE 1).
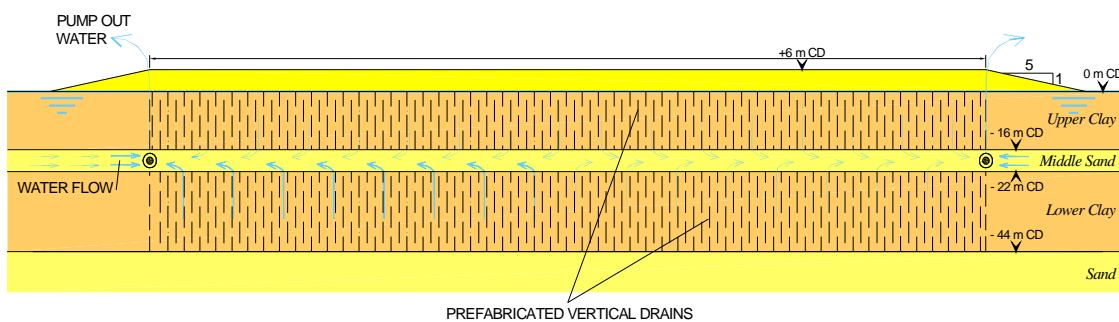
Note vertical drains terminated in the lower clay above the basal sand layer to prevent hydraulic connection

Figure1: Cross-Section of Ground Improvement with Pumping from Middle Sand (CASE 1)
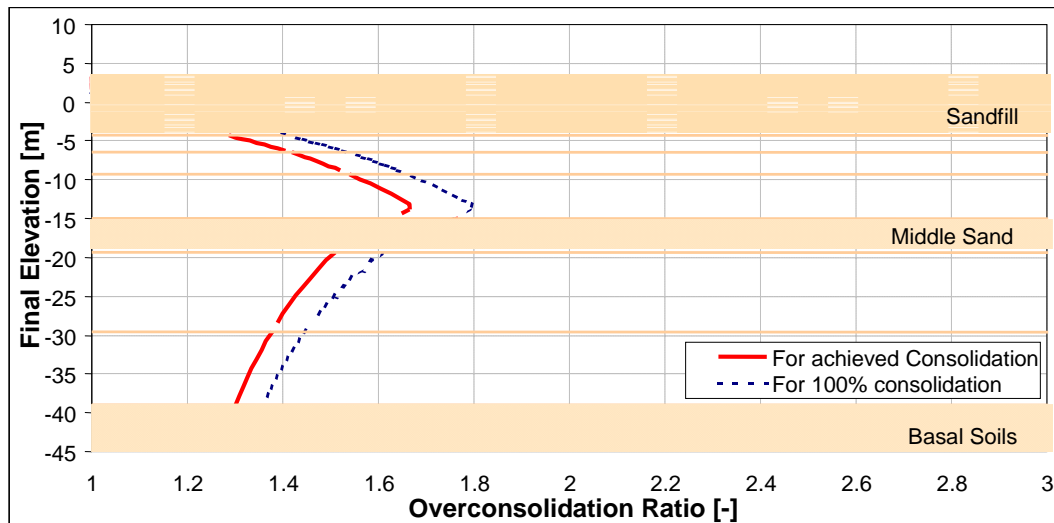
Note the above illustration does not include the benefit of removal of 1m sand surcharge.

Figure 2: Over-Consolidation Achieved by Temporary Groundwater Lowering to -14m (CASE 1).

➤ Simple shallow foundations for lightly loaded structures
➤ Pile rafts for more heavily loaded structures
➤ Load shared between raft and piles (raft transmits some load to the soil directly)
➤ Piles designed at Creep limit (provide constant force irrespective of settlement)
➤ Piles Terminate in Upper or Lower Clay (longer piles for heavily loaded rafts)

Base design case:
30% load transmitted raft to soil
70% load transmitted to piles

Figure 3: Range of Foundations: Shallow Foundations up to Piled Rafts into Lower Clay (CASE 1).
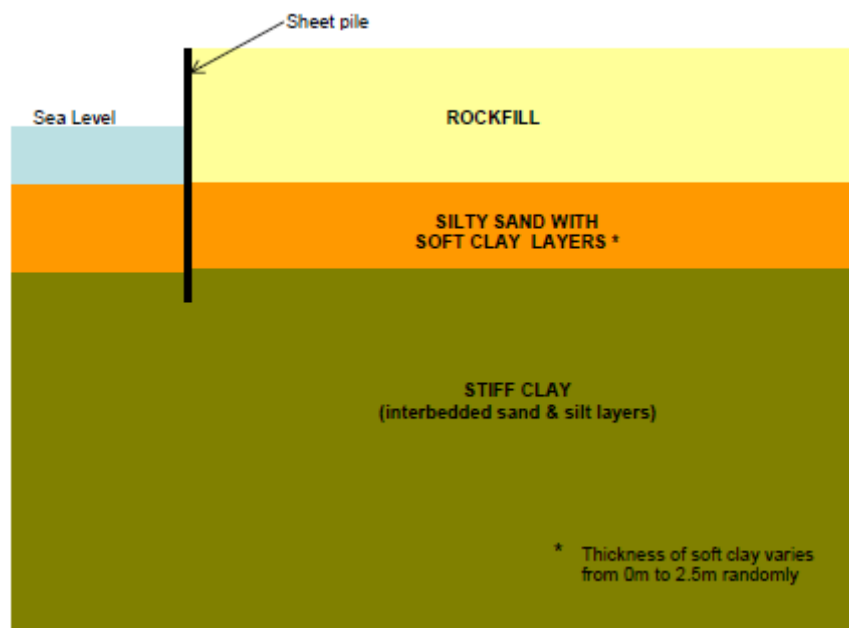
Figure 4: Artificial Island (CASE 2).
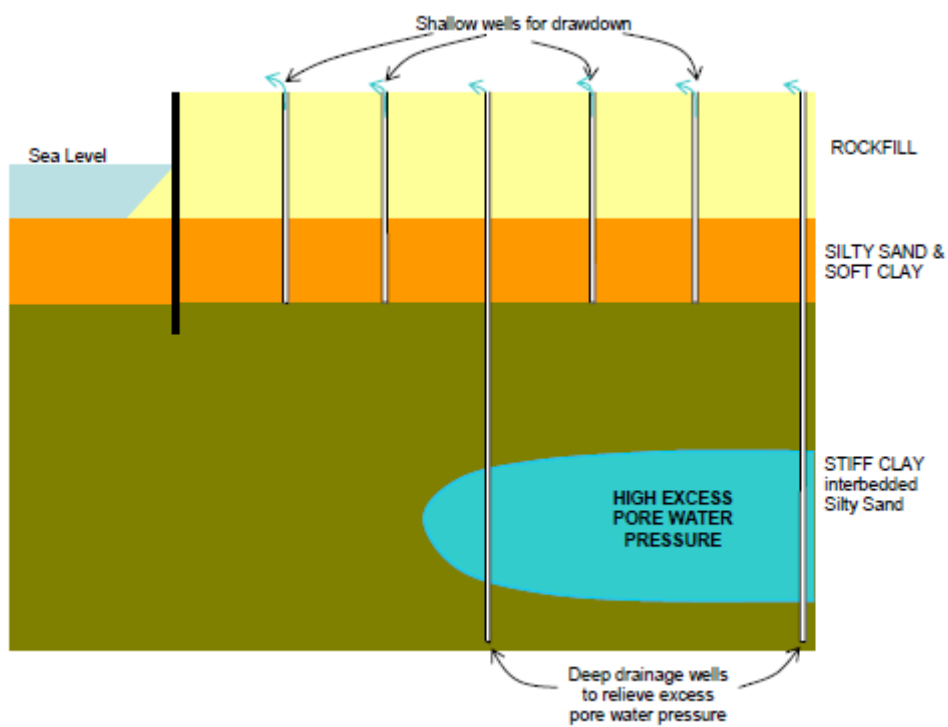
Figure 5:   Shallow Wells for Drawdown and Deep Wells for Excess Pore Water Pressure (CASE 2).
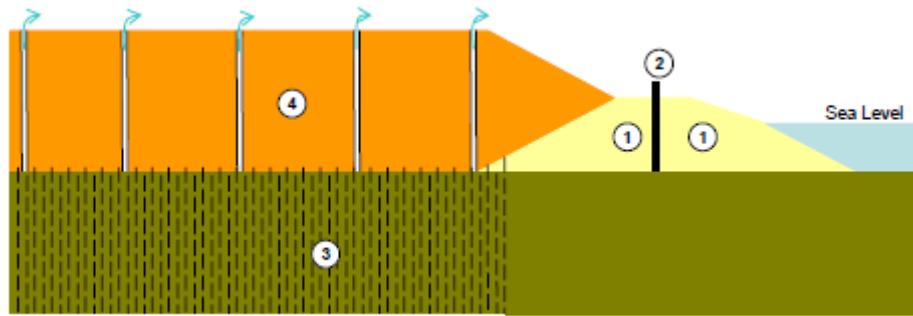
(1) Construct outer embankment (soil improvement and reinforcement not shown)
(2) Install sheet pile cut-off into soft estuarine clay
(3) Install vertical drains
(4) Place sumps and pumps and fill reclaimed area.

Figure 6: Shallow Wells for Drawdown as Part of Land Reclamation (CASE 3)

Back analysis of a trial embankment settlement based on CPTu and oedometric test results.

Teresa Mateos (Acciona Ingeniería, Spain, tmateosg@acciona.es)

ABSTRACT

Main results from a monitorized trial embankment are shown in this paper. A "High Speed Rail Track", SE of Spain, is to cross a swampy area with soft sediments up to 35m thick, thus implying big settlements under future embankments weight because of the high deformability of concerned soils.

In order to better assessing the problem, 32 dynamic continuous penetration tests, 67 drillings with continuous borelog recovery and 13 CPTU tests were performed to obtain proper geotechnical information about these soils. Among other tests, 16 one-dimensional consolidation tests in oedometric cell were made on undisturbed samples, and 41 dissipation tests during CPTUs execution to determine consolidation coefficients.

A trial embankment was proposed with previous installation of prefabricated vertical drains 20m deep and instrumentation consisting in settlement plates, horizontal inclinometers and surveying landmarks. After more than 15 months settlement still go on progress.

Back analysis proved that one key factor is the distance between draining borders and this was estimated after CPTU careful interpretation. Thus, a good adjustment was got for a good forecasting on final settlements and time evolution when using Barron solution for horizontal and vertical consolidation.

1.   INTRODUCTION

The studies included in this paper were developed in order to get accurate settlement prediction under a long embankment which is being built for a new "High speed rail track" in southeast of Spain.

The new rail track has been designed along earth fills 4 to 8 m height. Due to the great deformability of the marsh sediments underneath, important settlements are forecast along the embankment. Consequently, it is necessary to do a settlement prediction as accurate as possible, both in magnitude and in temporal development.

Estimation of settlements is one of the less accurate geotechnical calculation. At least we may say that the magnitude of the settlement estimated for a certain load, geometry and soil profile can be half or twice the estimated value. Much more difficult is to estimate consolidation time. This value depends on two parameters which are difficult to know properly: the consolidation coefficient, both vertical and horizontal, whose magnitude changes related to a potential law, and the distribution of drain levels along the geotechnical profile.

This paper shows how an accurate knowledge of the distribution of drained levels improves the forecasting of temporal consolidation development. The improved geotechnical profile including all the drain levels in the soil is defined by the study of CPTu records.

In order to check this approach a trial embankment has been built over a section treated with vertical drains 20 m deep distributed in a triangular mesh whose side is 1.66 m long. Data from this embankment have been recorded for more than 15 months.
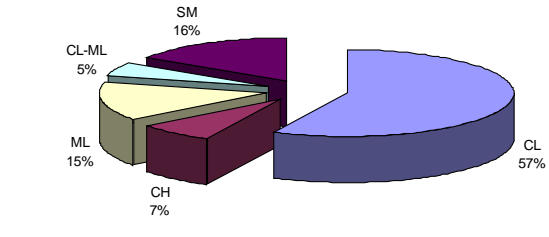
2.   SOIL GEOTECHNICAL PROFILE

Soil profile in the area of the study is composed by 32 meters of marsh sediments overlaying alluvial fan sediments. It is possible to define three different marsh levels:

- 0 – 2 m.- preconsolidated marsh sediments.
- 2 – 20 m.- upper marsh sediments.
- 20 – 32 m.- lower marsh sediments.

Marsh soils are composed mainly by low plasticity clays (CL) and locally by silty sands (SM). These three levels in marsh sediments are define according to their geotechnical properties, specially undrained shear strength and deformability, as it is resumed in the next table.

Table 1: Geotechnical properties of marsh sediment

	S_u (kPa)	E (kPa)	
Preconsolidated level	70	7000	
Upper marsh sediments	30/40	3500	
Lower marsh sediments	40 + 3,85 kPa/m	7500	

Values of deformation modulus where obtain from results of presiometrics tests and by correlations between cone tip resistance measured in CPTu tests. The obtained values were really closed to that estimated from the back analysis of the trial embankment data.

The second relevant parameter, vertical consolidation coefficient, was estimated from the results of oedometric tests. A total of 16 tests where done. Distribution of these results is shown in the next figure. It can be seen that a value of 5.10^{-4} cm^2/s could be representative of the vertical drained behaviour of these soils.
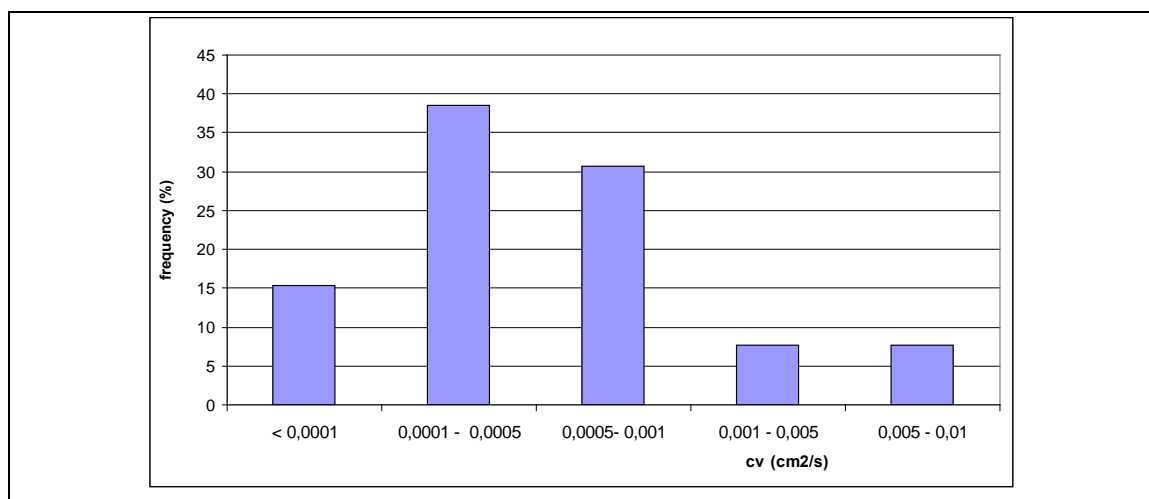
Figure1: Cv values obtained from oedometric tests.

The horizontal consolidation coefficient was estimated from the dissipation tests in CPTu. A total of 41 tests were performed. Frequency distribution of these results is shown in figure 2.
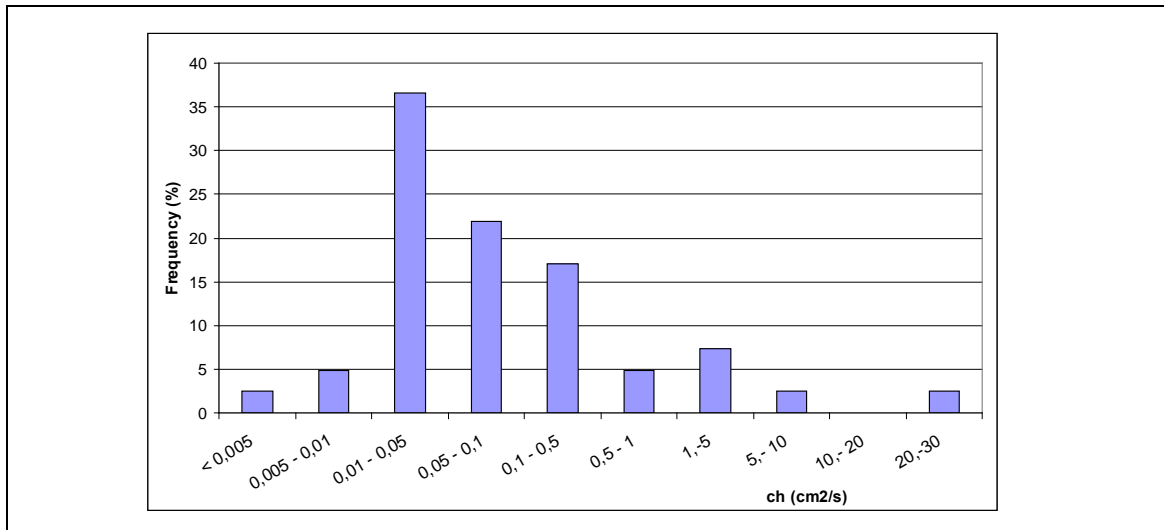
Figure 2 : Cr values obtained from dissipation tests(CPTu).

Results from CPTu test were also employed to define the drained levels distribution in the soil profile. Interpretation of borehole log data usually gives a simplify soil profile because it is difficult to identify thin granular levels in mainly cohesive soils. But, it is almost impossible that in a soil 32 m thick there is no granular sedimentation episode. Even more, marsh sediments usually include mainly clay levels and depositional episodes related to channel dynamics where sand and silts are accumulated. This fact explains the granulometric distribution shown in table 1 and results in high radial consolidation coefficient values as have been recorded in dissipation tests (Figure 2). These results reveal the jointed draining behaviour of clay and silty sand levels. On the other hand, results of vertical consolidation coefficients concern just to draining behaviour of clay levels because samples to be tested have been chosen with a high component of particles passing 200# sieve.

Borehole log interpretation jointed to laboratory data gives us the profile shown in the next figure. According to these results, there are only one or two granular levels in the profile and whose lateral continuity is not assured.

These swampy soils are situated over alluvial fan sediments with a higher strength and much less compressibility as it is shown in figure 3.
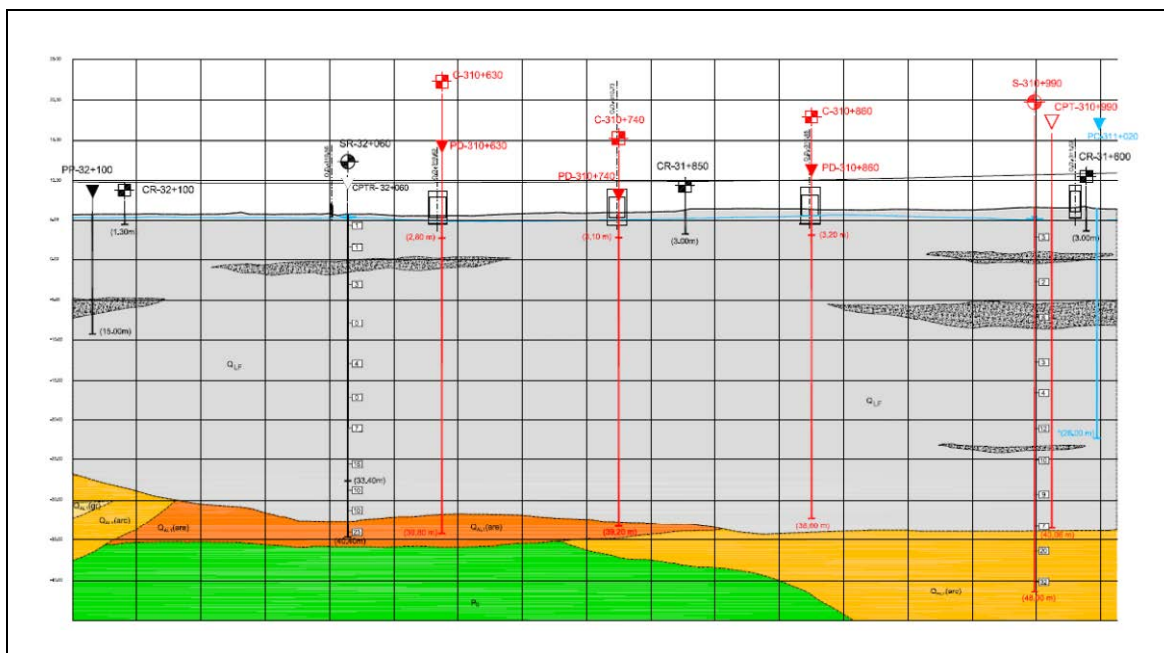
Figure 3: Soil profile from borehole data. In grey marsh sediment (Q_{LF}); in orange sandy alluvial ($Q_{AL(are)}$); yellow, clay alluvial ($Q_{AL(arc)}$) and green, Pliocene sediments.

Meanwhile, if CPTu data are analysed it is discovered that there are many granular levels in the profile. Results of CPTu tests closed to the trial embankment are shown in the next figure. The criterion to distinguish between drained and undrained levels is related to excess pore measured during static penetration. In the figure, hydrostatic pressure is shown jointed to the excess pore record. If the cone is penetrating trough an impermeable layer the excess pore pressure measured will be over the hydrostatic pressure. On the contrary, if it is penetrating trough a permeable layer there won't be excess pore pressure over the hydrostatic pressure.

According to these records, there are permeable layers every two meters in the six first meters of the profile and between eleven to thirteen meters. Then there is another granular level at sixteen meters depth and others levels less defined at twenty and twenty seven meters depth. So, the real distribution of permeable levels is much more complex than the figure elaborated by the borehole data. An accurate localization of these levels is a key factor in forecasting of consolidation time as it is explained in the next paragraphs.
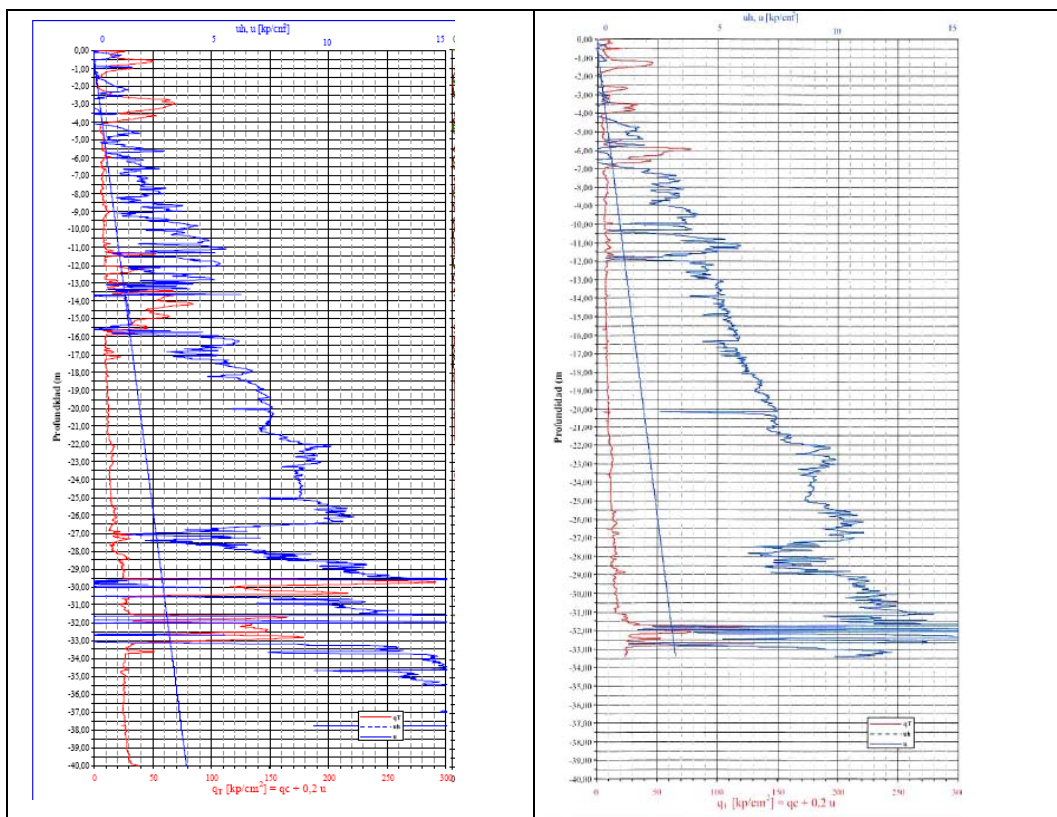
Figure 4: Excess pore pressure registered by CPTu tests close to the trial embankment.

3.   TRIAL EMBANKMENT

A trial embankment has been built in order to get a better understanding of consolidation behaviour of marsh soils. The trial embankment is 4 m height, 25.45 m wide and 64 meters long. It has been instrumented with settlement plates (PA), vertical (INC) and horizontal (LCA) inclinometers and surveying landmarks (H). Distribution of these equipments is shown in the next figure.

The embankment has been built after a treatment by vertical drains – in a triangular mesh, 1,6 m in side- had been applied to reduce consolidation time. Drain's length is 20 m, so there are another 12 m of marsh sediments where consolidation time is not accelerated and it is only related to dissipation of excess pore pressure in the vertical direction.
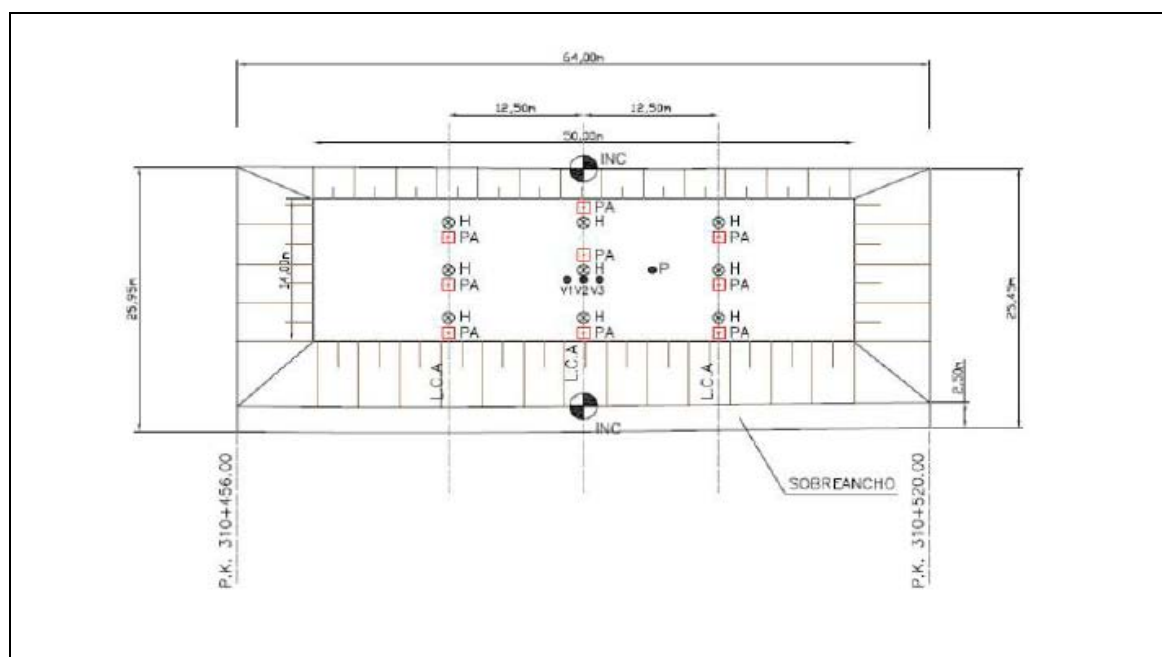
Figure 5: Trial embankment geometry and instrumentation.

Photo1: Treatment by vertical drains.

Data obtained since the beginning of the construction to September 2011 are shown in the next figures. These data show that most of the settlement develops at the time of the embankment construction and in the next two months. Since then, the velocity of settlement has been continuously decreasing and now is less than 0.5 cm per month.
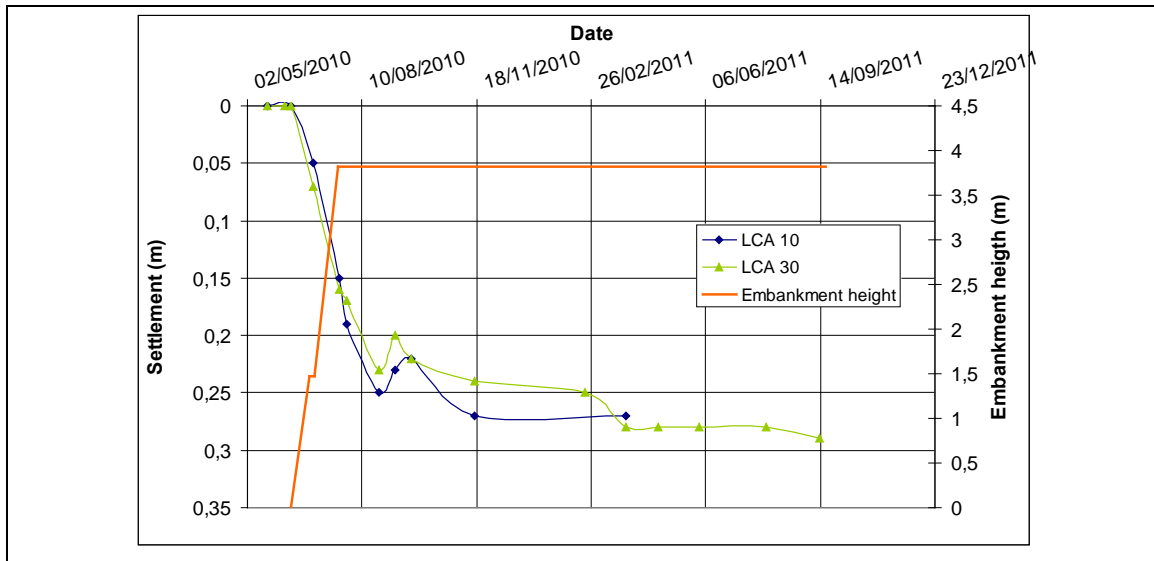
Figure 6: Settlement data from horizontal inclinometers (LCA) along embankment axe.
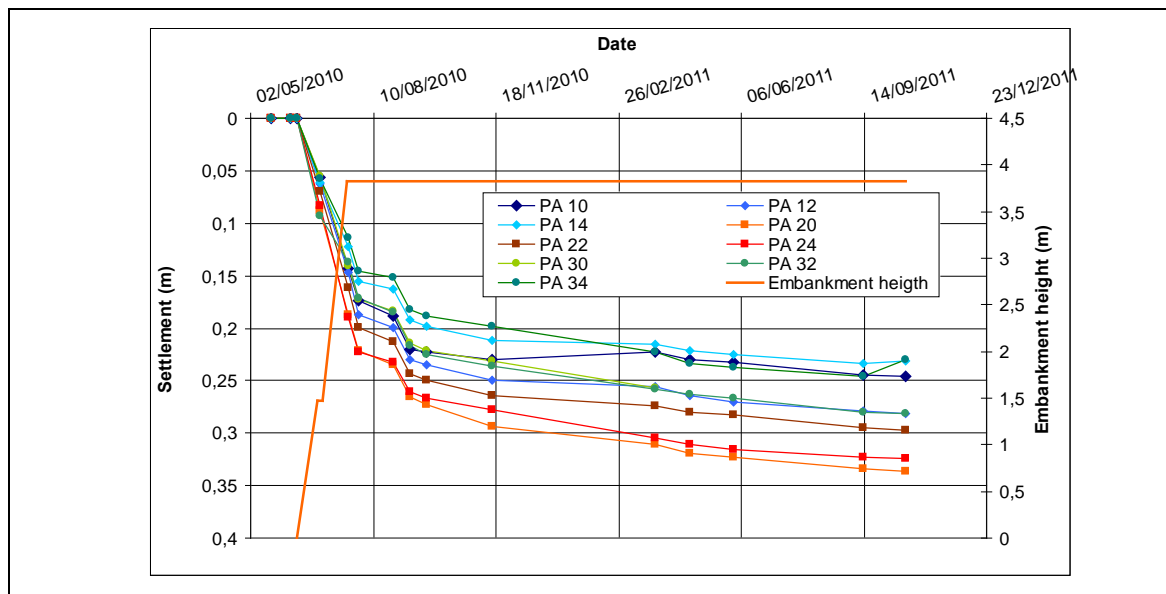
Figure 7: Settlement data obtained from settlement plates. PA 12, PA 22 and PA 32 are located over the embankment axe.

4.   BACK ANALYSIS

Data were first analysed by Asaoka method in order to get a prediction of the magnitude of final settlement. From this analysis a magnitude close to 30 cm was obtained. Then, with this figure in mind, the initial value of the deformation modulus was corrected in order to obtain a similar value of settlement. Calculations were done employing an elastic solution for trapezoidal load to estimate the vertical load increase in depth due to the trial embankment (Jimenez Salas, 1981). Changes in the value of the elastic modulus estimated from is situ tests have represented less than 30 % in the magnitude originally determined of the upper marsh level. This level is the most relevant in settlement estimation in this profile as it is the softest level. Also, it is the level where the load increment is highest.

The values of the consolidation coefficients were chosen from results in figures 1 and 2. Vertical consolidation coefficient was selected equal to 5.10^{-4} cm^2/s. This value express for the draining behaviour of mainly clay levels. In the case of the horizontal consolidation coefficient values obtained from dissipation CPTu tests are too high in relation to vertical coefficient to characterize the horizontal

draining behaviour of clay levels, so a value of 2.10^{-3} cm^2/s has been selected for calculation. Results of c_r could stand for mixture behaviour of silty sand and clay levels.

Vertical consolidation was estimated according to Terzaghi one-dimensional consolidation theory, meanwhile horizontal consolidation by the solution included in the Spanish geotechnical recommendation for foundation in linear works (Guía de Cimentaciones para Obras de Carretera. Ministerio de Fomento, 2002). Also, Barron solution was employed to accomplish for horizontal and vertical consolidation together.

To compute horizontal consolidation distance between draining borders is the distance between vertical drains in the triangular mesh designed. For vertical consolidation the distance between draining levels is estimated according to the criterion described in point 3. Values employed in calculation are shown in the next figure where vertical distribution of draining levels is drawn related to CPTu results. Of course, this distribution is a simplification of soil profile but, on the other side, it represents draining levels location in a much more complex way that results obtained from boreholes and laboratory data.

Modelization results are shown in figure 9. Settlement develops mainly during the three first months. Then settlement velocity is progressively decreasing. Still there is some deformation measured in the soil profile due to the fact that vertical drains are only 20 meters long. Consequently, there are 12 m of marsh sediment where consolidation is only related to vertical drainage, so it develops according to a slower rate.
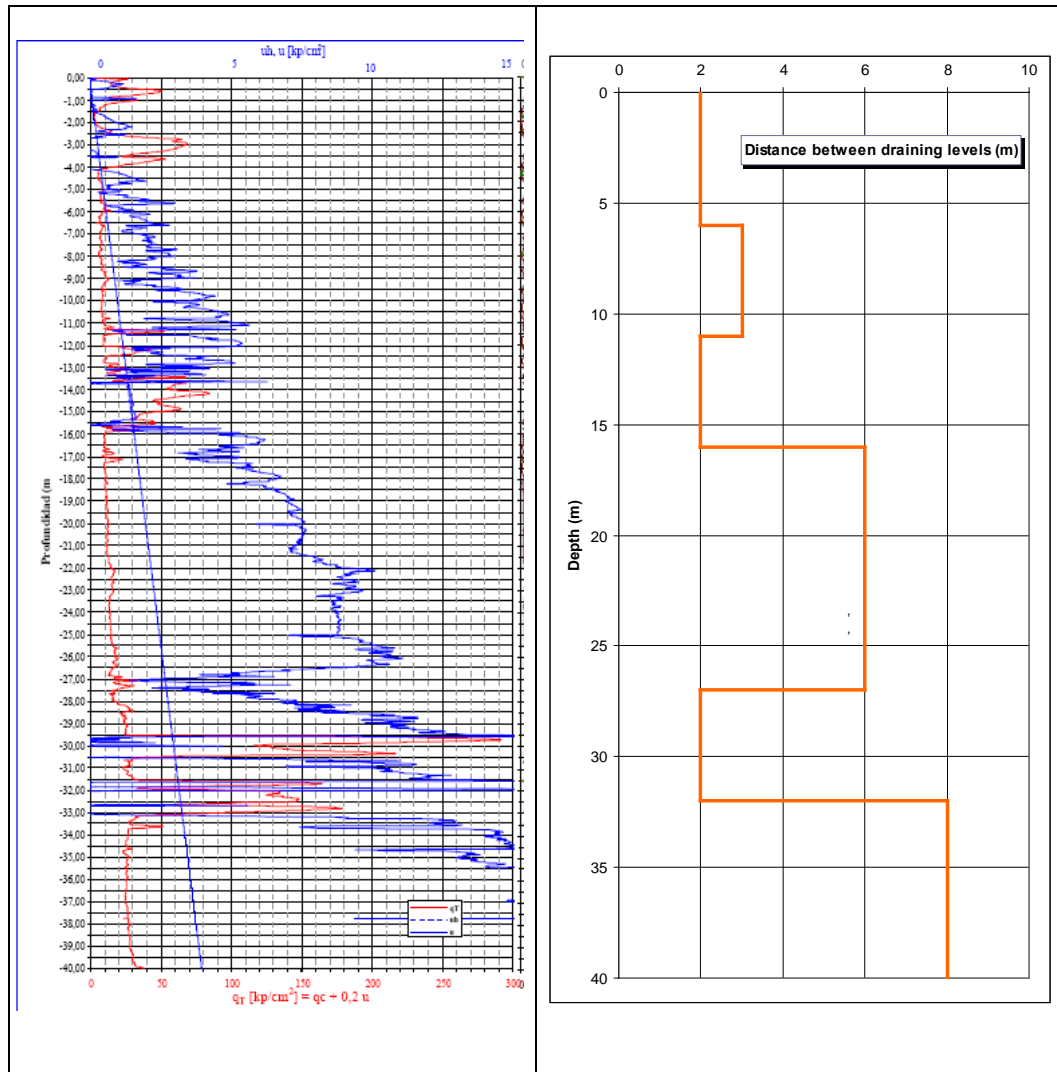
Figure 8: Distribution of drain levels according to excess pore pressure record.
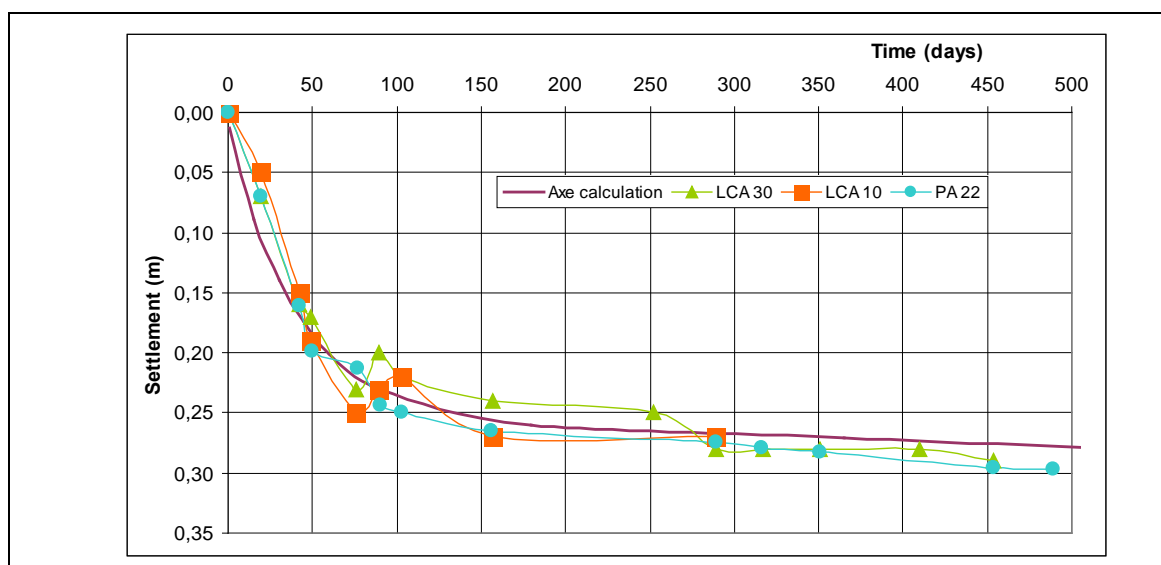
Figure 9: Comparison between instrumentation data and calculation results.

Evolution of consolidation in depth can be observed in figure 10. Calculations show that the settlement going on is due to vertical drainage in non treated soil, deeper than 20 m. The difference between total settlement and settlement at 20 m depth is the same, so the rate of settlement development will be slow.
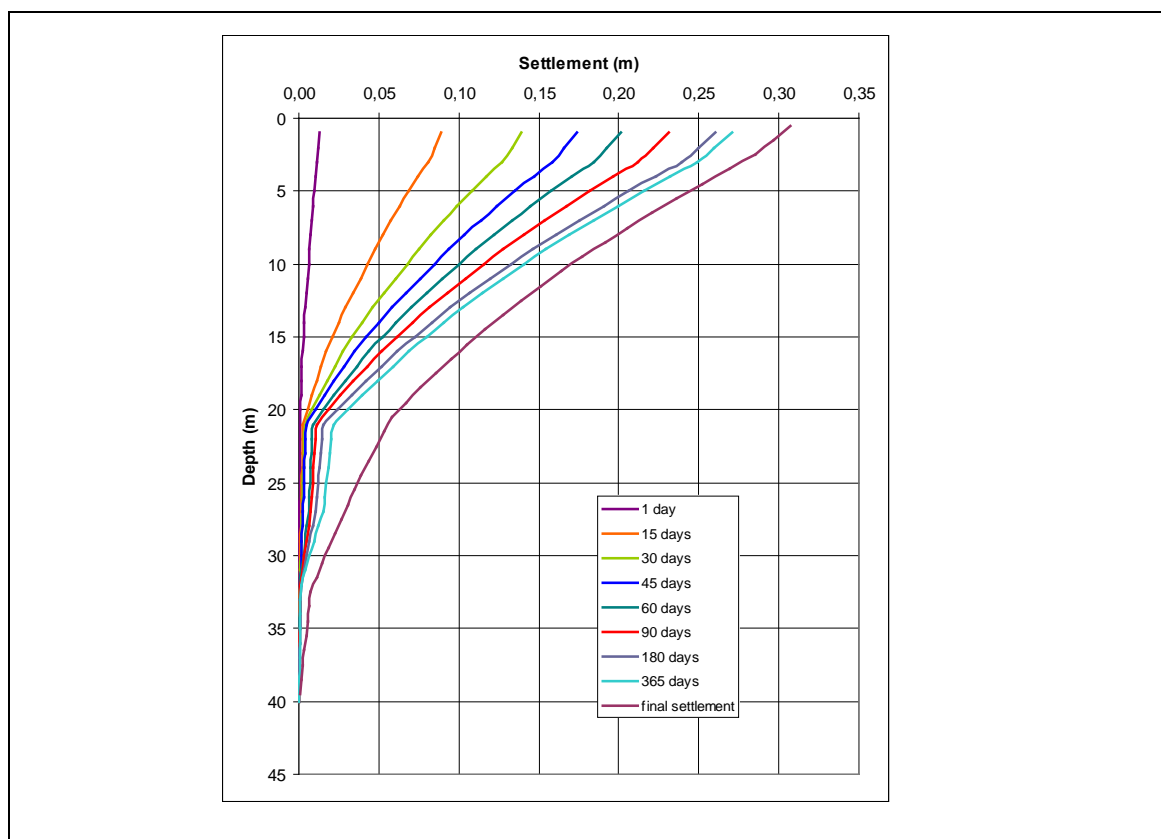
Figure10: Settlement development in depth

5.   DISCUSSION

Results from an instrumented trial embankment have been analysed in order to check a settlement estimation approach based on oedometer and CPTu tests results. Main parameters that control settlement development are consolidation coefficients and distribution of draining levels across the geotechnical profile. Both parameters are difficult to define accurately.

The approach used in this example characterize vertical consolidation coefficient directly from results of oedometric tests, assuming that samples tested represent the behaviour clay levels in the profile. On the contrary, results of radial consolidation coefficient obtained from dissipation tests in CPTu are thought to be too high related to vertical consolidation coefficient in clay levels. These results may be representative of the draining behaviour both the silty sand and clay levels together. Calculations done are really sensitive to these parameters due to the distance between vertical drains. As this distance is small (1.6 m) and the value of this parameter changes according to a potential law, it actual value has been obtained by a trial an error fitting.

Distribution of draining levels across the geotechnical profile has been obtained from a careful analysis of CPTu results. It has been shown that this type of analysis provides a complex distribution of draining borders in the soil which is probably more real than the profile resulting from borehole description. Also, this distribution is probably better related to results from oedometer tests and helps to discriminate the group of parameters to be used in consolidation calculation.

To simulate the real consolidation behaviour of a soil profile we have to choose between some options. One is to characterize the global soil profile behaviour. In this case we probably would select soil profile resulting from boreholes description and results from dissipation test for consolidation coefficients. Or even, we would have chosen results from oedometric tests multiplied 10 to 20 times because back analysis data indicate that it represents better the real soil draining behaviour (Lerouil et al, 1990).

On the other side, we would chose a value of the consolidation coefficient obtained directly from oedometric tests done with samples of clay levels and a distribution of draining levels reliable, as it results from analysis of CPTu test. This approach has been employed in the case studied in this paper and in other studied sites (Arroyo & Mateos, 2006). We think that results obtained represent the real behaviour of the soil studied. Subsequently, the results from oedometer tests and CPTu profiling provide an accurate description of soil consolidation behaviour and estimations for settlement development.

REFERENCES

Arroyo, M. & Mateos, T. "Embankment design with DMT and CPTu" (2006). Second international Flat dilatometer conference. Washington (USA).

Jimenez Salas, et alr, 1981"Geotecnia y Cimientos, Tomo II. Editorial Rueda, Spain.

Lerouil, S., Magnan, J.P. & Tavenas, F. (1990). "Embankments on soft clays". Ellis Horwood Series in Civil Engineering.

Ministerio de Fomento (Spain). "Guía de cimentaciones en Obras de Carreteras" (2002).

Preloading of a hydraullic fill for foundation of LNG tanks

Fernando Román, Technical University of Madrid (UPM), Spain, fernando.roman@upm.es
Rafael Jimenez, Technical University of Madrid (UPM), Spain rafael.jimenez@upm.es
Julio C. García Suarez, Enagás S.A., Spain, jcgarcia@enagas.es
Ana Coz, Eng. Geologist, Spain, anacoz@gmail.com

ABSTRACT

A liquefied natural gas (LNG) plant is currently being constructed on a hydraulic fill in El Musel Port (Gijon, Northern Spain). The hydraulic fill is mainly composed of marine sands dredged from nearby locations, and it was placed on site using rainbow and pipeline discharge and the bottom dump method. Preloading was selected among several alternatives as the ground improvement method employed to reduce settlements of the LNG tanks. This paper presents the results of the geotechnical characterization campaign conducted at the site (SPT, CPTU, DPSH) and at the laboratory. In addition, the main features of the preloading employed are presented, as well as the results of the monitored settlements (both during preloading and during the construction of the tanks).

1. INTRODUCTION

In a recent extension to El Musel Port (Gijon, northern Spain), almost three kilometers of new docks have been constructed, as well as 145 hectares of new surface behind the docks. Most of this new (reclaimed) land has been constructed by means of hydraulic fills with dredged material. The volume of fill material is above 32 million cubic meters. Gijon Port Authorities (APG) developed in 2009 a new surface of 260.000m2, of which 220.000m2 were occupied by ENAGAS (the Spanish Technical Manager of the Gas system and Common Carrier for the high pressure gas network) to build a regasification plant of Liquefied Natural Gas (LNG). (For a review of similar uses of hydraulic fills, see Whitman (1970).)
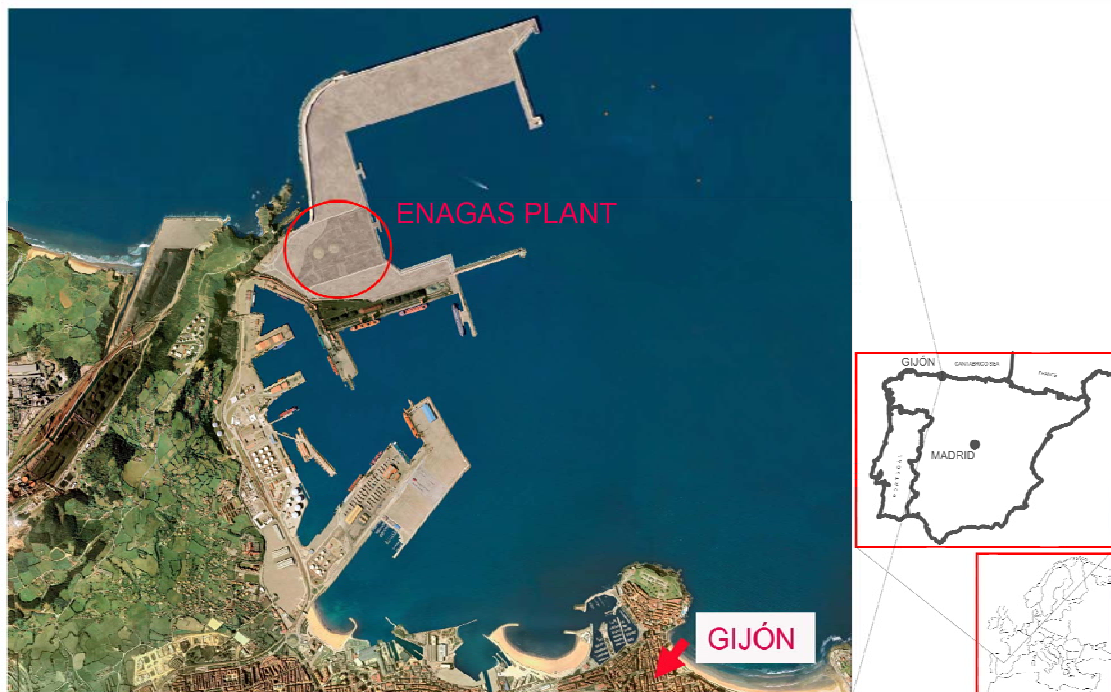
Figure 1: Location of Enagás Plant

The main structures in the new regasification plant are two tanks for storage of the LNG. Their dimensions are 78,2 m of diameter and 50,5 m of maximum height, with an storage capacity of 150.000 m3 each. The tanks have an exterior ring of pre-stressed concrete of 80 cm thickness, and a concrete

dome reinforced with a steel structure. The foundation mat has a diameter of 82,4 m and a thickness of 0,70 m, that is increased to 1,2 m under the 5,4 m wide area below the exterior concrete ring. The service load transmitted by the tank is 200 kPa, and the load during the hydraulic test is 285 kPa.

Before the port extension, the sea bed was located between -15 and -20 m O.D.. Between 2006 and 2008, the APG started to fill the "Enagas area" with approximately 600.000 m3, which elevated the sea bed up to -8 m O.D. in some points in the southwest corner. During 2009, an additional 4,5 million m3 have been filled using two dredges and the rainbow discharge, bottom dump, and pipeline discharge methods (Lee et al., 1999). The final height of the fill is +6,40 m O.D., which means that the fill thickness ranges from 21 to 26 meters. The materials below the fill include thin Quaternary layers of dense sands and gravels underlayed by bedrock composed of limestone, marls, and quartzite.
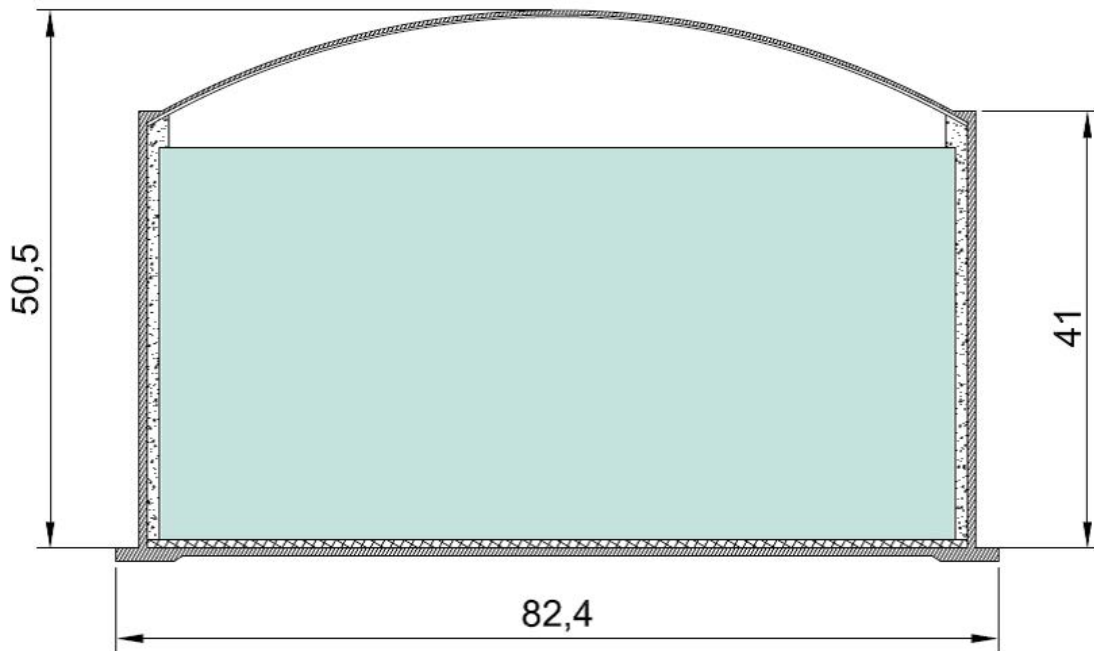
Figure 2: Schematic cross-section of the LNG storage tank

2.   GROUND INVESTIGATION

The following works were performed:
- 25 boreholes (rotary core drilling), with "undisturbed" samples taken every 3 m and with SPT tests conducted immediately after each sample taken.
- 55 continuous dynamic penetration tests (DPSH)
- 2 continuous BORROS dynamic penetration tests (DPH)
- 23 cone penetration tests with pore pressures measurement (CPTU), and with 6 dissipation tests.
- 6 seismic cone tests (SCPTU) with measurement of wave velocities
- 10 exploratory ditches.

Even though the position of the boreholes and tests conducted was mainly selected depending on the position of the facilities in the plant, it was also intended that the overall dataset would allow a good characterization of the site.
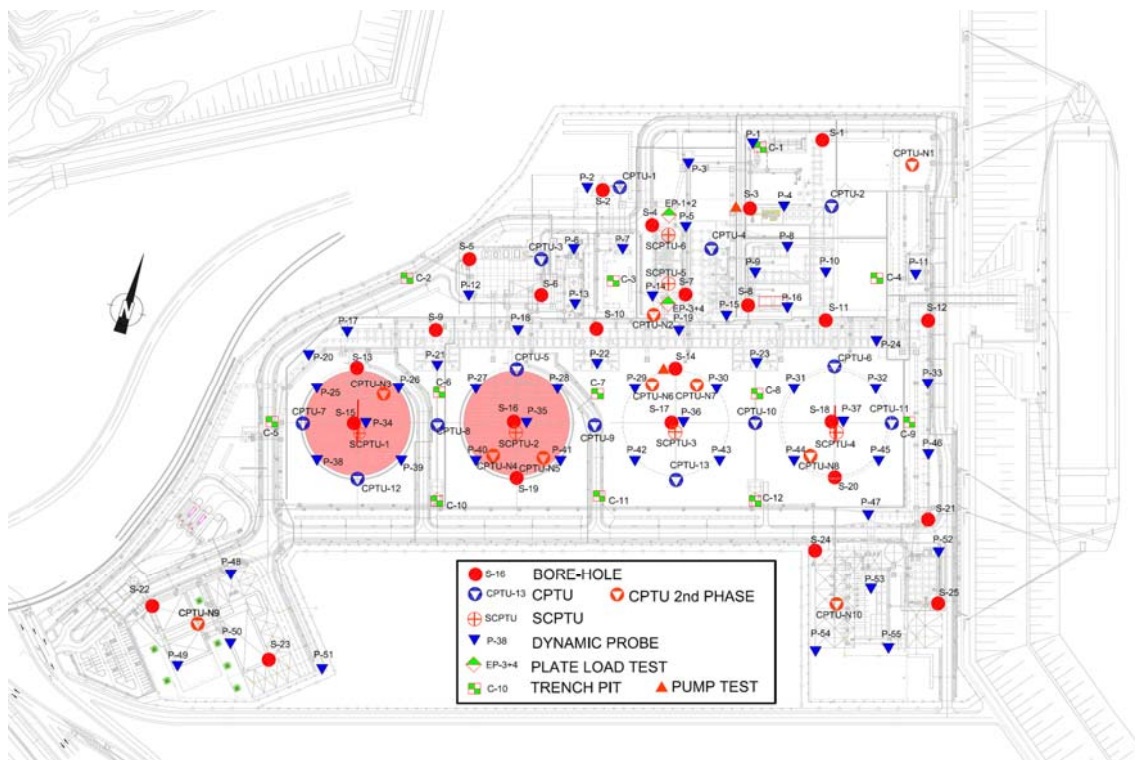
Figure 3: Lay out of the site characterization program

3.   GEOTECHNICAL CHARACTERIZATION

3.1.   Composition, granulometry, plasticity

The fill materials are sands (with variable silt content) whose particles are mainly composed of shell fragments (50 to 60%; see Photo 1). Because of such composition, tests were conducted to study whether there were variations (due to particle breakage) after the material was compacted (Modified Proctor).
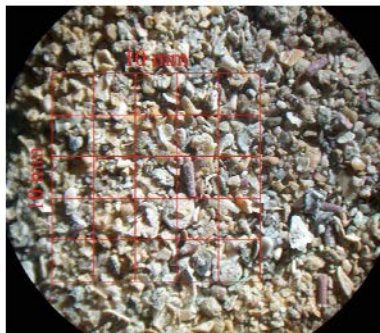
Photo 1: Sand sample (size of the grid is 10 mm)

Figure 4 shows the granulometric curves of all the samples taken from the borehole samples. In most cases, the fines content (measured as particles smaller than 0,080mm) is below 30%. Figure 5 shows the fines content as a function of depth. Particles smaller than 0,4mm are always non-plastic.
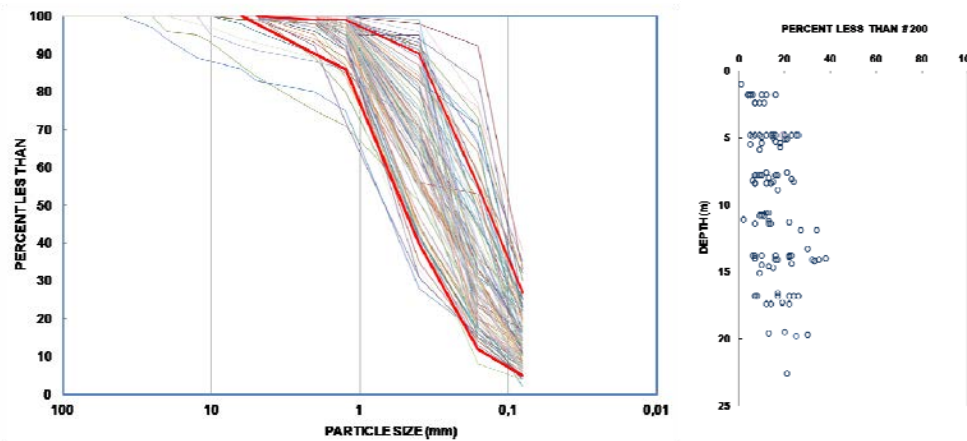
Figures 4 & 5: Size analysis curves and distribution of passing 0,080 mm with depth

3.2. **Dynamic penetration resistance (SPT, DPSH and BORROS)**

SPT tests were conducted inside the boreholes taking special care so as to avoid the heave of the bottom once that the sample was extracted before the test. SPT test results are shown in Figure 6 (a red line indicates the average of tests at each depth). Table 1 lists representative SPT values for each depth.

Table 1: Representatives values of SPT

Depth (m)	N_{30}SPT
(Over phreatic level)	7 - 15
3,5 a 8,5	3 - 7
8,5 a 13	4 - 9
13 a 18	6 – 14
18 a 22	8 – 17
22 a 24	15 -23
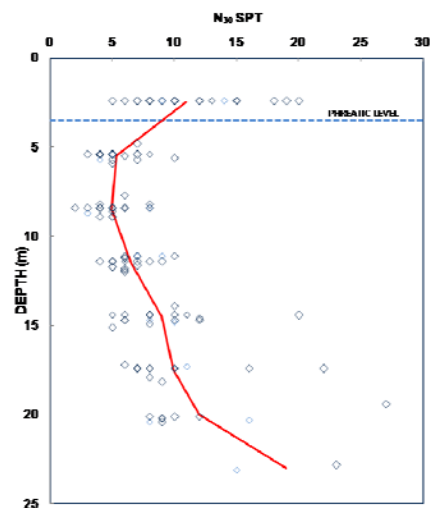
Figure 6: SPT versus depth

Dynamic penetration tests (DPSH) have been employed to estimate the density of the sands at the site. Figure 7 shows their evolution with depth, and Table 2 lists representative values. To serve as a contrast, two BORROS dynamic penetration tests were conducted as well.

Table 2: Representatives values of DPSH

Depth (m)	N_{20} DPSH	
(Over phreatic level)	5 – 11	
3,5 a 8	1 – 4	
8 a 13	3 – 8	
13 a 16	6 – 10	
16 a 18	8 – 15	
18 a 24	12 -18	
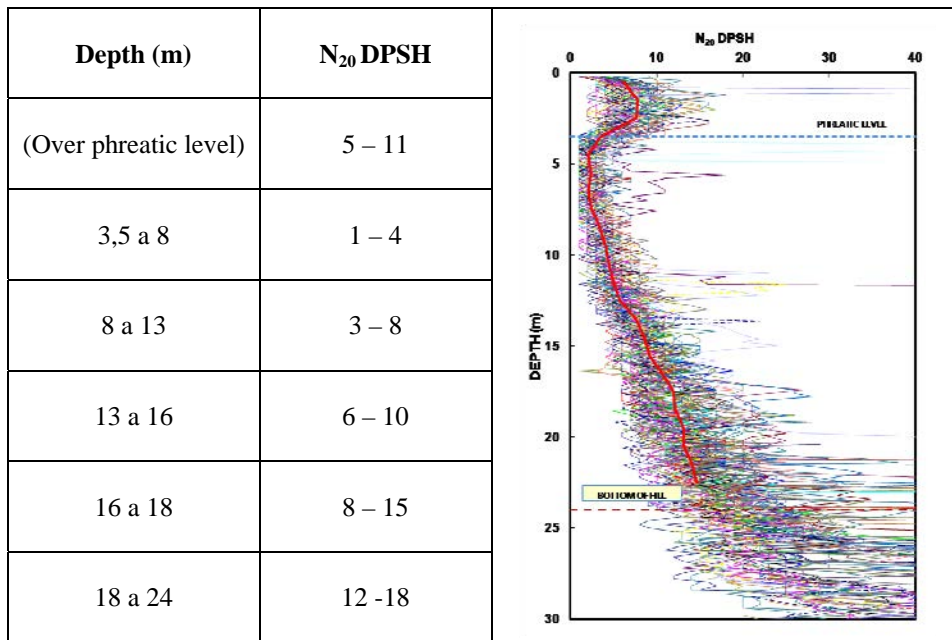
Figure 7: N_{20} DPSH versus depth

The following correlation could be established:

$$N_{20\,DPSH} = 0,67 \cdot N_{20\,BORROS} \tag{1}$$

We have also correlated the results of DPSH and SPT tests (for SPT, with the normalization to obtain $N_{1(60)}$.) In DPSH tests, the rods have a somewhat greater lateral friction than in SPT and, therefore, the energy loss is greater. At shallow depths, the energy loss due to lateral friction is small and, therefore, similar in both tests; that produces SPT values approximately 1,5 times the DPSH values (30cm are introduced in SPT vs. 20cm in DPSH). With depth, both values become similar, and that is why in the SPT $N_{1(60)}$ values there is a correction for rod length (C_R=0,75) but there is not a similar correction for the DPSH. Figure 8 shows the relationship between SPT and DPSH values with depth (**$N_{1(60)}$ /N_{20}**), and Table 3 shows representative value of such ratio. (Note that at depths indicated with (*) –i.e., between depths 3, 5 and 8m-- there is a greater dispersion of values because both SPT and DPSH are quite small).

Table 3: Representatives values of $N_{1(60)}$ /N_{20} DPSH

Depth (m)	$N_{1(60)}$ /N_{20} DPSH	
(Over phreatic level)	1,2 -2,2	
3,5 a 7	1,2 – 2,2 (*)	
7 a 10	1 – 1,7 (*)	
10 a 24	0,8 -1,2	
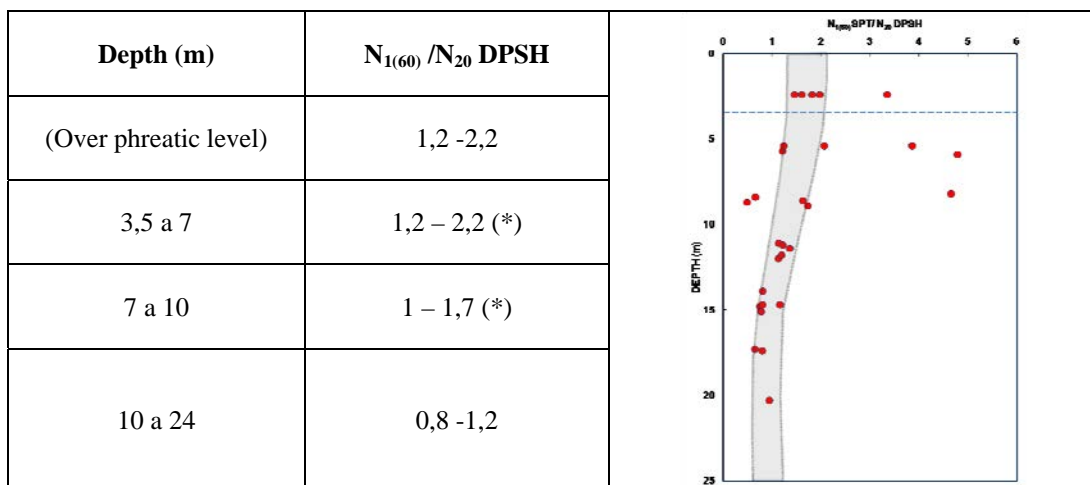
Figure 8: $N_{1(60)}$ /N_{20} DPSH versus depth

3.3. Static Cone Penetration Tests (CPTU)

CPTU has been widely employed for characterization of hydraulic fills (see e.g., Lee (2001); Na et. al (2005)). The CPT penetration resistance (as given by tip resistance and sleeve friction) are shown in Figs 9 and 10.

Figures 9 & 10: Tip resistance and sleeve friction vs. depth.
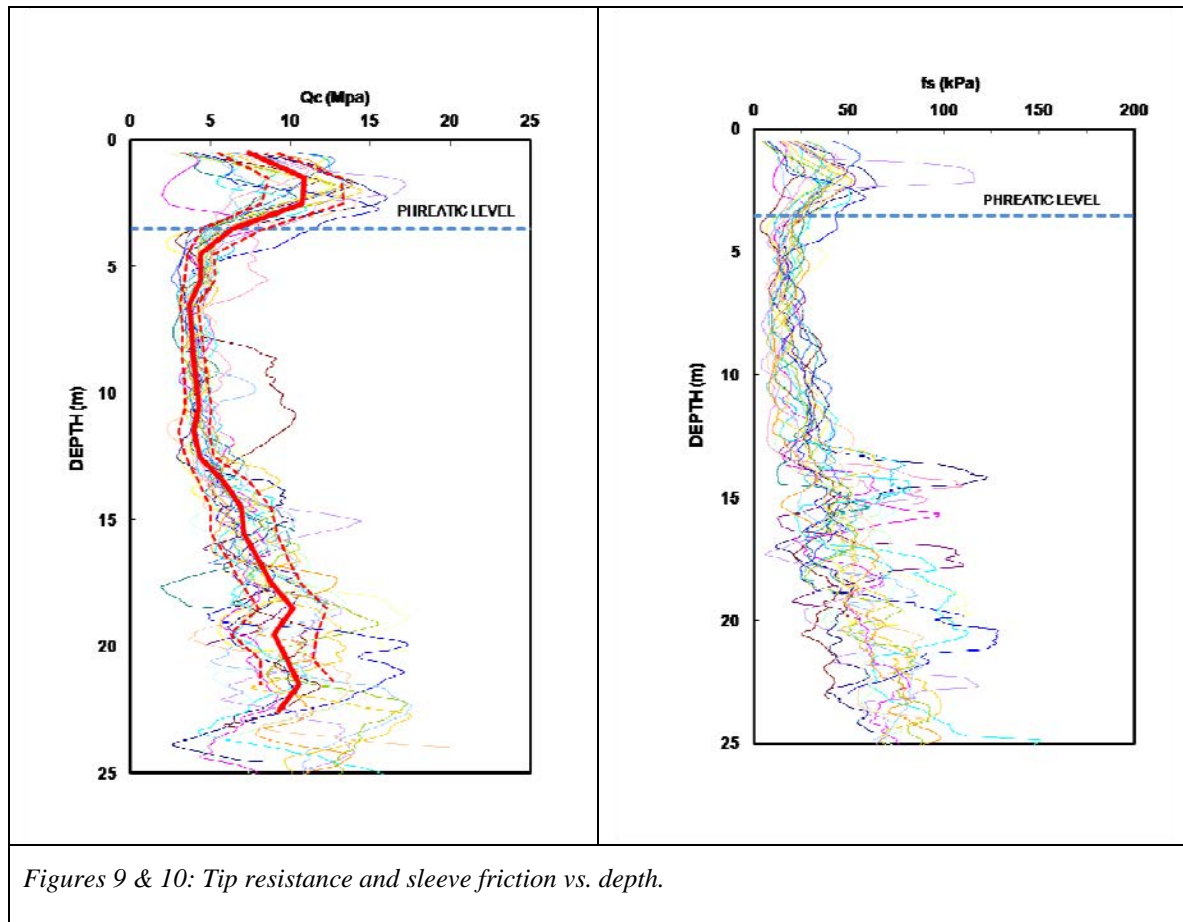
Table 4 shows the representative values that correspond to the selected area in Figure 9.

Table 4: Representative values of Q_C

Depth (m)	Qc (MPa)
(Over phreatic level)	7 - 14
3,5 a 13	3 - 6
13 a 16	4 – 10
16 a 24	6 – 13

If we correlate the static penetration (tip resistance, Qc) with the dynamic penetration resistance (SPT or DPSH) (see e.g., Robertson et al. (1983)), we obtain the results shown in Figures 11 to 13. (Table 5 summarizes results.) We could also establish the following correlation:

$$Q_c = (0,8 \ a \ 1) \cdot N_{1(60)} \tag{2}$$

Figures 11 &12: Correlation between Qc and $N_{1(60)}$, and $Qc/N_{1(60)}$ ratio versus depth
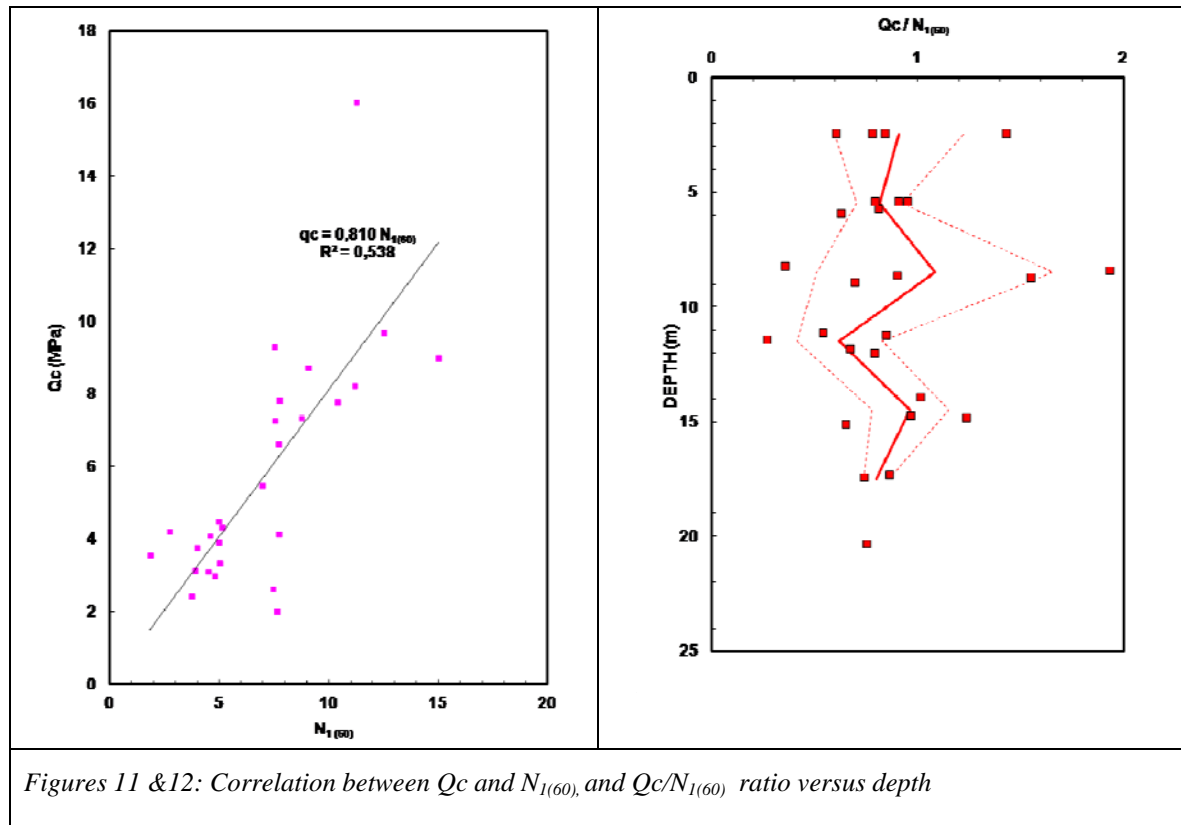
Table 5: Representative values of Q_C/N_{20} DPSH

Depth (m)	Qc/N$_{20}$DPSH
(Over phreatic level: 3,50 m)	1,0 -1,6
3 a 7	1,5 – 2 (*)
7 a 10	1,0 – 1,6
10 a 24	0,7 - 0,9

Figure 13: Ratio Qc/N$_{20}$DPSH versus depth.

3.4.   Seismic wave velocities measured in SCPTU

Seismic wave velocities measured with the SCPTU tests are shown in Figure 14. Figure 15 shows the relationship between velocity of S-waves and static cone tip penetration resistance (Qc).

Figures 14 & 15: Wave (S) velocity obtained from SCPTU and variation of Vs/Qc, versus depth
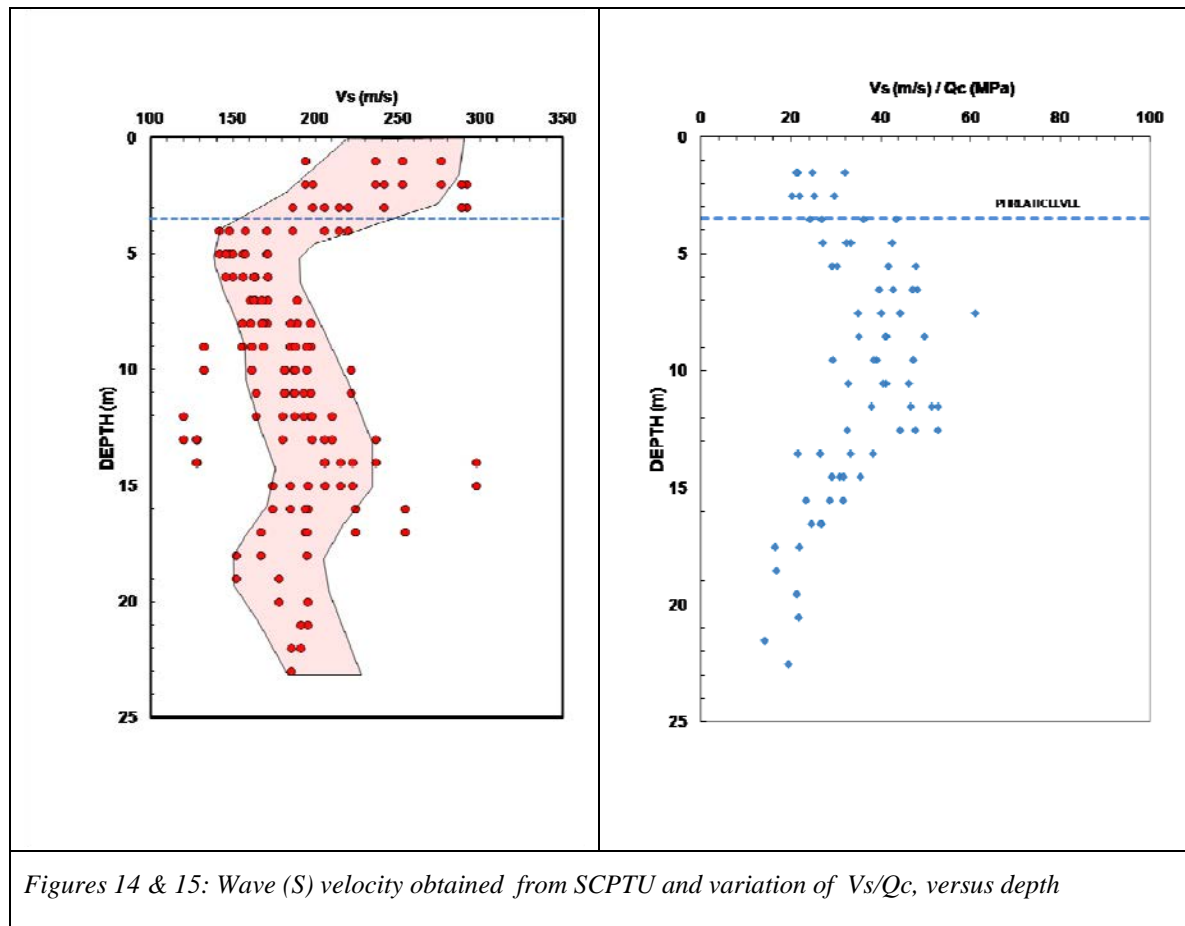
4.   PRELOADING AS GROUND IMPROVEMENT

Several ground improvement alternatives were considered, including dynamic compaction, vibrocompaction, jet-grouting and preloading. Preloading was selected as the most efficient treatment in this case. It has the advantages that it reproduces the stress state that the foundation is going to have in service and, given the limited amount of fines in this case, it was expected to be a fast treatment with limited waiting times. In addition, in this case, the material used for preloading in the first tank could be "reused" for the second one.

4.1.   Representative cross section
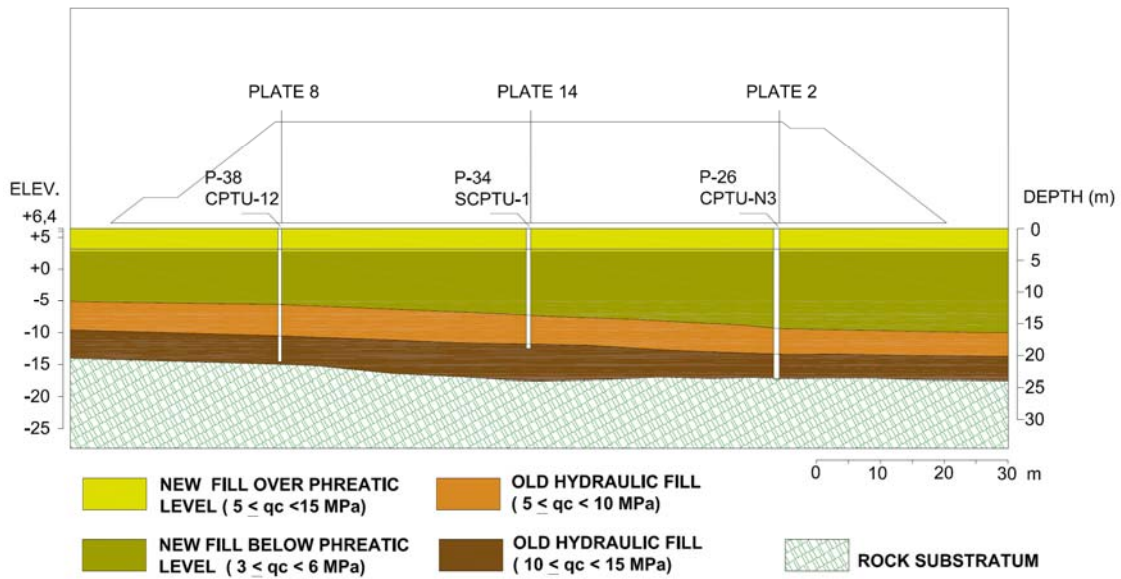
Figure 16: Representative cross-section under Tank 1

4.2.   Preload Dimensions

The preloading magnitude has to be equivalent to the load transmitted to the foundation during the hydraulic proof (285 kPa). Since during the earthworks it could be verified that the apparent density was over 20 kN/m^3, the height could be limited to 16 m. The shape of the preloading fill was a conical frustum with a 130 m diameter base and a 80 m diameter top. Photo 2 shows the aspect of the completed preloading.

Photo 2: Completed Preload of Tank Nr 1

4.3.   Monitoring

In each tank, the following monitoring has been employed: 14 settlement plates (12 in the perimeter and 2 in the center); 2 sets of extensometers with measurements at three depths, 3 inclinometers with their quadrant oriented towards the adjacent tank. (Piezometers have not been employed given the high permeability of the sands.)

4.4.   Results

Figure 17 shows the load (expressed as preloading height) vs settlement curve observed during preloading construction and unloading. Note that during unloading the recovered deformation (upwards movement)

during preloading removal was 8,6 times smaller than the settlement during first loading. Figures 18 and 19 show the results of the more inclinometer with the highest deformations, as well as the variation of maximum measured displacements with time and with fill height.
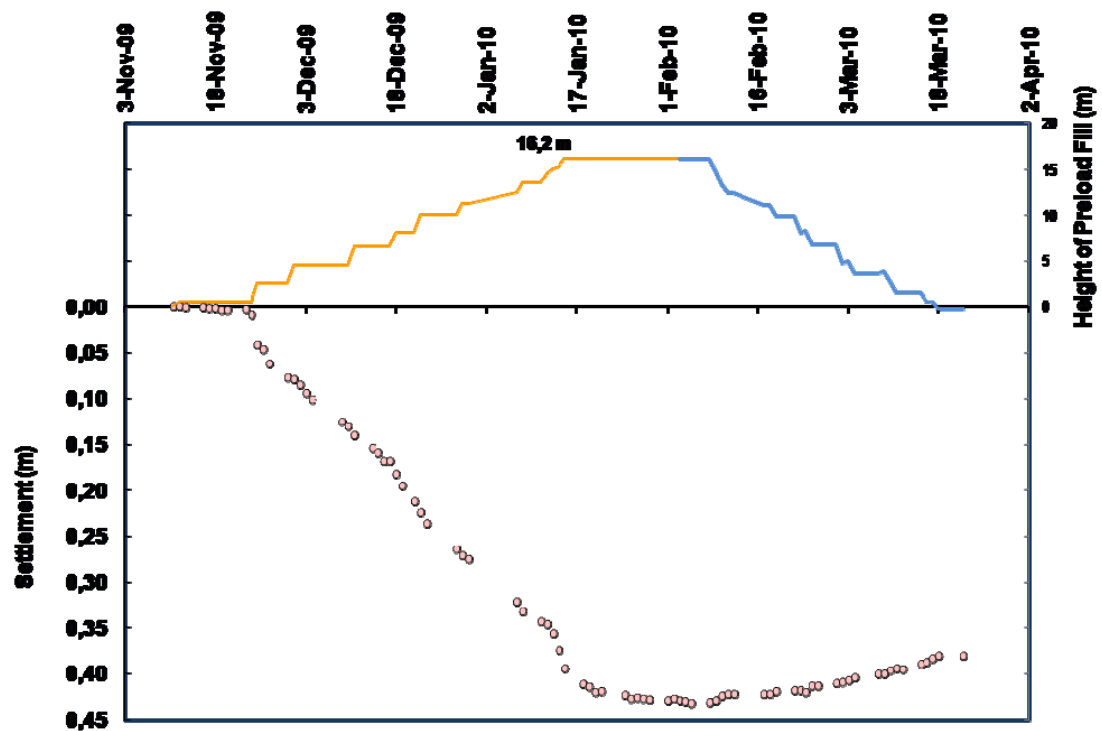
Figure 17: Preload height and settlement vs time
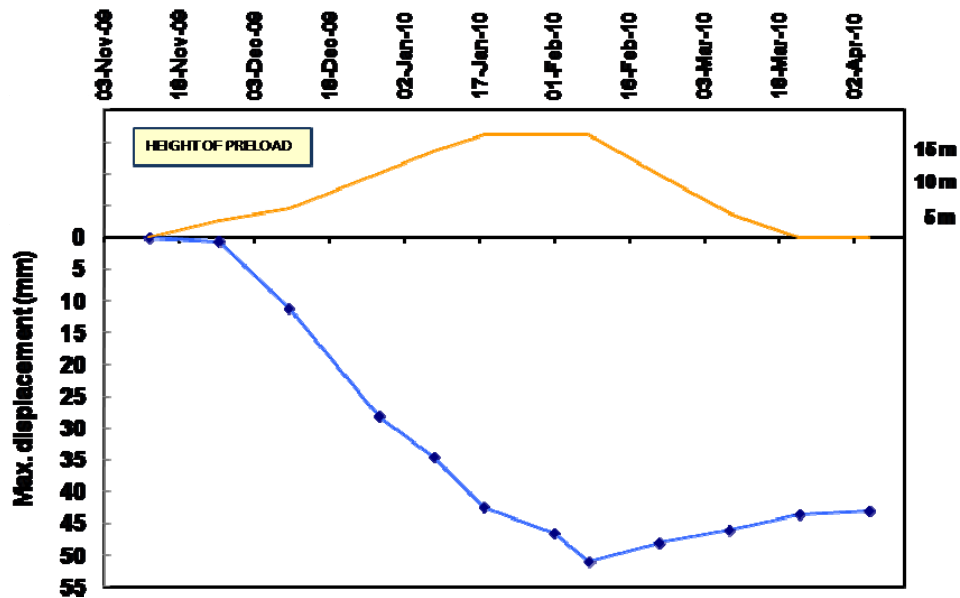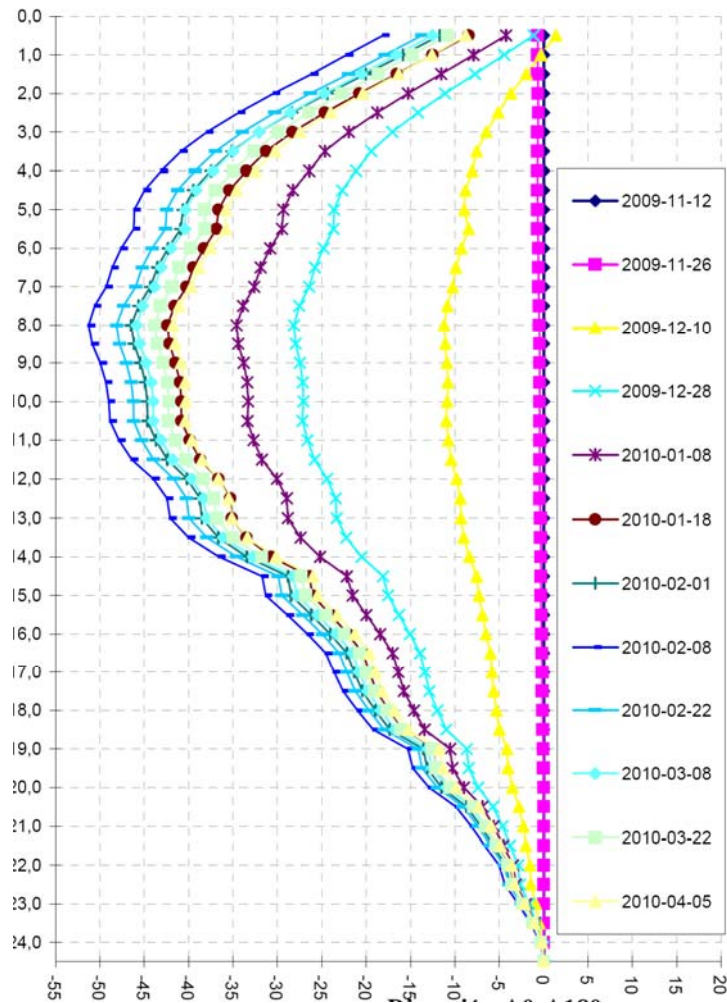
Figures 18 & 19: Results of Inclinometer Nr 1 and evolution of maximum displacement versus time and height of preload.

The deformation moduli of each layer should be proportional to the CPTU tip resistance Qc. The relationship between them has been shown in Figure 20, where to additional lines (representing Em= 3 to 5 Qc) have been presented as well. The upper layer corresponds to the less dense layers, whereas the lower line corresponds to the denser sand levels.
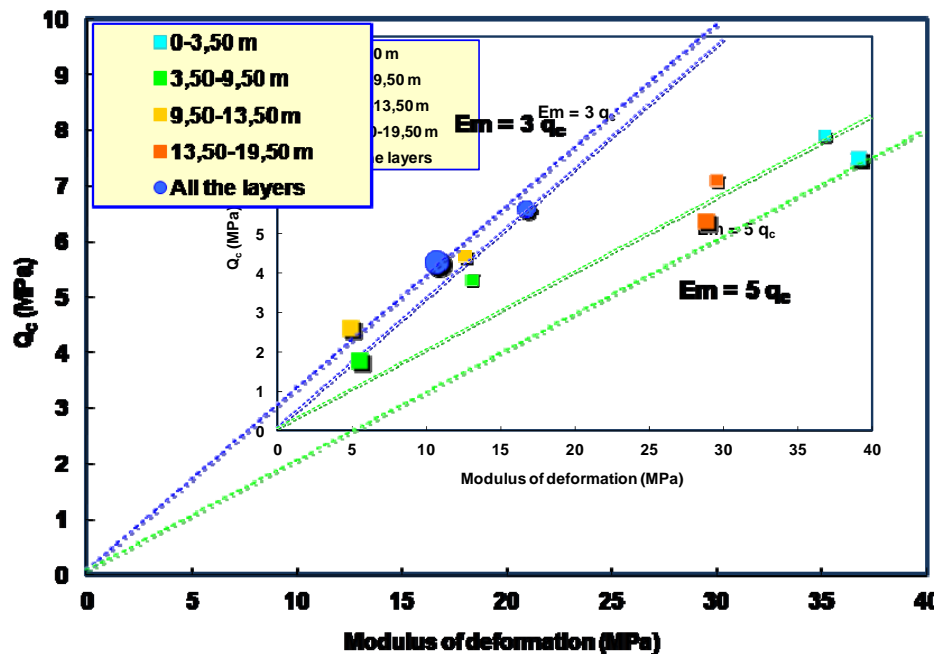
Figure 20: Correlation between Qc and Em

5. SETTLEMENTS DURING CONSTRUCTION OF THE EXTERIOR RING

Figure 21 shows the settlement as the exterior "ring" concrete structure is being constructed. The maximum load once that such ring is constructed will be of 230 kPa acting approximately over a width of 5-6 meters. The observed settlement is being smaller than predicted.
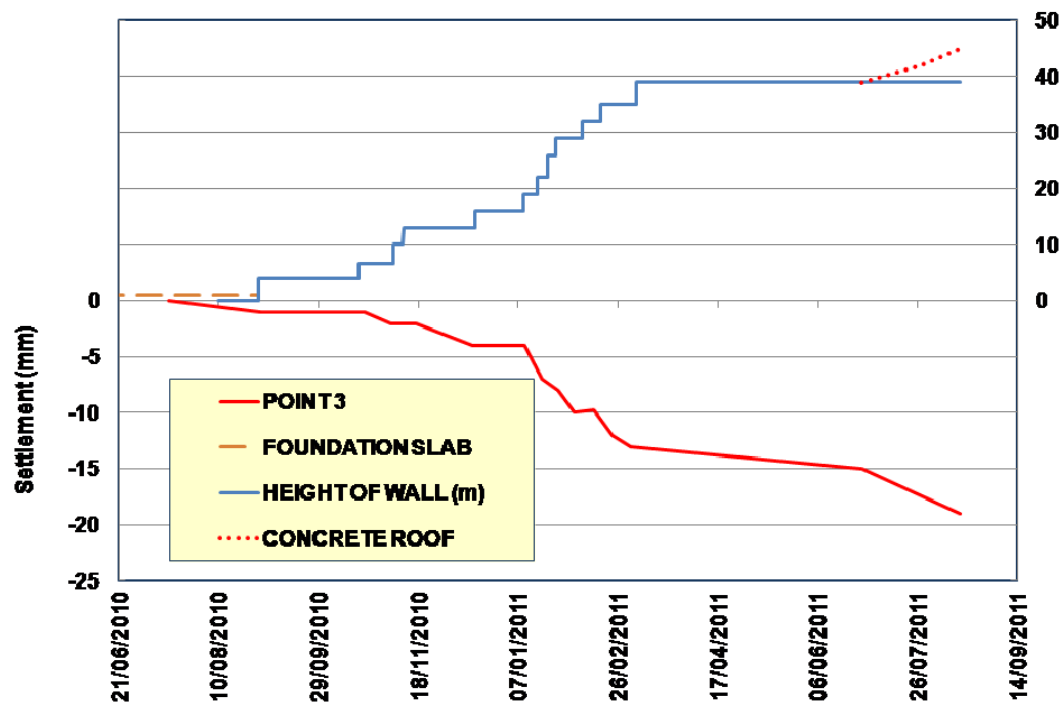
Figure 21: Settlement during the concrete ring construction

6.   CONCLUSIONS

A large hydraulic fill has been recently constructed in El Musel (Gijon, Spain) using dredged sands of marine origin from nearby locations. The main purpose of such fill is the construction of industrial facilities for Enagas and, in particular, the construction of two large dimension LNG tanks for a regasification plant.

This article presents the results of the site and geotechnical characterization programs (boreholes, dynamic and static penetration, etc.) and it also presents some correlations that could be established for the available materials in this case.

In addition, we discuss the monitoring details and observed behavior of a preloading scheme that was chosen as a ground improvement alternative for the foundation of the tanks. Preloading has been shown to be an efficient improvement alternative for the tank foundations in this case, with limited settlements during unloading-reloading that are below the accepted thresholds.

7.   ACKNOWLEDGEMENTS

FLUOR is the project manager of the works. The main engineering contractor of tanks at the site is a Joint-Venture between DURO FELGUERA and FCC. GEOCISA conducted and managed the site characterization program. Their support, as well as the support of ENAGAS engineering department, is gratefully acknowledged.

REFERENCES

Lee, K.M. (2001). "Influence of placement method on the cone penetration resistance of hydraulically placed sand fills". Canadian Geotechnical Journal. 38(3). pp. 592–607.

Lee, K.M., Shen, C.K., Mitchell, J.K. (1999). "Effects of placement method on geotechnical behavior of hydraulic fill sands". Journal of Geotechnical And Geoenvironmental Engineering (ASCE);125(10). pp. 832–846.

Na, Y.M., Choa, V., The, C.I., Chang M.F. (2005). "Geotechnical parameters of reclaimed sandfill from the cone penetration test". Canadian Geotechnical Journal; 42. pp. 91–109.

Robertson, P.K., Campanella, R.G. and Wightman, A. (1983). "SPT-CPT Correlations". Journ. Of Geotech. Eng. ASCE, 109(11).

Whitman, R.V. (1970). "Hydraulic fills to support structural loads". Journal of the Soils Mechanics and Foundations Division (Proceedings of the American Society of Civil Engineers); 96(SM1). pp. 23–47.

Radial Consolidation Modelling Incorporating Downdrag Effect for a Multi-Layer Soil

Cholachat Rujikiatkamjorn, Centre for Geomechanics and Railway Engineering, Faculty of Engineering, University of Wollongong, NSW, Australia, cholacha@uow.edu.au

Buddhima Indraratna, Centre for Geomechanics and Railway Engineering, Faculty of Engineering, University of Wollongong, NSW, Australia, indra@uow.edu.au

ABSTRACT

A system of vertical drains (PVDs) with preloading is a successful method for promoting horizontal drainage and accelerating soil consolidation. A piecewise technique is used to capture the radial consolidation in the multi-layer soil system to incorporate (a) the effect of soil downdrag and (b) smear zone where soil permeability varying linearly. The effect of soil dragged down from the upper soil layer into the lower layer has been analysed in terms of required time for consolidation. It can be seen that the consolidation of the multi layer soil depends on the interaction between 2 adjacent layer, penetration depth, and drain spacing. Design procedures are described with a worked out example.

1.   INTRODUCTION

Recently, most infrastructures are required to be constructed on marine or estuarine clays that are of low shear strength, unless substantially improved before infrastructure construction. Ground improvement technique is essential prior to the construction of the permanent structures. Preloading with prefabricated vertical drains (PVDs) is one of the most viable methods for improving the shear strength of soil and to reduce its lone term settlement. Employing PVDs, the drainage path length can be shortened significantly from the soil layer thickness to half of the drain spacing. Furthermore, the lateral permeability is usually higher than the vertical one; hence, the consolidation time can be reduced (Jamiolkowski et al. 1983). This system has been applied successfully to improve foundation soils for airports, rail and road embankments (Indraratna and Redana 2000; Li and Rowe 2002).

PVDs are usually installed using steel mandrel (casing) driving through soft ground creating smear zone nearby PVDs. The soil in the smear zone is disturbed and remoulded with an associated permeability reduction, which is unfavourable to radial consolidation. The extent of remoulding relies on the mandrel size, shape, installation technique and soil type (Eriksson et al., 1999; Lo, 1998; Bo et al. 2003). Sensitivity clays with prominent macro fabric generally demonstrate the greatest smear effects. A number of studies have shown that the disturbance increases towards the drain (Chai and Miura, 1999; Hawlader et al., 2002; Sharma and Xiao, 2000; Indraratna and Redana, 2000; Madhav et al., 1993; Bergado et al., 1991). Laboratory studies illustrate a linear horizontal permeability reduction towards the drain. The permeability close to the drain is usually assumed to be the same as the vertical permeability (Hansbo, 1981; Indraratna and Redana, 2000). The vertical permeability remains relatively unchanged. In layered soil, the disturbance of the lower layer is not only caused by the lateral displacement of soil surrounding PVDs but also the down-dragged remoulded soil in the upper layer forming an additional smear zone (Casagrande and Poulos, 1969; Hird and Moseley, 2000).

Barron (1948) proposed the radial consolidation theory considering the effects of smear (for equal strain) and well resistance (for equal and free strain). These solutions involved Bessel functions. Consolidation solutions were further advanced including: rigorous solutions for vertical and horizontal drainage for equal strain with well resistance (Yoshikuni and Nakanodo, 1974, Onoue et al., 1988). Hansbo (1981) proposed a much simpler solution incorporating both smear effect and well resistance into Barron's formulation. Indraratna et al (2005a, b) included the effect of vacuum pressure and non-linear soil compressibility and permeability for radial consolidation. In the all solutions, a smear zone permeability is simply assumed as a constant. Subsequently, Walker and Indraratna (2007) and Basu and Prezzi (2007) used a linear decay in horizontal permeability towards the drain representing a more realistic variation of soil permeability within the smear zone. However, none of them considered the effect of soil dragged down from the upper layer to create additional smear in the underlying layer.

A piecewise-linear technique is a method that divides the soil properties into small segments based on material coordinates so that the soil properties can be considered as a constant for a particular segment. This method offers a more general solution compared to the exact solutions that can be applicable for any particular conditions (Walker 2006). Fox et al. (2003) has applied this method for radial consolidation

accounting for vertical strain and flow, soil self-weight, and variable hydraulic conductivity and compressibility during the consolidation process.

In this paper, a radial consolidation model using a piecewise technique will be proposed to investigate the smear effect in layered soil. The effects of permeability of the penetrating upper soil layer on the underlying soil layer are discussed in terms of the degree of consolidation. The intrusion of the upper soil layer into the underlying soil layer creates an additional zone where the remoulded permeability of this zone can be increased or decreased depending on the initial permeability of the upper soil layer. In the intrusion zone located in the lower soil layer, the permeability change can be divided into 3 distinct zones including (a) smear zone due to the dragdown of the upper soil layer, (b) smear zone due to the remoulding of the underlying soil, and (c) the undisturbed lower soil layer. So far there is no existing technique to take this effect into consideration. The piecewise-linear technique has been considered as an appropriate approach to determine the effect of soil dragdown on the overall consolidation. An array of design charts with a worked-out example is illustrating the role of down-dragged soil.

2.   THEORETICAL DEVELOPMENT

The main assumptions for radial consolidation considering equal vertical strain condition are assumed to be applicable to a unit cell (Hansbo 1981), and they are:

(1) Laminar flow through the saturated and homogeneous soil (Darcy's law) is valid. Flow is not allowed to occur at the outer boundary (Fig. 1), and for relatively long vertical drains (drain length is usually more than 10 times the drain spacing), only the lateral flow is permitted to occur (i.e. no vertical flow) (Rujikiatkamjorn and Indraratna, 2007).

(2) Soil deformation is uniform at the upper boundary of the unit cell and the small strain theory is valid.

(3) Based on the equal strain concept (Barron 1948, Indraratna et al. 2005a, Walker and Indraratna 2007) that all vertical strains at any given depth z are assumed to be equal, as the radial consolidation prevails.

To enable the use of index notation the inner radius r_w and outer radius r_e have been replaced with r_0 and r_m respectively. Figure 1 shows a unit cell with an external radius r_e, drain radius r_w, and an initial drainage path length *l*. Any radial distribution of lateral permeability (k_h) can be approximated by dividing the soil into *m* segments as in Fig. 2. k_h is constant within each segment.
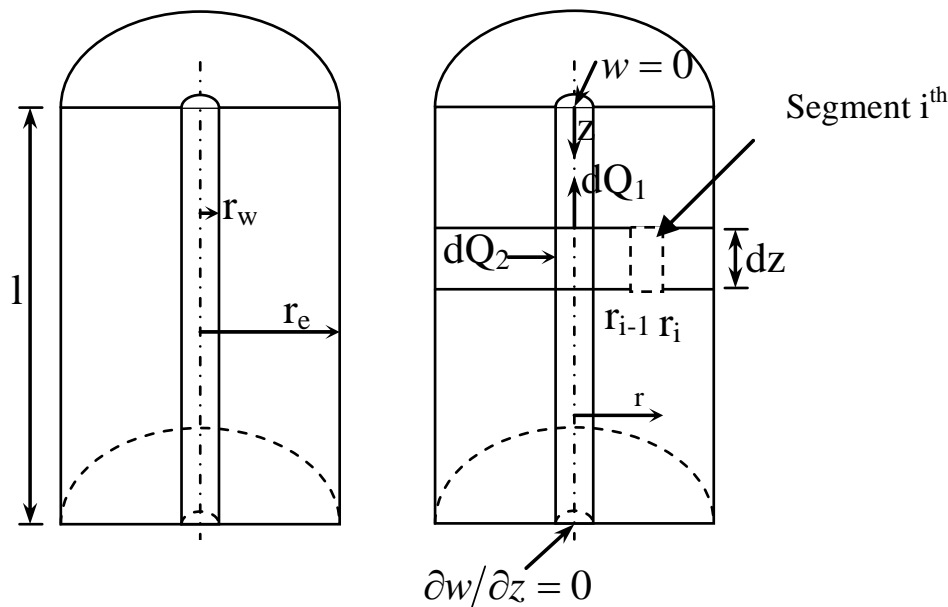
Figure 1: Axisymmetric unit cell (Rujikiatkamjorn and Indraratna, 2010)

Material Property
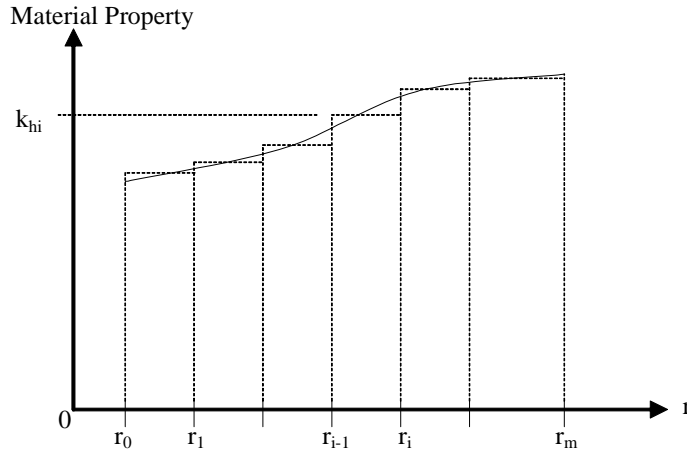
Figure 2: Discretised radial permeability (Rujikiatkamjorn and Indraratna 2010)

Rujikiatkamjorn and Indraratna (2010) proposed that the pore pressure expression for $\bar{u}$ can be in the following form:

$$\bar{u} = \frac{\gamma_w r_e^2}{2\bar{k}_h} \frac{\partial \varepsilon}{\partial t} \left(\mu + \mu_w \right) \tag{1}$$

The `μ parameter is revealed as:

$$\mu = \frac{n^2}{n^2 - 1} \sum_{i=1}^{m} \kappa_i \left[\frac{s_i^2}{n^2} \ln\left(\frac{s_i}{s_{i-1}} \right) - \frac{1}{2} \left(\frac{s_i^2}{n^2} - \frac{s_{i-1}^2}{n^2} \right) - \frac{\left(s_i^2 - s_{i-1}^2 \right)^2}{4n^4} + \psi_i \left(\frac{s_i^2}{n^2} - \frac{s_{i-1}^2}{n^2} \right) \right] \tag{2}$$

where μ_w is the contribution of the well resistance given by:

$$\mu_w = \frac{\bar{k}_h}{q_w} \pi z (2l - z) \left(1 - \frac{1}{n^2} \right) \tag{3}$$

3. SMEAR ZONE DEFINITION FOR MULTI-LAYER SOIL

During the PVD installation via a steel mandrel, the soil adjacent to the mandrel is dragged down by friction. It is well known that mandrel action remoulds the soft clay causing a reduction in permeability. The high total vertical stresses due to the mandrel further decreases the lateral permeability. In addition, the mandrel action that forces soil to be dragged down from upper layers to the underlying regions distinctly divides the clay seam into multi-layer permeability zones (Fig. 3). The consolidation process of the underneath soil layer can be retarded, if the soil permeability in the upper layer is lower. As the dragdown of soil affects the consolidation of lower soil layer, a two-layer soil system can be used to determine the consolidation response of the lower layer (Fig. 4). The dragdown effect influences the variation pattern of soil permeability of underlying layer. In the analysis, the permeability of lower soil layer with the intrusion zone was divided into 3 zones, the undisturbed zone, the smear zone due to the remoulding of lower soil layer and the smear zone due to the intrusion of the upper soil layer. Indraratna and Redana (2000) show that the lateral permeability can vary in the order of 10 within the multilayer soil in which the soil compressibility remains relatively constant, and the variation of the extent of the smear zone (d_s) is insignificant. On the basis of the above, the assumptions can be made:

1. Horizontal permeabilities of soil in layers 1 (upper) and 2 (lower) are k_{h1} and k_{h2}, respectively. Based on linear decay in horizontal permeability towards the drain proposed by Indraratna and Walker (2007), the smear zone characteristics (i.e. s and κ) in both layers remain the same.
2. Both soil layers have the same compressibility and overlapping of smear zone does not occur.
3. Figure 4c presents the variation of soil permeability after mandrel installation at Sections 1-1, 2-2 and 3-3. Sections 1-1 and 3-3 represent the normal situation when the soil is homogeneous. In Section 2-2 where the intrusion of the soil layer (radius $d_i/2$) occurs (infiltration zone), the permeability variation can be expressed as:

$$k_h = k_{h,upper}\left[\frac{A_1}{r_w}r + B_1\right]; \qquad\qquad d_w/2 < r < d_i/2 \tag{4}$$

$$k_h = k_{h,lower}\left[\frac{A_2}{r_w}r + B_2\right]; \qquad\qquad d_i/2 < r < d_s/2 \tag{5}$$

$$A_1 = \frac{\kappa_{upper}-1}{s-1} \tag{6}$$

$$A_2 = \frac{\kappa_{lower}-1}{s-1} \tag{7}$$

$$B_1 = \frac{s-\kappa_{upper}}{s-1} \tag{8}$$

$$B_2 = \frac{s-\kappa_{lower}}{s-1} \tag{9}$$

As observed from Casagrande and Poulos (1969) and Hird and Moseley (2000), the diameter of intrusion as a function of depth (z) in layer 2 can be expressed as:

$$\alpha = \frac{(d_s + d_w)}{2}\left[1 - z/H_2\right] \qquad\qquad 0 < z < H_2 \tag{10}$$

The normalised penetration depth (D) can be defined as a function of the penetration length due to upper soil layer (d_2) and the lower clay thickness (H_2):

$$D = d_2 / H_2 \tag{11}$$
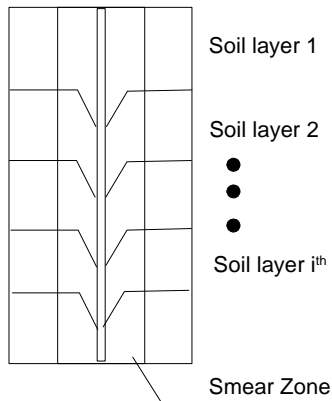
Figure 3: Downdrag effects due to mandrel installation in layered soil (Rujikiatkamjorn and Indraratna 2010

The normalised penetration depth illustrates how deep the upper soil layer can be dragged down into the immediately underlying soil layer. When D is more than 1 (i.e. the lower soil layer is quite thin compared to penetration length due to upper soil layer), the entire underlying soil is affected by the down-dragging. When D is less than unity, the down-dragged soil from upper layer partially is pushed into the underlying soil layer. The value of D has to be acquired by thorough field investigations as it relies on the interface characteristics between the soil and the mandrel. To analyse this problem, a piecewise-linear technique (Equation 2) will be used together with Equations (3)-(11) to obtain the parameter μ. For modern drains, the well resistance is ignored.

4.   EFFECT OF DOWNDRAG OF UPPER SOIL LAYER ON THE LOWER SOIL LAYER

To investigare the downdrag effect, the soil layer 2 (underlying soil) in Fig. 4b is divided into n small layers horizontally having thickness of H_2/n. In each thin horizontal layer slice i^{th}, the μ_i parameter can be determined using the proposed piecewise linear technique (Equations 2) and the variation of the

permeability in the intrusion zone can be calculated based on Equations (3)-(11). The average degree of consolidation for soil layer 2 can be determined from:

$$U_h = \frac{1}{n} \sum_{i=1}^{n} \left[1 - \exp\left(-\frac{8T_h}{\mu_i} \right) \right] \tag{12}$$
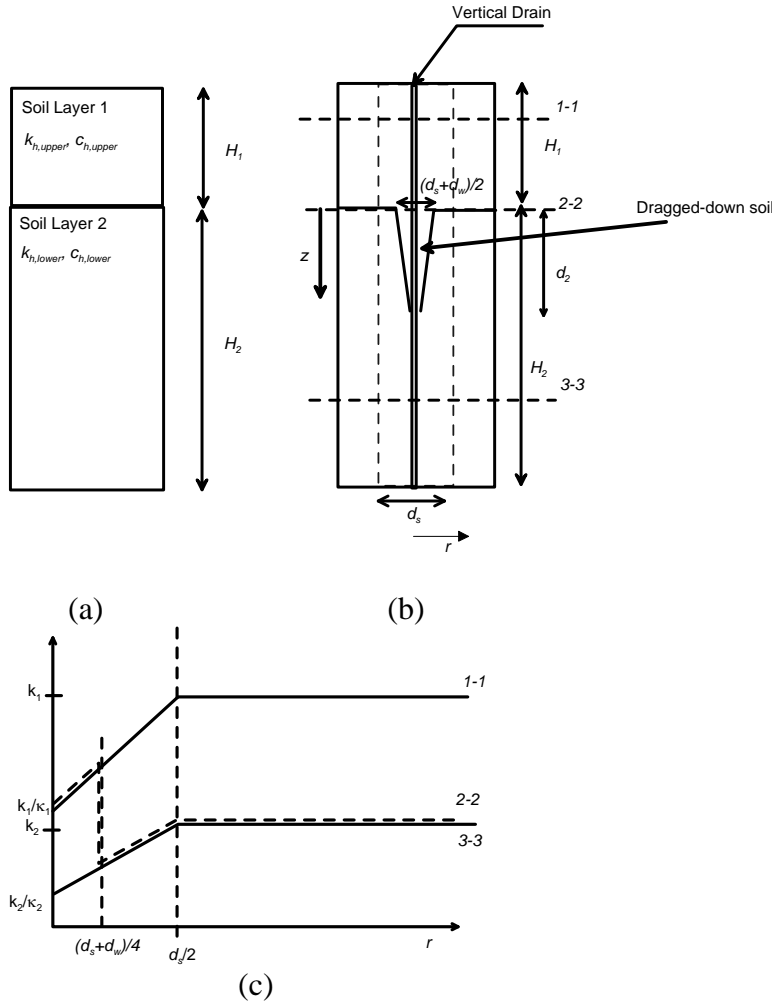
Figure 4: (a) Soil system with upper and lower soil layer, (b) Downdrag and smear effect due to mandrel installation in two-layer soil, (c) permeability variations along the radial direction at various horizontal cross sections (Rujikiatkamjorn and Indraratna 2010)

μ_i depends on smear zone characteristics (κ and s), permeability ratio between upper and lower soil layers ($k_{h,upper}/k_{h,lower}$), penetration depth (D), and drain spacing (n).

The overall time factor at 90% degree of consolidation (T_{h90}) of soil layer 2 can be determined from:

$$0.9 = \frac{1}{n} \sum_{i=1}^{n} \left[1 - \exp\left(-\frac{8T_{h90}}{\mu_i} \right) \right] \tag{13}$$

Figure 5 presents the variation of T_{h90} with normalised penetration depth (D) where n and s are assumed to be 30 and 5, respectively. When the horizontal permeability in the upper soil layer ($k_{h,upper}$) is lower than that in the underlying soil layer ($k_{h,lower}$) (i.e. $k_{h,upper}/k_{h,lower}<1.0$), T_{h90} significantly increases with an increase in penetration depth, retarding the consolidation in the second soil layer. However, when $k_{h,upper}/k_{h,lower} >1.0$, T_{h90} slightly decreases and becomes constant after D is less than 2. This implies that the horizontal permeability of the overlying soil layer can accelerate or retard the consolidation of the underlying soil layer.
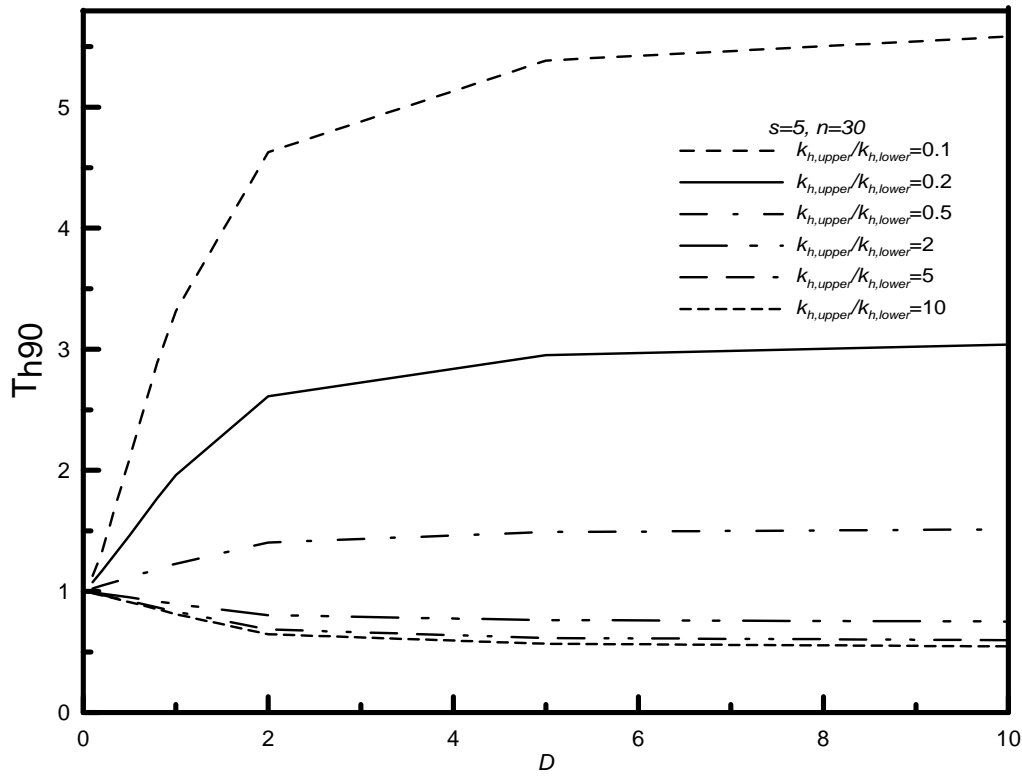
Figure 5: Time factor at 90% degree of consolidation with normalised penetration depth (Rujikiatkamjorn and Indraratna 2010)

5.   DESIGN PROCEDURES FOR MULTI-LAYER SOIL

Several vertical drains design procedures applicable for a single layer soil use horizontal time factor (T_h) vs. degree of consolidation curves (U_h) to determine the drain spacing (S) (Hansbo 1981; Zhu and Yin 2005; Rujikiatkamjorn and Indraratna 2007). The determination of the drain spacing can become a cumbersome task when the downdrag effect of upper soil layer combines with an iteration process. The required drain spacing (S) for a given soil layer considering the downdrag effect of upper soil layer to achieve 90% degree of consolidation can be determined by:

A. Assume a drain influence zone of d_e;

B. Determine d_w from $d_w=2(b+d)/\pi$ (Hansbo 1981);

C. Determine n_1 from $n= d_e /d_w$;

D. Based on n_1, D, κ,$k_{h,upper} / k_{h,lower}$, and s, determine T_{h90}

E. Calculate d_e from $d_{e2} = \sqrt{\dfrac{c_h t}{T_{h90}}}$ where c_h = radial coefficient of consolidation, t = required time.

Determine n_2 from $n = d_{e2} /d_w$ If the above parameters are the same as those given in the Figures, extrapolation and interpolation can be used to find $n_{2.}$;

F. If $n_1 \neq n_2$, select n_3 from $n_3=(n_{2+} n_1)/2$. Repeat procedures *(d)* and *(e)* until $n_1= n_2$

G. Determine drain influence zone (d_e) from $d_e=1.13S$ for PVDs with square pattern installation and $d_e=1.05S$ for PVDs with triangular pattern installation;

The overall degree of consolidation of n-layer soil (U) can be determined by

$$U_h = \frac{\displaystyle\sum_i^n U_{hi}\Delta h_i}{\displaystyle\sum_i^n \Delta h_i} \tag{14}$$

where, U_{hi} is the degree of consolidation of soil layer i^{th} and Δh_i is the thickness of soil layer i^{th}.

For the upper soil layer, the degree of consolidation based on linear smear zone can be determined from Eq. (2) where μ can be expressed by (Walker and Indraratna 2007):

$$\mu_L = \ln\left(\frac{n}{s}\right) - \frac{3}{4} + \frac{\kappa\ (s_L - 1)}{s\ - \kappa}\ln\left(\frac{s}{\kappa}\right) \tag{15}$$

For the case when $s_L = \kappa_L$ the μ parameter is:

$$\mu = \ln\left(\frac{n}{s}\right) - 1.75 + s \tag{16}$$

6. WORKED-OUT EXAMPLE

The above methodology is illustrated by the following example. The foundation soils are divided into 2 layers, whereby $t = 1.2$ years and well resistance is ignored. The required soil parameters for normally consolidated clay for each soil layer are assumed to be:

Layer 1 (Upper layer):
$c_{h1} = 0.5$ m^2/year, $\kappa= 5$, $s_1 = 5$, $k_{h,\ upper}=1\times10^{-10}$ m/s, $H_1=7$m

Layer 2 (Lower layer):
$c_{h2} = 1.0$ m^2/year, $\kappa= 5$, $s_2 = 5$, $k_{h,\ lower}=2\times10^{-10}$ m/s, $H_2=3$m, $D= 0.5$

PVDs with $d_w = 0.06$ m are expected to be installed in square pattern

Determine the drain spacing (S) when degree of consolidation of layer 2 is 90% and overall degree of consolidation for both upper and lower soil layer.

Solution:

Considering second soil layer
a) Assume $d_e =0.9$m;
b) $n_1 =0.9/0.06 = 15$, $k_{h,upper}\ /\ k_{h,lower} = 0.5$;
c) Based on n_1, D, K, $k_{h,upper}\ /\ k_{h,lower}$, and s, determine $T_{h90} = 1.46$.
d) $n_2 = \sqrt{\dfrac{1\times1.2}{1.46}}\Big/0.06 =15.1$, $n_1\approx n_2$, therefore $n= 15.0$
e) Based on n_3, D, K, $k_{h,upper}\ /\ k_{h,lower}$, and s, determine $T_{h90} = 1.48$.
f) $n_4 = \sqrt{\dfrac{1\times1.2}{1.48}}\Big/0.06 = 15.0$, therefore $n= 15$ and $d_e =0.9$m
g) For the upper soil layer, the degree of consolidation determined from Eqs. (2) is 75%.
h) The average degree of consolidation for both soil layers based on Equation (14) is 80%. For comparison, the overall degree of consolidation is 92% if the downdrag effect of soil is ignored in the lower layer.

7. CONCLUSIONS

Prefabricated vertical drains speed up soil consolidation via a short horizontal drainage path, and are now employed worldwide in many soft soil improvement projects. A radial consolidation model using a piecewise technique to capture variation of permeability is proposed. The consolidation of the multi-layer soil depends on the permeability of upper and lower soil layers, penetration depth, and drain spacing. When the horizontal permeability in the upper soil layer is less than that of the underlying soil layer, consolidation time of the underlying soil layer can be retarded depending on the upper soil penetration depth. On the other hand, the consolidation process can be accelerated further when the downdrag upper soil layer has a higher permeability. The proposed design method is most beneficial to the practitioner as a preliminary tool for the design of embankments stabilized by prefabricated vertical drains in a multi-layered soil affected by the downdrag.

8.   ACKNOWLEDGEMENT

REFERENCES

Barron, R.A. 1948. Consolidation of fine-grained soils by drain wells. Transactions, ASCE, 113, 718-742.
Basu, D. and Prezzi, M. 2007. Effect of the smear and transition zones around prefabricated vertical drains installed in a triangular pattern on the rate of soil consolidation. International Journal of Geomechanics, ASCE, Vol. 7, No. 1, pp. 34-43.

Bergado, D.T., Asakami, H., Alfaro, M.C., and Balasubramaniam, A.S. 1991. Smear effects of vertical drains on soft Bangkok clay. Journal of Geotechnical Engineering, ASCE, 117(10), 1509-1530.

Bo, M. W., Chu, J., Low, B. K., and Choa, V. 2003. Soil improvement; prefabricated vertical drain techniques, Thomson Learning, Singapore.

Casagrande, A. and Poulos, S. 1969. On the effectiveness of sand drains. Can. Geotech Journal., 6 pp. 287-326.

Chai, J. C. and Miura, N. 1999. Investigation of factors affecting vertical drain behaviour. Journal of Geotechnical and Geoenvironmental Engineering, ASCE, 125(3), 216-226.

Eriksson, U., Hansbo, S. and Torstensson, B.A. 1999. Soil improvement at Stockholm-Arlanda Airport. Ground Improvement, 4(2), 73-80.

Hawlader, B., Imai, G. and Muhunthan, B. 2002. Numerical study of the factors affecting the consolidation of clay with vertical drains. Geotextiles and Geomembranes, 20, 213-239.

Hansbo, S. 1981. Consolidation of fine-grained soils by prefabricated drains. "Proc. 10th International Conference Soil Mechanics and Foundation Engineering, Stockholm, 677-682.

Hird, C.C. and V.J. Moseley 2000. Model study of seepage in smear zones around vertical drains in layered soil. Geotechnique, 50(1), 89-97.
Indraratna B., and Redana I.W. 2000. Numerical modeling of vertical drains with smear and well resistance installed in soft clay. Canadian Geotechnical Journal, 37(1):133-145.

Indraratna, B., Rujikiatkamjorn, C. and Sathananthan, I. 2005a. Radial Consolidation of Clay using Compressibility Indices and Varying Horizontal Permeability. Canadian Geotechnical Journal , Vol. 42, pp. 1330-1341.

Indraratna, B., Rujikiatkamjorn, C. and Sathananthan, I. 2005b. Analytical And Numerical Solutions for a Single Vertical Drain including the Effects of Vacuum Preloading. Canadian Geotechnical Journal, Vol. 42, Issue 4, pp. 994-1014.

Jamiolkowski, M., Lancellotta, R., and Wolski, W. 1983. Precompression and speeding up consolidation. In Proceedings of 8th European Conference on Soil Mechanics and Foundations, Helsinki, Finland, 3, pp.1201-1206.

Li, A.L., and Rowe, R.K. 2002. Combined effect of reinforcement and prefabricated vertical drains on embankment performance. Canadian Geotechnical Journal, 38:1266-1282.

Lo, D. 1998. Vertical drain performance: myths and facts. Transactions, Hong Kong Inst. Eng, 5(1), 34-50.

Madhav, M. R., Park, Y.-M. and Miura, N. 1993. Modelling and study of smear zones around band shaped drains." Soils and Foundations, 33(4), 135-147.

Onoue, A. 1988. Consolidation of multi-layered anisotropic soils by vertical drains with well resistance. Soil and Foundations, Japanese Geotechnical Society, 28(3), 75-90.

Rujikiatkamjorn, C. and Indraratna, B. 2007. Analytical solutions and design curves for vacuum-assisted consolidation with both vertical and horizontal drainage. Canadian Geotechnical Journal, 44 (2), 188-200.

Rujikiatkamjorn C. and Indraratna, B. 2010. Radial consolidation modelling incorporating the effect of smear zone for a multi-layer soil with downdrag of caused by mandrel action. Canadian Geotechnical Journal, 47(9): 1024–1035.

Sharma, J.S. and Xiao, D. 2000. Characterization of a smear zone around vertical drains by large-scale laboratory tests. Canadian Geotechnical Journal, 37(6), 1265-1271.

Walker, R. and Indraratna, B. 2007. Vertical drain consolidation with overlapping smear zones. Géotechnique, Institution of Civil Engineers, UK, 57(5). pp. 463-467.

Yoshikuni, H. and Nakanodo, H. 1974. Consolidation of Fine-Grained Soils by Drain Wells with Finite Permeability. Soil and Foundations, Japanese Geotechnical Society, 14(2), 35-46.

EKGs Application for Hydro-Mechanical Behaviour Changing in Saturated Clay

Shariatmadari Nader, Iran University of Science and Technology, Iran, shariatmadari@iust.ac.ir
Karbalaieali Sogand, Iran University of Science and Technology, Iran, s_karbalaie@civileng.iust.ac.ir
Saeidijam Saeid, Iran University of Science and Technology, Iran, Saeidijam@iust.ac.ir

ABSTRACT

Solution for stabilization of mine tailings, waste lagoons, saturated clay slopes, and issues like that is an important subject which is undertaken by both classic and modern combinatory methods. One of the methods is Electrokinetic Geosynthetic or "EKG" which is formed by composition of Electrokinetic functions e.g. Electrosmosis beside Geosynthetics functions e.g. filtration and drainage. The innovative material form of EKGs is electrical conductive polymer drainage (ePVD) enhances dewatering rate, self-weight consolidation, and on the top of that it decreases the power consumption through the treatment. In this paper changing in dewatering rate, settlement and strength characteristics are studied in new cell and EKG design. In addition, some tests are run to show the situation of saturated soft clay in isolated self-weight consolidation, Electrokinetic enhanced consolidation, Electrokinetic Geosynthetic enhanced consolidation. Electrokinetic geosynthetic treatment improved dewatering more than electrokinetic. As result, the rate of water content decrease in EKG improved suitably than that of both EK and without EKG. On the other hand, Final Vertical settlement measure in EKG and EK tests increased than that of self-weight consolidation which caused the rate of vertical settlement during both EKG and EK treatment increased.

1.   INTRODUCTION

Generally problematic clays are characterized by low shear strength, high compressibility, and high water content will caused these clays to lose the bond of soil particles and its bearing capacity will decreased. Also dewatering under self-weight consolidation is very slow which takes an inappropriate long time. This characteristics cause many problem for soft clay and tailings for instance, dewatering rate, drainage, settlement, etc which need high effort to challenge.

In situ dewatering of such problematic material is highly desirable. The most likely technique to achieve this dewatering would traditionally include the installation of prefabricated vertical drains (PVDs). In order for these drains to work it is necessary to create a flow gradient in it, which is traditionally achieved by the application of a surcharge load. The drawbacks of this approach include the cost of importing and placing the fill, potential instability of the fill because of the low shear strength of the in situ material (Daniel Tjandra, 2007).

Recently there are many significant developments in soil improvement methods as the solution for problems on soft soils on new or existing construction (C. Liaki, 2010), (Colin JFP Jones, 2010). One of those soft soil improvements is the application of electrokinetic geosynthetics to strengthen soft soil bearing capacity. One way of reducing the water content of such material is by electroosmotic dewatering (Hamir, 2001), (A.B Fourie, 2007).

This paper presents results of electrokinetic geosynthetics laboratory experiments. The goal of the present research is to investigate physical properties of the Kaolin including water content, settlement as well change of strength in one dimension consolidation due to electrokinetic geosynthetics treatment.

2.   ELECTROKINETIC THEORY

In geotechnical engineering there are many researches of application of electric current to clays in order to strengthen the soil. This method has an advantage such as an application on low permeability soil and fine grained soil. Electrokinetic is a soil improvement method by supplying electric current to electrodes which are dug in the soil.

The applied electric current leads to electrolysis reaction in the electrodes. Oxidation of water at the anode generates an acid front while reduction at the cathode produces a base front by following electrolysis reactions:

$$\text{Anode}: 2H_2O - 4e^- \rightarrow O_2 + 4H^+ \tag{1}$$

$$\text{Cathode}: 2H_2O + 2e^- \rightarrow H_2 + 2OH^- \tag{2}$$

The electrolysis reactions are then followed by H^+ migration to the cathode and OH^- migration to the anode, which is called electro migration, and the pore water migration from the anode to the cathode is electro osmotic. The latest one would strengthen the soil bearing capacity in the vicinity of the anode. (A.B Fourie, 2007)

If in a compressible soil, electroosmosis draws water to a cathode where it is drained away and no water is allowed to enter at the anode, then consolidation of the soil between the electrodes occurs in an amount equal to the volume of water removed. Water movement away from the anode causes consolidation in the vicinity of the anode. The effective stress must increase concurrently. The pure water pressure must decrease, because the total stress in the vicinity of anode remains essentially unchanged. Consolidation continues until the hydraulic force balances the electroosmotic force driving water toward the cathode. (Mitchell, 1993)

3.   RESEARCH METHODOLOGY AND EXPERIMENTAL PROCEDURE

3.1.   Characteristics of Soil Sample

Modeling of natural clays by Kaolin sample as marine clays, mine and tunneling tailings is common (A.B Fourie, 2007), (Kalumba, 2009). In this research, application of electrokinetic geosynthetics method is conducted to Kaolin with index properties in table 1 and Fig1.

Table 1: Index properties of Kaolin

Specific Gravity *(gr/cm3)*	Liquid Limit	Plastic Limit	Permeability *(cm/sec)*	pH
2.68	52	32	6.32×10^{-8}	9
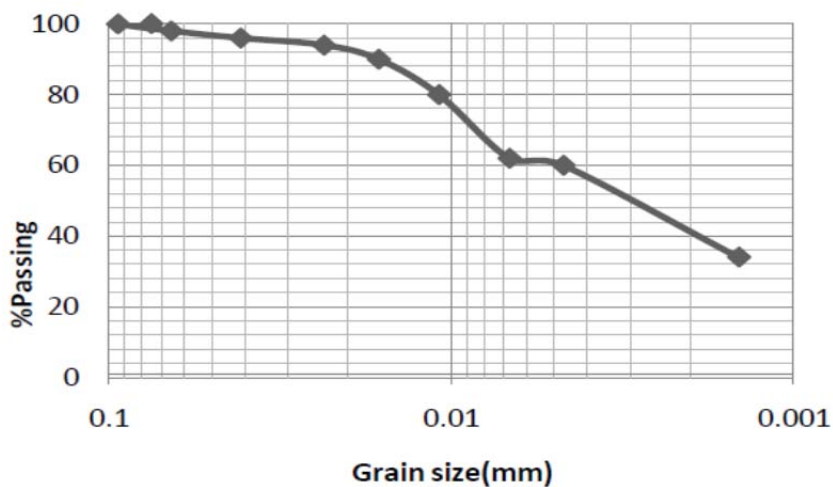
Figure 1: Particle size distribution of Kaolin

3.2.   Details of Electrokinetic Geosynthetics (EKGs) used as Electrodes

One of the side effects to the use of electrokinetic dewatering is high corrosion rate of metal electrodes. There have been experiments of graphite electrodes or metal electrodes with a carbon coating, but with a little success (Bergado, 2003). Description of EKGs development and comparative tests as well as copper electrodes showed no clogging of the EKGs or loss of material through EKG (Hamir, 2001). Therefore, there was excellent potential for further research in the EKGs' usage for dewatering and self-weight consolidation of soft soils.

The EKGs consisted of an electrically conductive geonet core manufactured using the counter-rotating dies method utilizing a stationary outer die. The geonet was extruded from a specially formulated conductive compound based on conductive carbon black dispersed in a modified high density

polyethylene resin. The polymer was designed for extrusion applications and was originally developed for the minimization of electrostatic discharge hazards in electrostatic sensitive environment (A.B Fourie, 2007). The durability of the EKG electrode is vastly superior to that of metallic electrodes. More details of EKGs were described in (Pugh, 2002), Photo1.

Photo 1: view of EKG used in the tests

3.3. Laboratory Test using an Electroosmotic Cell

This research is conducted by supplying different current of 18 and 30 volts in the anode and cathode with duration of 72 hours. The electrodes are EKGs. A schematic experimental set up of the electroosmotic process is presented in fig 2. Also two series of test run by metal electrodes to show the differences between EKG and EK treatments. Different sets of laboratory tests were carried out by 75,100,150% water content. The initial set of laboratory tests were designed to test the dewatering rate of Kaolin without an applied voltage gradient.

Table 2: Test properties

NO	Test Name	Test Duration (Days)	Initial Water Content(%)	Soil/Water (Kg/Kg)	Electrode Material	Voltage
1	w100V0(2)	4	100	10/10	-	0
2	EKGw100V18(2)	3	100	10/10	EKG	18
3	EKGw150V18	3	150	10/15	EKG	18
4	EKGw75V18	3	75	10/7.5	EKG	18
5	EKGw100V30	3	100	10/10	EKG	30
6	EKw100V30-10	3	100	10/10	Galvanize Steel	30-10
7	EKw100V10-6	3	100	10/10	Galvanize Steel	10-6
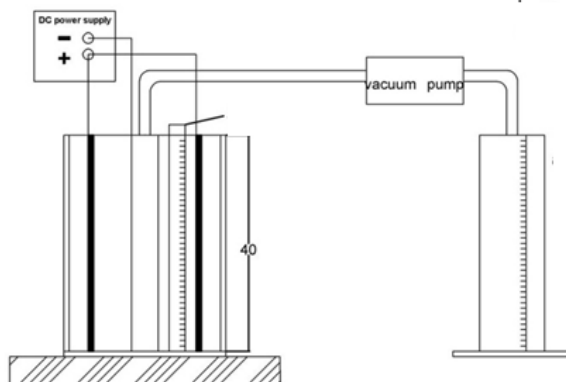
Figure 2: Electroosmotic cell

Photo 2: View *of the laboratory experiment*

This research is conducted by the laboratory testing procedure as follows. The central perforated cylindrical is wrapped by filter paper and coated by EKG, then slurry mixture of Kaolin and water is placed in an open cube Plexiglas box, its dimensions are $30\times30\times40$ cm^3. Afterwards the anode which is wide EKG is placed through the slurry,Photo2. The electric current was supplied to the EKGs continuously within the 72hours. In the final stage several laboratory tests like 1D Consolidation and fall cone were carried out to investigate the index properties of the soil sample taken at vicinity of anode and cathode.

4.   RESULT AND DISCUSSION

4.1.   Water content and Dewatering result

The result of test with diverse voltage and variable water contents are presented in fig.3 , which shows the variation in water content in the vicinity of anode for 8 series of test. The rate of electroosmotic dewatering increases as the initial solids content decreases (Gray, 1967). Due to the electroosmotic dewatering in the system water content at the anode area was decreasing with the increase of time. Besides, the water content at the cathode area was decreasing but not as much as the anode (fig. 4.). The decreased water content naturally strengthened the soil.
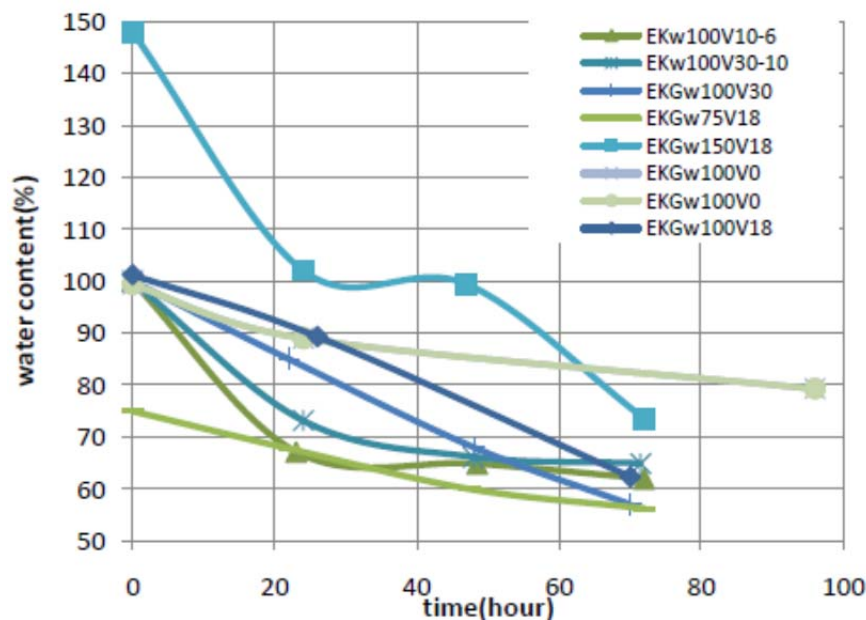
Figure 3: Variation of water content in Anode vicinity with time
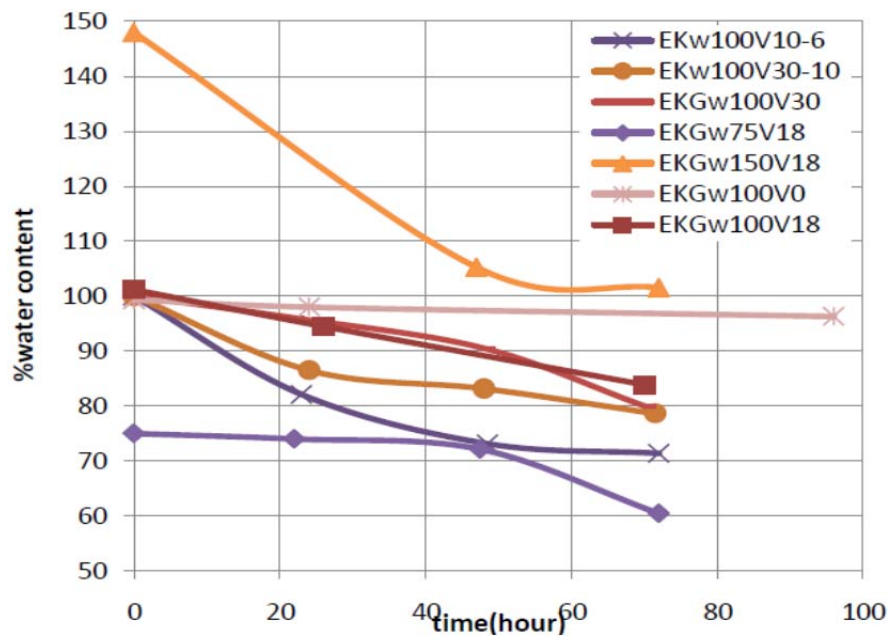
Figure 4: Variation of water content in Cathode vicinity with time

4.2.   Settlement

The result of test bench (without applied voltage) showed final vertical strain 0.10 after more than 72hours while the EKG treatment for most of tests increase this index twice as much as test bench's.(fig. 5)
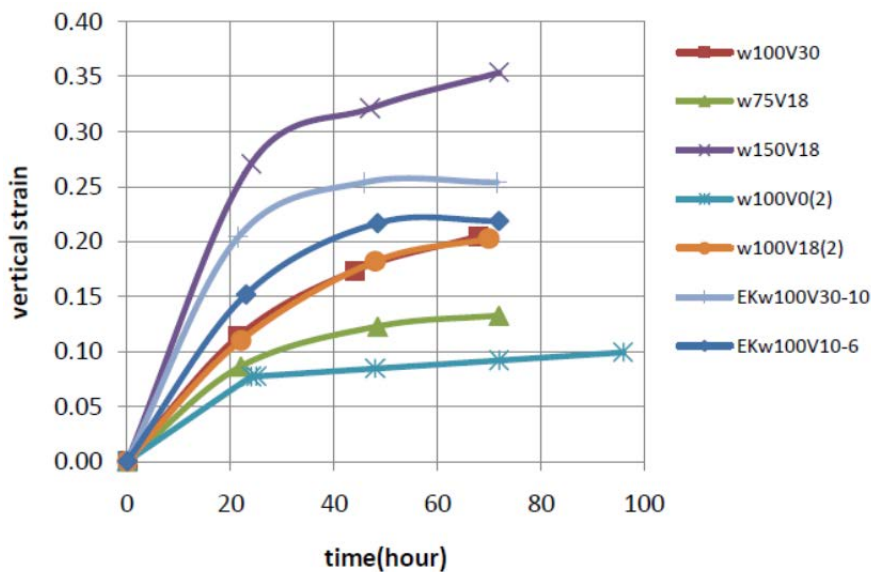
Figure 5: Variation of vertical strain due to dewatering with time

4.3.   Stress-Strain behavior due to1D Consolidation after EKG

In 1D consolidation result for the series of EKG and EK test with same water content but different voltage and electrodes, EKG test with 30V were found to increase the strength of soil by strain hardening more than the others tests. Also EKG test with 18V and EK test with variable voltage in the range of 30 to 10V show the similar result in lower stress levels ; 0.25, 0.5, 1, 2 kg/cm^2 ,although the energy consumption in the first test is 180 kWh and in second one is 450 kWh. The cost of treatment can be significantly reduced by using EKGs instead of conventional metallic electrodes.

Also, Fig.6 shows variation of vertical strain with different levels of stress. Generally the series of tests with lower initial water content led to lower final water content at the end of EKG treatment.
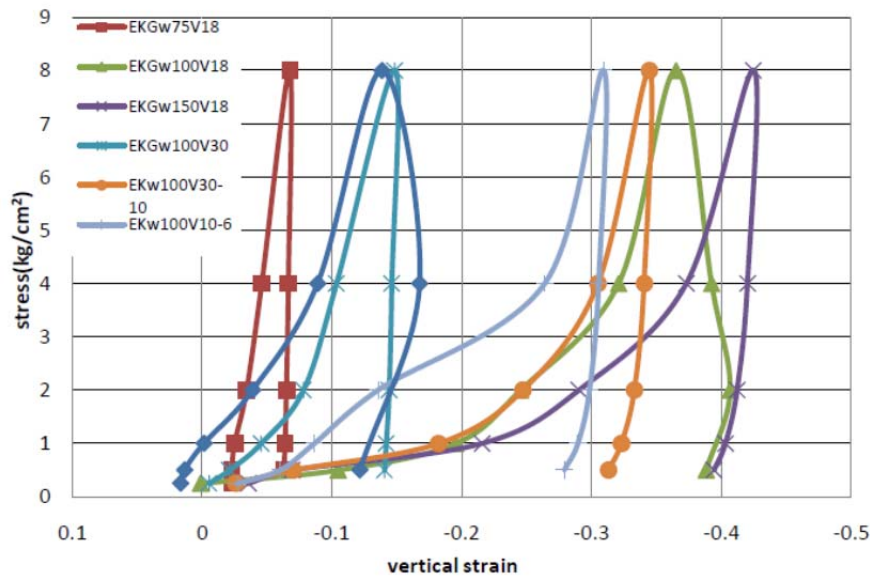
Figure 6: stress-strain diagram after EKG and EK treatment in Oedometer test

By investigating stress for same strain %10, can be seen stress for EK and EKG treatment with same initial water content were 1.27 and 3.72 kg/cm2 respectively. It shows the usage of Electrokinetic Geosynthetics as electrodes heightened the strength gained by the electroosmotic dewatering and consolidation.

4.4. Energy consumption and cost

The result of energy consumption shows the cost of treatment can be significantly reduced by using a low voltage and the provision of electrodes that are not subject to rapid corrosion. Conventional metallic electrodes (especially the anode) corrode rapidly beside it causes a significant loss of efficiency in EK treatment (A.B Fourie, 2007).this can be overcome by the use of EKG material.
For the soil in this research (Kaolin) EK treatment with galvanized metallic electrodes dewatering took place at an electrical energy consumption rate of 45 kWh/dry tone. While the rate of EKG test was 25 kWh/dry tone in same water content mixture.
Fig. 7 shows the increase in Energy consumption rate with increase in initial water content but constant applied voltage.
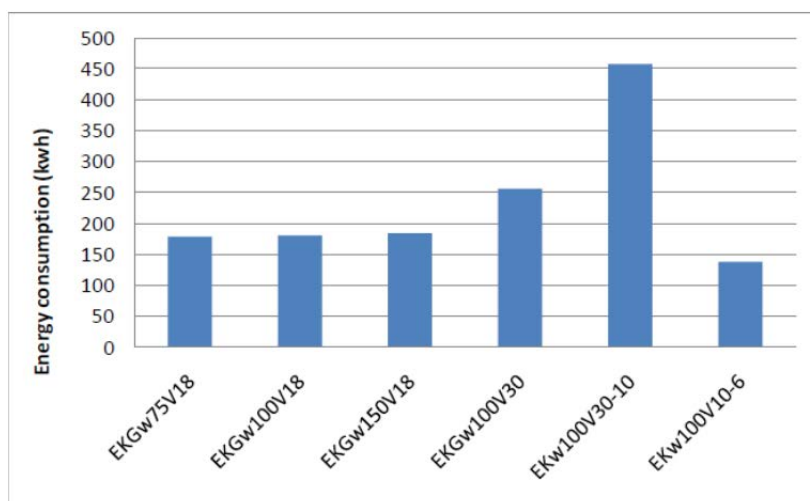
Figure 7: Energy consumption in EKG and EK tests

5.   CONCLUSION

The following is a summary of the conclusion from this experimental study:
1.   Electrokinetic geosynthetic treatment improved dewatering efficiency more than Electrokinetic.
2.   The rate of water content decrease in EKG improved suitably than that of both EK and self-weight consolidation.
3.   Final Vertical settlement measure in EKG and EK tests increased twice as much as that of self-weight consolidation.
4.   The rate of vertical settlement during both EKG and EK treatment increased.
5.   The energy consumption in EKG test is not as much as EK test with same water content. So the cost of treatment can be significantly reduced by using EKGs instead of conventional metallic electrodes.

6.   ACKNOWLEDGEMENTS

REFERENCES

A.B Fourie, D. J. (2007). Dewatering of mine tailings using electrokinetic geosynthetics. Can.Geothech.J. Acar, Y. B. (1995). Electrokinetic Remediation: Basics and Technology Status. Journal of Hazardous Materials .

Bergado, D. (2003). Electroosmotic consolidation of soft Bangkok clay using copper and carbon electrodes with PVD. Geotechnical Testing Journal.

C. Liaki, C. D. (2010). Physico-chemical effects on clay due to electromigration. Journal of Applied Electrochemistry .

Chang-Yu Ou, S.-C. C.-H. (2009). Soil improvement using electroosmosis with the injection of chemical solutions: field tests. Can. Geotech. J.

Colin JFP Jones, J. L.-B.-f. (2010). RECENT RESEARCH AND APPLICATIONS IN THE USE OF ELECETRO-KINETIC GEOSYNTHETICS.

Daniel Tjandra, P. S. (2007). Improving marine clays with electrokinetics method. Civil Engineering Dimension.

Gray, D. H. (1967). Fundamental Aspects of Electro-Osmosis in Soils. J. Soil Mech. Found. Div.

Hamir, R. J. (2001). Electrically conductive geosynthetics for consolidation and reinforced soil. Geotextiles and Geomembranes.

J Q. Shang, S. M. (2001). Electrokinetic Strengthening of Marine Clay Adjacent to Offshore Foundations. international Offshore and Polar Engineering Conference. Stavanger, Norway: The International Society of Offshore and Polar Engineers.

Jame K. mitchell, K. S. (2005). Foundamentals of soil behavior. Wiley.

Kalumba, D. G. (2009). Dewatering of Tunneling Slurry Waste. JOURNAL OF ENVIRONMENTAL ENGINEERING.

Mitchell, J. (1993). Fundamentals of Soil Behavior (2 ed.). New York: Wiley.

Pugh, R. C. (2002). The application of electrokinetic geosynthetic materials to uses in the construction industry. PhD Thesis, Newcastle University.

Finite Element Modeling of Vacuum Consolidation using Drain Elements and Unsaturated Soil Conditions

Richard Witasse, Plaxis bv, Delft, The Netherlands, rw@plaxis.com
Jérome Racinais, Menard, Nozay, France,
Fanny Maucotel, Menard, Nozay, France,
Vahid Galavi, Plaxis bv, Delft, The Netherlands,
Ronald Brinkgreve, Plaxis bv and Delft University of Technology, r.brinkgreve@plaxis.nl
Cyril Plomteux, Menard, Nozay, France,

ABSTRACT

Vacuum consolidation is a method used for preloading and consolidating soft and very soft saturated fine-grained soils. The procedure consists of installing vertical and horizontal vacuum transmission pipes under an airtight impervious membrane and evacuating the air below the membrane producing an atmospheric pressure on the soil.

This article aims at presenting the set-up and the results of a finite element analysis performed for a reclamation project in Vietnam. In this context the two-dimensional behaviour of an embankment on soft soils incorporating prefabricated vertical drains is analyzed with the geotechnical finite element package PLAXIS 2D.

This FE analysis is carried out in the framework of a fully coupled flow-stress analysis with unsaturated soil condition. For this purpose, a new drain element has been implemented on which negative pore pressure (vacuum induced suction) can be applied as a flow boundary condition. Advanced constitutive modelling for the nonlinear behavior of the constitutive soft soil layers is also considered.

Results obtained in this context are finally presented and the added value of the proposed two-dimensional FE analysis is clearly highlighted.

1.   INTRODUCTION

In this study, a finite element (FE) model is employed to analyze consolidation and lateral displacement of soft ground with prefabricated vertical drain (PVD) under vacuum consolidation.

A two-dimensional idealization is used for simplicity. Soft Soil model is used to idealize the soft ground. An equivalent permeability, based on the equal discharge rate in the model and in the field, is used to characterize flow. Field vacuum pressure is simulated by specifying negative pore pressure-time history on the PVD boundaries and sand blanket. Varying the negative pressure inputs, several FE simulations are performed to predict the field behaviour on soft clay for a real reclamation work in Vietnam.

The purpose of this article is to demonstrate the capability of the finite element method to properly model vacuum consolidation and highlight its interest in the design process of ground improvement using such a process.

2.   GENERAL DESCRIPTION OF THE PROJECT AND SITE CONDITIONS

The project is the construction of a container port along the Cai Mep River. The riverbank length is approximately 500m, and container storage yard depth ranges between 600 to 750m. The total area covered by the port land is about 330,000 m² (excluding berth). The port comprises an offshore berth (reinforced concrete slab deck on piles), along which the ships will moor, and on which will be installed the unloading cranes. The berth is located 100 to 150m away from the river shore, and a "reclamation" area, where sand fill will be installed over the existing natural ground (swamp). Due to the draft of the ships, the natural riverbed will be dredged down. The reclamation area will welcome the container storage area, surrounding service roads, and ancillary buildings. The berth and the reclamation area will be connected by three approach bridges, also RC deck on piles. Due to its very poor mechanical properties, the natural soil will settle of a very large amount under the load of the sand fill. Therefore, ground improvement is foreseen to address this issue.

Figure 1: General port layout

The piece of land represents about 72 Ha, but only 33 Ha will be reclaimed in this phase of the project. The remaining area may be developed in further phases of the project. The length of reclaimed land along the river is 508m. The longitudinal length of reclaimed land varies between 650 and 700m. A schematic drawing of the reclaimed area is reproduced in Figure 1.

An 800m long berth will be constructed some 150m away from the edge of the reclamation, in the river. The natural ground is swamp and mangroves; a third of the area is under the mean water level. A backfill of several meters thick will be necessary to raise the overall platform above water level and provide proper working and circulation platform for the port utilities. Due to the important amounts of backfill and the soft subsoil condition, settlements in the range of several meters are anticipated. Moreover, dredging is foreseen along the berth to allow necessary water draft for the vessels to approach the berth. This dredging will impact the overall stability of the riverbank land. Therefore, extensive ground improvement works have been designed to address those important settlements and ensure the stability of the riverbank.

3.   TWO-DIMENSIONAL PLANE STRAIN FINITE-ELEMENT ANALYSIS

The finite element mesh along with the mechanical and hydraulic boundary conditions are given in Figure 2. The overall model dimensions are 450 m and 135 m in horizontal and vertical directions respectively.

The finite element model has been set-up in plane strain situation using 15-nodes triangular elements which provide a high order of displacement and pore pressure interpolation. The mesh has been further refined in the vacuum treatment area.

Prefabricated vertical drains (PVD) are inserted into the soft soil layers and a drainage layer (clean coarse sand blanket with horizontal drain network) is installed above to convey water to the periphery of the treated zone. The PVD are a slender, synthetic drainage element comprised of a drainage core wrapped in a geotextile filter and they have rectangular cross-section (band-shaped). The prefabricated vertical drains (PVD) have been modelled as special drain elements and interface elements have been introduced over the sand blanket to represent the impervious membrane.
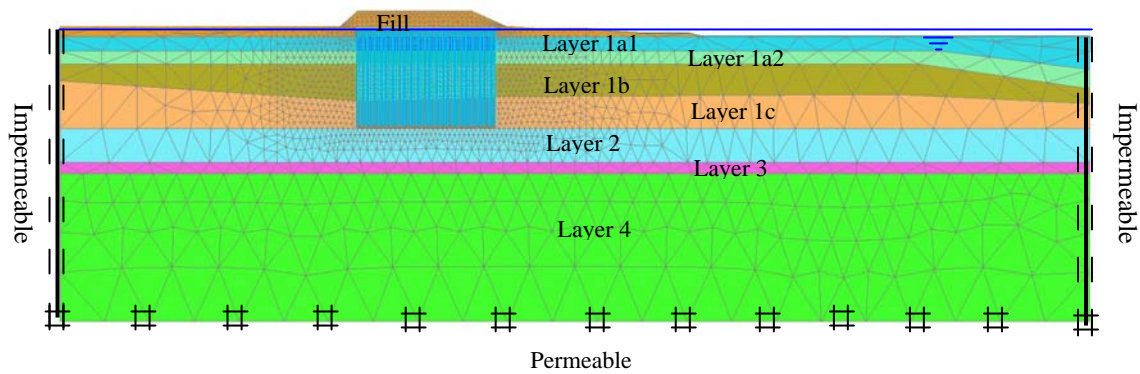
Figure 2: FE mesh

3.1.   Soil profile and material properties

The modelled ground formation is composed of 7 soil layers on top of which the sand fill will be brought for constructing the embankment. The assumed model properties have been summarized in Table 1. Material properties have all been defined in terms of effective stiffness and effective strength parameters. Undrained behaviour has also been assumed for all constitutive materials of layer 1.

Table 1: Assumed model parameters

Soil layer	Layer 1a1	Layer 1a2	Layer 1b	Layer 1c
Depth (m)	[0.5, -5.8]	[-5.8, -11.5]	[-11.5, -28]	[-28, -40]
Model type	Soft-Soil	Soft-Soil	Soft-Soil	Soft-Soil
Drainage type	Undrained	Undrained	Undrained	Undrained
Unit weight (kN/m^3)	15.2	15.2	15.7	16.2
Compression index $\lambda*$	0.135	0.135	0.135	0.131
Swelling index $\kappa*$	$2.27.10^{-2}$	$2.70.10^{-2}$	$2.48.10^{-2}$	$2.66.10^{-2}$
Initial void ratio e_0	2.06	2.06	1.81	1.62
Overcons. press. POP (kPa)	32.75	0	0	0
Poisson ratio v	0.15	0.15	0.15	0.15
Cohesion c (kPa)	7.6	7.6	7.6	7.6
Friction angle φ	23.6	23.6	23.6	23.6
Equiv. hor. perm k_h (m/day)	$1.5.10^{-5}$	$1.5.10^{-5}$	$1.5.10^{-5}$	$1.5.10^{-5}$
Ver. perm k_v (m/day)	$1.5.10^{-5}$	$1.5.10^{-5}$	$1.5.10^{-5}$	$1.5.10^{-5}$

Soil layer	Fill	Layer 2	Layer 3	Layer 4
Depth (m)	[11.7, 0.5]	[-40, -55]	[-55, -60]	[-60, -125]
Model type	Mohr-Coulomb	Mohr-Coulomb	Mohr-Coulomb	Mohr-Coulomb
Drainage type	Drained	Drained	Non porous	Non porous
Unit weight (kN/m^3)	18	17.5	19	19
Young's modulus E (kPa)	20.10^3	30.10^3	40.10^3	60.10^3
Poisson ratio v	0.3	0.33	0.25	0.25
Cohesion c (kPa)	1	1	1	1
Friction angle φ	30	30	30	30
Horizontal perm k_h (m/day)	1	0.1	1	1
Vertical perm k_v (m/day)	1	0.1	1	1

3.2.   Modelling of the vertical drains

Practically the drains will be installed following a regular square pattern of 1m by 1m through the top clay layers (layer 1). In the 2D model presented in Figure 2 PVD have been modelled as vertical linear elements. As we are assuming plane-strain modelling, real in-situ vertical soil permeability values need to be modified to account for the fact the drainage path is different than in reality as presented in Figure 3.

(a) Axisymmetric radial flow   (b) Plane strain flow
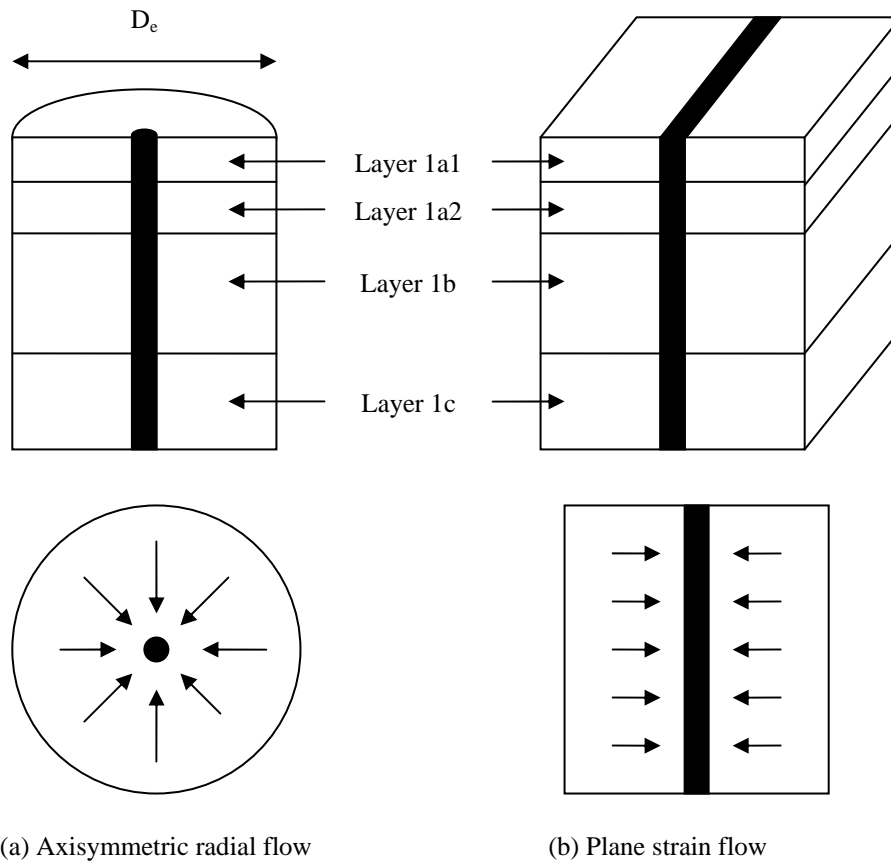
Figure 3: Comparison of axisymmetric unit cell radial flow into plane strain flow

The equivalent horizontal soil permeability has been obtained by considering a 1D consolidation problem of a layered soil containing a central drain (cf Figure 3) such that the FE calculation of the degree of consolidation perfectly matches the analytical solution given by Barron (1948). In this context it has been found that the initial in-situ horizontal permeabilities should be divided by a factor 3 in order to get comparable kinetics of the degree of consolidation as shown in Figure 4. One shall also note in this context that the equivalent horizontal permeability values have been set up without considering any void ratio dependency.
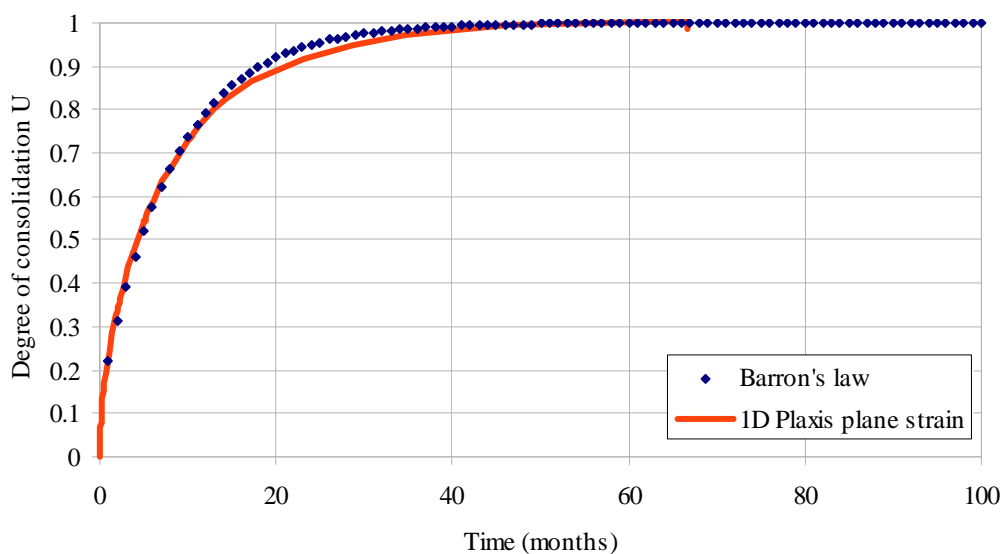
Figure 4: Comparison of 1D PLAXIS plane strain consolidation results with Barron's law

4. FINITE ELEMENT SIMULATION OF THE EMBANKMENT CONSTRUCTION WITH VACUUM LOADING

Finite element calculations have been carried out in the framework of a fully coupled flow-deformation analysis assuming unsaturated soil conditions and 2D plane strain situation (Galavi, 2010).

The governing equations of such an elasto-plastic consolidation as considered in PLAXIS 2D is based on a total pore pressure approach and follow Biot's theory (Biot, 1941). The formulation is based on small strain theory and Darcy's law for fluid flow is assumed. Bishop's effective stress (Bishop & Blight, 1963) is utilised in this formulation defined by:

$$\sigma = \sigma' + \mathbf{m}\chi p_w \approx \sigma' + \mathbf{m}S_e\,p_w \qquad (1)$$

σ is the total stresses, σ' is the effective stresses, p_w is the pore water pressure and $\mathbf{m}$ is a vector containing unity terms for normal stress components and zero terms for the shear stress components. χ is an effective stress parameter called matric suction coefficient and varies from 0 to 1 covering the range from dry to fully saturated conditions and approximated by the effective degree-of-saturation S_e in PLAXIS 2D.

The vacuum consolidation pressure is applied along the drain through a uniform total water head defined as the one represented by the steady state pore water pressure minus the suction excess pore pressure induced by the vacuum p_{va}.

$$h_{va}^{drain} = z - \frac{p_{steady} - p_{va}}{\gamma_w} \qquad (2)$$
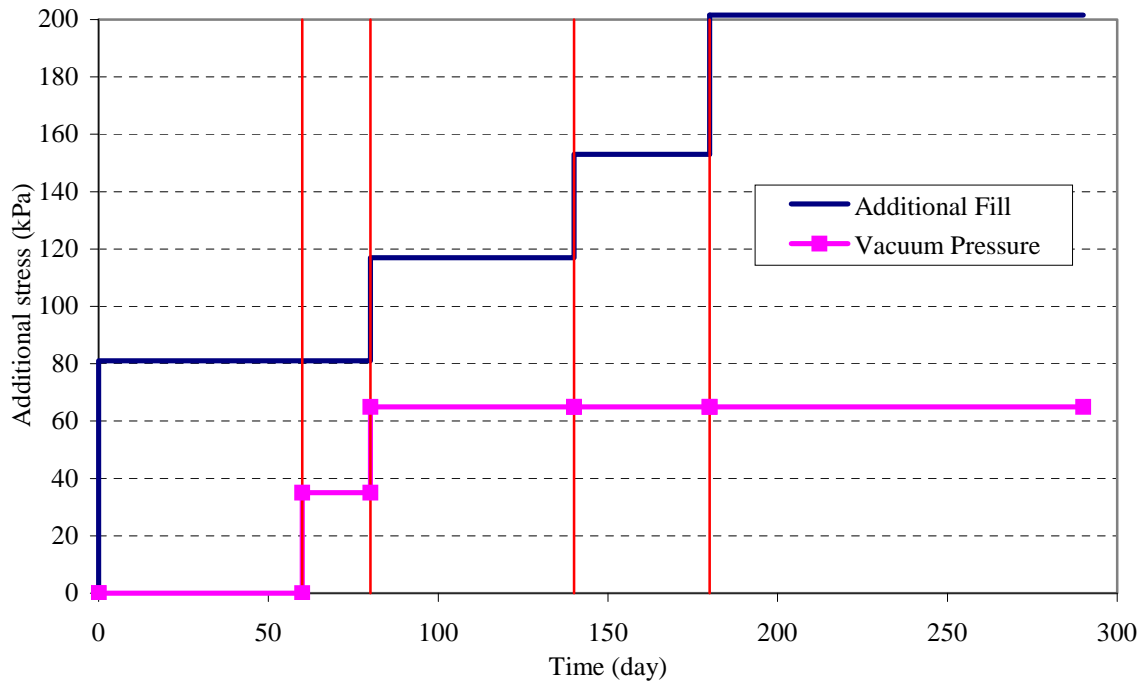
Figure 5: Additional fill and additional vacuum pressures

For the current project, the following construction stages have been defined:

Phase 0: Initial stress definition assuming drained behaviour for all constitutive soil layers (K0-procedure)
Phase 1: Drains installation without vacuum (Plastic analysis assuming instantaneous loading)
Phase 2: Consolidation over 60 days (Coupled flow-stress analysis)
Phase 3: Installation vacuum at 35 kPa (Coupled flow-stress analysis with depression applied over 1 day)
Phase 4: Consolidation over 20 days (Coupled flow-stress analysis)

Phase 5: Add 2m fill and increase vacuum depression to 65 kPa (Coupled flow-stress analysis with

additional depression and loading applied over 1 day)
Phase 6: Consolidation over 60 days at 65 kPa vacuum pressure (Coupled flow-stress analysis)
Phase 7: Add 2m Fill (Coupled flow-stress analysis with loading applied over 1 day)
Phase 8: Consolidation over 40 days at 65 kPa vacuum pressure (Coupled flow-stress analysis)
Phase 9: Add 2.7m Fill (Coupled flow-stress analysis with loading applied over 1 day)
Phase 10: Consolidation over 110 days at 65 kPa vacuum pressure (Coupled flow-stress analysis)

The evolution of the distributed pressure load created by constructing the different fill layers as well as the effective vacuum pressure are summarized in Figure 5.

5. NUMERICAL RESULTS

5.1. Stresses and active pore pressures

Eight Gauss points K, L, M, N, O, R, P and Q located respectively at the centre of layers 1a1, 1a2, 1b and 1c have been chosen to follow the main parameters in this analyses: total vertical stress, effective vertical stress and active pore pressures (see Figure 6).
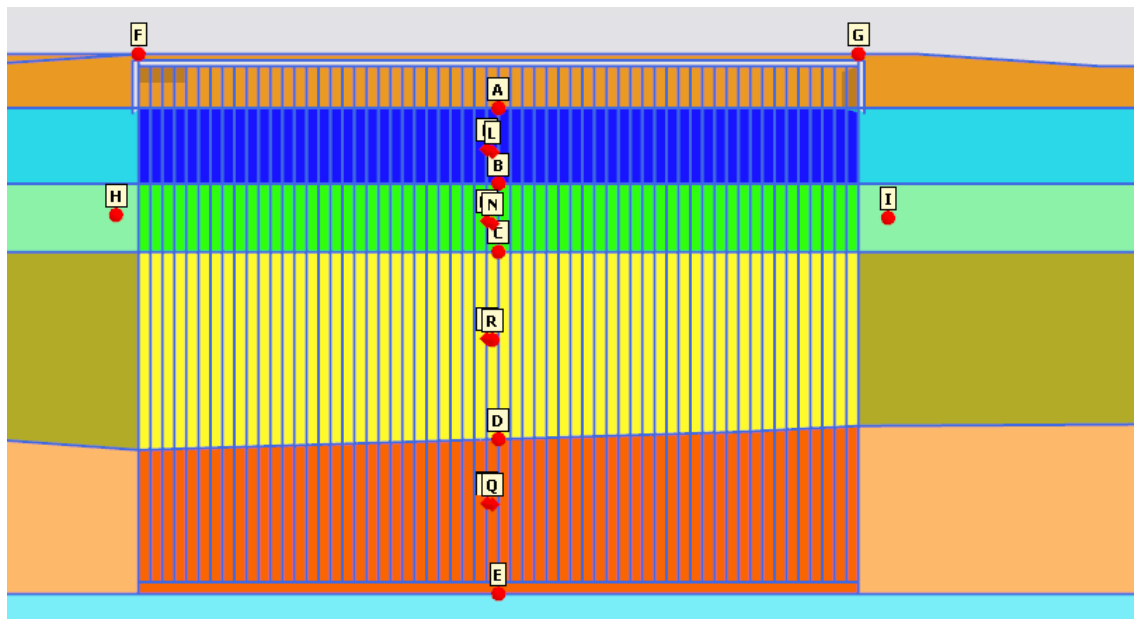
Figure 6: Location of Gauss points and nodes for results post-processing

Figure 7 presents the evolution of total vertical stresses at different depths in the middle of each constitutive clay layers in the vacuum area and show the expected following results
- The total stress value increases immediately after each fill layer and then remains constant
- The vacuum (applied between 60 and 80 days) does not affect the total stress value
- The evolution of the total stress at different depth is in good agreement with analytical results according to the construction sequence

In Figure 8 the variation of the active pore pressure ($p_{steady} + p_{excess}$) with time is given. It can be seen that
- The construction of each fill layer systematically leads to an instantaneous increase of the pore pressure in between the drains equal to the applied total stress
- The pore pressure then decreases during the following consolidation period
- The vacuum treatment (applied between 60 and 80 days) leads to a further decrease of the active pore pressure equal to the applied vacuum pressure

 Figure *9* finally presents the evolution of the effective stresses at the same previously considered depths. Although the effective stresses are not fully stabilized at the end of the calculation it shows the positive influence of the vacuum which increases the rate of the effective stress increase very valuable to evaluate the possible amount of the mobilized friction with time.
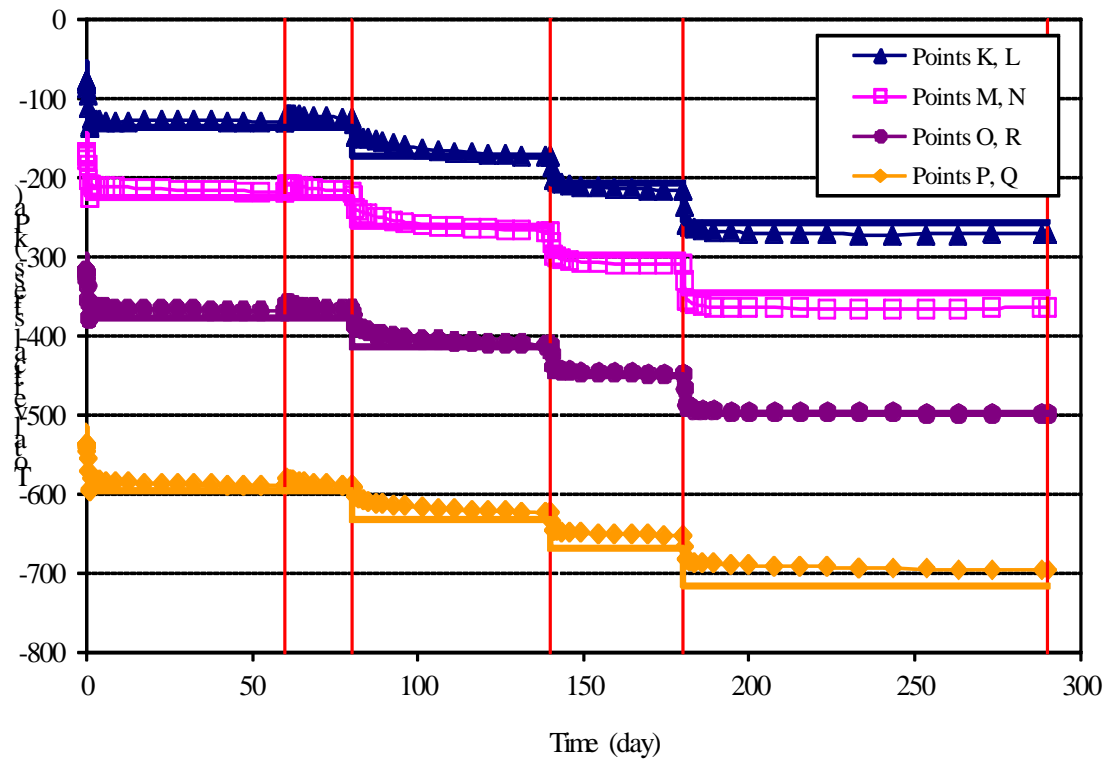
Figure 7: Total vertical stresses variation with time
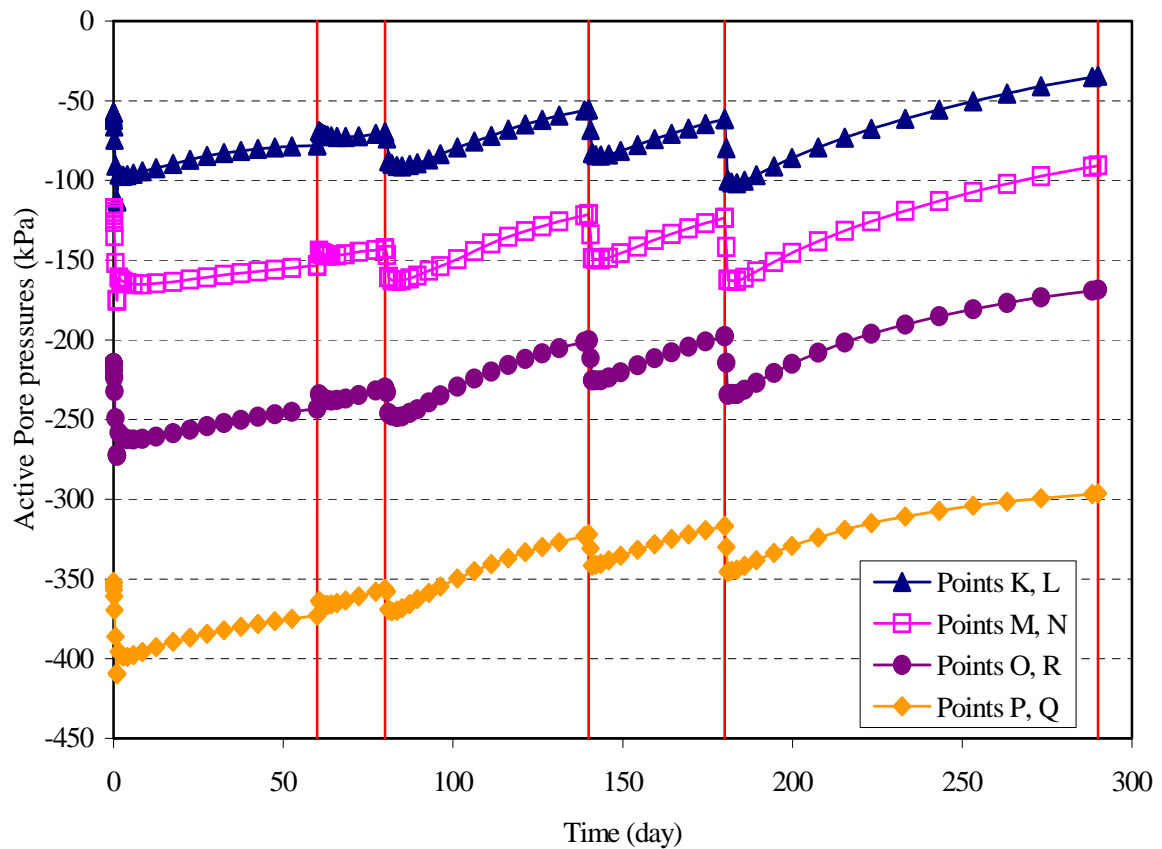
Figure 8: Active pore pressures variation with time
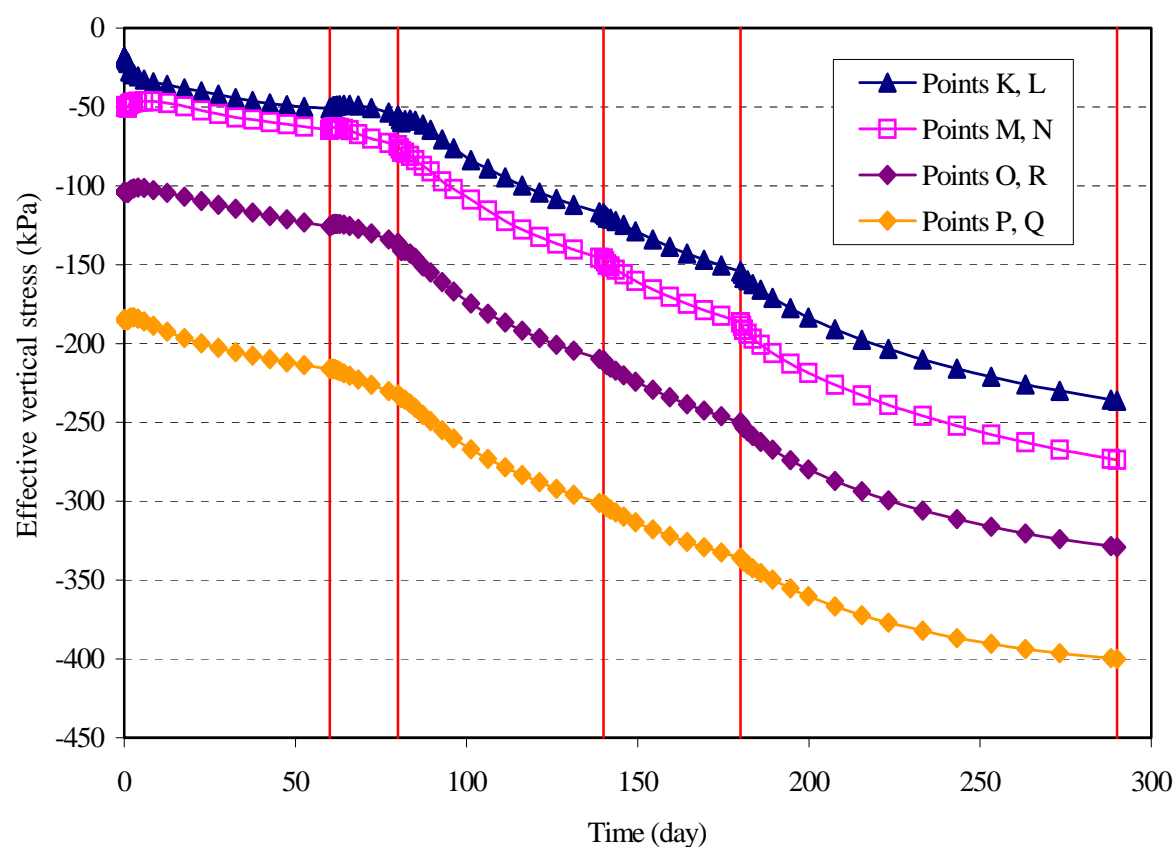
Figure 9: Effective vertical stresses with time

Total displacements u_x

Maximum value = 0,9282 m (Element 1755 at Node 40875)

Minimum value = -0,6213 m (Element 5163 at Node 24228)
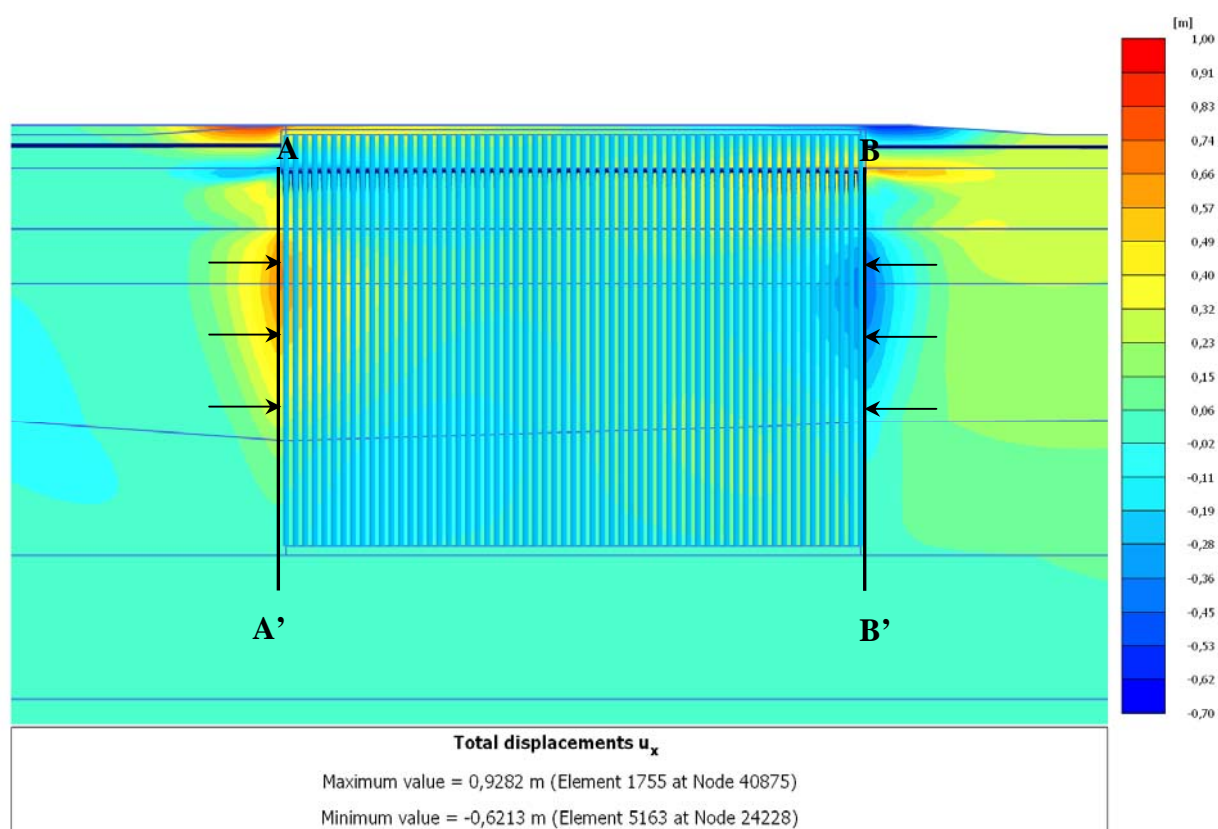
Figure 10: Global view of horizontal displacements at 290 days

(a) Cross section A-A'   (b) Cross section B-B'
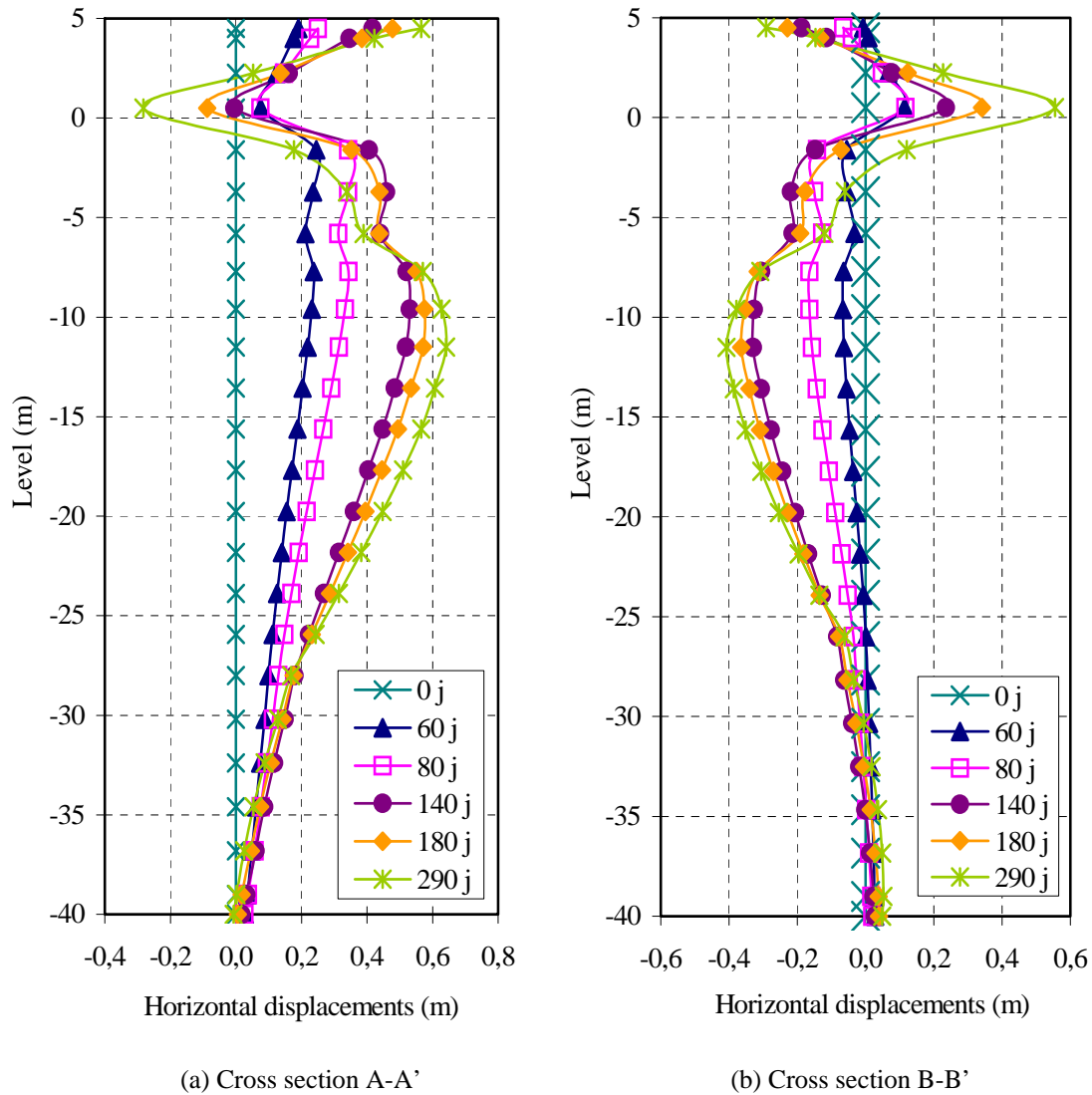
Figure 11: Horizontal displacements at the edge of vacuum consolidation area

5.2.   Horizontal displacements

Figure 10 and Figure 11 summarize the evolution of the lateral displacement induced by the vacuum pressure. These figures show the ability of the vacuum consolidation process to generate lateral displacement inwards the treated area like expected for a porous medium subjected to an isotropic depression. Such information on the amount of generated lateral displacement could be very useful in situations where the integrity of surrounding building would be of concern and have to be addressed during design stage as well.

5.3.   Factor of safety

Figure 12 presents the typical slope failure mechanism obtained using a phi-c reduction analysis (at 290 days for the situation presented where the vacuum treatment is active) and table 2 summarizes the different values of the factor of safety reached just after each fill raising and at the end of the calculation. The factors of safety are obtained using a phi-c reduction analysis after phase 5 (81 days), phase 7 (141 days), phase 9 (181 days) and phase 10 (290 days) for the situations with and without vacuum treatment. The situation without vacuum is considering an additional load equal to the vacuum pressure in order to generate in the soil an equivalent state of effective stresses and comparable settlement rate after each fill construction and generated fair comparison for the factors of safety.
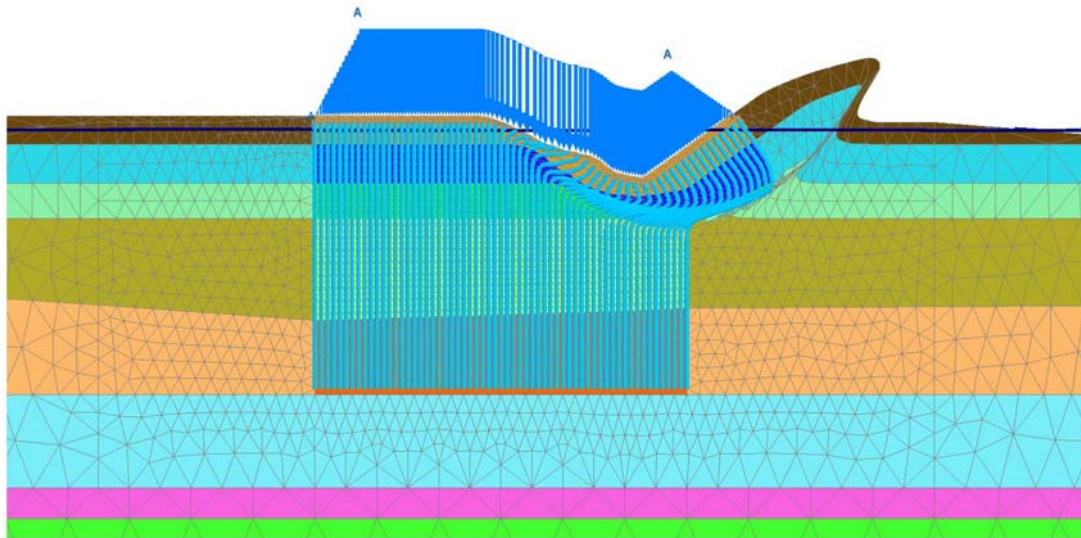
Figure 12: Failure mechanism after 6,7m fill construction

Table 2: Factors of safety

	Factor of Safety	
	Vacuum	**No vacuum - equivalent vacuum load**
Phase 5: After 2 m fill (81 days)	2.57	1.12
Phase 7: After 4 m fill (141 days)	2.07	1.16
Phase 9: After 6.7 m fill (181 days)	1.52	1.00
Phase 10: Final (290 days)	1.96	2.04

During the construction (at 81 days, 141 days and 181 days), the factor of safety obtained with the vacuum treatment active is considerably larger than the one obtained with an equivalent vacuum load representing a rough increase from 53% to 130%.

6.   CONCLUSIONS

The response of a soft clay deposit to vacuum consolidation has been discussed and investigated by finite element method (FEM) with practical application to a reclamation work project conducted in Vietnam. The capability of the finite element method to properly model vacuum consolidation has been clearly highlighted. More particularly it has been found that the developed FE model could show the following:

- Higher rate of effective stress increase as the applied vacuum pressure gets higher
- Vacuum pressure induced inward lateral displacement
- Increase of factor of safety when vacuum consolidation is active

REFERENCES

Barron, R.A. (1948), Consolidation of fine-grained soils by drain wells, Trans. ASCE No. 2346, pp. 718-754.

Biot, M.A. (1941). "General theory of three dimensional consolidation". Journal of Applied Physics, 12, 155-164.

Bishop, A.W. & Blight, A.K.G. (1963). "Some aspects of effective stress in saturated and partially saturated soils". Géotechnique, 13: 177-197.

Galavi, V. (2010), "Groundwater flow, fully coupled flow deformation and undrained analyses in PLAXIS 2D and 3D", Technical report, Plaxis BV, Delft, The Netherlands

PLAXIS 2D User's Manuals (2010), Edited by Brinkgreve, R.B.J., Swolfs W.M. and Engin, E., Plaxis BV, Delft, The Netherlands

Rixner, J.J., Kraemer, S.R., and Smith, A.D. (1986), Prefabricated vertical drains, Vol. 1 (Eng'g. Guidelines), Federal Highway Administration, Report No. FHWA-RD-86/168, Washington D.C.

Electro-osmotic Consolidation for Improvement of Geotechnical Engineering Properties of Tropical Peat

J.H.S. Yee, School of Engineering and Science, Curtin University, Malaysia, sharon.yee@student.curtin.edu.my
A.M.R.G. Athapaththu, School of Engineering and Science. Curtin University, Malaysia, athapaththu@curtin.edu.my
H.H. Lau, School of Engineering and Science, Curtin University, Malaysia, lau.hieng.ho@curtin.edu.my

ABSTRACT

Peat, which commonly shows high compressibility and weak shear strength properties, has drawn continuing interests among geotechnical researchers due to its problematic behaviour found in civil engineering projects. Though there have been some progress in solving problems in such materials found in Singapore, Indonesia, Netherlands, Ireland and some area of Canada etc., it is well known that the properties of peat differs from one area to another. As for the state of Sarawak in Malaysia, it was found that most of the major cities are located along the coast where peat made up about 13% of the overall state land area. In order to understand the behaviour of peat available locally, a series of laboratory experiments were carried out and their basic characterics were studied. It was found that most of the properties have significant variations with the same materials found in other countries. The research was extended to examine possible stabilization techniques available in the literature. In recent years, electro-osmotic consolidation is studied to examine its viability as a means of stabilization for peat and organic soft soils. To further understand electro-osmotic consolidation in peat, a series of laboratory model tests were carried out using commercially available prefabricated vertical drains as electrodes. In this paper, the geotechnical characterization of peat, the experimental set-up as well as the results of the tests conducted are presented. The tests were carried out to investigate the change in water content, void ratio, and settlement as well as changes in undrained shear strength due to electro-osmotic consolidation. Voltage distribution across the soil was measured to provide a better visualization of the effective area of electro-osmotic consolidation. It was found that with the application of electro-osmosis, water content of the peat was reduced while the shear strength increased up to 1400%. Settlement that occurred during electro-osmotic consolidation was at a faster rate when compared to self weight consolidation.

1. INTRODUCTION

Many of the civil engineering project works such as roads and buildings in many parts of the state of Sarawak experience post-construction settlement. The post-construction settlement can be in various degress from minor to major. Major post-construction settlement could be problematic as it involves continuous rectification works to maintain the functionability of the constructed works and safety of the users or occupants. Various methods of ground stabilization have been developed to overcome post-construction settlement. Some of the techniques are such as removal, replacement and surcharging with or without vertical drains. Post-construction settlement occurs in areas with soft soil, typically peat and organic soils in the populated coastal areas of the state. These soils are of high moisture content and low bearing capacity, making it poor foundation material for construction. Continuous research are carried out to provide better understanding and to develop a database for peat and other soft organic soils in Malaysia. Better understanding of basic physical and geomechanical properties would lead to properly treat and stablize soft soil so that post-construction settlement can be mitigated. Construction on peat without proper stabilization and treatment would lead to problems such as immediate settlement, long-term secondary compression (Duraisamy *et al.* 2007).

1.1. Electro-osmosis

Electrokinetic phenomena is a grouping of several different effects that can be observed in porous bodies filled with fluids under influence of external force (Acar & Alshawabkeh, 1993). For stabilization of soil, it is necessary to remove excess pore water in order for consolidation to occur. The electrokinetic phenomena of interest for this research would be electro-osmosis, which is defined as the movement of fliud under an applied electric field. Based on this effect, electrodes are used to apply direct current to saturate soil mass, creating a potential difference in the soil between anode and cathode. Positive ions in the soil would be attracted to the negative electrode. During their migration, the positive ions drag surrounding free water molecules along toward the cathode. At the cathode, the water can be collected

and removed from the system. When no water is added to the system, removal of the water results in consolidation in the soil mass. Flow rate of electro-osmosis generally is expressed as

$$Q_e = k_e i_e A \tag{1}$$

where ke is the coefficient of electro-osmotic permeability (m^2/Vs), ie is the applied voltage gradient (V/m) and A is the cross sectional area of flow (m^2).

Using the concept of electro-osmosis, studies were carried out on its application in terms of ground contaminant remediation (Yeung 2006), dewatering (Kalumba *et al.* 2009), geotechnical treatment of soils which includes increasing pile capacity and consolidation and strengthening of fine-grained soil (Micic *et al.* 2001). The electro-osmotic permeability for fine-grained soils is found to be up to four orders greater than hydraulic permeability (Glendinning *et al.* 2008). This is an advantage for consolidation in fine-grained soil as it would lead to shorter consolidation time. One of the reason for higher coefficient of permeability is that it is more dependent on applied voltage rather than geophysical property of the soil.

Various studies on electro-osmotic consolidation were carried out in parts of Europe, Canada and South East Asia. Extensive research have been done on strengthening of clay (Barker *et al.* 2004, Bergado *et al. 2003,* Bjerrum *et al.* 1967, Jeyakanthan *et al.* 2011, Rittirong *et al.* 2008). More recently, the feasibility of EO consolidation on peat is being considered. Initial laboratory tests carried out on Sarawak peat and organic soils have shown promising results on its application.

Over the years, different parameters that could govern electro-osmosis have been investigated. One of the factors would be the type of electrode used. Conventional electrodes such as copper is effective in terms of electric conductivity. However, with time, the acid front in the vicinity of the anode would corrode the electrode. When this occurs, the electrode-soil contact will be reduced and this in turn causes a decrease in the effective current applied to the soil. In order to overcome this problem, researchers have developed an electrode that is electrically conductive and yet corrosive resistant as well as chemically unreactive. To achieve this, a composite electrode was introduced, with electrically conductive geosynthetics (EKG) and other electrically conductive materials. (Hamir *et al.* 2001) compared conventional copper electrodes to EKG electrodes and found that the results were comparable with the added advantage of being less susceptible to corrosion.

This paper mainly presents the laboratory investigation of electro-osmotic consolidation on peat with respect to the effect of applied direct current. Different applied voltage gradient would result in different rate of electro-osmotic flow as well as differing degree of settlement and consolidation. One of the tests was maintained as self weight consolidation for the purpose of a control tank. Practicality and cost effectiveness of the application of the electro-osmotic consolidation in the field is directly related to the applied direct current. Other considerations for choosing electro-osmotic consolidation as a ground improvement technique are construction time, technical factors, targeted performance as well as safety considerations.

2.   EXPERIMENTAL METHODOLOGY

In general, the testing apparatus was designed with the considerations for measurement of drained water volume, soil sample deformation, applied voltage and current. For application of voltage, a benchtop direct current (DC) power supply is required. The testing tank is to be of a material that is non-conductive.

2.1   Peat Specimen

Peat used for the experiment was collected from Similajau, North Sarawak, Malaysia. Table 1 shows results of the geotechnical characterization tests carried out on the collected soil.

Table 1: Geotechnical properties of peat

Properties	Peat
Natural water content, w_n (%)	643
Organic content, N (%)	96
Atterberg limits (%)	
Liquid limit, w_l	323
Plastic limit, w_p	244
Plasticity index, PI	79

2.2   Experimental Set Up

The experimental set up was designed with considerations for direct current (DC) power supply for constrant voltage, drainage, settlement, voltage and current measurement. Initially the drained water was allowed to freely drain from drainage holes allowed for near the base at each end of the tank. Later as the tests progressed, a drainage well was included to collect the drained water. This was done to simulate field conditions where bottom drainage may not be always possible A vacuum extraction jar was used to remove collected water from the drainage well. Suction pressure was controlled so that only sufficient pressure was applied to extract the water without exerting extra pressure on the soil sample, similar to a submersible pump. A benchtop DC power supply was used to provide direct current for the experimental set up.

The test tank is constructed of glass with inner dimensions of L:B:H = 250:110:250mm. In tests with free bottom drainage, a 6mm diameter hole was provided near the base of the tank and drained water was collected in measuring cups. Commercially available electical vertical drains (EVD) were used as electrodes. The EVD is of a similar concept to the prefabricated vertical drains with the added ability to conduct electricity via its copper-polymer sandwich core. For the purpose of the experiment and in proportion to the test tank, strips of 15mm wide strips of EVD were used instead of the full 110mm width. The 2anodes-1cathode configuration used during the experiments was to simulate three dimensional flow withint the test bed. Figure 1 shows the layout plan for test with bottom.
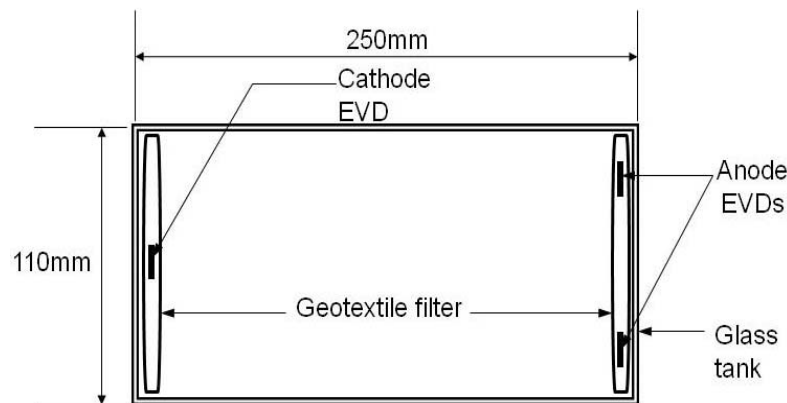
Figure 1: Plan of experimental tank with bottom drainage

Figure 2 shows the slight change in layout of the experimental tank. For tests carried out at a later stage, the drainage holes were sealed and a drainage well was included instead. The drainage well was formed using perforated 20mm outer diameter PVC pipe encased in filter geotextile. The drainage well was placed near the cathode for the collection of water as during electroosmosis, water travel toward the cathode. Both sets of tests were carried out under the cathode opened-anode closed conditions, where water was allowed to drain from the cathode and no water was added at the anode.
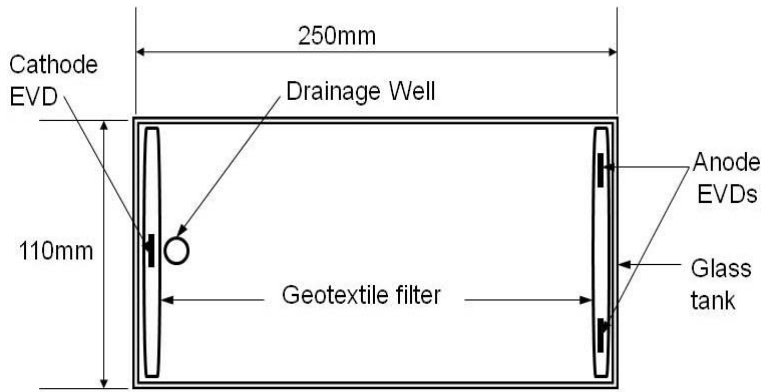
Figure 2: Experimental tank layout

The tanks were gradually filled with peat in thin layers and each layer was carefully tamped to remove any trapped air. This was done until a total thickness of approximately 200mm was achieved. For each of the filled tanks, initial moisture content was obtained. Laboratory vane shear tests were carried out on top of the test bed at two separate locations. To aid settlement measurements, discrete 10mm square glass plates were placed along the lenght of the test bed as surface settlement markers. Settlement measurements were taken at 24-hour intervals using a digital vernier calliper. For the second set of test, measurements of voltage along the soil bed and current was also measured. This was not done in the first set as the experiment was still in a preliminary stage and no provisions were made for voltage and current measurement.

The test tanks were prepared a day before application of direct current. In the case of bottom drainage, the drainage tubes at the bottom of the tank were kept closed during preparation until the start of the experiment. However, with the open drainage well in the second set of test, due to self weight, water began to collect in the well after preparation and before application of direct current. Before the start of the experiment, the water in the drainage well was collected and measured.

For the set of test with bottom drainage, three different DC voltages was applied, namely 100V/m, 120V/m and 140V/m for a period of 8 days. The test was stopped when the water drained out was too little to be measured after 12 hours from the previous reading. In the second set of test with drainage well, a comparison between self weight consolidation, EO consolidation at constant 80V/m and incremental voltage was carried out. In the incremental test tank, 10V/m was applied at the start of the experiment with 10V increment at 24-hour intervals, ending with 80V/m. Removal of water from the drainage well was done at 3-hour intervals during the day. The experimental tanks were covered to prevent evaporation.

At the end of the electro-osmotic consolidation tests, 3 laboratory vane shear tests were carried out at the top of the test bed. After that, soil extraction was done using Shelby tubes to obtain samples for determintation of shear strength at the bottom of the test bed. Upon completion of the laboratory vane shear tests, the peat in the Shelby tubes was extruded and divided into sections for determination of water content along the height of the soil bed.

3.   EXPERIMENTAL RESULTS

Results of the electro-osmotic consolidation test tanks in comparison to the self weight consolidation tank showed distinct differences in terms of settlement, changes in water content as well as shear strength. There is marked reduction of water content and strength gain in the peat after 8 days of electro-osmotic consolidation even when the applied voltage varied.

3.1   Settlement

Figure 3 shows the settlement measured at the centre of the test bed for the first set of test. With applied DC voltage, settlement can be seen as early as Day 1 onward. With the increase in applied voltage, there is also an increase in the rate of settlement. However, the effects of the increment are not as noticeable when the applied voltage was 140V/m as it more or less reflects the settlement at 120V/m.
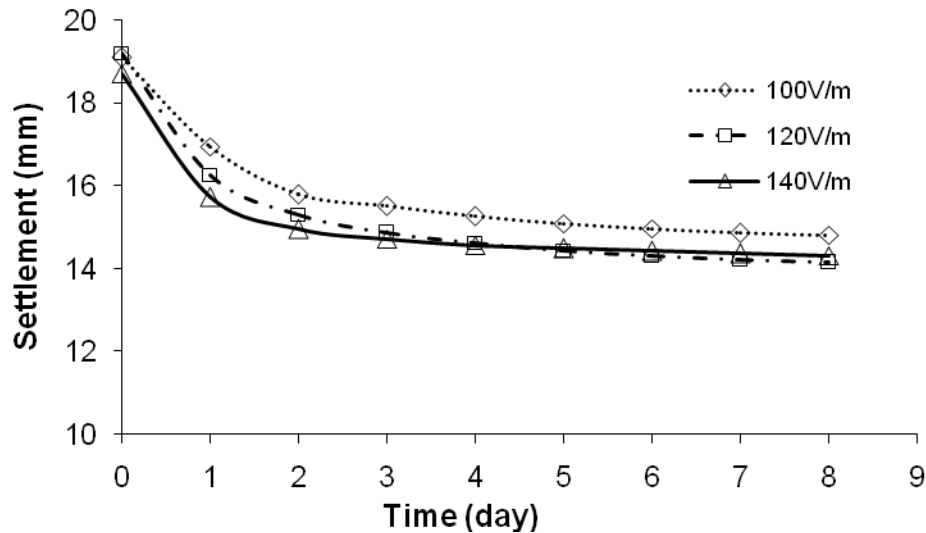
Figure 3: Settlement profile at centre of test tank for tests with bottom drainage

In Figure 4, it can be seen that under self weight condition, there was hardly any consolidation. Application of a fixed 80V/m direct current produced a trend similar to that shown in Figure 3. When incremental voltage was applied during electro-osmotic consolidation, the settlement occurred at a slower rate but toward the end of the experiment, magnitude of the settlement approximately matches the fixed voltage test tank.
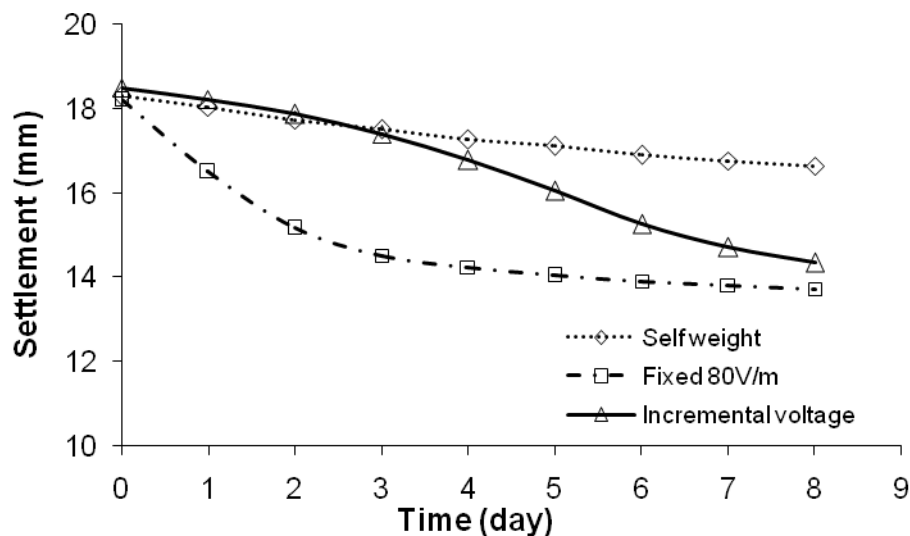
Figure 4: Settlement profile at centre of test tank for tests with drainage well

By comparing the settlement profile at the end of the tests, it clearly indicates that electro-osmotic consolidation induced a faster settlement rate. Ratio of the settlement, calculated as the percentage of change in the soil profile gives a range of 22% to 26% for settlement in electro-osmotic consolidation tanks at the end of 8 days. For the same period with self weight consolidation, the percentage of settlement at 8 days was 9%.

3.2   Changes in water content

Total volume of drained water over the period of 8 days is as tabulated in Table 2 below. Generally, in the test with electro-osmotic consolidation, the amount of water collected within Days 1 to 3 make up the bulk of the total volume. This is clearly illustrated in Figure 5, showing the amount of water collected during the testing period. However, in the case of incremental applied voltage, with the low initial applied voltage, the electro-osmotic flow will also be lower as expected. As the test progressed, the amount of water collected increased with the increase in applied direct current. Toward the end of the experiment, as

the water content in the peat had gradually reduced, the amount of water collected also decreased despite the increase in applied voltage.

Table 2: Changes in water content of peat

Test	Average initial water content, $w_{i\text{-}av}$ (%)	Average final water content, $w_{f\text{-}av}$ (%)	Total volume of water drained (ml)	Water removal efficiency (%)
Fixed 100V/m	555	397	1337	28
Fixed 120V/m	552	391	1590	29
Fixed 140V/m	554	417	1454	25
Self weight	663	610	334	8
Fixed 80V/m	654	473	1330	27
Incremental V	628	463	1138	26

The volume of water measured at 24 hours after the start of the experiment ranged from 58ml to 940ml for the electro-osmotic consolidation tanks. From the self weight consolidation tank, 51ml of water was collected. By 48 hours, volume of water collected from the electro-osmotic consolidation tanks increased to a range between 135ml to 1175ml. For the same period of time, water drained from the self weight consolidation tank was 99ml. Due to the inital low applied voltage, the incremental voltage tank showed lower volume of drained water as expected. However, the rest of the electro-osmotic tanks, water drained in a much larger volume when compared to self weight consolidation.
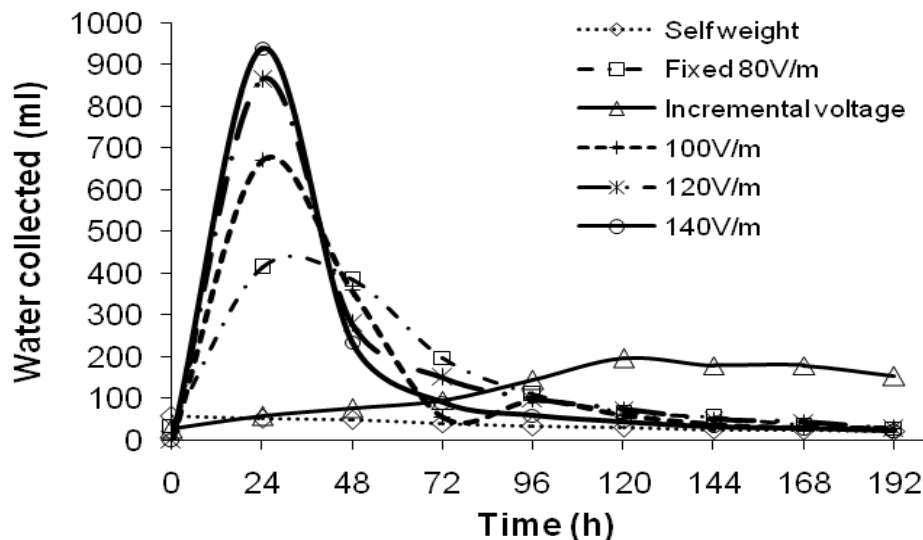
Figure 5: Volume of water collected

As there were some differences in the average inital water content between the two sets of experiments, water removal efficiency was used to compare the removal of water. This was calculated as the percentage of water content reduction (Yuan & Weng 2003). Range of water removal efficiency with electro-osmotic consolidation falls within 26% to 29% which is at least three times greater than self weight consolidation. A common observation in electro-osmotic consolidation tests is that the area in the vicinity of the anode will undergo greater reduction in water content as water flows from the anode towards the cathode.

3.3   Changes in Shear Strength

Laboratory vane shear tests were carried out at top of the peat bed after preparation of the experimental tanks. They showed initial undrained strength, S_{ui}, ranging between 0.92kPa to 1.32kPa. At the end of each test, vane shear strength tests were carried out at 7cm, 12.5cm and 18cm away from the cathode. The post electro-osmotic consolidation undrained shear strength showed a great improvement especially in the vicinity of the anode. This corresponded to the relatively lower water content of the same area. The post consolidation shear strength reached 43kPa at the anode in the test with applied 120V/m direct current. In the second set of test with drainage well, the problem with trapped water was sometimes encountered. This occured when the sample shrank away from the side of the test tank as water was gradually removed.

As free drainage from the bottom of the tank was not allowed, there is a tendency for water to fill the voids that formed in the sample. This occurance and the lower applied voltage accounted for the lower strength gain in the test tanks with drainage well, namely the fixed 80V/m and incremental voltage tests.
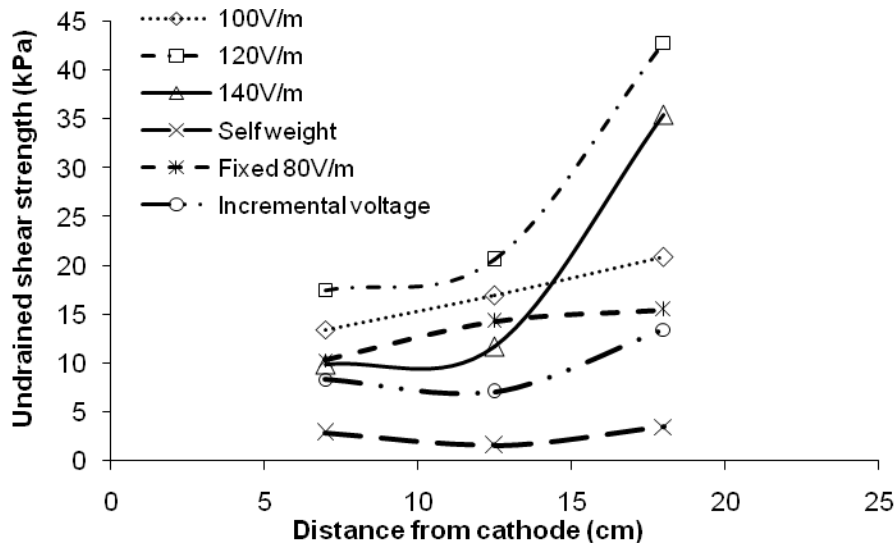
Figure 6: Post consolidation undrained shear strength, S_{uf}, at top of test bed

To investigate the reach of the electro-osmotic consolidation, laboratory vane shear tests were carried out on peat samples from bottom of the soil bed extracted using Shelby tubes. Post electro-osmotic consolidation undrained shear strength at the bottom of the peat bed shows similar trend to the top of the peat bed. Although the strength gain at the bottom of the peat bed is less than strength gain at the top, it still showed considerable strength gain. Figure 7 shows a relatively consistent strength gain at the bottom of the test bed in all of the different tests, in spite of the different applied voltage gradient.
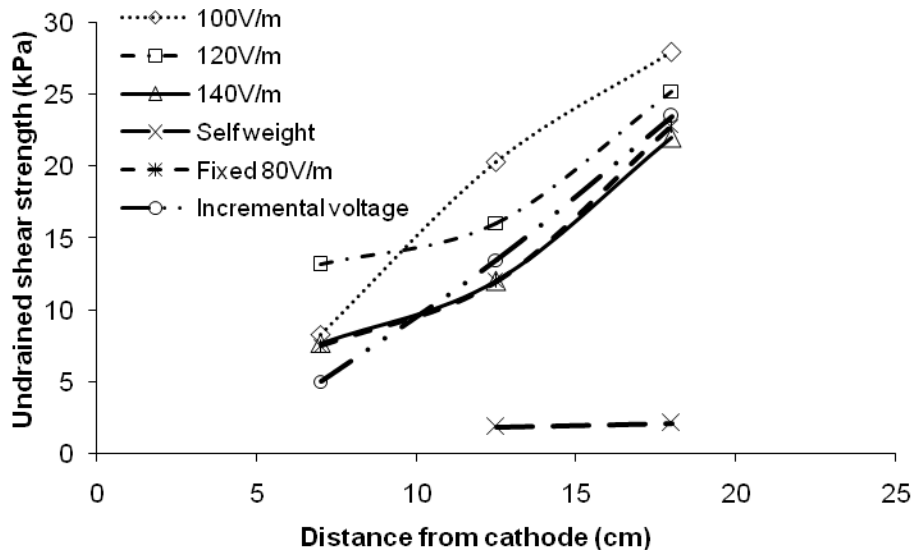
Figure 7: Post consolidation undrained shear strength, S_{uf}, at bottom of test bed

3.4 Other observations – Voltage and Current

In order to gauge the actual voltage applied along the length of the peat bed, measurements were taken from four different locations. Both Figures 8 and 9 show a drop in voltage almost immediately in the vicinity of the anode. The drop continued in a more gradual manner toward the direction of the cathode. This is known as the loss at electrode-soil contact. This phenomena was studied by Lefebvre and Burnotte (2002), where it was found that the power loss at the anode resulted in lower effective gradient transferred to the soil. Certain measures can be taken to control power loss, such as chemical treatment of the area in the vicinity of the anode using injection of saline solution.
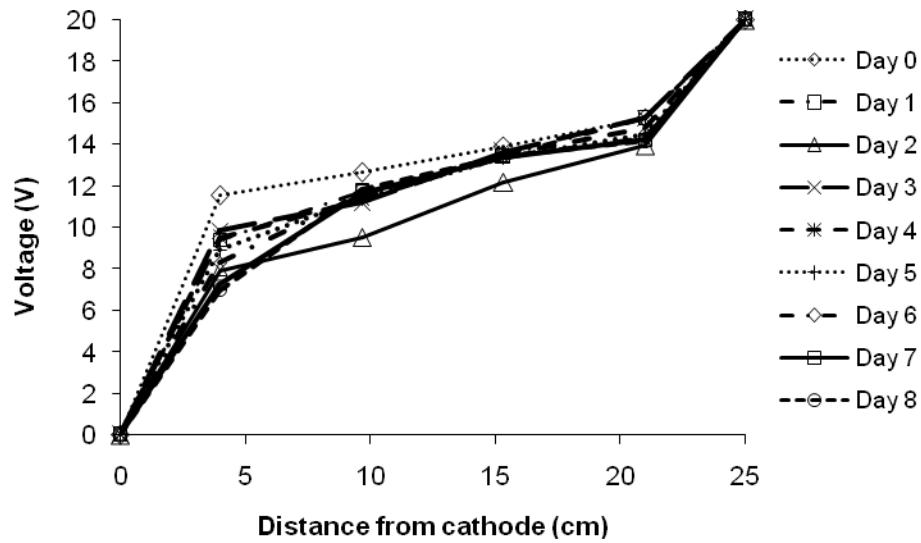
Figure 8: Voltage along test bed for test with incremental voltage gradient
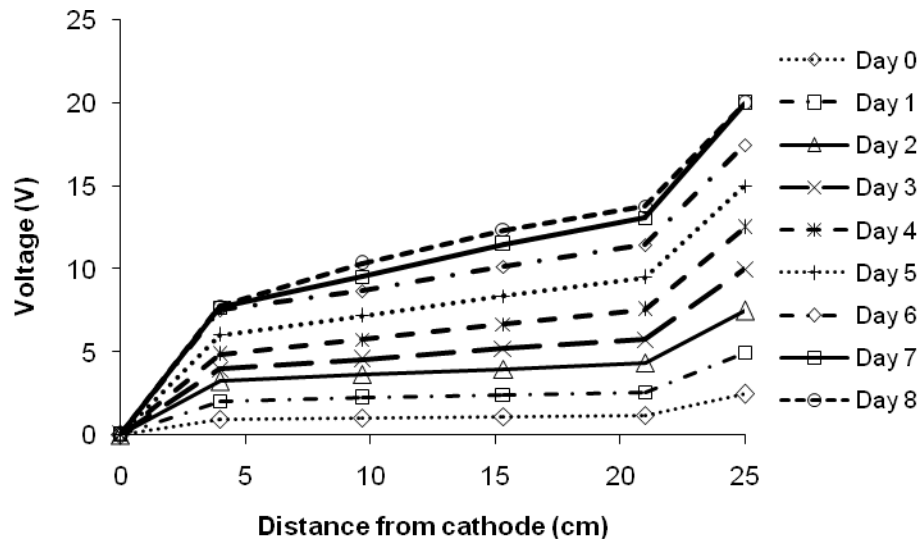
Figure 9: Voltage along test bed for test with incremental voltage gradient

Table 3: Measured current

	Fixed 80V/m	**Incremental Voltage**
Day 0	21.7 mA	1.3 mA
Day 1	32.0 mA	N/A
Day 2	26.0 mA	6.0 mA
Day 3	22.0 mA	9.5 mA
Day 4	19.0 mA	14.0 mA
Day 5	18.5 mA	17.0 mA
Day 6	16.0 mA	17.0 mA
Day 7	15.0 mA	16.0 mA
Day 8	13.0 mA	15.5 mA

The current measured for fixed 80V/m test tank is in agreement with gradual decrease in the effective voltage transmitted and increased soil resistivity. This in turn also decreases the current passing through the soil bed. This trend is not seen in the early stages of the incremental voltage test. As expected, with

the increase in applied voltage, the current would also increase. However, toward the end of the test period, even though the voltage applied was increased, the current did not increase.

4. CONCLUSION

Due to the movement of water from anode toward the cathode during electro-osmosis, the highest reduction in water is found near the anode. Higher applied voltage induced higher rate of electro-osmotic flow, greater water reduction and strength gain. However, no significant difference is seen between the applied 120V/m and 140V/m experimental results in terms of settlement or volume of water drained. Therefore, a limitation to the applied voltage should be considered, in terms of practicality, cost and safety. In terms of strength gain, with the reduction of water content, naturally the peat will consolidation and gain strength. The greatest improvement is seen near the anode and this directly reflected the greatest reduction in water content. By gradually increasing the applied voltage during electro-osmotic consolidation, the occurance of trapped water in the test tank with drainage well is reduced. Application of incremental voltage can be further investigated as it could contribute to lowering power consumption during electro-osmotic consolidation.

5. ACKNOWLEDGEMENT

REFERENCES

Acar, Y.B. and Alshawabkeh A.N., 1993, Principles of Electrokinetic Remediation, Environmental Science Technology, Vol. 27, No. 13, 2638-2647

Barker, J.E., Rogers, C.D.F., Boardman, D.I. and Peterson, J., 2004, Electrokinetic Stabilisation: an overview and case study, Ground Improvement, Vol. 8, No. 2, 47-58

Bergado, D.T., Sasanakul, I. and Horpibulsuk, S., 2003, Electro-Osmotic Consolidation of Soft Bangkok Clay using Copper and Carbon Electrodes with PVD, Geotechnical Testing Journal, Vol. 26, No. 3, 1-12

Bjerrum, L., Moum, J. and Eide, O., 1967, Application of Electro-osmosis to a Foundation Problem in a Norwegian Quick Clay, Geotechnique, Vol. 17, 214-235

Duraisamy, Y., Huat, B.B.K. and Aziz, A.A., 2007, Methods of Utilizing Tropical Peat Land for Housing Scheme, American Journal of Environmental Sciences, Vol. 3, No. 4, 258-263

Glendinning, S., Lamont-Black, J., Jones, C.J.F.P. and Hall, J., 2008, Treatment of lagooned sewage sludge in situ using electrokinetic geosynthetics. Geosynthetics International, Vol. 15, No. 3, 192-204

Hamir, R.B., Jones, C.J.F.P. and Clarke, B.G., 2001, Electrically conductive geosynthetics for consolidation and reinforced soil, Geotextiles and Geomembranes, Vol. 19, 455-482

Jeyakanthan, V., Gnanendran, C.T. and Lo, S.-C.R., 2011, Laboratory assessment of electro-osmotic stabilization of soft clay, Canadian Geotechnical Journal, Vol. 48, 1788-1802

Kalumba, D., Glendinning, S., Rogers, C.D.F., Tyrer, M. and Boardman, D.I., 2009, Dewatering of Tunneling Slurry Waste Using Electrokinetic Geosynthetics, Journal of Environmental Engineering, Vol. 135, No. 11, 1227-1236

Lefebvre, G. and Burnotte, F., 2002, Improvements of electroosmotic consolidation of soft clays by minimizing power loss at electrodes, Canadian Geotechnical Journal, Vol. 39, 399-408

Micic, S., Shang, J.Q. and Lo, K.Y., 2001, Electrokinetic Strengthening of Marine Clay Adjacent to Offshore Foundations, Proceedings of the Eleventh (2001) International Offshore and Polar Engineering Conference, Stavanger, Norway, June 17-22, 694-701

Rittirong, A., Douglas, R.S., Shang, J.Q. and Lee, E.C., 2008, Electrokinetic improvement of soft clay using electrical vertical drains, Geosynthetics International, Vol. 15, No. 5, 369-381

Yeung, A.T., 2006, Fundamental aspects of prolonged electrokinetic flows in kaolinites, Geomechanics and Geoengineering: An International Journal, Vol. 1, No. 1, 13-25

Yuan, C. and Weng, C.H., 2003, Sludge dewatering by electrokinetic technique: effect of processing time and potential gradient, Advances in Environmental Research, 7, 727-732

Multi-dimensional electro-osmosis consolidation of clays

J.Yuan, Delft University of Technology, Delft, The Netherlands, j.yuan-1@tudelft.nl
M.A.Hicks, Delft University of Technology, Delft, The Netherlands, m.a.hicks@tudelft.nl
J.Dijkstra, Delft University of Technology, Delft, The Netherlands, j.dijkstra@tudelft.nl

ABSTRACT

Electro-osmosis consolidation is an innovative and effective ground improvement method for soft clays. But electro-osmosis is also a very complicated process, as the mechanical behaviour, and hydraulic and electrical properties of the soil are changing rapidly during the treatment process; this makes electro-osmosis hard to describe and simulate. Traditional electro-osmosis consolidation theory cannot provide a satisfactory solution, because it does not directly consider the mechanical behaviour of the soil and the coupling between the soil deformation, electro-osmosis flow and pore pressure. A numerical model for the electro-osmosis consolidation of clay in multi-dimensional domains is presented, with the coupling of the soil mechanical behaviour, pore water transport and electrical fields being considered. Three fully coupled governing equations considering force equilibrium, pore water transport and electrical distribution are presented and solved using COMSOL. The model is verified against the well-known classical analytical solution for electro-osmosis consolidation. A two-dimensional numerical model is then simulated to investigate the settlement and excess pore pressure profile during the electro-osmosis consolidation process. It is found that the peak excess pore pressure is developed near the bottom of the anode and that the maximum settlement is developed near the top of the anode. Moreover, excess pore pressures and settlements develop very rapidly at the beginning of the electro-osmosis treatment, but then become slower with time.

1.   INTRODUCTION

A wide variety of ground improvement methods have been developed for economic foundation solutions on soft soils (for a state-of-the-art, see Chu et al. [1] and cited references). An alternative method, however, is the use of electro-osmosis. Electro-osmosis is important for many geo-engineering applications, such as improving friction pile capacity (Milligan [2]), the strengthening and stabilization of soft clays (Casagrande [3]; Lo et al. [4]; Burnotte et al. [5]), controlling the pore water at excavation sites (Bjerrum et al. [6]) and dewatering of mine tailings (Sprute and Kelsh [7]; Sprute et al. [8]; Lockhart [9]; Fourie et al. [10]). Consolidation in clays due to applying an electric current may occur as the result of two distinct mechanisms; the osmosis under electric gradients will cause fluid flow from anodes to cathodes resulting in pore pressure changes and a consequential increase in effective stress in the clay; a less important effect is the hardening of the soil due to the generation of heat and electro-chemical reactions during the process. Electro-osmosis consolidation is a coupling process involving mechanical behaviour, hydraulic flow and electrical flow.

The theory of one dimensional electro-osmosis consolidation was first developed by Esrig [11]. Based on Esrig's equation, Wan and Mitchell [12] presented an analytical solution for one dimensional preloading and electro-osmosis consolidation. Feldkamp and Belhomme [13] later provided a large-deformation one dimensional electro-osmosis consolidation model. A two dimensional finite-element solution was given by Lewis and Garner [14], who considered the coupling effect of the electric and hydraulic gradients. Shang [15] developed a two dimensional analytical model combining preloading and electro-osmosis consolidation of clay soils. Iwata and Jami [16] presented a numerical model to simulate the combined electro-osmosis dewatering and mechanical response using the Terzaghi-Voigt combined model to consider creep deformation. However, none of the models cited above directly consider the mechanical behaviour of soil or the full multi-physical coupling that occurs during the electro-osmosis consolidation process.

In this study, a numerical model for the electro-osmosis consolidation of clay in multi-dimensional domains is developed. Three fully coupled governing equations considering force equilibrium, pore water transport and electrical current flow are presented and solved using COMSOL. The proposed approach is verified via comparison with the analytical solution developed by Esrig [11]. The results of pore pressure changes for the two cases are compared. Finally, a two-dimensional numerical model is simulated to investigate the settlements and excess pore pressure profile during the electro-osmosis consolidation process.

2. THEORETICAL AND NUMERICAL FORMULATION

In this paper, an isotropic saturated soil with incompressible pore liquid and soil particles is considered. The governing equations for the electric potential and hydraulic head are derived based on the following assumptions: the current due to electrophoresis of the fine grained particles is negligible [11]; the flow of fluid due to the electrical and a hydraulic gradients may be superimposed to obtain the total flow [11]; Ohm's law is valid; Darcy's lay is valid; the electrical gradient caused by movement of ions is negligible compared to applied electrical field.

2.1. Mechanical equilibrium and stress-strain constitutive relationship

The stress equilibrium equation, for small deformations, can be expressed by

$$\mathbf{A}^T \boldsymbol{\sigma} + \mathbf{f} = \mathbf{0} \tag{1}$$

where **A** contains the spatial derivatives:

$$\mathbf{A} = \begin{bmatrix} \dfrac{\partial}{\partial x} & 0 & 0 & \dfrac{\partial}{\partial y} & 0 & \dfrac{\partial}{\partial z} \\ 0 & \dfrac{\partial}{\partial y} & 0 & \dfrac{\partial}{\partial x} & \dfrac{\partial}{\partial z} & 0 \\ 0 & 0 & \dfrac{\partial}{\partial z} & 0 & \dfrac{\partial}{\partial y} & \dfrac{\partial}{\partial x} \end{bmatrix}^T \tag{2}$$

and $\boldsymbol{\sigma}$ represents the total stress vector:

$$\boldsymbol{\sigma} = \begin{bmatrix} \sigma_x & \sigma_y & \sigma_z & \tau_{xy} & \tau_{yz} & \tau_{zx} \end{bmatrix}^T \tag{3}$$

and **f** represents the vector of body forces:

$$\mathbf{f} = \begin{bmatrix} F_x & F_y & F_z \end{bmatrix}^T \tag{4}$$

where F_x, F_y and F_z are the body forces in the x, y and z directions, respectively. According to the principle of effective stress, the total stress can be written as:

$$\boldsymbol{\sigma} = \boldsymbol{\sigma}' + \mathbf{m}p \tag{5}$$

where $\boldsymbol{\sigma}'$ and p are the effective stress vector and pore pressure, repetitively, and

$$\mathbf{m} = \begin{bmatrix} 1 & 1 & 1 & 0 & 0 & 0 \end{bmatrix}^T \tag{6}$$

The strain-displacement relationship can be written as:

$$\boldsymbol{\varepsilon} = \mathbf{A}\mathbf{u} \tag{7}$$

where $\boldsymbol{\varepsilon}$ is the total strain vector:

$$\boldsymbol{\varepsilon} = \begin{bmatrix} \varepsilon_x & \varepsilon_y & \varepsilon_y & \gamma_{xy} & \gamma_{yz} & \gamma_{zx} \end{bmatrix}^T \tag{8}$$

and **u** is the displacement vector:

$$\mathbf{u} = \begin{bmatrix} u & v & w \end{bmatrix}^T \tag{9}$$

where u, v and w are the displacements in the x, y and z directions, respectively.
The elastic constitutive relationship for soil is:

$$\boldsymbol{\sigma}' = \mathbf{D}\boldsymbol{\varepsilon} \tag{10}$$

where the elastic stress-strain matrix **D** is given by:

$$\mathbf{D} = \frac{E(1-\nu)}{(1+\nu)(1-2\nu)} \begin{bmatrix} 1 & \dfrac{\nu}{1-\nu} & \dfrac{\nu}{1-\nu} & 0 & 0 & 0 \\[2mm] \dfrac{\nu}{1-\nu} & 1 & \dfrac{\nu}{1-\nu} & 0 & 0 & 0 \\[2mm] \dfrac{\nu}{1-\nu} & \dfrac{\nu}{1-\nu} & 1 & 0 & 0 & 0 \\[2mm] 0 & 0 & 0 & \dfrac{1-2\nu}{2(1-\nu)} & 0 & 0 \\[2mm] 0 & 0 & 0 & 0 & \dfrac{1-2\nu}{2(1-\nu)} & 0 \\[2mm] 0 & 0 & 0 & 0 & 0 & \dfrac{1-2\nu}{2(1-\nu)} \end{bmatrix} \tag{11}$$

where E and ν are the elastic modulus and Poisson's ratio, respectively.

Hence, by substituting eq.(2)-eq.(11) into eq.(1) the mechanical equilibrium governing equation can be expressed by

$$\mathbf{A}^{\mathrm{T}}\mathbf{D}\mathbf{A}\mathbf{u} + \mathbf{A}^{\mathrm{T}}\mathbf{m}p + \mathbf{f} = \mathbf{0} \tag{12}$$

2.2. Pore water transport

The mass conservation of the pore water can be expressed by:

$$\frac{\partial n}{\partial t} + \nabla \cdot \mathbf{v} = 0 \tag{13}$$

where n is the porosity of the soil, t is time and $\mathbf{v}$ is the velocity of the pore water in the soil, which comprises two components. One is the hydraulic flow caused by the gradients of pore water pressure and the other is the electro-osmosis flow caused by electrical potential gradients. From Darcy's law the hydraulic flow can be expressed as:

$$\mathbf{v}_w = -\frac{k_w}{\gamma_w}\nabla\left(p + \gamma_w z\right) \tag{14}$$

where k_w, γ_w and z are the coefficient of hydraulic conductivity, the unit weight of water and the elevation, respectively.

The fluid flux due to electro-osmosis is [17]

$$\mathbf{v}_{eo} = -k_{eo}\nabla V \tag{15}$$

where k_{eo} is the coefficient of electro-osmosis conductivity and V is the electrical potential.

According to Esrig's assumption, these two independent flows can be combined to give the total flow:

$$\mathbf{v} = -\frac{k_w}{\gamma_w}\nabla\left(p + \gamma_w z\right) - k_{eo}\nabla V \tag{16}$$

Because the soil is saturated and incompressible, the change of porosity can be expressed in terms of the deformation as

$$\frac{\partial n}{\partial t} = \mathbf{m}^T \frac{\partial \varepsilon}{\partial t} = \mathbf{m}^T \mathbf{A}\frac{\partial \mathbf{u}}{\partial t} \tag{17}$$

Consequently, the equation of pore water mass conservation can be written in the following form by substituting eq.(16) and eq.(17) into eq.(13):

$$\mathbf{m}^T \mathbf{A}\frac{\partial \mathbf{u}}{\partial t} + \nabla \cdot \left(-\frac{k_w}{\gamma_w}\nabla\left(p + \gamma_w z\right)\right) + \nabla \cdot \left(-k_{eo}\nabla V\right) = 0 \tag{18}$$

2.3. Electrical transport

According to Ohm's law, the electrical current flow can be expressed by:

$$I = -\sigma_e \nabla V \tag{19}$$

where I is the electrical current and σ_e is the electrical conductivity of the soil.

By applying the conservation of charge and assuming the current is steady state:

$$-\nabla \cdot I + R_e = 0 \tag{20}$$

where R_e is the current source.

Substituting eq.(19) into eq.(20) gives;

$$\nabla \cdot (\sigma_e \nabla V) + R_e = 0 \tag{21}$$

2.4.   Final governing equations

The primary variables, that is, displacements, pore pressure and electrical potential, are coupled through the governing equations for mechanical equilibrium, pore water transport and electrical current transport, i.e. eqs. (12), (18) and (21) respectively. These governing equations are solved using the COMSOL Multiphysics PDE interface.

3.   VERIFICATION AND INVESTIGATION

The proposed approach is here verified against the well-known classical 1D analytical solution of electro-osmosis consolidation. Then two dimensional electro-osmosis consolidation is investigated using the proposed approach.

3.1.   1D Verification

Esrig [11] developed a one dimensional electro-osmosis consolidation theory, in which the governing equation can be expressed as

$$\frac{k_w}{\gamma_w} \frac{\partial^2 p}{\partial x^2} + k_{eo} \frac{\partial^2 V}{\partial x^2} = m_v \frac{\partial p}{\partial t} \tag{22}$$

where m_v is the coefficient of compressibility.

The analytical solution of above equation can be obtained through the method of variable separation and Laplace transform [18]:

$$p(x,t) = -\frac{k_{eo}}{k_w} \cdot \gamma_w \cdot V(x) + \frac{2k_{eo} \cdot \gamma_w \cdot V}{k_w \pi} \cdot \sum_{n=0}^{\infty} \frac{(-1)^n}{m^2} \sin \sin\left(\frac{m\pi x}{L}\right) \cdot \exp(-m^2 \pi^2 T) \tag{23}$$

where $m=n+1/2$, $T = k_w \cdot t / m_v \cdot L^2$ is the time factor, and L is the distance between the anode and cathode.

Furthermore, the maximum negative excess pore pressure developed at the anode is given by [19]

$$p_{\max} = -\frac{k_{eo}}{k_w} \cdot \gamma_w \cdot V \tag{24}$$

The one dimensional model is shown in Fig. 1 and is considered to be originally 1.0m thick. The material parameters are listed in Table 1 and are typical for a soft clay. These have been used for Esrig's solution and for the finite element analysis using COMSOL. For the latter, a two dimensional plane strain FEM model has been used, but with suitable boundary conditions to impose the one dimensional condition. 3-node triangular elements and a linear solver are used in this study.

Table 1: Material parameters

Variable	Physical meaning	Unit	Value
k_w	Hydraulic conductivity	m/s	2.0E-09
k_{eo}	Electro-osmosis conductivity	$m^2/V \cdot s$	2.0E-09
m_v	Coefficient of compressibility	1/Pa	1.0E-06
γ_w	Unit weight of pore water	kN/m^3	9.8E+03
E	Young's modulus	Pa	7.4E+05
ν	Poisson's ratio	-	0.3
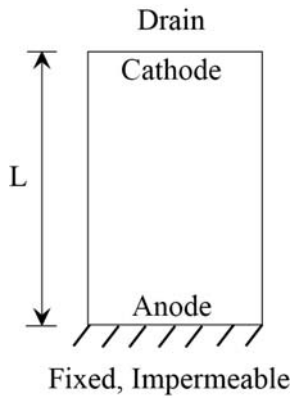
Figure 1: 1D electro-osmosis consolidation   *Figure 2: Excess pore pressure profile at anode*
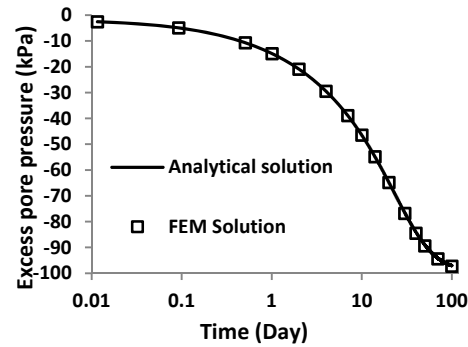
The initial excess pore pressure is set to zero throughout the problem domain. The cathode is the top boundary and is free draining, whereas the anode is the bottom boundary and is fixed and impermeable, as seen in Fig.1. The electrical potential is maintained at 10 volts at the anode. The left and right boundaries are impermeable with respect to both pore pressure and electrical potential, to ensure one-dimensionality. The simulation time is 100 days.

According to eq.(24), the maximum negative excess pore pressure developed at the anode will be -98.1 kPa. Fig. 2 shows the evolution of pore pressure with time at the anode due to electro-osmosis. The negative pore pressure develops rapidly at the beginning and reaches the maximum value at around day 100. An excellent correlation is found between the results of the proposed approach and Esrig's theoretical solution. This demonstrates that the proposed approach is able to correctly consider the coupling behaviour in 1D electro-osmosis consolidation.

3.2.   2D Investigation

A two dimensional electro-osmosis consolidation model has also been investigated using the proposed approach. The impact of the electro-osmosis consolidation is assessed by analysing the excess pore pressures and settlements.

A square domain of side length 1m is presented in Fig.3. In order to investigate the coupling behaviour in the soil, a surcharge load is applied on the top surface. The boundary conditions employed are as follows: the anode is along the left edge, which is set as impermeable and on rollers; the right edge is the cathode, and is free draining and on rollers; the bottom boundary is impermeable and fixed; the top surface is free draining and a uniform surcharge pressure, q=100 kPa, is applied. An electrical potential of 10 V is applied at the anode, and the initial conditions and material parameters are the same as for the previous one dimensional analysis, besides the use of a Yong's modules of E=1000 kPa.

The excess pore pressure profiles at day 0, day 10 and day 100 are shown in Fig. 4, in which automatic scaling has been used for the contours. At the start of the analysis, at day 0, the postive pore pressure developed is around 98.8 kPa because of the surcharge loading. As time progresses there are two evolution processes: the positive pore pressure reduces due to the free draining boundaries; at the same
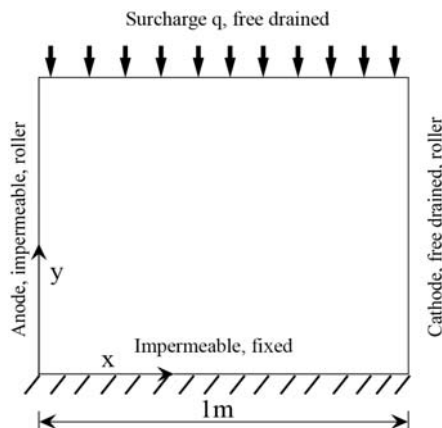
Figure 3: 2D Electro-osmosis consolidation model
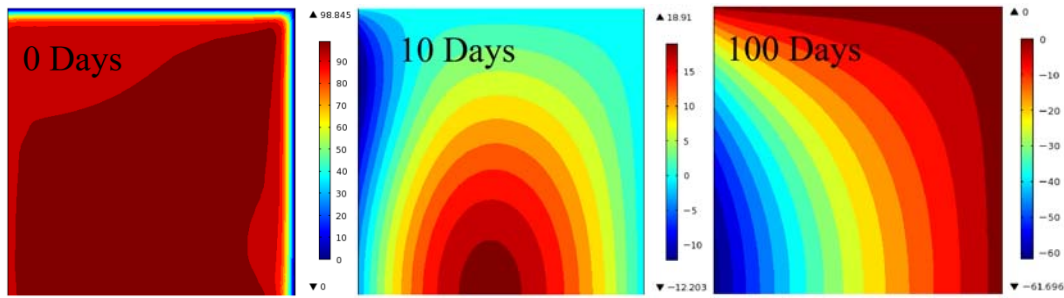
Figure 4: Excess pore pressure profiles at day 0, 10 and 100
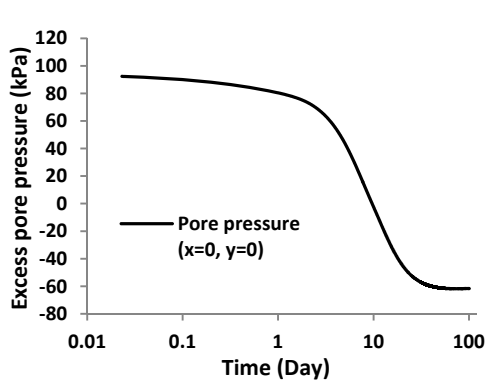
Figure 5: Excess pore pressure-time relationship
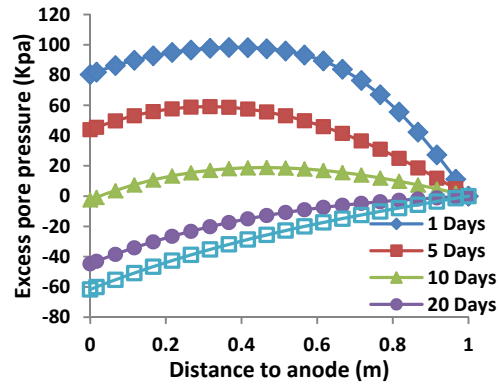
Figure 6: Excess pore pressure profiles along bottom boundary

time negative pore pressures develop at the anode caused by the electro-osmosis. At day 10, the maximum negative pore pressure of -12.2 kPa has developed near the top of the anode, whereas the largest postive pore pressure of 18.9 kPa is near the middle of bottom boundary. At day 100 the time dependent system reaches the steady state, with a maximum negative pore pressure of -61.7 kPa having been developed near the bottom of anode.

Fig. 5 shows the excess pore pressure–time relationship at the bottom of the anode ($x=0$, $y=0$ m). In the early stages of the analysis, the electro-osmosis dominates the pore water flow and the negative excess pore pressures grow rapidly near the anode. As the negative excess pore pressures increase, the hydraulic gradients becoming larger and the entire system reaches the steady state after around 40 days.

The excess pore pressure distributions along the bottom of the model at different times are shown in Fig. 6. The dissipation of the excess presures is related to both the distance to the cathode and anode, since the electro-osmosis causes the development of negative pore pressure changes along anode and the cathode is free draining. So, at early stages of the analysis the middle part has the highest pore pressure, but if the time is long enough the pore pressure profile stabilises. Note that the initial conditions and surcharge load do not influence the final profiles of this time dependent problem.

The settlement profiles at day 1, 10 and 100 are shown in Fig. 7. At day 1, the settlement is mainly developed near the cathode and is about 32 mm; this because there is free drainage at the cathode. Later, negative pore pressures developed by electro-osmosis become a dominating factor; at day 10, the settlement is almost uniform over the whole domain, and the maxmium value is around 68 mm near the anode. At day 100, the maxmium settlement is 92 mm near the anode.
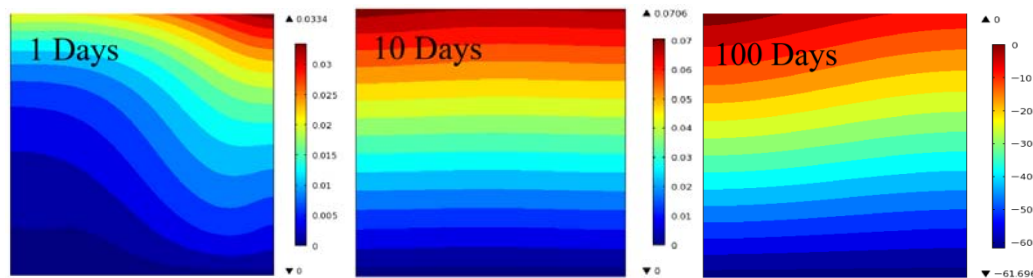
Figure 7: Displacement profiles at day 1, 10 and 100
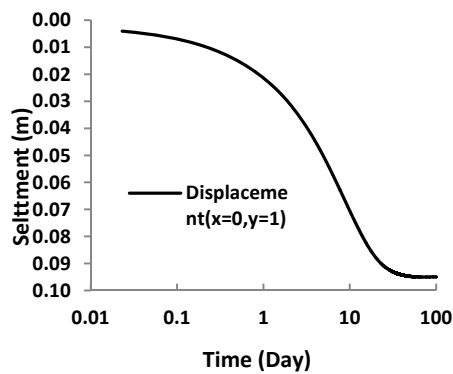
Figure 8: Settlement-time relationship   *Figure 9: Settlement profiles at top surface*
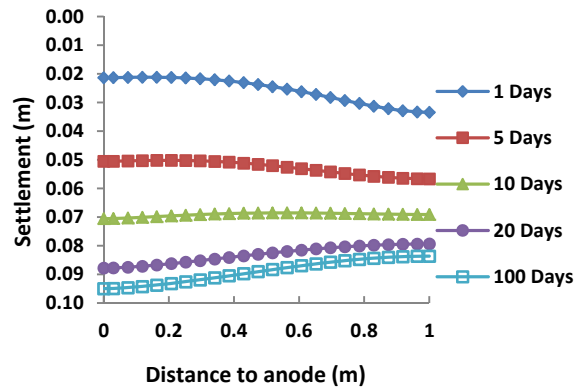
To investigate the surface settlement during electro-osmosis consolidation, the evolution of the surface settlement at the top of anode (x=0, y=1 m) with time is shown in Fig. 8. The settlement increases quickly between day 1 and day 10, and becomes stable by day 100 when the maxmium settlement has reached around 95mm. It can also be observed from Fig. 8 that most of the surface settlement takes place within the first 10 days. As mentioned before, the excess pore pressure plays an important role in the mechanical equilibrium, which controls the soil deformation as is evident by comparing Fig. 5 and Fig. 8.

Furthermore, the settlement profiles of the top surface at different times are shown in Fig. 9. At day 1 the settlement at the cathode is larger than at the anode; at this stage the settlement is mainly controlled by the surcharge load. As the negative pore pressure develops near the anode, the settlement at the anode surface increases quicker than at the cathode and, between days 5 and 10, the settlements are almost uniform along the top surface. As the excess pore pressures continue to grow near the anode, the settlement at the anode becomes larger than at the cathode at the steady state. Fig. 9 also shows that, by applying the combined surcharge loading and electro-osmosis consolidation, a more unifrom consolidation rate can be obtained.

4.   CONCLUSIONS

A formulation for the consideration of multi-dimensional electro-osmosis consolidation has been presented in this paper. Three coupled governing equations for force equilibrium, pore water transport and electrical transport are presented and solved using finite elements. The proposed approach is verified against a well-known analytical 1D solution of electro-osmosis consolidation.

A hypothetical two dimensional electro-osmosis consolidation problem considering surcharge load is then investigated. The settlements and excess pore pressure profiles during the electro-osmosis consolidation process are studied. It is found that the peak excess pore pressure is developed near the bottom of the anode and that the maximum settlement is developed near the top of the anode. Moreover, excess pore pressure and settlements develop very rapidly at the beginning of the electro-osmosis treatment, but then became slower with time.

In this new developed model, the mechanical behaviour of soil is considered and the soil settlements are obtained directly; hence the real coupling effect in the electro-osmosis process is modelled. Although unsaturated flow and material and geometric nonlinearity are not considered in this paper, the formulation is amenable to further development to include these factors.

REFERENCES

[1]   *Chu, J., S. Varaksin, U. Klotz and P. Menge, Construction Processes. "State of the art Report". 17th Int. Conf. Soil Mech. Geotech. Eng., Alexandria, Egypt, 2009. Vol. 4: p. 3006-3135.*

[2]   *Milligan, V., First application of electro-osmosis to improve friction pile capacity - three decades later. Proceedings - ICE: Geotechnical Engineering, 1995. 113(2): p. 112-116.*

[3]   *Casagrande, L., Stabilization of soils by means of electro-osmosis-State of the art. Journal of the Boston Society of Civil Engineers Section, American Society of Civil Engineers, 1983. 69(2): p. 255-302.*

[4] Lo, K.Y., I.I. Inculet and K.S. Ho, *Electroosmotic strengthening of soft sensitive clays. Can Geotech J, 1991. 28: p. 362-73.*

[5] Burnotte, F., G. Lefebvre and G. Grondin, *A case record of electroosmotic consolidation of soft clay with improved soil-electrode contact. Can Geotech J, 2004. 41(6): p. 1038-1053.*

[6] Bjerrum, L., J. Moum and O. Eide, *Application of electro-osmosis to a foundation problem in a Norwegian quick clay. Géotechnique, 1967. 17(3): p. 214-235.*

[7] Sprute, R.H. and D.J. Kelsh, *Dewatering fine-particle suspensions with direct current. In: Proc. Int. Symp. Fine Particle Processes,vol.2. 1980. La Vegas, Nevada , p.1828-1844.*

[8] Sprute, R.H., D.J. Kelsh and S.L. Thompson, *Electrokinetic densification of solids in a coal mine sediment pond : a feasibility study. Report of Investigations. 1982, Avondale, Md.: U.S. Dept. of the Interior, Bureau of Mines.*

[9] Lockhart, N.C., *Electro-dewatering of fine suspensions. Advances in Solid-liquid Separation, 1986: p. 241-274.*

[10] Fourie, A.B., D.G. Johns and C.F. Jones, *Dewatering of mine tailings using electrokinetic geosynthetics. Can Geotech J, 2007. 44(2): p. 160-172.*

[11] Esrig, M.I., *Pore pressures, consolidation and electrokinetics. J. Soil Mech. Found. Div., Am. Soc. Civ. Eng, 1968. 94(4 SM): p. 899-921.*

[12] Wan, T. and J.K. Mitchell, *Electroosmotic consolidation of soils. Journal of Geotechnical Engineering Division, ASCE, 1976. 101(5): p. 503-507.*

[13] Feldkamp, J.R. and G.M. Belhomme, *Large-strain electrokinetic consolidation: theory and experiment in one dimension. Geotechnique, 1990. 40(4): p. 557-568.*

[14] Lewis, R., *A finite element solution of coupled electrokinetic an hydodynamic flow in porous media. International Journal for Numerical Methodes in Enginerring 1972. 5: p. 41-55.*

[15] Shang, J.Q., *Electroosmosis-enhanced perloasing consolidation via vertical drains. Can Geotech J, 1998. 35: p. 491-499.*

[16] Iwata, M. and M.S. Jami, *Analysis of combined electroosmotic dewatering and mechanical expression operation for enhancement of dewatering. Drying Technology, 2010. 28(7): p. 881-889.*

[17] Casagrande, L., *Electro-osmotic stabilization of soils. Journal of the Boston Society of Civil Engineers, 1952. 39(1): p. 51-83.*

[18] Mitchell, J.K., *Fundamentals of Soil Behavior. 2nd ed ed. 1993, New York: John and Sons.*

[19] Mitchell, J.K., *In-place treatment of foundation soils. Journal of the Soil Mechanics and Foundations Division, 1970. 96(SM1): p. 73-110.*

SESSION 3
SOIL MIXING 1 – SOIL STABILIZATION (SURFACE MIXING AND
LABORATORY MIXTURES)

Improvement of Geotechnical Properties of Silty sand Soils Using Natural Pozzolan and Lime

Nader Abbasi, Iranian Agricultural Engineering Research Institute, Iran, nader_iaeri@yahoo.com
Masoud Mahdieh, Tehran Azad University, Iran, masoudmahdieh@yahoo.com
Mohammad Hadi Davoudi, Soil Conservation and Watershed Management Research Institute SCWMRI, Iran,
m.hadi.davoudi@gmail.com

ABSTRACT

Silty sand soils are the most important deposits of desert areas which are scattered in large parts of the world, including the central regions of Iran. Low density, large potential for collapse and low strength and bearing capacity in saturated condition are the main geotechnical characteristic of this kind of soils. So that, the structures founded on such a soil are faced with a large risk of damages and destruction. Since construction of different fundamental projects such as highway, railway, water conveyance canals and pipelines and etc, are unavoidable in mentioned areas and replacing of the bed material with proper and strength soils is often very expensive, stabilization and improvement of the geotechnical properties of the such weak soils could be considered. In this study the effect of different amounts of lime and natural pozzolan on geotechnical properties of a silty sand soil has been investigated. To do this, 20 treatments were prepared with adding five lime levels of 0, 1, 3, 5 and 7 percent (by weight) and four levels of pozzolan including; 0, 5, 10 and 15 percent. Compaction characteristics, compressive strength and bearing capacity of the treatments were determined using standard test procedures. For evaluation of compressive strength, cylindrical specimens (3.5cm in diameter and 7cm in length) were made and cured for three different ages including 7, 14 and 28 days in three replication. Result of compaction tests showed that adding of both lime and pozzolan alone and with together increase optimum moisture content and decrease the maximum dry density of treated soil samples. Statistical analysis using SPSS software showed that although adding of natural pozzolan and lime to the soil increases the compressive strength significantly, but adding of them with together is more effective. So that the compressive strength of a treatment having 3 percent lime and 15 percent pozzolan was found to be 16 times of untreated sample. Furthermore, the results of California Bearing Ratio, CBR test showed that the values of CBR in different treatment increased up to 12 times of untreated sample.

1. INTRODUCTION

Silty sand soils are most important kind of desert sediments that have high dispersal potential in different areas of the world, also in Iran. Weakness of mechanical properties of this soil such as bearing capacity and compressive strength and also unfamiliarity of some of other physical and mechanical properties of these soils have caused serious problems in structures founded on this kind of soils. With attention that wide part of iran is covered of desert areas and construction of different projects such as road and highway in these areas is inevitable, stabilization and strengthening of silty sand soils is necessary to reduce construction and maintenance costs and also for prevention of probable difficulties. Addition of lime to the soil was the most commonly used method for stabilization of different soils in past decades. Sakr et. al. (2009) studied the geotechnical and mineralogical properties of a lime treated high organic soft clay soil and showed that with increasing the curing age and lime percent, unconfined compressive strength increases. Furthermore, the required lime content for satisfactorily stabilization of the high organic soft clay was found to be 7%. Kabir and davudi (2010) showed that the unconfined compressive strength of a fine grained soil with classification of CL-ML soil treated by lime and sodium chloride increases as the additives content and curing time increases. Abdi and charkhyari (2009) studied feasibility of using of the slag of Esfahan Steel Plant to stabilization of clayey soils. For this purpose, the soil was mixed with 1%, 3% and 5% of lime and 10%, 15% and 20% of slag by weight of soil and the samples were cured for 1, 7, 27 and 90 days under a temperature of 35 degree centigrade and near 100% relative moisture. Results indicated that the unconfined compressive strength of samples treated by both lime and slag increases more efficiently and significantly in comparison those treated only by lime or slag. Also the increase of compressive strength was subsidiary of lime content and slag content in the mixture and also the curing time. Ji-ru and Xing (2002) investigated the individual and admixed effects of lime and fly ash on the geotechnical characteristics of expansive soil. The results of experiment showed that as the amount of lime and fly ash is increased, there is an apparent reduction in maximum dry

density, free swell and swelling capacity under 50 kPa pressure, and a corresponding increase in the percentage of coarse particles, optimum moisture content and CBR value. Mohamedzein et al., (2006) presented that the engineering properties of the desert sands can be improved significantly by the addition of incinerator ash. Saltan and findik (2008) used the pumice of the Isparta-Karakaya as stabilization material in the subbase layer and showed that pumice can be used as subbase material of highway and the stabilization material when building highway and every kind of road. Vakili et al (2010) showed that by adding lime and pozzolan to expansive soil the unconfined compressive strength increases as the amount of these materials and curing time increases. Lin et al (2007) used sewage sludge ash (SSA) and hydrated lime to stabilize soft cohesive subgrade soil. To do this, five different ratios of sludge ash to hydrated lime including; 0, 2, 4, 8, and 16 percent by weight were added to the cohesive soil. The results indicated that the unconfined compressive strength of treated specimens increased from three to seven times. Also, it was observed that 95% of CBR values of treated samples were close to high bearing capacity subgrade soil materials. Abdi and Baharluii (2010) studied the effects of poly propylene fibers and lime mixtures, on unconfined compressive strength and plasticity of a kaolinite soil. Specimens were prepared using four different percent of poly propylene fiber (0.05, 0.15, 0.25 and 0.35% by weight of dry kaolinite) and three different percent of lime (1, 3 and 5%) and cured under temperature of 35 degree of centigrade for 1, 7 and 28 days. Results of tests indicated that the increase of compressive strength is affected by lime and fiber contents and also curing time. Bagherian et al, (2005) studied the effects of Rice Husk Ash (RHA) on Atterberg limits, compaction characteristic, shear strength and bearing capacity of soils. They showed that by adding of 4 to 6 percent of lime and various percentages of RHA to the soil, CBR values increases significantly. Asnaashari and Jaafari (2010) studied the effect of various percentages of lime and tire yarn and curing time on bearing capacity through CBR tests. The specimens were made of mixing different amounts of the soil, lime and yarn, and then CBR tests were carried out on 7, 14 and 28-day samples. CBR results revealed that by addition of lime and tire yarn to the soil and increasing of curing age, CBR values increases. Baghdadi and Rahman (1990) studied the effects of cement kiln dust (CKD) on geotechnical properties of dune sand. The results of tests showed that by addition of CKD, compressive strength and CBR values increases significantly. Chen and Lin (2009) mixed incinerated sewage sludge ash (ISSA) with cement in a ratio of 4:1 and added this mixture with a soft and cohesive subgrade soil in four different rates of 2, 4, 8 and 16 percent They showed that unconfined compressive strength of specimens with the ISSA/cement addition improved approximately 3-7 times. In some samples, the ISSA/cement additive improved the CBR values by up to 30 times. In this research the effects of natural pozzolan and lime mixtures on a silty sand soil were studied.

2.   MATERIALS AND METHODS

2.1.   Preparation of the materials

Silty sand soil sample, Pozzolan and Lime were the main materials used in this research. The soil sample was provided from the road of Jandagh-Garmsar situated in central desert area of Iran as showed in Figure 1. The index properties and mineralogical characteristics of the soil sample were presented in Tables 1 and 2.

Table 1: Index properties of the studied soil sample

classification	Specific gravity	Maximum dry density (g/cm^3)	Optimum moisture content (%)	Plasticity
SM	2.52	2.01	9.96	N.P.

Table 2: Minerals of the studied soil sample

$CaSo_4,2H_2O$	SiO_2	$CaCO_3$	$NaAlSi_3O_8$	$KAlSi_3O_8$	$KAl_2Si_3AlO_{10}(OH)_2$	$(Mg,Fe)_6$
25	23	20	20	5	4	2

The Pozzolan used in this research is a natural kind of pozzolan provided from Abyek Cement Factory. The natural pozzolan was pulverized and passed from sieve No. 60 (0.25 mm). Also the lime was provided from Qom Lime Factory as hydrated form. X-Ray Diffraction (XRD) tests performed in order to determine the minerals of lime and pozzolan, as presented in table 3.

Table 3: Percentages of minerals in the materials used

	SiO2	Al2O3	Fe2O3	CaO	MgO	SO3	K2O
Lime	1.36	0.24	0.13	51.64	2.65	0.8	0.03
pozzolan	54.87	18.88	2.62	2.62	1.93	0.15	5.5

Figure 1: Location of sampling area

2.2.   Preparation of treatments

Considering that main purpose of the research is surveying effects of different contents of lime and pozzolan on characteristics of the soil and assessing suitable mixture for stabilization, numerous treatments were prepared and tested. For this purpose, four different levels of pozzolan including; 0, 5, 10 and 15% by dry weight of soil and also five different levels of lime; 0, 1, 3, 5 and 7 percent were mixed to the soil and so that 20 different mixtures (treatments) were prepared. Details of the treatments were presented in Table 4.

Table 4: Details of the test mixtures(treatment)

No.	Sign of treatment	Pozzolan contents (%)	Lime contents (%)	No.	Sign of treatment	Pozzolan contents (%)	Lime contents (%)
1	P0L0	0	0	11	P10L0	10	0
2	P0L1	0	1	12	P10L1	10	1
3	P0L3	0	3	13	P10L3	10	3
4	P0L5	0	5	14	P10L5	10	5
5	P0L7	0	7	15	P10L7	10	7
6	P5L0	5	0	16	P15L0	15	0
7	P5L1	5	1	17	P15L1	15	1
8	P5L3	5	3	18	P15L3	15	3
9	P5L5	5	5	19	P15L5	15	5
10	P5L7	5	7	20	P15L7	15	7

2.3.   Laboratory tests

Unconfined compressive strength and California Bearing Ratio, CBR, tests were used for assessing the mechanical behavior and characteristic of the treated specimens. Harvard miniature compaction test

apparatus having 3.1 cm in diameter by 7.1 cm height was used for construction of unconfined compressive strength test specimens. To do this, standard compaction test, according to ASTM D1557-02, was performed to determine the maximum dry density (MDD) and optimum moisture content (OMC) of the treated soil samples. Then treated soils containing OMC were placed in the mold at 5 equal layers and each layer was compacted with 16 impacts of standard hammer. Figure 2-*a* shows Harvard miniature compaction test apparatus and prepared cylindrical specimens. Then, the specimens were cured in plastic bag for 7, 14, and 28 days. Considering 3 replication for each treatment and 3 different curing ages, totally 180 test specimens were prepared and tested with a constant speed rate uniaxial test apparatus as shown in Figure 3-*b*. CBR tests were done in accordance with ASTM D1883-99 on different treatments at curing age of 14 days and under 2 different moisture condition of optimum moisture content and saturated. For the last condition, the CBR specimens were saturated for 4 days under 5.8 kg overburden pressure after curing time. The swelling of specimens was negligible to start the test so the samples were fixed in loading setting and penetration was carried out with a rate of 1.25 mm/min. Figure 3-*c* shows CBR test apparatus used in this study.

a-Harvard miniature compaction test apparatus

b- unconfined compressive strength

c- CBR test apparatus

Figure 2: Preparation of test specimen for compressive strength

3.   RESULTS AND DISCUSION

3.1.   Compaction tests

As mentioned in previous section, standard compaction test was performed in order to determine the effect of lime and pozzolan on optimum water content and maximum dry density of treated soils. Figure 3 and Figure 4 show the effects of pozzolan and lime on OMC and MDD of treated soil samples respectively. As it is obvious from the figures, optimum moisture content, OMC, of the samples increases

and maximum dry density, MDD, decreases as pozzolan and lime content increases. By increasing the amounts of additives, which is very finer than silty sand soil, then the treated sample tend to be finer and having bigger void ratio and thereby causes the increasing of OMC. Increasing of OMC will always lead to decrease the maximum dry density as the specific gravity of soil and additives particles are more than water. In the performed tests the value of OMC, increases from 9.96% for natural soil to 13% for P15L7 treatment. This finding confirms the earlier findings of different researchers (e.g. Abdi and Charkhyari, 2010).
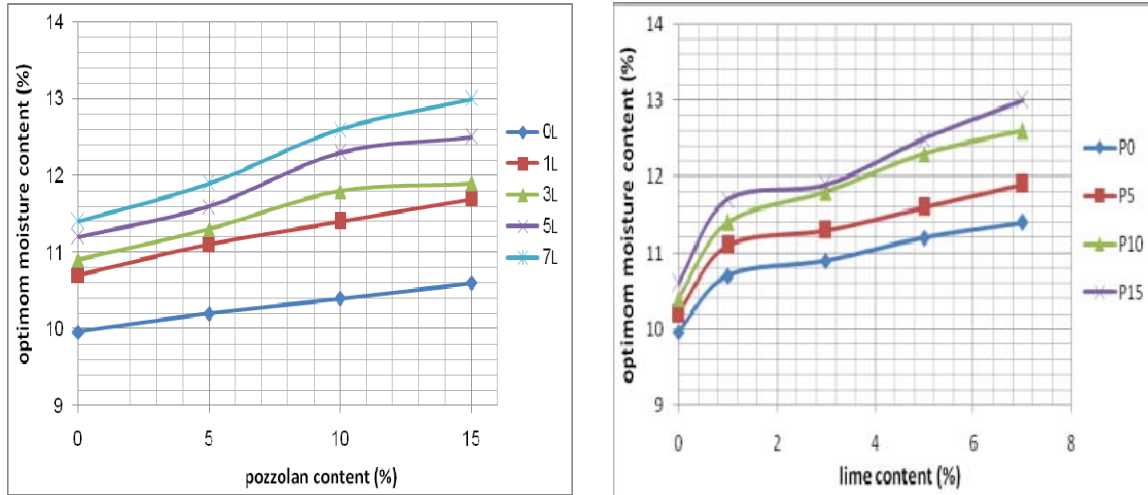
Figure 3: Effects of pozzolan and lime content on optimum moisture content of treated samples
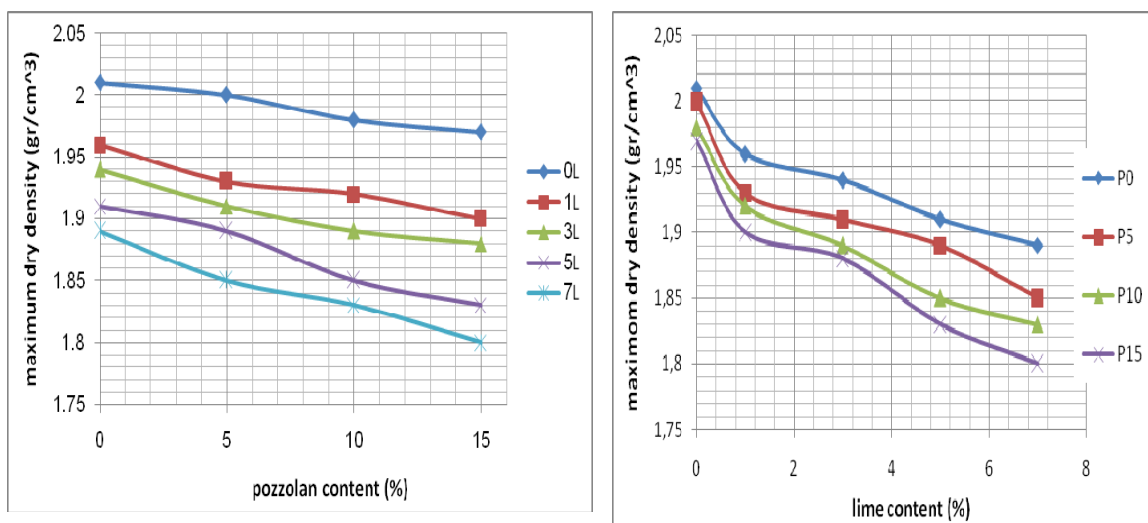
Figure 4: Effects of pozzolan and lime content on maximum dry density of treated samples

3.2.   Unconfined compressive strength tests

The variations of unconfined compressive strength versus lime and pozzolan contents are illustrated in Figures 5 and 6, respectively. In Figure 5, it is observed that increasing of lime content causes significant improvement in compressive strength of the soil at in all of the pozzolan contents, and the maximum strength is achieved at 5% lime approximately. Figure 6 indicates that pozzolan without lime can not affect the compressive strength significantly, while in the samples containing lime, increasing of pozzolan content lead to increasing of compressive strength and the maximum compressive strength increases as the pozzolan content increases. Also, the influence of curing time on compressive strength of the all samples is illustrated in Figure 7.
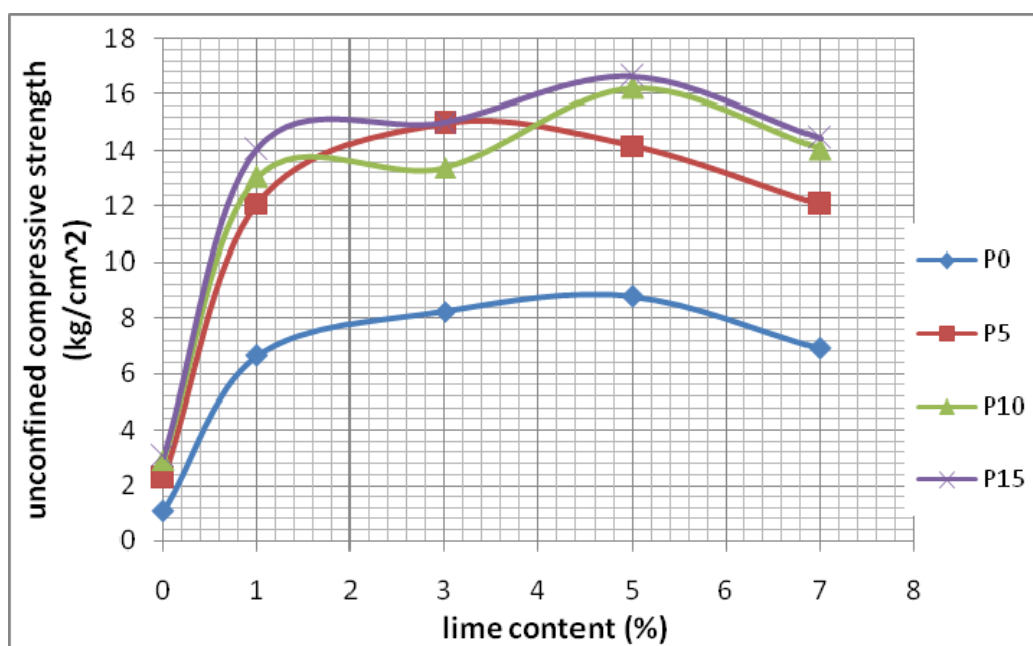
Figure 5: Effects of lime content on compressive strength of samples having different Pozzolan content
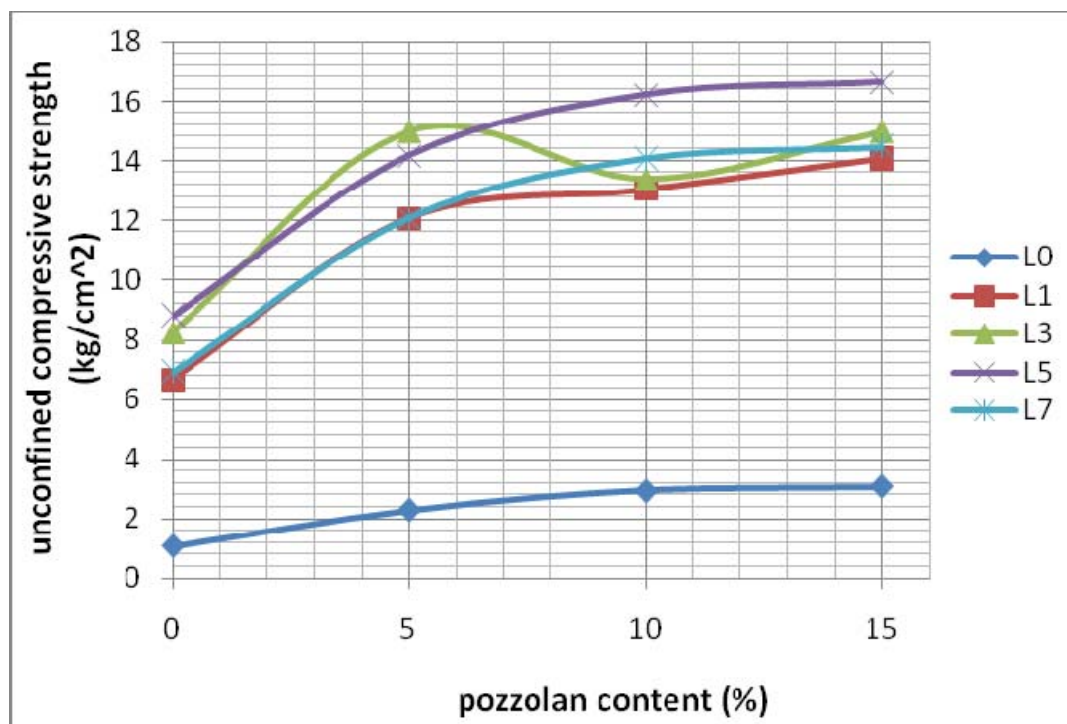
Figure 6: Effects of pozzolan content on compressive strength of samples having different lime content
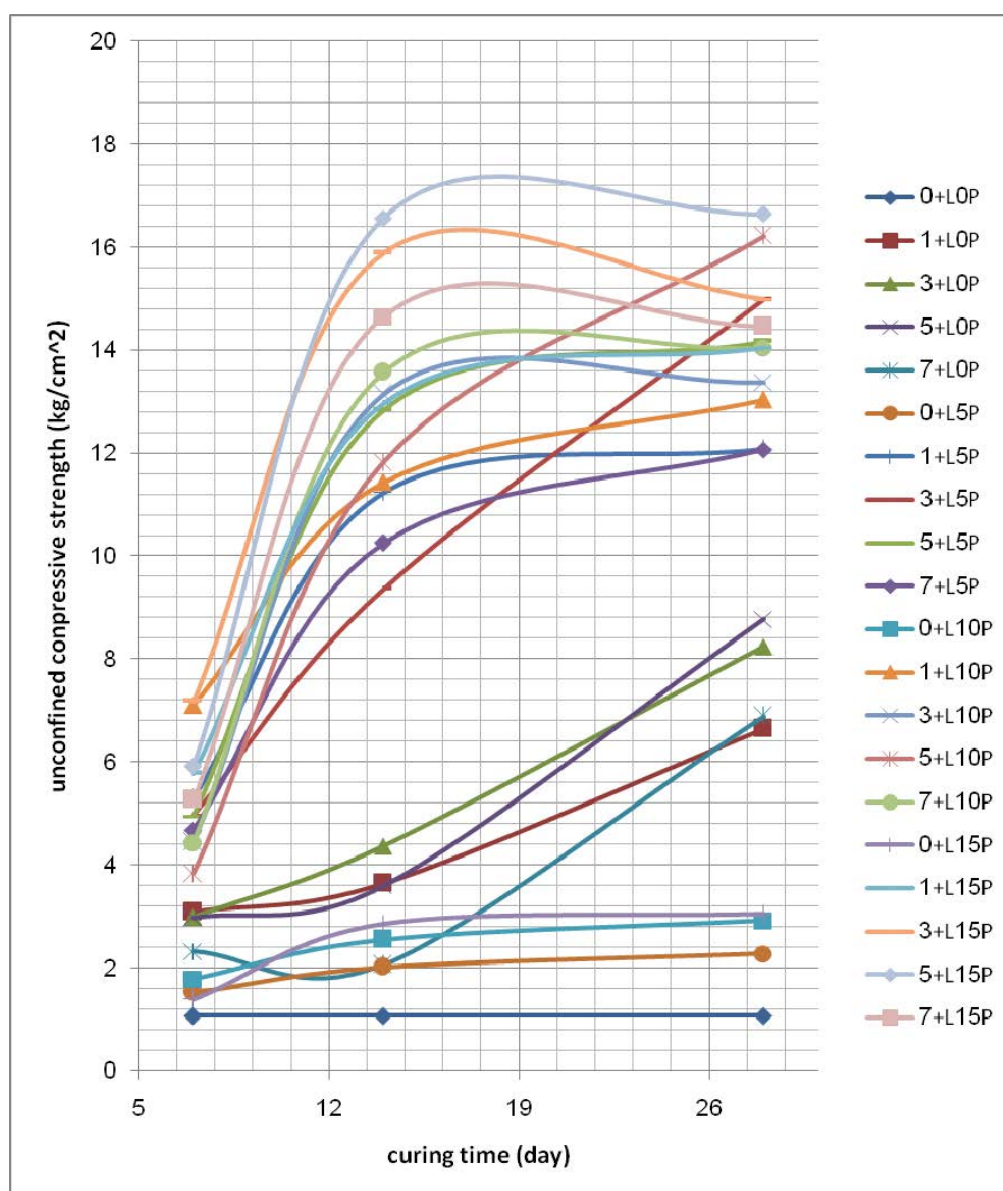
Figure 7: Effects of curing time on compressive strength of the samples

As it is obvious from Figure 7, almost in all of the treatments, by increasing the curing time, compressive strength increases while in the treatments containing only pozzolan, curing time doesn't affect the compressive strength, considerably. But in the samples containing lime, the strength of the samples is increased with curing time proportionally. Furthermore, it is found that the improvement of compressive strength in samples treated by pozzolan and lime with together is higher than those having only lime or pozzolan. It means that the application of lime and pozzolan with together is more efficient for strengthening of the silty sand soil. In addition, the rate of compressive strength growth is very high up to two weeks and after that it becomes gentle and even in some cases, it doesn't change. In order to compare the effects of pozzolan and lime with curing time more precisely, the experimental data were statistically analyzed by the commonly used statistical software, SPSS. The results of statistically analysis of presented in tables 5 to 8. Table 5 shows that there is no significant difference between replications at a significance level of 0.01 or with a probability level of 99%. But, there is significant difference between compressive strength of treatments containing different levels of lime, pozzolan and curing ages. Also, the table reveals that various parameters; i.e. lime, pozzolan and curing age; affect the compressive strength, significantly, meanwhile there exist interactions between these parameters. Tables 6, 7 and 8 show mean comparison analysis using Duncan method for assessment of the effect of Pozzolan, lime and curing ages on compressive strength of treatments.

Table 5: Results of variance analysis of effects of pozzolan, lime and curing age on unconfined compressive strength

Sources of the variations	Degree of	Root Mean Square of compressive
Replication	2	0.799ns
pozzolan	3	319.471**
Lime	4	389.799**
time	2	671.210**
Pozzolan X lime	12	13.457**
Pozzolan X time	6	35.065**
Lime X time	8	35.907**
Pozzolan X lime X time	24	3.784**
Total error	118	0.671ns
Total Mean (kg/cm2)	179	7.803
Coefficient of variation (%)		10.5

**: significant at a significance level of 1 % (0.01)   ns: Non-significant

Table 6: Effect of pozzolan content on mean of compressive strength of treatments

Pozzolan content (%)	Number of samples	Subset 1	2	3	4
0	45	3.96			
5	45		8.20		
10	45			8.94	
15	45				10.06

Table 7: Effect of lime content on mean of compressive strength of treatments

lime content (%)	Number of samples	subset 1	2	3
0	36	1.97		
7	36		8.72	
1	36		8.86	
3	36			9.53
5	36			9.88

Table 8: Effect of curing time on mean compressive strength of all the samples

curing time (day)	Number of samples	Subset 1	2	3
7	60	4.05		
14	60		8.83	
28	60			10.50

Table 6 indicates that in various curing time, by increasing pozzolan content, compressive strength increase where, by addition 5 percent pozzolan the average compressive strength of the samples increases from 3.96 kg/cm2 to 8.20 kg/cm2; i.e. more than 2 times; and then after it has less influences. Table 7 shows that lime percent based on the value of compressive strength can be classified in three subsets: no lime, extreme values of lime (7% and 1%) and medium lime (3 and 5%). According to this classification, the lime content of 3 percent which is in the third subset is assigned as the optimum lime content. The point to be mentioned is that, by adding only 1% lime, average compressive strength of the samples increases from 1.97 kg/cm2 to 8.86 kg/cm2 there after its influences decreases significantly. Table 8 presents the compressive strength increases as the curing age increase where at 28 days, the maximum value is achieved.

3.3.   California Bearing Ratio tests

As mentioned earlier, CBR tests were performed on different treatments at curing age of 14 days and under 2 moisture condition of optimum water content and saturated. The effects of pozzolan and lime

contents on CBR values are presented in Figures 8 and 9, respectively. Figure 8 shows the variation of CBR for the samples containing 5% lime and different content of pozzolan in both conditions of optimum water content and soaked after 14 days. It is clearly obvious from the Fig. 8 that the CBR values increases by increasing pozzolan content. Figure 9 also indicates that in the samples containing 10% pozzolan, CBR values increases by increasing lime percentage, whereas for lime percentages more than 5%, CBR values decreases. Totally, it is revealed that by adding lime and pozzolan admixtures to the soil, CBR values increases significantly. For example; CBR values of the treatment P15+L5 were 120 and 63 in optimum moisture and saturated conditions respectively which are 9 and 12 times of corresponding CBR value of natural soil. Also, it was found that the CBR values of saturated samples are approximately half of CBR values of those with optimum moisture content.
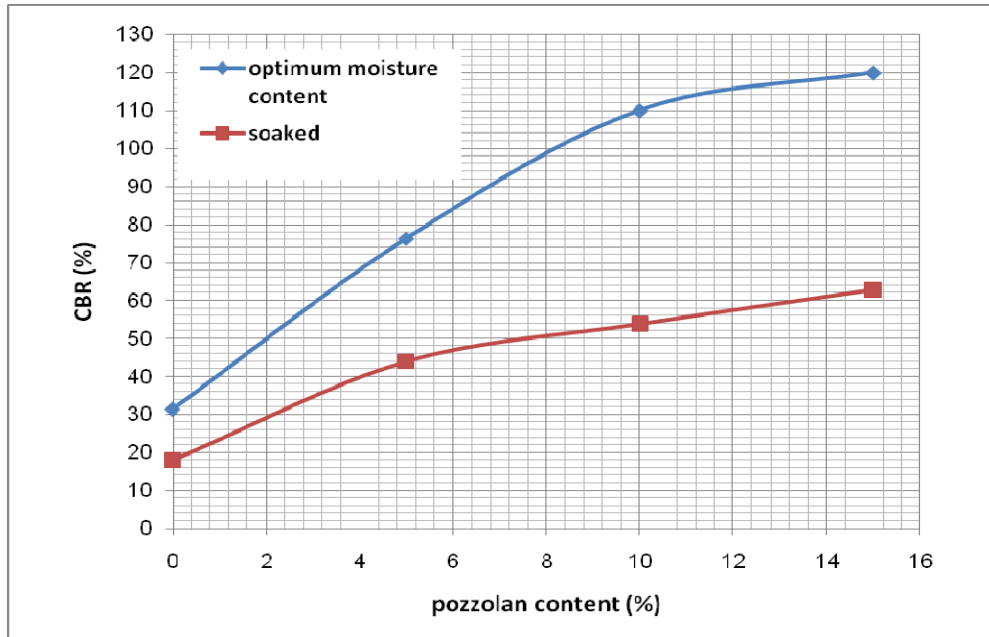
Figure 8: Effects of pozzolan content on CBR values of samples containing 5% lime
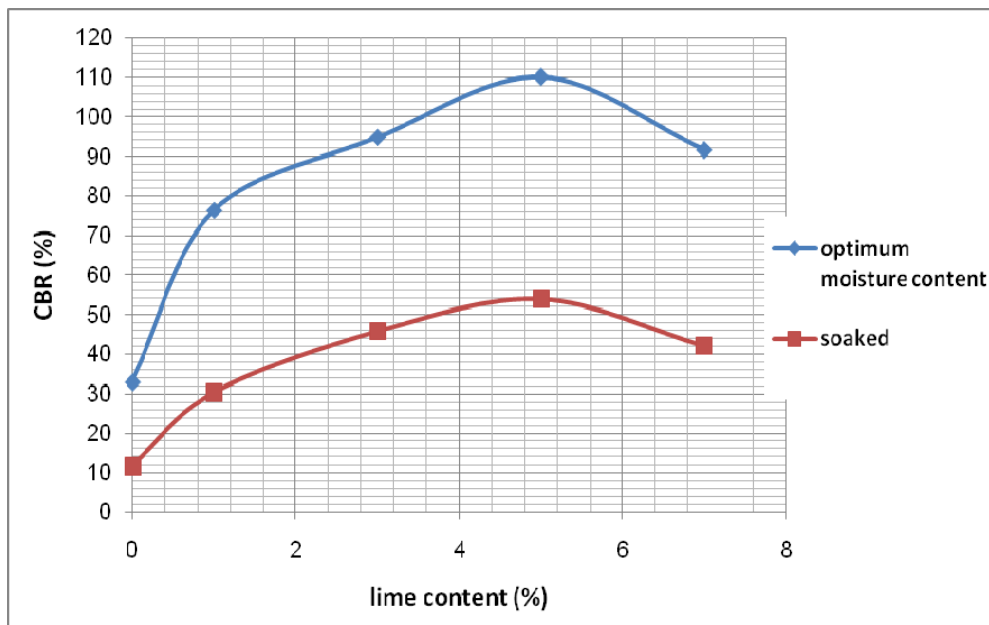
Figure 9: Effects of lime content on CBR values of samples containing 10% pozzolan

4.   CONCLUSIONS

Based on the results of different tests in this research, the following conclusions could be derived:

1. Adding lime or pozzolan or both of them to a silty sand soil, causes an increase in optimum moisture content and a decrease in the maximum dry density.
2. Application of pozzolan with alone has a little or negligible effect on compressive strength of silty sand soil.
3. Adding lime to the soil, improves compressive strength while using both of lime and pozzolan, causes substantial increasing in compressive strength even to 16 times in comparison of natural soil.
4. Curing time has important role on increasing of compressive strength of treated silty sand soil with lime and pozzolan.
5. The maximum values of compressive strength were achieved by applying of 15 percent pozzolan and 1, 3 and 5 percent lime at 7 , 14 and 28 days curing respectively.
6. Adding of lime and pozzolan causes increasing of California Bearing Ratio (CBR) values up to 9 times in optimum water content condition and up to 12 times in saturated condition in comparison of the natural soil.
7. Based on the statistical analysis of the results, a combination of 3 percent and 15 percent pozzolan was found as the most effective combination for stabilization of silty sand soil.

REFERENCES

Anon, 2000. Annual Book of ASTM Standards. Vol. 04.08, Soil and Rock

Asnaashari, M., Jabari,M.,2010. "Application of lime and tire yarn for Stabilization of clayey soils" , 5th national congress on civil Engineering, Tehran, Iran(in farsi)

ASTM C 618-03, (1998) Standard Specification for Coal Fly Ash and Raw or Calcined Natural Pozzolan for Use in Concrete.

Bagherian, A., Janializade , A. and Hesami,S., 2005. "The effects of Rice Ash and Lime on Bearing capacity of soils," , 2nd   congress of civil Engineering , Tehran, Iran, (in farsi)

Baghdadi, Z.A. , Rahman, M.A., (1990) The Potential of Cement Kiln Dust for The Stabilization of Dune Sand in Highway Construction, Journal of Building and Environment, Vol.25, No. 4, pp.285-289.

Chen, L., Lin, D., (2009) Stabilization Treatment of Soft Subgrade Soil by Sewage Sludge Ash and Cement , Journal of Hazardous Materials (2009) 162: 321-327.

Ji-ru, ZH., Xing, C., (2002) Stabilization of Expansive Soil by Lime and Fly Ash, Journal of Wuhan University of Technology – Mater. Sci. Ed. Vol. 17, No. 4.

Kabir, A. and Davoudi, M.H, 2010." The effect of sodium chloride and lime on unconfined impressive Strength of clays, 5th national congress on civil Engineering, Tehran, Iran(in farsi)

Lin, D., Lin, K., Hung, M., Luo, H., (2007) Sludge Ash/Hydrated Lime on The Geotechnical Properties of Soft Soil, Journal of Hazardous Materials (2007) 145: 58-64.

Mohamedzein, Y.E.A., Al-Aghbari, M.Y., and Taha, R.A., (2006) Stabilization of Desert Sands Using Municipal Solid Waste Incinerator Ash, Geotechnical and Geological Engineering, (2006) 24: 1767-1780.

Sakr, M.A., Shahin, M.A., Metwally, Y.M., (2009) Utilization of Lime for Stabilizing Soft Clay Soil of High Organic Content, Geotechnical and Geological Engineering, (2009) 27: 105-113.

Saltan, M., Findik, S.F., (2008) Stabilization of Subbase Layer Materials with Waste Pumice in Flexible Pavement, Building and Environment 43(2008): 415-421.

Volume Change Behaviour of a Sand-Bentonite Mixture Improved by Potassium Silicate

Mohsen Ajdari, Islamic Azad University, Branch of Estahban, Iran, m_ajdari@iauestahban.ac.ir

Hossein bahmyari, Islamic Azad University, Branch of Estahban, Iran

ABSTRACT

Artificially prepared sand-bentonite samples with different bentonite content were employed to investigate the role of the clay content in the swelling potential, swelling pressure and oedometric behaviour of the soil. Specimens were also compacted at various initial water contents to study the effect of the initial fabric of the soil on its volume change behaviour and also, to find the moisture content corresponds to the minimum drying-wetting induced swell and shrinkage of the material.

Furthermore, commercially available Potassium Silicate was evaluated as a potential stabilizer in improving the volume change features of the sand-bentonite mixtures. Three dosage levels of the Potassium Silicate solutions were utilized to stabilize the expansive clayey soil. Free swelling, drying-wetting and consolidation tests were conducted on the stabilized soil samples. The results indicate that the swelling potential of the improved soil specimens are much lower than that of the non-stabilized soils. Also, Potassium Silicate eliminates the shrinkage behaviour of the expansive clay. Besides, the oedometric behaviour of the stabilized and non-stabilized soils is similar and Potassium Silicate does not change the response of the soil samples to the mechanical loading.

1. INTRODUCTION

Expansive clays are among problematic soils which exhibit certain characteristics such as considerable swell-shrinkage behavior and the crack propagation during the drying-wetting process. Therefore, understanding the behavior of saturated and unsaturated expansive clays is essential in the design and construction of light structures, embankments and roads.

In this regard, considerable experimental researches have been done to investigate the hydro-mechanical behavior of these soils (Ajdari et al. 2011). Alonso et al. (1995) and Alonso et al. (2005) showed that the pre-consolidation stress of expansive clays is significantly affected by the initial dry density and hydraulic loading. Similar results were reported by Liangton (2003).

Shuai (1996) investigated the swelling pressure of the expansive soils. The experimental data from the loaded swell oedometer tests indicated that total heave has a linear relationship with logarithm of the surcharge load. Besides, different values of swelling pressure were measured from different test procedures. The rate of the swelling was significantly dependent on the permeability of the soil and low hydraulic conductivity results in a slow swelling process.

Rao et al., (2001) studied the swelling behavior of desiccated soils. The results of the tests indicated that the ultimate void ratio of the compacted clays subjected to drying-wetting cycles is independent of the initial compaction condition. Further, their investigation showed that the vertical deformation, void ratio and water content are reversible in the oedometer test after four cycles of drying-wetting.

Attom et al. (2001) conducted a set of swell tests on both undisturbed samples and three sets of specimens compacted employing different methods namely: dynamic, static and kneading compaction. Dynamic compaction provides the highest value of swell potential and swelling pressure followed by the static and kneading compaction.

Day (1994), Tripathy et al. (2002) and Lloret, et al. (2003) have shown that the swelling and shrinkage path of a single structure expansive soil occurs as a part of an S-shaped curve and in three different phases. Besides, Tripathy et al. (2002) stated that the swelling and shrinkage path is reversible in terms of void ratio and water content after several drying-wetting cycles. The results showed the increase in the swelling with an increase in the initial dry density.

Sridharan and Gurtug (2004) studied the swelling behavior of Cyprus expansive clay with variation in compaction energies from standard Proctor compaction to modified Proctor. The results demonstrated that there is a linear relationship between the swelling pressure and swelling potential irrespective of the level of compaction energy. Swelling potential increases linearly with the compaction energy.

Avsar et al. (2009) performed some swelling pressure and swelling percentage tests on the Ankara clay. The results showed that the swelling parameters determined in the vertical direction are greater than those determined in the horizontal direction. Besides, micro-structural study showed that the direction of the sheeting of the clay particles play a significant role in the swelling parameters of the soil. Employing the

conventional swelling test and Mercury Intrusion Porosimetry (MIP) method, Ferber et al. (2009) examined the coupled influence of the initial dry density and moisture content on the swelling potential and micro-structure of the expansive clay. The results indicated that sample preparation method affects the micro and macro-pores leading to the different swelling behavior. Such that, initial dry density governs the macro-pores and initial moisture content directs the micro-pores.

In this study, a comprehensive experimental investigation of the volume change behavior of some artificially prepared sand-bentonite mixtures was performed. Soil specimens were blended with different amount of distilled water to reach various moisture contents resulting in different initial soil fabrics. Then, wetted samples were dynamically compacted in the oedometer ring. Free swelling, consolidation and drying-wetting tests were performed subsequently and the role of initial fabric in the hydro-mechanical behavior of the samples is discussed. Details of the test program and results are considered in the next sections.

Furthermore, the south west of Iran is among the regions of reported examples of expansive clays. This follows the hypothesis that swelling clays are in abundance where the annual evapo-transpiration exceeds the precipitations. Structures founded on this type of material bear damages from the minor cracking of pavements or interior finishing of buildings, irreparable displacement of footings and superstructure elements (Chen, 1975; Nelson and Miller, 1992; Fityus et al., 2004). Estimated damages that occur around the world due to expansive clays volume change is about a few billion dollars per year. Therefore, finding suitable methods to stabilize the material and reduce the drying-wetting induced volume change of the expansive clays is essential. Consequently, numerous studies have been performed to investigate the various improvement techniques (Rao et al., 2001; Kumar and Sharma, 2004; Cai et al., 2006; Cokca, 2007; Yilmaz and Civelekoglu, 2009). Al-Rawas et al. (2005) compared the suitability of the different stabilization methods and indicated the superiority of the lime in the reduction of swelling potential and swelling pressure of the soil. Guney et al. (2007) showed that the drying-wetting cycles increase the swelling pressure of the lime-stabilized clays.

In this investigation, commercially available Potassium Silicate (PS) is considered as a stabilizer material. Different PS solutions were prepared by solving various amount of PS in unit volume of distilled water. The solutions were then blended with sand-bentonite mixture and the hydro-mechanical behavior of the stabilized soil was studied employing the free swelling, consolidation and drying-wetting tests. The comparison between the behavior of the stabilized and non-stabilized soils are presented and discussed in detail.

2.   MATERIALS AND EXPERIMENTAL PROGRAM

Two types of artificially prepared sand–bentonite mixtures with different percentage of bentonite content were taken to investigate the hydro-mechanical behavior of the expansive clays. Sand and bentonite were separately oven-dried at the temperature of 105°C for 24 hours. Coarse grain particles of the sand were removed by passing the soil through the 2 mm sieve. Bulk soil samples were prepared by blending a predetermined percentage of sand and bentonite with the desired water contents (Optimum Water Content (OWC), OWC-5% and OWC+5%) and stored in a humid chamber. After 48 hours, samples were dynamically compacted using the identical standard Proctor energy per unit volume of soil. Several classification tests were performed employing ASTM (1995) code procedure. Atterberg limits of the material were determined and specific gravity of the sand-bentonite was calculated. Maximum dry density and optimum moisture content were determined using the standard Proctor compaction test. Table 1 shows the index properties of the materials.

Table 1: Physical properties of the studied materials

	Bentonite Content	
Parameter	15%	25%
LL (%)	52	79
PI (%)	21	41
G_s	2.63	2.61
OWC (%)	14	16.5
$\gamma_{d,max}$ (kN/m^3)	18.7	17.7
USCS Classification	SM	SM

Distilled water was utilized for preparing the non-stabilized samples and Potassium Silicate (PS: K2SiO3, Batch Number: 123-44) solutions were employed for providing the stabilized specimens. PS solution was prepared employing the distilled water and exposed to the environment for two days. Three dosage of the PS solution was blended with dry soil (25% bentonite and 75% sand) to prepare the moist specimens and

wetted samples were stored for 48 hours to homogenize the moisture content in between the soil particles. These specimens were used to determine the hydro-mechanical behavior of stabilized sand-bentonite mixture.

Several cylindrical specimens, five centimeter in diameter and one centimeter in high were prepared to perform the oedometric tests. Free swelling tests under the vertical stress of five kPa followed by the conventional consolidation tests were done on the stabilized and non-stabilized samples. In consolidation experiments, the load was held on the sample for twenty four hours or until all excess pore pressure was dissipated. During this time the change in height was measured and the change in void ratio was determined. The load was doubled at the end of a 24 hour period and the process was repeated. The measurements were then used to determine the relationship between the vertical stress and void ratio.

In the free swelling test, water was introduced to a sample that was laterally restrained in the oedometer cell and the one-dimensional volume change was measured with time. Readings of the vertical displacement of the sample were taken at sequential time intervals. To keep the sample submerged in water, distilled water was added if necessary.

Drying-wetting cycles were imposed to the specimens followed by the consolidation under the applied vertical loads. Samples were air-dried in an oedometer located in a thermal control chamber (temperature of 21°C) for six days and then introduced to the distilled water for twenty four hours to do the wetting procedure. The suitable duration of the drying process was determined through a trial procedure by increasing the time of the drying and monitoring the rate of the shrinkage of the samples. The flowchart of the oedometric tests is shown in Figure 1.
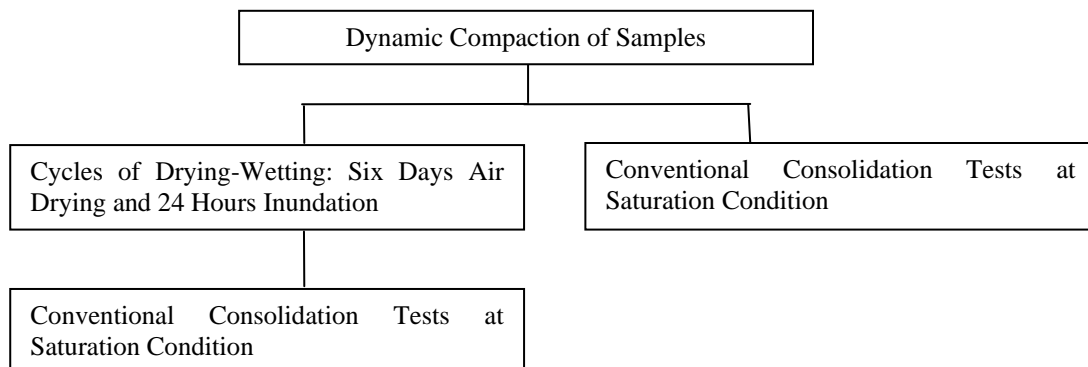
Figure 1: Layout of the Oedometric Tests

3.   TESTS RESULTS AND DISCUSSION

3.1.   Oedometric Response of Non-stabilized Soil

Figures 2 and 3 compare the oedometric behavior of the saturated soil samples and their volume change during the free swelling test. As is clear from these figures, swelling pressure and swelling potential of the samples decrease with an increase in the initial water content (Table 2). Obviously, it is due to the higher capacity of the dry specimens to absorb water during the saturation process. Besides, samples compacted in the dry side of the OWC have a flocculated texture. Absorbed water increases the thickness of the double layer water and changes the structure of the samples to the dispersed one resulting in a high amount of the volume increase (Ajdari et al. 2010). Therefore, more effort should be consumed to reach the initial volume of the samples and swelling pressure of these samples is more than that of others (Table 2).
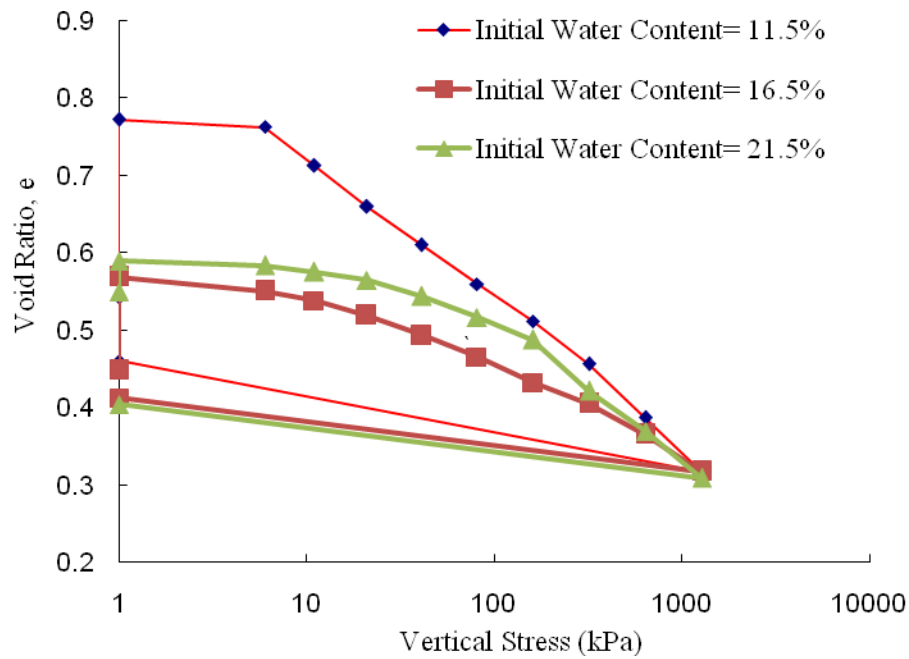
Figure 2: Consolidation Curves of Saturated Sand-bentonite Mixtures with the Bentonite Percent of 25
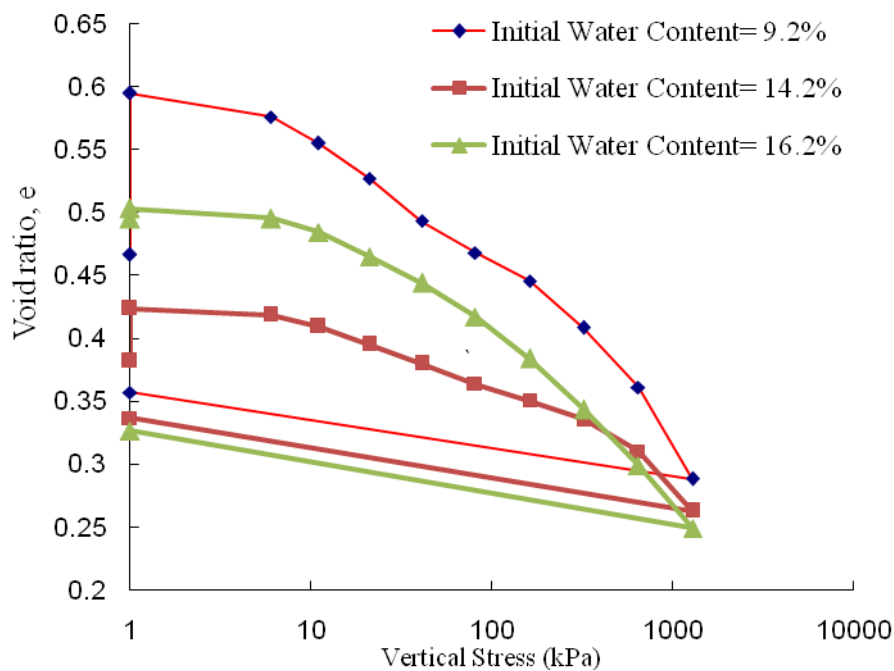
Figure 3: Consolidation Curves of Saturated Sand-bentonite Mixtures with the Bentonite Percent of 15

Also, these figures show that the samples compacted at OWC have lower coefficients of compressibility (Table 2). High initial unit weight of these specimens can be the cause of this behaviour. Furthermore, mechanical loading leads to the destructuring of the samples approaching asymptotically to a unique normal consolidation line at high applied net stresses (Ajdari et al. 2010). It is worth mentioning that, in general, more bentonite content results in a higher swelling pressure and swelling potential.

Table 2: Swelling and Oedometric Properties of the Sand-bentonite Mixture

Bentonite (%)	Initial Water Content (%)	Cc	Cs	Swelling Potential (%)	Swelling Pressure (kPa)
15	9.2	0.19	0.02	8.7	90
15	14.2	0.1	0.025	3	40
15	19.2	0.15	0.025	0.5	7
25	11.5	0.23	0.048	14.9	120
25	16.5	0.08	0.029	7.8	110
25	21.5	0.12	0.03	2.6	35

3.2. Responses of the Stabilized and Non-stabilized Soils upon Drying-Wetting Cycles

Figures 4 and 5 indicate the volume change behaviour of non-stabilized soils during wetting-drying cycles. Clearly, the amount of the volume change decreases with an increase in hydraulic loading cycles. Also, the more bentonite contents the more the volume change of samples. Besides, while, drying induced shrinkage of samples with bentonite content of 15% is negligible; specimens with bentonite content of 25% show a significant amount of shrinkage during the drying process.
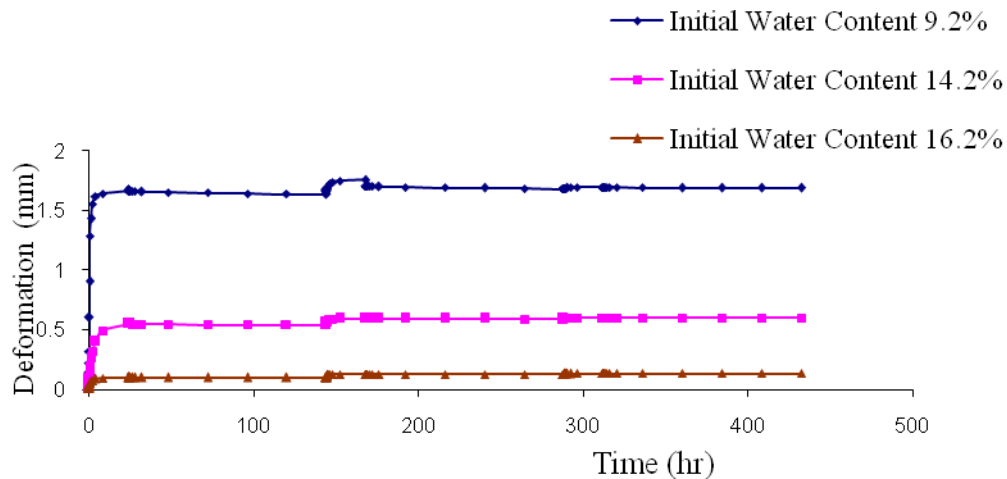
Figure 4: Wetting-drying Cycles at Constant Vertical Stress of 5kP, Bentonite Content=15%

The variation of the volume of the stabilized samples with time is indicated in Figure 6. PS reduces the amount of the wetting induced swelling and removes the drying induced shrinkage. The more concentration of the PS solution the less the amount of the soil expansion. Base on these results, this stabilization method is more suitable for arid areas and effectively eliminates the drying induced shrinkage of the soil media.
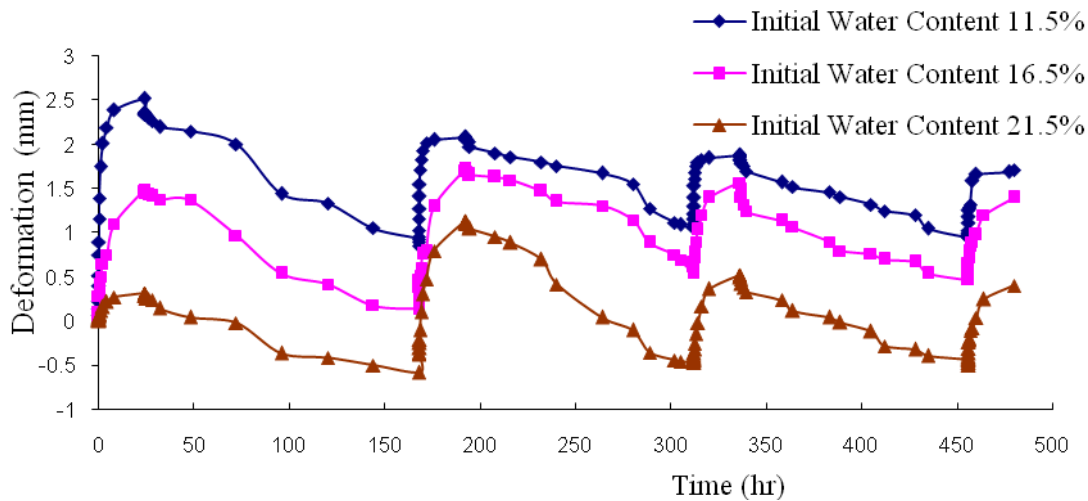
Figure 5: Wetting-drying Cycles at Constant Vertical Stress of 5kP, Bentonite Content=25%
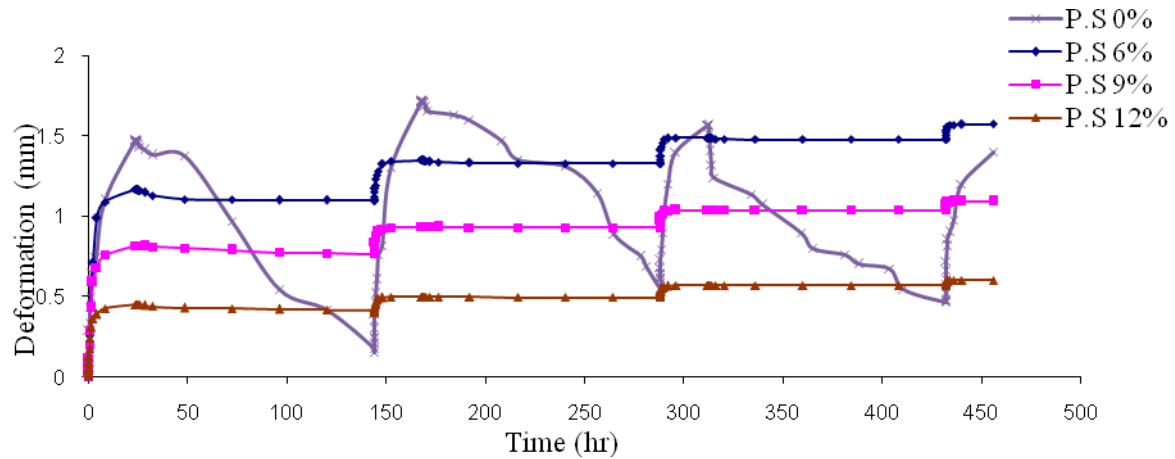
Figure 6: Wetting-drying Cycles of the non-stabilized and PS stabilized samples at Constant vertical Stress of 5kP, Bentonite Percent=25, Initial Water Content=16.5%

3.3. Oedometric Response of Stabilized Soil

Figure 7 indicates the oedometric response of the non-stabilized and PS stabilized soils. The mechanical behaviour of stabilized and non-stabilized samples is similar. In other words, an identical load step results in a similar change in void ratio in all specimens. Also, pre-consolidation pressures of all samples are about twenty kPa. The single difference between the oedometric curves of the specimens is the various initial void ratios resulted from the various swelling potential of non-stabilized and PS stabilized soil samples. Therefore, PS does not change the oedometric behaviour of the expansive sand-bentonite mixture.

To stabilize the thick layers of expansive clays, shallow thin layers of the soil can be mixed with PS. Vertical flow of the rain washes the stabilizing material into the deeper parts and these portions are hydrated by PS solution. More field tests are needed to verify the applicability of this method to treat the thick layers of swelling clays.
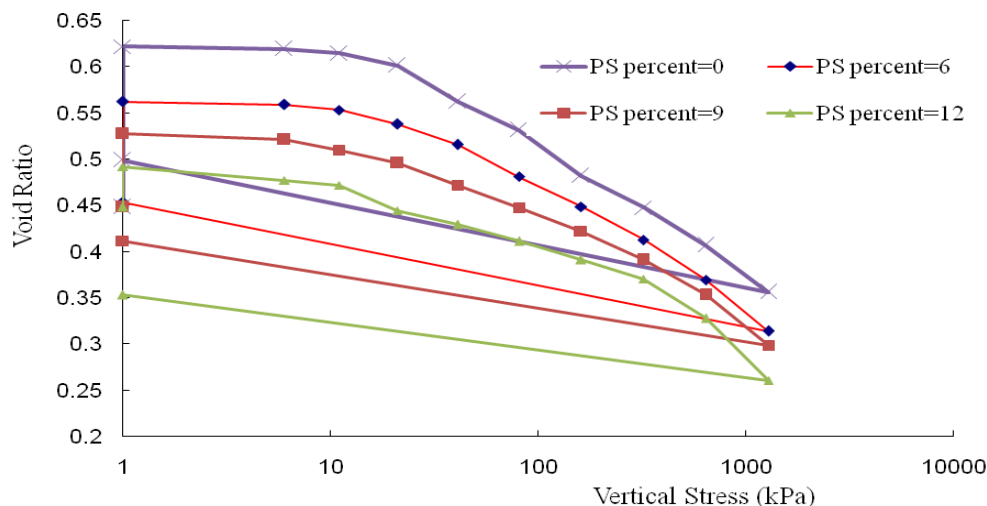
Figure 7: Consolidation Curves of Non-stabilized and PS Stabilized Sand-bentonite Mixture, Bentonite Percent=25, Initial Water Content=16.5

4.   CONCLUSIONS

Potassium Silicate was introduced as a stabilizer of expansive clays. Consolidation and wetting-drying tests were performed on the stabilized and non-stabilized samples. Although PS does not change the oedometric parameters of the plastic clay (C_c, pre-consolidation pressure and C_s), wetting induced swelling of the stabilized soil is less than that of non-stabilized samples and drying induced shrinkage of stabilized specimens is negligible. Also, oedometric results showed that the initial water content and bentonite content change the oedometric behaviour of the soil samples.

REFERENCES

Ajdari, M.; Habibagahi, G.; Nowamooz, H.; Masrouri, F. and Ghahramani, A. 2010, Shear Strength Behavior and Soil Water Retention Curve of a Dual Porosity Silt-Bentonite Mixture, Scientia Iranica, 2010, pp. 430-440.

Ajdari M, Habibagahi G, Nowamooz H, Masrouri F, Ghahramani A 2010, Hydro-mechanical response of expansive silt-bentonite mixture, Proceedings of UNSAT2010, Alonso and Gens, Taylor and Francis, Barcelona: 175-180.

Alonso, E.E.; Lloret, A.; Gens, A. and Yang, D.Q. 1995. Experimental Behaviour of Highly Expansive Double-Structure Clay. Proc. 1th Int. Conf. on Unsaturated Soils. Balkema. Paris. Vol. 1, pp. 11-16.

Alonso, E.E., Romero, E., Hoffmann, C., Garcia-Escudero, E., 2005. Expansive Bentonite-Sand Mixtures in Cyclic Controlled-Suction Drying and Wetting. Engineering Geology, 81, 213-226.

Al-Rawas, Amer Ali., Hago, A. W., Al-Sarmi, Hilal., 2005, Effect of lime, cement and Sarooj (artificial pozzolan) on the swelling potential of an expansive soil from Oman., Building and Environment, Vol. 40, pp. 681–687.

Attom, M.F.; Abu-Zreig, M.M. and Obaidat, M.T. 2001. Changes in Clay Swelling and Shear Strength Properties With Different Sample Preparation Techniques, Geotechnical Testing Journal, GTJODJ, Vol. 24(2), pp. 157-163.

Avsar, E., Ulusay, R. And Sonmez, H. 2009. Assessments of Swelling Anisotropy of Ankara Clay, Engineering Geology, 105, pp. 24-31.

Cai, Y., Shi, B., Ng, C. and Tang, C. 2006, Effect of polypropylene fibre and lime admixture on engineering properties of clayey soil, Engineering Geology.,Vol. 87, September, pp. 230–240.

Chen, F.H. 1975, Foundations on Expansive Soils, Elsevier Scientific Publication Company.

Cokca, E., 2001, Use of class C fly ashes for the stabilization of an expansive soil, Journal of Geotechnical and Geoenvironmental Engineering, ASCE, Vol. 127, No. 7, July, pp. 568-573.

Day, R. W., 1994, Swell shrink behavior of compacted clay, Journal of Geotechnical Engineering, ASCE, Vol. 120, No. 3, March, pp. 618-623.

Ferber, V., Auriol, J.C., Cui, Y. J. and Magnan, J. P., 2009. On the Swelling Potential of Compacted High Plasticity Clays, Engineering Geology, 104, pp. 200-210.

Fityus, S. G.; Smith, D. W. and Allman, M. A. 2004, Expansive Soil Test Site Near Newcastle, ASCE, J. of Geotech. and Geoenviron. Eng., Vol. 130, No. 7, pp. 686-695.

Guney, Yucel., Sari, Dursun., Cetin, Murat., Tuncan, Tuncan., 2007, Impact of cyclic wetting–drying on swelling behavior of lime-stabilized soil, Building and Environment, Vol. 42, pp. 681–688.

Kumar, B. R. P., Sharma, R. S., 2004, Effect of Fly Ash on Engineering Properties of Expansive Soils, Journal of Geotechnical and Geoenvironmental Engineering, ASCE, Vol. 130, No. 7, July, pp. 764-76.

Liangtong, Z. 2003, Field and Laboratory Study of an Unsaturated Expansive Soil Associated with Rain-induced Slope Instability, PhD Thesis, Hong Kong University.

Lloret, A., Villar, M.V.; Sanchez, M.; Gens, A.; Pintado, X. and Alonso, E. E. 2003, Mechanical Behaviour of Heavily Compacted Bentonite under High Suction Changes, Geotechnique, 53, 1, pp. 27-40.

Nelson, JD. and Miller, JD., 1992, Expansive soils: problems and practice in foundation and pavement engineering, New York, Wiley.

Rao, S. M., Reddy, B.V.V., Muttharam, M., 2001, The impact of cyclic wetting and drying on the swelling behaviour of stabilized expansive soils, Engineering Geology, Vol. 60, march, pp. 223–33.

Shuai, F., 1996, Simulation of the Swelling Pressure Measurements of Expansive Soils, PhD Thesis, Saskatchewan, Canada.

Sridharana,A. and Gurtug, Y., 2004, Swelling Behavior of Compacted Fine-Grained Soils, Engineering Geology, Vol. 72, pp. 9-18.

Tripathy, S.; Rao, K.S.S. and Fredlund, D.G., 2002, Water Content-Void Ratio Swell-Shrinkage Paths of Compacted Expansive Soils, Can. Geotech. J. Vol. 39, pp. 938-959.

Yilmaz, I. and Civelekoglu, B., 2009, Gypsum: An additive for stabilization of swelling clay soils, Applied Clay Science, January, pp. 1-7.

Nucleation centres in lime stabilised soils

Mr Paul Beetham, Loughborough University, UK, p.beetham@lboro.ac.uk
Dr. Tom Dijkstra, Loughborough University, UK, t.a.dijkstra@lboro.ac.uk
Prof. Neil Dixon, Loughborough University, UK, n.dixon@lboro.ac.uk

ABSTRACT

Nucleation centres, in the form of a small percentage of finely ground limestone powder, are often utilised to enhance the hydration of Portland cement. Cement mixing water has relatively low solubility and capacity to dissolve solutes from cement particles. Nucleation centres provide a surface of lower energy permitting hydration products to form in an expedited manner around these 'seeds'. The mixing water is then able to further dissolve the cement particle and strength development of the hardening paste is accelerated. The laboratory study presented here investigates whether similar nucleation processes may prove beneficial to lime stabilised soils. One of the mechanisms driving the formation of cement product may be dissolution, from the edge sites of clay particles, of silica and alumina. These diffuse and combine with calcium and water forming cementitious minerals and associated strength gain. If this mechanism is present, then the solubility of the dissolving chemistries may cause a bottleneck and limit the rate of strength gain. It is possible that widespread nucleation centres may negate this bottleneck. This paper presents the initial findings of a practically focussed study into the potential of nucleation centres in lime stabilised soils.

Early results have identified that the use of clay clods up to 20mm in diameter, introduces a structure interlinking weak areas around clay clod peripheries and influencing the manner of sample failure. Pozzolanic reaction at the surface of the clods is considered to considerably influence this failure mechanism. CBR results (soaked and unsoaked) tested at 8 and 32 days suggest that there has been greater pozzolanic development due to the addition of finely ground limestone. However, due to the triaxial test results not supporting the CBR results and possible dry density influences, the results are equivocal at this stage. Further work to remedy this is underway.

1. INTRODUCTION

Intermixing a small percentage of lime binder with poor quality host soils during earthwork construction has been employed as a ground improvement technique since the 1950's (Petry & Little, 2002). Where clay minerals have a significant influence upon the engineering properties of a fill material, this addition of lime has a typically ameliorative effect. It is usual to discuss the effects that result from lime / clay reaction in terms of the time scale over which they occur. The short term effects relate to modification of the properties by drying (if quick lime is used) and cation exchange process. These benefits are often utilised as a construction expedient, therefore, a common and descriptive reference to these rapid changes is 'lime improvement'. Where sufficient lime and clay reactivity is present, a secondary process involving time dependent, pozzolanic reactions may follow on. This growth of cementitious minerals further enhances the soils strength and durability (Sherwood, 1993) and may be given the amended distinction 'lime stabilisation'.

The laboratory activities presented in this paper focus on gaining an enhanced understanding of the pozzolanic reactions which occur within lime stabilisation. This project is driven by the need to provide practitioners (the project sponsors) with information of practical benefit. Therefore, preparation techniques were applied that reflect the processes engaged on site. This, combined with the control and consistency of a laboratory setting, should provide a means of identifying mechanisms which may influence field behaviour.

1.1. Literature Information

1.1.1. Pozzolanic reaction

Lime stabilisation takes places through growth of a cementitious product. This is a reaction that primarily involves calcium, silica, alumina and water and in a high pH environment. The products are similar in nature to those derived from Portland cement hydration and provide the binders that keep the clay

aggregations together (Greaves, 1996). The reaction products are usually described as calcium silicate hydrates or calcium aluminate hydrates (C-A-H). Other soil chemistries, such as sulphates, may alter the reaction products and cause potentially expansive minerals, such as ettringite and/or thaumasite to form (Hunter, 1988). For the purpose of this paper, such deleterious reactions are not specifically considered.

Whilst the pozzolanic reaction process is widely accepted as a concept, the detail surrounding a lime – clay cementitious reaction is poorly understood (Wilkinson et al., 2010). Boardman et al. (2001) noted a general lack of agreement amongst researchers, relating to the timescale and location of the reactions. This was attributed to the wide variety of clay soil compositions and complexity of clay mineral structures.

Two reaction processes have been discussed in the literature; a 'rapid surface alteration' and 'long term dissolution and precipitation'. The rapid surface alteration process was proposed by Diamond & Kinter (1965) and considered that some initial pozzolanic reactions occur over a similar timescale to the lime improvement process and through the alteration of the surface of a clay particle. They suggested that calcium hydroxide is initially and rapidly adsorbed onto a clay particle's surface. Cementation would then occur through $Ca(OH)_2$ reaction with $Al(OH)_X$ groups at the edge sites. The resultant C-A-H bridges and strengthens the edge / face contacts of the clays flocculated structure. This cementation at point of contact was considered by the authors to resist de-flocculation upon soaking, thereby accounting for the observed immediate improvement in swelling / plastic response to soaking.

Alternatively, dissolution and precipitation is a long term reaction, involving the release of aluminium and / or silica from clay particle edges under high pH conditions. New minerals are then precipitated at, or close to the dissolution sites (Diamond & Kinter, 1965; Sherwood, 1993; Boardman et al., 2001).

1.1.2. Nucleation in Portland Cement

In their state of the art review on "The Use of Limestone in Portland Cement", Hawkins et al. (2003) summarise how finely ground limestone acts as nucleation centres within hydrating cement. They note how widespread distribution of the $CaCO_3$ centres accelerates the formation of hydration products, notably ettringite and portlandite. This expedited hydration removes solutes from the supersaturated mixing water and cement clinker particles may dissolve at a faster rate. Winter (2009) noted that this results in increased early (1-2 day) strengths and, due to a more uniform microstructure, late strengths (28 days) may also be enhanced.

1.1.3. Nucleation in Lime Stabilised Soils

In view of the above it is considered that finely ground limestone may have similar potential benefit as nucleation centres within the lime stabilisation process. Boardman et al. (2001) reported the presence of water soluble aluminium or silicon, as dissolved from the edges sites of kaolinite and bentonite. These ions were identified within 7 days of lime addition and their number had substantially increased by 175 days cure. With regard to new mineral growth, Boardman et al. (2001) considered that there was no sign of this occurring by 7 days, although substantial growth had occurred by 301 days. It may be considered, therefore, that dissolution of the necessary reactants occurs at a relatively early stage, yet mineral growth is not simultaneous.

If a contribution towards this delay is that the nucleation of the new minerals is slow due to high-energy requirements, then the provision of a low energy surface, as may be provided by well distributed, finely ground limestone, may encourage pozzolanic growth at an early stage. Such a mechanism may encourage widespread and accelerated cementitious mineral growth, with accompanying strength gain.

Reports of beneficial effects of nucleation surfaces in a lime-clay system have been supposed elsewhere within the soil stabilisation literature. This was made, however, with reference to the use of ground granulated blast furnace slag (GGBS) to mitigate the deleterious effects of ettringite formation in soils of high sulphate content. In such systems Wild et al. (1996) considered that GGBS provides an alternative nucleation surface that would compete with kaolinite to instigate ettringite growth. Ettringite grown from the GGBS particles was reported to have an absence of the property which caused it to secrete substantial H_2O and swell upon specimen soaking. Furthermore, in reference to pozzolanic reaction between lime and fly ash, Jalali et al. (1997) explained that an induction period observed in the strength gain of these mixes followed classic nucleation and diffusional growth theories. In consideration of reports that nucleation rates may influence strength gain and that reaction products may be nucleated at interfaces

other than the clay particle surface, it was considered appropriate to trial the potential of finely ground limestone centres.

2.   METHODOLOGY

2.1.   Practical Considerations

Fundamental to this study was adopting preparation techniques which reflect the field practice of surface mixing lime stabilisation in the UK. This process uses mobile plant equipped with high torque rotational drums, arranged within a mixing chamber and appointed with multiple sharp teeth. The plant passes through a depth (nominally 300mm) of clay fill, and the action of the drums work to **denudate** the clay fill. Lime powder is added through an integral feed hopper. Mixing water may also be added via the mixing chamber. Upon completion of the mixing stages the binder should have been well distributed over the clod surface and, following any mellowing period requirements, the material is compacted with appropriate plant.

The clay clod sizes resulting from the above will be substantially reduced from their original size, however, there is often a practical limit to the degree of pulverisation that can be attained (Petry & Wohlgemuth, 1988), even with modern, high efficiency, machinery. Contractors are often required by specification to achieve a minimum degree of pulverisation e.g. the UK Highways Agency specification requires that 95% and 30% pass 28mm and 5mm sieves respectively (The Highways Agency, 2007). Hence, pulverisation beyond this minimum may not typically be pursued.

2.2.   Material preparation

The aim of the trial was to compare and contrast the engineering properties of lime stabilised mixes made with and without nucleation centres. Additionally, a core focus of the laboratory trial was to engage in preparation techniques which are faithful to the site process. Specifically this involved utilising clod sizes achievable in the field, using a clay soil at 'as dug' moisture contents and employing a binder addition / mixing process similar to field practice. Details of the clay soil are provided in Table 1. Both quick lime (Proviacal ST) and lime slurry (Proviacal SLS45) binders, supplied by Lhoist UK Ltd, were utilised. For the nucleation centres, a finely ground limestone was used, of Blaine surface area 480m^2/kg (Betocarb 80-BT supplied by Omya UK Ltd). The preparation procedure is detailed below.

Efforts were made to limit air drying effects which involved; use of a humidity room; clay storage in sealed sample bags and; at any interim periods of preparation, the clay clods were temporarily stored beneath a wet tented sheet, intended to provide a localised atmosphere of 95% R.H. The scale of test programme required that the test moulds were created in batches. This permitted all mould preparation to be completed within 2.5 hours of the final binder mixing stage (stage 5b in table 2). Each batch received identical preparation, undertaken in two stages; clay pulverisation / homogenisation and binder mixing.

Table 1: Details of the natural clay utilised in this study

> Description: Brown mottled grey soft to firm consistency low strength CLAY with rare fine to medium angular gravel of shale and rare rootlets. Sourced from a single trial pit at depths 1.5m to 3m below ground level within highly weathered Namurian age shale. Approx. Co-ordinates 40707 E 34979 N.
>
> Mineralogy (as identified by qualitative XRD on air and oven dried specimen): Kaolinite, quartz, illite. Reflections between 14 Å and 10 Å also suggest an expansive clay mineral, possibly interlayered smectite– illite, however, this could not be fully determined from air / oven dried patterns alone.
>
> Initial Consumption of Lime (from 3 tests**).** Average 3.53%. Range 3.4% -3.7%

2.2.1.   Clay pulverisation / homogenisation

The 'as dug' clay was pulverised by hand (small balls pulled away from the main clay mass). The resultant clods were passed through 20mm and then 14mm sieves. Each clod size group was thoroughly blended by hand. Each batch comprised 42.5kg of 'as dug' clay, which was composed of the same mass percentage of the two clod size groups i.e. <14mm = 13.7%; 14-20mm =86.3%, which were manually intermixed to ensure an even distribution.

2.2.2. *Mixing process*

Table 2 summarises the process followed for each batch. The mixing times were considered sufficient to ensure that the binder/water was uniformly distributed over the surface of all clods. The total water added was determined through initial reference to the Moisture Condition Value (MCV; as described by British Standards Institution, 2002), with the intention of achieving a target MCV of 9.0. This MCV was selected because it should provide sufficient water to enhance ion transportation (Barker et al., 2007) and permit pozzolanic reaction products to form. This is in comparison to a drier material where both may become limited (Bell, 1988). Perry et al. (1996) note that MCV's of 13.5 equate approximately with optimum moisture content (OMC), hence an MCV of 9.0 would certainly be wet of optimum, yet also workable on site. Once the mass of water required for this MCV was determined for the initial batch, this quantity was used for all subsequent batches. Batches were created for mixes with and without nucleation centres and for curing periods of 8, 32 and 189 days. Hence, there were a total of six batches treated with binder addition, along with a further batch of natural material (host soil) which was pulverised / homogenised, but not treated with lime.

2.3.   Test programme

It was intended that cementitious mineral growth would be observed by increases in values recorded for CBR (soaked and unsoaked) and strengths determined from 38mm unconsolidated undrained triaxial tests. Whilst it is acknowledged that the CBR test is not a strength test in the strict sense, it does reflect the properties of stiffness, shear strength and deformation (Biczysko, 1996), hence an increase in CBR value is an indication in the beneficial promotion of one, or all of these attributes. For simplicity it will be referred to herein as a strength indicator. With a view to linking any observed increases in strength with changes in moisture content and/or plasticity, classification tests after each curing period were also undertaken.

For the natural (untreated) batch, sub samples were conditioned, either by air drying or with added water), to achieve four separate moisture contents ranging between 27.7% (approx. corresponding with OMC) to 38.7%. A similar range of tests were performed on the natural material, however, other than for targeted comparison with the stabilised mixes these results will not specifically be reported.

Table 2: The preparation stages engaged to replicate the site process

Stage	Description	Detail
1	Binder 1 (quick lime) addition/ mixing	Quick lime addition to the average Initial consumption of lime value (3.53% by dry mass). Mixed for 10 minutes.
2	Mellowing	Clay clods thinned into an approx 50mm deep layer, covered with plastic and tamped. Material mellowed for 1 hour.
3	Disaggregation / Nucleation centres	Any lightly adhered clods separated manually. For mixes containing nucleation centres, 3.5% by dry weight was evenly spread over the surface.
4a	Binder 2A (SLS45)	Lime slurry addition in quantities to equal the same molar mass of CaO added in stage 2 (i.e. equivalent of 3.53% quicklime) Mixed for 6 minutes.
4b	Binder 2B (SLS45)	Further lime slurry added to bring total lime slurry addition to equate to an equivalent of 5% quicklime. Mixed for 4 minutes.
5a	Water A	50% of the mixing water added (523ml). Mix for 6.5 minutes.
5b	Water B	Remaining 50% of mixing water (523ml) added. Mix for 6.5 minutes

2.4.   Curing and Testing

All curing (in air or in water) was undertaken at a temperature of 20°C +/-2. All exposed sample surfaces were wrapped with several layers of cling film and the edges were sealed by parcel tape immediately after trimming to test dimensions. This was to prevent evaporation during curing. For CBR mould soaking, the process described by British Standards Institution (2004) was followed with the exception that the sample's top surface was left exposed to the water. The top perforated plate / surcharge rings were omitted as this comprises a more aggressive durability test. Soaking durations were 4 days for the 8 day cure samples and 28 days soaking for all others. Apart from stated deviations, testing was undertaken in accordance with the appropriate current British Standards. For the triaxial tests on stabilised samples, in

order to reflect the near surface environment of their typical application, cell pressures of 25, 50 and 75 kN/m^2 were used.

The following reference system is used: [Days cured]_[Test name (cell pressure)]_[If soaked]_[Binder Type] e.g. 7_CBR_S_Nuc or 32_TRI(50)_L.

3. RESULTS

At time of submission, results from the 8 day and 32 day curing periods were available. The 189 day cure results will be available by and presented at the IS-GI 2012 conference.

3.1. Classification tests

Table 3 contains the classification test results. This demonstrates that the mixing process increased the moisture content from 'as dug', however, it is apparent that the results of nucleation centre batches are, on average, 1.8% lower than the lime only mixes. This correlates with the reduction that would be expected from the extra 3.5% of solid mass added with the nucleation centres. In all cases the moisture content reduces following air curing and by 32 days this reduction was approx. 0.8%. Soaking appears to reinstate the moisture content to a similar, or slightly higher, level than the mixing value.

Following 8 days curing, liquid and plastic limits for both mixes had increased by 15-16%, which resulted in an effectively unchanged plasticity index (I_P) of 37-38%. The 32_L results indicated slight further increases in liquid limit (W_L) and plastic limit (W_P) combining to reduce I_P to 35%. The 32_Nuc results had a similarly reduced I_P of 34%, however, this was manifest through a small reduction in W_P with a notable reduction in W_L to 80%.

Table 3: Average moisture content and Atterberg limits for the binder treated batches. Atterberg's for natural material are shown for comparison. Moisture contents are the average of at least 4 tests (binder mixing) and up to 9 tests (cured batches). Atterberg's are the average of 2 (cured batches) or 3 (natural material) tests.

Batch	Moisture Content (%)				Atterberg Limits		
	Binder Mixing	Air Cure	Soak Cure	Difference between mix and air cure	W_P	W_L	I_P
Natural	Average natural moisture content = 35.4%				31	69	38
8_L	38.8	38.6	38.9	-0.2	48	85	37
32_L	38.8	38.0	39.4	-0.8	51	87	35
8_Nuc	37.3	36.7	37.4	-0.6	47	85	38
32_Nuc	36.7	35.9	37.0	-0.8	46	80	34

3.2. Strength Test Results

3.2.1. CBR

Table 4 illustrates the CBR results for all tested specimens. As might be expected, average CBR values for all specimens increase with prolonged curing. For both curing periods and conditions, the samples with the nucleation centres have higher CBR values than their lime only counterparts. The difference is most notable when comparing the 32 day soaked specimens, with the nucleation samples average CBR of 14.7% being 28% greater than the lime only average of 11.5%.

Table 4: Average CBR results for all tested specimen. All results are the average of 3 separate tests

	Air cure CBR (%)			% Increase from 8-32d (Ave)	Soaked CBR (%)			% Increase from 8-32d (ave)
	Top	Bottom	Ave		Top	Bottom	Ave	
8_CBR_L	9.7	12.0	10.9	35	9.4	11.2	10.3	12
32_CBR_L	14.2	15.1	14.7		10.0	12.9	11.5	
8_CBR_N	11.7	13.1	12.4	34	10.1	11.7	10.7	37
32_CBR_N	15.0	18.3	16.6		12.8	16.6	14.7	

3.2.2. 38mm unconsolidated undrained triaxial tests

Table 5 summarises the peak shear strength recorded on failure of the triaxial specimens and Figure 1 presents the stress / strain plots. For all samples the shear stress at failure increases with curing period and confining stress. For the 32 day cure samples, the strain at peak strength was notably reduced from those at 8 days. At 8 days cure it is clear that the nucleation samples are of superior strength. By 32 days, however, there is less discernable difference, especially at 75kN/m^2 confining stress, where shear strengths are almost identical at 154 and 156kN/m^2. This is considered further in Section 4.

Table 5: Triaxial test - shear stress at failure

	Shear Stress at failure		
Confining pressure (kN/m$_2$)	**25**	**50**	**75**
8_L (kN/m$_2$)	85	97	106
32_L (kN/m$_2$)	122	137	156
8-32 d increase (%)	*43*	*41*	*47*
8_Nuc (kN/m$_2$)	112	114	121
32_Nuc (kN/m$_2$)	130	144	154
8-32 d increase (%)	*16*	*26*	*27*
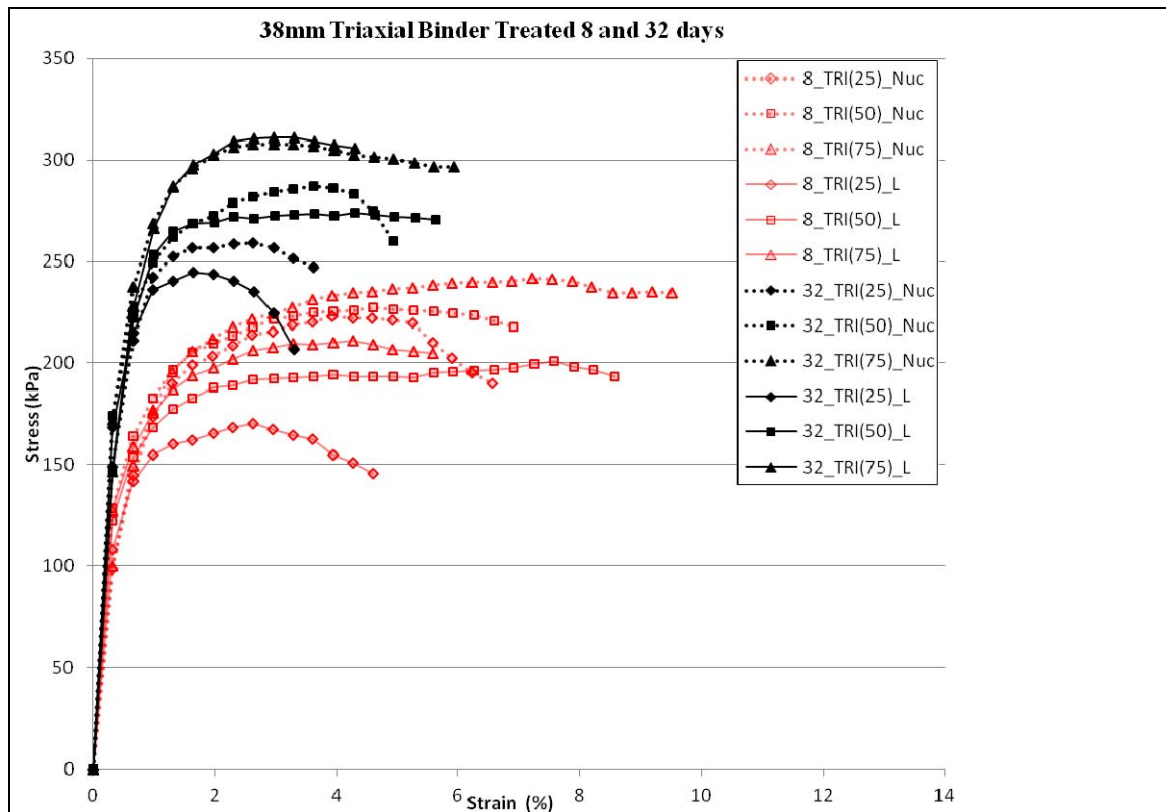
Figure 1: Stress / Strain plots from triaxial tests

3.3.   Sample Structure

3.3.1.   Triaxial tests

Observation of failure planes that developed during the triaxial tests on the binder treated samples indicated that the structure of the sample may have influenced the mode of failure. Figures 2a-d illustrate examples of the types of failure planes identified in the samples. Failure surfaces were typically rough, possessing either undulating, wavy or a stepped / jagged profile. Occasionally flat smooth areas were present, sometimes with striations (slickensides). Figure 2.a is an atypical example where slickensides have developed over much of the failure plane surface. The failure plane of some samples change considerably i.e. from a shallow to steep angle from the horizontal. This is either through abrupt angle changes (figure 2.b) or with a more gradual / curving profile (figure 2.d). Occasionally failure planes

were relatively straight (figure 2.c) although often minor stepping / jagged areas were still present. Other specimens displayed even more complex planes. Figure 2.a, illustrates a failure surface which appears relatively straight/diagonal on one side, yet with distance into the sample, rotates both out of plane and steepens to daylight in an irregular manner on the opposing side.

3.3.2. *CBR Tests*

Following completion of the CBR tests, the samples were broken up for classification testing. During this process for the 32 day cured samples, the presence of numerous isolated nodules surrounded by a matrix of softer material were identified. It was possible to scrape away the softer matrix to reveal the nodule's profile (figure 3.a). The larger nodules could be split in half with strong finger pressure (figure 3.b), which revealed they comprised intact clay material and not agglomerates of smaller clods. The nodules were typically stiff and friable which caused them to appear of lower moisture content than the relatively plastic matrix. The nodules were typically elongate and sub rounded with the long axis ranging in size from 10mm to 30mm. These features were present within lime and nucleation mixes and in the air cured and soaked CBR specimens. Although no attempt was made to measure this, it could be estimated that the nodules comprised approximately 30% of the sample volume.   It was also considered that the nodule representation appeared greater in the nucleation samples. However, in the absence of measurement, this is subjective. No nodules were observed in the 8 day cured samples, although, as they were not specifically sought at that stage, this does not evidence their complete absence.

a, 8_TRI(25)_N Slickensides on failure surface

b, 32_TRI(25)_L Abrupt change in failure plane

c, 32_TRI(75)_N. Wavy failure plane

d, 32_TRI(50)_L Curving failure plane

Figure 2 a-d: Triaxial sample failure planes evidencing a macrostructure within the sample. All photos were oven dried at 105°C prior to the picture being taken

Figure 3: a (left) 'Stiff' nodules recovered from 32_CBR_L. b (right) A nodule split in half.

4.   DISCUSSION

If the finely ground limestone centres were performing the function of nucleation centres, it may be anticipated that there would be a difference in strength values at an early stage, i.e. the 8 and 32 day curing periods selected. Indeed, the 8 day results reveal that all strength indicator tests for the nucleation centre mixes are greater than their lime only equivalents. This might be considered evidence of early nucleation. However, it may alternatively be considered that the strength difference is a residual function of the nucleation samples having a lower moisture content and therefore, higher dry density at preparation.

The 32-day results were less conclusive. The percentage increase in CBR results between the 8-32 day curing periods for both lime only and nucleation samples were near identical at 34% and 35%. Therefore, the nucleation specimens maintained the notably superior values identified at 8 days. The triaxial results, however, reveal that the lime only samples experienced a greater rate of strength gain (ca. 45%), than the lesser increase (16-27%) observed for the nucleation samples.   Accordingly, whilst the nucleation samples are typically of greater shear strength than the lime only, this is less marked at the lower confining stress and is not evident at $75kN/m^2$ cell pressure. Therefore, whilst the CBR results provide an indication that the nucleation mixes are stronger and certainly more durable to soaking, the triaxial tests do not provide complete agreement.

The consistency tests reveal some small changes with time. Most notably W_L and W_P results at 32 days are 5% and 7% lower (respectively) for the nucleation specimens. This difference may indicate different reaction rates. Literature reports on the change of Atterberg limits in response to lime treatment are variable and tend to focus on the modifications process. However, of the limited comments on Atterberg response over time, Sherwood (1993) suggests W_P and possibly W_L will increase as pozzolanic reactions develop.   As the W_L for the nucleation specimens appear to be reducing with curing time, strength increase and (presumed) pozzolanic reaction, this is an interesting contradiction.

It is suspected that the reason for a lack of clarity surrounding the results is the influence of the observed structure. For the natural clay samples (particularly the driest), it was suspected that the clod boundaries comprised a weakness which influenced failure. For the stabilised samples, clod boundaries may also comprise a weakness. However, the identification of hard nodules within the CBR samples suggests the shear strength would also be zonal, where an apparently weaker matrix separates the stiff nodules. With this structure, the failure planes would essentially link points of pre-existing weakness, stepping around strong locations, resulting in the irregular profiles described. Picarelli et al. (1988) noted that a similar mechanism occurred during undrained triaxial tests of an over-consolidated clay shale. Pre-existing planes within samples of this clay shale were considered to act as weaknesses, along which shear failure mobilised, but only following an initial period of high stiffness at small strains. At these small strains, it was considered that stress was relatively uniformly distributed through the entire sample. With increasing stress, the strain became localised at the weak planes and a dramatic reduction in stiffness occurred. Picarelli et al (1998) considered this rupture mechanism to be analogous to the failure of a jointed rock, where mass strength is dominated by the frictional resistance of the discontinuity and not by strength of the solid rock. This rock mechanics analogy may be completed by consideration of Hoek's (2007)

explanation that peak strength equates to the sum of cementing forces holding rock surfaces together plus frictional resistance. Hence, the stabilised soils would have a minimum 'cohesion' plus an increasing frictional contribution to shear strength with confining pressure. Such an increase with confining pressure is reflected by Figure 4.

It has been suggested that the stiff nodules have influenced the profile of the failure planes. Therefore, it is worthwhile considering how they developed. Petry & Wohlgemuth (1988) proposed that pozollanic reactions develop a coating on the surface of clay clods, which, in their study was considered to provide substantial durability against wetting/drying effects. It is possible that the stiff nodules noted in the present study have developed where pozzolanic reactions at the clod surface have essentially segregated the interior of the clod from the rest of the sample. This closed system appears to have been subject to different influences, with the internal region developing observably different engineering properties (stiff / friable) when compared with the matrix. The stiff nature of the nodule interior may be due to a lower moisture content and/or soil suction effects. Such a situation may be generated by the consumption of H_2O in the formation of the cementitous product at the periphery. Pozzolanic reaction within the nodule interior is another possibility. With a coating mechanism, it would be anticipated that where pozzolanic reaction has occurred at an accelerated rate, resilience to soaking would result. This may account for the superior soaked CBR values of the nucleation samples, thus potentially evidencing the nucleation process. It is suspected that further and widespread pozzolanic reaction at clod peripheries would cause the stiff nodules to increase in representation. By inspection this would lead to a reduction in the number of weak zones in the sample and sample strength would increase accordingly. If cementitious reaction is also able to bond adjoining clod surfaces together, then this may equate to the point where the underlying structure is overcome and the intact strength of the stiff clods would dominate. In such a scenario it would be anticipated that an inclined failure plane would shear triaxial samples at a relatively consistent angle, as might be anticipated for a 'normal' brittle failure. It will be interesting to see if this stage, or notable progression towards it, is evidenced in the 6 month results.

In view of the original aim, there is some suggestion in the CBR results, particularly the soaked CBRs, of early nucleation providing increased strength in the samples treated with finely ground limestone. Notwithstanding, the described interclod structure has provided weak planes, which appear to have influenced the results, in particular those of the triaxial tests. There is also the possibility that different moisture contents on preparation may account for some of the superior performance in nucleation samples. It may prove that with further curing time, i.e. upon testing of the 6 month cured samples, the strength difference and role may be clearer. It is necessary to use additional methods of enquiry in order to determine whether finely ground limestone do act as nucleation centres. The following additional works are currently underway:
1. Scanning Electron Microscopy analysis; to provide visual evidence (or otherwise) at a microscopic scale, of preferential nucleation around the limestone particle;
2. Further triaxial test specimens prepared at comparable moisture contents and cured for 8, 32 and 189 days. Intended to remove the moisture content anomaly and provide further information on the development of failure plane surfaces.
3. X-Ray Diffraction analysis of 32 and 189 day cures. To identify growth of new mineral phases.

5.   CONCLUSIONS

This paper has investigated the potential role that finely ground limestone, intermixed within a lime stabilised soil, may have as nucleation centres. An approach to producing test specimens in a manner which closely reflects UK site practice has also been described. The following conclusions are taken:
- The preparation method employed resulted in formation of a structure which appeared to influence the failure of all specimens. This structure was considered to form through the interlinking of weak areas around clay clod peripheries and its influence was observed through unusual failure planes in the triaxial specimens;
- Following 32 days curing, the development of stiff, friable nodules within a matrix of softer material was noted within all CBR mould specimens. The nodules were considered to have developed where pozzolanic reaction had occurred at the periphery of a clay clod. This coating appears to have led to enhanced engineering properties developing within the clod interior;
- Superior CBR values (most notably the soaked values) in the limestone treated specimens, may reflect the role that further and more widespread nucleation plays in enhancing the growth and distribution of the (above described) pozzolanic coating;
- At this stage it is not possible to conclude that finely ground limestone do provide a beneficial role as nucleation centres under the conditions investigated. This is due to the triaxial test results not

supporting the CBR results and possible dry density differences between the samples. Further works to remedy these conflicts is underway.

REFERENCES

Barker, J.E., Rogers, C.D.F. & Boardman, D.I., 2007, Ion migration associated with lime piles: A review, Ground Improvement, vol. 11, no. 2, pp. 87-98.

Bell, F.G., 1988, Stabilisation and treatment of clay soils with lime: Part 1, Ground Engineering, vol. 21, no. 1, pp. 10-15.

Biczysko, S.J., 1996, Long-Term Performance of Lime Stabilised Road Subgrade, Proceedings, seminar on Lime Stabilisation at Loughborough University, eds. C.D.F. Rogers, S. Glendinning & N. Dixon, Thomas Telford, pp. 62-71.

Boardman, D.I., Glendinning, S. & Rogers, C.D.F., 2001, Development of stabilisation and solidification in lime-clay mixes, Geotechnique, vol. 51, no. 6, pp. 533-543.

British Standards Institution, 2004, BS EN 13286-47: Unbound and hydraulically bound mixtures-Part 47:Test method for the determination of the California bearing ratio, immediate bearing index and linear swelling, BSI, London.

British Standards Institution, 2002, BS1377-4 Methods of test for soils for civil engineering purposes - Compaction related tests, BSI, Great Britain.

Diamond, D. & Kinter, E.B., 1965, Mechanisms of soil-lime stabilization: An interpretive review, Highways Research Board Record, vol. HRB 92, pp. 83-101.

Greaves, H.M., 1996, An Introduction To Lime Stabilisation, Proceedings, seminar on Lime Stabilisation, at Loughborough University, eds. C.D.F. Rogers, S. Glendinning & N. Dixon, Thomas Telford, pp. 5-12.

Hawkins, P., Tennis, P.T. & Detwiler, R.J.,2003, The Use of Limestone in Portland Cement: A state of the Art Review, Portland Cement Association, Illinois, USA.

Hoek, E., 2007,Practical Rock Engineering - Chapter 4: Discontinuities, . Available from: http://www.rocscience.com/education/hoeks_corner [accessed 7 November 2011].

Hunter, D., 1988, Lime induced heave in sulfate bearing clay soils, Journal of Geotechnical Engineering, vol. 114, no. 2, pp. 150-167.

Jalali, S., Abyaneh, M. & Keedwell, M., 1997, Differential Scanning Calorimetry Tests Applied to Lime-Fly Ash Soil Stabilization, Testing soils mixed with waste or recycled materials ASTM STP 1275, eds. M.A. Wasemiller & K.B. Hoddinott, American Society for Testing and Materials, pp. 181.

Perry, J., Macneil, D.J. & Wilson, P.E., 1996, The uses of Lime in Ground Engineering:a review of work undertaken at the Transport Research Laboratory, Proceedings, seminar on Lime Stabilisation, at Loughborough University, eds. C.D.F. Rogers, S. Glendinning & N. Dixon, pp. 27-41.

Petry, T.M. & Little, D.N., 2002, Review of stabilization of clays and expansive solis in pavements and lightly loaded structures - History, practice, and future, Journal of Materials in Civil Engineering, vol. 14, no. 6, pp. 447-460.

Petry, T.M. & Wohlgemuth, S.K., 1988, Effects of pulverization on the strength and durability of highly active clay soils stabilized with lime and portland cement, Transportation Research Record, vol. 1190, pp. 38-45.

Picarelli, L., Olivares, L., Maio Di, C. & Urciuoli, G., 1998, Properties and behaviour of tectonized clay shales in Italy, The geotechnics of hard soils - soft rocks; Proc. of the 2nd Int. symp. Vol.3, eds. A. Evangelista & L. Picarelli, Balkema A.A., pp. 1211.

Sherwood, P.T., 1993, Soil stabilization with cement and lime, HMSO, London.

The Highways Agency, 2007, Design Manual for Roads and Bridges, Vol 4.1, Part 6. HA74/07 Treatment of Fill and Capping Materials Using Either Lime or Cement or Both, Highways Agency, UK.

Wild, S., Kinuthia, J.M., Robinson, R.B. & Humpheys, I., 1996, Effects of ground granulated blast furnace slag (ggbs) on the strength and swelling properties of lime stabilised kaolinite in the presence of sulphates, Clay Minerals, vol. 31, no. 3, pp. 423-433.

Wilkinson, A., Haque, A. & Kodikara, J., 2010, Stabilisation of clayey soils with industrial by-products: part A, Proceedings of the ICE - Ground Improvement, vol. 163, no. 3, pp. 165-172.

Winter, N.B., 2009, Understanding Cement: An introduction to cement production, cement hydration and deleterious processes in concrete, WHD Microanalysis Consultants LTD, UK.

A non-traditional treatment for the compaction of fine-grained soils

Gaëtan Blanck, Laboratoire Environnement Géomécanique & Ouvrages,
Agence de l'Environnement et de la Maîtrise de l'Énergie, France, Gaetan.Blanck@ensg.inpl-nancy.fr
Olivier Cuisinier, Laboratoire Environnement Géomécanique & Ouvrages, France,
Olivier.Cuisinier@ensg.inpl-nancy.fr
Farimah Masrouri, Laboratoire Environnement Géomécanique & Ouvrages, France,
Farimah.Masrouri@ensg.inpl-nancy.fr

ABSTRACT

Sustainable development principles lead earthworks companies to use all natural extracted materials on construction sites. Most of the time, mechanical properties of these materials have to be improved, lime and cement being the traditional additives. In this context, the use of organic non-traditional products with limited environmental impact has been proposed, but their effects on soil behavior and stabilizing mechanisms are not well understood. The aim of this paper is to characterize the modification of geotechnical properties of three fine graded soils treated with an acid solution (AS) containing sulfonated limonene, a byproduct of the citrus industry. Investigations including Proctor compaction and unconfined compressive strength measurements were performed.

For one of the tested soils, the experimental results showed a reduction of the optimum Proctor water content that induced an improvement of the unconfined compressive strength of the treated soil. The modifications of compaction characteristics observed for two soils allowed a better compaction especially on the dry side of the Proctor curve. For dry soils, such modifications can reduce water and energy consumption during the compaction step. However, the effects of the treatment appeared to be highly dependent on soil nature.

1.   INTRODUCTION

Sustainable development in earthworks is a growing issue which tend to modify the companies practices. The aim of this environmental approach is to limit the impacts of earth constructions and imply to use most of natural materials extracted within the construction site, even materials with very low geotechnical characteristics. But sustainable development also involves the reduction of energy and water consumption in order to limit the emission of greenhouse gases. On the first hand, the common solution to improve the geotechnical properties of a soil is the addition of lime, cement or fly ash. On the other hand, in last two decades, lots of "non-traditional" additives have been developed. These additives are diverse in nature and some of them derivate from industrial transformation of renewable raw materials. Various additives have been tested for improving diverse purposes such as the compaction of dry soils for limiting dust generation (Scholen, 1995; Surdahl, 2007) or the stabilisation of erodible soils (Vinod *et al.,* 2010). Mechanical properties such as unconfined compressive strength (Santoni *et al.* 2002; Tingle & Santoni, 2003) or swelling potential of plastic soils (Rajendran & Lytton, 1997; Harris *et al.* 2006) were also studied.

Non-traditional stabilisers can be grouped into three large categories. The first one includes inorganic salts and acids. The second one includes organic products such as acid solutions of sulfonated naphthalene or limonene, enzymatic solutions, lignosulfonates and tree resin emulsions. The last category is composed of by-products of oil industry such as synthetic polymer or petroleum emulsions. In this study, a representative acid solution containing sulfonated limonene was tested.

Acid solutions are suspected to stabilise the soils by dissolution of clay minerals leading to the formation of more stable phases (Scholen, 1995). Cation exchange leading to flocculation-aggregation is also mentioned by this author but experimental results do not confirm these mechanisms. After acid treatments, Katz *et al.* (2001) and Rauch *et al.* (2003) observed that X-ray diffraction, specific surface area and cation exchange capacity of tested clayey soils were not modified by the treatment even for application rates as high as 50% of dry weight of soil. Moreover, scanning electron microscopy pictures obtained by Katz *et al.* (2001) showed similar structures for the acid treated and untreated soils. Marquart (1995) supposed that the effectiveness of acid treatments is affected by the presence of carbonate in the soil.

Soil treatment with non-traditional acid solutions was studied by different authors. Scholen, (1995) reported the use of acid solutions for the stabilisation of uncovered roads between 1991 and 1993. In 1995, no particular failure of the treated sections was reported. Visser, (2007) also reported results of *in situ* studies undertaken in South Africa on four low plastic soils (PI ranging from 4 to 12). The author noticed improvements of 10 to 130% of the I_{CBR} values measured on the treated sections after a curing period of 8 months.

Swelling properties of plastic soils treated with acid solutions were tested by Rauch *et al.* (2002) and Harris *et al.* (2006). Rauch *et al.* (2002) treated two plastic soils (IP = 37 and 38) with 0.017% of an acid solution containing sulfonated limonene but they did not observed any modification of the swelling potential of the soil. On the contrary, Harris *et al.* (2006) showed reduction of about 7% of the swelling potential of high plastic clay after the addition of 0.23% of an acid solution. The swelling potential of the untreated soil was measured to be between 17 and 23%. Other mechanical properties such as unconfined compressive strength of low plastic clay (Tingle & Santoni, 2003) and silty sand (Santoni *et al.* 2002) was not modified by the addition of different amount of an acid solution. In some studies (Rajendran & Lytton, 1997 and Rauch *et al.* 2003), modifications of the compaction properties of treated soils were shown, but no consistent trend was observed.

2. MATERIALS AND METHODS

2.1. Acid solution

The non-traditional additive selected for this study was an aqueous solution of sulphuric acid mixed with sulfonated D-limonene, a by-product of citrus processing. Recommended application rate by product's provider was $0.2 \, L/m^3$. As the density of the concentrated solution was $1.15 \, Mg/m^3$ and the maximal dry density of the soil estimated to be $16 \, kN/m^3$, a reference dosage of 0.014% of concentrated product by dry weight of the soil was applied. The product is stored in sealed containers according to provider's recommendations.

2.2. Soils

Three natural fine graded soils were tested. Before testing, the soils were sieved at 5 mm and dried at 60°C. Their geotechnical properties are listed in Table 1. As calcium carbonate is suspected to influence the effectiveness of the treatment, a soil with high calcium carbonate content was chosen for this study.

Table 1: Geotechnical properties of the three soils

Property	Silt 1	Silt 2	Silt 3
	Granulometry		
Passing 5 mm (%)	99.9	99.9	100.0
Passing 80 µm (%)	89.6	95.0	97.1
Passing 2 µm (%)	32	25	26
	Plasticity index		
Plastic limit (%)	29	28	28
Liquid limit (%)	50	37	39
Plasticity index	21	9	11
	Carbonate content		
$CaCO_3$ (%)	0.1	1.3	22.3

2.3. Treatment procedure

For the preparation of all samples, a first quantity of distilled water was added to the dry material to achieve a water content of 10%. Then, the soil was stored in sealed containers at 20°C for 16 hours to reach the moisture equilibrium. After this period, the required quantity of additive was mixed with the amount of water needed to obtain the total desired water content. The mixture was allowed to cure for one hour in a sealed container before samples preparation.

2.4. Experimental program

For each soil, the effect of the treatment at the reference dosage on the compaction properties and unconfined compressive strength (UCS) were tested. To test the sensitivity of compaction results and UCS to the dosage of acid solution (AS), dosages between 0.004 and 0.0032% were tested on the silt 1.

The effect of curing period on the UCS of the silt 1 was also tested by measuring UCSs of treated samples at different curing times between 1 and 60 days.

3.   EXPERIMENTAL RESULTS

3.1.   Compaction

Compaction tests were performed according to ASTM D 698-91 using a standard Proctor effort. The compaction curves of silt 1 treated with different dosages of AS are plotted on the Figures 1 and 2. Figure 1 shows compaction curves after reduction of the treatment dosage. Figure 2 shows the result of the reference dosage (0.014%) and of the addition of twice the reference dosage. Optimum water content (w_{opt}) and maximum dry unit weight (γ_{dmax}) are summarized in Table 2.
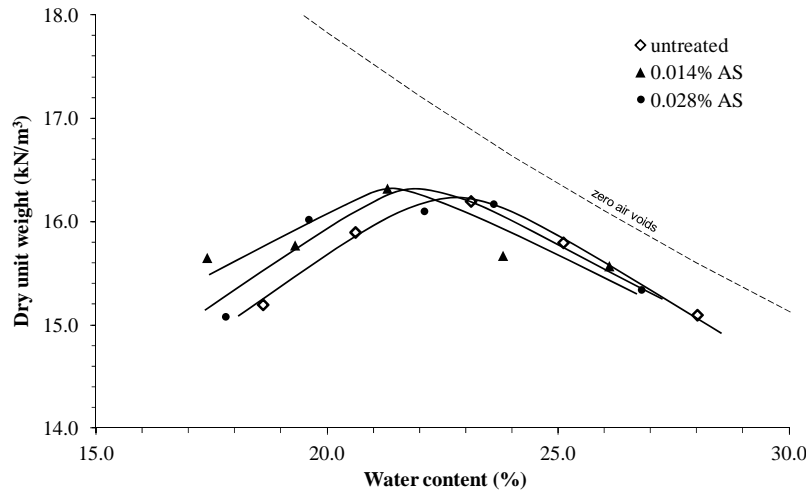
Figure 1: Compaction curves of the silt 1 after the addition of 0.004 to 0.014% of AS
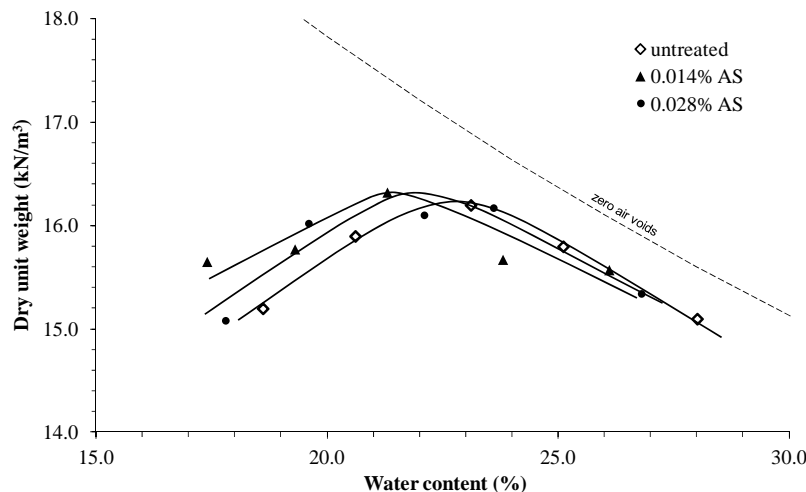
Figure 2: Compaction curves of the silt 1 after the addition of 0.014 and 0.028% of AS

The addition of 0.014% of acid solution by dry weight of silt 1 induced a reduction of 2% of the optimum water content, $w_{opt} = 21.2\%$ after treatment, instead of $w_{opt} = 23.1\%$ for the untreated soil. The maximum dry density was not affected by the treatment at the reference dosage. When the dosage of AS is reduced (Figure 1) or increased (Figure 2), the value of the observed reduction of w_{opt} remain constant but the maximal dry density is slightly modified with a maximal increase for the lowest dosage (Table 2). On the dry side of the compaction curve ($w < w_{opt}$) an increase in dry density was observed for all tested dosages. This result indicates that the treatment made the soil easier to compact.

Blanck - A non-traditional treatment for the compaction of fine-grained soils

Table 2: Standard Proctor compaction characteristics for the silt 1 treated at different dosages of acid solution

Silt 1		
Dosage (%)	Properties of compaction optimum	
	γ_{dmax} (Mg/m³)	w_{opt} (%)
Untreated	1.62	23.2
0.004%	1.65	21.0
0.007%	1.64	21.5
0.014%	1.63	21.3
0.028%	1.62	21.5

Figures 3 and 4 respectively show the effects on the compaction curves of the addition of 0.014% of AS for the silt 2 and 3.
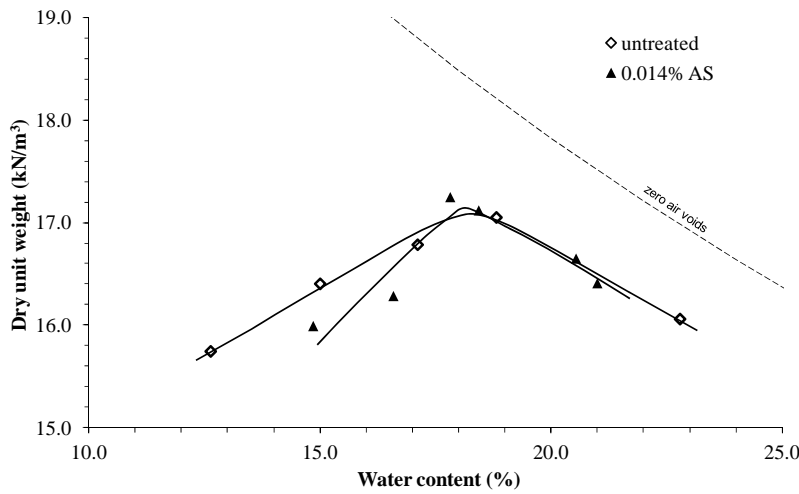
Figure 3: Compaction curves of the silt 2 after the addition of 0.014% of AS
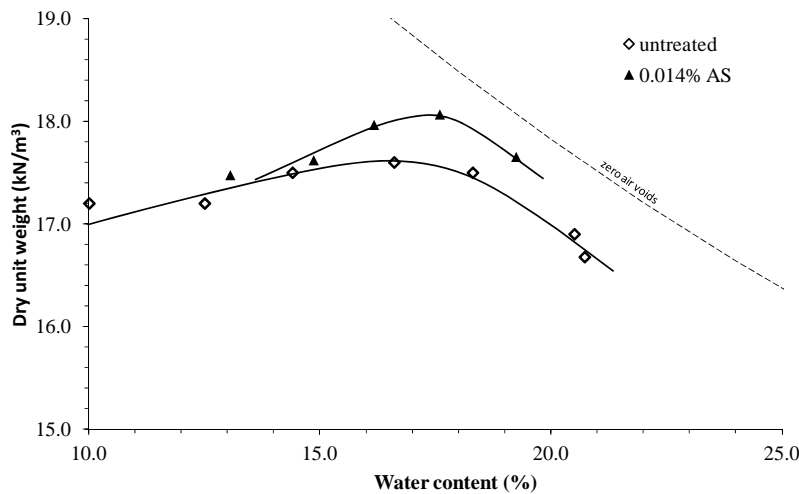
Figure 4: Compaction curves of the silt 3 after the addition of 0.014% of AS

The addition of AS to the silt 2 induced a reduction of the dry density obtained on the dry side of the compaction curve but the compaction optimum was not modified by the treatment. The silt 3 behaved differently after treatment. An increase of the maximal dry unit weight by 0.5 kN/m³ without modification of w_{opt} was observed (γ_{dmax} = 18.1kN/m³ after treatment and γ_{dmax} = 17.6 kN/m³ for the untreated soil).

Table 3: Standard Proctor compaction characteristics for the three soils

Properties of compaction optimum	Silt 1		Silt 2		Silt 3	
	untreated	AS 0.014 %	untreated	AS 0.014 %	untreated	AS 0.014 %
γ_{dmax} (Mg/m³)	16.2	16.3	17.1	17.2	17.6	18.1
w_{opt} (%)	23.1	21.2	18.5	18.3	16.5	17.5

3.2. Unconfined compressive strength

The effect of the acid treatment on the unconfined compressive strength resistance was studied for the three soils. For each curing time, three replicate specimens were statically compacted in one layer in a cylindrical mould of 100-mm-high and 50-mm-diameter. For each soil and treatment dosage, samples were compacted at their respective w_{opt} and γ_{dmax} as summarized in Table 2 and 3. To avoid desiccation, specimens were wrapped in a plastic film, covered by an aluminium sheet and stored in a plastic container at 20°C. Geometrical parameters, weight and water content were controlled at the confection and just before testing.

Figure 5 shows the results obtained after different curing periods for the three soils treated with 0.014% of acid solution. To judge of the dispersion of the results, standard deviation bars are drawn for each result. For the silt 1, the addition of 0.014% of acid solution induced an improvement of the UCS from 0.15 MPa to roughly 0.4 MPa. For both other soils, modifications of the UCSs were not significant in comparison with untreated samples. Moreover, no evolution of the UCSs values with the time was observed. This means that the initial increase in UCS was essentially due to the reduction of w_{opt} induced by the treatment for the silt 1 (Table 3).
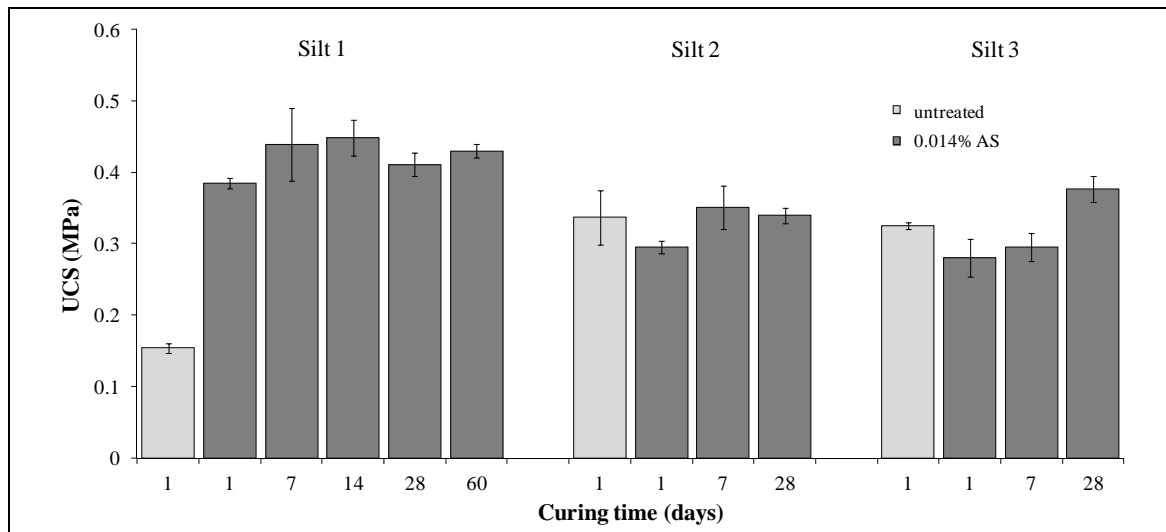
Figure 5: Evolution of unconfined compressive strengths for the studied soils treated with 0.014% of acid solution.

4. DISCUSSION

The experimental results on compaction and unconfined compressive strength of three silts treated with an acid non-traditional additive showed that:
- The treatment of the silt 1 induced a reduction of the optimal water content of about 2% for the four tested dosages. The maximal dry density was slightly increased by lowering the dosages and significant improvement of the dry densities were observed on the dry side of the compaction curve. This treatment induced an increase of unconfined compressive strength of about 300% in comparison of untreated soil. These results could have interesting implications for the compaction of dry soils which should normally be wetted. In this case, the treatment of the soil allows to compact it at a 2% reduced water content with an increase in its UCS resistance. Moreover, less compaction energy is required to achieve a specified dry density for $w < w_{opt}$. Thus, in arid or semi-arid countries where the water resources are lacking, the treatment with such an acid additive can improve the environmental balance of earthwork projects.

- For the silt 2, geotechnical properties were not significantly modified by the treatment. No particular application can be recommended in this case.
- The increase in the dry densities of the silt 3 indicates that the treatment made this soil easier to compact, thus as for silt 1, compaction energy savings can be made.

Globally, the treatment of the studied soils with the selected acid solution tends to make their compaction easier, but experimental results also appeared to be dependent on the soil nature. Moreover no conclusion can be drawn on the influence of the carbonate content on the efficiency of the treatment. For traditional treatments, the presence of chemical substances such as sulphates can make the treatment inefficient. As for traditional treatments, chemical substances may have activating or inhibiting effects on non-traditional treatments. For the acid solution tested in this study, the suspected presence of significant quantities of iron oxides in the silt 1 indicated by the pronounced red colour of the soil should be an activator of the treatment. But for the moment, the potential chemical mechanism of interaction between iron oxides and the treatment product is not known.

In order to gain a better understanding of the effects of this family of non-traditional additives, investigations should be done on the stabilization mechanisms of such products.

5. CONCLUSION

The treatment of three silts with an acid non-traditional additive induced mechanical properties modifications of the soils. Compaction properties and unconfined compressive strength were modified by the treatment especially for the silt 1. For the silts 1 and 3, the treatment allows a better compaction at lower water contents which have particularly interesting implications for the compaction of dry soils. In this case, the amount of water and energy needed to achieve a specified dry density are reduced contributing to lower the environmental impacts of earthworks projects.

REFERENCES

Harris P., Holdt J v., Sebesta S., Scullion T., 2006, Recommendations for stabilization of high-sulfate soils in Texas, Transportation Research Record : Journal of the Transportation Research Board, No. 1952, pp. 71–79, Washington D.C.

Katz L.E., Rauch A.F., Liljestrand H.M., Harmon J.S., Shaw K.S., Albers H., 2001, Mechanisms of soil stabilization with liquid ionic stabilizer, Transportation Research Record : Journal of the Transportation Research Board, No. 1757, pp. 50–57, Washington D.C.

Marquart D.K., 1995, Chemical Stabilization of three Texas Vertisols with Sulfonated Naphthalene, MS thesis, A&M University, College Station.

Rajendran D., Lytton R.L., 1997, Reduction of Sulfate Swell in Expansive Clay Subgrade in the Dallas District, Research Report TX-98/3929-1, Texas Transportation Institute, College Station.

Rauch A.F., Katz L.E., Liljestrand H.M., 2003, An analysis of the mechanisms and efficacy of three liquid chemical soil stabilizers : volume 1, Report FHWA/TX-03/1993-1, Center for transportation research, University of Texas, Austin

Rauch A.F., Harmon J.S., Katz L.E., Liljestrand H.M., 2002, Measured effects of liquid soil stabilizers on engineering properties of clay, Transportation Research Record : Journal of the Transportation Research Board, No. 1787, pp. 33 – 41, Washington D.C.

Santoni R.L., Tingle J.S., Webster S.L., 2002, Stabilization of silty sand with nontraditional additives, Transportation Research Record : Journal of the Transportation Research Board, No. 1787, pp. 61–70, Washington, D.C.

Scholen D.E., 1995, Stabilizer mechanisms in nonstandard stabilizers, Conference Proceedings 6 : Sixth International Conference on Low-Volume Roads, Vol.2, pp. 252–260, TRB National Research Council, Washington, D.C.

Surdahl R.W., Woll J.H., Marquez H.R., 2007, Stabilization and dust control at the Buenos Aires national wildlife refuge, Arizona, Transportation Research Record: Journal of the Transportation Research Board, No. 1989, Vol.1, pp. 312 – 321, Washington D.C.

Tingle J.S. et Santoni R.L., 2003, Stabilization of clay soils with non traditional additives, Transportation Research Record : Journal of the Transportation Research Board, No. 1819, Vol.2, pp. 72 – 84, Washington D.C.

Vinod J.S., Indraratna B., Mahamud M.A.A., 2010, Stabilisation of an erodible soil using a chemical admixture, Proceedings of the institution of civil engineers: Ground Improvement, Vol. 163, pp. 43-51.

Visser A.T., 2007, Procedure for evaluating stabilization of road materials with nontraditional stabilizers, Transportation Research Record : Journal of the Transportation Research Board, No. 1989, Vol.2, pp. 21 – 26, Washington D.C.

Chemical Stabilization of Subgrades for Better Support of Highway Infrastructure

Bhaskar Chittoori, Faculty Associate-Research, University of Texas at Arlington, USA, sinu@uta.edu
Anand J Puppala, University of Texas at Arlington, USA, anand@uta.edu

ABSTRACT

Majority of state highway agencies select stabilization methods based on soil types, and traffic loads. These practices vary from state to state in the USA. One common factor among these designs is the dependency of stabilizer selection based on soil plasticity properties. This practice is not always effective, yet no modifications are suggested to the designs. Recent research in Texas explored the causes of poor stabilization problems experienced in the field. This research eventually resulted in the understanding dominant clay mineral and durability issues related to soil-chemical reactions. This paper presents results of the experimental studies that provided insights into the importance of clay mineralogy factors as well as durability study results. Also, a proposed modification to existing design soil stabilization practices that account for clay mineralogy and permanency aspects of chemical treatments is presented.

1.   INTRODUCTION AND BACKGROUND

Pavements are usually designed based on the assumption that specified levels of improvement will be achieved for each soil layer in the pavement system (Huang, 2002). Each layer within the pavement system must resist shearing within the layer, avoid excessive elastic deformations that would result in fatigue cracking within the layer or in overlying layers, and also prevent excessive permanent deformation through densification. Improved or stabilized soil layer has the ability to distribute the load over a greater area which permits a reduction in the required thickness of the soil and surface layers (Sherwood, 1995). Generally, the soil quality improvements through stabilization include reduction of plasticity index or swelling potential, enhancements of workability and increase in durability performance and maintain sustained strength over a design time period. Typically, the tensile strength and stiffness of a soil layer can be improved through the use of chemical additives and thereby permit a reduction in the thickness of the stabilized layer and overlying layers within the pavement system (TM 5-822-14/AFJMAN 32-1019).

Soil stabilization has been a topic of interest and discussion for many years now, due to potential reduction in the construction and maintenance costs when the pavement infrastructure is built on problem grounds. Moreover, soil treatment enhances riding comforts to travellers. Extensive research was documented with regard to the engineering properties, reliability and durability of various types of stabilized materials (Tayabji, 1982; Haussman, 1989; Puppala et al., 2006). However, many state Departments of Transportation (DOTs) in the United States have had problems with subgrade failure due to a loss of stabilizer with time, or a stabilizer being ineffective in some soils while other soils with the same index properties respond well to that stabilizer (Little et al., 2000).

Mixing soils with stabilizing agents such as lime and cement, usually in low amounts, alter both physical and chemical properties of the stabilized soils. The commonly used stabilizers in the civil engineering practice are lime and cement, and sometimes these are used in combination. Other stabilizers including fly ash, pozzalons, blast furnace slag and several others are also used. The selection and determination of the percentage of chemical additives depend upon the soil classification and the degree of improvement desired. In general, smaller dosages of chemical additives are required to alter soil properties such as gradation, workability, and plasticit. Slightly larger dosages are needed to improve the strength and durability. Overal a balance mix design is needed to satisfy both the criteria. Figure 1 presents a typical stabilizer design procedure.

In several pavement sections built on chemically treated high plastic clays, the amount of stabilizer was often found to be not sufficient to produce a stable subgrade foundation system to support the pavement structure. These problems are attributed to the limitations of the stabilizer design methods for selecting and designing the optimal additive content for subsoil layers. One such limitation is the lack of understanding of the complex interactions between the clay mineralogy of a given soil and the chemical

additives used for soil stabilization. Also, the design procedure is time consuming and hence, the specifications are bypassed and the design is conducted based on the local experience. However, several premature failures of pavements on stabilized subgrade soils and poor long-term performance of the treated soils have prompted a research study to incorporate both clay mineralogy and durability issues in the stabilizer mix design guidelines.

Pavement projects constructed over stabilized subsoils have achieved satisfactory results. However, challenges still remain in the optimal design and use of stabilized subgrade materials as treated bases to support pavements. Other challenges in stabilization designs include developing a better understanding of the long-term performance of the stabilized materials, better construction methods and use proper quality assurance/quality control (QA/QC) procedures that are effective predictors of the long-term performance of pavement infrastructure with minimal distress problems (Little et al., 2000). One measure of this long-term efficacy of a stabilized material is the performance of the treated material due to moisture conditioning. Currently stabilization design guides have not accounted for the durability of the stabilization and also leaching of chemicals due to constant moisture ingress into the treated soils (Chittoori et al, 2008; Pedarla et al., 2011).

In this research, an attempt is made to address these limitations in the soil stabilization by studying clay mineralogy aspects into the stabilization design process. Durability studies to address the long-term effectiveness of the stabilization are also incorporated into the stabilization design principles.
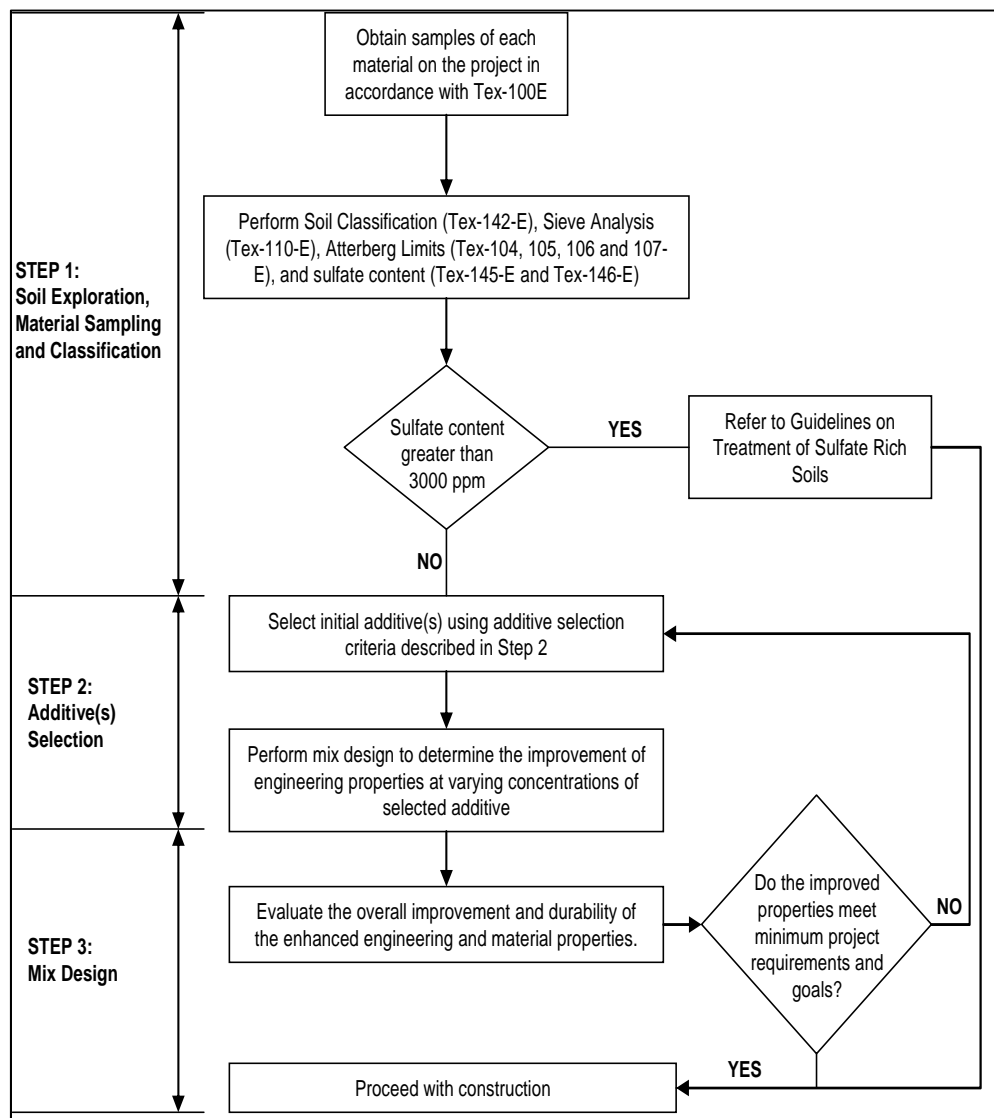

Figure 1: Flowchart for subgrade soil treatment (from TxDOT Guidelines)

2.   EXPERIMENTAL STUDIES

This research study was conducted in two phases. The first phase consisted of developing a model for the determination of dominating clay mineral in the soils. A total of twenty soils were collected with the help of Texas Department of Transportation (TxDOT) districts from different parts of Texas to include various types of clay mineralogies expected in the state of Texas. Fifteen of the twenty soils collected were used for developing the model and the remaining five were used for validating the developed model. Three chemical properties of soil namely Cation Exchange Capacity (CEC), Specific Surface Area (SSA) and Total Potassium (TP) are used for the determination of the dominating clay mineral. The reader is referred to Chittoori and Puppala (2011) for further details of the developed model.

For the second phase, six soils with distinct mineralogies were selected. Stabilizer mix design was performed on these soils and the stabilized soils are investigated for long-term durability by subjecting the compacted soil specimens to moisture fluctuations simulating summer and winter seasons in the field conditions. Table 1 shows the gradation and Atterberg details of the soils along with their soil classification. The mix design was perfoemd as per TxDOT design manual using lime as an additive and the amount of lime required to achieve a minimum strength requirement of 50 psi was established.

Table 1: Gradation, Atterberg limits and soil classification details for soils under study

S No.	Soil	Gradation, %				Atterberg Limits			Classification
		Gravel	Sand	Silt	Clay	LL	PL	PI	USCS
1	Austin	0	5	38	57	41	17	34	CH
2	Bryan	0	13	40	47	45	14	31	CL
3	El Paso	0	37	42	21	30	14	16	CL
4	Fort Worth	0	11	37	52	61	32	29	CH
5	Keller	0	18	45	37	25	14	11	CL
6	Paris	0	9	45	46	60	24	36	CH

Once the additive amount was determined, durability of the chemically treated soils was investigated by exposing the treated soil specimens to various cycles of wetting and drying conditions in the laboratory environment. During these processes, volume change, strength and stiffness properties were determined and monitored. These properties provided insights into the effects of seasonal moisture content fluctuations on the soil property variations. ASTM D 559 method is the standard method often used for these wet-dry cycles based durability investigations on chemically treated soils. Hence, the procedure outlined by ASTM D-559 method was closely followed, which simulates both wet and dry cycle conditions close to local weather conditions in a reasonably short time period. Soil specimens were allowed to swell and shrink in both lateral and vertical directions. Prior studies by Punthutaecha et al. (2006) have proved that the volumetric swell/shrink strains obtained by allowing lateral movements along with vertical movements are in close agreement with the field measured volume changes than those obtained by restraining the lateral movement.

According to the ASTM D 559 the soil specimens should be prepared and cured. Each wet-dry cycle consists of submerging the soil sample in water for 5 hours and then placing them in a 60°C oven for 42 hours. After removal from the oven, the specimen is subjected to volume change and strength measurements. The test was then continued until 21 wet-dry cycles or until the specimens failed. The test setup can be seen in Figure 2. During wetting and drying periods sample size changes were measured in all the three dimensions. The Vertical movement is measured with the help of a dial gauge and the radial movements are measured using a "pi tape". The wetting/drying was continued for 21 cycles. After 3, 7, 14 and 21 cycles the specimens were subjected to UCS tests.

3.   RESULTS AND DISCUSSION

Table 1 summarises the results obtained from this study highlighting the number of cycles sample survived and the total volumetric change the sample experienced in those number of cycles. It should be noted here that the stabilizer design was carried out by following current TxDOTs plasticity index based design procedure and this study clearly showed that three out of six soils would have had premature failures if treated by using this procedure.
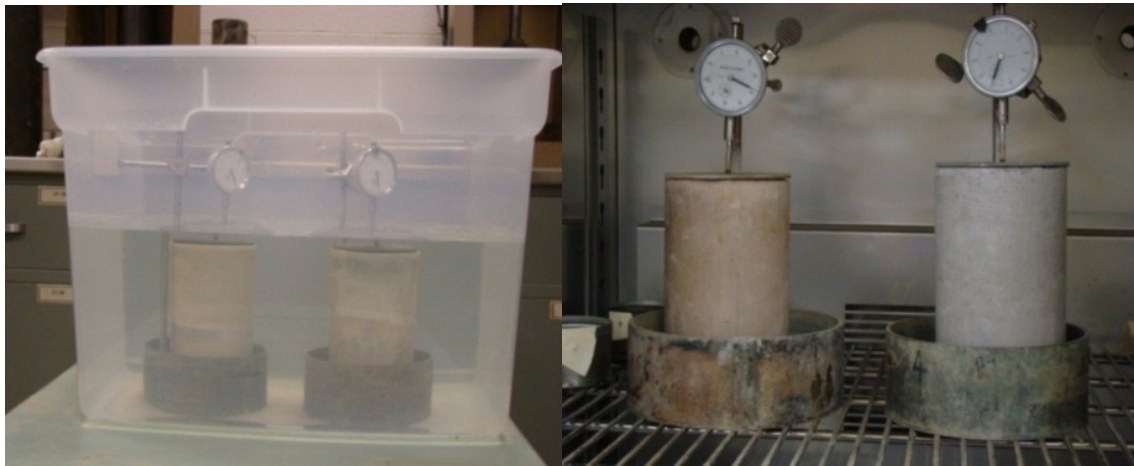
a)   b)

Figure 2: Apparatus used for the wet/dry studies: a) Wetting b) Drying

In order to understand the shortcomings of the design process and the variables affecting the stabilizer design methods, the following two plots were made. Figure 3 shows a plot between the plasticity index or PI of the soil and the number of wet/dry cycles that the soil specimen survived in durability studies. This figure shows that as the PI of the soil increases, the likelyhood of having premature failures is higher. This indicates the fallacy of the he current stabilizer design procedures when using it to design stabilizers for high plastic soil. However, Bryan soil with a PI of 31 survived all twenty one cycles with low volume changes hence this counters the previous argument that the current design procedures do not hold good for higher PI soils. Overall, this indicates that the PI of the soil alone is not the deciding factor for the stabilization performance of a given soil. Hence further investigations were attempted to determine the clay mineralogies including the percentage of the Montmorillonite of the tested soils.

Table 2: Summary of test results

Soil	PI, %	Dominating clay mineral	% M	Additive content, (% by weight)	# of cycles sample survived	Total volumetric change, %
Austin	34	M	53	6%	7	15
Bryan	31	K	37	8%	21	6
El Paso	16	I	23	8%	21	12
Fort Worth	29	M	60	6%	10	15
Keller	11	K	20	6%	21	5
Paris	36	M	70	8%	7	15

Note: M – Montmorillonite, K – Kaolinite, I – Illite, PI – Plasticity Index

Figure 4 presents a plot between the percentage Montmorillonite of the treated soil and the number of wet/dry cycles the sample survived after stabilization. This plot shows that as the percentage of Montmorillonite of the soil increases the likelyhood of having premature failures is higher. This confirms that the current stabilizer design procedures need to be changed for high Montmorillonite soils. Also, this clearly explains the reason behind Bryan soil with a PI value of 31, survived all twenty one cycles with very little volume change; as this behavior is attributed to low percentage Montmorillonite content in this soil.
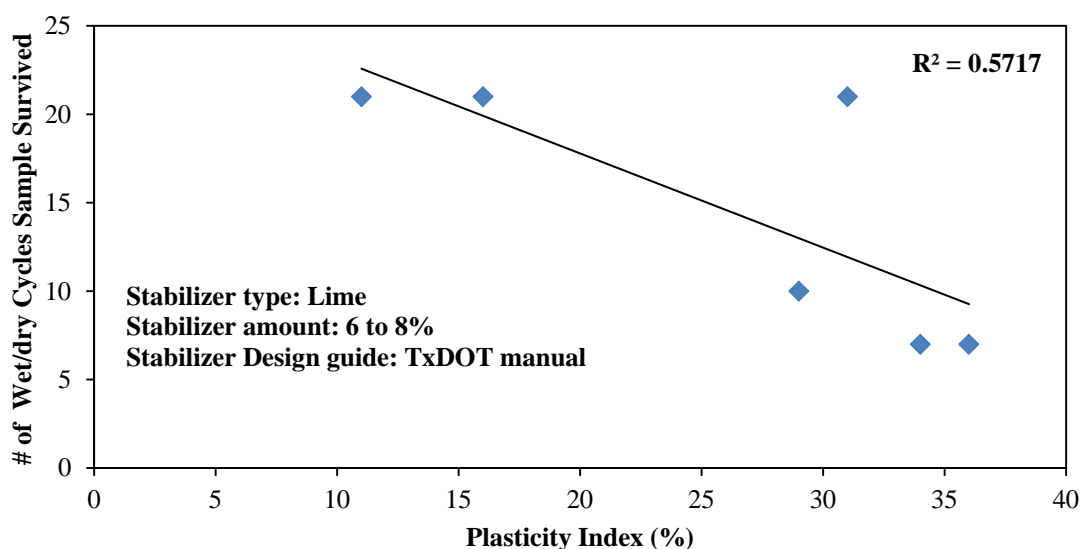
Figure 3:Variation of # of cycles lime stabilized sample survived with plasticity index of the soil
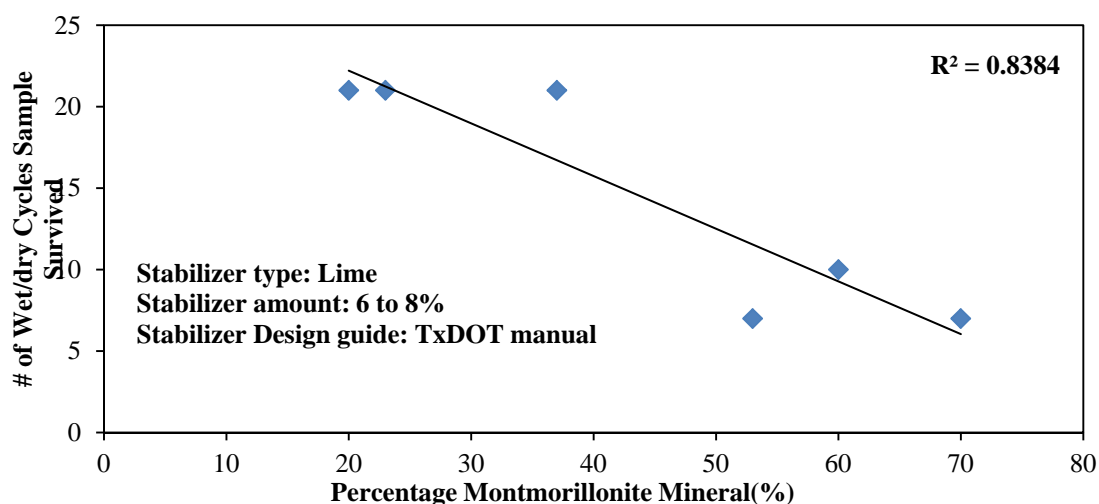
Figure 4: Variation of # of cycles lime stabilized sample survived with percentage Montmorillonite mineral of the soil

Overall, in this study, it was found that the selection of type and concentration of additives based on gradation and plasticity is not adequate. For example, two subgrades with the same plasticity indices (PIs) react differently to the same stabilizer depending on the dominant clay type in the fines. A lack of a more refined soil classification that considers the clay mineralogy creates a dilemma whether a certain chemical treatment method could be used for all types of clayey subgrades. Hence, better and more reliable strategies are needed for screening clay mineralogy for successful use of a given stabilizer. Hence, based on the current laboratory testing, the following recommendations are made:

Aside from the gradation and PI properties, the clay mineralogy impacts the concentration of the additives the most. It is recommended to include this information in the stabilization design process. Direct measurements of the clay mineralogy utilizing X-Ray Diffraction (XRD) and Scanning Electron Microscope (SEM) are not practical for day-to-day use since they are expensive to perform and require advanced instrumentation. Hence a set of simple chemical tests, such as cationic exchange capacity (CEC), specific surface area (SSA) and total potassium (TP) are recommended to estimate the dominating clay minerals in the subgrades.

Figure 5 presents the flowchart that is being used in the field as per the current TxDOT stabilization guide lines for reference with the insertion of additional chemical analyses and an accelerated mix design steps based on the present research observations.
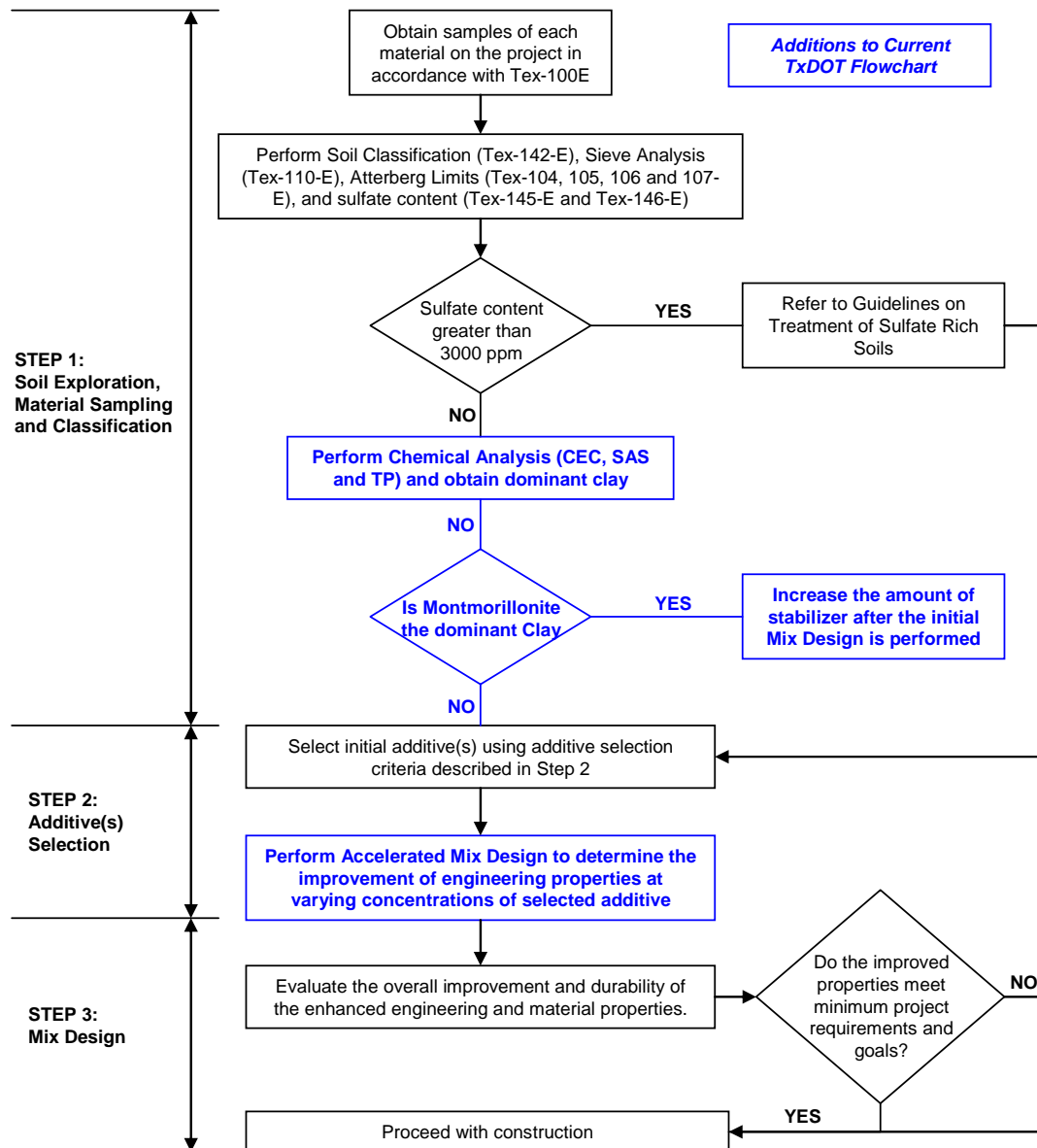
Figure 5: Proposed guidelines for subgrade soil treatment

4.   SUMMARY AND CONCLUSIONS

In this research an attempt is made to identify the causes of these premature failures and based on these causes, new/improved guide lines are outlined for the better design of stabilizers in the field. One of the causes of the problem was lack of understanding of the chemical interactions between the stabilizer and the soil minerals. Also, durability and permanency related stabilization studies were needed to understand the effect of the clay mineralogy on the long-term performance of stabilized expansive soils.

The second task was to assess the effects of clay minerals on the long-term durability of stabilized expansive clays by conducting wetting/drying (W/D) studies replicating moisture fluctuations expected during summer and winter seasons in the field. It has been interpreted from tests performed on several soils and their results that the effects of clay mineralogy on the long-term performance of stabilized expansive soils is evident. The results of all the eight soils showed that if the dominating clay mineral was montmorillonite, then durability of stabilizers will be a concern. A proposed design chart with modifications by incorporating clay mineralogy measurements is also presented for future stabilization mix designs.

REFERENCES

Huang, H.Y. (2004). "Pavement analysis and design." 2nd ed., Prentice Hall, Boston.

Sherwood, P. T. (1995). "Soil Stabilization with Cement and lime: State of the Art-review." HMSO, London.

TM 5-822-14/AFJMAN 32-1019 – "Soil Stabilization for pavements", Technical manual for Army, Navy and Air Force - "http://armypubs.army.mil/eng/DR_pubs/DR_a/pdf/tm5_822_14.pdf"

Tayabji, S. D., Nussbaum, P. J. and Ciolko, A. T. (1982). "Evaluation of Heavily Loaded Cement-Stabilized Bases." Transportation Research Record, TRB, National Research Council, Washington, D.C., 839, 6-11.

Hausmann, M. R. (1989). "Engineering Principles of Ground Modification." McGraw-Hill, New York.

Pedarla, A., Chittoori, B. and Puppala, A. (2011). "Influence of mineralogy and plasticity index on the stabilization effectiveness of expansive clays", Transportation Research Record, Journal of Transportation Research Board, No. 2212, pp. 91-99.

Puppala, A. J., Punthutaecha, K. and Vanapalli, S. K. (2006). "Soil-water characteristic curves of stabilized expansive soils." Journal of Geotechnical and Geoenvironmental Engineering, 132 (6), 736-751.

Little, D. N., Males, E. H., Prusinski, J.R. and Stewart, B. (2000). "Cementitious Stabilization." 79th Millennium Rep. Series, Transportation Research Board.

Little, D. N. (1995). "Stabilization of pavement sub-grades and base courses with lime." Technical report made for Lime association of Texas.

Porbaha, A. and Puppala, A. J. (2003). "In Situ Techniques for Quality Assurance of Deep Mixed Columns." Proceedings of the Third International Conference (ASCE).

Chittoori, B. and Puppala, A. J. (2011). "Quantitative Estimation of Clay Mineralogy in Fine-Grained Soils", Journal of Geotechnical and Geoenvironmental Engineering, Vol. 137, No. 11, 997-1008.

Chittoori, B., Puppala, A., Nazarian, S., & McDaniel, M., (2008), "Subgrade Characterization for Better Ground Improvement Design" ASCE Geotechnical Special Publication 162, Geo-Congress, New Orleans, February, 2008.

Punthutaecha, K., Puppala, A. J., Vanapalli, S. K. And Inyang, H. (2006), " Volumetric change behaviours of expansive soils stabilized with recycled ashes and fibers." Journal of Materials in Civil Engineering, ASCE, Vol. 18, No. 2, 295-306.

Rational criteria for the assessment of the target mechanical strength and stiffness of artificially sand-cement mixtures

Nilo Cesar Consoli, Federal University of Rio Grande do Sul, Brazil, consoli@ufrgs.br
António Viana da Fonseca, Faculty of Engineering, University of Porto, Portugal, viana@fe.up.pt

ABSTRACT

The treatment of soils with cement is an attractive technique when a project requires improvement of a local soil for the construction of subgrades for rail tracks, roads, as a support layer for shallow foundations and to prevent soil liquefaction. The key-parameters for the control of strength and stiffness of artificially cemented soils are being associated to porosity/cement ratio. This framework is based in very simple and expeditious unconfined compression, tensile and bender elements tests, towards more complex triaxial tests, and else, for the purpose of establishing a general frameworks for soil-cement admixtures. The possibility to establish a general indexation of geomechanical properties to a unique porosity/cement ratio is discussed in the field control of soil-cement layers. This thorough evaluation of the sensitivity of mechanical properties is very much relevant in a large number of structures, namely in transportation infrastructures, where demanding and time consuming tests (such as cyclic triaxial tests) would create practical difficulties for thorough and competent quality control. The possibility of enabling these projects with preliminary combination studies based on objective and physically well fundament indexes will be determinant in optimization of these applications.

1. INTRODUCTION

The use of traditional techniques in geotechnical engineering often faces problems because of high costs and/or environmental issues. In roads, for instance, the use of granular bases became unviable when the borrow site is far away from the construction site. Another example is the construction of foundations in soils with poor bearing capacities, where the costs of a deep foundation solution can be incompatible with the overall costs for low-budget building projects.

In these cases, an alternative is the improvement of local soil by the addition of Portland cement. The soil-cement technique has been used successfully in pavement base layers, slope protection or earth dams, as a base layer to shallow foundations and to prevent sand liquefaction (Ingles and Metcalf 1972; Dupas and Pecker 1979; Thomé et al. 2005).

In spite of the numerous applications, until 2007 there were no dosage methodologies based on rational criteria as in the case of the concrete technology, where the water/cement ratio plays a fundamental role in the assessment of the target strength. Up to 2006, the soil-cement ratio has been assessed by numerous laboratory tests that aim to find the minimum amount of cement that meets the target properties in terms of strength and durability. This approach probably results from the fact that soil-cement shows a complex behavior that is affected by many factors, for example, the physicochemical properties of the soil, the amount of cement, and the porosity and moisture content at the time of compaction (Moore et al. 1970; Clough et al. 1981; Consoli et al. 2000, 2003, 2006).

In 2007, Consoli et al. showed that for unsaturated soils it was not possible to establish a relationship between the unconfined compression strength and the water/cement ratio, the latter defined as the water mass divided by the cement mass, as used in concrete technology. These results differ from those obtained by Horpibulsuk et al. (2003) where the water/cement ratio was found to be a useful parameter in the analysis of the strength development of the materials the writers studied. However, in the studies by Horpibulsuk the high moisture contents were sufficient for the pores of the samples to be predominantly water filled, so that the water content would reflect the amount of voids. This is the same as happens in concrete, where the amount of water again reflects the amount of voids in the mortar.

Consoli et al (2007) went after an index based on parameters that could control the unconfined compression strength of soil-cement blends in unsaturated and saturated conditions. The authors found out that the porosity of the specimen and the amount of cement were the parameters that affect the most the compressive strength. The authors went further and showed that a unique index, named porosity-cement ratio (expressed as volume of voids – water plus air – divided by volume of cement V_v/V_{ce}; or alternatively expressed as porosity of the specimen divided by the volumetric cement content η/C_{iv}, the latter expressed as a percentage of the total volume), controlled the unconfined compressive strength of the soil-cement mixture. The authors have shown that points with the same porosity/cement ratio but

Consoli - Rational criteria for the assessment of the target mechanical strength and stiffness of artificially sand-cement mixtures

II-297

obtained by different combinations of cement content and densification show similar unconfined compressive strengths, and that for a given change in the volume of voids, a proportional variation in the cement volume would be enough to balance the strength gain or loss.

2. UNCONFINED COMPRESSIVE STRENGTH VERSUS SPLIT TENSILE STRENGTH OF ARTIFICIALLY CEMENTED SAND

Extending previous studies using a uniform sand-cement mixture, considering cement contents varying from 1% to 12% and voids ratio of 0.64, 0.70 and 0.78, corresponding respectively to high, medium and reduced relative densities, the porosity–cement ratio (η/C_{iv}) has been shown to be an appropriate parameter to assess not only the unconfined compression strength (q_u), but also the splitting tensile strength (q_t), as shown in Figure 1.
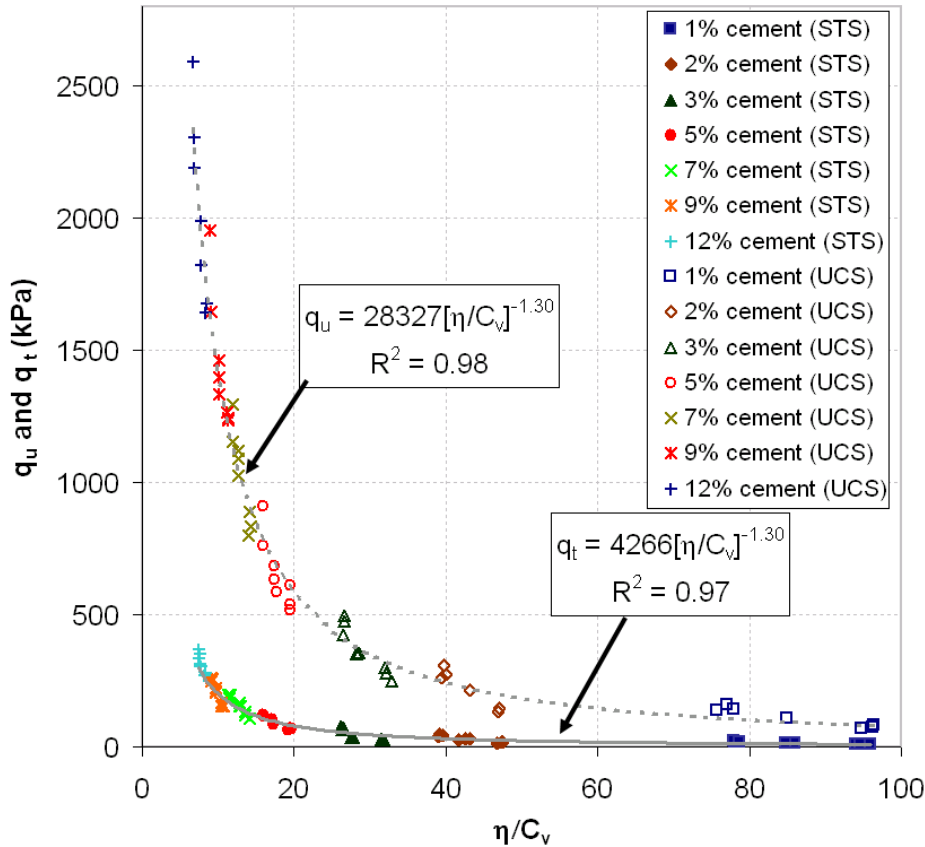
Figure 1: Variation of both splitting tensile (q_t) and unconfined compressive strength (q_u) with porosity/cement ratio.

A simple observation of Figure 1 suggests that the porosity/cement ratio is useful in normalizing results. A good correlation (R^2=0.97) can be observed between this ratio (η/C_{iv}) and the splitting tensile strength (q_t) of the sand-cement studied [see Eq. (1)], as well as between η/C_{iv} and the unconfined compressive strength (q_u) of the sand-cement studied [see Eq. (2) with R^2=0.98].

$$q_t\,(kPa) = 4{,}266\left[\frac{\eta}{C_{iv}}\right]^{-1.30} \tag{1}$$

$$q_u\,(kPa) = 28{,}327\left[\frac{\eta}{C_{iv}}\right]^{-1.30} \tag{2}$$

Examining Figure 1, as well as Eqs. (1) and (2), it is possible to observe that they present rather similar trends. In order to check whether a q_t/q_u relationship for the sand-cement mixture is a function of porosity, cement content or porosity/cement ratio, Eq. (1) is divided by Eq. (2) which yields the ratio:

Consoli - Rational criteria for the assessment of the target mechanical strength and stiffness of artificially sand-cement mixtures

II-298

$$\frac{q_t}{q_u} = \frac{4{,}266\left[\dfrac{\eta}{C_{iv}}\right]^{-1.30}}{28{,}327\left[\dfrac{\eta}{C_{iv}}\right]^{-1.30}} = 0.15 \tag{3}$$

The authors found that q_t/q_u was a scalar for the studied sand-cement blend, being independent of porosity, cement content or porosity/cement ratio. So, there was a straight proportionality between tensile and compressive strengths, which was valid for the whole range of porosity and cement content studied. As a consequence, the authors concluded that any rational dosage methodology considering the effect of different variables could be centered on tensile or compression tests, once they are intimately related through a scalar (0.15 for the sand cement studied herein).

3.   TRIAXIAL TESTING OF ARTIFICIALLY CEMENTED SAND

Figure 2 presents the deviator stress-axial strain-volumetric strain behavior of specimens with a unique effective confining pressure (200 kPa) and the three studied porosity/cement ratios, 10, 17, and 30. It can be seen that the conclusions obtained for V_v/V_{ce}=10 can be extended to V_v/V_{ce}=17 and V_v/V_{ce}=30 (and so for any value of the index). It can be clearly observed in Fig. 2 that the increase of the porosity/cement ratio from 10 to 30 comes together with a reduction in the brittleness of the cemented soil, changing from dramatically brittle (V_v/V_{ce}=10) to nearly ductile (V_v/V_{ce}=30) behavior.
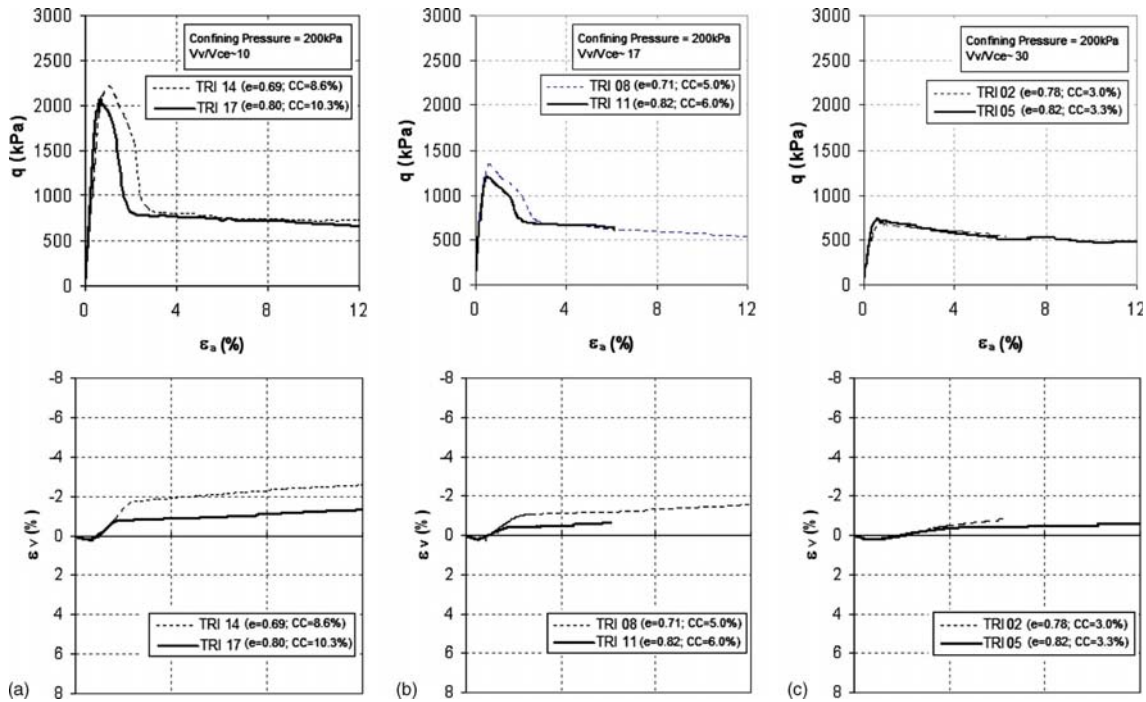
Figure 2: Stress-axial strain-volumetric strain curves for the drained triaxial tests for effective confining stresses of 200 kPa and (a) V_v/V_{ce}=10; (b) V_v/V_{ce}=17; and (c) V_v/V_{ce}=30.

Figure 3 presents the peak strength envelopes for V_v/V_{ce}=10, 17, and 30 considering all triaxial data for each porosity/cement ratio, as well as the q_u results. The cohesion intercept (c') and angle of shearing resistance (Φ') for each porosity/cement ratio are also presented in Fig. 3. Values of c' and Φ' reduce with increasing V_v/V_{ce} values. Eqs. (4) and (5) present the correlations of the porosity/cement ratio with peak strength parameters, cohesion intercept and friction angle, respectively.

$$c'(kPa) = 4{,}430\left[\frac{V_v}{V_{ce}}\right]^{-1.10} \tag{4}$$

$$\phi'(\deg rees) = 79\left[\frac{V_v}{V_{ce}}\right]^{-0.31} \tag{5}$$

Consoli - Rational criteria for the assessment of the target mechanical strength and stiffness of artificially sand-cement mixtures
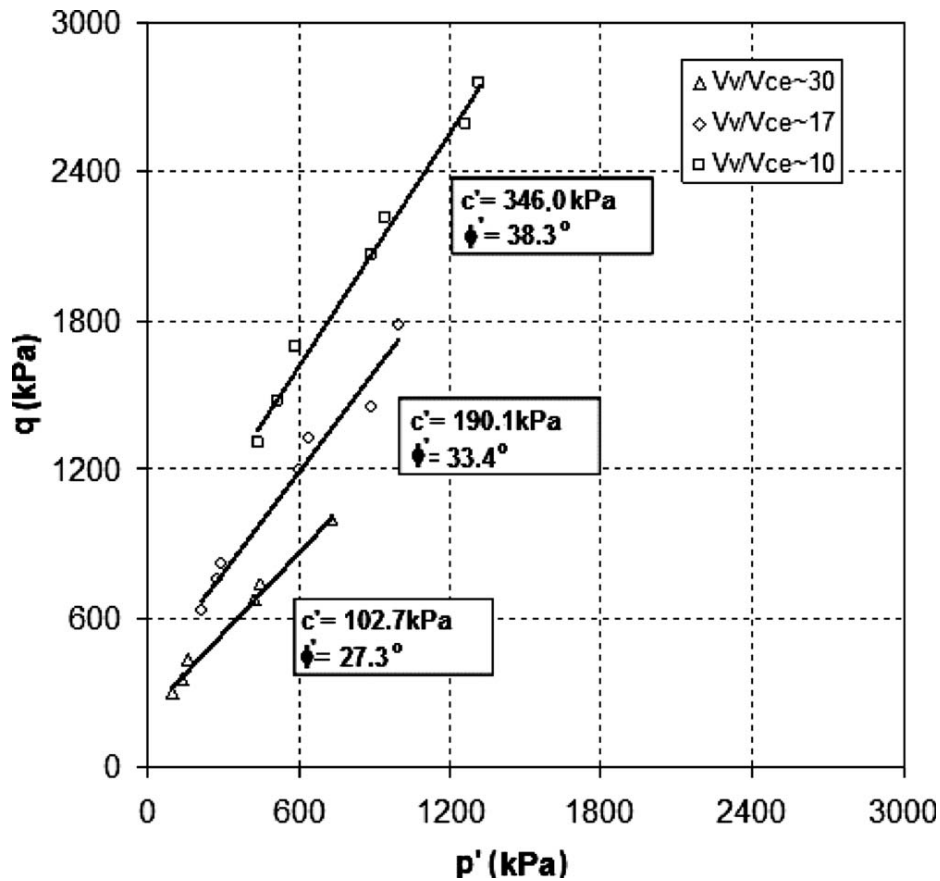
Figure 3: Peak strength envelopes for V_v/V_{ce}=10, 17, and 30 considering all triaxial data for each porosity/cement ratio.

4.   BENDER ELEMENTS TESTING OF ARTIFICIALLY CEMENTED SANDS

The influence of porosity/cement ratio on the initial stiffness of sand-cement blends has also been studied. The authors have found that the influence of porosity/cement ratio on the initial shear modulus (G_0) (Figure 4) of two artificially cemented sands (a uniform and a well graded) is quite similar to the shape found for the relationship between unconfined compressive strength and porosity/cement ratio for the same materials, since the shape of the curves were almost the same (see Eq. 6 – uniform sand, Eq. 7 – well graded sand and Fig. 4) compared to Fig. 1 and Eq. 2.

$$G_0(MPa) = 17,504\left[\frac{\eta}{(C_{iv})^{1.0}}\right]^{-0.99} \tag{6}$$

$$G_0(MPa) = 1x10^8\left[\frac{\eta}{(C_{iv})^{0.21}}\right]^{-3.33} \tag{7}$$

Consoli - Rational criteria for the assessment of the target mechanical strength and stiffness of artificially sand-cement mixtures

II-300
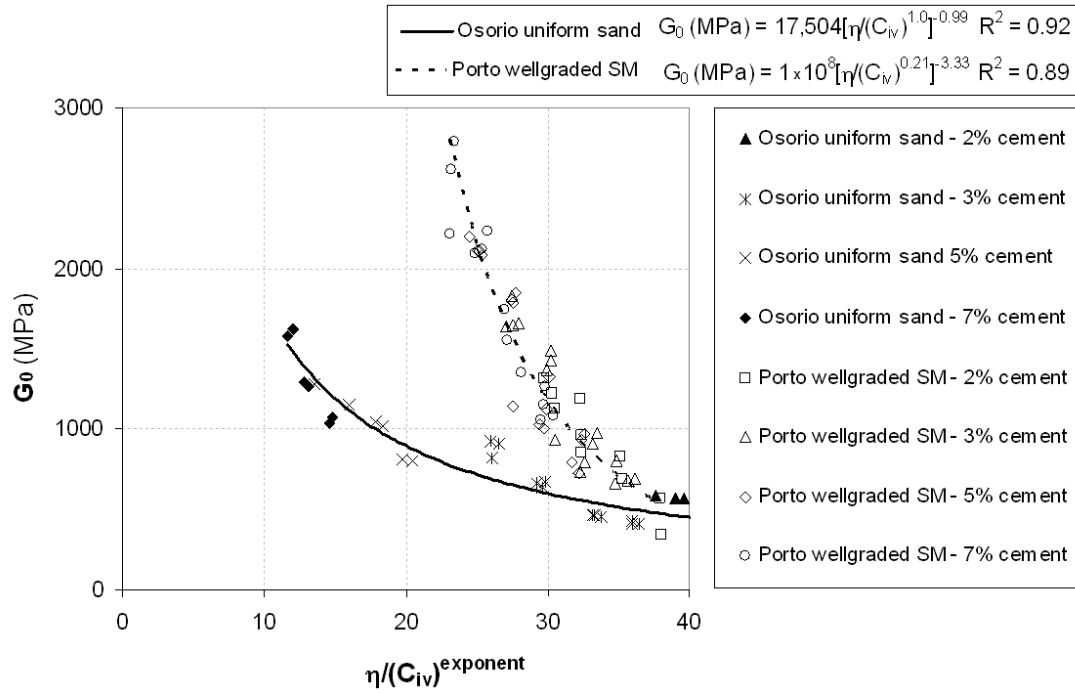
Figure 4: Variation of initial shear modulus (G_0) for cemented uniform sands with porosity/cement ratio.

For both the Osorio sand-cement and the Porto well graded sand-cement mixtures, assembling the data of the unconfined compressive strength (q_u) and initial shear modulus (G_0) with porosity/cement ratio allows relationships for G_0/q_u to be determined as a function of η/C_{iv} (see Eq. 8 – uniform sand, Eq. 9 – well graded sand and Figure 5).

$$\frac{G_0}{q_u} \cong 127 \left[\frac{\eta}{(C_{iv})^{1.0}} \right]^{0.97} \tag{8}$$

$$\frac{G_0}{q_u} \cong 25 \left[\frac{\eta}{(C_{iv})^{0.21}} \right]^{0..96} \tag{9}$$
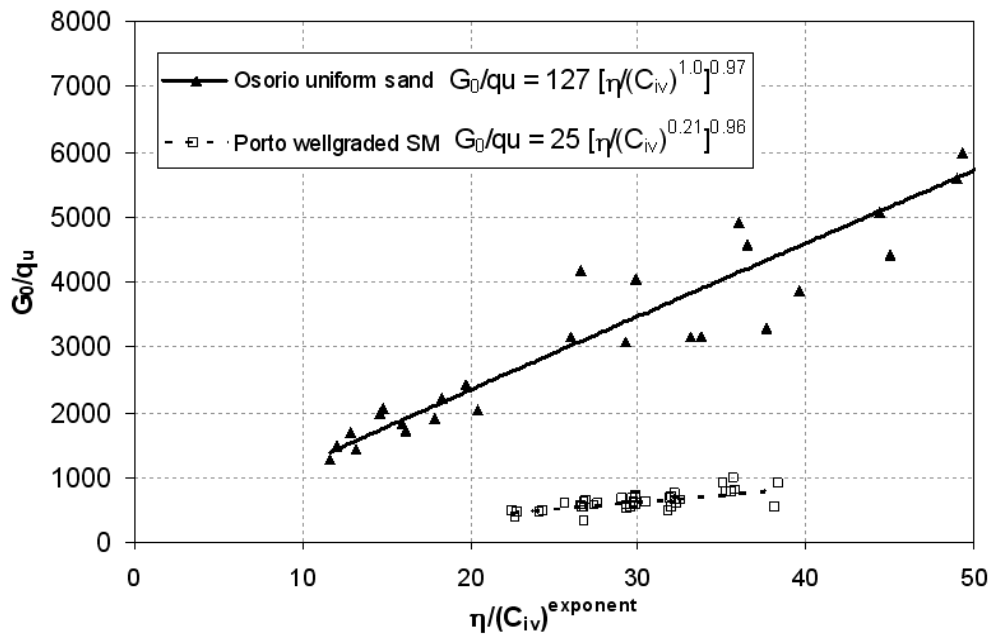
Figure 5: Relations between G_0 and q_u for cemented uniform sand and Porto well graded sand with porosity/cement ratio.

Consoli - Rational criteria for the assessment of the target mechanical strength and stiffness of artificially sand-cement mixtures

5. CONCLUSIONS

From the research presented in this manuscript regarding an index parameter that controls the mechanical behaviour of artificially cemented sandy soils, the following conclusions can be drawn:

- η/C_{iv} (or alternatively V_v/V_{ce}) is an appropriate parameter to assess the influence of both porosity and cement content on the initial stiffness, tensile and compressive (both unconfined and triaxial) strength of sand-cement mixtures;
- For a given soil matrix-cement blend, G_0/q_u varies almost linearly with η/C_{iv} (also named V_v/V_{ce}), revealing a consistent pattern of dependency between these geomechanical properties and that index;
- By using η/C_{iv} index, practitioners may choose the amount of cement and the target density appropriate to provide a mixture that meets the strength and stiffness required by their project.

6. ACKNOWLEDGEMENTS

REFERENCES

Clough, G. W., Sitar, N., Bachus, R. C. and Rad, N. S. (1981). "Cemented sands under static loading". Journal of Geotechnical Engineering Division, New York: ASCE, 107(6), 799-817.

Consoli, N.C., Rotta, G.V. and Prietto, P.D.M. (2000). "The influence of curing under stress on the triaxial response of cemented soils". Géotechnique, 50(1), 99-105.

Consoli, N. C., Vendruscolo, M. A. and Prietto, P. D. M. (2003). "Behavior of plate load tests on soil layers improved with cement and fiber". Journal of Geotechnical and Geoenvironmental Engineering, ASCE, 129(1), 96-101.

Consoli, N. C., Rotta, G. V. and Prietto, P. D. M. (2006). "Yielding-compressibility-strength relationship for an artificially cemented soil cured under stress". Géotechnique, London, 56(1), 69-72.

Consoli, N. C., Foppa, D., Festugato, L. and Heineck, K. S. (2007). "Key parameters for strength control of artificially cemented soils". Journal of Geotechnical and Geoenvironmental Engineering, ASCE, 133(2), 197-205.

Dupas, J., and Pecker, A. (1979). ''Static and dynamic properties of sandcement.'' J. Geotech. Engrg. Div., ASCE, 105(3), 419–436.

Horpibulsuk, S., Miura, N. and Nagaraj, T.S., (2003). "Assessment of strength development in cement-admixed high water content clays with Abram's law as a basis". Géotechnique, 53 (4), 439-444.

Ingles, O. G. and Metcalf, J. B. (1972). "Soil stabilization: Principles and practice". Butterworths, 374 p.

Moore, R. K., Kennedy, T. W. and Hudson, W. R. (1970). "Factors affecting the tensile strength of cement-treated materials". Highway Research Record: Soil Stabilization: Multiple Aspects, Washington - DC, HRB, 315, 64-80.

Thomé, A., Donato, M., Consoli, N. C. and Graham, J. (2005). "Circular footings on a cemented layer above weak foundation soil". Canadian Geotechnical Journal, 42(6), 1569-1584.

Consoli - Rational criteria for the assessment of the target mechanical strength and stiffness of artificially sand-cement mixtures

II-302

Application of Polypropylene and Carpet Fibres to Improve Mechanical Properties of Cement Treated Clay

Behzad Fatahi, Hadi Khabbaz and Behnam Fatahi

Centre for Built Infrastructure Research, School of Civil and Environmental Engineering, University of Technology Sydney (UTS), Sydney, Australia, Behzad.Fatahi@uts.edu.au

ABSTRACT

In this study, the influence of two types of fibre reinforcement, namely polypropylene and carpet waste fibres, on mechanical properties of cement treated kaolinite is investigated. The results of unconfined compressive strength testing of 63 cylindrical samples of cement treated kaolinite with varied cement and fibre contents are analysed to discern the relationships between these parameters and the key mechanical properties, including unconfined compressive strength and stiffness of treated soil. The fibre reinforcement increases the peak strength. The initial Young's modulus of the fibre reinforced cement treated kaolinite increases by adding polypropylene whereas slightly decreases when adding carpet fibres. The improvement of mechanical properties was far more pronounced with the introduction of polypropylene than carpet waste fibres. The implication of these findings is a cost effective and environmentally friendly alternative compare to increasing cement content in soil to achieve the required mechanical properties, particularly where the strength is a governing consideration.

1. INTRODUCTION

With the growth of cities and industries, sites that can be used without some ground modification are increasingly scarce. If the soil encountered at a particular site is not suitable for construction, design engineers have various options. They can bypass the poor soil, replace it with superior soil, redesign the structure for the poor condition, or improve the soil's properties by, for example, mixing it with materials such as cement, lime, gypsum, fly ash, milled slag and other cementitious by-products. Cement stabilisation techniques, including jet grouting and deep cement mixing (dry and wet), have been used worldwide, especially in South East Asia and North America and recently in Australia, for stability and deformation control of land reclamation and road construction projects, and in deep excavations in soft clay. Deep soil mixing (DSM) is an in situ soil improvement approach that mixes in situ soil with strengthening agents, usually cementitious, through hollow, rotating shafts with cutting tools, mixing paddles and/or augers mounted at various locations along the shafts. The compressibility of the soil is similarly altered, with the cement-treated soil having much higher preconsolidation pressure than the untreated soil. Exceeding preconsolidation pressure, due to heavy structural loads, leads to a sharp decrease in the void ratio and deformation (Uddin et al. 1997; Balasubramaniam et al. 1998; Topolnicki 2004), which has also been observed in natural soils (Burland 1990; Lapierre et al. 1990; Nagaraj et al. 1998; Liu and Carter 1999). This technology can be employed in conjunction with shallow foundations, instead of deep foundations, the cost of which may be prohibitive for low-budget roads, pavements, slope protection walls, and building projects.

As reported by Green Capital (2011), each year approximately 18 million tons of waste from the municipal, construction, demolition, commercial and industrial sectors are disposed (landfill) in Australia, among which significant portion belongs to polypropylene (PPP) waste material. In order to solve environmental problems generated by this waste production, different solutions are presented. One of solutions is to produce synthetic fibres specifically engineered as an additive to enhance materials performance. In addition, according to Freedonia Group (2002), the processed or clean waste associated to the large production rate of carpet are estimated to be around 7% amounting to $4.5 billion worth of goods, which are currently destined for landfill sites and/or incinerators. However, as reported by Miraftab and Lickfold (2008), growing public concern for the environment and tighter restrictions/costs on landfill sites in recent years has forced many wast producers to look for innovative methods to the waste product in the form of fibres to enhance performance of different materials.

Some studies with reference to the reinforcement of uncemented and cemented soils using fibre inclusions have been reported (e.g. Maher and Ho, 1993; Omine et al., 1996; Michalowski and Cermak, 2003; Prabakar and Sridhar, 2002). Mo et al. (1999) reported that the admixture of fibre and cement in

soil could greatly improve the toughness and strength of cement treated soil. The research results of Wu (2002) indicated that fibre-cement-fly ash stabilised soil of higher strength and toughness was obtained by adding a small amount of glass fibre into cement-fly ash treated soil and that its strength increased with increasing content and length of glass fibre. Cai et al. (2005) conducted a series of experiments on fibre-reinforced filled soil and found that the presence of fibre could markedly improve the toughness of filled soil and change the failure characteristics of soil. Prabakar and Sridhar (2002) found that the strength of soil was improved when shreds of plants such as jute, sisal, and coconut shells were mixed into soil. Taking the biological degradation of plant into account, some scholars attempted to adopt artificial synthetic fibre to improve the engineering properties of soil. Consoli et al. (2003) employed polypropylene fibres with different lengths and diameters at various fibre contents to reinforce sandy soil. It was concluded that the deviatoric stress of reinforced soil specimen increased with an increase in the fibre length, the fibre aspect ratio and the fibre content, whilst it decreased with an increase in the fibre diameter alone. Investigations by Yi et al. (2006) found polypropylene fibre introduction to soil improved the engineering properties (specifically the shear strength, toughness and plasticity). Their investigation also found that the extent of the strength improvement contributed by the fibre introduction was not affected by curing time. Investigations by Sahin (2009) and Chaosheng et al. (2006) showed the most significant effect, which increased polypropylene content, was on ductility, with those of a higher polypropylene content failing at a far greater strain. Neither found that the stiffness up to approximately 80% of the ultimate strength was affected by changing fibre content.

According to Miraftab and Lickfold (2008), nylon carpet pile waste can be successfully mixed with substandard soil up to a maximum of 10%, while enhancing the cohesion and strength of the soil as well as its internal friction. Michalowski and Cermak (2003) reported that the addition of a small amount of synthetic fibre increases the failure stress of the composite. Wang et al. (1994) investigated the relationship between the tensile strength of concrete with varying carpet fibre contents, and concluded that the presence of carpet fibre reinforcement improves the tensile strength, toughness, and reduced drying shrinkage. Wang et al. (2000) and Wang (1999) reported that using up to 3% fibre waste could enhance the internal friction, the shear strength, the compressive strength, and the load-bearing capacity of silty to clayey sand. Prabakar and Sridhar (2002), carried out a series of triaxial compression test, concluded that the increase in strength of fibre-reinforced soil is a function of the fibre weight fraction. Miller and Rifai (2004), based on their test results, indicated that fibre inclusion reduced the crack formation and the hydraulic conductivity of compacted clay soil. Yetimoglu et al. (2005) conducted an experimental study on California bearing ratio of soil and indicated that the presence of fibre in sand fill caused an appreciable increase in the peak piston load. The test results of Li et al. (1995) showed that fibre reinforcement could significantly improve the shear strength, and the tensile strength of clayey soil. The work of Zhang et al. (1998) indicated that the presence of fibre greatly improved the dynamic strength of silty clay samples under dynamic tension, as well as the toughness and plasticity of soil.

A substantial amount of research has been performed on reinforced sandy or clayey soils with fibres but there is a lack of study on the effect of fibres on cement treated clays, which may be utilised in deep soil mixing, particularly polypropylene and carpet fibres. In this study, effects of these two fibres, on the mechanical properties of cement improved kaolinite clay are investigated.

2.   EXPERIMENTAL PROCEDURE

The clay sample for testing was Q38 kaolinite clay with an average liquid limit of 50% and plastic limit of 29%. Q38 kaolinite clay is a dry milled kaolin China clay, of a white-cream colour. Kaolinite is one of the most abundant minerals in soil, and as such is often encountered in in-situ conditions. Kaolinite is formed by the breakdown of feldspar, which is induced by water and carbon dioxide and is often formed by the alteration of aluminium silicate minerals in a warm and humid environment (Craig, 2000; Murray, 1999). The admixture used in stabilising the experimental clay samples was Portland Type I cement, one of the most widely used construction materials in Australia and is representative of a typical cement used in DSM construction within Australia. In the design of soil-cement mixes, the cement content is the fundamental variable to be adjusted when considering the required strength of the composite mixture. Higher cement contents generally result in increased strength, durability and permeability characteristics. The exact cement content is dependent on the site requirements as well as the type of soil being stabilised. Soils of differing compositions react differently to cementious additives and as such designs are specific to in-situ conditions. Cement contents of 10%, 15% and 20% of the dry weight of the clay were adopted for the kaolinite samples, as well as a water content of 150% of the clay liquid limit, similar parameters to those adopted by Lorenzo and Bergado (2004).

For this study the polypropylene and carpet fibres in quantities of 0.1%, 0.2%, 0.5% for polypropylene and 0.5%, 0.75%, 1% for carpet fibre were used to reinforce the 10%, 15% and 20% cement stabilised clay, producing 54 samples (3 samples per mix) with the addition of 9 control samples without fibre reinforcement. This summed up to a total of 54 samples per fibre type. The quantity of fibre and cement was expressed as a percentage of the dry weight of the kaolinite clay. Monofilament Polypropylene fibre was used instead of fibrillated to prevent any clustering and tangling during the mix, allowing for a more homogeneous mix.

The test procedure was designed with guidance from AS 5101.4 – 2008 (method 4: Unconfined compressive strength of compacted materials), as well as relevant literature detailing experimental procedures on testing of soil-cement columns, such as Lorenzo and Bergado (2004), and Liu et al. (2008). The clay and fibres were initially mixed through with the water being added and mixing conducted to obtain reasonable workability. For kaolinite, a water content of 75%, which is 50% more than the liquid limit of the soil, was required to produce a mix of adequate workability. Cement slurry with a water to cement ratio of 1 to 1 was then added to the remoulded reinforced clay as the stabilising admixture. Alternating hand and mechanical mixing was introduced to ensure a homogenous mix for all samples. The resulting mixtures were of reasonable workability for placement into the moulds. In an effort to minimise entrapped air and to provide compaction, the mixture was placed into the mould in several layers and worked into the mould with palette knives. At this point, the moulds were placed on a vibration table to ensure entrapped air was minimised and the sample was uniform. It should be noted that plastic sheets were wrapped around the final specimens to minimise moisture loss and assist the cement hydration process. The specimens were left to cure in the controlled environment within the moulds and plastic wrapping for 7 days prior to de-moulding. It can also be noted that all specimens were stored in an identical controlled ambient environment of 25°C.

The specimens were placed in a curing bath immediately after de-moulding. The specimens remained in the curing bath for an additional 7 days. Thus, the total curing time for the samples was 14 days. After removal from the curing bath, the samples were weighed and dimensions measured. The specimens were then capped with gypsum in preparation for compressive testing to ensure an even surface for the application of load. The compression testing was conducted under the guidance of AS 5101.4–2008. The standard outlines the compressive machine used is to comply with the requirements for Grade B of AS 2193-2006 referring to the upper block of the machine having a spherical seat. The machine was set at a load rate of 1 mm/min. This was kept consistent for all specimens tested. An "S" type load cell was used as a transducer converting the force into an electrical signal readable on the load cells display. A data logger was used to transfer the data to a readable output. An LVDT displacement transducer was set up against the bearing block of the machine measuring the vertical displacement of the specimen under applied load. The LVDT readings were used to calculate the strain of the specimens.

3. RESULTS AND DISCUSSION

As anticipated, increases in the cement content resulted in increased strength. As illustrated in Figures 1 and 2, the analysis revealed a varying degree of strength gains through increasing the fibre reinforcement content. The polypropylene reinforced sample analysis showed a clear trend of increasing strength with increasing fibre content. Although the unconfined compressive strength of carpet reinforced samples increases, the change is less pronounced than the change for polypropylene fibres. For examples, addition of 0.5% and 1% polypropylene and carpet fibres increases the unconfined compressive strength of treated clay with 20% cement, by 25% and 20%, respectively.
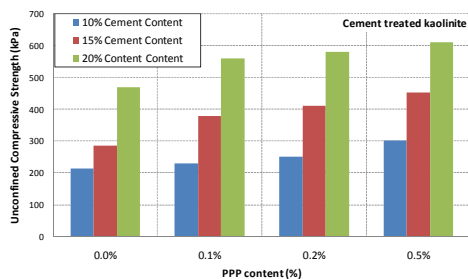

Figure 1: Variations of unconfined compressive strength of kaolinite-cement mixture with polypropylene fibre content
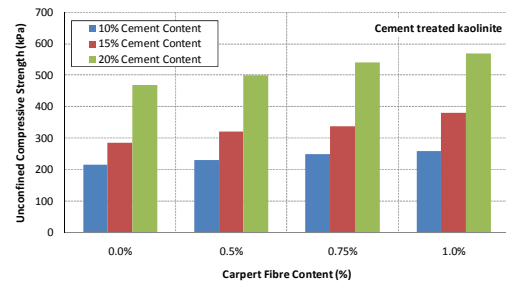
Figure 2: Variations of unconfined compressive strength of kaolinite-cement mixture with carpet fibre content

Figures 3 and 4 present the results of the relationship between the initial Young's modulus, the fibre content and the cement content. The samples reinforced with polypropylene fibres show an increasing stiffness with increasing fibre content. However, the stiffness of carpet reinforced cement treated clay decreases with fibre content. This may be the result of the introduction of a material more plastic than the cement treated clay, which potentially did not engage as well with the surrounding matrix. Figures 5 and 6 illustrate the relationship between the ratio of E_i to E_f, fibre content and cement content for cement treated Kaolinite.
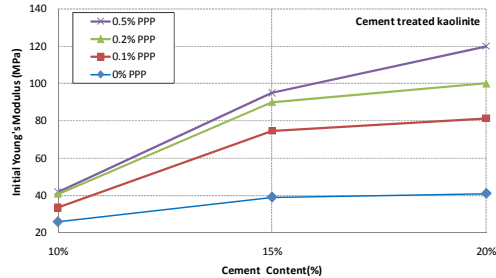
Figure 3: Variations of initial Young's modulus of kaolinite-cement mixture with polypropylene fibre content
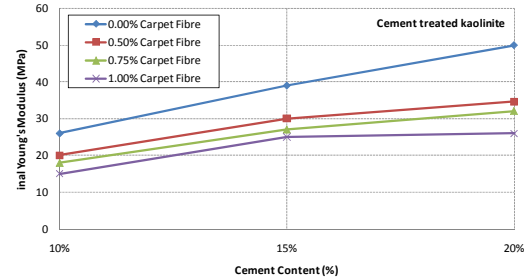
Figure 4: Variations of initial Young's modulus of kaolinite-cement mixture with carpet fibre content
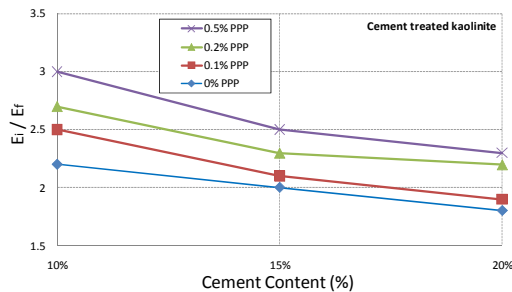
Figure 5: Variations of (E_i/E_f) of kaolinite-cement mixture with polypropylene fibre content
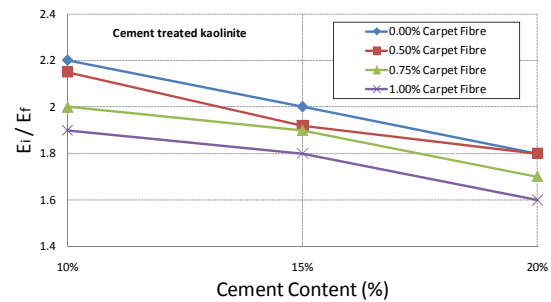
Figure 6: Variations of (E_i/E_f) of kaolinite-cement mixture with carpet fibre content

Figure 5 displays a trend of an increasing ratio of E_i to E_f with increasing polypropylene fibre content, with an decreasing ratio of E_i to E_f with increasing cement content. This suggests that increasing the polypropylene fibre increases the ductility of the material, whilst increasing the cement content decreases the ductility. However, as shown in Figure 6, the ratio of E_i to E_f decreases with carpet fibre content. According to Figures 5 and 6, ratio of E_i to E_f ranges between 1.8 and 3, and 1.6 and 2.2 for polypropylene and carpet fibre reinforced cements treated kaolinite within the four mentioned cement and fibre content ranges, respectively.

The results obtained are of significant values, as current literature does not address the potential of fibres to be used in conjunction with DSM to achieve the required design strength. Past research has primarily focused on strength gains associated with introducing a cementitious admixture to clay. Although the use of fibre in concrete columns is an accepted industry practice, literature investigating the effects of the fibre on the mechanical properties of the soil-cement column is scarce. This study covers different soils and cement contents with various fibre contents and clearly proves that adding fibres can be adopted to reduce the required cement content for kaolinite, particularly in applications where bearing capacity resulting from poor soil strength is the primary challenge to be overcome.

4.   CONCLUSIONS

In this study, effects of various polypropylene and carpet fibre contents on the unconfined compressive strength of cement treated kaolinite have been investigated. The specimens were cured for 7 days prior to de-moulding under controlled/sealed environment after which they were placed in a curing bath for an additional 7 days. Thus, the total curing time for the samples was 14 days. The results of this study indicated that introducing polypropylene fibres had a positive effect on the strength and stiffness properties of the soil-cement columns. This allows for less cement content to be used in reaching required strength of soil-cement mixes when polypropylene fibres are added to the cement treated clay. The

Young's modulus was also observed to increase with the application of more polypropylene fibres. However, the results show that although the unconfined compressive strength of cement treated kaolinite increases with carpet fibres, the stiffness of the tretaed soil slightly decreases with the carpet fibre content. It should be noted that adding fibre content to soil-cement mixes can reduce the cement usage for the DSM process, which effectively contributes to carbon footprint reduction. As discussed, the potential for utilisation of polypropylene and carpet waste fibres offers significant economic and environmental benefits, even if significantly greater quantities are required to produce similar results.

5.   ACKNOWLEDGMENTS

REFERENCES

Australian Standard. (2008). Method 4: unconfined compressive strength of compacted materials. Methods for preparation and testing of stabilized materials. AS 5101.4 – 2008.

Australian Standard. (2006). Calibration and classification of force-measuring systems, AS 2193 – 2006.

Balasubramaniam, A.S., Kamruzzaman, A.H. M., Uddin, K., Lin, D.G., Phienwij, N. & Bergado, D.T. (1998). "Chemical stabilization of Bangkok clay with cement, lime and flyash additives", Proc. 13thSoutheast Asian Geotechnical Conf., 253–258.

Burland, J. B. (1990). "On the compressibility and shear strength of natural clays", Geotechnique, 40(3), 329–378.

Cai, Y., Shi, B., Liu, Z. B., Tang, C. S., and Wang, B. J. (2005). "Experimental study on the effect of aggregate size on the strength of filled soils." Chinese J. Geotech. Eng., 27(12), 1482–1486.

Chaosheng, T., Yi, C., Bin, S., Charles, W.W. Ng., (2006). "Effect of polypropylene fibre and lime admixture on engineering properties of clayey soil", Department of Earth Science, Nanjing University.

Consoli, N. C. Casagrande, M. D. T. Prietto and P. D. M. Thome, A. (2003). "Plate Load Test on Fibre-Reinforced Soil", Journal of Geotechnical and Geoenviromental Engineering, ASCE, 129, 951-955

Craig, H. (2000). "Soil Mechanics", Chapman and Hall, London.

Freedonia Group (2002). "World Carpet and Flooring", Published by Freedonia Group, p. 355.

Green Capital (2011). Available from <http://www.greencapital.org.au/issues/waste.html>.Accessed on 12 July 2011.

Lapierre, C., Leroueil, S., & Locat, J. (1990). "Mercury intrusion and permeability of Louiseville clay", Can. Geotech. J., 27, 761–773.

Li, G.X., Chen, L., Zheng, J.Q., Jie, Y.X., (1995). "Experimental study on fibre-reinforced cohesive soil", Shuili Xuebao (in Chinese). Journal of Hydraulic Engineering, 6, 31–36.

Liu M. D. & Carter J. P. (1999). "Virgin compression of structured soils", Geotechnique, 49(1), 43–57.

Liu, S.Y., Zhang, D.W., Liu, Z.B., & Deng, Y.F. (2008)."Assessment of unconfined compressive strength of cement stabilized marine clay", Marine Georesources & Geotechnology, 26(1), 19-35.

Lorenzo, G. A. and Bergado, D. T. (2004). "Fundamental parameters of cement-admixed clay – New approach", Journal of Geotechnical and Geoenvironmental Engineering, 130(10), 1-9.
Maher, M. H., and Ho, Y. C. (1993). "Behavior of fibre-reinforced cemented sand under static and cyclic loads", Geotech. Testing J., 16(3), 330-338.

Michalowski, R.L., Cermak, J., (2003). "Triaxial compression of sand reinforced with fibres", *Journal of Geotechnical and Geoenvironmental Engineering* 129 (2), 125–136.

Miller, C.J., Rifai, S. (2004). "Fibre reinforcement for waste containment soil liners", *Journal of Environmental Engineering* 130 (8), 981–985.

Miraftab, M. and Lickford, A. (2008). "Utilization of Carpet Waste in Reinforcement of Substandard Soils", *Journal of Industrial Textiles*, 167- 174.

Mo, Y. J., Peng, H. T., Lei, T. W., Yang, S. P., and Zhang, X. P. (1999). "Study on tensile strength of fibre soil stabilization with Portland cement." *Journal of China Agricultural University*, 4(6), 106–109.

Murray, H.H. (1999). "Applied Clay Mineralogy Today and Tomorrow', *Clay Minerals*, 34, 39-49.

Nagaraj T.S., Pandian N.S. & Narasimha Raju P.S.R. (1998). "Compressibility behavior of soft cemented soils", *Geotechnique*, 48(2), 281–287.

Omine, K., Ochiai, H., Yasufuku, N., and Kato, T. (1996). "Effect of plastic wastes in improving cement-treated soils", *Proc., 2nd Int. Congr. on Envir. Geotech.*, A. A Balkema, Rotterdam, The Netherlands, 2, 875-880.

Prabakar, J., Sridhar, R.S., (2002). "Effect of random inclusion of sisal fibre on strength behaviour of soil", *Construction and Building Materials* 16 (2), 123–131.

Sahin, A. (2009). "Freezing-thawing behaviour of fine-grained soils reinforced with polypropylene fibres", *Technial Vocational School of Higher Education, Ataturk University, Erzurum, Turkey*

Topolnicki M. (2004). "In situ soil mixing. In Ground Improvement", 2nd ed (eds Moseley. & Kirsch), New York: Spon Press, 331–428.

Uddin, K., Balasubramaniam A.S. & Bergado D.T. (1997). "Eng. Behaviour of Cement-Treated Bangkok Soft Clay", *Geot. Eng.*, 28(1),89-121.

Wang, Y., Zureick, A.H., Cho, B.S. & Scott, D.E. (1994). "Properties of fibre reinforced concrete using recycled fibres from carpet industrial waste", *Journal of Material Science*, 29, 4191–4199.

Wang, Y. (1999). "Utilization of Recycled Carpet Waste Fibres for Reinforcement of Concrete and Soil", *Polymer-Plastic Technology Engineer*, 38(3): 533–546.

Wang, Y., Frost, J.D. and Murray, J. (2000). "Utilization of Recycled Fibre for Soil Stabilisation", *Proceedings of the Fibre Society, Guimaraes, Portugal*, 59–62.

Wu, G. X. (2002). "The research of enforcing role on glass fibre to stabilizing soil of cement-fly ash." *Journal of Heilongjiang Institute of Science*, 12(3), 24–27.

Yi, C., Bin, S., Charles, W.W. Ng., Chaosheng, T., (2006). "Effect of polypropylene fibre and lime admixture on engineering properties of clayey soil", *Department of Earth Science, Nanjing University*.

Yetimoglu, T., Inanir, M., Inanir, O.E., (2005). "A study on bearing capacity of randomly distributed fibre-reinforced sand fills overlying soft clay", *Geotextiles and Geomembranes* 23 (2), 174–183.

Zhang, X. J., Zhou, K. J., and Zhou, J. X. (1998). "Experimental study on dynamic properties of cohesive soil reinforced with fibres." *Chinese J. Geotech. Eng.*, 20(3), 45–49.

Numerical analysis of the behavior of cement treated sand

Hamid GHORBANBEIGI, Laboratoire Génie Civil et geo-Environnement de Lille LGCgE (EA4515), USTL, France,
ghorbanbeigi@gmail.com
Hussein MROUEH, Laboratoire Génie Civil et geo-Environnement de Lille LGCgE (EA4515), USTL, France,
Hussein.Mroueh@polytech-lille.fr
Laurent LANCELOT, Laboratoire Génie Civil et geo-Environnement de Lille LGCgE (EA4515), USTL, France,
Jian Fu SHAO, Laboratoire de Mécanique de Lille LML (UMR CNRS 8107), USTL, France,

ABSTRACT

This paper deals with the numerical analysis of the behavior of cement treated sand mixing, used as an alternative and economical solution of soil improvement for many geotechnical-engineering problems. Based on a series of triaxial tests of several mixtures of sand, cement, lime and silica fume, including curing time effect, it has been shown that cement treated sand behavior is governed by a non-linear elastoplastic response, that is highly dependent on cement and lime content, and time curing (Ajorloo, 2010). As a consequence, it is of importance to take into account such a behavior in the design and optimisation of the cement treated soil.

The mechanical behavior of the cement treated sand is firstly described using an elastic perfectly plastic model, based on the Mohr-Coulomb failure criterion. Elastic and plastic parameters are identified using an iterative calibration procedure, for several confining pressures. The effect of cement percentage and others binders on the mechanical parameters is then analysed for several amount of cement and lime mixture. Two more sophisticated constitutive models, Hardening Soil and Modsol model are then used to describe the material behavior. These laws are based on non-linear elastoplastic relationships.

1. INTRODUCTION

This paper deals with the numerical analysis of cement treated sand used as an alternative and economical solution of soil improvement for many geotechnical-engineering problems. Ajorloo (2010) has experimentally investigated the behavior of cement treated sand, and highlighted the effect of various parameters on the mechanical responses of various types of soil-cement in unconfined and triaxial compression tests. In fact, the effect of specimen age, cement percentage, lime and silica fume content and confining pressure on mechanical strength and permeability of cemented sand were investigated. Experimental investigations indicated that increase in confining pressure induces an increase of compressive strength and elastic modulus, and a more ductile behavior of soil cemented specimens. It was also obtained that increase of lime and silica fume content and increasing of curing time increases the compressive strength due the pozzolanic reactions. Based on these results, the aim of the present work is to describe the mechanical behavior of cement treated soil as a basis for safer and more cost-effective design of soil improvement in deep mixing method. Three types of non linear models (from an elastic perfect plastic model to an advanced elastoplastic constitutive model involving isotropic hardening) are proposed in the present work to reproduce the mechanical response of cement treated sand.

After a presentation of the methodology followed in this work, we will describe in details the constitutive models and the results obtained for various soil mixtures under triaxial compression condition.

2. METHODOLOGY

2.1. Experimental program

The experimental program proposed by Ajorloo (2010) has investigated the effects of various levels of cement, lime and silica fume (SF) ratios including 0%, 40% and 80 % lime (note that for all mixes, SF to cement ratio of 0.1 and SF to lime ratio of 0.3 are taken constant), on stiffness parameters and strength of a sandy soil-cement mix. The quantities of Portland cement used correspond to 50 to 200 kg per m^3 of silica sand (cement/sand =3.8 to 15%) and the mortars were prepared from a mixture of Portland cement, silica-sand in its minimum dry density (13.36 kN/m^3) and mass fractions of lime of 0%, 40% and 80%. The water-to-binders (C+L+SF) ratio varied from 0.778 to 2.22.

The parent soil used for this study is a silica loose granular sand (SP in the unified classification), with medium sized sub-angular grains ranging from 0.125 to 0.8 mm in diameter. The principal physical

characteristics are a mean diameter D_{50}=0.471 mm, a uniformity coefficient Cu=2.26, a unit weight of solid particles γ_s=25.96 kN/m^3, a minimum void ratio e_{min}=0.575 and a maximum void ratio e_{max}=0.943. The main binder is Portland cement, conforming to type II-Tehran, according to ASTM C 150-86 (1986). As shown in Table 1, mixture proportions were tested with different water to cementitious binders (cement+lime+SF) ratios (ranging from 0.75 to 2.22).

Mixtures are referenced with C standing for cement, L for lime and S for sand. Numbers following the aforementioned codes refer to the factor of cementitious materials used, in kg/m^3 of silica sand.

Table 1: Mixture proportions of sandy soil-cement mixes

Mix Code	L/C %	B/S %	W/B	Water (kg/m^3)	Cement (kg/m^3)	Lime (kg/m^3)	Silica fume (kg/m^3)	Silica Sand (kg/m^3)	Dry density g/cm
C50 L0	0	4.1	2.22	123.0	50	0	5.0	1336	1.391
C100 L0	0	8.2	1.26	139.0	100	0	10	1336	1.420
C150 L0	0	12.4	0.94	154.5	150	0	15	1336	1.440
C200 L0	0	16.5	0.78	172.0	200	0	20	1336	1.450
C50 L20	40	6.1	1.75	141.5	50	20	11.0	1336	1.500
C100 L40	40	12.2	1.09	177.0	100	40	22.0	1336	1.550
C150 L60	40	18.2	0.87	211.5	150	60	33.0	1336	1.500
C200 L80	40	24.2	0.76	246.0	200	80	44.0	1336	1.580
C50 L40	80	8.0	1.50	160.0	50	40	17.0	1336	1.660
C100 L80	80	16.0	1.00	214.0	100	80	34.0	1336	1.560
C150 120	80	24.0	0.84	268.5	150	120	51.0	1336	1.680
C200L160	80	32.0	0.75	322.0	200	160	68.0	1336	1.690

C=Cement, B=Binders (Cement+Lime+Silica Fume), S= Silica Sand, L= Lime, SF/C=10%, SF/L=30%

2.2. Numerical procedure

A finite element model was performed to reproduce the triaxial compression test. It includes 110 triangular two-dimensional elements under triaxial axi-symmetric condition (figure 1). Three-types of constitutive models were tested to reproduce the mechanical response of the cemented sand samples:
- A non-associated elastic perfectly plastic constitutive model, based on the failure criterion of Morh-Coulomb.
- Hardening-Soil model, which is an advanced model in the framework of classical theory of plasticity.
- MODSOL model (Khoshravan, 1995), which is an advanced elastoplastic model based on the concept of bounding surface (Dafalias and Popov, 1975), involving isotropic hardening.
-
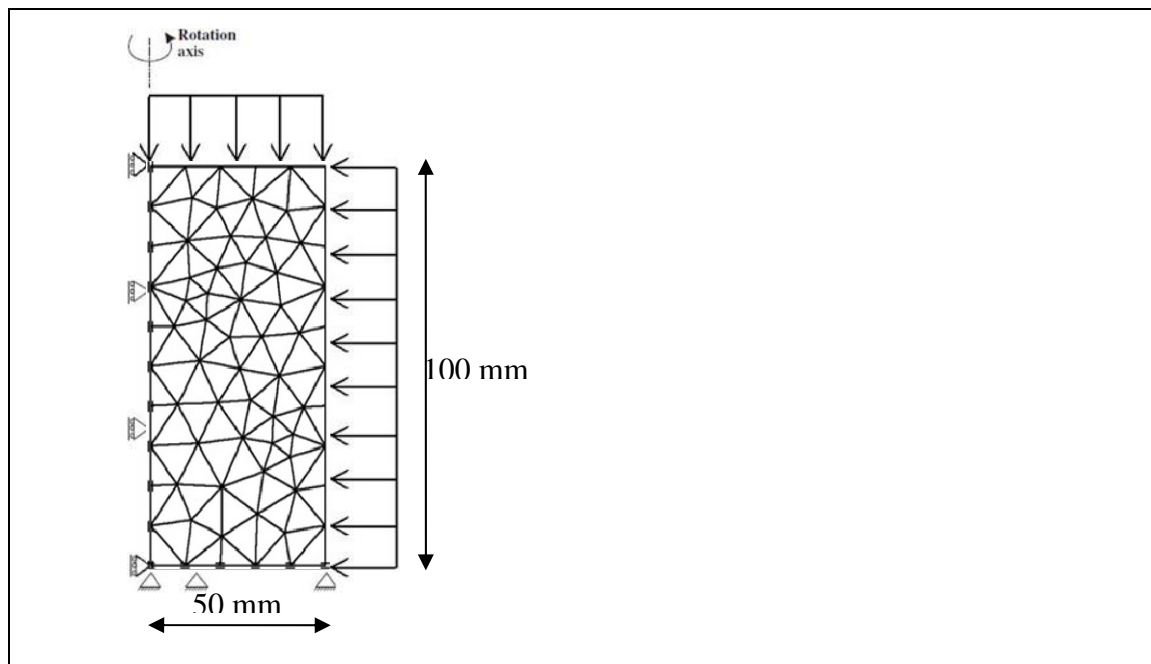
Figure 1: Cylindrical unit cell used for an axi-symmetric simulation

3.   NUMERICAL SIMULATION

3.1.   Mohr-Coulomb model

A non-associated elastic perfectly plastic constitutive model is firstly used in this study. This constitutive relation is popular in the analysis of the geotechnical structures, because of the availability of constitutive parameters for a wide range of soils. The elastic part is assumed to be linear and isotropic. It involves two constitutive parameters: Young Modulus E and Poisson ratio ν. The Mohr-Coulomb criterion is used to describe the yield function. Its expression is given by:

$$f = p \sin \varphi + \sqrt{J_2} \cos \theta - \sqrt{\frac{J_2}{3}} \sin \varphi \sin \theta - C \cos \varphi \tag{1}$$

C and φ designate the soil cohesion and the friction angle, respectively; p, J_2 and   stand for the mean stress, the second invariant of the deviatoric stress tensor and the Lode angle, respectively. Their expressions are given by:

$$p = \sigma_{ii}/3 \tag{2}$$

$$J_2 = \frac{1}{2} s_{ij}.s_{ij} \text{ where } s_{ij} = \sigma_{ij} - p\delta_{ij} \tag{3}$$

$$\theta = \frac{1}{3}\sin^{-1}\left(-\frac{3\sqrt{3}}{2}.\frac{J_3}{J_2^{3/2}}\right) \text{ where } J_3 = \frac{s_{ij}.s_{jk}.s_{ki}}{3} \tag{4}$$

The plastic potential is expressed as:

$$g = p \sin \psi + \sqrt{J_2} \cos \theta - \sqrt{\frac{J_2}{3}} \sin \varphi \sin \theta \tag{5}$$

Where ψ is the dilatancy angle.

3.1.1.   *Identification of parameters by Mohr-Coulomb model (MC-model)*

The set of constitutive parameters used in Mohr-Coulomb model includes five parameters, which are easily calibrated by an iterative fitting procedure, based on the experimental results of triaxial test under several confining pressure (figure 2).

Figure 3 summarises the determination of the Mohr-Coulomb parameters. It shows that Young modulus is derived from deviatoric stress (q) and axial strain (ε_1) diagram. Poisson's ratio is given by the slope of the elastic part of volumetric strain (ε_v) vs. axial strain (ε_1) diagram. The friction angle and cohesion can be obtained from $p - q$ failure envelope. The dilatancy angle can be obtained from the plastic part of $\varepsilon_v - \varepsilon_1$ diagram. Figure 4 shows an example of the numerical simulation of the drained triaxial compression tests of the mixture C100-L0-28 under confining pressures of 100, 200 and 400 kPa, after 28 days curing. It shows that the rate of mobilization of the deviator stress increases with effective confining stress and illustrates the underlying mechanisms of the strength enhancement and volumetric dilation due to cementation effects. Table 2 gives the sets of parameters used for this simulation.
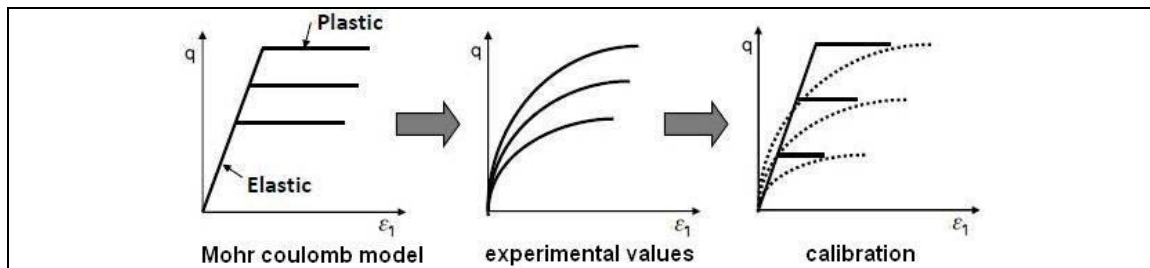
Figure 2: Iterative fitting procedure for the determination of Mohr-Coulomb parameters
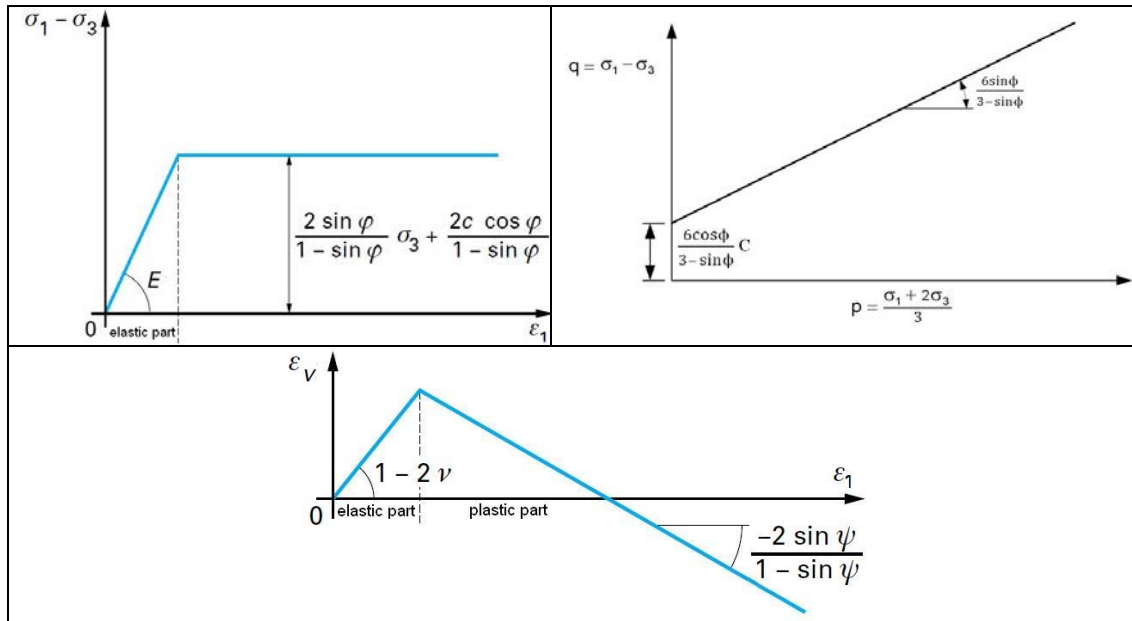
Figure 3: Triaxial drained test paths simulated by Mohr-Coulomb model

Table 2: Mohr Coulomb model set of parameters for C100-L0-28

E (kPa)	ν	φ (degree)	ψ (degree)	C (kPa)
220000	0.2	38	12	221.8

3.1.2. *Results of numerical simulations of triaxial drained paths*

By using the previous procedure, it has been possible to determine the evolution of parameters of Mohr-Coulomb model for various mixtures of cement treated sand, and for different curing times (28 and 180 days). Results are summarised in figure 5 for the Young modulus E, friction angle   and cohesion C. We can note that Young modulus increases with cement factor, lime content and curing time. It is also observed that the influence of cement factor is more important with the increase of lime content. The same trends are observed for the cohesion and friction angle that indicate an improvement of the treated sand with increase of cement and lime.
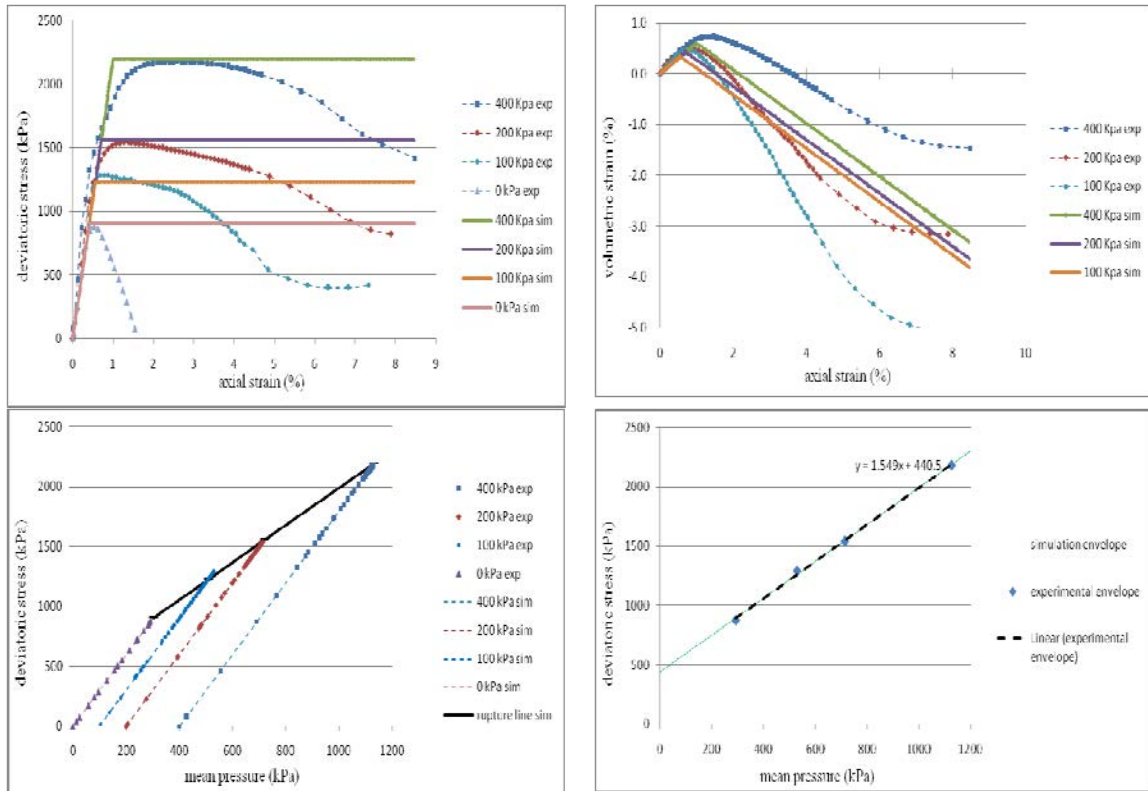
Figure 4: Simulation of the drained triaxial test on C100-L0-28 mixture using MC-model

3.2. Hardening-Soil model (HS-model)

The Hardening-Soil model is an advanced model in the framework of classical theory of plasticity. As for Mohr-Coulomb model, limiting states of stress are described by means of friction angle (φ), cohesion (c), and dilatancy angle (ψ). However, soil stiffness is described much more accurately by using three different input stiffnesses: the triaxial loading secant stiffness, E_{50}, the triaxial unloading reloading stiffness, E_{ur}, and the oedometer loading stiffness, E_{oed}.

In contrast to the Mohr-Coulomb model, the Hardening-Soil model also accounts for stress-dependency of stiffness moduli. This means that all stiffnesses increase with confining pressure. Hence, all three input stiffnesses relate to a reference stress.

With respect to its stiffness behavior the model involves a power law formulation for stress dependant stiffness. In fact, the model shows a hyperbolic stress-strain response when simulating a standard drained triaxial test (Figure 6).

28 days	180 days
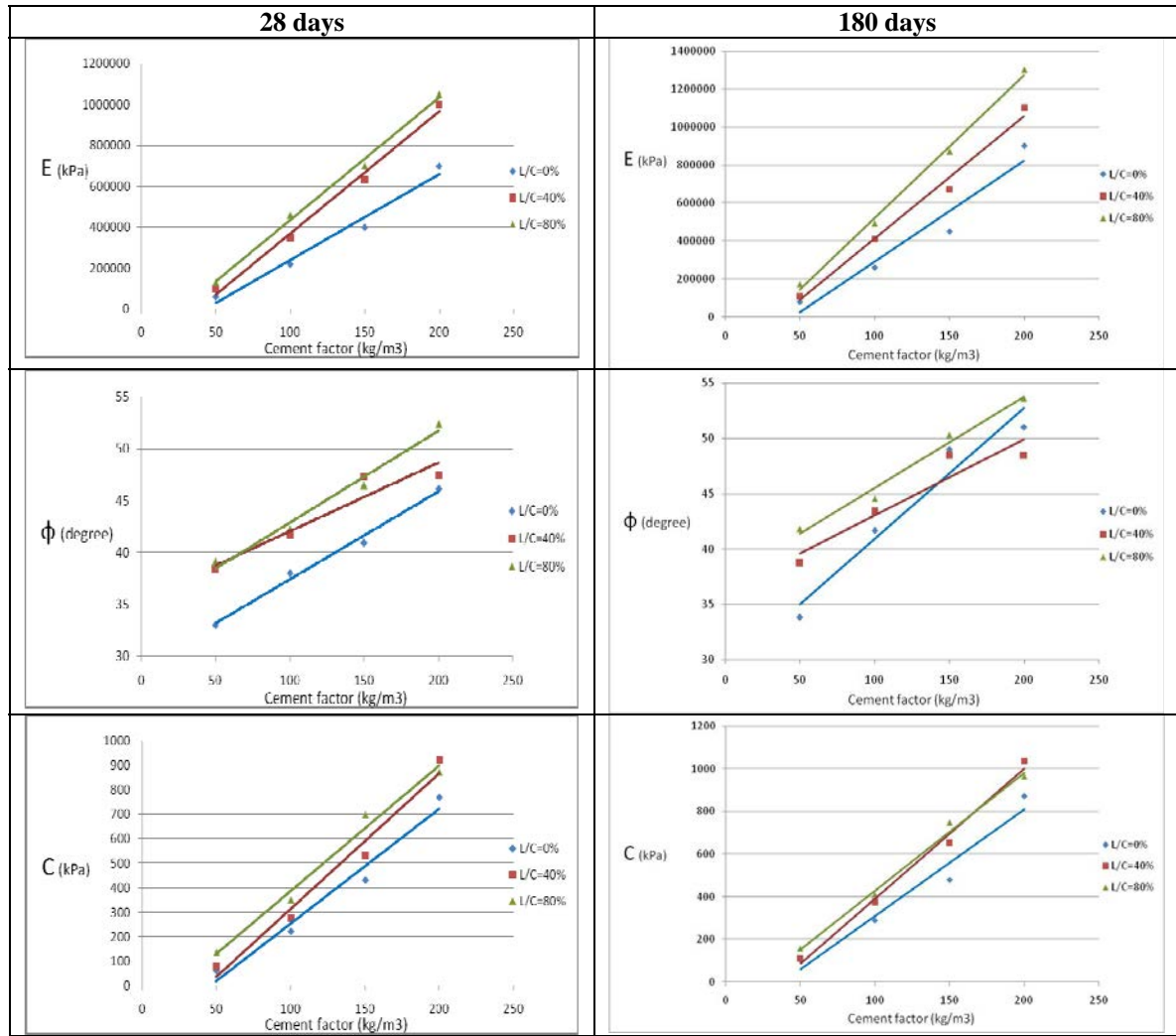
Figure 5: Evolution of strength parameters of MC-model with the increase of cement and lime at 28 and 180 days
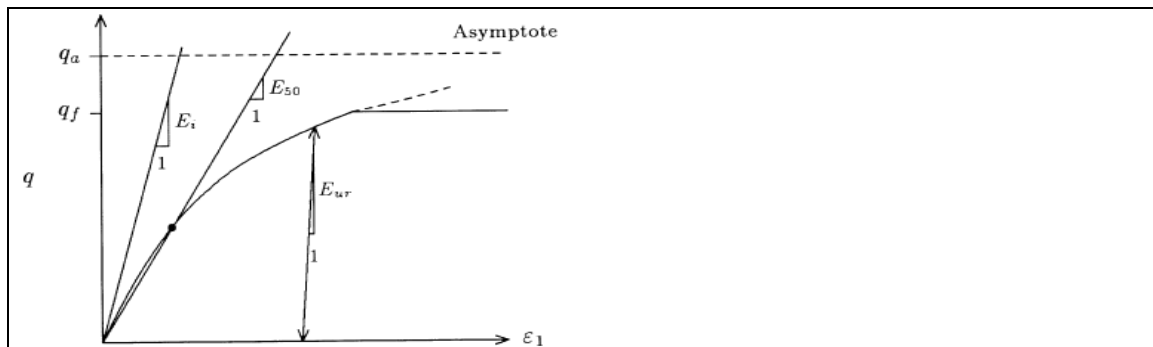
Figure 6: Hyperbolic stress-strain relation in primary loading for a standard drained triaxial test

Two types of hardening are present in this model, friction hardening (shear hardening) and cap hardening (compression hardening). Shear hardening is used to model irreversible strains due to primary deviatoric loading and compression hardening is used to model irreversible plastic strains due to primary compression in oedometer loading and isotropic loading. Failure is defined by means of Mohr-Coulomb failure criterion. By increasing the deviatoric loading, the failure surface approaches the Mohr-Coulomb failure line (Figure 7). Because of two types of hardening, the model is also accurate for problems involving a reduction of mean effective stress and at the same time mobilization of shear strength. Such situations occur in excavation (retaining wall problems) and tunnel construction projects.

The shear yield function is expressed as:

$$f_{13} = \frac{q_a}{E_{50}} \frac{(\sigma_1 - \sigma_3)}{q_a - (\sigma_1 - \sigma_3)} - \frac{2(\sigma_1 - \sigma_3)}{E_{ur}} - \gamma^p \tag{6}$$

Where γ^p is the plastic shear strain used as the relevant parameter for the frictional hardening, and q_a is the asymptotic failure deviatoric stress as shown in figure 6.

The plastic potential is expressed as:

$$g_{13} = \frac{(\sigma_1 - \sigma_3)}{2} - \frac{(\sigma_1 + \sigma_3)}{2} . sin\psi_m \tag{7}$$

Where ψ_m is the mobilized dilatancy angle.

Table 3 gives an example of the set of parameters obtained after calibration procedure for C100-L0-28, according to figure 8, for three levels of confining pressure: 100, 200 and 400 kPa. It shows a better simulation of the triaxial drained test, either for the deviatoric stress or volumetric strain vs. axial strain.
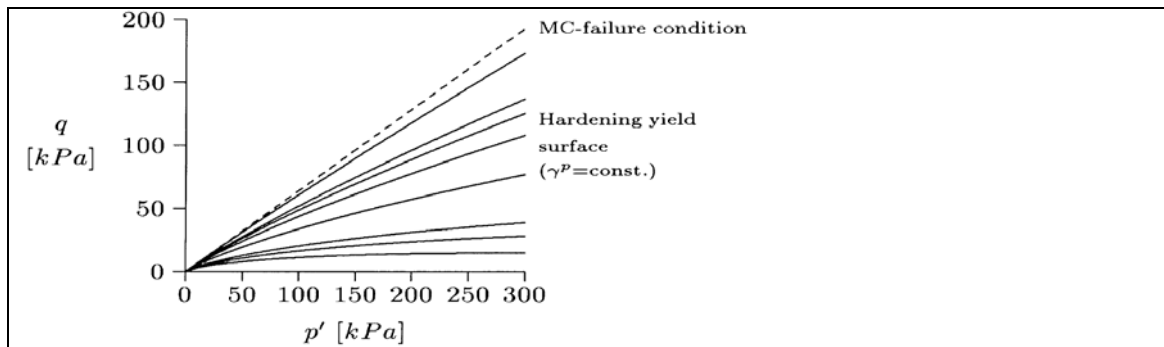
Figure 7: Successive yield loci for various values of the hardening parameter γ^p and failure surface

Table 3: Hardening soil model set of parameters for C100-L0-28

E_{50}^{ref} (kPa)	E_{oed}^{ref} (kPa)	E_{ur}^{ref} (kPa)	C (kPa)	φ (degree)	ψ (degree)	υ_{ur}	m	K_0^{nc}	R_f
100000	50000	325000	81.41	38.34	9	0.2	0.5	0.380	0.95
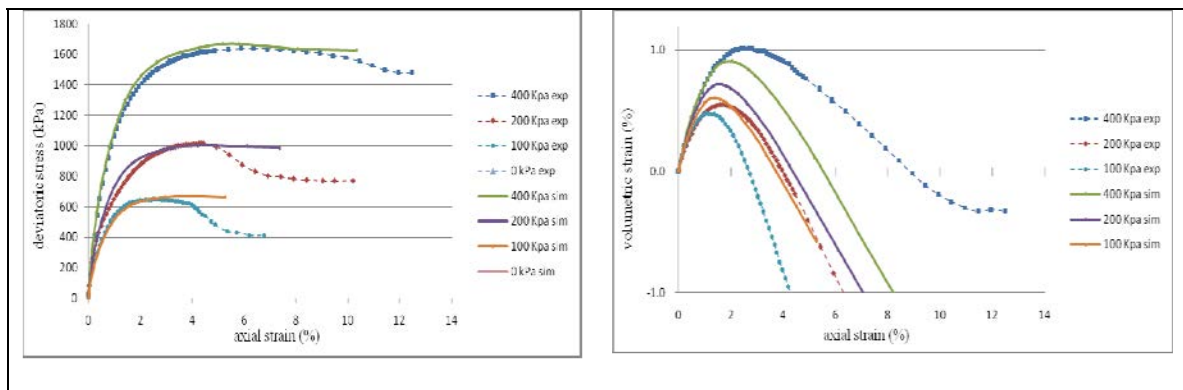
Figure 8: Numerical simulation for C50-L20-28 by Hardening Soil model

3.3.   Modsol Model

The third constitutive model tested in the paper is Modsol model which has been developed by I. Shahrour and W. Chehade (1992). It is based on the theory of elastoplasticity whereby any increment of deformation has a reversible elastic component and an irreversible plastic component. One of the hypotheses is to consider that the material is described by a non-associated flow rule. This model takes into account the fundamental aspects of observed behavior of granular materials, including: nonlinear elasticity, critical state and change of friction angle based on the mean pressure.

The elastic behavior of the model is assumed isotropic and non-linear. Young's modulus is assumed to depend on the average pressure in the form below:

$$E = E_0 \left(\frac{P}{P_0} \right)^n \tag{8}$$

Where:

E_0 and n are two parameters from the model ($0 < n < 1$)

P is the mean pressure

P_0 is a reference pressure

In contrast to Young modulus, the Poisson's ratio is taken constant and independent of mean pressure:

$$\nu = \nu_0 \tag{9}$$

The loading surface is conical in principal stress space, and it evolves according to a hardening rule. In monotonous loading the hardening rule is isotropic. The original Modsol loading surface was described as:

$$f_m = q - M_f \cdot p \cdot R_m \tag{10}$$

Where R_m represents the isotropic hardening function.

The hardening is assumed to depend only on deviatoric plastic deformations (ε_d^p) and takes values between 0 (initial elastic domain) and 1 at rupture. It is expressed as:

$$R_m = \frac{a \varepsilon_d^p}{b + \varepsilon_d^p} + c \left(\varepsilon_d^p \right)^2 \exp(-d \varepsilon_d^p) \tag{11}$$

a and b are two parameters of the model principally affecting the speed of evolution and the amplitude at peak.

c and d are two parameters that control the phenomenon of softening.

We note that this expression contains two terms: a hyperbolic term generally used for soils, and an exponential term that takes into account the softening of materials observed in the behavior of dense sands.

The coefficient M_f is given by:

$$M_f = \frac{6 sin\varphi}{3 - sin\varphi \cdot sin3\theta} \tag{12}$$

where φ and θ represent respectively internal frictional angle at peak and the angle of Lode.

Since the original Modsol model was developed to predict purely frictional sands behavior and that the soil used in this study was very cohesive due to the use of cement (cohesion between 60 kPa to 1 MPa), it was necessary to add the cohesion on the loading surface, in order to make the purely frictional model take into account the cohesion of the mixture. The new loading surface is then expressed as:

$$f_m = q - M_f \cdot p \cdot R_m - C \tag{13}$$

Where C is the cohesion of soil held as constant (independent from the mean pressure)

The projection of the load surface in the deviatoric plane is assumed to coincide with a rounded Mohr-Coulomb criterion.

The gradient of plastic potential is given by the following equation:

$$\frac{\partial g_m}{\partial p} = \frac{exp\left(-\alpha_0 \varepsilon_d^p\right)}{M_c \, p} \left(M_c - \frac{q}{p} \right) \tag{14}$$

α_0 is a parameter to control the expansion rate and to cancel it in high amounts of deviatoric deformations. For $\alpha_0 = 0$ we find the flow rule of the Cam-Clay model.

$$\frac{\partial g_m}{\partial q} = \frac{1}{M_c \, p} \tag{15}$$

M_c represents the q/p ratio in the transition from contracting domain to dilating domain. It is assumed to depend on the Lode angle and characteristic angle φ_{cv}. It is described by:

$$M_c = \frac{6 sin\varphi_{cv}}{3 - sin\varphi_{cv} \cdot sin3\theta} \tag{16}$$

φ_{cv} is the internal friction angle at constant volume in the triaxial compression test.

Thus the model includes 13 parameters in its modified version, which includes the cohesion: $E_0, v_0, n, \varphi_b, \varphi, P_n, \alpha_0, \varphi_{cv}, a, b, c, d, C$

Due to the contractive-dilative behavior of Modsol model the stress-strain and volumetric deformations are well predicted in low and high cement quantities. Calibration procedure on drained triaxial tests under 100, 200 and 400 kPa confining pressures for various mixtures is then carried on. As an example, we obtained for the mixture C50-L20-28 the sets of parameters given on table 4, and the corresponding curves for both deviatoric stress and volumetric strain vs. axial strain are plotted on figure 9. It is observed that the use of Modsol enhances the simulation of triaxial behavior of cemented sand, with a better fitting of softening behavior.

Table 4: Modsol set of parameters for C50-L20-28

E_0 (kPa)	v_0	n	φ_b (°)	φ (°)	φ_{cv} (°)	α_0	a	b	c	d	C (kPa)
110000	0.1	0.2	35	0	37	7	1.012	0.0008	850	55	120
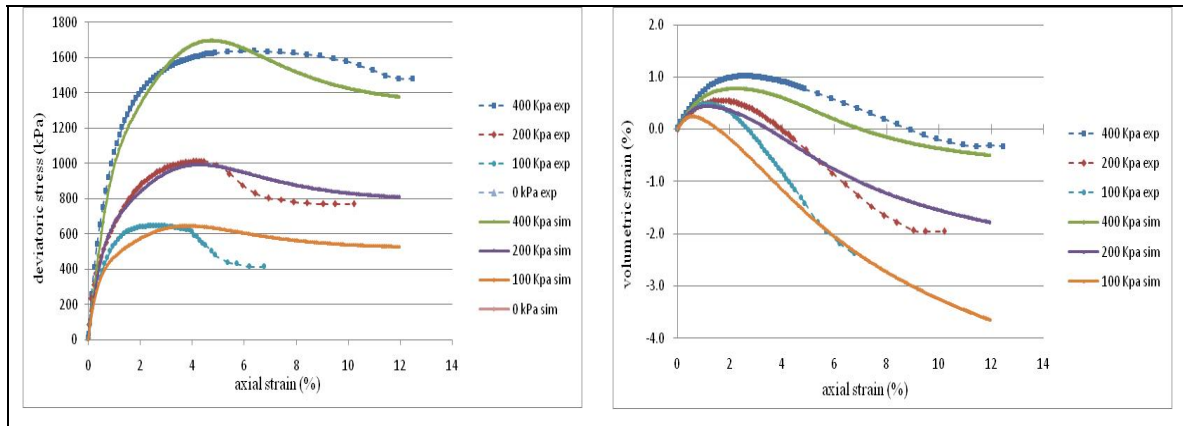
Figure 9: Numerical simulation for C50-L20-28 by MODSOL model

4. CONCLUSIONS

This paper dealt with the simulation of behavior of cemented treated sand under triaxial conditions. Depending on the amount of binders, it has been noted that the treated sand exhibits a moderate material softening behavior. In this context, it has been shown that, although Mohr-Coulomb is a simple constitutive model, it is an effective model for the identification of the soil strength parameters because of its simplicity, accuracy and efficiency. When increasing the amount of binders, it may be necessary to use a more complex constitutive model to reproduce the softening observed for large strain. Indeed, with the increase of cement and time curing, the testing data show very pronounced strain softening with significant volumetric dilatation under triaxial loading. Thus, the contracting-dilating effect of the material leads to a complex behavior that is better simulated using Modsol model, because of its ability to reproduce the hardening and softening behavior of the mixed soil.

It is expected that the damage evolution plays a key role in material softening and failure process. This may be the inelastic behavior related to irreversible frictional sliding of contact planes. This aspect has

not been taken into account in the present work, and should be the next step to predict the behavior of cemented treated sand under triaxial condition.

REFERENCES

Ajorloo A.M. (2010), "Characterization of the Mechanical Behavior of Improved Lose Sand for Application in Soil Cement Deep Mixing", Ph.D. thesis, University of Sciences and technologies of Lille, France.

ASTM C 150-86. Standard specification for portland cement. 1990 Annual book of ASTM standards 4.02, 89-93.

Bardet J.P. (1997), "Experimental soil mechanics", ISBN 0-130374935-5, PRENTICE HALL
Upper Saddle River, New Jersey 07458

Dafalias, Y. F., and Popov, E. P. (1975). "A model of nonlinear hardening materials for complex loading." Acta Mechanica, 21, 173–192.

Jiang, H. (2010) A note on the Mohr-Coulomb and Drucker–Prager strength criteria, Mechanics Research Communications, doi:10.1016/j.mechrescom.2011.04.001

Khoshravan Azar. A. (1995), "Problemes de sols satures sous chargement dynamique : Modele cyclique pour les sols et validation sur des essais en centrifugeuse", Ph.D. thesis, Ecole Centrale de Lille, Laboratoire de Mecanique de Lille, France.

Magnan J.P. & Mestat P. (1997), "Lois de comportement et modélisation des sols", Techniques de l'Ingénieur, traité Construction, C218.

Mroueh H. (1994), "Validation of two rheological models on the calculation of an earth dam", Masters (DEA) dissertation, Ecole Centrale de Lille, Laboratory of Mechanic of Lille

Q.Z. Zhu, J.F. Shao, M. Mainguy (2010), "A micromechanics-based elastoplastic damage model for granular materials at low confining pressure", International Journal of Plasticity, 26 (2010) 586-602.

Schanz T, Vermeer P.A., Bonnier P.G. (1999), "The hardening soil model Formulation an verification", Beyond 2000 in Computational Geotechnics – 10 Years of PLAXIS © 1999 Balkema, Rotterdam, ISBN 90 5809 040 X

Soil Cement Stabilization - Mix Design, Control and Results during Construction

Jose N. Gomez S., ECS Mid-Atlantic, LLC, U.S.A., Jgomez@ecslimited.com

David M. Anderson, ECS Mid-Atlantic, LLC, U.S.A., Danderson1@ecslimited.com

ABSTRACT

An active two-lane US State Highway located in Northampton County, Virginia, U.S.A., required roadway improvements. Surface features consisted of 2 to 3 inches of asphalt pavement, underlain by a coarse sand base. In order to improve the roadway structure, a soil-cement stabilization was recommended and implemented for the upper 8 inches of the existing roadway structure.

Soil-cement stabilization consisted of pulverizing the existing asphalt and mixing it with existing base materials. The recycled asphalt and base materials were then combined with 4% cement by weight and moisture content was manipulated in order to maintain soils within the optimum moisture content.

In order to design the required cement ratio of the soil-cement mix, several samples of existing asphalt and base were obtained. Standard Proctor tests were performed to determine the maximum dry density and optimum moisture content of these materials when manipulated with varying cement contents. Soil-cement mixes were prepared with varying cement contents ranging from 4% to 6% by weight. The mix design requirement was to establish the cement content necessary to have a minimum unconfined compressive strength of 250 psi (1724 kpa) at 7 days.

This paper presents the soil-cement mix design, field-laboratory procedure and results. The construction sequences and the basic design example of the soil-cement mix are also given in this paper. Lastly, the results of the soil-cement improvements are shown.

1. INTRODUCTION

In general, pavement structure surfaces and/or aggregate bases become deteriorated throughout the years due to vehicular traffic and extensive weathering. This is a normal aging process that occurs during the life expectancy of a roadway. Roadway maintenance programs are typically conducted in a timely manner in order to maintain the integrity of the pavement structure to the required operational standard to assure safety and comfort to users. There are several methods to repair or stabilize pavement structures; one of these methods, known as Full Depth Reclamation - FDR (Utilizing soil cement stabilization means), calls for pulverizing the existing asphalt and mixing it with existing base materials; the recycled asphalt and base materials are then combined with cement to develop a strong compacted base material achievable only within the optimum moisture content. Intensive laboratory work is required to determine the optimum cement content for the resulting recycled mix.

The subject State Route 636 contained a severe pitch in excess of 5% and surface features consisted of 2 to 3 inches of asphalt pavement, underlain by a coarse sand base. The pavement structure was in a fatigued condition and Full Depth Reclamation practices were considered to be advantageous in order to reduce the pitch and provide a suitable base for the proposed roadway and at the same time improve the pitch of the existing roadway.

A total of eight (8) sample locations were selected for exploration at intervals no greater than 1,320 feet according to the Virginia Department of Transportation (VDOT) requirements. Asphalt and base materials were removed, pulverized and mixed to a maximum depth of 8 inches below the top of pavement.

All samples were subject to extensive, laboratory controlled testing and all data was recorded and analyzed according to VDOT and ASTM standards. The mix design requirement was to establish the cement content necessary to have a minimum unconfined compressive strength of 250 psi (1724 kpa) at 7 days. According to the research, it was found that a cement content of 4% cement by weight was acceptable for the blend of pulverized asphalt and existing base materials.

This paper contains the interpretation and results of our field exploration and soil cement mix design for Route 636 reclamation, located on Cobbs Station Road in Northampton County, Virginia, U.S.A. The owner of the project is VDOT, Hampton Roads District; the reclamation project was conducted by Slurry Pavers Incorporated and the design and field quality control (QC) were performed by ECS Mid-Atlantic, LLC (ECS). The authors of this paper would like to thank Michael J. Galli of ECS for providing input and review of this paper. Works were carried out during the summer of 2010.

2.   PROJECT CHARACTERISTICS

The subject roadway reclamation project is located along State Route 636 – Cobbs Station Road in Northampton County, Virginia, U.S.A. The project is located in what is called the Easternshore at the Mid-Atlantic portion of the country (coastal region). The roadway reclamation project consisted of the widening of the existing roadway along a length of approximately 5,000 feet (1,524 meters), and stabilizing the existing pavement cover and base by means of soil cement stabilization. The total thickness of the stabilized portion was approximately 8 inches (0.2 meters).

In order to accomplish soil-cement stabilization using the FDR technique, the existing asphalt was pulverized and mixed with existing base materials. The recycled asphalt and base materials are then combined with a specified amount of Portland Cement and the moisture content is manipulated in the field in order to maintain the soils at levels of optimum moisture content as determined in the soils laboratory by means of the Standard Proctor test. The soil cement material (or reclaimed material) is then roller compacted in one lift of approximately 8 inches with cement, moisture, and aggregate blended at specified levels required to achieve the minimum compressive strength.

3.   EXPLORATION PLAN AND RESULTS

3.1   Site Conditions

At the time of the subsurface investigation and design analysis, the existing roadway was active and located within a coastal region; the ground water table was within 2 to 3 feet below the ground surface. The roadway is paralleled by drainage ditches and is surrounded by agricultural facilities.
Photo 1 and 2 depict project site before starting the reclamation works.

Photo 1

Photo 2

3.2   Existing Pavement Structure Conditions

It was observed that the existing roadway consists of 2 to 3 inches of asphalt pavement. Approximately 6 to 8 inches of coarse sand fill material was encountered underlying the asphalt pavement. Laboratory testing determined the actual field moisture content with the added asphalt material is approximately 4%. The underlying coarse sand fill appeared to be well graded and consistent throughout the existing roadway.

The existing roadway had an approximate pitch of 5% and the reclamation process is intended to aid in reducing the existing pitch and fatigued pavement structure. The reclamation process was anticipated to include only the asphalt pavement and base materials; no subgrade soils were anticipated to be included within the mix design. Samplings of the road base are depicted within Photos 3 and 4.

Photo 3   *Photo 4*

4.   SOIL CEMENT MIX DESIGN

4.1   Method Description

Soil samples were extracted from the existing roadway at intervals no greater than 1,320 linear feet (402 meters) within each lane. Sample extraction was controlled in order to ensure the proper depth and ratio of pavement to base soils was consistent with anticipated construction procedures. Bulk samples and asphalt pavements were pulverized and blended within the laboratory using mechanical means to gradations similar to typical blending of the field equipment.

Laboratory testing consisted of full gradation analysis, Standard Proctor testing, molding of cylinders for compressive strength testing; compacted to 97% maximum dry density having cement contents of 4%, 5%, and 6%. Average maximum dry density and optimum moisture content were within 127 pcf and 5.6%, respectively. Density results are depicted within Figure 1.
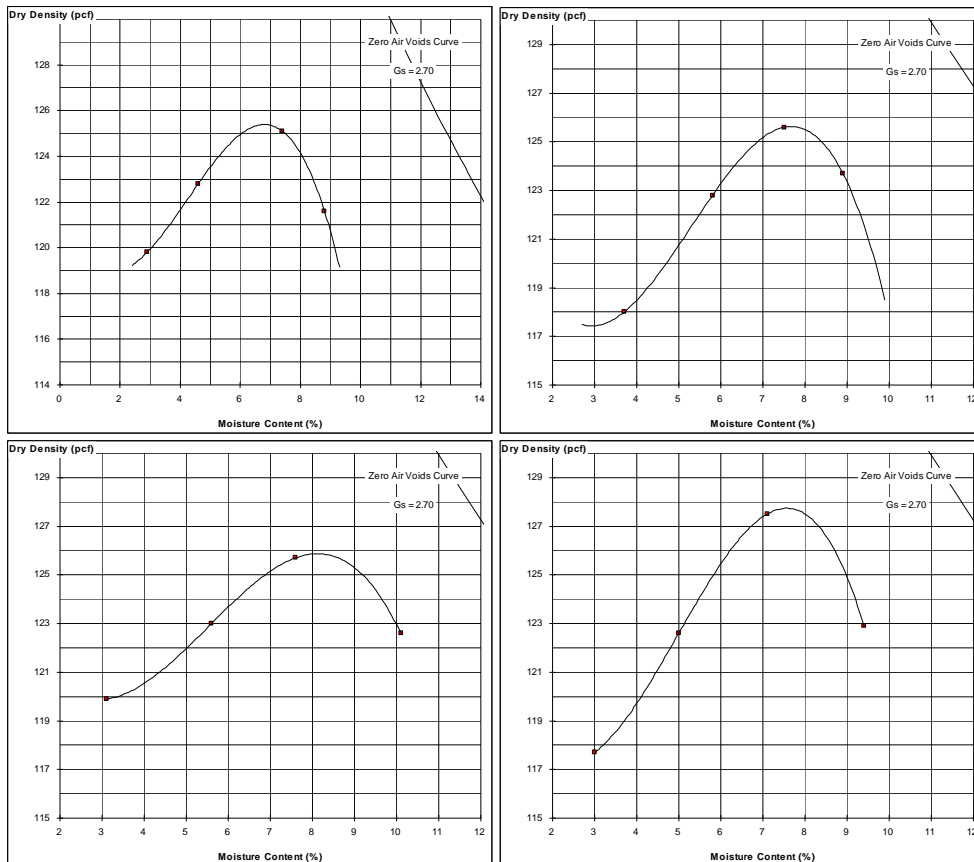
Figure 1

4.2   Unconfined Compressive Strength Results

A total of 24 cylinder samples were formed using differing cement contents of 4%, 5% and 6% by weight. Samples were prepared to 97% maximum dry density using Standard Proctor compaction test procedures.

Average compressive strengths for soil cement cylinders made from the blended base material with cement contents of 4%, 5% and 6% were 379.5 psi, 448.9 psi and 483.1 psi, respectively. As indicated within Figure 2, soil cement strengths increase progressively as cement content increases. Compressive strength increased in average by approximately 18% from 4% to 5% cement content, and 27% increase from 4% to 6% cement content.

Soil cement cylinders made from samples 1 through 8, taken on the existing roadway, were tested at 7 days and compressive strengths greater than 250 psi were observed for all samples tested.

All soil cement cylinders made from the asphalt blended base material have an observed maximum dry density of approximately 127 pcf and an observed optimum moisture content of approximately 5.6%. These results are similar to those obtained in the lab without cement.

Compressive strength results according to all 8 samples tested are as depicted below within Figure 2; the bolded curve corresponds to the average one used for selecting the cement percentage as explained in next section.
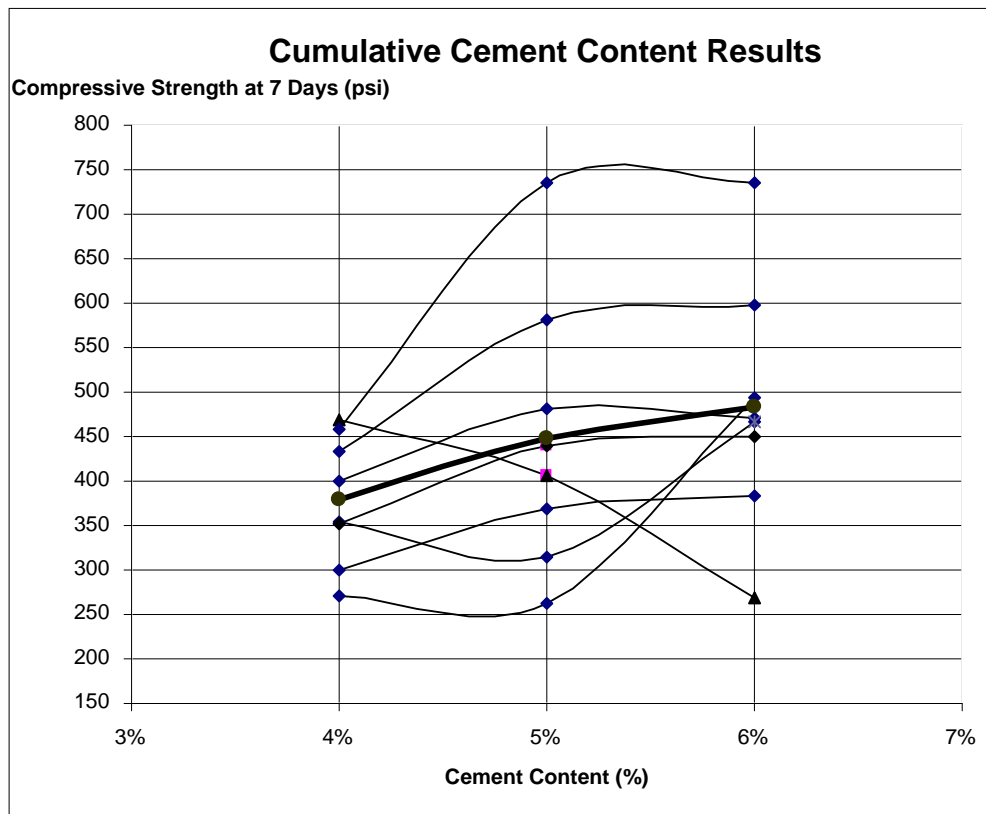
Figure 2

The bold line depicts the average of soil cement compressive strengths and thinner lines depict the results of each individual sample.

Photo 5 and 6 depict the results of compressive strength testing. Failure planes followed Coulomb type of failure.

Photo 5

Photo 6

4.3   Cement Content Selection

According to VDOT and ASTM requirements, soil cement cylinders taken from FDR procedure must have a compressive strength of 250 psi (1724 kpa) at 7 days. Design cement content was determined based on weight and cement contents were developed at 4%, 5% and 6% accordingly.

The blended soil mix was considered to have a maximum dry density of 127 pcf across the project site. Blending of the mix is depicted within Photos 7 and 8; it was very important to obtain a uniform mix to assure a high quality sample, representative of likely field conditions.

Photo 7

Photo 8

Based on a thorough analysis of all results and data made available at the time of this study, the following soil cement design parameters were to be applied to the soils specific to the State Route 636 Pavement Rehabilitation. Optimum cement content was recommended to be at least 4% by weight for base materials blended with asphalt pavements encountered on site, in order to obtain a compressive strength of 250 psi (1724 kpa) at 7 days.

5.   CONSTRUCTION PRACTICES DURING RECLAMATION

5.1   Construction Reclamation Method

Full Depth Reclamation methods were used in the rehabilitation of the subject roadway with reclamation extending to depths of 8 inches below the top of the existing pavement structure and complete blending of the asphalt pavement with the existing base materials. Some leveling of the roadway occurred after moisture conditioning and the addition of Portland Cement in order to adjust grades and elevations per drainage requirements.

5.2 Quality Control and Results

During the course of construction full time quality control measures were provided and included the verification of cement content, adequate moisture and density via nuclear gauge testing and minimal sand cones, proper compaction and mixing techniques, and timely mixing and placement of soils.

After a period of 7 days, coring of the rehabilitated base was attempted. Coring of the stabilized mix proved to be unsuccessful because the samples crumbled, likely due to the coring method itself or the resulting stabilized sandy matrix did not have the adequate strength to hold together with the applied pressures of the coring operation. It was not possible to conduct in-situ plate testing to determine the strength of the stabilized soil-cement mix. Due to the inability to obtain quality field specimens after construction to verify in-situ conditions, acceptance was based on density results, adequate means of rehabilitation, and observed stability of the roadway.

6. CONCLUSIONS

Field collection of the soil samples must be strictly maintained to specific proportions, replicating construction conditions, in order to adequately obtain proportioned samples. Additionally, the gradation of asphalt, as pulverized within the lab, must be compared to historical pulverizing of the subject equipment. Best practice for the contractor is to maintain a log of asphalt gradations upon crushing in order to properly determine sufficient pulverizing methods within the laboratory.

The addition of cement should be measured not only by rate of application, but also by means of weight spread over a fixed area. Additional measures to ensure adequate cement content are to collect field samples for additional laboratory testing for Portland Cement content verification.

Soil-cement mix design using traditional mixing and compacting soil laboratory test methods probed to be a reliable procedure to establish the optimum cement percentage for the mix. Standard Proctor test was required to determine maximum dry density and optimum water content. It is recommended for further studies to compare results with Modified Proctor test to verify the ability to core the in-situ material at early ages.

Full Depth Reclamation processes do not allow for compacting soils in multiple lifts; therefore, it is critical that adequate compacting equipment, such as a heavy compaction roller, be used for the compaction of stabilized soils.

Coring of the finished product was not possible on this specific project at 7 days; therefore, acceptance of the subject roadway was based on adequate levels of density and observed stability of the roadway. Based on observations and test procedures utilized on this project, it was determined that field quality control verification for FDR procedures utilizing soil cement means and sandier soils, in lieu of high aggregate content, should be pill-formed during construction for curing within the laboratory and testing at 7 days.

REFERENCES

Asphalt Recycling and Reclaiming Association. Basic Asphalt Recycling Manual. U.S.A: ARRA, FHA, USDOT; 2001.

ASTM D1632 - 07 Standard Practices for Making and Curing Soil-Cement Compression and Flexure Test Specimens in the Laboratory

Influence of tire chips on the mechanical properties of cement treated soil

Massimo Grisolia, Sapienza University of Rome, Italy, massimo.grisolia@uniroma1.it
Enrico Leder, Sapienza University of Rome, Italy, enrico.leder@uniroma1.it
Ignazio Paolo Marzano, Sapienza University of Rome, Italy, paolo.marzano@uniroma1.it
Taka-aki Mizutani, Port and Airport Research Institute, Japan, mizutani-t@pari.go.jp
Yoshiyuki Morikawa, Port and Airport Research Institute, Japan, morikawa@pari.go.jp

ABSTRACT

The paper presents results of a laboratory investigation on the influence of tire chips on the mechanical properties of cement-stabilised clayey sand, as used in soil mixing applications such as low permeability cut-off walls. The used soil was made up of 64% Soma Sand, 27% Kawasaki Clay, and 9% of gravel. Three different tire chips contents were used to compare the performance of different mixtures. Unconfined compressive strengths were determined at specific time intervals in order to follow the curing and the increase of strength with time. The effect on the hydraulic conductivity was also investigated. The test results showed that the strength and the secant modulus reduce with the tire chips content showing less fragile behaviour. Micro-focus X-ray Computed Tomography (CT) scanner was also used to investigate how the tire chips content influence the cracks pattern development and the failure mechanism with a positive effect on the hydraulic conductivity. From the study it can be drown that tire chips mixed with cement-treated soil could be successfully used in environmental applications to minimize the barrier breakage in the event of serious deformation due to differential settlements or earthquake events.

1. INTRODUCTION

Waste tire disposal has become a major environmental issue in many countries. The Landfill Directive 1999/31/EC (Council of the European union, 1999) forbade the landfill disposal of whole tires since 2003 and of shredded tires since 2006. Therefore, several beneficial and sustainable uses of waste scrap tires have been proposed worldwide in the last years, and some of them have already been applied in engineering works. Research on scrap tire-derived products such as tire chips as geomaterials has been conducted since the early 1990s, mainly in the US and Canada (Kikuchi et al., 2008). Shredded tires can be used for lightweight fill for embankment construction, retaining wall and bridge abutment backfill, vibration damping layer, drainage layer (Edil & Bosscher, 1992; Humphrey 2003). The environmental effects of using tire-derived geomaterials in the geo-environment were discussed by Edil (2007) showing that human health concerns are minimal for several application. Recent experiences related to scrapped tires for geotechnical applications include sand mixed with shredded tires to reduce liquefaction potential during earthquakes (Yasuhara, 2007) and cement treated clay with tire chips as a sealing material at a coastal waste disposal site (Hazarika et al., 2010). The effect of tire chips on the engineering properties of cement treated soil, as used for the construction of a seepage cut-off wall for a waste disposal site was studied in order to evaluate the performance of the barrier in the presence of large deformations. It has to be considered that a coefficient of permeability of 1.0E-09 m/s or less is usually required for cut-off wall as used for permanent seepage control. The effect of the tire chips fraction on the physical properties of cement treated soil was first investigated based on the results of computed tomography (CT) scanning with image processing analysis. Then a series of permeability and X-ray CT scan as a nondestructive observational method (Otani & Obara, 2004) tests were conducted during the process of unconfined compression (UC) test, and permeability change and failure mechanism were examined.

2. LABORATORY TESTS

2.1. Materials and mixing procedure

The used soil was an artificial clayey sand, characterized by a water content, $w_n = 16$ %. The soil was made from 64% of "Soma Sand", 27% of "Kawasaki clay" and 9% of clean Gravel (particle size: from 2.5 to 5 mm) (Photo 1). Properties of soils are shown in Table 1. The tire chips were shredded from used car tires to a separate size of few mm as shown in Photo 1. Average particle size was $D_{50} = 2$ mm, density 1,15 g/cm^3 and elastic modulus E = 4-6 Mpa.

Table 1: Details of the soils used (ρ_s = soil particle density, w_n = natural water content, L.L. = liquid limit, L.P. Plastic limit, D_{10}, D_{50}, D_{60} = percentage diameters)

Kawasaki clay	ρ_s	w_n	L.L.	L. P.	75 µm – 2mm	5 µm - 75µm	< 5µm
	2.68 g/cm³	57 %	48.6 %	23 %	14 %	42 %	44 %
Soma Sand	ρ_s	D_{60}	D_{50}	D_{10}	75 µm – 2mm	5 µm - 75µm	< 5µm
	2.65 g/cm³	0.37 mm	0.35 mm	0.25 mm	99.7 %	0.3%	0 %
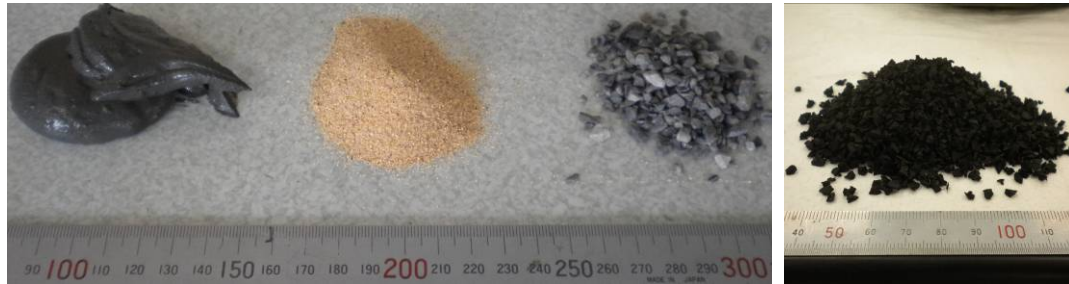
Photo 1: Elements of the artificial soil and tire chips used.

Three types of mixtures were studied, using different tire chips contents, t_c (%) = 0, 10 and 20 % defined as the ratio of the weight of tire chips introduced to the dry weight of the soil. The compositions of the three mixtures obtained are shown in Table 2. The grout used for the stabilisation was made by ordinary Portland cement (cement content = 10%, defined as the ratio of the weight of cement introduced to the dry weight of the soil) and water (water:cement ratio = 1). The water content of the soil was adjusted to the desired value, then tire chips were added and the material was homogenised by mixing. The grout was then added and the materials were mixed for 10 minutes (according to JGS 0821-2000) using a "Hobart" type mixer. Stabilised material was then placed in plastic moulds (5 cm inner diameter and 10 cm height) in three layers, compacted by the "Tapping" technique, according to Leder et al. (2011). The samples obtained were stored in curing tanks for a maximum period of 28 days, at high relative humidity (~95%) and a constant temperature of ~ 20°C.

Table 2: The mixture's compositions tested (weight percentage)

Mixture	Clay (%)	Silt (%)	Sand (%)	Gravel (%)	Water (%)	Cement (%)	Tire (%)
M-1, t_c = 0	8.61	8.36	48.97	6.52	20.29	7.25	0.00
M-2, t_c = 10%	8.14	7.90	46.29	6.16	17.81	6.85	6.85
M-3, t_c = 20%	7.62	7.39	43.32	5.77	16.67	6.41	12.82

2.2.   Experimental procedure

Specimens were tested at 7 and 28 days. Specimens were first sealed with a membrane and set in the triaxial compression apparatus. A series of permeability test and X-ray CT scan were conducted during process of UC test, using the devices shown in Photo 2. The compression test was conducted with no confining pressure, while the permeability test was conducted applying an hydraulic gradient equal to 20 (according to ASTM D5084, 2000). CT scanning was conducted only for specimens cured for 28 days. In order to determine the initial state of the specimen set in the apparatus, X-ray CT scanning with image processing analysis was conducted at first, then initial permeability was evaluated. After the permeability test, the pressures were released, and the first compression step was conducted. Compression was interrupted at fixed strain, were X-ray scan and permeability test were performed again. This procedure was repeated several times, until the specimen reached the 2/3 of peak strength, according to JIS 1216:2009. Additional unconfined compression tests were performed on supplementary specimens.
The micro-focus X-ray CT scanner used is the same described by Kikuchi et al. (2007).
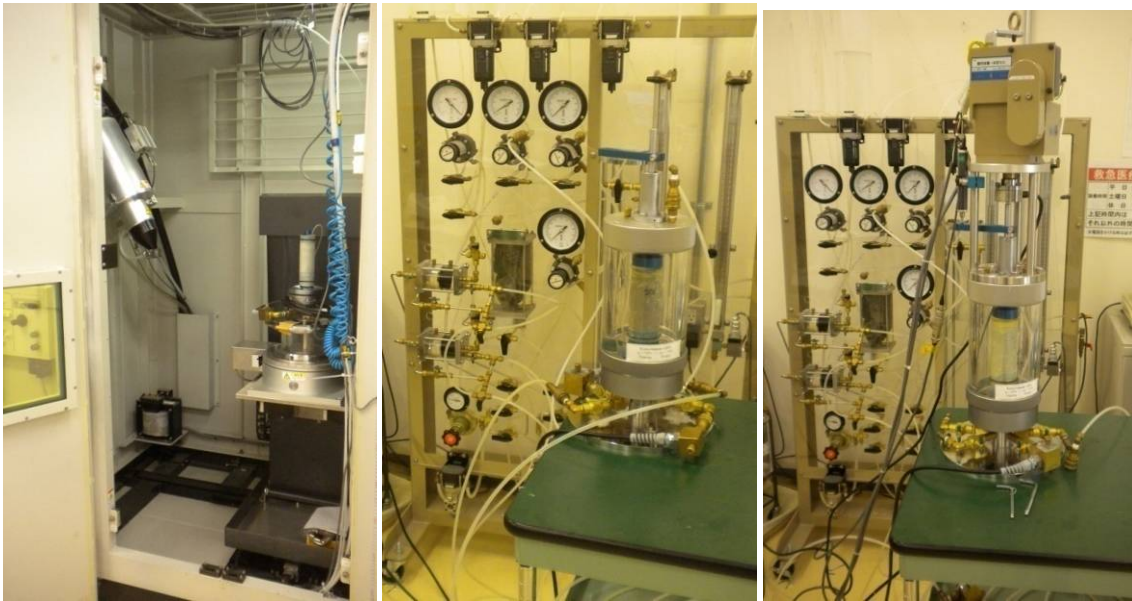
Photo 2: From left to right: X-Ray CT scanner, Triaxial apparatus and press used.

3. RESULTS AND DISCUSSION

The results of the experimental work are presented below in three different sections to show the effects of the tire chips addition on the physical and mechanical properties of the treated soil. For each mixture, three specimens for the UC test and one specimen for the permeability test and CT scanning during the compression process were used.

3.1. X-ray CT scan analysis

CT images of cross section were obtained for the specimens tested at 28 days (Figure 1). For each specimen a total of 500 slices of 0.2 mm height were obtained. CT image data are evaluated quantitatively using the so-called "grey level", which is a numerical number proportional to the material density. In CT images darker regions represent lower density zones, while lighter regions represents higher density ones. Therefore, air voids and cracks are black, tire chips are dark grey, soil-cement matrix is light grey and cement lumps and gravel pieces are white. It was possible to obtain a relation between the initial wet density of the specimen and the average grey value (Figure 2). After calibration, specimen density could be evaluated using the CT scanning results. Figure 3 shows the estimated density distributions with height for each specimen, evaluated from gray levels, considering initial ($\varepsilon = 0\%$) and peak states. During the compression test the density varies along the height of the specimens. The different specimens presents similar density variations, irrespective of tire chips presence, it means that the tire chips are uniformly mixed in the specimens M-2 and M-3, no segregation occurred.

Initial state, $\varepsilon = 0\%$

Scale: |⟵ 1 cm ⟶|

M-1 Specimen ($t_c = 0$)   M-2 Specimen ($t_c = 10\%$)   M-3 Specimen ($t_c = 20\%$)
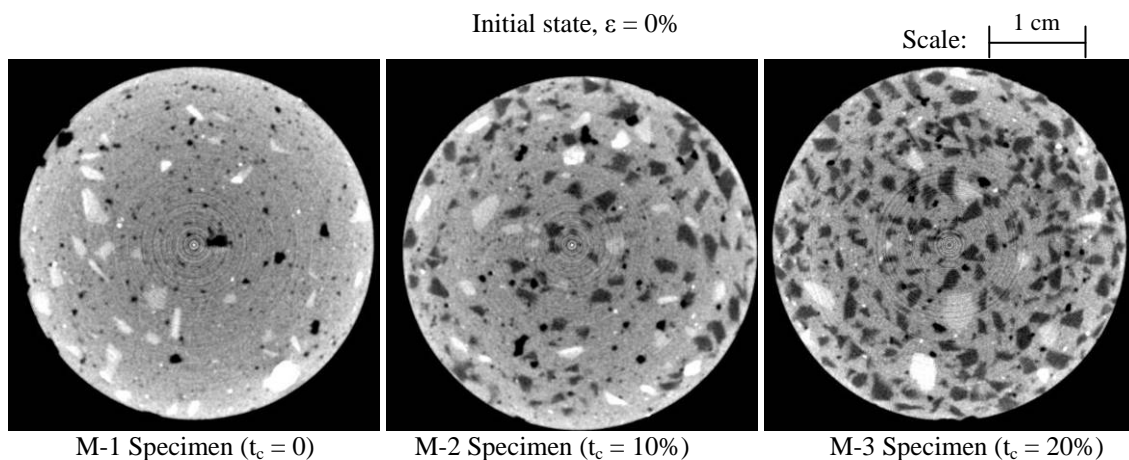
Figure 1: Cross sectional images of the specimens tested, chosen at middle heigth.
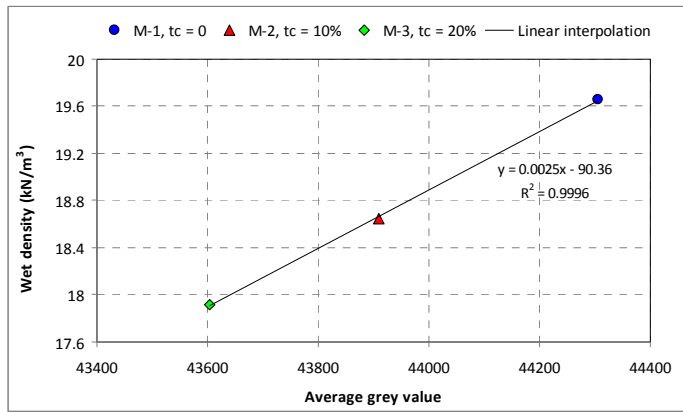
Figure 2: Relation between wet density and average grey value.
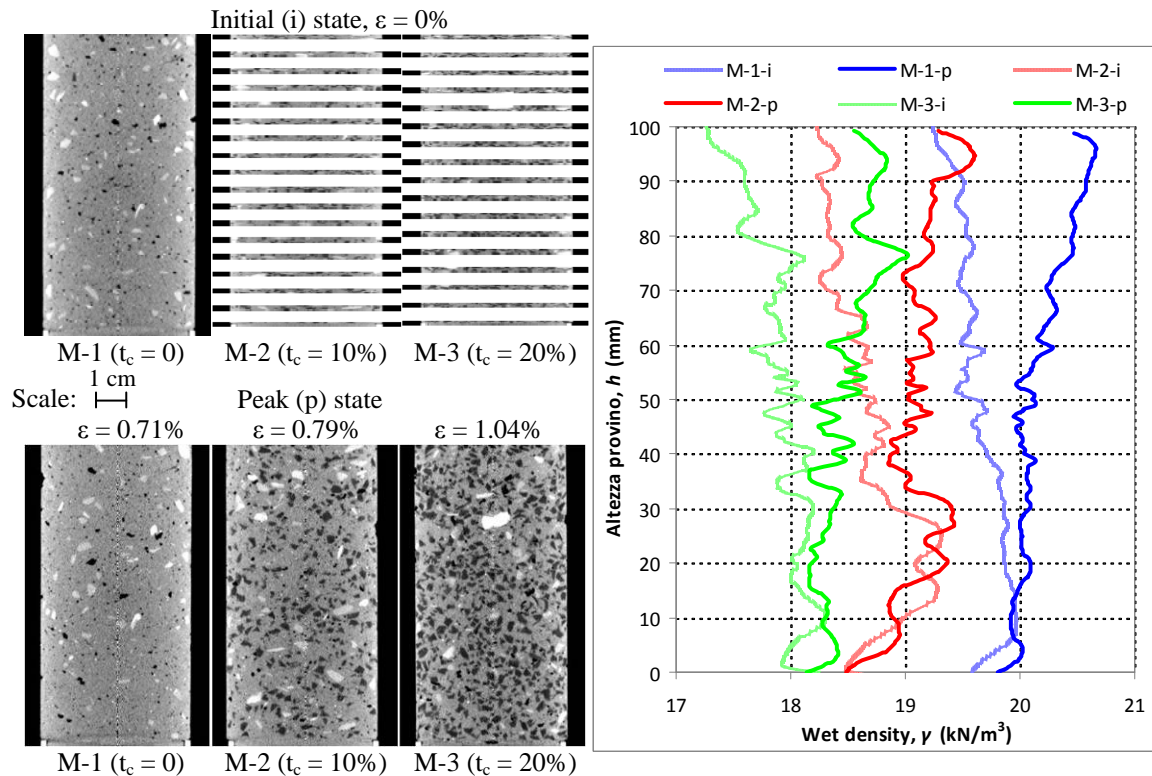
Figure 3: Longitudinal section images and density disributions of the specimens tested

3.2.   Unconfined compressive strength

The unconfined compressive strength, qu (kPa) at different curing time for the three mixtures was obtained. Figure 4 shows the relationship between the stress and axial strain of specimens tested. The points marked with "●" in the graphs show were permeability test and CT scanning were conducted. The shape of the curves obtained for the specimens subjected to permeability test presented lower accuracy than the other ones, this could be due to the testing conditions adopted (repeated loading and unloading cycles). Anyway, as can be seen in Figure 4, it was possible to obtain a significant comparison between the different mixtures, as the results were characterized by the same disturbance level. The results obtained are summarized in Table 3, were the average *qu* strenght, values are reported (considering only the three specimens tested in UC test). The axial strain required to reach peak strength increases with the tire chips content, showing ductile behaviour. Lower *qu* strength and secant modulus, E_{50} (determined from the stress strain curve for a mobilization of 50 % of the *qu* strength), passing from mixture M-1 to M-2 and M-3, were obtained. Higher strength values of the specimens with curing time have been observed: similar ratios between the *qu* strength values at 7 to 28 days, namely *qu*$_{28}$/*qu*$_7$, were found for the three mixtures, with or without tire chips.
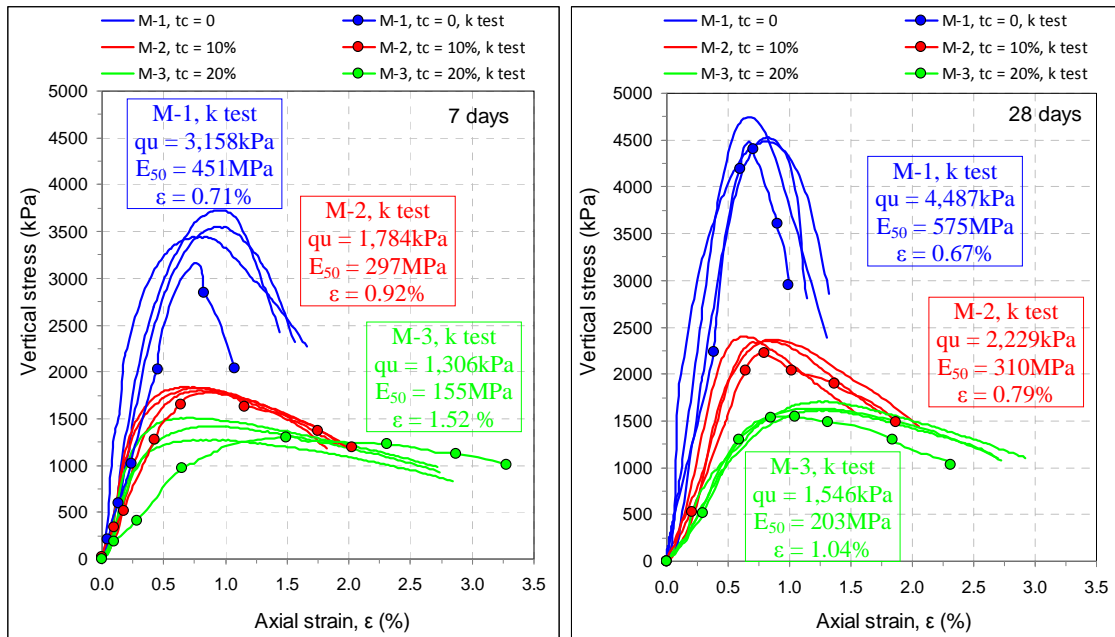
Figure 4: Relationships between the stress and axial strain of specimen tested at different curing times.

Table 3: Comparison between obtained average values for the three mixtures:

Specimen code	UCS, *qu* (kPa)	Secant modulus, E_{50} (Mpa)	Strain at failure, ε_f (%)	Permeability, k (m/s)	qu_{28}/qu_7	k_{28}/k_7
M-1 7days	3573.7	654.4	0.88	2.46E-10	-	-
M-2 7days	1824.2	334.8	0.81	4.14E-10	-	-
M-3 7days	1403.8	319.7	1.02	2.72E-10	-	-
M-1 28days	4,584.9	839.6	0.76	9.65E-11	1.28	0.39
M-2 28days	2,373.5	394.9	0.78	1.41E-10	1.30	0.34
M-3 28days	1,650.6	231.5	1.20	9.65E-11	1.18	0.35

The specimens display no large change from the initial condition to the stress peak condition, however little cracks took place near failure condition, then more cracks occurred after reaching the maximum stress. Figure 5 shows cross-sectional images of each specimen in the initial condition, around stress peak condition and at different axial strains. These images were chosen at the middle height of each specimen. Initial little cracks were localized more in the upper part of the specimens, and they could be seen by magnification. The appearance of the cracks in the respective cross sections was different between specimens M-1, without tire chips, and specimens M-2 and M-3. Specifically M-1 specimens presented a single wide crack along all the specimen and its thickness widened as axial strain increased. In contrast, the cracks in M-2 and M-3 were thin and developed successively in a reticulated pattern as axial strain increased. Thus, the crack formation mode was changed by the presence of tire chips.

M-1 (t_c = 0)

| ε = 0.39% | ε = 0.59% | ε = 0.71% | ε = 0.90% | ε = 0.99% |

M-2 (t_c = 10%)

| ε = 0.64% | ε = 0.79% | ε = 1.02% | ε = 1.37% | ε = 1.87% |

M-3 (t_c = 20%)

| ε = 0.85% | ε = 1.04% | ε = 1.32% | ε = 1.84% | ε = 2.31% |

Scale: 1 cm
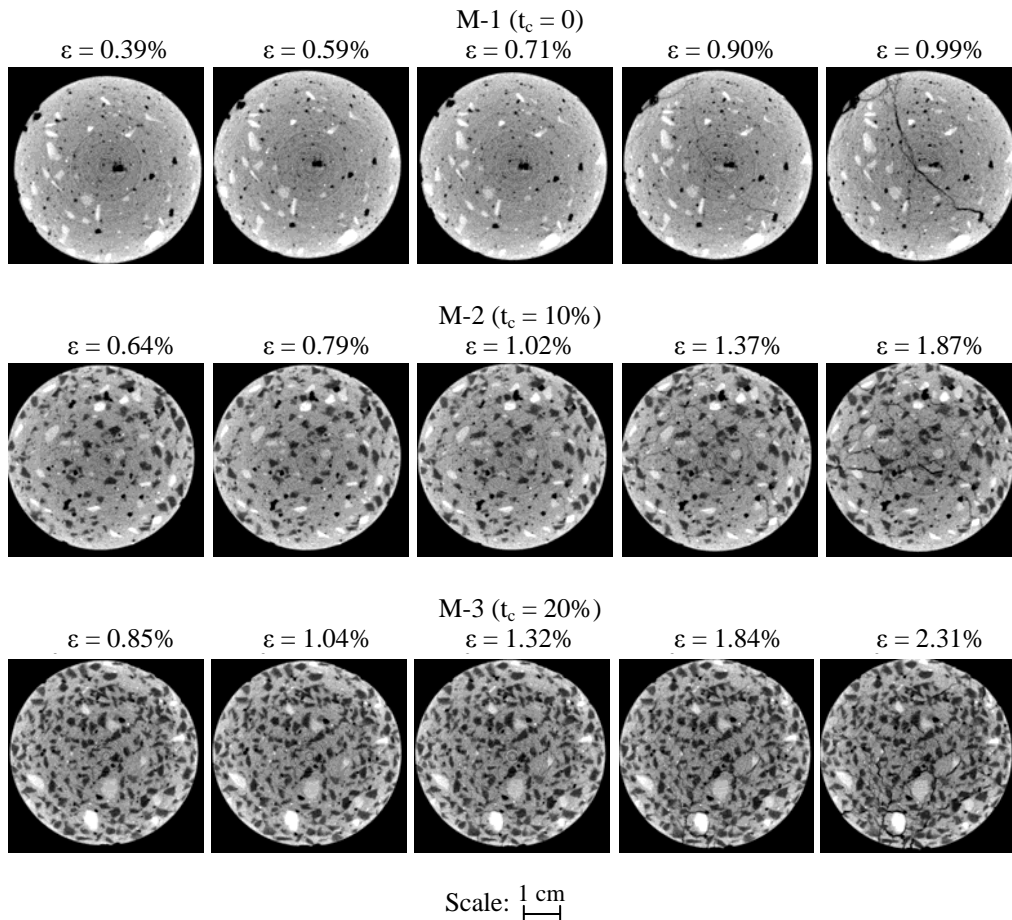
Figure 5: Cross sectional images of the specimens tested at 28 days, taken at different axial strains, chosen at middle height.

3.3. Hydraulic conductivity

Similar coefficient of permeability, k (m/s) and ratios between the coefficients at 7 to 28 days, namely k_{28}/k_7, were found for the three mixtures, irrespective of the tire chips content (Table 3). For all the specimens, permeability values were sufficiently lower than k = 1.0E-09 m/s, considered as a target value when dealing with low permeability barrier. Figure 6 shows the relationship between the hydraulic conductivity and the axial strain for specimens M-1, M-2 and M-3. Permeability increases with compression process, in different way depending upon the tire chips content, faster for specimen with no tire chips. It can be seen that hydraulic conductivity increased faster near and after peak strain.

M-3 specimen could provide k < 1.0E-09 m/s until larger strain, ε = 1%. It was considered that the large cracks which formed in the M-1 specimen created large water-bleeding channels and thus increased the hydraulic conductivity. On the other hand, the M-2 and M-3 specimens maintained lower permeability since thin cracks developed successively around the tire chips, preventing growth into wider ones until larger axial strain were reached. This led to a lower permeability at same strain value for the specimens with tire chips. Figure 7 shows the relationship between the hydraulic conductivity and the cracks volume for each specimen (cracks volume was measured by means of open source software "ImageJ").
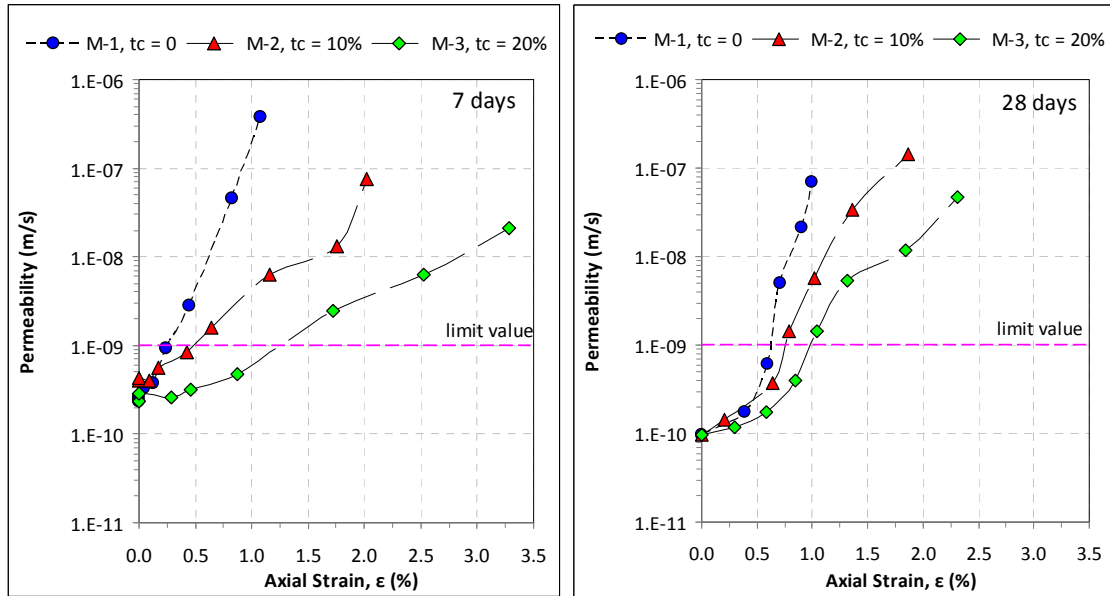
Figure 6: Relationship between the hydraulic conductivity and axial strain of the specimens tested.
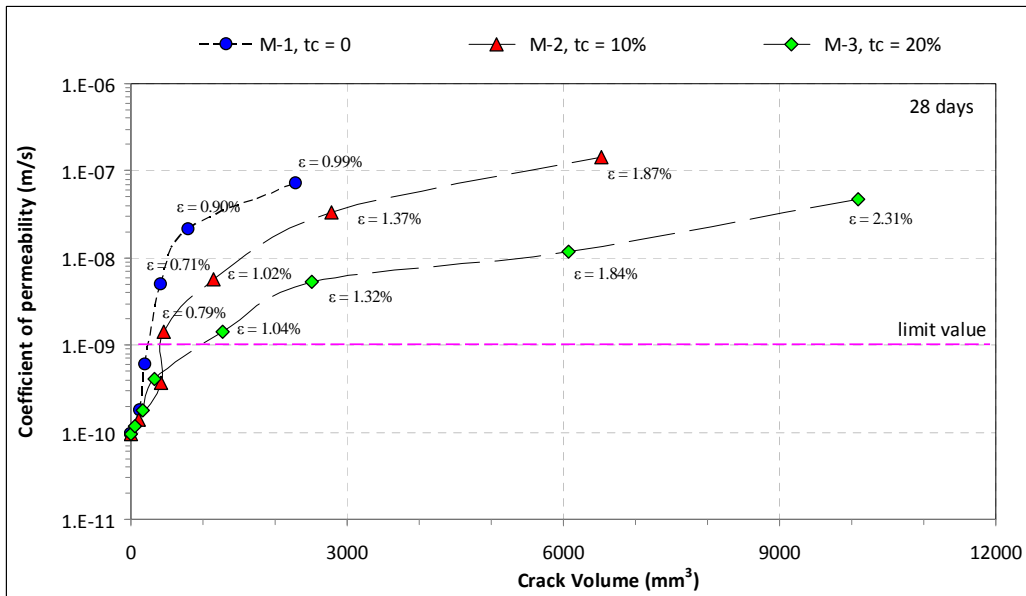
Figure 7: Relationship between the hydraulic conductivity and crack volume of the specimens tested.

From Figure 7 it can be seen that permeability values increased at the beginning also for little volume of cracks. Considering the same cracks volume permeability resulted to be higher for the specimen without tire chips. This may be due to the shape and the number of cracks, as shown in Figures 5 and 8: for the specimen without tire chips, there was a single large crack; for specimens with tire chips, widespread thin cracks were found.

Scale: ⊢—⊣ 1 cm

M-1 (t_c = 0)   M-2 (t_c = 10%)   M-3 (t_c = 20%)
ε = 0.99% ε = 1.87% ε = 2.31%
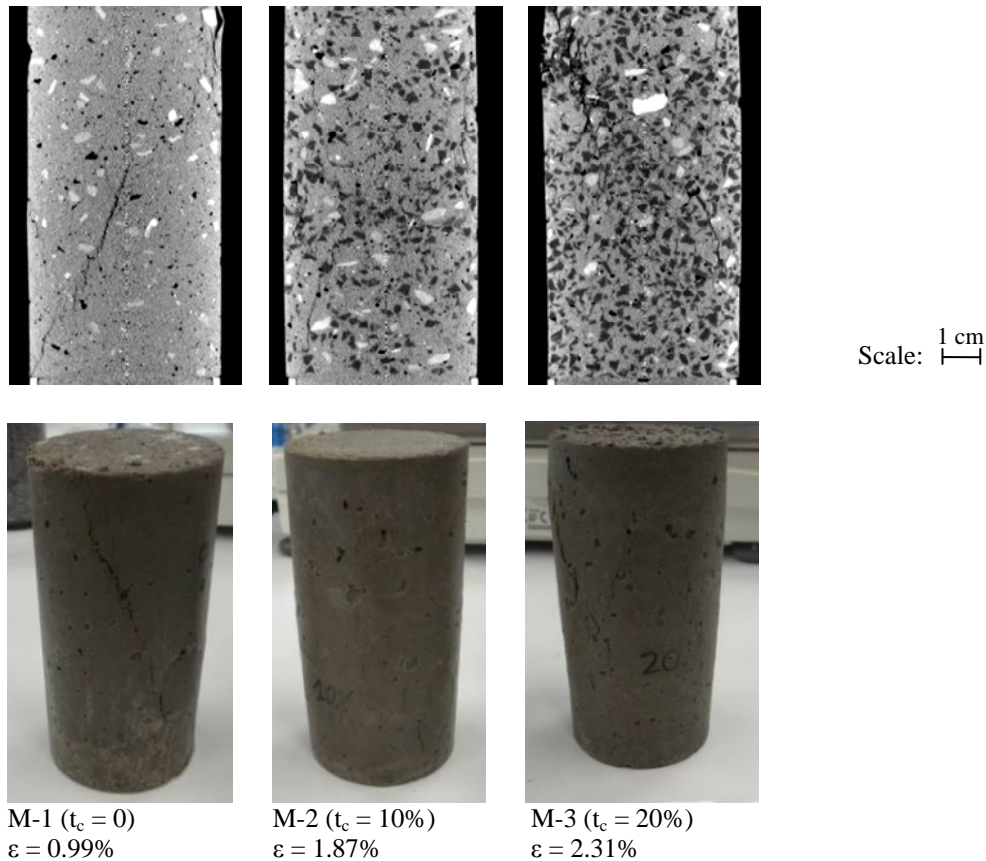
Figure 8: Specimens at 28 days, after compression test.

4.   CONCLUSIONS

Using a micro-focus X-ray CT scanner useful information on the structure and failure mechanism during shear deformation were retrieved. It was observed that the addition of tire chips keep down the hydraulic conductivity of cement treated soil after larger strain. Increasing the tire chips content lower q_u strength and secant modulus (E_{50}) and higher strain at failure (ε_f) were generally obtained . The results presented in this study demonstrate the success of using cement treated soil with tire chips to increase the cut-off wall efficiency, since the addition of tire chips can minimize the barrier breakage in presence of large deformation such as differential settlements or earthquakes. The outcomes presented in this paper constitute a preliminary useful base, which requires further research and development, to adapt in the construction techniques in field applications.

5.   AKNOWLEDGMENTS

REFERENCES

ASTM D5084 (2000), Measurement of Hydraulic Conductivity of Saturated Porous Materials Using a Flexible Wall Permeameter, American Standard Test Methods.

Council of the European union (1999),Directive 1999/31/EC of 26 April 1999 on the landfill of waste. Official Journal of the European Communities.

Edil, T.B.& Bossher, P.J. (1992), Development of Engineering Criteria for Shredded Waste Tires in Highway Applications, Research Report GT-92-9, University of Wisconsin, Madison, Wisconsin.

Edil, T.B. (2007), A review of Environmental Impacts and Environmental Applications of Shredded Scrap Tires, Proc. Int. Workshop on Scrap Tire Derived Geomaterials – Opportunities and Challenges, Hazarika, Yasuhara Editors, Taylor & Francis Group, London, pp. 3 - 18.

Hazarika, H., Yasuhara, K., Kikuchi, Y., Karmokar, A.K., Mitarai, Y. (2010), Multifaceted potential of tire-derived three dimensional geosynthetics in geotechnical applications and their evaluation, Geotexiles and Geomembranes 28, 2010, pp. 303 - 315.

Humphrey, D.N. (2003), Civil Engineering applications of tire shreds, Report, California Intergrated Waste Management Board, California Environmental Protection Agency.

ImageJ software: http://rsb.info.nih.gov/ij/index.html

Japanese Geotechnical Society (2000). Practice for Making and Curing Stabilized Soil Specimens Without Compaction, JGS 0821-2000.

Japanese Geotechnical Society (2009). Method for unconfined compression test of soils, JIS A 1216:2009.

Kikuchi, Y., Nagatome, T., Mitarai, Y. (2007) Change of engineering properties of cement treated clay by mixed with tire chips, Proc. Int. Workshop on Scrap Tire Derived Geomaterials – Opportunities and Challenges, Hazarika, Yasuhara Editors, Taylor & Francis Group, London, pp. 139 - 148..

Kikuchi, Y., Sato, T., Nagatome, T., Mitarai, Y., Morikawa, Y. (2008) Change of failure mechanism of cement treated clay by adding tire chips, Proc. of the 4th Asian Regional Conference on Geosynthetics, Shangai China.

Leder, E., Kitazume M., Grisolia M., Morikawa Y., Marzano I.P., Ninomiya Y., Kuwahara T. (2011) "Applicability of different molding procedures for the preparation of stabilised specimens". The 46th Japan National Conference on Geotechnical Engineering (CD-ROM), pp. 615-616, Kobe, 5th-7th July 2011

Otani, J. and Obara, Y. (2004), X-ray CT for geomaterials: soils, concrete, rocks, Proc. Int. Workshop GeoX2003, Kimamoto, Japan.

Yasuhara, K. (2007), Recent Japanese experiences on scrapped tires for geotechnical applications, Proc. Int. Workshop on Scrap Tire Derived Geomaterials – Opportunities and Challenges, Hazarika, Yasuhara Editors, Taylor & Francis Group, London, pp. 19 - 42.

Laboratory study on the applicability of molding procedures for the preparation of cement stabilised specimens

Massimo Grisolia, Sapienza University of Rome, Italy, massimo.grisolia@uniroma1.it
Masaki Kitazume, Port and Airport Research Institute, masaki_k@ac.auone-net.jp
Enrico Leder, Sapienza University of Rome, Italy, enrico.leder@uniroma1.it
Ignazio Paolo Marzano, Sapienza University of Rome, Italy, paolo.marzano@uniroma1.it
Yoshiyuki Morikawa, Port and Airport Research Institute, Japan, morikawa@pari.go.jp

ABSTRACT

An international collaborative study has been undertaken to establish common understanding of the key issues involved in Quality Assurance/Quality Control of deep mixing techniques. This paper focuses on comparing different laboratory techniques used in treatability procedures of deep mixing technology applications. The applicability of different molding procedures in function of the initial consistency of the mixture has been investigated, considering the specimens mechanical properties and test results repeatability. The results of a first series of tests, performed on Kawasaki marine clay with different initial water contents, are presented. Six mixtures with different consistency were produced using ordinary Portland cement added to the soil in dry form changing the amount of binder. Four molding techniques, namely Dynamic Compaction, Tapping, Rodding and No Compaction were used. The results provide a base to select the right molding technique in function of the soil-binder mixture consistency that produces the best specimens quality.

1. INTRODUCTION

In situ Deep Mixing is a treatment technology which improves the properties of soils by the introduction and mechanical mixing of a binder with the soil (CDIT, 2002). Laboratory testing of stabilised soils is extensively used in the Quality Assurance/Quality Control processes in deep mixing projects (Åhnberg & Holm, 2009). The paper focuses on a practical aspect of laboratory mix tests on a cement stabilised clay, dealing with the applicability of different molding techniques. This is one of the major theme currently being studied in the international collaborative study that has been undertaken to establish common understanding of the key issues involved in Quality Assurance/Quality Control of Deep Mixing works (Terashi & Kitazume, 2009). In the present work the results of a first series of tests are presented. Six mixtures with different consistency and four molding techniques, namely Dynamic Compaction, Tapping, Rodding and No Compaction were used. Unconfined compression test were performed on the specimens produced. Some indications on the applicability of each molding technique with the consistency of the mixture were obtained considering three different parameters, namely: 1) the "Normalised q_u strength and wet density values, N": when the molding technique produces the better homogenisation and reduces the air voids of the specimens, it guarantees higher strength and wet density values; 2) the "q_u strength and wet density relative errors, E": the molding method which assures the highest repetitiveness thus reducing variability represents a suitable technique; 3) the "R-squared value of the wet density- q_u strength relationship, $R^2(\gamma\text{-}q_u)$": this parameter considers the relationship which exists for real soil, where strength increases with the wet density. The analysis of these parameters were useful for an evaluation on the applicability of each used molding technique.

2. TESTING PROGRAM

The experimental work consisted in a laboratory investigation on the effect of different molding techniques on the unconfined compressive strength, q_u (measured according to the JIS A 1216:2009) and wet density, γ (defined as the specimen's weight divided by the volume of the mold) of cement stabilised clay specimens under various mixing conditions.

2.1. Materials and testing conditions

Kawasaki clay (soil properties on Figure 1) with different initial water contents, w_n(%) and ordinary Portland cement, added with three cement contents, a_c(%) (defined as the weight of the introduced dry cement divided by the dry weight of the soil to be stabilised) were used to produce six soil-cement mixtures with different consistency. The properties of the mixtures tested are shown in Table 1. The

effective total mixture water content, w_m (%) was measured just before the molding phase, together with the hand vane shear strength, c_u (kPa), which was related to the initial consistency of each mixture. According to the values obtained, the mixtures were then divided into three groups, namely *A*, *B* and *C*, passing from softer ($c_u < 10$ kPa, Group A), to stiffer ($c_u > 20$ kPa, Group C) mixtures. Cement to mixture water ratio, C/M_w (%) (ratio of the weight of dry cement to the weight of the total mixture water) was also measured.

Kawasaki Clay	
Specific gravity, G_s (g/cm^3)	2.676
Natural water content, w_n (%)	57.0
Liquid limit, w_L (%)	48.6
Plastic limit, w_P (%)	29.6
Plasticity index, I_P (%)	19.0
Sand content (%), 75 µm – 2 mm	14.0
Silt content (%), 5 µm – 75 µm	42.0
Clay content (%), < 5 µm	44.0

Figure 1: Kawasaki clay properties.

Table 1: Testing conditions

Group	Mixture m#	Cement content, a_c (%)	Water content, w_n (%)	Hand vane strength, c_u (kPa)	Mixture water content, w_m (%)	Cement/Mixture water, C/w_m (%)
A (cu: 3-10 kPa)	m1	5	72	3.01	66.08	7.10
	m2	5	60	7.46	54.51	8.63
B (cu: 10-20 kPa)	m3	20	60	13.15	46.50	36.18
	m4	30	60	15.49	43.23	53.36
C (cu: 20-30 kPa)	m5	30	54	21.75	39.86	57.21
	m6	30	49	28.54	35.59	63.92

2.2. Molding techniques

The stabilised clay was placed in plastic molds (cylindrical shape, 50 mm in diameter and 100 mm in hight) in three layers. In particular four different molding techniques were used, as shown in Photo 1:
- Dynamic Compaction (namely *D.C.*): Each layer was compacted by a falling weight (1.5 kg) using a special apparatus. Fall height was set at 10 cm, while number of blows at 5.
- Tapping (namely *TA.*): For each layer, the mold was tapped against floor 50 times.
- Rodding (namely *RO.*): Performed using a 8 mm diameter steel rod; consisted in slowly tamping the mixture with the rod for each layer and eventually push down the material attached to the rod. Number of poking per layer was set to 30.
- No Compaction (namely *N.C.*): simply consisted in filling the mold by either pouring or placing in the case of higher consistency mixture.

Grisolia - Laboratory study on the applicability of molding procedures for the preparation of cement stabilised specimens

II-336

Photo 1: Molding techniques used, from left to right: Dynamic Compaction, Tapping, Rodding, No Compaction.

2.3. Testing procedures

The Hobart type mixer was used for the soil-binder mixing. The water content of the natural clay was adjusted to the desired value after which the soil was made homogeneous by mixing. Dry ordinary Portland cement was then added to the soil and they were mixed for 10 minutes (according to JGS 0821-2000). Afterwards the stabilised soil was placed into plastic molds and compacted using the molding techniques described before. To prevent water evaporation from the specimen each mold was covered with the sealant and stored in special curing tanks at 95% relative humidity. To reduce the effect of the time of rest between the hydration of binder and the completion of molding of the mixture consistency, according to Kitazume et al. (2009), all the stabilised soil was molded in less than 45 minutes since binder was added. After curing times of 28 days, the specimens were removed from the molds and then subjected to unconfined compression tests at a rate of 1.0 mm/min. Unconfined compression tests was conducted on triplicate samples for each case (mixture number and molding technique) analysed.

3. RESULTS

Figure 2 and Figure 3 show for each molding technique the relationship between the consistency of the mixtures studied and the q_u strength and wet density respectively. It can be seen from the figures below that the TA. technique had higher strength and density for low consistency mixtures, while RO. technique, together with the D.C. one, produced better results for stiffer mixtures. A group mixtures (m1 and m2) had a small amount of cement, therefore strength values were considerably lower if compared to the other ones.

As shown in the following paragraphs, it was observed a relation between the consistency of soil-cement mixture and the mechanical properties of the specimens obtained using different molding techniques. Some indications on the applicability of each molding technique under various mixing conditions were derived considering three different parameters namely: "Normalised q_u strength and wet density values, N", the "q_u strength and wet density relative errors, E" and the "R-squared value of the wet density- q_u strength relationship, $R^2(\gamma$- $q_u)$". Considering the different techniques adopted, several remarks arise from the problems encountered during the molding phase, which are linked to the trends of the three parameters studied as described in the study. The analysis of these parameters are discussed in the following paragraphs.

Grisolia - Laboratory study on the applicability of molding procedures for the preparation of cement stabilised specimens

II-337

Figure 2: q_u versus initial consistency for the different molding techniques.
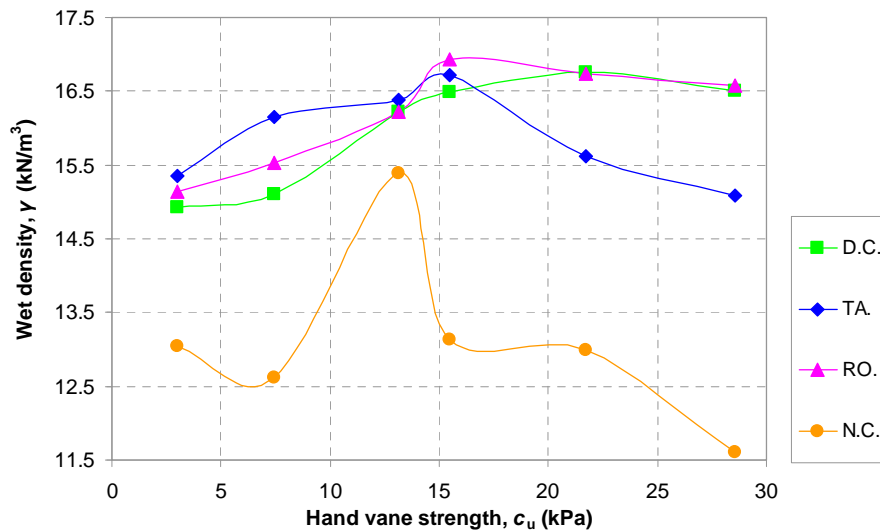
Figure 3: Wet density versus initial consistency for the different molding techniques.

3.1. Normalised q_u strength and wet density parameter, N

It was considered that the highest suitability for the molding technique adopted is related to the best obtained mechanical properties of the specimens produced (highest q_u and wet density values). The q_u strength and wet density values for each molding techniques were normalised with the maximum values measured for the mixture (m#), as described in eq. (1) and (2):

Normalised q_u strength: $\quad q_{uN} = \left(\dfrac{q_u}{q_{u\,\max}} \right)_{m\#} , \quad 0 < q_{uN} < 1$ (1)

Normalised wet density: $\quad \gamma_N = \left(\dfrac{\gamma}{\gamma_{\max}} \right)_{m\#} , \quad 0 < \gamma_N < 1$ (2)

The q_{uN} data obtained are shown in Figure 4. It is possible to see some trends of the q_{uN} with the mixture consistency for both curing times, which were not clearly shown in the previous Figure 2, overall for the lower consistency mixtures. The results also show that the molding technique has a lower influence on the wet density than that on the strength, since all data obtained excluding the N.C. results are closer to 1.

Grisolia - Laboratory study on the applicability of molding procedures for the preparation of cement stabilised specimens
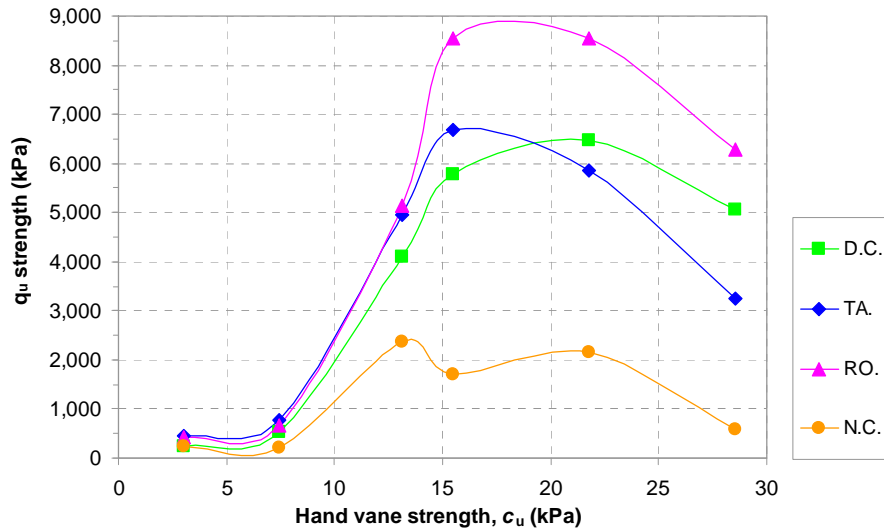
II-338
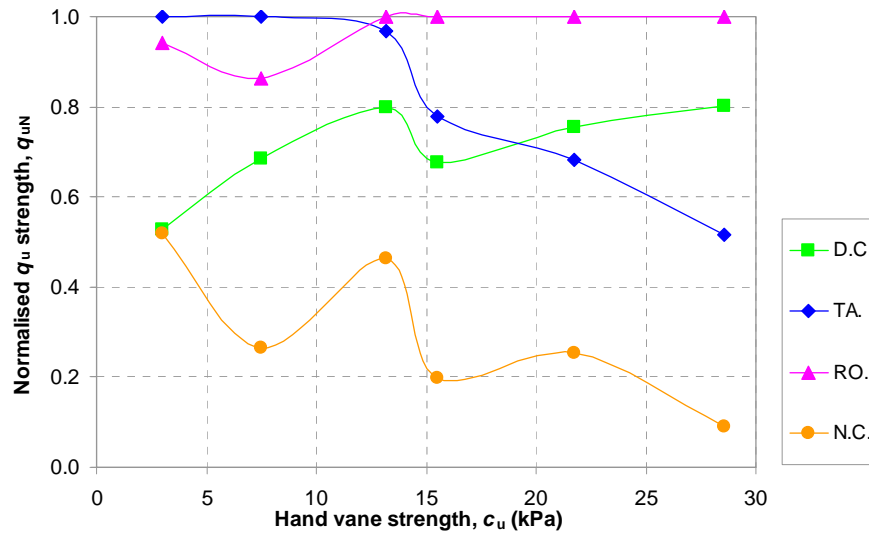
Figure 4: q_{uN} versus initial consistency for the different molding techniques.
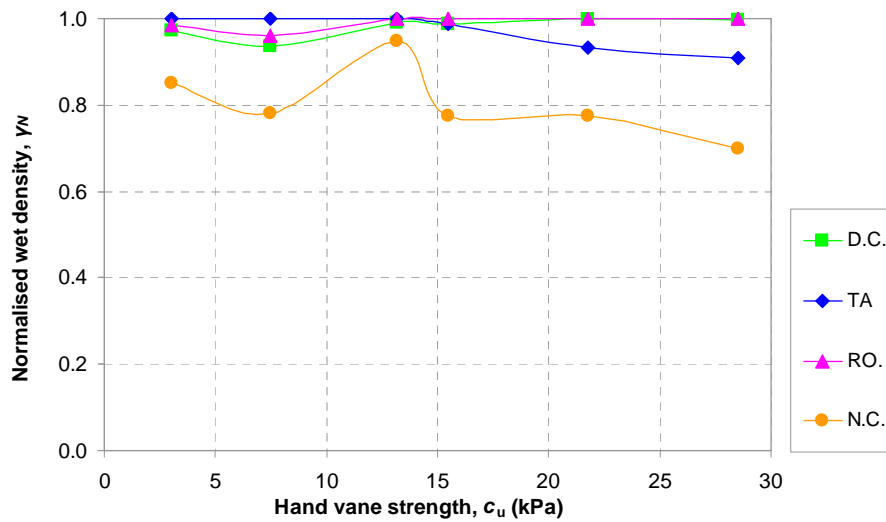
Figure 5: γ_N versus initial consistency for the different molding techniques.

In order to have some indication on the applicability of a molding technique, considering both the normalised strength and wet density results, it was introduced the N parameter, defined in the eq. (3):

$$N = \frac{1}{2}\left(\overline{q}_{uN} + \overline{\gamma}_N\right) \ , \ 0 < N < 1 \tag{3}$$

The $\overline{q}_{uN}$ and $\overline{\gamma}_N$ (mixture's group q_{uN} and γ_N average values) are evaluated for each molding technique. A molding technique that present N values higher than 0.9 it is considered suitable for that consistency. Figure 6 shows for each mixture group the N values. From Figure 6 it can be seen that the suitable techniques are: RO. for all groups and TA. for A and B groups.

Grisolia - Laboratory study on the applicability of molding procedures for the preparation of cement stabilised specimens

II-339
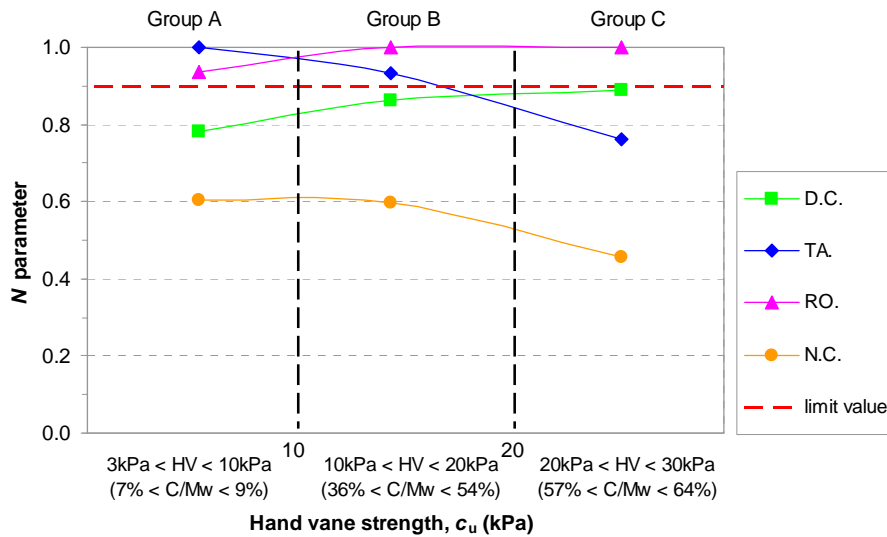
Figure 6: N parameter of the molding techniques versus group consistency.

3.2. q_u strength and wet density relative errors, E

In this study repetitiveness of the results obtained for each molding technique was evaluated using q_u strength and wet density relative error (E_{qu} and E_γ respectively), defined as the difference between maximum and minimum value divided by the average one, eq. (4) and (5):

$$E_{qu} = \frac{q_{u\max} - q_{u\min}}{q_{u\,average}}(\%) \tag{4}$$

$$E_\gamma = \frac{\gamma_{\max} - \gamma_{\min}}{\gamma_{average}}(\%) \tag{5}$$

E_{qu} and E_γ for the different molding techniques and mixtures consistency are shown in Figure 7 and Figure 8. The results show very high E_{qu} and E_γ when considering the *D.C.* technique in presence of low consistency mixtures. This is probably due to molding problems such as mixture squeeze out of the mold during compaction. The highest E_{qu} and E_γ were obtained for the *N.C.* technique, excluding m1 mixture, where pouring operation could be adopted instead of placing largely affected by the operator. The E_γ were very low compared to the E_{qu} ones. In order to minimise the influence of the operator on the final results, each molding technique was performed by the same person for all mixtures tested.
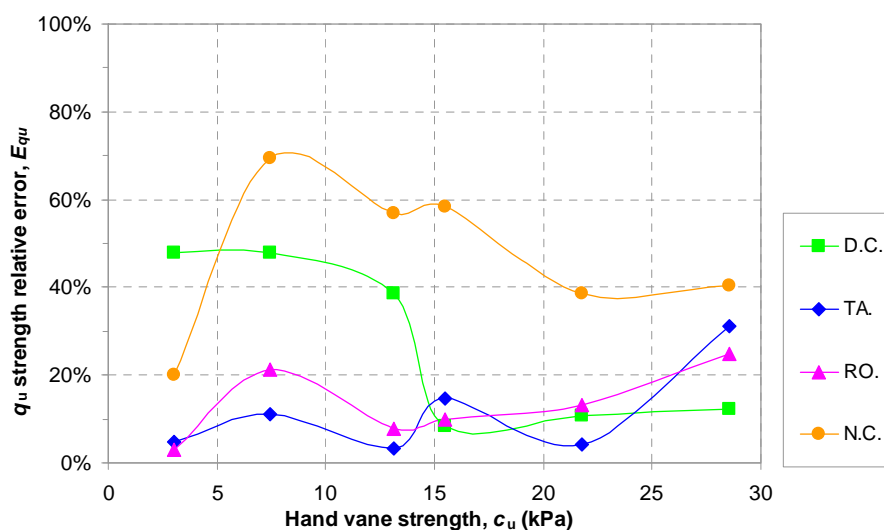
Figure 7: E_{qu} versus initial consistency for the different molding techniques.

Grisolia - Laboratory study on the applicability of molding procedures for the preparation of cement stabilised specimens

II-340
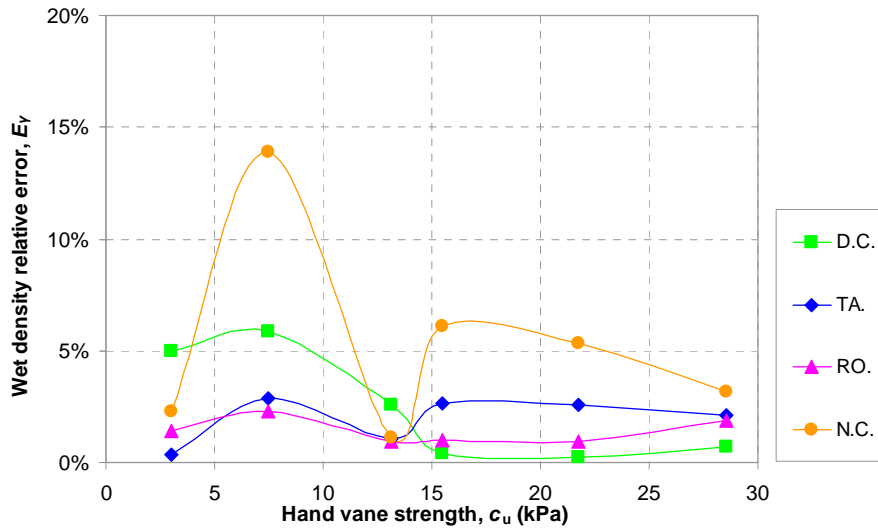
Figure 8: E_γ versus initial consistency for the different molding techniques.

It was introduced the E parameter, defined as the sum between the $\overline{E}_{qu}$ and the $\overline{E}_\gamma$ (mixture's group E_{qu} and E_γ average values) at 28 curing days, eq. [6]:

$$E = \overline{E}_{qu} + \overline{E}_\gamma \qquad (6)$$

Figure 9 shows for the three mixtures groups analysed the E values for each molding technique. A molding technique that presented results in terms of E lower than 10% was considered suitable. Figure 9 shows that the *TA.* technique resulted the only valid for softer mixtures, while *RO.* technique gave lowest errors for medium stiff mixtures (B group). Concerning the *C* group mixtures, the *D.C.* technique appeared to be better than others, but presented E value over 10%, thus indicating that none of the molding techniques used was appropriate in that range of stiffer consistency.
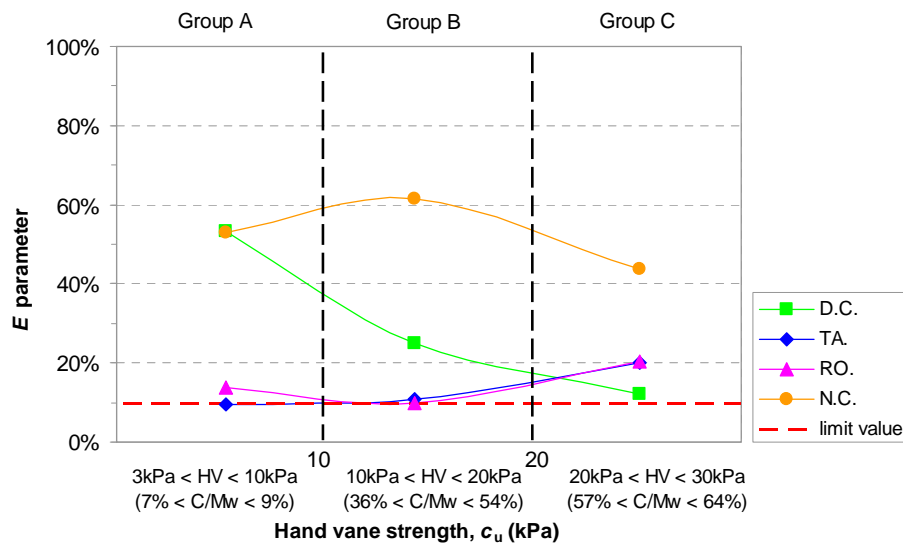
Figure 9: E parameter of the molding techniques versus group consistency.

3.3.   R-squared value of the wet density-q_u strength relationship, $R^2(\gamma$-$q_u)$

Figure 10 shows the wet density in function of the q_u strength data obtained for the proposed three mixtures groups. It can be generally seen that strength increases with wet density, in different way between the molding techniques utilised. For each group, data referring to the specific molding technique were fitted using a logarithmic interpolation. Non linear R-squared values, $R^2(\gamma$- $q_u)$, were then evaluated. A molding technique that presents $R^2(\gamma$- $q_u)$ higher than 0.90 it is assumed suitable. In Figure 11, the $R^2(\gamma$-$q_u)$ values obtained in function of the hand vane strength for the three groups are reported. From this

Grisolia - Laboratory study on the applicability of molding procedures for the preparation of cement stabilised specimens

II-341

Figure appear that the *TA.* and *RO.* techniques result suitable for *A* group mixtures, while *RO.* technique is valid for *B* group ones. Considering stiffer mixtures, the D.C. technique is considered appropriate.
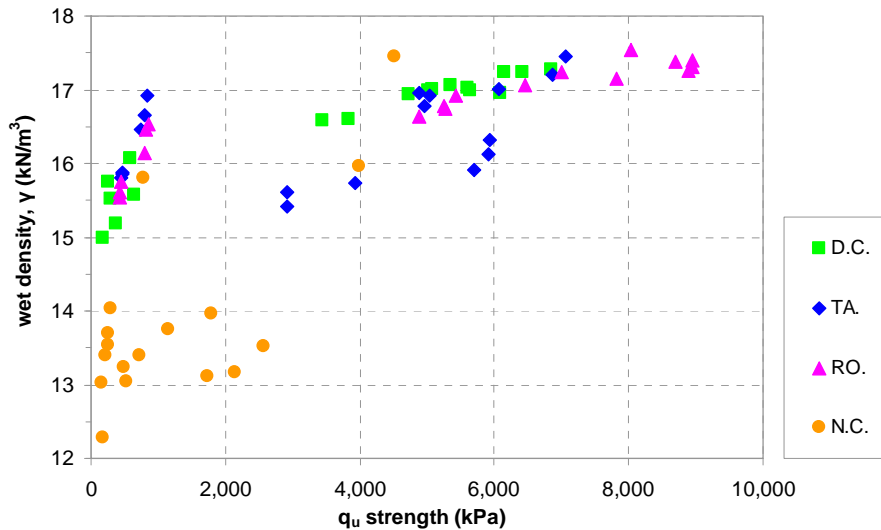
Figure 10: q_u strength versus wet density for the different molding techniques.
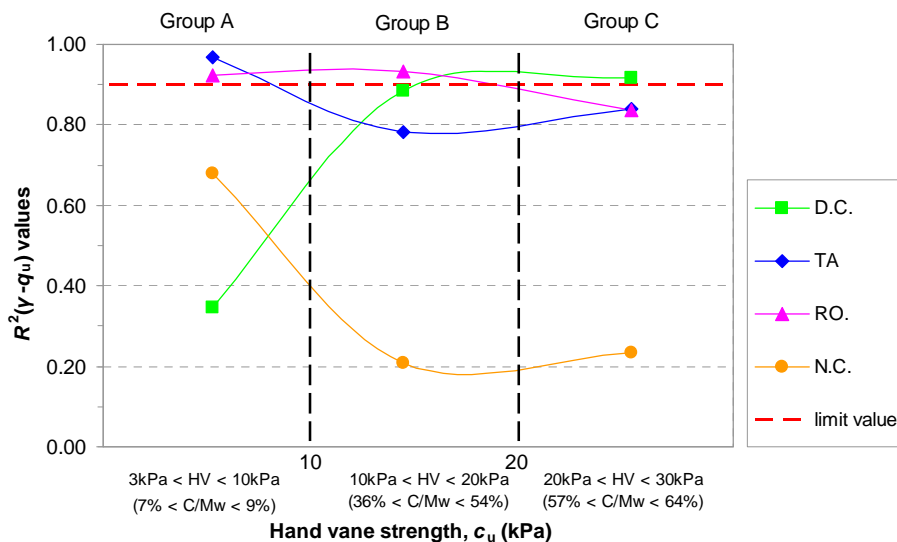
Figure 11: $R^2(\gamma$-$q_u)$ values of the molding techniques versus group consistency.

4.   CONCLUSIONS

The laboratory investigation on the influence of different molding techniques for the preparation of specimens provided useful indication for QA/QC procedures. Applicability of each molding technique for the preparation of stabilised specimens was found to be affected from the initial consistency of the mixture in different proportion. The definition and analysis of three parameters namely "densest specimens with the highest strength", "results repetitiveness" and "lower scatter qu-wet density relationship" gave indications on the applicability of a molding technique. It was possible to compare different techniques and choose the most suitables in function of the mixture consistency. Specifically, the *TA.* technique showed to have the highest applicability for the softer *A* group mixtures, while for *B* group ones the *RO.* technique was found to be the most applicable technique. Regarding the *C* group mixtures, *RO.* and *D.C.* techniques appeared to be the best ones (higher *N* and *R* parameter values respectively), even if the target limit values for the three parameters were not met all together. This fact underlines the lack of an appropriate molding technique in the case of high consistency mixtures. The results of this first series of tests on the effects of different molding techniques provide a basis to select the right technique to produce appropriate specimens of stabilised material. The results obtained would be integrated by the second series of tests, which is currently undergoing, with the aim of defining a global

Grisolia - Laboratory study on the applicability of molding procedures for the preparation of cement stabilised specimens

II-342

applicability index. Further research and development are needed to extend the results of the investigation towards the standardization for the correct selection of the molding technique for different kind of soils.

5.   AKNOWLEDGMENTS

REFERENCES

Åhnberg, H. & Holm, G. (2009). Influence of laboratory procedures on properties of stabilised soils specimens. In Proceedings International Symposium on Deep Mixing & Admixture Stabilization, Okinawa, Japan, 19-21 May 2009. CD-ROM, IC-9.

Coastal Development Institute of Technology (2002). The Deep Mixing Method - principle, design and construction, 123p.

Ismail, M.A., Joer, H.A. and Randolph, M.F. 2000. Sample Preparation Technique for Artificially Cemented Soils. Geotechical Testing Journal, ASTM, 23(2): 171-177.

JGS 0821-2000. Practice for Making and Curing Stabilised Soil Specimens Without Compaction (Translated version). Geotechnical Test Procedure and Commentary, Japanese Geotechnical Society.

JIS A 1216:2009. Method for unconfined compression test of soils. Japanese Geotechnical Society.

Kitazume, M. & Nishimura, S., Terashi, M., Ohishi, K. (2009). International Collaborative Study Task 1: Investigation into Practice of Laboratory Mix Tests as Means of QC/QA for Deep Mixing Method. In Proceedings International Symposium on Deep Mixing & Admixture Stabilization, Okinawa, Japan, 19-21 May 2009. CD-ROM, IC-2.

Kitazume, M., Ohishi, K., Nishimura, S., Terashi, M. (2009). International Collaborative Study Task 2 Report: Interpretation of comparative test program. In Proceedings International Symposium on Deep Mixing & Admixture Stabilization, Okinawa, Japan, 19-21 May 2009. CD-ROM, IC-3.

Marzano, I.P., Osman, A.A-M., Grisolia, M., Al-Tabbaa, A. (2009): Mechanical performance of different stabilised soils for application in stratified ground, Proc. 17th ICSMGE, Alexandria, Egypt.

Takahashi, H., Morikawa, Y., Ichikawa, E., Hayano, K., Ohkusa, Y. 2010. Model tests on compressibility and bearing capacity of lean-mixed granular cement treated soil. Journal of Japan Society of Civil Engineers, 66(2): 236-249.

Terashi, M. & Kitazume, M. (2009). Keynote Lecture: Current Practice and Future Perspective of QA/QC for Deep-Mixed Ground. In Proceedings International Symposium on Deep Mixing & Admixture Stabilization, Okinawa, Japan, 19-21 May 2009. CD-ROM, KL-3.

Grisolia - Laboratory study on the applicability of molding procedures for the preparation of cement stabilised specimens

II-343

On the strength and durability of cement-stabilised sands

Antoine Guimond-Barrett, IFSTTAR-LCPC, Université du Havre, France,
antoine.guimond-barrett@ifsttar.fr
Fabien Szymkiewicz, IFSTTAR-LCPC, France,
Philippe Reiffsteck, IFSTTAR-LCPC, France, philippe.reiffsteck@ifsttar.fr
Anne Pantet, Université du Havre, France,
Alain Le Kouby, IFSTTAR-LCPC, France, alain.lekouby@ifsttar.fr
Sylvine Guédon, IFSTTAR-LCPC, France,

ABSTRACT

Deep mixing is a general term for a large number of techniques in which binding agents are mechanically dispersed within the soil either in dry or slurry form using specially designed mixing tools. There is an increasing interest in the use of this technique not only for soil stabilisation but also to construct temporary and permanent foundation/structural (load bearing) elements and excavation retaining walls. Despite the available knowledge on factors affecting the development of strength of in-situ deep mixed soils, there are still no widely accepted dosage methodologies. Preliminary laboratory trials are frequently carried out in feasibility studies for soil mixing projects to evaluate the strength of the stabilised soil with different binder contents and curing times. The duration of these preliminary trials is usually quite long. This paper focuses on the mechanical properties of a silica sand stabilized with Portland blastfurnace slag cement in the laboratory. The effects of curing time and cement content, as well as the addition of bentonite and the presence of sulphates, are investigated by means of unconfined compressive strength tests and ultrasonic pulse wave velocity measurements. An empirical relation is proposed, applicable to sandy soils stabilised in the laboratory with slag cement and cured in endogenous conditions up to 90 days, to predict the development of strength with time based on measurements carried out after short curing periods. However, special precautions must be taken when using such relations as it is shown that numerous factors can modify the development of strength in cement-mixed sands. In some cases, the use of empirical relations can lead to erroneous predictions of strength.

1. INTRODUCTION

Deep mixing is a general term for a large number of techniques, in which binding agents are mechanically dispersed within the soil either in dry or slurry form using specially designed mixing tools (Porbaha, 1998). Originally, the main purpose of deep soil mixing was to enhance the stability and reduce settlements of structures such as embankments on soft soils of low shear strength or very high moisture contents (CDIT, 2002). Nowadays, improving the strength and deformation properties as well as the permeability of very soft soils by deep soil mixing is a commonly used stabilisation method. Lime and/or cement are the most frequently used binders, although recent studies have shown that many industrial by-products such as granulated ground blastfurnace slag and pulverised fuel ash can also provide suitable characteristics of the treated material when blended with cement (Jegandan et al, 2010).

In Europe, there is an increasing interest in the use of this technique not only for soil stabilisation but also to construct temporary and permanent foundation/structural (load bearing) elements and excavation retaining walls (Ganne et al, 2010).

The properties and types of soils encountered for these new applications of deep soil mixing differ greatly from those found in soft soil stabilisation projects. Sandy soils are the most suitable as the created materials are in many ways similar to mortars. According to Topolnicki (2004), the curing time required to reach the design strength is shorter for deep mixed sands (compared with fine grained soils) and the distribution of cement by the mixing tool throughout the soil is simpler. In sandy soil conditions, bentonite is often added to fluidize the mixture and prevent the mixing tool from being trapped if the construction time exceeds the setting time of the cement slurry. A large number of factors are known to influence the strength and deformation properties of the treated soils (Terashi, 1997). These factors are mainly related to the characteristics of the binder (type, amount), the soil conditions (soil type, moisture content, and organic content), the mixing conditions (degree of mixing) and the curing conditions. Certain chemical compounds present in the soil can also significantly affect strength increase in treated soils. The most widely known compounds to affect the durability of soil treatment with lime and/or cement are sulphates (Hunter, 1988).

Despite the available knowledge on factors controlling the strength development of in situ deep mixed soils, there are still no widely accepted dosage methodologies. Preliminary laboratory trials are frequently carried out in feasibility studies for soil mixing projects to evaluate the strength of the stabilised soil with different binder contents and curing times. The duration of these preliminary trials is usually quite long (up to 90 days). This paper focuses on the mechanical properties of sand stabilised with Portland blastfurnace slag cement by deep mixing. The aim of this study is to evaluate the effects of time and cement content on the strength of sandy soils when mixed in the laboratory with cement. The effects of the addition of bentonite and the presence of sulphates in the soil are also considered. The main objective of this research is to determine a simple method to estimate the increase in strength with time of sandy soils treated with cement in the laboratory. Such a method would minimise the number of trials needed and assist engineering judgments on the amounts of binder and curing periods needed to reach specific target strengths of cement-admixed sands for deep soil mixing applications.

2.   EXPERIMENTAL DETAILS AND PROCEDURES

2.1.   Experimental program

The experimental program carried out to investigate the effects of different cement contents, curing time, the addition of bentonite and the presence of sulfates on the strength of silica sand is presented in Table 1. The water and cement contents considered in this study are within the typical ranges of those used in in-situ deep soil mixing. The cement contents were selected between 70 to 400 kg/m^3. To ensure a sufficient fluidity of the fresh soil-cement mixtures, moisture contents of 19 % and 35 % were chosen. In mixes n°1 to 6, silica sand was mixed with various amounts of cement producing different cement / water ratios (C / W). The effects of bentonite on the strength of the sand-cement mixes were investigated by adding the equivalent of 50 kg of C2 Bentonite per cubic meter of sand in mix n°7. Bentonite was also added to the mixes with a moisture content of 35 % (n°8 to 11) to stabilise the mixtures. For mixes n°10 and 11, 10 g of calcium sulphate ($CaSO_4$, 2 H_2O) were added per kg of dry sand. The curing conditions were endogenous for all mixes except n°9 and 11. The specimens from those batches were stored in tap water (in which 1g of $CaSO_4$ / L was dissolved in the case of mix n°11). Unconfined compressive strength tests and ultrasonic pulse wave velocity measurements were carried out at different curing times up to 90 days.

Table 1: Experimental program

Mix n°	Cement content (kg/m^3)	Initial Moisture Content (%)	C/W	Bentonite (kg/m^3)	Sulphate Addition	Curing conditions
1	70	19	0.21	-	-	Endogenous
2	140	19	0.41	-	-	Endogenous
3	200	20	0.50	-	-	Endogenous
4	265	19	0.73	-	-	Endogenous
5	320	19	0.86	-	-	Endogenous
6	400	19	1.03	-	-	Endogenous
7	200	19	0.50	50	-	Endogenous
8	200	35	0.30	50	-	Endogenous
9	200	35	0.30	50		Immersed
10	200	35	0.30	50	10g/kg dry soil	Endogenous
11	200	35	0.30	50	10g/kg dry soil	Immersed (1g $CaSO_4$/L)

2.2.   Silica sand and binder characteristics

The soil used in this study is Fontainebleau sand, which is a silica sand from the south of Paris. The characteristics of this sand are listed in Table 2 and the grain size distribution is shown in Figure 1. Fontainebleau sand has a uniform distribution of sub-rounded quartz grains.

Table 2: Characteristics of the Fontainebleau sand

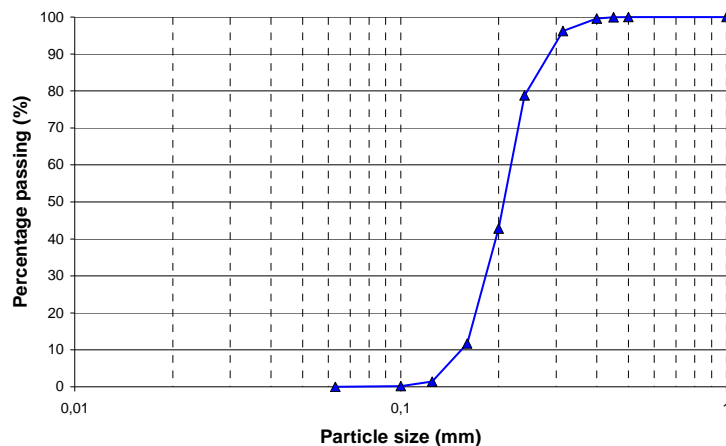| d_{60} (mm)	d_{50} (mm)	d_{30} (mm)	d_{10} (mm)	Cc	Cu
0.22	0.21	0.18	0.15	0.98	1.47

Figure1 : Grain size distribution - Fontainebleau sand

The cement used in this study is a Portland blastfurnace slag cement containing 85 % ground granulated blast furnace slag (European classification: CEM III/C 32,5 N CE PM-ES NF "HRC") (CEN 2005). This cement presents a slow strength development, and its initial setting time is 4 hours after hydration.

2.3.   Specimen preparation and testing procedures

2.3.1.   Specimen preparation

Firstly, the appropriate amounts of dry soil, cement and bentonite were manually blended in a recipient until a visually homogenous mixture was obtained. The weights of cement and bentonite for a given mix were determined assuming a dry unit weight of 1650 kg/m^3 for the Fontainebleau sand. The content of the recipient was poured in the mixer and tap water was added. The amount of water was calculated based on the target water content of the mixes, i.e. 19 % and 35 %. In the case of mixes n°10 and 11, the equivalent of 10 g of CaSO4 per kg of dry soil was mixed with the water before addition to the dry soil-cement mixture. The hydrated soil-cement was mixed for five to ten minutes with a laboratory mixer. The mixes were then poured in cylindrical moulds of 52 mm diameter. To reduce the trapping of air bubbles, the sand – cement pastes were compacted in three layers by lightly tapping the moulds on a horizontal surface. To ensure endogenous curing conditions, the moulds were sealed and placed in hermetic bags containing a wet textile to preserve the humidity during curing. They were stored at a constant curing temperature of 20°C. The specimens of mixes n°9 and 11 were de-moulded two to three days after preparation and immersed in tap water (with 1g of CaSO$_4$ / L for mix n°11). The samples were de-moulded or taken out of the water baths immediately before testing. Their extremities were cut and smoothed. The specimens were then measured, weighted and tested.

2.3.2.   Unconfined compressive strength tests

Unconfined compression tests were performed on specimens of approximately 100 x 50 mm (height to diameter ratio of 2) to evaluate their strength (q_u). The tests were conducted in accordance with NF EN 13286-42 (2003).The vertical load was statically applied at a constant displacement rate of 1.5 mm/min. The external axial displacement was measured using a LVDT. Unconfined compressive strength tests were carried out after 14, 28, and 90 days for all mixes. Tests after 7 days of curing were performed on all mixes except n°9 and 11 (immersed in water). The 56-days strength was measured in the case of mixes n° 1 to 6. For each curing time, the average strength of three specimens was determined.

2.3.3.   Ultrasonic pulse wave velocity measurements

Ultrasonic pulse wave velocity measurements were carried out to confirm the strength test results. The ultrasonic equipment used in this study consisted of a pulser/receiver PUNDIT device manufactured by Proceq. The device generates and receives ultrasonic waves with a digital display of the results. Measurements were conducted according to procedures described in NF EN12504-4 (2005). A frequency of 54 kHz was used throughout this study. The device can be used with different testing methods: direct transmission, semi direct transmission, and indirect transmission. The direct transmission method was used in this study. All prepared sand-cement specimens of mixes n°3 and n°7 to 11 were tested at curing times of 7, 14, 28, and 90 days. The transducers were pressed against the specimen by hand in order to ensure a uniform and constant pressure between transducers and specimen surfaces. Vaseline was used as

couplant between the transducer and specimen surface. The PUNDIT device was used to read the time required for ultrasonic waves to propagate from the pulser through the specimen to the receiver. The distance between the transducers, which is equal to the specimen height, was divided by the measured time to calculate the wave velocity. For every mix, three readings were performed on each specimen and three specimens were tested for each curing time.

3. EXPERIMENTAL RESULTS AND ANALYSES

3.1. Effects of cement content and curing time

The evolution of the unconfined compressive strength q_u with time for mixes n°1 to 6 is presented in Figure 2 (Szymkiewicz, 2011).
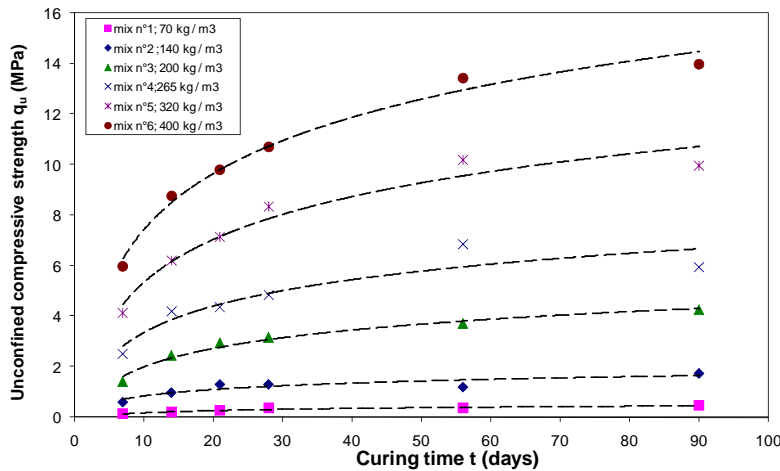
Figure 2: Unconfined compressive strength of Fontainebleau sand – cement mixes versus time

The results clearly show that the strength of the sand-cement mixes increases with cement content and curing time. The average unconfined compressive strengths after 7 days ranged from 136 kPa for a cement content of 70 kg / m³ (mix n°1) to approximately 6 MPa for a cement content of 400 kg / m³ (mix n°6). After 90 days, the average unconfined compressive strengths varied between 464 kPa (mix n°1) and 14 MPa (mix n°6). Figure 2 also shows that the rate of strength increase is higher during the first 28 days of curing. The rate of strength gain seems to decrease for longer curing times as q_u reaches a maximum value. The following relations were derived from the results obtained on mixes n°1 to n°6:

$$2.34 \leq \frac{q_{u90}}{q_{u7}} \leq 3.40 \tag{1}$$

$$1.93 \leq \frac{q_{u28}}{q_{u7}} \leq 2.70 \tag{2}$$

$$1.20 \leq \frac{q_{u90}}{q_{u28}} \leq 1.34 \tag{3}$$

With q_{u7} : unconfined compressive strength after 7 days; q_{u28} : unconfined compressive strength after 28 days ; q_{u90} : unconfined compressive strength after 90 days.
The unconfined compressive strength of Fontainebleau sand-cement mixes after 90 days is 2.34 to 3.40 times higher than the strength after 7 days of curing. The strength is multiplied by a factor of 1.93 to 2.7 between 7 and 28 days whereas between 28 and 90 days, the strength only increases by 20 to 34%. These ratios are slightly higher than those reported in the literature (Topolniki, 2004; Porbaha et al, 2000).
The ratios of strength increase between 7, 28 and 90 days are plotted against cement content in Figure 3. The ratios of 28 to 7-days strengths and 90 to 7-days strengths decrease as the cement content increases. The variation in strength between 28 and 90 days is almost constant for the cement contents chosen in this study. It appears that the strength increase between 7 and 90 days of curing is greater for low cement contents, most of the strength being acquired during the first 28 days of curing.
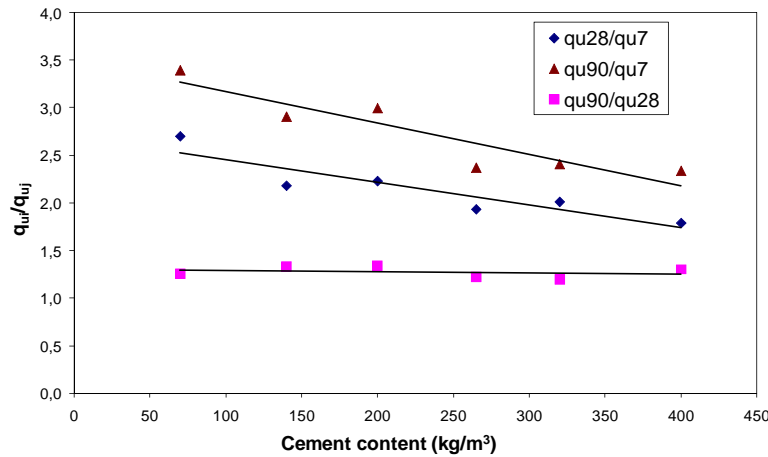
Figure 3: Increase in unconfined compressive strength of Fontainebleau sand – cement mixes after different curing times versus cement content

3.2. Prediction of the development of strength based parameters obtained after short curing times

The unconfined compression strengths of specimens from mixes n°1 to n°6 are plotted against the logarithm of time in Figure 4.
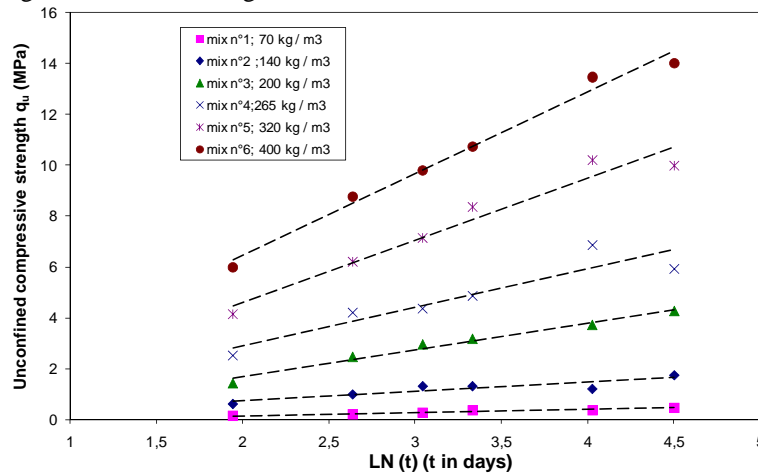
Figure 4: Unconfined compressive strength of Fontainebleau sand – cement mixes versus the logarithm of time Ln(t)

For all cement contents tested in this study, there exists a linear relation between q_u and the logarithm of time ln (t):

$$q_u(t) = \alpha \times \ln(t) - \beta \tag{4}$$

With t : curing time in days ($7 < t \leq 90$) ; $q_u(t)$ unconfined compressive strength after time t in MPa, α and β : experimental constants in Mpa.

In order to anticipate the development of strength based on tests performed after short curing times, the values of the experimental parameters α and β are assumed to be related to (and lower than) the 7-days strength q_{u7} :

$$\alpha = \lambda \times q_{u7} \tag{5}$$

$$\beta \approx 0.1 \times \alpha = 0.1 \times \lambda \times q_{u7} \tag{6}$$

Equation (4) becomes:

$$q_u(t) = \lambda \times q_{u7} \times (\ln(t) - 0.1) \tag{7}$$

With λ : an empirical reduction factor.

The 7-days strength q_{u7} partly takes into account the effects of the type of soil, type of binder and the initial curing conditions. It also partly reflects the quantity of binder used. The reduction factor λ is

introduced to take into account the decrease in the rate of strength gain with binder content recognized in Figure 3.

Moisture content is known to have a significant effect on the characteristics of soils stabilised with cement. A decrease in water content is typically observed after stabilisation which is related to chemical reactions occurring during the binder hydration process. Most of the decrease in water content occurs during the first week after stabilisation, but a continued decrease is normally observed up to at least one month after mixing. The moisture content of the stabilised soil w_f can roughly be calculated as (Anhberg, 2003):

$$w_f = \frac{\rho_{soil} \times \dfrac{w_N}{w_N + 1} - a \times x}{\rho_{soil} \times \dfrac{1}{w_N + 1} + (1 + a) \times x} \tag{8}$$

where ρ_{soil} is the bulk density of unstabilised soil (t/m^3); w_N is the natural water content of the unstabilised soil (in decimal number); x is the amount of dry binder added to the soil (t/m^3); and a is the content of non-evaporable water of the hydration product with respect to dry binder weight (in decimal number). The moisture content of the stabilised soil calculated from equation (8) decreases as the amount of binder increases.

It is proposed that the reduction factor λ introduced in equation (7) be taken as the ratio of the initial to final water contents w_f / w_i:

$$q_u(t) = \frac{w_f}{w_i} \times q_{u7} \times (\ln(t) - 0.1) \tag{9}$$

A good agreement is found when comparing the compressive strengths calculated from relation (9) for curing times between 14 and 90 days to the measured unconfined compressive strengths of specimens from mixes n°1 to n°6 (Figure 5).

The empirical relation (9) is applicable to sandy soils stabilised in the laboratory with slag cement in endogenous conditions for curing times up to 90 days. Its application to different soil types and different binders must be investigated. Preliminary investigations suggest that it is adaptable to fine grained soils through minor adjustments as similar relations have been proposed by other authors for clayey soils stabilised with Portland cement (Horpibulsuk et al, 2003; Nagaraj et al, 1997).
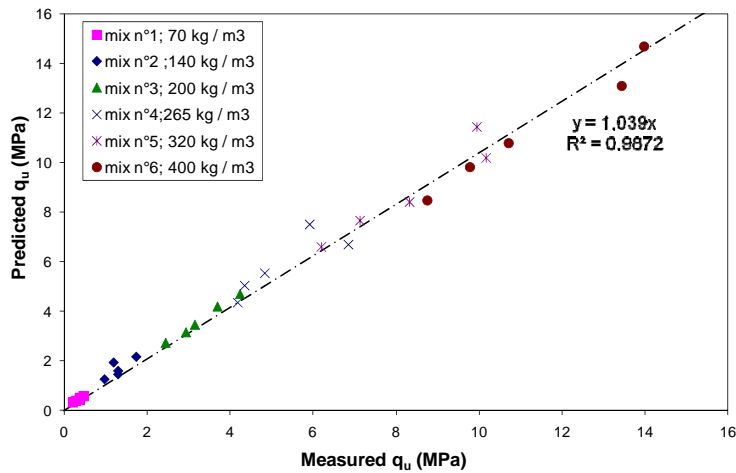
Figure 5: Unconfined compressive strength predicted using equation (9) versus measured strength.

3.3.   Effects of the addition of bentonite
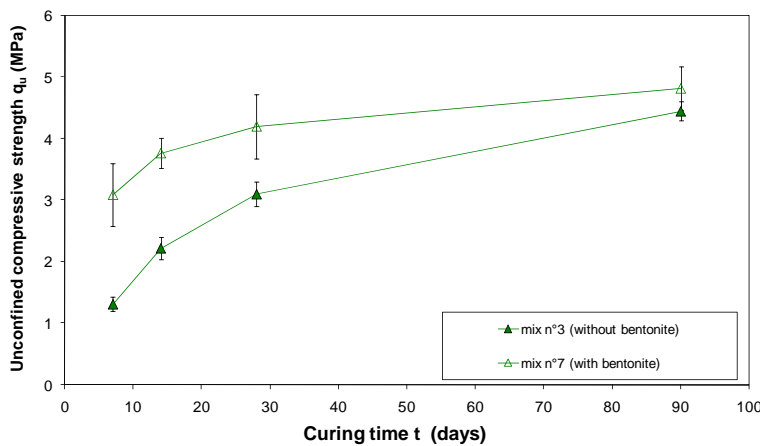
Figure 6: Effects of bentonite on the unconfined compressive strength of cement-stabilised Fontainebleau sand.

The results of unconfined compressive strength tests on specimens from mixes n°3 and n°7 are compared in Figure 6. After 7 days of curing, the average strength measured on specimens containing 50 kg/m³ of bentonite (mix n°3) is significantly higher than the strength of the specimens prepared without bentonite (mix n°7). The difference in strength progressively reduces after 90 days as the strengths of mixes n°3 and 7 are very close.

Figure 7: Effects of bentonite on ultrasonic pulse wave velocities measured in specimens of cement-stabilised Fontainebleau sand.

These results from unconfined compressive strength tests are confirmed by ultrasonic pulse wave velocity measurements (Figure 7). After 7 days of curing, the average ultrasonic wave velocity measured in specimens with bentonite is considerably higher (2640 m/s) than the velocity measured in specimens of mix n° 3 without bentonite ($\approx$ 2080 m/s). For longer curing periods, the wave velocities measured for mix n°3 progressively increase and ultimately exceed the velocities measured for mix n°7 after 90 days.

Although the final strengths obtained after 90 days of curing are approximately the same, the results presented in figure 6 clearly show that the addition of bentonite in sand-cement mixtures can significantly alter the strength development process in cement-stabilised sands.

Relation (9) was established based the results of tests on sand–cement mixes without bentonite (mixes n°1 to n°6) to estimate the strength development from strengths measured after short curing times. Due to the high strength measured after 7 days of curing, relation (9) significantly over-estimates the strength of specimens containing bentonite (mix n° 7).

3.4.   Effects of the presence of sulphates
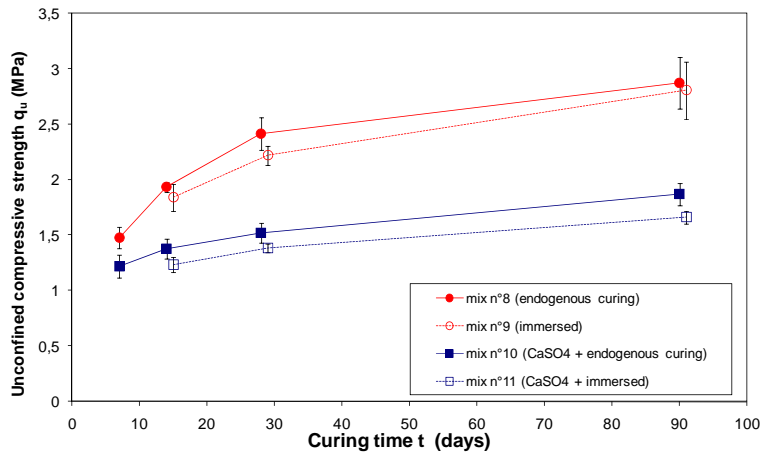
Figure 8: Effects of sulphates on the unconfined compressive strength of cement-stabilised Fontainebleau sand

The average unconfined compression strengths of specimens from mixes n°8 and n°9 are compared to the strengths measured on specimens of mixes n°10 and 11 in Figure 8.

The cement and moisture contents of these mixes are of 200 kg/m^3 and 35% respectively. They contain the equivalent of 50 kg/m^3 of bentonite. 10 g of CaSO4 per kg of dry soil was added to mixes n°10 and 11. Specimens of mixes n° 9 and 11 were immersed in water. Figure 8 clearly shows the detrimental effects of sulphates on the strength of stabilised soils. After 7 days, the average strength of the specimens of mix n°8 (without sulphates) is 1.21 times higher than the strength of specimens of mix n°10 (containing sulphates). This ratio increases with time to values of 1.41 after 14 days, 1.59 after 28 days and 1.53 after 90 days of curing. Immersion in water has a relatively small effect on average strength as the ratios of soaked to un-soaked strengths vary between 0.92 to 0.97 for the mixes without sulphates (n°8 and 9) and between 0.89 and 0.91 for the mixes in which sulphates were added (n° 10 and 11).
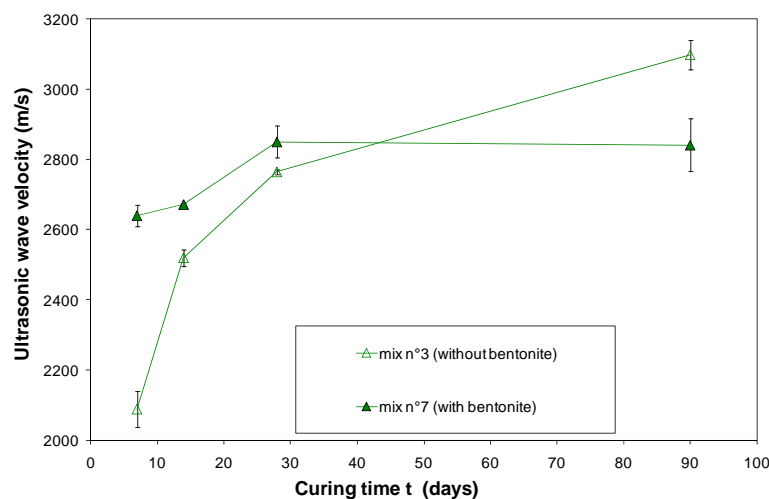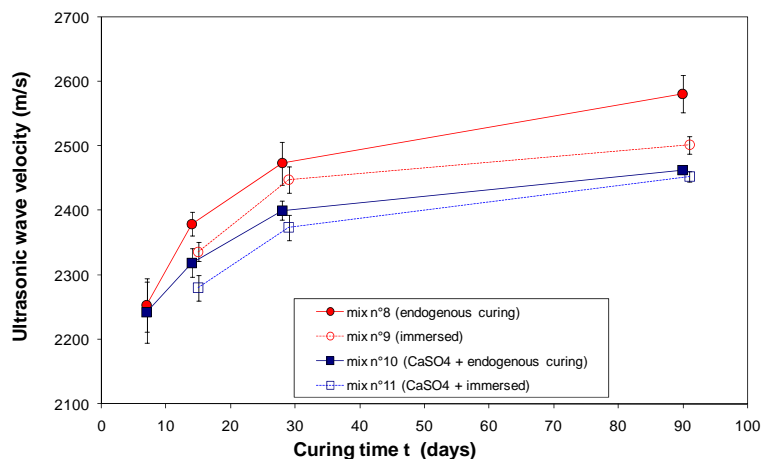

Figure 9: Effects of sulphates on ultrasonic pulse wave velocities measured in specimens of cement-stabilised Fontainebleau sand

The effects of sulphates on the unconfined compressive strength are also confirmed by ultrasonic pulse wave velocity measurements (Figure 9). The average ultrasonic velocities measured for specimens without sulphates are higher than those of the specimens containing sulphates, the difference also increasing with time. By their negative effect on the development of strength with time in stabilised soils, the presence of sulphates can be a factor that significantly complicates the estimation of strength gain from measurements carried out after short curing times. In this case, the proposed relation (9) is not applicable as it overestimates the strength of the mixes containing sulphates.

4.   CONCLUSION

The aim of this study was to evaluate the effects of time and cement content on the strength of sandy soils when mixed in the laboratory with cement. The main objective of this research was to determine a simple method to estimate the increase in strength with time of sandy soils treated with cement in the laboratory. An empirical relation is proposed, applicable to sandy soils stabilised in the laboratory with slag cement in endogenous conditions for curing times up to 90 days, to predict the development of strength with time based on measurements carried out after short curing times. Its application to different soil types and different binders must be investigated. This formula must also be tested on sandy soils stabilized by deep mixing in the field. This relation can contribute to minimise the number of laboratory trials needed and assist engineering decisions on the amounts of binder and curing periods needed to reach specific target strengths for deep soil mixing applications. However, special precaution must be taken when using such relations as it has been shown that numerous factors such as the addition of bentonite or the presence of sulphates can modify the development of strength with time in cement-mixed sands. In such cases, the use of empirical relations can lead to erroneous predictions of strength.

REFERENCES

AFNOR, NF EN 13286-41, 2003, Unbound and hydraulically bound mixtures - Part 41 : test method for the determination of the compressive strength of hydraulically bound mixtures

AFNOR, NF EN 12504-4,2005, Testing concrete. Determination of ultrasonic pulse velocity.

Ahnberg, H., S.-E. Johanson, H. Pihl and T. Carlsson, 2003, Stabilising effects of different binders in some swedish Soils, Ground Improvement, 7(1).

CDIT, 2002, The Deep Mixing Method - Principle, Design and Construction, Balkema, The Netherlands

CEN, 2005, Cement - Part 1: Composition, specifications and conformity criteria for common cements. EN 197-1. CEN.

Ganne, P., Huybrechts, N., De Cock, F., Lameire, B., & Maertens, J., 2010, SOIL MIX walls as retaining structures – critical analysis of the material design parameters. Geotechnical challenges in Megacities, Moscow, Russia.

Horpibulsuk, S., Miura, N., and Nagaraj, T. S., 2003, Assessment of strength development in cement admixed high water content clays with Abrams' law as a basis, Geotechnique, 53(4).

Hunter, D., 1988, Lime induced heave in sulfate bearing clay soils. Journal of Geotechnical Engineering 114.

Jegandan, S., Liska, M., Osman, A. A.-M., & Al-Tabbaa, A., 2010, Sustainable binders for soil stabilisation. ICE Journal of Ground Improvement.

Nagaraj,T. S., Miura, N., Yamadera, A. And Prakash, Y., 1997, Strength assessment of cement admixture soft clays – parametric study, International Conference on Ground Improvement Techniques, Macau.

Porbaha, A., 1998, State of the art in deep mixing technology: Part I. Basic concepts and overview. Ground Improvement, 2(2).

Porbaha, A., S. Shibuya and T. Kishida, 2000, State of the art in deep mixing technology, Part III : Geomaterial characterization of deep mixing, Ground Improvement, 4(3).

Szymkiewicz, F., 2011, Evaluation des caractéristiques mécaniques du matériau Soil-Mixing, PhD thesis, Université Paris-Est/IFSTTAR.

Terashi, M., 1997, Theme Lecture: Deep Mixing Method - Brief State of the Art. Paper presented at the 14th International Conference on Soil Mechanics and Foundation Engineering, Hamburg, Germany.

Topolnicki, M., 2004, Chapter 9 In situ soil mixing, In M. P. Moseley & K. Kirsch (Eds.), Ground Improvement (Second ed.), Abingdon, Oxon, Spon Press.

Rheological properties of cement-stabilised kaolin

Antoine Guimond-Barrett, IFSTTAR-LCPC/Université du Havre, France, antoine.guimond-barrett@ifsttar.fr
Ammar Touati, Université du Havre,
Anne Pantet, Université du Havre, France,
Philippe Reiffsteck, IFSTTAR-LCPC, France, philippe.reiffsteck@ifsttar.fr
Alain Le Kouby, IFSTTAR-LCPC, France, alain.lekouby@ifsttar.fr

ABSTRACT

Deep soil mixing is a process used to improve the mechanical properties of soft soils by mixing dry or wet binders with the existing soil. The strength and deformation properties of the treated soils depend on the initial soil conditions, the type and amount of binder used and the curing conditions. The homogeneity and strength of soils stabilised by deep mixing also depend on the mixing mechanisms that occur during construction. These mixing mechanisms are directly related to the rheological properties of the materials being mixed. Therefore, rheology is the starting point in understanding the processes involved in deep soil mixing although knowledge of the rheological characteristics of stabilised clays is very limited. The aim of the research presented in this paper is to investigate the effects of cement stabilisation on the rheological properties of kaolin clay. The flow properties of kaolin, cement slurries and kaolin–cement mixtures at various moisture contents were measured using a rheometer with two different geometries: parallel plates and the ball measuring system. For all mixtures tested, the shear stresses increase as the moisture content decreases. A good agreement was found between the stresses measured using the parallel plates and the ball measuring system for kaolin suspensions, validating the use of this shear geometry for subsequent studies on coarse grained soils. The results are discussed with respect to in situ soil mixing processes. It is proposed that observations made in the field on the relation between blade rotation speed and strength and homogeneity of treated soils can be explained by the shear-thinning behaviour of clays. The yield stress may be a relevant tool to study the workability of soil-cement mixtures.

1. INTRODUCTION

Ground improvement by deep mixing is today a widely accepted method used to improve the permeability, strength and deformation properties of soft soils. The aim of the installation process in deep soil mixing is to inject and spread a binder in dry or slurry form into the soil in order to produce a homogeneous soil-binder mixture. The execution process is very complex compared to other ground improvement methods. The mixing mechanisms that occur during deep mixing are difficult to monitor and present engineering challenges (Larsson, 2003). A large number of factors are known to influence the strength and deformation properties of the treated soils (Terashi, 1997). These factors are mainly related to the characteristics of the binders (type, amount), the soil conditions (soil type, moisture content, and organic content) and the curing conditions. The homogeneity and strength of soils stabilised by deep mixing also largely depend on the mixing conditions and mechanisms that occur during construction (degree of mixing, mixing tool). It has been observed that the mixing of fine grained soils with binders is particularly difficult in extremely cohesive soils of high moisture contents. The mixing mechanisms in deep mixing are directly related to the rheological properties of the materials being mixed. Therefore, rheology is the starting point in understanding the processes involved in deep soil mixing. Knowledge of the rheological characteristics of stabilised soils is very limited (Larsson, 2005).

In current practice, certain simple tests are performed on site to rank and compare flow properties of grouts, concrete and soil-binder mixtures using empirical parameters (Marsh cone, Abrams cone ...). These tests can be very useful in the field for rapid assessments of rheological characteristics but are limited to comparisons of the effects of different dosages on flow properties. They do not allow a quantitative assessment of rheological parameters or the understanding of fundamental physical and chemical interactions between the different constituents in the mixtures.

The use of rheometry allows a more quantitative study of the impacts of the addition of binders on the flow properties of soils. The type of soil and its rheological behaviour have a considerable impact on the efficiency of the mixing process. For coarse grained soils, classic shear geometries cannot be used and only a few rheometers exist that allow the determination of yield stress and viscosity.

The aim of this research is to study the effects of the addition of cement on the rheological characteristics of kaolin clay. In the present investigation, we focus on rheometrical measurements carried out with both

the parallel plates geometry and the ball measuring system (BMS). The objectives are (1) to validate the use of the BMS to measure the rheological parameters of soil-cement mixtures for subsequent studies on coarse grained soils and (2) to examine the effects of the rheological properties on the resulting solidified materials and the reactivity between soils, water and soil mixing conditions.

2. RHEOLOGY OF CLAYS AND CEMENT PASTES

Many authors (Coussot & Ancey, 1999; Lagaly, 1989; Roussel, 2005) have reported that cement slurries and clay–water suspensions could be described in the liquid state as shear-thinning yield stress fluids (Figure 1). The viscosity of shear-thinning fluids decreases as the shear rate increases.
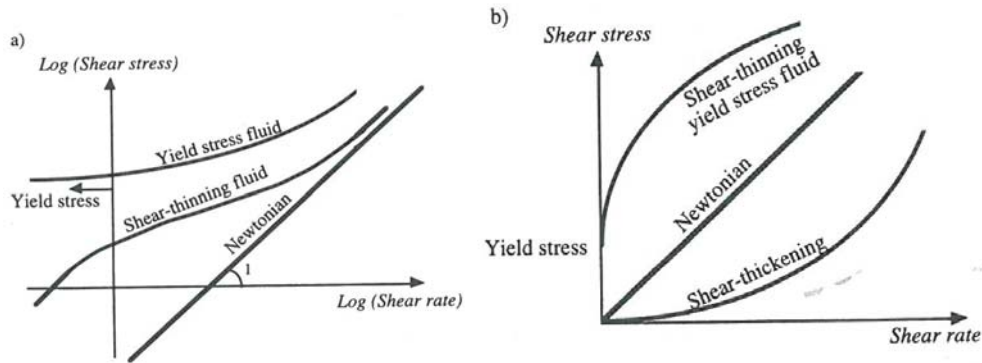
Figure 1: Main steady state behaviour types a) logarithmic diagram b) linear diagram (Coussot, 1997).

The simplest theoretical model for yield stress fluids is the Bingham model (equation 2).

$$\tau = \tau_0 + \eta\dot{\gamma} \tag{1}$$

Where τ_0 = yield stress (Pa), η = viscosity (Pa.s).

It is possible to fit this model to experimental data in a narrow range of large shear rates. However, key material properties may be disregarded by using this model. Consequently, it was proposed to fit a Herschel–Bulkley model (1926) to experimental data:

$$\tau = \tau_0 + K\dot{\gamma}^n \tag{2}$$

Where, K and n = experimental parameters; (n < 1 for shear shinning fluids).

Usually, the yield stress represents the strength resulting from the interparticle interaction forces under shear displacement. It corresponds to a critical value of shear stress below which it is not possible to have flow. However, the concept of yield stress is still widely discussed (Tattersal & Banfill, 1983, Barnes & Walters, 1995; Coussot et al, 1996; Barnes, 1999). Indeed, depending on the test procedure, many different values of yield stress can be defined. Even during a single test, different yield stresses can be measured or calculated. This is especially the case for fluids that exhibit a minimum in flow curves. This phenomenon is related to flocculation and deflocculation processes that depend on the hydration of the particles (clay and cement particles are particularly reactive in terms of swelling, phase modification and crystallisation).

3. MATERIALS AND METHODS

3.1. Characteristics of kaolin and binder

The clay used in this study is Speswhite kaolin. This kaolin has a liquid limit WL of 55% and a plasticity index PI of 25%.The cement used is a Portland slag cement containing 85 % ground granulated blast furnace slag (European classification: CEM III/C 32,5 N CE PM-ES NF "HRC") (CEN, 2005). This cement presents a slow strength development, and its initial setting time is 4 hours after hydration. The grain size distributions of the Speswhite kaolin and the cement are presented in Figure 2.
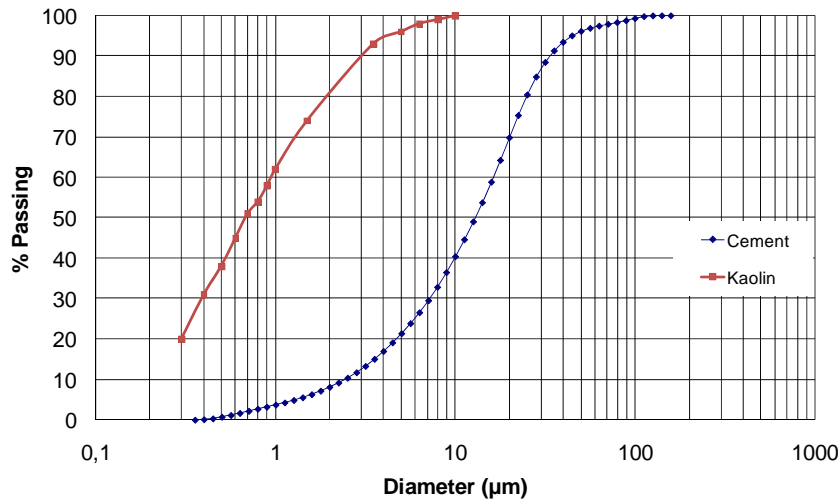
Figure 2: Grain size distributions of Speswhite kaolin and CEMIII cement.

3.2. Sample preparation

For the preparation of the clay samples, the appropriate amount of tap water to reach the target water content was added to the dry soil. Dry cement was then added to the humidified clay and mixed with a laboratory mixer for 5 to 10 minutes at a rotation speed of 2000 rpm. It is well known that the order in which the different constituents are added may have a significant effect on the properties of the mixture. The time between sample preparation and testing was less than 15 minutes. For the cement slurries, dry cement was mixed with tap water for 10 minutes also at a speed of 2000 rpm.

3.3. Testing apparatus and procedure

The tests were carried out using a MCR 501 rheometer manufactured by Anton Paar equipped with parallel plates and the ball measuring system.
The parallel plates geometry consists of two coaxial disks. The material placed between the disks is sheared by their relative rotation. The parallel plates used in this study were of 50 mm in diameter. The gap between the plates was 1 mm.
The ball measuring system consists of a 12 mm diameter sphere that is dragged through a sample volume of approximately 0.5 L (Figure 3) implemented in a standard rheometer (Schatzmann et al, 2009). The rotating speed was controlled and torque measurements were recorded by a computer. The shear stress and the shear rate were then calculated.

Figure 3: The BMS of Müller et al (1999) implemented in a standard rheometer (Schatzmann et al, 2009).

It is well known that clay–water suspensions are thixotropic materials (Coussot, 1997). To obtain consistent and reproducible measurements, specific rheometric procedures must be executed. The procedure used is similar to the method described by Pantet & Monnet (2007). In order to define a structural reference state, measurements with the parallel plate geometry started with an initial shearing

phase (constant shearing at a rate of 300 s^{-1} during 60 s), followed by a rest period of 120 s. Then, the material was subjected to increasing and decreasing shear rates. The difference between the increasing and decreasing values gives indications about the thixotropic properties (i.e. structural evolution) of the fluid. Flow curves were established for shear rates between 0.01 and 300 s^{-1} with the parallel plates geometry and between 0.01 and 50 s^{-1} with the ball measuring system.

3.4. Experimental program

The experimental program is presented in Tables 1 and 2. Kaolin was tested at 3 different moisture contents. Flow curves of cement slurries were established for 5 different water-cement ratios.

In total, 7 kaolin-cement mixes were tested. The cement contents C (weight of dry cement/weight of dry clay) varied between 5 and 20% (0.05 and 0.2) and the moisture contents between 0.43 and 1.74. To study the effects of an increase in cement content, 4 kaolin-cement mixtures were prepared with a water/clay ratio equal to 1 and with increasing cement/clay ratios between 0.05 and 0.20 (mixes n°1 to 4, Table 2). The 3 other kaolin-cement mixes were prepared with a cement/clay ratio of 0.15 and different water/clay ratios.

Table 1: Characteristics of the kaolin and cement suspensions

Soil	Moisture content (kaolin) / Water-cement ration (cement slurries) w = weight of water/weight of dry solids				
Kaolin	2.00	1.50	1.00	-	-
Cement	0.60	0.55	0.50	0.45	0.42

Table 2: Characteristics of the kaolin-cement mixes

Mix n°	C= weight of dry cement/weight of dry clay	W= weight of water/weight of dry solids	weight of water/weight of dry clay
1	0.05	0.95	1.00
2	0.10	0.91	1.00
3	0.15	0.87	1.00
4	0.20	0.83	1.00
5	0.15	1.74	2.00
6	0.15	1.30	1.50
7	0.15	0.43	0.50

4. EXPERIMENTAL RESULTS AND ANALYSES

4.1. Flow curves of kaolin

The flow curves obtained using the parallel plates and the ball measuring system for Speswhite kaolin at different moisture contents are presented in Figure 4. For both geometries, the shear stresses measured increase as the moisture content decreases. This can be explained by the increasing interaction between the clay particles as their concentration increases.

The yields stresses obtained for the two geometries, taken as the shear stress at a shear rate of 1s^{-1}, are compared in Table 3. An acceptable agreement is found between the yield stresses obtained using the parallel plates and the ball measuring system.

No thixotropic effects were observed for the Speswhite kaolin. Thixotropic behaviour exhibited by other clay minerals such as smectites is related to high reactivities and modifications in particle size and surface properties caused by the hydration process (Lagaly, 1989; Besq et al., 2003; Pantet & Monnet 2007).

Table 3: Yield stresses of kaolin at different moisture contents

Geometry	Yield stress (Pa)		
	W=1.0	W=1.5	W=2.0
Parallel plates (average)	300	55	7.5
Ball Measuring system	300	43	14

a)

b)
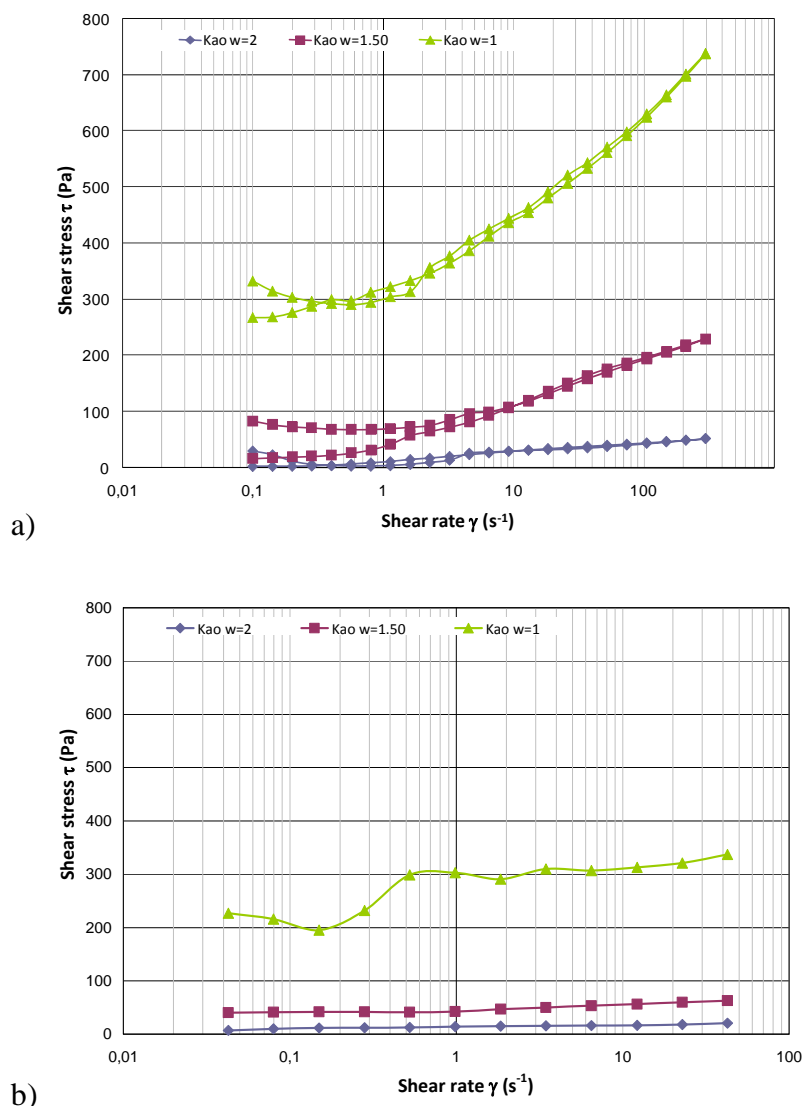
Figure 4: Flow curves for Kaolin using a) the parallel plates b) the ball measuring system.

4.2. Flow curves of cement slurries

The flow curves obtained using the ball measuring system for cement slurries with different concentrations are plotted in Figure 5. The yield stresses, taken as the shear stress at a shear rate of $1s^{-1}$, are given in Table 4.

Table 4: Yield stresses of cement slurries at different concentrations

Geometry	Yield stress (Pa)				
	W=0.6	W=0.55	W=0.50	W=0.45	W=0.42
Ball Measuring system	17	50	153	415	830

a)

b)
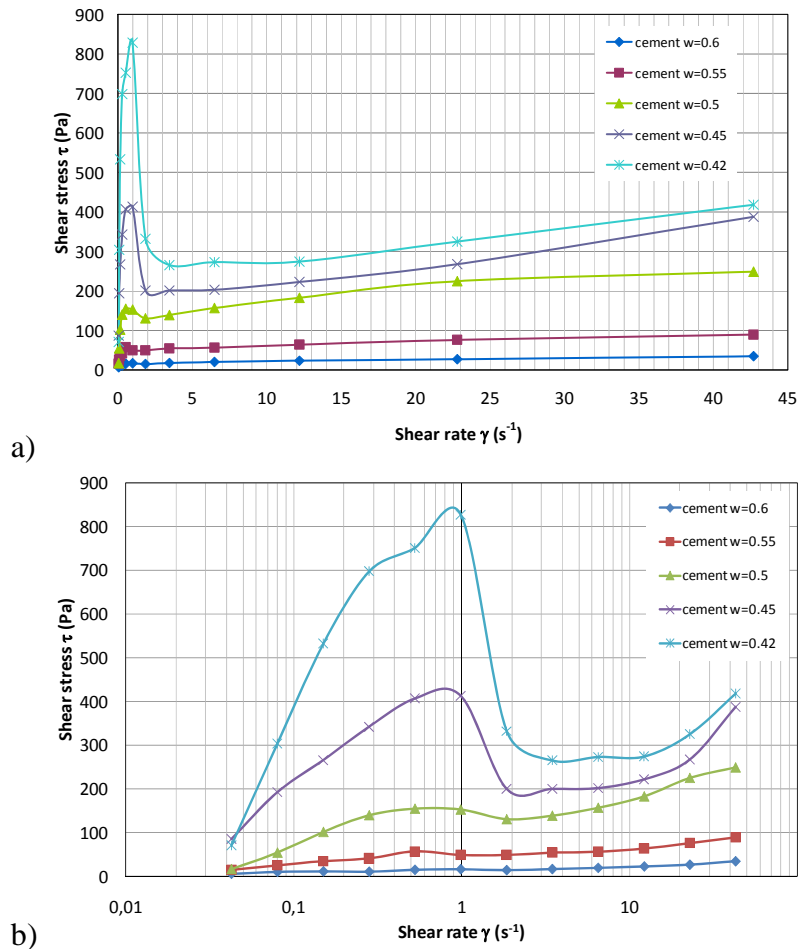
Figure 5: Flow curves for cement slurries a) linear scale b) logarithmic scale.

The measured flow curves are above the equilibrium state flow curves. These results demonstrate that the deflocculation process was insufficient to bring the structure to its equilibrium state. This type of flow curve is directly related to the duration of the experimental measuring cycle as reported by Roussel (2005, Figure 6).
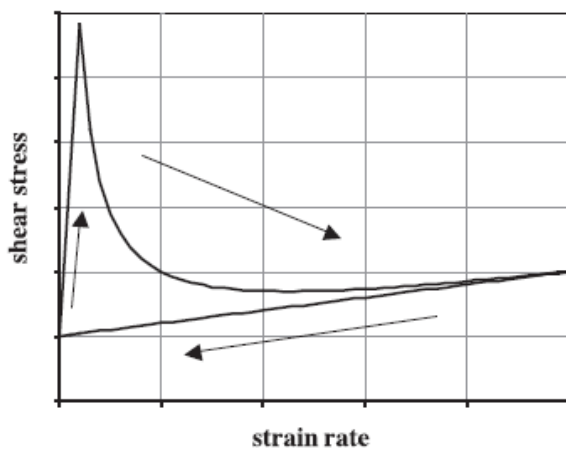
Figure 6: Cement paste flow curve: short cycle test; steady state not reached (Roussel, 2005).

4.3. Flow curves of clay-cement mixes

The flow curves obtained for clay-cement mixtures using the ball measuring system are plotted in Figures 7 and 8. The flow curves are similar to those obtained for the cement slurries. The behaviour, once the minimum is reached, is rheopetic and can be related to the hydration process. Figure 7 shows that the

addition of dry cement affects the measured shear stresses inasmuch as it causes an increase in particle concentration. The effect of moisture content on the rheological behaviour of cement-kaolin mixes is clearly visible in Figure 8 as the measured shear stresses drastically increase for moisture contents lower than 100%. The yield stresses (shear stress at a shear rate of $1s^{-1}$) are summarized in Table 5.
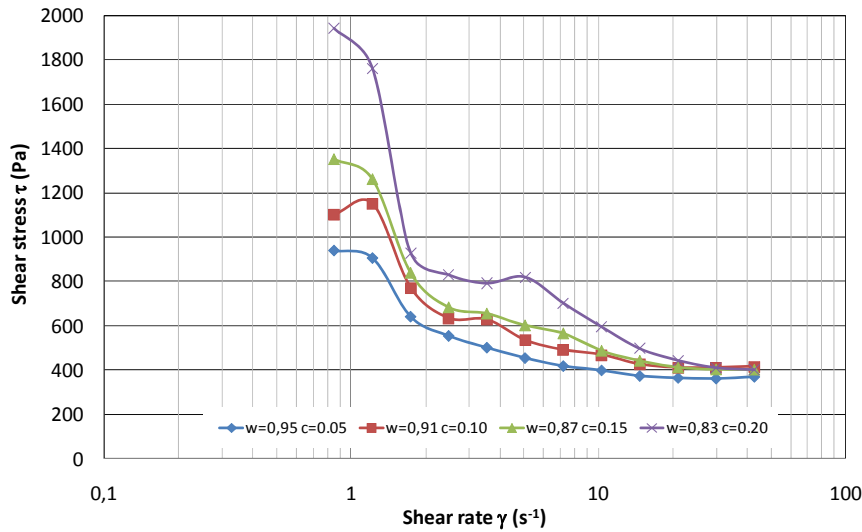
Figure 7: Flow curves for clay-cement mixes n°1 to 4 using the BMS (constant water / clay ratio; different cement contents).
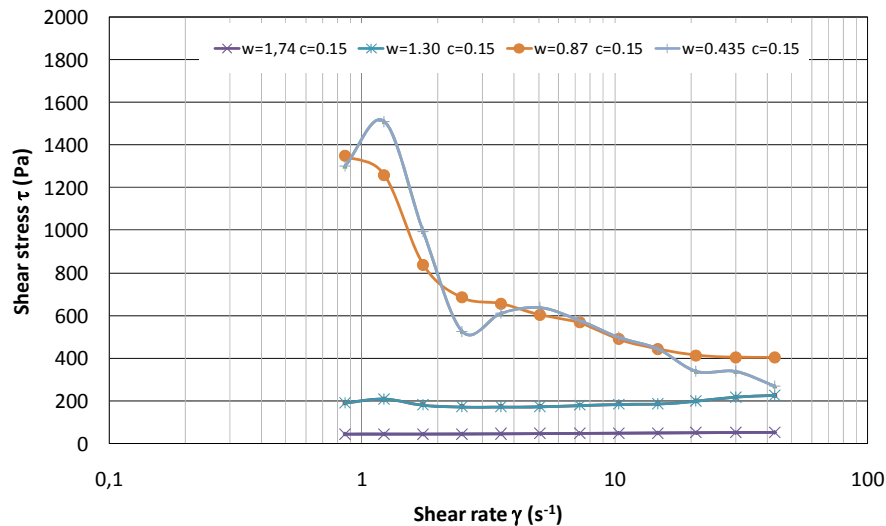
Figure 8: Flow curves for clay-cement mixes n°3 and n°5 to 7 using the BMS (constant cement content; different water / dry solid ratios).

Table 5: Yield stresses of kaolin-cement mixes measured with the BMS

Mix n°	1	2	3	4	5	6	7
C= weight of dry cement/weight of dry clay	0.05	0.10	0.15	0.20	0.15	0.15	0.15
W= weight of water/weight of dry solids	0.95	0.91	0.87	0.83	1.74	1.30	0.435
Yield stress (Pa)	906	1150	1260	1760	45	210	1510

5.   DISCUSSION

The results presented above can be related to observations made in the field regarding the installation process of deep soil mixing elements. Many others have reported that faster tool rotation speeds increase

the homogeneity and strength of treated soils (CDIT, 2002). In the case of fine grained soils, this can be explained by the shear-thinning behaviour of clays (i.e. lower viscosity at higher shear rates). As the blade rotation speed increases, the soil is subjected to increasing shear rates. Assuming that homogenising low viscosity fluids or suspensions is easier than mixing viscous fluids, the efficiency of the mixing process is improved at higher shear rates (blade rotation speeds). The clay-binder mixture produced is more homogeneous and therefore of higher strength after curing.

The effects of yield stress on the mixing process in deep mixing are less straightforward as the stresses produced by the rotation of the mixing tool are much higher than the yield stresses of clay suspensions. The yield stress may be related to the workability of soil-cement mixtures. In general, no compaction is performed during the installation of soil mixing columns. The soil-cement mixtures must therefore be sufficiently fluid to be self-compacting. This implies that the mixes should have a yield stress which is low enough to allow the mixture to flow under its own weight and fill the voids created by the passing of the mixing tool. The results obtained on kaolin-cement mixtures clearly show the predominant effect of moisture content on yield stress (Figure 9). Further research and experiments are needed in this direction as it may be possible to determine, for a particular soil-cement mixture, an optimum moisture content which does not significantly alter the strength of the treated soil after curing but at which the yield stress in the fresh state is sufficiently low for the mixture to be self-compacting. Further field experiments could allow the determination of yield stress thresholds for the workability of soil-cement mixtures.
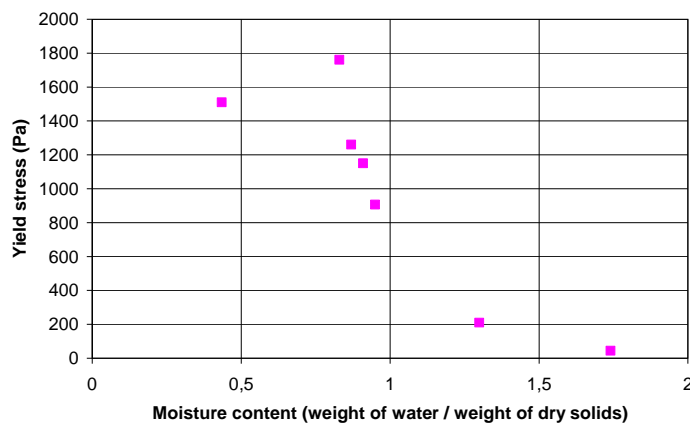
Figure 9: Yield stress versus moisture content for kaolin-cement mixes.

6.   CONCLUSION

In this paper, the flow properties of kaolin, cement slurries and kaolin–cement mixtures at various moisture contents were measured using a rheometer with two different geometries: the parallel plates and the ball measuring system. For all mixtures tested, the yield stresses decreased as the moisture content increased. A good agreement was found between the stresses measured using the parallel plates and the ball measuring system for kaolin suspensions, validating the use of this shear geometry for subsequent studies on coarse grained soils. The results are discussed with respect to in situ soil mixing processes. It is proposed that observations made in the field on the relation between blade rotation speed and strength and homogeneity of treated soils can be explained by the shear-thinning of clays. The yield stress seems to be a relevant tool to study the workability of soil-cement mixtures.

REFERENCES

Barnes, H.A., 1999, The yield stress–a review or–everything flows ? Journal of Non–Newtonian Fluids Mechanics, 81.

Barnes, H.A. & Walters, K., 1995, The yield stress myth ? Rheologica Acta, 24.

Besq, A., Malfoy, C., Pantet, A., Monnet, P., Righi, D., 2003, Physicochemical characterization and flow properties of some bentonite muds. Applied Clay Science, 23.

CEN, 2005, Cement - Part 1: Composition, specifications and conformity criteria for common cements. EN 197-1. CEN.

CDIT, 2002, The Deep Mixing Method - Principle, Design and Construction, Balkema, Rotterdam.

Coussot, P., 1997, Mudflow Rheology and Dynamics, Balkema, Rotterdam.

Coussot, P. & Ancey, C., 1999, Rhéophysique des pâtes et des supensions, EDP Sciences.

Coussot, P., Proust, S., Ancey.C.,1996, Rheological interpretation of deposits of yield stress fluids. Journal of Non-Newtonian Fluid Mechanics,66.

Hershel, W.M.,& Bulkley, R.,1926, Measurement of consistency as applied to rubber-benzene solutions, Proc Amer Soc Testing Materials. 26(II).

Larsson, S., 2003, Mixing Processes for Ground Improvement by Deep Mixing: KTH, Sweden.

Larsson, S., 2005, State of practice report - execution, monitoring and quality control. Paper presented at the Deep Mixing ´05. International Conference on Deep Mixing. Best Practice and Recent Advances.

Lagaly. G., 1989, Principles of flow of kaolin and bentonite dispersions. Applied Clay Science, 4.

Müller, M., Tyrach, J., Brunn, P.O., 1999, Rheological characterization of machine-applied plasters.ZKG Int 52.

Pantet, A. & Monnet, P., 2007, Liquid–solid transition of kaolinite suspensions, Mechanics of Materials, Volume 39, Issue 9.

Roussel, N., 2005, Steady and transient flow of fresh cement pastes, Cement and concretre research,35.

Schatzmann., M., Bezzola, G. R., Minor, H.-E., Windhab E. J., Fischer ,P., 2009, Rheometry for large particulated fluids: analysis of the ball measuring system and comparison to debris flow rheometry, Rheologica acta, vol. 48, n°7.

Tattersall, G.H. & Banfill, P.F.G., 1983, The rheology of fresh concrete. Pitman.

Terashi, M., 1997, Theme Lecture: Deep Mixing Method - Brief State of the Art. Paper presented at the 14th International Conference on Soil Mechanics and Foundation Engineering, Hamburg, Germany.

Influence of the clay content of a lime-treated soil on its compression strength

HASHEMI Mir Amid, Université Libre de Bruxelles, Belgium, mihashem@ulb.ac.be
KADIRI Hicham, Université Libre de Bruxelles, Belgium, hkadiri@ulb.ac.be
MASSART Thierry, Université Libre de Bruxelles, Belgium, thmassar@batir.ulb.ac.be
VERBRUGGE Jean-Claude, Université Libre de Bruxelles, Belgium, jverbrug@ulb.ac.be
FRANCOIS Bertrand, Université Libre de Bruxelles, Belgium, bertrand.francois@ulb.ac.be

ABSTRACT

Lime treatment is an efficient way to stabilize soils. However, its efficiency is very limited in sandy soil for which cement treatment is often more adapted. It is believed that very low clay content can be enough to drastically increase the properties of a sandy soil by lime treatment. Hence, adding a low quantity of clayey materials in addition to lime can make sand stabilization possible.

In this context, this paper presents the preliminary results of an experimental program carried out on different sand-bentonite mixtures treated with lime and then compacted at normal optimum Proctor conditions. Lime-treated soils have been uniaxially compressed at different curing times (up to 56 days). The results show that the strength properties of lime-treated soils are considerably increased because of relatively low contents of bentonite added in pure sand. Also, beyond a given bentonite content, the soil strength starts to decrease when bentonite is further added. In parallel, a comparison is also made with the Proctor compaction curves. Starting from pure sand, the Proctor optimum density increases with the bentonite content, reaches a maximum density and then decreases with addition of clay.

1.   INTRODUCTION

Clay soils can be stabilized by the addition of small percentages, by weight, of lime. The stabilization enhances many of the engineering properties of the soil (mainly the stiffness and the strength parameters). Its efficiency lies in the low quantity of lime addition and the ecological advantage because it uses the soil already in place without requiring soil replacement. Lime mostly reacts with the clay and silt part of the soil.

Lime treatment has its effect on soil at two different levels. First, lime modifies the soil instantaneously. Lime reacts quickly with clay by modifying its structure. It allows the clay minerals to merge to bigger aggregates (Little, 1995). It is for a matter of fact one of the reasons why lime is used in civil engineering. Lime increases the bearing capacity and diminishes the plasticity. Soils where mud makes the field work complicated can be treated with lime to allow a more efficient workability.

The second effect is soil stabilization. Long term pozzolanic reactions take place after soil modification (Eades, 1962). CSH and CAH formations from pozzolanic reactions increase the soil mechanical properties. They are similar to those in cement. However, in cement, when hydrated, calcium binds with silicates and aluminates to form CSH and CAH crystals. In clayey soils treated with lime, the same reaction takes place between the calcium of the lime and the silicates and aluminates of the clay minerals. However, the reaction is slower than of cement because it requires the dissolution of clay minerals into silicium and aluminium ions. And besides, the dissolution is possible only at high alkaline solution (pH > 10) (Keller, 1964). Research on soil stabilization has been made for the last decades. (Estéoule, Perret, 1979) and (De Bel, 2008) observed an increase on the compression resistance in phases in function of time. Many important parameters influence soil stabilization, such as water content and dry density of soil (Locat et. al., 1990). Also, higher temperatures increase the speed of the reaction (Estéoule and Perret, 1979), (Bollens, 2005), (De Bel, 2008). Organic matter decreases the efficiency of lime (Locat et. al., 1990), (Onitsuka et. al., 2003). The clay mineral type is an important parameter of soil stabilization (Bell, 1996). Montmorillonite has a better efficiency for lime adsorption than kaolinite. CEC value is an important factor to be considered.

Lime production, compared to cement production, releases less carbon dioxide. Lime industry emits 785kg of CO_2 for 1000kg CaO (EIA, 2002) whereas every ton of cement produces 900kg of CO_2 (Mahasenan et. al., 2003).

Consequently, it becomes more ecologically-efficient to use lime for soil stabilization if time is not an important factor. However, sandy soils cannot be treated in the same way. These are usually treated with cement (NRS, 1969). The idea is to make lime stabilization possible with sand by adding clay minerals. This paper contributes to the understanding of the effect of a small amount of bentonite on the efficiency of sandy soils treated with lime.

In the present work, different proportions of sand-bentonite mixtures going from pure sand to pure treated bentonite have been studied. From (Kenney et. al., 1992), (Sivapullaiah et. al., 1998), (Ferber, 2005), the studied mixtures of sand and bentonite have all a maximum optimum dry density at a known composition which is higher than the optimum dry density of sand and bentonite taken separately. Proctor tests for our compositions have also been carried out to point out this property for the lime treated mixtures.

Three different compositions have first been chosen for unconfined compression tests: 30%, 45% and 60% bentonite mixed with 70%, 55% and 40% sand respectively. Further investigations on compression resistance are still being done in lower bentonite contents. The quantity of lime added to the three compositions has been fixed to 2% after the Eades & Grim test (Eades and Grim, 1966). All the percentages are in mass. After lime treatment, Normal Proctor Compaction Tests have been made on different lime treated compositions. Sand-bentonite samples have been prepared by static compaction at dry density and water content at normal proctor optimum conditions. Unconfined compression tests have been performed at different curing times up to 56 days.

2. METHODOLOGY

2.1. Choice of compositions

The sand used in the experience is homometric (i.e. the particles have all more or less the same size. The reason for taking homometric sand is to have the simplest sand possible and the easiest to consider in theoretical and numerical modeling. It corresponds to the skeleton of the mixture. The second part of the mixture is bentonite. This part stands for the clayey cohesive matrix that reacts with lime. There is no overlapping between the particle size of sand and bentonite. Bentonite is taken because of its high reactivity with lime (principally montmorillonite), its cheapness and its availability in the market. Since sodium bentonite is known to have a very high swelling index, calcium bentonite is chosen to avoid any discomfort with manipulation.

2.2. Eades & Grim procedure (ASTM D-6276)

This test allows calculating the quantity of lime necessary to fully provide the mixture (Eades, Grim, 1966). The measurement is done via the pH of the lime-soil solution. Once pH reaches 12.4, Eades & Grim optimum is reached which means that the quantity of lime added is considered as sufficient. The measurement is done through different containers each having 20g of soil in 100ml of distilled water. Then for each container, different quantities of lime are added in mass percentage between 0.5% and 10.0% by steps of 0.5%. The solution is then mixed during an hour at a fixed frequency and, at the end, the pH is taken. The Eades & Grim optimum is the lowest value of lime percentage having reached 12.4.

2.3. Proctor Compaction (ASTM D-3668 78)

In order to correspond to in situ field conditions, tested samples should be at 98.5% of the Normal Proctor Optimum (OPN) density. Consequently, a preliminary step before sample preparation is the determination of the Optimum Proctor Curve. The following procedure has been carried out. The soil is mixed with a mechanical mixer. Once the Eades & Grim procedure is done, the optimal quantity of lime is added to the mixture and distilled water is poured in the mixer in different moisture contents. The wet soil is then put in a plastic bag to mellow for 24 hours at 20°C. After 24h, compaction takes place. The results give the Normal Proctor Optimum density and the Optimum moisture content to use for the samples preparation.

2.4. Unconfined compression test (ASTM D-5102 96)

Unconfined compression test allows measuring both compression resistance and rigidity of the mixtures. Five samples of each composition and for each curing time have been prepared. The sand and the bentonite are mixed with the amount of lime calculated with the Eades & Grim process. Then, distilled water is added at Optimum Moisture Content. The soil is put in a plastic bag for 24h mellowing. Finally, five samples are made at 98.5% of OPN. Their dimensions are of 70mm length and 36mm diameter. First, a plastic film is wrapped around the sample and then, an aluminum film. Finally, the sample is immersed in paraffin to avoid any exchange of water and air with the exterior. The samples are then put at 20°C and stay for curing at 7, 14, 28 and 56 days. After curing, compression tests are performed to determine the force displacement curve and obtain both compression strength and rigidity.

3.   MATERIALS

3.1.   Main characteristics

The bentonite used is a calcium bentonite in order to avoid any excessive swelling upon wetting. Its swelling index is 7ml/2g, which is relatively low in comparison to the swelling index of sodium bentonite included between 20 and 30ml/2g. The main characteristics are reported in Table 1. The mineralogy of the bentonite is mainly montmorillonite. There is also muscovite and quartz and traces of kaolinite and calcite.
The used sand is called Mol Sand M32. Its specific density is 2.65 g/cm³. Its mineralogy is mainly quartz and orthoclase feldspath.

Table 1: Ca-Bentonite properties

Natural moisture content	10 ± 2 %
Specific density	2,65 g/cm³
Compacted dry density	0,80 ± 0,05 g/cm³
Methyl blue value	30 ± 3 g/100g
CEC	60 ± 10 meq/100g
pH	8,5 ± 0,5
Water absorption capacity	> 160 %
Swelling index	max. 8 ml/2g
Liquid limit (w_l)	115 %
Plastic limit (w_p)	33 %
Plasticity index (I_p)	82 %

3.2.   Particle sizes

The bentonite has 65% of fine particles (< 2µm), 28% silt (2µm < D < 67µm) and 7% sand (> 67µm). The sand is homometric with a D_{50} of 260µm. Figure 1 reports the grain size distribution curve of the two soils.
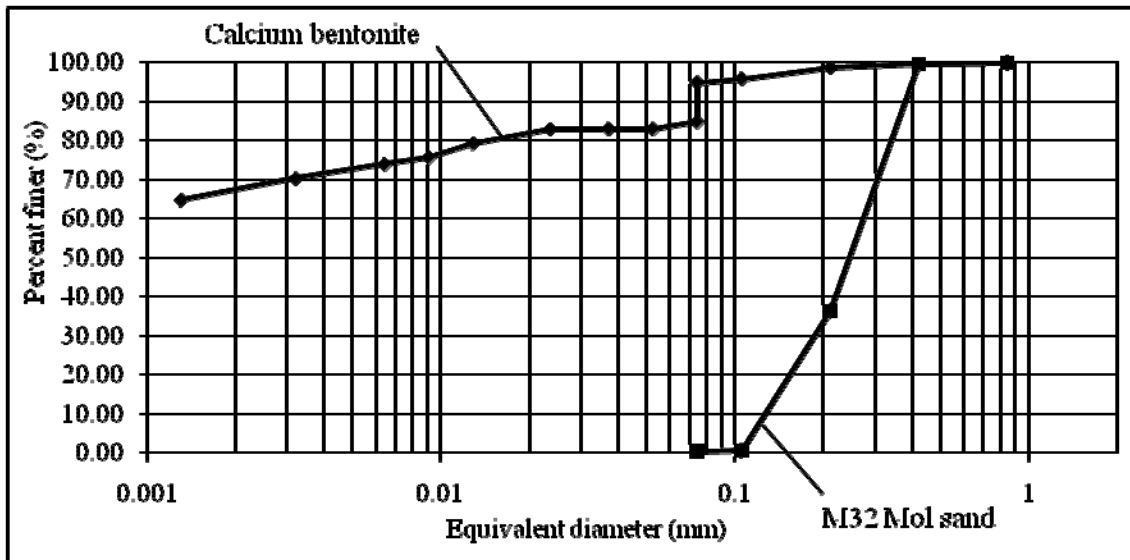
Figure 1: Particle size of the calcium bentonite and the Mol sand

4.   RESULTS

4.1.   Eades & Grim Procedure

Eades & Grim tests have been made on compositions between 30% and 100% of bentonite. On Figure 2, proportions are written as % of bentonite.
The relation between optimum lime content and bentonite proportion is linear (Fig. 3). A mixture with higher bentonite content demands more lime to be fully treated.
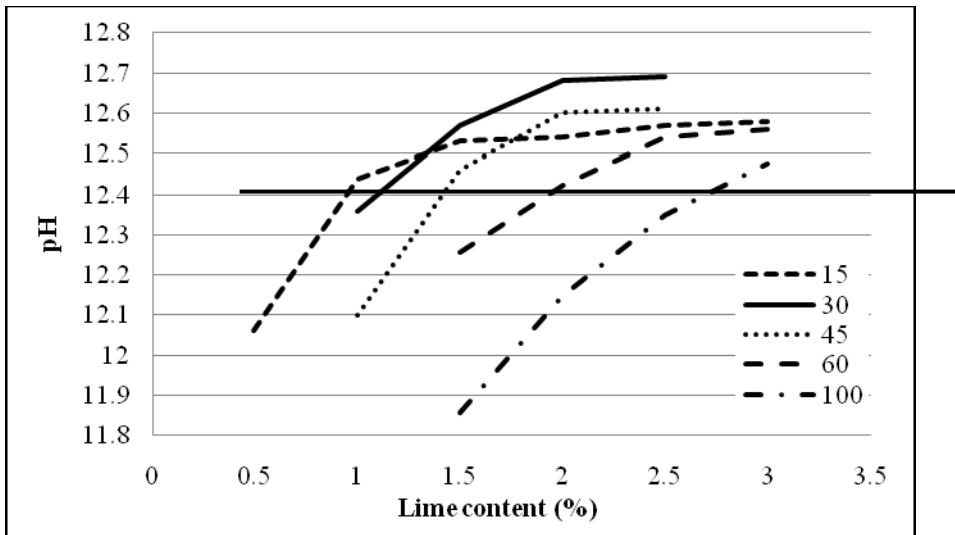
Figure 2: Eades & Grim tests on sand-bentonite mixtures (legend shows the bentonite percentage)
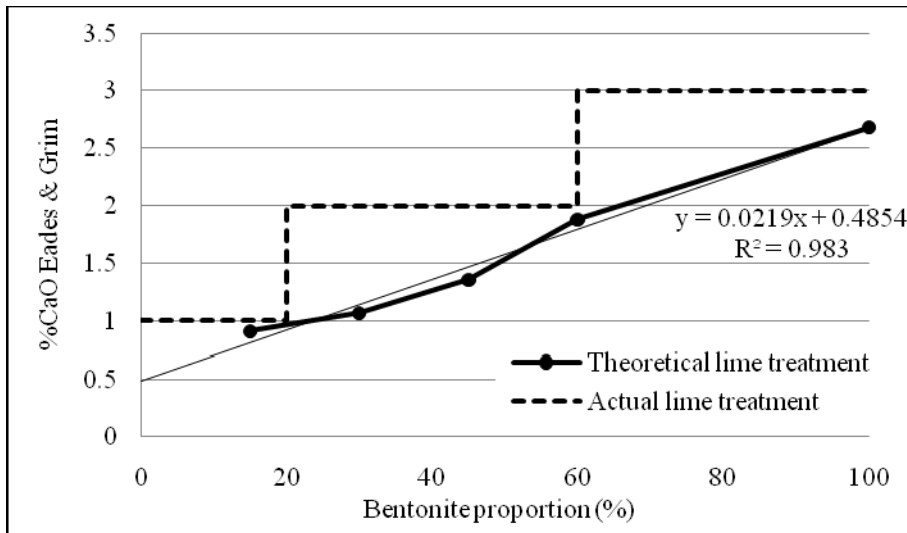
Figure 3: Relation between optimum lime content and bentonite proportion

Eades & Grim procedure shows (Figure 3) that mixtures between 5% and 20% bentonite can be treated with 1% lime, those between 30 and 60% with 2% lime, and the pure bentonite with 3% lime.
So doing, it allows having a small quantity of spare lime in addition to the lime that will theoretically react with clay.

4.2. Proctor Optima

Normal Proctor Compaction tests have been made on mixtures going from pure sand to pure bentonite. Results in Figure 4 shows that there exists a mixture with the highest Normal Proctor Optimum: the mixture with 10% bentonite. It reaches a density of 17.3 kN/m³.
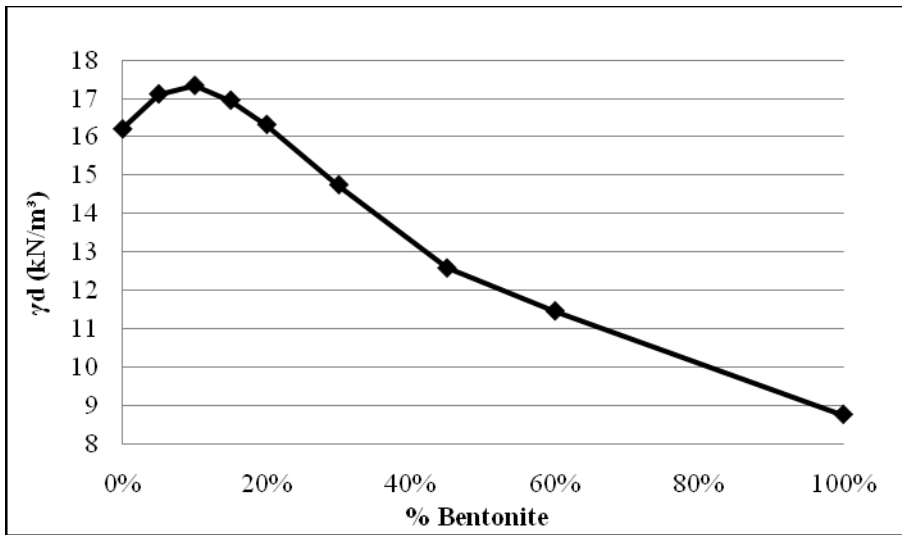
Figure 4: Normal Proctor Optimum of mixtures in function of their bentonite content

Dry density reached from Proctor compaction of pure sand is of course higher than in the case of pure bentonite. However, the addition of a small amount of bentonite in a pure sand enhances the obtained optimum dry density, because fine particles fill the macro voids between sand particles. However, if too much bentonite is added, clay starts to separate the sand particles from each other which progressively reduces the resulting dry density (cf. Figure 5).

For similar sand-bentonite mixtures, (Kenney et. al., 1992), (Sivapullaiah et. al., 1998) and (Ferber, 2005) obtained a maximum dry density at around 20% of bentonite. In our case, the optimal bentonite content seems a bit lower. It may be explained by the fact that the soil is treated. So the treated clay aggregates fill more rapidly the voids hence they are bigger.
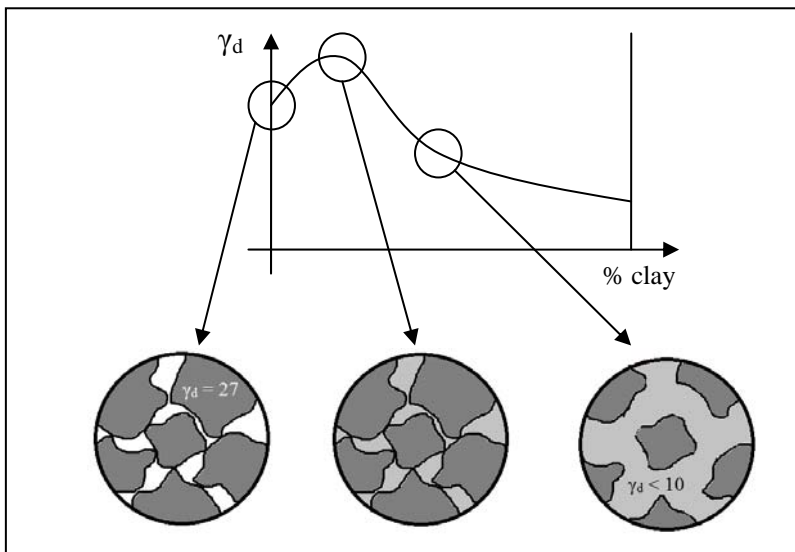
Figure 5: Distribution of clay aggregates between sand particles

Figure 6 shows that with bentonite content below 10%, the optimum water content stays the same (i.e. 15%), and above 10%, rises linearly.
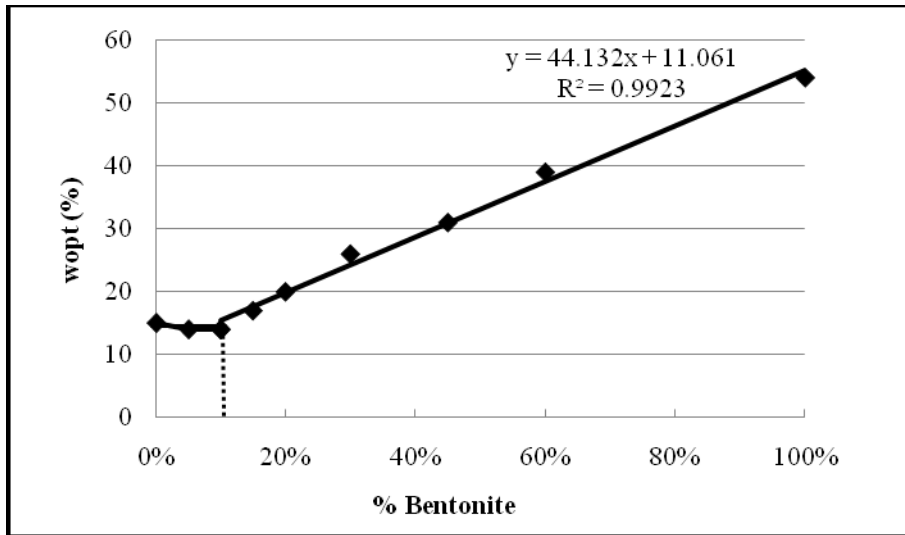
Figure 6: Optimum water content of mixtures in function of bentonite content

4.3. Unconfined compression tests

The unconfined compression strength (UCS) of sand-bentonite mixtures with 30%, 45%, and 60% of bentonite have been evaluated at different curing times: 0, 7, 14, 28, 56 days. All samples have been cured at 2% lime except the one at 0 day which is the mixture without treatment.

Figure 7 shows in function of the curing time, the compression resistance of the mixtures. The symbols show the exact value of each sample and the lines their mean value for each curing time. As already known, compression resistance increases with time. The mixture at 30% bentonite is more resistant than the others. After 56 days, its compression resistance is 350% higher, and its rigidity multiplied by 10.
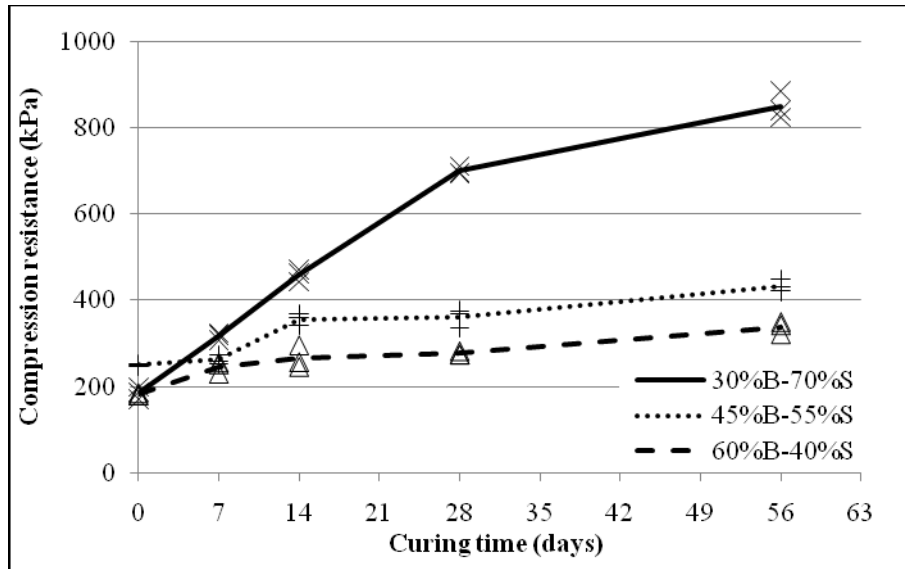
Figure 7: Compression resistance of the three mixtures in function of curing time

Figure 8 shows the rigidity of the mixtures in function of time. It has the same trend than figure 7. The more there is bentonite in the mixture the less rigid it is.

For the rigidity, it can be observed that there is a linear change of the curves in relation to the bentonite proportion. In the compression resistance graphs, it is different. The mixture at 30% bentonite is much higher than the other two.
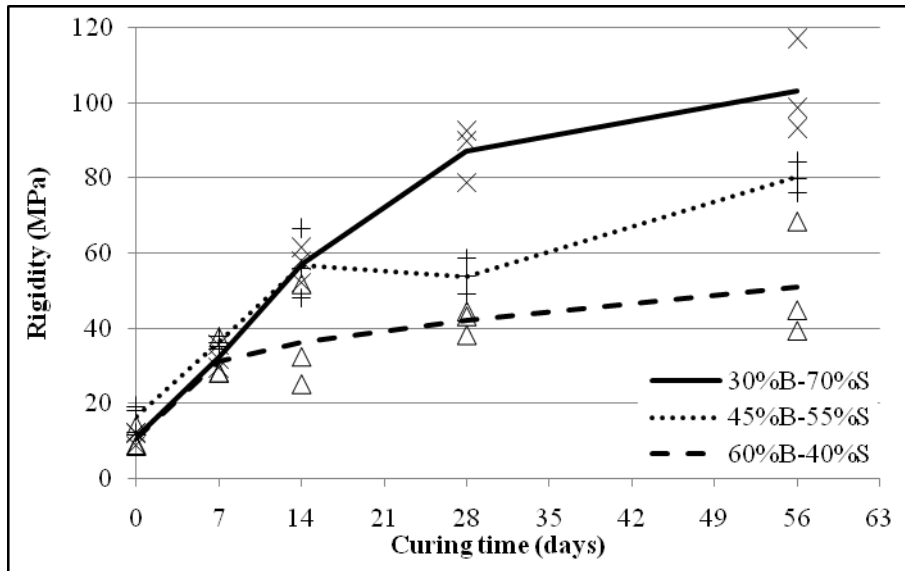
Figure 8: Rigidity of the three mixtures in function of curing time

The rigidity seems to follow a linear law in function of bentonite proportion as a weighted mean between pure treated bentonite and pure sand rigidities. On the other hand, the compression resistance does not follow a linear law. It may depend on the contact surface between sand particles and clay aggregates. In fact, there are three different types of rupture in these studied mixtures: the sand particle rupture, the clay aggregate rupture and the contact rupture between sand particles and clay aggregates. Considering the sand unbreakable, there are two possible rupture modes left. Figure 9 shows that all three compositions have approximately the same lime consumption in function of time. The total quantity of lime consumed after 56 days is practically of 1.2% mass for all compositions. Lime consumption is the same while clay content is different. Consequently, the proportion of bentonite that has already reacted with lime is higher for lower bentonite content. So, for high bentonite content mixtures, clay should not have reacted completely and clay aggregates have only reacted at their surface leaving a soft fragile core. The consequence is that the rupture mode should be inside the clay aggregates and not in the bonding between clay aggregates and sand particles.
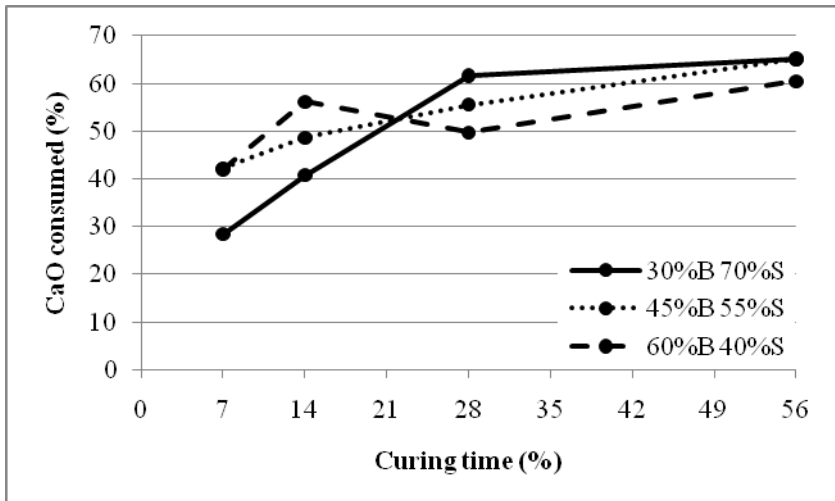
Figure 9: Lime consumption of the three mixtures in function of curing time

Further investigations are still being done for the moment to determine whether the clay aggregates break or the contact between those and the sand particles. Unconfined compression tests for lower bentonite contents are still under investigation for compositions between 5% and 20% bentonite where a maximum of Optimum Proctor density has been found.

5.   CONCLUSION

Sand takes an important part in the process of soil stabilization even if it does not directly react with lime. A soil having an important part of clay does not necessarily behave better than a more sandy soil when treated with lime. This interesting phenomenon gives us a reason to investigate further in detail the

interaction between lime treatment and sand. This paper shows that lime treated bentonite behaves like a binder between sand particles. For the moment only three compositions have been studied showing that the one with the lowest bentonite content is the most resistant and the most rigid. On the other hand, in the case of pure sand (0% bentonite), there is no compression resistance thus proving there is a maximum compression resistance for a composition between 0% and 30% of bentonite. This "optimal" composition may be related to the composition of highest Proctor density shown in this paper (i.e. 10% bentonite).

REFERENCES

Bell F.G., 1996, Lime stabilization of clay minerals and soils, Engineering Geology n°42, pp. 223-237.

Bollens Q., Verbrugge J.C, 2005., Time dependant evolution of the shear strength of a silty soil treated with lime, TREMTI 2005, Communication C008.

De Bel R., Gomes A.C., Verbrugge J.C., 2009, Contribution of loamy soil treatment to improve embankments performance, Geotechnical Special Publication n°189 ASCE pp. 186-191.

Eades J.L.,Grim R.E., 1966, A quick test to determine lime requirements for lime stabilization, Highway Research Record n°139 pp 61-72.

Eades J.L., 1962, Nichols F.P., Grim R.E., Formation of new minerals with lime stabilization as proven by field experiments in Virginia, Highway Research Board Bulletin n°335, pp. 31-39.

EIA, Energy Information Association, 2002, Emissions of Greenhouse Gases in the United States 2001, Diane Publishing.

Estéoule J., Perret P., 1979, Etude expérimentale des phénomènes de stabilization des sols fins par la chaux, Bull. Liaison Labo. P. et Ch. n°99, janv-févr, pp. 99-109.

Ferber V., 2005, Sensibilité des sols fins compactés à l'humidification : apport d'un modèle de microstructure, PhD pp. 283.

Keller W.D., 1964, Process of origin and alteration of clay mineral, Soil Clay Mineralogy, C.I. Rich, G.W.Kunze (ed.), University of North Carolina.

Kenney T.C., Van Veen W.A., Swallow M.A., Sungaila M.A., 1992, Hydraulic conductivity of compacted bentonite-sand mixtures, Canadian Geotechnical Journal 29-3, June 1992: 364-374.

Little D.N., 1995, Handbook for stabilization of pavement subgrades and base courses with lime, Kendall/Hunt Pub. Co. pp. 219.

Locat J., Bérubé M.A., Choquette M., 1990, Laboratory investigations on the lime stabilization of sensitive clays: shear strength development, Can. Geotech. J. 27, pp. 294-304.

Mahasenan N., Smith S., Humphreys K., 2003, The Cement Industry and Global Climate Change: Current and Potential Future Cement Industry CO2 Emissions, Greenhouse Gas Control Technologies - 6th International Conference, pp. 995-1000.

NRS, National Research Council (U.S.). Building Research Advisory Board, 1969, Chemical Soil Stabilization, National Academies, pp. 49.

Onitsuka K., Modmoltin C., Kouno M., Negami T., 2003, Effect of organic matter on lime and cement stabilized Ariake clays, J. Geotech. Eng. JSCE, N°729/III-62, pp. 1-13.

Sivapullaiah P.V., 1998, Sridharan, A., Stalin, V.K., Evaluation of bentonite and sand mixtures as liners, Environmental Geotechnics, Sêco e Pinto (ed.) 1998 Balkema, Rotterdam, volume 1, 17-21.

Recycled Bassanite in Conjunction with Coal Ash for Stabilization of Soft Clay Soil

Takeshi Kamei, University of Miyazaki, Japan, kamei@civil.miyazaki-u.ac.jp
Aly Ahmed, Beni-Suef University, Beni-Suef, Egypt, and Gunma University, Japan, alyahmed@geotech.ce.gunma-u.ac.jp
Toshihide Shibi, Shimane University, Japan, shibi@riko.shimane-u.ac.jp

ABSTRACT

The huge growth of waste materials in Japan is one of the most challenges nowadays. Therefore, most of attentions are directed to keep sound environment by using wastes as alternative materials in earthwork projects to reduce these quantities and cut down the cost of ground improvement. Gypsum wastes and coal ash are considered two examples of such wastes that contribute with negative effect on surrounding environment in terms of contamination and cost which spend in their disposing. So, this study focuses on the use of recycled Bassanite, which is produced from gypsum wastes, in conjunction with coal ash to improve the strength of very soft clay soil. For this purpose, recycled Bassanite is mixed with coal ash in different contents and this admixture used as a stabilizer agent to enhance the performance of tested soil. Bassanite-coal ash admixture is treated with a small content of cement to prevent the solubility of Bassanite, when it is subjected to wet environment, since the Bassanite is soluble material. Test results show that Bassanite-coal ash admixture has a significant effect on the strength improvement of tested soil by increasing the compressive strength. The strength increased with the increase of admixture content and curing time. The increase of Bassanite level in admixture content has a significant effect on the strength increase compared to coal ash level. The increase of admixture content increases the unit weight of stabilized soil and reduces the water content. The use of coal ash alone without the addition of recycled Bassanite for tested soil is not recommended to use since it has no positive effect on strength.

1. INTRODUCTION

Great research efforts have been done to study the use of different types of waste and recycled materials as alternative to cementation materials in soil stabilization for different types of soils. Examples of these waste and recycled materials include recycled Bassanite/gypsum, fly ash, cement kiln dust (CKD), blast furnace slag, incinerated sewage ash, stone dust, rice husk ash and industrial lime waste (Miller and Azad, 2000; Arora and Aydilek, 2005, Jha and Gill, 2006; Lin et al., 2007; Kamei et al., 2007; Khattab et al., 2008; Maslehuddin et al., 2008; Chen and Lin, 2009; Ahmed et al., 2009; Ugai and Ahmed, 2009; Ahmed et al., 2010; Ahmed et al., 2011a). Recycled Bassanite/gypsum, produced from gypsum waste plasterboard, has a potential to use as stabilizer material since gypsum is one of the common cementation materials used in construction industry. Application of recycled Bassanite, which is derived from gypsum waste materials, in soil stabilization was recently introduced in Japan by Kamei (2007). Therefore, literature about the use of recycled Bassanite/gypsum as a stabilizer material in ground improvement projects is limited. This section presents the available studies which focused on the use of recycled Bassanite/gypsum as a stabilizer material. Recycled Bassanite/gypsum was derived from gypsum waste plasterboard material by heating at a temperature ranged from 140 to 160 °C for a certain time. Four different contents of recycled Bassanite based on dry soil weight were used to enhance the strength of tested soils and investigate their influence on mechanical properties in terms of unit weight and moisture content. The recycled Bassanite was mixed with two different soil types, sand and clay, to investigate the effect of the soil type on the performance of the Bassanite stabilized soil. Results showed that the addition of recycled Bassanite had a significant effect on increasing the strength and mechanical properties of tested soils. Recycled Bassanite had a significant effect on increasing the strength in case of sandy soils compared to clayey soils. Increasing the Bassanite content in the soil mixture significantly increases the dry unit weight and decreases the water content (Kamei et al., 2007). Ahmed (2011a; 2010) conducted a series of mechanical tests included unconfined compression, splitting tensile and capillary rise on silty sand soil stabilized with recycled Bassanite to investigate the performance of cohesion less soil stabilized with recycled Bassanite. Results indicated that strength enhanced by the addition of recycled Bassanite. The increase of recycled Bassanite content had a significant effect on the enhancement of the compressive strength compared to tensile strength. Capillary rise time increased with the increase of Bassanite content and curing time (Ahmed et al., 2010; Ahmed et al., 2011a). Another study investigated the durability of cohesion less soil stabilized with recycled Bassanite against the actions of wetting-drying and freezing-

thawing cycles. In this study four different contents of recycled Bassanite and furnace cement were used as a stabilizer material to improve the strength and durability of silty sand soil. The 7-days cured samples were subjected to different numbers of wetting-drying and freezing-thawing cycles before testing for unconfined compression, volume change and soil loss. Results indicated that soil stabilized only with recycled Bassanite and without treatment of cement is not survive against the actions of both freezing-thawing and wetting-drying cycles since Bassanite is a soluble material. The addition of small content of furnace cement was found enough to improve the durability and strength against the actions of freezing-thawing and wetting-drying cycles. Freezing-thawing cycles had a negative effect on the durability of Bassanite stabilized specimens compared to the effect of wetting-drying cycles. The actions of both freezing-thawing and wetting-drying cycles had no significant effect on volume change. The increase of Bassanite content had a significant effect on the enhancement of durability and strength against the actions of weathering conditions (Ahmed and Ugai, 2011). Mechanical and environmental properties of clayey soil stabilized with recycled Bassanite were investigated through laboratory and site investigations. In this study, recycled Bassanite was mixed with two different types of cement Portland and furnace slag type B in dry state and then mixed with soft clay soil. Results indicated that Bassanite treated with cement had a positive effect on strength improvement as well as mechanical and environmental properties of tested soil. The investigated contents of Bassanite used in this case did not show any adverse effect on the environment in terms of hydrogen sulfide emission or the release of Fluorine, hexilvanent chromium and Boron (Ahmed at al., 2011b). To sum up, recycled Bassanite, produced from gypsum waste plasterboard, has a potential to be used as a stabilizer material in soil stabilization because it has a cementation property which develops enough hardening between soil particles and then the strength improves.

It is well known that coal ash has a great history of use in the area of soil stabilization especially for stabilization of clayey soils since it has self-cementing property and pozzolanic reactions. The coal ash was added to the stabilized cement/lime soils since it promotes the activity of pozzolanic reactions between cementation materials and soil, subsequent the strength improved. The performance of using coal ash in road construction and soil stabilization were investigated by Rifai (2009). In this study, a series of tests includes XRD, swelling, California bearing ratio, atterberg limits and leaching of heavy metals were conducted to investigate the impact of adding the coal ash on the physical, mechanical and environmental properties of coal ash-soil mixture. Results indicated that the addition of coal ash improved the index properties of soft clay soil, increased the bearing capacity and decreased the swelling potential. Environmental results indicated that the heavy metal levels measured in stabilized soil coal ash were within the permitted limits (Rifai et al., 2009). The coal fly ash type F was used as a stabilizer to strength the characteristics of peat or highly organic soils. Four different contents of coal ash class F ranged from 5 to 20% were mixed with tested soil based on dry soil weight. Results indicated that the increase of the ash content increased the dry density, decreased the moisture content, and improved the compressive strength. These results proved that coal ash had a potential to be used as a stabilizer material for tropical peat soil (Kolay et al., 2011). Another study investigated the geotechnical properties of fly ash included atterberg limits, specific gravity, compaction characteristics and compressive strength as well as its application for stabilization of soft clay soil was conducted by Geliga and Ismail (2010). They used different proportions of fly ash and soft clay soil sample. Results of this study indicated that the increase of fly ash content more than 80% in soil-fly ash mixture had no positive effect on strength improvement while the highest improved strength was obtained with 60% of fly ash content. The use of fly ash alone was not recommended since the strength of fly ash samples is not strong. The optimal range of fly ash in soil-fly ash mixture was found between 50 to 60% (Geliga and Ismail, 2010). Thus, fly ash has a potential to be used as a stabilizer and solidified agent for soil stabilized with recycled Bassanite since it has self-cementing and pozzolanic activity.

The main objective of this study is to explore the use of recycled Bassanite, produced from gypsum waste plasterboard, in conjunction with coal ash to enhance the strength, performance and mechanical properties of very soft clay soil. The specific objective of this study is to investigate the use of coal ash as a stabilization agent for soil stabilized with Bassanite to reduce the amount of cement which is needed to prevent the solubility of Bassanite when water is introduced. Furthermore, to investigate the performance and strength of soil stabilized with Bassanite when coal ash is added.

2. MATERIALS AND TESTING

Four different materials used in this study are very soft clay soil, recycled Bassanite, coal ash and furnace slag cement type-B. The tested soil used is artificial clay soil named in market as MC clay and it was brought from an industrial clay company in Japan. Physical properties and chemical components of tested soil were determined based on laboratory tests and presented in Tables 1 and 2, respectively. The tested

soil can be classified as clay with high plasticity according to unified soil classification system, USCS. To achieve the soft state for the tested soil, the oven-dry soil was mixed with water with a content of 140% based on dry soil weight for a certain time, subsequently it became in a very soft state. The selection of water content 140% for tested soil is related to the natural very soft clay soils spread in some locations in Japan have approximately the same water content based on several records (Nakase and Kamei, 1984).

Table 1: Physical properties of tested soil

Property	Density (Mg/m^3)	Liquid limit, %	Plastic Limit, %	Plasticity Index	Compositions, (%)		
					Sand	Silt	Clay
Value	2.68	73.10	36.70	36.40	0.00	35.30	64.70

Table 2: Chemical compsoitions of tested soil

Element	SiO$_2$	Al$_2$O$_3$	Fe$_2$O$_3$	TiO$_2$	CaO	MgO	K$_2$O	Na$_2$O
(%)	68.10	24.80	0.14	0.15	0.02	0.02	1.54	0.56

Recycled Bassanite/gypsum used in this study was produced from gypsum waste plasterboard and the production process was presented in details in previous works (Ahmed et al., 2011a; Ahmed et al., 2010; Kamei et al., 2007). In brief, the air dried gypsum waste plasterboards were crushed and then screened to remove any undesired materials such as paper, wood, fibers, paints and stones. The crushed gypsum wastes were heated under temperature of 140-160 °C for a certain time to remove the three molecules of water, from its chemical composition, and then recycled Bassanite/gypsum was produced, which is hemi hydrae calcium sulphate, $CaSO_4.1/2H_2O$. Four different contents of Bassanite-soil ratio (B/S) of 0, 5, 10 and 20% were used to study the influence of recycled Bassanite content on strength, performance and mechanical properties of tested soil.

Coal ash used in this study was brought from Energia Eco Material Co., LTD in Japan. Originally the used coal ash was produced from electrical power plant in south of Japan. In fact fly ash characteristics are different from site to another because it depends on the type of fuel/coal used and the additives used during the combustion process. There are two types of fly ash namely C and F. Type C is derived from sub-bituminous coals and consists primarily of calcium alumina-sulphate glass, tri calcium aluminates and free lime. Type C is also referred to as high calcium fly ash since it has 20 to 30% calcium compounds, consequently type C has a self-cementing property (Scott et al., 2005; Rafai et al., 2010). Type F is derived from bituminous and anthracite coals and it consists basically of alumina-silicate glass, with quartiz mullite and magnetite (Rafai et al., 2010). Mineral composition of coal ash is identified using x-ray diffraction method and presented in Table 3 while physical properties of coal ash is presented in Table 3. Table 3 shows that the used coal ash contains amounts of SiO2, Al2O3, and Fe2O3 with a content of 93.53%, LOI is 2.2%, respectively and the retained on sieve#325 equals 18.9%. According to ASTM C 618-78, the used coal ash is categorized as class F since the amount of (SiO2 + Al2O3 + Fe2O3) more than 70%, LOI is less than 6% and the retained on sieve#325 is less than 34%. Subsequently the coal ash class F cannot be used alone for solidification of soil-Bassanite mixture since it has no self-cementing property compared to fly ash class C and that is why small amount of cement is introduced. Three different contents of fly ash-soil ratio (A/S) of 0, 10 and 20% were used to investigate the effect of additives coal ash on the performance of soil stabilized with recycled Bassanite.

Table 3: Physical properties and compositions of used coal ash

Property	Physical Properties			Compositions, (%)		
	Dry density, (Mg/m^3)	Retained on Sieve#325, (%)	LOI (%)	Sand	Silt	Clay
Value	2.17	18.90	2.20	6.90	71.10	22.00

Table 4: Chemical compositions of used coal ash

Element	SiO$_2$	Al$_2$O$_3$	Fe$_2$O$_3$	SO$_3$	CaO	MgO	K$_2$O	Na$_2$O
(%)	66.90	22.40	4.28	0.29	1.96	1.16	0.86	0.39

Furnace slag cement type-B is used in this research with a content of 5% and it is labelled as cement soil ratio herin, (C/S). In fact the main reason for using cement is to solidify the stabilized soil-Bassanite mixture since Bassanite is soluble material. Furnace cement Type-B is produced from waste materials and by-product Portland cement and it has 30 to 60% furnace slag in its composition.

Cylindrical soil specimens with a 50-mm diameter and 100-mm height were modeled by using cylindrical steel moulds having internal dimensions of 50 mm in diameter and 100 mm in height. To prevent any friction between soil mixture and the internal sides of the mould, oil was used to lubricate the inner sides before sample placing. The investigated contents of recycled Bassanite, coal ash and cement were mixed in dry state and then mixed with the tested soil. The mixing process was conducted by using automatic mixer and prolonged for a certain time to ensure that the mixture is uniform. The mixture was placed in the mould in three layers and pressed with steel rod and then subjected to a specific number of blows using plastic hummer for each layer to prevent the formation of air bobbles in soil mass. The stabilized soil samples were extracted from the mould after 24 hours and then subjected to different curing times of 1, 3, 7 and 28 days at room temperature of (21 ± 1 °C). More attention was considered during sample preparation and extraction to produce homogenous samples. It is important to report that each cylinder has the same volume and then the density of stabilized soil was determined since the weight of soil mixture is known. To achieve more accuracy for results, three specimens were used for each test and the average result was used to plot the curves.

The effects of recycled Bassanite and coal ash on soil properties and strength improvement were evaluated using the unconfined compression test. It is attributed to compressive strength is considered one of the most important parameters in earthwork design as well as evaluation the performance of soil stabilization. The unconfined compressive test was conducted in accordance ASTM D 2166-66. The load was applied to the tested sample with a displacement rate of 1mm/min and the loading process continued till the occurrence of failure or the strain reached to more than 5%.

3.   RESULTS AND ANALYSIS

The effects of addition coal ash and recycled Bassanite on ultimate unconfined compression strength for tested soils are presented in Figures 1 to 3. Ultimate strengths were derived from stress-strain relationships while these relations not presented herein as result the increase the number of curves. From these figures and based on stress-strain relationships, the addition of recycled Bassanite and coal ash in most cases improved the compressive strength. Generally, when clay soil mixed with such cementation and pozzoalnic materials there are some chemical reaction takes place between them, which provided the strength improve. However, still there are some factors controlling the activity of such chemical reaction, which provide strength improve, such as moisture content, stabilizer content, type of tested soil and stabilizer, curing condition, weathering condition and time. Furthermore, the strength improve is not only due to the induced chemical reaction between clay and stabilizers but also there are some factors control the strength improve. For example, the tested soil in this study has high moisture content of 140% and then the strength improve, especially in the early time, is mainly depends on the potential of stabilizer for absorption of water. Results presented in Figures 1 to 3 indicated that the improvement in strength increased with the increase of Bassanite-soil ratio. The permanent improvement in strength is mainly related to the formation of ettringite, which is responsible for the development of hardening between soil particles as presented in Figure 4. This figure shows the formation of ettringite based on SEM images which taken after 28 days of curing for different investigated cases. The images indicate that the quantity and size of ettringite improved with the increase of Bassanite-soil ratio. Besides to the role of ettringite on strength improve, there are other factors promote the strength improve. Firstly, the desire of recycled Bassanite to absorb the water from moist soil to recover the three molecules of water that were missed during manufacturing process. Subsequently, when water absorbed from the moist soil, the strength increased since the number of voids in soil matrix reduced. Secondly, when Bassanite mixed with moist soil dissolves fairly and breaks down to calcium (Ca^{++}) and sulphate (SO_4^{--}) ions that called dissociation process (Ahmed et al., 2011a). Calcium has two positive charges attracts the clay particles, which have negative charges and flocculation for clay particles is occurred. It is well known that flocculation for clay particles enhanced the strength by increasing the links between soil particles. The improvement in strength is not only due to the additives of recycled Bassanite while the additive of coal ash has also a significant effect on strength improve as presented in previous Figures. The SEM results proved that the additive of coal ash improved the formation of ettringite as presented in Figure 5. These images indicate that the increase of coal ash-soil ratio increased the quantity and size of ettringite formation since coal ash is pozzolanic material. It has been known that coal ash has a highly reactive pozzolanic, which helps to develop the ettringite early compared to samples that stabilized without coal ash (Reeves et al., 2006).
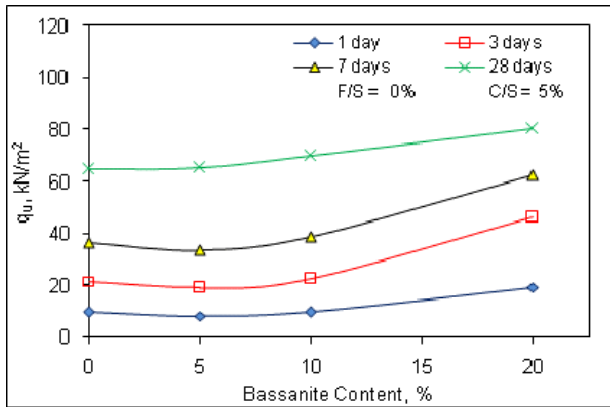
Figure 1: Effect of Bassanite content on ultimate strength at different curing times and Coal ash content 0.00%
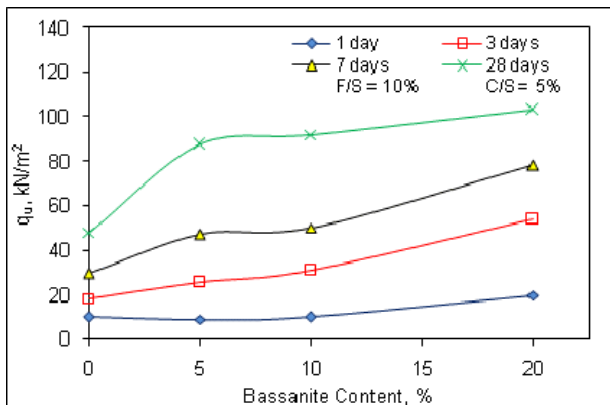
Figure 2: Effect of Bassanite content on ultimate strength at different curing times and Coal ash content 10.00%
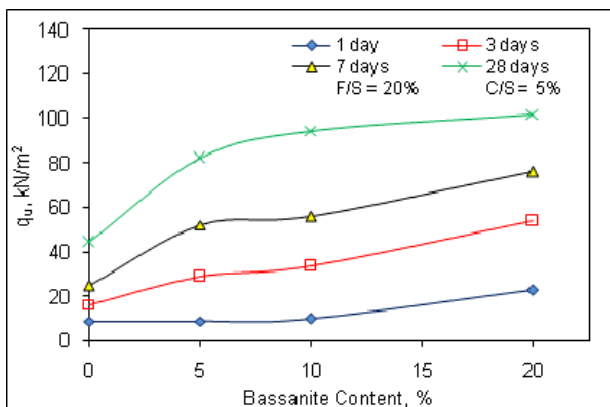
Figure 3: Effect of Bassanite content on ultimate strength at different curing times and Coal ash content 20.00%

The increase of Bassanite-soil ratio is associated with the increase of ultimate compressive strength as presented in Figures 1 to 3 for different curing periods investigated. Figure 1 indicates that the effect of Bassanite-soil ratio on strength increase is not significant up to Bassanite content of 10% and afterward the strength increased with the increase of Bassanite-soil ratio content. It is attributed to the amount of Bassanite used in the soil mixture is not enough to develop hardening between soil particles and also coal ash is not used in this case. While the increase of Bassanite-soil ratio more than 10% results in more water absorption from the tested soil and consequently the strength increased with the increase of Bassanite-soil ratio content. Figurers 2 and 3 show that the effect of Bassanite-soil ratio in case of additives coal ash is much pronounced in the later curing times compared to the early curing times. It is attributed to the presence of coal ash promotes the chemical reaction between soil particles and Bassanite to develop the ettringite since coal ash has a pozzolonic activity. This reaction may be needed more time

to complete since the water content of tested soil is high. Subsequently, the permanent improvement in strength is noticeable in the later curing time compared to the early curing time especially in case of small content of Bassanite used. The increase of strength due to the increase of Bassanite-soil ratio is attributed to the increase of Bassanite proportion in soil mixture. Subsequently, the possibility of absorbing more water from the moist soil is increased since the surface area of Bassanite increased due to the increase of Bassanite proportion in soil mixture.
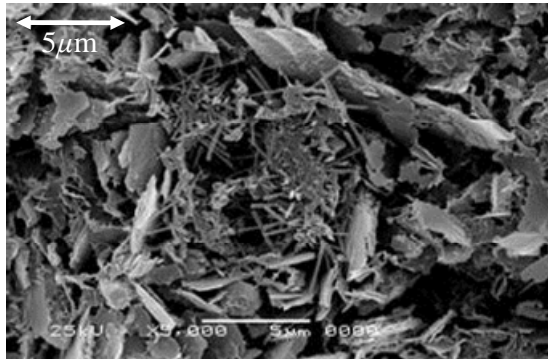
4a) In case of Bassanite content = 0.00%
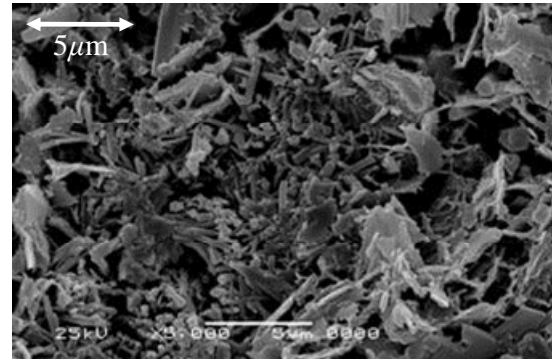
5a) In case of coal ash ratio = 0.00%
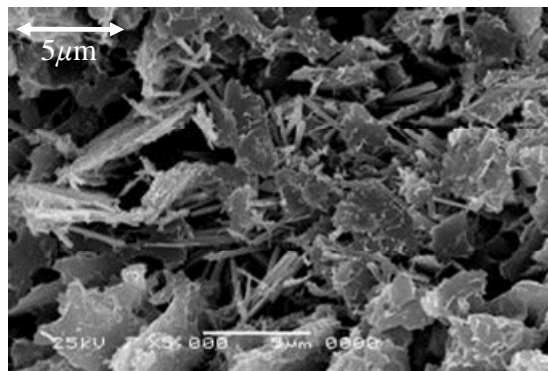
4.b) In case of Bassanite content = 10.00%
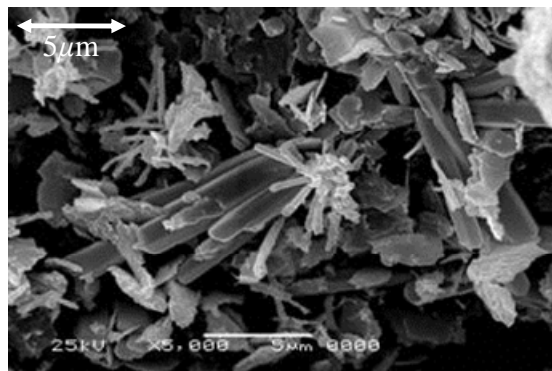
5.b) In case of coal ash ratio = 10.00%
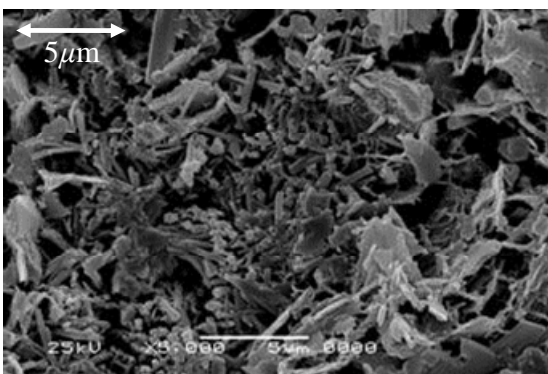
4c) In case of Bassanite content = 20.00%
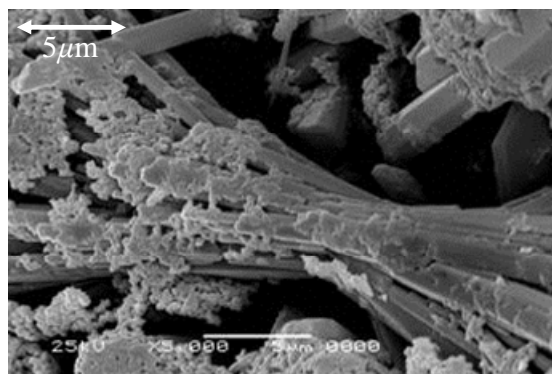
5c) In case of coal ash ratio = 20.00%

Figure 4: SEM images for soil stabilized with different contents ofBassanite and no coal ash

Figure 5: SEM images for soil stabilized with different contents of coal ash and 20% Bassanite

The effect of curing time on soil stabilized with recycled Bassanite and coal ash are presented in Figure 6. This Figure indicates that the increase of curing time is associated with the increase of strength for all the investigated samples. This result meets the concept of curing time affect on the behavior of stabilized cement soil. From Figure 6, the strength increased rapidly from curing times 1 to 7 and then the strength increased smoothly. It can be concluded that the effect of curing days in strength increase is much pronounced in the early curing days compared to the later curing days and this results are in agreement

with the results presented in previous work done by Ahmed et al. (2011a). It is attributed to the fact that Bassanite has early setting time compared to cement, thus samples stabilized with recycled Bassanite has early strength. In fact it is a very important property to reduce the construction time and open the site for compaction process directly after mixing process, especially when the tested soil has high water content as in this case. Figure 6 shows that the effect of Bassanite-soil ratio on strength improvement is clearer with the increase of coal ash-soil ratio. It is attributed to the presence of coal ash in stabilized sample promotes the formation of ettringite and then the effect of Bassanite-soil ratio is clearer compared to the identical untreated samples with coal ash. Thus, this experiment shows the role of using coal ash as a stabilizing agent to promote the activity of recycled Bassanite in soil improvement projects.

The effect of Bassanite-soil and coal ash-soil ratios on water content and dry unit weight is presented in Figures 7 and 8, respectively. From Figure 7, the increase of Bassanite-soil ratio is associated with water content decrease and dry unit weight increase. This result is in agreement with the results presented in previous works that investigated the effect of additives only Bassanite for silty sand soil on moisture content and dry unit weight relationship carried out by Ahmed et al. (2010) and Ahmed et al. (2011a). The decrease of moisture content is related to the tendency of Bassanite to absorb the water from the moist soil as presented previously and consequently water content decreased. In fact decreasing the water content in stabilized soil results in increasing the dry unit weight since the relation between them is indirect. The decrease in water content results in the decrease in the number of voids in the soil matrix for the same soil weight and consequently increase in the dry unit weight. In addition, the effect of additives of coal ash has a slightly effect on water content decrease and dry unit weight increase for the tested soil compared to the effect of the Bassanite. It is attributed to Bassanite has more potential to absorb water compared to coal ash. Subsequently, the effect of additives coal ash on dry unit weight increase is small since coal ash has a slightly effect on water content decrease.
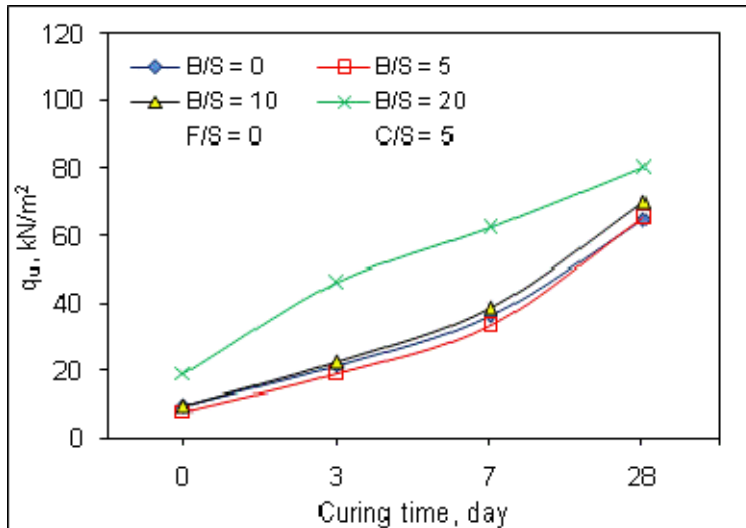
6a) In case of coal ash ratio (F/S) = 0.00%
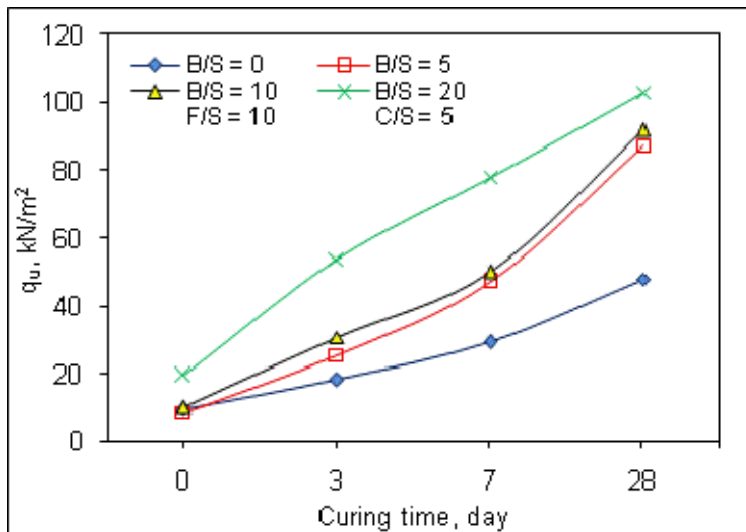
6b) In case of coal ash ratio (F/S) = 10.00%
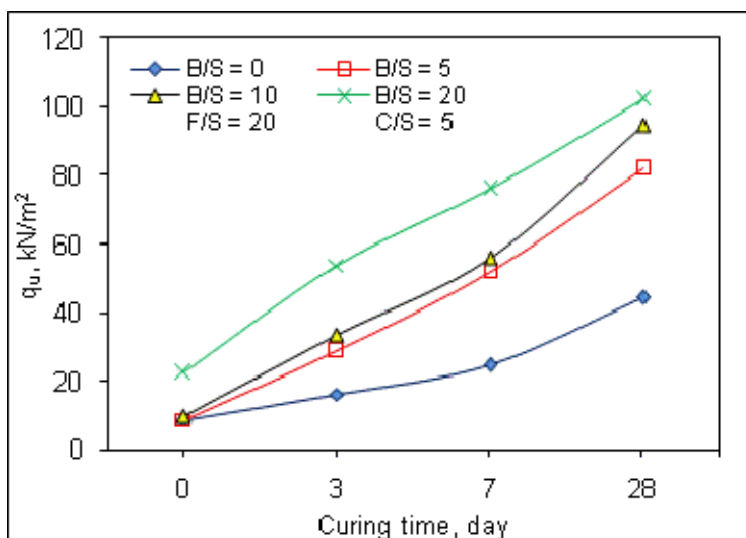
6c) In case of coal ash ratio (F/S) = 20.00%

Figure 6: Effect of curing time on ultimate strength for samples stabilied with different Bassanite and coal ash content
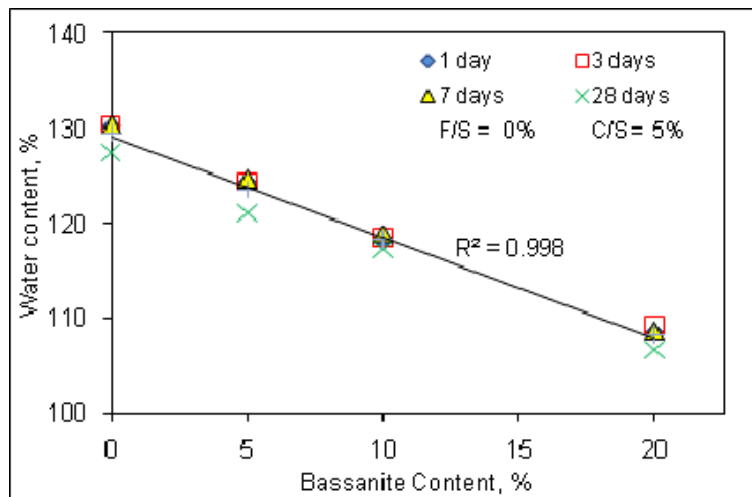
7.a) In case of coal ash ratio (F/S) = 0.00%
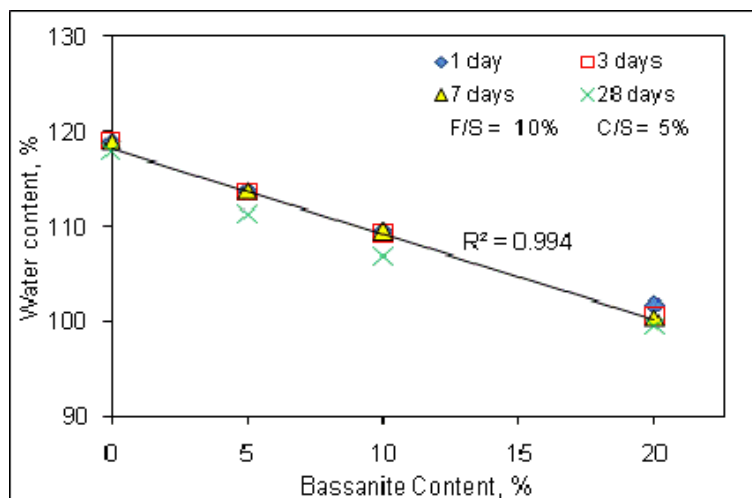
7b) In case of coal ash ratio (F/S) = 10.00%
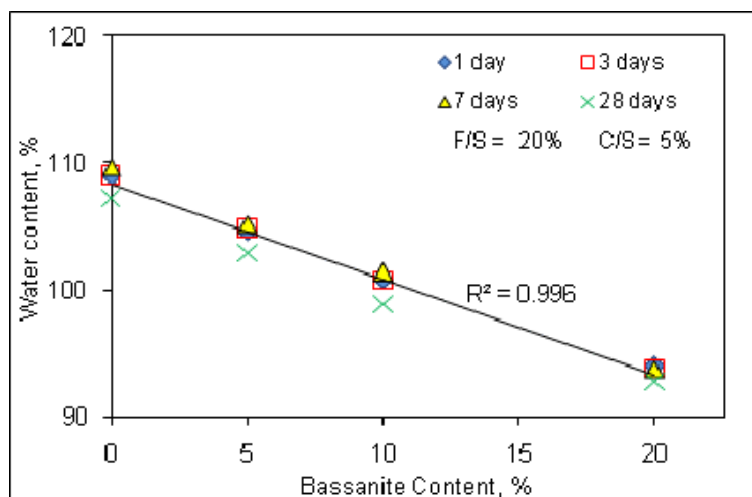
7c) In case of coal ash ratio (F/S) = 20.00%

Figure 7: Effect of Bassanite and coal ash contents on water content for stabilized soil specimens
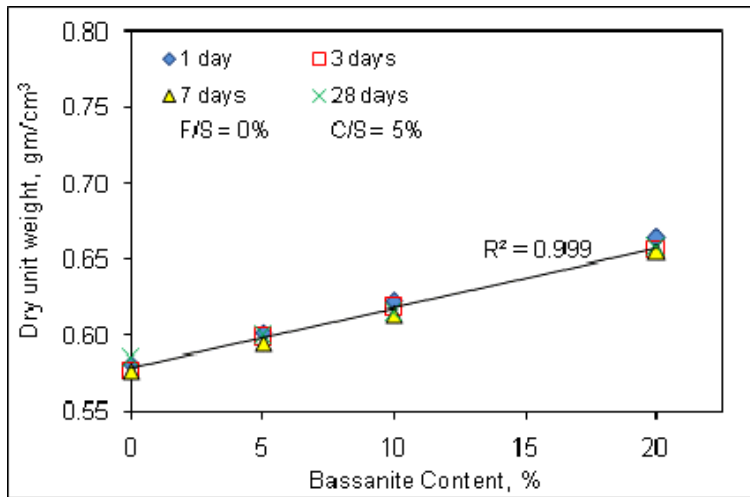
8a) In case of coal ash ratio (F/S) = 0.00%
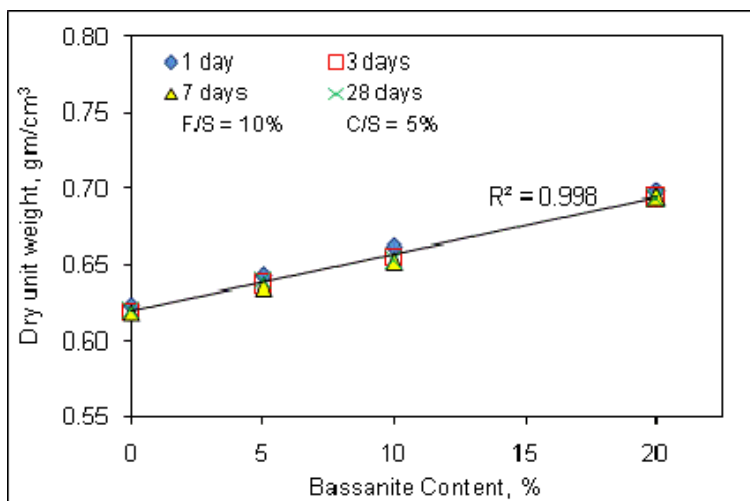
8b) In case of coal ash ratio (F/S) = 10.00%
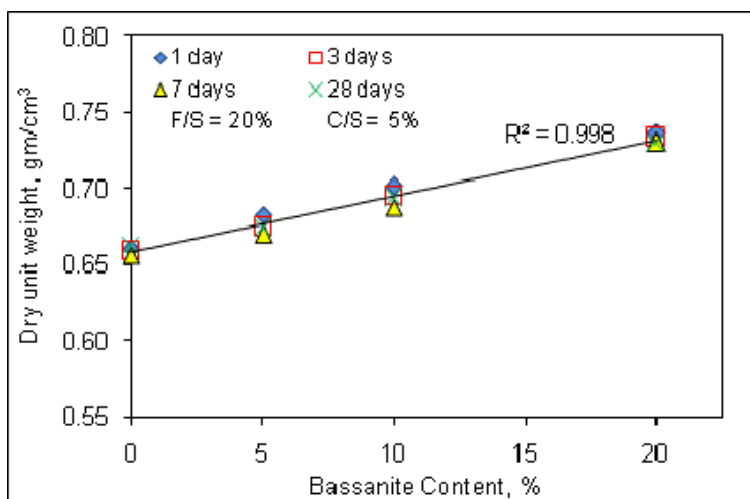
8c) In case of coal ash ratio (F/S) = 20.00%

Figure 8: Effect of Bassanite and coal ash contents on on dry unit weight for stabilized soil specimens

4.   CONCLUSIONS

Based on the test results, the following conclusions can be drawn:
1. Recycled Bassanite and coal ash have a positive effect on the strength improvement of very soft clay soil. The strength enhanced with the increase of Bassanite-soil and coal ash-soil ratios in soil mixture.
2. Increasing the contents of Bassanite and coal ash in soil mixture have a significant effect on water content decrease and dry unit weight increase.
3. The addition of coal ash without Bassanite has a slightly negative effect on the strength increase because the used coal ash has not self-cementing property.
4. Increasing the content of coal ash has a significant effect on the formation of ettringite compared to Bassanite. The formation of ettringite increased with the increase of both Bassanite and coal ash contents in soil mixture.
5. The effect of curing time on strength improve in the early times is much pronounced compared to that effect of the later curing time.

5.   ACKNOWLEDGMENTS

REFERENCES

Ahmed A. and Ugai K., (2011), "Environmental effects on durability of soil stabilized with recycled gypsum". Journal of Cold Regions Science and Technology, 66(2-3): 84-92.

Ahmed A., Shehata M. and Easa S, (2009), "Use of factory-waste shingles and cement kiln dust to enhance the performance of soil used in road works". Advances in Civil Engineering Journal, 9 pages, Article ID 143750, 2009: doi:10.1155/2009/143750.

Ahmed A., Ugai, K., Kamei T, (2011a), "Investigation of recycled gypsum in conjunction with waste plastic trays for ground improvement". Journal of Const. and Building Materials, 25(1): 208-217.

Ahmed A., Ugai K., Kamei T., (2011b), "Environmental Evaluation for Clayey Soil Stabilized with Gypsum Waste Plasterboard in Japan". In the Proceeding of the International GeoHunan 2011 Conference, June 9-11, Hunan, China, Geotechnical Special Publication, ASCE, 217(2011): 9-17.

Ahmed A., Ugai K. and Kamei T., (2010), "Application of gypsum waste plasterboard and waste plastic trays to enhance the performance of sandy soil". In the Proceedings of Geo-Shanghai 2010, Ground Improvement and Geosynthetics, GSP, ASCE, 207(2010): 165-173.

Arora S. and Aydilek A.H. (2005), "Class F fly ash-amended soils as highway base materials." Journal of Materials in Civil Engineering, ASCE, 17(6): 640-649.

Chen L. and Lin D. F, (2009), "Stabilization treatment of soft subgrade soil by sewage sludge ash and cement". Journal of Hazardous Materials, 162 (2009): 321–327

Geliga E.A. and Ismail D.S.A, (2010), "Geotechnical properties of fly ash and its application on soft soil stabilization." UNIMAS E-Journal of Civil Engineering, 1(2): 1-6.

Jha J.N. and Gill K.S., (2006), "Effect of rice husk ash on lime stabilization." Journal of the Institution of Engineers (India), 87(2006): 33-39.

Kamei T., Kato T. and Shuku T., (2007), "Effective use for bassanite as soil improvement materials - Recycling of waste plasterboard-". Geotechnical Society Electronic Journal, 2(3): 245-252 (In Japanese)

Khattab S.A.A., Al-Juari K.A.K. and Al-Kiki I.M.A., (2008), "Strength, durability and hydraulic properties of clay soil stabilized with lime and industrial waste lime". Al-Rafidain Engineering Journal, 16(1): 102-116.

Kolay P.K., Sii H. Y. and Taib S.N.L. (2001), "Tropical peat soil stabilization using Class F pond ash from coal fired power plant." World Academy of Science, Engineering and Technology Journal, 74 (2011): 15-19.

Kunitomo, H., (2009), "Recycling of coal ash: current activities and challenges for the future". In the Proceedings of Symposium on effective use of coal ash in 2009, 23p (In Japanese).

Lin D. F., Lin K. L., Hung M. J., Luo H. L., (2007), "Sludge ash/hydrated lime on the geotechnical properties of soft soil". Journal of Hazardous Materials, 45(2007): 58–64.

Maslehuddin M., Al-Amoudi O.S.B, Shameem M., Rehman M.K. and Ibrahim M., (2008), "Usage of cement kiln dust in cement products – Research review and preliminary investigations". Journal of Construction and Building Materials, 22 (2008): 2369–2375.

Miller G.A. and Azad S., (2000), "Influence of soil type on stabilization with cement kiln dust." Journal of Construction and Building Materials, 14(2000): 89-97

Nakase A. and Kamei T., (1984), "In situ void ratio, strength and overburden pressure anomalies in seabed clays, Seabed Mechanics". International Union of Theoretical and applied Mechanic, (1984): 9-14.

Reeves G.M., Sims I. and Cripps J.C. (eds)., (2006), "Clay Materials Used in Construction". Geological Society, London, Engineering Geology Special Publication, (21): 525pp.

Rifai A., Yasufuku N., and Tsuji K., (2009), "Characterization and effective utilization of coal as soil stabilization on road construction". Ground Improvement Technologies and Case Histories, Geotechnical Society of Singapore (GeoSS) 2009: doi:10.3850/GI025, (2009): 469-474.

Scott M. Mackiewicz and E. Glen Freguso, (2005), "Stabilization of soil with self-cementing coal ashes." In the proceedings of 2005 World of Coal Ash (WOCA), April 11-15, 2005, Lexington, Kentucky, USA, 7P.

Ugai K. and Ahmed A., (2009), "Evaluation of using gypsum waste plasterboard in ground improvement". In Proceeding of the Workshop on Recycling Waste Plasterboard, March 13, 2009, Memorial Hall, Chuo University, Tokyo, Japan

Influence of specimen preparation on unconfined compressive strength of cement-stabilized Kaolin clay

Masaki Kitazume, Tokyo Institute of Technology, Japan, kitazume@cv.titech.ac.jp

ABSTRACT

The Deep Mixing Method, a ground modification technique that improves the mechanical and physical properties of the ground, is often used in many applications such as increasing bearing capacity, liquefaction mitigation and remediation of contaminated ground. Laboratory mix tests are essential to quality assurance and quality control of deep mixing methods. With the increasingly globalizing DMM market in the background, it is desired to establish common understanding of the nature of laboratory mix tests and internationally accepted guidelines to conduct them, in order to guarantee the quality of DMMs. The procedures used for the preparation of stabilized specimens in the laboratory greatly affect the properties of the stabilized soils. The influence of different moulding techniques for the preparation of specimens has been studied. The tests were carried out on Kaolin clay stabilized with ordinary Portland cement. Several mixtures with different consistency and several moulding techniques, namely Tapping, Rodding, Dynamic Compaction and Static Compaction were used. The results show the influence of moulding techniques on the unconfined compressive strength (UCS) and wet density of the stabilized specimens.

1.   INTRODUCTION

The Deep Mixing Method is a ground modification technique that improves the mechanical and physical properties of soils with the introduction and mechanical mixing of a binder with the soil. Laboratory testing of stabilized soils is extensively used in the Quality Assurance/Quality Control processes in deep mixing projects (Åhnberg & Holm, 2009). In Japan, the procedure of laboratory mix test has been standardized and applied to many construction works (Japanese Geotechnical Society, 2009). The paper focuses on a practical aspect of laboratory mix tests on a cement stabilized clay, dealing with the applicability of different molding techniques. This is one of the major theme currently being studied in the international collaborative study that has been undertaken to establish common understanding of the key issues involved in Quality Assurance/Quality Control of Deep Mixing works (Terashi and Kitazume, 2009). In the present work four mixtures with different consistency and four molding techniques, namely Tapping, Rodding, Dynamic Compaction and Static Compaction were used. Unconfined compression tests were performed on the specimens produced. Generally speaking, when soil cement mixture consistency at the time of molding is low (liquid type) or could be easily reduced through knocking or vibrations, Tapping and Rodding techniques could be used efficiently. In the same case the mixture squeeze out of the mold during compaction take place if using the Static or Dynamic Compaction, which could not be adopted. On the other hand, when the materials consistency becomes higher (plastic or stiff type), the Dynamic and Static compaction techniques are often adopted since they could provide higher compaction energy, while tapping or no compaction techniques could not be applied with success.

The eventual purpose of the study is to assess the sensitivity of stabilized soil's strength (and other properties) to operators' choice of techniques, test facilities, interpretation of the standards and variability in operators' proficiency and in execution routines. While a general picture covering a variety of soils may be obtained after compiling contributions from other collaborators, this paper is a fast report of detailed test results obtained for a 'typical' clay.

2.   TESTING PROGRAMME

The experimental work consisted in a laboratory investigation on the effect of different molding techniques on the unconfined compressive strength, q_u and wet density, γ (defined as the specimen's weight divided by the volume of the mold) of cement stabilized clay specimens under various mixing conditions. A total of 160 specimens were tested. The paper addresses these topics through series of strictly controlled laboratory mix tests.

2.1. Material and testing conditions

The Kaolin clay was stabilized and tested in unconfined compression, with ordinal Portland cement (OPC) as a binder. The physical properties of the Kaolin clay tested are summarised in Table 1. The composition of the OPC used abides by the JIS prescription (Japanese Industrial Standards, R5210: 2003); see Table 2. The binder content was changed as 10, 20, 30 and 40% for each moulding technique. Ten soil specimen were prepared for each mixing condition and moulding technique, and the total of 160 specimen were prepared. At 28 days curing, the soil specimens were subjected to the unconfined compression test, in which the compression at the axial strain rate of 1%/min.

Table 1: Physical properties of Kaolin clay

Specific Gravity, Gs	2.61
Liquid Limit, w_L (%)	77.5
Plastic Limit, w_P (%)	30.3
Plastic Index, I_P	47.2
Compression Index, C_c	0.56
Swelling Index, C_s	0.10
K_0	0.6
c_u/p	0.24

Table 2: Requirements for Normal Portland Cement (JIS R5210: 2003)

Components	Standard values
Calcium oxide	< 5.0 %
Sulphur trioxide	< 3.0 %
Ignition loss	< 3.0 %
Total alkali	< 0.75 %
Chloride ion	< 0.035 %

2.2. Testing procedures

The unstabilized Kaolin clay was adjusted to the initial water content of 120% and made uniform by mixing. The powder of OPC was mixed with the clay, and they were mixed for 10 minutes to make uniform mixture. After the mixing, the stabilized soil was moulded by the following procedures. The soil and cement mixtures are sealded with a plastic sheet and sured in high humidit box. The stabilized clay was placed in plastic molds (cylindrical shape, 50 mm in diameter and 100 mm in hight) in three layers. In particular four different molding techniques were used, as shown in Photo 1:

(1) Tapping
For each layer, the mold was tapped against floor 50 times (taken as standard value).

(2) Rodding
Performed using a 8 mm diameter steel rod; consisted in slowly tamping the mixture with the rod for each layer and eventually push down the material attached to the rod. Number of poking per layer was set to 30.

(3) Dynamic Compaction
Each layer was sompressed by the weight of rod (1.6 kg) and compacted by a falling weight (0.6 kg) using a special apparatus. Fall hight was set at 10 cm, while number of blows at 5.

(4) Static Compaction
Each layer was statically compressed by the weight (4.82 kg) for 10 seconds by using a heavy rod, in which the vertical pressure of 25 kPa pressure was applied.

(a) Tapping

(b) Rodding

(c) Dynamic compaction

(d) Static compaction

Photo 1: Moulding techniques

3.   INFLUENCE OF MOULDING TECHNIQUES

3.1.   Observation of specimens

Photos 2 show typical examples of the specimens produced by various moulding techniques. The figures clearly show that relatively uniform specimens without any large air pockets and cavities were produced by the Tapping technique irrespective of the amount of binder. In Rodding technique, some air pockets and cavities are found in the specimens. In the Dynamic Compaction and Static Compaction techniques, several air pockets and cavities with relatively large volume are found in the specimens, especially in the Static Compaction technique. It was found in producing specimens that the soil binder mixture was stuck the loading platen. In particular, the suction that develops upon removal of the loading platen is suspected to be responsible for the sub-horizontal discontinuities.

| *Tapping* | *Rodding* | *Dynamic compaction* | *Static compaction* |

(a) binder content of 10%

| *Tapping* | *Rodding* | *Dynamic compaction* | *Static compaction* |

(b) binder content of 20%

| *Tapping* | *Rodding* | *Dynamic compaction* | *Static compaction* |

(c) binder content of 30%

| *Tapping* | *Rodding* | *Dynamic compaction* | *Static compaction* |

(d) binder content of 40%
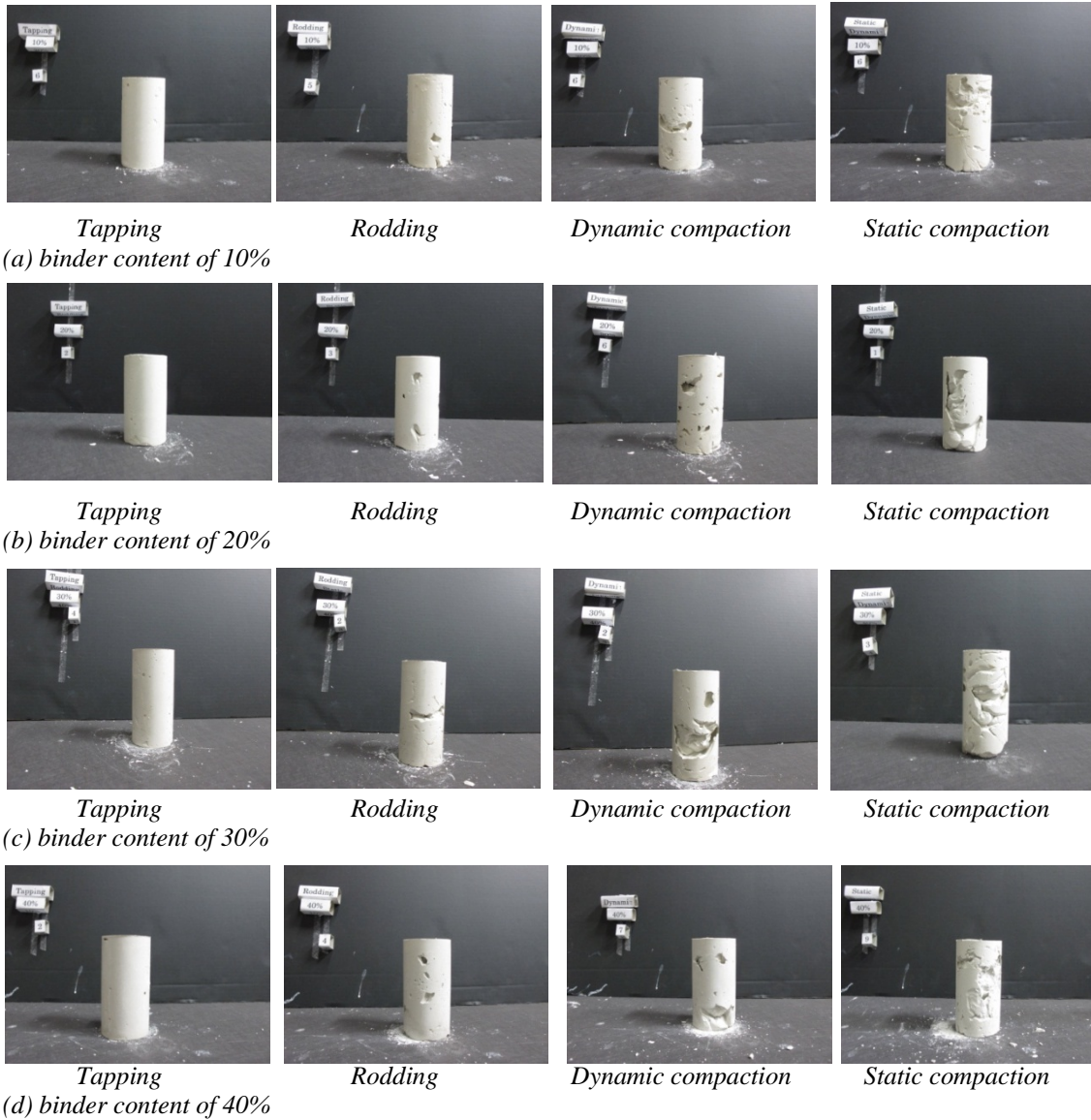
Photo 2: Observation of specimens.

3.2. Wet density

The wet desnity of specimen, max., min. and average, produced with different moulding techniques are plotted against the binder contents in Figure 1. The wet desnity increases with increasing the binder content irrespective of the moulding technique. The varietion in the wet desnity is different from the moulding technique: the smallest deviation in the maximun and minimum density is observed in the Tapping technique. However, quite large variation in the wet density is found in the Dynamic Compaction and Static Compaction techniques.

(a) Tapping

(b) Rodding

(c) Dynamic compaction

(d) Static compaction
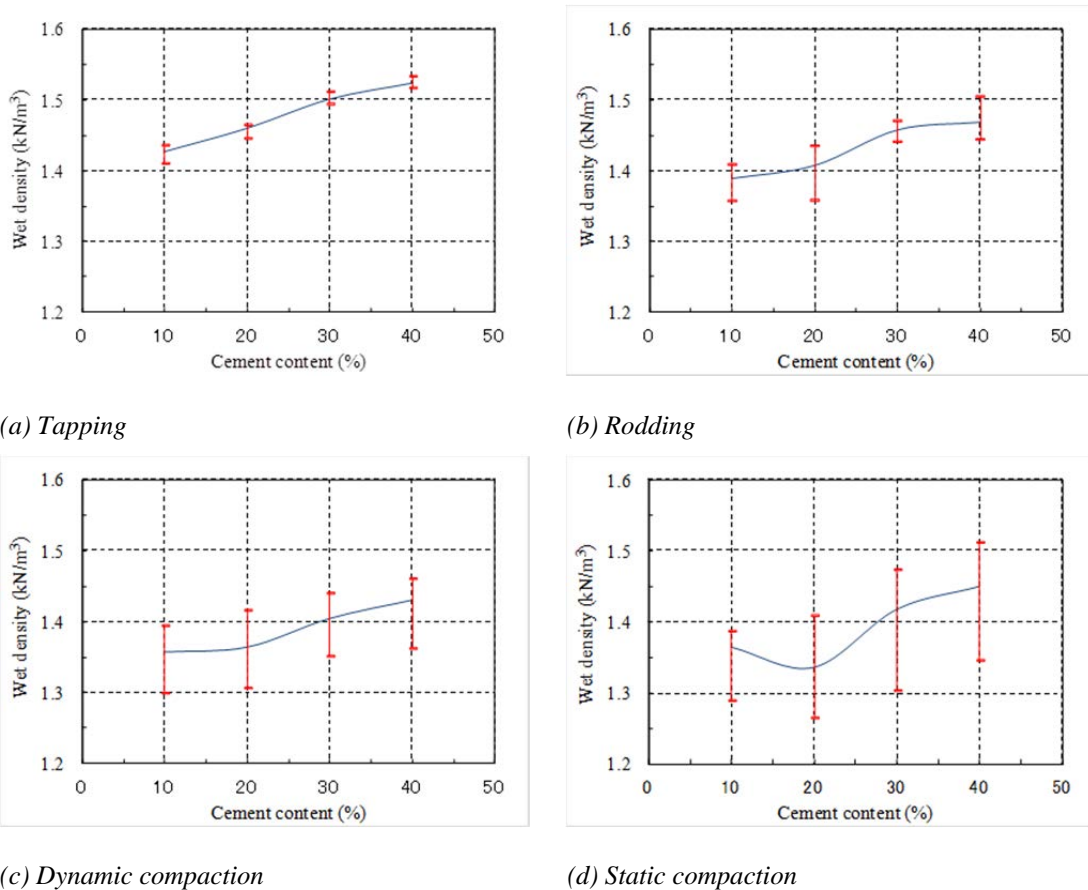
Figure 1: Wet unit weight of specimens produced by different moulding techniques

In order to clearify the influence of the moulding technique, the density ratio is shown in Figure 2, which is defined as the density of arbitary moulding technique by that of the Tapping technique. The figure shows that the largest density is found in the Tapping technique irrespective of the binder content. The Static Compaction technique gives the smallest went density.
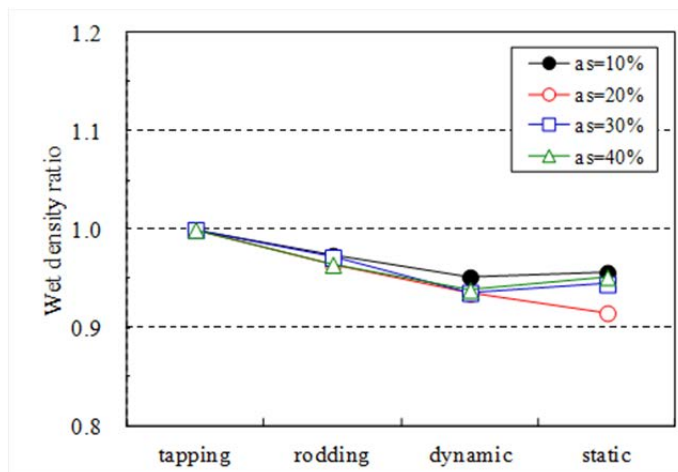
Figure 2: Wet density ratio of specimens

The coefficient of variation in the wet density is shown in Figure 3. Again, the smallest *CV* value is found in the Tapping technique, and the largest in the Static Compaction technique. In the Static Compaction technique, the *CV* value increases rapidly when the binder content becomes 20%, and is almost constant for further increase of the binder content.
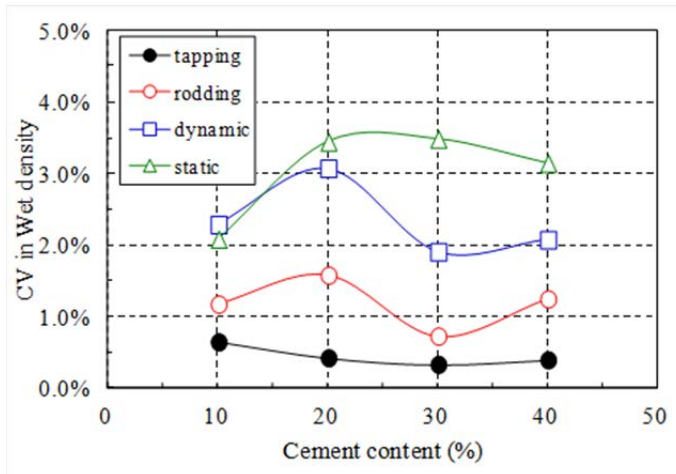
Figure 3: Coefficient of variation in Wet unit weight of specimens

3.3. Unconfined compressive strength

The unconfined compressive strength of the specimens produced by different techniques is plotted against binder contents in Figure 4. A clear hierarchy was observed, with the Tapping technique giving the highest strength. Compared to the results from the Tapping technique, the Dynamic Compaction and Static Compaction techniques resulted in approximately 30% and 50% lower q_u, respectively, for the binder content of 10% or more. The effect can be accounted by the heterogeneity of the specimens caused during moulding. The loose structure of the statically compacted specimens is clear, while the Tapping technique led to denser specimens. The photographs of the specimens, as shown in Photo 2, confirm that the specimen by the Static Compaction technique contained large air pockets and cavities. While the Static Compaction techniques are sometimes used for fibrous, compressible soils, a caution may be needed if a uniform specimen is desired.

(a) Tapping

(b) Rodding

(c) Dynamic compaction

(d) Static compaction
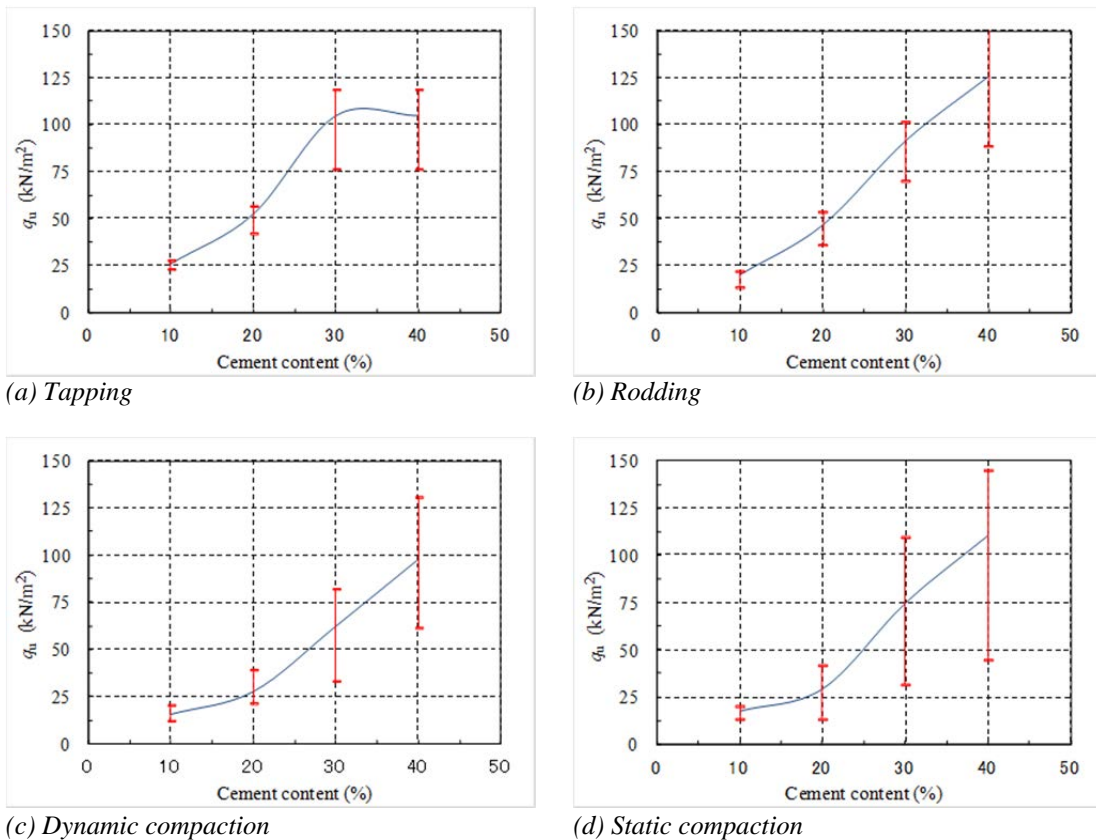
Figure 4: Unconfined compression strength of specimens produced by different moulding techniques

In order to clearify the influence of the moulding technique, the strength ratio is shown in Figure 5, which is defined as the unonfined compressive strength of arbitary technique by that of the Tapping technique. The figure shows that the largest strngth is found in the Tapping technique for the binder content of 10, 20 and 30%. The strength ratio is considerably small of the order of 50 to 75% in the Dynamic Compaction and Static Compaction techniques. However, when the binder content is 40%, the highest strength ratio is found in the Rodding technque of the order of about 120%, while the smallest is found in the Dynamic Compaction technique.
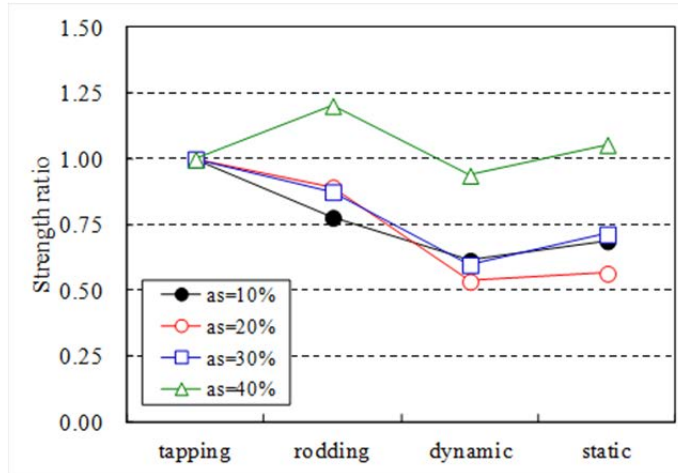
Figure 5: Strength ratio of specimens

The coefficient of variation in the unconfined compressive strength is shown in Figure 6. When the binder content is 10%, relatiely small *CV* value are found irrespctive of the binder content while the smallest *CV* value is found in the Tapping technique. The *CV* values slightly increase in the Tapping and Rodding techniques with increasing the binder content. In the Dynamic Compaction and Static Compaction techniques, on the other hand, the *CV* values increase rapidly to around 25% with increasing the binder content. As shown in Photo 2, the specimens produced by these techniques contain large volumn air pockets and cavities, which cause inuniformity in the strength.
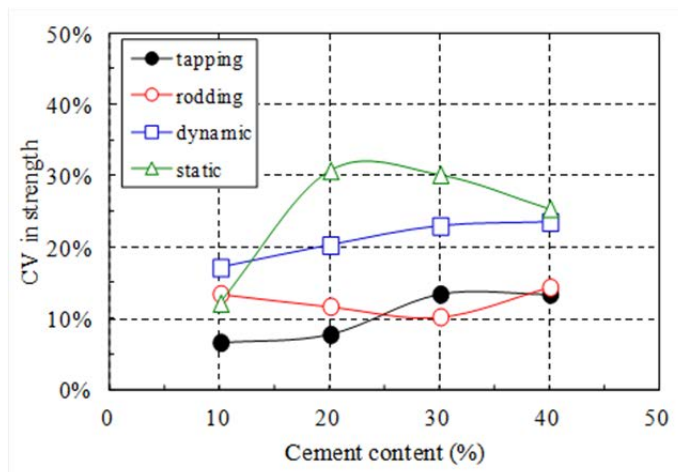
Figure 6: Coefficient of variation in unconfined compressive strength of specimens

3.4.   Relationship between unconfined compressive strength and wet density

Figure 7 shows the relationship between the unconfined compressive strength and the wet density of the specimens produced by diferent moulding techniques. There are clear relationship between them, in which the strength increases almost linearly with increasing the wet density irrespective of the moulding technique.
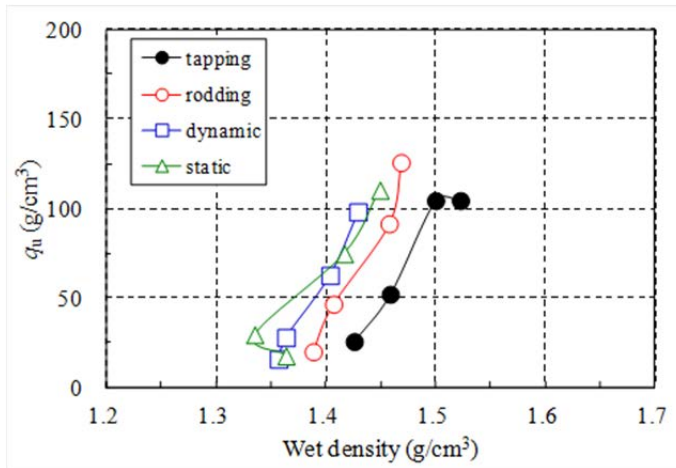
Figure 7: Relationship between unconfined compressive strength and wet density of specimens produced by different moulding techniques

Figure 8 shows the relationship between the coefficient of variation in the unconfined compressive strength and that in the wet density. The magnitude itself is different in the moudling technique, which can be caused by the degree of uniformity of the specimen as shown in Photo 2. The smallest *CV* value in strength and wetdensity is found in the Tapping technique, while the largest *CV* value is found in the Dynamic Compaction and Static Compaction techniques. It is noted that the *CV* value in the strength increas almost linearly with increasing the *CV* value in wet density.
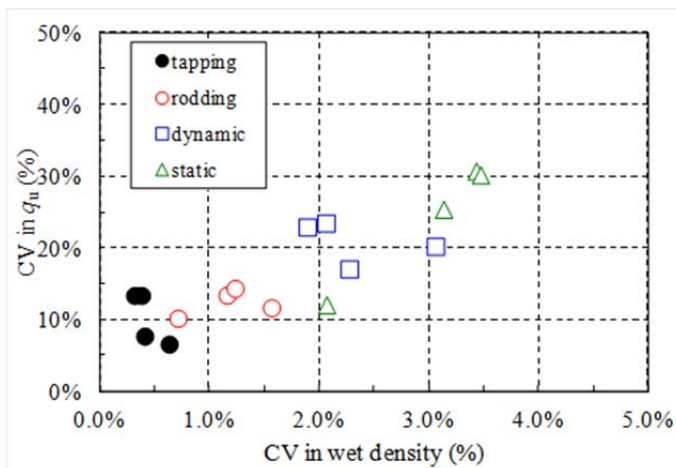
Figure 8: Relationship between coefficient of variations in unconfined compressive strength and wet density of specimens produced by different moulding techniques

4.   CONCLUSIONS

A comprehensive series of laboratory mix tests was performed to investigate the effect of moulding technique on the wet density and unconfined compressive strength of the cement stabilized Kaolin clay. The tests clearly show that the moulding techniques considerably affect the wet density and strength of the stabilized clay. For the tested inorganic clay with high water content, the tapping technique provids the quite uniform specimen and the densest specimens with highest shear strength. The Rodding technique also provids uniform specimen with small variation in the wet density and strength. The Dynamic Compaction and Static Compaction techniques, on the other hand, provid specimens containing large volume of air pockets and cavities, and provide small density and strength with a lot of scatter.

The work was undertaken as part of an international collaborative study. Within the programme, similar studies on laboratory mix tests are being performed on different soils in different laboratories, and the results are forthcoming.

5.   ACKNOWLEDGEMENTS

REFERENCES

Japanese Geotechnical Society, 2009, Practice for Making and Curing Compacted Stabilized Soil Specimens Using a Rammer, JGS0811-2009 (in Japanese).

Japanese Geotechnical Society, 2009, Practice for Making and Curing Statically Compacted Stabilized Soil Specimens, JGS0812-2009 (in Japanese).

Japanese Geotechnical Society, 2009, Practice for Making and Curing stabilized Soil Specimens Without Compaction, JGS0812-2009 (in Japanese).

Terashi, M. and Kitazume, M., 2009, Keynote Lecture: Current Practice and Future Perspec-tive of QA/QC for Deep-Mixed Ground, Proc. of the International Symposium on Deep Mixing & Admixture Stabilization, Okinawa, pp. 59-97.

Åhnberg, H. and Holm, G., 2009, Influence of laboratory procedures on properties of stabilised soil specimens, Proc. of the International Symposium on Deep Mixing & Admixture Stabilization, Okinawa, pp.167-172.

Immediate modification of clays with quicklime: alteration of grain-size distribution

Alan J. Lutenegger, University of Massachusetts, Amherst, USA, lutenegg@ecs.umass.edu

ABSTRACT

The immediate, short-term, alteration of clays soils with quicklime (CaO) was investigated through measured changes in the grain-size distribution of clays after reaction with lime. Laboratory results obtained on eight different clays mixed with quicklime varying from 0.5% to 15% by dry weight of the soil are presented. The clays represent a wide range of deposits with differing amounts of initial clay content, plasticity, specific surface, and Activity and as such represent a wide range in mineralogy. Results of standard hydrometer tests show dramatic reduction in the clay fraction (both % < 0.002 mm and % < 0.001 mm) which is accompanied by an increase in the silt and fraction. These data clearly demonstrate the varying degree of the immediate quicklime reaction with the clay to flocculate the particles and create silt and sand sized particle clusters or peds. The results also demonstrate the influence of initial soil composition and mineralogy on the lime reactivity. The test methods and results are presented and results are discussed in the context of the limited previously published results available from the literature.

1.   INTRODUCTION

Since the 1940s one of the most common methods used to alter the engineering behavior of fine-grained soils had been by the addition of lime, either hydrated lime, $CaOH_2$, or quicklime, CaO. The principal soil stabilization processes associated with the addition of quicklime are: 1) the exothermic reaction between quicklime and soil water, producing heat and consuming soil water; 2) rapid modification of the soil plasticity through initial cation exchange; and 3) long term pozzolanic reactions producing cementatious calcium silicate and calcium aluminate hydrates. The degree of improvement of the engineering properties depends on the soil mineralogy and clay content, the amount of lime added and time.

The short term reactions of lime with soils, especially soft high water content clays, are of interest to contractors who may use lime to improve workability and constructability but are also of general interest to help explain the observed changes and overall improvement in behavior. In fine-grained soils composed predominantly of clays, initial modification produced by the addition of lime is to change the soil consistency through initial hydration and cation exchange.

Several previous investigations have clearly shown that the addition of lime alters the grain-size distribution of fine-grained soils, especially montmorillonitic clays, as determined by the conventional hydrometer analysis (e.g., Lund and Ramsey 1959; Thomas et al. 1965; Uppal and Chadda 1967; Basma and Tuncer 1991; Tuncer and Basma 1991; Osula 1996; Narasimha Rao and Rajasekaran 1996; Rajasekaran and Narasimha Rao 1998; Rao et al. 2001; Cokca 2001; Sakr et al. 2009). Generally, these studies have shown that there is an immediate reduction in the clay sized fraction, which increases with increasing lime content, and, depending on the soil, often a dramatic increase in the sand fraction (i.e., % retained on the No. 200 sieve). Obviously, no new sand grains are formed, only aggregates of silt and clay that are resistance to dispersion affected in the hydrometer test and which produce the appearance of particles larger than 0.075 mm. Laguros and Jha (1977) suggested the term "Aggregate Index" as a numerical indication of the degree of apparent aggregation of particles achieved as a result of using an admixture to soils. The Aggregate Index, AI, was defined as:

$$AI = \frac{\text{\% non clay-size material of stabilized soil}}{\text{\% non clay-size material of raw soil}} \qquad (1)$$

The purpose of this study was to determine the immediate effect of lime treatment on the grain-size distribution of a number of fine-grained soils of differing composition. The objective was to document any changes in grain-size produced by the lime to provide insight into the immediate modification mechanism produced by the lime reaction and to investigate the influence of soil characteristics on the degree alteration to enable engineers to predict the effectiveness of lime treatment on other soils.

2.   INVESTIGATION

2.1   Soils

Fine-grained, predominantly montmorillonitic, soils representing a wide range in geologic origin, composition, clay content, plasticity, Activity and Specific Surface were selected for testing. A summary of soil properties of the eight soils tested in given in Table 1. A Casagrande Plasticity Chart for these soils is shown in Figure 1 and the Activity Chart is shown in Figure 2. Specific Surface (SSA) was determined by the EGME method described by Cerato and Lutenegger (2002).

Table 1: Summary of Soil Characteristics.

Soil No.	Name	L.L.	P.I.	Clay (% < 0.002mm)	A	SSA (m²/g)
1	Ainsworth	53.2	27.5	46.5	0.59	268
2	Black Cotton	82.0	58.0	61.0	0.95	361
3	Wyoming Bentonite	153.0	100.0	90.2	1.11	594
4	London Clay	64.1	30.3	56.6	0.73	165
5	Texas Sodium	130.0	68.0	65.3	1.31	455
6	RS-101	59.7	39.3	46.5	0.86	
7	Heiden Clay	67.1	46.7	54.6	0.87	134
8	SWy-2	519.1	484.1	96.0	8.01	637
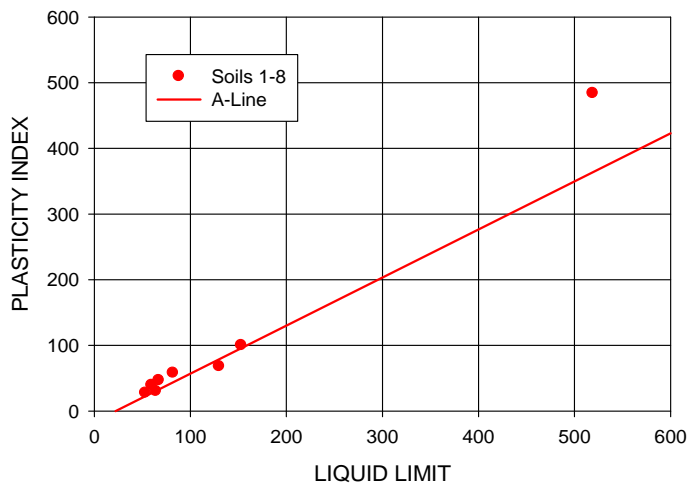
Figure 1: Casagrande Plasticity Chart
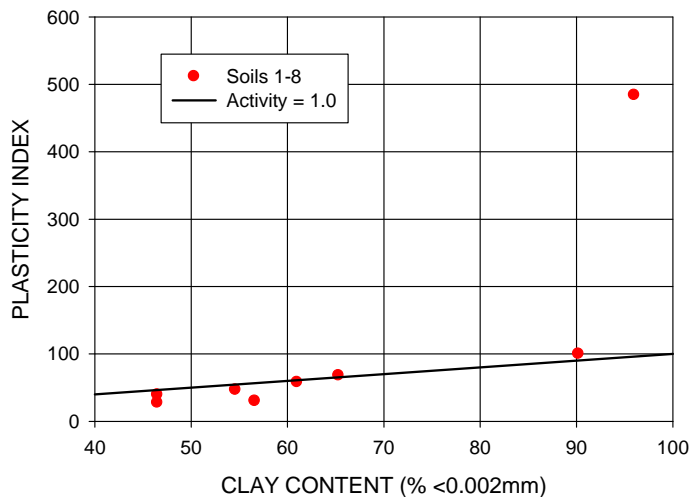
Figure 2: Activity Chart

The range in soils was selected to provide an opportunity to evaluate the influence of soil characteristics on the effectiveness of lime modification.e shrinkage characteristics. All eight soils classify as high plasticity clays (CH) with Liquid Limit greater than 50 and all but one fall on the A-Line. Soil 8 is is a pure soium montmorillonite and falls above the A-Line closer to the U-Line. Seven of the eight soils are considered Active clays according to Skempton's Activity with Activity ranging from 0.59 to 1.31 but generally close to A = 1.0. Soil 8 has a very high Activity of 8.01.

2.2   Test Procedures

Individual samples were initially air dried and pulverized by hand using a ceramic mortar and rubber tipped pestle to pass a No. 40 (0.420 mm) sieve. Each sample was then mixed with distilled/deionized water to an initial water content slightly above the Liquid Limit (as determined by the Casagrande Cup). Mixtures were then covered and allowed to temper for about 12 hours. Various amounts of laboratory grade quicklime (CaO) was then added to the soil/water pastes to produce the desired % lime (by dry weight of soil) ranging from 0.5% to 15%. The lime was thoroughly mixed into the paste by hand for several minutes using a stainless steel spatula. After mixing, the samples were left open and allowed to air dry. After air drying, the samples were again crushed to pass the No. 40 sieve before performing hydrometer tests.

Hydrometer tests were conducted on untreated and treated samples using the standard procedure described in ASTM D422. Sodium hexamataphosphate was used as the dispersing agent.

3.   RESULTS

Figure 3 shows the measured clay content (<0.002 mm) as a function of the lime content for all eight soils. In some cases, the reduction in clay content occurs rapidly as the lime reacts with the clay but in other cases, there is a much sloweer reduction in the clay content as lime is added. In cases wher the reduction occurs rapidly, there is also a "leveling off" point beyond which the reduction in clay is less dramaitic with additional lime. This is likely to occur when the available cly is so small that further lime has no possibility to produce a reaction. The immediate initial reduction in clay content results from immediate cation exchange and calcium ions being shared in the clay interlayer.

A comparison of the results obtained from these eight samples may be made by considering the reduction in clay content at a fixed percentage of added lime. If we arbitrarily select a lime content of 4% as being a reasonable amount of lime to add to a soli we can compare the effectiveness of the lime on all eight soils. The percent change in clat content can be determined from:

% Change = [(ICF – LCF)/ICF] x 100%   (2)

where:
ICF = Initial Clay Fraction
LCF = Lime Treated Clay Fraction

Figure 4 shows the variation in % change in clay content of all eight soils as a function of the Activity. It can be seen that Activity is not a good indicator of the effectiveness of lime to alter the grain-size of the soils. Similarly, Liquid Limit and Plasticity Index did not show strong correlations with the change in clay content. On the other hand, Figure 5 shows the variation in % change in clay content as a function of the Initial Clay Content and it can be seen that there is more of a trend in these data. Figure 6 shows the % change in cay content with Specific Surface and indicates a strong relationship suggested by these data. This might be expected if all of the soils have similar mineralogic composition. There is some evidence in the literature that suggests that for predominantly montmorillonitic soils lime reactivity may be related to specific surface area (e.g., Moore and Jones 1971) but is less important for illitic soils. Similar correlations between specific surface area and the amount of Portland Cement required for effective stabilization have been noted by Diamond and Kinter (1958) and Dos Santos (1961).
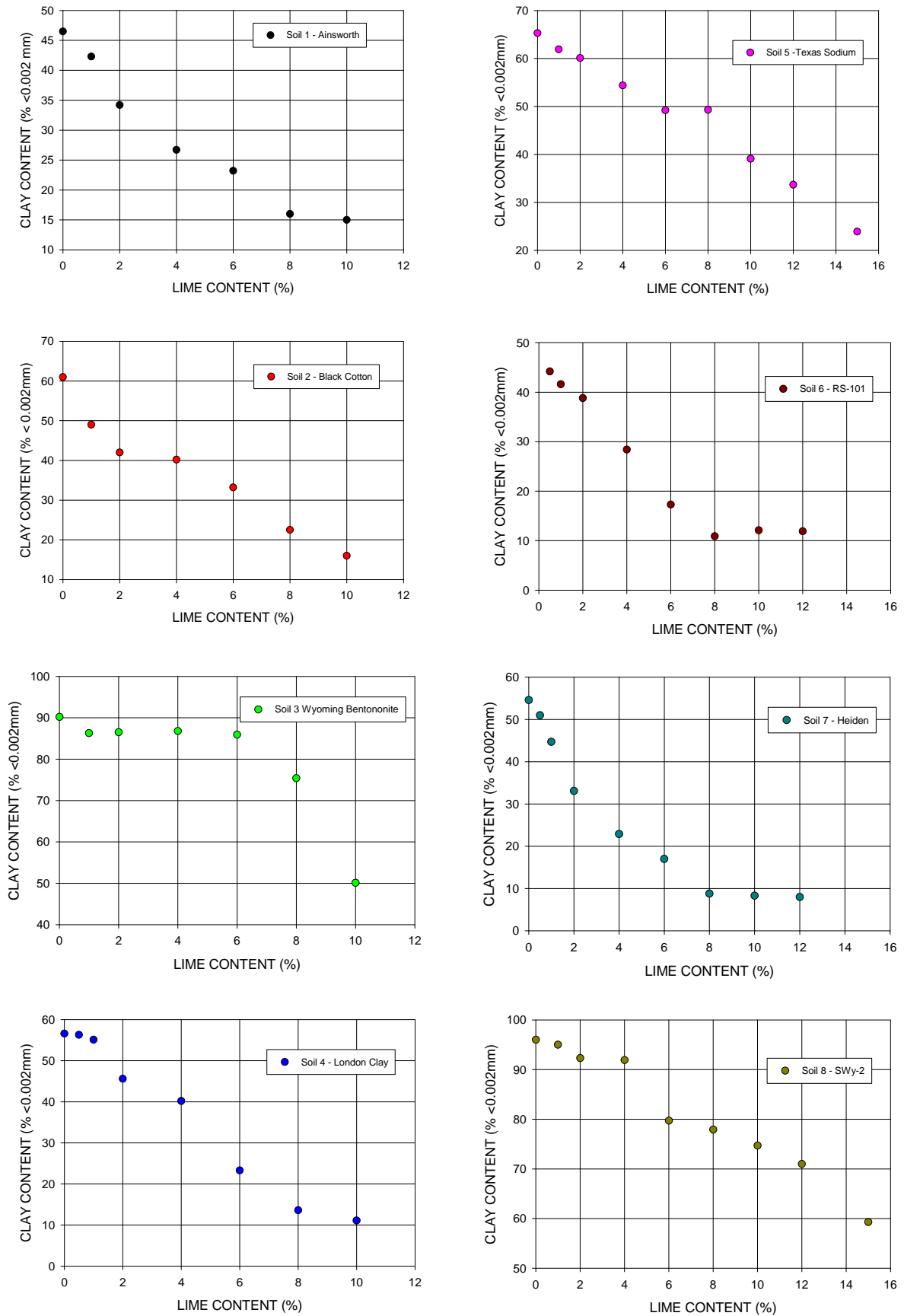
Figure 3: Variation in Clay Content with Lime Content
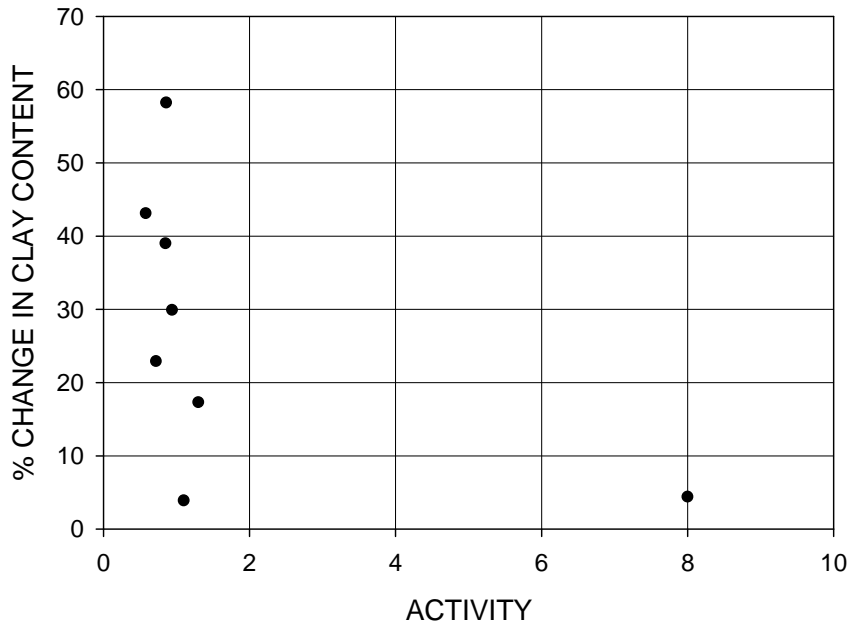
Figure 4: Variation in % Change in Clay Content with 4% Lime and Activity
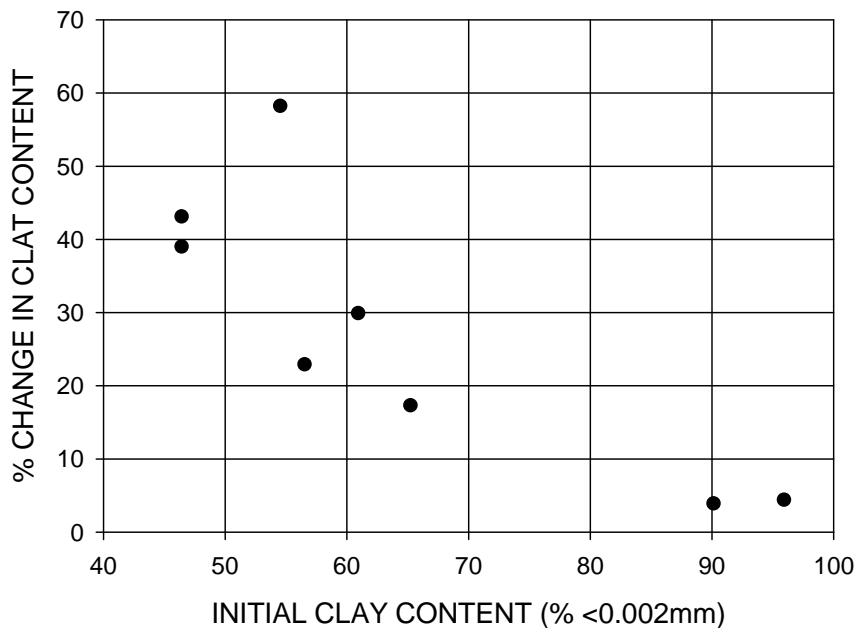
Figure 5: Variation in % Change in Clay Content with 4% Lime and Initial Clay Fraction

Changes in the clay fraction for differnt soils as indicated in Figure 3 show a wide range of response to the addition of lime although for most of the soils there is a gradual and continuous decrese in clay content with increasing lime content. Clearly the alteration of the clay fraction and the formation of particle aggregates is complex and shows differing behavior over the full range of added lime. For soils with very high clay content and Specific Surface, small amounts of lime do not have any significant effect on the soil as the number of added calcium cations is so low in comparison to the number of sites available for exchange and sharing of cations. In these soils (e.g., Texas Sodium; Swy-2) even the addition of 15% lime does not appear to fully satisfy the potential for cation exchange as there is no leveling off in the reduction of the clay content. In other soils, it can be seen that there is a clear point beyond which additional lime produces no additional significant change in the clay fraction, suggesting that, like the Lime Fixation Point, determined by soil plasticity, this additional lime would be available for long-term pozzolanic reactions.
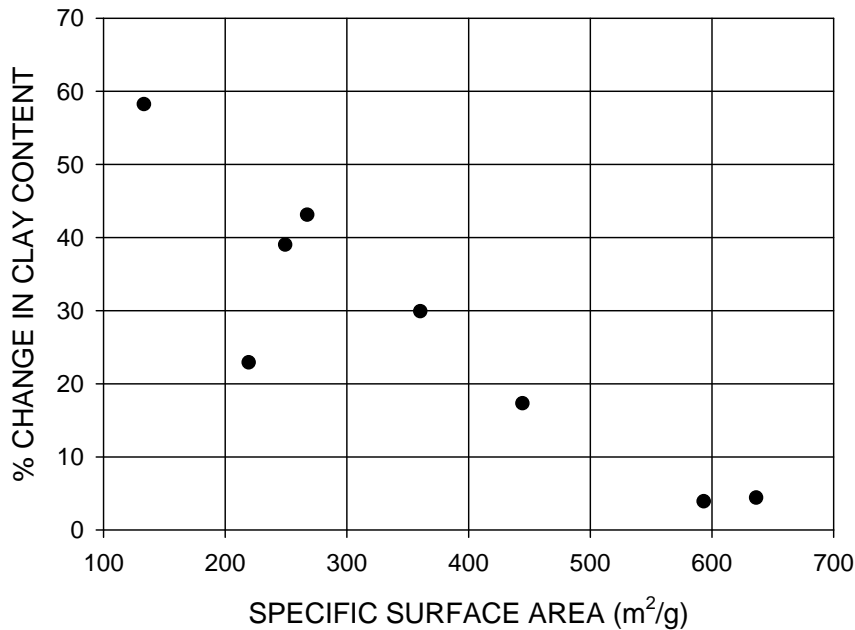
Figure 6: Variation in % Change in Clay Content with 4% Lime and Specific Surface

4.   SUMMARY

Test results on the change in clay fraction of eight high plasticity clays of varying origin and characteristics with added quicklime have been presented. The results show that in all cases, the addition of lime produces an immediate alteration in the grain-size with a decrease in clay content as measured by standard hydrometer tests. The degree of alteration is different for different soils. However, for a fixed amount of added lime, in this case 4% by dry weight, the change in clay content produced by the lime appears to be strongly related to the Specific Surface. Additional tests on soils with other dominat clay mineral species are needed to provide further verification.

REFERENCES

Basma, A.A. and Tuncer, E.R., 1991. Effect of Lime on Volume Change and Compressibility of Expansive Clays. Transportation Research Record 1295, pp. 52-61.

Cerato, A.B. and Lutenegger, A.J., 2002. Determination of Surface Area of Fine-Grained Soils by the Ethylene Glycol Monoethyl Ether (EGME) Method. Geotechnical Testing Journal, ASTM, Vol. 25, No. 3, pp. 315-321.

Cokca, E., 2001. Use of Class C Fly Ashes for the Stabilization of an Expansive Soil. Journal of Geotechnical and Geoenvironmental Engineering, ASCE, Vol. 127, No. 7, pp. 568-573.

Diamond, S. and Kinter, E.B., 1958. A Rapid Method Utilizing Surface Area Measurements in Predicting the Amount of Cement Needed to Stabilize Plastic Soils. Public Roads, Vol. 30, No. 2, pp. 63-70.

Dos Santos, M.P.P., 1961. Progress in the Design and Construction of Soil-Cement Roads. Proceedings of the 5th International Conference on Soil Mechanics and Foundation Engineering, Vol. 2, pp. 217-220.

Laguros, J.G. and Jha, K., 1977. Stabilization of Oklahoma Shales. Report No. ODOT 73-04-02, ORA158-602. University of Oklahoma, School of Civil Engineering and Environmental Science, Norman, Ok.

Lund, and Ramsey, 1959. Experimental Lime Stabilization in Nebraska. Highway Research Board Bulletin 231, pp. 24-38

Moore, J.C. and Jones, R.L., 1971. Effect of Soil Surface Area and Extractable Silica, Alumina and Iron on Lime Stabilization Characteristics of Illinois Soils. Highway Research Record No. 351., pp. 87-92.

Narasimha Rao, S. and Rajasekaran, G., 1996. Reaction Products Formed in Lime-Stabilized Marine Clays. Journal of Geotechnical Engineering, ASCE, Vol. 122, No. 5, pp. 329-335.

Osula, D.O.A., 1996. A Comparative Evaluation of Cement and Lime Modification of Laterite. Engineering Geology, Vol. 42, pp. 71-81.
.
Rajasekaran, G. and Narasimha Rao, S., 1998. Particle Size Analysis of Lime-Treated Marine Clays. Geotechnical Testing Journal, ASTM, Vol. 21, No. 2, pp. 109-119.

Rao, S.M., Reddy, B.V.V. and Muttharam, M., 2001. Effect of Cyclic Wetting and Drying on the Index Properties of Lime Stabilized Expansive Soil. Proceedings of the Institution of Civil Engineers, Ground Improvement, Vol. 5, No. 3, pp. 107-110.

Sakr, M.A., Shanin, M.A. and Metwally, Y.M., 2009. Ulilization of Lime for Stabilizing Soft Clay Soil of High Organic Content, Geotechnical and Geological Engineering, Vol. 27, pp. 105-113.

Thomas, C.E., Jones, W.G. and Davis, W.C., 1965. Lime and Phosphoric Acid Stabilization in Missouri. Highway research Record 92, pp. 43-68.

Tuncer, E.R. and Basma, A.A., 1991. Strength and Stress-Strain Characteristics of a Lime Treated Cohesive Soil. Transportation Research Record 1295, pp. 70-79.

Uppal, H.L. and Chadda, L.R., 1967. Physico-Chemical Changes in the Lime Stabilization of Black Cotton Soil (India). Engineering Geology, Vol. 2, No. 3, pp. 179-189.

Stabilizing clays using basic oxygen steel slag (BOS)

Hamed Mirzaeifar, Islamic Azad University-Pardis Branch Tehran, Iran, h.mirzaeifar@pardisiau.ac.ir
M.R. Abdi, Faculty of Civil Engineering, KNT University, Tehran, Iran, abdi@kntu.ac.ir

ABSTRACT

Rapid industrialization has resulted in generation of large quantities of wastes, most of which do not find any effective use and create environmental and ecological problems. The use of various slags as by-products of steel industry is well established in civil engineering applications. However, the use of BOS slag in the area of soil stabilization has not been fully researched and developed. This paper presents the results of unconfined compressive strength (UCS) and durability tests conducted on kaolinite samples stabilized with various percentages of lime (i.e. 1, 3 and 5%) and treated with various percentages of BOS slag (i.e. 10, 15 and 20%). Tests determined strength development of compacted cylinders, moist cured in a humid environment at 35° C and durability by freezing and thawing method. Results show that using lime and BOS slag as additives either singularly or concurrently for stabilizing kaolinite improves soil properties in terms of increased UCS and durability by resistance to freezing and thawing. The improvements are shown to be dependent on the lime and the BOS slag contents as well as the curing period.

1.   INTRODUCTION

Generation of large quantities of wastes due to rapid industrialization is one of the challengable issues in civil environmental engineering. At the same time, disposal of industrial waste or by-products has become more difficult and expensive because of the increasing stringent environmental regulations and shortages of suitable nearby disposal sites. It has been observed that some of these wastes have high potential and can be gainfully utilized as raw mix/blending ingredient in cement manufacturing or other industries. Usage of industrial wastes will not only help in solving the environmental pollution problems associated with their disposal but also help in conservation of natural resources such as limestone and aggregates.

Steel slag aggregates show an inclination to expand because of the presence of free lime and magnesium oxides that have not reacted with the silicate. They can hydrate and expand in humid environments. Steel slag intended for use as aggregate should be stockpiled outdoors for several months to expose the material to moisture from rain or application of water by spraying. The purpose of such storage (ageing) is to allow potentially destructive hydration and its associated expansion to take place before using the material. Processed steel slag has favourable mechanical properties for aggregate use, including good abrasion resistance, good soundness characteristics, and high bearing strength. Steel slag aggregate has long been used as granular base, in embankments, highway shoulders, hot mix asphalt pavements, railway ballast and hydraulic structures. More recently slag uses have been expanded to include use as a cement additive and landfill cover material [21].

The chemical composition and mineralogy of steel slag is similar to that of Portland cement. It is considered a weak Portland cement because of its low tricalcium silicate (C3S) content [12, 18]. According to Altun and Yilmaz [3], the reactivity or hydraulic properties of BOS slag is dependent on its chemical composition, mineral phase, and alkalinity. Wild et al. [24]examined the effects of partial substitution of lime with ground granulated blast furnace slag (GGBS) on the strength properties of lime stabilized sulphate-bearing clay soils. In their laboratory investigation they used lime-stabilized kaolinite containing different levels of added gypsum and lime stabilized gypsum bearing Kimmeridge clay to which lime was progressively substituted with GGBS. They used cylindrical specimen cured in a humid environment at 30° C. Their results showed that substitution of lime with GGBS in stabilizing gypsum containing clays produces significant improvements in strength development. Poh et al. [23] conducted a laboratory investigation of using three BOS slag fines from different steel production sites in United Kingdom for stabilizing English China Clay (ECC) and Mercia Mudstone (MM). Results showed that using mixtures of BOS slag fines produces improvements in strength and durability (soaked UCS/unsoaked UCS) as well as reducing expansion.

2.   PURPOSE OF RESEARCH

Considering that steel slag has similar chemical composition and mineralogy to Portland cement, there might be potential for furthering its use in soil stabilization. Based on the literature review, the use of BOS slag in soil stabilization has not been extensively examined so far. This research will examine the potential use of Basic Oxygen Steel slag singularly or in combination with lime for improving strength and durability of fine-grained soils.

3.   MATERIALS AND LABORATORY TESTING PROGRAM

3.1.   Materials

Kaolinite was used as the clay soil in this investigation to reduce the effects of material variability in tests results. Index characteristics of kaolinite determined according to appropriate ASTM standards are summarized in Table 1. According to Unified Soil classification System, kaolinite is classified as CL. The lime used for the investigation was hydrated lime with particles passing No. 200 sieve having specific gravity of 2.3. Basic Oxygen Steel (BOS) slag aggregates passing sieve No. 4 (i.e. $420\,\mu m$) with a specific gravity of 3.32 were used. Considering the size of the samples this was necessary to separate the coarse particles and promote possible chemical reactions by increasing specific surface. Grain size distribution curves for the clay and the BOS slag are shown in Figure 1.

Table 1: Kaolinite index characteristics

Characteristic	Value
Particle size distribution (% by mass) < 0.075mm	100(%)
Specific gravity	2.6
Plastic limit (%)	2.6
Liquid limit (%)	45
Plasticity index (%)	19
Max. dry density (Mg/m³)	1.69
Optimum moisture content (%)	21
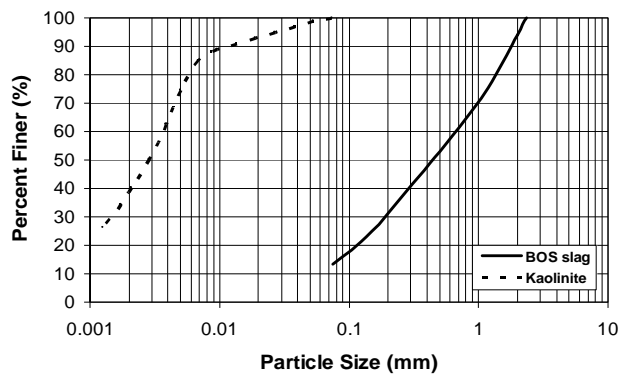
Figure 1: Particle size distribution curves for kaolinite and BOS slag

3.2.   Mixtures

Mixtures studied together with their respective maximum dry density (MDD) and optimum moisture content (OMC) is presented in Table 2. Results show that lime addition resulted in slightly reducing MDD and increasing OMC of the soil, whereas BOS slag addition had exactly the opposite effect. Kaolinite treated with a particular percentage of lime and various amounts of BOS slag also showed slight increase in MDD and reduction in OMC. The decrease in dry density of lime treated kaolinite samples is attributed to the immediate formation of cementitious products at particle contact points. These products reduce compactibility and thus density of the treated soil. The air within the macro-pores formed is easily expelled to be replaced by water without increasing the volume, thus causing the increase in optimum moisture content [1, 4]. The slight increase in MDD and the reduction in OMC of BOS slag treated kaolinite are attributed to the coarser slag particles promoting better compaction.

3.3.   Sample Preparation

Cylindrical test specimens with 38mm diameter and 76mm height were prepared with MDD and OMC values shown in Table 2. After mixing and compaction of the samples, they were labeled and wrapped in several layers of cling film and placed in airtight plastic containers. They were then transferred to a controlled chamber set at 35°C and approximately 100% relative humidity and cured for 1, 7, 28 and 90 days. To ensure repeatability in sample preparation, preliminary investigations were conducted on two of the mix compositions. A maximum variation of 7% was observed in UCS result which was considered satisfactory. For the main tests, results that varied more than 5% were discarded.

Table 2: Compaction characteristics of mixtures

Mixtures	Max. dry density (Mg/m³)	Optimum Moisture (%)	Mixtures	Max. dry density (Mg/m³)	Optimum Moisture (%)
K	1.69	21	K+1%L+15%B	1.77	19.5
K+1%L	1.68	21.4	K+1%L+20%B	1.81	18.5
K+3%L	1.67	22	K+3%L+10%B	1.73	20.5
K+5%L	1.65	23	K+3%L+15%B	1.76	19.7
K+10%B	1.74	19.7	K+3%L+20%B	1.79	19
K+15%B	1.77	19	K+5%L+10%B	1.70	21
K+20%B	1.81	18	K+5%L+15%B	1.73	20.5
K+1%L+10%B	1.74	20	K+5%L+20%B	1.76	19.7

Notations: K= kaolinite, L=lime, B=BOS Slag

4.   TESTING

Tests were conducted on both treated and untreated kaolinite samples to determine the changes in compressive strength and durability by resistance to freezing and thawing (F/T). X-ray fluorescence (XRF) and X-ray diffraction (XRD) analysis were also carried out on kaolinite, lime and BOS slag to determine their chemical and mineralogical compositions.

4.1.   Unconfined compression tests

To determine the effects of lime and BOS slag addition on strength of kaolinite, unconfined compressive strength (UCS) tests were performed in accordance to ASTM D: 2166-87. After completion of UCS tests, samples were collected for moisture content determination to ensure that moisture loss was not significant and uniformity was achieved with samples prepared using the same procedure.

4.2.   Durability Tests

Durability of untreated and treated soil samples were examined by conducting freeze / thaw (F/T) tests in accordance to ASTM D 560**.** At the designated curing periods, samples were taken out of the curing chamber, cooled, weighted and then stood on carriers and placed in a freezer. On removal after 24 hours of freezing, the specimens were transferred to a humidity chamber and kept for a further 24hr. Each cycle of freezing / thawing lasted 48 hours to complete. Because of the variety of mix compositions, number of samples as well as time limitations, a maximum of 4 cycles of F/T were used. On completion of designated F/T cycles, samples were subjected to UCS tests. Brushing of samples after F/T was not carried out as it is conducted manually and could be affected by the consistency of the technician. In this regard, Shibata and Baghdadi reported a good correlation between F/T durability as measured by mass loss (i.e. brushed) and residual strength (i.e. unbrushed) for soil - cement specimens. Baghdadi and Shibata [5] also reported that replacing brushing by measuring the compressive strength of specimens after they are subjected to cycles of wet – dry or freeze – thaw provides a more consistent and convenient measure of the deterioration of the material. Durability in terms of residual strength after freezing and thawing as well as being based on the calculated index of "UCS after F/T / UCS before F/T" has been determined. This index, denoted by "Di" is a measure of the resistance of a specimen to the deteriorating effect of freezing and thawing on its strength. Poh et al. [23] used the "soaked UCS / unsoaked UCS" as the index for determining the durability of stabilized soils.

5.   RESULTS

5.1.   Unconfined compression tests

5.1.1. Lime stabilized samples

Compressive strength development of untreated and stabilized kaolinite samples with 1, 3 and 5% lime is shown in Figure 2. As expected, untreated samples do not show any strength development with curing time. Lime addition enhanced strength development which increased with increasing lime content. Strength development is very significant between 7 and 28 days of curing with the trend continuing up to 90 days but at a reduced rate. Samples stabilized with 1% lime, showed no gain in strength after 28 days whereas those stabilized with 3 and 5% lime, show continued strength development even after 90 days of curing. Kaolinite samples stabilized with 3% lime in particular show a substantial increase in strength. Increasing lime content from 3% to 5%, although resulted in higher compressive strengths, but the changes are not substantial. Considering the results, it can be concluded that 1% lime was not sufficient to produce enough pozzolanic compounds needed for significant strength development and 5% is the optimum lime content for the kaolinite studied. Strength development showed to be dependent on the lime content as well as the curing time. The observations made are in agreement with the results reported by Abdi [1] and Arabi [4]. Taking strength of untreated kaolinite as the base, addition of 1, 3 and 5% lime respectively resulted in 160, 558 and 642% improvement after 90 days of curing (see Table 3).
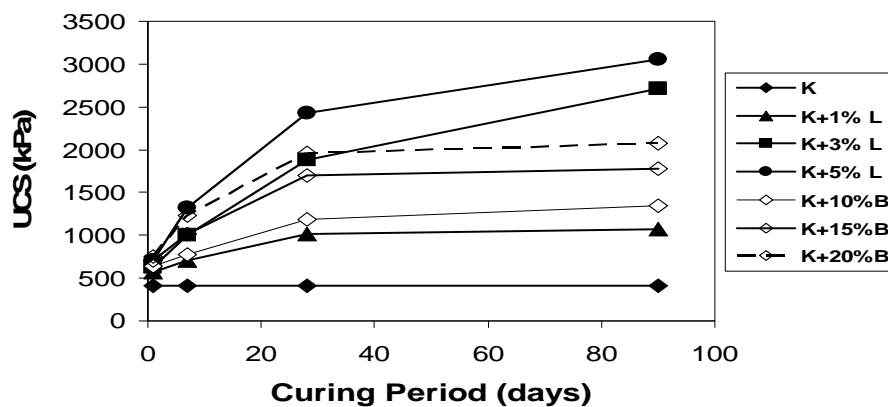
Figure 2: UCS versus curing period for lime and, BOS slag treated kaolinite

Table 3: UCS and the percentage increase after 90 days curing

Mixture	UCS (kN/m²)	Increase (%)	Mixture	UCS (kN/m²)	Increase (%)
K	412	0	K+1%L+15%B	2112	413
K+10%B	1347	227	K+1%L+20%B	2586	528
K+15%B	1776	331	K+3%L+10%B	3091	650
K+20%B	2077	404	K+3%L+15%B	3480	744
K+1%L	1074	160	K+3%L+20%B	3606	775
K+3%L	2713	558	K+5%L+10%B	4130	902
K+5%L	3061	642	K+5%L+15%B	4714	1044
K+1%L+10%B	1872	354	K+5%L+20%B	4861	1080

Notations: K= kaolinite, L=lime, B=BOS Slag

5.1.2. BOS slag treated samples

Compressive strength of BOS slag treated kaolinite samples are also shown in Figure 2. It can be observed that by the addition of 10, 15 and 20% BOS slag to kaolinite, strength enhancement is achieved. The most significant increase in strength is displayed by samples treated with 10% BOS slag and further increases (i.e. 3 and 5%) although resulted in higher compressive strengths, but the changes are not substantial. Strength gain by all samples mainly occurred during the first 28 days of curing and remained almost constant from 28 to 90 days. Considering the results, 20% BOS slag seem to be the optimum content for the kaolinite examined. The changes observed in this investigation are slightly different to the results reported by Poh et al. [23]. Although they also reported increase in strength by adding BOS slag

fines to English China Clay and Mercia Mudstone, it was stated that strength gain showed continuing even after 90 days of curing. The difference in observations are attributed to the fact that Poh et al. [23] used ground BOS slags with particles finer than 63 μm compared to 420 μm minor particles used in this investigation. The finer slag particles probably promoted more extensive chemical reactions, taking longer to complete. Addition of 10, 15 and 20% BOS slag respectively resulted in 227, 331 and 404% improvement in strength after 90 days curing (see Table 3).

5.1.3. Lime/BOS slag treated samples

Figure 3 shows the effects of 10, 15 and 20% BOS slag addition on strength development of lime stabilized kaolinite samples. Concurrent addition of lime and BOS slag to kaolinite samples resulted in enhanced UCS compared to UCS of samples treated with only lime or BOS slag. Lime acts as an activator increasing the hydration of BOS slag which can be distinguished by comparing their UCS with the UCS of lime only treated samples. Kaolinite samples treated with higher percentages of lime and BOS slag, displayed substantially higher UCS. Figure shows that even after 90 days of curing the gain in UCS of samples treated with 3 and 5% lime is still continuing. The UCS and the associated percentage increases after 90 days of curing compared with untreated kaolinite are presented in Table 3. Poh et al. [23] reported greater improvements in UCS development by using quicklime. In the current investigation greater UCS enhancement might have been reached if CaO instead of Ca(OH)2 and BOS slag in powder form were used.
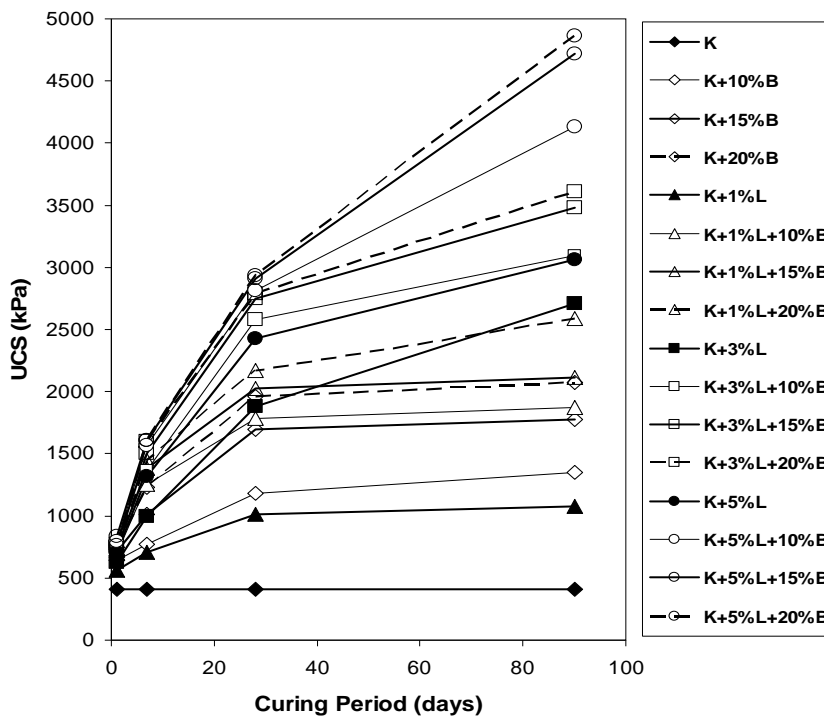
Figure 3: UCS versus curing period for untreated , lime , BOS slag and lime + BOS slag treated kaolinite

5.2. Durability

5.2.1. Lime/BOS slag addition

Effects of concurrent addition of lime and BOS slag on durability of kaolinite are presented in Figures 4(a) and (b). Each figure shows the results for a particular curing period (i.e. 7and 28 days). Figure 4(a) shows that apart from the sample stabilized with only 1% lime, all other samples showed good resistance to 4 cycles of F/T. The positive effects of lime/BOS slag addition on durability of kaolinite became intensified at longer curing periods (i.e. Fig. 4(b)). Generally the higher the initial UCS, the higher the residual strengths after F/T which is a function of both lime and BOS slag content as well as the curing period. Samples stabilized with 3 and 5% lime and treated with 10, 15 and 20 % BOS slag showed the same trend of changes as mentioned above but of different magnitude. Using higher lime contents combined with BOS slag significantly improves kaolinite resistance to freezing and thawing which is attributed to the formation of more extensive cementitious reaction products. These products not only

change the nature of clay particles through modification but also bind the particles promoting greater resistance to deteriorating effects of ice formation.

Summary of the UCS results determined before and after conducting freeze/thaw tests with durability index (i.e. Di) are presented in Table 4. It can be seen that for kaolinite samples treated with a certain percentage of BOS slag, increasing lime content resulted in enhancing the durability index, "Di". For example, for the K+10%B mixture stabilized with 1, 3 and 5% lime and cured for 1-day, durability indices of 0.48, 0.60 and 0.71 were respectively determined. The higher the durability index, the greater the resistance of a sample to the deteriorating effects of F/T. Considering that the durability index for untreated kaolinite is "zero", the overall conclusion drawn is that the addition of lime and BOS slag to kaolinite either singularly or in combination significantly increases its durability. The durability enhancement is a function of lime and BOS slag content as well as curing period. Poh et al. [22] also reported that durability index in terms of "soaked UCS / unsoaked UCS" for ECC and MM to increase when treated with BOS slag. The amount of improvement was stated to be function of the slag type.

Table 4: UCS of 90 day cured samples before and after freezing with durability index, Di

C/P (days)	IUCS (kPa)	FUCS (kPa)	Di	IUCS (kPa)	FUCS (kPa)	Di	IUCS (kPa)	FUCS (kPa)	Di
	K+1%L+10%B			K+3%L+10%B			K+5%L+10%B		
1	700	333	0.48	740	459	0.60	792	561	0.71
7	1252	432	0.36	1368	729	0.53	1569	989	0.63
28	1785	543	0.30	2579	1361	0.53	2810	1949	0.69
90	1872	591	0.32	3091	1496	0.48	4130	2131	0.52
	K+1%L+15%B			K+3%L+15%B			K+5%L+15%B		
1	740	366	0.49	770	496	0.64	836	566	0.68
7	1384	613	0.44	1504	733	0.49	1608	1002	0.62
28	2029	951	0.47	2746	1451	0.53	2909	1986	0.68
90	2112	1101	0.52	3480	1790	0.51	4714	2529	0.54
	K+1%L+20%B			K+3%L+20%B			K+5%L+20%B		
1	723	417	0.58	744	522	0.70	766	613	0.80
7	1444	631	0.44	1600	891	0.56	1608	1157	0.72
28	2172	1333	0.61	2790	1674	0.60	2937	2107	0.72
90	2586	1428	0.55	3606	1883	0.52	4861	2671	0.55
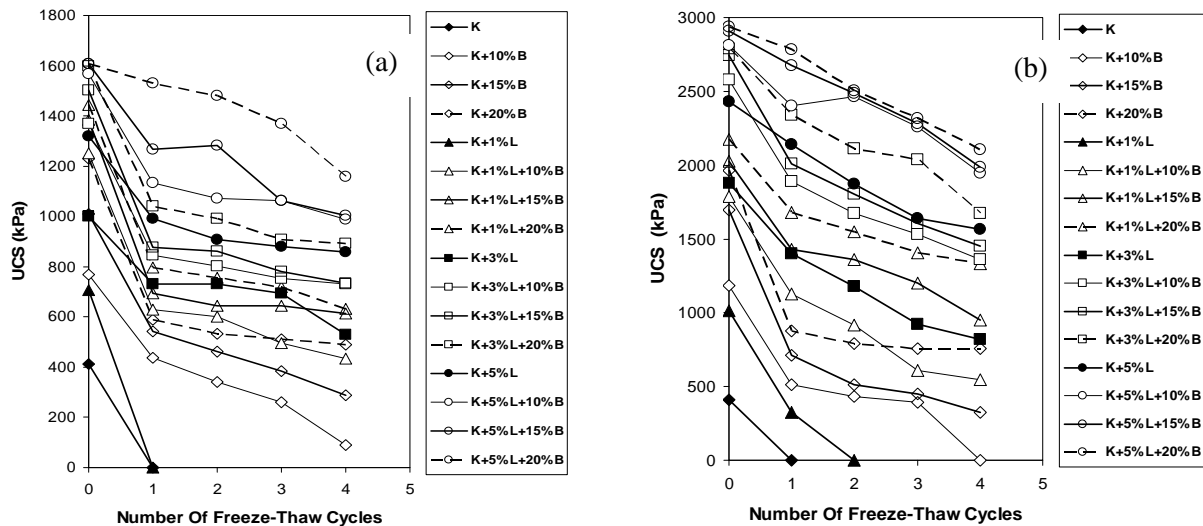
Figure 4: UCS versus Number of freeze – thaw cycles for untreated, lime treated, BOS slag treated and BOS slag/lime treated kaolinite cured for (a) 7-days, (b) 28-days

6.   CONCLUSIONS

Results of the investigation showed that using lime and BOS slag either singularly or concurrently for stabilizing kaolinite improves soil properties in terms of increased UCS and durability by resistance to freezing and thawing. The improvements are shown to be dependent on the lime and the BOS slag contents as well as the curing period. Use of these additives for stabilizing kaolinite initiated short term

"modification" (i.e. reduced plasticity) and long term "pozzolanic" (i.e. increased strength) reactions which occur concurrently.

In general, lime proved to be a more effective additive in stabilizing kaolinite compared to BOS slag. Their concurrent addition significantly enhanced strength development and resistance to freezing and thawing. These improvements are mainly attributed to the additional modification and pozzolanic reactions between the CaO content of lime and BOS slag and the clay minerals. Breakup of the Si-O and Al-O layers as suggested by Poh et al. [23] may also contribute to the changes. Reactions between the silica and the alumina present in the clay particles and lime or BOS slag cause the formation and growth of cementitious products such as calcium silicate and aluminate hydrates (i.e. C-S-H, C-A-H and C-A-S-H). These compounds affect not only strength development but also permeability and subsequently resistance to F/T. The improvement in frost resistance of kaolinite when treated with lime or BOS slag is not principally a function of changes in porosity but is predominantly due to the development of inter-particle bonding and strength. Particle bonding is influenced by the amount of reaction products which is a function of the lime and the BOS slag contents, the amount of silica and alumina present in the mixture as well as the curing period. XRD analysis of BOS slag showed the presence of mineral phases C_3S, C_2S, C_4AF, and C_2F which also comprise OPC. These indicate that BOS slag possesses some of the cementitious properties of OPC.

Considering the overall results, there is potential for using BOS slag as a stabilizer for fine-grained soils. Whenever an improvement in strength and frost resistance of road materials such as sub-grade or sub-base is required, BOS slag stabilization should be considered as an appropriate alternative. It would be more effective as a stabilizer if used in conjunction with lime.

REFERENCES

[1] *Abdi, M. R.: 1991, Effects of calcium sulphate on lime stabilized kaolinite, PhD Thesis, University of Glamorgan, Wales, U.K.*

[2] *Allen, J. J., Currin, D. D. and Little, D. N.: 1977, Mix design, durability and strength requirements for lime-stabilized layers in airfield pavements, Transport Res. No. 641.*

[3] *Altun, I. A. and Yilmaz, I.: 2002, Study on steel furnace slags with high MgO as additives in Portland cement, Cement and Concrete Research, No. 32, 1-3.*

[4] *Arabi, M.: 1987, Lime stabilization of clays, PhD Thesis, University of Glamorgan, Wales, U.K.*

[5] *Baghdadi, Z. A., and Shibata, S. A.: 1999, On durability and strength of soil-cement, Journal ISSMF, Ground improvement, 3(1), 1-6.*

[6] *Barret, P., Menetrier, D. and Cottin, B.: 1977, Study of silica-lime solution reactions, Cement and Concrete Research, Vol. 7, No. 1, 61-68.*

[7] *Bernard, D., Alkire, M. and Jashimuddin, J.: 1984, Freeze-thaw durability of lime stabilized clay soils, Journal of Technical Topics in Civil Eng., ASCE, Vol.110, No.1.*

[8] *Collins, R. J. and Ciesielski, S. K.: 1994, Recycling and reuse of waste material and by-products in highway construction, National Cooperative Highway Research Program Synthesis of Highway Practice 199, Transportation Research Board, Washington, DC.*

[9] *Croft, J. B., (1964), The processes involved in the lime-stabilization of clay soils, Australian Road Research Board, Proc., 2nd Conf. Vol. 2, Part 2, 1169-1200.*

[10] *Dempesy, B. J. and Thompson, M. R.: 1973, Vacuum saturation method for predicting freeze/thaw durability of stabilized materials, Highway Res. Rec. No. 442.*

[11] *Eades, J. L. and Grim, R. E.: 1960, Reaction of hydrated lime with pure clay minerals in soil stabilization, Highway Research Board, Bull. No. 262, 51-63.*

[12] *Emery, J. J.: 1982, Slag utilization in pavement construction extending aggregate resources, ASTM Special Technical Publication 774, American Society for Testing and Materials, Washington, DC.*

[13*] Esmer, E., Walker, R. D. and Krebs, R. D.: 1969, Freeze-thaw durability of lime-stabilized clay soils, Highway Res. Rec. No. 263.*

[14] *JEGEL, 1993, Steel slag use in hot mix asphalt concrete, Final report, prepared by John Emery Geotechnical Engineering Limited for the Steel making Slag Technical Committee, April.*

[15] *Kawamura, M. and Diamond, S.: 1975, Stabilization of clay soils against erosion loss, Clay and Clay Minerals, Vol. 23, 444-451.*

[16] *Khan, M. A., Usmani, A., Shah, S. S., and Abbas, H.: 2008, A study of multilayer soil-fly ash layered system under cyclic loading, Int. Journal of Civil Eng., Vol. 6, No. 2, 73-89.*

[17] *Lea, F. M.: 1970, The chemistry of cement and concrete, 3rd Edition, Edward Arnold, London.*

[18] *Lee, R. A.: 1974, Blast furnace and steel slag: Production, properties and uses, Edward Arnold, London.*

[19] *Murphy, J. N., Meadowcroft, T. R., and Barr, P. V.: 1997, Enhancement of the cementitious properties of steelmaking slag, Can. Metall. Q., 36(5), 315-331.*

[20] *Noble, D. F.: 1967, Reactions and strength development in Portland cement-clay mixture, Highway Research Record No. 198, 39-56.*
[21] *Noureldin, A.S., and McDaniel, R.S.: 1990, Evaluation of steel slag asphalt surface mixtures, Presented at Transportation Research Board 69th Annual Meeting, Washington, DC, January.*

[22] *Proctor, D. M., Fehling, K. A., Shay, E. C., Wittenborn, J. L., Green, J. J., Avent, C., Bigham, R. D., Connolly, M., Lee, B., Shepker, T. O. and Zak, M. A.: 2000, Physical and chemical characteristics of blast furnace, basic oxygen furnace, and electric arc furnace steel industry slags, Environmental Science and Technology, Vol. 34, No. 8.*

[23] *Poh, H. Y., Ghataora, G. S., and Ghazireh, N.: 2006, Soil stabilization using basic oxygen steel slag fines, Journal of Materials in Civil Engineering, ASCE, March/April, 229-240.*

[24] *Wild, S., Kinuthia, J. M., Jones, G. I., and Higgins, D. D.: 1998, Effects of partial substitution of lime with ground granulated blast furnace slag (GGBS) on the strength properties of lime-stabilized sulphate-bearing clay soils, Engineering Geology, Volume 51, Number 1, November, 37-53(17).*

Effectiveness of lime stabilisation in organic clay

Mohd Yunus, N. Z., University of Nottingham, United Kingdom, E-mail: evxnzm@nottingham.ac.uk
Wanatowski, D., University of Nottingham, United Kingdom, E-mail: dariusz.wanatowski@nottingham.ac.uk
Stace, L. R., University of Nottingham, United Kingdom, E-mail: rod.stace@nottingham.ac.uk

ABSTRACT

The presence of organic matter is one of the most important factors affecting the effectiveness of lime stabilisation of clays. It was reported in the literature that humic acid is the main constituent of organic matter responsible for reducing the strength of lime stabilised organic clay. However, the effects of humic acid content on the lime stabilisation process of organic clay are not fully understood. In this paper, an investigation on the effects of humic acid content on the strength of lime-stabilised organic clay is presented. Artificial organic clay with different humic acid contents of 0.5%, 1.5% and 3.0% was stabilised with 5%, 8%, 10% and 15% of hydrated lime. The strength of the lime-treated organic clay was analysed using the Unconfined Compression Strength (UCS) tests at different curing periods. The results showed that the UCS of untreated organic clay was affected by the presence of humic acid and the improvement of strength in the lime-stabilised clay with high humic acid content was not very successful. However, the experimental results also showed that the effectiveness of lime stabilisation in organic clay can be improved by addition of small amount of chloride salts.

1. INTRODUCTION

The use of lime as a stabilising agent, mainly in clayey soils, has been widely known for decades. The availability and cost make lime a very popular chemical additive in soil stabilisation methods. It is well recognised that lime stabilisation increases shear strength of soil and reduces potential for soil settlement (e.g. Sherwood 1993; Bell 1996; Moseley & Kirsch 2004; James et al. 2008).

However it was reported that the shear strength of organic clay was affected by the presence of organic matter in lime-soil solution (Huat et al. 2005; Chen & Wang, 2006; Koslanant et al. 2006; Chen et al. 2009). The presence of organic matter has a tendency to coat the soil particles making it difficult for lime to come in contact with clay minerals. Furthermore, it appears that organic matter reduces the pH value to the point where dissolution of clay minerals no longer takes place, which obstructs pozzolanic reaction during lime stabilisation. Humic acid was identified as the main compound that could detriment the hardening of the lime-clay reaction (Clare & Sherwood 1956; Onitsuka et al. 2002; Tremblay et al. 2002; Zhu et al. 2009). This suggests that for the purpose of lime stabilisation it is more important to determine the amount of this organic compound rather than the total amount of organic matter in clay. For example, Koslanant et al. (2006) and Harris et al. (2009) reported that the presence of at least 1% humic acid in clay can retard the pozzolanic reaction and lead to unsuccessful lime stabilisation of clay.

Due to the disadvantages of humic acid, salts are recommended as additives for stabilisation of organic clay when the required shear strength cannot be obtained with lime alone. A small percentage of a salt can develop an additional strength of lime treated organic clay due to formation of highly hydrated silicate gels and a marked increase in the sodium-calcium ratio in soil (Ramesh et al. 1999; Onitsuka et al. 2003; Koslanant et al. 2006; Murty & Krishna 2006; Abood et al. 2007; Sharma et al. 2008; Manchikanti & Raju 2008; Davoudi & Kabir 2011; Kazemian et al. 2011).

This paper presents the experimental study carried out on artificial organic clay with different humic acid contents. The effects of humic acid on the strength of organic clay are investigated. In addition, a preliminary investigation on the influence of salts (calcium chloride and sodium chloride) on the effectiveness of lime stabilisation of organic clay is reported. The results of laboratory tests are discussed and verified with microstructure analysis carried out on selected clay specimen using the Scanning Electron Microscope (SEM).

2.   SOIL TESTED

An artificial organic clay was used in this research. The soil samples were prepared by mixing commercial kaolin with different percentages of commercial humic acid powder (0%, 0.5%, 1.5% and 3%) according to dry mass of kaolin. Table 1 summarizes chemical composition of organic clay with different humic acid contents. In general, the presence of humic acid in soil can be identified from the existence of carbon and oxide ions based on chemical element analysis. It can be seen from Table 1 that the total amounts of carbon and oxide ions increase with increasing humic acid content. In addition, the presence of humic acid can be identified by the increase in total amount of sulphur and phosphorus. As a result, the amount of pozzolan minerals such as silica and alumina decreases with an increase of humic acid content.

Table 1: Chemical composition of artificial organic clay with different humic acid contents

Element	Wt (%)		
	Kaolin with 0.5% humic acid	Kaolin with 1.5% humic acid	Kaolin with 3.0% humic acid
C	2.80	2.74	20.16
O	50.45	54.54	48.97
Na	0.36	0.41	0.81
Mg	0.65	0.64	0.56
Al	16.94	18.47	12.8
Si	24.74	21.52	14.07
P	0.18	0.28	0.16
S	0.05	0.12	0.42
Cl	0.00	0.01	0.19
K	3.42	0.79	0.59
Ca	0.02	0.04	0.33
Ti	0.00	0.02	0.18
Fe	0.39	0.40	0.74

The physical properties of the artificial organic clay are summarized in Table 2. It can be seen that the specific gravity of clay prepared with humic acid is low when compared to inorganic kaolin clay. As shown in Table 2, the liquid limit of clay decreased with increasing humic acid content whereas the plastic limit increased with increasing humic acid content. As a result, the Plasticity Index was reduced with increasing humic acid content. Table 2 also shows that the maximum dry density of organic clay decreased as the humic acid content increased.

Table 2: Physical properties of organic clay with different humic acid contents

Index Properties	Kaolin	Kaolin with 0.5% humic acid	Kaolin with 1.5% humic acid	Kaolin with 3.0% humic acid
Liquid limit (%)	65	64	63	61
Plastic limit (%)	30	33	34	35
Plasticity Index (%)	35	31	29	26
Specific gravity	2.61	2.53	2.51	2.47
pH	5.52	5.34	5.16	5.07
Optimum moisture content (%)	30.6	30.9	30.6	33.4
Maximum dry density (kg/m^3)	1440	1429	1425	1404

3.   SPECIMEN PREPARATION

All the soil specimens tested in this study were prepared using standard procedures described in the ASTM and British Standards (ASTM D3551-02, ASTM D5102-96, and BS-1377). As recommended by the standards, before mixing, the specimens were oven-dried at 60°C until the constant weight was obtained. All the specimens of untreated clay tested in this study were prepared by mixing relevant amounts of dry kaolin with 0.5%, 1.5%, and 3% of humic acid by dry mass of kaolin. Mixing of dry materials was continued until a uniform appearance of the kaolin-humic acid mixture was obtained. Water was then added and further mixing was performed until a homogeneous appearance of the soil paste was achieved. This paste was then used for plasticity and compaction tests.

The results obtained from the compaction tests were used to prepare specimens for strength testing. Each of the specimens of lime-treated organic clay was prepared according to the maximum dry density (MDD) and optimum moisture content (OMC) of the untreated clay with corresponding humic acid content. By knowing the volume of mould and the MDD, the required dry mass of soil was calculated. The appropriate quantity of hydrated lime was then calculated based on the dry mass of the untreated soil. Then, these amounts of dry soil and dry lime were mixed with water according to the OMC. For specimens stabilized with lime and salt additives i.e., calcium chloride ($CaCl_2$) and sodium chloride (NaCl), 0.5%, 2%, or 5% of a salt was added at this stage. The process of mixing was conducted as quickly as possible to ensure that lime was not exposed to air for too long. This was necessary to avoid the carbonation process that could affect the strength characteristics of lime-treated specimens.

The specimens were compacted into the mould at a specified moisture content to achieve the specified dry density. A small amount of grease was applied inside the mould to minimize friction. The specimens were then extruded from the mould and wrapped in cling film to preserve the water content and to keep them free from carbon dioxide (CO_2). The specimens were cured in desiccators at 20°C and with humidity more than 90% for 7, 28, and 90 days. The specimens were 76 mm in height and 38 mm in diameter.

4.   RESULTS AND DISCUSSIONS

The shear strength of untreated (artificial organic clay) and treated (lime-treated and lime-salt treated) specimens were determined by the Unconfined Compressive Strength (UCS) test. Microstructure analysis was also performed on selected specimens to verify results obtained from the UCS testing.

Firstly, the effect of humic acid content on the undraied shear strength of untreated organic clay was investigated to obtain benchmark data for comparison with lime-treated organic clay. Figure 1 shows the relationship between the undrained strength (Su) of clay and the humic acid content. The Su values were determined as the half of the UCS values. It can be seen from Figure 1 that the shear strength of organic clay decreases with increasing humic acid content. For instance, the organic clay with 3% humic acid content experienced the strength loss of about 44.6% compared to inorganic clay (i.e., with 0% humic acid content).
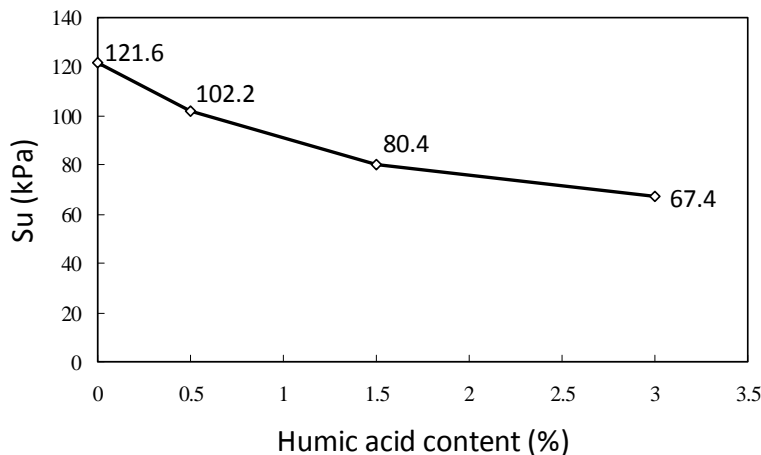
Figure 1: Effect of humic acid content on the shear strength of organic clay.

In order to examine the effectiveness of lime stabilisation in organic clay, several UCS tests on lime-treated organic clay were also carried out. However, an appropriate amount of lime to be added was first determined by means of the initial consumption lime (ICL) test. The ICL value is defined as the minimum amount of lime in a treated-clay required to provide a pH of 12.40 (BS 1924). This is essential to ensure that the amount of lime added to organic clay is sufficient for the occurrence of modification and stabilization processes. Results obtained from the ICL tests on organic clay with different humic acid contents showed that approximately 2% of lime was needed to achieve pH of 12.4 regardless of the humic acid content (Mohd Yunus et al. 2011). However, more than 2% of lime is normally required to ensure a long term strength gain achieved from the lime stabilization process (Clare and Sherwood 1956; Huat et al. 2005; Harris et al. 2009). Therefore, 5% was chosen as the minimum lime content for stabilisation of the soil tested in this study. In addition, organic clay was stabilized with 8%, 10% and 15% of lime to analyze the effect of lime content on the shear strength of lime-treated organic clay.

The results of the UCS tests carried out on lime-treated organic clay with different humic acid contents (0%, 0.5%, 1.5%, 3%) and lime contents (5%, 8%, 10%, 15%) at 7 days are shown in Figure 2. It can be seen from Figure 2 that the undrained shear strength of all the specimens with 5% lime content increased significantly compared to the strength of untreated clay (i.e., 0% lime). However, the shear strength of specimens with higher than 5% lime contents reduced gradually with increasing lime content regardless of the humic acid content in the clay. Therefore, 5% was considered as the optimum lime content (OLC) for each type of organic clay tested in this study. Figure 2 also shows that the shear strength of organic clay decreases with increasing humic acid content which proves that the presence of humic acid in organic clay diminishes the shear strength. The results presented in Figure 2 suggest that the shear strength of organic clay can be improved efficiently by means of lime stabilisation.
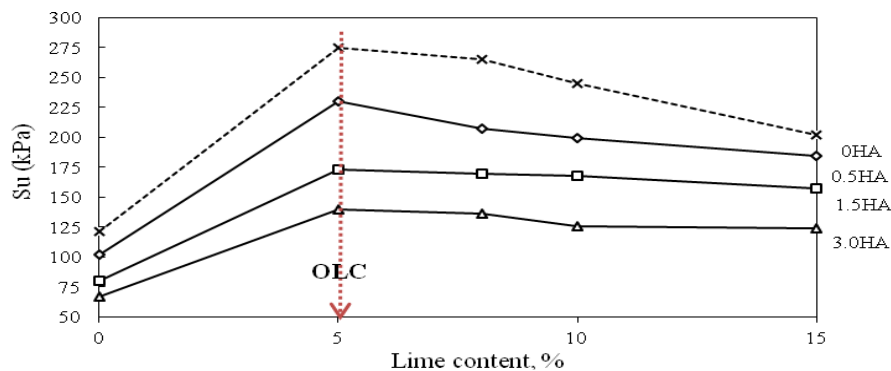
Figure 2: Effect of lime content on the undrained shear strength of clay at 7 days of curing.

Since the OLC of 5% determined after 7 days of curing was identical for each type of organic clay, further investigation of the development of lime-clay reactions with time was focused on 5% lime content. Figure 3 presents the values of the undrained shear strength of lime-treated specimens after 7, 28 and 90 days of curing.

Figure 3: Effect of curing period on the undrained shear strength of lime-treated organic clay.

It is evident from Figure 3 that the undrained shear strength of lime-treated organic clays with 0.5%, 1.5% and 3.0% humic acid contents decreases with increasing curing time. For example, the shear strength of specimens with 0.5%, 1.5% and 3.0% humic acid contents reduced from 230 kPa, 174 kPa and 140 kPa at 7 days to 212 kPa, 130 kPa and 96 kPa at 90 days of curing. This is oposite to the behaviour of inorganic koalin clay (i.e. 0% humic acid), in which the shear strength increased with increasing curing period, as shown in Figure 3.

It should be pointed out that despite exhibiting the loss in strength at longer curing periods, the undrained shear strengths of lime-treated organic specimens at 90 days are still higher than those of untreated specimens (see Figure 1). However, from practical point of view, lime stabilisation cannot be considered as a potential improvement method for organic clays, if the shear strength of lime-treated organic clay is uncertain in long term.

In other to illustrate more clearly the long term effect of humic acid on the strength of organic clay, the results obtained from the UCS tests were presented in terms of strength loss in Figure 4. the strength loss (%) was calucalted according to Equation (1).

$$\text{Strength loss} = \frac{Su_{7d} - Su_{id}}{Su_{7d}} \ 100\% \tag{1}$$

where Su_{7d} is the undrained shear strength at 7 curing days for each humic acid content and Su_{id} is the undrained shear strength at other curing periods (i.e. 28 or 90 days) for each humic acid content.

The experimental results plotted in Figure 4 show that the strength losses from 7 to 90 days for kaolin prepared with 0.5%, 1.5% and 3% humic acid contents were about 4.1%, 13.4% and 14.4%, respectively. Meanwhile, the total strength losses of the same clays from 7 to 90 days were 7.8%, 25.1% and 31.7%, respectively. Thus, the strength loss increased with increasing humic acid content and with increasing curing period. Figure 4 also shows that the strength loss is more significant for higer humic acid contents. A slight loss in strength was observed for organic clay with 0.5% of humic acid, while a substantial loss in strength could be seen for clays with 1.5% and 3% of humic acid. The results shown in Figure 4 clearly demonstrate that lime stabilization of organic clay with high humic acid contents is not very efficient in long term. Similar observations were reported by other researchers (Koslanant et al. 2006; Harris et al. 2009; Zhu et al. 2009). As mentioned earlier, this behaviour is different from that observed for lime-stabilised inorganic clays, where the shear strength increases with curing time (Bell, 1996; James et al. 2008).

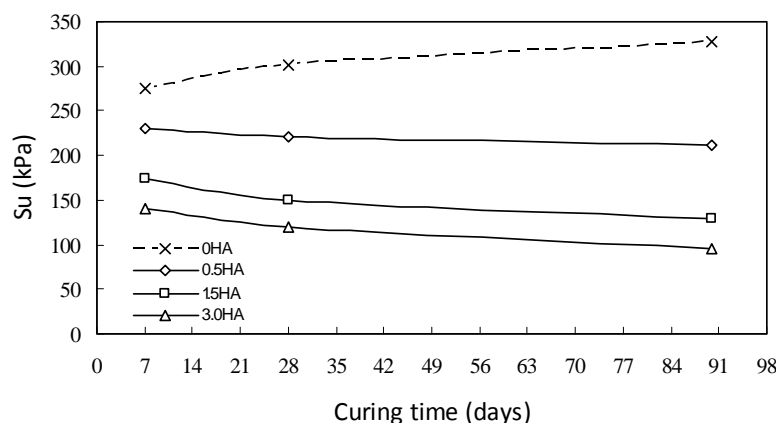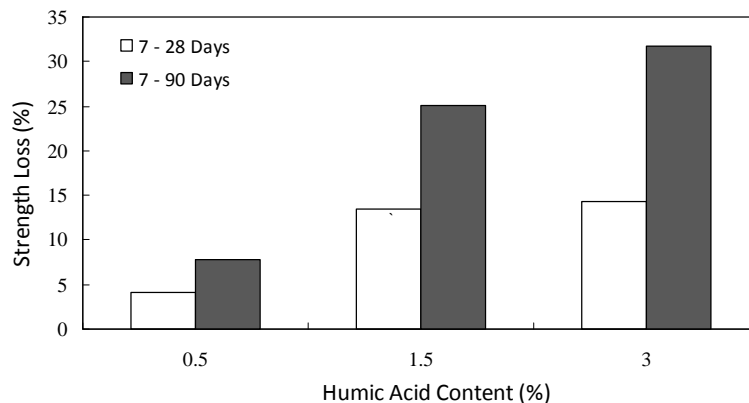*Figure 4: Strength loss of lime-treated organic clay with different humic acid contents.*

Selected specimens of untreated and lime-treated organic clay sheared in the UCS tests were also analysed in the scanning electron microscope (SEM). An example of SEM micrograph of untreated organic clay with 1.5% of humic acid is shown in Figure 5. Some cracks can be observed on clay particles, as shown in Figure 5. Such cracks were more noticeable in clay with 3% humic acid content but were not present in clay specimens with 0% and 0.5% humic acid contents (Mohd Yunus et al. 2011). The occurrence of cracks on individual particles suggests that the breakage of particles took place during shearing due to obstruction of humic acid.
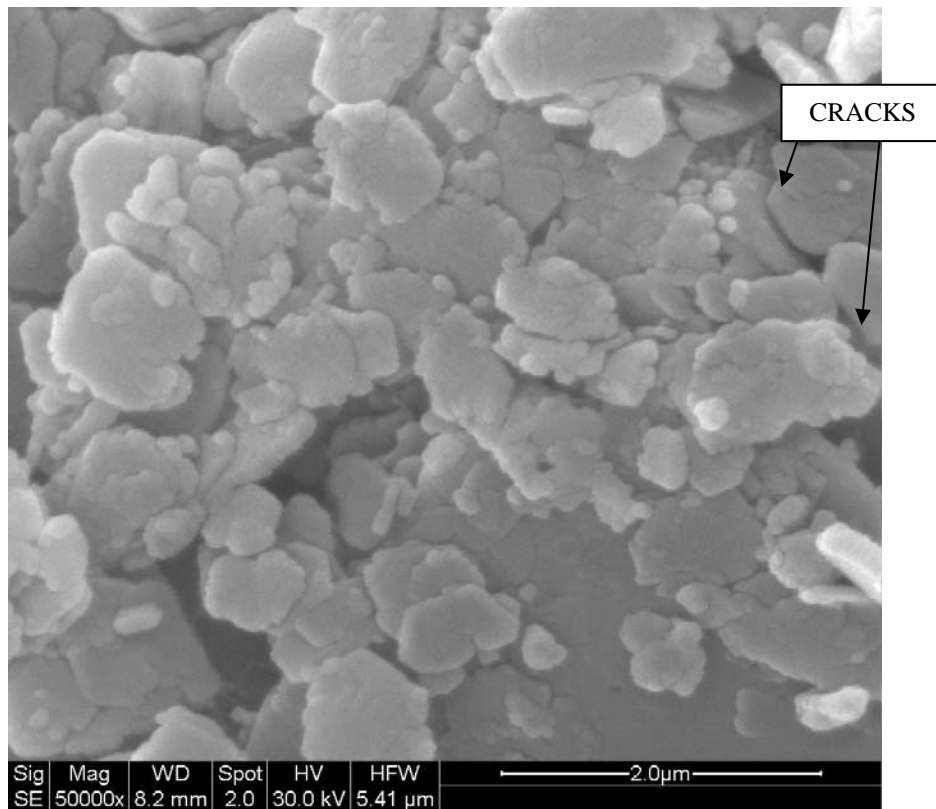
Figure 5: SEM micrograph of untreated clay with 1.5% humic acid content.
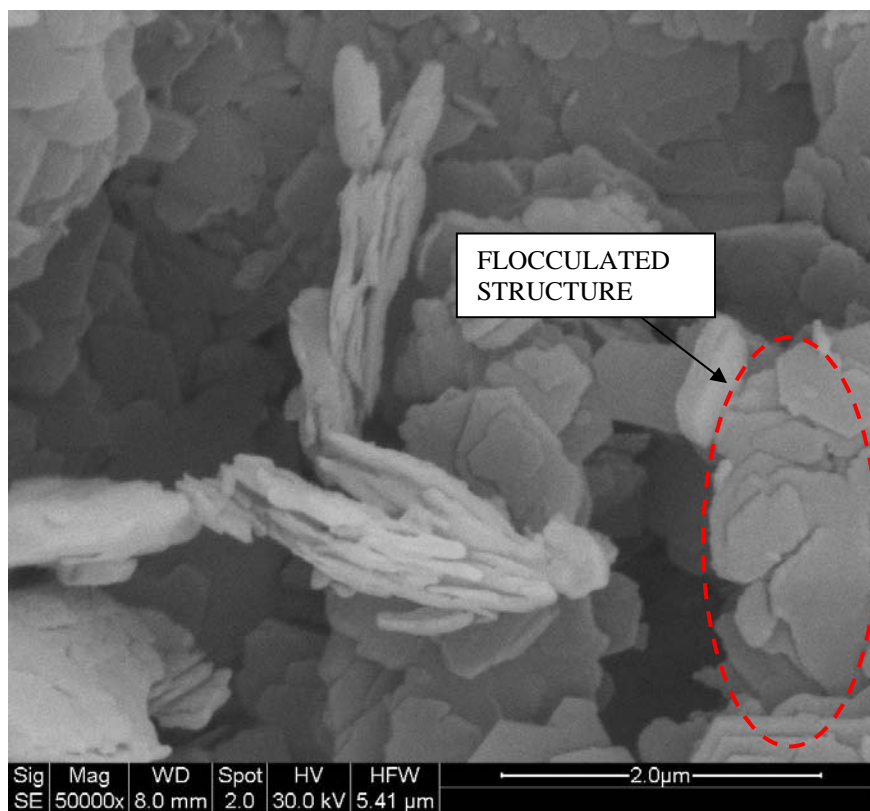
Figure 6: SEM micrograph of lime-treated organic clay with 1.5% humic acid content.

The SEM micrograph of the specimen with 1.5% of humic acid treated with 5% of lime and cured for 28 days is shown in Figure 6. The duration of 28 days curing period represents stabilization process. Therefore, it is expected that cementing products such as Calcium Silicate Hydrate (CSH) and Calcium

Aluminate Hydrate (CAH) are fully formed in the soil structure. Unfortunately, even after being treated with 5% lime content, the image revealed no significant cementing structure in the specimen. On the other hand, as a result of lime stabilisation, the crack appearance was reduced and well flocculated structure, where particles clump to each other to form bigger units (i.e. aggregate), was observed in the lime-treated specimen, as shown in Figure 6. The SEM micrographs shown in Figures 5 and 6 confirm that the effect of lime in organic clays was limited to modification process, which alters only physical structure of soil. The long term stabilisation process was obstructed by the presence of humic acid. This could be the reason why the shear strength of lime-stabilised organic clay reduced at longer curing periods.

The findings obtained from experiments on lime-treated organic clay revealed that lime may not be a suitable for stabilising organic clay with more than 1.5% humic acid content. Although the shear strength was still higher than that of untreated organic clay, the improvement in long term was not very successful. However, other binders or additives can be introduced to eliminate detrimental effects of humic acid (Harris et al. 2005, Koslanant et al. 2006; Zhu et al. 2009). In this study, two chloride salts (calcium chloride ($CaCl_2$) and sodium chloride (NaCl)) were considered as potential additives that could improve the effectiveness of lime stabilisation in organic clay. The analysis was carried out for the clay with 1.5% humic acid content stabilised with 5% of lime.

The results of the UCS tests carried out on lime-stabilised organic clay with addition of calcium chloride ($CaCl_2$) and sodium chloride (NaCl) at 7 and 28 days are shown in Figure 7(a) and 7(b), respectively. It can be observed from Figure 7 that the strength of lime-treated clay with salt additives increases from 7 to 28 days for both types of salts, which is a good indicator of effectiveness of this improvement method. However, it appears that the undrained shear strength reduces with increasing salt content. This suggests that 0.5% is the optimum salt content for the organic soil tested in this study. These observations are consistent with previous studies by Danmarks & Haliburton (1999), Davoudi & Kabir, (2011), Kazemian et al. (2011) who suggested that the influence of salts to gain additional increase in strength of lime-treated specimens was only effective when low quantity of salts was added to the soil. On the other hand, the results presented in Figure 7 are in contrast to those obtained by Onitsuka et al. (2002), Koslanant et al. (2006), and Abood et al. (2007) who reported that the strength of lime-stabilised organic clay increased with salt contents.

(a)   *(b)*
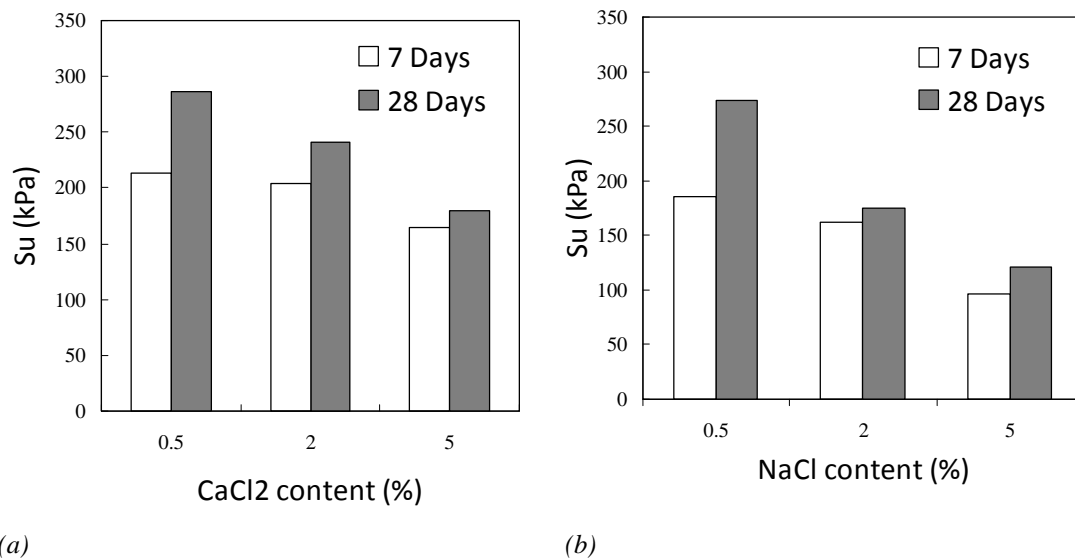
Figure 7: Effect of salt content on the undrained shear strength of lime-treated organic clay at different curing periods: (a) Calcium chloride, (b) Sodium chloride.

The effectiveness of lime stabilisation of organic clay with salt additives is investigated further in Figure 8, where the undrained shear strength values obtained from specimens with different types of salt are compared at the same curing periods. The results obtained at 7 days and 28 days of curing are plotted in Figures 8(a) and 8(b), respectively. The undrained shear strengths of lime-treated specimens without salts additives, determined at 7 days (174 kPa) and 28 days (150 kPa) of curing, are also shown in Figures 8(a) and 8(b), respectively.
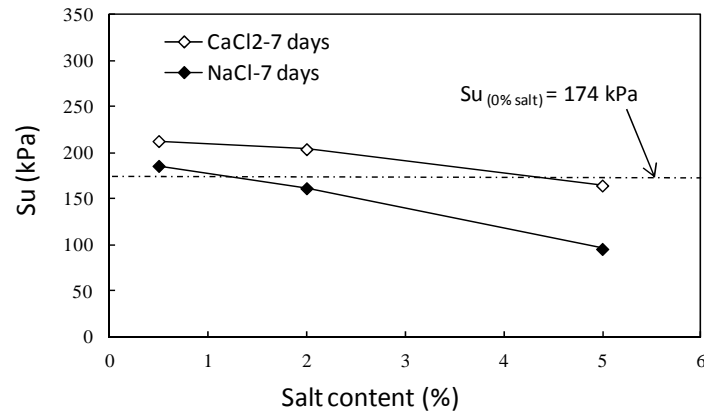
(a)
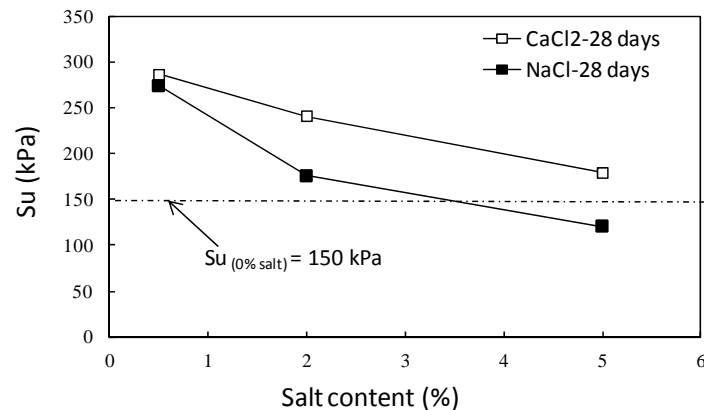
(b)

Figure 8: Comparison of undrained shear strengths of specimens stabilised with lime and chloride salts at different curing periods: (a) 7 days, (b) 28 days.

It can be observed from Figure 8 that the strength of lime-treated clay stabilised with $CaCl_2$ was higher than that of clay stabilised with NaCl, both at 7 and 28 days or curing. However, as mentioned before, the undrained shear strength reduced with increasing salt content. Figure 8(a) shows that the addition of 0.5% and 2.0% of $CaCl_2$ and 0.5% of NaCl increases the strength of lime-treated organic clay after 7 days of curing. On the other hand, an additional 2% and 5% of $CaCl_2$ or 5% of NaCl in specimens resulted in the strength lower than that of specimens without any salts. Similar observations were reported by Sharma et al. (2008). Nonetheless, with longer curing time, chloride salts successfully improved the shear strength of lime-stabilised organic clay, except for 5% of NaCl, as shown in Figure 8(b).

The results presented in Figure 8 agree well with analysis carried out by Modmoltin & Vootipruex (2009). They reported that the dual function of Ca^{2+} ions promotes better ion exchange activity and contributes more significantly towards formation of cementing products such as CSH and CAH. Na^+ ions, on the other hand, can only accelerate dissolution of silica (Danmarks & Haliburton, 1999; Koslanant et al. 2006; Modmoltin & Vootipruex, 2009). It is also possible that the effect of chloride salts on the shear strength of lime-stabilised organic clay may be related to the charge balance on the clay particle surfaces. Clay surfaces are known to be negatively charged thus may attract the cations from salts. Excessive calcium and sodium ions from lime and chloride salts may create an unbalanced net charge. The excessive positive charge that does not participate in cation exchange activity will be scattered on surrounding clay. Consequently, the clay particles may be dispersed, leading to deflocculating of large aggregates and reduction of the shear strength due to the presence of large amount of $CaCl_2$ and NaCl. However, further investigation is required to fully understand the way in which the chloride salts affect the behaviour of lime-stabilised organic clay.

5.   CONCLUSIONS

In this paper, the effectiveness of lime stabilisation of organic clay was investigated. The influence of salts on the strength of lime-treated organic clay was also analysed. Based on the experimental results obtained in the study, the following conclusions can be made.

1. The shear strength of lime-treated organic clay reduced when the lime content exceeded 5%. Thus, 5% of lime was identified as the optimum lime content (OLC) for the organic clay tested in this study.
2. The shear strength of the lime-treated organic clay reduced at longer curing periods. The total strength loss determined between 7 and 90 days of curing was 7.8%, 25.1% and 31.7%, for clay with 0.5%, 1.5%, and 3% humic acid, respectively. These results show that the presence of more than 1.5% humic acid in the organic clay reduces significantly the efficiency of lime stabilisation process.
3. The SEM images of lime-treated organic clay revealed the appearance of well aggregated microstructure created during stabilization process. However, a significant number of cracks were detected in clay with higher humic acid contents. In addition, large voids between aggregates were detected in organic clay with 1.5% and 3% of humic acid. This may explain why the undrained shear strength of lime-treated organic clay reduces with increasing humic acid content.
4. The results obtained from the UCS tests carried out on specimens with 1.5% of humic acid treated with 5% of lime show that the strength of lime-treated organic clay can be successfully improved with addition of 0.5% of chloride salts. Therefore, there is a real potential for the use of chloride salts in lime stabilisation of organic clay in geotechnical practice. However, further study is required to understand chemical reactions that occur between clay, humic acid, lime and salts during stabilisation process in order to provide specific recommendations on types and amounts of salts that need to be used to optimise design and construction procedures.

REFERENCES

Abood, T. T., Kasa, A. and Chik, Z., 2007, Stabilisation of silty clay using chloride compunds, Journal of Engineering Science and Technology, Vol. 2, No. 1, pp. 102-110.

ASTM Standard D3551-08, 2008, Standard Practice for Laboratory Preparation of Soil-Lime Mixtures Using Mechanical Mixer, Annual Book of ASTM Standards, Vol. 04.08, ASTM International, West Conshohocken, PA.

ASTM, Standard D5102-96, 2004, Standard Test Method for Unconfined Compressive Strength of Compacted Soil-Lime Mixtures, Annual Book of ASTM Standards, Vol. 04.08, ASTM International, West Conshohocken, PA.

Bell, F. G., 1996, Lime stabilization of clay minerals and soils, Engineering Geology, Vol. 42, No. 4, pp. 223-237.

British Standard 1377, 1990, Methods of test for soils for civil engineering purposes, British Standard Institution, London.

British Standard 1924, 1990, Stabilized materials for civil engineering purposes. Part 2: Methods of test for cement-stabilized and lime-stabilized materials, British Standard Institution, London.

Chen, H. and Wang, Q., 2006, The behaviour of organic matter in the process of soft soil stabilization using cement, Bulletin of Engineering Geology and Environment, Vol. 65, No. 4, pp. 445-448.

Chen, D.-H., Si, Z. and Saribudak, M., 2009, Roadway heaving caused by high organic matter, Journal of Performance of Constructed Facilities, ASCE, Vol. 23, No. 2, pp. 100-108.

Clare, K. E and Sherwood, P. T., 1956, Further studies on the effect of organic matter on the setting of soil-cement mixtures, Journal of Applied Chemistry, Vol. 6, No. 8, pp. 317-324.

Danmarks, B. and Haliburton, T. A. 1999, Effects of sodium chloride and sodium chloride-lime admixtures on cohesive Oklahoma soils, Highway Research Record, Washington, No. 315, pp. 102-111.

Davoudi, M. H. and Kabir, A., 2011, Interaction of lime and sodium chloride in a low plasticity fine grain soils, Journal of Applied Sciences, Vol. 11, No. 2, pp. 330-335.

Harris, P., Harvey, O., Sebesta, S., Chikyala, S. R., Puppala, A. and Saride, S., 2009, Mitigating the effects of organics in stabilized soil, Technical Report No. 0-5540-1, Texas Transportation Institute, United States.

Huat, B., Maail, S. and Ahmed Mohamed, T., 2005, Effect of chemical admixtures on the engineering properties of tropical peat soils, American Journal of Applied Sciences, Vol. 2, No. 7, pp. 1113-1120.

James, R., Kamruzzaman, A. H. M., Haque, A. and Wilkinson, A., 2008, Behaviour of lime-slag-treated clay, Proceedings of the ICE - Ground Improvement, Vol. 161, No. 4, pp. 207-216.

Kazemian, S., Huat, B. K. and Barghchi, M., 2011, Effect of calcium chloride and kaolinite on shear strength and shrinkage of cement grout, International Journal of the Physical Sciences, Vol. 6, No. 4, pp. 707-713.

Koslanant, S., Onitsuka, K. and Negami, T., 2006, Influence of salt additive in lime stabilization of organic clay, Geotechnical Engineering, Journal of the Southeast Asian Geotechnical Society, Vol. 37, pp. 95-101.

Mohd Yunus, N. Z, Wanatowski, D. and Stace, L. R., 2011, Effect of humic acid on physical and engineering properties of lime-treated organic clay, Proceedings of the International Conference on Chemical and Materials Engineering, 28-30 November 2011, Venice, Italy.

Manchikanti, S. and Raju, R., 2008, A laboratory study on the effect of electrolytes on properties of expansive soil used in pavement sub-grade, Journal of the Institution of Engineers (India), Part CV, Civil Engineering Division 87.

Modmoltin, C. and Voottipruex, P., 2009, Influence of salts on strength of cement-treated clays. Proceedings of the ICE - Ground Improvement, Vol. 162, No. 1, pp. 15-26.

Moseley, M. P. and Kirsch, K., 2004, Ground improvement, 2nd edition, Spon Press, London.

Murty, V. R. and Krishna, P. H., 2006, Stabilisation of expansive clay bed using calcium chloride solution. Proceedings of the ICE - Ground Improvement, Vol. 10, No. 1, pp. 39-46.
Onitsuka, K., Modmoltin, C., Kouno, M. and Negami, T., 2002, The effect of humic acid on lime stabilized Ariake Clay, Proceedings of the 12th International Offshore and Polar Engineering Conference, Kitakyushu, Japan, pp. 577-583.

Onitsuka, K., Modmoltin, C., Kouno, M. and Negami, T., 2003, Effect of organic matter on lime and cement stabilized Ariake clays, Proceedings of Japanese Society of Civil Engineers, No. 729, pp. 1-13.

Ramesh, H. N., Siva Mohan, M. and Sivapullaiah, P. V., 1999, Improvement of strength of fly ash with lime and sodium salts. Proceedings of the ICE - Ground Improvement, Vol. 3, No. 3, pp. 163-167.

Sharma, R. S., Phanikumar, B. R. and Rao, B. V., 2008, Engineering behaviour of a remolded expansive clay blended with lime, calcium chloride, and rice-husk ash, Journal of Materials in Civil Engineering, Vol. 20, No. 8, pp. 509-515.

Sherwood, P. T., 1993, Soil stabilization with cement and lime, State of the Art Review, HMSO Publications, London.

Tremblay, H., Duchesne, J., Locat, L. and Leroueil, S., 2002, Influence of the nature of organic compounds on fine soil stabilization with cement, Canadian Geotechnical Journal, Vol. 39, pp. 535-546.

Zhu, W., Chiu, C. F., Zhang, C. L. and Zeng, K. L., 2009, Effect of humic acid on the behaviour of solidified dredged material, Canadian Geotechnical Journal, Vol. 46, pp. 1093-1099.

Strength increase in time of an alluvial clay, typical of the coast of Brazil´s Northeastern, mixed with different dosages of cement

Geraldo Vanzolini Moretti, Moretti Engenharia Consultiva, São Paulo, SP, Brazil,
geraldo@morettiengenharia.com.br
António Viana da Fonseca, University of Porto, Porto, Portugal, viana@fe.up.pt
João Alexandre Paschoalin Filho, Nove de Julho University, São Paulo, Brazil,
joao@morettiengenharia.com.br
David de Carvalho, State University of Campinas, SP, Brazil, david@feagri.unicamp.br

ABSTRACT

This study presents the increase over time of the strength of an alluvial clay, typical of the northeast coast of Brazil, mixed with different dosages of cement. In laboratory, water was added to samples obtained until the moisture content reached its liquid limit. Then the clay was homogenized using a planetary mixer with steel reservoir with a capacity of 5 lts and stainless steel beater. The following dosages of cement were used: 200, 400 and 600kg/m³. The cement used was of type Portland made with blast furnace slag (compressive strenght ≥ 32MPa for 28 days) and water /cement ratio of 0.8. After completion of mixing, the sample was homogenized during five minutes. The specimens were molded using a cylindrical steel mold with height and diameter of 50mm and 100mm, respectively. Soon after remoulded, they were immersed in water, and subsequently taken to failure in laboratory tests of uniaxial compression according to the recommendations of the Brazilian Association of Technical Standards (ABNT: NBR 14992/03 - "Determination of compressive strength). The tests were performed after 7, 28, 56 and 120 days. The soil samples were collected in an area located on the coast of Pernambuco State, northeastern Brazil. The site collection is characterized by a superficially homogeneous layer composed by highly organic clay-silts to very soft clays, with gray color and a thickness ranging between 12 and 15m. The groundwater level is found at 1.60m depth. Data analysis, determined by tests conducted, enabled the evaluation of the increase with time of the compressive strength of the soil-cement mixture, and the influence of dosage in the resistances values obtained

1. INTRODUCTION

1.1. Soft Soil stabilization by means of chemical elements addition

With the expansion of urban areas, increasing the necessity of occupation, sites that were not historically occupied due to geotechnical engineering, such as dominant soft soils, are now being increasingly occupied.

This situation concerns the technical means to find alternative solutions for mitigation of structural problems caused in the superstructures of the buildings by soil settlements.

One approach to this problem also includes, as an alternative for the treatment of these soils by means of chemical additives, the execution of pre-compaction, removal and replacement of material, among others (Nelson & Miller, 1992).

The soil stabilization by adding cement to improve the geotechnical characteristics of soft soil consists in a new technique, which has found wide acceptance in recent years by the improvement of technical means, with higher versatility and competitiveness compared to other more heavy classical solutions. (Hausmann, 1990).

The concept of using lime in marine organic clays stabilization was first published in technical journals written by PHRI (Port and Harbour Research Institute) in 1968 (Yanase, 1968).

The first studies carried out by PHRI aimed to pursue two main goals: a) to investigate how the lime reacts with Japanese marine clays; b) to develop equipment that would allow the constant supply of stabilizing agent and a proper and uniform mixing during the operation. These surveys also revealed that many Japanese marine clays showed strength gains in the order of the 100kN/m^2 to 1MN/m^2, in terms of unconfined compression strength.

In 1967 a new methodology for clay stabilization using active lime was developed by Kjeld Paus. The method was then called "Swedish Lime Column Method (SLCM)" (Broms & Boman, 1975).

Broms & Boman (1975) reported this new technique to the Geotechnical International Community at the 5th Asian Regional Conference of Soil Mechanics and Foundations Engineering. The first publication

Moretti - Strength increase over time of an alluvial clay, typical of the coast of Brazil´s Northeastern, mixed with different dosages of cement

II-421

containing design recommendations was written by Broms & Boman was published in 1977 (Broms & Boman, 1977).

In Northern Europe countries, the main objective of improving soil using columns of soil-lime is to reduce the road settlements in landfills, to improve stability of compacted embankments, excavation slopes and other geotechnical structures. The mixing of lime and cement is also currently used to prepare columns with higher resistance (Rathmayer, 1996).

As an example of application of this technique, Rathmayer (1996) comments that in 1992 Sweden and Finland carried out more than one million linear feet of stabilized soil column. The author also reports that recently some new stabilizing agents, composed of ash and recycled residues, are being increasly used in the treatment of organic soils and saturated

The selection of the stabilizing agent and the sellection of the dosage will depend on the local ground conditions (soil type) and the level of improvement needed (Taki & Yang, 2005).

The concentration of stabilizing agents is usually expressed in weight per volume of soil mass to be treated. According to Bruce (2001) and Jacobson *et al* (2003) this value reaches 6 and 12% of the dry weight of soil under treatment.

## 1.2. Basic mechanisms of soft soil stabilization

For many different types of soils, Portland Cement and Lime are the most commonly used stabilizing agents, however there is a range of other agents available today that can be used with success.

The basic mechanisms of admixture stabilization using cement or lime were extensively studied for several decades in transport infrastructures' engineering. This is because lime or cement treated soils have been used for sub-base or base materials in road constructions for long (Ingless & Metcalf, 1972). In the following paragraphs, the basic mechanisms lime and cement stabilization are briefly reviewed.

The most common types of cement used as stabilizing agent are the following: Portland cement, cement made from blast furnace slag and special cements.

Portland cement is obtained by the addition of gypsum and clinker. The clinker is formed by minerals: $3CaO.SiO_2$, $2CaO.SiO_3$, $3CaO.Al2O_3$, $4CaO.Al2O_3.Fe2O3$.

The cementitious mineral $3CaO.SiO2$, for example, reacts with water hydrating the cement in what follows, herein expressed by:

$$2(3CaO.SiO_2)+6H_2O=3CaO.2SiO_2.3H_2O+3Ca(OH)_2 \tag{1}$$
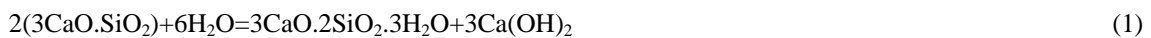
During the cement hydration, calcium hydroxide is released. The product of hydration of cement induces an increase of strength up to significant values, while the calcium hydroxide contributes to the pozzolanic reaction, occurring along the stabilization of lime.

The cement blast furnace slag is obtained by mixing Portland cement and blast furnace slag. When well ground, the blast furnace slag will not react with water, but has the potential to generate pozzolanic reaction products under conditions of high alkalinity.

In the cement blast furnace slag, SiO_2 and AlO_3, contained in the slag, are released by stimulation of a large quantity of Ca^{2++} and SO_4^{2-} released by the cement, so that a well hydrated and abundant silicate aggregation is formed.

Special cement type stabilizing agents are cements that are specially prepared for the purpose of stabilizing soil or similar materials by reinforcing certain constituents of the ordinary cement, by adjusting the grain size or by adding other constituents more effective for particular soil types (*Japan Cement Association*, 1994). The improvement effectiveness of organic soils seems to be affected by the ratio $((SiO_2+Al_2O_3)/CaO)$ of the constituent elements in cement type stabilizing agents (Hayashi *et al*, 1989). The delay of stabilization or gain control of resistance over time can be obtained by adjusting the amount of ingredients such as gypsum and limestone.

Although the improvement by lime or cement is based on similar chemical reactions, the rate of strength increase differs.

In both cases, reduction of water content due to hydration precedes all other reactions if a dry-powder stabilizer is added. The reduction of water content leads to a slight increase of strength, following a reaction common to both stabilizing agents. This is due to a cation exchange, which leads to an improvement in the plasticity of soils.

After these reactions, substantial hardening of the mixture starts. In the case of lime treatment, the pozzolanic reaction between lime and clayey soils is slow but lasts for years. In contrast to this, in the case of cement treatment, the formation of cement hydration product is relatively rapid and most of the strength increase due to cement hydration is completed within several weeks. The lime liberated during the hydration of cement also reacts with clayey soils, although the strength increases very slowly, but it tends to last for a long time.

Moretti - Strength increase over time of an alluvial clay, typical of the coast of Brazil´s Northeastern, mixed with different dosages of cement

II-422

The magnitude of the strength increase of treated soil by lime or cement is influenced by a number of factors, because the basic strength increase mechanism is closely related to the chemical reaction between the soil and the stabilizing agent. The factors can be roughly divided into four categories: I) Characteristics of stabilizing agent, II) Characteristics and condition of soil, III) Mixing conditions, and IV) Curing conditions, as show in Table 1 (Terashi, 1997).

Table 1: Factors affecting the strength increase (Terashi, 1997).

I- Characteristics of stabilizing agent	1- Type of stabilizing agent
	2- Quality
	3- Mixing water additives
II – Characteristics and conditions of soil (especially important for clays)	1-Physical chemical and mineralogical properties of soil
	2-Organic content
	3-pH of pore water
	4-Water content
III- Mixing Conditions	1- Degree of mixing
	2-Timing of mixing/re-mixing
	3-Quantity of stabilizing agent
IV- Curing Conditions	1-Temperature
	2-Curing time
	3-Humidity
	4- Wetting and drying/freezing and thawing, etc

The characteristics of stabilizing agent mentioned in Category I strongly affect the strength of the treated soil. Therefore, the selection of an appropriate stabilizing agent is, in a real sense, an important issue. (*Japan Cement Association, 1994*).

2.   RESEARCH OBJECTIVES

This paper, aiming to contribute to the increasing technical knowledge about the mobilization of resistance with time of soft soil stabilized with cement, presents and discusses results from axial compression tests conducted on specimens manufactured in the laboratory using marine soft alluvial clay stabilized with Portland cement CPII-E-32, as well as the influence of different dosages of Portland cement on the increase of compressive strength. Finally, this paper will also discuss the influence of curing time on strength increase.

3.   CHARACTERISCS OF THE EXPERIMENTAL SITE

The site where the soft soil samples were collected is located on the coast of Pernambuco, a state in Northeart of Brazil, near the city of Goinia and has 300m of extension, an is part of a project of enlargement of a national roadway.

This project involves a significant volume of new embankements founded over deep layers of soft soil with low resistance and variable thickness.

The subsoil is composed by a layer of sandy silt-clay of approximately 1.0 m of thickness followed by a layer of organic clay from 12.0 to 15.0 m, a layer of silty clay, 2.0m a layer of silt and clay. The water table level was detected at a depth of 1.60 m.

4.   MATERIALS AND METHODS

The following activities and methodologies were carried out to develop this research:

a) Soil samples colection:
To conduct the laboratory tests soft clayey soil samples were collected, using Shelby samplers, in the following depths: 2,6 e 11m.

b) Elemental geothecnical characterization tests:
Aiming to characterize the collected soil samples, the following laboratory tests were carried out in accordance with their respective Brazilian Standards (ABNT:NBR): Liquid Limit (ABNT:NBR 6459/1984), Plasticity Limit (ABNT NBR 7180/1984), Grain Size Distribution (ABNT: NBR7181/1984), Natural Moisture Content, and Particle Density.

Moretti - Strength increase over time of an alluvial clay, typical of the coast of Brazil´s Northeastern, mixed with different dosages of cement

II-423

c) Clayey samples homogenization

After collecting, water was added to soil samples until the moisture content approached their Liquid Limit. Then the clayey samples were homogenized by planetary mixer with steel tank capacity of 5 litres and stainless steel beater.

d) Mixing procedures

To create the mixture of soil-cement the following dosages were adopted: 200, 400 and 600kg / m³. The cement used was of type Portland made with blast furnace slag (compressive strenght $\geq$32MPa for 28 days) and water / cement ratio of 0.8. This cement have adition of ground granulated blast-furnace slag and carbonatic material, reaching a compressive strenght of 32 MPa. After completion of mixing, the sample was additionally homogenized for five minutes. After this period the homogeneity of the mixture was evaluated verifying the occurrence of pellets and clumps of cement.

e) Specimens and Curing Time

For molding the specimens cylindrical steel molds were used, with height and diameter of 50 and 100 mm, respectively. Then, the cylindrical specimens were immersed in water (temperature of 20°C) for 7, 28, 56 and 120 days on curing.

f) Determination of compressive strength

Aiming to obtain the compressive strength of the specimens, laboratory tests were carried out according the recommendations of the Brazilian Association of Technical Standards (ABNT: NBR 14992/03 - "Determination of compressive strength).

5.   ACHIEVEMENTS AND DISCUSSIONS

Table 2 shows the geotechnical parameters obtained by the elemental characterization tests carried out. The grain size distribution of the studied soil is presented on Table 3.

Table 2: Geotechnical parameters obtained by simple characterization tests.

Depth (m)	Liquid Limit (%)	Plasticity Index (%)	Natural Moisture Content (%)	Volume Weight (kN/m^3)
2	64	25	120	13,8
6	65	26	126	13,9
11	71	30	100	14,4

Table 3: Grain Size distribution

Depth (m)	Sand (%)	Silt (%)	Clay (%)
2	10	28	62
6	2	20	78
11	6	20	74

Table 4 presents the compressive strength obtained for different curing times using cement dosage of 200kg/m³. Figure 1 shows the values presented on Table 4.

Table 4: Compressive strength for different curing times using cement dosage of 200kg/m3.

Specimen	Compressive strength (MPa)			
	Curing time (days)			
	7	28	56	120
1	1.3	2.9	2.9	4.0
2	1.1	3.0	3.3	3.6
3	1.0	2.7	3.0	3.7
4	1.2	2.5	3.5	3.7
Average value (MPa)	1.2	2.8	3.2	3.8
Standard deviation (sd) (MPa)	0.1	0.2	0.3	0.2
Coefficient of variation (cv) (%)	11.2%	8.0%	8.7%	4.6%

Moretti - Strength increase over time of an alluvial clay, typical of the coast of Brazil´s Northeastern, mixed with different dosages of cement

II-424
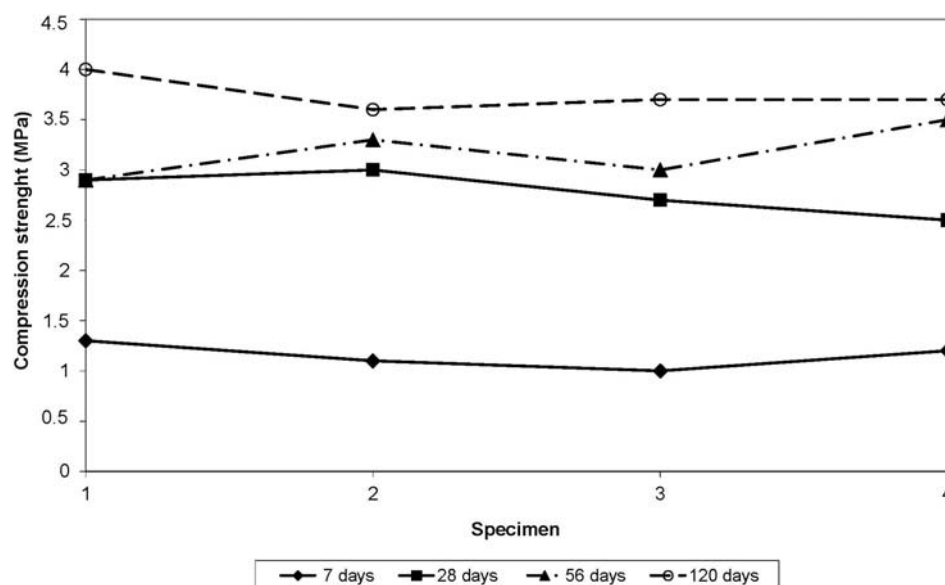
Figure 1: Compressive strength for different curing times using cement dosage of 200kg/m³.

Table 5 presents the compressive strength obtained for different curing times using cement dosage of 400kg/m³. Figure 2 shows the values presented on Table 5.

Table 5: Compressive strength for different curing times using cement dosage of 400kg/m³.

	Compressive strength (MPa)			
Specimen	Curing time (days)			
	7	28	56	120
1	1.5	4.7	5.2	9.3
2	1.5	4.7	6.0	7.0
3	1.4	4.4	5.9	7.0
4	1.4	4.5	4.8	7.0
Average value (MPa)	1.5	4.6	5.5	7.6
Standard deviation (sd) (MPa)	0.1	0.1	0.6	1.2
Coefficient of variation (cv) (%)	4.0%	3.3%	10.5%	15.2%
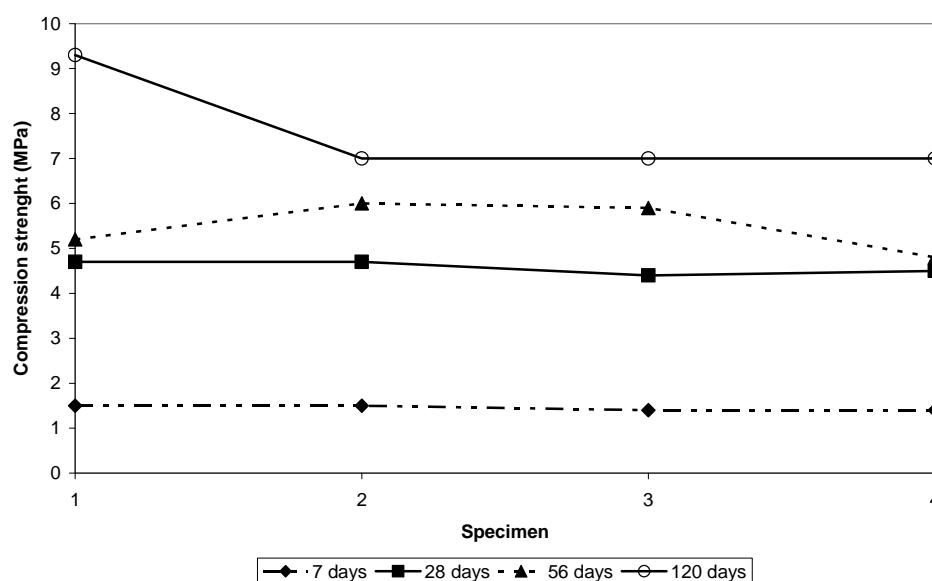
Figure 2: Compressive strength for different curing times using cement dosage of 400kg/m3.

Moretti - Strength increase over time of an alluvial clay, typical of the coast of Brazil´s Northeastern, mixed with different dosages of cement

Table 6 presents the compressive strength obtained for different curing times using cement dosage of 600kg/m^3. Figure 3 shows the values presented on Table 6.

Table 6: Compressive strength for different curing times using cement dosage of 600kg/m3.

	Compressive strength (MPa)		
Specimen	Curing time (days)		
	7	28	56
1	1.7	7.9	8.5
2	1.9	7.6	9.4
3	2.2	7.9	8.9
4	2.4	7.7	8.4
Average value (MPa)	2.05	7.78	8.8
Standard deviation (sd) (MPa)	0.31	0.15	0.45
Coefficient of variation (cv) (%)	15%	2%	5%
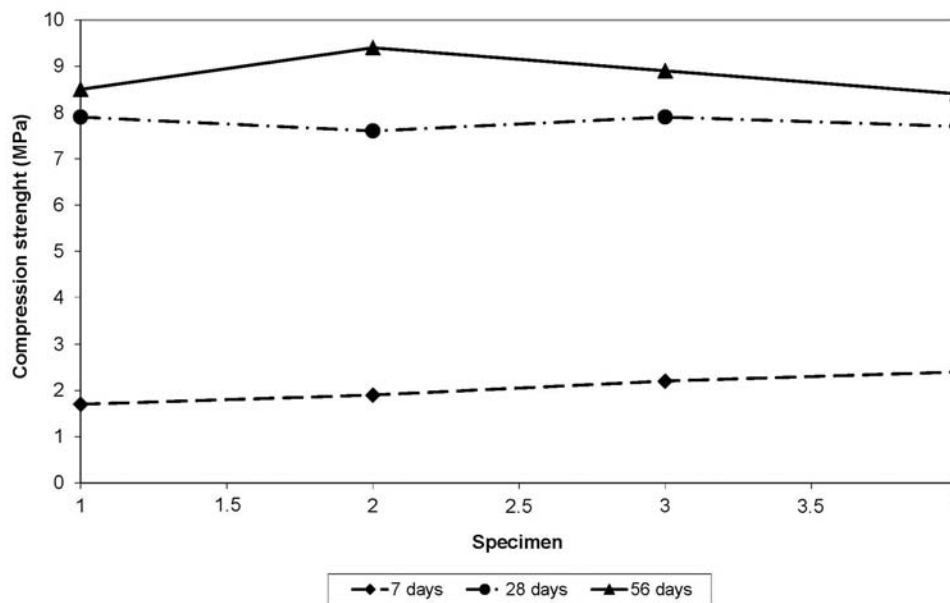
Figure 3: Compressive strength for different curing times using cement dosage of 600kg/m3.

As shown in the previous tables, the compressive strengths for 7 days curing time considering cement dosages of 200, 400 e 600kg/m^3 are, respectively: 1.2MPa *(sd=0.1MPa, cv=11.2%); 1.5MPa (sd= 0.1MPa, cv=4%)* and *2.05MPa (sd=0.31MPa, cv= 15%).* The compressive strengths for 28 days curing time considering cement dosages of 200, 400 e 600kg/m^3 are the respectively: 2.8MPa *(sd=0.2MPa, cv=8%), 4.6MPa (sd=0.1MPa, cv=3.3%)* and *7.8MPa (sd=0.1MPa, cv= 2%).* The compressive strengths for 56 days curing time considering cement dosages of 200, 400 e 600kg/m^3 are, respectively: 3.2MPa *(sd=0.3MPa, cv=8.7%), 5.5MPa (sd=0.6MPa, cv=10.5%)* and *8,.8MPa (sd=0.45MPa, cv=5%).* The compressive strengths for 120 days curing time considering cement dosages of 200, 400 e 600kg/m^3 are, respectively: 3.8MPa *(sd=0.2MPa, cv=4.6%)* and *7.6MPa (sd= 1.2MPa, cv=15.2%).* The low values observed of *cv* and *sd* indicate the good homogeneity of the mixture.

Figure 4 presents the variation of compressive strength with the different used cement dosages for different curing times (7, 28, 56 and 120 days).

Moretti - Strength increase over time of an alluvial clay, typical of the coast of Brazil´s Northeastern, mixed with different dosages of cement

II-426
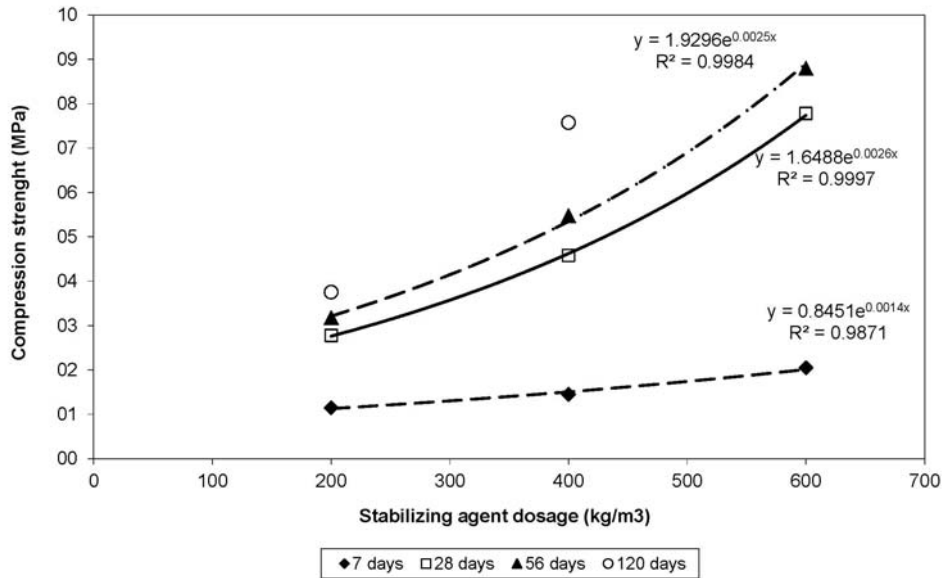
Figure 4:Compressive strength versus cement dosages

All curing times revealed the same trend of increasing compressive strength with the cement dosage. The exponential regressions showed good correlations between compressive strength and stabilizing agent dosages ($R^2 > 0.98$).

Figure 5 shows correlations between differents compressive strengths (q_u) obtained for different dosages of stabilizing agent in different curing times.
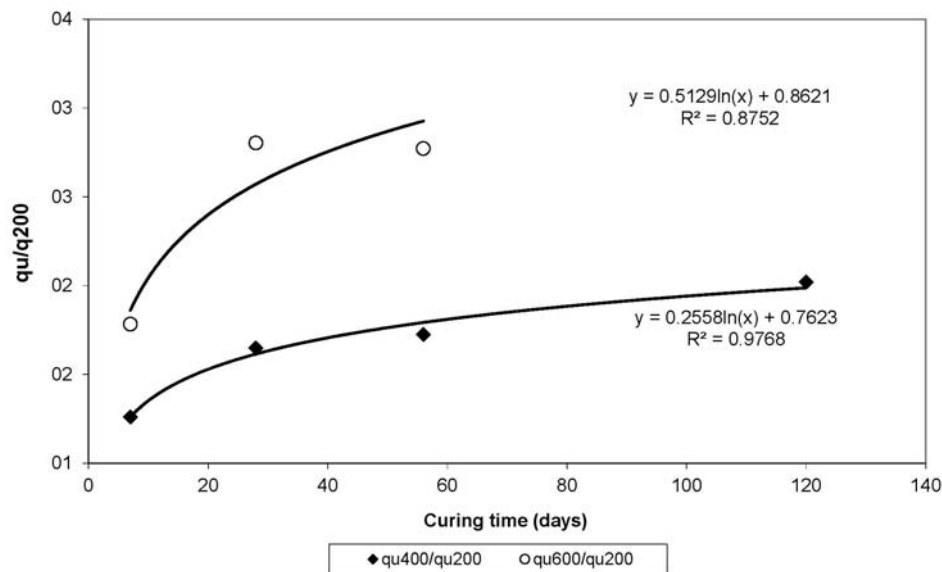
Figure 5: Correlations between different compressive strengths and curing time

As shown in Figure 5, the values of q_u obtained considering dosage of 600kg/m³ and 7 days of curing time were $1.8 \cdot q_{u200}$, increasing to $2.8 \cdot q_{u200}$ for 28 days of curing time and keeping the same value for 56 days.

The values of q_u obtained considering cement dosage of 400kg/m³ and 7 days of curing time were $1.3 x q_{u200}$, increasing to $1.65 \cdot q_{u200}$ for 28 days, $1.72 \cdot q_{u200}$ for 56 days and $2.0 \cdot q_{u200}$ for 120 days of curing time.

Figure 5 also shows that the obtained correlations (q_{u600}/q_{u200} and q_{u400}/q_{u200}) present an increase of 50% between the first controlling date of curing time (7 days) and the last one (120 days). This fact shows that the compressive strength results obtained in early ages may not represent the real difference between the

Moretti - Strength increase over time of an alluvial clay, typical of the coast of Brazil´s Northeastern, mixed with different dosages of cement

II-427

stabilizing agent dosages and compressive strength. In these very early days the sensitivity of these mixtures to the difference in the cementing agent is not sufficient.

Figure 6 shows the average increase of the compressive strength with curing time, considering the studied cement dosages.
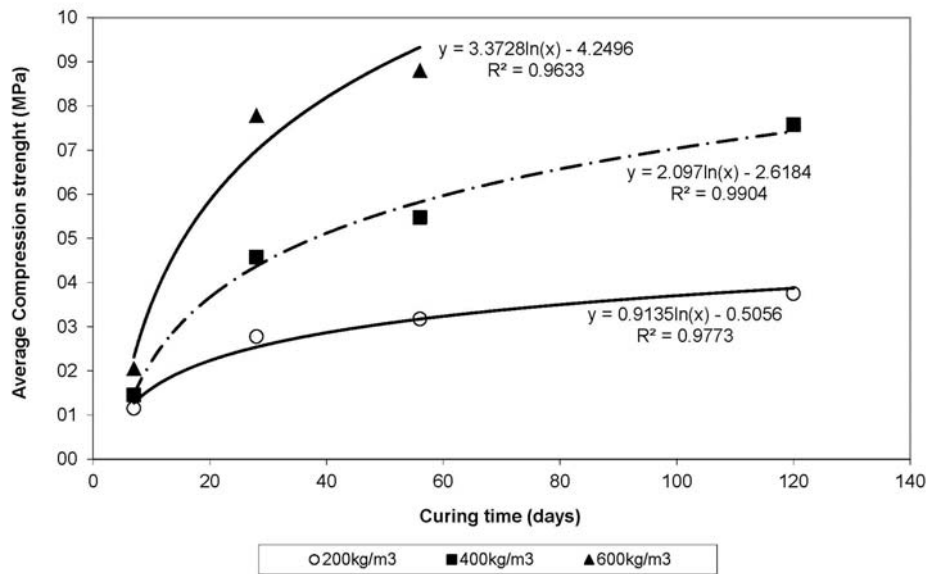
Figure 6: Increase of average compressive strength versus curing time

As shown in Figure 6 the compressive strength increasing in the first curing days can be represented by a logarithmic curve. The compressive strength increases fast in the first days, however decreases gradually with time. The logarithmic regressions showed correlations presenting $R^2 > 0.96$.

Figure 7 presents compressive strength *versus* curing time, however the horizontal axis (curing time) time is represented by a logarithmic scale.
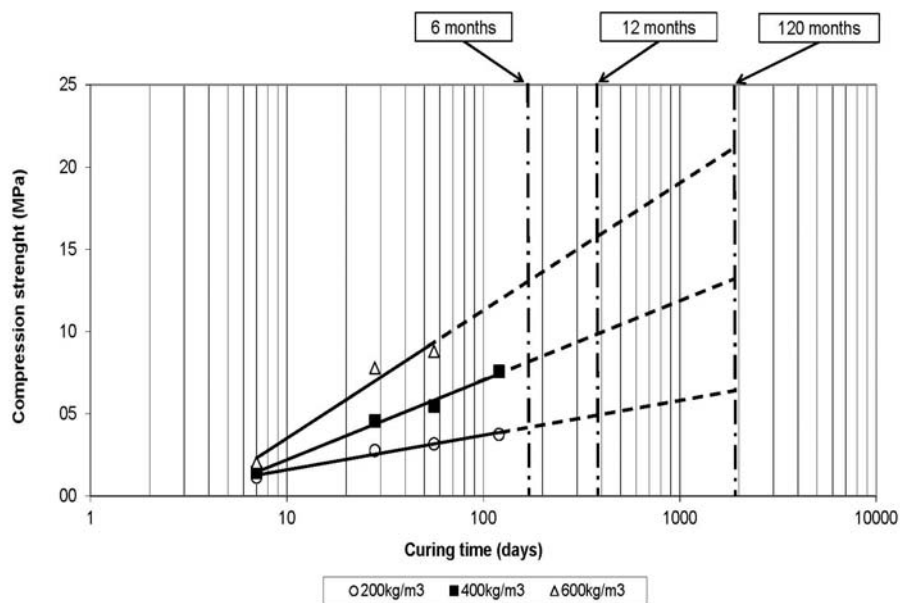
Figure 7: Compressive strength vsversus curing time

As presented in Figure 7, assuming that the best relationship between the compressive strength *versus* curing time is logarithmic (*as seen in Figure 6*) considering a period of 10 years it is estimated that qu could reach approximately the double of the maximum value obtained for 120 days of curing time.

Moretti - Strength increase over time of an alluvial clay, typical of the coast of Brazil´s Northeastern, mixed with different dosages of cement

II-428

6.   CONCLUSIONS

The following conclusions can be drawn from the work presented above:

a) The homogenization procedures used to stabilize with the clayey soil involved in this project were satisfactory. This fact can be based in the low coefficients of variation obtained, ranging between 2% and 15% within the same group of samples (samples molded with the same dosages and tested in the same curing time).

b) The curves that represented the gain of compressive strength, obtained for the tested samples in the same curing time within the adopted cement dosages ranges, showed a exponential variation law with high adjustment (R^2 values between 0.98 and 0.99).

d) The relationship between the compressive strength obtained for different stabilizing agent dosages in the same curing time varied considerably, increasing when the tests were carried out with 7 days or 28 days. Considering the two studied relationships, for the dosages of 400 and 600kg/m³ in relation to the one of 200kg/m³ (q_{u600}/q_{u200} and q_{u400}/q_{u200}), the observed strength gain was about 50% between tests performed with 7 days and 28 days, respectively. After this period the samples increased in strength, however, their relationship did not vary significantly. Thus, it is concluded that controlling tests should be performed with a curing time of no less than 28 days, as there is the risk of assuming inaccurate trends for the variation of strength in mixtures studied with samples cured with lower times.

e) The values of compressive strength obtained for each cement dosage in different curing times, showed that the increase is logarithmic type. In the first curing days, the gain of strength was faster, decreasing gradually in time. The logarithmic regressions obtained showed R^2 values ranging between 0.96 and 0.99. Thus it can be concluded that the adoption of a logarithmic law to represent the gain in strength with time is appropriate when soft soils stabilized with Portland Cement.

REFERENCES

Brazilian Association of Technical Standards (ABNT). ABNT:NBR-6459/1984. Soil-Determination of Liquid Limit. Rio de Janeiro, 1984. 6p. In Portuguese.

Brazilian Association of Technical Standards (ABNT). ABNT: NBR-7180/1984. Soil- Determination of the Plasticity Limit. Rio de Janeiro, 1984. 3p. In Portuguese.

Brazilian Association of Technical Standards (ABNT). ABNT:NBR-7181/1984. Soil- Grain Size Distributio Analysis. Rio de Janeiro, 1984. 13p. In Portuguese.

Brazilian Association of Technical Standards (ABNT). ABNT:NBR-7215/196. Portland Cement - Determination of Compressive Strength. Rio de Janeiro, 1996. 8p. In Portuguese.

Babasaki, R. M., Terashi, T., Suzuki, A. Maekaea, M. (1996) JGS TC report: Factors influencing the strength of improved soil. Proceedings 2and International Conference on Ground Improvement Geosystems, Grouting and Deep Mixing, Vol. 2, Balkema, Tokyo, pp913-918. 1996.

Broms, B., Boman, P. (1979) Lime columms – a new foundation method. Journal of Geotechnical Engineering, ASCE, Vol. 105, GT4, pp. 539-556

Bruce, D. (2001) An introduction to deep mixing methods as used in geotechnical applications, volume 3, the verification and properties of treated ground. Report No FHWA-RD-99-167 U.S. Department of Transportation, Federal Highway Administration, Washington, D.C.

Enami, A., Hibino, S. (1991) Improvement of foundation ground using a deep mixing blender with free blades.

Journal of Japanese Society of Soil Mechanics and Foundation Engineering, N 39, Vol.10, pp 37-42.

Hayashi, H.S., Noto.,Toritani, N. (1989) Cement improvement of Hokkaido peat. Proceedings. Symposioum on High Organic Soils: pp101-106. 1989

Moretti - Strength increase over time of an alluvial clay, typical of the coast of Brazil´s Northeastern, mixed with different dosages of cement

II-429

Hausmann, M.R. (1990) Engineering principles of ground modification, McGraw Hill. New York, 320p.

Ingless, O.G., J.B., Metcalf. (1972) Soil stabilization, principles and practice. Butterworth.pp120-135.

Jacobson, J. R., Filz, G.M., Mitchell, J. K. (2003) Factors affecting strength gain in lime-cement columms and development of a laboratory testing procedure. Report No. VTRC 03-CR16, Virginia Transportation Research Council, Charlottesville, Va.

Japan Cement Association. (1994) Soil improvement manual using cement stabilizer. pp15-30.

Lorenzo, G.A, Bergado, D.T. (2004). Fundamental parameters of cement admixed Clay-New approach. JGGE, n.130, vol.10,pp.1042-1050.

Nelson, J.D., Miller, J. D. (1992) Expansive soils: Problems and Practice in foundation and pavement engineering. John Wiley and Sons, Inc., New York.

Puppala, A.J, Bhadriraju, V., Porbaha, A. (2005) Quality assurance practices and protocols for in-situ testing of deep mixed columns. Proceedings of International Conference on Deep Mixing: Best Practice and Recent Advances, Swedish Deep Stabilization Research Centre, Stockholm, Sweden, pp 613-619.

Rathmayer, H. (1996) Deep mixing methods for soft subsoil improvement in the Nordic Countries. Proceedings 2and International Conference on Ground Improvement Geosystems, IS-Tokyo 96, Balkema, Rotterdam, The Netherlands, 869-878.

Taki, O, Yang, D.S. (2005) Soil-cement mixed wall technique. Geotechnical Engineering Congress, ASCE, Reston, Va., 298-309.

Terashi, M., H. Tanaka & T. Okumura. (1979) Engineering properties of lime treated marine soils and the DSM method. Proceedings of the 6th Asian Regional Conference on Soil Mechanics and Foundation Engineering, vol.1, pp. 191-194.1979

Terashi, M. Theme Lecture: (1997) Deep Mixing Method-Brief State of the Art. Proceedings of the 14th International Conference on Soil Mechanics and Foundation Engineering, vol.4, pp.2475-2478.

Yanase, S. (1968) Stabilization of marine clays by quicklime. Report of the Port and Harbour Research Institute, n.7, vol.4, pp.85-132.

Moretti - Strength increase over time of an alluvial clay, typical of the coast of Brazil´s Northeastern, mixed with different dosages of cement

II-430

Case Study Analysis of OPMC Improved Foundation Ground, Pavement and Other Geo-structures Employing the GECPRO Model

J.N. Mukabi, Kensetsu Kaihatsu Limited, Kenya, mukabinj@gmail.com

ABSTRACT

The degree of effective improvement of the OPMCS (Optimum Mechanical and Chemical Stabilization) technique in enhancing the vital geotechnical engineering properties of ground and geomaterials is illustrated through some typical results based on laboratory and in-situ experimental testing performed on various geomaterials within the East and Central African region. A case example of the most recent application of the OPMC technology in realizing Value Engineering (VE) design and construction of a runway pavement for the Isiolo International Airport in the Eastern State of Kenya is also provided, whilst case study analyses are carried out for a road pavement structure in Juba, a pad foundation in the Jonglei Flood Plains of Southern Sudan and a retaining wall along a steep slope in Addis Ababa, Ethiopia.

The results from this Study demonstrate that the degree of improvement of the consolidation properties, bearing capacity, shear strength and Young's modulus (elastic stiffness) are mainly a function of the quantitative and qualitative level of OPMCS.

1   INTRODUCTION

1.1   Brief Background of OPMCS R&D

Fulfillment of specifications within acceptable construction practices requires high-quality geomaterials which are usually expensive and mostly involve long haulage distances of such materials thereby increasing the period of construction and, most of all, the project cost. On the other hand, the use of "substandard" geomaterials, which, in singularity, are mostly deficient in mechanical stability and other geo-properties, certainly requires the application of innovatively researched ground and material improvement techniques.

The OPMCS is an extrapolation of the OBRM (Optimum Batching Ratio Method), which was developed during the prevalence of the late 1997 to early 1998 El-Nino floods causing detrimental damage to pavement structures and bridge foundations along the 330km Tana Basin Project Road that was under construction in the Coast/North-Eastern States of Kenya during this occurence .

OBRM is fundamentally based on the theory that regards soil as an assembly of particles whose integrated motion can be characterized theoretically by basic concepts and fundamental principles of continuum mechanics and models that consider probabilistic perspectives of microscopic state and multi-dimensional analysis (Mukabi, 2001a [1]). The application of this technology was first reported by Mukabi and Shimizu, 2001b [2] and Mukabi et al (2001c) [3]. OPMCS was later developed during the construction of the 240km Addis Ababa ~ Debre Markos international trunk road connecting Ethiopia to Sudan in the West and Eriteria in the East.

1.2   OPMCS – Cost Aspect and Maintenance requirement Ratios

Through the application of the OPMCS technology, most road projects have realized cost savings of 30 ~ 40% and reduction of maintenance requirement of up to 60% for pavement layers and composite structures (Kogi et al, 2011 [4]).

1.3   OPMCS as an Environmental Mitigation Measure

Mukabi et al, 2007b [5] and Kogi et al, 2011 [4] have reported achievement of the following through the application of the OBRM and OPMCS technologies: 1) reduction of volume of materials used by approximately 40% in most cases; 2) less disturbance of land for borrow pits; 3) reduced amounts of disposable soil during construction; 4) reduced risk of collapse of geo-engineering structures and; 5) environmentally friendly due to; utilization, as much as possible, of locally available material and reduction of dust, distances (lengths of access roads) to borrow pits, geomaterial quantities required and land acquisition, among other factors. Whilst developing these methods, comprehensive appraisals and

Mukabi - Case Study Analysis of OPMC Improved Foundation Ground, Pavement and Other Geo-structures Employing the GECPRO Model

II-431

environmental assessments that would lead to sustainable development with minimal negative environmental impacts, were undertaken [5].

The example depicted in Figure 1 was part of the design for Wau~Abyei Trunk road constructed in the northern oil fields of the Republic of Southern Sudan.
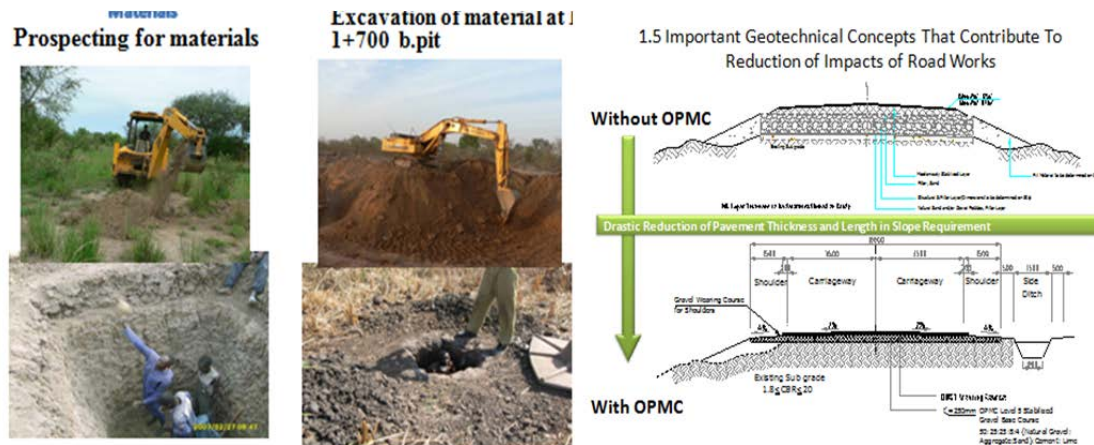

Figure 1: Contribution of OPMCS to reduction of environmental impacts of road works ([4] & [5]).

A summary of the approach, considerations and contribution of OBRM and OPMCS from an environmental and geotechnical engineering perspective are discussed in [5].

2   RECENT APPLICATION OF OPMCS TECHNOLOGY – RUNWAY PAVEMENTS

The most recent application of the OPMCS is manifested in the design and on-going construction of the runway pavements, taxi way, aprons and parking bays of the Isiolo International Airport located in the Eastern State of Kenya.

Figure 2 is a typical depiction of some of the basic results realized from laboratory experimental testing, whilst Figures 3 and 4 show the plan and one of the typical cross-sections of the pavement structures.
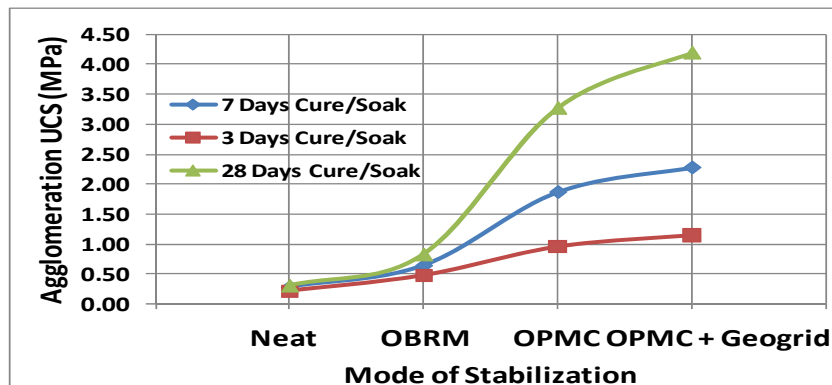
Figure 2: Enhanced strength as a result of particle agglomeration for varying modes of stabilization

It can be noted from this figure that: a) the UCS is significantly enhanced as the soil particles agglomerate progressively with time particularly for the cemented geomaterial; b) soil particle agglomeration is dependent on the mode of stabilization; c) the effects of geogrid reinforcement are more noticeable with increased agglomeration possibly due to the influence of confinement in increasing the degree of interlocking of particles culminating in reduction of voids ratio, and d) the degree of soil particle agglomeration is higher under OPMC stabilization in comparison to geogrid reinforcement thus confirming the theory that, in comparison to other influencing factors, cementation processes have greater impact on agglomeration mechanisms.

Mukabi - Case Study Analysis of OPMC Improved Foundation Ground, Pavement and Other Geo-structures Employing the GECPRO Model

II-432
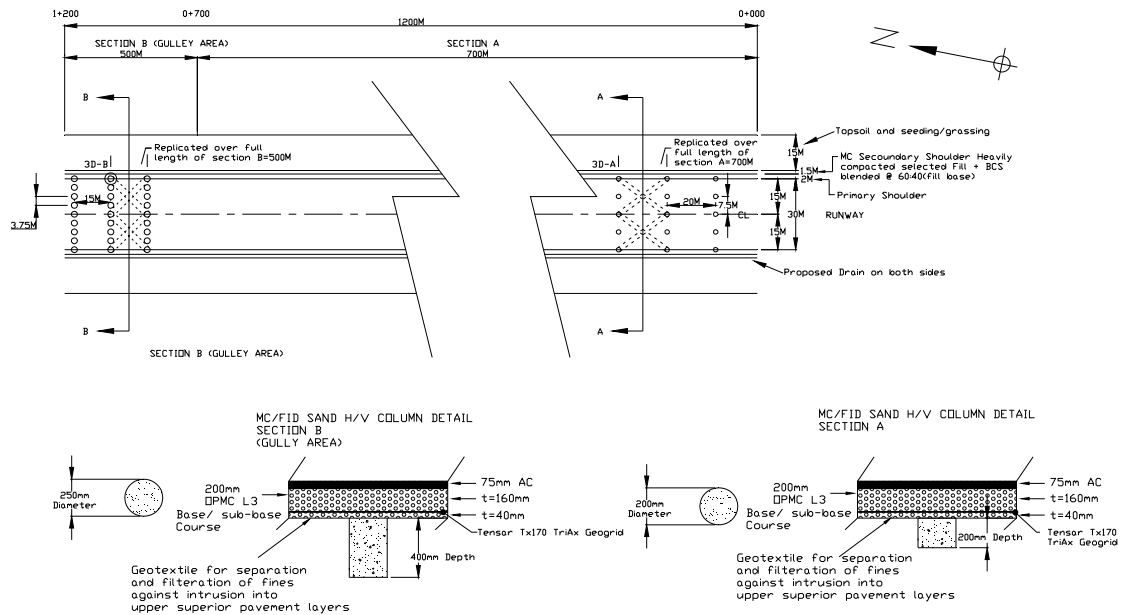
Figure 3: Plan View and MC Sand Column details for BCS subgrade improvement for Isiolo Int'l Airport
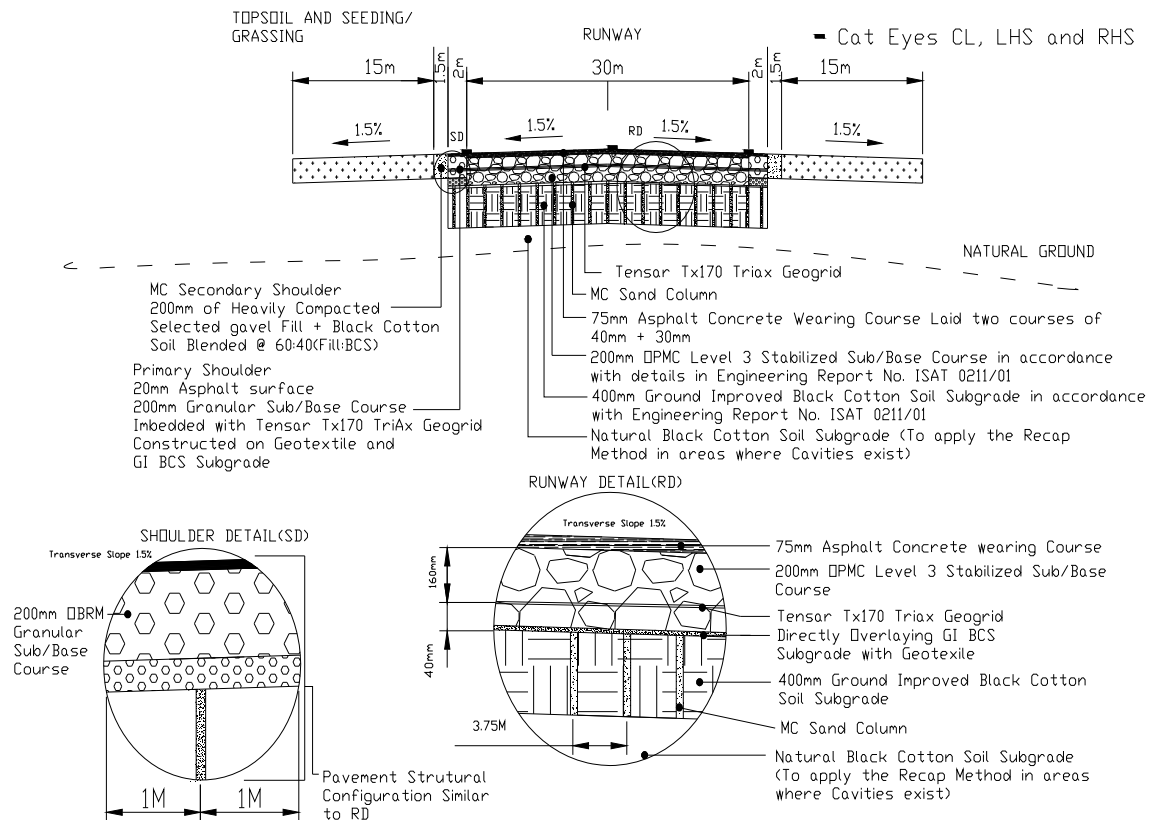
Figure 4: Detail of typical cross-section B and detail of Isiolo International Airport pavement structure

The site location of this project is predominated by Black Cotton Soils (BCSs), which are highly problematic and expansive in nature. Consequently, as can be observed from Figure 4, Ground Improvement (GI) was undertaken by adopting the Moisture Control Sand Column (MCSC) method proposed by Mukabi et al, 2010b [6]. Both laboratory and field experimental testing results indicate that, on the average, this method typically enhances the bearing capacity, strength and deformation resistance of BCS subgrades by more than five - fold (Kensetsu Kaihatsu, 2011 [7]) .

The uniqueness of this design includes the: 1) combination of OPMCS and geosynthetics; 2) use of geotextile as a separation, filtration and stress mobilization interface; 3) use of geogrid as a reinforcement and tensile stress control component, and 4) realization of high composite structural enhancement factor.

Mukabi - Case Study Analysis of OPMC Improved Foundation Ground, Pavement and Other Geo-structures Employing the GECPRO Model

II-433

3 BRIEF INTRODUCTION OF THE GECPROM – GEOMATHEMATICO-EMPIRICAL MODEL

3.1 Preamble

An appreciably versatile mechanistic-empirical geo-mathematical model (GECPROM) encompassing most of the concepts developed in this Study as well as other related studies, is proposed. GECPROM is designed to probe and estimate changes in vital seismic geo-properties for clayey geomaterials and ground. The significant advantage of this model is that various geotechnical changes and geostructural behavior can be modeled from a single sophisticated experimental test, whilst simultaneously catering for the effects of drainage conditions, loading rate, and consolidation stress-strain-time history. The complete and perfect model would, categorically, have to be multidimensional with relativistic coaxiality, relations and consequences. The GECPROM is primarily designed to be adopted at the study or investigative stage facilitating basic data and information that can then be applied for design of foundations, pavements and other geostructures and/or comprehensive experimental testing and research regimes, input for global and constitutive models, counter/cross-checking and designating the confidence levels of laboratory and field experimental testing, construction control, risk analysis and technical mitigation measures in seismic zones besides the integral role of prediction of ground response and retrospective behavior.

This model is to be further developed to incorporate the Consolidation and Shear Stress Ratio (CSSR) and Modified Critical State Theory (MCST) modules (Mukabi and Hossain, 2011e [8] and Mukabi, 2011d [9]), in order to effectively complement the ESDAM (Environmental, Strength and Deformation Analysis Model), which is under development based on some of the concepts developed in the process defined in the sedimentary model that merges the Simsafadim-Clastic and Discrete Element model.

3.2 Probing and prediction of shear and elastic moduli

The fundamental equation for the shear modulus developed from CSSR model functions is expressed as:

$$[G_o]_{p'} = \left\{ \mathcal{A}_{p_o'} \left[(K_{cs})^\alpha \times \left(\frac{p'}{p_o} \right)^\beta \right] + \mathcal{B}_{p_o}^{K_{cs}} \right\} \times [G_o]_{p_o'} \tag{1}$$

where $[G_o]_{p'}$ is the initial shear modulus at a variable stress point p', $K_{cs} = \sigma_r'/\sigma_a'$ is the arbitrary or designated consolidation stress ratio traced to p', $[G_o]_{p_o'}$ is the initial shear modulus determined at in-situ overburden pressure, $\mathcal{A}_{p_o'} = 0.95$ and $\mathcal{B}_{p_o'} = 0.35$ are geomaterial experimental constants, the values of which are applicable for most natural stiff to hard clayey geomaterials, while $\beta = 1.16$ and $\alpha = 0.4$ for stress states in the 1st quadrant and $\alpha = -1$ for stress states in the 4th quadrant accordingly [8].

In developing the model functions it is important to consider the relativistic rates of change of $[G_o]_{p'}(\Delta, \delta)$ at least within the 1st quadrant of the $\{p', q\}$ stress plane for stress ratio and orientation whereby, $\psi_{p'} = p'/p_o'$ and $\delta_k = K_{cs}$ and the total derivative is expressed in a generalized form as:

$$\frac{d[G_o]_{p'}}{d\psi_{p'}} = \frac{\partial[G_o]_{p'}}{\partial\psi_{p'}} + \left(\frac{\partial[G_o]_{p'}}{\partial\delta_k} \right) \times \frac{d\delta_k}{d\psi_{p'}} \tag{2}$$

$$\therefore \frac{d[G_o]_{p'}}{d\psi_{p'}} = \mathcal{A}_{p_o'} \left[(K_{cs})^\alpha \times \beta \left(\frac{p'}{p_o} \right)^{\beta-1} \right] + \left\{ \mathcal{A}_{p_o'} \left[\alpha K_{cs}^{\alpha-1} \times \left(\frac{p'}{p_o} \right)^\beta \right] + \frac{\mathcal{B}^{K_{cs}}}{K_{cs}} \right\} \times \frac{d\delta_k}{d\psi_{p'}} \tag{3}$$

3.3 Geo-mathematical determination of Initial Yield Strain (IYS) for varying conditions

GECPROM retrospectively reflects and mirrors the conditions applied during the testing at stress point p_o'. Unlike the initial shear and elastic moduli which can be ideally considered to be only stress state dependent, the Initial Yield Strain $\{(\varepsilon_a)_{ELS}(Y_I)\}$ representing the threshold of the initial sub-yield surface, Y_I, which is dependent on various factors such as consolidation stress-strain-time history, shear strain rate, drainage conditions and OCR [1], is rather complicated in terms of modeling it in singularity. In the generalized state therefore, the $(\varepsilon_a)_{Y_I}$ is expressed as a function of multi-variables in the form;

$$(\varepsilon_a)_{Y_I} = \Omega[p' \sim q]f\big(\sigma_{ss}, L_{CSSH}, \delta_{SCT}, \phi_{OCR}, \alpha_{cp}, \varphi_{DC}, \dot{\varepsilon}_{SR}\big) \tag{4}$$

where, σ_{ss} is the current stress state, $\mathcal{L}_{CSSR}$ represents the consolidation stress-strain history, $\varphi_{SCT} = (d\varepsilon_a/dt)_{SCT}$ is the secondary consolidation time (ageing), ϕ_{OCR} is the overconsolidation ratio factor, φ_{DC}

Mukabi - Case Study Analysis of OPMC Improved Foundation Ground, Pavement and Other Geo-structures Employing the GECPRO Model

II-434

defines the drainage conditions and $\dot{\varepsilon}_{SR}$ is the strain rate effect. However, corroborative deduction made from [8] and [9] indicates that the variables can essentially be simplified as: $f[(\sigma_{ss}, \mathcal{L}_{CSSR}, \varphi_{DC}, \dot{\varepsilon}_{SR})]$
The generalized analytical function of the resulting $(\varepsilon_a)_{Y_I}^R$ expressed in compound terms is:

$$(\varepsilon_a)_{Y_I}^R = \oiint \oiint \oint_{\{\Delta q, \varepsilon_a\}}^{\{\Delta q Y, \varepsilon_{aY}\}} f(\sigma_{ss}, L_{CSSR}, \varphi_{DC}, \alpha_{cp}, \dot{\varepsilon}_{SR}) d\sigma_{ss} \\ dL_{CSSR} d\varphi_{DC} d\alpha_{cp} d\dot{\varepsilon}_{SR} \tag{5}$$

3.3.1 Stress States (σ_{ss}) and Bounding Limits (BL)

The basic generalized equation defining the impact of stress states is expressed as:

$$[\varepsilon_a]_{Y_I}^{\sigma_{ss}} = \frac{\left\{ \mathcal{A}_{p_o}^{\varepsilon,} \left[(K_{cs})^l \times \left(\frac{p'}{p_o}\right)^m \right] + \mathcal{B}_{p_o, \varepsilon}^{K_{CS}^r} \right\}^\alpha}{\psi_{(\varepsilon_a)_{Y_I}}} \times [(\varepsilon_a)_{Y_I}]_{p_o'}, \left| \psi_{(\varepsilon_a)_{Y_I}}^{\leq 1, \alpha = +1}_{>1, \alpha = -1} \right. \tag{6}$$

where, constants $\mathcal{A}_{p_o}^\varepsilon = 0.98$, $\mathcal{B}_{p_o', \varepsilon} = 0.32$, $l = 0.4$, for stress states in the 1st quadrant and, $l = -1$, in the 4th quadrant, while $m = 1.16$ [8].
Carrying out 2nd order partial differentiation w.r.t ρ we obtain,

$$\left(\frac{\partial^2 (\varepsilon_a)_{Y_I}^{\sigma_{ss}}}{\partial \rho_{p'}^2}\right)_\kappa = \mathcal{A}_{p_o'} \left[(K_{cs})^l \times m(m-1) \left(\frac{p'}{p_o}\right)^{m-2} \right] \times [(\varepsilon_a)_{Y_I}]_{p_o'} < 0^{-1} \tag{7}$$

Performing the same w.r.t κ we obtain,

$$\left(\frac{\partial^2 (\varepsilon_a)_{Y_I}^{\sigma_{ss}}}{\partial \rho_{p'}^2}\right)_{\rho_{p'}} = \left\{ \mathcal{A}_{p_o'} \left[l(l-1) K_{cs}^{l-2} \times \left(\frac{p'}{p_o}\right)^m \right] + \left[\frac{K_{cs} \mathcal{B}^{K_{CS}^{(n-2)}} - m K_{CS}^{(n-1)} \mathcal{B}^{K_{CS}^{(n-1)}}}{(K_{CS}^n)^2} \right] \right\}^{-1} \times [(\varepsilon_a)_{Y_I}]_{p_o'} < 0 \tag{8}$$

3.3.2 Consolidation Stress-strain history ($\mathcal{L}_{CSSH}$)

$$[\varepsilon_a]_{Y_I}^{\sigma_{ss}} = A_{L_{CSSH}}^\varepsilon \ln(\delta_{SCT} \times \phi_{OCR}) + [(\varepsilon_a)_{Y_I}]_{NC}^{tp} \tag{9}$$

where $\mathcal{A}_{L_{CSSH}}^\varepsilon = 1.9 \times 10^{-3}$ is a constant, δ_{SCT} is the secondary consolidation factor, ϕ_{OCR} is the overconsolidation factor and $[(\varepsilon_a)_{Y_I}]_{NC}^{tp}$ is the initial yield strain determined under normally consolidated conditions at a standard time period designated after the end of primary consolidation.

3.3.3 Drainage conditions (φ_{DC})

$$[\varepsilon_a]_{Y_I}^{\varphi_{DC}} = \left[\frac{\left(\Delta \sigma_a' - 2\nu \Delta \sigma_r'\right)}{\left(\Delta \sigma_a' - \Delta \sigma_r'\right)} \right]^{\beta(d/u)} \times \left[\frac{\sigma_r'}{\sigma_a'} \right]_{KC} \times [(\varepsilon_a)_{Y_I}]_{\{d/u\}} \tag{10}$$

where $\Delta \sigma_a'$, $\Delta \sigma_r'$ are the effective axial and radial stresses respectively determined at the threshold of $[(\varepsilon_a)_{Y_I}]_{\{d/u\}}$, $[\sigma_r'/\sigma_a']_{KC}$ is the stress ratio during consolidation, $\beta(d) = -1$, $\beta(u) = +1$ (d: drained and u: undrained) and ν is the Poisson's ratio. For perfectly drained conditions $\nu \doteq 0.2$ and $\nu \doteq 0.5$ for perfectly undrained state. Under partially undrained conditions ν_{pd} can be determined as;

$$\nu_{pd} = \left\{ \frac{(E_o)_d}{(E_o)_u} (1 + \nu_u) \right\} - 1 \tag{11}$$

where $(E_o)_d$, $(E_o)_u$ are the initial drained and undrained elastic moduli respectively.

3.3.4 Cyclic prestraining (α_{cp})

$$[\varepsilon_a]_{Y_I}^{\alpha_{cp}} = \mathcal{A}_{\alpha_{cp}}^\varepsilon \ln \alpha_{cp} + [(\varepsilon_a)_{Y_I}^R]_{(tp)}, \left| \frac{\partial^2 (\varepsilon_a)_{tp}}{\partial \alpha_{cp}^2} = 0 \text{ and,} \left[\frac{\partial^3 (\varepsilon_a)_{tp}}{\partial \alpha_{cp}^3} \right]_{\delta R} < 0 \tag{12}$$

3.3.5 Strain rate $(\varepsilon_a)_{Y_I}^{\dot{\varepsilon}_{SR}}$

$$[\varepsilon_a]_{Y_I}^{\dot{\varepsilon}_{SR}} = \left[A_{\dot{\varepsilon}_{SR}} \ln\left(\frac{\dot{\varepsilon}_{ASR}}{\dot{\varepsilon}_{RSR}}\right) + B_{\dot{\varepsilon}_{SR}} \right] \times (\varepsilon_a)_{Y_I}^{\dot{\varepsilon}_{SR}} \tag{13}$$

Mukabi - Case Study Analysis of OPMC Improved Foundation Ground, Pavement and Other Geo-structures Employing the GECPRO Model

II-435

where the subscripts *SR* denote Strain Rate, *ASR*: Applied Strain Rate during testing or arbitrarily designated and *RSR*: Reference Strain Rate.

3.4 Deriving shear strength from elastic stiffness and generation of secant modulus prediction curves

Developing an appreciably reliable correlation between shear strength at failure and the elastic (Initial) stiffness is important in determining a more precise parameter (q_{max}) closely related to a ground property (E_0). The GECPROM module for this relation is:

$$q_{max} = A_{\psi E_0} \times \exp[B_{\varphi_{CSS}} \ln\{m^{-1} \times (\sigma_a)_{max} \times E_0] - C_{\varphi_{CSS}} \tag{14}$$
$$A_{\psi E_0} = 0.134, \qquad B_{\varphi_{CSS}} = 0.418, \qquad C_{\varphi_{CSS}} = 0.936, and\ m^{-1} = 1.32$$

Figures 6 (a) and (b) depict the experimental and modeled characteristic curves for stress ~ strain behavior and the decay of stiffness plotted as a function of strain level for intact and reconstituted specimens sampled and tested in Japan adopting sophisticated Triaxial testing equipment.

For generating the prediction curves that characterize the secant and initial moduli, E_S, E_0 , Eqs. (15) and (16) are applied respectively, in conjunction with other equations proposed by [8].

$$E_S = \frac{d\Delta q}{d\Delta\varepsilon_a} = \psi_{E_S} \times \left\{ G = \frac{E_S}{2(1+v)} \alpha_{E_S}(\varepsilon_a)^m + \beta_{E_S}(\varepsilon_a)^n + \gamma_{E_S} \right\} \times 10(MPa) \tag{15}$$

$$\left| \begin{matrix} m = 1 \\ n = 0 \end{matrix} \right. when\ 0 \leqq \varepsilon_a \leqq 0.1 \ , and \left| \begin{matrix} m = 2 \\ n = 1 \end{matrix} \right. when\ \varepsilon_a > 0.1$$

and,

$$E_o = [\alpha_{E_o}(\varepsilon_a)_{=0.001\%} + \beta_{E_o}] \times 10(MPa) \tag{16}$$

where α_{E_o} and β_{E_o} are determined simultaneously at ε_a=0.001% and 0.01%.

3.5 Application examples in modelling and prediction

Figures 5 (a) and 5 (b) compare experimental test results of stiff pleistocene clays sampled and tested in Japan. In these figures all the curves modeled by the GECPROM show a very good agreement in comparison to the experimental trends. It can also be inferred that the curves for the reconstituted specimens deviate significantly from those of the intact ones in all cases.
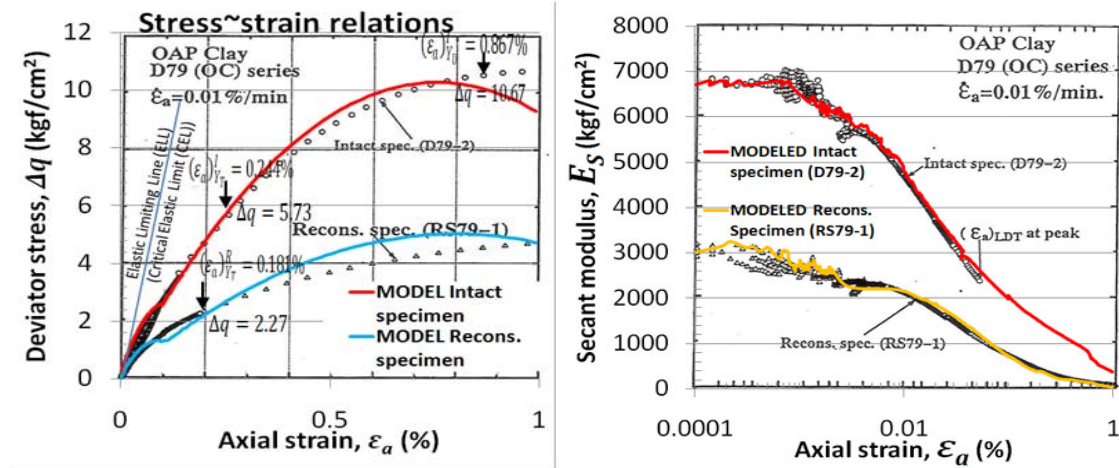
Figure 5 : (a) Comparison of modeled and measured stress~strain relations for Over-Consolidated (OC) OAP clay for intermediate strains {(ε$_a$)$_{ELS}$(Y$_I$)} ~ {(ε$_a$)$_{TYS}$(Y$_T$)}, (ε$_a$ ≤ 1%); (b) Comparison of modeled and experimentally determined strain level dependency of stiffness decay curves including predicted curves {(ε$_a$)$_{ELS}$(Y$_I$)} ~ {(ε$_a$)$_{FYS}$(Y$_F$)}, (ε$_a$ ≤ 1%); for intact and reconstituted specimens [8]

4 CASE STUDY ANALYSIS

4.1 Survey, Monitoring and Testing Regimes

Details of the survey, monitoring and testing procedure are reported in the "Innovative Laboratory and In-situ Methods of Testing in Geotechnical Engineering" and the Juba River Port Access Road Engineering

Mukabi - Case Study Analysis of OPMC Improved Foundation Ground, Pavement and Other Geo-structures Employing the GECPRO Model

II-436

Report No. SST1[10]. A summary of the main tests citing the purpose of the test and the engineering parameters determined in relation to the Case Study Analysis is presented in Table 1.

Table 1: Summary of main tests, purpose and engineering parameters determined

Prop.	Description of Test	Purpose of Test/Engineering Parameters Determined in Reference to this Case Study Analysis	Ref. Eq.
1 (BPP)	Moisture ContentVariation Field and Lab. Density	Comparative Analysis for mainly quantifying Moisture-Suction Variation, ΔM_c, ρ	1,2 &3
2 (MS)	Sieve Analysis	Comparative Analysis to determine state of Mechanical Stabilization, η, δ, M_s^f, B_c, f_{BSR}, $f_{opt}R_r^c$	4,5,6 7&8
3 (SC)	3.1 Field Deflection Testing 3.2 Innovative Soil Profiling 3.3 ST Geophysical Sounding	1. Determine Existing Structural Capacity, f_{SC}^e 2. Predict Structural Capacity Soundness, f_{SC}^t 3. Compute Maintenance Requirement Ratio, M_{RR}	17 20
4 (UCS) (SS) (EM)	4.1 Dynamic Cone Penetration 4.2 Laboratory UCS 4.3 Laboratory CUTC 4.4 Modified Laboratory VDL	1. Determine Consolidation Properties, SC, STC, LTC, Creep ($\dot{\varepsilon}_a$), CAS (σ_a^c), CLS (σ_r^c), CSRF(δ_{CSR}) 2. CS (q_u, C_u), Modulus of Deformation (E_{50}), EEM (E_E), 3. Deviator Stress, (q), Axial Stress, (σ_a), Lateral Stress, (σ_r), Angle of Shearing Resistance, (Φ), Elastic Modulus, (E), Shear Modulus (G), Modulus of Deformation, (E_s, G_γ), Secondary Yield Strain, Y_S, Mean Effective Stress (p') 4.Degree of Particle Interlocking(ϕ_I'), ϕ_I'/C_u ratio($^I/_S$), Shear Strength (τ_f), Dynamic Modulus (E_D),	21 To 36
5 (EM)	In-situ Geophysical Testing	Initial Elastic Modulus, (E_0), Shear Modulus (G_0) Geophysical Profile (G_P)	21 32
6	Innovative Stage Loading Tests	Refer to Mukabi et al. (2012a)[1]	

Notes: Prop – Property, BPP - Basic Physical Properties, SC – Structural Capacity, ST - Structural Thickness, SS- Shear Strength, UCS – Unconfined Compressive Strength, CUTC – Consolidation Undrained Triaxial Compression, VDL – Vibrational Dynamic Loading, SC , STC, LTC, – Secondary , Short Term and Long Term Consolidation, CAS – Consolidation Axial Stress, CLS – Consolidation Lateral Stress, CSRF – Consolidation Shear Stress Factor, US – Compressive Strength, EEM – Empirical Elastic Modulus, EM - Elastic Modulus

4.2 Juba River Port Access Road – Road Pavement Structure

The Juba River Port Access Road traverses areas that are predominantly overlain with high problematic and expansive Black Cotton Soils (BCS) within swampy stretches. During the implementation of an Emergency Project grant aid funded by the Japan International Cooperation Agency (Government of Japan), it was necessary to adopt cost-effective methods of improving the existing ground for purposes of reducing the quantities that would be required for the upper pavement layers (subbase and base courses) mainly due to lack of suitable road construction materials within reasonable haulage distances. Full-fledged field experimental sections with three varying pavement structural configurations were designed, as shown in Figures 6 ~ 8, and implemented under otherwise similar environmental conditions for purposes of determining the most optimum and cost-time-effective VE design, appropriate methods of construction and reduction in the Maintenance Requirement Ratio [4]and [10].

Figure 6: Typical Cross section of Type II-1 of the Juba River Port Access Road depicting the experimental trial section pavement structure without OPMC stabilization and without subgrade improvement, constructed in swampy areas with expansive Black Cotton Soils

Mukabi - Case Study Analysis of OPMC Improved Foundation Ground, Pavement and Other Geo-structures Employing the GECPRO Model
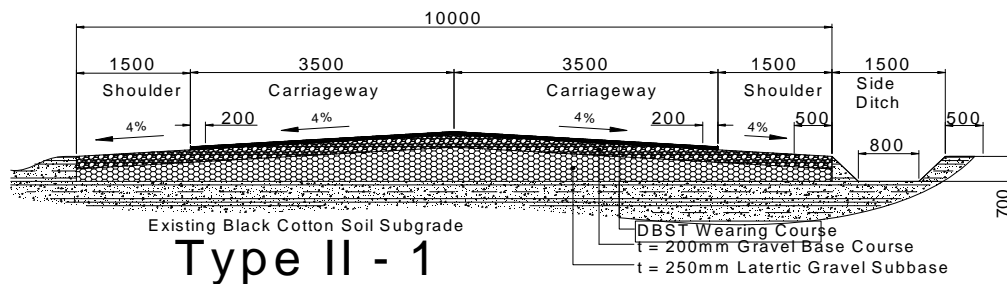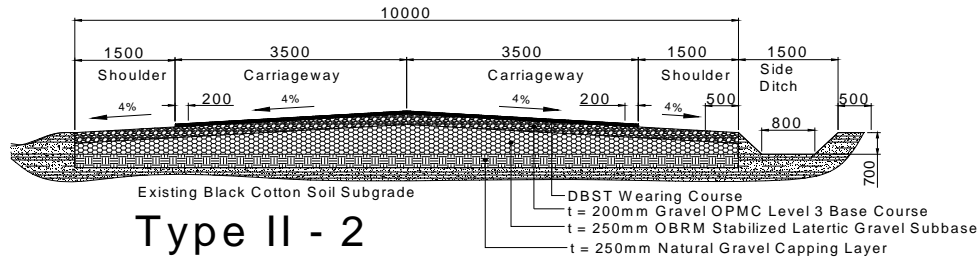
II-437

Figure 7: Typical Cross section of Type II-2 of the Juba River Port Access Road depicting the experimental trial section pavement structure with OPMC Level 3 stabilization and OBRM stabilization for Base/Subbase as well as partial Black Cotton Soil subgrade improvement
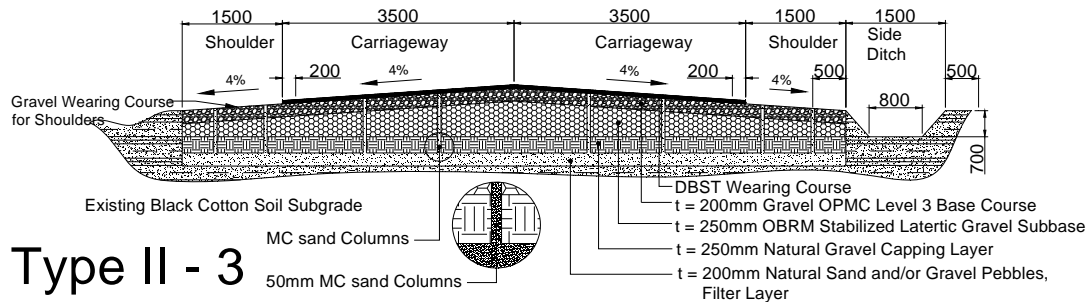

Figure 8: Typical Cross section of Type II-3 of the Juba River Port Access Road depicting typical pavement structure with OPMC Level 5 and OBRM stabilization for Base/Subbase with well improved Black Cotton Soil subgrade constructed in swampy areas under extreme conditions

4.3 In-situ Modeling of Response of Varying Pavement Structural Configurations

Monitoring, laboratory testing of samples hand-curved and/or cored from the experimental trial sections and in-situ measurements were undertaken consistently for a period of 3 years (1092 days) as can be noted from Figure 9 (a), which depicts the effect of particle agglomeration on shear strength development characteristics mainly as a result of cementation and secondary consolidation due to heavy dynamic traffic loading. A high rate of progressive strength development can be observed in the initial phase.
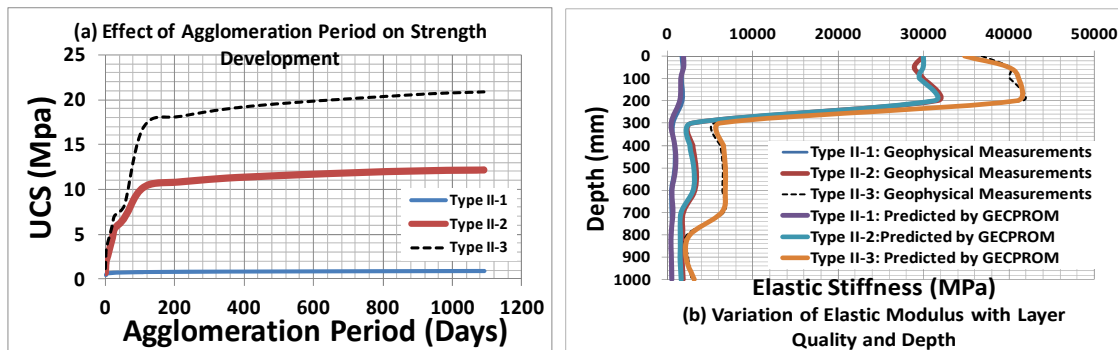

Figure 9: (a) Influence of agglomeration of strength developement wit time, and (b) Variation of elastic stiffness with pavement layer quality, configuration and depth for measured and predicted results

Figure 9 (b) shows the quantitative variation of the elastic stiffness with layer quality, configuration and depth for the three different types of trial sections. The results reported were measured on the 1092nd day, while the behavior of the varying pavement structures was modeled by using the GECPROM [8].

4.4 Oil exploration project in Jonglei Flood Plains in Southern Sudan

The scope of the project included the design and construction of pad foundations, access roads, airstrips and base camps foundations. The design criteria took into consideration various environmental and load factors; including dead loads, live loads, static and dynamic loading effects during drilling operations and construction equipment. Some representative results from the design studies, which portray dependency

Mukabi - Case Study Analysis of OPMC Improved Foundation Ground, Pavement and Other Geo-structures Employing the GECPRO Model

II-438

of stress-strain characteristics on the mode of stabilization as well as type and location of geosynthetics reinforcement, are depicted in Figure 10, while a typical design cross section is shown in Figure 11.
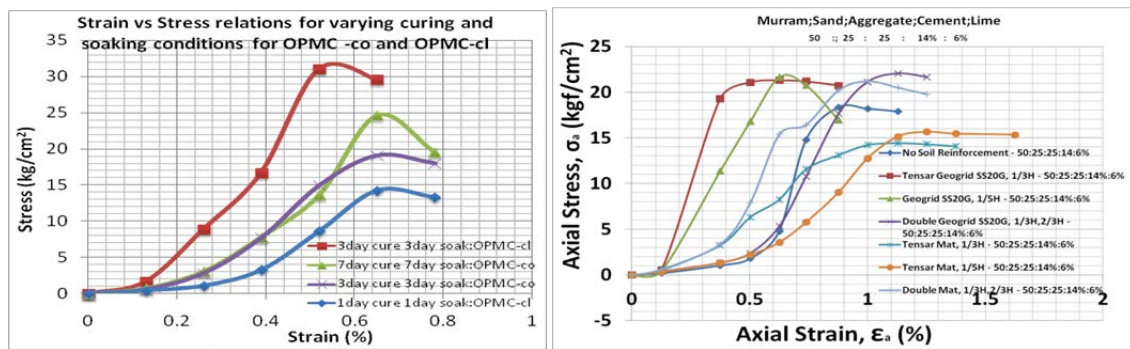

Figure 10: OPMC-cl and OPMC-co Stress – strain relations for varying curing, soaking and geosynthetics reinforcing conditions for specimens constituent of geomaterials sampled in Jonglei
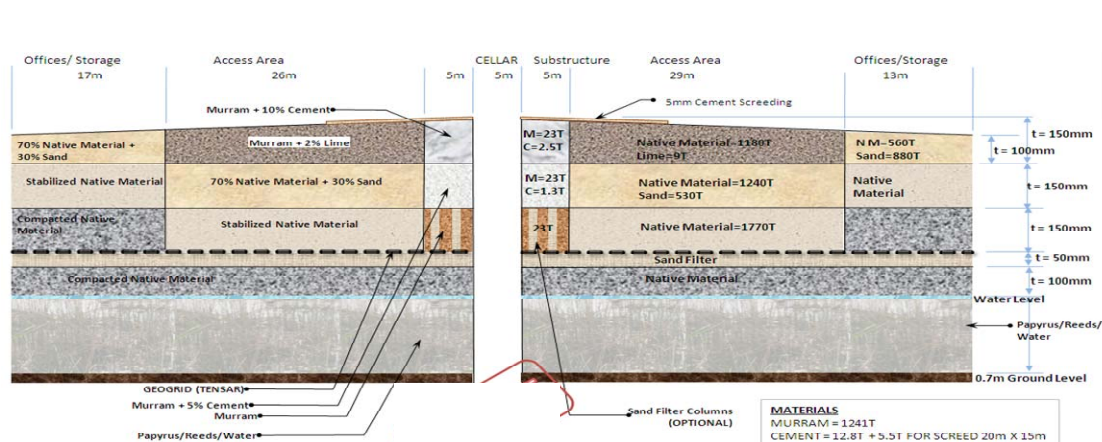

Figure 11: Typical Cross-section of the drilling rig pads foundation employing OPMC and geogrid reinforcement

4.5   Addis Ababa ~ Debre Markos International Trunk Road – Retaining Wall

During a road and bridges rehabilitation programme under Grant Aid funding by the Government of Japan, slope failure occurred at a stretch around Sta. 9+310km from the city centre of Addis Ababa along the Addis Ababa~Goha Tsion~Debre Markos International Trunk road traversing through the Blue Nile, and which forms an integral part of the all-important north-western corridor connecting to the western part of The Sudan, whilst branching off to the east towards Gonder to the Eriterian border.

As a result, longitudinal cracks were prevalent within the asphalt concrete and significant shear failure occurred right through the pavement structure and subgrade. Due to environmental and financial constraints, it became imperative that a cost-effective method utilizing locally available material as much as possible be employed. OPMCS technology was employed in improving the available geomaterials and existing subgrade. Typical experimental test results and design cross section are shown in Figures 12 and 13 respectively. Enhanced performance in terms of deformation resistance can be observed in Figure 12.

Mukabi - Case Study Analysis of OPMC Improved Foundation Ground, Pavement and Other Geo-structures Employing the GECPRO Model
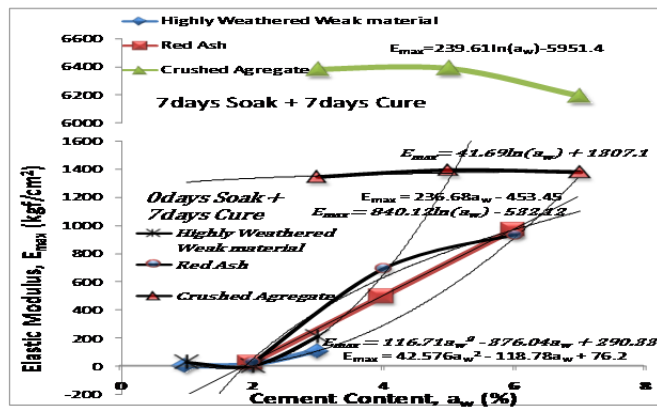
II-439

Figure 12: Effect of cementation and curing time on soil particle agglomeration of varying OPMC stabilized geomaterials with respect to elastic modulus
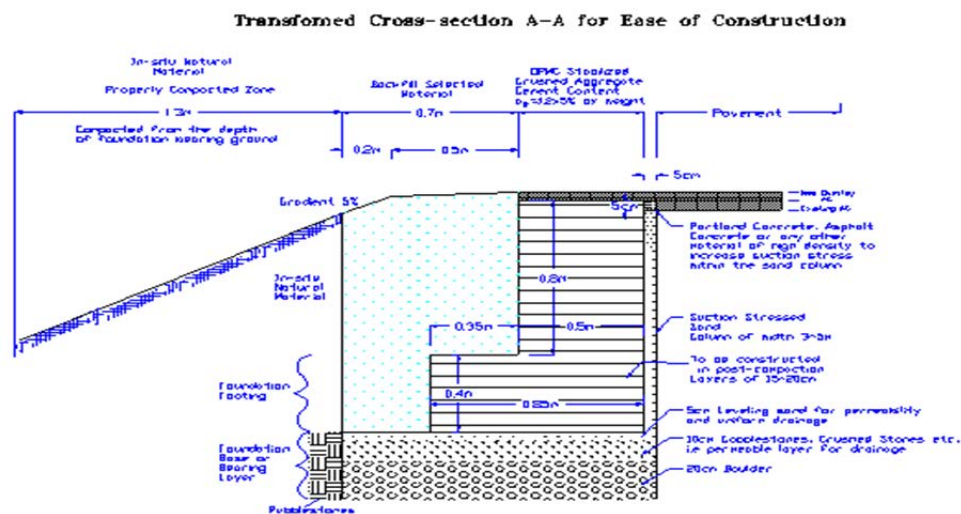

Figure 13: Cross-section A-A showing the foundation, stabilized retaining wall, improved layer configuration and geomaterials and ground improvement stabilization zones

5   CONCLUSIONS

The Case Study Analysis undertaken in this Study indicate that:
1. OPMCS technology is substantially effective in improving the vital geotechnical engineering parameters, and that the degree of enhancement is mainly a function of it's qualitative level .
2. OPMCS can be classified as a Value Engineering technology. This technology has also been proven to be useful as an environmental mitigation tool.
3. The GECPROM can be effective in predicting multi-layered pavement structural behavior.

REFERENCES

[1] *Mukabi, J.N, 2001a, "Theoretical and empirical basis for a method of determining the optimum batching ratio for mechanical stabilization of Geomaterials", Proceedings, 14th International Road Federation, Road World Congress, Paris, CD-ROM.*

[2] *Mukabi, J.N & Shimizu, N, 2001b, " Strength and deformation characteristics of mechanically stabilized road construction materials based on a new batching ratio method", Proceedings, 14th International Road Federation, Road World Congress, Paris, CD-ROM.*

[3] *Mukabi J.N, Kimura Y, Shimizu, N, Mwangi SN, Omollo A, Njoroge BN, 2001c, " Evaluation of some Kenyan Geomaterial properties for embankment design based on a quasi-empirical approach", Procs. 15th Int. Conf. on SMGE, Istanbul, pp2159-2166.*

Mukabi - Case Study Analysis of OPMC Improved Foundation Ground, Pavement and Other Geo-structures Employing the GECPRO Model

II-440

[4] *Kogi, S.K, Mukabi, J.N, Ndeda, M, Wekesa, S, 2011, "Analysis of Enhanced Strength and Deformation Resistance of Some Tropical Geomaterials through Application of In-situ Based Stabilization Techniques", Proceedings. 1st International Conference. on Geotechnique, Environment & construction Materials, GEOMAT, Mie, Japan.*

[5] *Mukabi J.N., Toda, T. & Shimizu, N, 2007b, "Application of a new mechanical stabilization technique in reducing the cost and impact of rural road construction, Proceedings of the 23rd World Road Congress, Paris, France, CD-ROM.*

[6] *Mukabi J.N, Kimura Y, Murunga P.A, Njoroge B.N, Wambugu J, Sidai V, Onacha K., Kotheki S, Ngigi A, 2010c, "Case example of design and construction within problematic soils", in Procs. Int. Geotech. Conf. on Geotechnical Challenges in Megacities, Geomos, Moscow, vol. 2, pp 1172-1179.*

[7] *Kensetsu Kaihatsu Limited, 2011, "Isiolo Airport Pavement Design, Engineering Report No. ISAT 0211/O2", submitted to Kenya Airports Authority, Government of Kenya, Nairobi.*

[8] *Mukabi, J.N & Hossain, Z, 2011e "Characterization and modeling of various aspects of pre-failure deformation of clayey Geomaterials – Applications in modelling", Proceedings. 1st International Conference. on Geotechnique, Environment & construction Materials, GEOMAT, Mie, Japan.*

[9] *Mukabi J.N, 2011d "Characterization and modeling of various aspects of pre-failure deformation of clayey Geomaterials – Fundamental theories and Analyses", Proc. 1st Int. Conf. on GEOMAT, Mie.*

[10] *Kensetsu Kaihatsu Limited, 2007, "Juba River Port Access Road Pavement Design, Eng. Report No. SST1", submitted to Japan International cooperation Agency, JICA, & Katahira & Eng. Int., Japan.*

[11] *Kensetsu Kaihatsu Limited, 2007b "A Comprehensive Engineering Report on the Study, Design and Construction of Drilling Pad Foundations in Jale, Jonglei State, Southern Sudan", submitted to White Nile Oil Exploration Company, London, England*

[12] *Mukabi, J.N, Hatakeyama, R, Tasfaye, A, 2007e, "Employing Cost-effective Countermeasures to Slope Failure Based on Newly Developed OPMC Stabilization Concepts, Proceedings of the 14th African Regional Conference on Soil Mechanics Geotechnical Engineering, Yaounde, Cameroon.*

Mukabi - Case Study Analysis of OPMC Improved Foundation Ground, Pavement and Other Geo-structures Employing the GECPRO Model

II-441

Remedy of Deep Soil Mixing Quality for Montmorillonite Clay Deposited in the Mekong and Mississippi Deltas

Mitsuo Nozu, Ngo Tuan Anh, Naotoshi Shinkawa & Kazunori Matsushita, Fudo Tetra Corporation
E-mail:mitsuo.nozu@fudotetra.co.jp

ABSTRACT

Wet type deep mixing (DM) columns have been installed in the southern region of Vietnam and in Louisiana, the United States, to increase the stability of slopes and mitigate ground settlement. Prior to DM production, laboratory mixing tests need to be executed carefully. Certain types of clay, such as Montmorillonite clay deposited in major river deltas in the South of Vietnam and in the Southern United States, are not easy to mix with cement in laboratory tests. Difficulties also arise in mixing on site.

This paper describes the clay property and considers a case study of a laboratory mixing test and differences with Japanese clay mixing results. In addition, suitable admixtures to remedy the mixing quality for more difficult clays are introduced, without significantly increasing the cement volume.

1.   INTRODUCTION

In South Vietnam, according to many references and standards (Miki, 1998, JGS, 2000, Kitazume et.al., 2001, BS 2005, Nozu 2005, Tung et.al., 2009, S. T. G. Peng et.al, 2009), deep mixing (DM) has been used in recent years for soft clay improvement to increase the stability of slopes and to reduce consolidation settlement. Prior to DM production, laboratory mixing tests need to be executed carefully. The cement dosage can vary considerably due to the required performance, such as unconfined compression strength, soil condition, and local cement property.

This paper begins with a description of clay properties and a case study of laboratory mixing tests using the local clay deposited in major river deltas in Vietnam and the United States, and considers differences with Japanese clay mixing results. These areas include Montmorillonite clay, which tends to absorb water so that sufficient mixing quality is hard to achieve (Nozu 2010). In addition, suitable admixtures to remedy the mixing quality for that kind of clay are introduced, without significantly increasing the cement volume.

Figure 1.1 DM on-land rig and off-shore barge in Vietnam

2.   SOIL PROFILE AND CEMENT PROPERTY

The soil profile at two large river deltas where DM method has been applied is shown in Table 2.1. In the South of Vietnam, marine clay is deposited to a thickness of around 20 to 30 m without a sand seam. (The shear strength of marine clay is typically around cu=10+1.5z, kPa.) The coefficient of consolidation (cv) is also rather low at around 10-60 cm^2/day, because of its fine clay particles. This suggests that a consolidation acceleration method like a plastic board drain is likely to be difficult to use in this area.

In the United States, the Mississippi river delta has soft clay layers such as a "peat" layer with a thickness of 4 to 5 m, at a depth of 5 m, and a "fat clay" layer with a thickness of 10 to 15 m, at a depth of 10 m. In fat clay, the natural water content is approximately 20% lower than the liquid limit so that it is hard to make it fluid and hard to mix it with cement (see Photo 4.1, Nozu 2010).

Table 2.1 Soil conditions in major river deltas in Vietnam and the United States

		Cc (%)	LL (%)	Ip	wn (%)	Density (g/cm3)	Su (kPa)	Su/p	cv (cm2/day)	pH
South Vietnam		40-70	75-100	35-64	65-95	2.67-2.78	20-60	0.2-0.25	10-60	5.4-5.8
U.S. (Mississippi)	Peat	-----	-----	-----	99-500	-----	15-20	-----	-----	5.0-7.6
	Fat clay	60-80	60-80	20-60	45-60	2.67-2.78	10-40	≒0.2	10-50	7.0-8.0
Japan(Ariake-kai)		50-55	55-140	50-80	42-200	2.58-2.66	8-40	0.25-0.45	50-200	6.5-7.5
Japan(Hachirogata)		40-70	150-200	54-77	74-100	2.65	130-160			

2.1 X-ray diffraction analysis

X-ray diffraction analysis (see Figure 2.1) has been performed to investigate the micro structure of these clays. The analysis has revealed montmorillonite crystals, formed by metamorphic tuff, to some extent in both Vietnam marine clay and U.S. fat clay.

Montmorillonite readily absorbs water. Subsequently, mixing with cement may be difficult because of local gel reaction and the lack of a separation property (Figure 2.3). Montmorillonite has an octahedron-type crystal structure that readily accepts water. This crystal is very rare and is not usually deposited in soft ground in Japan.
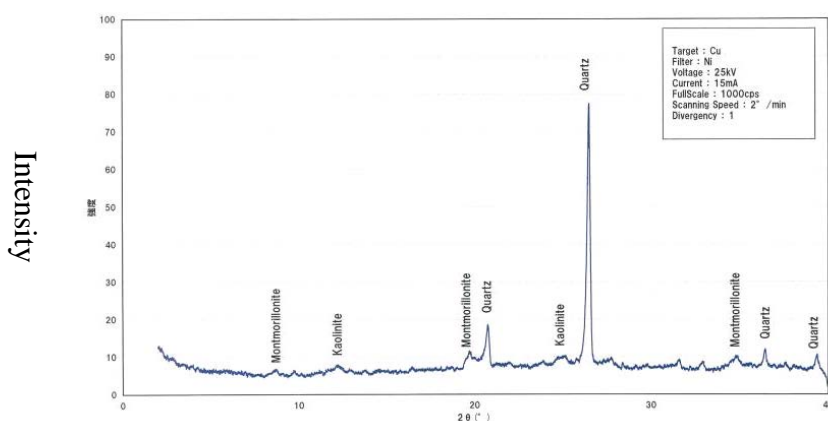

Figure 2.1 X-ray diffraction analysis results of South Vietnam marine clay
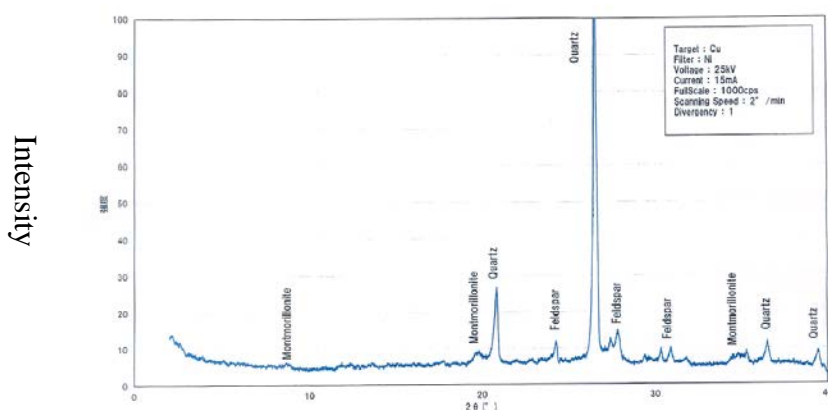

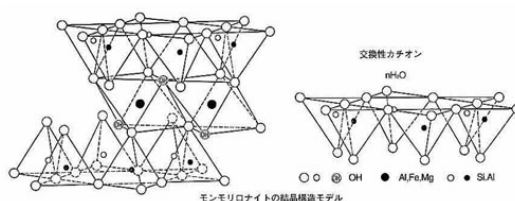Figure 2.2 X-ray diffraction analysis results of Mississippi delta clay

Figure 2.3 Crystal structure of montmorillonite

2.2 Element quantitative analysis

Table 2.2 shows the results of element quantitative analysis obtained using a fluorescent X-ray device.

Table 2.2 Results of element quantitative analysis

(%)	South Vietnam	New Orleans
SiO_2	53.5	65.0
Fe_2O_3	17.6	9.3
AL_2O_3	11.8	8.6
SO_3	9.0	4.4
K_2O	3.4	5.1
TiO_2	2.3	1.6
CaO	1.9	5.4
MnO	0.2	0.2

2.3 Electric conductivity

Table 2.3 shows the electric conductivity of each kind of soil. The electric conductivity of South Vietnam and New Orleans fat clay is comparatively high, such as 230-992 micro Siemens/cm.

Table 2.3 Electric conductivity of suspended soils

	South Vietnam	New Orleans	Japan Osaka Bay
Electric conductivity(mS/cm)	992	230	4.5
pH	8.0	10.0	
Ignition loss (%)	11.5	6.1	

2.4 Ion exchange capacity

Table 2.4 shows the cation exchange capacity (CEC) and each cation amount.

Table 2.4 CEC and Cation amount

(meq/100g)	South Vietnam	New Orleans
CEC	18.4	20.2
Ca^{2+}	39.6	40.0
Mg^{2+}	17.8	14.2
Na^+	37.2	11.7
K^+	3.3	2.2
Total	97.9	68.1

2.5 CEMENT PROPERTY

Cement content in each region is summarized in Table 2.5. Both Vietnam and the United States have Ordinary Portland Cement (OPC) and Portland Blast Furnace Cement (PBFC). However, the fineness of each cement type is significant and hydration time is short in comparison with Japanese cement.

In the Vietnam cement standard, fineness values such as 3780 cm^2/g for OPC and 3970 cm^2/g for PBFC are relatively high. This means that it is easy to obtain a hydration reaction at an early stage using Vietnam cement.

Table 2.5 Cement content in each region

		Vietnam		U.S.	Japan		
					JIS R 5210		JIS R 5211
		OPC	PBFC	OPC	NP[1]	HEP[2]	PBFC B[3]
Specific surface (cm^2/g)		3780	3970	3790	$\geqq 2500$	$\geqq 3300$	$\geqq 3000$
Setting time	Initial (min)	110	165	96	$\geqq 60$	$\geqq 45$	$\geqq 60$
	Final (h)	2h45min	3h55min	3h58min	$\leqq 10$		
Chemical(%)	MgO	-----	-----	2.9	$\leqq 5.0$	$\leqq 5.0$	$\leqq 6.0$
	SO_3	2.1	2.4	2.9	$\leqq 3.0$	$\leqq 3.5$	$\leqq 4.0$

*1) NP: Normal portland cement
*2) HEP: High early strength portland cement
*3) PBFC B: Portland blast furnace slag cement (Type B)

3.   LABORATORY MIXING TEST RESULTS

Figure 3.1 shows a comparison of the cement dosage and 28-day UCS strength relationship for each region. Figure 3.2 shows the cement dosage and UCS relation for peat and fat clay in the United States. It is clear that with PBFC, a higher UCS is obtained at all regions, while in both the United States and Vietnam, the UCS is lower than it is in the Japanese case. The reasons for the low UCS are believed to be as follows:

(1) Small clay particles compared with cement particle,
(2) Mixing hardness; Photo 3.1 is the filling condition for a mold in the United States. The clay readily absorbs mixing water so it is hard to fill the mold. In addition, unmixed clay remained because of condensation through an exchange of ions between the cement and the clay. Aoyama et. al. (2002) indicated a tendency to condensation with only clay itself before the hydration reaction if the clay contains a significant ion component (Figure 3.3).
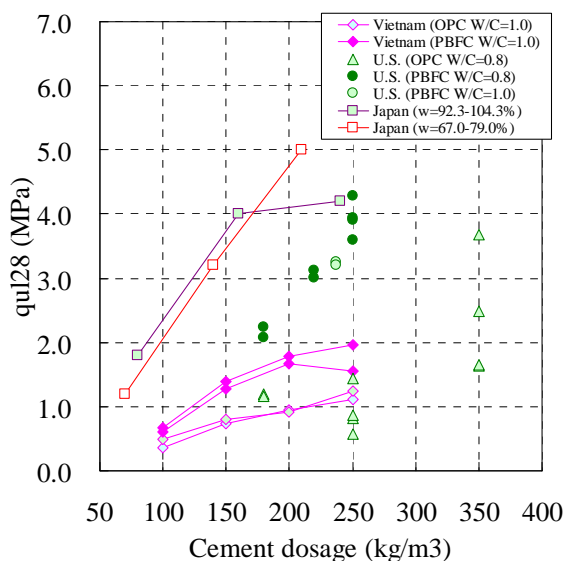

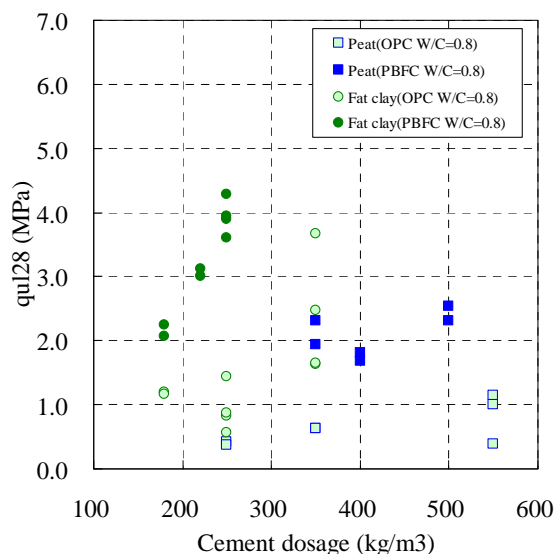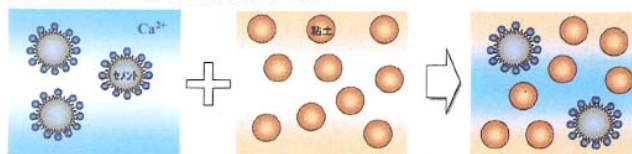Figure 3.1 Cement dosage and 28-day strength in each region

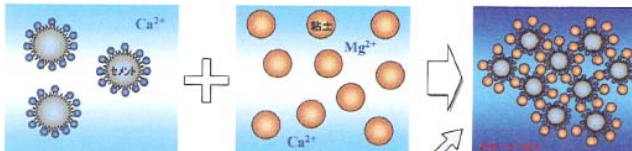Figure 3.2 Cement dosage and 28-day strength of peat and fat clay in the United States

Photo 3.1 Filling condition to molds

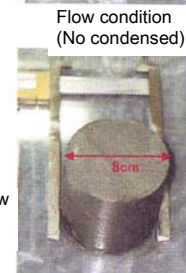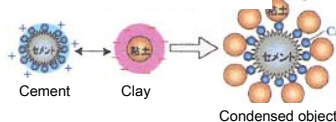Figure 3.3 Condensation property (Aoyama, et. al. 2005)

---

4. MEASURES TO MITIGATE CONDENSATION

To mitigate condensation during cement mixing, some admixtures have been tested in a laboratory mixing test and table flow test using South Vietnam clay, including Montmorillonite clay. In this moment, two kinds of admixtures are selected: Admixture A and Admixture B. They are shown as Table 4.1 in detail. These two admixtures have the function of increasing liquidity.

Table 4.1 Comparison of each admixture

	Admixture A	Admixture B
Producer	BASF	KAO
Purpose	Retarding water reducing	Increase liquidity for cement mix soil
Place of Production	Almost all countries	Japan and Thailand

4.1 Unconfined Compression Strength (UCS) test

In the laboratory mix test, cement dosage 160kg/m3, W/C (water cement ratio) 1.0, and admixtures 1% and 2% were employed, and a UCS test was conducted using South Vietnam clay. The results are shown in Table 4.2, Figure 4.1, and Figure 4.2.

   According to the results, the UCS effect is roughly the same with Admixture A 2% and Admixture B 1%. In addition, a comparatively large increase in UCS at 28 days compared with 7 days UCS was observed.

Table 4.2 UCS test results

CASE	Admixture	28day qu kPa	7day qu kPa
CASE 1	No	1,627.8	288.4
		1,233.4	461.0
		1,507.2	565.8
CASE 2	Admixture A 1%	1,746.6	444.4
		1,570.7	439.2
		1,446.9	465.8
CASE 3	Admixture B 1%	2,056.0	581.5
		1,987.5	486.7
		1,987.5	482.0
CASE 4	Admixture A 2%	2,043.6	592.0
		2,101.6	583.5
		2,105.9	466.2
CASE 5	Admixture B 2%	1,961.4	517.1
		2,110.1	501.4
		1,683.0	453.5

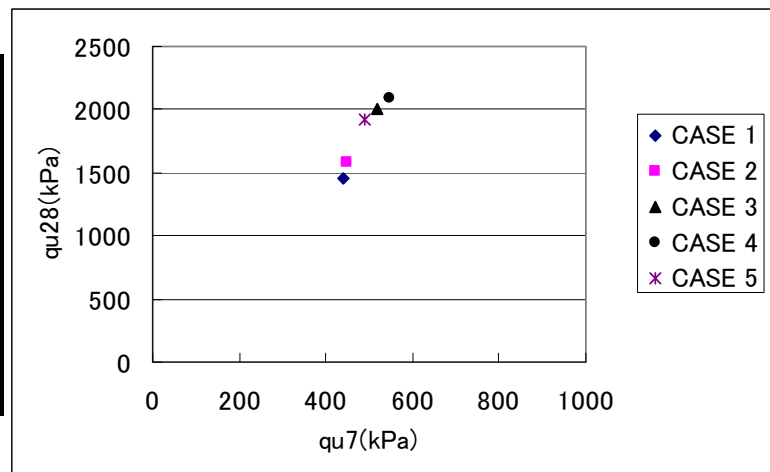*qu7:7days UCS
*qu28: 28days UCS

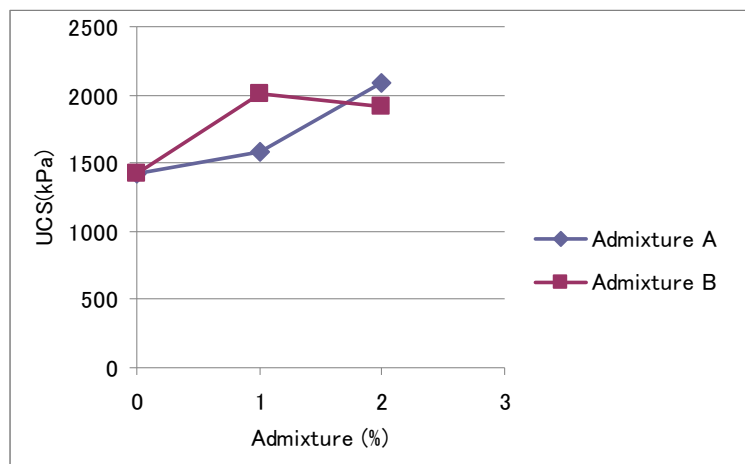Figure 4.1 Relationship between qu7 and qu28.

Figure 4.2 Admixture amount and UCS relationship

4.2 Table flow test

Table flow test (Photo 4.1) were conducted using the same Vietnam clay. Diameter of the flow cone is 100mm and 15 times shocks are given to the mix soil and the subsequent diameter expansion is measured. The results are shown in Figure 4.3. According to the results, there is a significant effect in terms of increased liquidity when using admixture, although the volume of admixture at this time was as high as 4% and 8%. Considering its strong retarding effect, actual amount of admixture should be restricted as less than 2%.

Photo 4.1 Table flow test device
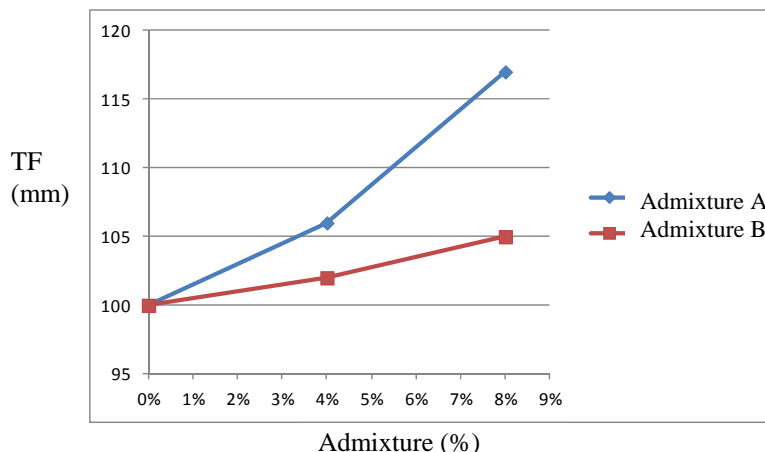
Figure 4.3 Results of table flow test

4.3 Image of Principle of Fluidity Increase by admixture

Very fine clay such as 'Montmorillonite' has tendency of being high negative ion charge rate. In this case, it is easy to have following 'Gel reaction' due to ion exchange just after cement mixing. This 'Gel reaction=condensation' cause difficulties of well mixing on site.

However, when the oxycarboxylic acid is used as the admixture (retarder), the calcium ion will be covered by the acid and therefore it is becoming neutral electrically. So, the Gel reaction is not occurred and therefore cement and soil are able to be mixed well. After that the retarder will be removed gradually and the mixed soil will have sufficient strength due to hydration / Pozzolana reaction (Figure 4.4).

(a) No admixture

(b) Admixture (Oxycarboxylic acid)
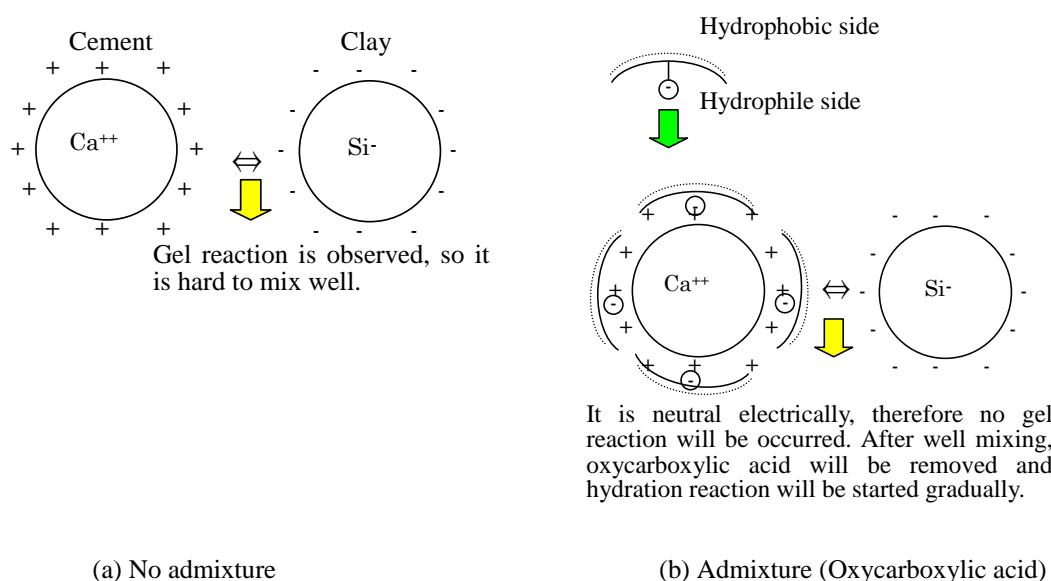
Figure 4.4 Image of Fluidity Increase by Admixture

5. CONCLUSIONS

The strength characteristics in a laboratory cement mixing test were investigated using Vietnam delta clay and Mississippi delta clay. Each local soils include Montmorillonite clay and have high electric conductivity. It causes serious condensation problems such as unmixed zone inclusion when cement is mixed with the clay. Therefore, various admixtures were tested to mitigate condensation and increase liquidity to achieve the desired mixing quality and a sufficient UCS value.

Consequently, when Deep Mixing in such Montmorillonite clay is planned, careful consideration to ensure good mixing quality is required.

REFERENCES

*Aoyama K., et.al, 2002, Influence of physical and chemical property of soil against initial condition and strength of cement mixed soil, Journal of Geotechnical Engineering, Japanese Society of Civil Engineers, No.721/VI-57,pp.207-219., JAPAN*

British Standard,2005, Execution of special geotechnical works-deep mixing, BS EN 14679

Japanese Geotechnical Society, 2000, Practice for making and curing stabilized soil specimens without compaction, JGS 0821-2000, Japanese Geotechnical Society (in Japanese).

Kitazume, M. and Terashi, M.,2001, The Deep Mixing Method, A.A. Balkema Publishers
.
Miki, H. and Nozu, M., 1998, Manual for Design and Construction of Cement Column Method, (JICA, Public Works Research Institute (MOC))-THAILAND (Department of Highway), Joint Study on Soft Clay Foundation.

Nguyen bach Tung, et.al, 2009, Soft Soil treatment with Wet Mixing Soil Cement Column of Japanese technology in Mekong River Delta, Deep Mixing '09 in Okinawa.

Nozu, M., 2005, Regional Report in Asia, Deep Mixing '05 in Stockholm.

Nozu, M. and Nakai, N., 2010, Strength characteristic at laboratory cement mixing test using soft clay deposited at the mouth of long rivers, Vietnam Geotechnical Day.

Sam Tam Gak Peng et.al, 2009, Soil Improvement works for the Design and Development of SP-PSA International Port Company Ltd project in Baria-Vung Tau, Vietnam, Deep Mixing '09 in Okinawa.

Stiffness of Soil-Cement-Fly Ash by means of Shear Wave Velocity

K. Piriyakul, Department of Civil and Environmental Engineering Technology, College of Industrial Technology, King Mongkut's University of Technology North Bangkok, Thailand, keeratikanp@kmutnb.ac.th

S. Pochalard, Civil Engineer, Division of Campus Buildings and Site, Suan Dusit Rajabhat University, Thailand, sakol.poc@gmail.com

ABSTRACT

This paper presents the bender element technique to determine the stiffness of Bangkok clay mixed with the Portland cement type 1 and fly ash by means of shear wave velocity. The Bangkok clay is mixed with 20% by weigh of Portland cement type 1 and varied the amount of fly ash (0, 10, 15, 20, 25 and 30% by weight). The soil-cement samples were cured for 3, 7, 14, 28 and 90 days. Then, these samples are performed the bender element test and the unconfined compression test. The results reported that the optimum of replacement fly ash is about 15-20% and showed that the stiffness of soil-cement-fly ash mixing is increased with increasing the curing time. However, both results of the shear wave velocity and the undrained shear strength are higher than the result of 0% replacement of fly ash which is the long term behaviour of cement mixed with fly ash.

1.   INTRODUCTION

Currently, the Soil Mechanics Laboratory of the Department of Civil and Environmental Engineering Technology, King Mongkut's University of Technology North Bangkok has developed a new technique for determination of the initial shear modulus, G_0, by means of elastic shear wave. This measurement uses the principles of wave propagation showing a direct correlation between the shear wave velocity and G_0 as described in [1]. [2] used similar piezoelectric ceramic sensors to assess the disturbance of soil samples and [3] used piezoelectric ceramic sensors to examine the anisotropy of clay soil. This initial shear modulus is widely considered to be an important parameter in earthquake engineering and the prediction of soil-structure interaction. The shear wave is generated and received by piezoelectric transducers placed at opposite ends of the soil specimen. The shear wave velocity is calculated from the tip to tip distance between the two transducers and the time required by the shear wave to cover this distance as shown in Equation 1.

$$V_s = L/t \tag{1}$$

where V_s is the shear wave velocity, L is the tip to tip distance between two transducers, and t is the required time to cover this distance. After obtaining the shear wave velocity, the initial shear modulus, G_0, is calculated using the relationship of elastic continuum mechanics as shown in Equation 2.

$$G_0 = \rho.V_s{}^2 \tag{2}$$

where ρ is mass density of the material.

2.   OPERATION OF PIEZOELECTRIC TRANSDUCER

The principle of piezoelectric transducer is based on the properties of piezoelectric ceramic materials. A voltage applied to faces of a combination of two piezoelectric ceramic materials causes one to expand while the other contracts, causing the entire element to bend as described by [4] and shown in Figure 1. Similarly, a lateral disturbance of the piezoelectric transducer will produce a voltage so the piezoelectric transducer can be used as both shear wave transmitter and receiver. Measurement of time delay between sending and receiving of the shear wave will provide the shear wave velocity.
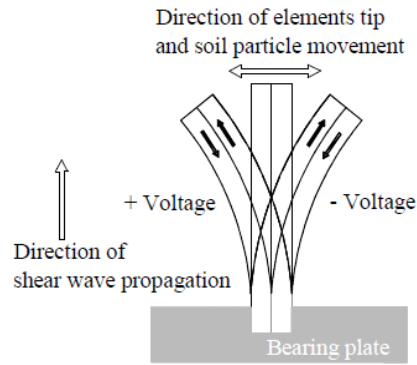
Figure1: Operation of piezoelectric ceramic sensor (after [4])

There are two types of piezoelectric transducers. One is a series connected piezoelectric transducer and the other is a parallel connected piezoelectric transducer. The series connected piezoelectric transducer is shown in Figure 2a. Noting that the polarization is oriented in opposite directions for each plate. An electrical wire lead is attached to each of the outer electrode surfaces. The parallel connected piezoelectric transducer is shown in Figure 2b. In this second type of piezoelectric transducer, the polarization has the same direction for both plates. The electrical connections are attached such that the two outer electrode surfaces are the same pole and the center electrode is the other pole. To attach an electrical wire lead to the center electrode, a portion of the element must be ground away. The series connected piezoelectric transducer is better to use as receiver. On the other hand, the parallel connected piezoelectric transducer is better to use as transmitter. However, this research uses only the parallel type for both transmitter and receiver transducers due to the advantage in measurement of sending signal.
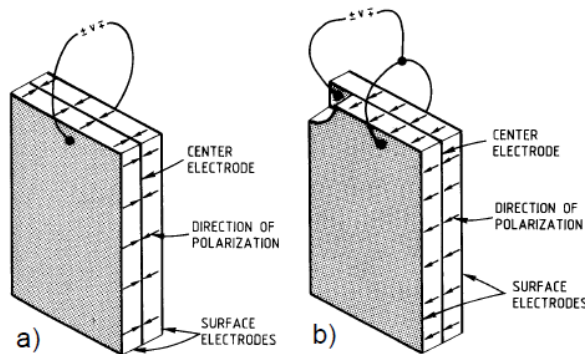
Figure2: a) Series and b) Parallel connected elements (after [1])

Figure 3 shows the piezoelectric transducer using in this research. This sensor is a non-magnetic piezoceramic with non-magnetic electrodes and non-magnetic reinforcing materials. This sending sensor (T220-A4NM-303Y) is manufactured from the Piezo System, Inc. The size of the sending sensor is 12.7 mm in width, 15.9 mm in length and 0.51 mm in thickness. The research uses this sensor to send the shear wave because of the strong sending signal.
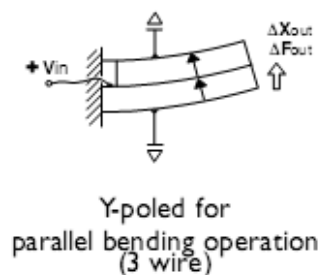
Figure3: Schematic of the piezoelectric ceramic sensor
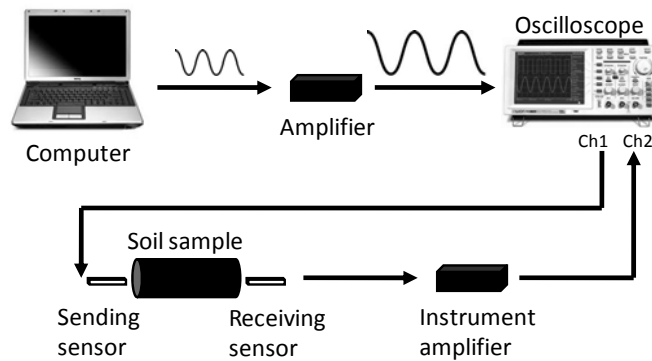
Figure 4: Schematic of shear wave measurement and associated electronics

Figure 4 shows the schematic test set-up. A personal computer generates a signal through a sound card with 5V peak to peak as suggested by [5]. This signal is amplified to 40V peak to peak. An oscilloscope is used to measure the arrival time between a sending signal and a receiving signal. A voltage pulse is applied to the sending transducer, this causes it to produce a shear wave. When the shear wave reaches the other end of the soil sample, distortion of the receiving transducer produces another voltage pulse. The receiving transducer is directly connected to the oscilloscope to compare the difference in time between the sending and the receiving signals. The shear wave velocity measurements are usually performed with frequencies ranging between 2 to 12 kHz, at strains estimated to be less than 0.0001 %. At low frequencies, signals can be influenced by a near-field effect. At high frequencies, the receiving signal is very weak and difficult to interpret. In most cases, signals are averaged 32 times in order to get a clear signal. The measurement of shear wave velocity in soil sample by means of piezoelectric ceramic sensors is clearly described by [6].

3. BANGKOK CLAY MATERIAL

The geological condition of Bangkok is reported by [7] that Bangkok is situated on a large plain underlain by alluvial and deltaic sediments of the Chaophraya basin. This plain is about 13,800 km2 in area and is generally known as "the lower central plain". The plain was under a shallow sea 3,000 to 5,000 years ago and the regression of the sea took place around 2,700 years ago, leaving the soft deposits, which form the lower central plain. This plain consists of thick clay known as Bangkok clay on its top layer, and its thickness is about 15 to 20 m in the Bangkok city area. The soft clay has very low shear strength, and is highly compressible, as it has never been subjected to mechanical consolidation.

The Bangkok clay at 10-12 m depth is sampled for this research. The engineering properties are found that the specific gravity is 2.72, the natural water content is 66.3%, the mass density is 1,470 kg/m^3 and the liquid limit is 88%. 108 experiment Bangkok clay samples are prepared at the liquid limit by mixing 20% by weight of Portland cement Type 1 and varying the replacement fly ash of 0, 10, 15, 20, 25 and 30%. Then, these samples are cured 3, 7, 14, 28 and 90 days in order to perform the bender element test and the unconfined compression test.

4. EXPERIMENTAL RESULTS

Figure 5 shows the undrained shear strength, S_u, versus the percent replacement of fly ash. From the experimental results, the research found that the optimum percent replacement of fly ash is about 15%.
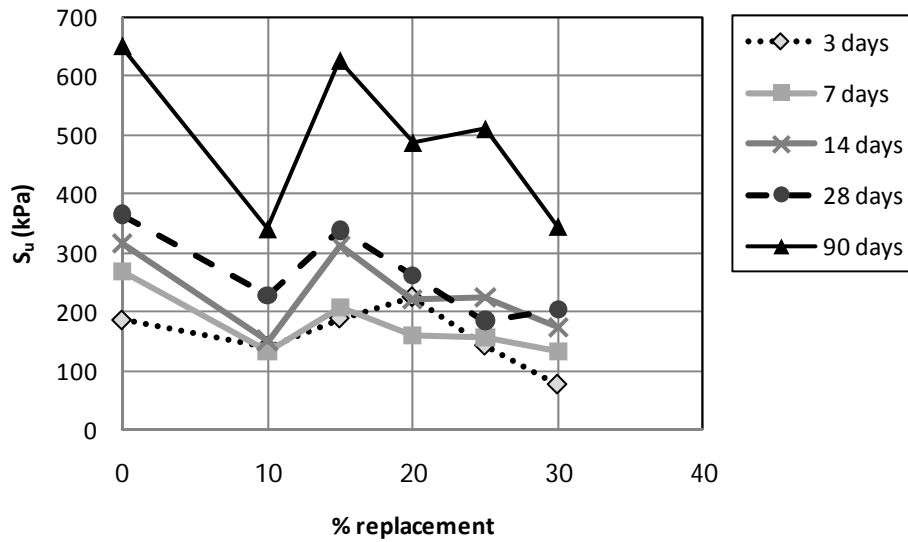
Figure 5: The undrained shear strength, S_u, versus the percent replacement of fly ash

In the similar way, Figure 6 shows the shear wave velocity, V_s, versus the percent replacement of fly ash. From the experimental results, the research found that the optimum percent replacement of fly ash is about 15-20%. From the 90 days results, the V_s is maximum at 20% replacement of fly ash which reports the long term behaviour of fly ash and cement mixed.
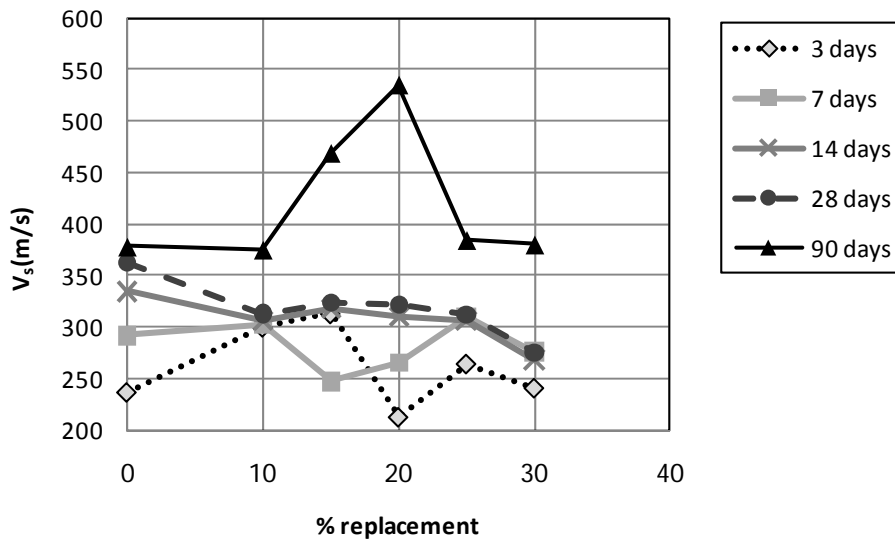
Figure 6: The shear wave velocity, V_s, versus the percent replacement of fly ash
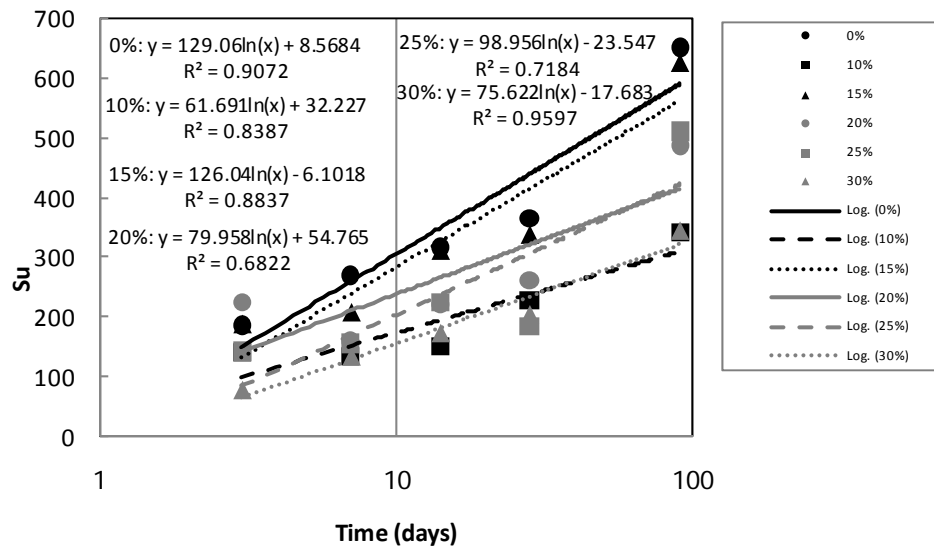
Figure 7: The undrained shear strength, S_u, versus time

Figure 7 shows the undrained shear strength, S_u, versus the time in logarithmic scale. From the experimental results, the S_u is increased with increasing the curing time. The results of 15% replacement of fly ash are almost the same as the result of 0% replacement of fly ash.

Figure 8 shows the undrained shear strength, V_s, versus the time in logarithmic scale. From the experimental results, the V_s is increased with increasing the curing time. The results of 15 and 20% replacement of fly ash are higher than the result of 0% replacement of fly ash which reports the long term behaviour of fly ash and cement mixed. But the results of 25 and 30% replacement of fly ash are lower than the result of 0% replacement of fly ash.
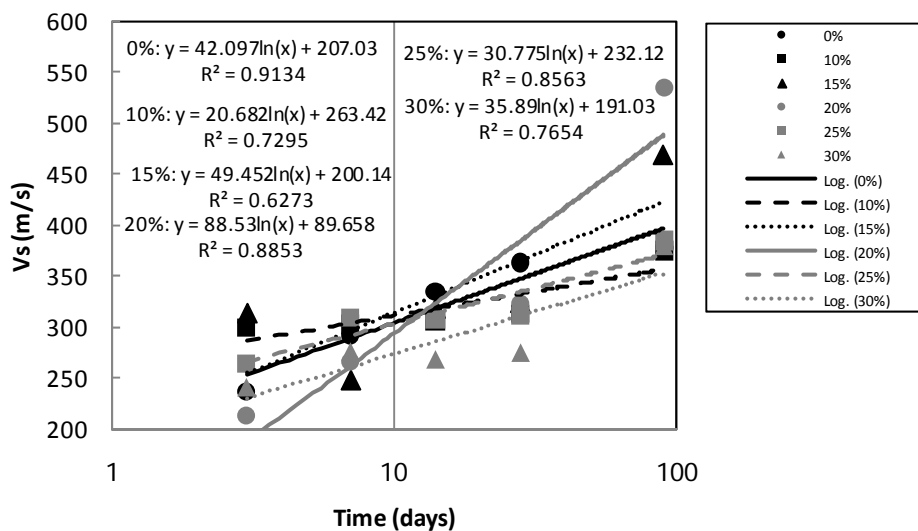
Figure 8: The shear wave velocity, V_s, versus time
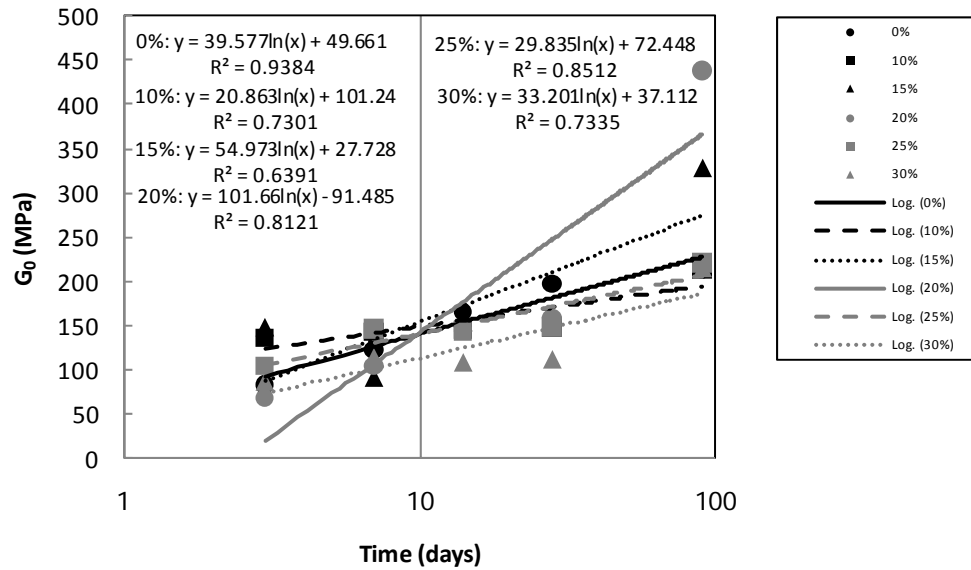
Figure 9: The initial shear modulus, G_0, versus time

In the similar way, Figure 9 shows the initial shear modulus, G_0, versus the time in logarithmic scale. From the experimental results, the G_0 is increased with increasing the curing time. The results of 15 and 20% replacement of fly ash are higher than the result of 0% replacement of fly ash which also reports the long term behaviour of fly ash and cement mixed.
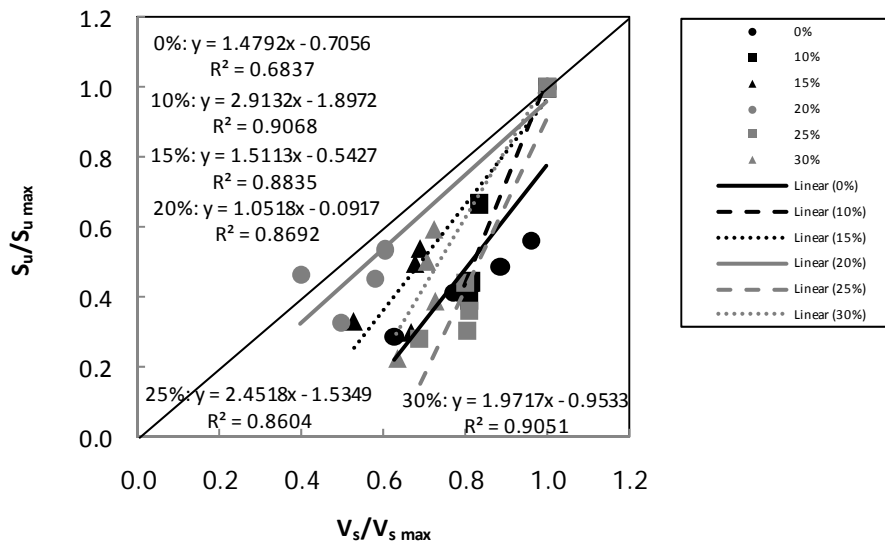
Figure 10: The ratio of $S_u/S_{u\ max}$ versus the ratio of $V_s/V_{s\ max}$

Figure 10 shows the ratio of $S_u/S_{u\ max}$ versus the ratio of $V_s/V_{s\ max}$. From the experimental results, all data are higher the result of 0% replacement of fly ash. However, the result of 20% replacement of fly ash reports the good agreement between the ratio of $S_u/S_{u\ max}$ and the ratio of $V_s/V_{s\ max}$.
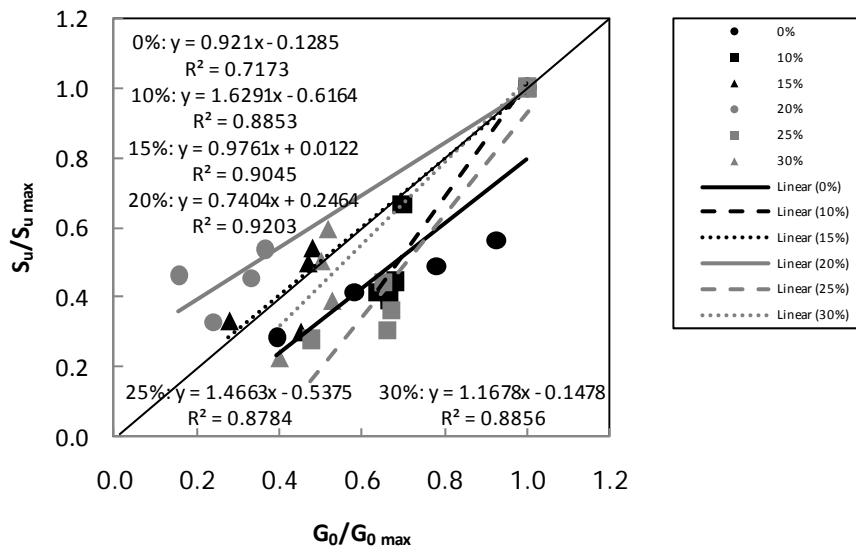
Figure11: The ratio of $S_u/S_{u\,max}$ versus the ratio of $G_0/G_{0\,max}$

In the similar way, Figure 11 shows the ratio of $S_u/S_{u\,max}$ versus the ratio of $G_0/G_{0\,max}$. From the experimental results, The results of 15% replacement of fly ash are in good agreement with the result of 0% replacement of fly ash. Moreover, all results are higher the result of 0% replacement of fly ash especially in the long term.

5. CONCLUSIONS

The research can conclude the stiffness of Bangkok clay mixed with the 20% of Portland cement type 1 and the fly ash replacement of 0, 10, 15, 20, 25 and 30% by using the shear wave velocity as follows;

- The optimum percent replacement of fly ash is about 15-20%.
- The S_u is increased with increasing the curing time. The results of 15% replacement of fly ash are almost the same as the result of 0% replacement of fly ash.
- The V_s is increased with increasing the curing time. The results of 15 and 20% replacement of fly ash are higher than the result of 0% replacement of fly ash which reports the long-term behaviour of fly ash and cement mixed.
- The G_0 is increased with increasing the curing time. The results of 15 and 20% replacement of fly ash are higher than the result of 0% replacement of fly ash which reports the long term behaviour of fly ash and cement mixed.
- From the ratio of $S_u/S_{u\,max}$ versus the ratio of $V_s/V_{s\,max}$, all data are higher the result of 0% replacement of fly ash. However, the result of 20% replacement of fly ash reports the good agreement between the ratio of $S_u/S_{u\,max}$ and the ratio of $V_s/V_{s\,max}$.
- From the ratio of $S_u/S_{u\,max}$ versus the ratio of $G_0/G_{0\,max}$, the results of 15% replacement of fly ash are in good agreement with the result of 0% replacement of fly ash. Moreover, all results are higher the result of 0% replacement of fly ash especially in the long term.

6. ACKNOWLEDGEMENT

REFERENCES

[1] *Dyvik, R. and Madshus, C. (1985). Laboratory measurement of G_{max} using bender elements, The ASCE Annual Convention, (pp. 186-196.). Detroi.*

[2] *Piriyakul, K. (2010). Soil disturbance assessment in soil sampling of open tube sampler and rotary core drilling. The Journal of Industrial Technology, 6(1): 1-6.*

[3] *Piriyakul, K. (2010). Examination of anisotropy of clay using shear wave velocity. The Journal of Industrial Technology, 6(2): 25-29.*

[4] *Kramer, S. L. (1996). Geotechnical Earthquake Engineering. Prentice-Hall International Series. Prentice Hall, Upper Saddle, New Jersey.*

[5] *Mohsin, A. K. M. and Airey, D. W. (2003). Automating G_{max} measurement in triaxial tests. The Prefailure Deformation Characteristics of Geomaterials, (pp. 73-80). Lyon.*

[6] *Brignoli, E. G. M., Gotti, M. and Stokoe, K. H. (1996). Measurement of shear waves in laboratory specimens by means of piezoelectric transducers. Geotechnical Testing Journal, 19: 384-397.*

[7] *Tuladhar R., Yamazaki F., Warnitchai P. and Saita J. (2004). Seismic microzonation of great Bangkok area using microtremor observations. The Journal of Earthquake Engineering and Structural Dynamics, 33: 211-225.*

A study on strength and swelling characteristics of three expansive soils treated with fly ash

T. L. Ramadas, Research Scholar, JNTUCEK, Department of Civil Engineering,
J.B. Institute of Engineering and Technology, India, ramadasjntu@gmail.com
N. Darga Kumar, Department of Civil Engineering, JNTUCEH, Hyderabad, Andhrapradesh, India,
ndkumar@jntuh.ac.in
Dr. G. Yesuratnam, JNT University Hyderabad, Andhrapradesh, India

ABSTRACT

This paper discusses the results pertinent to fly ash treated three expansive soils collected from different places in AP state, India. The test results such as Atterberg limits, Compaction, Unconfined compression stress (UCS), California Bearing Ratio (CBR) and Swelling properties obtained in the laboratory were discussed and presented. From the results, it is noticed that the plasticity and swelling characteristics of three expansive soils treated with fly ash reduced drastically and not much improvement is noticed in the UCS. Overall the results showed encouraging trend towards use of fly ash treated expansive soils in the construction.

1.   INTROUDCTION

Industrial development has necessitated construction of infrastructure facility such as highways, airports seaports and residential buildings. For these projects the difficult soil conditions such as expansive soils, soft clays and reclaimed soils play a crucial role during initiation and construction of project. Stabilization is the process of improving the properties of soil by changing its gradation. Two or more types of natural soils are mixed to obtain a composite material which is of superior to any of its components. To achieve the desired grading, sometimes the soils with coarse particles are added or the soils with finer particles are removed. The blended soil possesses both internal friction and cohesion. When properly placed and compacted, the blended material becomes stable and also load carrying capacity would be increased. Many of the important engineering properties of clay soils are improved by the addition of lime. Flyash is a waste by product from thermal power plants, which uses coal as fuel. It is estimated that about 110 million tons of fly ash is being produced from different thermal power plants in India consuming several thousand hectares of fertile land for its disposal causing severe health and environmental hazards (Sing and Murthy 1998). In order to utilize fly ash in bulk quantities, ways and means are being explored all over the world to use it for the construction of embankments and roads (Hausmann, 1990). Seasonal moisture variations bring about volume changes in expansive soils (Hausmann, 1990). Continued efforts are being made all over the world to devise innovative methods to solve the problems posed by expansive soils. Several measures such as application of adequate surcharge load, pre-wetting, moisture control, CNS layer technique (Katti, 1979) are in practice to treat these soils.

Inspite of continuous efforts made and incentives offered by the government, hardly 5 to 10% of the ash is being used for gainful purposes like brick making, cement manufacture, soil stabilization and as fill material (Murthy, 1998; Boominathan and Hari, 1999). Erdal Cocka (2001) studied the effect of flyash on expansive soil and confirmed that the plasticity index, activity and swelling potential of the samples decreased with increasing percentage stabilizer and curing time. The optimum content of flaysh in decreasing the swell potential was found to be 20%. Pandian et. al.(2002). Studied the effect of two types of Indian fly ashes such as Raichur fly ash (Class F) and Neyveli fly ash (ClassC) on the CBR characteristics of the black cotton soil. The flyash content was increased from 0 to 100%. The CBR of black cotton soil (BC soil), which consists of predominantly of finer particles, is contributed by cohesion. The CBR of flyash, which consists predominantly of coarser particles, is contributed by its frictional component. The low CBR of BC soil is attributed to the inherent low strength, which is due to the dominance of clay fraction. The addition of flyash to BC soil increases the CBR of the mix up to the first optimum level causes a decrease up to 60% and then up to the second optimum level there is an increase. Thus the variation of CBR of flyash-BC soil mixes can be attributed to the relative contribution of frictional or cohesive resistance from flyash or BC soil, respectively. In Neyveli fly ash also there is an increase of strength with the increase in the flyash content, here there will be additional pozzolonic reaction forming cementitious compounds resulting in good binding between BC soil and flyash particles.

In general, the specific gravity of fly ash has low value as compared to the specific gravity of soils; hence ash fills tend to result in low dry densities. The reduction in unit weight is of advantage in case of its use as a backfill material for retaining walls since the pressure exerted on the retaining structure as well as the foundation structure would be less. Flyash can be used economically embankment construction in the vicinity of thermal power stations when lead distances are less than 10 to 15 km. In case of rigid pavements, usage of flyash leads to considerable savings even if flyash is to be transported more than 50 km or perhaps 100 km. Compaction characteristics of soil-flyash mixes were studied by several investigators since they are very important in the construction of embankment, roads, and back filling in retaining walls. Several investigators reported that maximum dry unit weight increase and the optimum moisture content decreases due to addition of flyash (Pandian, 2004).

Phanikumar and Sharma (2004) presented the effect of fly ash on free swell index (FSI), swell potential, swelling pressure, plasticity, compaction, strength and hydraulic conductivity of expansive soil. It is brought that increase in flyash content reduces plasticity characteristics and the FSI was reduced by about 50% by the addition of 20% fly ash. The undrained shear strength of the expansive soil blended with flyash increases with the increase in the ash content. However, these techniques are successful only to partial extent and hence the attempts to devise better techniques are still going on. In the present work, an attempt is being made to bring out the behavior of fly ash treated three expansive soils collected from Bhimavaram, Amlapuram and Warangal in Andhra Pradesh, India.

2. EXPERIMENTAL STUDY

2.1. Material used

The expansive soil was collected from the Amlapuram-**A**, Bhimavar-**B**, and Warnagal-**W** and Flyash was collected from Vijayawada Thermal Power Station (VTPS) in Andhra Pradesh. The basic properties of the soils are presented in Table 1. The chemical properties of fly ash are presented in Table 2. Maximum dry density, MDD and Optimum moisture content, OMC of fly ash are 14 kN/m^3 and 18% respectively. The liquid limit, W_L and soaked CBR of fly ash are 30% and 6% respectively.

Table-1: Properties of three expansive soils

S.No	Property	Soils		
		Soil A	Soil B	Soil W
1	Liquid Limit, (%)	98	76	64
2	Plastic Limit, (%)	36	30	26
3	OMC, (%)	26	25	23
4	MDD, (kN/m^3)	16	16.2	16.4
5	UCS, kPa	80	100	130
6	DFSI, (%)	180	150	100
7	Soaked CBR, (%)	1.5	1.75	2.0
8	IS Classification	CH	CH	CH

Table-2: Chemical properties of fly ash (Courtesy VTPS, Vijayawada)

Chemical Constituent	Symbol	Value in %
Silica	Sio_2	61 to 64.29
Alumina	Al_2O_3	21.6 to 27.04
Ferric oxide	Fe_2O_3	3.09 to 3.86
Titanium dioxide	Tio_2	1.25 to 1.69
Manganese oxide	MnO	Up to 0.05
Calcium oxide	CaO	1.02 to 3.39
Magnesium oxide	MgO	0.5 to 1.58
Phosphorous	P	0.02 to 0.14
Sulphar trioxide	SO_3	Up to 0.07
Potassium oxide	K_2O	0.08 to 1.83
Sodium oxide	Na_2O	0.26 to 0.48
Loss of ignition	-	0.20 to 0.85

2.2. Admixture Proportions and Tests Conducted

The proportions of flyash used along with three soils in the study are 0%, 10%, 15%, 20%, 25%, 30%, 40% and 50% respectively. The following tests were conducted on the soil samples mixed at different proportions of flyash. The liquid limit and plastic limit tests were conducted as per IS: 2720 (Part 5) - 1985. Heavy compaction test was carried out according to IS: 2720(Part 8)-1983. Unconfined compressive strength (UCS) tests were conducted at OMC as per IS: 2720 (Part 10) - 1991. Free swell index (FSI) tests were conducted as per IS: 2720 (Part -XL) - 1977. The California Bearing Ratio (CBR) tests were conducted as per IS: 2720 (Part 16) – 1987.

3. RESULTS AND DISCUSSION

Atterberg's limits, IS heavy compaction, Unconfined compressive strength, Differential free swell, Swell pressure and Swell potential tests were conducted on three expansive soils treated with fly ash of different percentages. The results are discussed below.

3.1. Liquid Limit and Plastic Limit

From the Figs.1 and 2, it is observed that as the percentage of flyash increases, there is a marked reduction in liquid limit and plastic limit of clays tested. From this, it can be deduced that the flow characteristics and plastic characteristics of the soil sample are gradually decreasing with increase in the percentage of flyash. This reduced plasticity of clay is very much required to avoid the failure patterns in the road construction over the expansive sub grade soils. At 50% of fly ash addition to clays caused around 20 to 25% reduction in liquid limit. The reduction in plastic limit observed is about 8 to 10% at 50% addition of fly ash to the three expansive clays. From the reduction in liquid limit and plastic limits of three expansive clays, there could be obviously reduction in plasticity index of clay soils. As the plasticity index of clay reduces, the adverse effects posed by expansive clays also would be reduced. This phenomena in turn is encouraging one for construction.
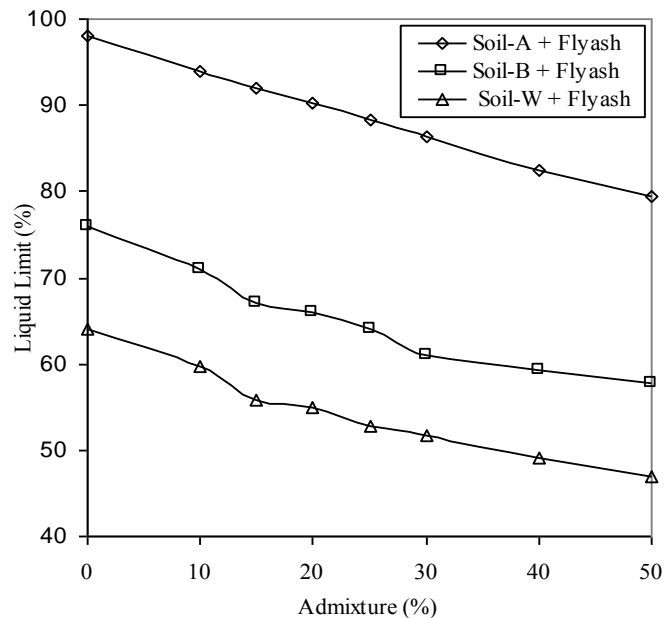
Figure 1: Influence of fly ash on Liquid Limit for three soils
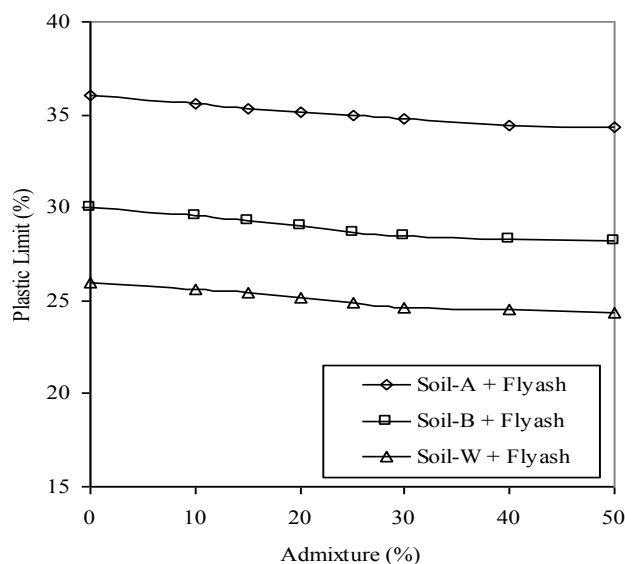
Figure 2: Influence of fly ash on Plastic Limit for three soils

3.2. Compaction Characteristics

In any construction activity, the soil alone or admixed soil would be compacted at its OMC so as to enhance the stability aspects of the subgrade and in turn structure found on it. The variation of compaction characteristics such as OMC and MDD for the three expansive clays treated with flyash are presented in Figs. 3 and 4. The addition of flyash to the three expansive clays caused reduced optimum moisture content increased maximum dry density. Nearly about 25% addition of flyash to all the soils showed optimum levels of maximum dry densities. At 25% addition of flyash to the Amlapuram, Bhimavaram and Warangal soils the maximum dry density values observed are 17.6 kN/m^3, 17.4 kN/m^3 and 18 kN/m^3. From this data, it is observed that there is about 8 to 10% increase in maximum dry density for all the three expansive soils is noticed at 50% addition of fly ash. In all the three expansive clays, around 30% reduction in OMC is observed at 50% addition of fly ash to the clays. Increase in MDD is marginal but there is a considerable decrease in OMC. From this aspect, it can be understand that reduced amount of water to be mixed during preparation of fly ash expansive soil subgrade in road works. This behavior is very much required during compaction of subgrade for construction purpose.
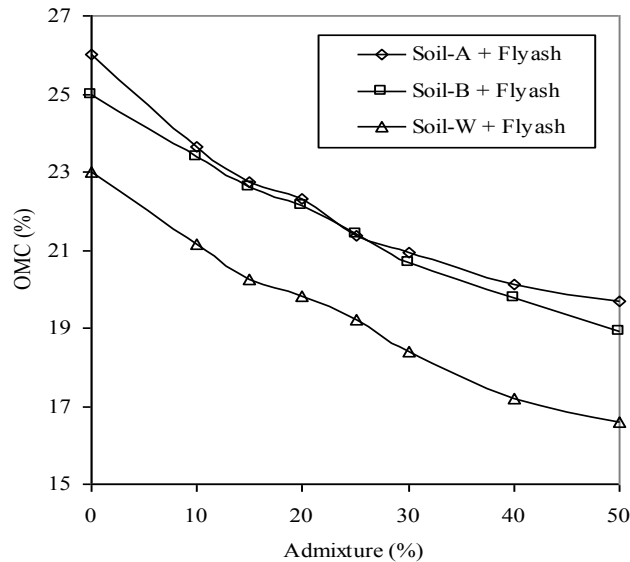
Figure 3: Influence of fly ash on OMC for three soils
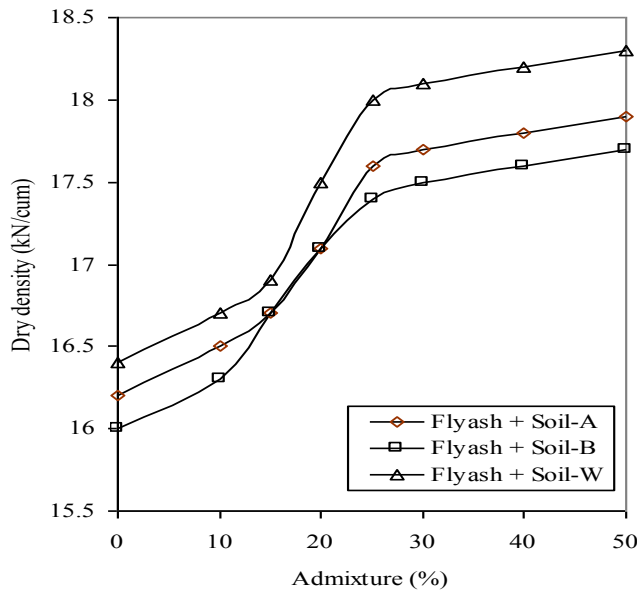
Figure 4: Influence of fly ash on MDD for three soils

3.3.   Unconfined compressive strength (UCS)

Unconfined compression stress of a clay soil is the indication of the bearing power of soil. Generally, the UCS test would be conducted on clay samples because these samples can stand on their own without any lateral confinement. The variations of unconfined compressive strength for all the three clay soils are presented in Fig.5. From this figure, it is observed that there is a good improvement in unconfined compression strength of clay at about 25% addition of flyash to three expansive soils and from 25% fly ash addition to the soils onwards caused reduction in UCS of samples. This can attributed to up to about 25% fly ash addition to the clay samples would have resulted flocculation of particles in the mixture. To cause collapse of the mixture needs more stress level and hence the mixture has resulted in more strength. From 25% of fly ash addition onwards the structure of clay fly ash mixture would have change to dispersed. The addition of flyash to three expansive soils has resulted in increase of strength 10 to 12% at about 25% of fly ash addition to the three expansive clay soils. From this it can be understand that up to about 25% of flash can be used by dry weight in subgrade clay soil improvement for construction purpose.
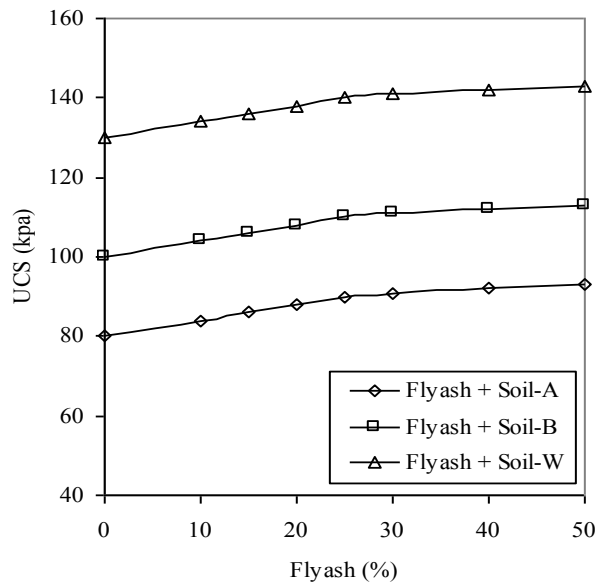
Figure 5: Influence of fly ash on UCS for three soils

3.4.   Soaked California Bearing Ratio (SCBR)

In arriving the flexible pavement thickness one of the useful parameters is subgrade soil is CBR value. The soaked CBR results obtained on fly ash treated expansive clay soils are presented in Fig. 6. From this figure, it is observed that as the percentage of admixture such as fly ash increases, the CBR also increasing and this trend is observed linear up to about 25% fly ash. And from 25% fly ash addition to clay samples onwards, the soaked CBR value showing similar value irrespective of % of fly ash. The optimum value of CBR is found in all the three expansive clays at 25% of fly ash.
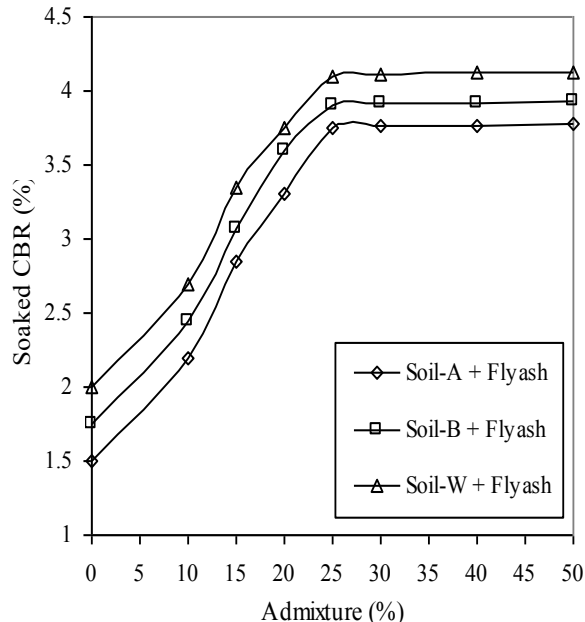
Figure 6: Influence of fly ash on S.C.B.R for three soils

3.5.   Differential free swell index (DFSI)

Fig. 7 presents the variation in of DFSI with the addition of fly ash. From this figure, it is observed that as the % of fly ash increases, the DFSI of the three expansive soils is decreasing. It can be attributed that as the fly ash content increases, the diffused double layer thickness of clay would have decreased and hence, the swelling has resulted in down trend. Further from this figure, it is noticed that the decrease in DFSI is gradual and it is noticed for all the % of fly ash.
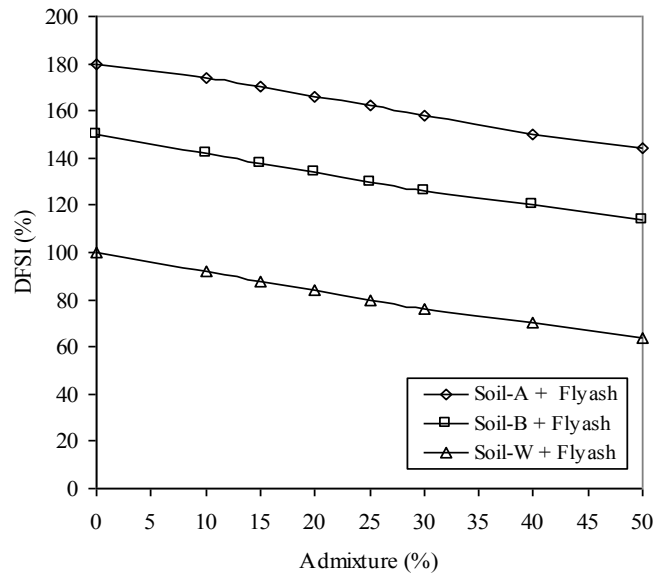
Figure 7: Influence of fly ash on DFSI for three soils

3.6.   Swell Pressure and Swell Potential
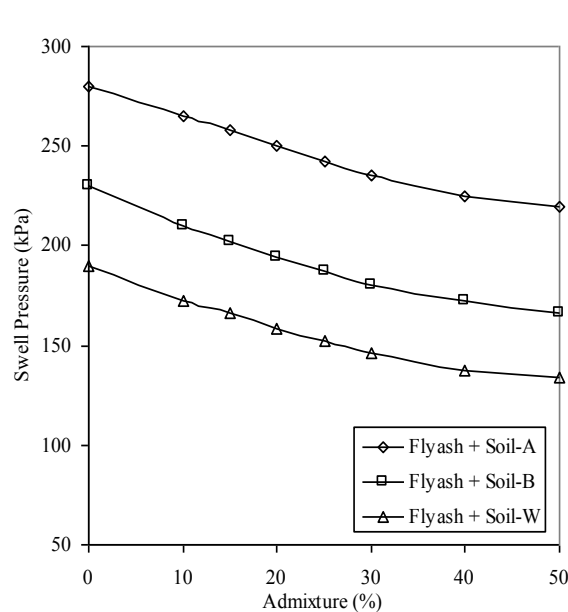
Figure 8: Variation of Swell pressure with % fly ash
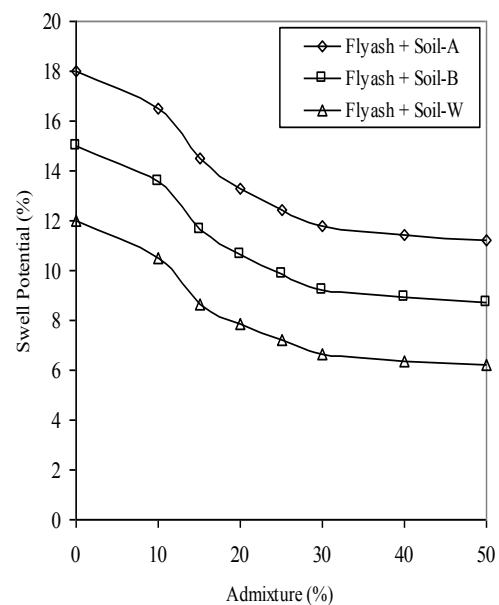
Figure 9: Variation of swell potential with % fly ash

The variation in swell pressure and swell potential in three expansive soils treated with different % fly ash are presented in Figs. 8 and 9 respectively. From the Fig.8, it can be seen that the swell pressure is decreasing gradually as the % of fly ash increases in all the three expansive clays tested. In all the three clays at the fly ash content of 50%, it is noticed that the decrease in swell pressure is around 35 to 40%. Fig. 9 presents the swell potential variation. From this figure, it can be noticed that as the % of fly ash increases from 0% to 50%, the swell potential is decreasing in a curvilinear trend. From this trend it is observed that at a 50% of fly ash content addition to the clay the swell potential in all the three expansive clays has decreased to about 50%. This reduction in swell pressure and swell potential are very encouraging conditions to work with expansive clays in construction.

4.   CONCLUSIONS

The following conclusions are drawn from the above results.

- When fly ash is added to the three expansive soils the Atterberg's limits, OMC, FSI are decreased and strength properties are increased.

- The optimum percentage of fly ash is found to be 25% from the strength and CBR results are concerned. Hence, without compromising the property of clay 25% of fly ash can be effectively added in the construction on expansive clayey subgrades.

- The swell pressure and swell potential are decreasing for all the fly ash proportions.

REFERENCES

[1] *Singh, D. V and Murthy (1998). Fly ash in India-Problems and Possibilities. Proceedings of experience sharing meet on use of fly ash in roads and embankments, CRRI, New Delhi, pp-5-20.*

[2] *Hausmann, M. R. (1990). Engineering principles of Ground modification. Mc Graw Hill Book Co., New Delhi.*

[3] *Katti, R. K. (1979). Search for solutions to problems in Black cotton soils. First IGS Annual Lecture, Indian Geotechnical Journal, Vol.9, pp 1-8.*

[4] *Bhoominadhan. A., and Hari S., (1999). Behavior of fly ash under static and cyclic loading. Proceedings of IGC-99, Calcutta, pp.324-326.*

[5] *Erdal Cokca (2001). Use Of Class C Fly Ashes for the Stabilization – of an Expansive Soil. ASCE Journal of Geotechnical and Geoenvironmental Engineering Vol. 127, July, pp. 568-573.*

[6] *IS: 2720 (Part XL), 1977. IS code of practice for determination of free swell index.*

[7] *IS: 2720 (Part 8) - 1983. IS code of practice for determination of water content – dry density relation using heavy compaction.*

[8] *IS: 2720 (Part 16) – 1987. IS code of practice for laboratory determination of CBR.*

[9] *IS: 2720 (Part 5) - 1985. IS code of practice for determination of liquid limit and plastic limit.*

[10] *IS: 2720 (Part 10), 1991. IS code of practice for determination of unconfined compressive strength.*

[11] *Pandian,N. S., Krishna, K. C. and Leelavathamma, B., (2002). Effect of Fly Ash on the CBR Behaviour of Soils. Indian Geotechnical Conference, Allahabad, Vol.1, pp.183-186.*

[12] *Pandian, N. S., (2004). Fly ash characterization with reference to geotechnical applications. J. Indian Institute of Science., Vol. 84, pp.189–216.*

[13] *Phanikumar, B. R., and Radhey S. Sharma (2004). Effect of Flyash on Engineering properties of Expansive Soil. ASCE Journal of Geotechnical and Geoenvironmental Engineering, Vol. 130, No 7, pp. 764-767.*

Alkali Activation of Industrial By-Products
for use in Soil Stabilisation

P. Sargent, *School of Civil Engineering and Geosciences, Newcastle University, United Kingdom,*
paul.sargent@ncl.ac.uk

M. Rouainia, *School of Civil Engineering and Geosciences, Newcastle University, United Kingdom,*
m.rouainia@ncl.ac.uk

P. N. Hughes, *School of Civil Engineering and Geosciences, Newcastle University, United Kingdom,*
p.n.hughes@ncl.ac.uk

S. Glendinning, *School of Civil Engineering and Geosciences, Newcastle University, United Kingdom,*
stephanie.glendinning@ncl.ac.uk

ABSTRACT

Presented in this paper is an overview of findings recently obtained from a laboratory study, which examined the potential of industrial-by-products and alkali activation for use in stabilising a synthetic soft soil. Geotechnical and mineralogical tests were performed on activated and non-activated samples for curing periods up to 56 days. Comparisons in performances to widely used CEM-I cement binders were made. Results from the study indicate that IBP-stabilisation (particularly with the use of ground granulated blast furnace slag) and alkali activation can improve soil's mechanical properties. Activation was observed to initiate pozzolanic reactions and subsequent strength enhancements with time. However, such improved material performances due to alkali activation did not always result in durability improvements.

1.   INTRODUCTION

Significant areas of land within flood plains in the UK predominantly comprise soft alluvial soils. Whilst wet or dry, such soils can present difficulties when loaded upon given their low strengths, poor bearing capacities and unfavourable shrinkage-swelling and differential settlement characteristics. To allow for any engineering development to occur on such poor quality soils, various stabilisation techniques may be adopted to improve the geotechnical properties of such soils. A technique that is popularly used in countries including Sweden and Japan, where soils are predominantly of poor quality is deep soil mixing. Amongst numerous other material properties, deep mixing is known for its ability to enhance a material's strength, durability and volume stability (Sherwood, 1993), and has been used in the UK since the early 1990's (Al-Tabbaa and Evans, 1998). Hence, this paper concentrates on the use of deep mixing.

Initially developed in Sweden during the 1970's, deep mixing uses cementitious and high-alkali binders such as lime and cement (Ahnberg et al., 2003). This technique would reduce the moisture contents and hence the potential of shrinkage-swelling within soft soils, thereby improving the soil's strength and compaction properties (Rogers et al., 2000). Generally, deep soil mixing contracts tend to use binder dosages of 5 – 15 % weight by mass within soils. To create deep mixed soil columns, a rotary auger is first drilled to a specified treatment depth. Once drilling has been completed, binder is then injected into the ground through the auger's bladed mixing tool to mix the soil and binder together, whilst the auger is retrieved and the drill's direction of rotation is reversed. The quality of the deep mixed column is further improved due to the auger's bladed mixing tool's fin orientation, which incurs a level of compaction during mixing. Figure 1 illustrates the deep soil mixing stabilisation process.

One of the most popular binders that has been widely used in soil mixing over the past 30 years is ordinary Portland cement (CEM-I); whereby Jegandan et al. (2010) state that it is favoured over lime with regards to its ability to provide considerable strength improvements over short time periods. Pore water within stabilised soil columns reacts with the calcium silicate/-aluminate based binders, resulting in the formation of calcium silica hydroxide (CSH) and/or calcium aluminate hydroxide (CAH) gels. Such gel forming reactions ultimately provide improved strengths within soils and are referred to as "pozzolanic". As stated by Davidson et al. (1965), Pozzolanic reactions take place over long time periods when soil pH

conditions are $\geq$ 10.50. As stabilised soils undergo curing, stronger cementitious soil matrices result, referred to by Sherwood (1993) as "Geopolymer" materials.
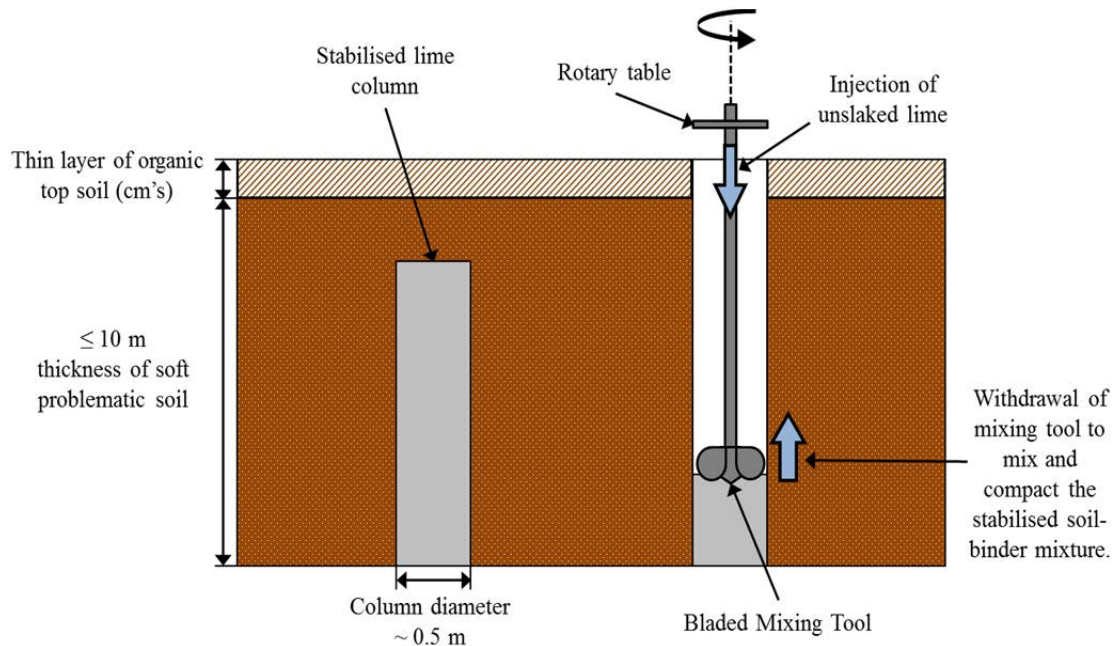
Figure 1: Illustration of the deep dry mixing technique using lime.

Although the usage of CEM-I and lime as soil binders in deep mixing have clearly demonstrated their ability to enhance the geotechnical properties of soft soils, a number of environmental issues have been identified in their use. One of the most concerning issues is related to the high amounts of energy required for their manufacture. On this basis, there has become the need to seek new more environmentally sustainable binder materials that would be able to produce improved engineering performances similar to those demonstrated by CEM-I and lime within similar curing periods. A recent more environmentally sustainable approach that has recently been adopted in selecting new binder materials is recycling industrial by-products (IBP's); whereby those that are pozzolanic in nature would be preferred.

To further improve the mechanical performances of deep mixed soils, the addition of alternative alkali materials to lime have also been sought to increase soil pH with a view to activating pozzolanic reactions and the subsequent formation of cementitious bonds. Encouraging work by Palomo et al. (1999) identified that sodium hydroxide and/or sodium silicate showed encouraging potential as alternative alkali activators for use in deep soil mixing, due to their observed ability to raise soil pH and increase rates of mechanical property improvement. Thus, the primary aim of this study was to assess the performance and viability of using alternative alkali activators (AA) within a deep mixed IBP-stabilised synthetic silty sandy clay.

2. SOIL AND BINDER MATERIAL CHARACTERISTICS

This study conducted geotechnical, chemical and mineralogical testing to determine the suitability and performance of a number of IBP's and alkali activation in stabilising an artificially manufactured silty sandy clay. This artificial soil was created by utilising a rotary mixer in the laboratory to typify a UK alluvium soil, which tends to be found abundantly on floodplains within river valleys where housing and industrial developments are common. Alluvium typically comprises high proportions of silt and/or clay, which has low levels of cohesion in both wet and dry conditions. This can inherently present wall failure hazards within excavations and slope instability for embankment projects. Additionally, such soft soils are often characterised by low levels of stiffness and consequently lead to problems associated with bearing capacity, should such soils be loaded upon. The artificial silty sandy clay consisted of 70 % fine silica sand and 30 % grade E kaolin, which were provided by WBB Minerals Ltd and English China Clay International Europe Ltd, respectively. The soil also had an optimum gravimetric water content of 15 %, based on compaction testing conducted in accordance with BS 1377: Part 4 (BSI, 1990). Data regarding the soil's grading curve and Atterberg limits are presented below in Figure 2.
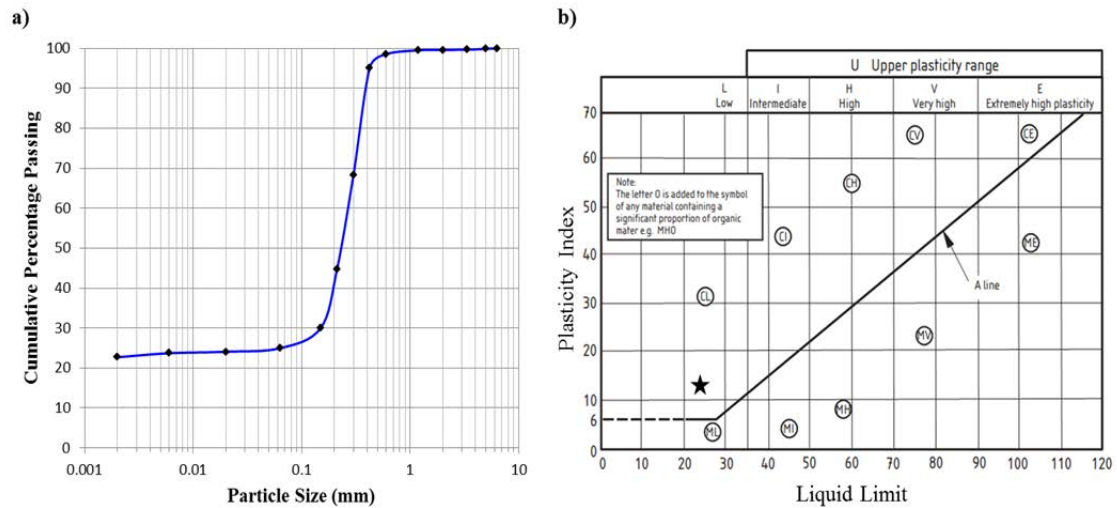
Figure 2: Particle size distribution and Atterberg limit data for the artificial alluvium tested (BSI, 1990).

The IBP's utilised as binders for this study included ground granulated blast furnace slag (GGBS), pulverised fly ash (PFA) and red gypsum (RG). GGBS (supplied by Frodingham Cement Ltd) is a pozzolanic latent hydraulic cement produced from pig iron manufacture; the chemical composition of which closely resembles that of CEM-I. PFA, which was provided by ScotAsh Ltd, is a synthetic pozzolanic waste material that results from combustion within coal-fired power plants. Finally, large stockpiles of RG filter cake are found the world over, which are produced as by-products of sulphuric acid neutralisation during the manufacture of Titanium Dioxide (see Table 1 for the chemical composition of RG). For this project, RG was supplied by Huntsman Tioxide Europe Ltd.

Table 1: A summary of the chemical composition of red gypsum. Courtesy of Hughes et al. (2011).

Component	Content (% dry weight)	Component	Content (mg/kg)
Gypsum ($CaSO_4.2H_2O$)	*58.5 – 59.3*	*Chromium (Cr)*	*500 – 800*
Iron Oxide (Fe_2O_3)	*32.9 – 36.6*	*Zinc (Zn)*	*200 – 400*
Titanium (Ti)	*1.0 – 1.3*	*Strontium (Sr)*	*100 – 300*
Aluminium (Al)	*0.1 – 0.8*	*Nickel (Ni)*	*50 – 60*
Magnesium (Mg)	*0.5 – 0.6*	*Cobalt (Co)*	*20 – 30*
Manganese (Mn)	*0.2 – 0.5*	*Barium (Ba)*	*1 – 3*
Silicon (Si)	*0 – 0.5*	*Lead (Pb)*	*1 – 2*
Chlorine (Cl)	*0.002 – 0.2*		

Recent studies, such as those by Hughes et al. (2011), have identified that utilising lime as an alkali activator within an IBP-stabilised alluvium resulted in inconsistencies with regards to significant strength developments. It may be considered that the relatively poor strength and durability performances observed for certain stabilised soil mixtures may have been attributed to the low pH levels produced by the lime activator used. Hence, based on the work by Palomo et al. (1999), this study used a sodium hydroxide - sodium silicate activator, which was prepared with a ratio of 1:2.

3.   SAMPLE MIXING METHODOLOGY

To produce stabilised samples, binders were mixed with the artificial alluvium at a dosage of 10 % by dry weight for 10 minutes within a rotary mixer. For AA samples, the sodium hydroxide-sodium silicate mixture was added at a dosage of 20 % by dry weight of the IBP binder used. Non activated (C) IBP-stabilised samples and CEM-I stabilised samples were also prepared and tested for comparative purposes. Once the stabilised soil mixtures had been prepared, samples were then manufactured by tamping into split sample moulds and compressed using a hydraulic press to produce optimum sample bulk densities of 2.2 Mg/m^3. Once compressed, samples were then placed within wax-sealed PVC moulds and cured for periods of 7, 14 and 28 days within a temperature controlled room at 20 ^{o}C and 55 % relative humidity. For testing at each curing period, samples were extruded from their moulds and then trimmed to the required dimensions in accordance to the necessary BSI (1990) and ASTM (1996) standards.

4.   TESTING PROGRAMME AND RESULTS

Some of the important material properties to take into account when examining the engineering performance of the aforementioned stabilised soil mixtures include: compressive strength, durability, pH levels and mineralogy. For this study's experimental programme, the strength test conducted was unconfined (uniaxial) compressive strength (UCS) (BS 1377: Part 7: Clause 7, BSI 1990). UCS samples were retained post-testing after each curing period in order to determine any changes in water content over the 28 day testing programme (BS 1377: Part 2, BSI, 1990). For durability testing, samples were submerged in water and underwent wetting-drying cycles (ASTM, 1996, D 559 – 96 clause 5.3) and freezing-thawing cycles (ASTM, 1996, D 560 – 96 clause 5.3). pH levels (BS 1377: Part 3: Clause 9, BSI 1990) of samples were recorded to determine whether alkali activation was necessary to raise the pH up to 10.5 to initiate pozzolanic reactions and subsequent strength developments.

4.1   Compressive Strength

To assess the UCS performance of the deep mixed IBP binder-soil mixtures, testing was conducted in adherence to BS 1377: Part 7 (BSI, 1990). Samples of dimensions 76 mm (long) x 38 mm (diameter), were tested on a uniaxial Instron 5585H loading frame; whereby three repeats were conducted for each stabilised soil mixture after each curing period. A consistent strain rate of 0.5 mm min^{-1} was used for all UCS tests. After a 28 day curing period, testing results presented in Figure 3 indicate that activated samples containing the GGBS binder produced the most rapidly improved strengths compared with activated samples mixed with PFA, RG or CEM-I. The GGBS-AA sample achieved a compressive strength of 6339 kPa. Contrastingly, based on the low compressive strengths of 488 kPa and 344 kPa achieved for PFA-AA and RG-AA samples, respectively; alkali activation using sodium hydroxide – sodium silicate had negligible effects on strength development. Whether the PFA or RG stabilised samples had been activated or not; they were observed to have experienced remarkably slow rates of strength development.
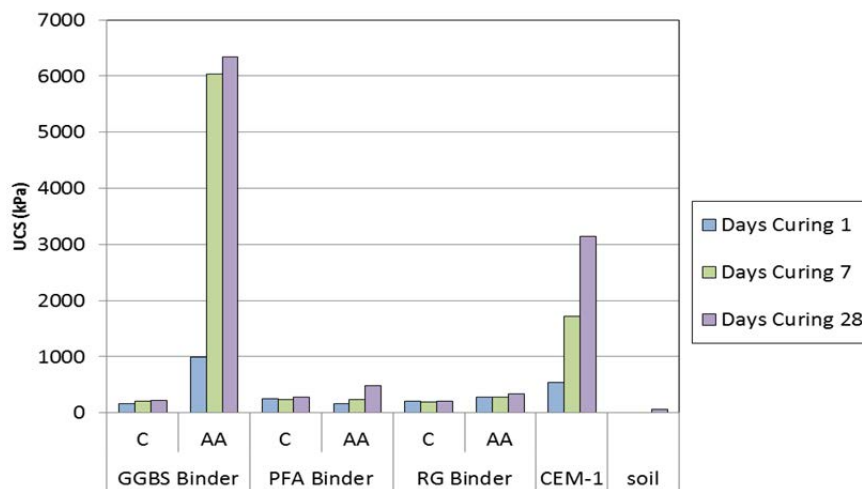
Figure 3: UCS behaviour for the non-activated and alkali activated samples tested.

Work by Fraay et al. (1989) claims that for non-activated PFA samples, delays in strength development may occur as a result of PFA's inertness and that a curing period of at least 7 days would normally be required before any marked strength gains are observed. However, from the results presented in Figure 3, no clear significant strength enhancements were seen over the 28 day testing period. Finally with regard to the GGBS-AA and CEM-I stabilised samples that rapidly reached high strength values, these samples were observed to experience brittle failure; whereas those characterised by much slower strength development experienced more plastic behaviour upon failure.

4.2   Wet-Dry and Freeze-Thaw Durability

The durability testing programme studied changes in volume and water content of IBP-soil samples and their resistance to soil-cement losses when subject to wetting and drying (ASTM, 1996, D 559 – 96 clause 5.3) and freezing-thawing (ASTM, 1996, D 560 – 96 clause 5.3) cycles over a 24 day period. Testing results from the wetting-drying component are presented in Figure 4 and Table 2. Other than the alkali

activated GGBS and PFA samples which survived the full 12 testing cycles, all other IBP-stabilised samples disintegrated very shortly after their initial immersion in water. The water content and volumetric changes experienced by the GGBS-AA and PFA-AA samples remained relatively uniform over the testing period. The CEM-I stabilised sample initially exhibited very similar water content and volumetric change behaviour to the GGBS-AA and PFA-AA samples, but disintegrated after 4.5 cycles of testing.
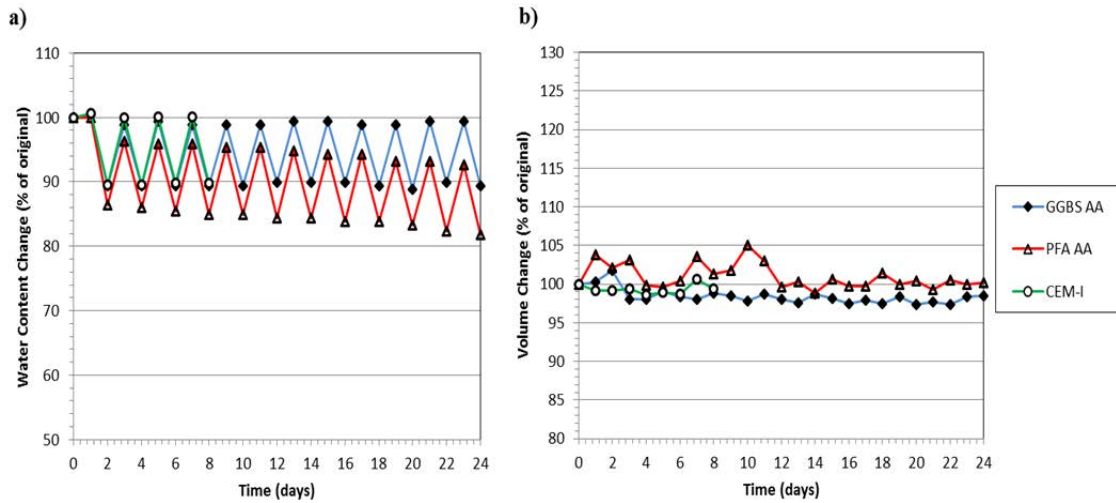
Figure 4:a) Water content and b) volumetric changes experienced by samples during wet-dry durability testing.

The results from the freezing-thawing testing are shown in Figure 5 and Table 2. As observed during wetting-drying testing, the alkali activated GGBS and PFA samples were the only soil-binder mixtures to survive the full 12 cycles of testing and that all non-activated samples disintegrated upon first immersion. Unlike that seen during the wetting-drying testing, the RG-AA sample was able to survive 3 cycles; however this was accompanied by a significant increase in volume during the third cycle. With the exception of the GGBS-AA soil-binder mixture which exhibited the least change in water content and volume change; samples water contents generally showed more variation than that observed during wetting-drying testing, whereby the general trend showed decreasing water contents. The most notable water content observation from the freeze-thaw programme was the dramatic decrease in PFA-AA's water content, which occurred between the seventh and twelfth cycles. Generally, considerably higher fluctuations in volume were recorded for samples during freezing-thawing testing compared with wetting-drying testing; whereby the sample which exhibited the greatest amount of variation was also found to be PFA-AA. As similarly seen during wetting-drying testing, the CEM-I sample survived 4.5 cycles and showed relatively little volume change and a slight reduction in water content.
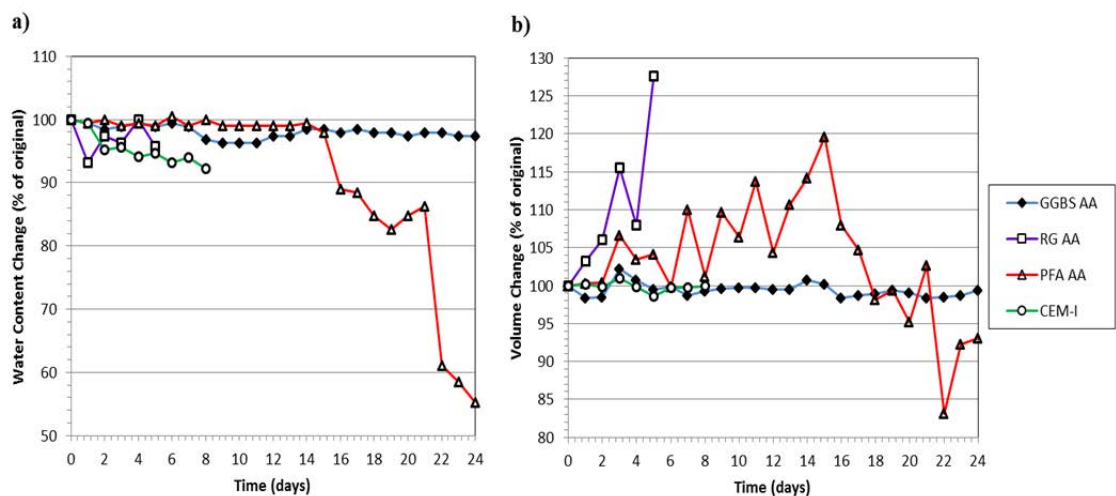

Figure 5: a) Water content and b) volumetric changes experienced by samples during freeze-thaw durability testing.

Table 2: Summary of the average number of cycles survived by the soil-binder mixtures tested during the wetting-drying and freezing-thawing testing programme.

Soil – Binder Mixture	Average no. of cycles survived	
	Wetting-Drying	Freezing-Thawing
Soil + GGBS-AA	12	12
Soil + GGBS-C	0	0
Soil + PFA-AA	12	12
Soil + PFA-C	0	0
Soil + RG-AA	0	3
Soil + RG-C	0	0
Soil + CEM-I	4.5	4.5

4.3   Moisture Content

To ensure that the moisture content within the samples tested were sufficiently high to allow for hydration and the development of cementitious bonds, UCS samples were retained post-strength testing for moisture content determination according to BS 1377: Part 2 (BSI, 1990) procedures. However, given the mineralogical and chemical structure of RG-based samples, a slight deviation from the BSI (1990) procedure was required in order to measure their moisture contents. Drying RG samples at 110 $^{\circ}$C would consequently remove RG's structural water and convert the gypsum to anhydrite; thereby potentially resulting in inaccurate moisture content data. Therefore, for this study it was decided that RG samples be dried at a lower temperature of 45 $^{\circ}$C for double the length of the standard drying period.

According to the data presented in Table 3, IBP-stabilised samples were measured to have moisture contents of 11 to 14 % over the 28 day testing period, regardless of whether they were alkali activated or not. Generally, each IBP-stabilised sample experienced very little variation from their initial moisture content over the 28 days, which severely contrasts to the distinct reduction in moisture content by the CEM-I stabilised sample. Hence, this would indicate that sufficient water was present within the IBP-stabilised samples for hydration reactions to occur during testing.

Table 3: Summary of the average variations in water content with increasing curing time experienced by the soil-binder mixtures studied.

Soil – Binder Mixture	Water Content (%)		
	1 day curing	7 days curing	28 days curing
Soil + GGBS-AA	*12.9*	*12.3*	*12.2*
Soil + GGBS-C	*12.8*	*12.9*	*12.7*
Soil + PFA-AA	*11.2*	*12.6*	*12.7*
Soil + PFA-C	*11.7*	*12.3*	*12.1*
Soil + RG-AA	*14.1*	*14.5*	*14.1*
Soil + RG-C	*12.5*	*13.3*	*12.9*
Soil + CEM-I	*15.29*	*13.25*	*11.92*

4.4   pH Levels

A recent study by Hughes et al. (2011) revealed that soft soils mixed with IBP binders whose pH levels were lower than 10.50 often resulted in poor strength improvements; thereby indicating that the addition of further alkalis would be required to activate pozzolanic reactions and thus CSH/CAH bond formation. Hence during this study, UCS samples were retained post-UCS testing after 28 days and tested for their pH in adherence to BS 1377: Part 3 (BSI, 1990) procedures. Samples were tested by using a Camlab Ultrameter 6P; the results are presented in Figure 6. The range of pH values recorded from this testing programme varied between 6.23 and 11.90. Non-activated samples had average pH levels of 6.23, 9.0 and 9.77 for RG-C, GGBS-C and PFA-C, respectively; thereby indicating that pozzolanic reactions did not occur within these samples. Whereas for these samples alkali activated equivalents, each achieved pH levels that were in excess of 10.50; specifically values of 11.10, 11.47 and 11.70 for RG-AA, GGBS-AA and PFA-AA, respectively. Additionally, the pH value achieved by the CEM-I stabilised sample (11.90) was comparable to the pH values obtained by the three alkali activated IBP-soil mixtures.
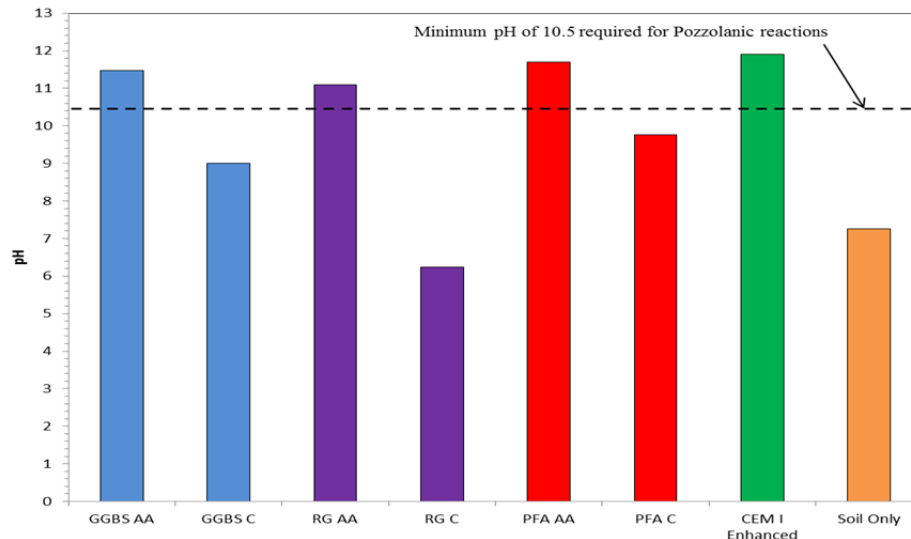
Figure 6: Bar chart showing the average pH values obtained by all non-activated and alkali activated samples over a curing period of 28 days.

5.   DISCUSSION

5.1   Strength

Compressive strength testing results generally suggest that more cementitious bonds were formed over the 28 day curing period within alkali activated samples compared with those which had not. Overall the GGBS-AA binder was seen to produce the most improved strengths over the 28 day testing period, surpassing those reached by the conventionally used CEM-I binder. Non-activated PFA-based samples exhibited delayed compressive strength gains, which are thought to be the result of PFA being inert and with a minimum of 1 week being required for such developments to become apparent (Fraay et al., 1999).

The poor UCS performances and plastic behaviour characteristics of RG-stabilised samples were consistently recorded over the testing period and were therefore not considered to be attributable to delayed strength gains. This would suggest that RG as a lone binder was not suitable for seeking improved engineering performances within soft alluvium, even when alkali activated using sodium hydroxide/sodium silicate. Factors which are likely to have contributed towards such performances include chemical compositional changes to RG during sample preparation; specifically the removal of RG's natural water content as its filter cake was dried, thereby resulting in a degraded mineralogical structure. Another factor associated with RG's sample preparation which may have contributed towards its poor performance was that once its original filter cake form had been dried, it required grinding down to a powder using a mortar and pestle. This in turn may have produced a powder that was less uniform in terms of particle size compared with the GGBS and PFA powders also used during this study. Away from RG's method of preparation for mixing, it should also be considered that a study by Beretka et al. (1996) showed RG not to have a pozzolanic nature and thus may be expected not to produce as impressive strength performances as other IBP binders such as GGBS.

Alkali activation was observed to cause strength and therefore stiffness enhancements within GGBS samples. However, the high stiffness nature of GGBS-AA samples inherently meant that they were likely to experience brittle failure and therefore considered to be potentially unsuitable, should they be dynamically loaded upon. Such observations in material behaviour upon sample failure would suggest that a denser network of cementitious bonds and CSH/CAH gels were present within alkali activated samples. Hence, the results obtained from the UCS programme infer that the strength of IBP-stabilised soils and the overall performance of alkali activation are predominantly controlled by the length of curing (in agreement with findings by Hughes et al., 2011); their level of alkali activation and the chemical/water composition of the soil and IBP's used.

5.2   Durability

Both wetting-drying and freezing-thawing durability results demonstrated that the GGBS-AA binder provided the most improved durability performance when added to the artificial alluvium, closely followed by PFA-AA. In severe contrast, RG-stabilised samples provided negligible improvements in durability, based on the disintegration of RG-AA and RG-C samples upon immersion during wetting-

drying testing and the RG-C sample during freeze-thaw testing. Although the RG-AA sample survived 3 cycles of freeze-thaw testing before disintegrating, this performance would still be classed as poor and unacceptable for construction standards. As discussed above for strength, the method used to prepare RG for mixing resulted in a non-uniform coarse-grained material, and thereby characterised by a lower density and higher permeability compared with GGBS or PFA powders. This consequently enabled water to more freely infiltrate RG-stabilised samples whilst submerged during testing and therefore be at high risk of disintegration before completing the 12 cycle wetting-drying/freeze-thaw testing periods. This occurrence has been recorded by Hughes (2005), whereby a GGBS-RG-AA sample failed in a brittle manner during thawing after the seventh cycle of freeze-thaw testing. Ultimately, water which entered the sample had frozen, causing contraction and consequently sample cracking. Hughes (2005) was also of the view that this sample degradation may also have been caused by reactions between RG and hydrated compounds, thereby forming unfavourable Ettringite along with shrinkage and/or swelling. Hence, as shown by the GGBS-AA sample; alkali activation demonstrated its ability to produce denser and less permeable soils and therefore decrease the chances of water absorption and sample shrinkage/swelling. However, as the results from RG-AA and PFA-AA samples suggest, alkali activation using the sodium hydroxide/sodium silicate mixture did not consistently result in improved durability properties.

5.3 pH and Mineralogy

pH and UCS testing results indicate that alkali activation was required to allow pozzolanic reactions and subsequent strength enhancements to occur. This would suggest that a soil's pH strongly influences any potential strength development it may experience. Compressive strengths greater than 1 MPa were only recorded for samples in this study that had been alkali activated and had achieved a pH $\geq$ 10.50, namely GGBS-AA (11.47); thereby permitting pozzolanic activity. However, some samples with sufficiently high pH levels for pozzolanic activity to occur, such as PFA-AA and RG-AA specimens, did not develop high strengths. A study by Wilkinson et al. (2010b) suggests that the strength of certain stabilised soils may increase as pH decreases. This therefore puts the relationship between soil pH and strength development under further scrutiny. Should any oxidation and/or pH degradation processes occur with stabilised soils, it may be possible for pozzolanic reactions along with any associated strength improvement to become impeded. Thus, it is strongly advised that samples be well sealed and stored within air-tight containers and that the precise quantities of alkali activator to be added to soils pre-mixing are accurately calculated, to ensure the pH will remain $\geq$ 10.50 over an adequate curing period (i.e. minimum of 28 – 56 days).

Previous mineralogical studies by Rodriguez-Navarro et al. (2000), Little et al. (2005) and Hughes (2005) have shown that through analysis techniques such as XRD, minerals including Ettringite, Thaumasite and Thenardite may be found within stabilised clay soils where calcium-based binders have been used. The presence of the aforementioned minerals within stabilised soils or concrete would be considered as highly unfavourable, as they can potentially lead to material degradation through shrinkage, swelling, sulphate attack and severely compromise the engineering integrity of the material in question. Although a mineralogical analysis was not conducted as part of this study, it is highly recommended that mineralogical techniques such as scanning electron microscopy and XRD be conducted in future studies in searching for the presence of potentially structurally unfavourable minerals within stabilised soil specimens. Additionally, it would be interesting to search for any correlation between the formation of structurally unfavourable minerals and pH during such mineralogical studies, as Hughes (2005) suggested that Ettringite or Thaumasite tend to form within soils characterised by low pH levels.

5.4 Moisture Content

To allow the hydration of binders and the formation of cementitious gels/minerals within stabilised soils, it is necessary for a suffice amount of water to be present. For this study, samples were initially mixed so that they had a moisture content of 15 %. Post-UCS testing for each curing period, sample's moisture contents were recorded. It was generally found that moisture contents decreased over the 28 day curing period by only 1 – 3 %. Given this relatively low reduction in moisture content, the samples tested are interpreted as containing enough water for hydration. It should also be noted that a proportion of samples' moisture contents is depleted due to pozzolanic reactions; involving calcium hydroxide being transferred by water to amalgamate with aluminate and siliceous minerals. These undergo dissolution to produce cementitious CAH/CSH gels. From this study, certain alkali activated samples (e.g. GGBS-AA) and the CEM-I sample showed higher compressive strengths with decreasing moisture contents. This observation is in agreement with a study by Duxson et al. (2007), who concluded that water is consumed during the dissolution of geopolymer-based reactions. This would also indicate that AA samples tend to have lower moisture contents than C samples; although it should be borne in mind that this may not always be the case, whereby C samples' moisture content may be equally depleted by evaporation pre-testing. One final

factor which may influence a sample's water content and hydration reactions is the negative pore pressures generated when compacting samples within the split-sample mould. Such negative pore pressures have also been documented by Hughes et al. (2011), which may result in higher strengths being achieved. Hughes et al. (2011) also state that soils with high clay contents would inherently have low levels of permeability and thus greatly inhibit the amount of water available within the soil for hydration.

6. CONCLUSIONS

Based on the results obtained from the laboratory testing programme carried out, a number of conclusions can be made:

- The use of IBP binders and alkali activation with a sodium hydroxide/sodium silicate mixture have demonstrated their plausibility in being successfully used as more environmentally sustainable replacements for lime and CEM-I in soft soil stabilisation. Namely, the strength and durability performances shown by the GGBS-AA specimens were commendable and would be suitable for construction specifications.

- The replacement of CEM-I with IBP binders for deep dry soil mixing projects could be accomplished with very little plant or equipment modifications, along with negligible degradation in the overall efficiency of the soil mixing process. However, the use of sodium silicate solution as an alkali activator on site may present financial and practicality problems. An alternative high-alkali waste product in the form of a powder would be preferred both in terms of the environment and finance.

- From the IBP binders tested, the GGBS-AA mixture proved to be the most effective in producing high strength gains of > 6 MPa and effective resistance to wet-dry and freeze-thaw cycles over 28 days. Hence, GGBS-AA would be the most suitable replacement for CEM-I in projects where engineering specifications require high strength and stiffness levels. However, other engineering scenarios where medium levels of stiffness are required, for instance high speed railway line foundations which frequently experience dynamic loading induced by passing trains; GGBS-AA would not be suitable as brittle failure of stabilised soil columns may result.

- pH testing results confirmed alkali activation was required to increase the pH of stabilised soils to at least 10.50, in order for pozzolanic activity to potentially take place. Evidence from this study suggest that pH bears an influence on a stabilised soil's strength development; whereby increasing pH allows pozzolanic reactivity and subsequent increases in strength. However, findings from other recent studies contend that this does not always apply; thereby warranting further investigation.

- Alkali activation using sodium hydroxide and sodium silicate did not harmoniously enhance sample durability. Given the poor overall geotechnical performances of the PFA and RG binders, careful evaluations ought to be conducted for IBP's when being considered for selection as binders for deep soil mixing projects. Additionally, careful consideration must be paid towards both the soil that is to be stabilised and the loading conditions to be imposed over stabilised soil columns, on an individual case basis. This approach is recommended to be taken until a more extensive and detailed understanding has been developed on binder/alkali activator properties for soil stabilisation.

- Findings from this study are expected to be valuable to the construction sector in procuring the most optimum sustainable binder mix designs for deep soil mixing, in terms of quality and economics for problematic soft alluvium soils. However, if this research is to be of use to the geotechnical community, future works should focus on demonstrating the potential of IBP binders within other documented problematic soils and determining whether utilising IBP binders is financially feasible compared with more traditional binders, by conducting a series of field trials and costing studies.

REFERENCES

Ahnberg, H., Johansson, S.-E., Pihl, H. and Carlsson, T., 2003, "Stabilising effects of different binders in some Swedish soils", Ground Improvement, 7, No. 1, pp. 9-23.

Al-Tabbaa, A. and Evans, C. W., 1998, "Pilot in situ auger mixing treatment of a contaminated site, Part 1: treatability study", Proceedings of the Institute of Civil Engineers, Geotechnical Engineering, 131, pp. 52-59.

American Society for Testing and Materials (ASTM), 1996, Designation: D 559 – 89 Standard Test Methods for Wetting and Drying Compacted Soil-Cement Mixtures, Annual Book of ASTM Standards, 4.08, West Conshocken: Pa.

American Society for Testing and Materials (ASTM), 1996, Designation: D 560 – 96 Standard Test Methods for Freezing and Thawing Compacted Soil-Cement Mixtures, Annual Book of ASTM Standards, 4.08, West Conshocken: Pa.

Beretka, J., Cioffi, R., Marroccoli, M. And Valenti, G., 1996, "Energy-saving cements obtained from chemical gypsum and other industrial wastes", Waste Management, 16, pp. 231-235.

BSI, 1990, BS: 1377 Incorporating Amendment No. 1, Methods of test for Soils for Civil Engineering Purposes, British Standards Institution, Milton Keynes.

Davidson, L. K., Demirel, T. and Handy, R. I., 1965, "Soil Pulverization and Lime Migration in Soil Lime Stabilisation", Highway Research Record, 1965 (92), pp. 103-126.

Duxson, P., Fernandez-Jimenez, A., Provis, J. L., Lukey, G. C., Palomo, A. and Deventer, J. S. J, 2007. Geopolymer technology: the current state of the art. Journal of Materials Science, Advances in Geopolymer Science and Technology. 42, 2917-2933.
Fraay, A. L. A., Bijen, J. M. and Haan, D. Y. M., 1989, "The reaction of fly ash in concrete: a critical examination", Cement and Concrete Research, 1989 (19), pp. 235-246.

Hughes, P. N. and Glendinning, S., 2004, "Deep dry mix ground improvement of a soft peaty clay using blast furnace slag and red gypsum", Quarterly Journal of Engineering Geology and Hydrogeology, 37, pp. 205-216.

Hughes, P. N., 2005, "The Use of Synthetic Red Gypsum as a Construction Material", PhD Thesis, School of Civil Engineering and Geosciences, Newcastle University, UK.

Hughes, P. N., Glendinning, S., Manning, D. A. C. and White, M. L., 2011, "Use of red gypsum in soil mixing engineering applications", Proceedings of the Institution of Civil Engineers, Geotechnical Engineering, vol. 164, GE3, pp. 223-234.

Jegandan, S., Liska, M., Osman, A. A-M. and Al-Tabbaa, A., 2010, "Sustainable binders for soil stabilisation", Proceedings of the Institution of Civil Engineers, Ground Improvement, 163, G11, pp. 53-61.

Little, D. N., Herbert, B. and Kunagalli, S. N., 2005, "Ettringite Formation in Lime-Treated Soils: Establishing Thermodynamic Foundations for Engineering Practice", Transportation Research Record: Journal of the Transportation Research Board, No. 1936: Soil Mechanics 2005, Transportation Research Board of the National Academies.

Palomo, A., Grutzeck, M. W. and Blanco, M. T., 1999, "Alkali-activated fly ashes. A cement for the future", Cement and Concrete Research, vol. 29, pp. 1323-1329.

Rodriguez-Navarro, C., Doehne, E. and Sebastian, E., 2000, "How does sodium sulphate crystallised? Implications for the decay and testing of building materials", Cement and Concrete Research, 30, pp. 1527-1534.

Rogers, C. D. F., Glendinning, S. and Holt, C. C., 2000, "Slope stabilisation using lime piles – a case study", Ground Improvement, 4, pp. 165-176.

Sherwood, P. T., 1993, "Soil stabilisation with cement and lime – state of the art review", Transport Research Laboratory, Department of Transport, HMSO publications, ISBN 0-11-551171-7.

Wilkinson, A., Haque, A. and Kodikara, J., 2010b, "Stabilisation of clayey soils with industrial by-products: part B", Proceedings of the Institution of Civil Engineers, Ground Improvement, 163, G13, pp. 165-172.

Soils treatment with hydraulic binders: physicochemical and geotechnical investigations of a chemical disturbance

L. SAUSSAYE[1,2],
M. BOUTOUIL[1,2],
F. Baraud, UCBN ERPCB EA, Caen, France fabienne.baraud@unicaen.fr
L. Leleyter, UCBN ERPCB EA, Caen, France, lydia.reinert@unicaen.fr

1. *ESITC Caen, France*
ecr.geotech@esitc-caen.fr ; dir.recherche@esitc-caen.fr

2. *UCBN ERPCB Labo EA-3914 Caen* , France

ABSTRACT

The reuse of soils after adding binder agents is becoming more and more applied. This treatment technique results in the improvement of the physical and mechanical characteristics of the soils, allowing them to be reused in several geotechnical applications.

However, in some cases, the treated soil (hydraulic binders-soil mixes) shows harmful effects such as swelling and reduction of mechanical strengths. This behavior could be linked to the presence in the soils of specific chemical compounds, such as chlorides, sulfates, nitrates and phosphates at high levels.

Our ongoing research work is aiming at the assessment of the influence of assumed disruptive chemical compounds. Nature and levels effects on treated soil physical and mechanical properties are studied.

In this paper, three soils from Normandy region – France, were subjected to comprehensive tests including geotechnical classification and chemical characterisation before being treated with quicklime and hydraulic binder.

First, the study reports the initial characterisation of 3 types of soils. The results show 3 soils with similar geotechnical parameters but a large variance regarding the anionic concentrations.

Then, are reported the results of the ability of the soils to be treated, before and after adding deleterious compounds. Volumetric swelling and indirect tensile strength are investigated. It appears that the 3 soils enriched with chloride or sulfate, between 1 and 10g.kg^{-1} of dry soil, present different behaviors, both at the level of the physical and the mechanical performances.

1.   INTRODUCTION

Solidification with hydraulic binders is essential to improve the engineering properties of soils in order to use them in capping layer or subbase with the required performances. The geotechnical parameters necessary for these applications are reported in the technical guide "Treatment of soils with lime and / or hydraulic binders – Application to the construction of pavement base layers" (GTS) (LCPC-SETRA, 2007).

Soil solidification faces limits of effectiveness. A failure is declared when there is an important volumetric swelling and/or a reduction of mechanical strengths. The technical guide hypotheses that some chemical compounds can have deleterious effects on the solidification of hydraulic binders. It attempts the presence in the soil of potentially disruptive chemical elements (such as chloride or sulfate ions). But it brings no detail on the concentrations of disorder.

The influence of these anions is discussed in several studies about cement-based material. To compare the results on these materials with treated soils, the concentrations are reported in percent of the mass of hydraulic binders.

The most widely known compound to alter soil solidification with lime and cement is sulfate (Sherwood, 1962; Mitchell, 1986 ; Hunter, 1998 ; Baryla *et al.*, 2000 ; Harris, 2004; Little *et al.*, 2005).

First, sulfates (gypsum, hemihydrates or anhydrite) are necessary compound to regulate the setting of the tricalcic aluminates (C_3A) of the hydraulic binders. So cement can contain 0.1 to 4.0 % of SO_3.

Cau Dit Coumes and Courtois (2003) note that under Na_2SO_4 form, at a weak concentration of 0.02 %, sulfates induce a setting delay of a cement paste CEMI 52.5. On the other hand, at a concentration superior to 0.30 %, they induce an acceleration of the setting and hydration.

But, beyond the changes of hydration kinetics, sulfates are especially targeted as being a source of swelling even of cracking of the cement material. The association of several sources of sulfate and alumina leads to the

Saussaye - Soils treatment with hydraulic binders: physicochemical and geotechnical investigations of a chemical disturbance

II-479

development of ettringite (hydrated calcium trisulfoaluminate and monosulfoaluminate) which becomes harmful to the materials durability.

Others sulfate compounds can develop by reaction between external sulfides and sulfates (pyrite and gypsum of the soil, the marine sea sprays, etc.) and cement hydrates. For example is noticed the formation of gypsum with the portlandite $Ca(OH)_2$ and the CSH, the formation of ettringite with CAH, the formation of thaumasite $CaCO_3$. $CaSiO_3.CaSO_4.15H_2O$ from the ettringite $3(CaO).Al_2O_3.3CaSO_4.32H_2O$ (Cabane, 2004).

Jallad *et al*. (2003) show that the stability of the thaumasite can be affected by the presence of the other chemical species such as phosphates and ammonium, at pH lower than 12, demonstrating then the likely interactions of the other soil components in the cement hydration reactions.

The descriptions of Le Borgne (2010), on a silt treated with 1.5 % of quicklime and 6 % CEMII, involve that sulfate ions, under $CaSO_4.2H_2O$ form, have a disruptive effect on lime and cement hydration between 0.1 and 1 %. The swelling is superior to 10 % but the mechanical performances remaining sufficient for the GTS application. The indirect tensile strength (ITS) with 0.1 % is improved beyond 10 % compared to soil without additive whereas 1 % had no effect. Xing *et al.* (2009) indicate a delay of setting for 0.2 %.

The GTS indicates a threshold of $10g.kg^{-1}$ of dry soil to take seriously into account the risk of sulfate reaction. Cabane (2004), with a literature review of case study for sulfate reaction in treated soils, reports a threshold of $3g.kg^{-1}$.

It is generally accepted that the interaction between chloride in solution and a cement paste has a beneficial influence on the concrete durability. Calcium chloride ($CaCl_2$), added at 1 % or 2 %, is an ideal accelerating admixture for cement.

The negative action of chloride is rather associated with chemical phenomena of crystallisation of salt, coming from exogenous contributions (i.e. NaCl of sea water), within the concrete.

The chloride ions of NaCl, introduced into a cement paste of CEMI 52.5, at a concentration lower than 0.03 % to the cement mass, delay the hydration of aluminates (C_3A, C_4AF) (Cau Dit Coumes and Courtois 2003).

The delay of hardening and cracking is attributed to the formation of calcium chloroaluminate $Ca_2Al(OH)_6Cl.2H_2O$ from the hydration of the calcium aluminates (Malone *et al.* 1997 ; Cau Dit Coumes and Courtois 2003 ; Barberon *et al*. 2005 ; Lubelli *et al.* 2006).

In the presence of concentrations higher than 0.3 %, expansive oxychloride minerals, $3CaO.CaCl_2.15H_2O$ and $CaO.CaCl_2.2H_2O$, appear (Cau Dit Coumes and Courtois 2003).

Saikia *et al*. (2006) underline that in a metakaolin-lime paste containing 3.25 % of chloride compared to the binders mass, the initial formation of the Friedel's salt $3CaO.Al_2O_3.3CaCl_2.10H_2O$ is later counterbalanced by the formation of strätlingite $2CaO.Al_2O_3. SiO_2.8H_2O$ (CASH).

At higher concentrations, for 5 to 10 % of chloride, the Friedel's salt is stable on the long term. The Friedel's salt formation leads to the destabilisation of the portlandite $Ca(OH)_2$.

Moreover, an important fraction of chloride is adsorbed on the CSH surface (Saikia *et al.* 2006 ; Elakneswaran *et al.* 2009).

About treated soil, Le Borgne (2010) indicates that the presence of chloride does not lead to a modification of the setting reaction kinetics of a silt treated with 1.5% of quicklime and 6% CEMII. The addition of NaCl, at weak (1%) or strong concentration (2%), has no effect on indirect tensile strength (ITS) after immersion.

Xing *et al.* (2009) show the behavior in unconfined compression at 7, 28 and 90 days of soils rich in salts, integrating chloride concentrations of 0.75 to 8%, under NaCl form, treated with 21 % of cement CEMI 32.5. At 4 %, chloride ions decrease UCS about 20 % (1.24MPa) compared to a soil with 0.75 % (1.50MPa).

Xing *et al.* (2009) led a physicochemical analysis in parallel of unconfined compression tests on treated soils. An increase of the Cl^- concentration beyond 4 % reduces the CSH formation and, then, it reduces the UCS. The Cl^- ion is the first to react with Ca^{2+} and Al^{3+} to form $Ca_2Al(OH)_6Cl(H_2O)_2$, mineral which settles on the surface of clays, without improving the cohesion. Chloride ions also react with C_3A to form $3CaOAl_2O_33CaCl_3.10H_2O$, the Friedel's salt, and so delay the development of the calcic compounds, CAH and CSH. Then, this effect of chlorides on soil solidification is similar to the effect of chlorides on cement or concrete hardening.

This research work is led in partnership with practitioners of soils treatment, namely Mastellotto company and Cimbéton association. They need to define a concentration threshold beyond which each compound alters the soil solidification processes. This paper intends to assess the influence of chloride and sulfate ions on solidification of three soils from Normandy region (France) treated with the same hydraulic binders formulation.

This study continues, in a complementary way, the experimental works led by Le Borgne (2010). To determine the concentration threshold beyond which a compound may have a negative impact on the effectiveness of soil solidification with lime and cement, Le Borgne (2010) mixed two selected soils with a potential deleterious

Saussaye - Soils treatment with hydraulic binders: physicochemical and geotechnical investigations of a chemical disturbance

II-480

compound at two concentrations representative of what can be found in the field. The influence of sulfate, under gypsum ($CaSO_4.2H_2O$), and chloride, under sodium chloride (NaCl) form, on the mechanical performance of a soil mixed with quicklime and cement are evaluated for five high concentrations with suitability tests of soils to treatment.

2. MATERIALS AND EXPERIMENTAL PROCEDURES

2.1. Materials

Three soils from the Normandy region, in France, were selected and sampled by the Mastellotto company. They are subjected to a geotechnical classification and a physicochemical characterisation.
According to the french GTR soil classification system, two soils are classified as fine and silty soil A1 and the third one as sandy to gravel soil with a fraction 0/50mm A1. The main properties of the three soils selected for this study are given in Table 1.

Table 1 : Main geotechnical properties of soils

	Soil 1 (LL)	Soil 2 (LS)	Soil 3 (LD)
Dmax (mm)	50	80	8
Fraction ≤ 80µm (%)	77	34	85
Fraction ≤ 2µm (%)	10	10	9
BVs (g.100g^{-1} of dry soil)	0,8	1,1	1,0
Natural moisture content w_N (%)	19,5 - 21,0	13,5 - 15,0	16,4 - 16,9
Optimum moisture content w_{OPN} (%)	16	17	15
Maximum dry density ρ_{dOPN} (Mg.m^{-3})	1,68	1,76	1,72
Immediate Bearing Index à w_N	≤ 3	13 – 16	≤ 3
GTR classification	A1th	(C1)A1m	A1th
LL, LS, LD : references to the location of sampling			

The physicochemical analyses allow to determine the anionic concentrations of the water soluble fraction of the three soils. The interstitial solution of s is so extracted in the distilled water with liquid / solid ratio of 10 during one hour. The extract is then filtered at 0.45µm and analysed by ionic chromatography. Each soil is divided into five samples and each sample is divided into 5 replicates, so 25 measures are realised for each soil.
The table 1 gives the minimum and maximum chloride and sulfate concentrations of the water soluble fraction of each soil and compared them to the frequent contents of the interstitial solution of soil indicated by Calvet (2003). The 3 soils present different anions concentrations, within the range of the most frequent reported values.

Table 2 : Water soluble fraction concentrations of soils

	Soil 1 (LL)	Soil 2 (LS)	Soil 3 (LD)	Frequent values (Calvet, 2003)
Anions concentrations of soil solution (mg.kg^{-1} of dry soil)				
Cl^-	16-115	59-145	32-95	16-142
SO_4^{2-}	81-136	75-147	45-83	13-182

According to the methylene blue value (i.e. clay activity) observed for the three soils, the option of a mixed treatment, quicklime-cement, was selected.
The quicklime selected, according to NF P98-101 standard, have a high content of free lime, greater than 90%.
Cement CEMII 32.5 is selected according to GTS 2000 prescriptions. The cement CEMII/B (S-LL) 32.5R is based on pure Portland cement (65 to 79% of clinker) containing limestone and slag as a secondary constituent (21 to 35%). It meets the prescriptions of NF EN 197-1 standard.
A pretreatment with 1% of quicklime is performed before the addition of 6% of cement CEMII. This formulation is used by the Mastellotto company for soil 1. Then, this treatment is also applied for the two other soils. All contents are expressed on the dry mass of the soil.

Saussaye - Soils treatment with hydraulic binders: physicochemical and geotechnical investigations of a chemical disturbance

II-481

The normal Proctor compaction characteristics of the different mixtures are determined according to NF EN 13286-2 standard. The wet soil is first mixed with lime for a few minutes. After 1h±10min, cement is added, and the mixture is compacted. The compaction references are used to prepare the samples.

Three cylindrical samples with a height of 50 mm and a diameter of 50 mm are prepared for each combination to be tested (soil and tested physicomechanical parameter). All samples are compacted by static axial compression in a cylindrical mold (according to the NF EN 13286-53 standard). The moisture content corresponds to the optimum water content. The dry density of the samples is at 96% of the maximum dry density.

2.2. Experimental procedures

Regarding the few quantitative data available on the chemical disruptive of the soils treatment with hydraulic binders, five study concentrations are selected : 1, 3, 5, 7 and 10g of anion potentially disruptive per kg of dry soil. The selected values are reported and converted in content on the hydraulic binders mass in Table 3, for comparison with the literature values.

The anions are added under NaCl and $CaSO_4.2H_2O$ form. It is likely that the associated cation (Na^+ or Ca^{2+}) has an influence on the solidification process of treated soil, but this effect will not be taken into account in this study.

Table 3 : Anionic concentrations added to soils

Anion	Chemical form	Anions concentrations added to soils (mg.kg^{-1} of dry soil)				
Cl$^-$	NaCl	1	3	5	7	10
SO$_4^{2-}$	CaSO$_4$.2H$_2$O	1	3	5	7	10
% of anion compared to the mass of hydraulic binders		2	5	8	12	17

Each soil is mixed with one deleterious compound at one given concentration. To obtain homogeneous samples, the chemical compound of interest is dissolved in fresh water (Guichard, 2006 ; Harris, 2004). Chromatographic analysis is performed to check the effective concentration of the chemical compound in the prepared solution. But the water soluble fraction of the soil is not analysed after the solution addition. So it remains difficult to estimate the anion fraction actually available to react with the hydraulic binders. The dry soil and the solution necessary to the samples compaction (water content to obtain optimal water content after treatment) are manually mixed a few minutes and then stored seven days in hermetic conditions at 20 °C. The soil is mixed with a mechanical mixer and the water content is subsequently determined.

Three samples of treated soils were prepared for each combination to be tested (soil, chemical element nature and concentration and suitability test). The physical and the mechanical behaviors of a mixture is then determined and compared to the performances of the control samples, i.e. the treated soil without any added chemical compounds.

The selected procedures correspond to three standards, NF P94-100, NF EN 13286-42 and NF EN 13286-49, which appear in the GTS (LCPC-SETRA, 2000) to define the suitability of a soil for a given treatment.

Two kinds of mechanical tests are selected to assess the influence of each chemical compound on the soil solidification. The first is a physical test to measure the volumetric swelling of samples. The second is a mechanical test to assess the indirect tensile strength (ITS).

The two series of samples are kept immersed in a bath at 40°C during seven days. So, the suitability test to treatment is an accelerated testing procedure, allowing to glimpse quickly the physicochemical reactions potentially disruptive of the hydration of the hydraulic binders, thus of the solidification of the treated soil.

The assessment criterias to decide on the suitability of a soil to a treatment are reported in Table 2. In this case, these thresholds allow to determine a level of disturbance of potentially disruptive anions added in the solution of soil.

Saussaye - Soils treatment with hydraulic binders: physicochemical and geotechnical investigations of a chemical disturbance

II-482

Table 4: Assessment criteria for suitability of a soil to treatment (LCPC-SETRA, 2000)

Suitability to treatment	Volumetric swelling (%) (NF EN 13286-49)	Indirect tensile strength ITS (MPa) (NF EN 13286-42)
Suitable	VS < 5 **and**	$R_{it} > 0.20$
Doubtful	$5 \leq VS \leq 10$ **or**	$0.10 \leq R_{it} \leq 0.20$
Unsuitable	VS > 10 **or**	$R_{it} < 0,1$

Without potentially disruptive element, the three soils are doubtful to the treatment with, certainly, very weak volumetric swelling but especially with insufficient ITS (Table 3).

The performances follow the order soil 1 < soil 2 < soil 3. This behavior can be explained partially by an optimal dry density ρ_{dOPN} which evolves in this order and confers initially on the material a compactness which takes a large part in the development of mechanical performances.

From this observation, it emerges that the results must be interpreted, at first, soil by soil before to compare the behavior of soils after integration of a potentially disruptive element.

Table 5 : Suitability of undisturbed soils

1%CaO + 6% CEMII/B 32.5R	Soil 1 (LL)	Soil 2 (LS)	Soil 3 (LD)
Volumetric swelling (%)	0.13	0.17	0.14
ITS (MPa)	0.14	0.17	0.19
Suitability	*doubtful*	*doubtful*	*doubtful*

3. RESULTS AND DISCUSSION

The suitability tests results are plotted in figures 1 to 4. In these figures, the bars associated with every point correspond to the maximal dispersion of the results obtained, i.e. the dispersion between minimum and maximum values obtained on 3 samples.

While all the values of volumetric swelling are saved, the strength measures are validated for dispersion lower or equal to 20 % of the average value.

The plot at 0g.kg^{-1} corresponds to a "control sample", that's to say, a sample without any added disruptive compound.

3.1. Influence of sulfate on soil solidification

The figure 1 shows the indirect tensile behavior of soils with sulfate addition.

The ITS of the soil 1 increases, compared to control soil, for concentrations of 1 and 3g of SO$_4^{2-}$.kg^{-1} of dry soil. The level of performance reached is then stable between 3 and 10g of SO$_4^{2-}$.kg^{-1} of dry soil. The mean value of ITS reached is then of 0.20MPa.

For the soil 2, an increase of ITS is observed after the addition of 1 then 3g of SO$_4^{2-}$.kg^{-1} of dry soil. A decrease of ITS is then noticed in 5g.kg^{-1}, with a resistance lower than that of the control soil. This weak ITS is maintained for 7 and 10g of SO$_4^{2-}$.kg^{-1} of dry soil, without evolution.

If the values of ITS for sulfate concentrations included between 1 and 3g.kg^{-1} exceed the threshold of suitability of 0.20MPa, that is not anymore the case between 5 and 10g.kg^{-1}.

For the soil 3 with 1g or 3g of SO$_4^{2-}$.kg^{-1} of dry soil, ITS increases from 0.19MPa for control soil to a constant value of 0.26MPa. Then for increasing concentrations, at 3 to 10g of SO$_4^{2-}$.kg^{-1} of dry soil, increasing ITS values are measured (0.26MPa to 0.43MPa).

Saussaye - Soils treatment with hydraulic binders: physicochemical and geotechnical investigations of a chemical disturbance

II-483

So, the mechanical behaviors of the 3 soils differ beyond a threshold of 3g of $SO_4^{2-}.kg^{-1}$ of dry soil, especially for the soil 2, for which the high sulfate concentrations lead to a loss of mechanical performances that produces a soil unsuitable to the treatment with 1 % of quicklime and 6 % of CEMII/B 32.5R.
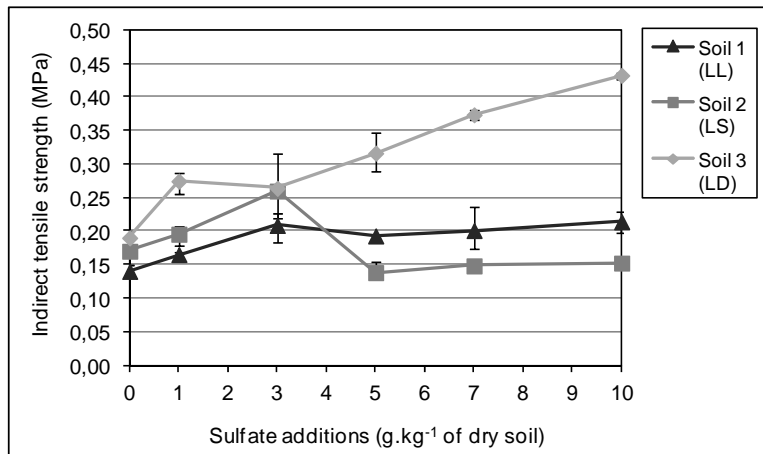

Figure 1 : Influence of sulfate (under CaSO₄.2H₂O form) on the ITS of the treated soils

The figure 2 reports the evolution of the volumetric swelling according to the sulfate concentrations in soils.

For the soil 1, the swelling increases at first slightly with 1g of SO_4^{2-} then with 3g of $SO_4^{2-}.kg^{-1}$ of dry soil. For higher concentrations, the curve exceeds the 5 % threshold for a 7g.kg^{-1} addition, reaching a 7.51 % mean value for 10g of $SO_4^{2-}.kg^{-1}$ of dry soil.

Regarding the soil 2, if a light increase of the swelling is noticed with 1 and 3g of $SO_4^{2-}.kg^{-1}$ of dry soil, a rough increase is then found for 5g of $SO_4^{2-}.kg^{-1}$ of dry soil making uncertain the suitability of the soil to the treatment. The increase of the swelling continues then for 7 then 10g of $SO_4^{2-}.kg^{-1}$ of dry soil. The soil becomes unsuitable to the treatment with 1 % of lime and 6 % of CEMII / B 32.5R with an overtaking of the 10 % threshold.

The soil 3 shows an increase of swelling with 1g of $SO_4^{2-}.kg^{-1}$ of dry soil, that continues with the increase of the sulfate concentration and brings it to an average swelling of 4.82 % for 10g of $SO_4^{2-}.kg^{-1}$ of dry soil.

The three soils are affected by a volumetric swelling superior to what is observed for the control soil. The physical behaviors of the 3 soils differ beyond a threshold of 3g of $SO_4^{2-}.kg^{-1}$ of dry soil. Beyond this concentration, the sulfate content lead sometimes to an important swelling that produces a soil unsuitable to the treatment with 1 % of quicklime and 6 % of CEMII/B 32.5R.
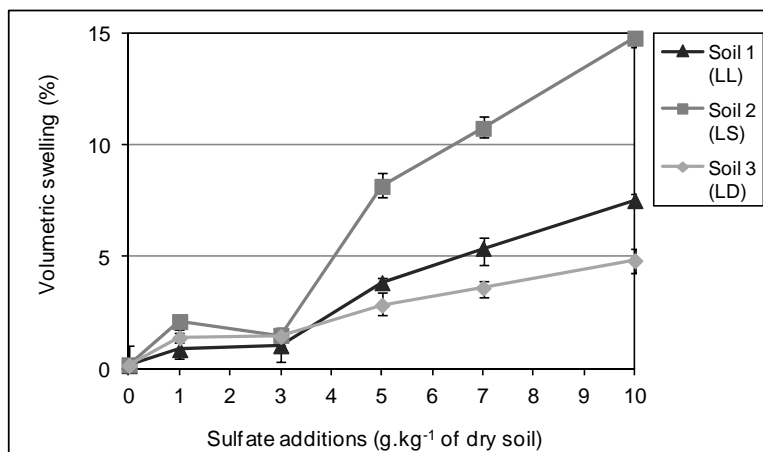
Figure 2: Influence of sulfate (under CaSO₄.2H₂O form) on the volumetric swelling of the treated soils

The results show that the presence of sulfates is not systematically associated with an alteration of the soil solidification process. So, if an important swelling is noticed, it is not inevitably associated with a mechanical failure. Indeed, ITS and volumetric swelling test don't give the same information and then cannot be compared.

Saussaye - Soils treatment with hydraulic binders: physicochemical and geotechnical investigations of a chemical disturbance

II-484

Le Borgne (2010) shows that during the study of the silt treated with 1.5 % of lime and 6 % of CEMII, the accelerated procedure led to a significant swelling of the samples, up to with 14.8 % with 6.20g of $SO_4^{2-}.kg^{-1}$ of dry soil. The ITS with 0.62g $CaSO_4.2H_2O.kg^{-1}$ is improved beyond 10% compared to soil without additive whereas 6.20 $g.kg^{-1}$ of dry soil have no effect.

Such a behavior is observed for the soil 2, but not for soil 1 and 3 : these results highlight that the impact of sulfate on the treated soils performance is dependent on the soil type.

Cuisinier *et al*. (2011) hypotheses that the fact that the silt exhibited more swelling than the sand can be related to the presence of the clay fraction in the silt. Clay particles contain aluminum that is essential for ettringite formation and therefore for swelling.

In this case another hypothesis competes : the soil 2, more sandy, is also the most inert towards sulfate addition. Then, it can be considered that sulfate, less bound to the soil particles, are more available to react with the hydraulic binders and thus to disrupt their hydration mechanisms.

3.2. Influence of chloride on soil solidification

The figure 3 represents the results of indirect tensile strength (ITS) of the 3 soils added with chloride.

For the soil 1, the ITS increases with the addition of 1g of $Cl^{-}.kg^{-1}$ of dry soil. Regarding to the dispersion of measures, the ITS remain constant between 1 and 10g of $Cl^{-}.kg^{-1}$ of dry soil.

However, the ITS increase does not allow the soil 1 to exceed the threshold of 0.20MPa which would have defined this soil as suitable to the treatment with 1 % of quicklime and 6 % of CEMII/B 32.5R.

For the soil 2, the ITS increases for 1g of $Cl^{-}.kg^{-1}$ of dry soil. It remains at the same level until 7g of $Cl^{-}.kg^{-1}$. At 10g of $Cl^{-}.kg^{-1}$, it is substantially equal to that of the control samples.

The ITS is below the threshold of 0,20MPa for 0g. This threshold is exceeded for 1g of $Cl^{-}.kg^{-1}$ of dry soil. The errors bars indicate that it is validated for concentrations of 3 to 7g of $Cl^{-}.kg^{-1}$ of dry soil.

In the case of the soil 3, after an increase of ITS for 1g of $Cl^{-}.kg^{-1}$, constant at $3g.kg^{-1}$, a surprising decline is registered with $5g.kg^{-1}$. For 7g of $Cl^{-}.kg^{-1}$ of dry soil, the level of performance is equivalent to that measured for 3g. The ITS increases again for 10g of $Cl^{-}.kg^{-1}$ of dry soil.

Except for a contribution of 5g of $Cl^{-}.kg^{-1}$ of dry soil, for whom the moderate ITS is included between 0.17 and 0.24 MPa, the threshold of 0.20MPa allowing to declare the soil suitable to the treatment is widely reached, with an average of 0.24MPa for 1g of $Cl^{-}.kg^{-1}$ to 0.28MPa for 10g of $Cl^{-}.kg^{-1}$ of dry soil.

The ITS of the three soils are included between 0.15 and 0.25MPa, with a weak improvement compared to the control soils whatever is the added concentration.
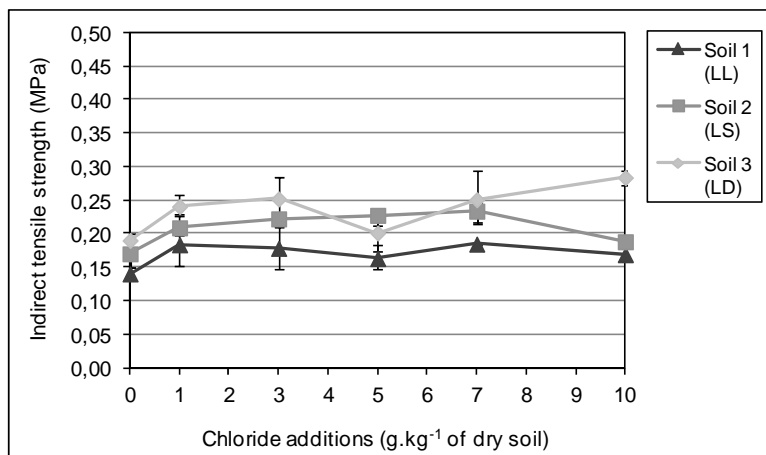
Figure 3: Influence of chloride (under NaCl form) on the ITS of the treated soils

The figure 4 presents the results of volumetric swelling of the 3 soils added with chloride.

Regarding the soil 1, the volumetric swelling for 1g of $Cl^{-}.kg^{-1}$ of dry soil is equivalent to that measured on control samples. Then, it increases gradually between 3 and 10g of $Cl^{-}.kg^{-1}$ of dry soil, to reach an average value

Saussaye - Soils treatment with hydraulic binders: physicochemical and geotechnical investigations of a chemical disturbance

II-485

of 0.93 %, which is clearly inferior to the 5 % threshold making a soil suitable to doubtful, regarding to the considered treatment.

The soil 2 shows an increase of the volumetric swelling with 1g of $Cl^-.kg^{-1}$ of dry soil. This swelling remains stable between 1 and $5g.kg^{-1}$. An inflection of the curve from 5g of $Cl^-.kg^{-1}$ of dry soil brings it to a mean value of 2.34 % for 10g of $Cl^-.kg^{-1}$ of dry soil.

The soil 3 swells weakly until $5g.kg^{-1}$. For higher concentrations, a curve inflection is observed with a regular increase until 3.28 % for 10g of $Cl^-.kg^{-1}$ of dry soil.

The volumetric swelling of the three soils lightly increase with the addition of chloride ions and stay under a value of 5%.
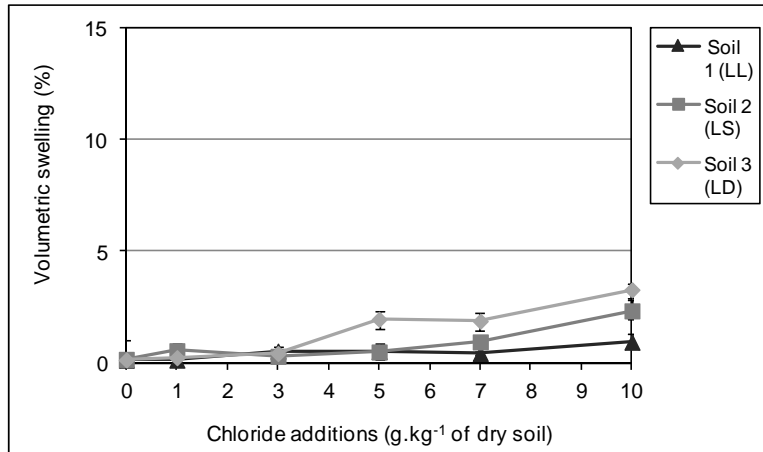

Figure 4: Influence of chloride (under NaCl form) on the volumetric swelling of the treated soils

The three soils, in spite of close geotechnical classes, react differently to the addition of chloride.
It seems nevertheless that after a first increase of ITS with 1g of $Cl^-.kg^{-1}$, the level of performance reaches a constant value until a concentration of 7g of $Cl^-.kg^{-1}$ of dry soil. The order of performance is the following : soil 1 < soil 2 < soil 3.
Regarding the volume swelling, an increase with the increase of the chloride content is noticed for the three soils. The swellings remain lower than 5 % in all cases and evolve in this order : soil 1 < soil 2 < soil 3.
So, it is noted that the increase of the volumetric swelling of soils with the increase of the chloride concentration cannot be correlated to a decrease of the mechanical performance, contrary to what is generally agreed.
In this study, the addition of chloride slightly improves the mechanical behavior for concentrations between 2 and 12% while the volumetric swelling remains weak.
About treated soil, Le Borgne (2010) indicates that the presence of chloride did not lead to a modification of the setting reaction kinetics. He shows that in a configuration with silt treated with 1.5% of quicklime and 6% CEMII, the addition of 1 or 2% NaCl have no effect on ITS after immersion.
Xing *et al.* (2009) lead a physicochemical analysis in parallel to unconfined compression strength (UCS) tests on treated soils. An increase of the Cl^- concentration beyond 4% reduces the CSH formation. Then, it reduces the UCS. The Cl^- ion is the first to react with Ca^{2+} and Al^{3+} to form $Ca_2Al(OH)_6Cl(H_2O)_2$, mineral which settles on the surface of clays, without improving the cohesion. Chloride ions also react with C_3A to form $3CaOAl_2O_3 3CaCl_3.10H_2O$, the Friedel's salt, and so delay the development of the calcic compounds, CAH and CSH. Then, this effect of chlorides on soil solidification is similar to the effect of chlorides on cement or concrete hardening.
In this study, in spite of important additions of chloride, these mechanical performance decreases are not observed.

4. CONCLUSION

In this paper, the influence of two potential deleterious compounds on soils treatment with lime and cement was considered. The effects of chloride and sulfate anions on three treated soils were studied from the suitability test point of view. These soils have close geotechnical classes but different water fraction soluble anionic concentrations.

Saussaye - Soils treatment with hydraulic binders: physicochemical and geotechnical investigations of a chemical disturbance

II-486

Soils were mixed with one deleterious compound at 1, 3, 5, 7 and 10g of anion per kg of dry soil. Volumetric swelling and mechanical strength were determined, in particular cure conditions, both for the disturbed and the control soils, allowing the quantification of the influence of each compound.

It has been demonstrated that:

- the considered compounds, chloride and sulfate ions, can have a significant effect on the mechanical performances of a soil ;

- the performance of soils after treatment is improved by the presence of chloride, under NaCl form. As a consequence, it is not possible to classify this element as deleterious ;

- the influence of sulfate on the soil solidification processes and the mechanical performance are shown to depend on the soil nature ;

- with sulfate, under $CaSO_4.2H_2O$ form, important swellings are measured for 2 of the 3 soils ;

- with sulfate, for only one of these soils, the swelling comes along with a consequent decrease of the mechanical performances ;

- the single presence of a significant amount of a given compound in the soil cannot be considered as a pertinent factor to assess the soil suitability for treatment with lime and cement.

Among the parameters of influence, the curing conditions (temperature, humidity, etc.) are also important. This study does not exclude potential long term effects of the considered chemical compounds on the treated soil strength. Suitability tests demonstrated the real effect of each compound quantitatively. So, to complete this study, the ITS and UCS are determined on soil doping with each compounds after different curing times, from 28 to 180 days, to assess the evolution over time of the mechanical performance in normal cure, at constant water content and at 20°C.

REFERENCES

Barberon F., Baroghel-Bouny V., Zanni H., Bresson B., D'Espinose de la Caillerie J.B., Malosse L., Gan Z., 2005, Interactions between chloride and cement-paste materials, Magnetic Resonance Imaging, vol. 23, Issue 2, pp.267-272

Baryla J.-M., Chenais V., Gavois L., Havard H., 2000, Effet de sulfates et sulfures sur des marnes traitées à la chaux et au liant routier sur un chantier autoroutier, Bulletin de Liaison des Laboratoires des Ponts et Chaussées 224, pp.39-48

Cabane N., 2004, Sols traités à la chaux et aux liants hydrauliques : contribution à l'identification et à l'analyse des éléments perturbateurs de la stabilisation, PhD Thesis, Centre des Matériaux de Grande Diffusion de l'Ecole des Mines d'Alès

Calvet R., 2003, Le sol : propriétés et fonctions - Tome 2, Phénomènes physiques et chimiques, applications agronomiques et environnementales, Ed. Dunod / France agricole, 511 p.

Cau Dit Coumes C., Courtois S., 2003, Cementation of a low-level radioactive waste of complex chemistry - Investigation of the combined action of borate, chloride, sulfate and phosphate on cement hydration using response surface methodology, Cement and Concrete Research, vol. 33, Issue 3, pp.305-316

Cuisinier O., Le Borgne T., Deneele D., Masrouri F., 2011, Quantification of the effects of nitrates, phosphates and chlorides on soil stabilization with lime and cement, Engineering Geology, vol.117, pp.229-235

Elakneswaran Y., Nawa T., Kurumisawa K., 2009, Electrokinetic potential of hydrated cement in relation to adsorption of chlorides, Cement and Concrete Research, vol. 39, Issue 4, pp.340-344

Guichard C., 2006, Eléments perturbateurs de la prise dans les sols traités aux liants hydrauliques : Définition, détection, seuils et remèdes, Projet de Fin d'Etudes, Institut National des Sciences Appliquées de Strasbourg

Saussaye - Soils treatment with hydraulic binders: physicochemical and geotechnical investigations of a chemical disturbance

II-487

Harris, J.P., Sebesta, S., Scullion, T., 2004, Hydrated lime stabilization of sulfate-bearing vertisols in Texas, Transportation Research Record 1868, pp.31-39.

Jallad K.N., Santhanam M., Cohen M.D., 2003, Stability and reactivity of thaumasite at different pH levels, Cement and Concrete Research, vol. 33, pp.433-437.

LCPC-SETRA, 2000, Traitement des sols à la chaux et/ou aux liants hydrauliques (GTS) - Application à la realization des remblais et couches de forme - guide technique, 240 p.

LCPC-SETRA, 2007, Traitement des sols à la chaux et/ou aux liants hydrauliques (GTS) - Application à la réalisation des assises de chaussées - guide technique, 82 p.

Le Borgne T., 2010, Effects of potential deleterious chemical compounds on soil stabilisation. PhD thesis, Université de Nancy, 242 p.

Little D.N., Herbert B., Kunagalli S.N., 2005, Ettringite formation in lime-treated soil : establishing thermodynamic foundation for engineering practice, Transportation research record, vol. 1936, 243pp.

Lubelli B., Van Hees R.P.J., Huinink H.P., Groot C.J.W.P., 2006, Irreversible dilation of NaCl contaminated lime–cement mortar due to crystallization cycles, Cement and Concrete Research, vol. 36, Issue 4, pp.678-687

Malone P.G., Poole T.S., Wakeley L.D., Burkes J.P., 1997, Salt related expansion reactions in portland-cement-based wasteforms, Journal of hazardous materials, vol. 52, Issue 2-3, pp.237-246

Mitchell J.K., 1986, Practical problems from surprising soil behavior, Journal of the Geotechnical Engineering Division 112, pp.259-289.

Saikia N., Kato S., Kojima T., 2006, Thermogravimetric investigation on the chloride binding behaviour of MK–lime paste, Thermochimica Acta, vol. 444, Issue 1, pp.16-25

Sherwood P.T., 1962, Effect of sulfates on cemented lime-stabilized soils, Highway Research Board Bulletin 353, National Academy of Sciences-National Research Council Publication 1048, Washington, D.C., pp.98-107

Xing H., Yang X., Xu C., Ye G., 2009, Strength characteristics and mechanisms of salt-rich soil-cement Engineering Geology, vol. 103, pp.33-38

Wang L., 2002, Cementitious stabilization of soils in the presence of sulphate, PhD thesis, University of Louisiane, 111 p.

Saussaye - Soils treatment with hydraulic binders: physicochemical and geotechnical investigations of a chemical disturbance

II-488

Effect of fabric on elastic properties of a lime treated clayey sand

B. Sonon, Université Libre de Bruxelles (ULB), Bruxelles, Belgium, bsonon@ulb.ac.be
M. A. Hashemi, Université Libre de Bruxelles (ULB), Bruxelles, Belgium, mihashem@ulb.ac.be
J.-C. Verbrugge, Université Libre de Bruxelles (ULB), Bruxelles, Belgium, jverbrug@ulb.ac.be
B. François, Université Libre de Bruxelles (ULB), Bruxelles, Belgium, Bertrand.Francois@ulb.ac.be
T.J. Massart, Université Libre de Bruxelles (ULB), Bruxelles, Belgium

ABSTRACT

Soil stabilization processes usually acting only on a specific active part of the soil constituents are significantly affected by inert constituents through the microstructural fabric. Thus, computational homogenization may be used to understand this dependence to the fabric through morphological studies. The high heterogeneity and complexity of soils make this approach difficult, mainly at RVEs definition and discretization stage. We present here an integrated framework for soil homogenization allowing morphological studies thanks to an efficient RVE generator coupled with an XFEM setting for mechanical simulation. The link between these tools is the use of Level Set functions for the geometrical description of RVEs. The efficiency of this framework is illustrated with homogenizations of deformation moduli of lime treated soils with a morphological study on the effect of an active constituent properties evolution.

1. INTRODUCTION

The lime treatment of soils, as well as many ground improvement techniques, involve chemical activity between a mineral addition and some constitutive minerals of the soil [1]. The usual heterogeneity of soils implies that only a specific part of minerals are concerned by the reaction (e.g. the clay in lime treatment processes), a (large) part of the materials being unaffected. Depending on the type of solicitation (i.e. mechanics, hydraulic, thermal, ...), the evolution of the response of a treated soil emerges from the relation between active and inert constituents through the material fabric.

Beside efforts being made to understand, describe and quantify the fundamental mechanisms involved in the reactive part, there is an interest in developing models that can use those results to deduce and compare the emergent property modifications of soils having different inert content and morphology. Computational homogenization can be used for this purpose by modeling through microstructural descriptions the detailed behavior of a Representative Volume Element (RVE) under solicitation. This approach is in active development and has already been used to derive macroscopic behavior of simple microstructural material [4,12,6], mainly for mechanical solicitations. The application of this methodology to soils brings up several difficulties, mainly related the material heterogeneity.

Those difficulties may differ depending on the type of the solicitation studied and the method used for it. However, in most of the case, problems first arise when (**a**) trying to define an RVE and (**b**) discretize RVEs for numerical computations (e.g. finite element-type model). We focus here on these two points, other potential difficulties will be addressed in future works.
(**a**) Using computational homogenization in order to study the fabric role in soil improvement requires the use of a large number of RVEs with controlled morphological characteristics. Those RVEs have to fit the measurable macroscopic descriptors (i.e. grain size distribution, volume fraction, void content, ...), as well as permit generations of several RVE maintaining constant each controlled parameter among RVEs while keeping the random generation.
(**b**) Each RVE that has to be computationally tested is subject to a computation set up, including a mesh generation for finite element-type modeling. This particular step is theoretically not a problem but is practically very demanding and human-time consuming, especially in 3D. This dramatically limits the complexity and the number of RVE that can be used and consequently lowers the feasibility of a fabric study. An automated procedure of discretization should avoid this limitation and allow more exhaustive case studies.

We present here an integrated framework for generation and homogenization of large sets of soil RVEs under mechanical solicitations, allowing a morphological parameter study. This is illustrated in the context of lime treatment of clayey sand, for which the ratio clay(active)/sand(inert) is suspected to play an important role. To restrict ourselves to the two above mentioned difficulties, we study the impact of

this ratio on a homogenized deformation modulus, assuming a uniform increase of the clay's Young modulus to be representative of a lime treatment.

The present manuscript is structured in three main sections. *Section 2* presents descriptors for soil morphology that can be used to define RVEs. Two methodologies to produce sets of RVE varying the sand/clay ratio are presented. *Section 3* introduces tools used to generate such RVEs and use them in microstructural mechanical modeling. The home-developed RVE generator and the well-known XFEM method of discretization are briefly introduced. *Section 4* describes the homogenization procedure and presents obtained results.

2.   FROM SOIL TO RVE DEFINITION

Introduction describes soils as multi-phase systems that can be studied and understood. This section describes soils morphology and leads to RVEs definition for our illustrating study. An RVE generator integrating the following considerations was presented previously in [9] and is introduced in *Section 3*.

2.1.   Multi-phase system

Physically speaking, soils are three-phases systems, including a solid skeleton (grains and fine aggregates), water (free or adsorbed in solid phases) and air, filling the remaining spaces. In the context of soil treatment, a phenomenological description, mechanically and chemically derived is preferred. Phases are attributed to constituents based on their chemical activity within the treatment and on their structural behavior within the fabric under mechanical solicitations. The chosen description has also to be based on separable phases, to allow experimental identification of their properties. Three phases are thus distinguished for our purpose: inert grains, clayey matrix (including treatment's addition - lime -, water and air) and the macro-voids.

Inert grains are considered to be the part of the grain size distribution $>2\mu m$ and may be assumed to be stable minerals which do not play any direct role on the treatment processes. The part $<2\mu m$, due to its electro-chemical properties, can be considered to be a distinct phase together with a certain quantity of lime from the treatment and micro-voids containing water and air. This phase play an important cohesive role, acting as a matrix, coating and bridging inert grains together. This clay/water/air/lime mix is considered as a continuous medium with specific properties, concentrating the evolving processes of the treatment. In mechanical modeling, the properties that should be provided for this phase depends on the cure progress. The treatment could therefore initially be modeled using a postulated or measured evolution for this lime-clay phase. Experimentally speaking, this phase is separable if the void and water content of this mix can be quantified and reproduced in testing samples. Finally, remaining spaces are the macro-void phase, which can be filled by air and/or water. It can be defined as the total porosity of the soil except the micro-voids detected in the clayey phase.

The microstructure of a soil is highly three-dimensional and there is no trivial way to find a 2D mechanically equivalent description of a given 3D sample. The mostly used 2D simplified model for grains assemblies description consist of 2D disks. But this can be used only for qualitative illustrations and mechanism analysis. Some morphological aspect concerning voids topology only emerge in 3D and the number of kinematically admissible mechanisms is also different. There is also no comparison possible in terms of volume fractions. The only available indication is the ratio between the volume of a sphere and the area of a disk of the same radius, but it is not enough to derive a 2D-3D equivalency rule for volume fractions in complex microstructures of soils.

The approach we present here can be formulated in 2D as well as in 3D, and should be used in 3D for quantitative purpose (i.e. quantitative comparison with experiments). However, we limit the present results to 2D developments for the ease of illustration and the low cost of computations. The presented results are thus by essence of qualitative nature.

2.2.   Descriptors for RVE definition

The developed RVE generator is built to integrate the use of experimentally measurable parameters allowing the description of the soil microstructure in terms of the three identified phases.

(**a**) The size distribution of solid grains and voids and the volumetric constitution of soil are used to derive volumetric fractions of the three phases. The $2\mu m$ threshold is used to separate clay minerals and micro-voids from inert grains and macro-voids respectively.

(**b**) The size distribution of inert grains can be extracted from the global solid grain size distribution using the 2µm threshold. Relative sizes of grain in an assembly has a major impact on the spatial organization of the microstructure, and then on the stress path pattern under mechanical loading. It should be correctly reproduced by the generator.

(**c**) The grain shapes can be characterized and reproduced qualitatively. The generator therefore has to integrate various shapes, from the quite simple geometry of crystalline minerals to the more rounded and/or irregular shape resulting from the soil constituents history (alteration, fragmentation, rolling, ...).

(**d**) The micro-voids included in the lime-clay mix are not explicitly described in the RVE, except if it is required, by mapping the matrix properties with a density map obtained by micro-tomography, and if this density can be used in a density-dependent constitutive model. The macro-void sizes and shapes can be seen as a consequence of the compaction rate and of the spatial arrangement of grain and clayey matrix in the microstructure.

(**e**) The clay bridges morphology, especially the fraction linking effectively two grains and transmitting stresses may be an important parameter in the structural system of the fabric. The generator is built to allow these parameters to be controllable in terms of volume fraction of bridging clay, relatively to the global clay fraction. Point (**d**) and (**e**) are correlated because the morphology of clay bridges constraints the sizes and shapes of macro-voids and conversely.

2.3.   Morphology of RVE for clayey sand

In this contribution, we chose to focus on the clay/sand ratio of clayey soils as the main morphological parameter to study. In terms of the assumed phases described before, this type of soil with bi-modal distribution of solid grain size is simply described as a distribution of sand grains of quasi uniform size highly-bridged by a clay matrix (*Figure 1.a*). We may use simple shapes for sand grains, as that can be observed on micrographs (*Figure 1.b*).

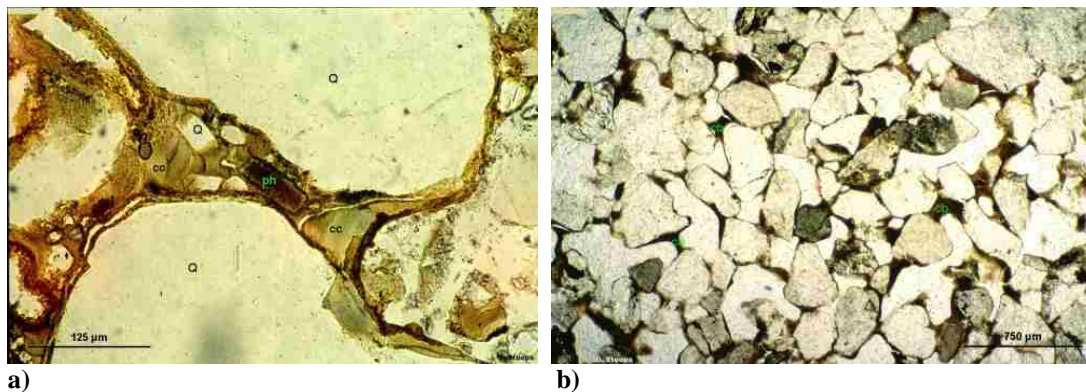**a)**   **b)**

Figure 1: Micrograph of clayey sand. a) Clay bridge detail. [2] b) General view of microstructure (dark : clay, light grey-yellow : sand grains, white : voids) [2]

The method used for RVE generation will be introduced in *Section 3*, we describe here the RVE construction process from a morphological point of view.

The RVE construction begins with the generation of a population of grains in the RVE by LS-RSA (see *Section 3.2*), using quite simple and regular shapes and a uniform distribution of size within a moderate range (*Figure 2.a*). Then remaining areas are divided in macro-voids and clay, this operation should create the previously mentioned and illustrated clay bridges. This is performed by using the product of the two distances from a point **x** to the two nearest sand grains to impose a criteria O(**x**) of bridge presence on this point **x**. The chosen form of O(**x**) (see *Section 3.3*) allow coating and bridging the sand grains in a single operation (*Figure 2.b*), providing moreover a tuning coefficient to adapt the bridge quantity for a given sand, macro-void and total clay quantity. This parameter is certainly not the first one to study, even if it could be of major importance, it is not directly identifiable with actual experimental observations. It is then fixed here to an intermediate value and kept constant for every RVE used.
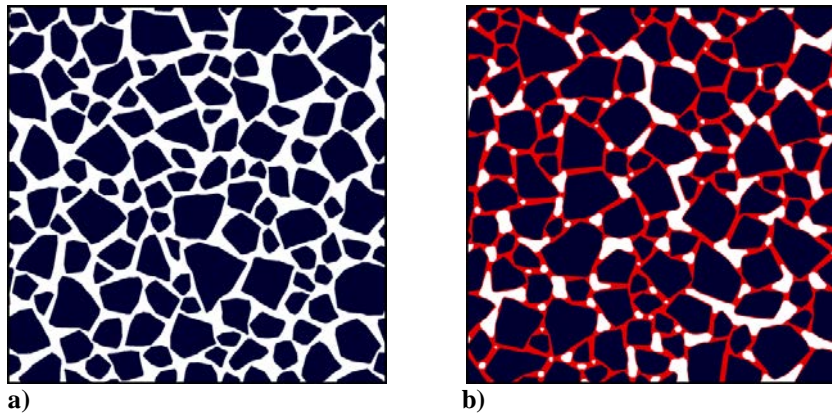
a)   **b)**

*Figure 2: Generation process for clayey sand. **a**) Generation of sand grain distribution, shapes mimic plane sections of quasi-regular sand grains. **b**) Generation of the bridging clayey matrix using distances rules.*

The methodology to vary the sand/clay ratio starting from one of such RVEs is to modify it smoothly by slightly moving phase boundaries in order to obtain a set of RVEs with the same global pattern but with an evolution of the studied ratio. There are basically to ways to proceed, both are performed in the study. (**a**) From a given microstructure, move the boundary between clay and voids to increase clay fraction and keep grain fraction unchanged, decreasing the ratio sand/clay but decreasing also the macro-voids (*Figure 3*). (**b**) From a given microstructure, move the boundary between clay and grains to increase the clay fraction, decreasing the grain fraction and keeping the macro-voids unchanged (but changing nonetheless the total void content because of micro-voids in clay) (*Figure 4*). This second procedure, preserving the void/solid ratio can be preferred but leads to "visually less realistic" microstructures for low sand/clay ratio. Moreover, under the same compaction energy, real samples with different sand/clay ratio will not be compacted to the same density, which is more reflected by the (**a**) case. It should be mentioned that strategies (**a**) and (**b**) do not allow varying the sand/clay ratio within the same range.

*Figure 3: Result of procedure (**a**) on a random sand grain distribution. Volume fraction of these RVE are reported in the Table 1, under label step 1, 3 and 5 for right, center and left RVE respectively.*
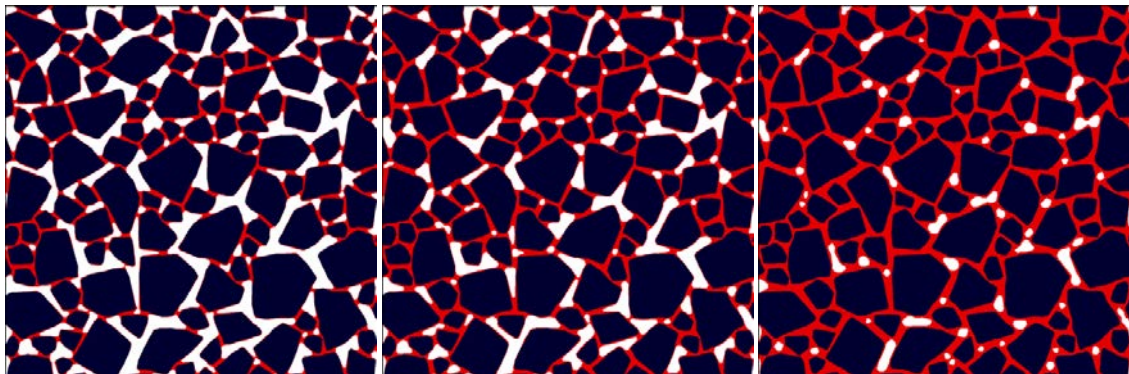

*Figure 4: Result of procedure (**b**) on a random sand grain distribution. Volume fraction of these RVE are reported in the Table 2, under label step 1, 3 and 5 for right, center and left RVE respectively.*
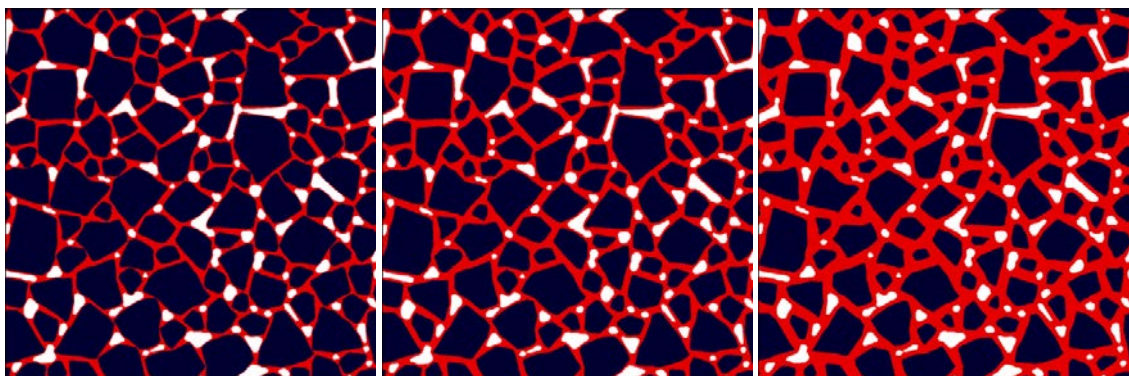
The RVE size should take part of the RVE definition, and this after having performed a variability study on homogenized quantity for several RVE sizes. The chosen size should be large enough to minimize variations on homogenized quantities but being small enough to be computed as discussed in [3]. Given the illustration purpose, this size dependency study is not performed here.

3. FROM RVE DEFINITION TO MICROSTRUCTURAL MODELING

This section gives an overview of different computational tools used to build the homogenization framework. *Section* 3.2 and 3.3 concern the RVE generator we develop, which is described more in details in [9]. *Section* 3.4 introduces the well-known XFEM methodology, largely described and illustrated in [10,7,5]. Those two methodologies use the Level Set functions as a geometrical tool which is the topic of *Section* 3.1.

3.1. Geometrical representation

The morphologically controlled random generation and the automated discretization of defined RVEs require several highly complex and cumbersome geometrical operations. The Level Set formalism [8] offers the possibility to handle heavy geometries with a fixed number of data which do not depend on the geometry complexity. The use of Level Set functions here is also highly motivated be the existence of XFEM techniques allowing the use of these functions as geometrical input for computations instead of meshes.

In 2D, Level Set functions are functions of $\mathbf{x}$ defining implicitly a planar curve φ by the solution of

$$\varphi \equiv LS_\varphi(\mathbf{x}) = 0 \qquad\qquad (1)$$

Various functions can be used as Level Set to define interfaces in a RVEs but the signed distance to the defined interface offers additional opportunities. Functions such as the first and second nearest neighbor function, denoted here $LS_1(\mathbf{x})$ and $LS_2(\mathbf{x})$ (*Figure 5*) can be constructed from signed distance functions of grains of a distribution and are extensively used as map by the RVE generator during the grain distribution stage. The clay bridges generation uses distance rules to define morphological quantities measured trough the microstructure by combinations of distance functions.
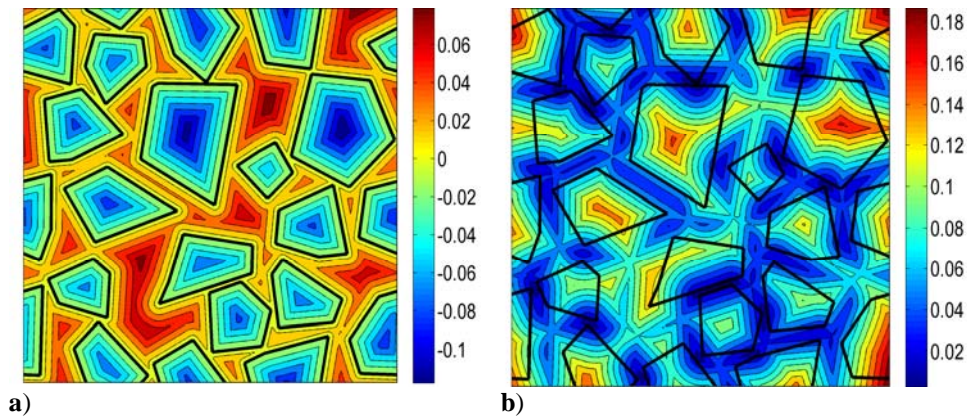

a)   **b**)

*Figure 5: Distance functions of an arbitrary distribution of grains. **a**) LS₁(**x**) **b**) LS₂(**x**).*

3.2. Generating a grain distribution

The generation of the grain distribution is performed by a Level Set controlled Random Sequential Addition (LS-RSA). This method adds grains one by one at random locations constrained by a criterion in terms of distances to previously added grains. For example, overlapping of grains is avoided by imposing the new grain to be added at more than a minimal distances related to the grain size. Other distances criteria in terms of neighboring distances can be used to control the global spatial organization of the generated microstructure. Actually, generating RVEs with a large quantity of grains with highly distributed sizes, enforcing a given density in most of the case require to impose the neighboring distances to be relative to the particle sizes or particle densities to achieve homogeneous and random packings. Otherwise, generation of RVEs with very high fraction of grains require an optimal spatial organization minimizing all inter-grain distances.

Functions $LS_1(\mathbf{x})$ and $LS_2(\mathbf{x})$ are maintained during the RSA procedure on a regular fine grid on the RVE and the random generation position is restricted to points of this grid respecting imposed criteria. Different criteria are illustrated in *Figure 6* and are briefly described here. (*Figure 6.a*) Non-overlapping criterion, only points satisfying $LS_1(\mathbf{x}) > R$ are accessible to the location generation for a grain of radius R

(red area). (*Figure 6.b*) Minimizing neighboring distances, only points which combines smaller values of $LS_1(\mathbf{x})$ and $LS_2(\mathbf{x})$ in addition to pass the non-overlapping criterion are selected. (*Figure 6.c*) Specific value of neighboring distances can be used to reach a given grain density in an homogeneous packing.

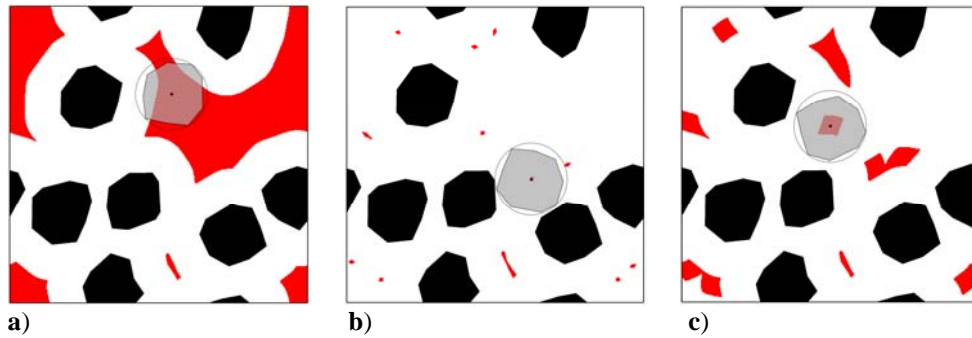**a**)   **b**)   **c**)

Figure 6: Criteria for the random position generation restriction.

The Level Set description of the grain boundaries offers the possibility to modify their shape and size after the generation by directly acting on their Level Set. For example, the (**b**) procedure explained in *Section 2* adds iteratively an increasing constant value to the Level Set of each grain. This causes the inward movement of grain boundaries and the decrease of their volume without topological change of their shapes.

3.3.   Generating clay bridges

Level Set functions of all the grains in the generated distribution can be used to construct a global descriptor of the microstructure. The generation of bridges can be formulated in terms of neighboring distances by placing bridges "where two particles are close to each other". This expression can be quantified and expressed in terms of functions built on sums or products of previously introduced LS_1 and LS_2 functions. Several approaches are available but are not discussed here. The following simple function is used :

$$O(\mathbf{x}) = LS_1(\mathbf{x}).LS_2(\mathbf{x})^{\kappa} - t \tag{2}$$

to extract the interfaces separating macro-voids and clay from $O(\mathbf{x}) = 0$. The exponent κ is the tuning coefficient mentioned in *Section 2* and t is the parameter used to vary to resulting clay volume fraction without changing the bridging morphology in procedure (**a**).

It should be mentioned here that this equation can be also iteratively solved to find t when an imposed resulting volume fraction is required from experimental evidences. We use the direct resolution here by imposing t, which causes the slight variations observed in clay fraction when the same t is used to built clay bridges on different random grain distributions. The measured amplitude of those variations for RVEs used in the results are given for information (see *Section 4.1*).

3.4.   Using XFEM to compute RVE mechanical responses

The automated discretization for finite element computation of RVE for mechanical modeling uses an XFEM setting [10,7]. This allows the use of one single regular mesh for the discretization of many large RVEs sets provided that Level Set functions are available to define grains and voids geometries of each RVEs. Level Set functions given by the generation process are used in the XFEM procedure to construct additional shape functions representing deformation modes related to material discontinuities within heterogeneous finite elements. Those shape functions, called enrichment, are directly derived from the Level Set functions and used to introduce the geometry of grains and voids in the mechanical computation independently of the used mesh (*Figure 7*).
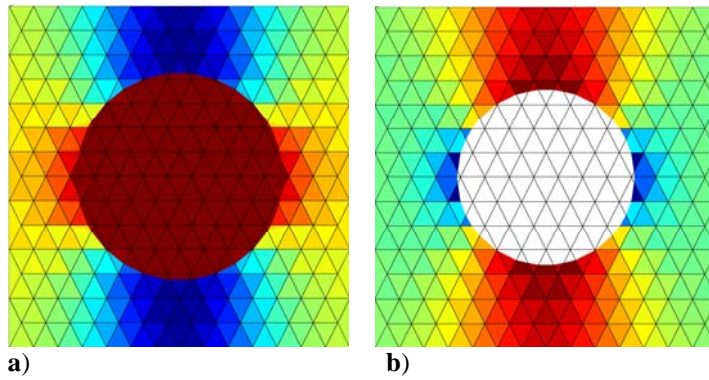
a)   b)

*Figure 7: Vertical strain distribution under vertical compression computed with regular meshes and XFEM. Red stands for low and blue for high compressive strain value. **a**) A stiff inclusion in a soft material. **b**) A void in a soft material.*

The implemented XFEM setting is based on tri-linear elements and the enrichment used is the F^2 enrichment presented in [7]. The multi-enrichment strategy proposed in [11] is used to resolve touching grains situations. Some examples of XFEM computation are given in *Figure 8*.
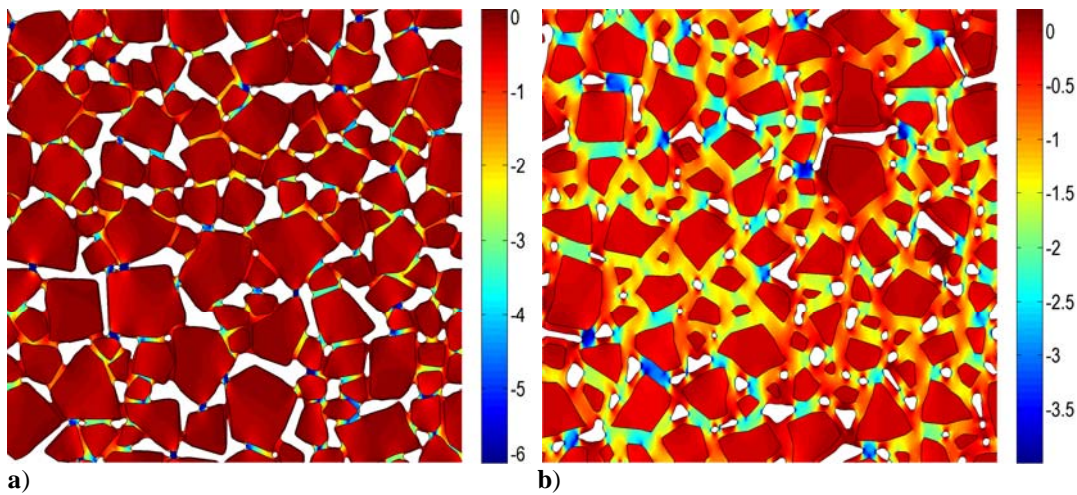

a)   b)

*Figure 8: Vertical strain distribution under vertical compression of RVEs from the procedure (**a**) and (**b**) computed with XFEM. The used clay Young modulus is 20 MPa, see section 4 for other parameters. **a**) Procedure (**a**), step 2. **b**) Procedure (**b**), step 5.*

4.   FROM MICROSTRUCTURAL MODELING TO HOMOGENIZATION

As an illustration of the introduced framework, we proceed now to elastic homogenization of RVEs applying on them an increase of the local clay Young modulus to roughly simulate a lime treatment.

4.1.   Homogenization set up

An *RVE set* is a set of RVEs produced from the same sand grain distribution with different sand/clay ratio, produced by the (**a**) or (**b**) procedure. Each RVE of a *set* is subsequently homogenized for different increasing Young moduli for the lime-clay matrix. Finally several *sets* are generated by both procedures to be aware of the dispersion linked with the randomness of RVEs and to be able to evaluate averaged quantities. We suppose here an homogenous soil so that each *RVE set* is generated with the same governing parameters, the randomness originates only from the initial sand grain distribution. One could be interested in including a natural variability of macroscopic soil descriptors trough RVEs generations. It is not done here even if slight variations of volume fraction are observed through RVEs at a same level of procedure (**a**) or (**b**). Theses variations are linked with a detail of the generation method and can be avoided as explained in *Section 3.3*.

Homogenization of deformation moduli is performed by modeling uni-axial compressions on RVEs in oedometric conditions and within the elastic domain of materials. Such homogenized moduli are thus not Young moduli. They should be seen as compressibility (oedometric) moduli, having only a physical

meaning for episodes of slow uniform loadings of large areas on highly surconsolidated soils. We consider that voids are water saturated and we model the result of stabilized deformations under effective stresses after drained compressions by ignoring water pressure contributions in computations. A 2D plane strain assumption is used. These simple conditions are chosen for the simplicity of the mechanical model required. Enlarging the domain of solicitations (e.g. by loading until plasticity and failure) brings specific difficulties that cannot be aborted here.

30 *RVE sets* of type (**a**) are generated with a sand grain volume fraction of 0.7±0.01 and with a clay volume fraction increasing from 0.106±0.008 to 0.256±0.01. This correspond respectively to macro-void volume fractions from 0.194±0.012 to 0.044±0.008 and average sand/clay repartition from 86.8 / 13.2 % to 73.2 / 26.8 %.

25 *RVE sets* of type (**b**) are generated with a macro void volume fraction of 0.089±0.01 and with clay volume fractions increasing from 0.189±0.01 to 0.499±0.02. This correspond respectively to sand grain volume fractions from 0.722±0.01 to 0.412±0.02 and average sand/clay repartition from 79.2 / 20.8 % to 45.2 / 54.8 %.

Each RVE is homogenized with increasing value of clay's Young modulus from 0.1 to 40 MPa to represent locally the lime treatment effect. The clay's Poisson ratio is fixed to 0.3 and the sand grains use quartz crystal values, 100 GPa for Young modulus an 0.1 for Poisson ratio.

The two following table summarize the *RVE sets* composition :

*Table 1: Average volume fraction of RVEs from procedure (**a**)*

	Clay	**Macro-voids**	**Sand**	**Sand/Clay**
Step 1 :	0.106	0.194	0.700	86.8 / 13.2 %
Step 2 :	0.142	0.158	0.700	73.2 / 16.8 %
Step 3 :	0.169	0.131	0.700	80.5 / 19.5 %
Step 4 :	0.210	0.090	0.700	76.9 / 23.1 %
Step 5 :	0.256	0.044	0.700	73.2 / 26.8 %

*Table 2: Average constitution of RVEs from procedure (**b**)*

	Clay	**Macro-voids**	**Sand**	**Sand/Clay**
Step 1 :	0.189	0.089	0.722	79.2 / 20.8 %
Step 2 :	0.283	0.089	0.689	68.9 / 31.1 %
Step 3 :	0.370	0.089	0.541	59.4 / 40.6 %
Step 4 :	0.437	0.089	0.474	52.1 / 47.9 %
Step 5 :	0.499	0.089	0.412	45.2 / 54.8 %

4.2.   Results presentation

Homogenized moduli are plotted here versus the clay (**I**) Young modulus (figures on the left) or (**II**) volume fraction (figures on the right). Graphs (**I**) illustrate the effect of our idealized treatment. The different blue curves are constructed by averaging and linearly interpolating the results obtained from all the RVEs having the same clay volume fraction and homogenized with the same clay modulus. The transition from dark to light denotes the increase of the clay volume fraction. Graphs (**II**) invert the role of clay Young modulus and volume fraction, the transition from dark to light for the reds curves denotes then an increase of the clay Young modulus. The value of the clay Young modulus of each red curve of a (**II**) graph can be read in the corresponding (**I**) graph and conversely.

4.2.1.   Case (a)

These first computations exhibit clearly a linear dependency of the homogenized modulus with the clay volume fraction (*Figure 9.II*). The studied volume fraction range is to sharp to conclude, but this means that in this domain of behavior, increasing the clay volume fraction by expanding an existing clay fraction does not modify the microstructural system but simply linearly increases its stiffness. The same results plotted in terms of relative increase of homogenized modulus degenerate in a single curve due to this linear behavior and this is not plotted here.
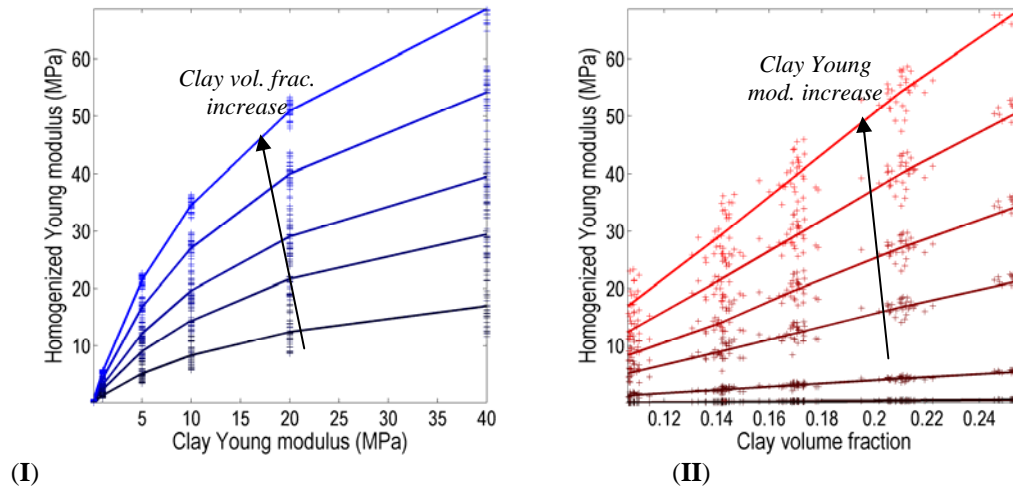
*Figure 9: Results of case (**a**) in terms of homogenized moduli.*

4.2.2. Case (b)

Computations of RVEs of case (**b**) reveal a different behavior (*Figure 10*). First here, the homogenized modulus decreases for an increase of the clay volume fraction because the added clay replaces a volume of grain which is the stiffer material. This relation is however not strictly linear anymore, note that the studied range of clay volume fraction more significant in this case.
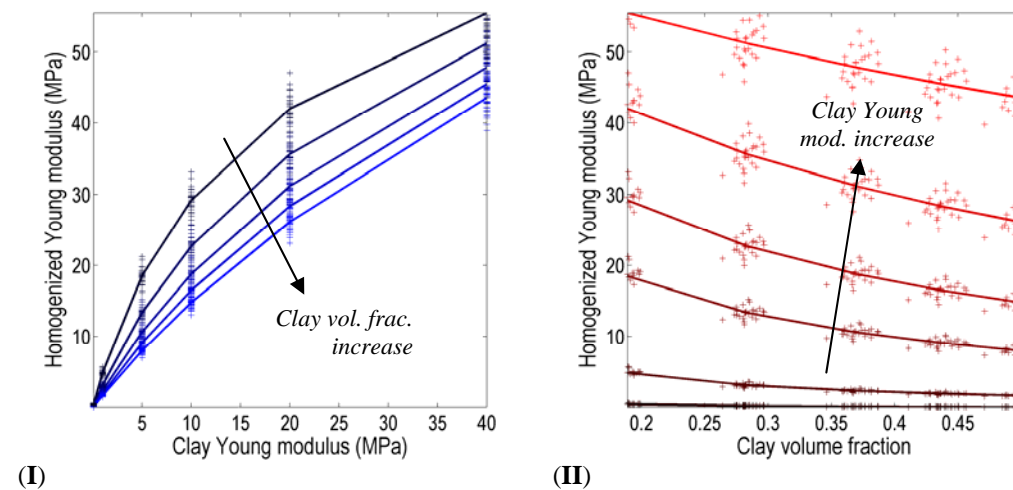
*Figure 10: Results of case (**b**) in terms of homogenized moduli.*

These results are clearly in agreement with intuition. Actually, trends of set (**a**) reflect probably more the increase of solid fraction that anything else while those of the set (**b**) reflect the decrease of the grain fraction, the main stiffness source. But this time, homogenized modulus relative increase shows a dependence to the morphology (*Figure 11.I*). The rate of increase of homogenized moduli is lower for low clay contents than for higher contents, there is a modification of the microstructural system. The increase of the inter-grain distances (see *Figure 4*) correlated to the clay volume fraction increase in the (**b**) procedure is a good potential explanation of this.

(**I**)   (**II**)

*Figure 11: Results of case (**b**) in terms of homogenized modulus relative increases.*
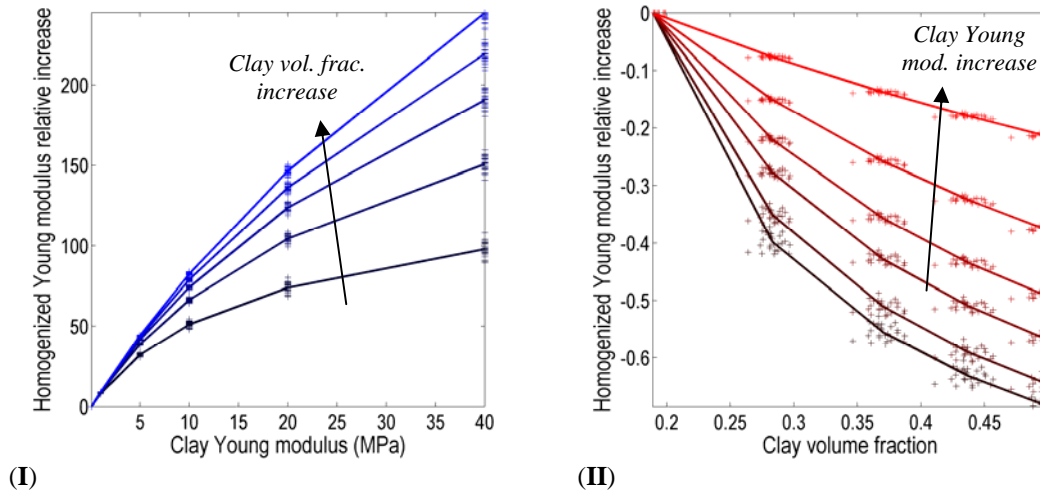
The variability on homogenized quantities related to RVEs size is well appreciated thanks to the large number of homogenized RVEs. This variability is substantial but does not interfere for trends extraction and should not be an inconvenient for engineering usage of this kind of results.

5.   DISCUSSION

A methodology to apply homogenization technique for simple mechanical loading on soils is presented. The influence of a lime treatment modifying the clay properties in a specific soil can be studied by providing this information at the microstructural scale. The microstructural description is fine enough to distinct inert and active phases and large enough to be averagely representative of an macroscopically homogeneous soil. A simple morphological parameter is studied, the ratio sand/clay of a clayey sand and the results seem to agree with intuitions.

However, this 2D study cannot be properly compared to experimental results. First, because 2D volume fractions used in this study cannot be linked with experimental sample measured 3D composition. Furthermore, neither the (**a**) nor (**b**) procedures lead to RVE set compositions which match with sample set compositions usually used in experiments and because those procedures involve other parallel modifications in the microstructures. Using proctor optimum in experiments leads to intermediate but not predictable situations. For a 3D experimentally reliable study, *RVE sets* should be produced to respect exactly the composition of a prepared sample set used for experiments. This require to be able to measure the clay phases micro-porosity to deduce the macro-voids content from the global porosity. This can be performed by mercury absorption or X-ray tomography by measuring the local clay density.

This study is only an example, a lot of geomaterials and constituent evolutions can be analyzed through this framework. More complex mechanical behaviors and loading can be analyzed with plasticity and density dependent constitutive models for clay fractions while damage models should be pertinent for highly cemented phases (i.e. at long curing time of a lime treatment). Any large or localized deformation occurring during loading on such RVEs leads to the inefficiency of the presented framework that should be adapted for such situations. However, this framework can also be used for various problem including heat conduction, electrostatic potential repartition, seepage, ...

From a strict computational point of view, this contribution demonstrates the efficiency of the coupling between LS-XFEM discretization and the LS-RSA generator. This particular efficiency is absolutely required to perform this kind of multi-scale morphological study. The 1650 computations of this study require around 60 hours on 12 CPU but only a light afternoon of human-time for preparation.

REFERENCES

[1] F.G. Bell, Lime stabilization of clay minerals and soils, Engineering Geology, 42 (1996) 223-237

[2] P. Bullock, N. Fedoroff, A. Jongerius, G. Stoops, T. Tursina, U. Babel, Handbook for Soil Thin Section Description, Cambridge University Press, New York (1999)

[3] I.M. Gitman, H. Askes, L.J. Sluys, Representative volume: Existence and size determination, Engineering Fracture Mechanics, 74 (2007) 2518-2534

[4] S.-M Kim, R.K. Abu Al-Rub, Meso-scale computational modeling of the plastic-damage response of cementitious composites, Cement and Concrete Research, 41 (2011) 339-358

[5] G. Legrain, P. Cartraud, I. Perreard, N. Moës, An X-FEM and Level Set computational approach for image-based, International Journal for Numerical Methods in Engineering, 86 (2011) 915-934

[6] T.J. Massart, T. Pardoen, Strain gradient plasticity analysis of the grain-size-dependent strength and ductility of polycrystals with evolving grain boundary confinement, Acta Materialia, 58 (2010) 5768-5781

[7] N. Moës, M. Cloirec, P. Cartraud, J-F. Remacle, A computational approach to handle complex microstructure geometries, Computer Methods in Applied Mechanics and Engineering, 192 (2003) 3163-3177

[8] J.A. Sethian, Level Set Methods and Fast Marching Methods, Cambridge University Press, New York (1999)

[9] B. Sonon, B. François, T.J. Massart, A unified Level Set based methodology for fast generation of complex microstructural multi-phased RVE, Computer Methods in Applied Mechanics and Engineering, submitted

[10] N. Sukumar, D.L. Chopp, N. Moës, T. Belytschko, Modeling holes and inclusions by level sets in the extended finite-element method, Computer Methods in Applied Mechanics and Engineering, 190 (2001) 6183-6200

[11] A.B. Tran, Q-C. He, C. Toulemonde, J. Sanahuja, A multiple level set approach to prevent numerical artefacts in complex microstructures with nearby inclusions within XFEM, International Journal for Numerical Methods in Engineering, 85 (2011) 1436-1459

[12] C. Wellmann, C. Lillie, P. Wriggers, Homogenization of granular material modeled by a three-dimensional Discrete Element Method, Computers and Geotechnics, 35 (2008) 394-405

Laboratory study of the workability of the Deep Soil-Mixing material and in situ applications

Fabien Szymkiewicz, IFSTTAR-LCPC/Université Paris-Est, France, fabien.szymkiewicz@ifsttar.fr
Friede-Stéphanie Tamga, Université Pierre et Marie Curie, France, friedestephanie.tamga@sfr.fr
Alain Le Kouby, IFSTTAR-LCPC/Université Paris-Est, France, alain.lekouby@ifsttar.fr
Philipphe Reiffsteck, IFSTTAR-LCPC/Université Paris-Est, France, philippe.reiffsteck@ifsttar.fr
Jean-Louis Tacita, IFSTTAR-LCPC/Université Paris-Est, France, jean-louis.tacita@ifsttar.fr

ABSTRACT

Originally, the main purpose of deep soil mixing was to enhance the stability and reduce settlements of structures such as embankments on soft soils of low shear strength or very high moisture contents. Nowadays, with development of the Deep Mixing Method, the scope of applications is widening and ranges from cut off walls (built in the heart of a dike or realized to confine pollutions) to temporary and permanent structural elements and retaining walls. Indeed, the execution is easier, with limited excavated material, and cost less than for traditional methods. With these new applications, the required hydraulic and mechanical properties of the Soil-Mixing material have also evolved. However, its workability must also be studied because it is critical for continuity and homogeneity purposes, which are capital properties considering the new applications. This paper presents a laboratory experimental program carried out to determine the evolution of the workability of a Soil-Mixing material with the increase of cement content. The sensitivity to water was studied as well.

1. INTRODUCTION

Nowadays, Deep Mixing is a common method used for soil improvement (CDIT 2002), pollution confinement or as an alternative solution for the realization of structural elements (Rocher-Lacoste and al., 2010).

These new applications require a better understanding of the method and of the material. Therefore, an increasing number of studies on the hardened material are carried out worldwide, to assess the effectiveness of a new binder (Anberg and Johanson, 2005; Jegandan et al., 2010) or to study the influence of the grain size distribution of the treated soils (Szymkiewicz et al., 2010) or the influence of laboratories procedures on the strength of the final material (Ahnberg and Holm, 2009; Kitazume and Nishimura, 2009; Marzano et al., 2009), for example. However, few studies focus on its workability.

Deep Mixing is a method that is implemented without compaction of the material. Therefore, it implies that this material should be self-compacting, meaning that it is fluid enough to flow under its own weight. Water is therefore a critical component. However, as for all cementitious materials, the lower the cement / water ratio (C/E), the lower the strength (Jacobson et al. 2005; Modmoltin et Voottipruex 2008).

This paper presents a new experimental approach to determine the range of workability of the Deep Mixing material, as well as results on cement treated soils ranging from low plastic silts to very plastic clays such as montmorillonite and for cement content (C) ranging for 30 to 800 kg/m^3. Finally, a direct on site application is described, showing the importance to study the workability of the material.

2. EXPERIMENTAL APPROACH

Workability, in the case of the Deep Mixing method, controls homogeneity, and therefore controls the strength, impermeability and durability of the material.

The experimental approach chosen for this study is the geotechnical approach, for two reasons. The first is that for Deep Mixing, the cement content is in most cases inferior to 30 % (roughly 450 kg/m^3) of the dry mass of soil to be treated. Therefore, the material is mostly made of soil. The second reason is that right after the realization of the mix, the cement can be considered as a fine soil. This fine fraction should have an influence on the workability of the mix, as it is well known that the liquid limit of a soil is dependent on its fine content. (Verdeyen et al. 1956; Boussaid et al. 2003) showed that the evolution of the liquid limit is a linear function of the soil clay content The objective was to assess the impact of the cement content on the workability.

In geotechnical engineering, the Atterberg limits (plastic limit w_P and liquid limit w_L) represent the transition between a solid state and a plastic state and between a plastic state and liquid state respectively.

In the case of the Deep Mixing material, the workability limit can be assumed to be almost equal to the liquid limit. Indeed, the liquid limit is defined as the water content at which the material flows at a stress level between 2 and 2.5 kPa. We assume that above this limit, the material is self-compacting. Furthermore, being close to the limit means that the material is still very viscous and dense, meaning that the shearing of the paddles will have an optimal effect on the dispersion of the particles (Larsson 2003). This effect will be less pronounced if the material has a higher water content, and therefore is closer to or over the limit w_F (flocculation limit).

To determine the material workability limit, we chose to use the cone penetration test. It is a reliable, simple and quick test widely used, and therefore transposable in a majority of laboratories.

Figure 1 shows the concept of the cone penetration test, as well as the different states of the soil and the limits corresponding to the transition zones.
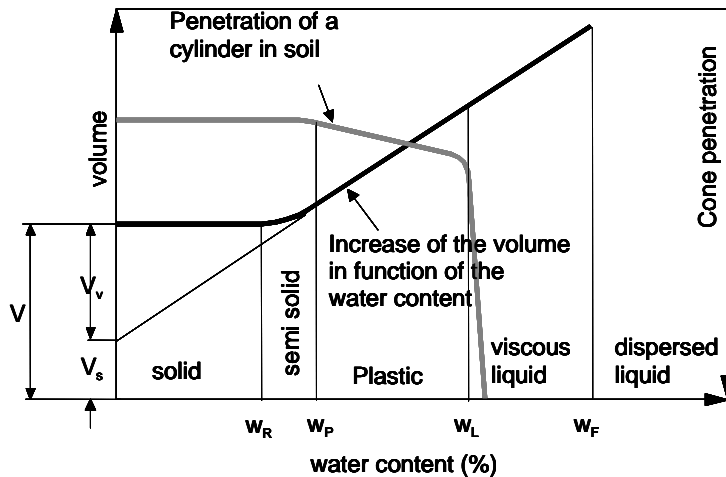

Figure 1: Principle of the cone test penetration and Atterberg limits

3.   MATERIALS AND PROCEDURES

3.1.   Materials

Workability of the Deep Mixing material is a question mainly related to the cohesive soils. Indeed, mixing a non cohesive soil such as sand is easier than mixing silt, for example. Cohesive soils are the most susceptible to present inclusions of non treated soils after treatment. Therefore, we chose to test five soils ranging from low plastic silts to a very highly plastic clay (a montmorillonite), to assess the influence of the cement content on different type of soils.

The cement used for this experimental program is a Portland blastfurnace cement containing 85 % ground granulated blast furnace slag, with the rest Portland clinker and a little gypsum (European classification: CEM III/C 32,5 N CE PM-ES NF"HRC") (CEN 2005).

Figure 2 represents the grain size distributions of the natural clayey soils and of the sand, and Table 1 shows the geotechnical characteristics of these soils and of the different mixed soils.
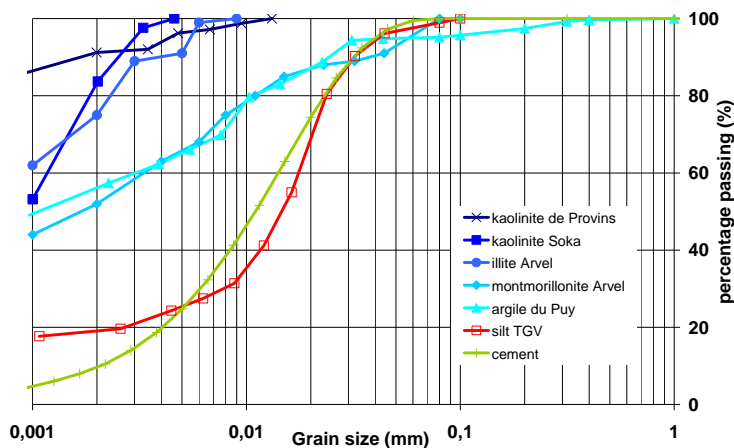

Figure 2: Grain size distribution of the different soils

Table 1: Liquid limit and VBS (methylen blue value) (AFNOR 98) of the different soils

Soil	w_L (%)	VBS
silt TGV	30	2.3
illite du Puy	49	5.4
montmorillonite Arvel	112	28
kaolinite de Provins	77	6.67
illite Arvel	56	5.9

3.2.   Procedures

3.2.1.   Soils preparation and mixing

Before any realization of mixes, the soils are prepared, meaning that they are dried and reduced in powder. The soil is then manually mixed with the cement in a dry state, again until achievement of a visual homogeneity. Water is finally added in such quantity as to reach the target water content of the mix. Again, the mixing is done manually.

Each sample of soil is prepared individually, meaning that for a serie of tests on a given soil at a given cement content, four or five samples are prepared.

3.2.2.   Testing

Once the mixing is complete, the testing part can begin. We have always followed the French Standard NF P94-052-1 (AFNOR, 1995) concerning the determination of the atterberg limits, with only two differences. To ensure that our sample is always five minutes old, once a measure has been realized, the complete sample is discarded, instead of being allowed to dry to enable us the have the four points linking penetration to water content. This is due to the fact that we work on cementious materials, and that with time hydration could occur. The second difference lies in the fact that, again due to the nature of the material, we could not afford to perform a traditional water content test on the samples without initiating a possible hydration of the cement. Thus, the water content is instead determined from calculations based on the total mass of water (known) added to the masses of soil and cement (also known).

3.2.3.   Expression of results

Figure 3 shows an example of the raw data resulting from the realization of the cone penetration test on the different soils used for this study.
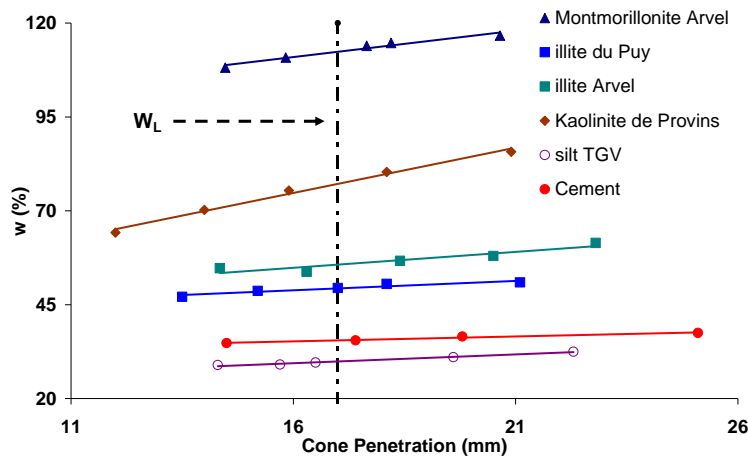
Figure 3: Relationship w – Penetration for all non treated soils

From this figure, it is possible to determine the liquid limit w_L. We can also note that the slopes of the lines, a coefficient that we will call subsequently *a*, vary with the different soil types.

These slopes can be defined as the inverse of the sensitivity of the material to water around the liquid limit. The higher is *a*, the lower is the water sensitivity, meaning that the propensity of the material to become more fluid, and thus workable, around the liquid limit with an addition of water is high.

Table 2 shows the values of *a* for the different soils tested.

Table 2: Value of the water sensitivity a for all non treated soils

Soil	*a*
montmorillonite Arvel	1,40
kaolinite de Provins	2,41
illite Arvel	0,85
argile du Puy	0,50
limon TGV	0,47
cement	0,26

The cement and the kaolinite de Provins shows the highest and lowest water sensitivity respectively, meaning that to achieved a 25 mm penetration with the cone, the water addition will be bigger for this clay than for the cement.

4. RESULTS

4.1. Mixes of natural soils and cement

4.1.1. Influence of the cement content on the liquid limit

The Figures 4 a, b, c, d and e show the relationship between water content and cone penetration for the illite du Puy (a), montmorillonite Arvel (b), illite Arvel (c), kaolinite Provins (d) and silt TGV (e), for different strengths of cement.
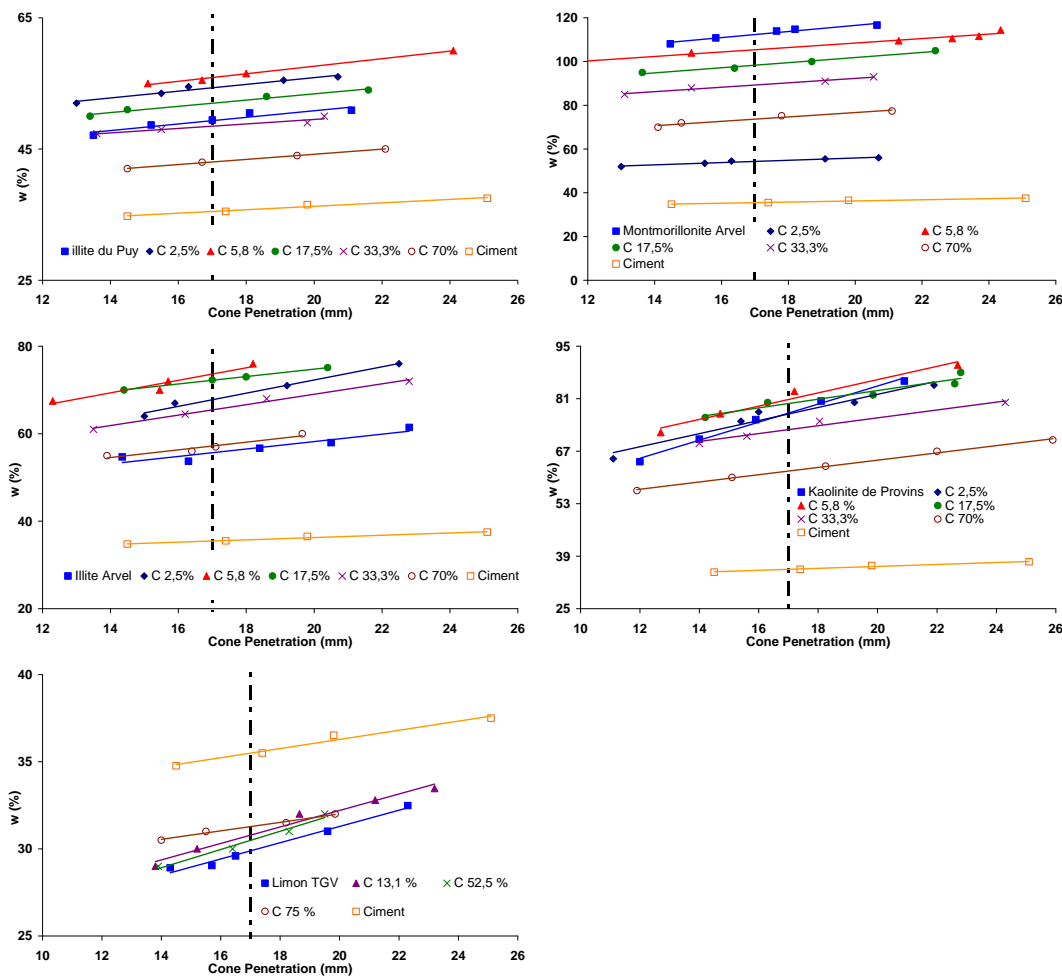

Figure 4 : Evolution of the water content w in functionof the cone penetration for the mixes illite duPuy – cement (a), montmorillonite Arvel – cement (b), illite Arvel – cement (c), kaolinite de Provins –cement (d), and silt TGV (e)

The evolution of the liquid limit as a function of the cement content is represented in Figure 5, for all the soils tested. This evolution differs, depending on the soil. The liquid limit doesn't vary or decreases gradually when the cement content increases, for the silt TGV and montmorillonite Arvel respectively. On the other hand, for the illites and kaolinites, we observe a different evolution. The liquid limit increases until the cement content reach 5.8 %, then decreases steadily and somewhat linearly. This increase is different for each soil, however. w_L increases only by 3.6 points for the kaolinite de Provins, whereas it increases by 18 points for the illite Arvel, meaning an increase of 32 % of the liquid limit. This is a result to take into account, for on site applications, as we will see later.
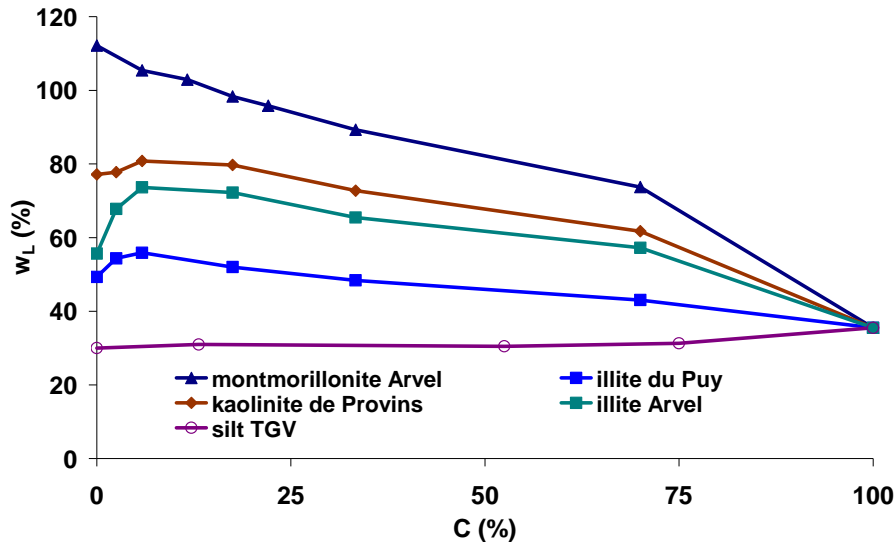

Figure 5: Evolution of the liquid limit in function of the cement content for all soils

These results are contrary to our hypothesis that the fresh cement (5 minutes after hydration in this case) acts only as a fine soil. If such was the case, the relation would be purely linear, and calculable, knowing the liquid limit of the two constituents. On the other hand, (Brandl 1981; Locat et al. 1996; Chew et al. 2004) obtained the same results at a much older age (at least equal to 7 days). Our results show that the liquid limit of the material at time t_0 is already affected by the cement, and that in the same way that after 7 days or more of curing.

However, some results are surprising: the silt, a low plastic soil, should present an increase in w_L at a low cement content, but this is not the case. In addition for the illites and kaolinite, after the peak, the relationship between the liquid limit and cement content appears to be linearly decreasing, until it reaches the cement w_L (36%). Therefore, the liquid limit of the material Soil-Mixing drops below the liquid limit of the non treated soil between a dosage of 33% for the clay du Puy, and a dosage greater than 70% for the illite Arvel. These results differ from those in the literature by the fact that for other authors the liquid limit seems to stabilize for cement contents greater than 10% (albeit for curing time equal or greater than 7 days).

We can conclude that for highly plastic soils plastics (VBS between 5 and 8), the addition of cement to the soil is detrimental to the workability for the range of dosages commonly accepted.

4.1.2. *Influence of the cement content on the water sensitivity of the mix*

Figure 6 shows the evolution of the water sensitivity of the treated soils in function of the cement content. Overall, *a* decreases as the dosage increases until reaching the value corresponding to the cement. However, for the illites du Puy and Arvel in particular, the coefficient increases to reach a peak between 3 and 6% of cement, as the liquid limit does. This would mean that the soil is made less sensitive to water and possibly less workable for a small addition of cement. In the same manner as the workability limit, this observation does not make sense if we consider the cement as a simple fine fraction: the trend should be linear and decreasing. However the overall trend is downward, which makes more sense.
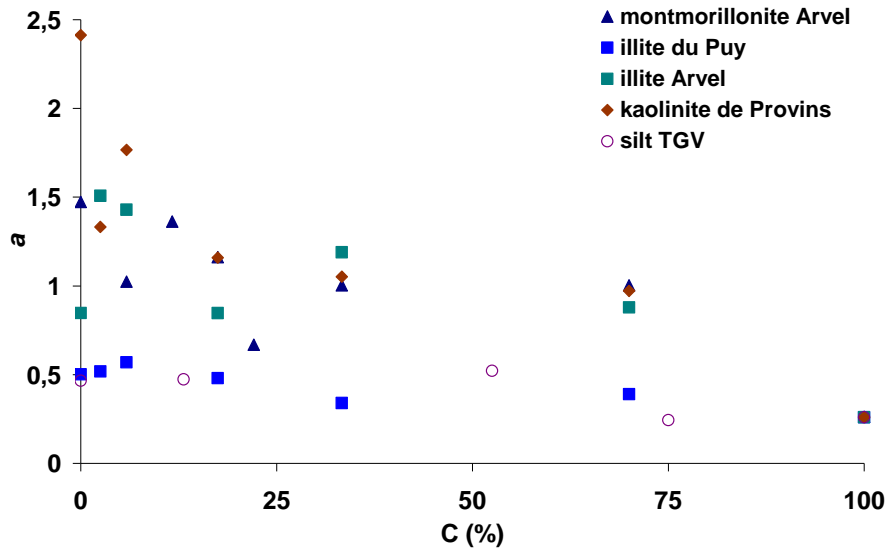
Figure 6: Evolution of the water sensitivity in function of the cement content for all soils

4.2.   On site applications

It is reported in the literature that it is necessary, for Deep Mixing, to work at a water content at least higher than that of the soil in place (Bergado and al. 2005). In this part we will compare, for different soils, the evolution of the highest achievable C / W depending on the cement content calculated following the literature recommendations on the one hand and calculated according to our observations on the other hand, in order to show a possible difference in the upper limit of the range of workability of the material. This is shown in Figures 7, 8 and 9 for the silt TGV, illite Arvel and montmorillonite Arvel. The highest achievable C / W is the maximum achievable C / W obtained for a minimum water content, which in the case of Deep Mixing is equal to the liquid limit of the material.

For some materials like the low plastic silt, the difference is null between the two calculation methods, since the liquid limit of the material does not seem to depend on the cement content (Figure 7).
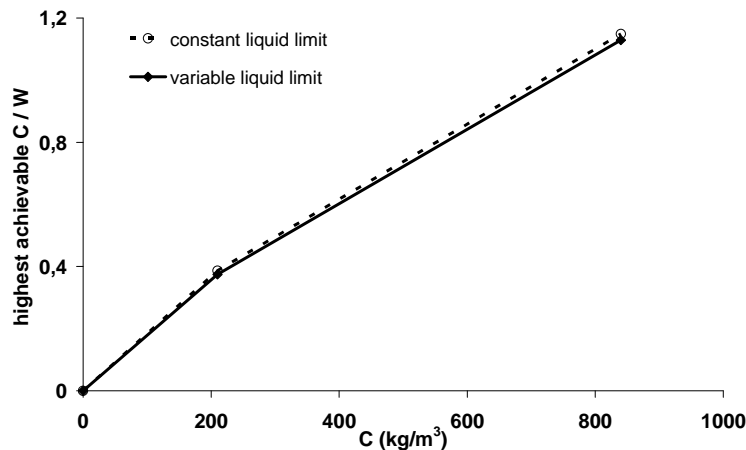
Figure 7: Maximum achievable C / W – C relationship, depending on the liquid limit determination method, for the silt TGV

For plastic and very plastic soils (VBS between 5 and 8), we saw that the liquid limit increases to reach a peak around 70 kg of cement per cubic meter. There is a wide variation of the maximum achievable C / W depending on whether one uses as liquid limit the soil w_L or that of the Soil-Mixing material w_L. The maximum achievable C / W is always smaller when the material liquid limit is taken into account. As a result, the range of workability is smaller (Figure 8).

Figure 8: Maximum achievable C / W – C relationship, depending on the liquid limit determination method, for the illite Arvel

On the contrary, for very highly plastic clays like montmorillonite and bentonite, the range of workability is greater if one takes into account the liquid limit of the material, since the minimum amount of water to be added to ensure the self-compacting quality of the material decreases.

For example, for the illite Arvel, the operator will have to inject an additional 230 litres of water, for a target cement content of 210 kg/m^3 if considering the liquid limit of the material instead of that of the non treated soil for a truly self-compacting material. This value is not negligible and it is therefore necessary to change the on site instructions to ensure the self-compacting and therefore the continuity of the material (Figure 9).
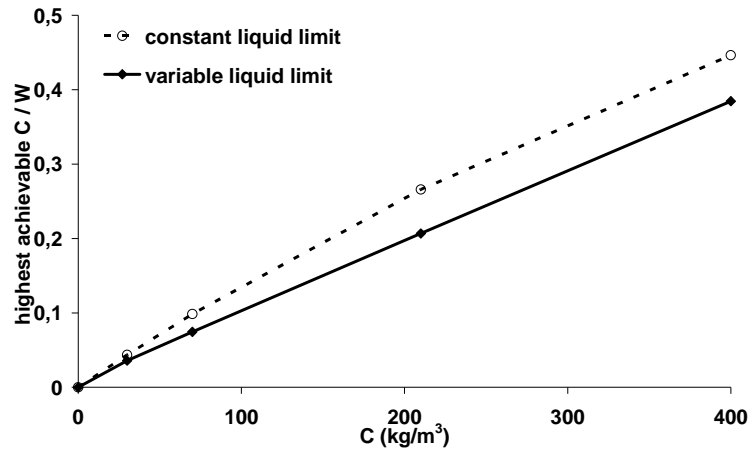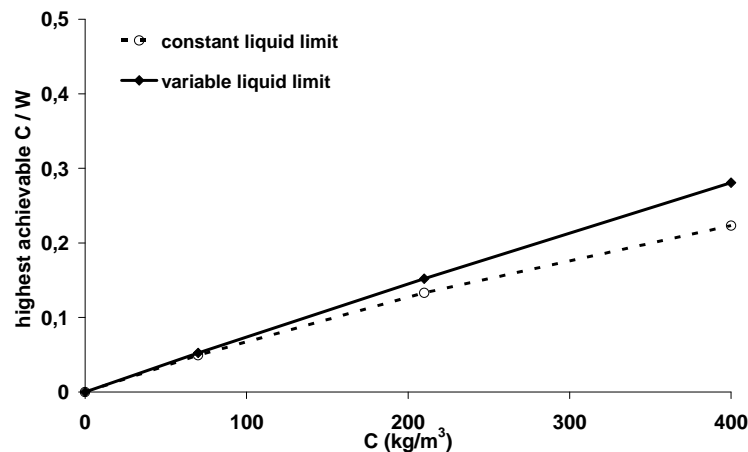

Figure 9: Maximum achievable C / W – C relationship, depending on the liquid limit determination method, for the montmorillonite Arvel

5. CONCLUSIONS

This paper presents the results of a study aiming to define the range of workability of the Soil-Mixing material with the limit of workability of the material that we associate with the liquid limit. Indeed, being over the liquid limit ensure the self-compacting quality of the material in a fresh state.

We have shown that changes in the workability of the material Soil-Mixing is not linear with the amount of cement added. This differs from results obtained on non-cementitious mixtures consisting of sand and clay, and questions our assumption of assimilating the cement to a fine soil at a very young age. The results obtained are comparable to those obtained by different authors for much higher hydration time (7 or more days).

The results show the existence of a range of cement content for which the workability limit of the treated soil is superior to that of the non treated material: the greatest difference is noticed for a cement content of about 6 %, and the workability limit of the material may in some cases not return to below the liquid limit of the non treated soil before being treated with a cement content at least equal to 50 % of cement. For these soils, the maximum achievable C / W at low cement content is smaller than the maximum

achievable C / W calculated from the soil liquid limit. This is an essential result that implies that to review the on site instructions, since it is in this range of cement content that contractors work. This difference varies widely (and may even be negative as in the case of montmorillonite). A maximum percentage increase of 32% was obtained on an illite.

The range of workability of the materials will therefore evolve according to the amount of cement added and the type of soil encountered.

The water sensitivity of the Soil-Mixing material shows a tendency to increase with the dosage in cement. This is an important parameter that must be taken into account on site: although it is acknowledged that it is important to provide instruction to reach at least the material liquid limit, it is better to stand a little above, for safety reasons (on site, the heterogeneity of soil parameters is a problem) and to facilitate the implementation of the work. But we have demonstrated that the water sensitivity of a soil can vary greatly: its knowledge will allow for a higher C / W or to not overdose cement mixture (depending on the Soil-Mixing method used). Indeed, the sensitivity varies from 1 to 5: the same amount of water added in two different soils will allow to move away more or less rapidly from the transition zone plastic state - liquid state.

Determination of Atterberg limits of soil, advocated by the standard NF EN 14679 (AFNOR, 2005), is therefore not sufficient. Determining the liquid limit of the treated soil is essential to be able to give instructions to achieve a continuous and homogeneous material.

An interesting perspective to this study will be to study more precisely, for cement-soil mixes, the influence of the mineralogy and quantity of fine on the evolution of the liquid limit. By mixing sand and clay with various cement content, it will be possible to assess the influence of the clay and determine if the Soil-Mixing material in a fresh state still presents the behaviour of a soil.

REFERENCES

AFNOR (1995). Détermination des limites d'Atterberg - Partie 1 : limite de liquidité - Méthode du cône de pénétration. NF P94-052-1. AFNOR.

AFNOR (1998). Mesure de la capacité d'adsorption de bleu de méthylène d'un sol ou matériau rocheux. Détermination de la valeur de bleu méthylène d'un sol ou d'un matériau rocheux par l'essai à la tache. NF P 94-068. AFNOR.

AFNOR (2005). Exécution de travaux géotechniques spéciaux - Colonnes de sol traité. NF EN 14679. AFNOR.

Ahnberg, H. and G. Holm (2009). Influence of laboratoriy procedures on properties of stabilised soil specimens. Deep Mixing '09, Okinawa.

Ahnberg, H. and S.-E. Johanson (2005). Increase in strength with time in soils stabilised with different types of binder in relation to the type and amount of reaction products. Deep Mixing '05, Stockholm, 195-202.

Bergado, D. T., G. A. Lorenzo, C. Taechakumthorn and A. S. Balasubramiam (2005). Compression Behavior of High Water Content Cement-Admixed Clay. Deep Mixing '05,Stockholm, 221-230.

Boussaid, K., V. Ferber, J. Garnier and L. Thorel (2003). Intermediate soils for physical modelling, International Symposium on Geotechnical Measurements, Karlsruhe, 335-340.

Brandl, H. (1981). Alteration of soil parameters by stabilization with lime. 10th International Conference on Soil Mechanics and Foundation Engineering, Stockholm, 587-594.

CEN (2005). Cement - Part 1: Composition, specifications and conformity criteria for common cements. EN 197-1. CEN.

CDIT (2002). The Deep Mixing Method - Principle, Design and Construction, 121 pages

Chew, S. H., A. H. M. Kamruzzaman and F. H. Lee (2004). "Physicochemical and Engineering Behavior of Cement Treated Clays " Journal of Geotechnical and Geoenvironmental Engineering: 696-706.

Jacobson, J. R., G. M. Filz and J. K. Mitchell (2005). Factors Affecting Strength of Lime- Cement Columns Based on a Laboratory Study of Three Organic Soils. Deep Mixing '05, Stockholm, 87-94.

Jegandan, S., M. Liska, A. A.-M. Osman and A. Al-Tabbaa (2010). "Sustainable binders for soil stabilisation". ICE Journal of Ground Improvement 163(1), 53-61.

Kitazume, M. and S. Nishimura (2009). Influence of specimen preparation and curing conditions on unconfined compression behaviour of cement-treated clay. Deep Mixing '09, Okinawa.

Larsson, S. (2003). Mixing processes for ground improvement by deep Mixing, Swedish Deep Stabilization Research Center. 12.

Locat, J., H. Tremblay and S. Leroueil (1996). "Mechanical and hydraulic behaviour of a soft inorganic clay treated with lime." Canadian Geotechnical Journal(33): 654-669.

Marzano, I. P., A. Al-Tabbaa and M. Grisolia (2009). Influence of sample préparation on the strength of cement-stabilised clays. Deep Mixing '09, Okinawa.

Modmoltin, C. and P. Voottipruex (2008). "Influence of salts on strength of cement-treated clays." Ground Improvement 162(G11): 15-26.

Rocher-Lacoste, F., A. Le Kouby, F. Szymkiewicz, S. Lechevallier and B. Fraysse (2010). "The soil-cement column, an alternative foundation and soil improvement method : static load tests", 11th International Conference: Geotechnical Challenges (ICGC) in Urban Regeneration, DFI 2010, London

Szymkiewicz, F., A. Le Kouby, P. Reiffsteck and S. Fanelli (2010). "Influence de la granulométrie sur la résistance à la compression d'un sol-ciment : comparaisons entre deux sols", AUGC 2010, La Bourboule

Verdeyen, J. and V. Roisin (1956). Stabilité des terres, sols routiers, soutènements, talus, Editions Eyrolles.

Some laboratory soil mixing trials of Irish peats

Timoney M., NUI, Galway, Ireland, martin.timoney@nuigalway.ie
Quigley P., Arup, Ireland, paul.quigley@arup.com
McCabe B.A., NUI, Galway, Ireland, bryan.mccabe@nuigalway

ABSTRACT

Highly organic soils such as peat can prove problematic due to their high water content and compressibility when encountered in construction projects. Peat is widespread in Ireland, covering about 17.2% of the country. Many secondary roads in Ireland have been constructed on peat, especially in western Ireland. Road widening and improvement schemes are complicated by extensive settlement and stability issues. Dry Soil Mixing (DSM) is envisaged as a potential method of enabling road widening without adversely affecting the adjacent road.

DSM involves the injection of dry cementitious and pozzolanic binders in to the soil which then react with the pore water of the soil resulting in improved strength and stiffness characteristics. The stabilisation of organic soils is more challenging than that of inorganic soils, as humic acids hinder the hydration processes and the reactions required for the development of strength, creating insoluble products that coat the soil particles, preventing them from binding properly.

This paper presents new laboratory test data from a series of stabilisation trials carried out on Irish peats, using different binders, including cement, rapid hardening cement and ground granulated blast furnace slag. The results show that ratio of water to the total binder content is a key determinant of stabilised strength.

An investigation of the Embodied Energy required in three hypothetical projects shows the production of the binders required in the stabilisation to be the significant contributor and not transportation of the binder to the site. The release of gases from the peat during DSM could be a significant contributor to emissions.

1. INTRODUCTION

Soil stabilisation is a method of improving the characteristics of a soil through the addition of cementitious and/or pozzolanic binders. Outcomes include increased strength, better deformation characteristics and confinement/remediation of contaminated ground. The stabilisation of organic soils is more difficult than that of inorganic soils, requiring greater binder contents to achieve the required strength as organics in the soil react with the binders creating insoluble products that coat the soil particles delaying and inhibiting the strengthening reactions.

Dry Soil Mixing (DSM) involves the injection of dry binders, such as cement, lime, ground granulated blast furnace slag (GGBS), *etc.,* into the soil. Two mixing methods exist: Deep Dry Soil Mixing, where the soil is stabilised in columns; and Mass Stabilisation, where the soil is stabilised in blocks up to 5m deep. The added binder then reacts with the pore water, initiating the strengthening reactions. DSM provides an alternative method of ground improvement to conventional *excavate and replace* methods used where peat is encountered.

Timoney et al. (2012) provide a detailed review of the stabilisation of organic soils including the various parameters which affect the stabilised strength, including binder type, curing temperature and prestress, as well as detailing the reaction characteristics of different binders. The authors compiled a large database of dry soil mixing stabilisation results from European and Japanese published data, investigating relationships between the strengths achieved and the initial moisture content, binder content, curing time and water to binder ratio. The focus of this paper is on Irish peats; new data is presented and interpreted in the context of existing data and the embodied energy associated with DSM in Irish peats is discussed.

2. PEAT

Peat is a highly organic soil type formed from decaying of plants and vegetation rich in carbohydrates to humus, a process known as humification. Peats can be classified into three simple categories in terms of their degree of humification (Hártlen, 1996):

(a)   *Fibrous* peat which has a low degree of humification. This form will have a distinct plant structure and will produce a brown to colourless cloudy to clear water when squeezed.
(b)   *Pseudo-fibrou*s peat has a mid to high degree of humification. The plant structure is now less identifiable and a mushy mass will be extruded when squeezed.
(c)   *Amorphous* is the classification used for the most highly humified peat. Very little, if any, of the plant structure remains and on squeezing no free water is released.

Von Post (1922) provides a very detailed system for classifying peats, taking into account degree of humification, moisture content, type of plants and fibres. This was later extended by Hobbs (1986) to include organic content, smell, plasticity, pH and tensile resistance. One of the main classifications in the system is von Posts degree of humification, H classification. H is a scale ranging from 1 (least humified) to 10 (most humified) representing the state of decay and Hártlen's (1996) categories fall as follows: *fibrous* peats lie in the range H1-H4, *pseudo-fibrous* in the range H5-H7 and *amorphous* between H8 and H10.

2.1.   Moisture Content, Strength and Compressibility

Peats, due to manner in which they are formed (discussed later) have very high organic content, typically between 80 and 99%, and very high moisture contents ranging up to many hundreds and even thousands of percent. Typically moisture contents are seen to reduce with an increasing degree of humification due to the manner in which water is stored in each degree of humified peat. Fresh peats have high void ratios and water is stored freely in these voids but with increasing degrees of humification the voids reduce and a lesser amount of water is held by capillary action and eventually by physical, chemical and osmotic processes bound to the peat particles. Due to these very high moisture contents the bulk density is typically found to be close to that of water due to the low specific gravity of the organic constituents making up the peat and in partially saturated peats can be below that of water.

From the authors' experience of current literature on dry soil mixing laboratory and field trials in peat, unconfined compression strengths for peat are seldom reported due to the difficulties in sampling and testing. Peat soils have very low strengths, with unconfined compression strengths typically less than 15kPa. Fibrous peats have higher strengths than amorphous peats as the fibres act to reinforce the peat in the vertical direction but their spongy nature, high void ratio and lack of soil structure results in high compressibility and large deformations when stressed. Further details on the strength of Irish peats can be found in Long (2005).

2.2.   Irish Peat Bogs

In Europe many countries have significant areas of peat deposits; 10m hectares of Finland, 1.5m hectares of Sweden and 3m hectares of Norway are covered in peat. In Ireland peat covers 17.2% of Ireland's landmass, giving a total of nearly 1.2m hectares (Hobbs, 1986). These peats are found in three main forms: raised bogs, blanket bogs and fen peats. Figure 1 shows the coverage of raised and blanket bogs across Ireland.
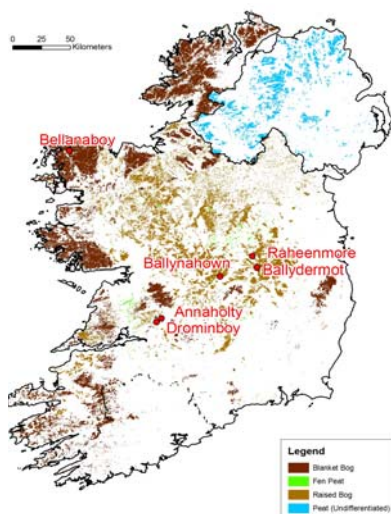

Figure 1: Irish Peatlands Map (courtesy of Geological Survey of Ireland and Geological Survey of Northern Ireland).

2.2.1　Raised Bogs

Raised bogs, normally found in Ireland's midlands, have thicknesses typically between 9 and 12m and make up 0.31m hectares of Irelands peat (Bord na Móna, 2011). They initially began as lakes or hollows, as shown in Figure 2 which were fed by nutrient rich inflows. These nutrients allow plants and vegetation to grow particularly around the edges which results in lake filling and as the bog grows, flow through it becomes impeded resulting in paludification or swamping of the area. As plants and vegetation die off peat is formed and the level of the bog rises above the water table resulting in reliance by the vegetation on precipitation for its nutrient supply. Once the hollow has reached a level surface further growth occurs in an upward dome shape (Hammond, 1981).
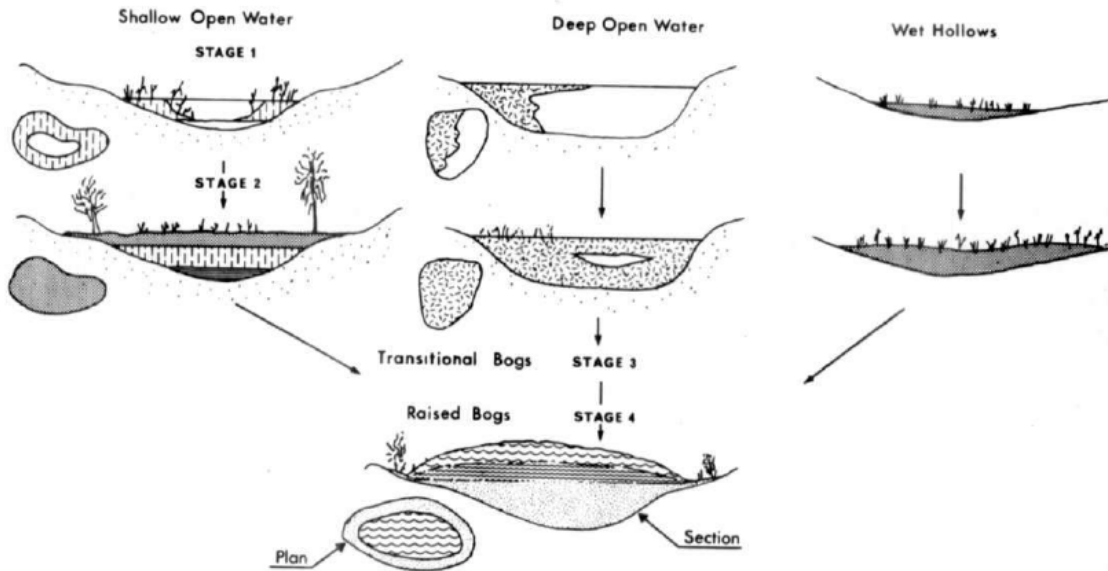

Figure 2: Raised Bog formation stages (Hammond 1981)

2.2.2　Blanket Bogs

Blanket bogs are the main type of bog found in Ireland, particularly in the west of Ireland and in mountainous regions. They are up to 4,000 years old and typically form shallow coverings with depths ranging from 1 to 6m (average of around 2.6m); higher altitude blanket bogs are generally thin with deeper profiles located in depressions and over flat areas (Hobbs, 1986).

The formation of blanket bogs is climate controlled, *i.e.*, cool summers and high precipitation levels on slopes (<20°) where drainage is impeded. In a similar way to raised bogs they initially begin in shallow hollows through water logging caused by the low nutrient precipitation, as shown in Figure 3. As the hollows fill the bog spreads outwards and connects with nearby formations to form a blanket of peat.
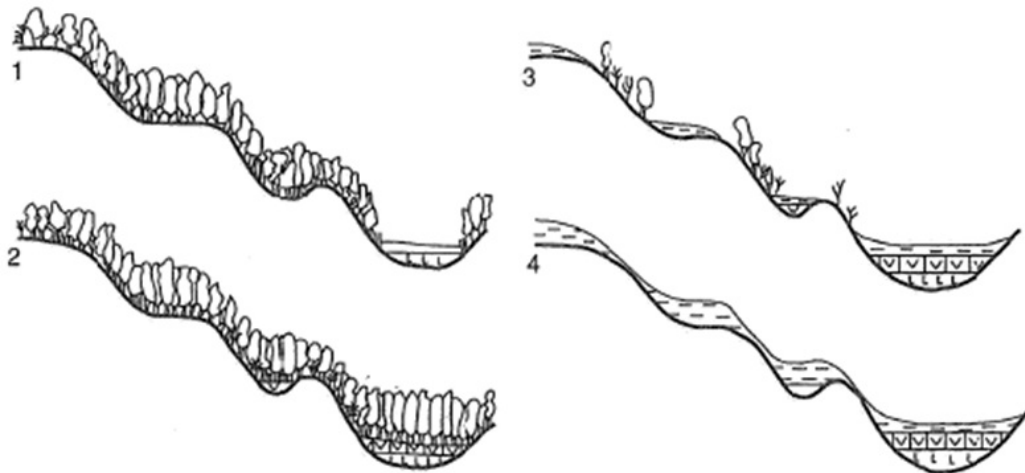

Figure 3: Blanket bog formation (Moore 1987)

2.1.3 Fen Peat

Fen peats derive from the decay of vegetation once fed by groundwater rich in calcium and other nutrients. In Ireland they tend to be shallow with depths of around 2.2m and are mainly found in the midlands at the base of raised bogs. These are Ireland's oldest bogs, with formation beginning about 9,000 years ago but many Irish fens have been drained for cultivation purposes but have only provided poor pasture (Hammond, 1981).

3. IRISH STABILISATION TRIALS

A number of laboratory stabilistion trials have been carried out on Irish peast and are collated in Table 1. This paper compares the results across four categories: strength, stiffness, 1-D compression and creep.

Table 1: Collated Irish peat stabilisation trials

Reference:	Source:	w_i (%)	ρ (kg/m^3)	Organic Content (%)	von Post H	pH	WTBR
Raheenmore	Hebib & Farrell, 2003	1200	1,075	98-99	2	5.3	3.97, 4.96 6.62
Ballydermot	Hebib & Farrell, 2003	850	1,125	94-98	6-9	4.9	4.03, 5.03
Bellanaboy	Quigley & O'Brien, 2010	1019	1,000	98	7-8	4.7	3.64,4.55 6.07
Ballynahown	Timoney *et al*, 2011	800	950	97-98	3	4.8	2.81, 3.38 4.22, 5.63
Annaholty	Ramboll, 2006	991-1664	1,100	88-99	-	5.0	4.06, 5.07 6.77
Druminboy	Ramboll, 2006	861-1580	1,100	88-96	-	5.5	4.05, 5.06 6.74

3.1. Strength

Strength and stiffness measurement were carried out using unconfined compression testing using the methodology in EurosoilStab (2001) and illustrated in Figure 4.
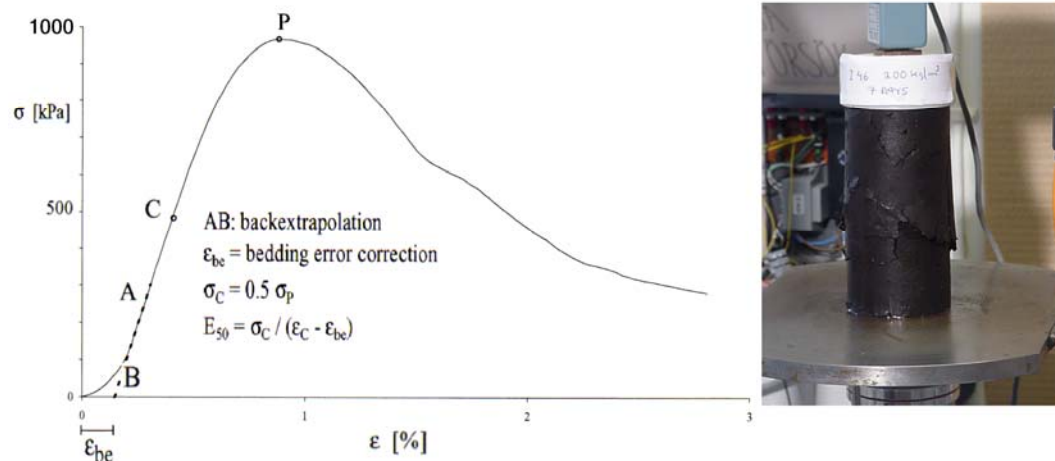
Figure 4: Methodology for determining strength and stiffness (left) with typical specimen (right)

Timoney et al. (2012) used the Water to Binder Ratio (WTBR, η) defined in equation 1 as a means of combining the influence of water content and binder quantity on the stabilised strength. The WTBR relates the mass per unit volume of water (m_w) in the soil to the mass per unit volume of binder (m_b) added in the stabilisation process. The mass of water is a function of the soil's initial water content (w_i) as no additional water is added during in the DSM process.

$$\eta = \frac{m_w}{m_b} = \frac{\rho}{m_b\left(1+\dfrac{1}{w_i}\right)} \tag{1}$$

The η value was calculated using the initial water content (w_i), the density of the peat (ρ) and the mass of binder per unit volume (m_b). The relationship between the 28 day unconfined compression strength (UCS$_{28}$) and *η*, annotated by binder type, is shown Figure 5. Where two binder constituents were used, the proportions are 50:50 unless otherwise stated. The site location is also annotated beside the data point. Figure 5 highlights a general tendency for increased UCS$_{28}$ values at low η values as might be expected, with some high UCS$_{28}$ values achieved for *η* <4.5. Research at NUI Galway has shown that these values of η are lower than would be necessary to achieve comparable strength gains in organic clays.
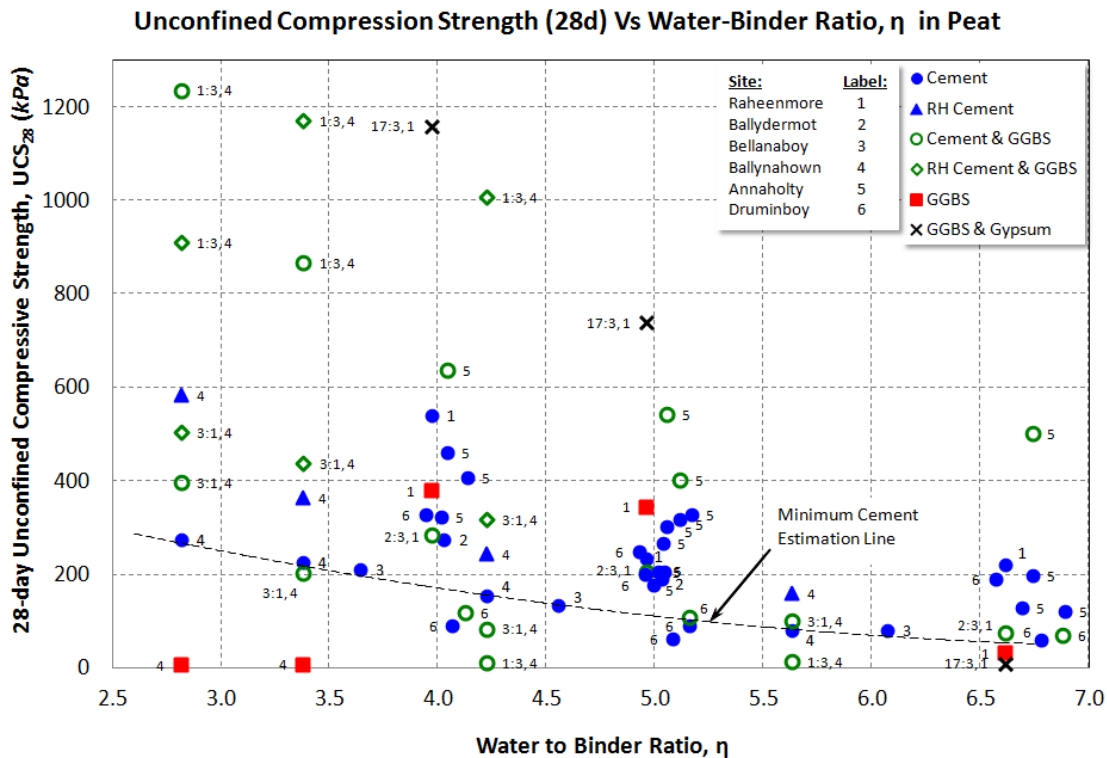

Figure 5: Unconfined Compression Strength (28d) vs Water-Binder Ratio, η in Irish Peats

The trend of reducing UCS$_{28}$ with *η* appears clearest for the cement binders, and an approximate lower bound line is shown in Figure 5 to aid designers estimate the minimum likely strength for a given binder dosage. The Rapid Hardening (RH) cements provide greater stabilised strengths at 7 and 28 days than Ordinary Portland Cement. Mixes with 3:1 cement to GGBS gave results similar to the cements alone. However, the 1:3 cement to GGBS mixes, only performed on the Ballynahown peat, showed very high strengths at binder contents of 250 and 300kg/m³ but poor strengths at 150 and 200kg/m³. These results may indicate the existence of a binder threshold, particular to the peat in question, which must be exceeded before any strength gain will occur. Axelsson et al. (2002) reports the binder threshold to be the content required to neutralise humic acids present in the soil and allow stabilisation to occur, while Hebib and Farrell (2003) detailed 150kg/m³ as the minimum content required for stabilisation in their trials. Quigley and O'Brien (2010) also report that a binder concentration of 150kg/m³ of Ordinary Portland Cement is required to minimise post mixing strains.

GGBS is a latent hydraulic binder and requires activation by calcium hydroxide, provided by the cement in the plotted data or by gypsum in the case of the Raheenmore peat (where very good strength gains are seen with an 85:15 GGBS and gypsum binder). The Ballynahown peat showed that a lack of activation can result in very poor strength gains, but further work is needed to understand why reasonable strengths were seen when GGBS alone was used with the Raheenmore peat.

EuroSoilStab (2001) shows an overall comparison of the results for stabilisation trials in peat across Europe and shows Irish peats to have relatively poor strength gains. The data in Figure 5 suggests high strengths can be achieved when using certain binders and high binder contents (up to 300kg/m³). It should

be noted that these strengths may not be achieved in the field. Parameters such as mixing homogeneity, prestress loading, curing temperature and *insitu* water content at the time of mixing may result in lesser strengths; Hayashi and Nishikawa (1999) detail the factor between field and laboratory results as between 2 and 5, with an average of 3, while experience in Norway by Braaten *et al.*, (1999) showed that field strengths in fact well exceeded strengths achieved in the laboratory.

3.2. Stiffness

The stiffness of stabilised peat (E_{50} – see Figure 1 for definition) was calculated using the methodology outlined in EurosoilStab (2001). Figure 6 shows a pattern of increasing stiffness at 90 days in rough proportion to the cement binder concentration. A review of undrained shear stength at 90 days suggests that a relationship of $E_{50} = 150c_u$ gives a reasonable first estimate of stiffness (Figure 7).

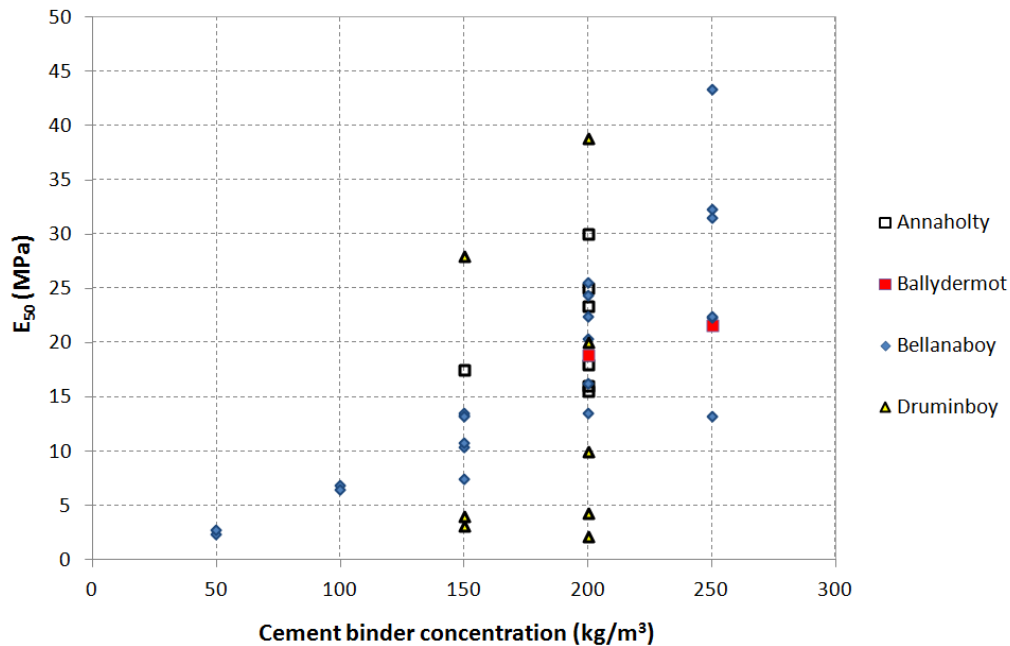

Figure 6: Compariion of stiffness at 90 days for various cement only binder concentrations.
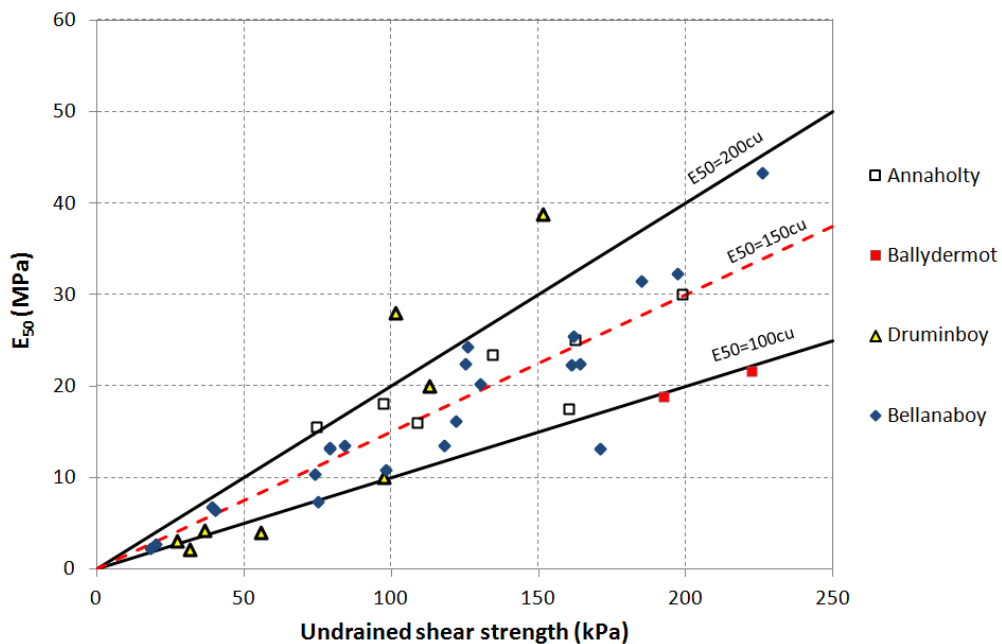
Figure 7: Correlation between undrained shear strength and stiffness at 90 days for various cement only binder concentrations.

The binder concentratuion was found to have an important role in the early stiffness of the stabilised peat. Following mixing, the stabilised Bellanaboy peat was placed in moulds and a confining stress of 18kPa was placed on top. The axial strain was measreed as the specimens consolidated under the initial stress (Figure 8). At cement concentration of 150kg/m³ and above there was sufficient binder to minimise further compression after Day 1. The lower cement concentrations resulted in increasing the axial strains over the next 5 to 6 days.
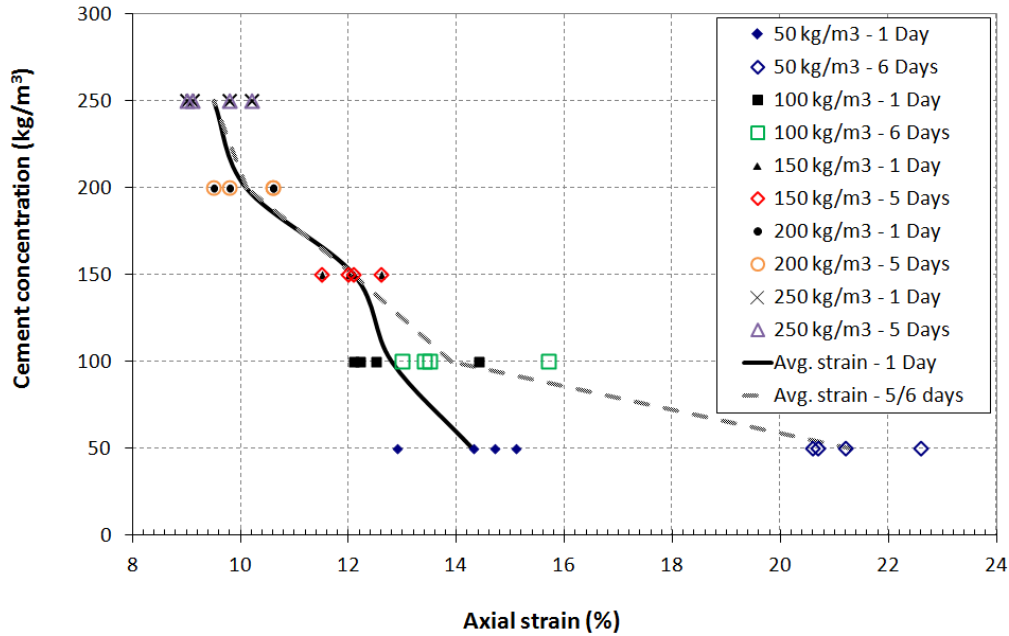
Figure 8: Axial strains in specimens following mixing

3.3. Compressibility

Oedometer tests using a standard 75mm diameter by 20mm high specimens carried out on peat stabilised with 200kg/m³ of cement from Bellanaboy (Quigley and O'Brien, 2010) and Ballydermot (Hebib, 2001). The results are plotted together on Figure 9 and show a similar stress strain response. The yield stress appeared to vary between 100kPa and 150kPa for both studies.
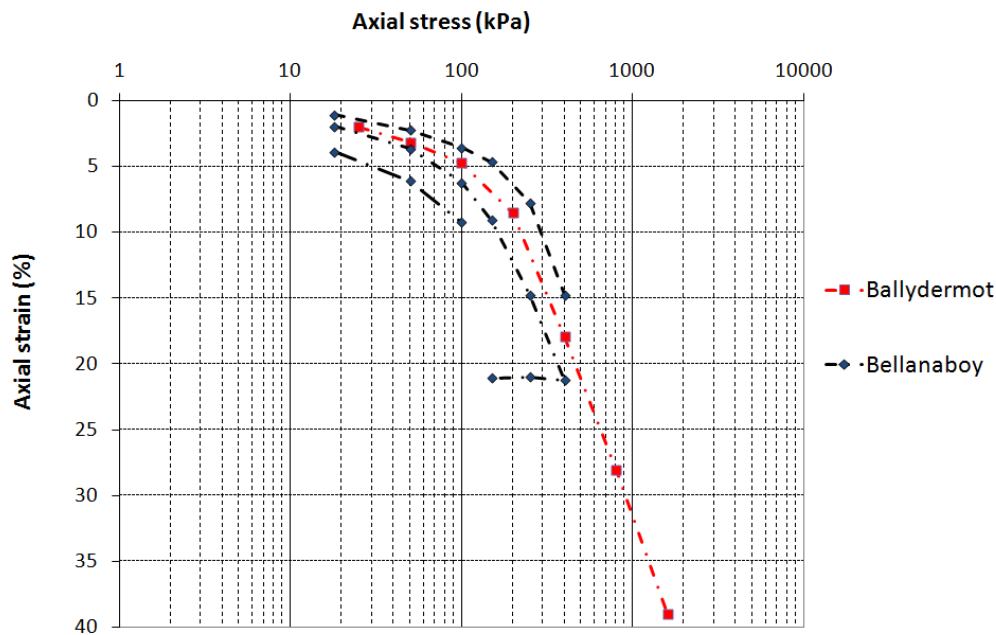
Figure 9: One dimensional consoldiation testing

3.4. Creep

The secondary consolidation coefficient, C_α, was measured on the linear section of the log time versus deformation plot after each load increment increase. C_α is defined as:

$$C_\alpha = \frac{\left(\Delta H_i \Big/ H_{i0}\right)}{\log\left(t_2 \Big/ t_1\right)} \qquad (2)$$

where H_i is the height of the specimen at the end of primary settlement during each load increment and t_1 and t_2 are the start and end time of the creep measurement. The variation between the blanket bog at Bellanaboy and the raised peat at Ballydermot is shown in Figure 10 and shows a gradual increase up to 100 to 150kPa before increasing more sharply once the yield stress of the stabilised peat is exceeded. Typical C_α values for virgin peat vary between 3% to 6%.

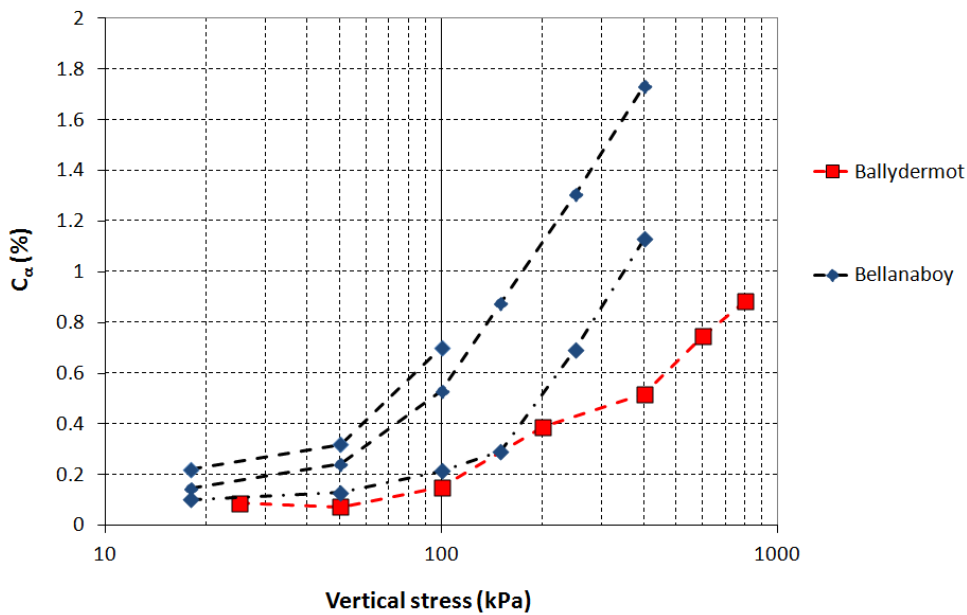*Figure 10: Comparison creep measurements between blanket bog (Bellanaboy) and raised bog (Ballydermot).*

4. EMBODIED ENERGY OF PEAT STABILISATION

There is an increasing awareness of sustainability issues in construction and sustainability is likely to have a greater influence on the choice of construction method. A common comparison tool in evaluating the sustainability of construction methods is the embodied energy (EE). Embodied energy is the energy required to manufacture and supply to the point of use, a product, material or service and is measured in Joules. An EE comparison was carried out for three hypothetical sites in Ireland for treating a 50m long by 5m wide by 5m deep peat block. There is currently a single source of GGBS binder in Ireland while cement production plants are located at various locations across Ireland, shown in Figure 11. The sites A, B and C are located 100km, 200km and 300km away from the GGBS source respectively and are all assumed to be 100km from an OPC production site. The binder concentration is assumed to be 250kg/m³. Crushed aggregates are readily available across Ireland and the three sites are assumed to be 30km from a suitable quarry.

In this calculation, three types of process are shown, covering materials, installation and transportation energies. Of these, the material energy calculation involves finding the total volume of each material used, calculating its weight, and multiplying this by its Embodied Energy Intensity (EEI) value. The transportation energy is that which is required to move all equipment and materials to and from the site. This is calculated using the litres of fuel consumed by the vehicles multiplied by the respective EEI value for the fuel. The installation energy is calculated by multiplying the amount of fuel used by the machinery with its EEI value. All three values of the material, transportation and installation energy are then summed to give the total embodied energy. The Embodied Energy Intensity values have been adapted from Hammond and Jones (2011) and are provided in Table 2. The results shown in Figure 12 suggest

that the material production is responsible for the largest proportion of EE and transport EE is not a significant variable.

Table 2: Embodied Energy Intensity values

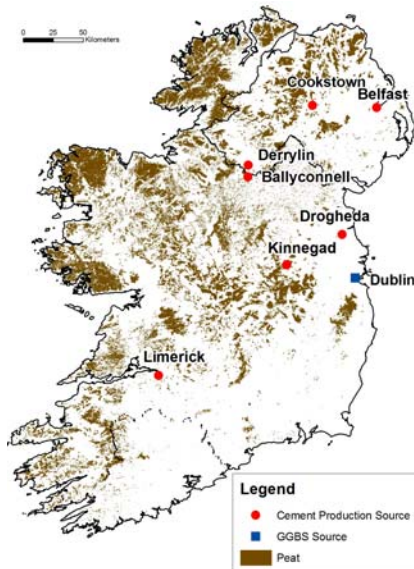| Material	Unit	EEI (MJ/unit):
Ordinary Portland Cement	Kg	5.4
Ground granulaed blast slag	Kg	2.4
Crushed rock	Kg	0.11
Geotextile	Kg	78.1
Diesel fiel	L	45.0

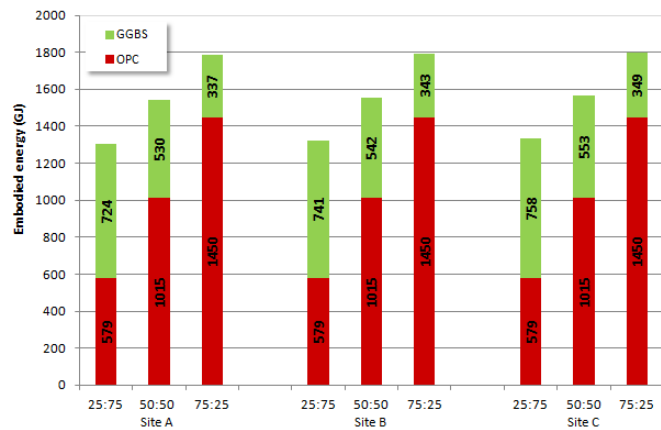*Figure 11 : Cement and GGBS depots in Ireland*

Figure 12 : Embodied Energy calculations for stabilised peat

Typically in construction projects there is a good correlation between embodied energy and CO_2 emissions (e.g. Inui et al., 2011). However, peat bogs are a vast natural reservoir of organic carbon. The invasive nature of soil mixing disturbs a large volume of peat, potentially releasing large volumes of CO_2, methane and other gases. Nayak et al.,(2008) provide some guidance on calculating the carbon losses for excavations and drainage works in peat. It is noteworthy that the excavate and replace approach, often favoured in Ireland when peat is encountered, is also a cause of CO_2 release. However, further research is required to evaluate the carbon loss from peat bogs and the influence of various types of construction.

5. CONCLUSION

Peat is a highly organic soil type unlike other soils, formed from the decay of the dead remains of plant and vegetation. It has a very high moisture content and compressibility. Strengths are very low and in many cases very difficult to quantify due to the fibrous nature and difficulties in undisturbed sampling.
The data in this paper shows that significant strength gains can be obtained by stabilising Irish peats. Unlike stabilisation in other soils, peat requires larger binder concentrations to produce the required strength improvement. The plotted data shows a trend of increasing strength with reducing WTBR. This trend is clearest for cement binders based on the data from the four different sites across a range of degrees of humification. Also visible is the variation in strength that can occur where the same binder is used in two different peats, in particular binders which included a GGBS portion. Cement and GGBS data from the Ballynahown peat show the possible existence of a binder threshold between 200 and 250kg/m^3. The plot may be used as a design guide for future Irish stabilisation projects, although trials are still be required to determine the achievable strengths.

A study of the Embodied Energy required to carry out a peat stabilisation project showed the transportation of the binder to site to be insignificant compared to the amount of embodied energy spent in production binder. It is also noted that carbon stored within the peat body released during mixing can

contribute to the carbon emissions of the project but further research is required to quantify this and compare with alternative construction methods such as excavate and replace and piling.

REFERENCES

Axelsson, K., S.-E. Johansson, and R. Andersson (2002), Report 3: Stabilization of Organic Soils by Cement and Puzzolanic Reactions - Feasibility Study, S.D.S.R. Centre,Swedish Deep Stabilization Research Centre c/o Swedish Geotechnical Institute: Linkoping. p. 44.

Bord na Móna (2011) website, http://www.bordnamona.ie/our-company/our-businesses/feedstock/peat/. Accessed 30/11/2011.

Braaten, A., Aaboe, R. and Oset, F. (1999) Development of in-situ control methods for lime/cement columns. Dry Mix Methods for Deep Soil Stabilization. Stockholm, Sweden. 295-301.

EuroSoilStab (2001), Development of design and construction methods to stabilise soft organic soils, in Design Guide: Soft Soil Stabilisation., BRE & IHS.

Hammond, G. and C. Jones (2011), Inventory of Carbon & Energy (ICE) Version 2.0: Department of Mechanical Engineering, University of Bath, UK.

Hartlén, J., (1996), Embankments on Organic Soils. Developments in Geotechnical Engineering, 80., Amsterdam: Elsevier. 424.

Hayashi, H. and J. Nishikawa, (1999), Mixing efficiency of dry jet mixing methods applied to peaty ground, in Dry Mix Methods for Deep Soil Stabilization, Stockholm, Sweden. p. 333-338.

Hebib, S. (2001), Experimental study of the stabilisation of Irish peat, PhD thesis, Trinity College, Dublin.

Hebib, S. and E.R. Farrell (2003), Some experiences on the stabilisation or Irish peats. Canadian Geotechnical Journal, Vol. 40, p. 107-120.

Hobbs, N.B., (1986), Mire morphoplogy and the properties and behaviour of some British and foreign peats. Quarterly Journal of Engineering Geology, 1986. 19: p. 7-80.

Inui, T., Chau, C., Soga, K., Nicolson, D. and O'Riordan, N.(2011), Embodied energy and gas emissions of retaining wall structures. Journal of Geotechnical and Geoenvironmental Engineering, ASCE, .

Long, M. (2005), Review of peat strength, peat characterization and constitutive modeling of peat with reference to landslides, Studia Getechnica et Mechanica, Vol. XXVII, No. 3 – 4.

Nayak, D.N., Miller, D., Nolan, A., Smith, P. and Smith, J., (2008), Calculating carbon savings from wind farms on Scottish peat lands - a new approach.

Moore, P.D. (1987), Man and mire: a long and wet relationship. Trans. Botanical Society of Edinburgh, 45, 77-95.

Quigley, P. and J. O'Brien (2010), A Feasibility Study of Dry Soil Mixing for a Blanket Bog, in Bridge and Infrastructure Research in Ireland 2010 (BRI10) and Concrete Research in Ireland 2010 (CRI10).: Cork, Ireland.

Rambol (2006). Report on peat stabilistaion tests for N7. Unpublished report.

Timoney, M.J., B.A. McCabe, and A.B. Bell, (2012), Experiences of Dry Soil Mixing in Highly Organic Soils. ICE Ground Improvement, Accepted for publication 2012.

von Post, L.,(1922), Sveriges Geologiska Undersøknings torvinventering och nogra av dess hittils vunna resultat (SGU peat inventory and some preliminary results). Svenska Mosskulturføreningens Tidskrift, Jønkøping, Sweden, 36, 1-37. 1922.

Consolidation of dredged mud in the Venice Lagoon

Daniele Vanni, Trevi SpA, Italy, dvanni@trevispa.com
Giovanni Preda, Trevi SpA, Italy, gpreda@trevispa.com

ABSTRACT

The issue concerning the management of sediments resulting from drainage maintenance activities and reclamation activities strongly affects the development of many Italian ports, some of which are located within the Contaminated Sites of National Interest. According to current regulations, most of sediments are disposed of within containment structures along the coast or waste dumps. It is worth underlining that, due to the massive presence of fine fractions in the dredged sediment, it is often necessary to enhance its geotechnical features through subsequent stabilization interventions, in order to re-use such spaces as productive port areas. The separation of the different granulometric sections and the optimization of treatments for each of them would allow a maximum efficiency of the sediment management process. For that reason, the Surveyor for the Social, Economic and Environmental Emergency concerning the major navigation port canals of Venice Lagoon (Commissario Delegato per l'Emergenza Socio Economico Ambientale relativa ai Canali Portuali di Grande Navigazione della Laguna di Venezia) has authorised the testing of an innovative process for the treatment of dredged sediments, which also includes the stabilization of the dredged sediment's fine fraction through the continuous injection of cement grout, so as to enhance its mechanical features before the final disposal. The testing procedure consists in draining and subsequently treating 200 m3 of sediments coming from different areas within the canals of Porto Industriale di Marghera. The last step of the treatment envisages collocation of a plant for the continuous addition of cement grout to the dredged sediment's fine fraction. The paper illustrates the chosen technological process and the main results obtained. Finally, we believe that the implementation of said method can be extremely important; in fact, not only does it explore innovative technologies and management processes which have never been investigated before in Italy, but it also tries to find out a new approach to the "sediment issue", thus being listed among the main methods for an eco sustainable management of drainage and treatment activities.

1.   PREFACE ABOUT THE METHOD

The need for carrying out large scale sediments' dredging works (for maintenance, deepening and land reclamation works), both for fresh water and in coastal environments, involves remarkable technical and environmental problems, both with regard to the carrying out of the same activity and for the following management of very large quantities of resulting sediments. Particularly, this strongly affects the commercial development of many Italian ports. According to the current Italian Regulations, the dredged sediments can be reused as they are, if suitable, or they must be disposed of in special facilities (Confined Disposal Facilities CDF) that are made in the harbour areas or dumps on the ground according to their contamination level. Unfortunately, the availability and the local capacity of said structures is almost always lower than the volumes of the sediments to be dredged; moreover, because of the presence, sometimes remarkable, of fine fractions into the referenced sediment, reusing said areas as harbour productive areas is often quite problematic, unless subsequent consolidating interventions are carried out. On the other hand, the market demand for inerts is always very high, both for the beach nourishment (that is necessary due to the steady erosion of seashores to which coasts are bound) and for all civil activities, especially in order to allow the construction of infrastructures for the connection with the national networks, in view of the development and modernization of harbours and coast areas. A process of "sediments' management" covering the separation of the various granulometric fractions and the optimization of the treatments per each of them, would allow reconciling the above requirements. In this connection, the Law Decree dated 24th January 2012, nr 1, which reforms the Law 84/94 on the organizing and administrative system of harbours, envisages that also "every single particle size" of the sediment can be placed in CDF. Said provision deserves special attention since, by allowing the reflux of single granulometric fractions, it also introduces the possibility of recovering or reusing part of them. In this view, it is fundamental to approach this topic from a multidisciplinary point of view. The very nature of the sediment, the various contaminations, the removal techniques and the possibility of decontamination, retrieval and/or reflux, involve several technical and scientific disciplines. The above considerations paved the way to collaboration between the Trevi Group – a worldwide leader in the field of Geo-Engineering and in the construction of related equipment - and 3V Green Eagle – a leader

company in the detoxication of wastes that are highly contaminated through the Wet Oxidation technology. The two companies have developed a process made of several activities that allows working on the whole sediments' management, from the dredging to the final destination, always aiming at reusing whatever possible of the resource. The Surveyor for the Social, Economic and Environmental Emergency concerning the major navigation port canals of Venice Lagoon has authorised, by means of the Decree Nr. 29 dated 30th November 2011, the testing of the innovative treatment process in order to verify its effectiveness.

2.   DESCRIPTION OF THE TESTING PROCESS

Testing ended in February 2012 and it was possible to check the efficacy of the granulometric separation of the sediments through physical treatments, the detoxication of water and mud through the Wet Oxidation system and the consolidation in line of the material to be sent to the confined waste disposal or to the dump. Depending on the contamination of the material, 2 technological approaches have been developed:

-   Dredging and treatment of the sediments that are slightly contaminated, such as to be reused following to treatments that are purely physical. (lot 1 and 2);
-   Dredging and treatment of contaminated or highly contaminated sediments (lot 3bis).
-   The two scenarios can be schematised as follows:
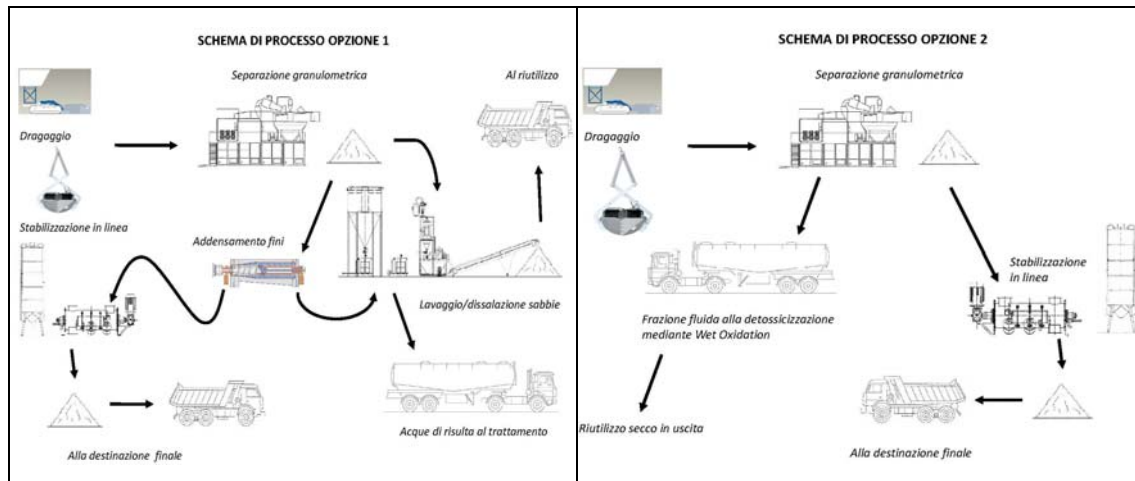
Figure 1: Layout of the process, option 1 –Layout of the process, option 2

Within the experimental activities, the dredging of Nr.3 batches has been carried out in areas located along the Brentella Canal and the West Industrial Canal of the industrial area in the Marghera Port (Figure 2). Lots 1 and 2 had a volume equal to about 60 m3 and the lot 3 bis was equal to about 40 m3. The dredged material was transported by means of a pontoon-barge until reaching the quay that was made available and, from there, it was then transferred into demountable watertight caissons and transported to the site area by means of authorized trucks.

Figure 2: Dredging Points of the sediment

Each sediment lot has been individually treated in order to allow a precise assessment of the efficiency of the suggested treatment. Said evaluation has been carried out by taking and analysing samples of the fractions at the entrance and at the exit of the treatment, in cooperation with ARPA Veneto (Regional Agency for the Environmental Prevention and Protection of the Veneto Region) which has supervised the activities. It was proceeded as follows:

− Nr.3 batches were dredged in the preset points. The material was sent to the quay together with their relevant Assignment Bills;
− Each batch was loaded on a truck and transported into demountable watertight caissons up to the plant that was authorized for the treatment. The arriving sediment was stored into the demountable caissons until the moment when it was treated.
− The first batch was treated. The plant has got three outlets:
  • Sand and coarse solids at the bottom of the desanding unit, stored in a suitable steel tank;
  • Thickened silt coming out of the centrifuge, then stored into a suitable steel tank;
  • Water coming out of the centrifuge, then stored into suitable steel tanks.
− Once the entering material was all sorted out, and the samples were taken for the characterization, the plant was washed and each fraction disposed of. At this point it was possible to start the treatment of the following batch.

Photo 1: Site Area

2.1. Pre-treatment of sediments: separation of coarse waste and blocks and fluidification of the entering material.

The material dredged with hydraulic bucket had a consistency that was too high in order to be sent to the plant. Therefore, a pre-treatment station was arranged for where the sediment was unloaded. The sediment is then made pass through a grid through which the coarse waste and rocks are gotten rid of which were in quite a large quantity in the first dredged sediment batch. The sediment was then fluidified with the cleared water coming out of the centrifuge used to thicken the fine particles, until reaching a thickness equal to about 1,30 - 1,40 t/m3 and pumped to the top of the desanding unit.

2.2. Granulometric separation of the fractions by means of vibrosieving, double phase of cycloning and centrifugation.

The granulometric separation has two main goals: the homogenization of the physical features and the minimization of the volumes to be sent to their final destination. It increases the efficiency of the whole managing process. The bumps and the forces the sediment has to undergo when passing through the plant add to the separation of the agents contaminated by the coarse solid fraction and to the transfer to the liquid fraction. Virtually, the suggested separation process is developed according to the following phases: the mud undergoes a first process of vibrosieving, where the whole coarse material having a diameter of > 2 mm is separated; following, the fluid containing the remaining solid fraction enters a first stage of cycloning (Cut Point $d50 = 60$ μm), where the sandy fraction is separated. This material is made shoveable and unloaded at the bottom of the plant. The fluid containing the remaining solid fraction enters a second phase of cycloning (Cut Point $d50 = 20$ μm), where the silty fraction having a diameter over 0,040 mm is separated. Moreover, there is the separation of the very fine particles by means of

centrifugation. The solid phase looks like a thickened mud and can be sent to the CDF or to the dump after a possible consolidation. The fluid phase is sent to the treatment or, like in the case of experimentation, it is reused as process fluid inside the treatment, so that the minimum quantity of water is used.

Photo 2: Coarse solids being washed on the refining sieve and sandy material being washed in the secondary sieve.

2.3.   Stabilization in line of the material to be sent to the CDF.

In order to use the surface occupied by the CDFs as a harbour infrastructure (once the disposals have been filled in), it is very often necessary to assign geomechanical features to the higher sediments. This is usually obtained by consolidating the mass through the addition of suitable binders. The stabilization of the material can be made before the assignment or, as alternative, at the same time or after the reflux. In this last case (following intervention), punctual techniques can be employed such as the Deep Mixing, by treating the whole volume with punctual treatments performed with cutters having an horizontal or vertical axis. The main limits to the application of the punctual stabilization after the reflux are the overall cost of the treatment, the logistic difficulties (working areas are not usually negotiable), the impossibility to stabilize the whole mass and, to end with, the increased delivery times of the work. As a matter of fact, by working on the whole mass, it's pretty difficult to get an homogeneous consolidation, both for technical problems and because the used geometries of the treated points are circular or rectangular and so they would imply an expensive overlapping of treated areas; moreover, if there is the HDPE liner on the bottom and on the walls of the CDF, the stabilization can't be total, since, otherwise, the cutting tools would damage it. Therefore a thickness of 0,50 – 1,00 m of unconsolidated sediment remains at the bottom. Said material can heavily impact the settlements of the place in the medium-long term. Instead, in the case of a preliminary stabilisation or one that is contemporary to the reflux, the whole volume is treated in a homogeneous way, before the laying, and the areas can be immediately used. The experimental activities have proved the efficaciousness of a mixing technique, where sediments are combined with "in line" binders, simultaneously with the reflux into the CDF, only for the lot Nr.2. Said technology allows a remarkable homogeneity of the stabilised material. From an operating point of view, the cement grout (CEM II/B LL 32,5 and fresh water), that is produced according to a receipt that is such as to optimise the addition of water to the process, has been directly introduced in the entrance of the centrifuge, so that there is a deep mixing of the binder's particles with the solid matrix and the material that is coming out which begins then to immediately harden. The centrifuge allows the automatic control of the quantity of grout to be added on the basis of the delivery volume and the unit weight of the entering fluid mud. The binders' quantity in kilos per tons of dry solid in the solid discharge that is produced by the decanter is calculated on the basis of the features required from the material and to its final use. Said phase of the process is deepened in the following chapters.

Photo 4: Treatment plant – Thickened silty and clayey fraction coming out from the centrifuge

2.4.   Treatment of water and mud: detoxication through Wet Oxidation

In the case of very high contamination, the liquid flow with silt and clay and the water used in the process contain concentrations of contaminants that don't allow their transport to the biological treatment plants, since they aren't biodegradable. The disposal of water and mud is therefore pretty difficult. For said reason a technological, innovative process has been chosen in order to sort out this phase. It is called Wet Oxidation. This process can treat concentrations of COD and contaminants such as to allow them to be sent as they are to the plant, without having to be pre-treated. The plant carries out the "Wet-Oxidation" of the organic component of the mud with pure oxygen at high temperature and pressure. During the reaction of oxidation, complex molecules are transformed into carbon dioxide, water and simple organic molecules (alcohols, aliphatic acids, etc.); the halogenated substances make up the correspondent chloride halides, the sulphide substances produce sulphates and the nitrogenous organic compound produce ammonia and/or nitrates. Inorganic substances are basically unchanged, metal ions can change into oxide correspondents. Reaction conditions don't allow the formation of dangerous substances (i.e. dioxins). The Wet-Oxidation is particularly efficacious with more complex and toxic molecules that can be found into contaminated silts such as: "Cyanides"; "PCB"; "IPA"; "Hydrocarbons C>12"; for these substances the conversion reaches about 100%. The remaining COD derives from the simple organic and partially oxided molecules (aliphatic acids, alcohols, etc …) which represent the intermediate products of the reaction, for whose oxidation longer reaction times would be requested as well as more drastic conditions. Due to its composition, the remaining COD coming out of the Wet-Oxidation plant is completely biodegradable. The effluent of the process, after the sedimentation and the filtration, consists in an inorganic residue and a water reflux that are totally biodegradable so that it can be sent to a biological depurating plant. Gases discharged by the plant, after the condensation and the washing, are exclusively: carbon dioxide, produced in the reaction, and the oxygen that was fed in excess. The process performed in the plant consists in the moisture oxidation of organic substances that are diluted or suspended into a water solution which occurs at a high temperature (200 – 350 °C) and with a consequently high pressure (in order to keep the solution at the liquid state and guarantee a sufficient partial pressure of the oxiding gas in the reaction environment). The oxiding gas can be oxygen, air or a mixture of the two (enriched air). The oxidation progressively demolishes the organic molecules with a final production of water and carbon dioxide. In view of a possible execution of a "TOP" plant for the moisture oxidation of silts that are remarkably polluted, it was deemed important to carry out a specific experimental campaign, performed with a pilot autoclave, aimed at the optimization of the process, both from the point of view of finding the most suitable operating conditions to be adopted and from the point of view of the materials with which the plant will be built. As for the operating conditions, the focus was on the research of the temperature and, following, of the lowest pressure at which there is a sufficient reduction of the concentration of the specific pollutants per each single silt, by keeping in mind that the plants' energy consumptions depend on the reaction temperature since the silts, even when they are highly polluted, have a modest content of organic substance and therefore the thermal contribution of the reaction heat is almost irrelevant. Also the effect on the reduction of the specific pollutants was checked, as well as the "quality" of the inorganic residue of the "pH" changes into the reaction environment. Moreover, the effect on the completion of the reaction when using air instead of pure oxygen was tested, considering it as being more or less rich in oxygen. The possibility of using enriched air, obtainable with plants that are quite simple, such as those with semi permeable membranes or the adsorbing ones that are compressible through quite

simple equipment, could allow the system to work disregarding the available amount of liquid oxygen of cryogenic origin.

Photo 5: Loading of the pilot system Wet Oxi – Fractions entering and coming out of the Wet Oxi

3. STABILIZATION AND CONSOLIDATION IN LINE OF THE FINE SEDIMENTS' FRACTION

3.1. Design hypothesis

As already mentioned in chapter 2.3, it's often necessary to give the material into the CDF some special geomechanical features, in order to be able to use the occupied surface as harbour infrastructure. The strength and deformability values that are usually required from the materials making up the bottom of harbour or street infrastructures are as follows:

− E50 = 50000 kPa in the strength interval ELL = 150 – 250 kPa next to the foundation level of the road paving;
− E50 = 20000 kPa in the strength interval ELL = 50 – 150 kPa on the level which is at a depth of 1,00 m below the foundation level of the road paving;
− E50 = 15000 kPa in the strength interval ELL = 50 – 150 kPa on the level which is at a depth of 2,00 m or more below the foundation level of the road paving.

On the basis of said design data, tests of in line consolidation have been carried out, by measuring the quantity of binders in order to reproduce the required features.

3.2. Performed tests

The in line injection of binders into the fluid suspension of silt and clay has been tested on the sediments of batch nr.2, before they entered the centrifuge decanter. In order to ensure the uniformity of the properties of the thickened and stabilized silt, Soilmec (the engineering company of the Trevi Group) has developed a new centrifuge decanter capable of managing in real time the deliveries of the polyelectrolytes and of the cement grout according to the features of the entering suspension:

− At the beginning of the activities, the specific gravity γs of the entering suspension was analysed and the type and quantity of polyelectrolyte to be added to the fluid suspension were determined in order to have the best separation solid/liquid inside the centrifuge;
− The suspension was taken from the stocking tank by means of an eccentric screw pump;
− Polyelectrolytes and cement grout are produced in other plants and then stored and kept stirring in suitable volumes.
− The delivery volume and the thickness of the entering fluid suspension are instantly measured by means of a mass delivery gauge. Measures are sent to the PLC of the decanter which controls, in real time, the delivery of the volumetric pumps of the polyelectrolyte and cement grout.

The fluid suspension had variable features during the execution of the tests. In particular, the volume weight varied in the range γ = 11,3 – 12,9 kN/m3 and the water content in the range 175 – 450%. The specific weight γs varied in the range 26,8 – 29,1 kN/m3.

Through suitable calibrations of the decanter it was possible to carry out 2 types of test (Photo 6):

1. Maximum separation of solid-liquid material so that the material was brought to the minimum possible volume when binders were added to it.
2. Achievement of a material added with binders having features such as to be sent to its disposal through pumps or pneumatic transport.

In both cases, the just treated material has been sampled into the stocking tank. Samples have been shaped in cylindrical specimens with a diameter of 80mm and a height of 240 mm, according to what envisaged by Designation ASTM C31/C 31M-03°. Samples were then hardened under water, in order to simulate the conditions of being cast into the CDF. The average features of the two materials are reported in the following table (Table 1):

Table 1: Average features of the materials to be added with cement

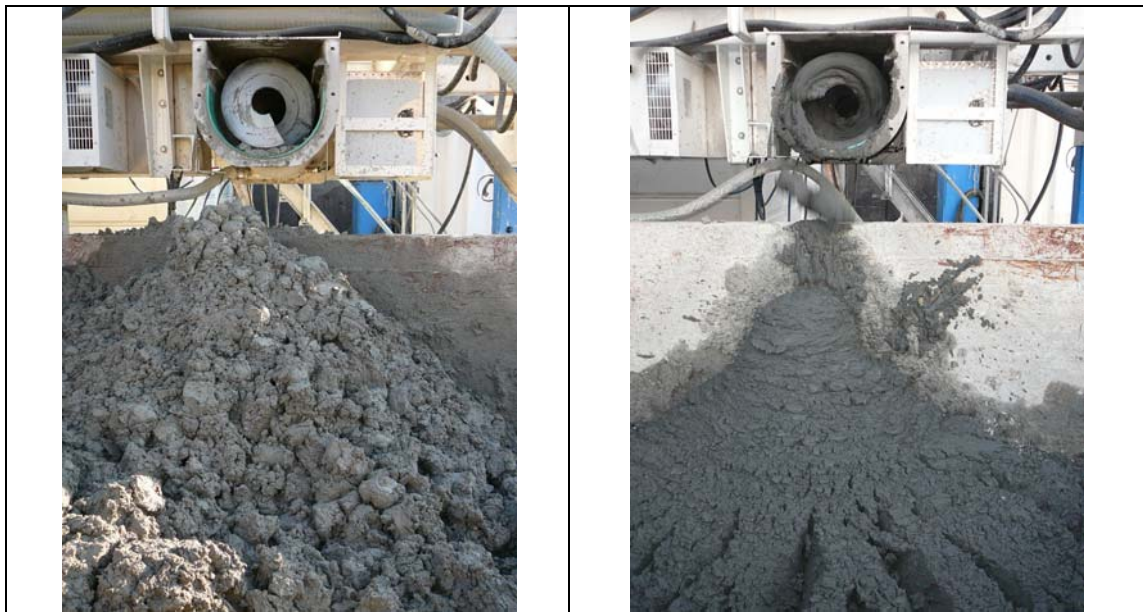| Test	Sand %	Silt %	Clay %	Water Content w%	Unit Weight γ kN/m3	Specific Weight γs kN/m3
1				82,1	14,60	26,79
2	6,1	50,2	43,8	113,9	14,06	27,04

Photo 6: Material for tests type 1 – Material for tests type 2

3.2.1. Tests type 1: shoveable material

Several tests have been carried out on this material, by adding different quantities of cement in kilos per tons of Dry Solid present into the thickened material. Particularly, nr 4 tests have been carried out:

Table 2: Quantity of introduced cement

Group of samples	Cement kgcem/tonDS	Cement kgcem/ton	Cement kgcem/m3
C	110	66	95
D	45	26	38
E	65	37	54
F	85	51	76

The following table reports the results obtained after 15 and 30 days of hardening, divided into groups of tested samples. The groups of samples A and B have been made with the thickened material coming out of the centrifuge decanter, without adding cement:

Table 3: results of the tests carried out after 15 days of hardening

Group	γ kN/m3	γs kN/m3	w %	ELL kPa	Def. %	E_{01} kPa	E_{50} kPa	Cem kg/tonDS
A-B	14,60	26,79	82,1	-	-	-	-	-
C	14,46	-	66,6	135,6	1,96	11743	11531	110
D	14,63	-	72,1	20,0	3,20	1656	938	45
E	14,44	-	74,1	49,0	2,95	2934	2576	65
F	14,98	-	68,1	55,2	2,64	4083	3333	85

Table 4: results of the tests carried out after 30 days of hardening

Group	γ kN/m3	γs kN/m3	w %	ELL kPa	Def. %	E_{01} kPa	E_{50} kPa	Cem kg/tonDS
B	-	26,79	75,8	-	-	-	-	-
C	15,18	-	66,5	151,8	1,71	20447	14737	110
D	14,76	-	68,8	25,3	3,2	1055	1063	45
E	14,69	-	74,5	43,6	2,73	2922	2344	65
F	14,84	-	64,8	41,6	1,42	4965	4789	85

3.2.2. Tests type 2: pumpable material

Several tests have been carried out on this material by adding different quantities of cement in kilos per tons of Dry Solid present in the thickened material. Particularly, nr.3 tests have been carried out:

Table 5: Quantity of introduced cement

Group of samples	Cement kgcem/tonDS	Cement kgcem/ton	Cement kgcem/m3
H	75	35	50
I	100	47	66
L	45	22	31

The following table reports the results obtained after 15 and 30 days of hardening, divided into groups of tested samples. The group of samples G was made with the thickened material coming out of the centrifuge decanter without adding cement:

Table 6: results of the tests performed after 15 days of hardening

Group	γ kN/m3	γs kN/m3	w %	ELL kPa	Def. %	E_{01} kPa	E_{50} kPa	Cem kg/tonDS
G	14,05	27,04	113,9	-	-	-	-	-
H	14,08	-	112,2	10,0	2,78	934	554	75
I	14,06	-	111,5	21,7	3,58	1269	978	100
L	-	27,07	104,1	-	-	-	-	45

Table 7: results of the tests performed after 15 days of hardening

Group	γ kN/m3	γs kN/m3	w %	ELL kPa	Def. %	E_{01} kPa	E_{50} kPa	Cem kg/tonDS
G	13,61	27,04	109,4	-	-	-	-	-
H	13,69	-	112,6	11,9	3,67	781	501	75
I	13,59	-	111,3	28,6	4,25	1340	1082	100
L	13,64	-	104,1	-	-	-	-	45

4.   CONCLUSIONS

When drafting this report, experimental activities are on the verge of being concluded. The analyses on the taken samples are being processed. Nonetheless, what described above reveals the scope of the problem, its complexity, the variety of technologies which can be used to manage the sediments, the undisputed environmental and social-economic advantages which could derive by using such a different approach from their usual transport to the dump. Experimentation is reaching an end and its goal is to develop several technologies and assess the advantages that the cycle seems to offer:

a) Production of reusable material; b) Elasticity of the process; c) Integration with already confirmed processes; d) Reduction of the contamination. The reduction of the contamination allows to downgrade the sediment and therefore the reuse of the resource or its being sent to a confined waste disposal (instead of being unloaded on the ground) with consequent savings. The material sent to the confined waste disposal can be combined with the stabilisation of the material in line or with other technologies, in order to make the areas immediately reusable as harbour quays and to avoid problems and costs involved by subsequent stabilising works.

Particularly, the experimentation of the stabilisation in line shows that it is possible to obtain a material aligned with the required design features and only through a single technological process of reflux-consolidation, hence allowing the Harbour Authorities to save money. The interaction between polyelectrolytes and cement grout is to study in order to better anticipate the geomechanical behaviour of the treated mass.

To end with, we deem that such an experimentation can be extremely important. As a matter of fact, it not only explores technologies and management processes that are innovative, but it also tries to find out a new approach to the "sediment issue", thus being listed among the main methods for an eco sustainable management of drainage and treatment activities.

5.   ACKNOWLEDGEMENTS

REFERENCES

EPA, 1994, Assessment and Remediation of Contaminated Sediments (ARCS) Program, Remediation Guidance Report.

EPA, USACE, TAMS, Malcolm Pirnie Inc., 2004, Lower Passaic River Restoration Project – Dredging Technology Review Report.

Kitazume M., Satoh T., 2005, Quality Control in Central Japan International Airport Construction, Ground Improvement 9, No. 2, 59-66.

ICS UNIDO, 2007, Survey of Sediment Remediation Technologies.

Evangelisti I., 2009, Trattamento mediante Wet Oxidation della componente organica dei sedimenti, Atti dell'evento Speciale Assoreca-ALA, REMTECH Expo 2009.

Oota M., Mitarai Y., Iba Hiroyuki, 2009, Deep Mixing 2009, Kitazume, Terashi, Tokunaga & Yasuoka (eds), 569-574.

Vanni D., Preda G., Evangelisti I., 2010, Un approccio multidisciplinare e innovativo alla gestione dei sedimenti, ECO Bonifiche Rifiuti Demolizioni, Novembre – Dicembre 2010.

Grubb D.G. et Alii, 2010, Stabilized Dredged Material. I: Parametric Study, Journal of Geotechnical and Geoenvironmental Engineering, ASCE.

Grubb D.G. et Alii, 2010, Stabilized Dredged Material. II: Geomechanical Behavior, Journal of Geotechnical and Geoenvironmental Engineering, ASCE.

PLATINUM SPONSORS

ABEF

BESIX

Cofra

DEME
Dredging, Environmental
& Marine Engineering

menARD

SOLETANCHE
BACHY

GOLD SPONSORS

APAGEO

DENYS

EIFFAGE

fUGRO

Holcim

LIEBHERR

Tensar.

TERRASOL

TERRE ARMEE
SUSTAINABLE TECHNOLOGY

CATHIE
ASSOCIATES

SILVER SPONSORS

ISCHEBECK
TITAN

Wicks

KELLER

ORGANIZING SECRETARIAT

BBRI

Belgian Building Research Institute

With the support of TIS-SFT

TIS
Speciale funderingstechnieken